THE ALZHEIMER'S DISEASE CHALLENGE

EDITED BY: Athanasios Alexiou, Mohammad A. Kamal and Ghulam Md Ashraf
PUBLISHED IN: Frontiers in Aging Neuroscience, Frontiers in Neuroscience, Frontiers in Neuroinformatics, Frontiers in Neurology and Frontiers in Human Neuroscience



frontiers Research Topics



frontiers

Frontiers eBook Copyright Statement

The copyright in the text of individual articles in this eBook is the property of their respective authors or their respective institutions or funders. The copyright in graphics and images within each article may be subject to copyright of other parties. In both cases this is subject to a license granted to Frontiers.

The compilation of articles constituting this eBook is the property of Frontiers.

Each article within this eBook, and the eBook itself, are published under the most recent version of the Creative Commons CC-BY licence. The version current at the date of publication of this eBook is CC-BY 4.0. If the CC-BY licence is updated, the licence granted by Frontiers is automatically updated to the new version.

When exercising any right under the CC-BY licence, Frontiers must be attributed as the original publisher of the article or eBook, as applicable.

Authors have the responsibility of ensuring that any graphics or other materials which are the property of others may be included in the CC-BY licence, but this should be checked before relying on the CC-BY licence to reproduce those materials. Any copyright notices relating to those materials must be complied with.

Copyright and source acknowledgement notices may not be removed and must be displayed in any copy, derivative work or partial copy which includes the elements in question.

All copyright, and all rights therein, are protected by national and international copyright laws. The above represents a summary only. For further information please read Frontiers' Conditions for Website Use and Copyright Statement, and the applicable CC-BY licence.

ISSN 1664-8714
ISBN 978-2-88963-128-5
DOI 10.3389/978-2-88963-128-5

About Frontiers

Frontiers is more than just an open-access publisher of scholarly articles: it is a pioneering approach to the world of academia, radically improving the way scholarly research is managed. The grand vision of Frontiers is a world where all people have an equal opportunity to seek, share and generate knowledge. Frontiers provides immediate and permanent online open access to all its publications, but this alone is not enough to realize our grand goals.

Frontiers Journal Series

The Frontiers Journal Series is a multi-tier and interdisciplinary set of open-access, online journals, promising a paradigm shift from the current review, selection and dissemination processes in academic publishing. All Frontiers journals are driven by researchers for researchers; therefore, they constitute a service to the scholarly community. At the same time, the Frontiers Journal Series operates on a revolutionary invention, the tiered publishing system, initially addressing specific communities of scholars, and gradually climbing up to broader public understanding, thus serving the interests of the lay society, too.

Dedication to Quality

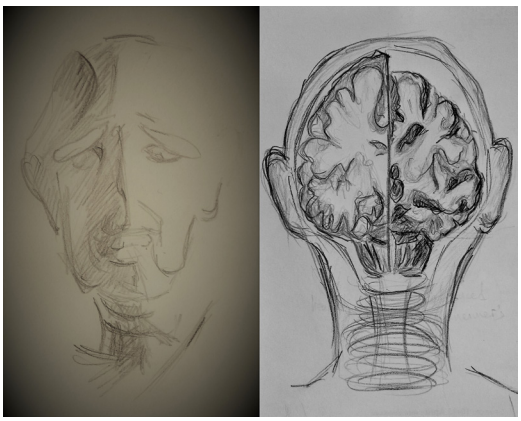
Each Frontiers article is a landmark of the highest quality, thanks to genuinely collaborative interactions between authors and review editors, who include some of the world's best academicians. Research must be certified by peers before entering a stream of knowledge that may eventually reach the public - and shape society; therefore, Frontiers only applies the most rigorous and unbiased reviews.
Frontiers revolutionizes research publishing by freely delivering the most outstanding research, evaluated with no bias from both the academic and social point of view. By applying the most advanced information technologies, Frontiers is catapulting scholarly publishing into a new generation.

What are Frontiers Research Topics?

Frontiers Research Topics are very popular trademarks of the Frontiers Journals Series: they are collections of at least ten articles, all centered on a particular subject. With their unique mix of varied contributions from Original Research to Review Articles, Frontiers Research Topics unify the most influential researchers, the latest key findings and historical advances in a hot research area! Find out more on how to host your own Frontiers Research Topic or contribute to one as an author by contacting the Frontiers Editorial Office: researchtopics@frontiersin.org

THE ALZHEIMER'S DISEASE CHALLENGE

Topic Editors:
Athanasios Alexiou, Novel Global Community Educational Foundation, Australia
Mohammad A. Kamal, King Fahd Medical Research Center, King Abdulaziz University, Saudi Arabia
Ghulam Md Ashraf, King Fahd Medical Research Center, King Abdulaziz University, Saudi Arabia



"Alzheimer's Brain" by Polina Simou is licensed under CC-BY.

Alzheimer's disease is undoubtedly the major health challenge of our Century with significant social and economic consequences. This Frontiers eBook offers a contribution of 39 innovative papers on the multidimensional and crucial problem of Alzheimer's disease management and treatment. Several perspectives, research updates, and trials describing methods on potential diagnosis and treatment are presented including biological mechanisms, biomarkers and risk factors for an early and efficient prognosis, diagnosis and prevention. Additionally, while the rapidly increasing Alzheimer's disease population demands holistic solutions and clinical studies with new therapeutic target approaches, several of the contributive papers present promising drugs targeting Alzheimer's disease treatment.

We give our deepest acknowledgment to all the authors for their important and innovative contributions, to the reviewers for their valuable recommendations on improving the submitting studies and all the Frontiers Editorial team for continuous support.

Citation: Alexiou, A., Kamal, M. A., Ashraf, G. M., eds. (2019). The Alzheimer's Disease Challenge. Lausanne: Frontiers Media SA. doi: 10.3389/978-2-88963-128-5

Table of Contents

07 ***Editorial: The Alzheimer's Disease Challenge***
Athanasios Alexiou, Mohammad A. Kamal and Ghulam Md Ashraf

SECTION 1
BIOMARKERS AND RISK FACTORS

12 ***Blood-Derived Plasma Protein Biomarkers for Alzheimer's Disease in Han Chinese***
Zaohuo Cheng, Jiajun Yin, Hongwei Yuan, Chunhui Jin, Fuquan Zhang, Zhiqiang Wang, Xiaowei Liu, Yue Wu, Tao Wang and Shifu Xiao

22 ***Investigation of Gal-3 Expression Pattern in Serum and Cerebrospinal Fluid of Patients Suffering From Neurodegenerative Disorders***
Ghulam M. Ashraf and Saleh S. Baeesa

30 ***On the Extraction and Analysis of Graphs From Resting-State fMRI to Support a Correct and Robust Diagnostic Tool for Alzheimer's Disease***
Claudia Bachmann, Heidi I. L. Jacobs, PierGianLuca Porta Mana, Kim Dillen, Nils Richter, Boris von Reutern, Julian Dronse, Oezguer A. Onur, Karl-Josef Langen, Gereon R. Fink, Juraj Kukolja and Abigail Morrison

54 ***Analysis of Alzheimer's Disease Based on the Random Neural Network Cluster in fMRI***
Xia-an Bi, Qin Jiang, Qi Sun, Qing Shu and Yingchao Liu

64 ***Decreased Bilateral FDG-PET Uptake and Inter-Hemispheric Connectivity in Multi-Domain Amnestic Mild Cognitive Impairment Patients: A Preliminary Study***
Xiao Luo, Kaicheng Li, Qingze Zeng, Peiyu Huang, Yeerfan Jiaerken, Tiantian Qiu, Xiaojun Xu, Jiong Zhou, Jingjing Xu and Minming Zhang for the Alzheimer's Disease Neuroimaging Initiative (ADNI)

77 ***Influence of* APOE *and* RNF219 *on Behavioral and Cognitive Features of Female Patients Affected by Mild Cognitive Impairment or Alzheimer's Disease***
Alessandra Mosca, Samantha Sperduti, Viorela Pop, Domenico Ciavardelli, Alberto Granzotto, Miriam Punzi, Liborio Stuppia, Valentina Gatta, Francesca Assogna, Nerisa Banaj, Fabrizio Piras, Federica Piras, Carlo Caltagirone, Gianfranco Spalletta and Stefano L. Sensi

85 ***Identification of a Novel Hemizygous SQSTM1 Nonsense Mutation in Atypical Behavioral Variant Frontotemporal Dementia***
Lin Sun, Zhouyi Rong, Wei Li, Honghua Zheng, Shifu Xiao and Xia Li

92 ***Challenges for Alzheimer's Disease Therapy: Insights From Novel Mechanisms Beyond Memory Defects***
Rudimar L. Frozza, Mychael V. Lourenco and Fernanda G. De Felice

105 ***Auditory Memory Decay as Reflected by a New Mismatch Negativity Score is Associated With Episodic Memory in Older Adults at Risk of Dementia***
Daria Laptinskaya, Franka Thurm, Olivia C. Küster, Patrick Fissler, Winfried Schlee, Stephan Kolassa, Christine A. F. von Arnim and Iris-Tatjana Kolassa

118 ***Metabolic Abnormalities of Erythrocytes as a Risk Factor for Alzheimer's Disease***
Elena A. Kosenko, Lyudmila A. Tikhonova, Carmina Montoliu, George E. Barreto, Gjumrakch Aliev and Yury G. Kaminsky

SECTION 2
COMORBIDITIES AND OTHER RELATED DISORDERS

135 ***Fighting the Cause of Alzheimer's and GNE Myopathy***
Shreedarshanee Devi, Rashmi Yadav, Pratibha Chanana and Ranjana Arya

149 ***Alzheimer's Disease and Type 2 Diabetes: A Critical Assessment of the Shared Pathological Traits***
Shreyasi Chatterjee and Amritpal Mudher

172 ***Sleep Disorders Associated With Alzheimer's Disease: A Perspective***
Anna Brzecka, Jerzy Leszek, Ghulam Md Ashraf, Maria Ejma, Marco F. Ávila-Rodriguez, Nagendra S. Yarla, Vadim V. Tarasov, Vladimir N. Chubarev, Anna N. Samsonova, George E. Barreto and Gjumrakch Aliev

182 ***Repetitive Transcranial Magnetic Stimulation (rTMS) Modulates Lipid Metabolism in Aging Adults***
Weicong Ren, Jiang Ma, Juan Li, Zhijie Zhang and Mingwei Wang

188 ***Divergent Roles of Vascular Burden and Neurodegeneration in the Cognitive Decline of Geriatric Depression Patients and Mild Cognitive Impairment Patients***
Qing Ye, Fan Su, Liang Gong, Hao Shu, Wenxiang Liao, Chunming Xie, Hong Zhou, Zhijun Zhang and Feng Bai

200 ***Subregional Structural Alterations in Hippocampus and Nucleus Accumbens Correlate With the Clinical Impairment in Patients With Alzheimer's Disease Clinical Spectrum: Parallel Combining Volume and Vertex-Based Approach***
Xiuling Nie, Yu Sun, Suiren Wan, Hui Zhao, Renyuan Liu, Xueping Li, Sichu Wu, Zuzana Nedelska, Jakub Hort, Zhao Qing, Yun Xu and Bing Zhang

SECTION 3
TREATMENT STRATEGIES
3.1 HUMAN TRIALS

209 ***Perspective Insights Into Disease Progression, Diagnostics, and Therapeutic Approaches in Alzheimer's Disease: A Judicious Update***
Arif Tasleem Jan, Mudsser Azam, Safikur Rahman, Angham M. S. Almigeiti, Duk Hwan Choi, Eun Ju Lee, Qazi Mohd Rizwanul Haq and Inho Choi

220 ***Application of Ferulic Acid for Alzheimer's Disease: Combination of Text Mining and Experimental Validation***
Guilin Meng, Xiulin Meng, Xiaoye Ma, Gengping Zhang, Xiaolin Hu, Aiping Jin, Yanxin Zhao and Xueyuan Liu

229 ***Targeting Beta-Amyloid at the CSF: A New Therapeutic Strategy in Alzheimer's Disease***
Manuel Menendez-Gonzalez, Huber S. Padilla-Zambrano, Gabriel Alvarez, Estibaliz Capetillo-Zarate, Cristina Tomas-Zapico and Agustin Costa

237 ***Insulin Resistance as a Therapeutic Target in the Treatment of Alzheimer's Disease: A State-of-the-Art Review***
Christian Benedict and Claudia A. Grillo

250 ***Ethnopharmacological Approaches for Dementia Therapy and Significance of Natural Products and Herbal Drugs***
Devesh Tewari, Adrian M. Stankiewicz, Andrei Mocan, Archana N. Sah, Nikolay T. Tzvetkov, Lukasz Huminiecki, Jarosław O. Horbańczuk and Atanas G. Atanasov

274 ***Dissecting Endoplasmic Reticulum Unfolded Protein Response (UPR^{ER}) in Managing Clandestine Modus Operandi of Alzheimer's Disease***
Safikur Rahman, Ayyagari Archana, Arif Tasleem Jan and Rinki Minakshi

284 ***Autophagy and Alzheimer's Disease: From Molecular Mechanisms to Therapeutic Implications***
Md. Sahab Uddin, Anna Stachowiak, Abdullah Al Mamun, Nikolay T. Tzvetkov, Shinya Takeda, Atanas G. Atanasov, Leandro B. Bergantin, Mohamed M. Abdel-Daim and Adrian M. Stankiewicz

302 ***Tai Chi Chuan and Baduanjin Mind-Body Training Changes Resting-State Low-Frequency Fluctuations in the Frontal Lobe of Older Adults: A Resting-State fMRI Study***
Jing Tao, Xiangli Chen, Jiao Liu, Natalia Egorova, Xiehua Xue, Weilin Liu, Guohua Zheng, Ming Li, Jinsong Wu, Kun Hu, Zengjian Wang, Lidian Chen and Jian Kong

3.2 MOUSE MODELS STUDIES

312 ***Effects of Oligosaccharides From* Morinda officinalis *on Gut Microbiota and Metabolome of APP/PS1 Transgenic Mice***
Yang Xin, Chen Diling, Yang Jian, Liu Ting, Hu Guoyan, Liang Hualun, Tang Xiaocui, Lai Guoxiao, Shuai Ou, Zheng Chaoqun, Zhao Jun and Xie Yizhen

326 ***Prebiotic Effect of Fructooligosaccharides From* Morinda officinalis *on Alzheimer's Disease in Rodent Models by Targeting the Microbiota-Gut-Brain Axis***
Diling Chen, Xin Yang, Jian Yang, Guoxiao Lai, Tianqiao Yong, Xiaocui Tang, Ou Shuai, Gailian Zhou, Yizhen Xie and Qingping Wu

354 ***The Role of Fluoxetine in Activating Wnt/ß-Catenin Signaling and Repressing ß-Amyloid Production in an Alzheimer Mouse Model***
Min Huang, Yubin Liang, Hongda Chen, Binchu Xu, Cuicui Chai and Pengfei Xing

367 ***Royal Jelly Reduces Cholesterol Levels, Ameliorates Aß Pathology and Enhances Neuronal Metabolic Activities in a Rabbit Model of Alzheimer's Disease***
Yongming Pan, Jianqin Xu, Cheng Chen, Fangming Chen, Ping Jin, Keyan Zhu, Chenyue W. Hu, Mengmeng You, Minli Chen and Fuliang Hu

381 ***The Histamine H3 Receptor Antagonist DL77 Ameliorates MK801-Induced Memory Deficits in Rats***
Nermin Eissa, Nadia Khan, Shreesh K. Ojha, Dorota Łazewska, Katarzyna Kieć-Kononowicz and Bassem Sadek

392 ***Sex Differences in the Cognitive and Hippocampal Effects of Streptozotocin in an Animal Model of Sporadic AD***
Jian Bao, Yacoubou A. R. Mahaman, Rong Liu, Jian-Zhi Wang, Zhiguo Zhang, Bin Zhang and Xiaochuan Wang

404 ***Corrigendum: Sex Differences in the Cognitive and Hippocampal Effects of Streptozotocin in an Animal Model of Sporadic AD***
Jian Bao, Yacoubou A. R. Mahaman, Rong Liu, Jian-Zhi Wang, Zhiguo Zhang, Bin Zhang and Xiaochuan Wang

406 ***Differential Roles of Environmental Enrichment in Alzheimer's Type of Neurodegeneration and Physiological Aging***
Vladimir V. Salmin, Yulia K. Komleva, Natalia V. Kuvacheva, Andrey V. Morgun, Elena D. Khilazheva, Olga L. Lopatina, Elena A. Pozhilenkova, Konstantin A. Shapovalov, Yulia A. Uspenskaya and Alla B. Salmina

SECTION 4
MODELING AND DIAGNOSIS

418 ***Analyzing the Behavior of Neuronal Pathways in Alzheimer's Disease Using Petri Net Modeling Approach***
Javaria Ashraf, Jamil Ahmad, Amjad Ali and Zaheer Ul-Haq

443 ***Streptozotocin Impairs Proliferation and Differentiation of Adult Hippocampal Neural Stem Cells* in Vitro*-Correlation With Alterations in the Expression of Proteins Associated With the Insulin System***
Ping Sun, Gabriela Ortega, Yan Tan, Qian Hua, Peter F. Riederer, Jürgen Deckert and Angelika G. Schmitt-Böhrer

456 ***An Algorithm for Preclinical Diagnosis of Alzheimer's Disease***
Tapan K. Khan

469 ***Cognitive Function and Brain Atrophy Predict Non-pharmacological Efficacy in Dementia: The Mihama-Kiho Scan Project2***
Ken-ichi Tabei, Masayuki Satoh, Jun-ichi Ogawa, Tomoko Tokita, Noriko Nakaguchi, Koji Nakao, Hirotaka Kida and Hidekazu Tomimoto

476 ***A Brainnetome Atlas Based Mild Cognitive Impairment Identification Using Hurst Exponent***
Zhuqing Long, Bin Jing, Ru Guo, Bo Li, Feiyi Cui, Tingting Wang and Hongwen Chen

484 ***Use of Peptides for the Management of Alzheimer's Disease: Diagnosis and Inhibition***
Mohammad H. Baig, Khurshid Ahmad, Gulam Rabbani and Inho Choi

490 ***A Novel Early Diagnosis System for Mild Cognitive Impairment Based on Local Region Analysis: A Pilot Study***
Fatma E. A. El-Gamal, Mohammed M. Elmogy, Mohammed Ghazal, Ahmed Atwan, Manuel F. Casanova, Gregory N. Barnes, Robert Keynton, Ayman S. El-Baz and Ashraf Khalil for the Alzheimer's Disease Neuroimaging Initiative

frontiers in Neuroscience

EDITORIAL
published: 24 July 2019
doi: 10.3389/fnins.2019.00768

Editorial: The Alzheimer's Disease Challenge

Athanasios Alexiou[1,2]*, *Mohammad A. Kamal*[1,3,4] *and Ghulam Md Ashraf*[3,5]

[1] Novel Global Community Educational Foundation, Hebersham, NSW, Australia, [2] AFNP Med, Wien, Austria, [3] King Fahd Medical Research Center, King Abdulaziz University, Jeddah, Saudi Arabia, [4] Enzymoics, Hebersham, NSW, Australia, [5] Department of Medical Laboratory Technology, Faculty of Applied Medical Sciences, King Abdulaziz University, Jeddah, Saudi Arabia

Keywords: AD, amyloid-β, diagnosis, treatment procedures, risk factors, mechanisms

Editorial on the Research Topic

The Alzheimer's Disease Challenge

BIOMARKERS, RISK FACTORS, AND PATHOPHYSIOLOGICAL MECHANISMS OF AD

Alzheimer's Disease is a major health challenge with significant social and economic consequences. Ten papers submitted to this Research Topic discuss the biological mechanisms and potential biomarkers for an early and efficient diagnosis, including genetic factors, imaging data, and comorbidities.

Cheng et al. examined the efficacy of certain plasma proteins as potential diagnostic biomarkers of AD using plasma samples from 98 AD patients and 101 healthy elderly controls from Wuxi and Shanghai Mental Health Centers. They discovered that a combination of the plasma proteins BDNF, AGT, IGFBP-2, OPN, cathepsin D, SAP, complement C4, and TTR may provide a diagnostic biomarker for AD in the Chinese population. Even though the sample size of the study was small and various factors can alter plasma protein levels, this plasma panel could provide a solution for the AD population in the future. Additionally, physicians must take into consideration that AD overlaps with other types of dementia, and that multiple comorbidities occur simultaneously. Therefore, a future challenge lies in determining whether this protein panel can exclusively reflect AD, and no other dementia diseases.

Ashraf and Baeesa identified a potentially strong effect of galectin-3 in serum and cerebrospinal fluid (CSF) samples of AD and amyotrophic lateral sclerosis patients, suggesting it as a promising biomarker of these chronic diseases. The authors collected CSF and serum samples from 31 AD patients, 19 amyotrophic lateral sclerosis patients, and 50 normal healthy controls, and performed a comparative analysis of the galectin-3 expression pattern. They also administered a set of neuropsychological assessments that revealed a strong correlation between the galectin-3 levels and cognitive decline in AD patients, and the activation of inflammation and apoptosis, suggesting the necessity of exploring other galectins in relation to neurodegeneration.

Even though functional Magnetic Resonance Imaging (fMRI) is a well-established diagnostic method for every stage of AD development, Bachmann et al. highlight the importance of different methods of graph construction and analysis of fMRI data. Several methods such as the Ward clustering, the Atlas-based clustering, the region growing, and selection algorithm were evaluated in their study based on a sample of 26 healthy controls, 16 subjects with mild cognitive impairment (MCI), and 14 with AD. The results were analyzed with respect to statistical significance of the

OPEN ACCESS

Edited and reviewed by:
Einar M. Sigurdsson,
New York University, United States

***Correspondence:**
Athanasios Alexiou
alexiou@ngcef.net

Specialty section:
This article was submitted to Neurodegeneration, a section of the journal Frontiers in Neuroscience

Received: *14 April 2019*
Accepted: *09 July 2019*
Published: *24 July 2019*

Citation:
Alexiou A, Kamal MA and Ashraf GM (2019) Editorial: The Alzheimer's Disease Challenge. Front. Neurosci. 13:768. doi: 10.3389/fnins.2019.00768

mean difference in graph properties, the sensitivity of the results to model parameter choices, the relative diagnostic power based on a statistical model, and support vector machines, leading to the conclusion that there are differences between the techniques and their biological interpretations.

Another neuroinformatics study on fMRI data from Bi et al. proposes a new method named the random neural network cluster, which consists of multiple neural networks, to improve the efficient discrimination of AD patients from healthy controls. The authors used the random Elman neural network cluster on the data of 25 AD patients and 36 healthy controls, imported from the AD Neuroimaging Initiative dataset, to select significant features for the identification of abnormal brain regions, to provide accurate AD diagnosis in large samples and high-dimensional data. With an accuracy of >90%, the authors provide the diagnosis of AD by identifying 23 abnormal regions such as the precentral gyrus, the frontal gyrus, and the supplementary motor area, compared to the healthy controls.

Luo et al. evaluated neuroimaging data, including fluorine-18 positron emission tomography—fluorodeoxyglucose of patients with single domain amnestic MCI (sd-aMCI) and multiple domains amnestic MCI (md-aMCI), concluding that the presence of inter-hemispheric connection patterns within the samples. More specifically, the authors evaluated 49 controls, 32 SD-aMCI, and 32 MD-aMCI patients, and presented very promising and clear evidence suggesting inter-hemispheric connectivity as a potential biomarker to monitor disease progression in aMCI patients, simultaneously demonstrating that different damage patterns of inter-hemispheric connectivity may contribute to distinct clinical symptoms in sd-aMCI and md-aMCI.

Although the ε4 variant of apolipoprotein E (ApoE4) gene has already been associated with AD development, Mosca et al. identified a new interaction between the ApoE4 and the RNF219 gene, which correlated with MCI. Here, 83 MCI and 90 AD patients participated, and were initially assessed using neuropsychological evaluations and then genotyped for the APOE and RNF219 polymorphic variants. The authors revealed that AD patients with the ApoE4 and RNF219/G variants presented certain behavioral conditions (including anxiety) that might be useful as potential neuropsychiatric biomarkers.

Sun et al. reported through a single case study the potential pathogenic significance of the SQSTM1 S224X mutation and frontotemporal dementia. The authors described a single case of a 59-year-old woman—with memory decline, mild personality changes, and subtle atrophy of frontal/temporal lobes—in whom an SQSTM1 mutation resulted in the absence of the SQSTM1/p62 protein. Obviously, a larger set of genetic data is necessary to identify the role of this mutation in dementia.

Despite the controversial role of many pathophysiological mechanisms involved in AD development, Frozza et al. highlighted the symptoms and lesions that may affect the patient and that should therefore be considered in drug development approaches in a recent review. While current treatments have a more symptomatic character, the authors described heterogeneous and complex AD signs including mood and behavioral changes, inflammation, and metabolic disturbances, which could lead to the development of hybrid drugs in the search for efficient AD therapy.

Laptinskaya et al. took advantage of the low cost and non-invasive electroencephalography technique to provide a novel and innovative method of neuropsychological assessment for the elderly. In this study 59 participants were classified with subjective memory impairment, 19 as naMCI, and 24 as aMCI, and the authors designed an extended version of the auditory mismatch negativity (MMN) which highly correlated with episodic memory at baseline, and which was underlined, at the 5-year-follow-up, as a potential biomarker for early diagnosis and AD monitoring.

Another research group provided evidence of the potential double role of erythrocyte energy metabolism as a biomarker of impaired cognitive function and as part of new therapeutic procedures (Kosenko et al.). Kosenko et al. discussed the association between the metabolic and antioxidant defense alterations in the circulating erythrocyte population and the neurobiological changes observed in the AD brain, along with the potential usefulness of restoring erythrocyte energy metabolism as an effective treatment.

COMORBIDITIES AND OTHER RELATED DISORDERS

Several lesions, symptoms, and comorbidities are commonly present in AD and other related disorders. Six papers featured in this Research Topic discuss common clinical observations and mechanisms between AD and other disorders including GNE myopathy (GNEM), type 2 diabetes mellitus (T2DM), sleep disturbances, hyperlipidemia, and vascular risk. While GNEM is characterized by numerous pathophysiological lesions similar to those of AD, in a detailed review on GNEM and AD-related impairments, Devi et al. draw interesting conclusions on common mechanisms such as the aggregation of amyloid-β (Aβ) and the accumulation of phosphorylated tau and other misfolded proteins. Moreover, in spite of the fact that AD affects mainly brain neurons while GNEM is a rare disease that affects muscle cells, they both share similar disruptions in cellular functions and other common etiologies, including mitochondrial dysfunction, oxidative stress, upregulation of chaperones, and cell death.

In a very detailed review, Chatterjee and Mudher described the strong association and the crossing pathways of T2DM with AD, as a high-risk factor in the elderly population, even though differences can be found between the familial and the sporadic cases. The authors presented novel findings showing that insulin resistance in T2DM can lead to AD-like pathology through abnormal Aβ and tau accumulation, resulting from the loss of synapses, impaired autophagy, and increased neuronal apoptosis.

The correlation between early-onset AD, cognitive impairment, and sleep disorder symptoms are described by Brzecka et al. The authors reviewed evidence from the literature on the influence of low quality sleep, including apneas or disordered breathing, on the circadian fluctuations of the concentrations of Aβ in the interstitial brain fluid and in the CSF

related to the glymphatic brain system, which could be associated with cognitive decline and AD pathology.

Ren et al. examined the impact of hyperlipidemia on dementia by applying repetitive transcranial magnetic stimulation (rTMS) on the right dorsolateral prefrontal cortex. The authors observed, in 30 randomly recruited and screened elderly subjects (14 assigned to the rTMS group and 16 to the control group), that rTMS reduces serum lipid levels such as cholesterol and triglycerides, and increases thyroid stimulating hormone and thyroxine levels. Those results show that rTMS may play an effective role in the activity of the hypothalamic-pituitary-thyroid (HPT) axis.

While depression and MCI are both known to contribute to the progression of dementia, Ye et al. reported novel findings in remitted geriatric depression and aMCI patients. In this study, 41 remitted geriatric depression subjects, 51 aMCI subjects, and 64 healthy elderly subjects underwent MRI scans and neuropsychological tests both at baseline and at a 35-month follow-up, and each group was further divided into a declining subgroup and a stable subgroup. Remitted geriatric depression groups with cognitive decline have shown greater vascular risk than the corresponding remitted geriatric depression stable groups, according to the authors, suggesting a relationship with vascular burden. Additionally, compared to the stable aMCI group, the aMCI decline group had a lower left hippocampal volume, which is indicative of neurodegeneration.

Nie et al. focused on the relationships between deep gray matter and loss of brain function due to AD and MCI. Comparing gray subregions of 30 AD patients and 30 MCI patients with 30 normal controls, the authors concluded that even without a decrease in the volume of a gray structure, atrophy might occur in several of its subregions. This atrophy measurement on a subregional level could be characterized as a potential biomarker for early AD diagnosis.

TREATMENT STRATEGIES

The rapidly increasing AD population demands holistic solutions and clinical studies with new therapeutic target approaches. Fifteen papers in this Research Topic present innovative promising drugs targeting AD prevention and treatment.

Jan et al. reviewed the failure of the drugs so far approved for treatment in AD, and shift toward a series of drugs to offer a holistic treatment against Aβ deposition and phosphorylated tau. The authors discuss risk factors that affect AD progression, such as mitochondrial dysfunction, endoplasmic reticulum stress and mitophagy, and the potential role of exosomes as efficient drug delivery vehicles for AD therapy.

Another approach involves text mining from traditional Chinese medicine (TCM) database to identify potential drugs and related protein target mechanisms (Meng et al.). Meng et al. retrieved articles from PubMed using AD-related keywords and focused on identifying compounds and proteins involved in AD development. The authors validated their results by applying protein-protein interaction (PPI) networks, western blotting, and co-immunoprecipitation in an AD cell model, in addition to identifying ferulic acid as a potential efficient component of AD treatment.

Menendez-Gonzalez et al. approached the topic of Aβ clearance by designing an alternative method known as the CSF-sink therapeutic strategy for the management of AD, which is based on previously published Aβ-immunotherapies. While Aβ-immunotherapies are directly influencing the CNS, the authors of this review imply that decreases in the concentration of Aβ in the CSF may lead to Aβ removal from the interstitial fluid, and that an increase in the elimination of Aβ by enzymatic degradation may slow down both protein aggregation and AD progression.

In another review study that associates T2DM with AD pathology, Benedict and Grillo presented pieces of evidence that relate the abnormalities in insulin signaling in AD. The authors proposed the existence of common mechanisms in AD pathology and disrupted insulin signaling, and that the pharmacological restoration of normal brain insulin signaling could offer a new therapeutic strategy against AD.

In their review study, Tewari et al. discussed the application of ethnomedicinal methods as dementia novel treatments. The authors evaluated the anti-inflammatory, antioxidative, and antiapoptotic neuroprotective effects of five different plants as potential future drug candidates.

Rahman et al. discussed the molecular signatures of unfolded protein response in elderly subjects, and the resulting neuropathology and memory loss. The role of the endoplasmic reticulum in brain signaling and age-related AD and the neuroprotective effects of modulating the endoplasmic reticulum unfolded protein response in AD are analyzed. Additionally, the authors described the use of astrocytes as potential pharmacological targets in AD therapeutics.

Uddin et al. analyzed the mechanisms and the genes that are related to autophagy and affect AD development. The authors suggested that even though normal autophagy is important for the healthy growth of aged neurons, certain dysfunctions might influence mediators of AD, such as the metabolism of Aβ and tau, the mTOR pathway, neuroinflammation, and the endocannabinoid system.

In a study of two cohorts of older adults, who were recruited independently, Tao et al. examined the effects of Tai Chi Chuan and Baduanjin training on subjects with age-related memory decline. The fractional Amplitude of Low-Frequency Fluctuations in specific frequency bands was proved to provide benefits on memory processes by comparing a Tai Chi Chuan-Baduanjin treatment group with a control group. It is suggested that a 12-week training plan can be used as a therapeutic procedure to improve brain mechanisms.

As microbial infections are a crucial risk factor for neurodegeneration, affecting the vagus nerve, metabolites, neurotransmitters, and immune signaling pathways, Xin et al. investigated the role of oligosaccharides from *Morinda officinalis* (OMO) as a prebiotic that may potentially lead to memory improvement in AD. The authors administered OMO to APP/PS1 transgenic mice and identified potential clinical biomarkers of AD through metabolomics and bioinformatics. Various behavioral experiments revealed that OMO can significantly improve memory in this animal model of AD. The

study showed the significance of several metabolites as early indicators of AD development in the animal model, presenting rather strong evidence on the defensive role of OMO on the brain-gut-microbiota axis in AD, providing insights into new potential therapeutic targets for this condition.

Chen et al. provided data from OMO on the brain-gut-microbiota axis of mice to seek for potential drug development for AD. Authors administered OMO to rats with AD-like symptoms. Significant and systematic deterioration were identified in AD-like animals, including in learning and memory abilities, histological changes, production of cytokines, and microbial community shifts, leading to the conclusion of an indirect role of gut microbiota on neurodegeneration. Although microbiota populations that were targeted with OMO were shown to be normally stable and diverse, the authors suggested the use of OMO in future drug designs.

Studies on a mouse model created by Huang et al. analyzed new strategies based on the properties of fluoxetine (FLX) to confront the depression and anxiety of AD subjects. The authors administered FLX via intragastric injection to an APP/tau/PS1 mouse model of AD, suggesting that enabling the Wnt/β-catenin signaling pathway from FLX could decrease amyloidosis in the brain of AD patients. FLX was shown to enhance the protein phosphatase 2A, which then increases β-catenin and inhibits GSK3β activity, both of which affect the Wnt/β-catenin pathway. This leads to the arrest of AD progression and represents a therapeutic formula that should be tested for its potential effectiveness.

Pan et al. tested royal jelly as a potential drug for preventing Aβ activity. Using 24 male white-haired, black-eyed rabbits, which were housed individually under a 12-h light/dark cycle and were provided with food and water *ad libitum*, the authors showed that royal jelly significantly reduces total cholesterol, low density lipoprotein cholesterol, and brain Aβ, lowering the expression of *BACE1* and *RAGE*, while increasing the expression of *LRP-1* and *IDE*. Further, it was noticed that it could be possible to achieve clearance of Aβ, along with an antioxidant impact and positive effects on neuronal metabolism.

Eissa et al. investigated the histamine H3 receptors in relation with AD, experimenting with donepezil on male rats using a passive avoidance paradigm and a novel object recognition task. The authors described the role of H3 receptor antagonists in modulating neurotransmitters and their potential therapeutic perspective.

Bao et al. investigated rat sporadic AD (sAD)—and the differences in pathological conditions in correlation with the sex of the subjects—using a Sprague-Dawley rat model. The findings showed that an intracerebroventricular infusion of streptozotocin results in memory impairment in male but not in female rats. Specifically, there was an increase in the phosphorylation of tau, in Aβ40/42, GSK-3β, and BACE1, with a complete reduction in dendritic and synaptic plasticity in male subjects. Furthermore, male rats showed lower estradiol levels in serum and in the hippocampus than females.

Salmin et al. focused on the application of environmental enrichment (EE) as a potential treatment tool for the efficient management of AD in rats. The authors compared the effects of EE on hippocampal neurogenesis *in vivo* and neurosphere-forming capacity of hippocampal stem/progenitor cells *in vitro*, on a model with AD type of neurodegeneration and a model with physiological brain aging. The authors showed that EE enhances memory signatures related to stem cells in the hippocampus, progenitor cells, and differentiated neurons in young adult rats or in AD model rats and amyloid-based treated rats, but not in the aged rats.

AD MODELING AND DIAGNOSIS

Seven papers in this Research Topic recognized and discussed the problem of the unsuccessful design of drug trials due to the usual late diagnosis of AD and the corresponding irreversible brain alterations.

Ashraf et al. focused on the clearance of Ab plaques by modulating calpastatin signaling, amyloid precursor protein pathways, and Ca^{2+} channels. The authors used stochastic Petri nets to model and simulate these pathways, and identified mechanisms involved in neuronal cell death. The study examined the decrease of plaque production and accumulation by targeting the calpain-calpastatin complexes, and the authors proposed the designing of inhibitors against active calpain using *in silico* methods and *in vitro* experiments.

A study by Sun et al. included experiments on sAD rats treated with streptozotocin. The results showed that different types of hippocampal neural stem cells derived from adult Wistar rats are affected by streptozotocin, and that the expression of metabolism-related genes/proteins is altered in many ways, leading to degenerative disorders.

Khan discussed the necessity of applying complex models for the diagnosis of AD, instead of using a single biomarker. The authors proposed a theoretical preclinical diagnostic algorithm combining heterogeneous evidence, including neuroimaging data, CSF biomarkers, and genetic markers. Additionally, the authors highlighted the diagnostic accuracy, the patient selection in a clinical trial, the universal standardization of diagnostic protocols, the high cost of diagnosis, and the potential ethical challenges as the crucial challenges that must be addressed to apply this algorithm with efficacy in the future.

Tabei et al. compared the effect of non-pharmacological interventions between dementia groups, including physical exercise with music and cognitive stimulation tasks. The authors enrolled 46 patients with mild-to-moderate dementia, 25 of them performed a task consisting of physical exercise with music, and 21 subjects performed cognitive stimulation tasks. It should be noted, however, that the results might be influenced by the limitations of the study, such as the non-inclusion of healthy controls, or the rapid intervention period of the study. The authors concluded that patients with mild-to-moderate dementia, accompanied by cognitive decline and extensive cortical atrophy, did not experience the same improvement after non-pharmaceutical therapy, concluding to the importance of individualized non-pharmacological interventions.

Long et al. discuss the function of MCI assessment as a crucial checkpoint of AD effects. This study enrolled 69 MCI patients

and 63 healthy controls. None of the MCI patients had taken any medications that could interfere with cognitive functions. The authors proposed and examined the Hurst exponent of fMRI data from several brain regions, including the left middle frontal gyrus, the right hippocampus, the bilateral parahippocampal gyrus, the bilateral amygdala, the left cingulate gyrus, the left insular gyrus, the left fusiform gyrus, the left superior parietal gyrus, the left orbital gyrus, and the left basal ganglia as proof of MCI identification.

Baig et al. present the role of peptide-based compounds for the diagnosis and treatment of AD in a review study. For the achievement of an early and accurate diagnosis, the authors revealed the importance of peptide-based inhibitors of Aβ, including β-site amyloid precursor protein cleaving enzyme 1, glyceraldehyde-3-phosphate dehydrogenase, tyrosine phosphatase, and the potassium channel KV1.3.

El-Gamal et al. discussed the importance of an efficient early AD diagnosis. The authors designed and programmed a computer-aided diagnosis system for the analysis of Pittsburgh Compound B-Positron Emission Tomography scans, and for the individualized diagnosis based on the analysis of brain regions. The system was validated from an Alzheimer's disease neuroimaging initiative dataset containing 19 normal controls and 65 MCI subjects.

CONCLUSION

We hope that this Frontiers Research Topic will enrich the understanding of the AD challenge, with the efforts and commitment of all the authors to whom we give our acknowledgment, and to the reviewers who have contributed by improving and clarifying these diverse contributions through their valuable comments. Finally, we are grateful to the Specialty Chief Editor for Neurodegeneration Prof. Einar M. Sigurdsson for his valuable comments and the Frontiers Editorial team of all the sections for their continuous support.

AUTHOR'S NOTE

The repeated unsuccessful clinical trials on the amyloid-beta targeting medications and the pessimistic calculations of the cost burden of Alzheimer's disease (AD) will have an impact in the next few decades, posing serious challenges for humanity with severe social implications. To date, holistic solution for the disease has yet to be identified, although quite a few alternative diagnostic and treatment procedures have been presented during the past years, considering the latest Alzheimer's classification. The range of scientific fields actively involved in the race for a cure for AD has been impressively extended, allowing the combination of creative ideas using modern technology with innovative therapeutic agents and traditional pharmaceutical practices. In this way, common etiologies and mechanisms in other related disorders or aspects of neurodegeneration could be identified. This Research Topic titled 'Alzheimer's disease as a current challenge' offers a contribution of 38 innovative papers on the multidimensional and crucial social problem of AD management. A total of 284 authors presented their different perspectives, research updates and studies in several sections of the Frontiers journals, describing methods on potential diagnosis and treatment.

AUTHOR CONTRIBUTIONS

All authors listed have made an equal, substantial, direct and intellectual contribution to the work, and approved it for publication.

ACKNOWLEDGMENTS

We give our acknowledgments to the authors, to the reviewers, to the Specialty Chief Editor for Neurodegeneration Prof. Einar M. Sigurdsson for his valuable comments, the Frontiers editorial team of all the Sections for their continuous support, and the Editage for English language editing.

Conflict of Interest Statement: The authors declare that the research was conducted in the absence of any commercial or financial relationships that could be construed as a potential conflict of interest.

Copyright © 2019 Alexiou, Kamal and Ashraf. This is an open-access article distributed under the terms of the Creative Commons Attribution License (CC BY). The use, distribution or reproduction in other forums is permitted, provided the original author(s) and the copyright owner(s) are credited and that the original publication in this journal is cited, in accordance with accepted academic practice. No use, distribution or reproduction is permitted which does not comply with these terms.

frontiers in Aging Neuroscience

ORIGINAL RESEARCH
published: 17 December 2018
doi: 10.3389/fnagi.2018.00414

Blood-Derived Plasma Protein Biomarkers for Alzheimer's Disease in Han Chinese

Zaohuo Cheng[1]†, Jiajun Yin[1]†, Hongwei Yuan[1], Chunhui Jin[1], Fuquan Zhang[1], Zhiqiang Wang[1], Xiaowei Liu[1], Yue Wu[1], Tao Wang[2] and Shifu Xiao[2]**

[1] Wuxi Mental Health Center, Nanjing Medical University, Wuxi, China, [2] Shanghai Mental Health Center, Shanghai Jiao Tong University School of Medicine, Shanghai, China

It is well known that Alzheimer's disease (AD) is one of the most common progressive neurodegenerative diseases; it begins gradually, and therefore no effective medicine is administered in the beginning. Thus, early diagnosis and prevention of AD are crucial. The present study focused on comparing the plasma protein changes between patients with AD and their healthy counterparts, aiming to explore a specific protein panel as a potential biomarker for AD patients in Han Chinese. Hence, we recruited and collected plasma samples from 98 AD patients and 101 elderly healthy controls from Wuxi and Shanghai Mental Health Centers. Using a Luminex assay, we investigated the expression levels of fifty plasma proteins in these samples. Thirty-two out of 50 proteins were found to be significantly different between AD patients and healthy controls ($P < 0.05$). Furthermore, an eight-protein panel that included brain-derived neurotrophic factor (BDNF), angiotensinogen (AGT), insulin-like growth factor binding protein 2 (IGFBP-2), osteopontin (OPN), cathepsin D, serum amyloid P component (SAP), complement C4, and prealbumin (transthyretin, TTR) showed the highest determinative score for AD and healthy controls (all $P = 0.00$). In conclusion, these findings suggest that a combination of eight plasma proteins can serve as a promising diagnostic biomarker for AD with high sensitivity and specificity in Han Chinese populations; the eight plasma proteins were proven important for AD diagnosis by further cross-validation studies within the AD cohort.

Keywords: Alzheimer's disease, biomarker, plasma protein, early diagnosis, Han Chinese

OPEN ACCESS

Edited by:
Athanasios Alexiou, Novel Global Community Educational Foundation (NGCEF), Australia

Reviewed by:
Md. Sahab Uddin, Southeast University, Bangladesh
Girish Kumar Gupta, Maharishi Markandeshwar University, India

***Correspondence:**
Zaohuo Cheng
chengzaohuo@126.com
Shifu Xiao
xiaoshifu@msn.com

† These authors have contributed equally to this work

Received: *04 April 2018*
Accepted: *30 November 2018*
Published: *17 December 2018*

Citation:
Cheng Z, Yin J, Yuan H, Jin C, Zhang F, Wang Z, Liu X, Wu Y, Wang T and Xiao S (2018) Blood-Derived Plasma Protein Biomarkers for Alzheimer's Disease in Han Chinese. Front. Aging Neurosci. 10:414. doi: 10.3389/fnagi.2018.00414

INTRODUCTION

Recently, the Centers for Disease Control and Prevention in the United States reported a 54.5% increase from the 1999 rate of 16.5 deaths per 100,000 patients with Alzheimer's disease (AD) (Taylor et al., 2017), which is one of the most common progressive neurodegenerative diseases and is characterized by the interaction of both genetic and environmental factors, resulting in memory dysfunction and behavioral changes (Hooli and Tanzi, 2009). In 2013, the number of older people in China was almost 200 million, and the proportion of the population that was aged 65 years and older increased to 14.3% (Sun et al., 2015). The World Alzheimer Report 2015 updated the estimates of the global prevalence, China is the region with the most people living with dementia (9.5 million), and the prevalence for the population aged 60 and older is 6.19% (Prince et al., 2015;

Wu et al., 2018). Currently, disease-modifying therapy and an ideal diagnostic tool for AD are largely lacking, severely influencing patients' quality of life and leading to a heavy financial burden for patients' families.

Preclinical Alzheimer's, the newly defined disease stage, demonstrates that brain changes are progressively initiated 10 to 20 years before the onset of dementia symptoms (Bateman et al., 2012). Thus, identifying biomarkers for preclinical Alzheimer's contributed to the early recognition and prediction of the progression of AD. Notably, the diagnostic tool should be inexpensive, easy to perform, and non-invasive (The Ronald and Nancy Reagan Research Institute of the Alzheimer's Association and the National Institute on Aging Working Group, 1998). Recent scientific evidence suggests some potential diagnostic biomarkers such as β-amyloid (Aβ) (Blennow et al., 2015) and tau (Meredith et al., 2013) accumulation in cerebrospinal fluid (CSF), Pittsburgh compound B positron emission tomography (PiB-PET) (Leuzy et al., 2015), and peripheral blood protein (Zhao et al., 2015) and microRNA (miRNA) expression (Galimberti et al., 2014), among which blood-derived biomarkers have been extensively studied due to their less invasive source (Blennow, 2017; Kitamura et al., 2017; O'Bryant et al., 2017). Although previous studies have demonstrated plasma protein profiles may be a valuable diagnostic biomarker for the early stage of AD, the findings have not been widely replicated in different races (Kiddle et al., 2014; Shi et al., 2018).

Therefore, based on these findings, the present study focuses on plasma protein differences in healthy individuals and patients with AD, exploring a specific protein panel as a potential diagnostic biomarker for AD patients in Han Chinese.

MATERIALS AND METHODS

Study Population

We recruited 1,105 older people aged 56–95 years from 2015 to 2017. Eventually, 98 AD patients diagnosed with the criteria of the National Institute of Neurological and Communicative Disorders and Stroke and the Alzheimer's disease and Related Disorders Association (NINCDS-ADRDA) were recruited from Wuxi and Shanghai Mental Health Centers. The cognitive function of these participants was assessed by two skilled professional psychiatrists using the Mini-Mental State Examination (MMSE). The absence of depression was documented on the basis of a score of 10 or less on the Hamilton Rating Scale for Depression (HAMD). A brain computed tomography (CT) or magnetic resonance imaging (MRI) scan excluded other structural brain diseases, and neurologic examination showed no significant abnormalities. A total of 101 elderly healthy subjects were recruited through advertisements, and their demographic characteristics were carefully recorded.

Exclusion Criteria

Patients with any dementia other than AD, such as vascular dementia, dementia with Lewy bodies, frontotemporal dementia or Parkinson's disease, were excluded. In addition, a history of stroke or cerebrovascular disease, bone marrow transplantation, major psychiatric disorder, and a history of alcohol or drug abuse were causes for exclusion from the study.

Study Design

Plasma samples from AD and elderly healthy controls from Shanghai and Wuxi in China were obtained. In total, we examined plasma samples from 199 subjects: 98 with AD and 101 elderly controls with no dementia. Multiple protein differences were explored using Luminex xMAP technology. Statistical analysis was performed to assess the relative importance of these protein biomarkers for the diagnosis of AD.

This study was approved by the Ethics Committees of the Wuxi Health Mental Center. Either patients or their guardians signed informed consent. If participants failed to fill out the consent form more than twice, their guardians were asked to fill out the consent form on the patients' behalf.

Luminex Assays

Luminex xMAP technology (Austin, TX, United States) uses a solid phase approach to analyze multiple proteins. In brief, the xMAP technology is a flow cytometric-based platform that uses microspheres inserted with a ratio of two different fluorescent dyes. In theory, up to 100 differently colored beads can be generated with a theoretical multiplex capacity of up to 100 assays per well of a 96-well plate. The capture antibody is covalently coupled to the bead, and immunoassays are run under standard sandwich immunoassay formats (Hye et al., 2014).

The Luminex kits were obtained from Millipore (Billerica, MA, United States) and the assays were performed according to the manufacturer's instructions (Soares et al., 2009). Eleven Milliplex MAP multiplex panels covering 50 proteins (96-well plate format; EMD Millipore) were utilized: cat.# HCYTOMAG-60K (7-plex); cat.# HIGFBMAG-53K (2-plex); cat.# HMHEMAG-34K (2-plex); cat.# HMMP2MAG-55K (2-plex); cat.# HNDG1MAG-36K (7-plex); cat.# HNDG2MAG-36K (6-plex); cat.# HNDG3MAG-36K (10-plex); cat.# HND2MAG-39K (3-plex); cat.# HND3MAG-39K (7-plex); cat.# SKINMAG-50K (1-plex); and cat.# HKI6MAG-99K (3-plex). Properly diluted plasma samples were incubated with the antibody-coupled microspheres and then with biotinylated detection antibody before the addition of streptavidin-phycoerythrin. The captured bead complexes were measured with a FLEXMAP 3D system (Luminex Corporation, Austin, TX, United States) using the following instrument settings: events/bead, 50; sample size, 50 μL; discriminator gate, 8000–15,000. The raw data (mean fluorescence intensity) were collected and further processed for calculating protein concentration (Zhi et al., 2014; Al-Daghri et al., 2018).

Data Processing

Quality checks (QC) based on standard curve linearity, intraassay coefficient of variation, interassay coefficient of variation for reference sample, and percentage of missing data were performed to examine the performance of each assay followed by measuring median fluorescent intensity (MFI) using xPONENT 5.1 (Luminex Corporation). This was further exported into Milliplex Analyst 5.1 (VigeneTech, United States) to calculate

protein concentrations by a five-parameter logistic fit. Afterward, all analytes were subjected to the statistical analysis.

Statistical Analysis

All analysis results were expressed as the mean ± SD. Statistical analyses were performed using the Statistical Package for the Social Sciences software version 20.0 (SPSS Inc., Chicago, IL, United States). Pearson's chi-square test was used to compare gender between control subjects and AD patients. All 50 blood protein levels were non-normally distributed, and subsequently underwent ln or square root transformation. The results of transforming the variables are displayed in the table. An independent-sample *t*-test was used to compare age, education and MMSE score and overall protein differences between control subjects and AD patients. Discriminant analysis was performed to assess the relative importance of these biomarkers in classifying AD and controls. In the case of the stepwise method, Wilk's lambda method was used to build the prediction model. The discriminant analysis used a partial *F*-test (F to enter 3.84; F to remove 2.71) and a stepwise method (maximum number of steps = 64) to sequentially incorporate the set of 32 significant variables into the canonical discriminant function. To check the reliability of our analysis, leave-one-out cross-validation was used. Receiver operating characteristic (ROC) analyses were conducted under the non-parametric distribution assumption for standard error of area to determine the performance of the models for discriminating AD from controls.

RESULTS

Study Participants

The demographic and clinical characteristics of healthy controls and AD patients are presented in **Table 1**. Briefly, the mean age of AD patients and their healthy counterparts were 78.76 ± 8.06 and 78.33 ± 7.30 years, respectively. No significant difference was found in age, gender or education between these two groups. As expected, patients with AD had significantly lower MMSE scores than healthy controls ($P = 0.000$).

Differentially Expressed Protein

In this study, we applied Luminex assay technology to determine the expression profiles of 50 proteins in the plasma from AD patients and healthy controls. Of the fifty candidates, thirty-two proteins were found to be differentially expressed, with statistical significance between AD patients and healthy controls ($P < 0.05$) (**Table 2**).

Stepwise Discriminant Function Analysis

Afterward, we performed a stepwise discriminant function analysis to further determine how effectively AD patients and healthy controls can be distinguished based on the expressed protein levels and to assess the differential contribution to the diagnosis. Of the 32 significant plasma markers, a feature group of eight most discriminative proteins, including brain-derived neurotrophic factor (BDNF), angiotensinogen (AGT), insulin-like growth factor binding protein 2 (IGFBP-2), osteopontin (OPN), cathepsin D, serum amyloid P component (SAP), complement C4, and prealbumin (transthyretin, TTR), was sorted out by stepwise discriminant analysis (**Table 3**, all $P = 0.00$), indicating their potential contributions to diagnosis. To detect whether this 8-protein panel was efficient in differentiating AD from healthy controls, we carried out both original- and cross-validation, correctly classifying 86.7 and 84.7% of the cases, respectively (**Table 4**).

The Classification Performance of the 8-Protein Panel

Furthermore, we decided the classification performance of the eight-protein panel and each biomarker by calculating the discriminant score (**Table 5**) and receiver operating characteristic (ROC) curve (**Figure 1**), resulting in an 87.4% correct classification for AD and control subjects with high sensitivity (86.7%) and specificity (88.1%), which suggested that the combination of these eight differentially expressed plasma proteins produced the most accurate results in a threshold classification.

DISCUSSION

To date, disease-modifying treatments have not been successfully developed for AD. Continuous clinical trials for novel drugs have failed, suggesting early diagnosis and prevention of AD is crucial for postponing the progression of disease effectively. Approximately 500 mL of cerebrospinal fluid (CSF), which is in direct contact with the extracellular space of the brain, is absorbed into the blood daily (Davidsson et al., 2002; Davidsson and Sjogren, 2006; Hye et al., 2006). Plasma contains multiple biological components, including proteins, peptides, lipids, and metabolites, which also effectively reflect physiological activity and pathology in the central nervous system (CNS). To our knowledge, this is the first study to investigate potential plasma protein biomarkers in the Han Chinese population using a high-throughput multiplexed xMAP Luminex assay. Our present

TABLE 1 | Characteristics of AD patients and control subjects.

	Controls (*n* = 101)	AD (*n* = 98)	χ^2/*t*-test	*P*-value
Gender (M/F)	35/66	34/64	0.000	0.995
Age (years)	78.33 ± 7.30	78.76 ± 8.06	−0.393	0.695
Education (years)	5.77 ± 4.77	5.00 ± 4.37	1.175	0.241
MMSE score	25.70 ± 2.90	8.62 ± 7.58	20.783	0.000*

*Chi-square was used for the gender comparison. Independent-sample t-test was used for age, education, and MMSE score. *P < 0.05 indicated statistical significance.*

TABLE 2 | Blood protein levels of AD patients and control subjects.

	Data conversion	AD (n = 98)	Controls (n = 101)	t-Test	P-value
G-CSF (pg/ml)	Ln (x+1)	3.510 ± 1.166	3.052 ± 1.097	2.584	0.005**
IL-10 (pg/ml)	Ln (x+1)	1.039 ± 0.800	0.759 ± 0.730	2.578	0.011*
MCP (pg/ml)	Ln (x+1)	1.106 ± 1.715	1.100 ± 1.768	0.026	0.980
IL-1a (pg/ml)	Ln (x+1)	2.044 ± 1.567	1.659 ± 1.578	1.726	0.086
IL-3 (pg/ml)	Ln (x+1)	0.239 ± 0.276	0.147 ± 0.143	2.953	0.004**
IL-8 (pg/ml)	Ln (x+1)	1.896 ± 1.260	1.726 ± 1.205	0.972	0.332
MIP (pg/ml)	Ln (x+1)	0.511 ± 0.811	0.528 ± 0.825	−0.152	0.880
IGFBP-2 (ng/ml)	Ln (x+1)	4.933 ± 1.085	4.122 ± 1.090	5.263	0.000***
IGFBP-6 (ng/ml)	Ln (x)	6.179 ± 0.461	6.169 ± 0.502	0.137	0.891
B-2 Microglobulin (ng/ml)	Ln (x)	8.064 ± 0.874	7.529 ± 0.770	4.580	0.000***
Clusterin (ng/ml)	SQRT (x)	878.97 ± 162.09	729.87 ± 183.25	6.069	0.000***
Cystatin C (ng/ml)	SQRT (x)	30.248 ± 7.670	23.610 ± 8.306	5.852	0.000***
PP (pg/ml)	Ln (x)	4.802 ± 0.971	4.667 ± 0.791	1.084	0.280
TNFa (pg/ml)	SQRT (x)	2.778 ± 0.731	2.622 ± 0.724	1.511	0.132
MMP-2 (pg/ml)	Ln (x)	12.046 ± 0.286	11.976 ± 0.232	1.882	0.061
MMP-9 (pg/ml)	Ln (x)	10.37 ± 0.700	10.55 ± 0.589	−1.927	0.055
CP (ng/ml)	SQRT (x)	551.21 ± 229.25	557.25 ± 196.47	−0.200	0.842
AGP (ng/ml)	Ln (x)	13.155 ± 1.944	13.475 ± 1.200	−1.394	0.163
HP (ng/ml)	SQRT (x)	1434.3 ± 926.7	1714.9 ± 1025.6	−2.023	0.044*
sSOD1 (ng/ml)	Ln (x)	5.440 ± 0.656	5.443 ± 0.498	−0.031	0.975
AGT (ng/ml)	Ln (x)	4.476 ± 1.993	6.470 ± 1.729	−7.544	0.000***
Fetuin A (ng/ml)	SQRT (x)	371.97 ± 45.32	377.39 ± 55.23	−0.755	0.451
sSOD2 (ng/ml)	Ln (x)	3.773 ± 0.476	3.640 ± 0.352	2.232	0.027*
Contactin-1 (ng/ml)	SQRT (x)	11.44 ± 1.982	11.29 ± 1.570	0.592	0.554
Kallikrein-6 (ng/ml)	SQRT (x)	2.806 ± 0.628	2.555 ± 0.452	3.252	0.001**
OPN (ng/ml)	SQRT (x)	7.060 ± 1.489	5.874 ± 1.248	6.098	0.000***
a2-Macroglobulin (ng/ml)	SQRT (x)	1299.5 ± 304.59	1146.9 ± 329.78	3.388	0.001**
APO A1 (ng/ml)	SQRT (x)	625.61 ± 175.59	609.57 ± 250.79	0.521	0.603
APO CIII (ng/ml)	SQRT (x)	411.28 ± 113.22	368.82 ± 137.12	2.385	0.018*
APO E (ng/ml)	SQRT (x)	289.40 ± 71.73	253.24 ± 90.32	3.133	0.002**
Complement C3 (ng/ml)	SQRT (x)	184.42 ± 76.35	208.99 ± 73.32	−2.331	0.021*
Prealbumin (ng/ml)	SQRT (x)	457.61 ± 113.94	411.31 ± 128.43	2.687	0.008**
Complement factor H (ng/ml)	SQRT (x)	583.95 ± 115.00	502.41 ± 165.47	4.047	0.000***
CRP (ng/ml)	Ln (x)	9.255 ± 2.643	9.580 ± 1.352	−1.086	0.279
A1-Antitrypsin (ng/ml)	Ln (x)	7.649 ± 1.340	8.151 ± 1.190	−2.792	0.006**
PEDF (ng/ml)	SQRT (x)	61.96 ± 23.23	63.61 ± 17.57	−0.565	0.572
SAP (ng/ml)	Ln (x)	10.812 ± 2.551	11.656 ± 1.368	−2.921	0.004**
MIP-4 (ng/ml)	Ln (x)	4.140 ± 0.784	4.011 ± 0.637	1.277	0.203
Complement C4 (ng/ml)	SQRT (x)	156.81 ± 72.86	116.06 ± 49.76	4.594	0.000***
BDNF (pg/ml)	Ln (x)	8.006 ± 1.219	6.818 ± 0.942	7.705	0.000***
Cathepsin D (pg/ml)	SQRT (x)	608.92 ± 178.92	479.43 ± 154.10	5.476	0.000***
sICAM-1 (pg/ml)	SQRT (x)	365.19 ± 69.65	300.29 ± 84.30	5.910	0.000***
MPO (pg/ml)	SQRT (x)	12.080 ± 1.491	11.519 ± 1.494	2.649	0.009**
PDGF-AA (pg/ml)	Ln (x)	7.212 ± 0.969	6.322 ± 0.756	7.206	0.000***
RANTES (pg/ml)	Ln (x)	10.122 ± 1.025	9.138 ± 1.030	6.751	0.000***
NCAM (pg/ml)	SQRT (x)	608.35 ± 96.051	505.86 ± 126.59	6.446	0.000***
PDGF-AB/BB (pg/ml)	Ln (x)	8.270 ± 1.161	7.789 ± 0.621	7.185	0.000***
sVCAM-1 (pg/ml)	SQRT (x)	956.61 ± 185.54	778.87 ± 215.38	6.215	0.000***
PAI-1 Total (pg/ml)	SQRT (x)	366.67 ± 117.04	331.95 ± 124.71	2.024	0.044*
HSA (μg/ml)	SQRT (x)	208.60 ± 40.69	192.74 ± 51.37	2.410	0.017*

Significant P-value ($P < 0.05$, **$P < 0.01$, ***$P < 0.001$).*

TABLE 3 | Summary of canonical discriminant analysis (stepwise method).

Step	Entered variable	Wilk's lambda	Exact F	*P*-value	Standardized coefficients
1	BDNF	0.768	59.363	0.000	0.355
2	AGT	0.651	52.431	0.000	−0.459
3	IGFBP-2	0.557	51.731	0.000	0.395
4	OPN	0.522	44.492	0.000	0.330
5	Cathepsin D	0.490	40.134	0.000	0.286
6	SAP	0.453	38.665	0.000	−0.748
7	Complement C4	0.410	39.311	0.000	0.549
8	Prealbumin	0.398	35.967	0.000	0.258

At each step, the variable that minimizes the overall Wilk's lambda is entered: a. Maximum number of steps is 64; b. Minimum partial F to enter is 3.84; c. Maximum partial F to remove is 2.71; d. F level, tolerance, or VIN insufficient for further computation.

TABLE 4 | Discriminant classification results[b,c].

Clinical diagnosis		Predicted group membership		Total
		Controls	AD	
Original	Controls	89 (88.1%)	12 (11.9%)	101
	AD	13 (13.3%)	85 (86.7%)	98
	Total	107	92	199
Cross-validated[a]	Controls	87 (86.1%)	14 (13.9%)	101
	AD	15 (15.3%)	83 (84.7%)	98
	Total	106	93	199

[a]*Cross validation was performed only for those cases in the analysis. In cross validation, each case is classified by the functions derived from all cases other than that case.* [b]*86.7% of original grouped cases correctly classified.* [c]*84.7% of cross-validated grouped cases correctly classified.*

TABLE 5 | Summary of ROC curve analysis.

	AUC				Sensitivity	Specificity	Correct classification
	Area	Standard error[a]	Asymptotic significance[b]	95% CI			
BDNF	0.776	0.033	0.000	0.711∼0.841	0.704	0.743	72.4%
AGT	0.203	0.034	0.000	0.138∼0.269	0.776	0.634	70.4%
IGFBP-2	0.707	0.037	0.000	0.635∼0.779	0.673	0.634	65.3%
OPN	0.739	0.035	0.000	0.671∼0.808	0.643	0.723	68.3%
Cathepsin D	0.735	0.035	0.000	0.666∼0.804	0.571	0.762	66.8%
SAP	0.425	0.041	0.067	0.345∼0.504	0.449	0.634	54.3%
Complement C4	0.694	0.038	0.000	0.618∼0.769	0.643	0.644	64.3%
Prealbumin	0.619	0.038	0.004	0.541∼0.697	0.653	0.574	61.3%
Discriminant Score	0.958	0.012	0.000	0.934∼0.982	0.867	0.881	87.4%

[a]*Under the non-parametric assumption.* [b]*Null hypothesis: true area = 0.5.*

findings suggest that a set of eight plasma proteins (BDNF, AGT, IGFBP-2, OPN, cathepsin D, SAP, complement C4, and TTR) serves as a putative predictor panel for AD diagnosis with high sensitivity and specificity. Importantly, these proteins have been considered to be interesting and potentially significant in AD disease pathology in previous studies (Phillips et al., 1991; Iadecola and Davisson, 2008; Carecchio and Comi, 2011; Daborg et al., 2012; Mold et al., 2012; Tian et al., 2014; Willette et al., 2015; Buxbaum and Johansson, 2017).

Recently, blood-derived biomarkers for AD have been widely considered for being relatively painless, inexpensive and having diagnostic accuracy. Using predictive analysis of microarrays, a previous study demonstrated that a panel of 18 plasma proteins (CCL18, CCL15, CCL7, CXCL8, ICAM-1, TRAIL-R4, G-CSF, GDNF, EGF, CCL5, M-CSF, IL-3, IL-1α, TNF-α, PDGF-BB, IL-11, ANG-2, and IGFBP-6) achieved a diagnostic accuracy of 90% in distinguishing AD and mild cognitive impairment (MCI) (Ray et al., 2007), which was reported to be unable to distinguish patients with AD from the populations through enough diagnostic precision (Bjorkqvist et al., 2012). In addition, it also failed to reach comparable accuracy in discriminating patients with AD and healthy controls using 16 and 8 plasma proteins derived from this 18-protein panel, respectively (Soares et al., 2009; Marksteiner et al., 2011), which might be attributed

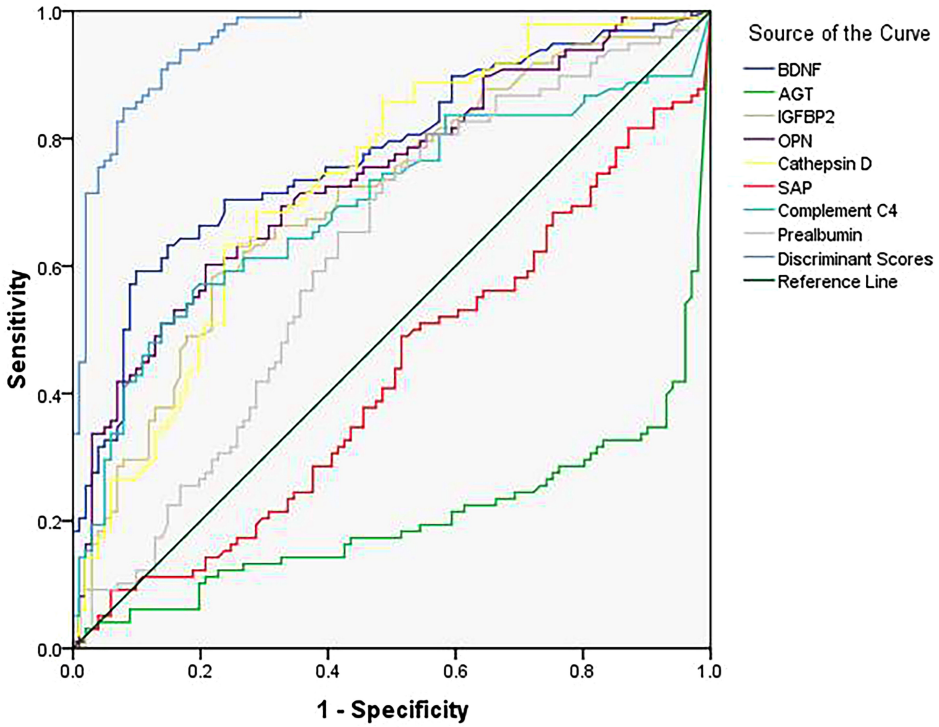


FIGURE 1 | Receiver-operating characteristic (ROC) curve for the 8-protein panel and each protein.

to only three of these 18 plasma proteins being differentially expressed between AD and healthy controls in an independent replication study. Afterward, Thambisetty et al. (2008) also performed a subsequent study to investigate 26 proteins that had been identified as potential AD biomarkers, including the 18-protein panel reported by Ray et al. (2007). Although only two proteins were found to be significantly different between AD and controls, they identified that a 10-protein panel (TTR, CLU, cystatin C, A1AcidG, ICAM-1, CC4, pigment epithelium-derived factor, A1AT, RANTES, and ApoC3) could predict the progression of MCI to AD with high diagnostic accuracy. However, of these proteins, ICAM-1 was a unique protein that overlapped with Ray's study. O'Bryant and colleagues used a panel from RBM to identify a list of 30 biomarkers to detect AD (O'Bryant et al., 2010, 2011).

It is well known that the pathological mechanism of AD is diverse. The fifty proteins selected in the present study, including those proteins that were reported in previous studies, are involved in the various signaling pathways associated with AD, including the immune response (Heneka et al., 2015), inflammatory (Harrison, 2013; Heneka et al., 2015) and antioxidant (Andrieu et al., 2015) processes, and metabolism (Arnoldussen et al., 2014; Counts et al., 2017). Of this 8-protein panel, three proteins, CC4, TTR, and IGFBP-2, overlapped with previous studies (Bennett et al., 2012; Uchida et al., 2015; McLimans et al., 2017) and affect immunology, Aβ fibril formation, DNA synthesis, and cell proliferation and death in AD.

The complement system is considered to be highly involved in the inflammatory response as a powerful component of innate immunity, consisting of more than 30 fluid-phase and cell-associated proteins as well as a wide range of specific receptors that interact to trigger the inflammatory response (Ricklin et al., 2010; Wagner and Frank, 2010). Recent genome-wide association studies (GWAS) have identified the association of complement receptor 1 with AD (Harold et al., 2009; Lambert et al., 2009; Seshadri et al., 2010; Naj et al., 2011). However, whether these complement molecules have any diagnostic value has not been fully elucidated. Elevated levels of complement 3 and 4 (C3 and C4) in cerebrospinal fluid (CSF) were found in AD, compared with MCI, patients (Daborg et al., 2012). Moreover, increased plasma levels of C4a protein were found in the plasma of AD patients (Bennett et al., 2012). Consistently, complement C4 was highly expressed in the plasma of AD participants in this study. We further showed that complement C4 had 64.3% accuracy for distinguishing AD from healthy individuals with 64.3% sensitivity and 64.4% specificity, indicating that complement C4 alone was inadequate as a biomarker for AD diagnosis.

Transthyretin (TTR) is a transport protein, also known as prealbumin, which has been found in cerebrospinal fluid (CSF) as an Aβ-binding protein and suppresses the toxicity of oligomers. Thus, the sequester protein, as an efficient inhibitor of Aβ fibril formation, may delay the pathologic progression of AD via the Aβ clearance signaling pathway (Buxbaum and Johansson, 2017). A previous study showed that TTR concentration was substantially decreased in the peripheral

blood of individuals with aMCI and AD, indicating that a set of sequester proteins, including TTR, can discriminate individuals with mild cognitive decline from healthy controls (Uchida et al., 2015). In contrast to this result, we found a significant increase in TTR concentration in AD patients when compared with normal controls, which might be attributed to the different ethnic populations revealing a number of influencing factors, such as heredity, environment, and lifestyle.

Among the candidate proteins, IGFBP2 was the one most frequently chosen. IGFBP-2 can influence DNA synthesis, cell proliferation and death, as well as glucose and amino acid uptake in cells by inhibiting IGF functions (Jones and Clemmons, 1995; Reyer et al., 2015). Overexpression of IGFBP-2 in mice led to decreased weights of the hippocampus, cerebellum, olfactory bulb, and prefrontal cortex (Schindler et al., 2017). In addition, IGFBP-2 was also reported to significantly increase in the serum of AD participants (Tham et al., 1993; McLimans et al., 2017), which was consistent with our findings. In addition, other insulin-like growth factors and the corresponding binding proteins were differentially expressed in both the CSF and serum from AD patients (Salehi et al., 2008), in which the expression of IGF-1 was reduced in serum (Vidal et al., 2016), while IGF-2 was highly expressed in CSF (Aberg et al., 2015). However, it has also been reported that serum, instead of CSF of IGF-1 and IGFBP3, was increased in AD (Johansson et al., 2013), both of which were more closely associated with AD in men than in women (Duron et al., 2012). Using a longitudinal case-control study, O'Bryant et al. (2010) found that serum protein-based biomarkers involving IGFBP-2 protein can be combined with clinical information to accurately classify AD (O'Bryant et al., 2010). Subsequently, using the multiplex panel, Doecke et al. (2012) identified an 18-plasma biomarker panel including IGFBP-2 that is useful for the diagnosis of AD (Doecke et al., 2012). These findings suggested that IGFBP-2 may be a key factor in a panel of protein biomarkers for the diagnosis of AD.

In addition, some proteins on the panel, including SAP, have been associated with hippocampal atrophy and the rate of change and progression to dementia (Thambisetty et al., 2010; Sattlecker et al., 2016). Importantly, we performed bioinformatics analysis and identified a close and interactive network among these proteins (data not shown), partly supporting the intimate relationship of the 8-protein panel with AD.

It is well known that recent clinical trials for the Aβ clearing strategies have failed (Galimberti and Scarpini, 2016; Mehta et al., 2017). Previous findings showed that 30% of cognitively normal elderly patients show signs of Aβ accumulation and, accordingly, a substantial number of AD patients show no signs of Aβ accumulation (Yang et al., 2012). In addition, several conflicting findings were demonstrated when using plasma Aβ peptides as markers for AD, suggesting that Aβ from peripheral blood may not reflect brain Aβ metabolism (Cummings, 2011; Hampel et al., 2012; Koyama et al., 2012). Importantly, Aβ can bind to a variety of proteins in blood, resulting in epitope masking and analytical interference (Marcello et al., 2009). In addition, methodology was also a limitation in the present study. The Milliplex MAP multiplex panels containing Aβ protein can only be used with CSF samples. To ensure the strong consistency of the results, the detection of plasma Aβ levels was not performed using other methods in this study.

Although many studies have identified plasma proteins related to AD [e.g., BDNF (Laske et al., 2007; Laske et al., 2011)], complement C4a (Bennett et al., 2012), IGFBP-2 (McLimans et al., 2017), TTR (Uchida et al., 2015), and SAP (Wilson et al., 2008), these are unlikely to be useful as a diagnostic test when used as single markers due to a lack of sensitivity and specificity. Based on the complexity of the pathogenesis of AD, as a relatively reliable biomarker for the diagnosis of AD, combinations of plasma proteins associated with various biological pathways may be necessary. Of note, accumulating evidence indicates that the replication and validation of results is urgent and important for exploratory studies. Thus, we plan to further validate our findings in a large-scale population that includes AD, MCI, and healthy controls.

The present findings should be interpreted considering some limitations. Since AD overlaps with other dementia forms, such as vascular dementia, frontotemporal dementia, and dementia with Lewy bodies, in the context of pathological traits, whether the same protein panel can accurately reflect their relationship to AD, but not to other dementia diseases, is a very important question. At present, only AD patients and healthy controls were included in this study, and no other dementia subtypes or disease stages were identified. In addition, our results may be influenced by the limited sample size. Moreover, due to the limitation of methodology, we did not detect plasma Aβ levels in the present study. Hence, more extensive studies including a large number of dementia subtypes should be conducted in the future. Furthermore, there are various factors, such as activity, diet, and medications, that can alter plasma protein levels.

CONCLUSION

Taken together, the present study identified a plasma 8-protein panel including BDNF, AGT, IGFBP-2, OPN, cathepsin D, SAP, complement C4 and TTR that showed the highest determinative score for AD and healthy controls. Thus, these findings suggest that a combination of eight plasma proteins is a valuable diagnostic biomarker for AD in the Chinese population, providing novel insight for the diagnosis of AD.

AUTHOR CONTRIBUTIONS

ZC and SX conceived and designed the experiments. ZC, JY, HY, CJ, FZ, ZW, XL, YW, and TW performed the experiments and contributed to reagents, materials, and analysis tools. ZC, JY, HY, and CJ analyzed the data. ZC, JY, and SX wrote the paper.

FUNDING

This study was supported by a grant from Jiangsu Province Science and Technology Department (BE2015615).

REFERENCES

Aberg, D., Johansson, P., Isgaard, J., Wallin, A., Johansson, J. O., Andreasson, U., et al. (2015). Increased cerebrospinal fluid level of insulin-like growth factor-II in male patients with Alzheimer's disease. *J. Alzheimers Dis.* 48, 637–646. doi: 10.3233/JAD-150351

Al-Daghri, N. M., Yakout, S. M., Wani, K., Khattak, M. N. K., Garbis, S. D., Chrousos, G. P., et al. (2018). IGF and IGFBP as an index for discrimination between vitamin D supplementation responders and nonresponders in overweight Saudi subjects. *Medicine* 97:e0702. doi: 10.1097/MD.0000000000010702

Andrieu, S., Coley, N., Lovestone, S., Aisen, P. S., and Vellas, B. (2015). Prevention of sporadic Alzheimer's disease: lessons learned from clinical trials and future directions. *Lancet Neurol.* 14, 926–944. doi: 10.1016/S1474-4422(15)00153-2

Arnoldussen, I. A., Kiliaan, A. J., and Gustafson, D. R. (2014). Obesity and dementia: adipokines interact with the brain. *Eur. Neuropsychopharmacol.* 24, 1982–1999. doi: 10.1016/j.euroneuro.2014.03.002

Bateman, R. J., Xiong, C., Benzinger, T. L., Fagan, A. M., Goate, A., Fox, N. C., et al. (2012). Clinical and biomarker changes in dominantly inherited Alzheimer's disease. *N. Engl. J. Med.* 367, 795–804. doi: 10.1056/NEJMoa1202753

Bennett, S., Grant, M., Creese, A. J., Mangialasche, F., Cecchetti, R., Cooper, H. J., et al. (2012). Plasma levels of complement 4a protein are increased in Alzheimer's disease. *Alzheimer Dis. Assoc. Disord.* 26, 329–334. doi: 10.1097/WAD.0b013e318239dcbd

Bjorkqvist, M., Ohlsson, M., Minthon, L., and Hansson, O. (2012). Evaluation of a previously suggested plasma biomarker panel to identify Alzheimer's disease. *PLoS One* 7:e29868. doi: 10.1371/journal.pone.0029868

Blennow, K. (2017). A review of fluid biomarkers for Alzheimer's disease: moving from CSF to blood. *Neurol. Ther.* 6, 15–24. doi: 10.1007/s40120-017-0073-9

Blennow, K., Mattsson, N., Scholl, M., Hansson, O., and Zetterberg, H. (2015). Amyloid biomarkers in Alzheimer's disease. *Trends Pharmacol. Sci.* 36, 297–309. doi: 10.1016/j.tips.2015.03.002

Buxbaum, J. N., and Johansson, J. (2017). Transthyretin and BRICHOS: the paradox of amyloidogenic proteins with anti-amyloidogenic activity for abeta in the central nervous system. *Front. Neurosci.* 11:119. doi: 10.3389/fnins.2017.00119

Carecchio, M., and Comi, C. (2011). The role of osteopontin in neurodegenerative diseases. *J. Alzheimers Dis.* 25, 179–185. doi: 10.3233/JAD-2011102151

Counts, S. E., Ikonomovic, M. D., Mercado, N., Vega, I. E., and Mufson, E. J. (2017). Biomarkers for the early detection and progression of Alzheimer's disease. *Neurotherapeutics* 14, 35–53. doi: 10.1007/s13311-016-0481-z

Cummings, J. L. (2011). Biomarkers in Alzheimer's disease drug development. *Alzheimers Dement.* 7, e13–e44. doi: 10.1016/j.jalz.2010.06.004

Daborg, J., Andreasson, U., Pekna, M., Lautner, R., Hanse, E., Minthon, L., et al. (2012). Cerebrospinal fluid levels of complement proteins C3. C4 and CR1 in Alzheimer's disease. *J. Neural. Transm.* 119, 789–797. doi: 10.1007/s00702-012-0797-8

Davidsson, P., and Sjogren, M. (2006). Proteome studies of CSF in AD patients. *Mech. Ageing Dev.* 127, 133–137. doi: 10.1016/j.mad.2005.09.021

Davidsson, P., Westman-Brinkmalm, A., Nilsson, C. L., Lindbjer, M., Paulson, L., Andreasen, N., et al. (2002). Proteome analysis of cerebrospinal fluid proteins in Alzheimer patients. *Neuroreport* 13, 611–615. doi: 10.1097/00001756-200204160-00015

Doecke, J. D., Laws, S. M., Faux, N. G., Wilson, W., Burnham, S. C., Lam, C. P., et al. (2012). Blood-based protein biomarkers for diagnosis of Alzheimer disease. *Arch. Neurol.* 69, 1318–1325. doi: 10.1001/archneurol.2012.1282

Duron, E., Funalot, B., Brunel, N., Coste, J., Quinquis, L., Viollet, C., et al. (2012). Insulin-like growth factor-I and insulin-like growth factor binding protein-3 in Alzheimer's disease. *J. Clin. Endocrinol. Metab.* 97, 4673–4681. doi: 10.1210/jc.20122063

Galimberti, D., and Scarpini, E. (2016). Emerging amyloid disease-modifying drugs for Alzheimer's disease. *Expert Opin. Emerg. Drugs* 21, 5–7. doi: 10.1517/14728214.2016.1146678

Galimberti, D., Villa, C., Fenoglio, C., Serpente, M., Ghezzi, L., Cioffi, S. M., et al. (2014). Circulating miRNAs as potential biomarkers in Alzheimer's disease. *J. Alzheimers Dis.* 42, 1261–1267. doi: 10.3233/JAD-140756

Hampel, H., Lista, S., and Khachaturian, Z. S. (2012). Development of biomarkers to chart all Alzheimer's disease stages: the royal road to cutting the therapeutic Gordian Knot. *Alzheimers Dement.* 8, 312–336. doi: 10.1016/j.jalz.2012.05.2116

Harold, D., Abraham, R., Hollingworth, P., Sims, R., Gerrish, A., Hamshere, M., et al. (2009). Genome-wide association study identifies variants at CLU and PICALM associated with Alzheimer's disease, and shows evidence for additional susceptibility genes. *Nat. Genet.* 41, 1088–1093. doi: 10.1038/ng.440

Harrison, N. (2013). Inflammation and mental illness. *J. Neurol. Neurosurg. Psychiatry* 84:e1. doi: 10.1136/jnnp-2013-306103.4

Heneka, M. T., Carson, M. J., El Khoury, J., Landreth, G. E., Brosseron, F., Feinstein, D. L., et al. (2015). Neuroinflammation in Alzheimer's disease. *Lancet Neurol.* 14, 388–405. doi: 10.1016/S1474-4422(15)70016-5

Hooli, B. V., and Tanzi, R. E. (2009). A current view of Alzheimer's disease. *F1000 Biol. Rep*. 1:54. doi: 10.3410/B1-54

Hye, A., Lynham, S., Thambisetty, M., Causevic, M., Campbell, J., Byers, H. L., et al. (2006). Proteome-based plasma biomarkers for Alzheimer's disease. *Brain* 129(Pt 11), 3042–3050. doi: 10.1093/brain/awl279

Hye, A., Riddoch-Contreras, J., Baird, A. L., Ashton, N. J., Bazenet, C., Leung, R., et al. (2014). Plasma proteins predict conversion to dementia from prodromal disease. *Alzheimers Dement.* 10, 799.e2–807.e2. doi: 10.1016/j.jalz.2014.05.1749

Iadecola, C., and Davisson, R. L. (2008). Hypertension and cerebrovascular dysfunction. *Cell Metab.* 7, 476–484. doi: 10.1016/j.cmet.2008.03.010

Johansson, P., Aberg, D., Johansson, J. O., Mattsson, N., Hansson, O., Ahren, B., et al. (2013). Serum but not cerebrospinal fluid levels of insulin-like growth factor-I (IGF-I) and IGF-binding protein-3 (IGFBP-3) are increased in Alzheimer's disease. *Psychoneuroendocrinology* 38, 1729–1737. doi: 10.1016/j.psyneuen.2013.02.006

Jones, J. I., and Clemmons, D. R. (1995). Insulin-like growth factors and their binding proteins: biological actions. *Endocr. Rev.* 16, 3–34. doi: 10.1210/edrv-16-1-3

Kiddle, S. J., Sattlecker, M., Proitsi, P., Simmons, A., Westman, E., Bazenet, C., et al. (2014). Candidate blood proteome markers of Alzheimer's disease onset and progression: a systematic review and replication study. *J. Alzheimers Dis.* 38, 515–531. doi: 10.3233/JAD-130380

Kitamura, Y., Usami, R., Ichihara, S., Kida, H., Satoh, M., Tomimoto, H., et al. (2017). Plasma protein profiling for potential biomarkers in the early diagnosis of Alzheimer's disease. *Neurol. Res.* 39, 231–238. doi: 10.1080/01616412.2017.1281195

Koyama, A., Okereke, O. I., Yang, T., Blacker, D., Selkoe, D. J., and Grodstein, F. (2012). Plasma amyloid-beta as a predictor of dementia and cognitive decline: a systematic review and meta-analysis. *Arch. Neurol.* 69, 824–831. doi: 10.1001/archneurol.2011.1841

Lambert, J. C., Heath, S., Even, G., Campion, D., Sleegers, K., Hiltunen, M., et al. (2009). Genome-wide association study identifies variants at CLU and CR1 associated with Alzheimer's disease. *Nat. Genet.* 41, 1094–1099. doi: 10.1038/ng.439

Laske, C., Leyhe, T., Stransky, E., Hoffmann, N., Fallgatter, A. J., and Dietzsch, J. (2011). Identification of a blood-based biomarker panel for classification of Alzheimer's disease. *Int. J. Neuropsychopharmacol.* 14, 1147–1155. doi: 10.1017/S1461145711000459

Laske, C., Stransky, E., Leyhe, T., Eschweiler, G. W., Maetzler, W., Wittorf, A., et al. (2007). BDNF serum and CSF concentrations in Alzheimer's disease, normal pressure hydrocephalus and healthy controls. *J. Psychiatr. Res.* 41, 387–394. doi: 10.1016/j.jpsychires.2006.01.014

Leuzy, A., Carter, S. F., Chiotis, K., Almkvist, O., Wall, A., and Nordberg, A. (2015). Concordance and diagnostic accuracy of [11C]PIB PET and cerebrospinal

fluid biomarkers in a sample of patients with mild cognitive impairment and Alzheimer's disease. *J. Alzheimers Dis.* 45, 1077–1088. doi: 10.3233/JAD-142952

Marcello, A., Wirths, O., Schneider-Axmann, T., Degerman-Gunnarsson, M., Lannfelt, L., and Bayer, T. A. (2009). Circulating immune complexes of Abeta and IgM in plasma of patients with Alzheimer's disease. *J. Neural. Transm.* 116, 913–920. doi: 10.1007/s00702-009-0224-y

Marksteiner, J., Kemmler, G., Weiss, E. M., Knaus, G., Ullrich, C., Mechtcheriakov, S., et al. (2011). Five out of 16 plasma signaling proteins are enhanced in plasma of patients with mild cognitive impairment and Alzheimer's disease. *Neurobiol. Aging* 32, 539–540. doi: 10.1016/j.neurobiolaging.2009.03.011

McLimans, K. E., Webb, J. L., Anantharam, V., Kanthasamy, A., Willette, A. A., and Alzheimer's Disease Neuroimaging Initiative. (2017). Peripheral versus central index of metabolic dysfunction and associations with clinical and pathological outcomes in Alzheimer's disease. *J. Alzheimers Dis.* 60, 1313–1324. doi: 10.3233/JAD-170263

Mehta, D., Jackson, R., Paul, G., Shi, J., and Sabbagh, M. (2017). Why do trials for Alzheimer's disease drugs keep failing? A discontinued drug perspective for 2010-2015. *Expert Opin. Investig. Drugs* 26, 735–739. doi: 10.1080/13543784.2017.1323868

Meredith, J. E. Jr., Sankaranarayanan, S., Guss, V., Lanzetti, A. J., Berisha, F., Neely, R. J., et al. (2013). Characterization of novel CSF Tau and ptau biomarkers for Alzheimer's disease. *PLoS One* 8:e76523. doi: 10.1371/journal.pone.0076523

Mold, M., Shrive, A. K., and Exley, C. (2012). Serum amyloid P component accelerates the formation and enhances the stability of amyloid fibrils in a physiologically significant under-saturated solution of amyloid-beta42. *J. Alzheimers Dis.* 29, 875–881. doi: 10.3233/JAD-2012-120076

Naj, A. C., Jun, G., Beecham, G. W., Wang, L. S., Vardarajan, B. N., Buros, J., et al. (2011). Common variants at MS4A4/MS4A6E. CD2AP, CD33 and EPHA1 are associated with late-onset Alzheimer's disease. *Nat. Genet.* 43, 436–441. doi: 10.1038/ng.801

O'Bryant, S. E., Mielke, M. M., Rissman, R. A., Lista, S., Vanderstichele, H., Zetterberg, H., et al. (2017). Blood-based biomarkers in Alzheimer disease: current state of the science and a novel collaborative paradigm for advancing from discovery to clinic. *Alzheimers Dement.* 13, 45–58. doi: 10.1016/j.jalz.2016.09.014

O'Bryant, S. E., Xiao, G., Barber, R., Reisch, J., Doody, R., Fairchild, T., et al. (2010). A serum protein-based algorithm for the detection of Alzheimer disease. *Arch. Neurol.* 67, 1077–1081. doi: 10.1001/archneurol.2010.215

O'Bryant, S. E., Xiao, G., Barber, R., Reisch, J., Hall, J., Cullum, C. M., et al. (2011). A blood-based algorithm for the detection of Alzheimer's disease. *Dement. Geriatr. Cogn. Disord.* 32, 55–62. doi: 10.1159/000330750

Phillips, H. S., Hains, J. M., Armanini, M., Laramee, G. R., Johnson, S. A., and Winslow, J. W. (1991). BDNF mRNA is decreased in the hippocampus of individuals with Alzheimer's disease. *Neuron* 7, 695–702. doi: 10.1016/0896-6273(91)90273-3

Prince, M., Wimo, A., Guerchet, M., Ali, G., Wu, Y., and Prina, M. (2015). *World Alzheimer Report 2015 The Global Impact of Dementia an analysis of Prevalence, Incidence, Cost, and Trends.* London: Alzheimer's Disease International.

Ray, S., Britschgi, M., Herbert, C., Takeda-Uchimura, Y., Boxer, A., Blennow, K., et al. (2007). Classification and prediction of clinical Alzheimer's diagnosis based on plasma signaling proteins. *Nat. Med.* 13, 1359–1362. doi: 10.1038/nm1653

Reyer, A., Schindler, N., Ohde, D., Walz, C., Kunze, M., Tuchscherer, A., et al. (2015). The RGD sequence present in IGFBP-2 is required for reduced glucose clearance after oral glucose administration in female transgenic mice. *Am. J. Physiol. Endocrinol. Metab.* 309, E409–E417. doi: 10.1152/ajpendo.00168.2015

Ricklin, D., Hajishengallis, G., Yang, K., and Lambris, J. D. (2010). Complement: a key system for immune surveillance and homeostasis. *Nat. Immunol.* 11, 785–797. doi: 10.1038/ni.1923

Salehi, Z., Mashayekhi, F., and Naji, M. (2008). Insulin like growth factor-1 and insulin like growth factor binding proteins in the cerebrospinal fluid and serum from patients with Alzheimer's disease. *Biofactors* 33, 99–106. doi: 10.1002/biof.5520330202

Sattlecker, M., Khondoker, M., Proitsi, P., Williams, S., Soininen, H., Kloszewska, I., et al. (2016). Longitudinal protein changes in blood plasma associated with the rate of cognitive decline in Alzheimer's disease. *J. Alzheimers Dis.* 49, 1105–1114. doi: 10.3233/JAD-140669

Schindler, N., Mayer, J., Saenger, S., Gimsa, U., Walz, C., Brenmoehl, J., et al. (2017). Phenotype analysis of male transgenic mice overexpressing mutant IGFBP-2 lacking the Cardin-Weintraub sequence motif: reduced expression of synaptic markers and myelin basic protein in the brain and a lower degree of anxiety-like behaviour. *Growth Horm. IGF Res.* 33, 1–8. doi: 10.1016/j.ghir.2016.11.003

Seshadri, S., Fitzpatrick, A. L., Ikram, M. A., DeStefano, A. L., Gudnason, V., Boada, M., et al. (2010). Genome-wide analysis of genetic loci associated with Alzheimer disease. *JAMA* 303, 1832–1840. doi: 10.1001/jama.2010.574

Shi, L., Baird, A. L., Westwood, S., Hye, A., Dobson, R., Thambisetty, M., et al. (2018). A Decade of Blood Biomarkers for Alzheimer's Disease Research: an evolving field, improving study designs, and the challenge of replication. *J. Alzheimes Dis.* 62, 1181–1198. doi: 10.3233/JAD-170531

Soares, H. D., Chen, Y., Sabbagh, M., Roher, A., Schrijvers, E., and Breteler, M. (2009). Identifying early markers of Alzheimer's disease using quantitative multiplex proteomic immunoassay panels. *Ann. N. Y. Acad. Sci.* 1180, 56–67. doi: 10.1111/j.1749-6632.2009.05066.x

Sun, R., Cao, H., Zhu, X., Liu, J.-P., and Dong, E. (2015). Current aging research in China. *Protein Cell* 6, 314–321. doi: 10.1007/s13238-015-0145-5

Taylor, C. A., Greenlund, S. F., McGuire, L. C., Lu, H., and Croft, J. B. (2017). Deaths from Alzheimer's Disease - United States, 1999-2014. *MMWR Morb. Mortal. Wkly. Rep.* 66, 521–526. doi: 10.15585/mmwr.mm6620a1

Tham, A., Nordberg, A., Grissom, F. E., Carlsson-Skwirut, C., Viitanen, M., and Sara, V. R. (1993). Insulin-like growth factors and insulin-like growth factor binding proteins in cerebrospinal fluid and serum of patients with dementia of the Alzheimer type. *J. Neural Transm. Park. Dis. Dement. Sect.* 5, 165–176. doi: 10.1007/bf02257671

Thambisetty, M., Hye, A., Foy, C., Daly, E., Glover, A., Cooper, A., et al. (2008). Proteome-based identification of plasma proteins associated with hippocampal metabolism in early Alzheimer's disease. *J. Neurol.* 255, 1712–1720. doi: 10.1007/s00415-008-0006-8

Thambisetty, M., Simmons, A., Velayudhan, L., Hye, A., Campbell, J., Zhang, Y., et al. (2010). Association of plasma clusterin concentration with severity, pathology, and progression in Alzheimer disease. *Arch. Gen. Psychiatry* 67, 739–748. doi: 10.1001/archgenpsychiatry.2010.78

The Ronald and Nancy Reagan Research Institute of the Alzheimer's Association and the National Institute on Aging Working Group (1998). Consensus report of the working group on: "Molecular and Biochemical Markers of Alzheimer's Disease". *Neurobiol. Aging* 19, 109–116. doi: 10.1016/S0197-4580(98)00022-0

Tian, L., Zhang, K., Tian, Z. Y., Wang, T., Shang, D. S., Li, B., et al. (2014). Decreased expression of cathepsin D in monocytes is related to the defective degradation of amyloid-beta in Alzheimer's disease. *J. Alzheimers Dis.* 42, 511–520. doi: 10.3233/JAD-132192

Uchida, K., Shan, L., Suzuki, H., Tabuse, Y., Nishimura, Y., Hirokawa, Y., et al. (2015). Amyloid-beta sequester proteins as blood-based biomarkers of cognitive decline. *Alzheimers Dement* 1, 270–280. doi: 10.1016/j.dadm.2015.04.003

Vidal, J. S., Hanon, O., Funalot, B., Brunel, N., Viollet, C., Rigaud, A. S., et al. (2016). Low serum insulin-like growth factor-i predicts cognitive decline in Alzheimer's disease. *J. Alzheimers Dis.* 52, 641–649. doi: 10.3233/JAD-151162

Wagner, E., and Frank, M. M. (2010). Therapeutic potential of complement modulation. *Nat. Rev. Drug Discov.* 9, 43–56. doi: 10.1038/nrd3011

Willette, A. A., Bendlin, B. B., Starks, E. J., Birdsill, A. C., Johnson, S. C., Christian, B. T., et al. (2015). Association of insulin resistance with cerebral glucose uptake in late middle-aged adults at risk for Alzheimer disease. *JAMA Neurol.* 72, 1013–1020. doi: 10.1001/jamaneurol.2015.0613

Wilson, M. R., Yerbury, J. J., and Poon, S. (2008). Potential roles of abundant extracellular chaperones in the control of amyloid formation and toxicity. *Mol. Biosyst.* 4, 42–52. doi: 10.1039/b712728f

Wu, Y.-T., Ali, G.-C., Guerchet, M., Prina, A. M., Chan, K. Y., Prince, M., et al. (2018). Prevalence of dementia in mainland China, Hong Kong and Taiwan: an updated systematic review and meta-analysis. *Int. J. Epidemiol.* 47, 709–719. doi: 10.1093/ije/dyy007

Yang, L., Rieves, D., and Ganley, C. (2012). Brain amyloid imaging–FDA approval of florbetapir F18 injection. *N. Engl. J. Med.* 367, 885–887. doi: 10.1056/NEJMp1208061

Zhao, X., Lejnine, S., Spond, J., Zhang, C., Ramaraj, T. C., Holder, D. J., et al. (2015). A candidate plasma protein classifier to identify Alzheimer's disease. *J. Alzheimers Dis.* 43, 549–563. doi: 10.3233/JAD-141149

Zhi, W., Ferris, D., Sharma, A., Purohit, S., Santos, C., He, M., et al. (2014). Twelve serum proteins progressively increase with disease stage in squamous cell cervical cancer patients. *Int. J. Gynecol. Cancer* 24, 1085–1092. doi: 10.1097/IGC.0000000000000153

Conflict of Interest Statement: The authors declare that the research was conducted in the absence of any commercial or financial relationships that could be construed as a potential conflict of interest.

Copyright © 2018 Cheng, Yin, Yuan, Jin, Zhang, Wang, Liu, Wu, Wang and Xiao. This is an open-access article distributed under the terms of the Creative Commons Attribution License (CC BY). The use, distribution or reproduction in other forums is permitted, provided the original author(s) and the copyright owner(s) are credited and that the original publication in this journal is cited, in accordance with accepted academic practice. No use, distribution or reproduction is permitted which does not comply with these terms.

frontiers in Neuroscience

ORIGINAL RESEARCH
published: 29 June 2018
doi: 10.3389/fnins.2018.00430

Investigation of Gal-3 Expression Pattern in Serum and Cerebrospinal Fluid of Patients Suffering From Neurodegenerative Disorders

Ghulam M. Ashraf[1]* *and Saleh S. Baeesa*[2]

[1] King Fahd Medical Research Center, King Abdulaziz University, Jeddah, Saudi Arabia, [2] Division of Neurosurgery, College of Medicine, King Abdulaziz University, Jeddah, Saudi Arabia

We performed this study to investigate the possibility of a definitive pattern of Galectin-3 (Gal-3) expression in the cerebrospinal fluid (CSF) and serum of Alzheimer's disease (AD) and Amyotrophic Lateral Sclerosis (ALS) patients. In our study, we collected the CSF and serum samples of 31 AD patients, 19 ALS patients and 50 normal healthy subjects (controls). Quantitative ELISA measured Gal-3 concentrations in CSF and serum samples. A comparative analysis was performed to analyze and understand the Gal-3 expression pattern. A number of neuropsychological assessments and statistical analyses were carried out to validate our findings. Recent researches have established the role of galectins in various neurodegenerative disorders (NDDs), but a definitive pattern of galectin expression is still elusive. A significant difference was observed in serum and CSF Gal-3 concentrations between AD patients and healthy controls. The difference in serum and CSF Gal-3 concentrations between ALS patients vs. controls was lesser as compared to AD patients vs. controls. The difference in serum and CSF Gal-3 concentrations of AD vs. ALS patients was not significant. The MMSE score and serum and CSF Gal-3 concentrations in AD and ALS patients, and controls exhibited a significant positive correlation. The findings of the present study are expected to provide an insight into the definitive pattern of Gal-3 expression in AD and ALS patients, and might thus establish Gal-3 as a strong biomarker. This in turn will open up new and promising research avenues targeting the expression of galectins to modulate the progression of NDDs, and pave the way for novel therapeutic options.

Keywords: Galectin-3, serum, cerebrospinal fluid, Alzheimer's disease, amyotrophic lateral sclerosis

OPEN ACCESS

Edited by:
Francesca Trojsi, Università degli Studi della Campania 'Luigi Vanvitelli', Naples, Italy

Reviewed by:
Yannick Vermeiren, University of Antwerp, Belgium
Jenny Sassone, Università Vita-Salute San Raffaele, Italy

***Correspondence:**
Ghulam M. Ashraf
ashraf.gm@gmail.com;
gashraf@kau.edu.sa

Specialty section:
This article was submitted to Neurodegeneration, a section of the journal Frontiers in Neuroscience

Received: *31 January 2018*
Accepted: *06 June 2018*
Published: *29 June 2018*

Citation:
Ashraf GM and Baeesa SS (2018) Investigation of Gal-3 Expression Pattern in Serum and Cerebrospinal Fluid of Patients Suffering From Neurodegenerative Disorders. Front. Neurosci. 12:430. doi: 10.3389/fnins.2018.00430

INTRODUCTION

Galectins are mammalian class of an otherwise large family, lectin, and characterized as glycoproteins, which have been reported to be expressed in almost all vital organs and involved in almost all significant biological functions (Hasan et al., 2007; Viguier et al., 2014). Gal-3 has been reported to exhibit an altered pattern of expression in patients suffering from NDDs like AD, ALS,

Abbreviations: AD, Alzheimer's disease; AGEs, advanced glycation end products; ALS, amyotrophic lateral sclerosis; ANOVA, analysis of variance; CNS, central nervous system; CSF, cerebrospinal fluid; FOME, Fuld object memory evaluation; LSD, least square difference; MMSE, Mini Mental Status Examination; NDDs, neurodegenerative disorders; PD, Parkinson's disease; ROC, receiver operating characteristic; SE, sensitivity; SKT, short cognitive test; TBI, traumatic brain injury; TMT, trail making test; VaD, vascular dementia.

PD, and VaD. While the exact molecular mechanisms behind the pathogenesis of various NDDs remain elusive, the experimental findings from the samples obtained from the patients continue to generate remarkable inputs related to possible pathogenetic channels of these disorders. Gal-3 is present in intracellular (cytosol and nucleus) as well as extracellular spaces, and has been reported to be expressed by almost all cell types (Hasan et al., 2007; Fortuna-Costa et al., 2014). Gal-3 being a multifunctional protein has been reported to be involved in plethora of physiological functions like immune activation, apoptosis, angiogenesis and fibrosis, which in turn have been intricately associated with the development and progression of various NDDs (Ashraf et al., 2010b, 2011; Radosavljevic et al., 2012; Tam and Pasternak, 2012). Gal-3 has also been reported to inhibit the peripheral nerve generation post axotomy (Narciso et al., 2009; DeFrancesco-Lisowitz et al., 2015), act as cell surface receptor for AGEs (Yamamoto and Yamamoto, 2012; Chen H. et al., 2017), and exacerbate the CNS damage in experimental autoimmune encephalomyelitis (EAE) (Jiang et al., 2009; de Oliveira et al., 2015). Microglial Gal-3 has significant role in neuroinflammation process in chronic ALS and TBI (Lerman et al., 2012; Boza-Serrano et al., 2014; Yip et al., 2017). A detrimental role of Gal-3 has been established in inflammation associated with CNS related prion infections (Mok et al., 2007). Gal-3 elevation induced by microglia during the progression of Lewy body dementia and ALS can act as effective indicator of neurodegenerative immune response (Zhou et al., 2010; Surendranathan et al., 2015; Garden and Campbell, 2016). Moreover, onset of remyelination has been favored by microglial Gal-3, either by directly effecting the differentiation of oligodendrocytes or through M2 cell polarization (Cherry et al., 2014; Franco et al., 2015; Rinaldi et al., 2016). Elevated levels of Gal-3 have been observed in the CSF of patients with TBI, ALS and newborn infants after birth asphyxia (Wuolikainen et al., 2011; Sävman et al., 2013; Yip et al., 2017). Gal-3 deregulates hippocampus-dependent memory formation via intracellular as well as extracellular mechanisms (Chen Y.C. et al., 2017). Proteomics approaches has established Gal-3 as a candidate biomarker for ALS (Zhou et al., 2010). Gal-3 has also been reported to be involved in AD neuropathogenesis, and could be a potential biomarker for AD (Wang et al., 2015). Moreover, Gal-3 has been identified in central as well as peripheral nervous system in Schwann cells, endothelial cells, microglia/macrophages, and astrocytes; and the activation of endothelial cells and microglia has been intricately associated with AD pathogenesis (Zlokovic, 2008; Ottum et al., 2015). These studies proclaim elevated Gal-3 expression pattern in AD and ALS patients.

The idea of the proposed research study cropped from the above-mentioned reports suggesting altered expression level of Gal-3 in various NDDs. The detrimental role of Gal-3 in diseases like ALS and AD suggest that lysosomal dysfunctions combined with reduced autophagy can further stimulate neurodegeneration. Elevated levels of Gal-3 in serum and CSF might induce enhanced inflammation, apoptosis and neurodegeneration. There are few individual studies on either serum or CSF, which suggest Gal-3 as possible biomarker of NDDs. The findings of the present study suggesting a definitive Gal-3 expression pattern in serum as well as CSF samples of AD and ALS patients will firmly affirm the role of Gal-3 as potential biomarker for these diseases.

MATERIALS AND METHODS

Ethics Statement

This study was carried out in accordance with the recommendations of National Institute of Neurological and Communicative Disorders and Stroke AD and Related Disorders Association and International Classification of Diseases, Tenth Revision, Diagnostic and Statistical Manual of Mental Disorders (Third Edition) (McKhann et al., 1984). The KAUH (King Abdulaziz University Hospital) ethical committee approved the protocol. All subjects gave written informed consent in accordance with the Declaration of Helsinki.

Patients and Neuropsychological Assessment

The AD (31) and ALS (19) patients as well as healthy individuals (50) serving as controls were recruited from Division of Neurosurgery, College of Medicine, King Abdulaziz University, Jeddah, Saudi Arabia under the careful supervision of Prof. Saleh Baeesa. Each participant was requested to provide written informed consent. The clinical severity of cognitive status was assessed by the standard MMSE (Mini Mental Status Examination) (Folstein et al., 1975). All the neuropsychological assessments were carried out by trained MD (Neurosurgery) students under the supervision of Prof. Saleh Baeesa, and included tests like SKT (Lehfeld and Erzigkeit, 1997; Flaks et al., 2006), TMT (Tombaugh, 2004), and FOME (Fuld, 1980). The cut off scores of all neuropsychological tests were adjusted for educational level and age. The participants were assessed with 21-item Hamilton depressive scale and euthymia was defined as a score of less than 8 (Hamilton, 1960). To exclude metabolic and vascular etiologies, magnetic resonance imaging (MRI) studies and blood tests (blood chemistry, blood lipid profile, complete blood count, folic acid, thyroid function, vitamin B12 dosage and syphilis test) were carried out. A consensus was developed before the clinical diagnoses by taking into account all the laboratory and clinical informations.

Sample Collection

CSF as well as serum samples were collected from 31 patients with AD and 19 patients with ALS. The collected samples were frozen at −80°C until assayed. Samples were also collected from 50 healthy elderly individuals, which served as controls. For CSF sampling, lumbar puncture (LB) using 20G spinal needle was performed using a 20 Gauge, 3.5 inch Quincke point spinal needle (Becton, Dickinson and Company) under local anesthesia in recumbent position at the L3/L4 spine interspace or below of each subject. Every CSF sample collected was

approximately 5–8 ml in volume. The CSF samples were collected in Falcon polypropylene tubes (BD Biosciences, Franklin Lakes, NJ, United States). The serum as well as CSF samples were collected early in the morning between 8 and 9 am. The collected CSF samples were centrifuged at 2500 rpm for 5 min to exclude blood contaminants. The samples were then aliquoted in smaller concentrations of 250 μl per aliquot and frozen instantly at −80°C until used for further analyses. While performing the experiments, we freeze thawed only the required number of aliquots as per the requirements of sample concentration needed for the experiment. All the patients and control individuals were fasting since the evening before at the time of LP, and were requested to abstain from smoking. Most of the CSF and serum samples were analyzed within 8 weeks of their collection. This duration was mainly attributed to the fact that before opening an ELISA kit, we made sure that we have collected at least 20 cumulative samples of CSF and serum.

Inclusion/Exclusion Criteria

- All the AD and ALS patients included in this study were diagnosed with the disease since at least 2 years.
- Only those patients and controls were included who gave their consent for the study either by themselves or with the help of their close kin.
- All the subjects under the prescription of NSAIDs or any other drugs interfering with the neuroinflammatory system at the time of sample collection were excluded.
- All the subjects reported for chain smoking were excluded; the information was confirmed by accompanying kin.

Limitations

- An important limitation of our study is relatively small sample size as compared with those used by large-scale multicentric studies.
- We collected the serum and CSF samples in a span of 2 years from almost all the NDDs patients like AD, PD, ALS, MCI, VaD, and MS based on their consent.
- For this study, we only selected the two group of patients with maximum number of samples, and those turned out to be AD (31 patients) and ALS (19 patients). The PD (7 patients), MCI (9 patients), VaD (7 patients) and MS (4 patients) were much lesser in number, and we chose to not include them in this study and wait for more samples to design an effective analyses.

Measurement of Gal-3 Concentrations in Serum, CSF and Control Samples

The concentrations of Gal-3 in serum, CSF and control samples were measured by Abcam's Galectin-3 *in vitro* SimpleStep ELISA^{TM} kit (ab188394). Briefly, 50 μL of all samples was added to respective wells of polystyrene 96-well plates which were pre-coated with antibodies against Gal-3 (i.e., anti-Gal-3-antibodies), followed by the addition of 50 μL antibody cocktail to each and every well. The treated plate was then sealed followed by incubation at RT (room temperature) for 1 h, and finally shaked at 400 rpm on a plate shaker at RT for 2 h. The plate was then washed three times with 350 μL wash buffer, the plate was inverted and blotted against clean paper towels to remove excess liquid. This was followed by the addition of 100 μL TMB substrate to every well, and incubation at 400 rpm on a plate shaker for 10 min in dark. In the last step, each well was added with 100 μL stop solution, and the plate was shaken for 1 min to mix the solutions. The endpoint reading was recorded at 450 nm in ELISA reader (ELx50, Biotek).

Data Interpretation and Statistical Analysis

The differences in cognitive performance, sociodemographic characteristics, and Gal-3 concentrations were analyzed by ANOVA test, with LSD tests for pairwise *post hoc* test between groups. Chi square tests were used to analyze the differences in gender distribution. The differences in scores of baseline and follow up neuropsychological tests for AD and ALS groups were analyzed by LSD test. ROC curves were built to determine the sensitivity (SE), specificity (SP), and area under the curve of Gal-3 biomarker for the discrimination between AD and controls, and ALS and controls.

RESULTS AND DISCUSSION

In relation to the present study, Gal-3 has been reported to be involved in the physiology of almost all types of immune cells (Rabinovich et al., 2012; Chung et al., 2013; Asayama et al., 2017). The information on the Gal-3 expression regulation, however, is quite limited and needs further elucidation. In the present study, we investigated the expression pattern of Gal-3 levels in serum and CSF of AD and ALS patients, and tried to explore the potential associations with the clinical symptoms of these disorders.

The AD patients were on average older than ALS patients were, and thus scored lower on MMSE test. No significant difference was found in years of education and gender distribution between AD, ALS and controls groups. The baseline characteristics and demographic parameters have been summarized in **Table 1**. The results of two consecutive neuropsychological evaluations performed at an interval of at least 1 year have been summarized in **Table 2**. In the ALS group, the scores in all neuropsychological tests remained stable over time, whereas in the AD group, there was a decline in TMT-A, FOME, and SKT scores in the same period.

Based on SE and SP values, ROC curves were drawn to determine the cutoff scores for serum as well as CSF Gal-3 concentrations (**Table 3**). Serum Gal-3 concentrations >8.32 ng/mL (SE = 87% and SP = 74%) and CSF Gal-3 concentrations >7.64 (SE = 83% and SP = 69%) best differentiated the AD, ALS and control groups. We also investigated whether the Gal-3 concentrations might alter the diagnostic accuracy. **Figure 1** represents the distribution of subjects according to the serum and

TABLE 1 | Demographic parameters and baseline characteristics.

Characteristics	AD	ALS	Control	*P*		
	(*n* = 31)	(*n* = 19)	(*n* = 50)	(AD vs. controls)	(ALS vs. controls)	(AD vs. ALS)
Age (years)	66.8 ± 7.8	64.1 ± 6.9	74.9 ± 7.3	0.06	0.07	0.03
Years of education	9.16 ± 5.67	10.65 ± 5.14	13.34 ± 6.12	0.03	0.04	0.38
Males	18	11	29	0.03	0.04	0.04
Females	13	8	21			
MMSE score	20.7 ± 5.2	23.4 ± 6.2	29.7 ± 0.8	<0.001	<0.001	<0.001
Serum Gal-3 (ng/mL)	11.19 ± 3.67	10.45 ± 3.48	8.76 ± 3.03	0.02	0.02	0.07
CSF Gal-3 (ng/mL)	8.37 ± 2.79	5.19 ± 2.23	7.92 ± 2.56	0.02	0.02	0.07

AD, Alzheimer's disease; ALS, amyotrophic lateral sclerosis; MMSE, Mini-Mental State Examination.

TABLE 2 | Neuropsychological performances of AD and ALS patients.

Test	ALS			AD		
	Baseline	Follow-up	*P*	Baseline	Follow-up	*P*
FOME	24.21 ± 6.26	24.19 ± 6.81	0.54	26.45 ± 5.84	21.2 ± 5.94	0.01
MMSE	21.86 ± 4.23	22.02 ± 4.16	0.62	24.84 ± 3.27	23.1 ± 3.96	0.65
TMT-A	68.2 ± 28.34	67.95 ± 24.2	0.12	70.55 ± 38.48	93.21 ± 41.22	0.05
TMT-B	144.28 ± 50.25	146.9 ± 54.23	0.51	159.75 ± 55.34	215 ± 88.65	0.06
SKT	2.95 ± 3.28	3.24 ± 4.19	0.43	5.84 ± 4.55	8.76 ± 5.18	0.02

AD, Alzheimer's disease; ALS, amyotrophic lateral sclerosis; FOME, Fuld object memory evaluation; MMSE, mini-mental state examination; TMT-A, trail making test A; TMT-B, trail making test B; SKT, short cognitive test.

TABLE 3 | Cutoff scores, sensitivity and specificity values of serum and CSF Gal-3 concentrations differentiating the AD patients from controls, ALS patients from controls, and AD patients and ALS patients.

	Cutoff	AD (*n* = 31) vs. controls (*n* = 50)		ALS (*n* = 19) vs. controls (*n* = 50)		AD (*n* = 31) vs. ALS (*n* = 19)	
		Sensitivity (%)	Specificity (%)	Sensitivity (%)	Specificity (%)	Sensitivity (%)	Specificity (%)
Serum Gal-3 (ng/mL)	>8.32	87	74	82	71	88	76
CSF Gal-3 (ng/mL)	>7.64	83	69	78	65	85	73

CSF Gal-3 concentrations in AD, ALS and control groups. Our findings suggested that the AD patients had a distribution almost similar those of ALS patients.

In order to incorporate the difference in age as a factor between AD and ALS patients, and controls; age was used as ANOVA covariate. Visible differences were observed in serum Gal-3 concentrations between the three different groups (AD, ALS, and healthy controls) (P = 0.005). Remarkable difference in the serum Gal-3 concentrations was observed between AD and ALS patients during the LSD test. **Figure 2** depicts that the difference in the serum Gal-3 concentrations between AD patients and healthy controls was significant [AD vs. controls (mean ± SD) 11.19 ± 3.67 vs. 8.76 ± 3.03 ng/mL; P = 0.02]. Similarly, **Figure 3** depicts that the difference in serum Gal-3 concentrations between ALS patients and controls was significant [ALS vs. controls (mean ± SD) 10.45 ± 3.48 vs. 8.76 ± 3.03 ng/mL; P = 0.02], but the difference was lesser as compared to AD vs. controls. **Figure 4** depicts that the difference in serum Gal-3 concentrations of AD and ALS patients was not significant [AD vs. ALS (mean ± SD) 11.19 ± 3.67 vs. 10.45 ± 3.48 ng/mL; P = 0.07]. **Figure 5** depicts that the MMSE score and serum Gal-3 concentrations in AD and ALS patients, and controls exhibited a significant positive correlation (P = 0.306; P < 0.001).

In order to incorporate the difference in age as a factor between AD and ALS patients, and controls; age was again used as ANOVA covariate. Visible differences were observed in CSF Gal-3 concentrations between the three different groups (AD, ALS, and healthy controls) (P = 0.005). Remarkable difference in the CSF Gal-3 concentrations was observed between AD and ALS patients during the LSD test. **Figure 6** depicts that the difference in the CSF Gal-3 concentrations between AD patients and healthy controls was significant [AD vs. healthy controls (mean ± SD) 8.37 ± 2.79 vs. 5.19 ± 2.23 ng/mL; P = 0.02]. Similarly, **Figure 7** depicts that the difference in CSF Gal-3 concentrations between ALS patients and controls was significant [ALS vs. healthy controls (mean ± SD) 7.92 ± 2.56 vs. 5.19 ± 2.23 ng/mL; P = 0.02], but the difference was lesser as compared to AD vs. controls. **Figure 8** depicts that the difference in CSF Gal-3 concentrations of AD and ALS patients was not significant

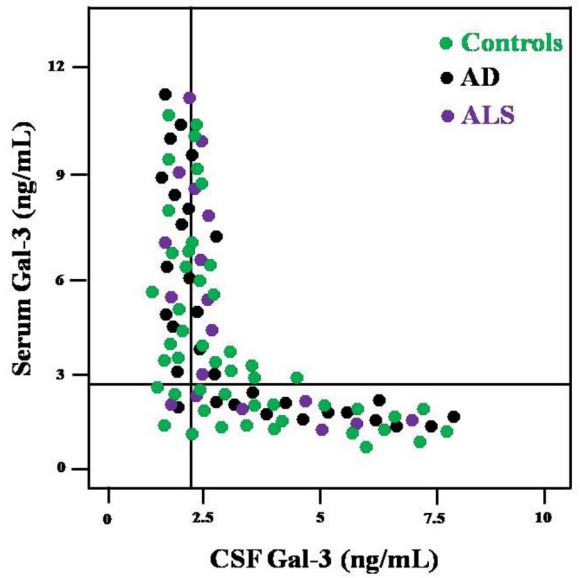


FIGURE 1 | Distribution of AD, ALS and control subjects according to the values of CSF Gal-3 (*x*-axis) and serum Gal-3 (*y*-axis).

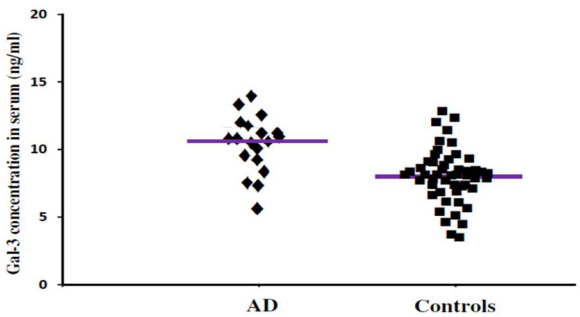


FIGURE 2 | The concentrations of Gal-3 in serum (ng/mL) of AD patients and healthy controls. AD patients showed enhanced Gal-3 concentrations in serum as compared to the healthy controls (AD vs. healthy controls [mean ± SD] 11.19 ± 3.67 vs. 8.76 ± 3.03 ng/mL; $P = 0.022$).

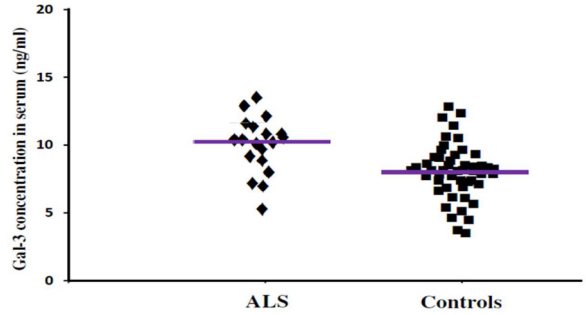


FIGURE 3 | The concentrations of Gal-3 in serum (ng/mL) of ALS patients and healthy controls. ALS patients showed enhanced Gal-3 concentrations in serum as compared to the healthy controls (ALS vs. healthy controls [mean ± SD] 10.45 ± 3.48 vs. 8.76 ± 3.03 ng/mL; $P = 0.019$).

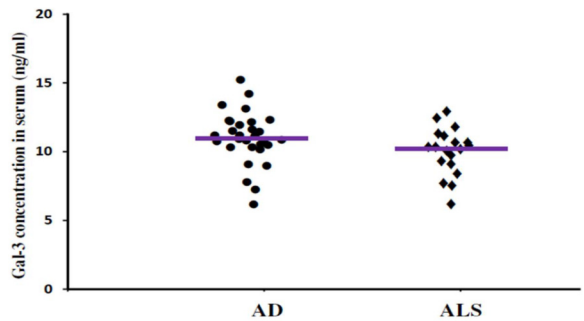


FIGURE 4 | The concentrations of Gal-3 in serum (ng/mL) of AD and ALS. There was no significant difference in the concentrations of Gal-3 in serum of AD and ALS patients (AD vs. ALS [mean ± SD] 11.19 ± 3.67 vs. 10.45 ± 3.48 ng/mL; $P = 0.719$).

[AD vs. ALS (mean ± SD) 8.37 ± 2.79 vs. 7.92 ± 2.56 ng/mL; $P = 0.07$]. **Figure 9** depicts that the MMSE score and CSF Gal-3 concentrations in AD and ALS patients, and controls exhibited a significant positive correlation ($P = 0.291$; $P < 0.001$).

The findings of our study demonstrated that the expression pattern of Gal-3 was significantly enhanced as compared to the controls in serum (**Figures 2**, **3**) as well as CSF samples (**Figures 6**, **7**) of AD and ALS patients. This enhanced expression of Gal-3 can be attributed to the activation and regulation of immune system in AD and ALS patients (Filer et al., 2009; Bauer et al., 2016; Yip et al., 2017). However, the difference in Gal-3 expression in serum (**Figure 4**) as well as CSF samples (**Figure 8**) between AD and ALS patients was not significant. This finding seems evident as the Gal-3 expression is altered to a considerable degree in AD as well as ALS patients, in reference to the control samples. This finding also suggests that Gal-3 is an aspecific marker that will discriminate every neurodegenerative/neuroinflammatory-related condition as opposed to a control population, and lacks specificity to discriminate between various dementias. A significant positive correlation between serum and CSF Gal-3 levels and MMSE score was observed (**Figures 5**, **9** and **Table 1**). The scores of neuropsychological tests remained stable in ALS patients over time, whereas in the AD group, there was a decline in TMT-A, FOME, and SKT scores in the same period (**Table 2**). This finding is well received, as there is hardly any memory loss is ALS patients, whereas there is a rapid loss of memory and cognitive skills in AD patients.

To our knowledge, the findings that serum and CSF Gal-3 levels are elevated in AD as well as ALS patients are one of the first of its kind to be reported from Saudi Arabia. Gal-3 functional roles have been reported in CNS (Bresalier et al., 1997; Reichert and Rotshenker, 1999). Gal-3 inductions are evident in various pathological processes of brain diseases such as prion diseases, ALS, AD, ischemic brain lesions, and PD (Jin et al., 2007; Lerman et al., 2012; Ashraf et al., 2015). The possible physiological role of Gal-3 in AD and

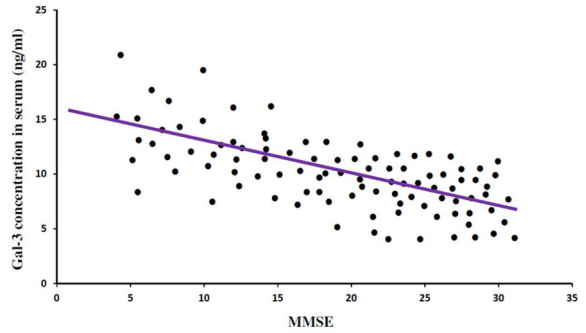


FIGURE 5 | Mini Mental Status Examination (MMSE) and serum Gal-3 concentrations. A significant correlation was observed between MMSE score as a measure of cognitive status and serum Gal-3 levels ($P = 0.306$; $P < 0.001$) in all the patients (AD = 31, ALS = 19, Controls = 50).

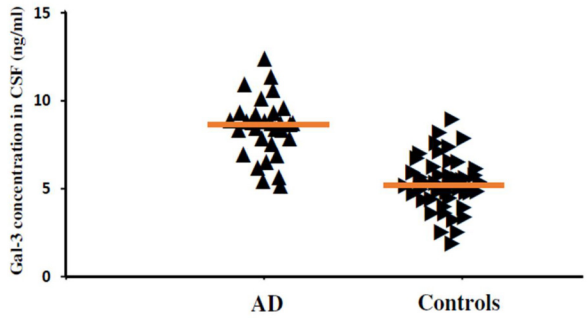


FIGURE 6 | The concentrations of Gal-3 in CSF (ng/mL) of AD patients and healthy controls. AD patients showed enhanced Gal-3 concentrations in CSF as compared to the healthy controls (AD vs. healthy controls [mean ± SD] 8.37 ± 2.79 vs. 5.19 ± 2.23 ng/mL; $P = 0.019$).

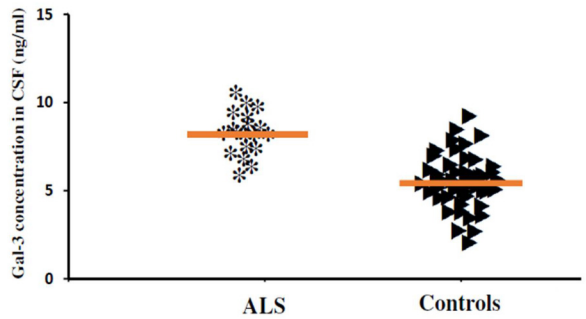


FIGURE 7 | The concentrations of Gal-3 in CSF (ng/mL) of ALS patients and healthy controls. ALS patients showed enhanced Gal-3 concentrations in CSF as compared to the healthy controls (ALS vs. healthy controls [mean ± SD] 7.92 ± 2.56 vs. 5.19 ± 2.23 ng/mL; $P = 0.017$).

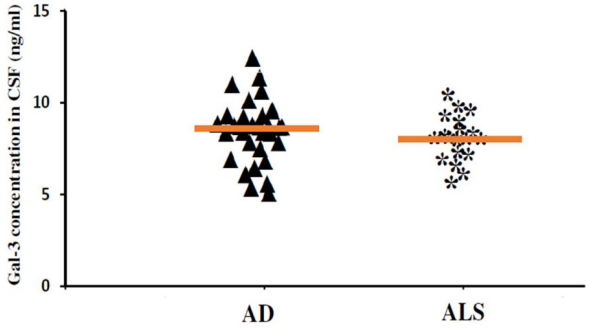


FIGURE 8 | The concentrations of Gal-3 in CSF (ng/mL) of AD and ALS. There was no significant difference in the concentrations of Gal-3 in CSF of AD and ALS patients (AD vs. ALS [mean ± SD] 8.37 ± 2.79 vs. 7.92 ± 2.56 ng/mL; $P = 0.734$).

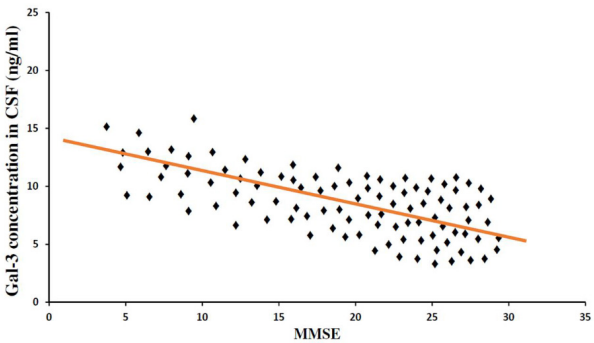


FIGURE 9 | Mini Mental Status Examination and CSF Gal-3 concentrations. A significant correlation was observed between MMSE score as a measure of cognitive status and CSF Gal-3 levels ($P = 0.306$; $P < 0.001$) in all the patients (AD = 31, ALS = 19, Controls = 50).

ALS can be investigated by exploring its already established biological functions like their role in inflammation and apoptosis (extracellular Gal-3 being proapoptotic, and intracellular Gal-3 being anti-apoptotic) (Yu et al., 2002; Nangia-Makker et al., 2007; Henderson and Sethi, 2009; Ashraf et al., 2010a; Siwicki et al., 2016). The activation of Gal-3 dependent TLR4 induces a sustained microglia activation, which in turn prolongs the inflammatory response in the brain (Burguillos et al., 2015). Gal-3 generates an enhanced inflammatory response by suppressing the production of interleukin 10 (IL-10), which is anti-inflammatory neuroprotective cytokine released by microglia during the progression of AD (Zhou et al., 2010; Di Bona et al., 2012). In a recent study, Gal-3 levels in plasma were reported to be highly enhanced in ALS patients with limb onset of the disease (Yan et al., 2016). This effect was especially more pronounced in female ALS patients and was found to be positively correlated with disease duration. In another study, Gal-3 deletion exacerbated microglial activation and accelerated the disease progression and demise in SOD1(G93A) mouse model of ALS (Lerman et al., 2012). These findings suggest Gal-3 as a crucial factor associated with ALS.

Based on above discussions, the elevated levels of Gal-3 in serum and CSF samples of AD and ALS patients investigated in our study potentially suggests activation of inflammation

and apoptosis, and impairment of neurodegenerative events in these patients. Our study successfully demonstrated a definitive association between the serum and CSF levels of Gal-3 and the cognitive status in AD and ALS patients and healthy individuals (controls). The secretory nature of Gal-3 and its detectable level in serum and CSF strongly proclaim this dynamic molecule as potential biomarker for AD and ALS in particular, and other NDDs in general. Our interesting findings suggest the need to explore and investigate the role of other galectins (Gal-1 to Gal-15) in various NDDs. These crucial findings strongly entail the need of future evaluation in prospective patient's cohort, which in turn can put galectins, especially Gal-3, in clinical trials.

AUTHOR CONTRIBUTIONS

GA conceived the study, performed all the experiments, analyzed the data, and compiled the whole manuscript. SB provided the CSF and serum samples.

FUNDING

This work was supported by the Deanship of Scientific Research (DSR), King Abdulaziz University, Jeddah, under Grant No. (141-764-D1435). The authors, therefore, gratefully acknowledge the DSR technical and financial support.

REFERENCES

Asayama, T., Tamura, H., Ishibashi, M., Kuribayashi-Hamada, Y., Onodera-Kondo, A., Okuyama, N., et al. (2017). Functional expression of Tim-3 on blasts and clinical impact of its ligand galectin-9 in myelodysplastic syndromes. *Oncotarget* 8, 88904–88917. doi: 10.18632/oncotarget.21492

Ashraf, G. M., Banu, N., Ahmad, A., Singh, L. P., and Kumar, R. (2011). Purification, characterization, sequencing and biological chemistry of galectin-1 purified from *Capra hircus* (goat) heart. *Protein J.* 30, 39–51. doi: 10.1007/s10930-010-9300-2

Ashraf, G. M., Bilal, N., Suhail, N., Hasan, S., and Banu, N. (2010a). Glycosylation of purified buffalo heart galectin-1 plays crucial role in maintaining its structural and functional integrity. *Biochemistry* 75, 1450–1457.

Ashraf, G. M., Rizvi, S., Naqvi, S., Suhail, N., Bilal, N., Hasan, S., et al. (2010b). Purification, characterization, structural analysis and protein chemistry of a buffalo heart galectin-1. *Amino Acids* 39, 1321–1332. doi: 10.1007/s00726-010-0574-7

Ashraf, G. M., Perveen, A., Tabrez, S., Jabir, N. R., Damanhouri, G. A., Zaidi, S. K., et al. (2015). Altered galectin glycosylation: potential factor for the diagnostics and therapeutics of various cardiovascular and neurological disorders. *Adv. Exp. Med. Biol.* 822, 67–84. doi: 10.1007/978-3-319-08927-0_10

Bauer, P. M., Zalis, M. C., Abdshill, H., Deierborg, T., Johansson, F., and Englund-Johansson, U. (2016). Inflamed in vitro retina: cytotoxic neuroinflammation and galectin-3 expression. *PLoS One* 11:e0161723. doi: 10.1371/journal.pone.0161723

Boza-Serrano, A., Reyes, J. F., Rey, N. L., Leffler, H., Bousset, L., Nilsson, U., et al. (2014). The role of Galectin-3 in α-synuclein-induced microglial activation. *Acta Neuropathol. Commun.* 2:156. doi: 10.1186/s40478-014-0156-0

Bresalier, R. S., Yan, P.-S., Byrd, J. C., Lotan, R., and Raz, A. (1997). Expression of the endogenous galactose-binding protein galectin-3 correlates with the malignant potential of tumors in the central nervous system. *Cancer* 80, 776–787. doi: 10.1002/(SICI)1097-0142(19970815)80:4<776::AID-CNCR17>3.0.CO;2-Q

Burguillos, M. A., Svensson, M., Schulte, T., Boza-Serrano, A., Garcia-Quintanilla, A., Kavanagh, E., et al. (2015). Microglia-secreted galectin-3 acts as a toll-like receptor 4 ligand and contributes to microglial activation. *Cell Rep.* 10, 1626–1638. doi: 10.1016/j.celrep.2015.02.012

Chen, H., Li, Y., Zhu, Y., Wu, L., Meng, J., Lin, N., et al. (2017). Advanced glycation end products promote ChREBP expression and cell proliferation in liver cancer cells by increasing reactive oxygen species. *Medicine* 96:e7456. doi: 10.1097/MD.0000000000007456

Chen, Y. C., Ma, Y. L., Lin, C. H., Cheng, S. J., Hsu, W. L., and Lee, E. H. (2017). Galectin-3 negatively regulates hippocampus-dependent memory formation through inhibition of integrin signaling and galectin-3 phosphorylation. *Front. Mol. Neurosci.* 10:217. doi: 10.3389/fnmol.2017.00217

Cherry, J. D., Olschowka, J. A., and O'Banion, M. K. (2014). Neuroinflammation and M2 microglia: the good, the bad, and the inflamed. *J. Neuroinflamm.* 11:98. doi: 10.1186/1742-2094-11-98

Chung, A. W., Sieling, P. A., Schenk, M., Teles, R. M., Krutzik, S. R., Hsu, D. K., et al. (2013). Galectin-3 regulates the innate immune response of human monocytes. *J. Infect. Dis.* 207, 947–956. doi: 10.1093/infdis/jis920

de Oliveira, F. L., Gatto, M., Bassi, N., Luisetto, R., Ghirardello, A., Punzi, L., et al. (2015). Galectin-3 in autoimmunity and autoimmune diseases. *Exp. Biol. Med.* 240, 1019–1028. doi: 10.1177/1535370215593826

DeFrancesco-Lisowitz, A., Lindborg, J. A., Niemi, J. P., and Zigmond, R. E. (2015). The neuroimmunology of degeneration and regeneration in the peripheral nervous system. *Neuroscience* 302, 174–203. doi: 10.1016/j.neuroscience.2014.09.027

Di Bona, D., Rizzo, C., Bonaventura, G., Candore, G., and Caruso, C. (2012). Association between interleukin-10 polymorphisms and Alzheimer's disease: a systematic review and meta-analysis. *J. Alzheimers Dis.* 29, 751–759. doi: 10.3233/JAD-2012-111838

Filer, A., Bik, M., Parsonage, G. N., Fitton, J., Trebilcock, E., Howlett, K., et al. (2009). Galectin 3 induces a distinctive pattern of cytokine and chemokine production in rheumatoid synovial fibroblasts via selective signaling pathways. *Arthritis Rheum.* 60, 1604–1614. doi: 10.1002/art.24574

Flaks, M. K., Yassuda, M. S., Regina, A. C., Cid, C. G., Camargo, C. H., Gattaz, W. F., et al. (2006). The short cognitive performance test (SKT): a preliminary study of its psychometric properties in Brazil. *Int. Psychogeriatr.* 18, 121–133. doi: 10.1017/S1041610205002577

Folstein, M. F., Folstein, S. E., and McHugh, P. R. (1975). Mini-mental state". A practical method for grading the cognitive state of patients for the clinician. *J. Psychiatr. Res.* 12, 189–198. doi: 10.1016/0022-3956(75)90026-6

Fortuna-Costa, A., Gomes, A. M., Kozlowski, E. O., Stelling, M. P., and Pavão, M. S. G. (2014). Extracellular galectin-3 in tumor progression and metastasis. *Front. Oncol.* 4:138. doi: 10.3389/fonc.2014.00138

Franco, P. G., Pasquini, L. A., Pérez, M. J., Rosato-Siri, M. V., Silvestroff, L., and Pasquini, J. M. (2015). Paving the way for adequate myelination: the contribution of galectin-3, transferrin and iron. *FEBS Lett.* 589, 3388–3395. doi: 10.1016/j.febslet.2015.08.001

Fuld, P. A. (1980). Guaranteed stimulus-processing in the evaluation of memory and learning. *Cortex* 16, 255–271. doi: 10.1016/S0010-9452(80)80061-X

Garden, G. A., and Campbell, B. M. (2016). Glial biomarkers in human central nervous system disease. *Glia* 64, 1755–1771. doi: 10.1002/glia.22998

Hamilton, M. (1960). A rating scale for depression. *J. Neurol. Neurosurg. Psychiatr.* 23, 56–62. doi: 10.1136/jnnp.23.1.56

Hasan, S. S., Ashraf, G. M., and Banu, N. (2007). Galectins – potential targets for cancer therapy. *Cancer Lett.* 253, 25–33. doi: 10.1016/j.canlet.2006.11.030

Henderson, N. C., and Sethi, T. (2009). The regulation of inflammation by galectin-3. *Immunol. Rev.* 230, 160–171. doi: 10.1111/j.1600-065X.2009.00794.x

Jiang, H.-R., Al Rasebi, Z., Mensah-Brown, E., Shahin, A., Xu, D., Goodyear, C. S., et al. (2009). Galectin-3 deficiency reduces the severity of experimental autoimmune encephalomyelitis. *J. Immunol.* 182, 1167–1173. doi: 10.4049/jimmunol.182.2.1167

Jin, J.-K., Na, Y.-J., Song, J.-H., Joo, H.-G., Kim, S., Kim, J.-I., et al. (2007). Galectin-3 expression is correlated with abnormal prion protein accumulation in murine scrapie. *Neurosci. Lett.* 420, 138–143. doi: 10.1016/j.neulet.2007.04.069

Lehfeld, H., and Erzigkeit, H. (1997). The SKT–a short cognitive performance test for assessing deficits of memory and attention. *Int. Psychogeriatr.* 9(Suppl. 1), 115–121. doi: 10.1017/S104161029700478X

Lerman, B. J., Hoffman, E. P., Sutherland, M. L., Bouri, K., Hsu, D. K., Liu, F.-T., et al. (2012). Deletion of galectin-3 exacerbates microglial activation and accelerates disease progression and demise in a SOD1 (G93A) mouse model of amyotrophic lateral sclerosis. *Brain Behav.* 2, 563–575. doi: 10.1002/brb3.75

McKhann, G., Drachman, D., Folstein, M., Katzman, R., Price, D., and Stadlan, E. M. (1984). Clinical diagnosis of Alzheimer's disease: report of the NINCDS-ADRDA Work Group under the auspices of department of health and human services task force on Alzheimer's Disease. *Neurology* 34, 939–944. doi: 10.1212/WNL.34.7.939

Mok, S. W., Riemer, C., Madela, K., Hsu, D. K., Liu, F.-T., Gültner, S., et al. (2007). Role of galectin-3 in prion infections of the CNS. *Biochem. Biophys. Res. Commun.* 359, 672–678. doi: 10.1016/j.bbrc.2007.05.163

Nangia-Makker, P., Nakahara, S., Hogan, V., and Raz, A. (2007). Galectin-3 in apoptosis, a novel therapeutic target. *J. Bioenerg. Biomembr.* 39, 79–84. doi: 10.1007/s10863-006-9063-9

Narciso, M. S., Mietto Bde, S., Marques, S. A., Soares, C. P., Mermelstein Cdos, D. S., El-Cheikh, M. C., et al. (2009). Sciatic nerve regeneration is accelerated in galectin-3 knockout mice. *Exp. Neurol.* 217, 7–15. doi: 10.1016/j.expneurol.2009.01.008

Ottum, P. A., Arellano, G., Reyes, L. I., Iruretagoyena, M., and Naves, R. (2015). Opposing roles of interferon-gamma on cells of the central nervous system in autoimmune neuroinflammation. *Front. Immunol.* 6:539. doi: 10.3389/fimmu.2015.00539

Peruzzotti-Jametti, L., Donegá, M., Giusto, E., Mallucci, G., Marchetti, B., and Pluchino, S. (2014). The role of the immune system in central nervous system plasticity after acute injury. *Neuroscience* 0, 210–221. doi: 10.1016/j.neuroscience.2014.04.036

Rabinovich, G. A., van Kooyk, Y., and Cobb, B. A. (2012). Glycobiology of immune responses. *Ann. N. Y. Acad. Sci.* 1253, 1–15. doi: 10.1111/j.1749-6632.2012.06492.x

Radosavljevic, G., Volarevic, V., Jovanovic, I., Milovanovic, M., Pejnovic, N., Arsenijevic, N., et al. (2012). The roles of Galectin-3 in autoimmunity and tumor progression. *Immunol. Res.* 52, 100–110. doi: 10.1007/s12026-012-8286-6

Reichert, F., and Rotshenker, S. (1999). Galectin-3/MAC-2 in experimental allergic encephalomyelitis. *Exp. Neurol.* 160, 508–514. doi: 10.1006/exnr.1999.7229

Rinaldi, M., Thomas, L., and Pasquini, L. A. (2016). Galectin-1 in myelin repair. *Oncotarget* 7, 81979–81980. doi: 10.18632/oncotarget.13455

Sävman, K., Heyes, M. P., Svedin, P., and Karlsson, A. (2013). Microglia/macrophage-derived inflammatory mediators galectin-3 and quinolinic acid are elevated in cerebrospinal fluid from newborn infants after birth asphyxia. *Transl. Stroke Res.* 4, 228–235. doi: 10.1007/s12975-012-0216-3

Siwicki, M., Engblom, C., and Pittet, M. J. (2016). Gal3 links inflammation and insulin resistance. *Cell Metab.* 24, 655–656. doi: 10.1016/j.cmet.2016.10.014

Surendranathan, A., Rowe, J. B., and O'Brien, J. T. (2015). Neuroinflammation in Lewy body dementia. *Parkinsonism Relat. Disord.* 21, 1398–1406. doi: 10.1016/j.parkreldis.2015.10.009

Tam, J. H., and Pasternak, S. H. (2012). Amyloid and Alzheimer's disease: inside and out. *Can. J. Neurol. Sci.* 39, 286–298. doi: 10.1017/S0317167100013408

Tombaugh, T. N. (2004). Trail making test A and B: normative data stratified by age and education. *Arch. Clin. Neuropsychol.* 19, 203–214. doi: 10.1016/S0887-6177(03)00039-8

Viguier, M., Advedissian, T., Delacour, D., Poirier, F., and Deshayes, F. (2014). Galectins in epithelial functions. *Tissue Barriers* 2:e29103. doi: 10.4161/tisb.29103

Wang, X., Zhang, S., Lin, F., Chu, W., and Yue, S. (2015). Elevated galectin-3 levels in the serum of patients with Alzheimer's Disease. *Am. J. Alzheimers Dis. Other Demen.* 30, 729–732. doi: 10.1177/1533317513495107

Wuolikainen, A., Moritz, T., Marklund, S. L., Antti, H., and Andersen, P. M. (2011). Disease-related changes in the cerebrospinal fluid metabolome in amyotrophic lateral sclerosis detected by GC/TOFMS. *PLoS One* 6:e17947. doi: 10.1371/journal.pone.0017947

Yamamoto, Y., and Yamamoto, H. (2012). Controlling the receptor for advanced glycation end-products to conquer diabetic vascular complications. *J. Diabetes Investig.* 3, 107–114. doi: 10.1111/j.2040-1124.2011.00191.x

Yan, J., Xu, Y., Zhang, L., Zhao, H., Jin, L., Liu, W.-G., et al. (2016). Increased expressions of plasma galectin-3 in patients with amyotrophic lateral sclerosis. *Chin. Med. J.* 129, 2797–2803. doi: 10.4103/0366-6999.194656

Yip, P. K., Carrillo-Jimenez, A., King, P., Vilalta, A., Nomura, K., Chau, C. C., et al. (2017). Galectin-3 released in response to traumatic brain injury acts as an alarmin orchestrating brain immune response and promoting neurodegeneration. *Sci. Rep.* 7:41689. doi: 10.1038/srep41689

Yu, F., Finley, R. L., Raz, A., and Kim, H. R. (2002). Galectin-3 translocates to the perinuclear membranes and inhibits cytochrome c release from the mitochondria. A role for synexin in galectin-3 translocation. *J. Biol. Chem.* 277, 15819–15827. doi: 10.1074/jbc.M200154200

Zhou, J.-Y., Afjehi-Sadat, L., Asress, S., Duong, D. M., Cudkowicz, M., Glass, J. D., et al. (2010). Galectin-3 is a candidate biomarker for ALS: discovery by a proteomics approach. *J. Proteome Res.* 9, 5133–5141. doi: 10.1021/pr100409r

Zlokovic, B. V. (2008). The blood-brain barrier in health and chronic neurodegenerative disorders. *Neuron* 57, 178–201. doi: 10.1016/j.neuron.2008.01.003

Conflict of Interest Statement: The authors declare that the research was conducted in the absence of any commercial or financial relationships that could be construed as a potential conflict of interest.

Copyright © 2018 Ashraf and Baeesa. This is an open-access article distributed under the terms of the Creative Commons Attribution License (CC BY). The use, distribution or reproduction in other forums is permitted, provided the original author(s) and the copyright owner(s) are credited and that the original publication in this journal is cited, in accordance with accepted academic practice. No use, distribution or reproduction is permitted which does not comply with these terms.

frontiers in Neuroscience

ORIGINAL RESEARCH
published: 28 September 2018
doi: 10.3389/fnins.2018.00528

On the Extraction and Analysis of Graphs From Resting-State fMRI to Support a Correct and Robust Diagnostic Tool for Alzheimer's Disease

Claudia Bachmann[1], Heidi I. L. Jacobs[2,3,4], PierGianLuca Porta Mana[5], Kim Dillen[6], Nils Richter[6,7], Boris von Reutern[6,7], Julian Dronse[6,7], Oezguer A. Onur[6,7], Karl-Josef Langen[8], Gereon R. Fink[6,7], Juraj Kukolja[6,7,9] and Abigail Morrison[1,10]*

[1] Institute of Neuroscience and Medicine (INM-6), Institute for Advanced Simulation (IAS-6), JARA BRAIN Institute I, Jülich Research Centre, Jülich, Germany, [2] Faculty of Health, Medicine and Life Science, School for Mental Health and Neuroscience, Alzheimer Centre Limburg, Maastricht University, Maastricht, Netherlands, [3] Division of Nuclear Medicine and Molecular Imaging, Department of Radiology, Harvard Medical School, Massachusetts General Hospital, Boston, MA, United States, [4] Department of Cognitive Neuroscience, Faculty of Psychology and Neuroscience, Maastricht University, Maastricht, Netherlands, [5] Kavli Institute for Systems Neuroscience, Norwegian University of Science and Technology (NTNU), Trondheim, Norway, [6] Cognitive Neuroscience, Institute of Neuroscience and Medicine (INM-3), Jülich Research Centre, Jülich, Germany, [7] Department of Neurology, University Hospital of Cologne, Cologne, Germany, [8] Cognitive Neuroscience, Institute of Neuroscience and Medicine (INM-4), Jülich Research Centre, Jülich, Germany, [9] Department of Neurology, Helios University Hospital Wuppertal, Wuppertal, Germany, [10] Faculty of Psychology, Institute of Cognitive Neuroscience, Ruhr-University Bochum, Bochum, Germany

OPEN ACCESS

Edited by:
Athanasios Alexiou, Novel Global Community Educational Foundation (NGCEF), Australia

Reviewed by:
Alessandro Giuliani, Istituto Superiore di Sanità, Italy
Rui Li, Institute of Psychology (CAS), China

***Correspondence:**
Claudia Bachmann
c.bachmann@fz-juelich.de

Specialty section:
This article was submitted to Brain Imaging Methods, a section of the journal Frontiers in Neuroscience

Received: *31 January 2018*
Accepted: *13 July 2018*
Published: *28 September 2018*

Citation:
Bachmann C, Jacobs HIL, Porta Mana P, Dillen K, Richter N, von Reutern B, Dronse J, Onur OA, Langen K-J, Fink GR, Kukolja J and Morrison A (2018) On the Extraction and Analysis of Graphs From Resting-State fMRI to Support a Correct and Robust Diagnostic Tool for Alzheimer's Disease. Front. Neurosci. 12:528. doi: 10.3389/fnins.2018.00528

The diagnosis of Alzheimer's disease (AD), especially in the early stage, is still not very reliable and the development of new diagnosis tools is desirable. A diagnosis based on functional magnetic resonance imaging (fMRI) is a suitable candidate, since fMRI is non-invasive, readily available, and indirectly measures synaptic dysfunction, which can be observed even at the earliest stages of AD. However, the results of previous attempts to analyze graph properties of resting state fMRI data are contradictory, presumably caused by methodological differences in graph construction. This comprises two steps: clustering the voxels of the functional image to define the nodes of the graph, and calculating the graph's edge weights based on a functional connectivity measure of the average cluster activities. A variety of methods are available for each step, but the robustness of results to method choice, and the suitability of the methods to support a diagnostic tool, are largely unknown. To address this issue, we employ a range of commonly and rarely used clustering and edge definition methods and analyze their graph theoretic measures (graph weight, shortest path length, clustering coefficient, and weighted degree distribution and modularity) on a small data set of 26 healthy controls, 16 subjects with mild cognitive impairment (MCI) and 14 with Alzheimer's disease. We examine the results with respect to statistical significance of the mean difference in graph properties, the sensitivity of the results to model and parameter choices, and relative diagnostic power based on both a statistical model and support vector machines. We find that different combinations of graph construction techniques yield contradicting, but statistically significant, relations of graph properties between health conditions, explaining the discrepancy across previous studies, but casting doubt on such analyses as a

method to gain insight into disease effects. The production of significant differences in mean graph properties turns out not to be a good predictor of future diagnostic capacity. Highest predictive power, expressed by largest negative surprise values, are achieved for both atlas-driven and data-driven clustering (Ward clustering), as long as graphs are small and clusters large, in combination with edge definitions based on correlations and mutual information transfer.

Keywords: Alzheimer's disease, MCI, graph theory, resting-state fMRI, diagnosis, model by sufficiency, negative surprise

1. INTRODUCTION

The two major challenges in Alzheimer's disease (AD) research consist in firstly, finding an effective treatment that at least slows down the disease progress, and secondly, developing diagnostic tools that can not only detect the disease at the earliest stage, during which no symptoms related to cognitive deficits are apparent (Sperling et al., 2011), but also provide information into the progression of the disease. For the latter challenge it is particularly desirable that the tools can be deployed within the existing medical infrastructure (i.e., not requiring specialized machinery or lab procedures), such that it is feasible to scan a wide range of the elderly population. Diagnosis procedures currently in use include psychological tests, detection of abnormal concentrations of disease specific biomarkers (Amyloid-β, tau proteins) in cerebrospinal fluid and analysis of structural magnetic resonance images (MRI).

Although abnormalities of Amyloid-β concentrations are proposed to be the earliest disease indicator, they are not very reliable in disease prognosis. Moreover, the changes in Amyloid-β concentrations show the strongest increase in the preclinical phase, and are thus uninformative with respect to the further progression of the disease. Tau pathology, which probably spreads along functional networks (Hoenig et al., 2018) better predicts cognitive deficits and progression of the disease (Nelson et al., 2012). However, the two methods measuring Amyloid-β and tau concentrations, lumbar puncture and PET are invasive (Schroeter et al., 2009; Sperling et al., 2011).

Possibly, synaptic dysfunction, another disease marker, corresponds to the onset of AD even before Amyloid-β pathology starts. Additionally, as it gradually worsens throughout the course of the disease, it could serve as diagnostic marker for all stages of AD. Dysfunction of synapses can be indirectly measured via invasive FDG-PET and non-invasive functional MRI, which might directly be combined with structural MRI scans (Schroeter et al., 2009; Sperling et al., 2011). However, a diagnostic framework based on functional MRI has yet to be established.

Although many fMRI studies have investigated changes of functional activity in AD (for a review see Dennis and Thompson, 2014), there is no consensus about which information should be used. Such studies typically examine disrupted cortical connectivity, either locally, considering single brain areas (e.g., Dillen et al., 2017) and their embedding in the network, or globally, analyzing the entire constructed brain graph and the statistics of its graph properties (Gits, 2016).

We argue that in order to develop a robust diagnosis tool applicable to all disease stages, it is preferable to consider global graph properties for the following reasons. First, global graph properties seem to be more robust across sessions; consequently, changes in these properties over time are more likely to reflect disease progression than statistical fluctuations (Telesford et al., 2010; Wang et al., 2014). Second, not all disease progressions follow a stereotypical pattern. Whereas structural evidence of AD is typically found predominantly in entorhinal cortex and hippocampus, in atypical cases atrophy occurs primarily in other areas, such as posterior cortex (Johnson et al., 2012). These atypical cases might be better captured by global properties, since they make use of the entire information provided by the brain. Furthermore, analyzing the statistics of graph properties rather than comparing the properties of single nodes allows the use of data-driven brain clustering, which results in different numbers and locations of brain clusters for each individual.

However, it is challenging to investigate the informativeness of global graph properties due to the innumerable methods of graph construction, comprising both the clustering of the voxels to define the graph's nodes, and the definition of functional connectivity to define its edges. Across the range of previous studies investigating graph properties in AD, a wide variety of methodological approaches for graph construction and properties assessment have been applied and are probably a major source of contradictory observations, such as the comparative length of the shortest path in AD subjects with respect to control being reported in two recent studies as both shorter (Zhao et al., 2012) and longer (Sanz-Arigita et al., 2010).

It is a further challenge to identify an appropriate evaluation method that not only enables us to compare the different graph construction methods, but also permits the results to be combined with other information indicating the probability of a particular health condition. This means that pure classifiers, although they achieve high discrimination performance (Khazaee et al., 2015, 2017) do not meet these requirements because they return a group membership ("AD," "MCI," or "control") and not a probability that can be combined with the results of other diagnostic tests (e.g., derived from Amyloid-β concentration measures) or individual patient risk factors (Porta Mana et al., 2018).

In this article, we address these issues by presenting a methodology for determining which combination of techniques

to extract and analyze graphs from resting state fMRI data provides the best basis for a diagnosis tool, assuming a given initial data set. Here, we apply our methodology to a small data set consisting of 26 control (C) elderly patients without any indication of any form of dementia or other cognitive problems, 16 mild cognitive impaired (MCI) subjects and 14 patients suffering from Alzheimer disease (AD) (Dillen et al., 2017). We evaluate the combinations of graph construction and analysis methods using a statistical model that partly compensates for the small data set and also yields probabilities rather than classifications, thus permitting the results to be combined with other probabilities, as discussed above. In addition, we evaluate the graph construction techniques with respect to robustness of results to method configuration parameters and similarity of results across different techniques.

Note that our aim here is not to demonstrate superior classification (for which our data set is in any case too small) or to propose a particular combination of techniques as optimal (as this may vary between settings), but primarily to provide a principled way for determining an appropriate combination of techniques for a given data set, and secondarily to highlight the sensitivity of graph theoretical analysis to the details of graph construction.

To understand how different methods for constructing graphs affect the resultant graph properties, and thus the ability to distinguish between patient groups, we evaluate a range of standard and non-standard methods to construct the graphs. The first step in graph construction consists in clustering adjacent voxels, such that the activity of the resulting region can be expressed by the average of time varying signal of the selected voxels (see **Figure 1**). The decision as to which voxels form a cluster is often based on atlases established for a standard brain with predefined brain regions. In order to map this standard atlas to the functional image or vice versa, registration algorithms are used. Problematic in this step, especially for subjects potentially suffering from neurodegenerative diseases, is the inhomogeneous shrinkage of the brain, which hampers a correct registration (Liu et al., 2017). In addition, individual brain regions derived from standard brain templates are likely to execute several cognitive processes in parallel, such that averaging the activity across the voxels of these functional inhomogeneous regions is not justified (Marrelec and Fransson, 2011). We therefore also include activity driven algorithms, namely region growing and selection (Lu et al., 2003) and Ward clustering, into our evaluation.

In the second step in graph construction, functional connectivity values are calculated based on the averaged signal of the regions. In most studies this is carried out based on the Pearson correlation coefficient, restricting the functional connectivity to non-directional connections. Here we cover a broader range of possible measures in the time domain: linear, non-linear model-free and model-based (Wang et al., 2014) that, depending on their exact realization, result in directed or undirected graphs.

We then calculate a variety of graph measures on the single nodes (weighted degree, cluster coefficient, closeness centrality), edges (weights, shortest path) and the entire graph (modularity). As several of these measures are only well-defined for binary graphs, many studies binarize the weighted graphs obtained from the previous steps into binary graphs, by setting weights above an arbitrary threshold $w_{\min}$ to 1, and those below it to 0 (e.g., Supekar et al., 2008). The drawback here is that there is no validation for an optimal threshold, and information that might be relevant in AD may be lost. To investigate this problem, we analyze the dependence of graph theoretic measures on $w_{\min}$, setting the weights below it to 0 but leaving the values above unchanged.

To assess the suitability of combinations of graph construction and analysis methods to inform a diagnosis tool, we set up a statistical analysis based on a training data set of known health conditions (healthy controls, mild cognitive impairment, and Alzheimer's disease), see section 5.6. The diagnostic usefulness of the analysis pipeline is then defined as the performance of the model against a labeled test data set. A model with good

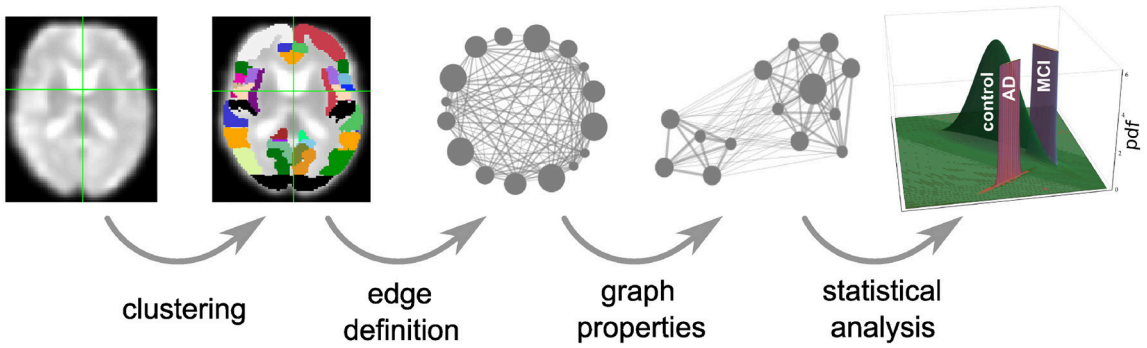


FIGURE 1 | Overview of intermediate steps for graph construction, properties derivation and statistical analysis. Each picture illustrates the result of a processing step starting from the preprocessed functional image (far left), which is clustered into regions, used as the nodes of the graph (second image). The averaged fMRI activity of each region is then used to calculate the edges of the graph (third image) and based on the calculated graph properties (fourth image) of all graphs, the statistical analysis estimates the probability density functions (pdf) of the three health conditions (last image) that are necessary for the evaluation of diagnostic performance based on the negative surprise measure. For the first three steps of the pipeline we investigate a range of different methods, see sections 2.1, 5.3, 5.4, and 5.5 for details.

performance can ultimately be employed in a clinical setting, to assess the probability that a patient has one of the three health conditions. For a more complete discussion of the development and use of the statistical model, see Porta Mana et al. (2018).

In this study we use a statistical model constructed from the following working hypothesis: the empirical means and correlations of graph data from previous patients with a given health condition are sufficient to predict the graph data of a new patient with that same health condition. This is a partially exchangeable model by sufficiency, and the resulting likelihood is a multivariate t distribution (Porta Mana et al., 2018), described in section 5.6. To assess which graph constructions have the greatest predictive power, we calculate their log-probabilities or *negative surprises* (Bartlett, 1952; Good, 1956, 1957a,b, 1983). To validate this approach, we also compare the results of the negative surprise with the classification performance achieved by a support vector machine (SVM).

Our results show that clustering resulting in small graphs with large clusters (Ward and atlas-based clustering) achieve highest negative surprises (and best SVM classification performance). Similarly, amongst the edge definition techniques, model-free methods (linear and non-linear correlations, mutually information transfer) obtain the highest negative surprise values. Conversely, calculating the graph's edge weights according to transfer entropy (model based) achieves limited diagnostic power but the ordering of the individuals based on their average graph properties is very robust toward the applied clustering method and choice of algorithm specific parameters. We further demonstrate that significant differences in the means of graph properties are very sensitive to method choice and to parameterization choices for a given method. Therefore such results, if taken at face value and not validated by alternate methods, may well be artifactual and not provide insight into the effects of a disease. Interestingly, the presence of significant differences in mean values of graph properties is not a reliable predictor of later diagnostic performance. In particular, atlas clustering results in only few significant differences but reaches the highest values for negative surprises and the best classification scores for the SVM. Finally, we show that the effect of setting a threshold on the graphs edge weights has only marginal effect on the negative surprise as long as threshold values are small.

2. RESULTS

2.1. Graph Construction

2.1.1. Vertex Definition by Means of Clustering

A universal property of the clustering algorithms examined here is the existence of a control parameter that regulates how the clusters are formed, and thus preserves a certain feature (or features) of the clusters. In atlas-based clustering, the preserved features are the number of clusters and the number of voxels per cluster. In Ward clustering, the number of resulting clusters is fixed, which we violate to a small extent by deleting very small clusters. In region growing and selection (RGS), the homogeneity of each cluster is preserved. The freedom that each of the algorithms leaves to the non-regulated features can either be considered as a drawback of the algorithm, because it makes graphs less easily comparable, or as an additional feature that might even improve the diagnosis performance.

Figure 2 shows the number of nodes/clusters, the average number of voxels per node and the average heterogeneity of the nodes for two configurations of the RGS algorithm, four configurations of the Ward algorithm, and the atlas algorithm (see section 5.3 and **Table 3**). Most strikingly, the node properties vary far more with respect to the clustering method chosen than with respect to the health condition.

By construction, the number of nodes for atlas clustering are the same for all individuals, and are the smallest over all the clustering methods (top panel). In Ward clustering the number of clusters is a parameter of the algorithm; it is not constant in **Figure 2** because we additionally include a parameter enforcing a minimum cluster size. Thus, the number of nodes for Ward clustering decreases as the minimum number of voxels per cluster p increases from 10 for "ward1" to 25 in "ward4." In RGS clustering we do not have such restrictions and the number of clusters is defined by the voxel dynamics. A consequence of this is that the number of clusters per graph are more widely spread.

The average number of voxels per cluster, shown in the middle panel of **Figure 2**, is unsurprisingly negatively correlated with the number of clusters. For purposes of comparison, the number of voxels for atlas clustering was first calculated for the standard space and then downscaled in proportion to the relation of the total number of voxels present in functional space to those in standard space. An inverse correlation can also be seen in the width of the distributions between the top two panels, for the non-atlas methods. In the case of RGS clustering, this can be explained by the fixation of the heterogeneity to one (see bottom panel of **Figure 2**), leading to quite homogeneous numbers of voxels per cluster, but to a wide range of the number of nodes, namely from 200 to 1200. Since this range is so large, it could be argued that graph properties that depend on this number would not be comparable in a meaningful fashion. In order to take care of such dependencies, we include the number of nodes in our statistical analysis (section 5.6). For Ward clustering we can observe that the numbers of nodes is inversely correlated not only with the average number of nodes and its variability, but also with the average heterogeneity and its variability. We observe the highest degree of heterogeneity for atlas clustering, presumably due to the high number of voxels per cluster.

Comparing node properties between the classes of clustering methods, atlas and ward4 clustering seem to be quite similar, which suggests they might result in similar graph properties and diagnosis performance. In particular, we note that these methods reveal a much smaller heterogeneity for the MCI group than for the control and AD groups.

2.1.2. Edge Definition by Means of Functional Connectivity

The edges of the graphs are constructed in four different ways, described in detail in section 5.4. Linear correlations (*corr*) are based on the Pearson correlation coefficient; non-linear correlations (H_2) result from a non-linear fit of piecewise linear correlations; mutual information transfer (*MIT*) measures the amount of shared information between two time varying signals

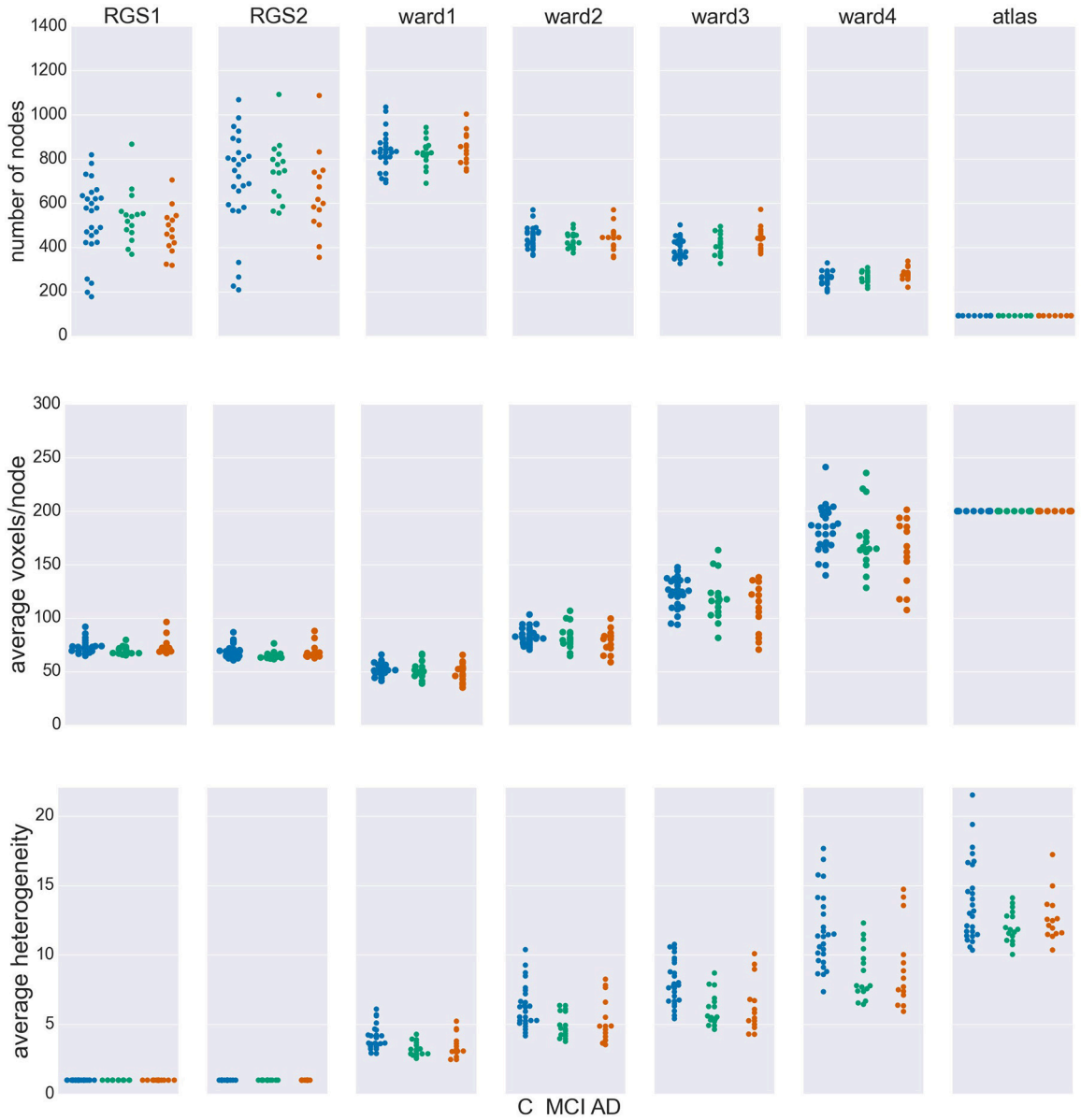


FIGURE 2 | Node properties across different clustering algorithms. For each of the seven clustering methods detailed in section 5.3 and **Table 3**, and each subject categorized in the health conditions: control (C, blue dots), mild cognitive impairment (MCI, green dots), and Alzheimer's disease (AD, orange dots) we calculate the total number of nodes/clusters generated **(Upper Panel)**, the average number of voxels per node **(Middle Panel)**, and the average cluster heterogeneity **(Lower Panel)**.

and transfer entropy (*TE*) describes in how far the future uncertainty is reduced by the preceding activity of the considered pair of nodes. As with the clustering algorithms described in the previous section, we defined differently parameterized variants of these four classes of technique (e.g., generating directed *D* or undirected *U* graphs) which are listed in **Table 4**.

For each combination of vertex (RGS, Ward or atlas) and edge definition technique (*corr*, H_2, *MIT*, *TE*), we averaged over the weights generated in each health condition for each variant of both techniques. For example, for the combination of region growing and transfer entropy (RGS *TE*) we averaged over all combinations of clustering implementation (RGS1 and RGS2) and edge detection (*BTEU*1, *BTEU*2, *BTED*1, *BTED*2). The results are shown in **Table 1** and exhibit a high variability in the mean connection weights. For instance, the combination RGS *TE* yields a maximal mean weight of 0.158 for controls, which is three times lower than the maximum mean weight of 0.493 obtained by the RGS H_2 combination. In particular, RGS clustering yields higher values compared with Ward and atlas clustering for model-free edge definitions (*corr*, H_2, *MIT*). The smallest values are obtained for *TE*. As a consequence, even small thresholds e.g., $w_{\min} = 0.3$ already cause *TE* graphs to disintegrate. Accordingly,

TABLE 1 | Mean and standard deviation of edge weight across different edge definitions.

Combination	$\hat{w}_C$	$\hat{w}_{MCI}$	$\hat{w}_{AD}$
Ward *corr*	0.328 ± 0.021	0.337 ± 0.04	0.315 ± 0.023
RGS *corr*	0.405 ± 0.076	0.363 ± 0.049	0.397 ± 0.113
atlas *corr*	0.319 ± 0.02	0.334 ± 0.054	0.307 ± 0.022
Ward H_2	0.443 ± 0.18	0.398 ± 0.081	0.414 ± 0.057
RGS H_2	0.452 ± 0.1	0.471 ± 0.126	0.493 ± 0.179
atlas H_2	0.36 ± 0.057	0.352 ± 0.039	0.355 ± 0.042
Ward *MIT*	0.201 ± 0.004	0.2 ± 0.007	0.197 ± 0.004
RGS *MIT*	0.221 ± 0.026	0.204 ± 0.011	0.218 ± 0.037
atlas *MIT*	0.196 ± 0.003	0.197 ± 0.008	0.193 ± 0.003
Ward *TE*	0.163 ± 0.013	0.158 ± 0.015	0.156 ± 0.018
RGS *TE*	0.158 ± 0.026	0.149 ± 0.02	0.152 ± 0.042
atlas *TE*	0.163 ± 0.016	0.17 ± 0.011	0.165 ± 0.011

Means and standard deviations are taken across the average edge weight of every individual graph in a health condition. Highest mean edge weights for each combination across the three health conditions are highlighted in gray.

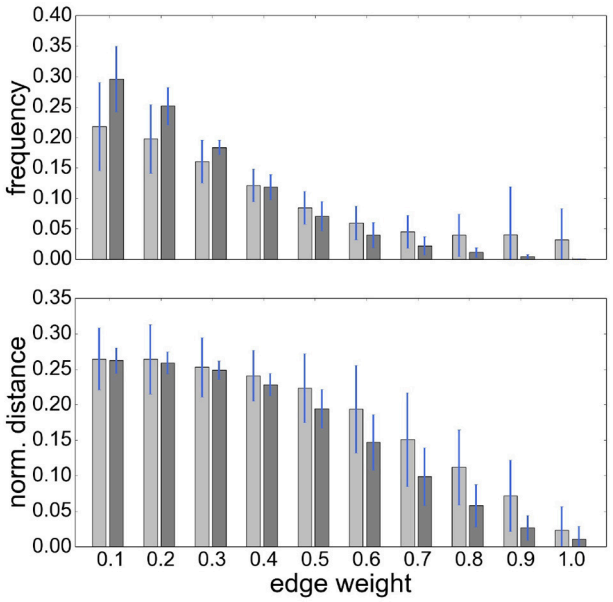


FIGURE 3 | RGS clustering yields stronger long-range connections then Ward clustering. Frequency **(Upper Panel)** and connection distance normalized to maximum graph distance **(Lower Panel)** across a range of graph edge weights calculated based on *BcorrU*1 for RGS1 (light gray bars) and ward2 (dark gray) clustering. Mean values and standard deviation (blue vertical lines) are calculated across single histogram values of all subjects independent of health condition.

not all graph properties can be calculated and used for statistical analysis, as shown in section 2.3.

It is also notable that there is no systematic relationship between the three health conditions—for RGS *corr*, the control graphs have the highest mean weight, for RGS H_2, the AD graphs; and for atlas corr, the MCI graphs. These results demonstrate that conclusions drawn on health conditions based on weight statistics should be treated with suspicion, as the outcome can be strongly influenced by the method of calculation. A possible explanation for the higher weights generated by RGS clustering is that it produces a greater number of shorter distances compared with the other clustering techniques. However, although **Figure 3** does indeed confirm that edge weights become smaller with cluster distance, it does not reveal a bias to shorter weights for RGS. In fact, the converse is true: RGS clustering yields stronger long-range connections for similar graph sizes [average number of graph nodes: 379.69 ± 147.99 (RGS), 311.43 ± 33.59 (Ward); average edge weights for distances longer than 0.8: 0.25 (RGS), 0.18 (Ward)]. Therefore we conclude that connecting homogeneous clusters allows stronger long-range connections to be extracted. However, the statistics of the RGS connections has a much larger variance then the ones derived from Ward clustering. This is only partly due to the variance in the number of nodes, since even if we choose three healthy subjects with similar graph size (RGS: 297 ± 2.16, Ward: 297.33 ± 6.6), we still get a higher standard derivation for RGS clustering in the weight distribution ($\sigma_{\mathrm{RGS}}/\sigma_{\mathrm{ward}} = 1.6$).

In the following we will treat the distribution of edge weights as a graph property since it contains information about graph structure.

2.2. Graph Properties

A recent survey by Gits (2016) of studies investigating graph properties in AD reveals no clear and systematic differences between heath conditions. For example, the mean clustering coefficient was found to be both significantly smaller (Supekar et al., 2008) and larger (Zhao et al., 2012) in AD compared to the aged-matched control group. We consider it likely that differences in methodology account for many of the contradictions. However, the stage of AD reached by the examined subject group may also play an important role. To investigate this aspect more closely, we examine the finding by Kim et al. (2015) that local efficiency, which corresponds to our definition of closeness centrality divided by the number of nodes in the network minus one, is increased for MCI, decreased for initial stages of AD and increased for severe AD stages with respect to the control group. The results of applying similar methods (atlas-based clustering combined with *BMITU*) are shown in **Figure 4**. The top panel shows the relationship between the health conditions when closeness centrality is calculated on the full, non-thresholded graph, which reproduces the findings of Kim et al. (2015), at least for initial stages of AD. However, if the measure is calculated on the graphs' rich club, i.e., the sub-graphs consisting of the nodes in the top 10% for degree, a different picture emerges, as shown in the middle panel of **Figure 4**. Here, AD has an increased closeness centrality with respect to both the control and mild cognitive impairment groups, which is in line with advanced AD stages in Kim et al. (2015).

More evidence that the outcome of a graph theoretical analysis can be highly sensitive toward the exact methodological implementation is given by considering the difference between

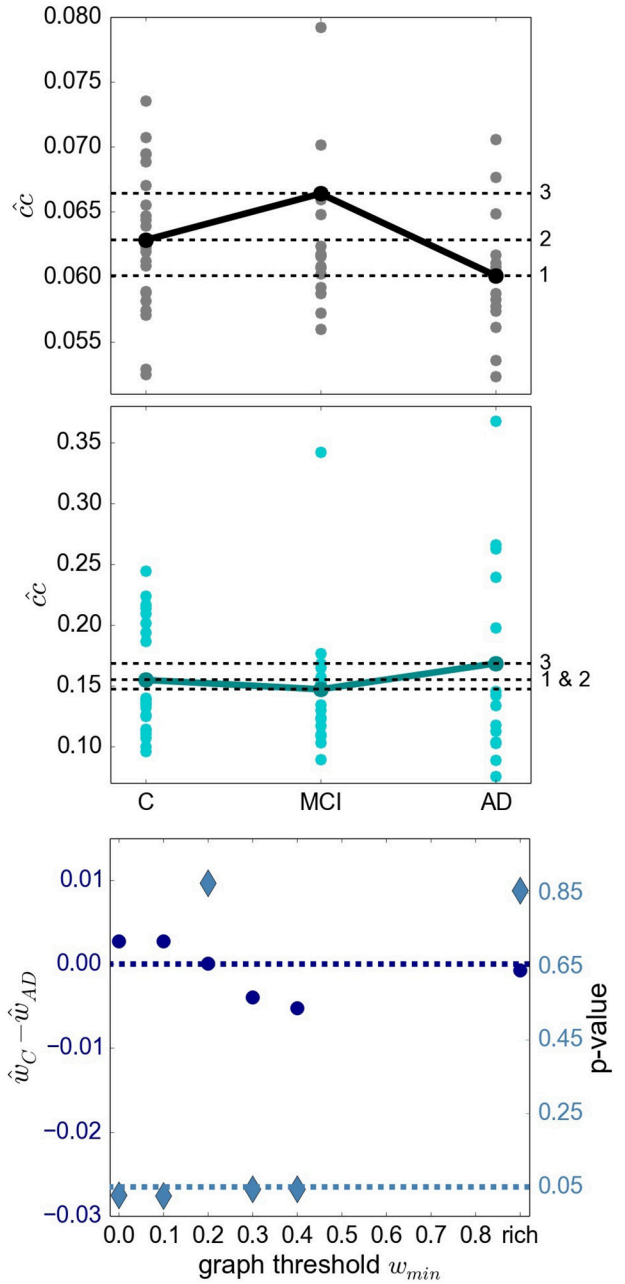


FIGURE 4 | Relationship of sub-graph properties across heath conditions is dependent on graph size. **(Upper Panel)** Average closeness centrality $\hat{cc}$ across graph nodes for complete graphs constructed with atlas *BMITU1* for the different health conditions C (left), MCI (middle) and AD (right). Each dot corresponds to the graph of an individual (connected dots indicate the mean values). **(Middle Panel)** As in top panel, but on the basis of the rich club graphs. **(Lower Panel)** Difference of the averaged ward1 *BMTID2* graph weights of the control group $\hat{w}_C$ and the AD group $\hat{w}_{AD}$ (left vertical axis, blue discs) and significance of this difference (right vertical axis, turquoise diamonds) as functions of the graph thresholding value $w_{\min}$. All $\hat{w}$ are positive and are only calculated as long as graphs are connected (which is the case for $w_{\min} < 0.5$). Average is taken across the weights of individual graphs. The dashed dark blue line indicates $\hat{w}_C - \hat{w}_{AD} = 0$; the dashed turquoise line indicates a significance level of 0.05.

the mean weights in the control and the AD conditions, and its significance (section 5.7.1), in dependence on the thresholding weight used to convert weighted graphs into simple graphs. This is illustrated in the bottom panel of **Figure 4**. Here, depending on where we set the threshold for considering an edge to be relevant, results having a significance level of $p < 0.05$ can be observed for both $\hat{w}_C > \hat{w}_{AD}$ ($w_{\min} \in \{0.0, 0.1\}$) and $\hat{w}_C < \hat{w}_{AD}$ ($w_{\min} \in \{0.3, 0.4\}$).

Extending this analysis, we find that contradictory significant results can be obtained for a variety of graph metrics across (and sometimes within) clustering methods. **Figure 5** shows the percentage of significant results obtained for health condition relationships in average edge weight, weighted degree, shortest path and clustering coefficient. Most strikingly, for most examined relationships, if significant differences are found at all, they are found in both directions, e.g., both for $\hat{d}_C > \hat{d}_{MCI}$ and for $\hat{d}_C < \hat{d}_{MCI}$ (weighted degree). Often a clustering algorithm favors a particular comparison direction, e.g., for the clustering coefficient, RGS clustering yields $\hat{clc}_{MCI} > \hat{clc}_{AD}$ whereas Ward and atlas clustering yields $\hat{clc}_{MCI} < \hat{clc}_{AD}$. However, we also find cases where significant differences are found in both directions with approximately equal frequency, such as $\hat{sp}_C > \hat{sp}_{AD}$ and $\hat{sp}_C < \hat{sp}_{AD}$ for Ward clustering. In addition, we find some clustering algorithms show a systematic behavior across metrics, e.g., for RGS $\hat{x}_C > \hat{x}_{MCI}$ with $x \in \{w, d, sp, clc\}$.

The largest number of significant differences is found for the comparison of controls with MCI, followed by the comparison of controls with AD. Only few significant differences of the means are found for AD and MCI. This relation among the groups is in line with the observed differences in heterogeneity observed for Ward and atlas clustering, for which MCI showed much lower heterogeneity and AD slightly lower values compared to controls (bottom panel of **Figure 2**).

Focusing on the clustering methods that bring about the most significant differences comparing the entire graph properties distributions results, we find the highest fraction for RGS, followed by Ward clustering. Atlas-based clustering yields only a few significant results. **Figure 6** shows the breakdown of the proportion of significant results for each clustering method on the edge definition technique (shown in collated form in **Figure 4**). Notably, transfer entropy (*TE*) only rarely produces significant differences. All other edge definition methods show a similar fraction of significant comparisons. The highest number of significant comparisons across the different graph properties is generated by RGS clustering combined with *MIT*.

To what extent a greater proportion of significant relationships is likely to make this graph construction method a good basis for a diagnostic tool depends on two aspects. First, the significance test is performed only on mean values, but ideally the overall distributions should overlap as little as possible. Second, the correlation between graph properties should be small in order to avoid redundant information.

In this section we considered only the first moments (means) of the graph properties taken from an individual brain. However,

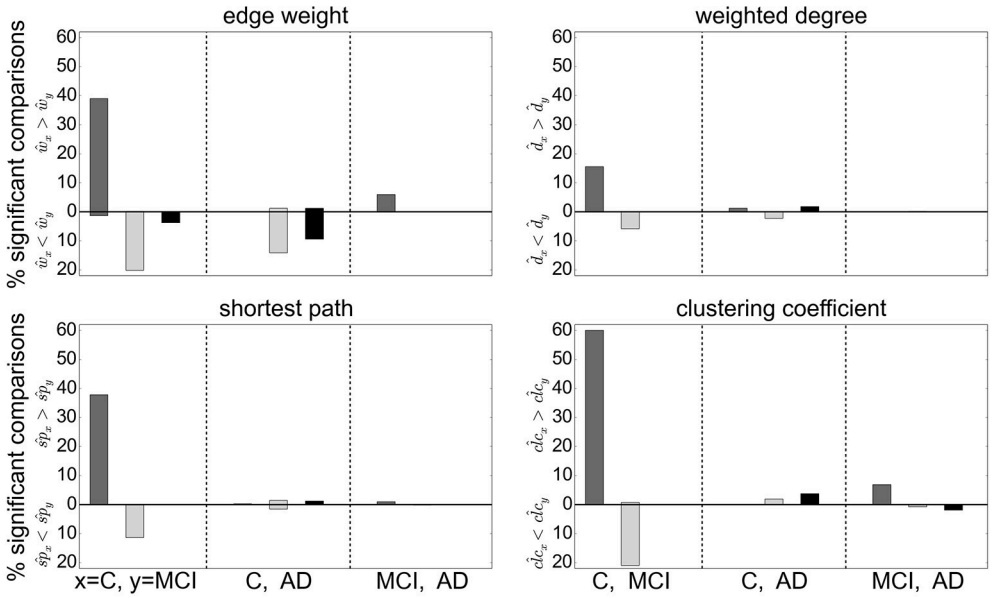


FIGURE 5 | Significant relationships in graph metrics between health conditions dependent on clustering methods. Percentage of significant differences for each clustering method RGS (dark gray), Ward (light gray), and atlas (black) for different averaged graph properties: edge weight **(Upper Left)**, weighted degree **(Upper Right)**, shortest path **(Lower Left)** and clustering coefficient **(Lower Right)**. Fraction of significant differences are calculated for each health condition over all graphs constructed with the corresponding clustering including all variants in parameters, edge definition techniques, thresholds and rich club sub-graphs. The abscissa labels show which pairs of health conditions are compared (C-MCI, C-AD, MCI-AD) and the ordinate labels the direction of the significant differences ("<," ">"). Significance is calculated as in the lower panel of **Figure 4**.

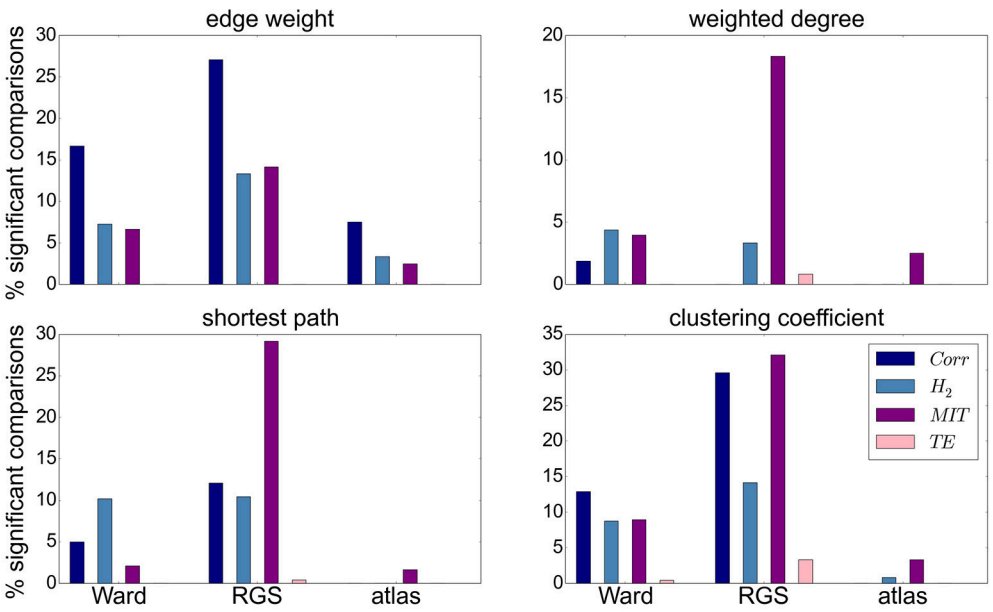


FIGURE 6 | Significant relationships in graph metrics between heath conditions dependent on edge definition methods. Percentage of significant differences for each clustering technique [Ward (left), RGS (middle), atlas (right)] for each class of edge definition method clustering method [*corr* (dark blue) , H_2 (light blue), *MIT* (purple), *TE* (pink)] for averaged graph properties: edge weight **(Upper Left)**, weighted degree **(Upper Right)**, shortest path **(Lower Left)** and clustering coefficient **(Lower Right)**. Fraction of significant differences are calculated for each health condition over all graphs constructed with the corresponding clustering and edge techniques including all variants in parameters, thresholds and rich-club sub-graphs. Significance is calculated as in the lower panel of **Figure 4**.

as explained in section 5.5, we use the first four moments of the individual distributions for our statistical analysis. Since the p-value of the other moments is not calculated, its influence on the statistical analysis cannot be considered.

In order to evaluate the methods based on robustness due to methodical variation, we investigate how the order of subjects (all subjects independent of their health conditions are ordered according to their average value of a certain graph property) is affected by the exact realization of the graph construction methods. Graphs constructed by methods based on similar underlying features of the data will tend to show a systematic ordering of subjects, regardless of the absolute values of the calculated graph metrics. **Figure 7** shows the commonalities and differences, which are illustrated with a dendrogram (see section 5.7.2) calculated on the Euclidean distance between the resulting ordered arrays of average graph weights. The continuous pink area show that graphs constructed using transfer entropy are most robust to the choice of clustering technique. Moreover, linear and non-linear correlations (dark and light blue) occupy contiguous blocks and so are most similar to each other. The leaves denoting atlas clustering (black) are rather spread out, indicating a high sensitivity of this method to the choice of edge definition.

In this section we have shown that the relationship of graph properties between health conditions strongly depends on the methods used for graph construction. For our data we find more significant mean differences for control-AD and control-MCI then for MCI-AD. With respect to clustering and edge definition methods, the largest number of significant differences are found for RGS and Ward clustering, and for model-free edge definitions. These results show that conclusions on how graph properties change due to AD have to be drawn carefully, and ideally validated by other methods, as they can be highly sensitive to the methods used for graph construction.

2.3. Evaluation of Graph Construction Methods Based on Negative Surprise

Having examined the consequences of particular choices for clustering and edge definition techniques in the previous sections, we now evaluate their combinations by considering their ability to help a clinician to discriminate among patient groups. This discrimination is achieved by using the graph data within a statistical model, which specifies the likelihood of the graph data. The model is described in section 5.6; the likelihood is a distribution which depends on a set of parameters. In general, the kind of graph data—i.e., their construction method—and the statistical model with its parameters are interdependent: they cannot be freely varied separately. Therefore our evaluations of the predictive power of the various graph construction methods have to be understood with a caveat: they depend on our specific choice of statistical model.

To quantify the discriminating power for each graph construction combination, we use a metric based on the final probabilities for the correct health conditions known as the log-probability, or *negative surprise* (Bartlett, 1952; Good, 1956, 1957a,b, 1983): a sure event, i.e., with unit probability, has surprise equal to zero; whereas an impossible event, i.e., with zero probability, has surprise equal to infinity, reflecting the fact that its occurrence would be contrary to all our expectations. A high surprise (in absolute value) therefore signals a low predictive power of the data we are using. The expectation or average of the surprises is the Shannon entropy (Shannon, 1948; Bartlett, 1952; McCarthy, 1956; Bernardo, 1979; Jaynes, 2003: section 11.3).

Another possibility, of a more decision-theoretical character, is to consider a metric based on the average utilities obtained with each particular graph-construction method. Given several possible courses of action (e.g., treat or dismiss) and their utilities or costs with respect to each health condition (e.g., treating an Alzheimer patient, dismissing a healthy patient, dismissing an Alzheimer patient, or treating a healthy one), the clinician

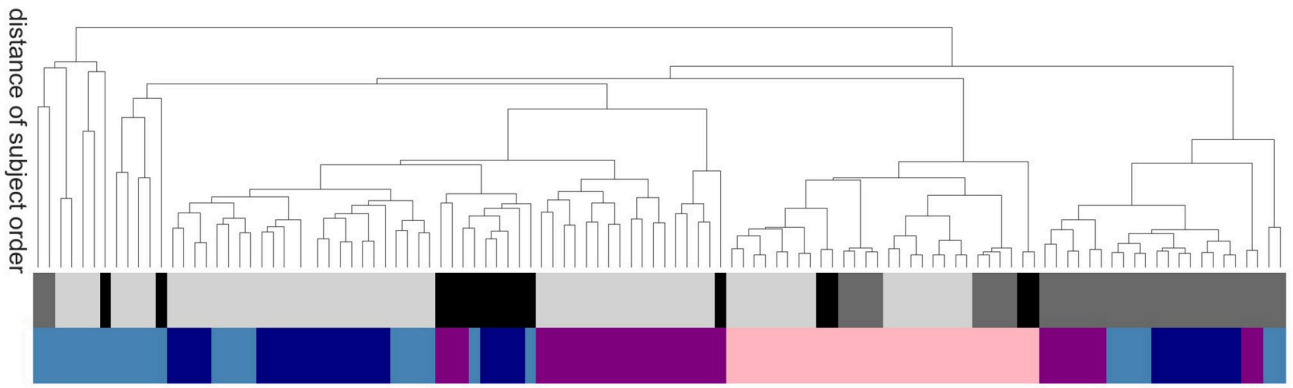


FIGURE 7 | Sensitivity of subject order to clustering and edge detection techniques. The dendrogram shows the distance of subject order, calculated by ordering all subjects according to their average graph edge weights and calculating the Euclidean distance between the resulting rank arrays. For better legibility, instead of naming the dendritic leaves, of which every leaf corresponds to a particular combination of clustering and edge definition techniques, e.g., ward2 *BTED2*, the top row of colors code for the class of clustering method: Ward (light gray), RGS (dark gray) and atlas (black); and the bottom row codes for the class of edge definition method: *corr* (dark blue), H_2 (light blue), *MIT* (purple) and *TE* (pink).

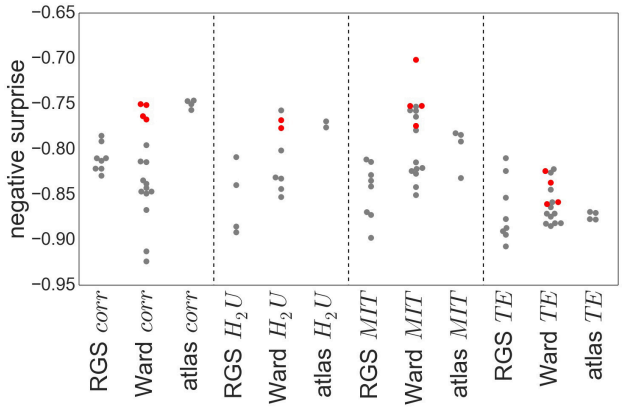


FIGURE 8 | Negative surprise of the different graph construction methods. Each dot represents a specific node clustering (e.g., RGS1) and edge definition (e.g., *BcorrU*1). Dots are grouped together according to their main class (e.g., RGS *corr*). Red dots highlight the results of ward4 clustering. Negative surprise expected by chance is −1.1.

should choose the action that maximizes the expected utility, the expectation being calculated from the final probabilities for the possible health conditions (Sox et al., 2013). This kind of metric therefore requires not only the final probabilities—which depend on the graph-construction method—but also a table of utilities.

Numerical tests show that the two kinds of metric yield similar results, at least for utility tables close to the identity (treating an ill patient and dismissing a healthy one have unit utility; the remaining combinations have zero utility). We therefore choose a metric based on the negative surprise, which is simpler and more intuitive than a utility metric.

In order to have an approximate idea of the relative predictive powers of the graph-construction methods we would like to use a statistical method that can be kept the same, as much as possible, across different methods. For this reason we choose a model based on the working hypothesis of sufficiency of mean and correlations of past data, as explained in the Introduction. This model ignores any restricted range of variability of graph quantities (e.g., positive or bounded). As explained in Porta Mana et al. (2018), this choice is non-standard but does not entail contradictions. The model has some free parameters; their values reflect the fact that the units of measure for the graph quantities make the latter of order unity. This choice of a generic, common statistical model allows us to sidestep the demanding problem of tailoring it for the different graph quantities from our 850 graph-construction methods.

Figure 8 shows the obtained negative surprises for all combinations of graph construction methods except H_2D, which is left out due to an inadequacy of the statistical model, resulting in unrealistic values between −1.26 and −0.66 with a mean and standard deviation of -0.94 ± 0.19.

The differences in negative surprise between the different graph construction method are in general small. The best results are obtained for ward4 clustering combined with mutual information (*MIT*) based edge definition. Across edge definition methods, linear correlation (*corr*) and mutual information give the best results and transfer entropy (*TE*) the worst. The rather poor performance of *TE* edge definition is in line with the small number of significant differences found for this method (compare **Figure 6**). Comparing the different clustering methods, atlas and ward4 clustering give the best results, as long as the edge definition is not *TE*. These two clustering methods have in common a very small number of graph nodes and (correspondingly) the highest number of voxels per cluster (compare **Figure 2**).

As explained above, the comparison of graph-construction methods can be affected by the statistical model and its parameters, especially for small datasets. As a complementary analysis we compare the negative surprises with the classification performances of a support vector machine (SVM, section 5.7.1) based on the same graph constructions. In a clinical setting, a misclassification between control and AD has more severe consequences than between MCI and AD. To avoid introducing an asymmetric misclassification penalty, we perform the classification between pairs of classes only (control-AD, C-MCI, MCI-AD).

Figure 9 shows the relationship between the SVM performance (measured as proportion of correct classifications) against the negative surprise. As long as *TE* edge definition is excluded, the two performance measures are positively correlated. In particular RGS clustering achieves low performance in both negative surprise and SVM classification. Furthermore, atlas clustering achieves a high classification performance across all edge definitions. The exact SVM classification results for each realization of graph construction method are depicted in **Figure S2** (see Supplemental Material).

Figure 10 demonstrates that thresholding graphs has only a minor effect on the negative surprise for small thresholds up to 0.2. No systematic relationship can be observed for the effect of larger thresholds; for example, increasing the threshold to 0.4 causes a decrease in negative surprise for RGS clustering with linear correlations or mutual information, but an increase for atlas clustering with transfer entropy edge detection. Likewise, the creation of highly connected and rich club sub-graphs typically decreases the negative surprise, but in some cases increases it (e.g., RGS H_2U). Overall the highest negative surprise (−0.66) is obtained for ward4 clustering combined with *BMITU*1 thresholded at $w_{\min} = 0.1$.

These results suggest that the best combination of graph construction techniques to use for this data set is the atlas-based or ward4 clustering combined with linear correlation methods or mutual information transfer. Thresholding the graph edges, which might reduce experimental noise and does lower computational complexity, has only a minor effect on the predictive power, as long as threshold values are small. Reducing the graphs complexity via larger thresholds or extracting the rich-club of the graph should be done with care, since the results can change in either direction. Although transfer entropy yields lower negative surprises then the model-free functional connectivity measures, we would not conclude that this edge definition performs worse in general, since it achieves high values in SVM classification. It is very likely that our choice of statistical

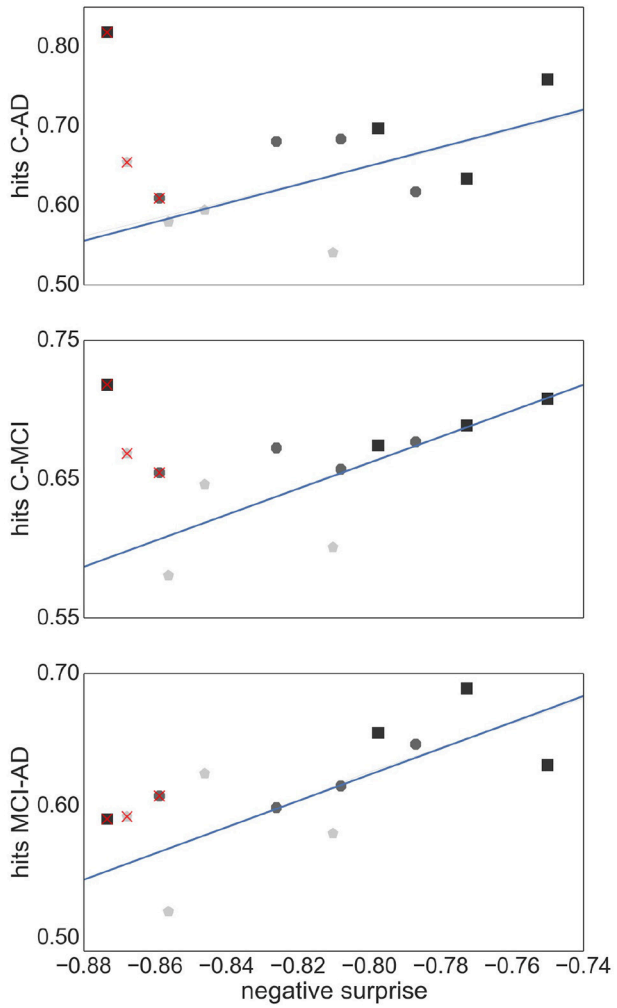


FIGURE 9 | Relationship between SVM classification performance and negative surprise. The average SVM performance achieved by each combination of clustering method and edge definition with respect to each pair of health conditions: control-AD **(Upper Panel)**, control -MCI **(Middle Panel)**, and MCI-AD **(Lower Panel)**, is plotted against the negative surprise calculated for all health conditions. Each marker corresponds to the averaged performance across the parameter space of a specific clustering method [atlas (black squares), Ward (dark gray octagons), RGS (light gray pentagons)] and a specific edge defintion (*corr*, H_2, *MIT*, *TE*). The regression line is calculated for all points but *TE* (superimposed red crosses). Pearson correlation coefficients *r* of the datasets are $r = 0.59$ **(Upper Panel)**, $r = 0.77$ **(Middle Panel)**, $r = 0.69$ **(Lower Panel)**.

model is not ideal, and a more tailored choice would improve performance.

3. DISCUSSION

In this article we have compared different techniques for constructing and analyzing graphs. By applying a statistical model, we have demonstrated a principled method for choosing a combination of techniques for a given data set. By examining the varied outcomes of the techniques, we have shown how sensitive the results of graph theoretical analyses, such as significant differences in mean properties, can be to the choice of clustering or edge definition technique.

With regards to the predictive power of the graph construction techniques, measured in terms of negative surprise, we find that Ward and atlas clustering yield the highest performance of the clustering techniques, and region growing and selection clustering (RGS) the lowest. In particular, the variant of Ward clustering that produces large clusters and small numbers of nodes (ward4) achieved the highest performance values. Analogously for the edge detection methods, we find better performance for the model-free methods (linear and non-linear correlations, mutual information transfer) than for the model-based method of transfer entropy. For this particular data set, a combination of ward4 clustering with mutual information derived edges achieves best results. Therefore, we would recommend this combination as the primary target for a more narrowly focussed investigation based on a larger data set.

The performances we obtain are above chance level but still far away from optimal prediction of the three health conditions. One reason for this sub-optimal prediction might lie in our choice of statistical model and its parameters. With our small data set (26 controls, 16 MCI, 14 AD) the model and its parameters have a high influence on the final probabilities, and thus on the performance (Porta Mana et al., 2018). We avoided tailoring the statistical model for the theoretic and practical reasons explained in section 2.3. Even if the model is not tailored, the results are consistent with the classification performance of support vector machines (see **Figure 9** and **Figure S2**), for the model-free edge definition techniques.

It remains unclear why Ward and atlas clustering are more successful than RGS, especially in combination with model-free edge definition. One possibility is that this is related to the large variability in graph sizes generated by RGS (**Figure 2**). In addition, the variance of weight distributions across subjects, and the variance of the cluster distances, are much larger in RGS then in Ward clustering (**Figure 3**). This could be related to the variance in the number of nodes; however, choosing graphs similar in size causes even higher variances (section 2.1). Therefore we assume that the number and connectivity of the small functional units extracted by RGS are highly variable across subjects. This variance might be even higher across subjects within a health condition than across health conditions, such that changes due to AD cannot be detected. This assumption might at first glance seem to contradict the high number of significant comparisons observed (**Figure 5**). However, we only calculate the significance level for the means of the distributions and not their entire shape. In addition, it is likely that some graph properties correlate with the graph size, and thus that apparent significant differences in graph properties are simply reflecting significant differences in numbers of nodes detected, and do not provide further information useful for classification or understanding the nature of the disease. Further investigation is needed on this matter.

The low negative surprise of transfer entropy (*TE*) compared with other model-free functional connectivity measures might

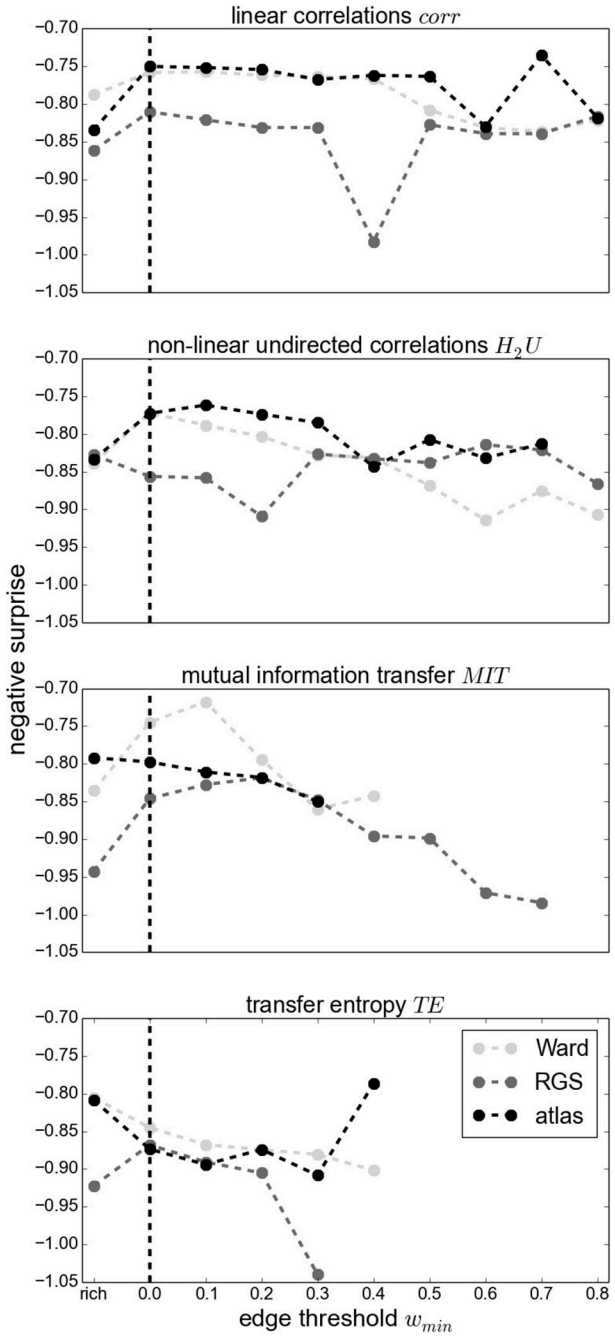


FIGURE 10 | Negative surprise for different graph edge thresholds $w_{\min}$ ($w_{\min} = 0$ for complete graphs, indicated by a vertical dashed line) and rich club graphs (rich) for different edge definitions: *corr* **(First Panel)**, H_2U **(Second Panel)**, *MIT* **(Third Panel)**, *TE* **(Fourth Panel)** and different clustering methods Ward (light gray), RGS (dark gray) and atlas (black). Each dot is the result of averaging across all possible parameters of a general graph construction method (for $w_{\min} = 0$ the average across all points of a swarm in **Figure 8**). Since some methods yield small edge weights, some graphs become unconnected for large $w_{\min}$ such that the statistical analysis is not conducted; no values are depicted in this case. Markers are connected for better visual comprehension.

have several reasons. The comparison of the negative surprise with the support vector machine classification suggests that a better choice of a statistical model is possible: the classification results for *TE* are similar to those of the model-free measures. In *TE* the data of a certain time interval in the past is used in order to calculate how much the uncertainty of the future is reduced. Here we use the data of the last 15 s. This time period might be poorly chosen, influencing the overall negative surprise. In addition *TE* is more sensitive to short recording periods than other methods, which may well also result in a reduced performance (Pereda et al., 2005).

With regards to the robustness of the graph theoretical outcomes, we discovered that relationships between mean graph properties, such as closeness centrality, edge weight or clustering coefficient (**Figures 4–6**) were sensitive to choice of clustering and edge definition techniques, to parameter choices for a given technique, and to the manner in which sub-graphs were defined (thresholding value and rich club). For most relationships between graph properties X, we could find significant ($p < 0.05$) differences in both directions, i.e., both $X_{\mathrm{AD}} > X_{\mathrm{C}}$ and $X_{\mathrm{AD}} < X_{\mathrm{C}}$, for specific choices of clustering and edge definition technique. This strongly suggests that a degree of suspicion should be applied to studies reporting such significant differences, especially if these results are argued to give insight into how a disease affects brain properties, unless the significance level is much more compelling or the reported differences can be validated with alternate methods.

We also investigated the sensitivity to method choice of the ordering of subjects according to a graph theoretic metric (**Figure 7**). In this analysis, transfer entropy was the most consistent. Nevertheless, the distributions of the negative surprises is as broad for transfer entropy as for other edge definitions (**Figure 8**). In general, the exact parameter selection within an edge definition method causes only slight changes in the negative surprise, more crucial is the exact realization of the clustering method: ward4 clustering generally achieves a better performance then ward3 clustering. These two variants differ only in the number of predefined clusters (see Supplemental Material **Figure S1**). Applying a lower threshold $w_{\min}$ on the graph's edge weights has little effect on the negative surprise for all methods, as long as only small weights (up to 0.2) are set to zero. Thresholding higher weights or extracting the graph's rich club has unpredictable effects on the results, and so should be used with caution (**Figure 10**). Atlas clustering was least consistent in the subject ordering analysis, suggesting that although it may provide a good basis for a diagnostic tool, care should be taken in reporting discoveries of particular relationships in graph properties between health conditions, as these may well turn out to be critically dependent on the edge definition method used.

Due to the intense computational requirements of the survey performed in this article, we recognize that it would be advantageous to develop heuristics for choosing between graph construction methods without performing the full calculation for each combination. Our results suggest that properties visible at the clustering stage, such as average heterogeneity, may give

some indication of predictive performance: graph constructions that result in different degrees of heterogeneity between the health conditions seem to be more discriminable by the later steps of the calculation. More research is needed in this area, which is outside the scope of the current study. In addition, it is tempting to consider *t*-test results of the mean graph properties as a heuristic. Our results suggest that this approach is largely inadequate. It holds for edge definition via transfer entropy, which gives very few significant results and the negative surprise is rather small compared with the model-free edge definitions. Conversely, region growing clustering yields most significant differences but a generally poor negative surprise. This may be due to graph properties being highly correlated, and so not providing additional information to the statistical model. In addition we used the first four moments (wherever possible) in our statistical model, rather than just the mean, which may also partially account for this apparent contradiction.

In addition to considering the predictive power and robustness of graph construction techniques, we can also evaluate them according to their practicality, i.e., speed of calculation and the extent to which they are easily available in established medical infrastructure and diagnostics. In general, applying graph theoretic measures to fMRI data for improving AD diagnosis makes sense, since MRI scans are already implemented in AD diagnostics for detecting structural changes such as hippocampal dystrophy caused by AD or AD-unrelated pathology (e.g., brain tumors). Softwares such as SPM (Tzourio-Mazoyer et al., 2002) and FSL (Jenkinson et al., 2012) are frequently used in medical research and mainly support clustering that is atlas and independent component analysis based. Ward clustering, which is the fastest of all these clustering methods, is a standard hierarchical clustering method and implemented in all standard programming softwares such as Python and Matlab. The region growing algorithm is not implemented in established softwares and is also computational very demanding. Given that it does not out-perform atlas or Ward clustering, we therefore do not recommend it. For edge definition and graph properties, several software packages are available based on Matlab (Wang et al., 2014; Kruschwitz et al., 2015) or Python[1], which provide a comprehensive range of edge definition and graph analysis methods.

In general we recommend using statistical models and not pure classifiers such as support vector machines as diagnostic tools, since statistical models calculate a probability of a diagnosis rather than assign a classification, i.e., "Given the fMRI scan, person x has a 80% probability of having Alzheimer's disease," rather than "Given the fMRI scan, person x has Alzheimer's disease." Probabilities can be easily combined with other probabilities of other diagnostic tests (Porta Mana et al., 2018) such as cognitive assessment, amyloid beta and tau protein occurrence in cerebrospinal fluid, blood tests, and structural MRI[2] (Johnson et al., 2012). This allows the medical doctor to conclude, for example: "Given the results of the cognitive test *and* cerebrospinal fluid analysis *and* structural and functional MRI scan, person x has a 95% probability of having Alzheimer's disease." After the estimation of the probability for a disease, she has to decide on a treatment, also taking into consideration such factors as "how harmful would the treatment be for a healthy person," which can be expressed in a utility function (Porta Mana et al., 2018). In addition, the statistical model used in this work allows an estimation of how much the model can be trusted, and therefore evaluate whether the sample size is sufficiently large (Porta Mana et al., 2018).

[1]https://github.com/dpisner453/PyNets.

[2]https://www.alz.org/research/diagnostic_criteria/.

3.1. Relationship to Previous Studies

Studies focusing on the graph properties extracted from resting-state fMRI in AD and its pre-stages generally have one of two aims. The first aim is to identify significant differences in the graph properties between health conditions, and to use these to gain insight into the effects of AD on the physical brain and its cognitive processes. These studies complement the picture revealed by investigations based on structural MRI and functional changes on the basis of EEG and MEG recordings. Typically a variety of graph properties (e.g., nodal degree, clustering coefficient, averaged shortest path, local efficiency, betweenness centrality, global efficiency, small worldness) are calculated, and used to motivate an account of how disease-related modifications to these properties result in a reduced capacity to transfer and process information.

However, such studies reveal entirely contradictory results. For example, the value of the clustering coefficient in AD with respect to controls has been reported to be increased, unchanged, and decreased, respectively (Supekar et al., 2008; Sanz-Arigita et al., 2010; Zhao et al., 2012). Analogous contradictions have been found for the comparative length of the shortest path (Supekar et al., 2008; Sanz-Arigita et al., 2010; Zhao et al., 2012). These contradictions could be caused by methodological differences or by not separating the different states of AD. Our results show ample evidence that the precise choice of graph construction techniques can easily account for contradictory findings, even for atlas based clustering, in which the number and size of clusters is held constant across all subjects (**Figure 5**). Evidence that the separation of different AD stages is relevant was provided by Kim et al. (2015), who demonstrated a non-monotonic behavior of global efficiency, local efficiency and betweenness centrality across different stages of AD and MCI. In our study, we could reproduce the pattern of increase and decrease of closeness centrality across conditions (**Figure 4**). However, we also demonstrate that the same analysis based on the rich club sub-graph yields a different pattern, and that contradictory (but significant) results can be obtained for the same graph construction techniques with different choices of threshold. We thus conclude that differences in graph properties between health conditions are currently ill-suited to provide an account of disease mechanisms in AD, unless either: (1) a specific method of graph construction can be shown to be more representative of the underlying connectivity than other methods, (2) the differences can be shown to be robust to choice of graph construction, (3) the differences can be validated by another analytical approach, or (4) the significance level is shown to be substantially more persuasive than $p < 0.05$.

The second category of studies use graph theoretical information as input for machine learning algorithms to classify the health conditions of the subjects. Note that for this purpose it is irrelevant if a difference between health conditions is not robust to method choice, as the goal is not to understand the effects of the disease but to robustly distinguish between conditions. Recent studies have reached very high performance: 100% accuracy in discriminating AD and control (Khazaee et al., 2015), and 93% for AD, MCI and control classification (Khazaee et al., 2017). In the latter work they extract more than two dozen local and global graph properties, resulting in roughly 3,000 features, since each of the local properties is calculated for all brain areas. Only a small subset of features is then used for classification, e.g., in-degree of the left middle temporal gyrus. They found that the classification power of local graph measures is larger than that of the global ones. Local changes in graph properties that do not propagate to global mean values have also been reported for area specific (frontal cortices, parietal and occipital regions) synchronization levels (Sanz-Arigita et al., 2010).

In this work we do not compare node-specific graph properties, because Ward and RGS clustering do not result in the same spatial location of clusters across subjects. Instead, we consider, wherever possible, the first four moments of the entire distributions of graph properties. This is more information than typically used for global measures, where often only the first moment (the mean) of a graph property distribution is taken into consideration. Nevertheless, it is still possible that considering single nodes, of which some may be more damaged by AD than others, could yield a better diagnostic performance. This requires further study in a survey considering only atlas based clustering. Again, this is out of scope of the current study, but we remark that the statistical model methodology we employ here would be equally applicable to such an investigation. The advantage of taking the entire distribution lies in the possibility of using purely data driven clustering algorithms (e.g., Ward clustering) that can be substantially faster than atlas based clustering, since they do not depend on a time and memory consuming registration of the individual brain image to standard space. In addition, the global distribution is more likely to be more robust against brain morphologic abnormalities such as brain tumors or brain shrinkage, and is more stable across recording sessions (Telesford et al., 2010; Wang et al., 2014). Finally, a short recording time might be expected to have a weaker influence on entire graph property distributions then on single nodes. Thus we conclude that global measures are preferable, if a good diagnostic performance can be reached. Although the goal of this work was not classification, we note that we obtain up to (80–90%) correct classification using an off-the-shelf support vector machine on leave-one-out subsets of our data for pairwise (C-AD, C-MCI, AD-MCI) comparisons. Whether global measures can reach the impressive performance shown by Khazaee et al. (2017) can only be investigated on a sufficiently large data set, ideally with several hundred participants.

3.2. Limitations of This Study

In each step of the graph construction and analysis pipeline (**Figure 1**) we set limits to the endless space of possible methods and their corresponding parameters. Here we will shortly summarize the reasons motivating the selection of the methods examined here and the exclusion of others, given the constraint of limited computational and temporal resources. As a general principle, we aimed to include the most commonly used method(s) and additional methods that we found to be reasonable, even if they are not currently frequently used.

Starting with the fMRI pre-processing, we had to decide whether to include global signal regression. The global signal (the average activity across all brain voxels) is assumed to originate partly from vascular and respiratory processes that do not represent neuronal activity. However, there is also evidence that it contains neuronal-signaling based components, since it is negatively correlated with the EEG signal and strongly correlated with the activity of the largest network in the brain (the default mode network, which plays a major role in rest state activity) when noise levels are low (Murphy and Fox, 2017). Without global signal regression, the Pearson correlation distribution derived from the signal of all voxels, or the average activity of clustered voxels, is biased to the right such that negative values are rare and small. The correction for the global signal centers this distribution, such that negative values are much more prominent. This also changes the properties of the graphs extracted from such data, for example an increase in modularity combined with fewer unconnected nodes has been reported (Schwarz and McGonigle, 2011; Hayasaka, 2013).

Speaking against global signal regression is the finding that correction for white matter, CSF and motions yield the most stable graph properties across sessions compared with additional applied global regression (Schwarz and McGonigle, 2011). In diagnostics it is important to have only small variance in the outcome across different sessions if the health condition of a subject is stable, such that small changes that indicate a worsening of the health condition can be rapidly detected. Moreover, we define the edges of our graphs as the absolute values of the functional connectivity values. As the negative part of the correlation distribution is small without global regression, different possible treatment of negative correlations (taking the absolute values or setting them to zero) should have only a small influence on the resulting graph properties, at least when the underlying functional connectivity are based on correlations. Consequently, we elect not to include global signal regression in our pipeline.

In the clustering step, the most commonly used method is to define clusters based on cortical regions defined by a brain atlas. We supplemented this with two data-driven clustering approaches: Ward clustering and RGS clustering. We selected Ward clustering, as it has been shown to perform better than alternative hierarchical clustering methods with respect to reproducibility and accuracy (Thirion et al., 2014). RGS, a method derived from image processing (Lu et al., 2003), was selected because we could adjust the method to produce functionally homogeneous clusters. In this formulation, the only free parameter of the algorithm is the minimal cluster size.

For both data-driven methods, we selected parameters such that graphs did not exceed a maximal size of 1,500 nodes, due to computational limitations. We excluded clustering based on independent component analysis, because of its laborious implementation and the requirement for domain expertise to distinguish noise from activity-related components. We also excluded all clustering algorithms that do not take functional consistency into account, e.g., dividing the voxels into cuboid patches, as has been proposed for structural data (Amoroso et al., 2017).

With regards to methods for edge definition, we limit our survey to functional connectivity measures that act in the time domain and not in the frequency domain, thus omitting frequency based wavelet analysis (Supekar et al., 2008), synchronization likelihood (Sanz-Arigita et al., 2010) and coherence (Wang et al., 2014). The most commonly used and simplest functional connectivity measure is the Pearson correlation coefficient (e.g., Zhao et al., 2012), which we name *BCorrU* in our work. We also test two additional model-free and one model-based method. A further model-based method based on Granger causality was excluded because it is too computationally expensive for larger graphs (Wang et al., 2014).

A thresholding operation is often applied to graphs extracted from fMRI, setting all values below $w_{\min}$ to zero. The aim of this step is to reduce experimental noise, which mainly manifests in the weaker edges, and to make the computation of graph properties computationally less demanding (Bordier et al., 2017). The threshold $w_{\min}$ can be defined in several ways: it can be set arbitrarily, without satisfying a certain demand, or such that certain properties of the graphs are preserved, e.g., average number of edges per vertex (Sanz-Arigita et al., 2010), node density (Zhao et al., 2012), small world behavior (Bassett et al., 2008) or a fixed cluster coefficient. Alternatively, it can be set such that information on the network's community structure is maximized; see, e.g., Bordier et al. (2017). In a variant of the thresholding approach, it has been proposed to transform the edge weights by applying a power law (Schwarz and McGonigle, 2011). In this study, for the sake of simplicity, we examine graph properties as a function of $w_{\min}$ without targeting any specific value of a graph property. Potentially, our results would reveal a different picture if $w_{\min}$ was optimized for each subject to attain, for example, a specific average nodal degree. However, comparison of these two different thresholding mechanisms resulted in no major difference in the relationships of graph properties between the control and AD groups (Sanz-Arigita et al., 2010).

We do not binarize our graphs (setting all values below $w_{\min}$ to zero and those above it to one) as is frequently done (e.g., Zhao et al., 2012), as this leads to a loss of information, and moreover some distributions of graph properties would become discrete (e.g., only ones and zeros for edge weights distributions), such that higher moments would be uninformative. The disadvantage of using weighted graphs lies in the limitation of possible graph properties. Most graph properties are well-defined for binary graphs and have been partly extended to weighted graphs. Here, we calculate the (normalized) weighted degree, shortest path, closeness centrality, clustering coefficient, and the modularity. We only investigate the most commonly used metrics and do not include more complex methods such as the minimal spanning tree (Çiftçi, 2011).

In addition to the restrictions of scope with regards to the examined techniques, a clear limitation of this study is the small data set. As our aim here is primarily to provide a methodology for evaluating and comparing analysis methods, rather than to draw conclusions on the effect of Alzheimer's disease on the graph properties of the cortex, a small data set is less problematic. Indeed, for the explorative survey carried out here, a large data set would have been prohibitively expensive with respect to computational resources. Moreover, many studies applying graph analysis to fMRI data are based on similarly sized data sets, which highlights the importance of raising awareness about the methodological artifacts we have identified.

The results of our survey indicate which combinations of methods are promising in view of Alzheimer diagnosis and should be investigated further in future studies based on larger data sets. Naturally, such studies could yield some quantitatively different results to those reported here, particularly with regard to the classification performance. Nonetheless, we would like to summarize some conclusions of the work that are unlikely to change with a larger data set. First, our results show that different combinations of methods can lead to contradictory findings with regard to significant differences in mean properties (section 2.2). This effect is unlikely to be resolved by a larger sample size. Second, methods showing good robustness with respect to parameter choice for a small sample size (e.g., *TE* edge definition, see **Figure 7**), are likely to remain robust with increasing sample size. Likewise, there is no reason to assume that methods performing well in all circumstances for the small data set, e.g., Ward clustering combined with *corr* edge definition (section 2.3), would perform worse for larger data sets. Finally, we assert that thresholding the graphs of a large data set with a small $w_{\min}$ (as shown in section 2.3) would similarly not result in a sudden jump in negative surprise.

3.3. Application of Approach to Other Analysis Techniques

We have demonstrated a systematic, quantitative approach for comparing and evaluating sequences of algorithms that result in classification of fMRI data based on the first four moments of simple graph theoretic metrics defined on the whole graph. However, the approach we present is equally well suited for assessing pipelines based on other metrics, as we briefly outline in the following.

One possibility is to consider the graph properties of individual nodes, as these have been shown to be very informative (Xia et al., 2014; Khazaee et al., 2015; Wang et al., 2016; Dillen et al., 2017).

This entails the use of atlas based clustering. We speculate that a global analysis of graph properties would be both faster and more robust to brain abnormalities and short recording

times, and so would be the preferable approach if equivalent performance levels can be attained.

A second possibility is to extend our approach to a hierarchical analysis. This could potentially be of great use, as previous studies based on PET imaging have suggested that in Alzheimer's disease, long range connections become weaker but local clustering increases (Pagani et al., 2016, 2017). These alterations would not be observable using the graph analyses so far considered, although we have taken the first step by calculating the modularity, which compares the ideal dissection of the given graph into modules with that of a random graph with similar edge weights.

To capture the graph meta-structures it is necessary to cluster graph nodes into modules, or sub-graphs. Modules can be defined either purely functionally, such that each node (ideally) has the strongest connections to the nodes in its own cluster, and the weakest connections to nodes of other clusters, or based on anatomic structures, such that nodes in a cluster are part of large, anatomo-functionally similar brain areas. Analogous to the variety of methods for spatial clustering and edge definition investigated in this study, there are many techniques used to cluster nodes into modules (e.g., k-clustering, hierarchical clustering and spectral clustering, for a review see Schaeffer, 2007 or anatomo-functional clustering, see Pagani et al., 2016), and likewise multiple options for analysing the characteristics of the resulting modular structure (e.g., module degree or participation coefficient; see Guimerá and Nunes Amaral, 2005). Such a comprehensive study is outside the scope of the current work, but could well provide great insight into health condition related alterations in the global network structure of the brain.

4. CONCLUSIONS

In order to achieve a robust and successful Alzheimer's disease diagnosis based on graphs extracted from fMRI data, we recommend clustering that results in rather small graphs with large clusters. Ward clustering, in which the number of clusters can be predefined, is fast, but requires programming knowledge to implement it. Atlas clustering is well established standard fMRI analysis software applications, but it is slow and might be affected by morphologic abnormalities in the brain, such as atrophy which is a common symptom of AD.

Edge weights should be calculated based on correlations or mutually information transfer, especially if a focus of the study is uncovering significant differences in mean graph properties between health conditions. We emphasize that the existence, magnitude *and direction* of such significant differences can be very sensitive to the methods chosen, and the parameterization of those methods, and so such findings should be reported with care, especially if a biological interpretation of said findings is claimed. Transfer entropy rarely gives significant results, but is more robust toward parameter changes in the algorithm and different clustering algorithms. Finding appropriate statistical models may be an additional challenge for this method.

Weak thresholding may be used for complexity reduction as it has little effect on performance. Applying a higher threshold or extracting the rich club sub-graph (The 10% of nodes with highest degree) causes unsystematic changes in the negative surprise and should therefore be used with caution, and validated against the full graph.

In summary, our quantitative evaluation and comparison of graph construction and analysis methods provides insight into how contradicting results come about in studies of graph properties of fMRI data, and identifies a number of potential methodological artifacts. Moreover, it provides a blueprint for establishing appropriate analysis pipelines, and serves as a well-founded starting point for future research on larger data sets.

5. METHODS

5.1. Data Acquisition

The recruitment and neuropsychological assessment of the study participants is given in Dillen et al. (2017). Demographic information is given in **Table 2**.

Anatomical MRI and resting state fMRI (rfMRI) images were obtained from a 3T MR-Brain-PET scanner (Siemens, Erlangen, Germany) in the Memory Clinic Cologne Juelich. The parameters for the single-shot echo planar imaging sequence of the functional (T2* weighted) image are the following: TR = 3,000 ms, TE = 30 ms, FA = 90°, FOV = 200 × 200 mm^2, matrix = 80 × 80, voxel resolution = 2.5 × 2.5 × 2.8, 50 oblique slices parallel to the infra-supratentorial line, gap = 0.28 mm, interleaved, scan time = 7 min. Parameters of the high-resolution T1-weighted structural image based on a magnetization-prepared rapid gradient echo sequence: TR = 2,250 ms, TE = 3.03 ms, FA = 9°, FOV = 256 × 256 mm^2, matrix = 256 × 256, voxel resolution = 1 mm isotropic, 176 sagittal slices, no gap, interleaved, scan time = 314 s. For more detail see Dillen et al. (2017).

5.2. Preprocessing of fMRI-Data and Extraction of Cortical Data

Image preprocessing is accomplished using FMRIB's Software Library tools (FSL; Woolrich et al., 2009; Jenkinson et al., 2012). We carry out the following steps for the structural T1-weighted image: skull-stripping (Smith, 2002) with bias field correction (Keihaninejad et al., 2010; Leung et al., 2011; Popescu et al., 2012) and for the functional T2-weighted image: discarding the first 10 volumes (out of 140 each taken after 3 sec), motion

TABLE 2 | Demographic information of participants.

	Controls	MCI	AD
Number	26	16	14
Age	62.38 [50, 73]	70 [55, 78]	71 [61, 78]
Sex	10 f, 16 m	7 f, 9 m	7 f, 7 m
Years of education	15.3 [8, 25]	12.75 [8, 21]	12.83 [7, 18]

Average and minimal and maximal values [min, max] are given for age and years of education; female (f), male (m).

correction (Beckmann and Smith, 2004), spatial smoothing using a 4 mm full width at half maximum Gaussian kernel, high-pass temporal filtering at 0.02 Hz and a six-parameter, rigid-body linear transformation procedure in MCFLIRT (Jenkinson et al., 2002). More details can be found in Dillen et al. (2017), where the same preprocessing is applied. In addition we carry out white matter and cerebrospinal fluid regression (FSL regfilt, MELODIC) to the functional image in order to reduce noise.

In order to extract only cortical voxels from the entire brain fMRI image, as needed for the data-driven clustering described in the next section, we first register cortical regions (frontal- , occipital-, temporal-, and insular-cortex) defined in the MNI structural atlas (Collins et al., 1995) to the structural and then to the functional space. For this registration we apply the transformation matrix obtained from registering the entire standard brain first to the individual structural brain (linear registration with FSL/FLIRT; Jenkinson and Smith, 2001; Jenkinson et al., 2002) and then to the functional space (non-linear registration with Advanced Normalization Tools, ANTs; Avants et al., 2011). In order to extract only gray matter tissue, we apply the gray matter image of the structural space (segmentation with FSL-FAST; Zhang et al., 2001) registered to functional space as described above, as a mask to the to the functional image.

5.3. Data-Driven and Atlas Based Clustering of Cortical Voxels

In order to construct graphs we cluster cortical voxels into regions using three different methods. Two of these methods, the Ward clustering and the region growing and selection algorithm (RGS) are data driven, such that only neighboring voxels with similar activity are combined into a single region. For these algorithms the number of regions per brain and the participating voxels in a region can differ for each individual and strongly depend on predefined algorithm-specific parameters. The atlas-based cluster algorithm, in contrast, produces the same number of clusters and a constant number of voxels per region across individuals, because the individual brains are mapped onto a standard brain.

5.3.1. Atlas-Based Clustering

For each subject we linearly register the rfMRI image first to the structural, skull-removed image (image segmentation for skull removing with SPM8, Wellcome Department of Cognitive Neurology, London, UKFSL; linear registration with FSL/FLIRT; Jenkinson and Smith, 2001; Jenkinson et al., 2002) and then, through a non-linear mapping, to the MNI standard brain [non-linear registration with Advanced Normalization Tools (ANTs; Avants et al., 2011); MNI 152 standard brain, non-linear 6th generation (Grabner et al., 2006)]. Regions of interest (ROIs) of the resulting functional image in standard space are extracted such that they match the 94 regions identified by the Oxford lateral cortical atlas (regions have a probability above 50%) (Desikan et al., 2006). A demonstration of how the brain is clustered according to the brain areas is given in the first panel of **Figure 12**.

TABLE 3 | Parameters used for the different clustering algorithms.

Method	Minimal number of voxels per cluster *p*	Number of clusters *k*	Threshold *T* of Pearson correlation coefficient
ward1	10	5,000	–
ward2	25	5,000	–
ward3	10	2,000	–
ward4	25	2,000	–
RGS1	55	–	0.75
RGS2	50	–	0.75
atlas	–	–	–

Ward clustering (ward), region growing and selection (RGS), atlas-based clustering (atlas).

5.3.2. Ward Clustering

Ward clustering (Python: *sklearn.cluster.AgglomerativeClustering*, Pedregosa et al., 2011) is a data-driven clustering algorithm, which is initiated by defining each voxel as a cluster and then, in each iteration step, merging the two neighboring clusters (even of different sizes) that after merging show minimal intra-cluster variance compared with all other possible variations of combining two adjacent clusters. In this way, the number of clusters is reduced by one in each iteration step. In our case the clustering stops after k clusters (**Table 3**) are formed. Afterwards, we discard away all clusters that contain less then p voxels (**Table 3**). An example of the outcome of Ward clustering algorithm is depicted in the second panel of **Figure 12**.

5.3.3. Region Growing and Selection

The region growing and selection algorithm is a modified version of the algorithm described in Lu et al. (2003). Region growing implies that each voxel serves as an initial seed (center) and neighboring voxels are added iteratively if they fulfill a certain growing criteria. (**Figure 11A**) The condition proposed for adding a voxel to a region is based on the Pearson correlation coefficient R between the averaged time-varying signals of the pre-merged region and the signal of the voxel to be tested (Lu et al., 2003). If this correlation is higher then a pre-defined threshold T (**Table 3**), the voxel is merged to the region. We tighten the growth criteria by imposing a second condition that allows the merging of voxels only if, in addition to exceeding the correlation threshold, the resulting cluster is also functionally homogeneous. Here, functional homogeneity means that the time-varying signals of all voxels can be expressed as instances of a single signal with varying levels of noise. The number of independent signals in a cluster can be estimated by the spatial functional heterogeneity h (Marrelec and Fransson, 2011):

$$h = n_0 + \frac{e_{n_0} - b_{n_0}}{(e_{n_0} - e_{n_0+1}) - (b_{n_0} - b_{n_0+1})}, \quad (1)$$

where e_n are the eigenvalues of the NxN covariance matrix of all N time varing signals in a cluster that exceed the eigenvalues generated by the broken-stick model b_n, such that $e_n > b_n = \sum_{i=n}^{N} 1/i$. The index n_0 accounts for the smallest eigenvalues that fulfill this inequality equation, such that

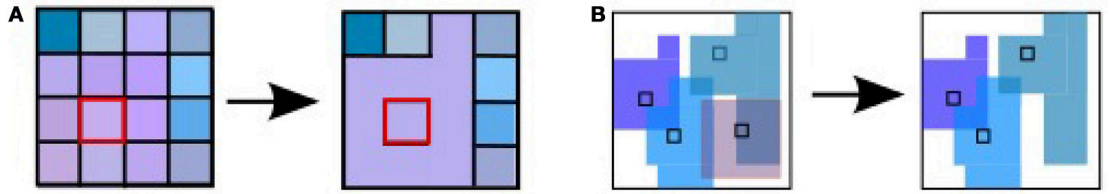


FIGURE 11 | Region growing and selection algorithm. **(A)** Region growing, left: each voxel (colored squares) serves as center for a cluster, right: example of a growing region (purple), only adjacent voxels that fulfill the fusion criteria are added to the growing cluster. **(B)** Region selection. Small regions (pink) with centers overlapping with larger regions (green) get deleted (from left to right) in a iterative manner. Remaining regions can still overlap as long as their centers do not cover other regions. This illustration is in 2D for simplicity, the algorithm used for fMRI data acts in 3D following the same rules.

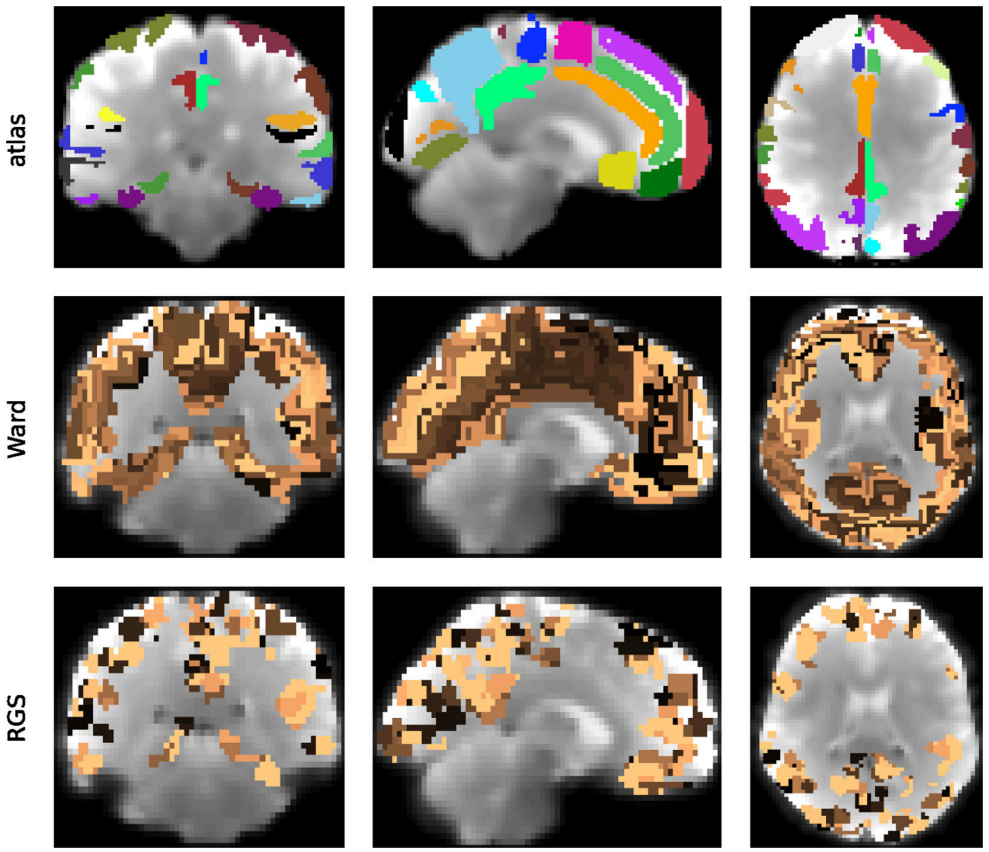


FIGURE 12 | Clustering of the cortical functional image. Illustrated are the clustering outcome of the atlas **(Upper Panel)** and the Ward clustering (ward4, **Middle Panel**) and RGS (RGS1, **Lower Panel**) algorithms for frontal, sagital and horizontal brain sections (from left to right) of a randomly chosen healthy individual. Individual clusters are depicted by a randomly chosen individual color, for clustering parameters see **Table 3**.

$e_{n_0} > b_{n_0}$ and $e_{n_{0+1}} < b_{n_{0+1}}$. A value of $h = 1$ indicates a homogeneous cluster.

The region selection algorithm iteratively selects the largest region and deletes all clusters that have their centers in that region, excluding the possibility that centers overlap with other regions. However, clusters can still overlap (**Figure 11B**). Applying this framework does not guarantee that clusters remain spatially connected after deleting regions with overlapping centers. Nevertheless, a check for spatial consistency reveals that only a negligible fraction of the clusters are disrupted in that way. Finally, we took only the clusters that comprised a minimum number of voxels p (**Table 3**). The outcome of RGS is illustrated in the last panel of **Figure 12**.

5.4. Edge Definition

A graph consists of nodes (vertices) that are connected through edges, that might be weighted or binary and directed or undirected. We construct individual brain graphs by defining

nodes that represent clusters as described in section 5.3, such that the mean activity of a cluster becomes a node attribute. We presume that all graphs are fully connected and edge weights are defined in terms of functional connectivity. Since functional connectivity can be calculated in several ways, we apply a range of different connectivity measures. In Wang et al. (2014) many such methods are evaluated, taking the structural connectivity of a toy model as reference. As a starting point, for each proposed category of functional connectivity, measured in time, we select the analysis measurement that captures structural connectivity best. We follow this strategy for all proposed measurement categories in Wang et al. (2014), leaving out only Granger causality measures, due to limited computational resources. We thus use linear and non-linear correlation (*corr* and H_2) and mutual information transfer (*MIT*) for the model-free category and transfer entropy (*TE*) for the model-based category. In all groups the bivariate methods perform better then the partial ones. In conclusion we select for each of the families the bivariate implementation that can be both directed and undirected. For consistency we use the same abbreviations for the different methods as in Wang et al. (2014) and the same Matlab toolbox Mulan[3] which they made public. Here we provide only a short description of the applied methods and more details can be inferred from Wang et al. (2014).

Linear correlation (*corr*) are measured based on the Pearson correlation coefficient (Rodgers and Nicewander, 1988) in a pair-wise manner. For directed connectivity (*BCorrD*) delays of up to 5 time steps (**Table 4**) are considered and the largest connectivity value is selected. We do not take into account time lags for undirected correlation (*BCorrU*).

Non-linear correlations (H_2) are based on piece-wise linear correlations of two time signals on which the non-linear curve is fitted (da Silva et al., 1989). Bivariate directed (BH_2D) and bivariate undirected (BH_2U) are defined as above for linear correlations.

Mutual information indicates how much information is shared between two time varying signals by means of Shannon entropy (Grassberger et al., 1991). For *BMITD1* individual histograms of two time series are contrasted to the joint histogram across different time delays. No delays are taken into account in *BMITU*.

Transfer entropy (Schreiber, 2000) describes how far in the past the activity of a node can reduce the uncertainty of the future activity of another node for which the past activity is also considered. Bivariate directed (*BTED*, Chicharro, 2011) and bivariate undirected (*BTEU*) are defined as above for linear correlations.

All methods were tested for a window size that comprises the whole time range (130 time points/6.5 min) and for a sliding window of 50 time points (2.5 min) with an overlap of 10 time points (0.5 min), see **Table 4**. If the methods revealed negative weights, the absolute value was considered. The resulting graphs are directed or undirected weighted graphs with values between zero and one for all methods except non-linear correlations, where values can exceed one.

TABLE 4 | Parameters of the different functional connectivity measures.

Method	Window size	Window overlap	Number of bins	Max. delay
*BcorrU*1	130	–	–	–
*BcorrU*2	50	0.2	–	–
*BcorrD*1	130	–	–	5
*BcorrD*2	50	0.2	–	5
*BH2U*1	130	–	10	–
*BH2U*2	50	0.2	10	–
*BH2D*1	130	–	10	5
*BH2D*2	50	0.2	10	5
*BMITU*1	130	–	5	–
*BMITU*2	50	0.2	5	–
BMITD1	130	–	5	5
*BMITD*2	50	0.2	5	5
*BTEU*1	130	–	–	5
*BTEU*2	50	0.2	–	5
*BTED*1	130	–	–	5
*BTED*2	50	0.2	–	5

Bivariate (B), undirected (U), directed (D), linear correlation (corr), non-linear correlation (H_2U), mutual information entropy (MIT), transfer entropy (TE).

Many studies transfer weighted graphs into binary ones by setting all values below a threshold $w_{\min}$ to zero and above to one e.g., Zhao et al. (2012). Following this strategy we also investigate the effect of setting all weights below $w_{\min}$ to zero but leaving higher weights unchanged. As far as the remaining graphs are still connected (left panels in **Figure 13**) and single nodes are not disconnected from the network (right panels in **Figure 13**) we study the disease diagnosis capacity for $w_{\min} \in \{0.1, 0.2, ...0.7, 0.8\}$. In addition we extract the rich club of the graphs. The rich club is a subgraph that comprises the nodes that are most strongly connected to the network. In this work we define the rich club as the 10% of nodes with highest degree.

5.5. Graph Properties

This section describes the different graph properties that are either characteristics of single nodes (weighted degree, closeness centrality, cluster coefficient), of pairs of nodes (shortest path) or of the entire network (modularity). In the first two cases we get a range of values for each graph. Since we do not know, which are the important features of the resulting distributions, we take the first four moments for our statistical analysis. Because graphs based on data-driven clustering contain different number of nodes and the calculated graph properties might be dependent on the number of nodes, we also include the number of nodes in the subsequent analysis (section 5.6).

5.5.1. Weighted Degree

The weighted degree $\deg_w$ describes how strongly a node is connected to all other vertices of the network, obeying the

[3]https://github.com/HuifangWang/MULAN.

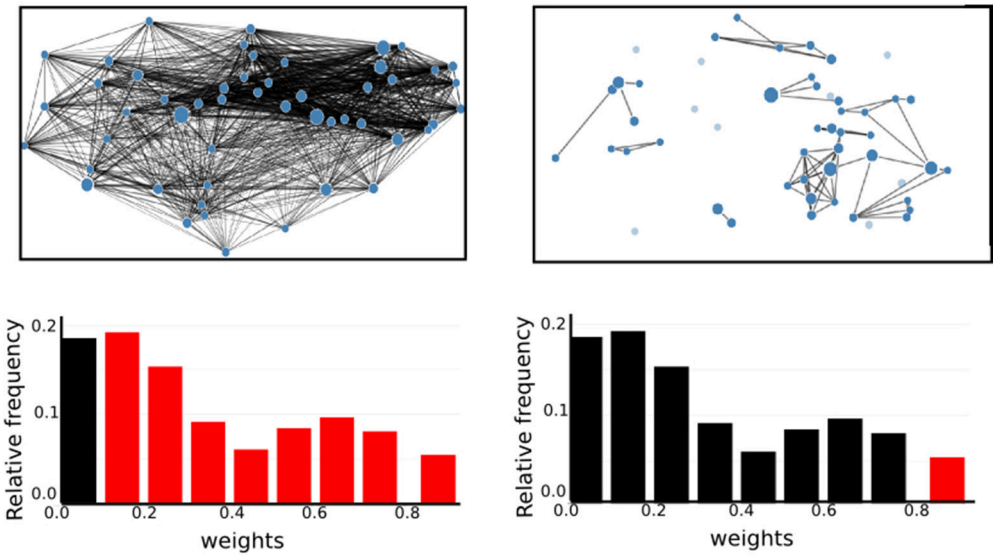


FIGURE 13 | High thresholds on graph edges cause the graphs to dissociate. **(Upper Panel)**, Illustration of graph with edge weights larger then 0.1 ($w_{\min} > 0.1$, **Left**) and larger then 0.9 ($w_{\min} > 0.9$, **Right**). In the according weight histograms **(Lower Panel)** the red bars correspond to the edges drawn in the upper graph. Edges corresponding to the black bars are not shown.

equation:

$$\deg_w(v) = \sum_{u \in V \setminus \{v\}} w_{uv} \tag{2}$$

where w_{uv} is the weight on the edge between nodes u and v of all nodes V in the graph. This definition implies a high dependency of the weighted degree on the number of nodes in a graph. To address this problem, we normalize the weighted degree

$$\deg_n(v) = \frac{\deg_w(v)}{\deg(v) \cdot w_{\max}} \tag{3}$$

with $w_{\max}$ being the maximal weight of the graph. The resulting values are between 0 and 1.

5.5.2. Shortest Path and Closeness Centrality

The shortest path $\text{dist}_w(u, v)$ between a pair of nodes u and v describes the path that minimizes the sum of the weights of its participating edges. A small shortest path should indicate a strong functional connectivity, therefore we consider the inverse of the graph weights for its calculation. Its computation is carried out using Dijkstra's algorithm (Rivest et al., 2000), which requires the weights to be positive.

Based on the shortest paths of a network we calculate closeness centrality $C_w(v)$ - a measure that indicates how strongly a node v participates in all shortest paths of the graph. It is given by:

$$C_w(v) = \frac{n-1}{\sum_{u \in V \setminus \{v\}} \text{dist}_w(u, v)} \tag{4}$$

Here, n is the number of all nodes V in the graph.

5.5.3. Clustering Coefficient

The clustering coefficient $cc(v)$ describes to what degree the neighbors of a node v are connected among each other and with node v. Since our network is weighted, we use the Zhang-Horvath clustering coefficient (Zhang and Horvath, 2005; Kalna and Higham, 2007), which is an extension to the "standard" algorithm applied to binary graphs:

$$cc(v) = \frac{\sum_{i \neq v} \sum_{j \neq i, j \neq v} \hat{w}_{vi} \hat{w}_{ij} \hat{w}_{jv}}{\left(\sum_{i \neq v} \hat{w}_{vi}\right)\left(\sum_{i \neq v} \hat{w}_{vi}^2\right)} \tag{5}$$

for i, j neighbors of v and $\hat{w}$ denoting the weights normalized by the highest weight in the network, such that $0 \leq \hat{w} \leq 1$.

5.5.4. Modularity

A graph can be partitioned into smaller components. Modularity measures the deviation of the properties of these components as compared to the components of a random graph with the same edge weights. Accordingly, the modularity of a partition p of a network G into communities c is given by Newman (2004):

$$Q(p) = \frac{1}{2m} \sum_{i,j \in V} \left(w_{ij} - \frac{\deg_w(i) \cdot \deg_w(j)}{2m}\right) \delta_{c_i c_j} \tag{6}$$

where $\delta_{c_i c_j}$ is 1, if the community c_i of node i is the same as the community c_j of node j, and 0 otherwise, and $m = \frac{1}{2} \sum_{i,j \in V} w_{ij}$ is the total sum of edge weights in a network. Although there are many different definitions in literature about what a community consists of, we define a community as a group of strongly interconnected nodes that make only weak connections to other communities. In addition, a node

can maximally contribute to one community. Hence we want to find the partition that maximizes modularity, which is computationally very demanding, so it is important to use a very effective algorithm. We therefore use the fast algorithm by Blondel et al. (2008), which is implemented in the Python packages community. Unfortunately this implementation is only suitable for undirected graphs, so we investigate modularity only for these type of graphs.

5.6. Statistical Model

The generated graph data is used as input for an exchangeable parametric statistical model. Let us recall that the purpose of the fMRI scan of a patient is to give the clinician a likelihood for the patient's health condition,

$$\mathrm{P}(\text{graph data from fMRI scan} \mid \text{health condition} \wedge \text{prior info}), \tag{7}$$

which she combines with the likelihoods from other tests and her initial probability assignment, to obtain via Bayes's theorem a final probability for the health condition (Sox et al., 2013):

$$\overbrace{\mathrm{P}(\text{health condition} \mid \text{results of all tests} \wedge \text{prior info})}^{\textit{final probability}} \propto$$

$$\textit{likelihoods} \begin{cases} \mathrm{P}(\text{graph data from fMRI scan} \mid \text{health condition} \wedge \text{prior info}) \\ \times \mathrm{P}(\text{results of other tests} \mid \text{health condition} \wedge \text{prior info}) \\ \times \cdots \end{cases}$$

$$\times \underbrace{\mathrm{P}(\text{health condition} \mid \text{prior info})}_{\textit{initial probability}}. \tag{8}$$

The prior information also includes test results from previous patients, so that the prediction becomes more accurate and reliable, the more patients have been previously observed.

The functional dependence of the likelihood on the graph data is determined by the statistical model we use, and may be different for each health condition. The statistical model is determined by additional assumptions or hypotheses. Such hypotheses and the functional form of the likelihood may depend on the particular space of graph data (e.g., real-valued, or positive, or bounded within a finite range, or combinations thereof), and therefore on the graph construction method.

As explained in section 2.3, our purpose is to assess as far as possible the relative predictive power of the different graph construction methods. We therefore would like the functional dependence on the graph data space to be minimal. In the present study we adopt the working hypothesis that only the first and second empirical moments—means and correlations—of the graph data from past patients with the same health condition are relevant to make predictions about a new patient. This hypothesis is adopted for all graph construction methods. We also assume our initial knowledge of the graph data to be approximately invariant under rescalings of their values (Minka, 2001). Finally, we do not take into account the natural range of variability (positive, bounded, etc.) of the graph data; this choice does not seem to impact the predictive power of the model (Porta Mana et al., 2018).

These assumptions almost uniquely determine the statistical model and the likelihood (Porta Mana et al., 2018): it turns out to be a multivariate t distribution (Minka, 2001; Kotz and Nadarajah, 2004; Murphy, 2007). More precisely: select a particular health condition, e.g., Alzheimer's disease. Denote with $\boldsymbol{f}_0$ the d-dimensional vector of graph data obtained from the patient's fMRI scan via a particular graph construction method, and with $(\boldsymbol{f}_i)$ the graph data of n previous patients with the selected health condition. Then the likelihood that the present patient has the selected health condition is

$$\begin{aligned} &\mathrm{p}[\boldsymbol{f}_0 \mid (\boldsymbol{f}_i), \kappa_0, \boldsymbol{\delta}_0, \nu_0, \boldsymbol{\Delta}_0, M] \equiv \mathrm{p}(\boldsymbol{f}_0 \mid \kappa, \boldsymbol{\delta}, \nu, \boldsymbol{\Delta}, M) \\ &\quad = \mathrm{t}\Big[\boldsymbol{f}_0 \Big|\ \nu - d + 1, \boldsymbol{\delta}, \tfrac{\kappa+1}{\kappa\,(\nu-d+1)}\boldsymbol{\Delta}\Big] \end{aligned} \tag{9}$$

$$\kappa = \kappa_0 + n, \quad \nu = \nu_0 + n, \tag{10}$$

with

$$\begin{aligned} &\boldsymbol{\delta} = \frac{\kappa_0\,\boldsymbol{\delta}_0 + n\overline{\boldsymbol{f}}}{\kappa_0 + n}, \quad \boldsymbol{\Delta} = \boldsymbol{\Delta}_0 + n\ \mathrm{Cov}(\boldsymbol{f}) \\ &\quad + \frac{\kappa_0\, n}{\kappa_0 + n}(\overline{\boldsymbol{f}} - \boldsymbol{\delta}_0)(\overline{\boldsymbol{f}} - \boldsymbol{\delta}_0)^{\intercal}, \end{aligned}$$

where t is a multivariate t distribution with $\nu - d + 1$ degrees of freedom, mean $\boldsymbol{\delta}$, and scale matrix $\frac{\kappa+1}{\kappa\,(\nu-d+1)}\boldsymbol{\Delta}$, and

$$\overline{\boldsymbol{f}} \coloneqq \frac{1}{n}\sum_i \boldsymbol{f}_i, \qquad \mathrm{Cov}(\boldsymbol{f}) \coloneqq \frac{1}{n}\sum_i (\boldsymbol{f}_i - \overline{\boldsymbol{f}})(\boldsymbol{f}_i - \overline{\boldsymbol{f}})^{\intercal} \tag{11}$$

are the empirical mean and covariance matrix of the previous graph data.

The parameters κ_0, ν_0, $\boldsymbol{\delta}_0$, $\boldsymbol{\Delta}_0$ should reflect our initial knowledge of the graph parameters. For the reasons explained above and in section 2.3, we fix one set of values identically for all graph construction methods: $\kappa = 1$, $(\boldsymbol{\delta}_0)_a = 0.5$, $\boldsymbol{\Delta}_0 = 2.5\boldsymbol{I}$, where $\boldsymbol{I}$ is the identity matrix. These values yield an initial distribution (before any data from previous patients) centered on positive values of unit order of magnitude, as all the graph data indeed are for each graph construction method.

5.7. Supportive Evaluation Measures of Graph Construction Methods

5.7.1. Significance Test

We measure the significance level of the mean values of a graph property distribution between pairs of the three healthy conditions (control-AD, control-MCI, MCI-AD) based on the Student's t-test, if variances are equal (F-test), and Welch's t-test otherwise. The underlying null hypothesis is that the means of the two data arrays are assumed to be equal, which is rejected for p-values smaller then 0.05.

5.7.2. Dendrograms of Subject Order

Subjects indexed from 1 to 56 (total number of participants) across all health conditions are ordered according to the mean values of a given graph property distribution. The indices of the ordering (the rank) calculated for each graph construction method is then used in order to construct the dendrogram. In the dendrogram, the Euclidean distance between two indices arrays

is indicated by the height of the top of the U-link linking the two arrays. In addition, arrays with a small distance are clustered together.

5.7.3. Support Vector Machines

For all complete graphs constructed by all different graph construction methods, we apply a support vector classification (Python: *sklearn.svm.SVC*) on each pair of health conditions (control-AD, control-MCI, MCI-AD). Hereby we choose the graph properties such that the performance of the algorithm maximizes. We use the default parameters and do not optimize performance by varying the kernel coefficient or the penalty parameter of the error term.

ETHICS STATEMENT

This study was part of a larger study, which was approved by the local ethics committee, in accordance with the declaration of Helsinki and performed after informed written consent of each participant. Healthy participants were reimbursed. AD patients were not reimbursed since imaging was part of their diagnostic procedures. We did, however, pay for and organize their traveling costs and lunch.

AUTHOR CONTRIBUTIONS

CB constructed the graphs and calculated and analyzed the graph properties. She also applied the statistical analysis, formulated together with PP, to the data. KD, HJ, NR, BvR, JD, OO, K-JL, GF and JK contributed to the conception of the study design and recruited patients. KD, NR, BvR, and JD organized and performed fMRI scanning. KD and HJ applied primary preprocessing to the fMRI data. The manuscript was written by CB, AM, and PP, with additional editing by HJ and JK.

FUNDING

We acknowledge partial support by the Helmholtz Alliance through the Initiative and Networking Fund of the Helmholtz Association and the Helmholtz Portfolio theme Supercomputing and Modeling for the Human Brain and the German Research Foundation (DFG; grant DI 1721/3-1 [KFO219-TP9]). This work was also supported by a DFG individual grant JA 2336/1-1 (HJ) and by a grant of the Marga and Walter Boll Foundation, Kerpen, Germany, to GF and JK.

ACKNOWLEDGMENTS

PP thanks Mari & Miri for continuous encouragement, affection, and support; the kind staff at Iris; and Buster Keaton and Saitama for filling life with awe and inspiration. We are grateful to Simone Buttler for her important help with regard to the calculation of graph properties, and Fahad Khalid and Andreas Müller of the SimLab Neuroscience at the Jülich Supercomputing Center for their expertise in graph visualization. We also acknowledge the support and expert advice by Alper Yegenoglu, Paulina Dabrowska, and Dr. Jyotika Bahuguna. We would like to thank Dr. Gabriele Stoffels, Dr. Christian Filss, and Nathalie Judov for their assistance and generous support. We also acknowledge the technical support and advice of Prof. Dr. Hans Herzog, Dr. Elena Rota Kops, Lutz Tellmann, and Dr. Daniel Pflugfelder. Finally, we are grateful to Kornelia Frey, Suzanne Schaden, and Silke Frensch for their important help in data acquisition. Thanks are extended to Prof. Dr. Nadim Jon Shah for support with the MRI.

SUPPLEMENTARY MATERIAL

The Supplementary Material for this article can be found online at: https://www.frontiersin.org/articles/10.3389/fnins.2018.00528/full#supplementary-material

REFERENCES

Amoroso, N., La Rocca, M., Bruno, S., Maggipinto, T., Monaco, A., Bellotti, R., et al. (2017). Brain structural connectivity atrophy in Alzheimer's disease. *arXiv 1709.02369* [preprint].

Avants, B. B., Tustison, N. J., Song, G., Cook, P. A., Klein, A., and Gee, J. C. (2011). A reproducible evaluation of ANTS similarity metric performance in brain image registration. *Neuroimage* 54, 2033–2044. doi: 10.1016/j.neuroimage.2010.09.025

Bartlett, M. S. (1952). The statistical significance of odd bits of information. *Biometrika* 39, 228–237. doi: 10.2307/2334019

Bassett, D. S., Bullmore, E., Verchinski, B. A., Mattay, V. S., Weinberger, D. R., and Meyer-Lindenberg, A. (2008). Hierarchical organization of human cortical networks in health and schizophrenia. *J. Neurosci* 28, 9239–9248. doi: 10.1523/JNEUROSCI.1929-08.2008

Beckmann, C. F., and Smith, S. M. (2004). Probabilistic independent component analysis for functional magnetic resonance imaging. *IEEE Trans. Med. Imaging* 23, 137–152. doi: 10.1109/TMI.2003.822821

Bernardo, J.-M. (1979). Expected information as expected utility. *Ann. Stat.* 7, 686–690.

Blondel, V. D., Guillaume, J.-L., Lambiotte, R., and Lefebvre, E. (2008). Fast unfolding of communities in large networks. *J. Stat. Mech.* 10:P10008. doi: 10.1088/1742-5468/2008/10/P10008

Bordier, C., Nicolini, C., and Bifone, A. (2017). Graph analysis and modularity of brain functional connectivity networks: searching for the optimal threshold. *Front. Neurosci.* 11:441. doi: 10.3389/fnins.2017.00441

Chicharro, D. (2011). On the spectral formulation of Granger causality. *Biol. Cybern.* 105, 331–347. doi: 10.1007/s00422-011-0469-z

Çiftçi, K. (2011). Minimum spanning tree reflects the alterations of the default mode network during Alzheimer's disease. *Ann. Biomed. Eng.* 39, 1493–1504. doi: 10.1007/s10439-011-0258-9

Collins, D. L., Holmes, C. J., Peters, T. M., and Evans, A. C. (1995). Automatic 3-D model-based neuroanatomical segmentation. *Hum. Brain Mapp.* 3, 190–208. doi: 10.1002/hbm.460030304

da Silva, F. L., Pijn, J. P., and Boeijinga, P. (1989). Interdependence of EEG signals: linear vs. nonlinear associations and the significance of time delays and phase shifts. *Brain Topogr.* 2, 9–18.

Dennis, E. L., and Thompson, P. M. (2014). Functional brain connectivity using fMRI in aging and Alzheimer's disease. *Neuropsychol. Rev.* 24, 49–62. doi: 10.1007/s11065-014-9249-6

Desikan, R. S., Ségonne, F., Fischl, B., Quinn, B. T., Dickerson, B. C., Blacker, D., et al. (2006). An automated labeling system for subdividing the human cerebral cortex on MRI scans into gyral based regions of interest. *Neuroimage* 31, 968–980. doi: 10.1016/j.neuroimage.2006.01.021

Dillen, K. N., Jacobs, H. I. L., Kukolja, J., Richter, N., von Reutern, B., Onur, O. A., et al. (2017). Functional disintegration of the default mode network in prodromal Alzheimer's disease. *J. Alzheimer. Dis.* 59, 169–187. doi: 10.3233/JAD-161120

Gits, H. C. (2016). Relating connectivity and graph analysis to cognitive function in Alzheimer's disease. *Michigan J. Med.* 1, 45–65. doi: 10.3998/mjm.13761231.0001.111

Good, I. J. (1956). The surprise index for the multivariate normal distribution. *Ann. Math. Stat.* 27, 1130–1135.

Good, I. J. (1957a). "The appropriate mathematical tools for describing and measuring uncertainty," in *Good Thinking: The Foundations of Probability and Its Applications*, Chap. 16 (Minneapolis, MN: University of Minnesota Press), 173–177. First publ. 1957.

Good, I. J. (1957b). Corrections to "The surprise index for the multivariate normal distribution." *Ann. Math. Stat.* 28:1055.

Good, I. J. (1983). *Good Thinking: The Foundations of Probability and Its Applications*. Minneapolis, MN: University of Minnesota Press.

Grabner, G., Janke, A. L., Budge, M. M., Smith, D., Pruessner, J., and Collins, D. L. (2006). Symmetric atlasing and model based segmentation: an application to the hippocampus in older adults. *Med. Image Comput. Comput. Assist. Interv* 9, 58–66. doi: 10.1007/11866763_8

Grassberger, P., Schreiber, T., and Schaffrath, C. (1991). Nonlinear time sequence analysis. *Int. J. Bifurcation Chaos* 1, 521–547. doi: 10.1142/S0218127491000403

Guimerá, R., and Nunes Amaral, L. A. (2005). Functional cartography of complex metabolic networks. *Nature* 433, 895–900. doi: 10.1038/nature03288

Hayasaka, S. (2013). Functional connectivity networks with and without global signal correction. *Front. Hum. Neurosci.* 7:880. doi: 10.3389/fnhum.2013.00880

Hoenig, M. C., Bischof, G. N., Seemiller, J., Hammes, J., Kukolja, J., Onur, O. A., et al. (2018). Networks of tau distribution in Alzheimer's disease. *Brain* 141, 568–581. doi: 10.1093/brain/awx353

Jaynes, E. T. (2003). *Probability Theory: The Logic of Science*. Cambridge: Cambridge University Press. Available online at: https://archive.org/details/XQUHIUXHIQUHIQXUIHX2, http://www-biba.inrialpes.fr/Jaynes/prob.html

Jenkinson, M., Bannister, P., Brady, M., and Smith, S. (2002). Improved optimization for the robust and accurate linear registration and motion correction of brain images. *Neuroimage* 17, 825–841. doi: 10.1006/nimg.2002.1132

Jenkinson, M., Beckmann, C. F., Behrens, T. E., Woolrich, M. W., and Smith, S. M. (2012). FSL. *Neuroimage* 62, 782–790. doi: 10.1016/j.neuroimage.2011.09.015

Jenkinson, M., and Smith, S. (2001). A global optimisation method for robust affine registration of brain images. *Med. Image Anal.* 5, 143–156. doi: 10.1016/S1361-8415(01)00036-6

Johnson, K. A., Fox, N. C., Sperling, R. A., and Klunk, W. E. (2012). Brain imaging in Alzheimer disease. *Cold Spring Harb. Perspect. Med.* 2:a006213. doi: 10.1101/cshperspect.a006213

Kalna, G., and Higham, D. J. (2007). A clustering coefficient for weighted networks, with application to gene expression data. *AI Commun.* 20, 263–271.

Keihaninejad, S., Heckemann, R. A., Fagiolo, G., Symms, M. R., Hajnal, J. V., and Hammers, A. (2010). A robust method to estimate the intracranial volume across MRI field strengths (1.5T and 3T). *Neuroimage* 50, 1427–1437. doi: 10.1016/j.neuroimage.2010.01.064

Khazaee, A., Ebrahimzadeh, A., and Babajani-Feremi, A. (2015). Identifying patients with Alzheimer's disease using resting-state fMRI and graph theory. *Clin. Neurophysiol.* 126, 2132–2141. doi: 10.1016/j.clinph.2015.02.060

Khazaee, A., Ebrahimzadeh, A., and Babajani-Feremi, A. (2017). Classification of patients with MCI and AD from healthy controls using directed graph measures of resting-state fMRI. *Behav. Brain Res.* 322, 339–350. doi: 10.1016/j.bbr.2016.06.043

Kim, H., Yoo, K., Na, D. L., Seo, S. W., Jeong, J., and Jeong, Y. (2015). Non-monotonic reorganization of brain networks with Alzheimer's disease progression. *Front. Aging Neurosci.* 7:111. doi: 10.3389/fnagi.2015.00111

Kotz, S., and Nadarajah, S. (2004). *Multivariate t Distributions and Their Applications*. Cambridge: Cambridge University Press.

Kruschwitz, J. D., List, D., Waller, L., Rubinov, M., and Walter, H. (2015). GraphVar: a user-friendly toolbox for comprehensive graph analyses of functional brain connectivity. *J. Neurosci. Methods* 245, 107–115. doi: 10.1016/j.jneumeth.2015.02.021

Leung, K. K., Barnes, J., Modat, M., Ridgway, G. R., Bartlett, J. W., Fox, N. C., et al. (2011). Brain MAPS: an automated, accurate and robust brain extraction technique using a template library. *Neuroimage* 55, 1091–1108. doi: 10.1016/j.neuroimage.2010.12.067

Liu, X., Gerraty, R. T., Grinband, J., Parker, D., and Razlighi, Q. R. (2017). Brain atrophy can introduce age-related differences in BOLD response. *Hum. Brain Mapp.* 38, 3402–3414. doi: 10.1002/hbm.23597

Lu, Y., Jiang, T., and Zang, Y. (2003). Region growing method for the analysis of functional MRI data. *Neuroimage* 20, 455–465. doi: 10.1016/S1053-8119(03)00352-5

Marrelec, G., and Fransson, P. (2011). Assessing the influence of different ROI selection strategies on functional connectivity analyses of fMRI data acquired during steady-state conditions. *PLOS ONE* 6:e14788. doi: 10.1371/journal.pone.0014788

McCarthy, J. (1956). Measures of the value of information. *Proc. Natl. Acad. Sci. U.S.A.* 42, 654–655.

Minka, T. (2001). *Inferring a Gaussian Distribution*. Tech. rep., MIT Media Lab, Cambridge, MA. Available online at: http://research.microsoft.com/en-us/um/people/minka/papers/Firstpubl.1998

Murphy, K., and Fox, M. D. (2017). Towards a consensus regarding global signal regression for resting state functional connectivity MRI. *Neuroimage* 154, 169–173. doi: 10.1016/j.neuroimage.2016.11.052

Murphy, K. P. (2007). *Conjugate Bayesian Analysis of the Gaussian Distribution*. Available online at: http://thaines.com/content/misc/gaussian_conjugate_prior_cheat_sheet.pdf

Nelson, P. T., Alafuzoff, I., Bigio, E. H., Bouras, C., Braak, H., Cairns, N. J., et al. (2012). Correlation of Alzheimer disease neuropathologic changes with cognitive status: a review of the literature. *J. Neuropathol. Exp. Neurol.* 71, 362–381. doi: 10.1097/NEN.0b013e31825018f7

Newman, M. E. J. (2004). Analysis of weighted networks. *Phys. Rev. E* 70:056131. doi: 10.1103/PhysRevE.70.056131

Pagani, M., Giuliani, A., Öberg, J., Chincarini, A., Morbelli, S., Brugnolo, A., et al. (2016). Predicting the transition from normal aging to Alzheimer's disease: a statistical mechanistic evaluation of FDG-PET data. *Neuroimage* 141, 282–290. doi: 10.1016/j.neuroimage.2016.07.043

Pagani, M., Giuliani, A., Öberg, J., De Carli, F., Morbelli, S., Girtler, N., et al. (2017). Progressive disintegration of brain networking from normal aging to Alzheimer disease: analysis of independent components of 18F-FDG PET data. *J. Nucl. Med.* 58, 1132–1139. doi: 10.2967/jnumed.116.184309

Pedregosa, F., Varoquaux, G., Gramfort, A., Michel, V., Thirion, B., Grisel, O., et al. (2011). Scikit-learn: machine learning in Python. *J. Mach. Learn. Res.* 12, 2825–2830.

Pereda, E., Quiroga, R. Q., and Bhattacharya, J. (2005). Nonlinear multivariate analysis of neurophysiological signals. *Prog. Neurobiol.* 77, 1–37. doi: 10.1016/j.pneurobio.2005.10.003

Popescu, V., Battaglini, M., Hoogstrate, W. S., Verfaillie, S. C. J., Sluimer, I. C., van Schijndel R. A., et al. (2012). Optimizing parameter choice for FSL-Brain Extraction Tool (BET) on 3D T1 images in multiple sclerosis. *Neuroimage* 61, 1484–1494. doi: 10.1016/j.neuroimage.2012.03.074

Porta Mana, P. G. L., Bachmann, C., and Morrison, A. (2018). Inferring health conditions from fMRI-graph data. *Open Science Framework. arXiv:1803.02626* [preprint]. doi: 10.31219/osf.io/r2huz

Rivest, R. L., Leiserson, C. E., and Cormen, T. H. (2000). *Introduction to Algorithms (MIT Electrical Engineering and Computer Science Series.)* Cambridge, MA: MIT Press.

Rodgers, J. L., and Nicewander, W. A. (1988). Thirteen ways to look at the correlation coefficient. *Am. Stat.* 42, 59–66. doi: 10.1080/00031305.1988.10475524

Sanz-Arigita, E. J., Schoonheim, M. M., Damoiseaux, J. S., Rombouts, S. A., Maris, E., Barkhof, F., et al. (2010). Loss of "small-world" networks in Alzheimer's disease: graph analysis of fMRI resting-state functional connectivity. *PLOS ONE* 5:e13788. doi: 10.1371/journal.pone.0013788

Schaeffer, S. E. (2007). Graph clustering. *Comput. Sci. Rev.* 1, 27–64. doi: 10.1016/j.cosrev.2007.05.001

Schreiber, T. (2000). Measuring information transfer. *Phys. Rev. Lett.* 85, 461–464. doi: 10.1103/PhysRevLett.85.461

Schroeter, M. L., Stein, T., Maslowski, N., and Neumann, J. (2009). Neural correlates of Alzheimer's disease and mild cognitive impairment: a systematic and quantitative meta-analysis involving 1,351 patients. *Neuroimage* 47, 1196–1206. doi: 10.1016/j.neuroimage.2009.05.037

Schwarz, A. J., and McGonigle, J. (2011). Negative edges and soft thresholding in complex network analysis of resting state functional connectivity data. *Neuroimage* 55, 1032–1146. doi: 10.1016/j.neuroimage.2010.12.047

Shannon, C. E. (1948). A mathematical theory of communication. *Bell Syst. Tech. J.* 27, 379–423, 623–656.

Smith, S. M. (2002). Fast robust automated brain extraction. *Hum. Brain Mapp.* 17, 143–155. doi: 10.1002/hbm.10062

Sox, H. C., Higgins, M. C., and Owens, D. K. (2013). *Medical Decision Making, 2nd Edn*. New York, NY: Wiley.

Sperling, R. A., Aisen, P. S., Beckett, L. A., Bennett, D. A., Craft, S., Fagan, A. M., et al. (2011). Toward defining the preclinical stages of Alzheimer's disease: recommendations from the National Institute on Aging-Alzheimer's Association workgroups on diagnostic guidelines for Alzheimer's disease. *Alzheimer. Dement.* 7, 280–292. doi: 10.1016/j.jalz.2011.03.003

Supekar, K., Menon, V., Rubin, D., Musen, M., and Greicius, M. D. (2008). Network analysis of intrinsic functional brain connectivity in Alzheimer's disease. *PLOS Comput. Biol.* 4:e1000100. doi: 10.1371/journal.pcbi.1000100

Telesford, Q. K., Morgan, A. R., Hayasaka, S., Simpson, S. L., Barret, W., Kraft, R. A., et al. (2010). Reproducibility of graph metrics in fMRI networks. *Front. Neuroinformat.* 4:117. doi: 10.3389/fninf.2010.00117

Thirion, B., Varoquaux, G., Dohmatob, E., and Poline, J.-B. (2014). Which fMRI clustering gives good brain parcellations? *Front. Neurosci.* 8:167. doi: 10.3389/fnins.2014.00167

Tzourio-Mazoyer, N., Landeau, B., Papathanassiou, D., Crivello, F., Etard, O., Delcroix, N., et al. (2002). Automated anatomical labeling of activations in SPM using a macroscopic anatomical parcellation of the MNI MRI single-subject brain. *Neuroimage* 15, 273–289. doi: 10.1006/nimg.2001.0978

Wang, H. E., Bénar, C. G., Quilichini, P. P., Friston, K. J., Jirsa, V. K., and Bernard, C. (2014). A systematic framework for functional connectivity measures. *Front. Neurosci.* 8:405. doi: 10.3389/fnins.2014.00405

Wang, Z., Zhang, M., Han, Y., Song, H., Guo, R., and Li, K. (2016). Differentially disrupted functional connectivity of the subregions of the amygdala in Alzheimer's disease. *J. X-Ray Sci. Technol.* 24, 329–342. doi: 10.3233/XST-160556

Woolrich, M. W., Jbabdi, S., Patenaude, B., Chappell, M., Makni, S., Behrens, T., et al. (2009). Bayesian analysis of neuroimaging data in FSL. *Neuroimage* 45, S173–S186. doi: 10.1016/j.neuroimage.2008.10.055

Xia, M., Wang, Z., Dai, Z., Liang, X., Song, H., Shu, N., et al. (2014). Differentially disrupted functional connectivity in posteromedial cortical subregions in Alzheimer's disease. *J. Alzheimers Dis.* 39, 527–543. doi: 10.3233/JAD-131583

Zhang, B., and Horvath, S. (2005). A general framework for weighted gene co-expression network analysis. *Stat. Appl. Genet. Mol. Biol.* 4:Article17. doi: 10.2202/1544-6115.1128

Zhang, Y., Brady, M., and Smith, S. (2001). Segmentation of brain MR images through a hidden Markov random field model and the expectation-maximization algorithm. *IEEE Trans. Med. Imaging* 20, 45–57. doi: 10.1109/42.906424

Zhao, X., Lui, Y., Wang, X., Liu, B., Xi, Q., Guo, Q., et al. (2012). Disrupted small-world brain networks in moderate Alzheimer's disease: a resting-state fMRI study. *PLOS ONE* 7:e33540. doi: 10.1371/journal.pone.0033540

Conflict of Interest Statement: The authors declare that the research was conducted in the absence of any commercial or financial relationships that could be construed as a potential conflict of interest.

Copyright © 2018 Bachmann, Jacobs, Porta Mana, Dillen, Richter, von Reutern, Dronse, Onur, Langen, Fink, Kukolja and Morrison. This is an open-access article distributed under the terms of the Creative Commons Attribution License (CC BY). The use, distribution or reproduction in other forums is permitted, provided the original author(s) and the copyright owner(s) are credited and that the original publication in this journal is cited, in accordance with accepted academic practice. No use, distribution or reproduction is permitted which does not comply with these terms.

frontiers in Neuroinformatics

ORIGINAL RESEARCH
published: 07 September 2018
doi: 10.3389/fninf.2018.00060

Analysis of Alzheimer's Disease Based on the Random Neural Network Cluster in fMRI

Xia-an Bi, Qin Jiang, Qi Sun, Qing Shu and Yingchao Liu*

College of Information Science and Engineering, Hunan Normal University, Changsha, China

As Alzheimer's disease (AD) is featured with degeneration and irreversibility, the diagnosis of AD at early stage is important. In recent years, some researchers have tried to apply neural network (NN) to classify AD patients from healthy controls (HC) based on functional MRI (fMRI) data. But most study focus on a single NN and the classification accuracy was not high. Therefore, this paper used the random neural network cluster which was composed of multiple NNs to improve classification performance. Sixty one subjects (25 AD and 36 HC) were acquired from the Alzheimer's Disease Neuroimaging Initiative (ADNI) dataset. This method not only could be used in the classification, but also could be used for feature selection. Firstly, we chose Elman NN from five types of NNs as the optimal base classifier of random neural network cluster based on the results of feature selection, and the accuracies of the random Elman neural network cluster could reach to 92.31% which was the highest and stable. Then we used the random Elman neural network cluster to select significant features and these features could be used to find out the abnormal regions. Finally, we found out 23 abnormal regions such as the precentral gyrus, the frontal gyrus and supplementary motor area. These results fully show that the random neural network cluster is worthwhile and meaningful for the diagnosis of AD.

Keywords: random neural network cluster, fMRI, classification, Alzheimer's disease, functional connectivity

OPEN ACCESS

Edited by:
Mohammad Amjad Kamal,
King Abdulaziz University,
Saudi Arabia

Reviewed by:
Rifai Chai,
University of Technology Sydney,
Australia
Na Li,
Central South University, China

****Correspondence:***
Xia-an Bi
bixiaan@hnu.edu.cn

Received: *03 February 2018*
Accepted: *22 August 2018*
Published: *07 September 2018*

Citation:
Bi X-a, Jiang Q, Sun Q, Shu Q and Liu Y (2018) Analysis of Alzheimer's Disease Based on the Random Neural Network Cluster in fMRI. Front. Neuroinform. 12:60. doi: 10.3389/fninf.2018.00060

INTRODUCTION

Alzheimer's disease (AD) is degenerative and irreversible which results from the cognitive decline. The progress of AD increases with age and the disease easily triggers the other psychiatric diseases, and eventually causing dementia. In 2006, the number of AD patients is 26.6 million all around the world and the number would be quadruple by 2050. Therefore, it is meaningful for clinician to track its progression and diagnose the disease. Currently, there have been many different neuroimaging techniques which can be applied to diagnose AD, such as ElectroEncephaloGram (EEG) (Engels et al., 2015), Single Photon Emission Computed Tomography (SPECT) (Prosser et al., 2015), Positron Emission Tomography (PET) (Pagani et al., 2017), Magnetoencephalographic (MEG) (Engels et al., 2016), and functional magnetic resonance imaging (fMRI) (Griffanti et al., 2015). Among these techniques, fMRI is widely used in the diagnosis of AD, because it adopts a non-invasive way and could be used to find the differences of brain regions between AD and healthy controls (HC) (Challis et al., 2015).

Machine learning is a method of pattern recognition and has been used for the study of AD in recent years (Moradi et al., 2015; Khazaee et al., 2016). Among many machine learning methods,

artificial neural network (ANN) is a useful classification method which evolves from human brain (Er et al., 2016). Several previous studies showed that neural network (NN) was able to be applied to diagnose neurological disease. Suk et al. (2016) proposed a method that combined deep learning and state-space model to classify Mild Cognitive Impairment (MCI) patients from HC, and the accuracy was 72.58%. Gao et al. (2017) employed an advanced convolution neural network (CNN) with 2D and 3D to diagnose AD, and the average accuracy reached to 87.6%. Ortiz et al. (2016) used deep learning architectures to classify AD patients from HC, and the accuracy approximately reached to 90%. Ortiz et al. (2013) used Learning Vector Quantization (LVQ) algorithm to classify AD patients from HC, and the accuracy was close to 90%. Luo et al. (2017) applied CNN to classify AD patients from HC, and the sensitivity and specificity of classification was 1 and 0.93 respectively. Suk et al. (2014) used deep learning to classify AD patients from HC, and the accuracy was close to 93.35%.

In existing studies, a single NN is often used to classify patients with neurological diseases and HC, and the accuracy of classification is considerable which indicates that NN is a powerful classification model (Hirschauer et al., 2015; Anthimopoulos et al., 2016). As the features of neuroimaging data are characterized by high dimension, significant information of original variables would be lost in the process of dimensionality reduction in traditional methods such as principal component analysis, local linear embedding and linear discriminate analysis (Mattioni and Jurs, 2003; McKeown et al., 2007; Mannfolk et al., 2010). In this paper, the method of the random neural network cluster is proposed to classify AD from HC. This method not only could be used in the classification, but also could be used for feature selection. The procedure of this method is as follows. Firstly, we chose Elman NN as the optimal base classifier from five types of neural networks [Back Propagation (BP) NN, Elman NN, PNN, Learning Vector Quantization (LVQ) NN and Competitive NN] based on the results of feature selection, and the accuracies of the random Elman neural network cluster could reach to 92.31% which is the highest and stable. Then we used the random Elman neural network cluster to select significant features and these features could be used to find out the abnormal regions. Finally, we found out 23 abnormal regions, such as the precentral gyrus, the frontal gyrus and supplementary motor area. These results fully show that the random neural network cluster is worthwhile and meaningful for the diagnosis of AD.

MATERIALS AND METHODS

Subjects

The experimental data was collected from the Alzheimer's Disease Neuroimaging Initiative (ADNI)[1] dataset which includes a variety of neuroimaging data. The ADNI study was approved by Institutional Review Board (IRB) of each participating site. All ADNI subjects together with their legal representatives should have written informed consent before collecting clinical, genetic and imaging data. The following two criteria need to meet when selecting data. One criterion is that the selected data should be resting-state fMRI data. Another criterion is that the selected data should have mini-mental state examination (MMSE) and clinical dementia rating (CDR) scores, and this criterion ensures that the selected data is homologous. Finally, 61 subjects were selected which consisted of 25 AD patients and 36 HC.

[1]http://adni.loni.usc.edu/

Data Collection and Preprocessing

Scanning images were acquired on a Philips Medical Systems 3 Tesla MRI scanner. Acquisition parameters included: pulse sequence = GR, *TR* = 3,000 ms, *TE* = 30 ms, matrix = 64*64, slice thickness = 3.3 mm, slice number = 48, flip angle = 80°.

To decrease the influence of signal-to-noise ratio of the fMRI images, the selected data should be preprocessed. The data was preprocessed based on the Data Processing Assistant for Resting-State fMRI (DPARSF) software (Chao-Gan and Yu-Feng, 2010; Wang et al., 2013). The process of the data preprocessing included: converting DICOM format into NIFTI format; removing first 10 time points; slicing timing (Sarraf et al., 2016); realigning (Jenkinson et al., 2002); normalizating images into the echo planar imaging (EPI) template (Misaki et al., 2010); temporal smoothing; removing the effect of low-level (<0.01 HZ) and high-level (>0.08 HZ) noise by a high-pass temporal filtering (Challis et al., 2015); removing covariates such as the whole brain signal and cerebrospinal fluid signal.

Functional Connectivity of Brain

After the preprocessing steps, the analysis of the functional connectivity of brain was followed. In this paper, we chose functional connectivity as the sample feature. The extraction of the functional connectivity is as follows. Firstly, the images of brain were divided into 90 regions defined by Automated Anatomical Labeling (AAL) brain atlas (Rolls et al., 2015). Secondly, the time series of each region were extracted. Thirdly, the Pearson correlation coefficient between two separated brain regions could be defined as the functional connectivity (Friston et al., 1993). Finally, 4,005 ($90 \times 89/2$) functional connectivity of each subject were taken as their features.

The Random Neural Network Cluster

The 4,005 functional connectivity belongs to the high-dimensional feature which causes the problems of computation difficulty and dimensions of disaster. Moreover, the high-dimensional features are likely to result in numerous redundant and irrelevant features which may decrease the classification performance. Therefore, the irrelevant features are needed to be removed by feature selection (Azar and Hassanien, 2015).

There are many methods of feature selection, such as principal component analysis, local linear embedding and linear discriminate analysis. However, in these methods, the process of selecting features may cause the loss of the original information, and the classification performance may be unsatisfactory (Zhou et al., 2015; Jolliffe and Cadima, 2016; Alam and Kwon, 2017).

To solve the problem above, this paper proposes the random neural network cluster by randomly selecting samples and features. The random neural network cluster could be used

to classify AD patients from HC and select features. In addition, the new method could achieve the purpose of reducing dimensionality, avoid losing significant information and improve classification performance.

The Design and Classification Accuracy of the Random Neural Network Cluster

The basic thought of the random neural network cluster is ensemble learning whose basic classifier is neural network. The detailed process of establishing the random neural network cluster is as follows. Firstly, the sample dataset D is randomly divided into a training set N_1 and a test set N_2, where $D = N_1 + N_2$. The real label of HC and AD is +1 and −1 respectively. Secondly, we randomly select n samples from the training set and m features from the 4,005 features. Thirdly, the selected samples and features are used to establish a single NN and the process of the second and third step is repeated for k times. Thus, k NNs are obtained which construct the random neural network cluster. It can be seen from this process that the method and the conventional process are essentially not the same in essence. **Figure 1** shows the formation of the random neural network cluster.

When a new sample enters the random neural network cluster, we could obtain k class labels from k NNs and the majority of class label is made as the predicted label of the new sample. Similarly, we could get the label of each sample in the test set N_2. Then the predicted label is compared with the real label to judge whether they are consistent, and we assume C as the number of consistent situations. The accuracy of the random neural network cluster equals to C/N_2.

Extracting Features From the Random Neural Network Cluster

As the features are randomly selected, the NNs constructed by these features have different characteristics. In this paper, the accuracy of each NN is used to evaluate the significance of selected features. The features that make significant contributions to the accuracy of the NN are called the "significant features". The process of extracting significant features is as follows.

Firstly, the test samples are used to obtain the accuracy of each NN in the random neural network cluster. If the accuracy of a NN is high, the corresponding features are significant. Next, the features in each NN with high accuracy are extracted to form a feature matrix. Finally, we count the frequency of each feature in the feature matrix, and extract the features with high frequency which are called as "significant features." **Figure 2** shows the process of selecting "significant features." The significant features tremendously contribute to the accuracy of a NN, thus they also make great contributions to the accuracy of the random neural network cluster. In this paper, we use the significant features to find the difference between AD patients and HC.

The Abnormal Brain Regions

As mentioned above, the significant features make great contributions to the accuracy of the random neural network cluster, thus we could find the difference between AD and HC through these significant features. In this paper, the significant features are regarded as the abnormal functional connectivity. As the functional connectivity is defined as the relationship of two brain regions, the extracted significant features could be used to find the abnormal brain regions between AD and HC. In order to estimate the abnormal degree of a brain region, the number of features related to a certain region is considered as the weight. When there is no functional connectivity related to a certain brain region, the weight of the region is 0. When the weight is greater, the abnormal degree of the brain region is higher.

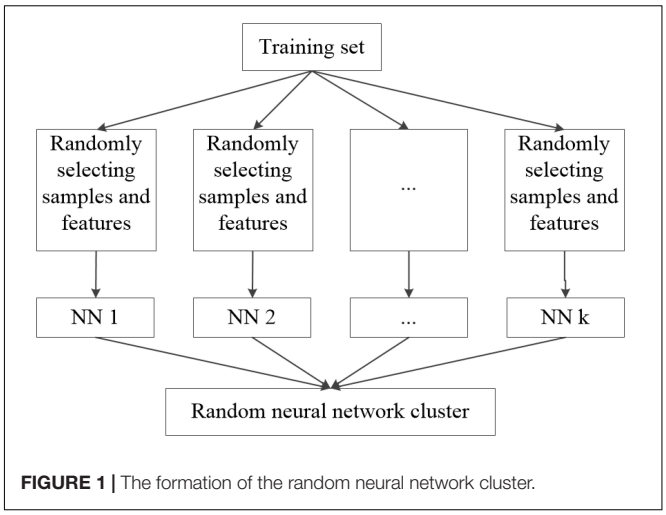


FIGURE 1 | The formation of the random neural network cluster.

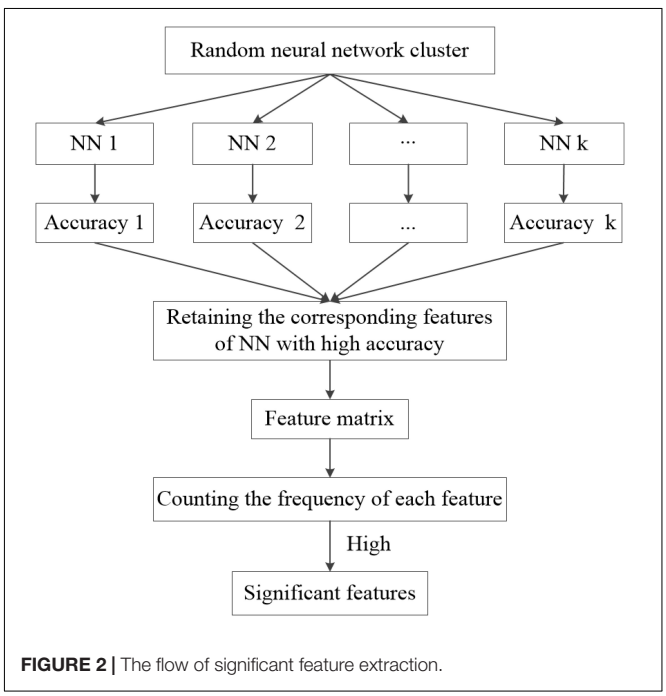


FIGURE 2 | The flow of significant feature extraction.

Experiment Design

The process of the experiment involves six steps in this paper.

Step 1. Building the random neural network cluster. Firstly, 61 subjects are divided into a training set and a test set according

to the proportion of 8:2. Thus, the number of training samples and test samples is 48 and 13 respectively. Then, 45 subjects are randomly selected from 48 training samples and 120 features are randomly selected from 4,005 features to build a NN. Similarly, we build 1,000 NNs to construct the random neural network cluster. The result of the random neural network cluster is calculated by using neural network toolbox.

Step 2. Selecting significant NNs. We select the NNs whose accuracy is >0.6 from the 1,000 NNs and call these NNs as significant NNs.

Step 3. Selecting significant features. The features corresponding to the significant NNs form the feature matrix. Then we count the frequency of each feature, and sort the features with a descending order. Finally, we retain the first 240 features which are regarded as the original significant features.

Step 4. Determining the optimal number of the significant features. We change the number of original significant features from 140 to 240 features with a step of 10 as the new significant features, thus there are 11 types of numbers of new significant features. Then we select 120 features from the new significant features to construct a NN. We select 120 features from the original significant features, and change the number of significant features from 140 to 240 features with a step of 10. Thus, we could obtain 11 random neural network clusters. The number of the significant features corresponding to the random neural network cluster with highest accuracy is the optimal number.

Step 5. We repeat the step1-step 4 by using five types of NNs. They are BP NN, Elman NN, PNN, LVQ NN, and Competitive NN. Then we choose one of them as the best base classifier who has the highest accuracy in step 4.

Step 6. Finding abnormal brain regions through the significant features in step 4 based on the best base classifier.

RESULTS

The Demographic Information of Participants

In this study, the selected 61 subjects include 25 AD patients and 36 HC. The gender and age difference between the AD group and HC group data are examined by two-sample *t*-test and chi-square test respectively. The result is shown in **Table 1**. It is referred that the two groups have no statistical significance in the gender and the age.

Classification Results

In this study, five different types of NNs are applied to construct five different types of random neural network clusters. The number of significant features in each random neural network cluster changes from 140 to 240 and the step is 10. Therefore, we can obtain 11 results for each type of random neural network cluster, and their parameters have been made appropriate adjustments to get better results. The accuracies of five types of random neural network clusters are shown in **Figure 3**. It is referred that the accuracies of random Competitive neural network cluster are not stable; the accuracies of random Elman neural network cluster and random Probabilistic neural network cluster are high, and their highest accuracy reaches to 92.31%; the accuracies of random BP neural network cluster and random LVQ neural network cluster are lower than the random Elman neural network cluster. The accuracies of the random neural network cluster changes when the number of features changes. As the highest accuracies of the random Elman neural network cluster are relatively stable and high, this paper chooses Elman neural network as the best base classifier. From **Figure 3** we can learn that when the number of significant features is 180, the accuracy is the highest. Therefore, 180 is the optimal number of significant features.

In order to better compare the performances of the random neural network cluster and a single NN, we display the corresponding 1,000 NNs' accuracies of five types of random neural network clusters in the **Figure 4**. From **Figures 3**, **4** we could learn that the accuracy of random neural network cluster is higher and more stable than a single NN except for the random Competitive neural network cluster. In addition, we also show the training errors, test errors and running time of five types of random neural network clusters in **Table 2**.

The Abnormal Brain Regions

The first 180 features constitute the optimal feature set which is used to find the abnormal brain regions between AD patients and HC. **Table 3** shows the abnormal brain regions with higher weight, their abbreviation and volume. **Figure 5** shows the abnormal degree of brain regions by using the Brain-NetViewer[2].

[2]http://www.nitrc.org/projects/bnv/

TABLE 1 | The information of participants.

Variables (Mean ± *SD*)	AD (*n* = 25)	HC (*n* = 36)	*P*-value
Gender(male/female)	12/13	20/16	0.784
Age	74.59 ± 7.03	77.00 ± 6.61	0.177

AD, Alzheimer's disease; HC, Healthy Control.

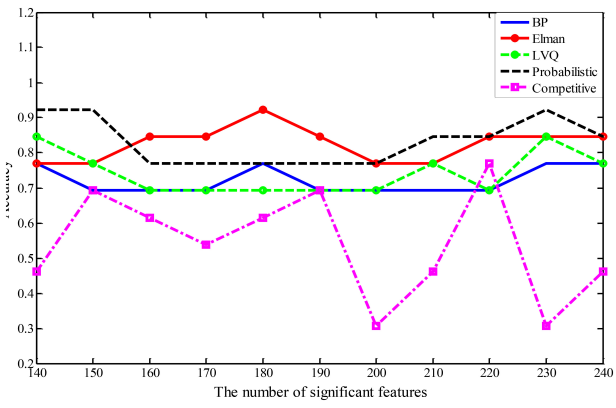


FIGURE 3 | The accuracies of five different types of random neural network clusters.

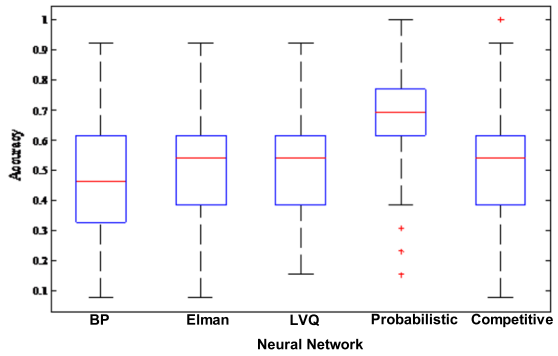


FIGURE 4 | The corresponding 1,000 NNs' accuracies of five types of random neural network clusters.

The node represents the brain region. The size of a node represents the weight of the brain region and it also indicates the abnormal degree of the brain region.

In this paper, we focus on the brain region whose weight is >17. **Figure 6** shows the functional connectivity between the 23 brain regions in the optimal feature set. **Figure 7** shows the functional connectivity between PreCG and other brain regions. The node in **Figures 6**, **7** also represents the brain region and the size of a node represents the weight of the brain region. Besides, the line represents the functional connectivity between two brain regions.

DISCUSSION

Classification Performance

A number of researchers have tried to classify and diagnose AD patients from HC in the past few years. For instance, Khazaee et al. (2016) applied machine learning methods to classify MCI patients, AD patients and HC, and the accuracy of AD and HC is 72%. Kim et al. (2016) applied DNN to classify schizophrenia (SZ) patients and HC based on fMRI image, and the accuracy is 85.8%. Zhang et al. (2014) proposed a kernel support vector machine decision tree (kSVM-DT) to classify MCI patients, AD patients and HC based on the MRI data, and the accuracy of AD and HC is 96%. However, there were several disadvantages in these studies. For instance, as the features of neuroimaging data are characterized by high dimension, significant information of original variables would be lost in the process of dimensionality reduction in traditional methods.

In this paper, the new method was proposed to avoid the loss of information and improve classification performance. We used five different types of NNs as the base classifier to build five different types of random neural network clusters. In the five types of random neural network clusters, the classification accuracies of the random Elman neural network cluster and the random PNN cluster could reach to 92.3%. As the resting-state fMRI data dynamically changes in a period of time and the Elman NN is able to deal with the time and spatial domain data, the Elman NN is more suitable for the fMRI data. The accuracies of the random Probabilistic neural network cluster could also reach to 92.3%, but the running time of the PNN is long which makes it not suitable for the base classifier of the random neural network cluster. Thus, we finally choose the random Elman neural network cluster as the best base classifier. To solve the problems caused by the high-dimensional data, the traditional methods suffer from the loss of some information in the process of reducing dimensionality. In this paper, we proposed a random neural network cluster which could be a good solution in dealing with the calculation of large samples and high-dimensional data. Moreover, the highest accuracies of the random Elman neural network cluster could reach to 92.3%. Therefore, this method could process high-dimensional data without information loss and improve classification performance.

The basic classifier used in this paper is the neural network. This classifier is indeed an existing classifier, and it is not the innovation point of this paper. The innovation of this article is the integrated cluster, which is the innovation in structure.

This paper researches on fMRI image, there is no innovation in the classification indicators of this article. But the classification indicators have been used in research. We used the random neural network cluster to classify the subjects and feature selection, and we got good results. That is the innovation in application.

TABLE 2 | The errors and running time of five types of random neural network clusters.

Base classifier (Mean ± *SD*)	Training errors	Test errors	Time (hour)
BP NN	0.2764 ± 0.0375	0.2797 ± 0.0388	2
Probabilistic NN	0.1709 ± 0.0712	0.1678 ± 0.0672	10
Elman NN	0.1782 ± 0.0519	0.1748 ± 0.0497	12
LVQ NN	0.2645 ± 0.0604	0.2587 ± 0.0622	48
Competitive NN	0.4627 ± 0.1532	0.4615 ± 0.1538	18

The Additional Details of the Random Neural Network Cluster

In the part of method, we have introduced many elementary details in our method and in this part we would introduce some additional details.

In order to make the random neural network cluster less complex, each NN occupies the same weight in the random neural network cluster. When determining the label of a new sample, each NN in the random neural network cluster predicts the label of the sample. The majority of class label is made as the predicted label of the sample which is equivalent to that the weight of each NN is the same. From **Figures 3**, **4** we could learn that the accuracy of a single NN is lower than the accuracy of the random neural network cluster. Moreover, when the number of significant features changes, the accuracies of five types of random neural network clusters are high and stable except for the random Competitive neural network cluster. This fully demonstrates that the robustness of the random neural network cluster is good.

TABLE 3 | Abnormal brain regions.

Regions	Abbreviation	Volume	Weight
The precentral gyrus	PreCG.L	[−39 −6 51]	19
The middle frontal gyrus	MFG.L	[−33 33 35]	
The olfactory cortex	OLF.L	[−8 15 −11]	
The orbital part of superior frontal gyrus	ORBsup.R	[18 48 −14]	18
The triangular part of inferior frontal gyrus	IFGtriang.L	[−46 30 14]	
The supplementary motor area	SMA.L	(−5 5 61)	
The orbital part of superior frontal gyrus	ORBsup.L	[−17 47 −13]	17
The orbital part of middle frontal gyrus	ORBmid.L	[−31 50 −10]	
The precentral gyrus	PreCG.R	[41 −8 52]	16
The dorsolateral of superior frontal gyrus	SFGdor.R	[22 31 44]	
The orbital part of middle frontal gyrus	ORBmid.R	[33 53 −11]	
The orbital part of Inferior frontal gyrus	ORBinf.L	[−36 31 −12]	
The orbital part of Inferior frontal gyrus	ORBinf.R	[41 32 −12]	
The olfactory cortex	OLF.R	[10 16 −11]	
The middle frontal gyrus	MFG.R	[38 33 34]	15
The rolandic operculum	ROL.L	[−47 −8 14]	
The rolandic operculum	ROL.R	[53 −6 15]	
The dorsolateral of superior frontal gyrus	SFGdor.L	[−18 35 42]	14
The opercular part of inferior frontal gyrus	IFGoperc.L	[−48 1319]	
The opercular part of inferior frontal gyrus	IFGoperc.R	[50 15 21]	
The triangular part of inferior frontal gyrus	IFGtriang.R	[50 30 14]	
The supplementary motor area	SMA.R	[9 0 62]	
The medial of superior frontal gyrus	SFGmed.L	[−549 31]	

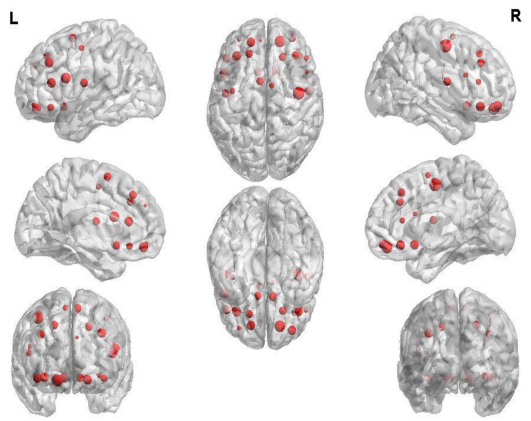


FIGURE 5 | The weight of brain regions.

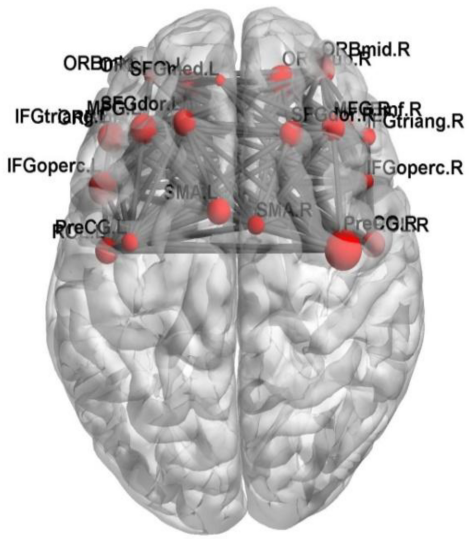


FIGURE 6 | The functional connectivity between the 23 brain regions.

In terms of the complexity of random neural network cluster, it is mainly reflected in the following two aspects. One aspect is that the number of base classifiers is large which makes the process of constructing a random neural network cluster complex. Another aspect is that we need to construct multiple random neural network clusters during finding the optimal feature set which also makes the method complex.

There are two types of parameters in our method. One type is the parameters of the random neural network cluster which are decided by the accuracy of the random neural network cluster through hundreds of experiments. Another type is the parameters of the NN which are decided by the neural network toolbox that automatically selects the optimal parameters.

The random neural network cluster is constructed by the training set and the performance is tested by the test set. The experimental results show that the random neural network cluster not only performs well on the training set, but also performs well on the test set. This fully demonstrates that

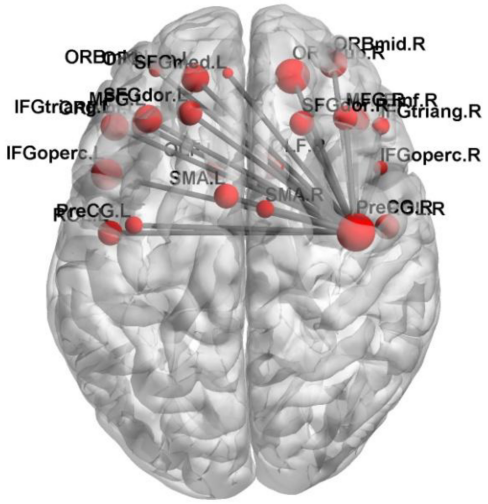


FIGURE 7 | The functional connectivity between PreCG and other brain regions.

the overfitting does not exist in the random neural network cluster.

Abnormal Brain Region Analysis

The functional connectivity differences between AD and HC could be used to find out the abnormal brain regions and we finally detected 23 abnormal brain regions between AD and HC. They are the PreCG, the OLF, the ORBsup, the IFGtriang, SMA, the SFGdor, the ORBmid, the ORBinf, the SFGmed.L, the IFGoperc, the ROL, and the MFG.

Previous studies have concluded that these abnormal brain regions are associated with AD patients. Khazaee et al. (2015) found that the lingual gyrus, the occipital gyrus and the superior frontal gyrus are abnormal brain regions in AD patients. Agosta et al. (2012) pointed out that the functional connectivity changed in the default mode network (DMN) and frontal networks in AD patients. Wang et al. (2007) discovered the decreased abnormal functional connectivity in the prefrontal and parietal lobes, meanwhile the increased abnormal functional connectivity in the occipital lobe in AD patients. Greicius et al. (2004) found that AD patients showed less deactivation in the anterior frontal, precuneus and posterior cingulate cortex. He et al. (2007) concluded that regional coherence of AD patients significantly decreased in the posterior cingulate cortex/precuneus. Binnewijzend et al. (2012) declared that the abnormal brain regions of AD patients located in the precuneus and posterior cingulate cortex. Golby et al. (2005) concluded that impaired activation changed in the temporal lobe and fusiform regions in AD patients. Grossman et al. (2003) found the activation of AD patients in the left poster lateral temporal and inferior parietal cortex. It is referred that our results are consistent with previous studies. In this paper, we focus on the precentral gyrus and the frontal gyrus which have larger weights.

Precentral Gyrus (PreCG)

The PreCG has the greatest weight in the abnormal brain regions. It is referred that the PreCG makes a great contribution to classify AD and HC in the random Elman neural network cluster. The PreCG locates in the primary motor area (Hopkins et al., 2017), and the superior part of PreCG is responsible for motor hand function (Yousry et al., 1997; Nebel et al., 2014).

Existing studies have found that the PreCG is abnormal in AD patients. Kang et al. (2013) showed that AD patients performed significant cortical thinning in superior and medial frontal gyrus, left precentral gyrus, postcentral gyrus, paracentral lobule, precuneus and superior parietal lobule. Bi et al. (2018) proposed a method of random support vector machine cluster to diagnose AD, and found out several disorder regions including inferior frontal gyrus, superior frontal gyrus, precentral gyrus and cingulate cortex. Zhang et al. (2015) pointed out that the middle occipital gyrus, the postcentral gyrus, the PreCG and precuneus were important in diagnosing AD. Brickman et al. (2015) discovered that the PreCG and right middle frontal gyrus were abnormal in AD patients based on T2-weighted MRI. Dani et al. (2017) used white matter hypointensity (WMH) volume to diagnose AD based on MRI and PET data, and they found out the difference between the PreCG, and the right medial and anterior part of orbital gyrus.

The abnormal functional connectivity between PreCG and other brain regions may lead to the physical movement dysfunction in AD patients. The above results revealed that PreCG may be a clinical diagnosis of AD in future.

Frontal Gyrus (FG)

The FG had a relatively higher weight in the abnormal regions. It is referred that the FG makes a great contribution to classify AD and HC in the random Elman neural network cluster. The left of inferior frontal gyrus is associated with language (Costafreda et al., 2006). The superior frontal gyrus contributes to higher cognitive functions and particularly the learning and working memory (WM) (Boisgueheneuc et al., 2006; Carter et al., 2006). Eliasova et al. (2014) explored that the improvement of attention and psychomotor speed resulted from the abnormity of the right IFG in AD patients.

Existing studies have found that the FG is abnormal in AD patients. Schultz et al. (2015) found out several abnormal brain regions in AD patients including the hippocampus, the posterior cingulate, the anterior cingulate and the middle frontal gyrus. Griffanti et al. (2016) pointed out that there was difference in orbito frontal network between AD patient and HC. Yetkin et al. (2006) evaluated brain activation in AD patients and HC based on fMRI while performing a WM task and found that AD group showed more activation in the right superior frontal gyrus, bilateral middle temporal, middle frontal, anterior cingulate and fusiform gyri. Karas et al. (2007) used voxel-based morphometry (VBM) to examine AD patients, and they found out several disorder regions including the left superior and inferior temporal gyrus, and the left superior frontal gyrus. Our experiment results are consistent with the existing studies.

The abnormal functional connectivity between FG and other brain regions may lead to the memory dysfunction in

AD patients. This abnormal brain region has significant effect on the identification of potentially effective biomarkers for the diagnosis of AD.

In this paper, the random neural network cluster is proposed to classify AD patients and HC and the abnormal brain regions are found out on the basis of fMRI data. Moreover, these findings suggest that the random neural network cluster might be an appropriate approach for diagnosing AD. This new method has some advantages. Firstly, the NNs make different contributions to the random neural network cluster which could make full use of each NN's characteristics, thus it could avoid losing information. Secondly, it is able to effectively deal with a large dataset even when there is many missing data. Finally, it is also able to select significant features from high-dimensional features. The new method presents a good classification performance with accuracy of 92.3% and detects several abnormal brain regions which would have influence in diagnosing AD. However, it has several limitations. Firstly, this paper only used the fMRI data and the future studies could integrate other imaging data to obtain comprehensive brain activity. Secondly, this paper only studied the brain activity, and the future studies could combine the brain and cerebellum activity. Thirdly, this paper only studies the brain difference between AD patients and HC, and the future studies could focus on the brain relationship in AD patients. Finally, the functional connectivity was regarded as feature in this paper, and the future studies could choose other attributions of the brain as feature such as clustering coefficient, degree and shortest path.

ETHICS STATEMENT

This study was carried out in accordance with the recommendations of National Institute of Aging-Alzheimer's Association (NIA-AA) workgroup guidelines, Institutional Review Board (IRB). The study was approved by Institutional Review Board (IRB) of each participating site, including the Banner Alzheimer's Institute, and was conducted in accordance with Federal Regulations, the Internal Conference on Harmonization (ICH), and Good Clinical Practices (GCP).

AUTHOR CONTRIBUTIONS

X-aB proposed the design of the work and revised it critically for important intellectual content. QSu and QJ carried out the experiment for the work and drafted part of the work. YL and QSh collected, interpreted the data, and drafted part of the work. All the authors approved the final version to be published and agreed to be accountable for all aspects of the work in ensuring that questions related to the accuracy or integrity of any part of the work are appropriately investigated and resolved.

FUNDING

This work was supported by the National Science Foundation of China (Nos. 61502167 and 61473259).

REFERENCES

Agosta, F., Pievani, M., Geroldi, C., Copetti, M., Frisoni, G. B., and Filippi, M. (2012). Resting state fMRI in Alzheimer's disease: beyond the default mode network. *Neurobiol. Aging* 33, 1564–1578. doi: 10.1016/j.neurobiolaging.2011.06.007

Alam, S., and Kwon, G. R. (2017). Alzheimer disease classification using KPCA, LDA, and multi-kernel learning SVM. *Int. J. Imaging Syst. Technol.* 27, 133–143. doi: 10.1002/ima.22217

Anthimopoulos, M., Christodoulidis, S., Ebner, L., Christe, A., and Mougiakakou, S. (2016). Lung pattern classification for interstitial lung diseases using a deep convolutional neural network. *IEEE Trans. Med. Imaging* 35, 1207–1216. doi: 10.1109/TMI.2016.2535865

Azar, A. T., and Hassanien, A. E. (2015). Dimensionality reduction of medical big data using neural-fuzzy classifier. *Soft Comput.* 19, 1115–1127. doi: 10.1007/s00500-014-1327-4

Bi, X.-A., Shu, Q., Sun, Q., and Xu, Q. (2018). Random support vector machine cluster analysis of resting-state fMRI in Alzheimer's disease. *PLoS One* 13:e0194479. doi: 10.1371/journal.pone.0194479

Binnewijzend, M. A. A., Schoonheim, M. M., Sanz-Arigita, E., Wink, A. M., van der Flier, W. M., Tolboom, N., et al. (2012). Resting-state fMRI changes in Alzheimer's disease and mild cognitive impairment. *Neurobiol. Aging* 33, 2018–2028. doi: 10.1016/j.neurobiolaging.2011.07.003

Boisgueheneuc, F. D., Levy, R., Volle, E., Seassau, M., Duffau, H., Kinkingnehun, S., et al. (2006). Functions of the left superior frontal gyrus in humans: a lesion study. *Brain* 129, 3315–3328. doi: 10.1093/brain/awl244

Brickman, A. M., Zahodne, L. B., Guzman, V. A., Narkhede, A., Meier, I. B., Griffith, E. Y., et al. (2015). Reconsidering harbingers of dementia: progression of parietal lobe white matter hyperintensities predicts Alzheimer's disease incidence. *Neurobiol. Aging* 36, 27–32. doi: 10.1016/j.neurobiolaging.2014.07.019

Carter, R. M., O'Doherty, J. P., Seymour, B., Koch, C., and Dolan, R. J. (2006). Contingency awareness in human aversive conditioning involves the middle frontal gyrus. *NeuroImage* 29, 1007–1012. doi: 10.1016/j.neuroimage.2005.09.011

Challis, E., Hurley, P., Serra, L., Bozzali, M., Oliver, S., and Cercignani, M. (2015). Gaussian process classification of Alzheimer's disease and mild cognitive impairment from resting-state fMRI. *NeuroImage* 112, 232–243. doi: 10.1016/j.neuroimage.2015.02.037

Chao-Gan, Y., and Yu-Feng, Z. (2010). DPARSF: A MATLAB toolbox for "Pipeline" data analysis of resting-state fMRI. *Front. Syst. Neurosci.* 4:13. doi: 10.3389/fnsys.2010.00013

Costafreda, S. G., Fu, C. H. Y., Lee, L., Everitt, B., Brammer, M. J., and David, A. S. (2006). A systematic review and quantitative appraisal of fMRI studies of verbal fluency: role of the left inferior frontal gyrus. *Hum. Brain Mapp.* 27, 799–810. doi: 10.1002/hbm.20221

Dani, M., Fan, Z., Wood, M., Mizoguchi, R., Morgan, R., Walker, Z., et al. (2017). amyloid deposition, tau aggregation and microglial activation correlate with vascular burden in vivo in Alzheimer's disease, Alzheimer's & Dementia. *J. Alzheimer's Assoc.* 13, 681–682. doi: 10.1016/j.jalz.2017.06.848

Eliasova, I., Anderkova, L., Marecek, R., and Rektorova, I. (2014). Non-invasive brain stimulation of the right inferior frontal gyrus may improve attention in early Alzheimer's disease: a pilot study. *J. Neurol. Sci.* 346, 318–322. doi: 10.1016/j.jns.2014.08.036

Engels, M. M., Stam, C. J., van der Flier, W. M., Scheltens, P., de Waal, H., and van Straaten, E. C. (2015). Declining functional connectivity and changing hub locations in Alzheimer's disease: an EEG study. *BMC Neurol.* 15:145. doi: 10.1186/s12883-015-0400-7

Engels, M. M. A., Hillebrand, A., van der Flier, W. M., Stam, C. J., Scheltens, P., and van Straaten, E. C. W. (2016). Slowing of hippocampal activity correlates with cognitive decline in early onset alzheimer's disease, an MEG study with virtual electrodes. *Front. Hum. Neurosci.* 10:238. doi: 10.3389/fnhum.2016.00238

Er, O., Cetin, O., Bascil, M. S., and Temurtas, F. (2016). A comparative study on parkinson's disease diagnosis using neural networks and artificial immune system. *J. Med. Imaging Health Inf.* 6, 264–268. doi: 10.1166/jmihi.2016.1606

Friston, K. J., Frith, C. D., Liddle, P. F., and Frackowiak, R. S. J. (1993). Functional connectivity: the principal-component analysis of large (PET) data sets. *J. Cereb. Blood Flow & Metab.* 13, 5–14. doi: 10.1038/jcbfm.1993.4

Gao, X. W., Hui, R., and Tian, Z. (2017). Classification of CT brain images based on deep learning networks. *Comput. Methods Programs* 138, 49–56. doi: 10.1016/j.cmpb.2016.10.007

Golby, A., Silverberg, G., Race, E., Gabrieli, S., O'Shea, J., Knierim, K., et al. (2005). Memory encoding in Alzheimer's disease: an fMRI study of explicit and implicit memory. *Brain* 128, 773–787. doi: 10.1093/brain/awh400

Greicius, M. D., Srivastava, G., Reiss, A. L., and Menon, V. (2004). Default-mode network activity distinguishes Alzheimer's disease from healthy aging: evidence from functional MRI. *Proc. Natl. Acad. Sci. U.S.A.* 101, 4637–4642. doi: 10.1073/pnas.0308627101

Griffanti, L., Dipasquale, O., Laganà, M. M., Nemni, R., Clerici, M., Smith, S. M., et al. (2015). Effective artifact removal in resting state fMRI data improves detection of DMN functional connectivity alteration in Alzheimer's disease. *Front. Hum. Neurosci.* 9:449. doi: 10.3389/fnhum.2015.00449

Griffanti, L., Wilcock, G. K., Voets, N., Bonifacio, G., Mackay, C. E., Jenkinson, M., et al. (2016). Donepezil enhances frontal functional connectivity in Alzheimer's disease: a pilot study. *Dementia Geriatric Cogn. Disord. Extra* 6, 518–528. doi: 10.1159/000450546

Grossman, M., Koenig, P., Glosser, G., DeVita, C., Moore, P., Rhee, J., et al. (2003). Neural basis for semantic memory difficulty in Alzheimer's disease: an fMRI study. *Brain* 126, 292–311. doi: 10.1093/brain/awg027

He, Y., Wang, L., Zang, Y., Tian, L., Zhang, X., Li, K., et al. (2007). Regional coherence changes in the early stages of Alzheimer's disease: a combined structural and resting-state functional MRI study. *NeuroImage* 35, 488–500. doi: 10.1016/j.neuroimage.2006.11.042

Hirschauer, T. J., Adeli, H., and Buford, J. A. (2015). Computer-aided diagnosis of Parkinson's disease using enhanced probabilistic neural network. *J. Med. Syst.* 39:179. doi: 10.1007/s10916-015-0353-9

Hopkins, W. D., Meguerditchian, A., Coulon, O., Misiura, M., Pope, S., Mareno, M. C., et al. (2017). Motor skill for tool-use is associated with asymmetries in Broca's area and the motor hand area of the precentral gyrus in chimpanzees (Pan troglodytes). *Behav. Brain Res.* 318, 71–81. doi: 10.1016/j.bbr.2016.10.048

Jenkinson, M., Bannister, P., Brady, M., and Smith, S. (2002). Improved optimization for the robust and accurate linear registration and motion correction of brain images. *NeuroImage* 17, 825–841. doi: 10.1006/nimg.2002.1132

Jolliffe, I. T., and Cadima, J. (2016). Principal component analysis: a review and recent developments. *Philos. Trans. R. Soc. A Mathemat. Phys. Eng. Sci.* 374:20150202. doi: 10.1098/rsta.2015.0202

Kang, K., Yoon, U., Lee, J.-M., and Lee, H.-W. (2013). Idiopathic normal-pressure hydrocephalus, cortical thinning, and the cerebrospinal fluid tap test. *J. Neurol. Sci.* 334, 55–62. doi: 10.1016/j.jns.2013.07.014

Karas, G., Scheltens, P., Rombouts, S., van Schijndel, R., Klein, M., Jones, B., et al. (2007). Precuneus atrophy in early-onset Alzheimer's disease: a morphometric structural MRI study. *Neuroradiology* 49, 967–976. doi: 10.1007/s00234-007-0269-2

Khazaee, A., Ebrahimzadeh, A., and Babajani-Feremi, A. (2015). Identifying patients with Alzheimer's disease using resting-state fMRI and graph theory. *Clin. Neurophysiol.* 126, 2132–2141. doi: 10.1016/j.clinph.2015.02.060

Khazaee, A., Ebrahimzadeh, A., and Babajani-Feremi, A. (2016). Application of advanced machine learning methods on resting-state fMRI network for identification of mild cognitive impairment and Alzheimer's disease. *Brain Imaging Behav.* 10, 799–817. doi: 10.1007/s11682-015-9448-7

Kim, J., Calhoun, V. D., Shim, E., and Lee, J.-H. (2016). Deep neural network with weight sparsity control and pre-training extracts hierarchical features and enhances classification performance: evidence from whole-brain resting-state functional connectivity patterns of schizophrenia. *NeuroImage* 124, 127–146. doi: 10.1016/j.neuroimage.2015.05.018

Luo, S., Li, X., and Li, J. (2017). Automatic Alzheimer's disease recognition from MRI data using deep learning method. *J. Appl. Mathemat. Phys.* 5, 1892–1898. doi: 10.4236/jamp.2017.59159

Mannfolk, P., Wirestam, R., Nilsson, M., Ståhlberg, F., and Olsrud, J. (2010). Dimensionality reduction of fMRI time series data using locally linear embedding. *MAGMA* 23, 327–338. doi: 10.1007/s10334-010-0204-0

Mattioni, B. E., and Jurs, P. C. (2003). Prediction of dihydrofolate reductase inhibition and selectivity using computational neural networks and linear discriminant analysis. *J. Mol. Graph. Model.* 21, 391–419. doi: 10.1016/S1093-3263(02)00187-0

McKeown, M. J., Li, J., Huang, X., Lewis, M. M., Rhee, S., Young Truong, K. N., et al. (2007). Local linear discriminant analysis (LLDA) for group and region of interest (ROI)-based fMRI analysis. *NeuroImage* 37, 855–865. doi: 10.1016/j.neuroimage.2007.04.072

Misaki, M., Kim, Y., Bandettini, P. A., and Kriegeskorte, N. (2010). Comparison of multivariate classifiers and response normalizations for pattern-information fMRI. *NeuroImage* 53, 103–118. doi: 10.1016/j.neuroimage.2010.05.051

Moradi, E., Pepe, A., Gaser, C., Huttunen, H., and Tohka, J. (2015). Machine learning framework for early MRI-based Alzheimer's conversion prediction in MCI subjects. *NeuroImage* 104, 398–412. doi: 10.1016/j.neuroimage.2014.10.002

Nebel, M. B., Joel, S. E., Muschelli, J., Barber, A. D., Caffo, B. S., Pekar, J. J., et al. (2014). Disruption of functional organization within the primary motor cortex in children with autism. *Hum. Brain Mapp.* 35, 567–580. doi: 10.1002/hbm.22188

Ortiz, A., Górriz, J. M., Ramírez, J., and Martínez-Murcia, F. J. (2013). LVQ-SVM based CAD tool applied to structural MRI for the diagnosis of the Alzheimer's disease. *Pattern Recognit. Lett.* 34, 1725–1733. doi: 10.1016/j.patrec.2013.04.014

Ortiz, A., Munilla, J., Górriz, J. M., and Ramírez, J. (2016). Ensembles of deep learning architectures for the early diagnosis of the Alzheimer's disease. *Int. J. Neural Syst.* 26:1650025. doi: 10.1142/S0129065716500258

Pagani, M., Nobili, F., Morbelli, S., Arnaldi, D., Giuliani, A., Öberg, J., et al. (2017). Early identification of MCI converting to AD: a FDG PET study. *Eur. J. Nucl. Med. Mol. Imaging* 44, 2042–2052. doi: 10.1007/s00259-017-3761-x

Prosser, A., Bolt, L., and Kipps, C. (2015). (99M)TC-HMPAO spect perfusion imaging predicts Alzheimer's disease cerebrospinal fluid biomarker status. *Alzheimer's & Dementia* 11, 407–408. doi: 10.1016/j.jalz.2015.06.363

Rolls, E. T., Joliot, M., and Tzourio-Mazoyer, N. (2015). Implementation of a new parcellation of the orbitofrontal cortex in the automated anatomical labeling atlas. *NeuroImage* 122, 1–5. doi: 10.1016/j.neuroimage.2015.07.075

Sarraf, S., DeSouza, D. D., Anderson, J., and Tofighi, G. (2016). DeepAD: Alzheimer's disease classification via deep convolutional neural networks using MRI and fMRI. *bioRxiv* [Preprint]. doi: 10.1101/070441

Schultz, S. A., Larson, J., Oh, J., Koscik, R., Dowling, M. N., Gallagher, C. L., et al. (2015). Participation in cognitively-stimulating activities is associated with brain structure and cognitive function in preclinical Alzheimer's disease. *Brain Imaging Behav.* 9, 729–736. doi: 10.1007/s11682-014-9329-5

Suk, H.-I., Lee, S.-W., and Shen, D. (2014). Hierarchical feature representation and multimodal fusion with deep learning for AD/MCI diagnosis. *NeuroImage* 101, 569–582. doi: 10.1016/j.neuroimage.2014.06.077

Suk, H.-I., Wee, C.-Y., Lee, S.-W., and Shen, D. (2016). State-space model with deep learning for functional dynamics estimation in resting-state fMRI. *Neuroimage* 129, 292–307. doi: 10.1016/j.neuroimage.2016.01.005

Wang, K., Liang, M., Wang, L., Tian, L., Zhang, X., Li, K., et al. (2007). Altered functional connectivity in early Alzheimer's disease: a resting-state fMRI study. *Hum. Brain Mapp.* 28, 967–978. doi: 10.1002/hbm.20324

Wang, L., Li, K., Zhang, Q.-E., Zeng, Y.-W., Jin, Z., Dai, W.-J., et al. (2013). Interhemispheric functional connectivity and its relationships with clinical characteristics in major depressive disorder: a resting state fMRI study. *PLoS One* 8:e60191. doi: 10.1371/journal.pone.0060191

Yetkin, F. Z., Rosenberg, R. N., Weiner, M. F., Purdy, P. D., and Cullum, C. M. (2006). FMRI of working memory in patients with mild cognitive impairment and probable Alzheimer's disease. *Eur. Radiol.* 16, 193–206. doi: 10.1007/s00330-005-2794-x

Yousry, T. A., Schmid, U. D., Alkadhi, H., Schmidt, D., Peraud, A., Buettner, A., et al. (1997). Localization of the motor hand area to a knob on the precentral gyrus, a new landmark. *Brain* 120, 141–157. doi: 10.1093/brain/120.1.141

Zhang, Y., Dong, Z., Phillips, P., Wang, S., Ji, G., Yang, J., et al. (2015). Detection of subjects and brain regions related to Alzheimer's disease using 3D MRI scans based on eigenbrain and machine learning. *Front. Comput. Neurosci.* 9:66. doi: 10.3389/fncom.2015.00066

Zhang, Y., Wang, S., and Dong, Z. (2014). Classification of Alzheimer disease based on structural magnetic resonance imaging by kernel support vector machine decision tree. *Progr. Electromagn. Res.* 144, 171–184. doi: 10.2528/PIER13121310

Zhou, Y., Peng, J., and Chen, C. L. P. (2015). Dimension reduction using spatial and spectral regularized local discriminant embedding for hyperspectral image classification. *IEEE Trans. Geosci. Remote Sens.* 53, 1082–1095. doi: 10.1109/TGRS.2014.2333539

Conflict of Interest Statement: The authors declare that the research was conducted in the absence of any commercial or financial relationships that could be construed as a potential conflict of interest.

Copyright © 2018 Bi, Jiang, Sun, Shu and Liu. This is an open-access article distributed under the terms of the Creative Commons Attribution License (CC BY). The use, distribution or reproduction in other forums is permitted, provided the original author(s) and the copyright owner(s) are credited and that the original publication in this journal is cited, in accordance with accepted academic practice. No use, distribution or reproduction is permitted which does not comply with these terms.

frontiers in Aging Neuroscience

ORIGINAL RESEARCH
published: 05 June 2018
doi: 10.3389/fnagi.2018.00161

Decreased Bilateral FDG-PET Uptake and Inter-Hemispheric Connectivity in Multi-Domain Amnestic Mild Cognitive Impairment Patients: A Preliminary Study

Xiao Luo[1†‡], Kaicheng Li[1†], Qingze Zeng[1], Peiyu Huang[1], Yeerfan Jiaerken[1], Tiantian Qiu[1], Xiaojun Xu[1], Jiong Zhou[2], Jingjing Xu[1] and Minming Zhang[1] for the Alzheimer's Disease Neuroimaging Initiative (ADNI)[§]*

[1] Department of Radiology, The Second Affiliated Hospital of Zhejiang University School of Medicine, Hangzhou, China,
[2] Department of Neurology, The Second Affiliated Hospital of Zhejiang University School of Medicine, Hangzhou, China

OPEN ACCESS

Edited by:
Mohammad Amjad Kamal,
King Fahad Medical Research Center,
King Abdulaziz University,
Saudi Arabia

Reviewed by:
Arun Bokde,
Trinity College Dublin, Ireland
Panteleimon Giannakopoulos,
Université de Genève, Switzerland

***Correspondence:**
Minming Zhang
zhangminming@zju.edu.cn

[†] These authors have contributed equally to this work.

[‡] orcid.org/0000-0003-1743-7842

[§] The data used in the preparation of this article were obtained from the Alzheimer's Disease Neuroimaging Initiative (ADNI) database (adni.loni.usc.edu). As such, the investigators within the ADNI contributed to the design and implementation of ADNI and provided data but did not participate in the analysis or writing of this report.

Received: 22 February 2018
Accepted: 14 May 2018
Published: 05 June 2018

Citation:
Luo X, Li K, Zeng Q, Huang P, Jiaerken Y, Qiu T, Xu X, Zhou J, Xu J and Zhang M for the Alzheimer's Disease Neuroimaging Initiative (ADNI) (2018) Decreased Bilateral FDG-PET Uptake and Inter-Hemispheric Connectivity in Multi-Domain Amnestic Mild Cognitive Impairment Patients: A Preliminary Study. Front. Aging Neurosci. 10:161. doi: 10.3389/fnagi.2018.00161

Background: Amnestic mild cognitive impairment (aMCI) is a heterogeneous condition. Based on clinical symptoms, aMCI could be categorized into single-domain aMCI (SD-aMCI, only memory deficit) and multi-domain aMCI (MD-aMCI, one or more cognitive domain deficit). As core intrinsic functional architecture, inter-hemispheric connectivity maintains many cognitive abilities. However, few studies investigated whether SD-aMCI and MD-aMCI have different inter-hemispheric connectivity pattern.

Methods: We evaluated inter-hemispheric connection pattern using fluorine-18 positron emission tomography – fluorodeoxyglucose (^{18}F PET-FDG), resting-state functional MRI and structural T1 in 49 controls, 32 SD-aMCI, and 32 MD-aMCI patients. Specifically, we analyzed the 18^{F} PET-FDG (intensity normalized by cerebellar vermis) in a voxel-wise manner. Then, we estimated inter-hemispheric functional and structural connectivity by calculating the voxel-mirrored homotopic connectivity (VMHC) and corpus callosum (CC) subregions volume. Further, we correlated inter-hemispheric indices with the behavioral score and pathological biomarkers.

Results: We found that MD-aMCI exhibited more several inter-hemispheric connectivity damages than SD-aMCI. Specifically, MD-aMCI displayed hypometabolism in the bilateral middle temporal gyrus (MTG), inferior parietal lobe, and left precuneus (PCu) ($p < 0.001$, corrected). Correspondingly, MD-aMCI showed decreased VMHC in MTG, PCu, calcarine gyrus, and postcentral gyrus, as well as smaller mid-posterior CC than the SD-aMCI and controls ($p < 0.05$, corrected). Contrary to MD-aMCI, there were no neuroimaging indices with significant differences between SD-aMCI and controls, except reduced hypometabolism in bilateral MTG. Within aMCI patients, hypometabolism and reduced inter-hemispheric connectivity correlated with worse executive ability. Moreover, hypometabolism indices correlated to increased amyloid deposition.

Conclusion: In conclusion, patients with MD-aMCI exhibited the more severe deficit in inter-hemispheric communication than SD-aMCI. This long-range connectivity deficit may contribute to cognitive profiles and potentially serve as a biomarker to estimate disease progression of aMCI patients.

Keywords: mild cognitive impairment, cerebral metabolism, corpus callosum, resting-state functional MRI, voxel-mirrored homotopic connectivity

INTRODUCTION

The amnestic mild cognitive impairment (aMCI) represents an intermediate stage between normal aging and Alzheimer's disease (AD) (Petersen et al., 2014). According to impaired cognitive domains number, aMCI patients could be further categorized into two subtypes: single-domain aMCI (SD-aMCI), characterized by relatively selective memory impairment and the multi-domain aMCI (MD-aMCI), indicating extensive deficits involving at least one other domain (Winblad et al., 2004; Busse et al., 2006). Previous epidemiology study shows that MD-aMCI has a higher risk of clinical progression than the SD-aMCI (Golob et al., 2007). Therefore, to investigate the mechanism underlying these aMCI subtypes may efficiently facilitate clinical early intervention and management. Recently, neuroimaging studies pointed out that the MD-aMCI displays more diffuse gray matter atrophy (Haller et al., 2010; Zhang et al., 2012) and lower brain activity than the SD-aMCI, mainly involving default mode network (DMN) and frontoparietal regions (Li et al., 2014). Despite these studies shedding light into the aMCI pathological mechanism to some extent, it remains unclear whether SD-aMCI and MD-aMCI have different inter-hemispheric connection pattern.

Compared to the other neuroimaging indices, insufficient attention paid to the direct inter-hemispheric connectivity of aMCI patients. Anatomically, the connectivity between hemispheres is a core mode of the brain intrinsic functional architecture. Moreover, this bi-hemispheric communication procedure substantially affects many cognitive domains, including executive and memory functions (Salvador et al., 2008; Stark et al., 2008; Saar-Ashkenazy et al., 2016). Until now, only two functional MRI studies directly explored the inter-hemispheric functional connectivity in aMCI patients. However, two studies drew the entirely different conclusion. Specifically, Wang et al. (2015) demonstrated that MCI patients exhibited an enhanced inter-hemispheric functional connectivity in the sensorimotor cortex to resist the cognitive decline; however, another work reported the negative result between aMCI and controls (Qiu et al., 2016). Given that aMCI is a heterogeneous condition, we thus hypothesized that this inconsistency might attribute to the different damage pattern of inter-hemispheric connectivity between SD-aMCI and MD-aMCI patients.

Notably, some previous findings focusing on corpus callosum (CC) supported this hypothesis. Anatomically, CC acts as the most robust commissural white matter bundle to maintain the functional connectivity between the hemispheres (Roland et al., 2017). Specifically, some studies demonstrated that the AD and MCI patients exhibit the CC shape change, atrophy, and impaired diffusivity indices impairment, especially in the posterior part (Janowsky et al., 1996; Di Paola et al., 2010; Ardekani et al., 2014; Rasero et al., 2017). Subsequently, some studies further demonstrated patients with MD-aMCI, but not SD-aMCI, have reduced mean diffusivity (MD) in the whole CC compared to controls; moreover, decrease of MD in the CC body is associated with decreased general cognition and executive ability (Li et al., 2013). On the other hand, as a valid diagnostic biomarker in dementia studies, fluorine-18 fluorodeoxyglucose (^{18}F FDG) positron emission tomography (PET) research also shows more diffuse hypometabolism in MD-aMCI than the SD-aMCI. Interestingly, these hypometabolism regions are mostly located in the bilateral homotopic precuneus (PCu) and the temporoparietal cortex (Caffarra et al., 2008; Cerami et al., 2015). Considering the evidence of CC degeneration and bilateral homotopic hypometabolism, we inferred that different inter-hemispheric connectivity damage pattern might exist between aMCI subgroups.

To test this hypothesis, we analyzed the structural T1 image, resting-state functional MRI (rsfMRI), ^{18}F PET-FDG, neuropsychological scales, and pathological biomarkers in a relatively large aMCI sample from ADNI database. Firstly, we analyzed inter-hemispheric homotopic functional connectivity by using a voxel-wise method, namely voxel-mirrored homotopic connectivity (VMHC) (Zuo et al., 2010; Luo et al., 2018b). The potential inter-hemispheric structural connectivity was evaluated by estimating CC volume. We divided CC into five part due to its different anatomical connection [i.e., genus connects the frontal areas, while body and splenium part connects the temporal and parietal areas (Fischl, 2012)]. Moreover, to test whether regions with inter-hemispheric disruption accompanied by metabolic abnormalities, we also analyzed ^{18}F FDG-PET data in a voxel-wise manner. Additionally, we also correlated neuroimaging indices with cognition and pathological biomarkers (reflecting by CSF and amyloid imaging). Our study aims to (i) compare the alteration of the inter-hemispheric connectivity and the metabolism between aMCI subtypes; (ii) explore the possible interactions between different neuroimaging modalities; and (iii) explore the relationships between neuroimaging indices and cognition.

MATERIALS AND METHODS

Alzheimer's Disease Neuroimaging Initiative

Data used in this study were obtained from the Alzheimer's disease Neuroimaging Initiative (ADNI) database[1]. The ADNI was launched in 2003 by the National Institute on Aging (NIA),

[1] adni.loni.usc.edu

the National Institute of Biomedical Imaging and Bioengineering (NIBIB), the Food and Drug Administration (FDA), private pharmaceutical companies, and non-profit organizations, as a $60 million, 5-year public–private partnership. The primary goal of ADNI has been to test whether serial magnetic resonance imaging (MRI), PET, other biological markers, and clinical and neuropsychological assessment can be combined to measure the progression of mild cognitive impairment (MCI) and early Alzheimer's disease (AD). Determination of sensitive and specific markers of very early AD progression is intended to aid researchers and clinicians in developing new treatments and monitor their effectiveness, as well as lessen the time and cost of clinical trials.

Subjects

All procedures performed in studies involving human participants were following the ethical standards of the institutional and national research committee and with the 1975 Helsinki Declaration and its later amendments or comparable ethical standards. The ADNI project was approved by the Institutional Review Boards of all participating institutions, and all participants at each site signed informed consent. Based on ADNI GO and ADNI 2 database, we identified 49 healthy right-handed subjects (normal controls, NC) and 64 aMCI patients, who had undergone structural scans, rsfMRI scans, FDG-PET scans, and neuropsychological evaluation. We downloaded the study data from the ADNI publicly available database before April 15, 2017. According to ADNI protocol, to be classified as healthy controls, the Mini-Mental State Examination (MMSE) for the subject should be between 24 and 30 (inclusive), and clinical dementia rating (CDR) score should be 0. Besides, the subject has no signs of depression (Geriatric Depression Scale, GDS <6) or possible dementia. To be defined as aMCI, the subject had an MMSE score between 24 and 30 (inclusive), memory complaint, objective abnormal memory evidence, and a CDR score of 0.5. Besides, aMCI patients' general cognition preserved well (cannot meet AD diagnostic criteria). Also, there were no signs of depression (GDS score <6) in aMCI patients.

Followed by exclusion standards: the subject who has a history of apparent head trauma, other neurological or major psychiatric disorder, and alcohol/drug abuse. Additionally, subjects were also excluded if they exhibited a significant vascular disease risk history, defined as Hachinski Ischemia Scale (HIS) scores higher than 4.

Neuropsychological Evaluation and MCI Subtypes Diagnosis

All subjects underwent comprehensive neuropsychological tests. Content includes general mental status (MMSE score, Alzheimer's Disease Assessment Scale, ADAS) and other cognitive domain, including memory function (Auditory Verbal Learning Test, AVLT; Wechsler Memory Scale-Logical Memory, WMS-LM, including immediate and delayed score), processing speed (Trail-Making Test, Part A, TMT-A), visuospatial function (Clock-Drawing Test, CDT), executive function (Trail-Making Test, Part B, TMT-B), and language ability (Boston Naming Test, BNT). According to the previous studies, we used the composite scores for executive functioning and memory (Crane et al., 2012; Gibbons et al., 2012).

The aMCI patients were divided into two subtypes by the performance in cognitive domains (Shu et al., 2012). Specifically, SD-aMCI refers to aMCI patients having an impairment in memory alone; MD-aMCI refers to aMCI patients having an impairment in memory and other cognitive domain (at least one). We defined impairment as the presence of a test scoring 1.5 standard deviations (SD) below the average score, from age- and education-matched healthy controls from ADNI. Specifically, the total number of healthy controls from ADNI is 198, mean age is 73.03 ± 6.20, and mean education attainment is 16.47 ± 2.45. No significant difference existed in terms of age and education level ($p > 0.05$) between ADNI controls and aMCI subjects (mean age: 73.33 ± 5.69; education level: 15.84 ± 2.45). Finally, we enrolled 49 out of 198 ADNI controls who undergone structural scans, rsfMRI scans, and neuropsychological evaluation for subsequent analyses. Meanwhile, 32 MD-aMCI and 32 SD-aMCI patients entered the subsequent analyses.

CSF Data

We downloaded the CSF dataset from the ADNI database. Based on CSF samples, $A\beta_{1-42}$, total tau (t-tau) and phosphorylated tau (p-tau_{181}) were measured (Bittner et al., 2016). These CSF biomarkers, including $A\beta_{1-42}$, t-tau, and p-tau_{181}, are also useful candidates as they are intimately related to amyloid plaques, neuronal death, and accumulation of tangles, respectively (Jovicich et al., 2016). Moreover, the ratio of p-tau/$A\beta_{1-42}$ was also calculated due to its association with cognition and disease progression (Landau et al., 2010). Notably, not all subjects in the present study had the CSF samples due to the invasive procedure of lumbar puncture. Thus, the final CSF sample for analyses included 26 out of the 49 NC, 30 out of the 32 SD-aMCI, and 28 out of the 32 MD-aMCI patients.

Amyloid PET Data

Given that amyloid PET shows more potent than CSF markers for MCI prognosis, we further downloaded the results of ^{18}F-florbetapir PET data from the ADNI database, namely UCBERKELEYAV45_11_14_17.csv (Bouallègue et al., 2017). The detailed processing procedure was described previously (Landau et al., 2013). In the following analysis, we used the results of composite SUVR value (intensity-normalized by a whole cerebellum region).

Image Acquisition

The 3.0-Tesla Philips MRI scanner was used to scan all participants. Based on MPRAGE T1-weighted sequence, structural images were acquired with the following parameters: repetition time (TR) = 2300 ms; echo time (TE) = 2.98 ms; inversion time (TI) = 900 ms; 170 sagittal slices; within plane FOV = 256 × 240 mm^2; voxel size = 1.1 × 1.1 × 1.2 mm^3; flip angle = 9°; and bandwidth = 240 Hz/pix. Based on echo-planar imaging sequence, rsfMRI images were acquired with the following parameters: time points = 140; TR = 3000 ms; TE = 30 ms; flip angle = 80°; the number of slices = 48; slice

thickness = 3.3 mm; spatial resolution = 3.31 × 3.31 × 3.31 mm^3; and matrix = 64 × 64. Meanwhile, PET images were obtained by either a 30-min six frame scan acquired 30–60-min post-injection or a static 30-min single-frame scan acquired 30–60-min post-injection.

Image Preprocessing

The image data were preprocessed by using the Data Processing Assistant for rsfMRI, DPASF[2], based on the Statistical Parametric Mapping (SPM 12)[3] and rsfMRI Data Analysis Toolkit, REST[4]. Briefly, we removed the first 10 image volumes of rsfMRI scans were for the signal equilibrium and the subjects' adaptation to the machine noise. The remaining 130 image volumes were corrected for both timing differences and head motion (24 Friston; Friston et al., 1996). We excluded the data with more than 2.0 mm maximum displacement in any directions (*X*-, *Y*-, and *Z*-axis) and 2.0 degrees of any angular motion. Subsequently, the T1-weighted images were co-registered to the mean rsfMRI image based on a thorough rigid-body transformation and normalized to the Montreal Neurological Institute (MNI) space, subsequent resliced into of 3 mm × 3 mm × 3 mm cubic voxels. Besides, we performed linear trends and temporal filter (0.01 Hz < f < 0.08 Hz). To remove any motion residual effects and other non-neuronal factors, we corrected covariates (including six head motion parameters, WM signal, CSF) in the following functional connectivity analysis. After preprocessing, we obtained each subject's 4D residual functional volume in native functional space. These 4D data were registered to the MNI152 space with 2 mm resolution (affine transformation). Due to the dispute of removing the global signal, we omit to regress out the global signal. Given the effect of the micro-motion artifact, we evaluated the frame-wise displacement (FD) value for each subject. Subjects were screened and excluded if FD value >0.5 mm on more than 35 volumes.

Voxel-Mirrored Homotopic Connectivity Analysis

For VMHC computation, firstly, the mean T1 image was generated from the average of 113 spatially normalized T1 images. Then, we flipped the left hemisphere along the midline of the *x*-axis to obtain the symmetric brain template, further, to create the final template. Subsequently, the each subject's T1 image was co-registered nonlinearly to the customized symmetric template. The same deformation field subsequently applied to the rsfMRI. More details regarding VMHC data processing are available in the literature (Anderson et al., 2010; Zuo et al., 2010). Based on Pearson's correlation, the homotopic RSFC between any pair of symmetrical inter-hemispheric voxels was estimated, then transformed to Fisher's *Z* map. Finally, we defined these resultant values as the VMHC and used it in following analyses.

[2]http://www.rfmri.org/DPARSF

[3]http://www.fil.ion.ucl.ac.uk/spm/

[4]http://www.resting-fmri.sourceforge.net/

Corpus Callosum Volume

We evaluated the CC volume and its subregions based on FreeSurfer software package (Version 5.1[5]) as described previously (Fischl, 2012; Reuter et al., 2012). In detail, FreeSurfer automatically segmented CC into five sections, with each section representing a fifth of the total area. We defined five segments as anterior (CC-A), mid-anterior (CC-MA), central (CC-C), mid-posterior (CC-MP), and posterior CC part (CC-P).

FDG-PET Voxel-Wise Analysis

We downloaded the ^{18}F FDG-PET data from the ADNI database in their most processed formats (PET Pre-processing protocol[6]). Specifically, pre-processed scans were generated following co-registration dynamic (to the first acquired frame), averaging frames, spatial re-orientation (AC–PC line), intensity normalization (within subject-specific mask), and smoothing (uniform isotropic spatial resolution 8 mm full width at half maximum kernel). The subsequent processing procedures of FDG-PET were conducted by combining T1 MRI images, which were similar to VMHC processing mentioned above. Firstly, each FDG-PET scan was co-registered to the individual's corresponding T1 MRI image in native space. Then, these structural scans were segmented, and the resulting GM partitions were spatially normalized using the SPM 12. The spatial normalization parameters (deformation fields) that had been estimated from the gray matter segment normalization were subsequently applied to the co-registered FDG-PET images so that both the GM, VMHC, and the FDG-PET images were in MNI space. To remove inter-individual nuisance variability in tracer metabolism, we intensity-normalized FDG-PET image via dividing it by the average FDG-PET value of the reference region (cerebellar vermis, defined by the AAL regions within the MNI atlas, manually checked by experienced radiologists, MMZ). Finally, we created the standardized uptake value ratio (SUVR) images for the following analysis.

Statistics

All statistical analyses were performed using IBM SPSS statistical software. The TMT-A, TMT-B, and ADAS-cog were log-transformed because of a positively skewed distribution. We used ANOVA to detect group differences in terms of age, education level, cognitive ability, and AD-related pathological results. We used the *post hoc* pairwise *t*-tests if ANOVA was significant ($p < 0.05$, corrected by Bonferroni).

Regarding VMHC results, the ANCOVA was used to explore different brain regions among the three groups, with controlling for age, education level, and gender. For the objective to explore, the threshold set at height $p < 0.05$ and cluster level $p < 0.05$ (Gaussian random field, GRF corrected). We performed the *post hoc* pairwise *t*-tests within the brain regions identified by the ANCOVA ($p < 0.005$ Bonferroni corrected). Regarding the FDG-PET SUVR image, we performed ANCOVA to explore metabolic differences, with controlling for age, education level,

[5]http://surfer.nmr.mgh.harvard.edu/

[6]http://adni.loni.usc.edu/methods/pet-analysis/pre-processing/

and gender [$p < 0.001$ at height and $p < 0.05$ at the cluster level (GRF corrected)]. Similarly, we performed the *post hoc* pairwise *t*-tests if ANCOVA was significant ($p < 0.005$, Bonferroni corrected). Also, we calculated the between-group CC subregions volume difference by using ANCOVA corrected by age, education level, gender, and total intracranial volume (TIV). We performed *post hoc* pairwise *t*-test if ANOVA was significant ($p < 0.05$, corrected by the least significant difference, LSD).

Further, we correlated imaging measures to cognitive abilities and also explored the possible interactions between neuroimaging modalities. To achieve the best visual effect, we overlapped between-group difference results of VMHC and FDG-PET SUVR image by the same statistical standard (ANCOVA, corrected by age, education level, and gender, $p < 0.05$ at height, $p < 0.05$ at the cluster level, GRF corrected). Meanwhile, to explore the possible interaction between CC subregions and other modalities, we performed voxel-wise regression analysis ($p < 0.05$ at height, $p < 0.05$ at the cluster level, GRF corrected). Notably, we calculated correlations limited to those indices having significant between-group differences.

RESULTS

Patient Characteristics

We displayed quantitative variables as the mean and its SD, and the categorical variable as absolute and relative frequency. **Table 1** shows the demographic characteristics, cognitive abilities, and pathological biomarkers for each group. There were no significant differences in terms of age, education level, and gender composition among the three groups. Regarding the general cognitive ability, we found that three groups exhibited the significant differences in the score of MMSE and ADAS-cog, with MD-aMCI displaying the worst performance. Regarding other cognitive domains, group effects were significant, with the best performance in NC and also the worst performance in MD-aMCI patients.

Regarding AD-related pathological biomarkers, MD-aMCI patients exhibited a significantly higher composite PET PiB SUVR value than NC ($p < 0.01$). Meanwhile, although MD-aMCI group presented a trend of the increased level of t-tau and p-tau$_{181}$ as well as decreased Aβ_{1-42}, no significant differences existed among groups ($p > 0.05$). Also, we also failed to detect the difference in the p-tau$_{181}$/Aβ_{1-42} ratio among groups.

Glucose Metabolism Differences

Three groups demonstrated the significant metabolic differences in the following regions: namely bilateral middle temporal gyrus (MTG), bilateral inferior parietal lobe (IPL), and left PCu. Subsequent pairwise group comparisons carried out on these clusters revealed that both aMCI patients exhibited a lower metabolism in bilateral MTG. Also, the MD-aMCI demonstrated a reduced metabolism in left PCu and bilateral IPL compared to the SD-aMCI and NC (**Figure 1** and **Table 2**).

Inter-Hemispheric Connection Differences

Among the three groups, we established the significant VMHC difference in these regions: namely middle MTG, PCu, postcentral gyrus (PCG), and calcarine gyrus (CG). As expected, subsequent pair-wise group comparisons suggested that MD-aMCI exhibited a decreased VMHC in MTG, CG, PCu, and PCG relative to SD-aMCI and NC ($p < 0.005$, corrected by Bonferroni); however, there were no significant differences of VMHC between SD-aMCI and NC (**Figure 2** and **Table 3**).

We observed the between-group effect on CC-MP subregion (**Figure 1**). Then, the *post hoc t*-test revealed that MD-aMCI exhibited the smallest CC-MP volume among groups, and no significant volume difference existed between SD-aMCI and NC ($p < 0.05$, corrected by LSD).

Neuroimaging Indices Correlate Cognitive Abilities and Pathological Biomarkers

All the correlation analyses we performed were within aMCI patients (**Figure 3**). We observed that reduced left IPL metabolism ($r = 0.27$) was related to worse executive ability ($p < 0.05$). In addition, regarding functional connectivity, we identified that reduced inter-hemispheric connection in PCu ($r = 0.39$), PCG ($r = 0.40$), and CG ($r = 0.54$) were related to worse composite score of executive functioning ($p < 0.001$). Also, the CC-MP volume was related to the composite score of executive functioning ($r = 0.40$, $p < 0.001$).

Regarding AD-related pathological biomarkers, we analyzed the correlation only within the indices having the between-group difference. Our results revealed that hypometabolism of left PCu ($r = -0.25$, $p < 0.05$) and right IPL ($r = -0.25$, $p < 0.05$) was related to the increased amyloid accumulation reflecting composite ^{18}F-florbetapir PET value.

Interaction Between Modalities

As expected, we noted that VMHC and PET-FDG SUVR between-group difference results overlapped well. Specifically, these overlapping included bilateral the MTG, the PCu, the IPL, and the PCG (Supplementary Material 1). Within these overlapping regions, we further observed that VMHC value related to SUVR uptake value within aMCI patient groups ($r = 0.27$, $p < 0.05$).

Within the aMCI patients, the mid-posterior CC volume was related to the bilateral MTG, PCu, CG, and insula ($p < 0.05$ at height and $p < 0.05$ at the cluster level, GRF-corrected Supplementary Material 2). However, we found no significance between mid-posterior CC volume and FDG SUVR uptake value ($p > 0.05$).

DISCUSSION

This study provides evidence that the MD-aMCI displayed simultaneous decreased bilateral metabolism and reduced inter-hemispheric functional connectivity in MTG, PCu, and

TABLE 1 | Comparison of demographic information, behavioral data, and pathological biomarkers.

	NC	SD-aMCI	MD-aMCI	*F* (χ^2)	*P*-value
Number	49	32	32		
Age	73.33 ± 4.60	72.43 ± 4.25	74.91 ± 5.27	2.29	0.11
Female	31	15	15	3.00	0.22
Education	16.24 ± 2.60	16.47 ± 2.24	15.25 ± 2.65	2.20	0.12
General mental status					
MMSE	29.02 ± 1.20	28.34 ± 1.68	27.16 ± 1.71	15.03	<0.001[bc]
Log-transformed ADAS	0.91 ± 0.17	1.07 ± 0.19	1.21 ± 0.20	24.21	<0.001[abc]
Spatial processing					
CDT	4.76 ± 0.48	4.75 ± 0.44	3.78 ± 1.18	19.69	<0.001[bc]
Language					
BNT	28.57 ± 1.44	28.09 ± 2.07	27.09 ± 11.36	0.55	0.58
Memory					
WMS-LM immediate	14.73 ± 2.76	9.88 ± 3.17	7.88 ± 2.83	60.49	<0.001[abc]
WMS-LM delayed	13.96 ± 2.99	7.97 ± 2.78	5.75 ± 3.06	84.93	<0.001[abc]
AVLT-Total	43.22 ± 9.01	37.34 ± 9.63	31.25 ± 8.78	16.85	<0.001[abc]
Processing speed					
Log-transformed TMTA	1.51 ± 0.12	1.47 ± 0.08	1.66 ± 0.15	23.82	<0.001[bc]
Executive function					
Log-transformed TMTB	1.86 ± 0.16	1.86 ± 0.13	2.18 ± 0.16	51.75	<0.001[bc]
Composite memory	1.05 ± 0.51	0.44 ± 0.59	0.06 ± 0.61	31.99	<0.001[abc]
Composite executive	0.80 ± 0.65	0.87 ± 0.51	−0.35 ± 0.51	47.82	<0.001[bc]
Pathological results					
$A\beta_{1-42}$ (pg/ml)	1222.19 ± 552.35	1132.06 ± 616.57	963.00 ± 438.94	1.85	0.16
t-tau (pg/ml)	248.52 ± 84.62	275.76 ± 90.51	300.33 ± 134.34	2.18	0.12
P-tau_{181} (pg/ml)	23.43 ± 9.46	25.69 ± 9.30	29.34 ± 15.01	2.30	0.11
p-tau/$A\beta_{1-42}$	0.03 ± 0.02	0.03 ± 0.02	0.04 ± 0.02	2.83	0.06
Composite PET-PiB	1.14 ± 0.19	1.20 ± 0.20	1.29 ± 0.25	4.54	0.01[b]

Data are presented as means ± SD. Notably, the mean levels of $A\beta_{1-42}$, t-tau, and p-tau_{181} in ***Table 1*** *only represent the subjects who had CSF samples.* [a]*Post hoc paired comparisons showed significant group differences between NC and SD-aMCI, after Bonferroni correction ($p < 0.05$).* [b]*Post hoc paired comparisons showed significant group differences between NC and MD-aMCI, after Bonferroni correction ($p < 0.05$).* [c]*Post hoc paired comparisons showed significant group differences between SD-aMCI and MD-aMCI, after Bonferroni correction ($p < 0.05$). MMSE, Mini-Mental State Examination; ADAS, the Alzheimer's Disease Assessment Scale-Cognitive Subscale; WMS-LM, Wechsler Memory Scale-Logical Memory; TMT, Trail-Making Test; CSF, cerebrospinal fluid; CDT, Clock-Drawing Test; AVLT, Auditory Verbal Learning Test; BNT, Boston Naming Test.*

parietal regions, accompanying with mid-posterior CC atrophy. However, except hypometabolism in bilateral MTG, no other differences existed between SD-aMCI and NC. Subsequently, the correlation analyses showed that these neuroimaging indices related to executive function across aMCI patients. Moreover, hypometabolism indices related to increased amyloid deposition. In summary, compared to SD-aMCI, the MD-aMCI exhibited the more severe deficit in inter-hemispheric communication. This long-range connectivity deficit may further contribute to cognitive abilities deficits and potentially serve as a biomarker to monitor the disease progression in aMCI patients.

Firstly, our findings suggested that both aMCI patients displayed hypometabolism in bilateral MTG, which is a region involving memory-related network (Ward et al., 2014; Munoz-Lopez et al., 2015). These deficits thus may contribute to the memory deficit in these patients. However, only the MD-aMCI simultaneously displayed inter-hemispheric functional connectivity decrease in MTG, supporting the notion that the MD-aMCI is a more advanced disease form than the SD-aMCI. Notably, one study pointed out that SD-aMCI displayed decreased regional activity in right MTG relative to NC (Luo et al., 2018a). Accordingly, we speculated that the intact inter-hemispheric connectivity in SD-aMCI might compensate its unilateral MTL impairment to some extent. Our neuropsychological results could support this interpretation, showing that MD-aMCI exhibited worse memory performance than SD-aMCI. Besides, other support evidence comes result from ^{18}F-florbetapir PET indicating that only the MD-aMCI has increased amyloid deposition than NC. Meanwhile, our findings validated previous studies, which reported that only MD-aMCI patients have cortical thinning, gray matter atrophy, and white matter tract deficit in MTG regions (Seo et al., 2007; Whitwell et al., 2007).

Many evidence suggests that amyloid accumulation preferentially starts in PCu, especially in the left side (Janke et al., 2001; Braak et al., 2006; Palmqvist et al., 2017). As expected, our results showed the MD-aMCI, but not the SD-aMCI, exhibited hypometabolism (left side) and reduced inter-hemispheric functional connection in PCu regions simultaneously. Moreover, we found that the reduced PCu inter-hemispheric functional

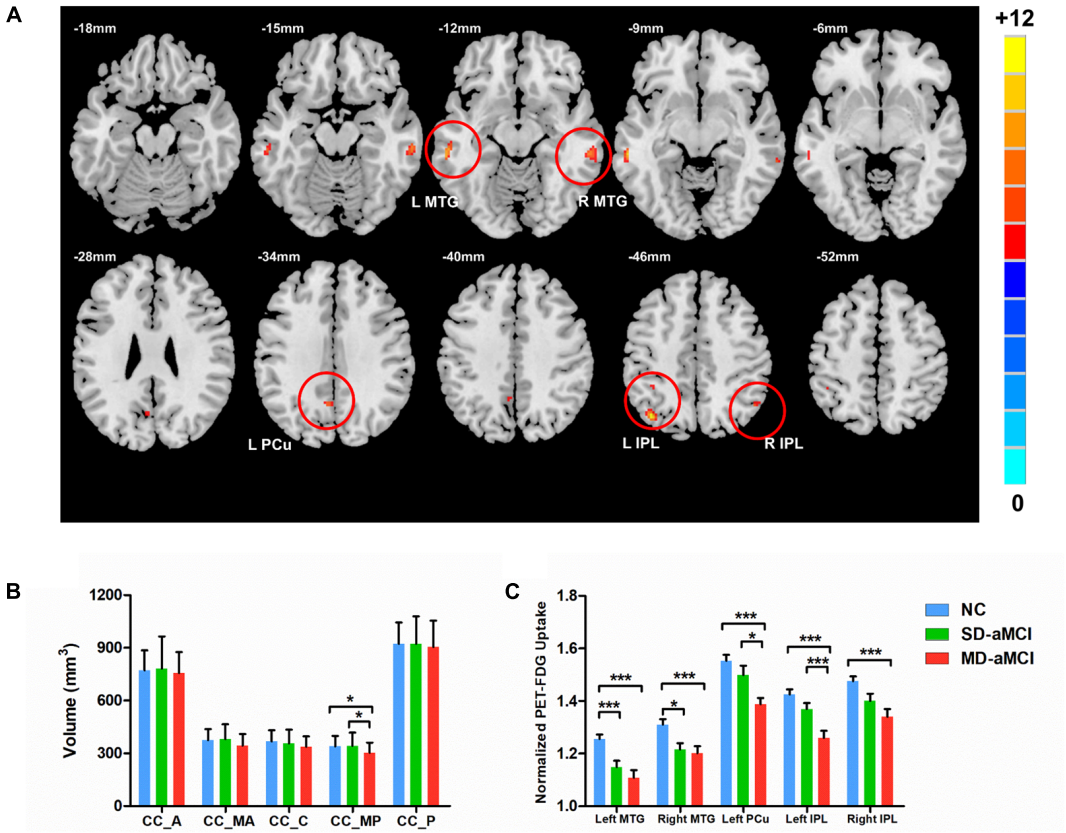


FIGURE 1 | Upper **(A)** shows the voxel-wise comparison result: brain areas with the significant difference of metabolism (normalized by cerebellum vermis) among NC, single-domain aMCI (SD-aMCI), and multi-domain aMCI (MD-aMCI), by controlling for age, education level, and gender. The threshold set $p < 0.001$ at height and $p < 0.05$ at the cluster level, GFR corrected. Lower figures show the histogram for MD-aMCI (red), SD-aMCI (green), and NCs (blue). Error bars represent SD. * represents $p < 0.05$ while *** represents $p < 0.001$, corrected for multiple comparisons. **(B)** The *post hoc* analyses were performed within the areas identified by the ANCOVA ($p < 0.05$). The MD-aMCI patients displayed the significantly decreased volume of the CC-MP compared to the other two groups. **(C)** We performed the *post hoc* analyses within the areas identified by the ANCOVA ($p < 0.005$). Among the three groups, the MD-aMCI patients exhibited the lowest metabolism in bilateral MTG, bilateral inferior parietal lobe (IPL), and left precuneus (L-PCu). Other abbreviation: A, anterior; MA, mid-anterior; C, central; MP, mid-posterior; and P, posterior.

connection associated with the worse executive function across aMCI patients. This relationship agrees with clinical manifestation in MD-aMCI patients, manifested by more than one cognitive domain impairment. Meanwhile, previous work also documented that MD-aMCI displayed impaired microstructure in PCu (Li et al., 2013). Specifically, by utilizing rsfMRI, one study demonstrated that the MD-aMCI exhibited lower regional activity in PCu than the SD-aMCI and NC. Coincidentally, their work also found that reduced PCu activity was related to worse executive ability (Li et al., 2014). As a central role in the primary executive networks, studies of the AD and MCI frequently reported that regional PCu deficit associated with the decreased executive ability (Sridharan et al., 2008; Chen et al., 2013; Luo et al., 2017a,b). Furthermore, we found that left PCu hypometabolism was related to amyloid deposition. Consequently, we speculated that amyloid-related neurotoxicity in unilateral PCu region might lead to the inter-hemispheric connectivity damage in corresponding areas.

Regarding the parietal cortex, the MD-aMCI exhibited hypometabolism in bilateral IPL and reduced inter-hemispheric PCG functional connectivity; additionally, we found that IPL hypometabolism was related to increased amyloid deposition. Therefore, we again interpreted that the hypometabolism in bilateral IPL may attribute to synaptic dysfunction caused by amyloid (Palop and Mucke, 2010; Tönnies and Trushina, 2017). Moreover, we observed that parietal cortex hypometabolism and inter-hemispheric dysfunction associated with worse executive ability. This relationship could attribute to the reason that both the IPL and PCG have extensive connections with the frontal region (i.e., frontoparietal circuit). Functionally, this circuit could send rich sensory information for processing speed and affect executive ability (Sullivan et al., 2001; Buckner et al., 2008; Luo et al., 2017b). Furthermore, some structural MRI studies support our results. One VBM study pointed out that patients with MD-aMCI exhibited GM reduction and increased mean diffusion in PCG (Li et al., 2013). Meanwhile, using diffusion spectrum

TABLE 2 | Brain areas with the significant difference of VMHC and PET-FDG among NCs, SD-aMCI, and MD-aMCI patients.

Regions	MNI coordinates			Cluster voxels	Peak intensity
	X	*Y*	*Z*		
VMHC					
Middle temporal gyrus	±51	−54	−3	128	8.30
Precuneus	±3	−57	60	133	7.60
Postcentral gyrus	±60	−21	24	317	8.86
Calcarine gyrus	±3	−75	9	195	9.60
PET-FDG					
L middle temporal gyrus	−60	−32	−10	59	11.08
	−44	−50	12	14	8.48
R middle temporal gyrus	62	−28	−14	52	9.37
L precuneus	−6	−54	38	38	8.86
L inferior parietal lobe	−38	−68	48	60	11.61
	−38	−42	48	24	9.46
R inferior parietal lobe	48	−58	44	13	8.60

Regarding VMHC results, the ANCOVA was used to explore differential brain regions among groups [controlling for age, education level, and gender, $p < 0.05$ at height and $p < 0.05$ at the cluster level, Gaussian random field (GRF) corrected]. Regarding the FDG-PET standardized uptake value ratio (SUVR) image, the ANCOVA was used to explore differential brain regions among the three groups (controlling for age, education level, and gender, $p < 0.001$ at height and $p < 0.05$ at cluster level, GRF corrected). The X, Y, and Z coordinates of the primary peak locations in the MNI space. MD-aMCI, multiple-domain amnestic mild cognitive impairment; SD-aMCI, single-domain amnestic mild cognitive impairment; MNI, Montreal Neurological Institute.

imaging (DSI), Chang et al. (2015) highlighted that the MD-aMCI groups have more impairment in the inferior cingulum bundle than the SD-aMCI groups, which anatomically connected with the parietal cortex.

Interestingly, MD-aMCI patients displayed reduced inter-hemispheric RSFC in CG, which is part of the extra-striate visual network and involved with the perception created by visual stimuli. Similarly, one rsfMRI study also illustrated that the MD-aMCI displayed decreased brain activity here (Li et al., 2014). On the other hand, most previous aMCI studies (without dividing into SD-aMCI and MD-aMCI) concluded that aMCI patients displayed increased intrinsic activity in CG (Han et al., 2011; Liu et al., 2012; Lou et al., 2016). This inconsistency may attribute to the aMCI heterogeneity. Besides, we found that decreased inter-hemispheric functional connectivity between bilateral CG was related to worse executive ability. Conceptually, the reaction time includes not only visual processing but also the time required for response execution (Thorpe et al., 1996). Moreover, optical encoding impairment could contribute to the reduction of processing speed (Brébion et al., 2015). Consequently, we interpreted this correlation as that the MD-aMCI patients were difficult to receive the information flows from visual sensors, further, exerting a negative influence on executive ability.

As the dominant white matter pathways, the CC links cortical hubs of the left and right hemispheres together. Here, we observed that MD-aMCI exhibited a smaller mid-posterior CC volume than the SD-aMCI and NC. Moreover, we found the selective mid-posterior CC degeneration in MD-aMCI corresponded well with the fMRI results discussed above. Specifically, regression analysis results showed that mid-posterior CC was significantly related to VMHC results, involving the bilateral MTG, PCu, CG, and PCG. In accord with our results, anatomical evidence showed that the bilateral MTG and PCu are strongly connected through the posterior CC (Cavanna and Trimble, 2006; van der Knaap and van der Ham, 2011; Wang et al., 2014). Additionally, we noted that smaller mid-posterior CC volume was related to worse executive function. This relationship suggests that CC degeneration might contribute to or even accelerate cognitive deficit (Agosta et al., 2015; Farrar et al., 2017; Luo et al., 2017b). Combined with the results of bilateral hypometabolism and inter-hemispheric disconnection, we hypothesized that mid-posterior CC atrophy may reflect the Wallerian degeneration secondary to neuronal loss caused by amyloid deposition (Bozzali et al., 2002).

Without the histological data, it was difficult to describe the exact mechanism underlying inter-hemispheric connectivity deficits in MD-aMCI patients. There are two reasons that may interpret the possible mechanism. Firstly, these deficits may result from the amyloid-related pathological process. Specifically, we found that the between-group difference results of PET-FDG and VMHC overlapped well, including the bilateral MTG, PCu, IPL, and PCG regions. Further, within these overlapping regions, the level of hypometabolism was significantly related to inter-hemispheric decrease. Nevertheless, only the metabolism indices were related to amyloid deposition. We, therefore, speculated that accumulated amyloid plaques in MD-aMCI patients might lead to synapse loss and hypometabolism, further, result in functional connectivity disruption with its contralateral regions (Tönnies and Trushina, 2017). Second, decreased inter-hemispheric functional connectivity may also result from the widespread white matter integrity disruption (White et al., 2009; Luo et al., 2016). Conclusively, these interpretations should be taken with caution due to the lack of animal study and diffusion tensor imaging (DTI) method, respectively.

Some limitations existed in our study. First, this cross-sectional study was failed to assess the long-term effects of hypometabolism and inter-hemispheric disconnection in the subsequent disease progression. Therefore, longitudinal studies are needed to explore the inter-hemispheric connection pattern following AD continuum, from healthy aging to clinical stages. Second, in accord with the inter-hemispheric functional connectivity results, correspondingly, MD-aMCI patients demonstrated selective mid-posterior CC degeneration. However, CC volume only identified the main inter-hemispheric connective tracts, rather than illustrating the precise definition of "inter-hemispheric structural connection." Therefore, future DTI studies by using tractography or network analysis are needed to provide more detailed information about inter-hemispheric white matter pathways in aMCI patients (Cavanna and Trimble, 2006; Rasero et al., 2017; Tucholka et al., 2018). In the current study, based on the ADNI 2 database, we noticed that subjects do not have both the DTI and the rsfMRI

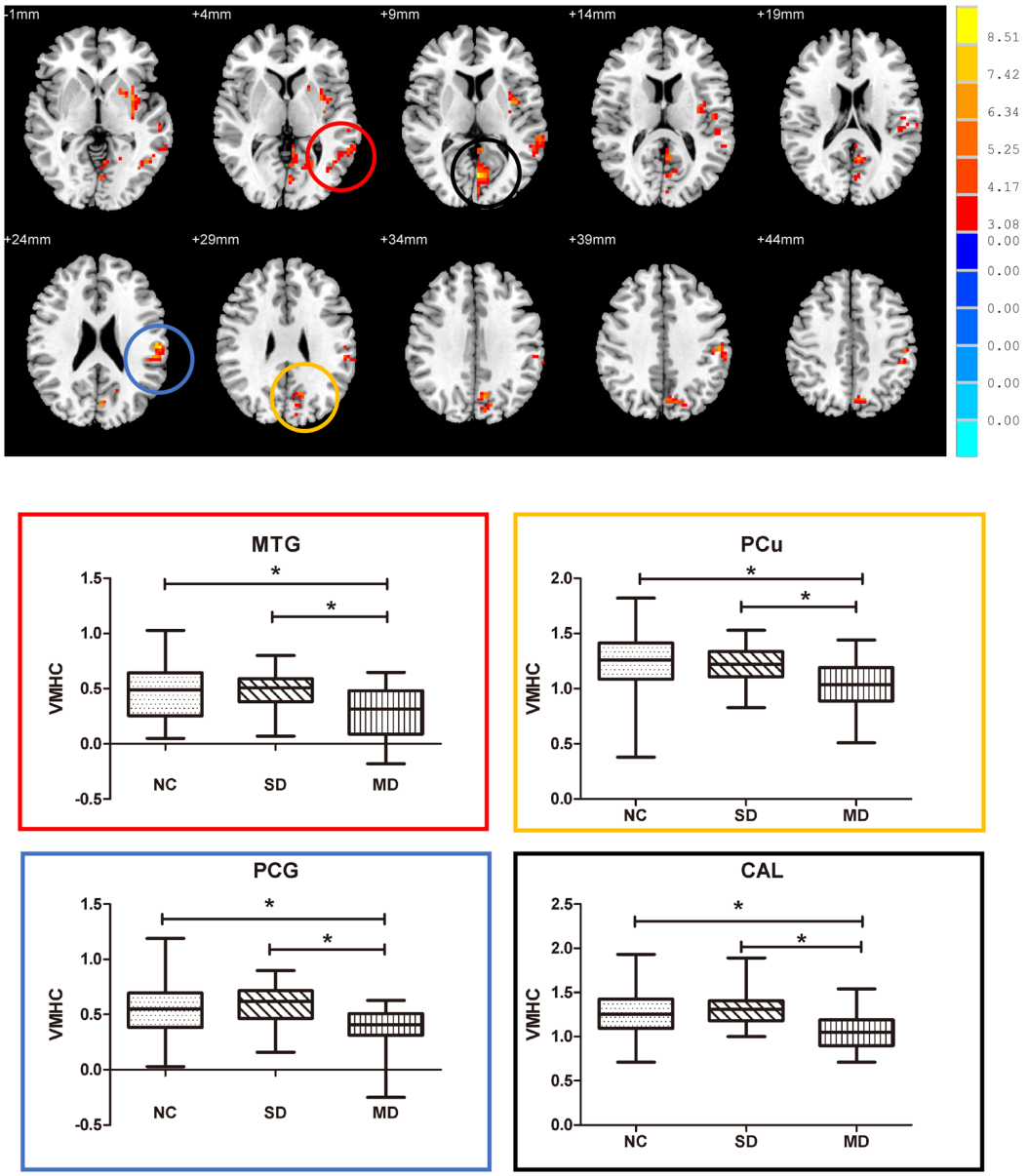


FIGURE 2 | Upper: brain areas with the significant difference of voxel-mirrored homotopic connectivity (VMHC) among normal control (NC), single-domain aMCI (SD-aMCI), and multi-domain aMCI (MD-aMCI), by controlling for age, education level, and gender. The threshold set $p < 0.05$ at height and cluster $p < 0.05$ at the cluster level, GFR corrected. Lower: we performed the *post hoc* analyses within the areas identified by the ANCOVA (corrected by Bonferroni). MD-aMCI patients displayed significantly decreased inter-hemispheric functional connectivity in bilateral middle temporal gyrus, precuneus (PCu), postcentral gyrus (PCG), and CG compared to NC and SD-aMCI patients ($p < 0.005$). But no significant difference existed between SD-aMCI patients and NC. Box graph displays mean VMHC value for middle temporal gyrus (MTG) (red), PCu (yellow), PCG (blue), and CG (black). *$p < 0.005$, Bonferroni corrected.

data. Finally, future studies with larger sample sizes are urgently required.

CONCLUSION

By using multi-modal neuroimaging methods, this study initially explored the mechanism underlying inter-hemispheric connection pattern in SD-aMCI and MD-aMCI patients. Firstly, our results support the notion that aMCI is heterogeneous. Specifically, MD-aMCI displayed more severe inter-hemispheric communication impairment while the SD-aMCI relatively preserved it. Moreover, our results demonstrate that different inter-hemispheric connectivity damage pattern contributes to distinct clinical symptoms in these two aMCI subtypes. Finally, our study shows that inter-hemispheric connectivity may serve as a potential biomarker to monitor disease progression in aMCI patients.

TABLE 3 | Comparisons of VMHC, FDG-PET SUVR, and corpus callosum subregions volume among groups.

	NC	SD-aMCI	MD-aMCI	*F*-value	*P*-value
Bi-hemispheric functional connectivity					
Middle temporal gyrus	0.48 ± 0.26	0.48 ± 0.17	0.28 ± 0.23	8.93	<0.001[bc]
Precuneus	1.23 ± 0.26	1.21 ± 0.17	1.02 ± 0.24	10.92	<0.001[bc]
Postcentral gyrus	0.54 ± 0.22	0.60 ± 0.18	0.37 ± 0.20	12.86	<0.001[bc]
Calcarine gyrus	1.25 ± 0.24	1.33 ± 0.20	1.06 ± 0.20	8.71	<0.001[bc]
Cerebral metabolism					
L Middle temporal gyrus	1.26 ± 0.12	1.14 ± 0.14	1.11 ± 0.16	11.72	<0.001[ab]
R Middle temporal gyrus	1.31 ± 0.14	1.22 ± 0.14	1.20 ± 0.15	6.94	<0.001[ab]
L Precuneus	1.55 ± 0.15	1.50 ± 0.20	1.39 ± 0.13	9.50	<0.001[bc]
L Inferior parietal lobe	1.42 ± 0.13	1.37 ± 0.13	1.26 ± 0.16	13.32	<0.001[bc]
R Inferior parietal lobe	1.48 ± 0.12	1.40 ± 0.16	1.34 ± 0.17	8.05	<0.001[b]
CC subregions volume					
CC-A	771.08 ± 113.95	781.06 ± 183.62	756.16 ± 120.71	0.26	0.77
CC-AP	374.65 ± 62.76	380.88 ± 87.48	343.75 ± 65.36	2.59	0.08
CC-C	367.82 ± 63.85	356.59 ± 77.61	337.59 ± 59.22	1.98	0.14
CC-MP	338.27 ± 61.17	342.06 ± 75.19	303.84 ± 56.78	3.61	0.03*
CC-P	921.65 ± 121.69	921.34 ± 157.03	904.50 ± 149.93	0.17	0.85

[a]*Post hoc paired comparisons showed significant group differences between NC and SD-aMCI, after Bonferroni correction ($p < 0.05$).* [b]*Post hoc paired comparisons showed significant group differences between NC and MD-aMCI, after Bonferroni correction ($p < 0.05$).* [c]*Post hoc paired comparisons showed significant group differences between SD-aMCI and MD-aMCI, after Bonferroni correction ($p < 0.05$).* **Post hoc paired comparisons showed significant group differences between NC and MD-aMCI as well as SD-aMCI and MD-aMCI, corrected by the LSD ($p < 0.05$). Data are presented as means ± SD. CC, corpus callosum; A, anterior; MA, mid-anterior; C, central; MP, mid-posterior; P, posterior.*

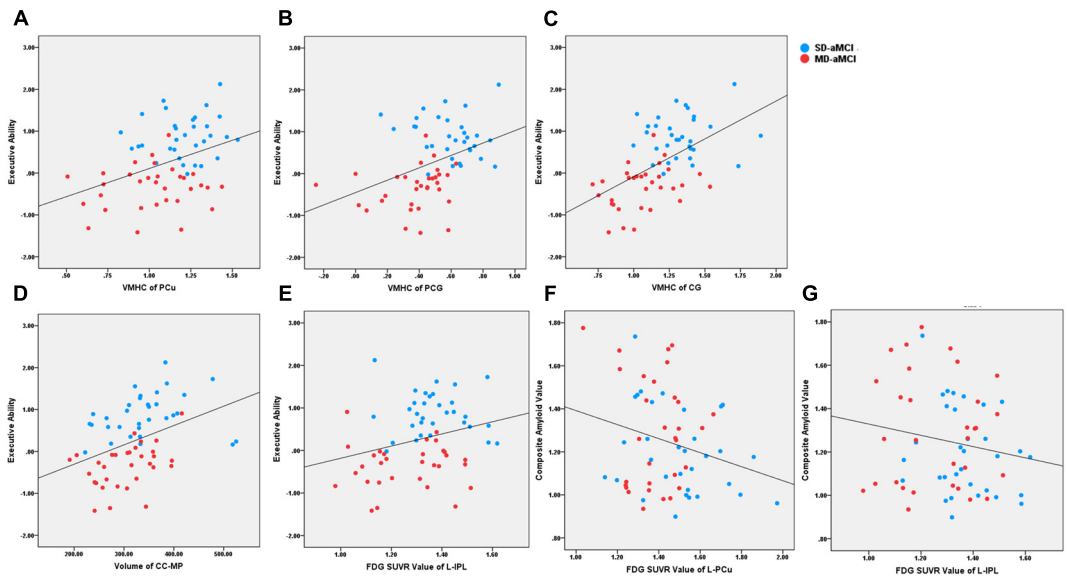


FIGURE 3 | It shows the scatter plot association between neuroimaging indices and behavioral/pathological data across aMCI patients. The blue and red dot represents the SD-aMCI and MD-aMCI patients, respectively. **(A–C)** Regarding functional connectivity, reduced inter-hemispheric functional connectivity in PCu ($r = 0.39$, $p < 0.001$), PCG ($r = 0.40$, $p < 0.001$), and CG ($r = 0.54$, $p < 0.001$) were related to the executive composite score. **(D)** The CC-MP volume was related to the executive composite score ($r = 0.40$, $p < 0.001$). **(E)** The PET-FDG SUVR uptake value in the left IPL ($r = 0.27$, $p < 0.05$) was related to executive function. **(F, G)** The PET-FDG SUVR uptake value in left PCu ($r = –0.25$, $p < 0.05$) and left IPL ($r = –0.25$, $p < 0.05$) were related to composite amyloid value reflecting by ^{18}F-florbetapir PET. Abbreviation: aMCI, amnestic mild cognitive impairment; PCu, precuneus; ITG, inferior temporal gyrus; AG, angular gyrus; CG, calcarine gyrus; PCG, postcentral gyrus; IPL, inferior parietal lobe; CC-MP, mid-posterior corpus callosum.

AUTHOR CONTRIBUTIONS

XL study design, analysis, interpretation, and writing. KL, QZ, and TQ analysis and interpretation of data, study concept, and design. PH, XX, MZ, YJ, JX, and JZ manuscript revision and statistical analysis.

FUNDING

This study was funded by National Key Research and Development Program of China (Grant No. 2016YFC1306600), Zhejiang Provincial Natural Science Foundation of China (Grant Nos. LZ14H180001 and Y16H090026), Young Research Talents Fund, Chinese Medicine Science, and Technology Project of Zhejiang Province (Grant No. 2018ZQ035). The data collection and sharing for this project were funded by the ADNI (National Institutes of Health Grant U01 AG024904) and DOD ADNI (Department of Defense Award No. W81XWH-12-2-0012). ADNI was funded by the NIA, the NIBIB, and through generous contributions from the following: AbbVie, Alzheimer's Association; Alzheimer's Drug Discovery Foundation; Araclon Biotech; Bio Clinica, Inc.; Biogen; Bristol-Myers Squibb Company; Cere Spir, Inc.; Eisai Inc.; Elan Pharmaceuticals, Inc.; Eli Lilly and Company; Euro Immun; F. Hoffmann-La Roche Ltd. and its affiliated company Genentech, Inc.; Fujirebio; GE Healthcare; IXICO Ltd.; Janssen Alzheimer Immunotherapy Research & Development, LLC.; Johnson & Johnson Pharmaceutical Research & Development LLC.; Lumosity; Lundbeck; Merck & Co., Inc.; MesoScale Diagnostics, LLC.; NeuroRx Research; Neurotrack Technologies; Novartis Pharmaceuticals Corporation; Pfizer Inc.; Piramal Imaging; Servier; Takeda Pharmaceutical Company; and Transition Therapeutics. The Canadian Institutes of Health Research is providing funds to support ADNI clinical sites in Canada. Private sector contributions are facilitated by the Foundation for the National Institutes of Health (www.fnih.org). The grantee organization is the Northern California Institute for Research and Education, and the study is coordinated by the AD Cooperative Study at the University of California, San Diego. ADNI data are disseminated by the Laboratory for Neuroimaging at the University of Southern California.

SUPPLEMENTARY MATERIAL

The Supplementary Material for this article can be found online at: https://www.frontiersin.org/articles/10.3389/fnagi.2018.00161/full#supplementary-material

REFERENCES

Agosta, F., Caso, F., Mattavelli, D., Copetti, M., Magnani, G., Canu, E., et al. (2015). Grey matter and white matter MRI markers of cognitive progression in early and late onset variants of Alzheimer's disease (P4.090). *Przegląd Lekarski* 34, 28–66.

Anderson, J. S., Druzgal, T. J., Froehlich, A., DuBray, M. B., Lange, N., Alexander, A. L., et al. (2010). Decreased interhemispheric functional connectivity in autism. *Cereb. Cortex* 21, 1134–1146. doi: 10.1093/cercor/bhq190

Ardekani, B. A., Bachman, A. H., Figarsky, K., and Sidtis, J. J. (2014). Corpus callosum shape changes in early Alzheimer's disease: an MRI study using the OASIS brain database. *Brain Struct. Funct.* 219, 343–352. doi: 10.1007/s00429-013-0503-0

Bittner, T., Zetterberg, H., Teunissen, C. E., Ostlund, R. E., Militello, M., Andreasson, U., et al. (2016). Technical performance of a novel, fully automated electrochemiluminescence immunoassay for the quantitation of β-amyloid (1–42) in human cerebrospinal fluid. *Alzheimer's Dement.* 12, 517–526. doi: 10.1016/j.jalz.2015.09.009

Bouallègue, F. B., Mariano-Goulart, D., and Payoux, P. (2017). Comparison of CSF markers and semi-quantitative amyloid PET in Alzheimer's disease diagnosis and in cognitive impairment prognosis using the ADNI-2 database. *Alzheimer's Res. Ther.* 9:32. doi: 10.1186/s13195-017-0260-z

Bozzali, M., Falini, A., Franceschi, M., Cercignani, M., Zuffi, M., Scotti, G., et al. (2002). White matter damage in Alzheimer's disease assessed in vivo using diffusion tensor magnetic resonance imaging. *J. Neurol. Neurosurg. Psychiatry* 72, 742–746. doi: 10.1136/jnnp.72.6.742

Braak, H., Alafuzoff, I., Arzberger, T., Kretzschmar, H., and Del Tredici, K. (2006). Staging of Alzheimer disease-associated neurofibrillary pathology using paraffin sections and immunocytochemistry. *Acta Neuropathol.* 112, 389–404. doi: 10.1007/s00401-006-0127-z

Brébion, G., Stephan-Otto, C., Huerta-Ramos, E., Ochoa, S., Usall, J., Abellán-Vega, H., et al. (2015). Visual encoding impairment in patients with schizophrenia: contribution of reduced working memory span, decreased processing speed, and affective symptoms. *Neuropsychology* 29, 17–24. doi: 10.1037/neu0000104

Buckner, R. L., Andrewshanna, J. R., and Schacter, D. L. (2008). The brain's default network: anatomy, function, and relevance to disease. *Ann. N. Y. Acad. Sci.* 1124, 1–38. doi: 10.1196/annals.1440.011

Busse, A., Hensel, A., Gühne, U., Angermeyer, M. C., and Riedelheller, S. G. (2006). Mild cognitive impairment: long-term course of four clinical subtypes. *Neurology* 67, 2176–2185. doi: 10.1212/01.wnl.0000249117.23318.e1

Caffarra, P., Ghetti, C., Concari, L., and Venneri, A. (2008). Differential patterns of hypoperfusion in subtypes of mild cognitive impairment. *Open Neuroimage J.* 2, 20–28. doi: 10.2174/1874440000802010020

Cavanna, A. E., and Trimble, M. R. (2006). The precuneus: a review of its functional anatomy and behavioural correlates. *Brain* 129, 564–583. doi: 10.1093/brain/awl004

Cerami, C., Della Rosa, P. A., Magnani, G., Santangelo, R., Marcone, A., Cappa, S. F., et al. (2015). Brain metabolic maps in Mild Cognitive Impairment predict heterogeneity of progression to dementia. *Neuroimage* 7, 187–194. doi: 10.1016/j.nicl.2014.12.004

Chang, Y. L., Chen, T. F., Shih, Y. C., Chiu, M. J., Yan, S. H., and Tseng, W. Y. (2015). Regional cingulum disruption, not gray matter atrophy, detects cognitive changes in amnestic mild cognitive impairment subtypes. *J. Alzheimers Dis.* 44, 125–138.

Chen, A. C., Oathes, D. J., Chang, C., Bradley, T., Zhou, Z.-W., Williams, L. M., et al. (2013). Causal interactions between fronto-parietal central executive and default-mode networks in humans. *Proc. Natl. Acad. Sci. U.S.A.* 110, 19944–19949. doi: 10.1073/pnas.1311772110

Crane, P. K., Carle, A., Gibbons, L. E., Insel, P., Mackin, R. S., Gross, A., et al. (2012). Development and assessment of a composite score for memory in the Alzheimer's Disease Neuroimaging Initiative (ADNI). *Brain Imaging Behav.* 6, 502–516. doi: 10.1007/s11682-012-9186-z

Di Paola, M., Di Iulio, F., Cherubini, A., Blundo, C., Casini, A., Sancesario, G., et al. (2010). When, where, and how the corpus callosum changes in MCI and AD A multimodal MRI study. *Neurology* 74, 1136–1142. doi: 10.1212/WNL.0b013e3181d7d8cb

Farrar, D. C., Mian, A. Z., Budson, A. E., Moss, M. B., Koo, B. B., and Killiany, R. J. (2017). Retained executive abilities in mild cognitive impairment are associated with increased white matter network connectivity. *Eur. Radiol.* 28, 340–347. doi: 10.1007/s00330-017-4951-4

Fischl, B. (2012). FreeSurfer. *Neuroimage* 62, 774–781. doi: 10.1016/j.neuroimage.2012.01.021

Friston, K. J., Williams, S., Howard, R., Frackowiak, R. S., and Turner, R. (1996). Movement-related effects in fMRI time-series. *Magn. Reson. Med.* 35, 346–355. doi: 10.1002/mrm.1910350312

Gibbons, L. E., Carle, A. C., Mackin, R. S., Harvey, D., Mukherjee, S., Insel, P., et al. (2012). A composite score for executive functioning, validated in Alzheimer's Disease Neuroimaging Initiative (ADNI) participants with baseline mild cognitive impairment. *Brain Imaging Behav.* 6, 517–527. doi: 10.1007/s11682-012-9176-1

Golob, E. J., Irimajiri, R., and Starr, A. (2007). Auditory cortical activity in amnestic mild cognitive impairment: relationship to subtype and conversion to dementia. *Brain* 130(Pt 3), 740–752. doi: 10.1093/brain/awl375

Haller, S., Nguyen, D., Rodriguez, C., Emch, J., Gold, G., Bartsch, A., et al. (2010). Individual prediction of cognitive decline in mild cognitive impairment using support vector machine-based analysis of diffusion tensor imaging data. *J. Alzheimers Dis.* 22, 315–327. doi: 10.3233/JAD-2010-100840

Han, Y., Wang, J., Zhao, Z., Min, B., Lu, J., Li, K., et al. (2011). Frequency-dependent changes in the amplitude of low-frequency fluctuations in amnestic mild cognitive impairment: a resting-state fMRI study. *Neuroimage* 55, 287–295. doi: 10.1016/j.neuroimage.2010.11.059

Janke, A. L., Zubicaray, G. D., Rose, S. E., Griffin, M., Chalk, J. B., and Galloway, G. J. (2001). 4D deformation modeling of cortical disease progression in Alzheimer's dementia. *Magn. Reson. Med.* 46, 661–666. doi: 10.1002/mrm.1243

Janowsky, J. S., Kaye, J. A., and Carper, R. A. (1996). Atrophy of the corpus callosum in Alzheimer's disease versus healthy aging. *J. Am. Geriatr. Soc.* 44, 798–803. doi: 10.1111/j.1532-5415.1996.tb03736.x

Jovicich, J., Minati, L., Marizzoni, M., Bartresfaz, D., Nobili, F., Blin, O., et al. (2016). Impairment of resting-state functional connectivity in the default-mode network closely tracks CSF biomarkers in MCI. *Alzheimers Dement.* 12:34. doi: 10.1016/j.jalz.2016.06.049

Landau, S., Harvey, D., Madison, C., Reiman, E., Foster, N., Aisen, P., et al. (2010). Comparing predictors of conversion and decline in mild cognitive impairment. *Neurology* 75, 230–238. doi: 10.1212/WNL.0b013e3181e8e8b8

Landau, S. M., Lu, M., Joshi, A. D., Pontecorvo, M., Mintun, M. A., Trojanowski, J. Q., et al. (2013). Comparing positron emission tomography imaging and cerebrospinal fluid measurements of β-amyloid. *Ann. Neurol.* 74, 826–836. doi: 10.1002/ana.23908

Li, H., Liang, Y., Chen, K., Li, X., Shu, N., Zhang, Z., et al. (2013). Different patterns of white matter disruption among amnestic mild cognitive impairment subtypes: relationship with neuropsychological performance. *J. Alzheimers Dis.* 36, 365–376. doi: 10.3233/JAD-122023

Li, X., Cao, M., Zhang, J., Chen, K., Chen, Y., Ma, C., et al. (2014). Structural and functional brain changes in the default mode network in subtypes of amnestic mild cognitive impairment. *J. Geriatr. Psychiatry Neurol.* 27, 188–198. doi: 10.1177/0891988714524629

Liu, Z., Zhang, Y., Yan, H., Bai, L., Dai, R., Wei, W., et al. (2012). Altered topological patterns of brain networks in mild cognitive impairment and Alzheimer's disease: a resting-state fMRI study. *Psychiatry Res. Neuroimage* 202, 118–125. doi: 10.1016/j.pscychresns.2012.03.002

Lou, W., Shi, L., Wong, A., Chu, W. C. W., Mok, V., and Wang, D. (2016). Changes of cerebral perfusion and functional brain network organization in patients with mild cognitive impairment. *J. Alzheimer's Dis.* 54, 397–409. doi: 10.3233/JAD-160201

Luo, X., Jiaerken, Y., Huang, P., Xu, X. J., Qiu, T., Jia, Y., et al. (2018a). Alteration of regional homogeneity and white matter hyperintensities in amnestic mild cognitive impairment subtypes are related to cognition and CSF biomarkers. *Brain Imaging Behav.* 12, 188–200. doi: 10.1007/s11682-017-9680-4

Luo, X., Jiaerken, Y., Yu, X., Huang, P., Qiu, T., Jia, Y., et al. (2017a). Affect of APOE on information processing speed in non-demented elderly population: a preliminary structural MRI study. *Brain Imaging Behav.* 11, 977–985. doi: 10.1007/s11682-016-9571-0

Luo, X., Jiaerken, Y., Yu, X., Huang, P., Qiu, T., Jia, Y., et al. (2017b). Associations between APOE genotype and cerebral small-vessel disease: a longitudinal study. *Oncotarget* 8, 44477–44489. doi: 10.18632/oncotarget.17724

Luo, X., Li, K., Jia, Y., Zeng, Q., Jiaerken, Y., Qiu, T., et al. (2018b). Abnormal of inter-hemispheric functional connectivity in elderly subjects with overweight/obesity. *Obes. Res. Clin. Pract.* doi: 10.1016/j.orcp.2018.01.003 [Epub ahead of print].

Luo, X., Qiu, T., Xu, X., Huang, P., Gu, Q., Shen, Z., et al. (2016). Decreased inter-hemispheric functional connectivity in cognitively intact elderly APOE ?4 carriers: a preliminary study. *J. Alzheime's Dis.* 50, 1137–1148. doi: 10.3233/JAD-150989

Munoz-Lopez, M., Insausti, R., Mohedano-Moriano, A., Mishkin, M., and Saunders, R. (2015). Anatomical pathways for auditory memory II: information from rostral superior temporal gyrus to dorsolateral temporal pole and medial temporal cortex. *Front. Neurosci.* 9:158. doi: 10.3389/fnins.2015.00158

Palmqvist, S., Schöll, M., Strandberg, O., Mattsson, N., Stomrud, E., Zetterberg, H., et al. (2017). Earliest accumulation of β-amyloid occurs within the default-mode network and concurrently affects brain connectivity. *Nat. Commun.* 8:1214. doi: 10.1038/s41467-017-01150-x

Palop, J. J., and Mucke, L. (2010). Amyloid-β–induced neuronal dysfunction in Alzheimer's disease: from synapses toward neural networks. *Nat. Neurosci.* 13, 812–818. doi: 10.1038/nn.2583

Petersen, R. C., Caracciolo, B., Brayne, C., Gauthier, S., Jelic, V., and Fratiglioni, L. (2014). Mild cognitive impairment: a concept in evolution. *J. Intern. Med.* 275, 214–228. doi: 10.1111/joim.12190

Qiu, Y., Liu, S., Hilal, S., Loke, Y. M., Ikram, M. K., Xu, X., et al. (2016). Inter-hemispheric functional dysconnectivity mediates the association of corpus callosum degeneration with memory impairment in AD and amnestic MCI. *Sci. Rep.* 6:32573. doi: 10.1038/srep32573

Rasero, J., Amoroso, N., La Rocca, M., Tangaro, S., Bellotti, R., Stramaglia, S., et al. (2017). Multivariate regression analysis of structural MRI connectivity matrices in Alzheimer's disease. *PLoS One* 12:e0187281. doi: 10.1371/journal.pone.0187281

Reuter, M., Schmansky, N. J., Rosas, H. D., and Fischl, B. (2012). Within-subject template estimation for unbiased longitudinal image analysis. *Neuroimage* 61, 1402–1418. doi: 10.1016/j.neuroimage.2012.02.084

Roland, J. L., Snyder, A. Z., Hacker, C. D., Mitra, A., Shimony, J. S., Limbrick, D. D., et al. (2017). On the role of the corpus callosum in interhemispheric functional connectivity in humans. *Proc. Natl. Acad. Sci. U.S.A.* 114, 13278–13283. doi: 10.1073/pnas.1707050114

Saar-Ashkenazy, R., Veksler, R., Guez, J., Jacob, Y., Shelef, I., Shalev, H., et al. (2016). Breakdown of inter-hemispheric connectivity is associated with posttraumatic symptomatology and memory impairment. *PLoS One* 11:e0144766. doi: 10.1371/journal.pone.0144766

Salvador, R., Martínez, A., Pomarol-Clotet, E., Gomar, J., Vila, F., Sarró, S., et al. (2008). A simple view of the brain through a frequency-specific functional connectivity measure. *Neuroimage* 39, 279–289. doi: 10.1016/j.neuroimage.2007.08.018

Seo, S. W., Im, K., Lee, J. M., Kim, Y. H., Kim, S. T., Kim, S. Y., et al. (2007). Cortical thickness in single- versus multiple-domain amnestic mild cognitive impairment. *Neuroimage* 36, 289–297. doi: 10.1016/j.neuroimage.2007.02.042

Shu, N., Liang, Y., Li, H., Zhang, J., Li, X., Wang, L., et al. (2012). Disrupted topological organization in white matter structural networks in amnestic mild cognitive impairment: relationship to subtype. *Radiology* 265, 518–527. doi: 10.1148/radiol.12112361

Sridharan, D., Levitin, D. J., and Menon, V. (2008). A critical role for the right fronto-insular cortex in switching between central-executive and default-mode networks. *Proc. Natl. Acad. Sci. U.S.A.* 105, 12569–12574. doi: 10.1073/pnas.0800005105

Stark, D. E., Margulies, D. S., Shehzad, Z. E., Reiss, P., Kelly, A. M., Uddin, L. Q., et al. (2008). Regional variation in interhemispheric coordination of intrinsic hemodynamic fluctuations. *J. Neurosci.* 28, 13754–13764. doi: 10.1523/JNEUROSCI.4544-08.2008

Sullivan, M. O., Jones, D. K., Summers, P. E., Morris, R. G., Williams, S. C. R., and Markus, H. S. (2001). Evidence for cortical "disconnection" as a mechanism of age-related cognitive decline. *Neurology* 57, 632–638. doi: 10.1212/WNL.57.4.632

Thorpe, S., Fize, D., and Marlot, C. (1996). Speed of processing in the human visual system. *Nature* 381, 520–522. doi: 10.1038/381520a0

Tönnies, E., and Trushina, E. (2017). Oxidative stress, synaptic dysfunction, and Alzheimer's disease. *J. Alzheimer's Dis.* 57, 1105–1121. doi: 10.3233/JAD-161088

Tucholka, A., Grau-Rivera, O., Falcon, C., Rami, L., Sánchez-Valle, R., Lladó, A., et al. (2018). Structural connectivity alterations along the Alzheimer's Disease continuum: reproducibility across two independent samples and correlation with cerebrospinal fluid Amyloid-β and Tau. *J. Alzheimer's Dis.* 61, 1575–1587. doi: 10.3233/JAD-170553

van der Knaap, L. J., and van der Ham, I. J. (2011). How does the corpus callosum mediate interhemispheric transfer? A review. *Behav. Brain Res.* 223, 211–221. doi: 10.1016/j.bbr.2011.04.018

Wang, P. N., Chou, K. H., Chang, N. J., Lin, K. N., Chen, W. T., Lan, G. Y., et al. (2014). Callosal degeneration topographically correlated with cognitive function in amnestic mild cognitive impairment and Alzheimer's disease dementia. *Hum. Brain Mapp.* 35, 1529–1543. doi: 10.1002/hbm.22271

Wang, Z., Wang, J., Zhang, H., Mchugh, R., Sun, X., Li, K., et al. (2015). Interhemispheric functional and structural disconnection in Alzheimer's disease: a combined resting-state fMRI and DTI study. *PLoS One* 10:e0126310. doi: 10.1371/journal.pone.0126310

Ward, A. M., Schultz, A. P., Huijbers, W., Dijk, K. R., Hedden, T., and Sperling, R. A. (2014). The parahippocampal gyrus links the default-mode cortical network with the medial temporal lobe memory system. *Hum. Brain Mapp.* 35, 1061–1073. doi: 10.1002/hbm.22234

White, T., Magnotta, V. A., Bockholt, H. J., Williams, S., Wallace, S., Ehrlich, S., et al. (2009). Global white matter abnormalities in schizophrenia: a multisite diffusion tensor imaging study. *Schizophr. Bull.* 37, 222–232. doi: 10.1093/schbul/sbp088

Whitwell, J. L., Petersen, R. C., Negash, S., Weigand, S. D., Kantarci, K., Ivnik, R. J., et al. (2007). Patterns of atrophy differ among specific subtypes of mild cognitive impairment. *Arch. Neurol.* 64, 1130–1138. doi: 10.1001/archneur.64.8.1130

Winblad, B., Palmer, K., Kivipelto, M., Jelic, V., Fratiglioni, L., Wahlund, L. O., et al. (2004). Mild cognitive impairment beyond controversies, towards a consensus: report of the international working group on mild cognitive impairment. *J. Intern. Med.* 256, 240–246. doi: 10.1111/j.1365-2796.2004.01380.x

Zhang, H., Sachdev, P. S., Wen, W., Kochan, N. A., Crawford, J. D., Brodaty, H., et al. (2012). Gray matter atrophy patterns of mild cognitive impairment subtypes. *J. Neurol. Sci.* 315, 26–32. doi: 10.1016/j.jns.2011.12.011

Zuo, X.-N., Kelly, C., Di Martino, A., Mennes, M., Margulies, D. S., Bangaru, S., et al. (2010). Growing together and growing apart: regional and sex differences in the lifespan developmental trajectories of functional homotopy. *J. Neurosci.* 30, 15034–15043. doi: 10.1523/JNEUROSCI.2612-10.2010

Conflict of Interest Statement: The authors declare that the research was conducted in the absence of any commercial or financial relationships that could be construed as a potential conflict of interest.

Copyright © 2018 Luo, Li, Zeng, Huang, Jiaerken, Qiu, Xu, Zhou, Xu and Zhang for the Alzheimer's Disease Neuroimaging Initiative (ADNI). This is an open-access article distributed under the terms of the Creative Commons Attribution License (CC BY). The use, distribution or reproduction in other forums is permitted, provided the original author(s) and the copyright owner are credited and that the original publication in this journal is cited, in accordance with accepted academic practice. No use, distribution or reproduction is permitted which does not comply with these terms.

frontiers in Aging Neuroscience

ORIGINAL RESEARCH
published: 13 April 2018
doi: 10.3389/fnagi.2018.00092

Influence of *APOE* and *RNF219* on Behavioral and Cognitive Features of Female Patients Affected by Mild Cognitive Impairment or Alzheimer's Disease

Alessandra Mosca[1,2,3†], Samantha Sperduti[1,4†], Viorela Pop[5], Domenico Ciavardelli[3,6], Alberto Granzotto[1,3], Miriam Punzi[1,3], Liborio Stuppia[4], Valentina Gatta[4], Francesca Assogna[7], Nerisa Banaj[7], Fabrizio Piras[7], Federica Piras[7], Carlo Caltagirone[7], Gianfranco Spalletta[7] and Stefano L. Sensi[1,3,5]**

[1] Department of Neuroscience, Imaging, and Clinical Science, Università degli Studi G. d'Annunzio Chieti e Pescara, Chieti, Italy, [2] Department of Neuroscience, Psychology, Drug Area and Child Health, University of Florence, Florence, Italy, [3] Molecular Neurology Unit, Center of Excellence on Aging and Translational Medicine, Università degli Studi G. d'Annunzio Chieti e Pescara, Chieti, Italy, [4] Department of Psychological, Health and Territorial Sciences, School of Medicine and Health Sciences, Università degli Studi G. d'Annunzio Chieti e Pescara, Chieti, Italy, [5] Department of Neurology and Pharmacology, Institute for Memory Impairments and Neurological Disorders, University of California, Irvine, Irvine, CA, United States, [6] School of Human and Social Science, Kore University of Enna, Enna, Italy, [7] Department of Clinical and Behavioral Neurology, Neuropsychiatry Laboratory, IRCCS Santa Lucia Foundation, Rome, Italy

OPEN ACCESS

Edited by:
Mohammad Amjad Kamal, King Abdulaziz University, Saudi Arabia

Reviewed by:
Khyobeni Mozhui, University of Tennessee Health Science Center, United States
Davide Ragozzino, Sapienza Università di Roma, Italy

***Correspondence:**
Gianfranco Spalletta
g.spalletta@hsantalucia.it
Stefano L. Sensi
ssensi@uci.edu

[†]These authors have contributed equally to this work.

Received: 22 November 2017
Accepted: 19 March 2018
Published: 13 April 2018

Citation:
Mosca A, Sperduti S, Pop V, Ciavardelli D, Granzotto A, Punzi M, Stuppia L, Gatta V, Assogna F, Banaj N, Piras F, Piras F, Caltagirone C, Spalletta G and Sensi SL (2018) Influence of APOE and RNF219 on Behavioral and Cognitive Features of Female Patients Affected by Mild Cognitive Impairment or Alzheimer's Disease. Front. Aging Neurosci. 10:92. doi: 10.3389/fnagi.2018.00092

The risk for Alzheimer's disease (AD) is associated with the presence of the ε4 allele of Apolipoprotein E (*APOE*) gene and, recently, with a novel genetic variant of the *RNF219* gene. This study aimed at evaluating interactions between *APOE*-ε4 and *RNF219*/G variants in the modulation of behavioral and cognitive features of two cohorts of patients suffering from mild cognitive impairment (MCI) or AD. We enrolled a total of 173 female MCI or AD patients (83 MCI; 90 AD). Subjects were screened with a comprehensive set of neuropsychological evaluations and genotyped for the *APOE* and *RNF219* polymorphic variants. Analysis of covariance was performed to assess the main and interaction effects of *APOE* and *RNF219* genotypes on the cognitive and behavioral scores. The analysis revealed that the simultaneous presence of *APOE*-ε4 and *RNF219*/G variants results in significant effects on specific neuropsychiatric scores in MCI and AD patients. In MCI patients, *RNF219* and *APOE* variants worked together to impact the levels of anxiety negatively. Similarly, in AD patients, the *RNF219* variants were found to be associated with increased anxiety levels. Our data indicate a novel synergistic activity *APOE* and *RNF219* in the modulation of behavioral traits of female MCI and AD patients.

Keywords: dementia, mild cognitive impairment (MCI), Alzheimer disease (AD), *APOE*, *RNF219*, genotype

Abbreviations: AD, Alzheimer disease; APOE, apolipoprotein E; APP, amyloid precursor protein; ART, Aligned Rank Transformation; BBB, blood–brain barrier; bp, base pair; CPM, Colored Progressive Matrices; GWASs, genome-wide-association studies; MCI, mild cognitive impairment; MMSE, Mini Mental State Examination; NPI, Neuropsychiatric Inventory; PCR, polymerase chain reaction; RAVL, Rey Auditory Verbal Learning; RNF, Ring Finger Protein.

INTRODUCTION

Alzheimer's disease is a complex syndrome characterized by a pleiotropic array of cognitive and behavioral symptoms (Selkoe, 2011). AD is mainly driven by the intraneuronal accumulation of β-amyloid, the extracellular formation of amyloid plaques and the appearance of intracellular neurofibrillary tangles composed of phosphorylated tau proteins. More recent lines of evidence support the idea that imbalance of β-amyloid production and clearance, along with phosphorylated tau and the interplay with other co-morbidity factors (metabolic, vascular, and inflammatory) work synergistically on a permissive condition represented by the aging brain to promote AD (Herrup, 2010; Corona et al., 2011; Selkoe and Hardy, 2016). Genetic and environmental factors also affect the onset and progression of the disease (Tanzi, 2012; Raskin et al., 2015).

Genome-wide-association studies have identified and confirmed more than 20 genetic variants associated with higher susceptibility to develop Late-Onset Alzheimer Disease (LOAD) of the sporadic type (Winblad et al., 2015). Among these, the ε4 allele is a specific variant of the Apolipoprotein E gene (*APOE*-ε4) and a significant risk factor for AD (Saunders et al., 1993; Bertram et al., 2007). The physio-pathological function of *APOE* is complex (Ossenkoppele et al., 2013; Tai et al., 2015) as the gene can interfere in many ways with the pillars of the disease (Ohm et al., 1999; Tanzi, 2012). As an integral part of cellular membranes, *APOE*-ε4 can influence the amyloidogenic processing of the APP and impair its clearance from the brain (Selkoe and Hardy, 2016). *APOE*-ε4 can also promote tau phosphorylation (Zhou et al., 2016) and affect metabolic and vascular factors such as hypertension, diabetes mellitus, as well as the metabolic syndrome. All these factors synergistically modulate the AD onset and progression (Duron and Hanon, 2008; Toledo et al., 2013). For instance, these factors target the physiological functioning of the neurovascular unit and the BBB integrity. Interestingly, *APOE*-ε4 has been recently shown to converge on this critical step by affecting the operation of the neurovascular unit and promoting the breakdown of proteins responsible for the BBB integrity (Montagne et al., 2015; Zhao et al., 2015). However, despite the growing body of evidence on the *APOE*-related pathogenic mechanisms, a definitive molecular roadmap on the ε4 haplotype targets remains elusive.

Recent data also indicate that a genetic variant of the *RNF219* gene may increase the risk for the AD (Rhinn et al., 2013). The rs2248663 A>G (*RNF219*/G) polymorphism of the *RNF219* gene encoding for a member of the RNF family, has been associated with earlier onset of AD when working in synergy with the *APOE*-ε4 (Rhinn et al., 2013). This accelerating effect is not present in non-ε4 and *RNF219*/A carriers, thereby indicating that the two genes may work on common pathogenic pathways. In the study, we set out to integrate with new evidence the original *RNF219* findings (Rhinn et al., 2013) and evaluated whether *APOE*-ε4 and *RNF219*/G work in synergy or independently to affect the behavioral or cognitive features of patients affected by mild cognitive impairment (MCI) or AD. To that aim, we analyzed a comprehensive set of behavioral and cognitive profiles in two cohorts of female MCI or AD patients that included carriers or non-carriers of *APOE*-ε4 and *RNF219*/G.

MATERIALS AND METHODS

Study Population

The study was approved by the Institutional and Ethics Committee of the I.R.C.C.S. Santa Lucia-Rome. All procedures were conducted in accordance with principles expressed in the Helsinki Declaration. We recruited 173 total volunteers (mean age ± standard deviation = 74 ± 7) including 83 MCI and 90 AD patients. All included subjects signed an informed consent form before enrolment. Clinical evaluations were conducted by trained psychologists and AD specialists (neurologists and psychiatrists).

Neuropsychological Assessment

Subjects were assessed with the following neuropsychological tests: MMSE, RAVL, Phonemic Verbal Fluency, CPMs, complex figure of Rey, Stroop test, and NPI. The main functional capacity was assessed by daily non-instrumental (ADL) (Wallace et al., 2007) and instrumental activities (IADL) (Lawton and Brody, 1969).

Mini Mental State Examination defines the global level of cognitive deterioration on a scale of 0–30 and targets general mental abilities, memory, attention, and language. A Score greater than or equal to 24 indicates the absence of cognitive deficits, scores ≤ 9 indicate the presence of severe cognitive deficits, scores between 10 and 18 indicate moderate cognitive deficits, and scores between 19 and 23 indicate mild cognitive deficits (Folstein et al., 1975). RAVL allows a quantitative assessment of the ability of immediate and delayed recall (Snyder and Harrison, 1997). The CPMs measure fluid intelligence (Basso et al., 1987). The complex figure of Rey is a visual-perceptual test that investigates the complex perceptual organization and long-term visual memory (Shin et al., 2006). The Stroop test examines aspects of attention and executive functions (Tremblay et al., 2016). The NPI was developed to provide a way to assess neuropsychiatric symptoms and psychopathology of patients with AD and other neurodegenerative disorders (Cummings et al., 1994). The NPI has been therefore employed to characterize neuropsychiatric profiles and is a structured interview that evaluates the following 12 behavioral domains: delusions, hallucinations, agitation, dysphoria, anxiety, apathy, irritability, euphoria, disinhibition, aberrant motor behavior, night-time behavioral disturbance, eating disorders, and weight changes.

DNA Extraction

For gene variants analysis, genomic DNA was isolated from blood samples by the PureLink Genomic DNA Mini Kit (Life Technologies, Carlsbad, CA, United States), quantified by an Agilent 8453 Spectrophotometer (Agilent, Santa Clara, CA, United States) and stored at −20°C.

APOE Genotyping

APOE genotyping was performed by direct sequencing. PCR amplification of the region containing the rs429358 and rs7412 sites that determine the ε2, ε3, or ε4 variants of the gene was carried out using the primers pair Forward: 5′-TAAGCTTGGCACGGCTGTCCAAGGA-3′ and Reverse: 5′-ACAGAATTCGCCCCGGCCTGGTACAC-3′, resulting in a 244 bp fragment (Hixson and Vernier, 1990). Purified PCR products were sequenced by the BigDye Terminator v3.1 Cycle Sequencing Kit (Life Technologies, Carlsbad, CA, United States) according to the manufacturer protocol. Sequence products were then separated on an ABI 3130xl automatic sequencer (Applied Biosystems, Paisley, United Kingdom) and analyzed using Sequencing Analysis Software (Applied Biosystems, Paisley, United Kingdom).

RNF219 Genotyping

RNF219 genotyping was carried out using High-Resolution Melting Analysis in 48-well plates on a StepOne^{TM} Real-Time PCR System run by StepOne Software v2.2.2 (Applied Biosystems, Paisley, United Kingdom) and analyzed with High-Resolution Melt Software v3.0.1 (Life Technologies, Carlsbad, CA, United States). We amplified a 103 bp fragment using the following primers pair: Forward: 5′-GG AAAAAGACAATGCAGGAAT-3′; Reverse: 5′-TTTTACCAA GGGCAACATTTC-3′. The PCR reaction, containing 20 ng of genomic DNA and the MeltDoctor HRM Master Mix (Applied Biosystems), according to the manufacturer protocols, was run as follow: enzyme activation at 95°C for 10 min; 40 cycles of denaturation and extension at 95°C for 15 s and 60°C for 1 min; melt curve with a denaturation at 95°C for 10 s, annealing at 60°C for 1 min, high resolution melting from 60 to 95°C with a ramp rate of 0.3% and final re-annealing at 60° C for 15 s. Fluorescence signals were measured during the amplification and melting steps.

Statistical Analysis

APOE and *RNF219* genotypic and allelic frequencies of female MCI and AD patients were calculated as previously described (Wigginton et al., 2005). For statistical analysis, we separated the MCI and AD cohorts in carriers and non-carriers of the two allelic variants ε4 and G. Allele frequencies of both *APOE* and *RNF219* polymorphisms were assessed for Hardy–Weinberg equilibrium (HWE) using a chi-square (χ^2) test with significance set at $p < 0.05$ (Wigginton et al., 2005).

One-way analysis of variance (ANOVA) followed by Fisher least significant difference (LSD) *post hoc* test was performed to investigate the significance of differences between age, education levels, MMSE corrected for age and education levels, the reported (by the patient or caregivers) age of appearance of the first symptom for MCI subjects, and age of onset for AD patients. Levene test was performed for assessment of homoscedasticity of the groups. Kruskal–Wallis test followed by multiple comparison of mean ranks was performed when the variances between groups were non-homogeneous.

Analysis of covariance (ANCOVA) was performed using a general linear model (GLM) approach and controlling for age and education level. *APOE* and *RNF219* genotypes were the independent factors, and the neuropsychological scores were the dependent variables. The main and interaction effects of the APOE and RNF219 genotypes were evaluated. The employed ANCOVA model is as follow: $Y_i = \beta_0 + \beta_1$ (age$_i$) $+ \beta_2$ (education level$_i$) $+ \beta_3$ (*APOE* genotype$_i$) $+ \beta_4$ (*RNF219* genotype$_i$) $+ \beta_5$ (*APOE* genotype$_i$ $\times$ *RNF219* genotype$_i$) $+ \varepsilon_i$, where Y_i indicates the specific i^{th} neuropsychological score, β_0 is the intercept, and ε_i is the error term associated with the model. In the case of ordinal variables or when the assumption of the homogeneity of the variance was rejected by the Levene test, the ART procedure was applied (Wobbrock et al., 2011; Feys, 2016). Multiple comparisons were performed using Fisher LSD *post hoc* test.

In all cases, *p*-values were corrected for multiple comparisons using the Benjamini–Hochberg correction at a false discovery rate (FDR) of 5%. *p*-Values < 0.050 were considered statistically significant. Statistical analysis was performed using Statistica 6.0 software (Statsoft, Tulsa, OK, United States).

RESULTS

Demographic and Clinical Features of MCI and AD Cohorts

The demographic and clinical characteristic of the study groups in the MCI or AD cohorts are shown in **Table 1**. The study subgroups were matched for age, education levels, and MMSE scores as well as for the reported age of the first symptoms (in the case of MCI subjects) or age of onset (in the case of AD patients).

Distribution of *APOE* and *RNF219* Genotypes in the MCI and AD Cohorts

The distribution of *APOE* and *RNF219* genotypes and relative frequencies in MCI and AD patients are shown in **Table 2**. Genotypes were in the Hardy–Weinberg equilibrium in MCI (*APOE* $p = 0.064$; *RNF219* $p = 0.36$) and AD (*APOE* $p = 0.64$; *RNF219* $p = 0.29$) patients.

Effects of the *APOE* and *RNF219* Genotypes on Behavioral Features of MCI Subjects

Our study revealed that, in MCI subjects, the anxiety-related NPI score depends on the interaction between *APOE* and *RNF219* genotypes ($p = 0.003$) (**Supplementary Table S1**). The *APOE* genotype alone showed a trend toward significant effect on the same NPI score ($p = 0.074$) (**Supplementary Table S1**). In contrast, we did not find significant effects of age or education on the anxiety trait ($p = 0.063$ and 0.16, respectively).

Post hoc multiple comparisons showed that MCI ε4/G carriers displayed increased levels of anxiety compared to other groups of patients. In fact, MCI patients carrying the ε4/G

alleles show higher levels of anxiety [median (interquartile range): 6 (6–9)] compared to MCI ε4/A carriers [median (interquartile range): 2 (0–4); $p = 0.009$], non-ε4/A carriers [median (interquartile range): 2 (0–4); $p = 0.017$] and non-ε4/G carriers [median (interquartile range): 1 (0–2.75); $p = 0.009$; **Figure 1**].

In contrast, we did not find significant main and/or interaction effects of *APOE* and *RNF219* variants on the other neuropsychological scores (**Supplementary Table S1**).

Effects of the *APOE* and *RNF219* Genotypes on Behavioral Features of AD Patients

In the case of AD patients, we found that *RNF219* variants had significant effects on anxiety-related NPI scores ($p = 0.015$). Similarly to the MCI group, in the AD cohort, we found that ε4/G carriers show higher anxiety-related NPI scores [median (interquartile range): 5.50 (1.75–8.25)] compared to

TABLE 1 | Demographic and clinical features of the study groups.

Characteristic	MCI				Levene test, *p*	One-way ANOVA or Kruskal–Wallis test, *p*
	APOE-ε*4* carrier		*APOE*-ε*4* non-carrier			
	G carrier	*G non-carrier*	*G carrier*	*G non-carrier*		
Number of participants	5	31	10	37		
Age, years; mean (SD)	72 (7)	71 (7)	69 (7)	73 (6)	0.80	0.34
Education level, mean (SD)	9 (5)	9 (5)	6 (3)	7 (3)	0.060	0.084
Reported age of first symptom, years; mean (SD)	70 (8)	68 (7)	67 (7)	71 (6)	0.76	0.39
MMSE, mean (SD)	25.5 (0.9)	25 (2)	27 (1)	26 (2)	0.069	0.22
Characteristic	**AD**				**Levene test, *p***	**One-way ANOVA or Kruskal–Wallis test, *p***
	APOE-ε*4* carrier		*APOE*-ε*4* non-carrier			
	G carrier	*G non-carrier*	*G carrier*	*G non-carrier*		
Number of participants	8	26	10	46		
Age, years; mean (SD)	79 (5)	74 (8)	79 (9)	77 (8)	0.41	0.19
Education level (years in school), mean (SD)	7 (4)	9 (5)	6 (4)	7 (3)	0.053	0.091
Age of onset, years; mean (SD)	77 (5)	72 (7)	77 (9)	75 (8)	0.52	0.18
MMSE, mean (SD)	21 (5)	20 (5)	17 (7)	20 (4)	0.41	0.21

Data are depicted as means and standard deviations (SD). Statistical analysis was performed using one-way analysis of variance (ANOVA) followed by Fisher least significant difference post hoc test or Kruskal–Wallis test followed by multiple comparison of mean ranks. Levene test was performed for assessment of homoscedasticity of the groups. False discovery rate (FDR) corrected p-values < 0.050 are shown in bold. MCI, patients with mild cognitive impairment; AD, patients with Alzheimer's disease; MMSE, mini-mental state examination score corrected for age and education levels; G carrier, RNF219/G polymorphism carrier, G non-carrier, RNF219/G polymorphism non-carrier; APOE genotype, APOE-ε4 genotype; ε4 carrier, APOE-ε4 genotype carrier; ε4 non-carrier, APOE-ε4 genotype non-carrier.

TABLE 2 | Allele and genotype frequencies of APOE and RNF219 polymorphisms in the MCI and AD groups.

		MCI (*n* = 83)			*AD* (*n* = 90)	
		n	*Frequency* (%)		*n*	*Frequency* (%)
APOE ε2/ε3/ε4 genotypes	ε2/ε2	0	0	ε2/ε2	0	0
	ε2/ε3	4	4.8	ε2/ε3	2	2.2
	ε3/ε3	43	51.8	ε3/ε3	54	60
	ε3/ε4	34	41	ε3/ε4	31	34.4
	ε4/ε4	0	0	ε4/ε4	2	2.2
	ε2/ε4	2	2.4	ε2/ε4	1	1.2
APOE ε2/ε3/ε4 alleles	ε2	6	3	ε2	3	2
	ε3	124	75	ε3	141	78
	ε4	36	22	ε4	36	20
RNF219 rs2248663 A > G genotypes	A/A	68	81.9	A/A	72	80
	A/G	15	18.1	A/G	18	20
	G/G	0	0	G/G	0	0
RNF219 rs2248663 A > G alleles	A	151	91	A	162	90
	G	15	9	G	18	10

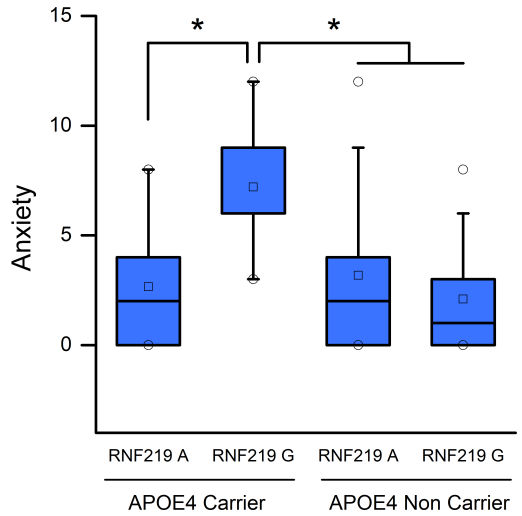


FIGURE 1 | Apolipoprotein E (APOE) and RNF219 interaction in the modulation of anxiety of MCI subjects. Box plots show a comparison of anxiety scores and statistical differences set at $p < 0.05$. Squares depict the mean values. The central horizontal bars represent the median values. The lower and the upper limits of the box represent the first and the third quartiles, respectively. Circles represent the minimum and maximum values of anxiety scores. Note that ε4/G carriers show increased anxiety-related NPI scores compared to ε4/A carriers ($p = 0.009$), non-ε4/A carriers ($p = 0.017$), and non-ε4/G carriers ($p = 0.009$). *Indicate statistically significant differences.

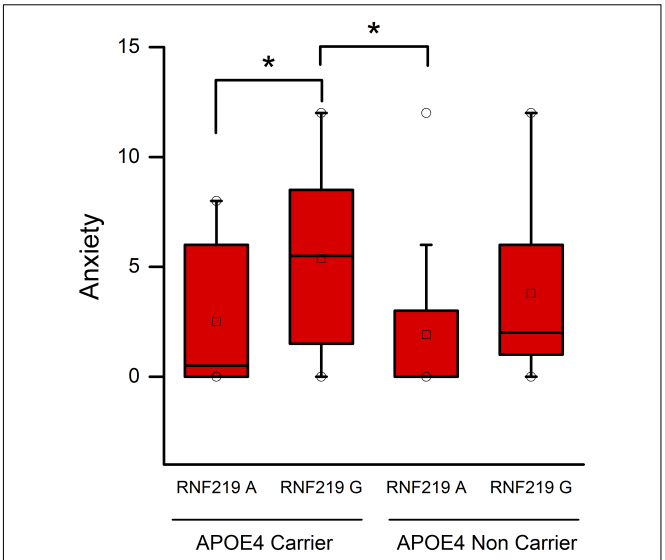


FIGURE 2 | Apolipoprotein E and RNF219 interaction in the modulation of anxiety of AD patients. Box plots show a comparison of anxiety NPI scores and statistical differences set at $p < 0.05$. Squares depict the mean values. The central horizontal bars represent the median values. The lower and the upper limits of the box represent the first and the third quartiles, respectively. Circles represent the minimum and maximum values of anxiety scores. Note that ε4/G carriers show higher anxiety-related NPI scores compared to ε4/A ($p = 0.041$) and non-ε4/A carriers ($p = 0.030$). *Indicate statistically significant differences.

ε4/A [median (interquartile range): 0.5 (0–5.5); $p = 0.041$; **Figure 2**] and non-ε4/A carriers [median (interquartile range): 0 (0–2.75); $p = 0.030$; **Figure 2**].

As for MCI subjects, we did not find any significant differences in other neuropsychological scores of the AD cohort (**Supplementary Table S2**).

DISCUSSION

In the study we explored whether *APOE*-ε4 and *RNF219*/G work in synergy or independently to affect the behavioral or cognitive features of MCI and AD patients (Rhinn et al., 2013).

In a preliminary phase of the study, we attempted to evaluate the synergistic effects of *APOE* and *RNF219* variants on behavioral and cognitive traits of male and female MCI or AD patients. However, after genotyping, we found that the sample size was too small to evaluate the effects of RNF genotype in males. Therefore, the study was redirected to investigate the impact of *APOE*-ε4 and *RNF219*/G only in female patients. We acknowledge that this is a limitation of our study and further studies will need to address effects on male patients.

In the study, we found that the *RNF219*/G variant, in synergy with the *APOE*-ε4 allele, amplifies the anxiety-related NPI scores. These scores are higher in *APOE*-ε4 and *RNF219*/G carriers of the MCI or AD cohorts (**Figures 1**, **2**).

Anxiety disorders are common late-life psychiatric features and have been associated with lower cognitive performance in older adults (Beaudreau and O'Hara, 2008). Several lines of evidence support the modifying effect of the *APOE*-ε4 status on the AD neuropsychiatric symptoms (Ungar et al., 2014). Reports indicate that anxiety and other behavioral symptoms are more prominent and severe in the population of female AD patients who are *APOE*-ε4 carriers (Steinberg et al., 2006; Xing et al., 2015), thereby supporting the notion of a relationship between the interaction of *APOE*-ε4 and gender in the phenotypical shaping of the AD-related behavioral features. The precise biological underpinning of the phenomenon is difficult to be identified. One possibility relies on the role played by estrogens in the disease progression of female patients. These hormones affect the synaptic plasticity of the AD brain as well as shape the response to AD-related pathology (Yaffe et al., 2000; Carroll and Rosario, 2012; Kang and Grodstein, 2012; Kramár et al., 2013). Hormonal changes can act on neurotrophic mechanisms and be responsible for behavioral symptoms. For instance, in females, decreased peri-menopausal levels of estrogens have been suggested to favor the onset and progression of dementia-related depression and anxiety (Aloysi et al., 2006). These estrogen-related effects can amplify the activity of *APOE*. In fact, it is well-known that *APOE*-ε4 allele acts as a negative modulator of neuropsychiatric features in AD patients (Spalletta et al., 2006; Steinberg et al., 2006; Panza et al., 2012). Moreover, levels of estradiol are known to be influenced by the expression of the *APOE*-ε4 allele and promote a worsening of neuropsychiatric symptoms in female *APOE*-ε4 carriers (Xing et al., 2012). Surprisingly, we did not find significant effects of the *APOE*-ε4 allele on neuropsychological

features such as apathy, aggressiveness, and depression. These symptoms have been previously shown in MCI or AD patients (Panza et al., 2011). A possible explanation of these divergent results may depend on the fact that our study has evaluated only female subjects while others have investigated mixed groups that included female and male patients.

The neurobiological effects of *RNF219* remain most unexplored. *RNF219* belongs to a family of proteins pleiotropically involved in many cellular functions. Some RNF proteins have been shown to modulate myelin formation (Hoshikawa et al., 2008) and the stability of GABAergic synapses (Jin et al., 2014). These proteins interfere with the activation of the ubiquitin system (Joazeiro and Weissman, 2000), a crucial mechanism for neuronal demise (Zheng et al., 2014). A role for selected RNF proteins has also been proposed in neurodegenerative processes (Pranski et al., 2013; Matz et al., 2014). In that regard, several genetic variants at the *RNF219* locus have been associated with the presence of cognitive deficits, brain atrophy and lipid deregulation (Barber et al., 2010; Cirulli et al., 2010; Furney et al., 2011). Of note, the *RNF219*/G variant has been recently associated with an earlier onset of AD (Rhinn et al., 2013).

Interestingly, recent studies in MCI patients have reported a positive relationship between the presence of high levels of anxiety and the likelihood of conversion to AD. Although the issue remains controversial (Devier et al., 2009; Breitve et al., 2016), it has been shown that anxiety is associated with the earlier conversion to AD (Gallagher et al., 2011; Mah et al., 2015). Therefore, our findings allow the speculation of a potential correlation between anxiety, RNF219/G, *APOE*-ε4 and the conversion to AD.

In our study, we did not find any significant correlation between the anxiety levels and an earlier onset age for the first cognitive symptoms for MCI subjects or AD clinical signs (data not shown). *RNF219*/G has been shown to favor an earlier presentation of the disease in AD patients who are carriers of the polymorphism. The discrepancy with our study may be related to the small sample size of our female study groups and/or a gender effect. Our findings instead show the presence of higher anxiety levels in patients who are carrying *APOE*-ε4 and *RNF219*/G. This result may support the idea of a synergistic effect of these alleles on the behavioral alteration of the disease. Future studies are needed to clarify whether and how *RNF219*/G plays in synergy with the gender and *APOE*-ε4 status to affect the neurodegenerative processes underlying dementia.

AUTHOR CONTRIBUTIONS

SLS and GS: designed the study. AM and SS: performed the experiments. AM, SS, DC, AG, MP, FaP, NB, FeP, FA, VP, LS, CC, GS, and VG: analyzed the data and interpreted the results. SS, AM, and SLS: wrote the paper. All authors approved the final version of the manuscript.

FUNDING

SLS was supported by research grants from the Italian Department of Education (PRIN 2011; Grant No. 2010M2JARJ_005) and the Italian Department of Health (Grant Nos. RF-2013-02358785 and NET-2011-02346784-1). GS and CC were supported by a grant of the Italian Department of Health (Grant No. NET-2011-02346784-1). AM was supported by a grant of the AIRAlzhOnlus-COOP Italia. FaP and FeP were supported by the Italian Department of Health (Grant No. RF-2013-02359074).

SUPPLEMENTARY MATERIAL

The Supplementary Material for this article can be found online at: https://www.frontiersin.org/articles/10.3389/fnagi.2018.00092/full#supplementary-material

TABLE S1 | Summary data and Analysis of Covariance (ANCOVA) of neuropsychological scores in MCI subjects. ANCOVA was performed in order to evaluate the main and interaction effects of APOE and RNF219 genotype controlling for age and education level. Significant *p*-values, corrected for multiple comparisons using the Benjamini–Hochberg correction at a false discovery rate (FDR) of 5%, are shown in bold.

TABLE S2 | Summary data and analysis of covariance (ANCOVA) of neuropsychological scores in AD patients. ANCOVA was performed in order to evaluate the main and interaction effects of APOE and RNF219 genotype controlling for age and education level. Significant *p*-values, corrected for multiple comparisons using the Benjamini–Hochberg correction at a false discovery rate (FDR) of 5%, are shown in bold.

REFERENCES

Aloysi, A., Van Dyk, K., and Sano, M. (2006). Women's cognitive and affective health and neuropsychiatry. *Mount Sinai J. Med.* 73, 967–975.

Barber, M. J., Mangravite, L. M., Hyde, C. L., Chasman, D. I., Smith, J. D., McCarty, C. A., et al. (2010). Genome-wide association of lipid-lowering response to statins in combined study populations. *PLoS One* 5:e9763. doi: 10.1371/journal.pone.0009763

Basso, A., Capitani, E., and Laiacona, M. (1987). Raven's coloured progressive matrices. *Funct. Neurol.* 2, 189–194. doi: 10.2466/03.04.PR0.115c25z8

Beaudreau, S. A., and O'Hara, R. (2008). Late-life anxiety and cognitive impairment: a review. *Am. J. Geriatr. Psychiatry* 16, 790–803. doi: 10.1097/JGP.0b013e31817945c3

Bertram, L., McQueen, M. B., Mullin, K., Blacker, D., and Tanzi, R. E. (2007). Systematic meta-analyses of Alzheimer disease genetic association studies: the AlzGene database. *Nat. Genet.* 39, 17–23. doi: 10.1038/ng1934

Breitve, M. H., Hynninen, M. J., Brønnick, K., Chwiszczuk, L. J., Auestad, B. H., Aarsland, D., et al. (2016). A longitudinal study of anxiety and cognitive decline in dementia with Lewy bodies and Alzheimer's disease. *Alzheimers Res. Ther.* 8:3. doi: 10.1186/s13195-016-0171-4

Carroll, J. C., and Rosario, E. R. (2012). The potential use of hormone-based therapeutics for the treatment of Alzheimer's disease. *Curr. Alzheimer Res.* 9, 18–34. doi: 10.2174/156720512799015109

Cirulli, E. T., Kasperaviciûte, D., Attix, D. K., Need, A. C., Ge, D., Gibson, G., et al. (2010). Common genetic variation and performance on standardized cognitive tests. *Eur. J. Hum. Genet.* 18, 815–820. doi: 10.1038/ejhg.2010.2

Corona, C., Pensalfini, A., Frazzini, V., and Sensi, S. L. (2011). New therapeutic targets in Alzheimer's disease: brain deregulation of calcium and zinc. *Cell Death Dis.* 2:e176. doi: 10.1038/cddis.2011.57

Cummings, J. L., Mega, M., Gray, K., Rosenberg-Thompson, S., Carusi, D. A., and Gornbein, J. (1994). The Neuropsychiatric inventory: comprehensive assessment of psychopathology in dementia. *Neurology* 44, 2308–2314. doi: 10.1212/WNL.44.12.2308

Devier, D. J., Pelton, G. H., Tabert, M. H., Liu, X., Cuasay, K., Eisenstadt, R., et al. (2009). The impact of anxiety on conversion from mild cognitive impairment to Alzheimer's disease. *Int. J. Geriatr. Psychiatry* 24, 1335–1342. doi: 10.1002/gps.2263

Duron, E., and Hanon, O. (2008). Vascular risk factors, cognitive decline, and dementia. *Vasc. Health Risk Manage.* 4, 363–381. doi: 10.2147/VHRM.S1839

Feys, J. (2016). New nonparametric rank tests for interactions in factorial designs with repeated measures. *J. Mod. Appl. Stat. Methods* 15, 78–99. doi: 10.22237/jmasm/1462075500

Folstein, M. F., Folstein, S. E., and McHugh, P. R. (1975). "Mini-mental state": a practical method for grading the cognitive state of patients for the clinician. *J. Psychiatr. Res.* 12, 189–198. doi: 10.1016/0022-3956(75)90026-6

Furney, S. J., Simmons, A., Breen, G., Pedroso, I., Lunnon, K., Proitsi, P., et al. (2011). Genome-wide association with MRI atrophy measures as a quantitative trait locus for Alzheimer's disease. *Mol. Psychiatry* 16, 1130–1138. doi: 10.1038/mp.2010.123

Gallagher, D., Coen, R., Kilroy, D., Belinski, K., Bruce, I., Coakley, D., et al. (2011). Anxiety and behavioural disturbance as markers of prodromal Alzheimer's disease in patients with mild cognitive impairment. *Int. J. Geriatr. Psychiatry* 26, 166–172. doi: 10.1002/gps.2509

Herrup, K. (2010). Reimagining Alzheimer's disease–an age-based hypothesis. *J. Neurosci.* 30, 16755–16762. doi: 10.1523/JNEUROSCI.4521-10.2010

Hixson, J. E., and Vernier, D. T. (1990). Restriction isotyping of human apolipoprotein E by gene amplification and cleavage with HhaI. *J. Lipid Res.* 31, 545–548.

Hoshikawa, S., Ogata, T., Fujiwara, S., Nakamura, K., and Tanaka, S. (2008). A novel function of RING finger protein 10 in transcriptional regulation of the myelin-associated glycoprotein gene and myelin formation in Schwann cells. *PLoS One* 3:e3464 doi: 10.1371/journal.pone.0003464

Jin, H., Chiou, T. T., Serwanski, D. R., Miralles, C. P., Pinal, N., and De Blas, A. L. (2014). Ring finger protein 34 (RNF34) interacts with and promotes γ-aminobutyric acid type-A receptor degradation via ubiquitination of the γ2 subunit. *J. Biol. Chem.* 289, 29420–29436. doi: 10.1074/jbc.M114.603068

Joazeiro, C. A. P., and Weissman, A. M. (2000). RING finger proteins?: mediators of ubiquitin ligase activity. *Cell* 102, 549–552. doi: 10.1016/S0092-8674(00)00077-5

Kang, J. H., and Grodstein, F. (2012). Postmenopausal hormone therapy, timing of initiation, APOE and cognitive decline. *Neurobiol. Aging* 33, 1129–1137. doi: 10.1016/j.neurobiolaging.2010.10.007

Kramár, E. A., Babayan, A. H., Gall, C. M., and Lynch, G. (2013). Estrogen promotes learning-related plasticity by modifying the synaptic cytoskeleton. *Neuroscience* 239, 3–16. doi: 10.1016/j.neuroscience.2012.10.038

Lawton, M. P., and Brody, E. M. (1969). Assessment of older people: self-maintaining and instrumental activities of daily living. *Gerontologist* 9, 179–186. doi: 10.1093/geront/9.3_Part_1.179

Mah, L., Binns, M. A., Steffens, D. C., and Alzheimer's Disease Neuroimaging Initiative (2015). Anxiety symptoms in amnestic mild cognitive impairment are associated with medial temporal atrophy and predict conversion to Alzheimer disease. *Am. J. Geriatr. Psychiatry* 23, 466–476. doi: 10.1016/j.jagp.2014.10.005

Matz, A., Lee, S. J., Schwedhelm-Domeyer, N., Zanini, D., Holubowska, A., Kannan, M., et al. (2014). Regulation of neuronal survival and morphology by the E3 ubiquitin ligase RNF157. *Cell Death Differ.* 22, 626–642. doi: 10.1038/cdd.2014.163

Montagne, A., Toga, A. W., and Zlokovic, B. V. (2015). Blood-brain barrier permeability and gadolinium: benefits and potential pitfalls in research. *JAMA Neurol.* 73, 13–14. doi: 10.1001/jamaneurol.2015.2960

Ohm, T. G., Scharnagl, H., März, W., and Bohl, J. (1999). Apolipoprotein E isoforms and the development of low and high Braak stages of Alzheimer's disease-related lesions. *Acta Neuropathol.* 98, 273–280. doi: 10.1007/s004010051080

Ossenkoppele, R., van der Flier, W. M., Zwan, M. D., Adriaanse, S. F., Boellaard, R., Windhorst, A. D., et al. (2013). Differential effect of APOE genotype on amyloid load and glucose metabolism in AD dementia. *Neurology* 80, 359–365. doi: 10.1212/WNL.0b013e31827f0889

Panza, F., Frisardi, V., Seripa, D., D'Onofrio, G., Santamato, A., Masullo, C., et al. (2012). Apolipoprotein E genotypes and neuropsychiatric symptoms and syndromes in late-onset Alzheimer's disease. *Ageing Res. Rev.* 11, 87–103. doi: 10.1016/j.arr.2011.06.005

Panza, F., Seripa, D., D'Onofrio, G., Frisardi, V., Solfrizzi, V., Mecocci, P., et al. (2011). Neuropsychiatric symptoms, endophenotypes, and syndromes in late-onset Alzheimer's disease: focus on APOE gene. *Int. J. Alzheimers Dis.* 2011:721457. doi: 10.4061/2011/721457

Pranski, E. L., Dalal, N. V., Sanford, C. V., Herskowitz, J. H., Gearing, M., Lazo, C., et al. (2013). RING finger protein 11 (RNF11) modulates susceptibility to 6-OHDA-induced nigral degeneration and behavioral deficits through NF-kB signaling in dopaminergic cells. *Neurobiol. Dis.* 54, 264–279. doi: 10.1016/j.nbd.2012.12.018

Raskin, J., Cummings, J., Hardy, J., Schuh, K., and Dean, R. A. (2015). Neurobiology of Alzheimer's disease: integrated molecular, physiological, anatomical, biomarker, and cognitive dimensions. *Curr. Alzheimer Res.* 12, 712–722. doi: 10.1186/s40478-014-0134-6

Rhinn, H., Fujita, R., Qiang, L., Cheng, R., Lee, J. H., and Abeliovich, A. (2013). Integrative genomics identifies APOE ε4 effectors in Alzheimer's disease. *Nature* 500, 45–50. doi: 10.1038/nature12415

Saunders, A. M., Strittmatter, W. J., Schmechel, D., George-Hyslop, P. H., Pericak-Vance, M. A., Joo, S. H., et al. (1993). Association of apolipoprotein E allele epsilon 4 with late-onset familial and sporadic Alzheimer's disease. *Neurology* 43, 1467–1472. doi: 10.1212/WNL.43.8.1467

Selkoe, D. J. (2011). Alzheimer's disease. *Cold Spring Harb. Perspect. Biol.* 3:a004457. doi: 10.1101/cshperspect.a004457

Selkoe, D. J., and Hardy, J. (2016). The amyloid hypothesis of Alzheimer's disease at 25 years. *EMBO Mol. Med.* 8, 595–608. doi: 10.15252/emmm.201606210

Shin, M.-S., Park, S. Y., Park, S. R., Seol, S. H., and Kwon, J. S. (2006). Clinical and empirical applications of the Rey–Osterrieth Complex Figure Test. *Nat. Protoc.* 1, 892–899. doi: 10.1038/nprot.2006.115

Snyder, K. A., and Harrison, D. W. (1997). The affective auditory verbal learning test. *Arch. Clin. Neuropsychol.* 12, 477–482. doi: 10.1093/arclin/12.5.477

Spalletta, G., Bernardini, S., Bellincampi, L., Federici, G., Trequattrini, A., and Caltagirone, C. (2006). Delusion symptoms are associated with ApoE epsilon4 allelic variant at the early stage of Alzheimer's disease with late onset. *Eur. J. Neurol.* 13, 176–182. doi: 10.1111/j.1468-1331.2006.01165.x

Steinberg, M., Corcoran, C., Tschanz, J. T., Huber, C., Welsh-Bohmer, K., Norton, M. C., et al. (2006). Risk factors for neuropsychiatric symptoms in dementia: the Cache County Study. *Int. J. Geriatr. Psychiatry* 21, 824–830. doi: 10.1002/gps.1567

Tai, L. M., Ghura, S., Koster, K. P., Liakaite, V., Maienschein-Cline, M., Kanabar, P., et al. (2015). APOE-modulated Aβ-induced neuroinflammation in Alzheimer's disease: current landscape, novel data, and future perspective. *J. Neurochem.* 133, 465–488. doi: 10.1111/jnc.13072

Tanzi, R. E. (2012). The genetics of Alzheimer disease. *Cold Spring Harb. Perspect. Med.* 2:a006296. doi: 10.1101/cshperspect.a006296

Toledo, J. B., Arnold, S. E., Raible, K., Brettschneider, J., Xie, S. X., Grossman, M., et al. (2013). Contribution of cerebrovascular disease in autopsy confirmed neurodegenerative disease cases in the National Alzheimer's Coordinating Centre. *Brain* 136(Pt 9), 2697–2706. doi: 10.1093/brain/awt188

Tremblay, M.-P., Potvin, O., Belleville, S., Bier, N., Gagnon, L., Blanchet, S., et al. (2016). The victoria stroop test: normative data in Quebec-French adults and elderly. *Arch. Clin. Neuropsychol.* doi: 10.1093/arclin/acw029 [Epub ahead of print].

Ungar, L., Altmann, A., and Greicius, M. D. (2014). Apolipoprotein E, gender, and Alzheimer's disease: an overlooked, but potent and promising interaction. *Brain Imaging Behav.* 8, 262–273. doi: 10.1007/s11682-013-9272-x

Wallace, M., Shelkey, M., and Hartford Institute for Geriatric Nursing (2007). Katz index of independence in activities of daily living (ADL). *Urol. Nurs.* 27, 93–94.

Wigginton, J. E., Cutler, D. J., and Abecasis, G. R. (2005). A note on exact tests of Hardy-Weinberg equilibrium. *Am. J. Hum. Genet.* 76, 887–893. doi: 10.1086/429864

Winblad, B., Amouyel, P., Andrieu, S., Ballard, C., Brayne, C., Brodaty, H., et al. (2015). Defeating Alzheimer's disease and other dementias: a priority for European science and society. *Lancet Neurol.* 15, 455–532. doi: 10.1016/S1474-4422(16)00062-4

Wobbrock, J. O., Findlater, L., Gergle, D., and Higgins, J. J. (2011). *The Aligned Rank Transform for Nonparametric Factorial Analyses Using Only ANOVA Procedures*. Available at: https://faculty.washington.edu/wobbrock/pubs/chi-11.06.pdf [accessed January 27, 2018].

Xing, Y., Qin, W., Li, F., Jia, X. F., and Jia, J. (2012). Apolipoprotein E ε4 status modifies the effects of sex hormones on neuropsychiatric symptoms of Alzheimer's disease. *Dement. Geriatr. Cogn. Disord.* 33, 35–42. doi: 10.1159/000336600

Xing, Y., Tang, Y., and Jia, J., (2015). Sex differences in neuropsychiatric symptoms of Alzheimer's disease: the modifying effect of apolipoprotein E ε4 status. *Behav. Neurol.* 2015:275256. doi: 10.1155/2015/275256

Yaffe, K., Haan, M., Byers, A., Tangen, C., and Kuller, L. (2000). Estrogen use, APOE, and cognitive decline: evidence of gene-environment interaction. *Neurology* 54, 1949–1954. doi: 10.1212/WNL.54.10.1949

Zhao, Z., Nelson, A. R., Betsholtz, C., and Zlokovic, B. V. (2015). Establishment and dysfunction of the blood-brain barrier. *Cell* 163, 1064–1078. doi: 10.1016/j.cell.2015.10.067

Zheng, C., Geetha, T., and Babu, J. R. (2014). Failure of ubiquitin proteasome system: risk for neurodegenerative diseases. *Neurodegener. Dis.* 14, 161–175. doi: 10.1159/000367694

Zhou, M., Huang, T., Collins, N., Zhang, J., Shen, H., Dai, X., et al. (2016). APOE4 induces site-specific tau phosphorylation through calpain-CDK5 signaling pathway in EFAD-Tg mice. *Curr. Alzheimer Res.* 13, 1048–1055. doi: 10.2174/1567205013666160415154550

Conflict of Interest Statement: The authors declare that the research was conducted in the absence of any commercial or financial relationships that could be construed as a potential conflict of interest.

Copyright © 2018 Mosca, Sperduti, Pop, Ciavardelli, Granzotto, Punzi, Stuppia, Gatta, Assogna, Banaj, Piras, Piras, Caltagirone, Spalletta and Sensi. This is an open-access article distributed under the terms of the Creative Commons Attribution License (CC BY). The use, distribution or reproduction in other forums is permitted, provided the original author(s) and the copyright owner are credited and that the original publication in this journal is cited, in accordance with accepted academic practice. No use, distribution or reproduction is permitted which does not comply with these terms.

frontiers in Aging Neuroscience

ORIGINAL RESEARCH
published: 06 February 2018
doi: 10.3389/fnagi.2018.00026

Identification of a Novel Hemizygous SQSTM1 Nonsense Mutation in Atypical Behavioral Variant Frontotemporal Dementia

Lin Sun[1†], *Zhouyi Rong*[2†], *Wei Li*[1], *Honghua Zheng*[2,3*], *Shifu Xiao*[1*] *and Xia Li*[1*]

[1] *Shanghai Mental Health Center, Alzheimer's Disease and Related Disorders Center, Shanghai Jiao Tong University School of Medicine, Shanghai, China,* [2] *Fujian Provincial Key Laboratory of Neurodegenerative Disease and Aging Research, Institute of Neuroscience, College of Medicine, Xiamen University, Xiamen, China,* [3] *Department of Neuroscience, Shenzhen Research Institute of Xiamen University, Shenzhen, China*

Frontotemporal dementia includes a large spectrum of neurodegenerative disorders. *SQSTM1*, coding for p62 protein, plays a vital role in the pathogenesis of FTD. Here, we report a case of a female patient with *SQSTM1* mutation S224X, who was 59 years old when she initially exhibited memory decline, mild personality changes, and subtle atrophy of frontal/temporal lobes in magnetic resonance imaging (MRI). Genetic testing revealed a nonsense mutation of the *SQSTM1* gene (S224X), resulting in premature termination of protein synthesis and a predicted truncated protein 217 amino acids shorter than the normal protein. Moreover, neither intact nor truncated SQSTM1 proteins was detectable in *SQSTM1* S224X mutant overexpressing HEK-293T cells. We assayed for *SQSTM1* cDNA in samples from the patient's peripheral leucocytes, and did not detect its mutation. The test of quantitative PCR showed significant decreased level of *SQSTM1* mRNA from peripheral leucocytes of the patient compared to five dementia controls. Our results identify a novel pathogenic *SQSTM1* S224X mutation in an atypical FTD patient accompanied with loss of SQSTM1/p62 protein expression probably due to *SQSTM1* gene haploinsufficiency.

Keywords: Frontotemporal dementia, FTD, *SQSTM1*, p62, S224X, nonsense mutation

OPEN ACCESS

Edited by:
Athanasios Alexiou, Novel Global Community Educational Foundation (NGCEF), Hebersham, Australia

Reviewed by:
Daniel Hesselson, Garvan Institute of Medical Research, Australia
Melissa Calegaro Nassif, Universidad Mayor, Chile

***Correspondence:**
Honghua Zheng
honghua@xmu.edu.cn
Shifu Xiao
xiaoshifu@msn.com
Xia Li
ja_1023@hotmail.com

[†] *These authors have contributed equally to this work.*

Received: *25 November 2017*
Accepted: *22 January 2018*
Published: *06 February 2018*

Citation:
Sun L, Rong Z, Li W, Zheng H, Xiao S and Li X (2018) Identification of a Novel Hemizygous SQSTM1 Nonsense Mutation in Atypical Behavioral Variant Frontotemporal Dementia. Front. Aging Neurosci. 10:26. doi: 10.3389/fnagi.2018.00026

INTRODUCTION

Frontotemporal dementia is the second common form of neurodegenerative dementia in presenile population, characterized by atrophy of frontal and/or temporal lobes, and is frequently linked to genetic mutations (Miller et al., 2015; Luis et al., 2016). The three primary clinical FTD subtypes include behavioral variant FTD (bvFTD), nonfluent variant primary progressive aphasia (nfvPPA), and semantic variant primary progressive aphasia (svPPA) (Miller et al., 2015; O'Connor et al., 2016). As the most common presentation, bvFTD presents as a progressive change in personality with abnormalities in social-emotional behavior, and its diagnosis remains difficult, with patients being erroneously considered as having Alzheimer's disease or psychiatric disorders (Pottier et al., 2016; Tosun et al., 2016). The definite diagnosis is based on three major pathological subtypes characterized by the presence of 43 kDa TAR DNA-binding protein (TDP43), tau, or fused in sarcoma (FUS) positive neuronal inclusions (Boutoleau-Bretonniere et al., 2015). Approximately 30–50% of FTD patients have a positive family history, and 10% exhibit an autosomal dominant

mode of inheritance. Mutations in the genes that encode microtubule associated protein tau (MAPT), progranulin and C9orf72 are the most common causes of FTD (Sun et al., 2017). Sequestosome 1 (SQSTM1), coding for p62 protein, is an adaptor protein that contains several protein-protein interaction motifs and serves as a signaling hub in a variety of key cellular processes including cell differentiation, transcriptional regulation, apoptosis, and oxidative stress response (Rea et al., 2014). SQSTM1, which has been identified in FTD in 2012 (Rubino et al., 2012), suggesting a role in the pathogenesis of neurodegenerative disease (Boutoleau-Bretonniere et al., 2015), is initially considered as a monogenic cause of Paget disease of bone (PDB) in 2002 (Laurin et al., 2002) and amyotrophic lateral sclerosis in 2011 (Fecto et al., 2011). Mutation in the *SQSTM1* gene is a rare cause of FTD and ALS (van der Zee et al., 2014). Rubino et al. only identified 3 missense mutations in the *SQSTM1* gene in 3 of 170 Italian patients with FTD, and 3 missense variants in 3 of 124 Italian patients with ALS (Rubino et al., 2012).

Here we report an atypical bvFTD patient with memory decline as an initial symptom and mild personality change emerging gradually, carried a novel pathogenic variant of the *SQSTM1* gene causing absent expression of SQSTM1/p62 protein.

MATERIALS AND METHODS

Genetic Procedures

Total genomic DNA was prepared and amplified from peripheral blood according to standard procedures. The quality of DNA was assessed by Qubit 3.0 (Thermo Fisher, USA) and agarose gel electrophoresis. Then the sequencing library was prepared according to the SureSelectXT Target Enrichment System Manual (Agilent, USA), and whole exome sequencing was performed by HiSeq X Ten (Illumina, USA). After this next-generation sequencing and bio-information analysis of the sequencing data, especially AD and FTD related genes including *APP*, *PSEN1*, *PSEN2*, *MAPT*, *GRN*, *CHMP2B*, *C9ORF72*, *VCP*, *FUS*, *SQSTM1*, *TREM2*, *TYROBP* etc., we found that there was a nonsense mutation in *SQSTM*1 gene. The nonsense mutation of *SQSTM1* gene were analyzed by Sanger sequencing (forward primer: 5′-AGCGTCTGCCCAGACTACGA-3′ and reverse primer: 5′-CAGGCACTTAGGCACCTCAG-3′, the values of Tm were 63.4 and 61.0 respectively, and the length of amplified product is 547 bp). Moreover, we detected *APOE* genotyping at locus of rs429358 and rs7412. The software of Mutation Taster was applied to predict the pathogenicity of the detected mutations (http://www.mutationtaster.org/).

Analysis of SQSTM1 Mutant Protein Expression

Plasmid DNA for wild type *SQSTM1* was prepared by inserting coding sequence of the human *SQSTM1* gene (NM_003900) into the pcDNA3.1/Myc-His vector, and the *SQSTM1* S224X mutation was obtained by PCR-based site-directed mutagenesis with c.671C>A. All constructs were verified by sequencing (Minbo Biotech, Xiamen, China). Human embryonic kidney cells (HEK 293T) were grown to 80% confluence and transfected with vectors by Turbofect Transfection Reagent (Thermo Fisher, USA) according to the manufacturer's instructions. Media were then replaced with fresh DMEM containing 10% FBS. Cells were then collected 24 h later for western blotting. Equal amounts of total proteins (20 μg) were subjected to SDS-PAGE and transferred to PVDF membrane (Millipore, USA). Membranes were incubated with antibodies specific for SQSTM1 Gly162 (Cell Signaling Technology, 8025, USA), SQSTM1 Gly410 (Cell Signaling Technology, 5114, USA), Myc (Proteintech, 16282-1-AP, USA), or GAPDH (Abcam, ab181602, USA). Proteins were quantified using ImageJ Software.

Characterization of SQSTM1 Gene Expression

The mutation S224X (c.671 C>A) of *SQSTM1* cDNA amplicons were obtained from the patient's mRNA sample by RT-PCR reaction. The cycling parameters of RT-PCR were 3 min at 95°C, followed by 30 s at 94°C, followed by 35 cycles of 60°C for 30 s, 72°C for 30 s, and a final extension of 72°C for 5 min. The pair of PCR primer sequence included the forward primer 5′-CTGTCTGAGGGCTCTCGC-3′ and reverse primer 5′-TCAACTTAATGCCCAGAGG-3′. The pyrosequencing and Sanger sequencing were performed following the manufacturer's protocols (Sangon, China). The analysis was used through PyroMark Software 1.0.11 software environment (Sangon, China).

Total cellular RNA was extracted from cell culture using TRIzol (Invitrogen, USA) according to manufacturer's procedures. Real-time PCR analysis was performed using 7900HT PCR instrument (ABI, USA). PCR conditions were at 95°C for 1 min, followed by 40 cycles at 95°C for 15 s, and 60°C for 30 s. For each biological replicate, three technical replicates were performed. The pair of PCR primer sequence included the forward primer 5′-TGGCGGAGCAGATG AGGAAG-3′ and reverse primer 5′-GGACTGGAGTTCACCTGTAGACG-3′.

Statistical Analysis

All data are presented as mean ± standard error of mean. The data were analyzed by one-way analysis of variance (ANOVA). Results were considered to be statistically different when $p < 0.05$.

Ethics and Patient Consent

We received approval from the regional ethical standards committee on human experimentation for our experiments using human materials. We also received written informed consent for research from the participants and guardians.

RESULTS

Case Report

The patient underwent a clinical evaluation at our institution and was then enrolled in the Foundation of China Alzheimer's disease and related disorders study. Additional data from the proband and her relatives were collected and analyzed.

A 65-year-old, right-handed female with 15 years of school education was first seen in our geriatric psychiatry department in December 2016 for memory difficulties over 6 years combined

with mild personality change over 1 year. She received surgical treatment for oophoroma in 2005 and drug treatment for hyperthyroidism in 2015, and gained full control of both diseases.

Her caregiver described the patient's forgetfulness at age 59, which had developed insidiously. She was referred to hospital because of memory decline and depression, and was prescribed antidepressant drugs. The patient refused to take the medications, and went on to care for her sick mother. At 5 years post-onset of symptoms, she began to lose her way and fall occasionally. In June 2015, she fell, resulting in cracking her head and bleeding. Her family brought her to hospital for testing. The brain computed tomography (CT) revealed cerebral atrophy, and electromyogram/ nerve conduction velocity (EMG/NCV) showed no positive finding. Subsequently, therapy with huperzine A was initiated. However, the patient took the medication irregularly, and her condition gradually aggravated. In May 2016, her family noticed her daytime somnolence, sluggishness, and reticence. Magnetic resonance imaging (MRI) showed mild atrophy of the cerebral cortex. Subsequently, combination therapy with Exelon and Escitalopram was started. In December 2016, the patient was brought to our department, and standard blood tests were normal. The neurological evaluation showed slow gait, normal muscular tension, brisk tendon reflexes, positive sign of bilateral palm-chin reflex, and negative Babinski sign. Her Mini Mental State Examination (MMSE) score was 20/30 and Montreal Cognitive Assessment (MoCA) score 15/30 (**Figures 1A,B**). Brain MRI in Dec 2016 revealed subtle atrophy in frontal and temporal lobes (**Figure 1C**). Although these findings did not lead to a definitive diagnosis, Memantine, Exelon, and Sertraline were administered as therapy. After 10 months, she was referred to our department again, and complained more serious memory decline. Her MMSE score was 12/30, and MoCA 10/30 (**Figures 1A,B**). However, brain MRI in Oct 2017 revealed no significant difference when compared with the last MRI (**Figure 1D**).

The family history is summarized in **Figure 2B**. There are no similar manifestations in the relatives of the patient.

Genetic Analysis

The mutation c.671 C>A, p. S224X of *SQSTM1* was detected by whole exome sequencing, and validated in gDNA by Sanger Sequencing (**Figure 2A**). This mutation has not been reported as pathogenic elsewhere, and is predicted to lead to premature termination of protein synthesis. The pathogenicity prediction of the nonsense mutation by Mutation Taster software was disease causing with a probability equal to 1. The Combined Annotation Dependent Depletion (CADD) predicted that Raw score was 6.91 and PHRED was 33. The mutation was not found in the dbSNP, 1000G, HGMD, or ExAC database. At the same time, we didn't detect the same mutation in 200 normal Chinese individuals. The mutation site of the *SQSTM1* gene was also assessed by evaluating the patient's unaffected younger sister, who did not carry the same mutation. Because the patient's father and mother were deceased, we could not determine whether the mutation was hereditary. The p.S224X heterozygous nonsense mutation is located at highly conserved position, as shown by a comparison of the corresponding sequences of 10 vertebrates (**Figure 2C**). The *APOE* genotype of the patient was *ε3/ε4*.

Analysis of SQSTM1 Mutant Protein Expression

HEK 293T cells were transfected with an empty-vector control or plasmids encoding either wild type or S224X mutant Myc-His tagged *SQSTM1* for 24 h. SQSTM1 was recognized in western blotting by different antibodies, which were SQSTM1 Gly162 and SQSTM1 Gly410 directed upstream and downstream, respectively, of the SQSTM1 mutation site (S224X). The SQSTM1

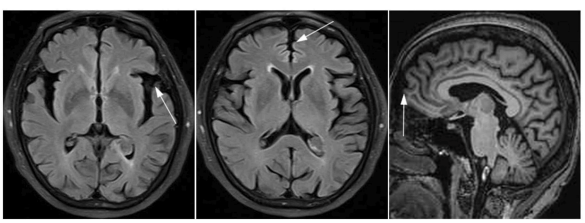
A

MMSE Category	2016.12 (6 year post onset)	2017.10 (6 year and 10 month post onset
orientation	7	4
attention and calculation	3	1
recall	3	3
language	5	3
execution	2	1
visual construction	0	0
total	20	12

B

MoCA Category	2016.12 (6 year post onset)	2017.10 (6 year and 10 month post onset)
visual-construction	1	1
alternate line	0	0
recall	0	0
attention and calculation	6	4
language	2	0
abstraction	1	1
orientation	5	4
Total	15	10

C



D

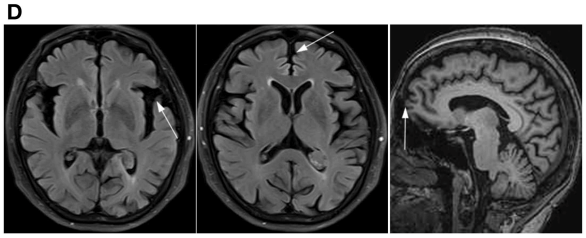


FIGURE 1 | Summary of MMSE and MoCA, and imaging data. Summary of MMSE **(A)** and MoCA **(B)** scores in Dec 2016 and Oct 2017 displayed the significant damage in cognitive function and decline trend with time. The brain MRI in Dec 2016 **(C)** and Oct 2017 **(D)** showed subtle atrophy of frontal and temporal lobes on transverse FLAIR weighted and sagittal T1 weighted sequences.

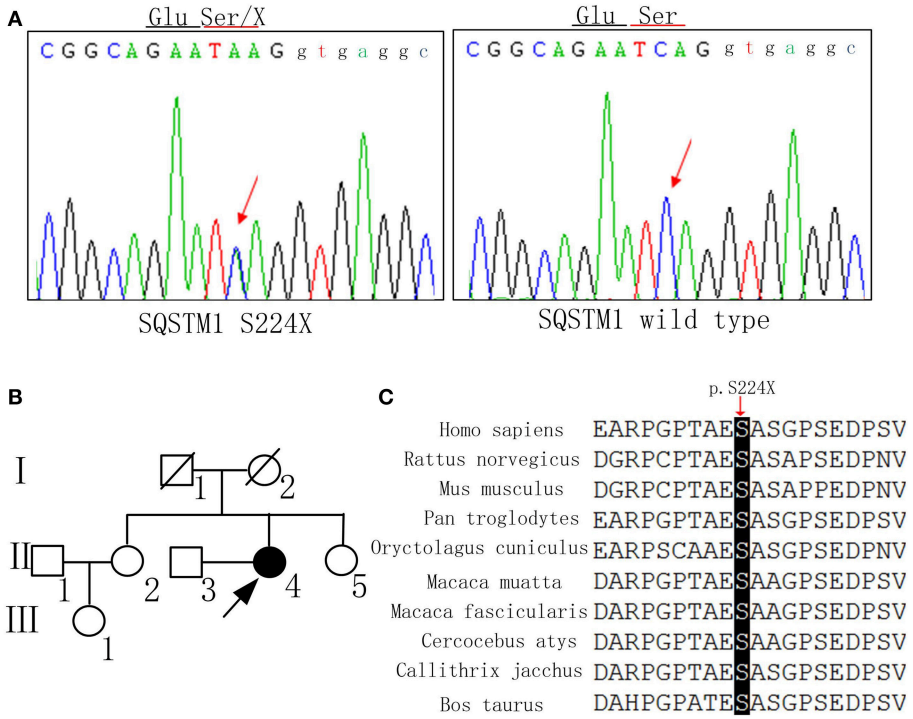


FIGURE 2 | DNA sequence, pedigree of the family, and gene conservation. **(A)** DNA sequence at codon 224 of *SQSTM1* gene from the patient and a control. The arrow indicates a mutated hemizygous site and a normal homozygous site, respectively. **(B)** The proband is indicated by an arrow (II-4). Her younger sister (II-5) also received the gene test and did not carry the same mutation. **(C)** The p.S224X heterozygous nonsense mutation occurs at highly conserved position, as shown by a comparison of the corresponding sequences of 10 vertebrates.

Gly162 antibody was used to detect truncated and intact SQSTM1 protein, and Gly410 to detect intact SQSTM1 protein (**Figure 3A**). Western blotting demonstrated that the levels of intact or truncated SQSTM1 protein in the S224X mutation group were all significantly reduced compared to wild type, similar to the vehicle ($p < 0.01$) (**Figure 3B**). Western blotting of Myc protein demonstrated no detectable Myc protein in the vehicle or S224X mutation group, only in the *SQSTM1* wild type group (**Figure 3A**).

Analysis of SQSTM1 Gene Expression

SQSTM1 cDNA was amplified by RT-PCR from mRNA extracted from peripheral blood leucocytes of the patient. We did not find the same mutation in *SQSTM1* cDNA (**Figures 3C,D**) through pyrosequencing or Sanger sequencing, which was inconsistent with DNA sequencing result. For analyzing the gene transcription differences between the *SQSTM1* S224X mutation and *SQSTM1* wild type, we included another five dementia controls (female: 3, male: 2, and age matched) without the *SQSTM1* mutation. The relative transcription of *SQSTM1* normalized to β-actin was analyzed using the concept of the threshold cycle (Ct) comparative method. Although the small sized of the samples adopted in the present study, it seemed that all dementia controls without *SQSTM*1 mutation presented an increased relative transcription level of *SQSTM1* mRNA (up to 3.06 ± 0.88-fold) with regards to the patient ($p < 0.05$) (**Figure 3E**).

DISCUSSION

The patient exhibited early-onset dementia combined with the initial symptom of memory decline, a gradual appearance of mild personality change, subtle atrophy of frontal/temporal lobes in MRI, negative appearance in EMG/NCV, and rapidly progressive course. The data of whole exome sequencing showed that AD related genes were all negative. These findings suggested an atypical bvFTD. The *SQSTM1* mutation (S224X) was found in the patient, which produced a stop codon and resulted in a predicted truncated protein 217 amino acids shorter than the normal SQSTM1 protein. *SQSTM1* has been reported to be associated with FTD-ALS type 3 (MIM: 616437). There isn't positive finding of EMG/NCV at present, but it still needs time to follow up the patient. The mutation is novel, not appearing in the dbSNP, 1000G, HGMD, ExAC database, and 200 normal Chinese individuals. The pathogenicity prediction by the Mutation-Taster application was disease causing, with a probability equal to 1. To determine the pathogenicity of this mutation, we overexpressed *SQSTM1* S224X mutant comparable to that of wild type *SQSTM1* in cell culture. Western blot of SQSTM1 recognized by Gly 410 and Gly 162 antibodies showed significant decrease of fully intact protein and truncated protein of SQSTM1. There

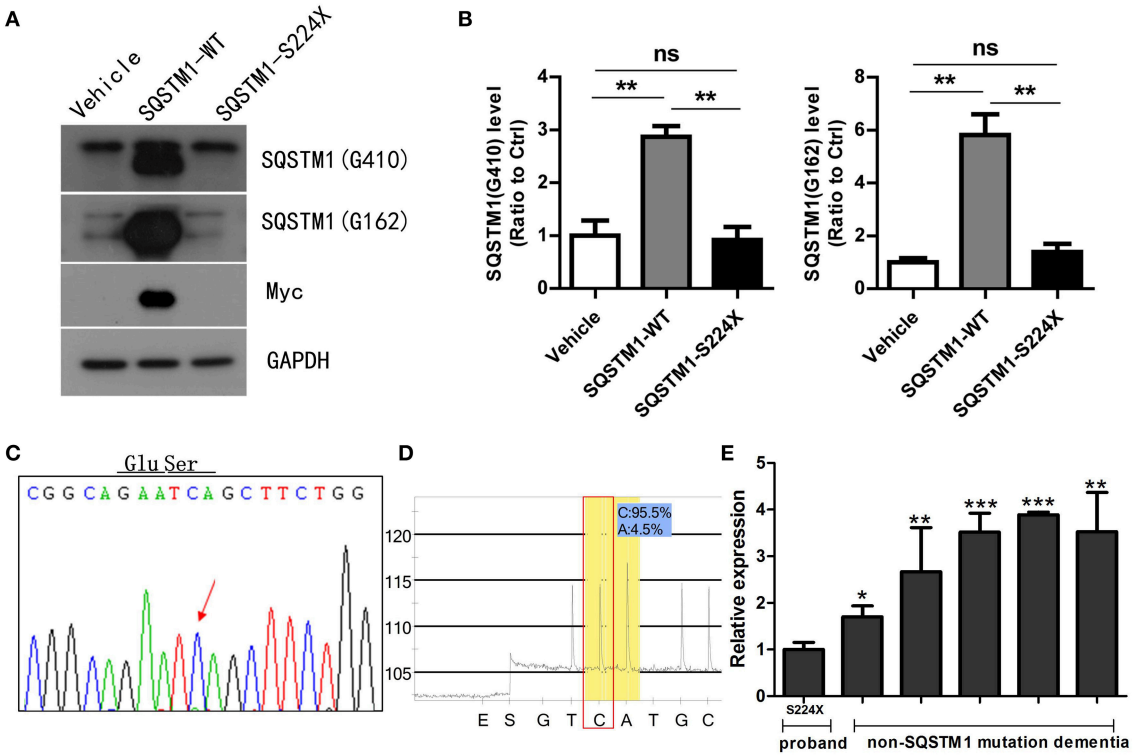


FIGURE 3 | Mutant SQSTM1 protein and cDNA levels. **(A)** HEK 293T cells were transfected with an empty vector or plasmids encoding either wild type or mutant Myc-His-tagged *SQSTM1* (S224X) for 24 h. Intact and truncated SQSTM1 proteins were recognized by western blotting with SQSTM1 (G410) and SQSTM1 (G162) antibodies, respectively. **(B)** The protein levels of SQSTM1 were quantified by densitometry and expressed as ratios to GAPDH. There were significantly reduced levels of intact or truncated SQSTM1 proteins in the S224X mutation group compared to wild type, similar to the vehicle. There was no expression of Myc protein in the vehicle or S224X mutation group, only in wild type. Data were plotted as mean ± SEM ($n = 3$). $^{**}p < 0.01$, One-way ANOVA. **(C,D)** *SQSTM1* cDNA from peripheral blood leucocytes of the patient was analyzed by Sanger sequencing and pyrosequencing. The mutation was not detected in *SQSTM1* cDNA through Sanger sequencing, and only 4% of mutation was detected through pyrosequencing. The arrow indicates the mutant site. **(E)** *SQSTM1* gene expression, measured by quantitative real-time PCR, normalized to β-actin, in peripheral blood leucocytes from the patient and five dementia controls without *SQSTM1* mutation. The expression of *SQSTM1* mRNA from the patient was significantly reduced compared to controls. Data were plotted as mean ± SEM ($n = 3$). $^{*}p < 0.05$; $^{**}p < 0.01$; $^{***}p < 0.001$, one-way ANOVA.

was no expressional difference between mutant protein and vehicle. Western blotting of the Myc tag demonstrated that the S224X mutation led to loss of SQSTM1 protein expression after eliminating the effect of endogenous SQSTM1 protein from HEK 293T cells. Furthermore, in *SQSTM1* cDNA from peripheral blood leucocytes of the patient, we didn't detect the mutation (S224X) by Sanger sequencing and pyrosequencing, and found significantly decreased level of *SQSTM1* mRNA compared to five dementia controls without SQSTM1 mutation. The above results suggested absent expression of SQSTM1/p62 protein in the S224X mutant overexpressing HEK-293T cells and significant decrease of *SQSTM1* mRNA level in the patient, which was possibly caused by nonsense-mediated mRNA decay (NMD), an mRNA degradation pathway regulating gene expression and mRNA quantity (Lopez-Perrote et al., 2016).

The *SQSTM1* gene encodes SQSTM1/p62 protein, a scaffolding protein, which regulates a variety of biological processes, including nuclear factor kappa B (NF-κB) signaling, apoptosis, transcription regulation, and ubiquitin-mediated autophagy (Rea et al., 2014). Collet et al. demonstrated that PDB patients with *SQSTM1* mutation (P392L, A381V, A390X, and L413F) had an increased level of SQSTM1/p62, and overproduction of the protein probably was involved in the pathophysiology of PDB (Collet et al., 2007). In FTD patients, *SQSTM1* mutations (E396X and R212C) are reportedly associated with p62 and TDP43 inclusions in brain (Kovacs et al., 2016). However, in the present study, we demonstrated that a novel *SQSTM1* mutation (S224X) causing loss of SQSTM1/p62 protein expression, not protein overproduction. Haack et al. identified three different biallelic loss-of-function variants (c.2T>A, p.?; R96X; E104Vfs*48) in *SQSTM1* gene in nine patients with neurodegenerative disorder, and confirmed absence of SQSTM1/p62 protein in these patients (Haack et al., 2016). In mice, the knock out of *SQSTM1* led to obesity and impaired glucose tolerance (Rodriguez et al., 2006). Furthermore, the chronic absence of SQSTM1/p62 promotes neurodegeneration with neurofibrillary tangles in hippocampal and cortical neurons manifesting with depression and short-term memory decline (Haack et al., 2016), which is similar to the clinical presentations of the present patient. There are multiple variants of *SQSTM1*

gene that cause diverse patterns of protein expression. Generally speaking, the imbalance of SQSTM1/p62 expression induced by *SQSTM1* mutations is probably involved in the pathological mechanisms of FTD.

SQSTM1/p62 plays a key role in a variety of vital cellular processes, but it is unexpected that its absence is compatible with survival above age of 40 years (Haack et al., 2016), and mice lacking SQSTM1/p62 were fertile and lived more than 1 year inspite of adult-onset obesity and diabetes (Komatsu et al., 2007). This phenomenon probably argues for a redundancy of involved pathways or effective compensatory mechanisms (Haack et al., 2016). The present patient likely reflected SQSTM1 gene haploinsufficiency due to a combination of protein instability and NMD. Meanwhile, the patient displayed the *APOE ε3/ε4* genotype, which confers an increased risk of developing Alzheimer's disease (AD). Whether APOE ε4 is a risk factor for FTD remains controversial. Ji et al. examined 432 patients with AD, 62 with FTD, and 381 controls. *APOE ε4* allele frequency was significantly increased in late-onset AD (24.86), early-onset AD (18.02), and FTD (16.13) patients compared with controls (7.34), which suggested that the ApoE ε4 genotype is a risk factor for AD and FTD (Ji et al., 2013). However, Gustafson et al. and Verpillat et al. reported no correlation between the ε4 allele and FTD, but a larger increase in the ε2 allele in FTD compared with controls (Gustafson et al., 1997; Verpillat et al., 2002). Whether the *APOE ε3/ε4* genotype in this case is promoting FTD requires further scrutiny.

In summary, we firstly identified a novel *SQSTM1* mutation (S224X) in an atypical bvFTD patient, and the mutation caused absence of SQSTM1/p62 protein, which was consistent with a reduced level of *SQSTM1* mRNA from peripheral leucocytes of the patient. The mechanisms underlying these observations are possibly associated with *SQSTM1* gene haploinsufficiency. Different variants of the *SQSTM1* gene result in diverse expression patterns, and imbalance of SQSTM1/p62 protein induces different pathogenic processes. In addition, there was a factor that limited the findings of the present study. Without a large family showing dementia and enough gene samples from family members, it is difficult to demonstrate that *SQSTM1* S224X was fully responsible for FTD. However, we have provided a clue for discussing the pathogenicity significance of *SQSTM1* S224X mutation in FTD, which should foster an understanding of the effect of *SQSTM1* mutation on FTD when the mutation can be verified in a large family showing dementia.

ETHICS STATEMENT

This study was carried out in accordance with the recommendations of "Shanghai Mental Health Center ethical standards committee on human experimentation" with written informed consent from all subjects. All subjects gave written informed consent in accordance with the Declaration of Helsinki. The protocol was approved by the "Shanghai Mental Health Center ethical standards committee". All subjects also gave written informed consent for the publication of this case report.

AUTHOR CONTRIBUTIONS

LS and ZR: performed the experiments; LS: wrote the paper; WL: collected the samples; XL, SX, and HZ: supervised the experiments.

ACKNOWLEDGMENTS

This study was supported by grants of National Key R&D Program of China (2017YFC1310501500), Western medical guidance project of Shanghai science and Technology Commission (17411970100), Natural Science Foundation of China (81301139 and 81771164), Precision medical research project of Shanghai Jiaotong University School of Medicine (15ZH4010), Natural Science Foundation of Guangdong Province of China (2016A030313821 and 2017A030313604), and the Educational Department of Fujian Province of China (JZ160403).

REFERENCES

Boutoleau-Bretonnière, C., Camuzat, A., Le Ber, I., Bouya-Ahmed, K., Guerreiro, R., Deruet, A., et al. (2015). A phenotype of atypical apraxia of speech in a family carrying SQSTM1 mutation. *J. Alzheimers. Dis.* 43, 625–630. doi: 10.3233/JAD-141512

Collet, C., Michou, L., Audran, M., Chasseigneaux, S., Hilliquin, P., Bardin, T., et al. (2007). Paget's disease of bone in the French population: novel SQSTM1 mutations, functional analysis, and genotype-phenotype correlations. *J. Bone Miner. Res.* 22, 310–317. doi: 10.1359/jbmr.061106

Fecto, F., Yan, J., Vemula, S. P., Liu, E., Yang, Y., Chen, W., et al. (2011). SQSTM1 mutations in familial and sporadic amyotrophic lateral sclerosis. *Arch. Neurol.* 68, 1440–1446. doi: 10.1001/archneurol.2011250

Gustafson, L., Abrahamson, M., Grubb, A., Nilsson, K., and Fex, G. (1997). Apolipoprotein-E genotyping in Alzheimer's disease and frontotemporal dementia. *Dement. Geriatr. Cogn. Disord.* 8, 240–243. doi: 10.1159/000106637

Haack, T. B., Ignatius, E., Calvo-Garrido, J., Iuso, A., Isohanni, P., Maffezzini, C., et al. (2016). Absence of the autophagy adaptor SQSTM1/p62 causes childhood-onset neurodegeneration with ataxia, dystonia, and gaze palsy. *Am. J. Hum. Genet.* 99, 735–743. doi: 10.1016/j.ajhg.2016.06.026

Ji, Y., Liu, M., Huo, Y. R., Liu, S., Shi, Z., Liu, S., et al. (2013). Apolipoprotein Epsilon epsilon4 frequency is increased among Chinese patients with frontotemporal dementia and Alzheimer's disease. *Dement. Geriatr. Cogn. Disord.* 36, 163–170. doi: 10.1159/000350872

Komatsu, M., Waguri, S., Koike, M., Sou, Y. S., Ueno, T., and Hara, T. (2007). Homeostatic levels of p62 control cytoplasmic inclusion body formation in autophagy-deficient mice. *Cell* 131, 1149–1163. doi: 10.1016/j.cell.2007.10.035

Kovacs, G. G., van der Zee, J., Hort, J., Kristoferitsch, W., Leitha, T., Höftberger, R., et al. (2016). Clinicopathological description of two cases with SQSTM1 gene mutation associated with frontotemporal dementia. *Neuropathology* 36, 27–38. doi: 10.1111/neup.12233

Laurin, N., Brown, J. P., Morissette, J., and Raymond, V. (2002). Recurrent mutation of the gene encoding sequestosome 1 (SQSTM1/p62) in Paget disease of bone. *Am. J. Hum. Genet.* 70, 1582–1588. doi: 10.1086/340731

López-Perrote, A., Castaño, R., Melero, R., Zamarro, T., Kurosawa, H., Ohnishi, T., et al. (2016). Human nonsense-mediated mRNA decay factor UPF2 interacts directly with eRF3 and the SURF complex. *Nucleic Acids Res.* 44, 1909–1923. doi: 10.1093/nar/gkv1527

Luis, E., Ortiz, A., Eudave, L., Ortega-Cubero, S., Borroni, B., van der Zee, J., et al. (2016). Neuroimaging correlates of frontotemporal dementia associated with SQSTM1 mutations. *J. Alzheimers. Dis.* 53, 303–313. doi: 10.3233/JAD-160006

Miller, L., Rollinson, S., Callister, J. B., Young, K., Harris, J., Mann, D. M., et al. (2015). Pickering-brown: p62/SQSTM1 analysis in frontotemporal lobar degeneration. *Neurobiol. Aging* 36, 1603.e5-1603.e9. doi: 10.1016/j.neurobiolaging.2014.08.035

O'Connor, C. M., Clemson, L., Hornberger, M., Leyton, C. E., Hodges, E., Mioshi, J. R., et al. (2016). Longitudinal change in everyday function and behavioral symptoms in frontotemporal dementia. *Neurol. Clin. Pract.* 6, 419–428. doi: 10.1212/CPJ.0000000000000264

Pottier, C., Ravenscroft, T. A., Sanchez-Contreras, M., and Rademakers, R. (2016). Genetics of FTLD: overview and what else we can expect from genetic studies. *J. Neurochem.* 138(Suppl. 1), 32–53. doi: 10.1111/jnc.13622

Rea, S. L., Majcher, V., Searle, M. S., and Layfield, R. (2014). SQSTM1 mutations–bridging Paget disease of bone and ALS/FTLD. *Exp. Cell Res.* 325, 27–37. doi: 10.1016/j.yexcr.2014.01.020

Rodriguez, A., Durán, A., Selloum, M., Champy, M. F., Diez-Guerra, F., Moscat, J., et al. (2006). Mature-onset obesity and insulin resistance in mice deficient in the signaling adapter p62. *Cell Metab.* 3, 211–222. doi: 10.1016/j.cmet.2006.01.011

Rubino, E., Rainero, I., Chiò, A., Rogaeva, E., Galimberti, D., Fenoglio, P., et al. (2012). SQSTM1 mutations in frontotemporal lobar degeneration and amyotrophic lateral sclerosis. *Neurology* 79, 1556–1562. doi: 10.1212/WNL.0b013e31826e25df

Sun, L., Chen, K., Li, X., and Xiao S. (2017). Rapidly progressive frontotemporal dementia associated with MAPT Mutation G389R. *J. Alzheimers Dis.* 55, 777–785. doi: 10.3233/JAD-160802

Tosun, D., Schuff, N., Rabinovici, G. D., Ayakta, N., Miller, B. L., Rosen, L., et al. (2016). Diagnostic utility of ASL-MRI and FDG-PET in the behavioral variant of FTD and AD. *Ann. Clin. Transl. Neurol.* 3, 740–751. doi: 10.1002/acn3.330

van der Zee, J., Van Langenhove, T., Kovacs, G. G., Dillen, L., Deschamps, W., Van Broeckhoven, C., et al. (2014). Rare mutations in SQSTM1 modify susceptibility to frontotemporal lobar degeneration. *Acta Neuropathol.* 128, 397–410. doi: 10.1007/s00401-014-1298-7

Verpillat, P., Camuzat, A., Hannequin, D., Thomas-Anterion, C., Puel, M., Belliard, S., et al. (2002). Apolipoprotein E gene in frontotemporal dementia: an association study and meta-analysis. *Eur. J. Hum. Genet.* 10, 399–405. doi: 10.1038/sj.ejhg.5200820

Conflict of Interest Statement: The authors declare that the research was conducted in the absence of any commercial or financial relationships that could be construed as a potential conflict of interest.

Copyright © 2018 Sun, Rong, Li, Zheng, Xiao and Li. This is an open-access article distributed under the terms of the Creative Commons Attribution License (CC BY). The use, distribution or reproduction in other forums is permitted, provided the original author(s) and the copyright owner are credited and that the original publication in this journal is cited, in accordance with accepted academic practice. No use, distribution or reproduction is permitted which does not comply with these terms.

frontiers in Neuroscience

REVIEW
published: 06 February 2018
doi: 10.3389/fnins.2018.00037

Challenges for Alzheimer's Disease Therapy: Insights from Novel Mechanisms Beyond Memory Defects

Rudimar L. Frozza[1]*, *Mychael V. Lourenco*[2,3] *and Fernanda G. De Felice*[2,4]*

[1] Oswaldo Cruz Institute, Fundação Oswaldo Cruz (FIOCRUZ), Rio de Janeiro, Brazil, [2] Institute of Medical Biochemistry Leopoldo de Meis, Rio de Janeiro, Brazil, [3] Institute of Biophysics Carlos Chagas Filho, Federal University of Rio de Janeiro, Rio de Janeiro, Brazil, [4] Department of Biomedical and Molecular Sciences, Centre for Neuroscience Studies, Queen's University, Kingston, ON, Canada

Alzheimer's disease (AD), the most common form of dementia in late life, will become even more prevalent by midcentury, constituting a major global health concern with huge implications for individuals and society. Despite scientific breakthroughs during the past decades that have expanded our knowledge on the cellular and molecular bases of AD, therapies that effectively halt disease progression are still lacking, and focused efforts are needed to address this public health challenge. Because AD is classically recognized as a disease of memory, studies have mainly focused on investigating memory-associated brain defects. However, compelling evidence has indicated that additional brain regions, not classically linked to memory, are also affected in the course of disease. In this review, we outline the current understanding of key pathophysiological mechanisms in AD and their clinical manifestation. We also highlight how considering the complex nature of AD pathogenesis, and exploring repurposed drug approaches can pave the road toward the development of novel therapeutics for AD.

Keywords: Alzheimer's disease, inflammation, metabolic derangements, memory defects, preclinical, therapy

OPEN ACCESS

Edited by:
Athanasios Alexiou, Novel Global Community Educational Foundation (NGCEF), Hebersham, Australia

Reviewed by:
Marzia Perluigi, Sapienza Università di Roma, Italy
Cheng-Xin Gong, Institute for Basic Research in Developmental Disabilities (IBR), United States

***Correspondence:**
Rudimar L. Frozza
rudimar.frozza@ioc.fiocruz.br
Fernanda G. De Felice
felice@bioqmed.ufrj.br

Specialty section:
This article was submitted to Neurodegeneration, a section of the journal Frontiers in Neuroscience

Received: *27 November 2017*
Accepted: *16 January 2018*
Published: *06 February 2018*

Citation:
Frozza RL, Lourenco MV and De Felice FG (2018) Challenges for Alzheimer's Disease Therapy: Insights from Novel Mechanisms Beyond Memory Defects. Front. Neurosci. 12:37. doi: 10.3389/fnins.2018.00037

INTRODUCTION

Increasing life expectancy has produced a dramatic rise in the number of cases of age-associated diseases, including dementia. Alzheimer's disease (AD) is the most frequent cause of dementia, accounting for 60–80% of all cases (Prince et al., 2016), and epidemiological studies indicate that AD will become even more incident by midcentury, constituting a major personal and societal tragedy. AD is primarily a condition of late life, roughly doubling in prevalence every 5 years after age 65 (Prince et al., 2013), and affects some 47 million people worldwide (Prince et al., 2013). This number is predicted to increase in the next two decades (Prince et al., 2016). The total cost of dementia was estimated around $818 billion in 2010 and has been projected to hit $1 trillion by 2018 worldwide (Prince et al., 2016). This becomes even more dramatic because nearly 60% of people affected by dementia live in low- and middle-income countries.

AD is a complex disorder. While the vast majority of AD cases are sporadic, affecting individuals older than 60 years, genetic mutations cause a rare (<0.5%) familial form of AD, whose symptoms develop earlier, typically between 30 and 50 years of age (Bateman et al., 2010). Further, there is a marked difference in the incidence of AD between women and men. It is estimated that nearly

two-thirds of the patients living with AD are women (Alzheimer's Association, 2017), raising the intriguing suggestion that there are biological mechanisms underlying the higher incidence of AD cases in women that still demand to be investigated.

AD is mainly characterized by progressive cognitive impairment. However, as disease progresses, other debilitating non-cognitive symptoms arise, including impaired sleep and appetite, and neuropsychiatric alterations (e.g., depression and apathy) (Ishii and Iadecola, 2015; Lanctôt et al., 2017). In addition, mounting epidemiological studies have supported a link between metabolic disorders and AD (Ott et al., 1996, 1999; Steen et al., 2005; Matsuzaki et al., 2010; Takeda et al., 2010; Crane et al., 2013; De Felice, 2013; De Felice and Lourenco, 2015; Chatterjee et al., 2016). Because AD has been considered a disease of memory, studies on AD pathogenesis have mainly concentrated on how memory and cognitive failure develop, while other symptoms and co-morbidities have remained largely overlooked.

Thus, it is not surprisingly that precise and reliable biomarkers are still lacking for early disease diagnosis. Although conclusive diagnostics has mostly been confirmed through *post-mortem* examination, it is now widely accepted that pathophysiological changes begin to develop decades prior to initial cognitive symptoms, in a preclinical or presymptomatic stage (Sperling et al., 2011a,b). Further, the addition of novel biomarkers to diagnostic criteria has prompted a shift in how AD is considered as pathological entity, increasing the appreciation that it should not be regarded as having discrete and defined clinical stages, but rather as multifaceted process moving along a continuum (Sperling et al., 2011a; van Maurik et al., 2017; **Figure 1**). Relatively accurate diagnosis and timely therapies will likely be achieved when neuropsychological, fluid and imaging biomarkers are used in combination (Viola and Klein, 2015; Dubois et al., 2016; Blennow, 2017).

Although advances in animal and clinical research over the past few decades have improved our knowledge on the pathophysiological course of AD, even drugs with successful preclinical assessment have not been effective in reversing or slowing down AD progression in large clinical trials. These constraints may be due to that clinical trials have predominantly focused on therapies based on anti-amyloid strategies, since the amyloid cascade hypothesis has been placed at the center of therapeutic prospection (Karran et al., 2011; Cummings et al., 2014; Hendrix et al., 2016). Such disappointing outcomes are also suggestive of problems in translating therapies from rodent model species to humans (De Felice and Munoz, 2016). The lack of adequate control for sex differences in animal models adds up to this translational impedance. Therefore, potential therapies that work in a sex of one animal species (usually male rodents) frequently fail to translate to human trials dominated by female participants (often 2:1 female:male in large trials). Furthermore, while neuropathological features of AD are widely recognized, the intricacies of the mechanism involving central and peripheral derangements have not been clearly defined.

Given that AD holds a complex pathology, it has now been believed that more effective treatments could be possible using disease-modifying therapies and drugs targeting multiple molecular pathways (Castellani and Perry, 2012; Cummings et al., 2014; Perry et al., 2014; Stephenson et al., 2014). These should importantly take sex differences into consideration, as recently noticed (Snyder et al., 2016; Zhao et al., 2016). In this review, we discuss recent advances in the AD field, as well as classical and novel mechanisms that might reveal potential new strategies to treat AD.

MOLECULAR PATHOGENESIS OF AD

Tau Phosphorylation, Amyloid Deposition, and Aβ Oligomers

The most distinctive features present in memory-associated brain regions of AD patients are the intracellular neurofibrillary tangles (NFTs) and the extracellular amyloid plaques. The major component of the NFTs is abnormally phosphorylated and aggregated tau protein (Querfurth and LaFerla, 2010; Medeiros et al., 2011; Morris et al., 2011), thereby destabilizing microtubules and compromising axonal transport (Querfurth and LaFerla, 2010; Ittner and Götz, 2011; Medeiros et al., 2011; Morris et al., 2011; Scheltens et al., 2016). It has been recently shown that tangles induce neuronal loss and spatial memory defects (Fu et al., 2017), putatively providing a link between tau pathology and cognitive deficits in early AD. Although pathological alterations of tau were thought to be downstream events of Aβ deposition, it is equally plausible that tau and Aβ act in parallel to enhancing each other's toxic effects and initiate the pathogenic events germane to AD (Small and Duff, 2008; Spires-Jones and Hyman, 2014; Bennett et al., 2017). Fresh evidence has also pointed to soluble, diffusible tau oligomers as important drivers of synaptotoxicity, and possible culprits for the marked progression of tau pathology across the brain (Fá et al., 2016; Carrieri et al., 2017; Piacentini et al., 2017; Puzzo et al., 2017; Reilly et al., 2017).

The amyloid cascade hypothesis suggests that brain accumulation of the amyloid-β peptide (Aβ), produced by sequential cleavage of the amyloid precursor protein (APP) by the β- and γ-secretase enzymes, is a central event in AD (Karran et al., 2011; Selkoe and Hardy, 2016). Soluble Aβ undergoes conformational changes to high β-sheet content, rendering it prone to aggregation into polymeric forms, including soluble oligomers and larger insoluble fibrils. These fibrils ultimately deposit into extracellular amyloid plaques in the AD brains (Stine et al., 2003; Blennow et al., 2006; Finder and Glockshuber, 2007; Lee et al., 2007).

Aβ is physiologically degraded by the peptidases insulin-degrading enzyme, neprilysin, and by endothelin-converting enzyme (Qiu et al., 1998; Iwata et al., 2001; Farris et al., 2003; Leissring et al., 2003). In addition, Aβ can be cleared out by transportation to peripheral circulation across multiple pathways, including the blood-brain barrier, interstitial fluid bulk flow, arachnoid villi, and glymphatic-lymphatic pathways (Tarasoff-Conway et al., 2015). Additionally, Aβ aggregates can be phagocited and degraded by microglia, perivascular macrophages, and astrocytes. Defective clearing systems could thus lead to an imbalance between production and clearance

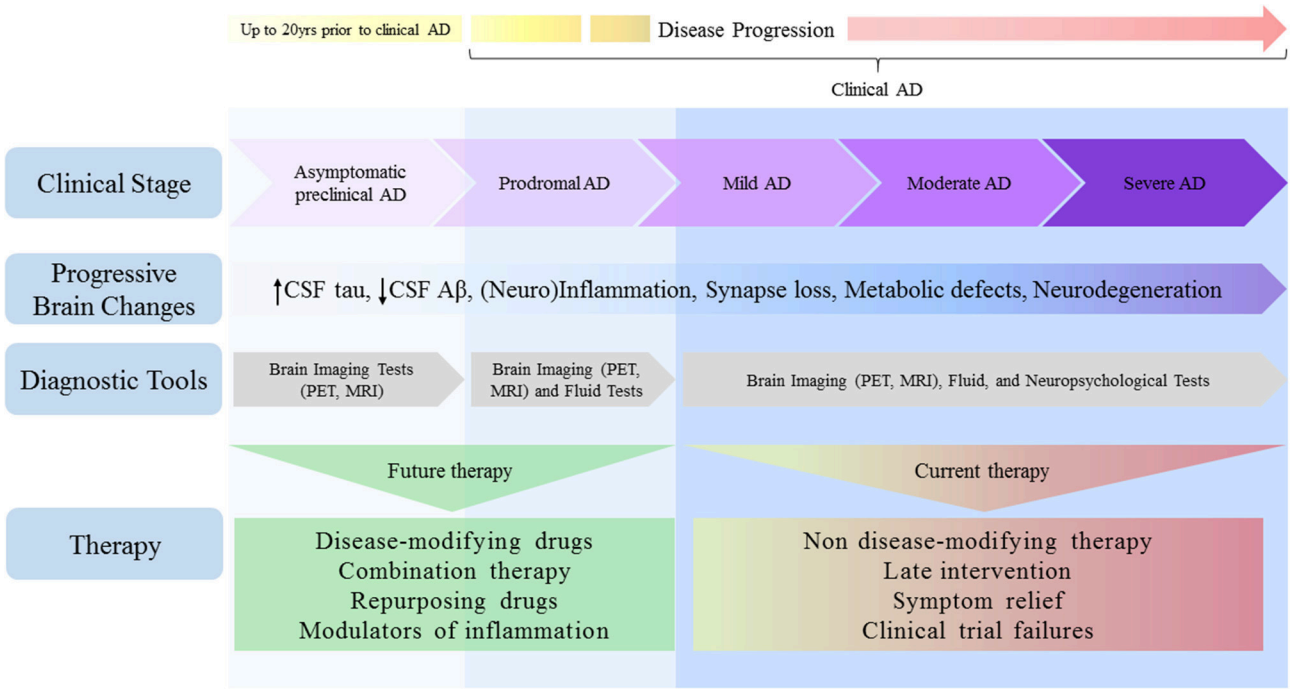


FIGURE 1 | Alzheimer's disease depicted as a continuum: challenges for therapy. Pathophysiological changes in the AD brain begin many years prior to clinical manifestations of disease and move along a continuum, spanning from clinically asymptomatic to severely impaired spectra. Although cognitive symptoms are absent in the preclinical stage, progressive amyloid deposition could drive the patient toward prodromal AD stage, characterized by short-term memory impairment without affecting activity of daily living. As disease progresses, however, many brain areas and their functions become impaired, culminating in severe memory loss and metabolic derangements, both of which affect autonomy. Despite the lack of *bona fide* biomarkers to date, earlier detection will ensure that treatments reach individuals in a timely manner. Given that therapies initially considered promising have disappointed in clinical trials, current AD research pipeline requires a shift toward the use of disease-modifying approaches, combination and/or repurposing therapies, and the search for agents selectively targeting specific modulators of inflammation.

of Aβ in the brain, thereby resulting in subsequent neuronal dysfunction and neurodegeneration (Hardy, 2002).

A growing body of evidence indicates, however, that plaque deposition is not the sole responsible for the impairments observed in AD. On the other hand, the notion that Aβ oligomers (AβOs) are the main toxins responsible for synapse dysfunction and cognitive deficits in AD has attracted considerable attention to improve our understanding of the mechanisms of the disease (Walsh and Selkoe, 2007; Selkoe, 2008; Ferreira and Klein, 2011; Ferreira et al., 2015; Yang et al., 2017). In this context, plaques have been thought to comprise a reservoir from which AβOs diffuse, or may even act sequestering soluble oligomers until they reach a physiological plateau (Selkoe and Hardy, 2016).

A considerable number of studies has reported that AβOs accumulate in the brain and CSF of AD patients (Georganopoulou et al., 2005; Haes et al., 2005; Anker et al., 2009; Xia et al., 2009; Herskovits et al., 2013; Viola et al., 2014; Murakami et al., 2016), and are found in association with synapses in the brains of patients presenting clinical signals of dementia (Koffie et al., 2009; Bjorklund et al., 2012; Perez-Nievas et al., 2013; Bilousova et al., 2016), adding clinical relevance to their role in AD. These studies suggest that synapse-associated AβOs promote detrimental modifications in synapse structure and composition, thereby leading to memory loss. This growing body of evidence props up an early notion that cognitive decline is not only a result of the extracellular accumulation of Aβ and intracellular accumulation of tau but also as a consequence of synapse failure and loss in AD (Terry et al., 1991; Masliah et al., 1992; Selkoe, 2002).

Despite intense research, the exact mechanisms of how AβOs exert their toxicity remains to be fully unveiled. Binding of Aβ aggregates to various receptors may disrupt key neuronal functions. However, the complete identity of receptors to which they bind and the underlying signaling pathways still remain to be fully elucidated (Ferreira et al., 2015).

We now know that AβOs bind to cell surface receptors and trigger multiple aberrant signaling pathways, including calcium signaling (Mattson, 2010; Ferreira et al., 2015), oxidative stress (Smith et al., 1998; Perry et al., 2002; De Felice et al., 2007), derangements in plasticity-related receptors and increased glutamate release from pre-synaptic terminals (Roselli et al., 2005; Shankar et al., 2007; Decker et al., 2010a; Ferreira et al., 2015). In addition, they promote tau hyperphosphorylation (De Felice et al., 2008; Jin et al., 2011), impaired axonal transport (Snyder et al., 2005; Decker et al., 2010b; Miñano-Molina et al., 2011; Bomfim et al., 2012), and drive inhibition of long-term potentiation (LTP) and memory impairment (Rowan et al., 2005; Shankar et al., 2008; Ferreira and Klein, 2011; Ferreira et al., 2015; Yang et al., 2017).

Inflammatory Markers in the Brain

AD pathogenesis appears to include strong interactions with immune mechanisms in the brain. AβOs induce aberrant reactivity of astrocytes and microglia, in the brains of mice and non-human primates (Bomfim et al., 2012; Ledo et al., 2013, 2016; Forny-Germano et al., 2014). Recent studies have further unveiled that disturbances in microglia, as well as interactions with peripheral immune cells, may play key roles in causing synapse loss and neurodegeneration in AD (Browne et al., 2013; Zhang et al., 2013; Baruch et al., 2015, 2016; Guillot-Sestier et al., 2015; Zenaro et al., 2015; Hong et al., 2016a,b). These studies are in line with emerging evidence suggesting that inflammation has a pivotal role in disease pathogenesis, as markers of inflammation, such as TNF-α, IL-1β, IL-6, and other cytokines, have been shown to be increased in the brain, CSF, and plasma of AD patients (Perry et al., 2010; Swardfager et al., 2010; Czirr and Wyss-Coray, 2012; Alcolea et al., 2014; Heneka et al., 2015a; Hong et al., 2016a; Salter and Stevens, 2017).

Increased pro-inflammatory signaling resulting from reactive microglial reduces Aβ clearance, promotes aberrant synaptic pruning (Lee and Landreth, 2010; Mandrekar-Colucci et al., 2012; Heneka et al., 2015a,b; Hong et al., 2016b), prompts Aβ and tau pathologies, and contributes to impaired synapse function (Wang W. Y. et al., 2015). Importantly, TNF-α-dependent mechanisms appear to drive memory defects (Lourenco et al., 2013) and depressive-like behavior in AD mice (Ledo et al., 2016), thereby indicating a causal role of inflammation in deleterious processes linked to AD.

Unfolded Protein Response and Defective Proteostasis

Pro-inflammatory pathways triggered by AβOs, notably via TNF-α, have been reported to induce neuronal stress (Lourenco et al., 2013), likely resulting in defective proteostasis. Furthermore, it has been recently demonstrated that AβOs stimulates eIF2α phosphorylation (Devi and Ohno, 2010, 2013, 2014; Lourenco et al., 2013; Ma et al., 2013; Baleriola et al., 2014). In the brain, eIF2α is a hub that controls protein synthesis-dependent learning and memory and mantain neuronal integrity in health and disease. When phosphorylated, however, eIF2α attenuates the initiation of global protein synthesis (Lourenco et al., 2015).

Aberrant eIF2α phosphorylation and inhibition of protein synthesis have emerged as major molecular pathways driving synapse and memory failure in AD models (Costa-Mattioli et al., 2007; Lourenco et al., 2013, 2015; Ma et al., 2013; Baleriola et al., 2014). In line with this notion, deletion of eIF2α kinases, including PKR, PERK, or GCN2 restores memory and synapse function in mouse models of AD (Lourenco et al., 2013; Ma et al., 2013).

Abnormal accumulation of misfolded proteins in the endoplasmic reticulum triggers the unfolded protein response (UPR), a set of signaling branches aimed at restore cellular homeostasis (Hetz, 2012; Dufey et al., 2014; Hetz and Saxena, 2017). However, when prolonged, UPR signaling might compromise neuronal functions, resulting in neurodegeneration (Lourenco et al., 2015; Freeman and Mallucci, 2016; Hetz and Saxena, 2017). There is now considerable evidence suggesting that AD brain display increased markers of UPR (Hoozemans et al., 2009; Hetz and Saxena, 2017), and that at least the PERK (Ma et al., 2013) and IRE-1a (Lourenco et al., 2013; Duran-Aniotz et al., 2017) branches of UPR are involved in memory defects in AD mice. Further, the chemical chaperone 4-phenylbutyrate alleviates AβO-induced memory defects in mice (Lourenco et al., 2013), thus highlighting the role of UPR in mediating neurotoxicity in AD. The combination of misfolded protein accumulation, activation of brain immune responses and defective proteostasis might thus comprise the very essence of synapse and memory failure in AD.

NOVEL PATHOPHYSIOLOGICAL MECHANISMS IN AD

Scientific breakthroughs during the past decades have expanded our knowledge on cellular and molecular aspects of AD. Nevertheless, AD remains largely idiopathic, and therapies that effectively combat disease progression are still lacking. Given that AD largely associates with memory loss, it is not surprising that the vast majority of studies deal with mechanisms implicated in cognitive deterioration. Hence, much less is known about how brain regions that are not directly linked to memory are affected in AD, as well as about mechanisms underlying its major comorbidities.

Numerous studies have investigated how Aβ impacts the hippocampus and the cortex (Ferreira and Klein, 2011; Musiek and Holtzman, 2015), known to be fundamentally involved in acquisition, consolidation, and recollection of new episodic memories. However, early studies indicated that brain regions not necessarily involved in learning and memory might also be affected in AD. It is noteworthy that AD patients exhibit significant non-cognitive deficits (summarized in the **Table 1**) such as sleep-wake disorders and neuroendocrine alterations attributable to hypothalamic dysfunction (Prinz et al., 1982; White et al., 1996; Csernansky et al., 2006).

Impaired Hypothalamic Function

Disturbances in hypothalamic nuclei have been reported in patients and animal models of AD (Duncan et al., 2012; Lim et al., 2014; Musiek et al., 2015; Musiek and Holtzman, 2016; Stevanovic et al., 2017). Since the hypothalamus is responsible for controlling circadian rhythm, impairments in its function can at least partially account for sleep disturbances. Nonetheless, although initial results have already shed light on how sleep becomes deregulated in AD (Ju et al., 2014; Musiek and Holtzman, 2016; Kincheski et al., 2017), studies investigating whether hypothalamic defects mediate sleep disturbances in AD are still needed.

Derangements in hypothalamic functions play a central role in peripheral metabolism deregulation and its consequences. For instance, hypothalamic inflammation and impaired proteostasis are critical pathogenic events in the establishment of peripheral insulin resistance in metabolic disorders (Zhang et al., 2008; Milanski et al., 2009; Denis et al., 2010; Arruda et al., 2011; Thaler

TABLE 1 | Novel pathophysiological mechanisms in AD.

Feature	Pathophysiological mechanisms	References
Impaired hypothalamic function	– Aβ deposits in hypothalamic nuclei leading to disturbances in circadian rhythm; – Reduced dendrite arborization and neurodegeneration; – Inflammation driving endoplasmic reticulum stress and insulin resistance.	Ogomori et al., 1989; Standaert et al., 1991; Duncan et al., 2012; Lim et al., 2014; Baloyannis et al., 2015; Clarke et al., 2015; Musiek et al., 2015; Musiek and Holtzman, 2016; Kincheski et al., 2017; Stevanovic et al., 2017
Metabolic derangement	– Reduced cerebral glucose metabolism; – Altered peripheral metabolism with hyperglycemia and hyperinsulinemia; – Defective glucose metabolism and insulin signaling induced by Aβ;	Chase et al., 1984; Janson et al., 2004; Rivera et al., 2005; Steen et al., 2005; Lester-Coll et al., 2006; De Felice et al., 2009; de la Monte, 2009; Matsuzaki et al., 2010; Moloney et al., 2010; Bomfim et al., 2012; Talbot et al., 2012; Crane et al., 2013; De Felice, 2013; Lourenco et al., 2013; De Felice and Ferreira, 2014; Clarke et al., 2015
Disturbances in monoamine signaling and mood	– Aβ induces both depressive-like behavior and decreases brain serotonin levels; – Increased microglial activity of IDO might partially explain reduced serotonin levels; – Reduced tryptophan and increased quinolinic acid in plasma might drive depressive-like behavior in AD; – Alterations in the dopaminergic system, including reduced levels of dopamine and its receptors might contribute to hippocampus-dependent memory deficits and reward circuitry dysfunction.	Gibb et al., 1989; Storga et al., 1996; Burns et al., 2005; Bonda et al., 2010; Gulaj et al., 2010; Jürgensen et al., 2011; Ledo et al., 2013, 2016; Romano et al., 2014; Masters et al., 2015; Nobili et al., 2017
Inflammation	– Pro-inflammatory cytokines are elevated in AD brains and mediate neurotoxic signals; – Brain inflammation underlies defective neuronal insulin signaling and peripheral metabolic deregulation; – Inflammation may drive synaptic failure in the monoaminergic systems, thereby linking cognitive and non-cognitive symptoms found in AD patients.	Heneka and O'Banion, 2007; Bonda et al., 2010; Lee and Landreth, 2010; Swardfager et al., 2010; Bomfim et al., 2012; Czirr and Wyss-Coray, 2012; Ledo et al., 2013, 2016; Lourenco et al., 2013; Alcolea et al., 2014; De Felice and Ferreira, 2014; Morales et al., 2014; Clarke et al., 2015; Heneka et al., 2015a,b; Yirmiya et al., 2015; Hong et al., 2016a,a; Santos et al., 2016; Nobili et al., 2017; Salter and Stevens, 2017

Aβ, amyloid-β peptide; AD, Alzheimer's disease; CNS, central nervous system; IDO, indolamine-2,3-dioxygenase; T2D, type 2 diabetes.

et al., 2012; Valdearcos et al., 2015). Nonetheless, very few studies so far investigated hypothalamic dysfunction in AD.

Early *post-mortem* studies identified Aβ deposits in hypothalamic nuclei of AD patients (Ogomori et al., 1989; Standaert et al., 1991), and neurodegeneration with marked retraction of dendrites in early AD (Baloyannis et al., 2015). Further, hypothalamic endoplasmic reticulum stress, inflammation, and insulin resistance were demonstrated in AβO-injected mice and non-human primates (Clarke et al., 2015). Dysfunction triggered by AβOs in the hypothalamus associated with development of persistent peripheral glucose intolerance, which was further demonstrated in several transgenic mouse models of AD (Clarke et al., 2015; Vandal et al., 2015; Stanley et al., 2016), and in human patients (Craft et al., 1992).

Defective Glucose Metabolism and Insulin Signaling

Altered peripheral metabolism with hyperglycemia and hyperinsulinemia, which are cardinal features of type 2 diabetes (T2D), were recently found to positively correlate with development of AD-like brain pathology in humans (Matsuzaki et al., 2010; Crane et al., 2013). Conversely, AD has been associated with increased T2D risk (Janson et al., 2004), suggesting that the connection between AD and T2D may comprise a two-way road. AD progression positively further correlates with reduction of cerebral glucose metabolism in the forebrain, including the posterior parietal lobe and portions of temporal and occipital lobes (Chase et al., 1984).

An important player accounting for impaired glucose metabolism in AD could arise from defects in insulin signaling pathways. AD brains exhibit lower levels of insulin and reduced insulin receptor (IR) expression and sensitivity (Rivera et al., 2005; Steen et al., 2005; Talbot et al., 2012). Further, impairments in insulin signaling downstream machinery have been reported in *post-mortem* brain tissue and in animal models of AD (Steen et al., 2005; Lester-Coll et al., 2006; de la Monte, 2009; Moloney et al., 2010; Bomfim et al., 2012; Craft, 2012; Talbot et al., 2012; Lourenco et al., 2013; Clarke et al., 2015). Recent studies have shown that AβOs are the toxins linked to impaired hippocampal insulin signaling by promoting internalization and cellular redistribution of insulin receptors, blocking downstream hippocampal insulin signaling (De Felice et al., 2009; Ma et al., 2009; Bomfim et al., 2012). Such body of evidence has established novel molecular parallels between AD and T2D.

The precise molecular mechanisms connecting impaired glucose metabolism and insulin signaling to AD pathogenesis remain to be fully determined. Nonetheless, mounting evidence has pointed to inflammation as a critical player linking AD and metabolic diseases, including T2D (De Felice and Ferreira, 2014;

Ferreira et al., 2014; Morales et al., 2014; Heneka et al., 2015b). Overproduction of pro-inflammatory cytokines, notably TNF-α, is a key feature of the pathophysiology of metabolic disorders (Hotamisligil, 2006, 2017). Notably, brain inflammation has recently been proposed to underlie defective neuronal insulin signaling (Bomfim et al., 2012; Lourenco et al., 2013), as well as peripheral metabolic deregulation in AD (Clarke et al., 2015).

Disturbances in Monoamine Signaling and Mood

Mounting evidence supports the notion that microglial activation and brain inflammation could further underlie mood disorders, including depressive behaviors (Yirmiya et al., 2015; Santos et al., 2016). Depression and/or apathy have been reported as frequent comorbidities in AD patients (Lyketsos and Olin, 2002), and have been regarded as risk factors for AD (Green et al., 2003; Ownby et al., 2006; Starkstein and Mizrahi, 2006; Geerlings et al., 2008).

Although clinical and epidemiological studies have revealed a strong connection between AD and depression, the mechanisms connecting these disorders at the molecular and cellular levels have only recently begun to be established. Clues into a mechanistic link between memory and mood disturbances in AD came from recent works showing that AβOs induce both depressive-like behavior and memory deficits in mice and associate with decreased brain serotonin levels (Ledo et al., 2013, 2016) in a similar way to that observed in transgenic mice model of AD (Romano et al., 2014). Reduced serotonin levels may be linked to increased levels and activity of indolamine-2,3-dioxygenase (IDO) follow microglial activation. Interestingly, AD patients were found to have reduced levels of plasma tryptophan and increased quinolinic acid (Gulaj et al., 2010), as well as increased IDO immunoreactivity in microglia (Bonda et al., 2010). Because inflammation plays a significant role in depression, these findings raise the possibility that AβO-induced brain inflammation may constitute a common denominator between cognitive and mood alterations in AD.

Alterations in the dopaminergic system have also been reported in AD patients and experimental models, including reduced levels of dopamine and its receptors (Gibb et al., 1989; Storga et al., 1996; Burns et al., 2005; Jürgensen et al., 2011; Nobili et al., 2017), and are commonly linked to cognitive and non-cognitive symptoms of the disease. It has been recently shown that inflammation and apoptosis take place in the ventral tegmental area, causing selective degeneration of the dopaminergic nuclei before senile plaque deposition, tangles or any sign of neuronal loss in cortical and hippocampal regions in a transgenic mouse model of AD (Nobili et al., 2017).

Given that dopaminergic neurons from ventral tegmental area not only modulate hippocampal synaptic plasticity (Rossato et al., 2009; McNamara et al., 2014; Broussard et al., 2016), but also target the nucleus accumbens and the cerebral cortex (Russo and Nestler, 2013), dopaminergic degeneration in ventral tegmental area might largely contribute to the deficits in hippocampus-dependent memory and reward circuits. These findings may provide an intriguing explanation to recent observations in AD patients indicating that the clinical diagnosis of dementia is associated with early non-cognitive symptoms, such as depression and apathy (Masters et al., 2015). Overall, these recent data suggest that inflammation may drive synaptic failure in the monoaminergic systems, thereby linking the cognitive and non-cognitive symptoms found in AD patients.

CHALLENGES FOR AD THERAPY

Despite intensive investigation of mechanisms of pathogenesis in AD during the past three decades, little has been achieved in terms of effective treatments or approaches to prevent or cure it. Taking into account the dramatic rise in the number of AD cases, huge economic and social hurdle will impact the society if no treatment is developed within the next few years. Additionally, it is noteworthy that advances in therapeutic strategies for AD that lead to even small delays in AD onset or progression would significantly attenuate the global burden of the disease.

Given the conceptual frameshift that occurred in the field in the past few years, AD has not only been viewed with discrete and defined clinical stages, but as a multifaceted process moving along a continuum. Thanks to the evolving biomarker research, it is now recognized that pathophysiological changes begin many years before clinical manifestations of AD. For example, changes in CSF tau levels have been shown to develop ∼15 years before the onset of clinical AD, while CSF Aβ42 levels may drop even earlier, up to 20 years before symptom onset (Bateman et al., 2012; Buchhave, 2012; Villemagne et al., 2013; Fagan et al., 2014).

The spectrum of AD spans from clinically asymptomatic to severely impaired (**Figure 1**). However, these boundaries are challenging, given that separation between healthy aging and preclinical AD is not well-defined in our current understanding. This unmet question will likely be addressed in the future, as early detection biomarkers have become a major research focus.

Sex differences should also be taken into account as a biological variable in AD pathogenesis as women constitute the majority of affected people, accounting for nearly two-thirds of AD patients (Alzheimer's Association, 2017). Reasons for the higher frequency of AD among women could be partly explained by the fact that women live longer. However, late-onset AD risk is greater in women even after controlling for their longer lifespan relative to men (Viña and Lloret, 2010). The biological underpinnings of the increased AD risk in women remain largely unknown.

Nonetheless, it is now accepted that the perimenopause to menopause transition disrupts multiple estrogen-regulated systems, thereby affecting multiple domains of cognitive function (Brinton et al., 2015; Christensen and Pike, 2015). Indeed, recent preclinical studies have implicated that a shift in the bioenergetics system of the brain during menopause onset could serve as an early initiating mechanism for increased AD risk in the female brain (Brinton et al., 2015; Mosconi et al., 2017a,b). These biological variables may lead to increased fatty acid catabolism, Aβ deposition, and impaired synaptic plasticity (Liu et al., 2008; Brinton, 2009; Yao and Brinton, 2012), which could serve as a mechanism that triggers AD (Brinton et al., 2015). As a result, it is conceivable that disappointing outcomes in clinical trials may be

partially explained by metabolic differences in women and men. Therefore, recommendations to include both female and male animals in preclinical research should be completely embraced by the research community.

While the amyloid cascade hypothesis has dominated research for the past 20 years, the shift toward disease-modifying drug development in the last decade might be imperative to develop approaches that interrupt the underlying disease processes.

Potential benefits for AD therapy can also emerge from combination pharmacotherapy. This strategy has proven effective for several diseases, including tuberculosis, HIV/AIDS, cardiovascular diseases, and cancer (Perry et al., 2014; Hendrix et al., 2016), and holds potential to enhance the efficacy of drugs that are ineffective on their own, but offer synergistic or additive benefits in combination.

Taking into account the well-known high failure rates in drug development targeting the central nervous system, strategies aimed at repurposing already marketed drugs become an interesting option to speed up drug discovery in AD (Appleby and Cummings, 2013). Given that metabolic derangements seem to play a pivotal role in AD, and that a myriad of drugs for metabolic disease have already been labeled for human use, repurposing such compounds may have the potential to accelerate drug development. That is because preclinical toxicology, human safety, tolerability, and pharmacokinetic assessments could move faster. Impaired brain insulin signaling or brain insulin resistance seems play a central role in the molecular pathogenesis of sporadic AD. Thus, targeting brain insulin signaling through the administration of drugs that have already been previously approved for the treatment of diabetes mellitus, such as insulin and drugs that improve insulin sensitivity, could expedite their development for the treatment of AD (Chen et al., 2016). It worthy to note that anti-diabetic compounds, such as insulin, exenatide, and liraglutide, have already been tested in ongoing clinical trials (clinical trial ID NCT01767909, NCT01255163, and NCT01843075, respectively).

Neuroinflammation, especially at the earliest stages, supports a vicious cycle of microglial activation, release of pro-inflammatory factors, and neuronal damage. Additionally, inflammatory mechanisms, such as those driven by TNF-α, may be orchestrated between the brain and the periphery, providing a likely link between AD and peripheral metabolic deregulation (De Felice and Ferreira, 2014; Ferreira et al., 2014; De Felice and Lourenco, 2015). The important role of neuroinflammation in AD is further supported by findings that gene variants for immune receptors, including TREM2, are associated with altered AD risk (Guerreiro et al., 2013; Heneka et al., 2015a).

A considerable body of evidence supports that inflammation could be a therapeutically relevant target in AD. Nevertheless, trials with anti-inflammatory compounds, such as non-steroidal anti-inflammatory drugs (NSAIDs), peroxisome proliferator-activated receptor-γ (PPAR-γ) activators, minocycline, and TNF-α signaling inhibitors have not yet provided exciting outcomes to date (Calsolaro and Edison, 2016), although lifelong use of NSAIDs has been associated with reduced risk of developing AD (Wang J. et al., 2015).

Additional therapeutic approaches with intravenous immunoglobulins and/or monoclonal antibodies are currently under evaluation, and results have not been conclusive yet. These uncertain results could be, to some extent, due to that anti-inflammatory drugs target generic rather than specific neuroinflammatory components in AD. Thus, specific modulators of inflammation at early disease stages will be essential to understand the potential of targeting inflammation in neurodegeneration.

CONCLUDING REMARKS

Although our understanding of AD has considerably increased over recent years, there is a still unmet requirement for effective therapeutics. Properly diagnosing AD is still one of the major hurdles in the field, as reliable biomarkers are lacking. There is fresh and compelling preclinical evidence that brain regions not necessarily involved in learning and memory might also be affected in AD, driving its major comorbidities. As most of therapeutic approaches have had disappointing outcomes so far, it is time to revisit the science underlining our current AD canons, and move toward the search for additional disease mechanisms and keys to treatment. Inflammation plays a critical role in the pathogenesis of AD and seems to drive the metabolic derangements that have been found to positively correlate with disease onset, leading to the emergence of cognitive and non-cognitive symptoms.

A deeper understanding of the complex features underlying major disease symptoms, including behavioral, mood, inflammation, and metabolic disturbances, may contribute to the development of novel and successful therapies. Given the differential prevalence of AD in men and women, sex differences should also be taken into account when studying AD pathophysiology, as they might reveal the need for separate therapeutic approaches. Drugs currently approved for use in AD are not disease-modifying, only confer mild and transient symptomatic management. Intervention at earlier stages using disease-modifying and combination therapy comprised of repourposed drugs and anti-inflammatory agents could pave the road toward successful outcomes in AD therapy.

AUTHOR CONTRIBUTIONS

RF, ML, and FD: planned, researched and wrote the manuscript.

ACKNOWLEDGMENTS

Work in the authors' laboratories has been supported by grants from National Institute for Translational Neuroscience (INNT/Brazil), Conselho Nacional de Desenvolvimento Científico e Tecnológico (CNPq/Brazil), Fundação Carlos Chagas Filho de Amparo à Pesquisa do Estado do Rio de Janeiro (FAPERJ), Alzheimer Society Canada and the International Society for Neurochemistry (ISN).

REFERENCES

Alcolea, D., Carmona-Iragui, M., Suárez-Calvet, M., Sánchez-Saudinós, M. B., Sala, I., Antón-Aguirre, S., et al. (2014). Relationship between β-secretase, inflammation and core cerebrospinal fluid biomarkers for Alzheimer's disease. *J. Alzheimer's Dis.* 42, 157–167. doi: 10.3233/JAD-140240

Alzheimer's Association (2017). 2017 Alzheimer's disease facts and figures. *Alzheimer's Dement.* 13, 325–373. doi: 10.1016/j.jalz.2017.02.001

Anker, J. N., Hall, W. P., Lambert, M. P., Velasco, P. T., Mrksich, M., Klein, W. L., et al. (2009). Detection and identification of bioanalytes with high resolution LSPR spectroscopy and MALDI mass spectrometry. *J. Phys. Chem. C* 113, 5891–5894. doi: 10.1021/jp900266k

Appleby, B. S., and Cummings, J. L. (2013). Discovering new treatments for Alzheimer's disease by repurposing approved medications. *Curr. Top. Med. Chem.* 13, 2306–2327. doi: 10.2174/15680266113136660162

Arruda, A. P., Milanski, M., Coope, A., Torsoni, A. S., Ropelle, E., Carvalho, D. P., et al. (2011). Low-grade hypothalamic inflammation leads to defective thermogenesis, insulin resistance, and impaired insulin secretion. *Endocrinology* 152, 1314–1326. doi: 10.1210/en.2010-0659

Baleriola, J., Walker, C. A., Jean, Y. Y., Crary, J. F., Troy, C. M., Nagy, P. L., et al. (2014). Axonally synthesized ATF4 transmits a neurodegenerative signal across brain regions. *Cell* 158, 1159–1172. doi: 10.1016/j.cell.2014.07.001

Baloyannis, S. J., Mavroudis, I., Mitilineos, D., Baloyannis, I. S., and Costa, V. G. (2015). The hypothalamus in alzheimer's disease. *Am. J. Alzheimer's Dis. Other Dementiasr.* 30, 478–487. doi: 10.1177/1533317514556876

Baruch, K., Deczkowska, A., Rosenzweig, N., Tsitsou-Kampeli, A., Sharif, A. M., Matcovitch-Natan, O., et al. (2016). PD-1 immune checkpoint blockade reduces pathology and improves memory in mouse models of Alzheimer's disease. *Nat. Med.* 22, 135–137. doi: 10.1038/nm.4022

Baruch, K., Rosenzweig, N., Kertser, A., Deczkowska, A., Sharif, A. M., Spinrad, A., et al. (2015). Breaking immune tolerance by targeting Foxp3^{+} regulatory T cells mitigates Alzheimer's disease pathology. *Nat. Commun.* 6, 7967. doi: 10.1038/ncomms8967

Bateman, R. J., Aisen, P. S., De Strooper, B., Fox, N. C., Lemere, C. A., Ringman, J. M., et al. (2010). Autosomal-dominant Alzheimer's disease: a review and proposal for the prevention of Alzheimer's disease. *Alzheimers. Res. Ther.* 3, 1. doi: 10.1186/alzrt59

Bateman, R. J., Xiong, C., Benzinger, T. L. S., Fagan, A. M., Goate, A., Fox, N. C., et al. (2012). Clinical and biomarker changes in dominantly inherited alzheimer's disease. *N. Engl. J. Med.* 367, 795–804. doi: 10.1056/NEJMoa1202753

Bennett, R. E., DeVos, S. L., Dujardin, S., Corjuc, B., Gor, R., Gonzalez, J., et al. (2017). Enhanced tau aggregation in the presence of amyloid β. *Am. J. Pathol.* 187, 1601–1612. doi: 10.1016/j.ajpath.2017.03.011

Bilousova, T., Miller, C. A., Poon, W. W., Vinters, H. V., Corrada, M., Kawas, C., et al. (2016). Synaptic Amyloid-β oligomers precede p-Tau and differentiate high pathology control cases. *Am. J. Pathol.* 186, 185–198. doi: 10.1016/j.ajpath.2015.09.018

Bjorklund, N. L., Reese, L. C., Sadagoparamanujam, V.-M., Ghirardi, V., Woltjer, R. L., and Taglialatela, G. (2012). Absence of amyloid β oligomers at the postsynapse and regulated synaptic Zn2^{+} in cognitively intact aged individuals with Alzheimer's disease neuropathology. *Mol. Neurodegener.* 7:23. doi: 10.1186/1750-1326-7-23

Blennow, K. (2017). A review of fluid biomarkers for alzheimer's disease: moving from CSF to blood. *Neurol. Ther.* 6(Suppl. 1), 15–24. doi: 10.1007/s40120-017-0073-9

Blennow, K., de Leon, M. J., and Zetterberg, H. (2006). Alzheimer's disease. *Lancet*. 368, 387–403. doi: 10.1016/S0140-6736(06)69113-7

Bomfim, T. R., Forny-Germano, L., Sathler, L. B., Brito-Moreira, J., Houzel, J.-C., Decker, H., et al. (2012). An anti-diabetes agent protects the mouse brain from defective insulin signaling caused by Alzheimer's disease–associated Aβ oligomers. *J. Clin. Invest.* 122, 1339–1353. doi: 10.1172/JCI 57256

Bonda, D., Mailankot, M., Stone, J., Garrett, M., S. M., Castellani, R. J., Siedlak, S. L., et al. (2010). Indoleamine 2,3-dioxygenase and 3-hydroxykynurenine modifications are found in the neuropathology of Alzheimer's disease. *Redox Rep.* 15, 161–168. doi: 10.1179/174329210X126505066 23645

Brinton, R. D. (2009). Estrogen-induced plasticity from cells to circuits: predictions for cognitive function. *Trends Pharmacol. Sci.* 30, 212–222. doi: 10.1016/j.tips.2008.12.006

Brinton, R. D., Yao, J., Yin, F., Mack, W. J., and Cadenas, E. (2015). Perimenopause as a neurological transition state. *Nat. Rev. Endocrinol.* 11, 393–405. doi: 10.1038/nrendo.2015.82

Broussard, J. I., Yang, K., Levine, A. T., Tsetsenis, T., Jenson, D., Cao, F., et al. (2016). Dopamine regulates aversive contextual learning and associated *in vivo* synaptic plasticity in the hippocampus. *Cell Rep.* 14, 1930–1939. doi: 10.1016/j.celrep.2016.01.070

Browne, T. C., McQuillan, K., McManus, R. M., O'Reilly, J.-A., Mills, K. H. G., and Lynch, M. A. (2013). IFN- production by amyloid -specific Th1 cells promotes microglial activation and increases plaque burden in a mouse model of alzheimer's disease. *J. Immunol.* 190, 2241–2251. doi: 10.4049/jimmunol.1200947

Buchhave, P. (2012). Cerebrospinal fluid levels of β-Amyloid 1-42, but Not of Tau, are fully changed already 5 to 10 years before the onset of alzheimer dementia. *Arch. Gen. Psychiatry* 69, 98. doi: 10.1001/archgenpsychiatry.2011.155

Burns, J. M., Galvin, J. E., Roe, C. M., Morris, J. C., and McKeel, D. W. (2005). The pathology of the substantia nigra in Alzheimer disease with extrapyramidal signs. *Neurology* 64, 1397–1403. doi: 10.1212/01.WNL.0000158423.05224.7F

Calsolaro, V., and Edison, P. (2016). Neuroinflammation in Alzheimer's disease: current evidence and future directions. *Alzheimer's Dement.* 12, 719–732. doi: 10.1016/j.jalz.2016.02.010

Carrieri, C., Cimatti, L., Biagioli, M., Beugnet, A., Zucchelli, S., Fedele, S., et al. (2017). Tau reduction prevents neuronal loss and reverses pathological tau deposition and seeding in mice with tauopathy. *Nat. Nanotechnol.* 481, 454–457. doi: 10.1126/scitranslmed.aag0481

Castellani, R. J., and Perry, G. (2012). Pathogenesis and disease-modifying therapy in Alzheimer's disease: the flat line of progress. *Arch. Med. Res.* 43, 694–698. doi: 10.1016/j.arcmed.2012.09.009

Chase, T. N., Foster, N. L., Fedio, P., Brooks, R., Mansi, L., and Di Chiro, G. (1984). Regional cortical dysfunction in Alzheimer's disease as determined by positron emission tomography. *Ann. Neurol.* 15(Suppl.), S170–S174.

Chatterjee, S., Peters, S. A. E., Woodward, M., Arango, S. M., Batty, G. D., Beckett, N., et al. (2016). Type 2diabetes as a risk factor for dementia in women compared with men: a pooled analysis of 2.3 million people comprising more than 100,000 cases of dementia. *Diabetes Care* 39, 300–307. doi: 10.2337/dc15-1588

Chen, Y., Zhang, J., Zhang, B., and Gong, C. X. (2016). Targeting insulin signaling for the treatment of Alzheimer's disease. *Curr. Top. Med. Chem.* 16, 485–492. doi: 10.2174/1568026615666150813142423

Christensen, A., and Pike, C. J. (2015). Menopause, obesity and inflammation: interactive risk factors for Alzheimer's disease. *Front. Aging Neurosci.* 7:130. doi: 10.3389/fnagi.2015.00130

Clarke, J. R., Lyra E Silva, N. M., Figueiredo, C. P., Frozza, R. L., Ledo, J. H., Beckman, D., et al. (2015). Alzheimer-associated Aβ oligomers impact the central nervous system to induce peripheral metabolic deregulation. *EMBO Mol. Med.* 7, 190–210. doi: 10.15252/emmm.201404183

Costa-Mattioli, M., Gobert, D., Stern, E., Gamache, K., Colina, R., Cuello, C., et al. (2007). eIF2α phosphorylation bidirectionally regulates the switch from short- to long-term synaptic plasticity and memory. *Cell* 129, 195–206. doi: 10.1016/j.cell.2007.01.050

Craft, S. (2012). Alzheimer disease: insulin resistance and AD—extending the translational path. *Nat. Rev. Neurol.* 8, 360–362. doi: 10.1038/nrneurol.2012.112

Craft, S., Zallen, G., and Baker, L. D. (1992). Glucose and memory in mild senile dementia of the alzheimer type. *J. Clin. Exp. Neuropsychol.* 14, 253–267. doi: 10.1080/01688639208402827

Crane, P. K., Walker, R., Hubbard, R. A., Li, G., Nathan, D. M., Zheng, H., et al. (2013). Glucose levels and risk of dementia. *N. Engl. J. Med.* 369, 540–548. doi: 10.1056/NEJMoa1215740

Csernansky, J. G., Dong, H., Fagan, A. M., Wang, L., Xiong, C., Holtzman, D. M., et al. (2006). Plasma cortisol and progression of dementia in subjects with Alzheimer-type dementia. *Am. J. Psychiatry* 163, 2164–2169. doi: 10.1176/ajp.2006.163.12.2164

Cummings, J. L., Morstorf, T., and Zhong, K. (2014). Alzheimer's disease drug-development pipeline: few candidates, frequent failures. *Alzheimers. Res. Ther.* 6, 37. doi: 10.1186/alzrt269

Czirr, E., and Wyss-Coray, T. (2012). The immunology of neurodegeneration. *J. Clin. Invest.* 122, 1156–1163. doi: 10.1172/JCI58656

Decker, H., Jürgensen, S., Adrover, M. F., Brito-Moreira, J., Bomfim, T. R., Klein, W. L., et al. (2010a). N-Methyl-d-aspartate receptors are required for synaptic targeting of Alzheimer's toxic amyloid-β peptide oligomers. *J. Neurochem.* 115, 1520–1529. doi: 10.1111/j.1471-4159.2010.07058.x

Decker, H., Lo, K. Y., Unger, S. M., Ferreira, S. T., and Silverman, M. A. (2010b). Amyloid- peptide oligomers disrupt axonal transport through an NMDA receptor-dependent mechanism that is mediated by glycogen synthase kinase 3 in primary cultured hippocampal neurons. *J. Neurosci.* 30, 9166–9171. doi: 10.1523/JNEUROSCI.1074-10.2010

De Felice, F. G. (2013). Alzheimer' s disease and insulin resistance : translating basic science into clinical applications. *J. Clin. Invest.* 123, 531–539. doi: 10.1172/JCI64595

De Felice, F. G., and Ferreira, S. T. (2014). Inflammation, defective insulin signaling, and mitochondrial dysfunction as common molecular denominators connecting type 2 diabetes to alzheimer disease. *Diabetes* 63, 2262–2272. doi: 10.2337/db13-1954

De Felice, F. G., and Lourenco, M. V. (2015). Brain metabolic stress and neuroinflammation at the basis of cognitive impairment in Alzheimer's disease. *Front. Aging Neurosci.* 7:94. doi: 10.3389/fnagi.2015.00094

De Felice, F. G., and Munoz, D. P. (2016). Opportunities and challenges in developing relevant animal models for Alzheimer's disease. *Ageing Res. Rev.* 26, 112–114. doi: 10.1016/j.arr.2016.01.006

De Felice, F. G., Velasco, P. T., Lambert, M. P., Viola, K., Fernandez, S. J., Ferreira, S. T., et al. (2007). Abeta oligomers induce neuronal oxidative stress through an N-methyl-D-aspartate receptor-dependent mechanism that is blocked by the Alzheimer drug memantine. *J. Biol. Chem.* 282, 11590–11601. doi: 10.1074/jbc.M607483200

De Felice, F. G., Vieira, M. N. N., Bomfim, T. R., Decker, H., Velasco, P. T., Lambert, M. P., et al. (2009). Protection of synapses against Alzheimer's-linked toxins: insulin signaling prevents the pathogenic binding of Abeta oligomers. *Proc. Natl. Acad. Sci. U. S. A.* 106, 1971–1976. doi: 10.1073/pnas.08091 58106

De Felice, F. G., Wu, D., Lambert, M. P., Fernandez, S. J., Velasco, P. T., Lacor, P. N., et al. (2008). Alzheimer's disease-type neuronal tau hyperphosphorylation induced by A beta oligomers. *Neurobiol. Aging* 29, 1334–1347. doi: 10.1016/j.neurobiolaging.2007.02.029

de la Monte, S. M. (2009). Insulin resistance and Alzheimer's disease. *BMB Rep.* 42, 475–481. doi: 10.5483/BMBRep.2009.42.8.475

Denis, R. G., Arruda, A. P., Romanatto, T., Milanski, M., Coope, A., Solon, C., et al. (2010). TNF-α transiently induces endoplasmic reticulum stress and an incomplete unfolded protein response in the hypothalamus. *Neuroscience* 170, 1035–1044. doi: 10.1016/j.neuroscience.2010.08.013

Devi, L., and Ohno, M. (2010). Phospho-eIF2α level is important for determining abilities of BACE1 reduction to rescue cholinergic neurodegeneration and memory defects in 5XFAD mice. *PLoS ONE* 5:e12974. doi: 10.1371/journal.pone.0012974

Devi, L., and Ohno, M. (2013). Deletion of the eIF2α kinase GCN2 fails to rescue the memory decline associated with alzheimer's disease. *PLoS ONE* 8:e77335. doi: 10.1371/journal.pone.0077335

Devi, L., and Ohno, M. (2014). PERK mediates eIF2α phosphorylation responsible for BACE1 elevation, CREB dysfunction and neurodegeneration in a mouse model of Alzheimer's disease. *Neurobiol. Aging* 35, 2272–2281. doi: 10.1016/j.neurobiolaging.2014.04.031

Dufey, E., Sepúlveda, D., Rojas-Rivera, D., and Hetz, C. (2014). Cellular mechanisms of endoplasmic reticulum stress signaling in health and disease. 1. An overview. *Am. J. Physiol. Physiol.* 307, C582–C594. doi: 10.1152/ajpcell.00258.2014

Dubois, B., Hampel, H., Feldman, H. H., Scheltens, P., Aisen, P., Andrieu, S., et al. (2016). Preclinical Alzheimer's disease: definition, natural history, and diagnostic criteria. *Alzheimers Dement.* 12, 292–323. doi: 10.1016/j.jalz.2016.02.002

Duncan, M. J., Smith, J. T., Franklin, K. M., Beckett, T. L., Murphy, M. P., St. Clair, D. K., et al. (2012). Effects of aging and genotype on circadian rhythms, sleep, and clock gene expression in APPxPS1 knock-in mice, a model for Alzheimer's disease. *Exp. Neurol.* 236, 249–258. doi: 10.1016/j.expneurol.2012.05.011

Duran-Aniotz, C., Cornejo, V. H., Espinoza, S., Ardiles, Á. O., Medinas, D. B., Salazar, C., et al. (2017). IRE1 signaling exacerbates Alzheimer's disease pathogenesis. *Acta Neuropathol.* 134, 489–506. doi: 10.1007/s00401-017-1694-x

Fagan, A. M., Xiong, C., Jasielec, M. S., Bateman, R. J., Goate, A. M., Benzinger, T. L. S., et al. (2014). Longitudinal change in CSF biomarkers in autosomal-dominant alzheimer's disease. *Sci. Transl. Med.* 6:226ra30. doi: 10.1126/scitranslmed.3007901

Fá, M., Puzzo, D., Piacentini, R., Staniszewski, A., Zhang, H., Baltrons, M. A., et al. (2016). Extracellular tau oligomers produce an immediate impairment of LTP and memory. *Sci. Rep.* 6:19393. doi: 10.1038/srep19393

Farris, W., Mansourian, S., Chang, Y., Lindsley, L., Eckman, E. A., Frosch, M. P., et al. (2003). Insulin-degrading enzyme regulates the levels of insulin, amyloid beta-protein, and the beta-amyloid precursor protein intracellular domain *in vivo*. *Proc. Natl. Acad. Sci. U.S.A.* 100, 4162–4167. doi: 10.1073/pnas.0230450100

Ferreira, S. T., Clarke, J. R., Bomfim, T. R., and De Felice, F. G. (2014). Inflammation, defective insulin signaling, and neuronal dysfunction in Alzheimer's disease. *Alzheimer's Dement.* 10, S76–S83. doi: 10.1016/j.jalz.2013.12.010

Ferreira, S. T., and Klein, W. L. (2011). The Aβ oligomer hypothesis for synapse failure and memory loss in Alzheimer's disease. *Neurobiol. Learn. Mem.* 96, 529–543. doi: 10.1016/j.nlm.2011.08.003

Ferreira, S. T., Lourenco, M. V., Oliveira, M. M., and De Felice, F. G. (2015). Soluble amyloid-β oligomers as synaptotoxins leading to cognitive impairment in Alzheimer's disease. *Front. Cell. Neurosci.* 9:191. doi: 10.3389/fncel.2015.00191

Finder, V. H., and Glockshuber, R. (2007). Amyloid-beta aggregation. *Neurodegener. Dis.* 4, 13–27. doi: 10.1159/000100355

Forny-Germano, L., Lyra e Silva, N. M., Batista, A. F., Brito-Moreira, J., Gralle, M., Boehnke, S. E., et al. (2014). Alzheimer's disease-like pathology induced by amyloid- oligomers in nonhuman primates. *J. Neurosci.* 34, 13629–13643. doi: 10.1523/JNEUROSCI.1353-14.2014

Freeman, O. J., and Mallucci, G. R. (2016). The UPR and synaptic dysfunction in neurodegeneration. *Brain Res.* 1648, 530–537. doi: 10.1016/j.brainres.2016.03.029

Fu, H., Rodriguez, G. A., Herman, M., Emrani, S., Nahmani, E., Barrett, G., et al. (2017). Tau pathology induces excitatory neuron loss, grid cell dysfunction, and spatial memory deficits reminiscent of early alzheimer's disease. *Neuron* 93, 533.e5–541.e5. doi: 10.1016/j.neuron.2016.12.023

Geerlings, M. I., Den Heijer, T., Koudstaal, P. J., Hofman, A., and Breteler, M. M. B. (2008). History of depression, depressive symptoms, and medial temporal lobe atrophy and the risk of Alzheimer disease. *Neurology* 70, 1258–1264. doi: 10.1212/01.wnl.0000308937.30473.d1

Georganopoulou, D. G., Chang, L., Nam, J.-M., Thaxton, C. S., Mufson, E. J., Klein, W. L., et al. (2005). From the cover: nanoparticle-based detection in cerebral spinal fluid of a soluble pathogenic biomarker for Alzheimer's disease. *Proc. Natl. Acad. Sci. U. S. A.* 102, 2273–2276. doi: 10.1073/pnas.0409336102

Gibb, W. R., Mountjoy, C. Q., Mann, D. M., and Lees, A. J. (1989). The substantia nigra and ventral tegmental area in Alzheimer's disease and Down's syndrome. *J. Neurol. Neurosurg. Psychiatry* 52, 193–200.

Green, R. C., Cupples, L. A., Kurz, A., Auerbach, S., Go, R., Sadovnick, D., et al. (2003). Depression as a risk factor for Alzheimer disease: the MIRAGE Study. *Arch. Neurol.* 60, 753–759. doi: 10.1001/archneur.60.5.753

Guerreiro, R., Wojtas, A., Bras, J., Carrasquillo, M., Rogaeva, E., Majounie, E., et al. (2013). TREM2 variants in Alzheimer's Disease. *N. Engl. J. Med.* 368, 117–127. doi: 10.1056/NEJMoa1211851

Guillot-Sestier, M. V., Doty, K. R., Gate, D., Rodriguez, J., Leung, B. P., Rezai-Zadeh, K., et al. (2015). Il10 deficiency rebalances innate immunity to mitigate Alzheimer-like pathology. *Neuron.* 85, 534–548. doi: 10.1016/j.neuron.2014.12.068

Gulaj, E., Pawlak, K., Bien, B., and Pawlak, D. (2010). Kynurenine and its metabolites in Alzheimer's disease patients. *Adv. Med. Sci.* 55, 204–211. doi: 10.2478/v10039-010-0023-6

Haes, A. J., Chang, L., Klein, W. L., and Van Duyne, R. P. (2005). Detection of a biomarker for Alzheimer's disease from synthetic and clinical samples using a nanoscale optical biosensor. *J. Am. Chem. Soc.* 127, 2264–2271. doi: 10.1021/ja044087q

Hardy, J. (2002). The amyloid hypothesis of Alzheimer's disease: progress and problems on the road to therapeutics. *Science* 297, 353–356. doi: 10.1126/science.1072994

Hendrix, J. A., Bateman, R. J., Brashear, H. R., Duggan, C., Carrillo, M. C., Bain, L. J., et al. (2016). Challenges, solutions, and recommendations for Alzheimer's disease combination therapy. *Alzheimer's Dement.* 12, 623–630. doi: 10.1016/j.jalz.2016.02.007

Heneka, M. T., Carson, M. J., Khoury, J., El, Landreth, G. E., Brosseron, F., Feinstein, D. L., et al. (2015a). Neuroinflammation in Alzheimer's disease. *Lancet Neurol.* 14, 388–405. doi: 10.1016/S1474-4422(15)70016-5

Heneka, M. T., and O'Banion, M. K. (2007). Inflammatory processes in Alzheimer's disease. *J. Neuroimmunol.* 184, 69–91. doi: 10.1016/j.jneuroim.2006.11.017

Heneka, M. T., Golenbock, D. T., and Latz, E. (2015b). Innate immunity in Alzheimer's disease. *Nat. Immunol.* 16, 229–236. doi: 10.1038/ni.3102

Herskovits, A. Z., Locascio, J. J., Peskind, E. R., Li, G., and Hyman, B. T. (2013). A luminex assay detects amyloid β oligomers in alzheimer's disease cerebrospinal fluid. *PLoS ONE* 8:e67898. doi: 10.1371/journal.pone.0067898

Hetz, C. (2012). The unfolded protein response: controlling cell fate decisions under ER stress and beyond. *Nat. Rev. Mol. Cell Biol.* 13, 89–102. doi: 10.1038/nrm3270

Hetz, C., and Saxena, S. (2017). ER stress and the unfolded protein response in neurodegeneration. *Nat. Rev. Neurol.* 13, 477–491. doi: 10.1038/nrneurol.2017.99

Hoozemans, J. J. M., van Haastert, E. S., Nijholt, D. A. T., Rozemuller, A. J. M., Eikelenboom, P., and Scheper, W. (2009). The unfolded protein response is activated in pretangle neurons in Alzheimer's disease hippocampus. *Am. J. Pathol.* 174, 1241–1251. doi: 10.2353/ajpath.2009.080814

Hong, S., Beja-Glasser, V. F., Nfonoyim, B. M., Frouin, A., Li, S., Ramakrishnan, S., et al. (2016a). Complement and microglia mediate early synapse loss in Alzheimer mouse models. *Science* 352, 712–716. doi: 10.1126/science.aad8373

Hong, S., Dissing-Olesen, L., and Stevens, B. (2016b). New insights on the role of microglia in synaptic pruning in health and disease. *Curr. Opin. Neurobiol.* 36, 128–134. doi: 10.1016/j.conb.2015.12.004

Hotamisligil, G. S. (2006). Inflammation and metabolic disorders. *Nature* 444, 860–867. doi: 10.1038/nature05485

Hotamisligil, G. S. (2017). Inflammation, metaflammation and immunometabolic disorders. *Nature* 542, 177–185. doi: 10.1038/nature21363

Ishii, M., and Iadecola, C. (2015). Metabolic and non-cognitive manifestations of Alzheimers disease: the hypothalamus as both culprit and target of pathology. *Cell Metab.* 22, 761–776. doi: 10.1016/j.cmet.2015.08.016

Ittner, L. M., and Götz, J. (2011). Amyloid-β and tau — a toxic pas de deux in Alzheimer's disease. *Nat. Rev. Neurosci.* 12, 65–72. doi: 10.1038/nrn2967

Iwata, N., Tsubuki, S., Takaki, Y., Shirotani, K., Lu, B., Gerard, N. P., et al. (2001). Metabolic regulation of brain Abeta by neprilysin. *Science* 292, 1550–1552. doi: 10.1126/science.1059946

Janson, J., Laedtke, T., Parisi, J. E., O'Brien, P., Petersen, R. C., and Butler, P. C. (2004). Increased risk of type 2 diabetes in Alzheimer disease. *Diabetes* 53, 474–481. doi: 10.2337/diabetes.53.2.474

Jin, M., Shepardson, N., Yang, T., Chen, G., Walsh, D., and Selkoe, D. J. (2011). Soluble amyloid -protein dimers isolated from Alzheimer cortex directly induce Tau hyperphosphorylation and neuritic degeneration. *Proc. Natl. Acad. Sci. U.S.A.* 108, 5819–5824. doi: 10.1073/pnas.1017033108

Jürgensen, S., Antonio, L. L., Mussi, G. E. A., Brito-Moreira, J., Bomfim, T. R., De Felice, F. G., et al. (2011). Activation of D1/D5 dopamine receptors protects neurons from synapse dysfunction induced by amyloid-β oligomers. *J. Biol. Chem.* 286, 3270–3276. doi: 10.1074/jbc.M110.177790

Ju, Y.-E. S., Lucey, B. P., and Holtzman, D. M. (2014). Sleep and Alzheimer disease pathology–a bidirectional relationship. *Nat. Rev. Neurol.* 10, 115–119. doi: 10.1038/nrneurol.2013.269

Karran, E., Mercken, M., and Strooper, B., De (2011). The amyloid cascade hypothesis for Alzheimer's disease: an appraisal for the development of therapeutics. *Nat. Rev. Drug Discov.* 10, 698–712. doi: 10.1038/nrd3505

Kincheski, G. C., Valentim, I. S., Clarke, J. R., Cozachenco, D., Castelo-Branco, M. T. L., Ramos-Lobo, A. M., et al. (2017). Chronic sleep restriction promotes brain inflammation and synapse loss, and potentiates memory impairment induced by amyloid-β oligomers in mice. *Brain Behav. Immun.* 64, 140–151. doi: 10.1016/j.bbi.2017.04.007

Koffie, R. M., Meyer-Luehmann, M., Hashimoto, T., Adams, K. W., Mielke, M. L., Garcia-Alloza, M., et al. (2009). Oligomeric amyloid associates with postsynaptic densities and correlates with excitatory synapse loss near senile plaques. *Proc. Natl. Acad. Sci. U.S.A.* 106, 4012–4017. doi: 10.1073/pnas.0811698106

Lanctôt, K. L., Amatniek, J., Ancoli-Israel, S., Arnold, S. E., Ballard, C., Cohen-Mansfield, J., et al. (2017). Neuropsychiatric signs and symptoms of Alzheimer's disease: new treatment paradigms. *Alzheimer's Dement. Transl. Res. Clin. Interv.* 3, 440–449. doi: 10.1016/j.trci.2017.07.001

Ledo, J. H., Azevedo, E. P., Beckman, D., Ribeiro, F. C., Santos, L. E., Razolli, D. S., et al. (2016). Cross talk between brain innate immunity and serotonin signaling underlies depressive-like behavior induced by Alzheimer's amyloid- oligomers in mice. *J. Neurosci.* 36, 12106–12116. doi: 10.1523/JNEUROSCI.1269-16.2016

Ledo, J. H., Azevedo, E. P., Clarke, J. R., Ribeiro, F. C., Figueiredo, C. P., Foguel, D., et al. (2013). Amyloid-β oligomers link depressive-like behavior and cognitive deficits in mice. *Mol. Psychiatry* 18, 1053–1054. doi: 10.1038/mp.2012.168

Lee, C. Y. D., and Landreth, G. E. (2010). The role of microglia in amyloid clearance from the AD brain. *J. Neural Transm.* 117, 949–960. doi: 10.1007/s00702-010-0433-4

Lee, S., Fernandez, E. J., and Good, T. A. (2007). Role of aggregation conditions in structure, stability, and toxicity of intermediates in the Abeta fibril formation pathway. *Protein Sci.* 16, 723–732. doi: 10.1110/ps.062514807

Leissring, M. A., Farris, W., Chang, A. Y., Walsh, D. M., Wu, X., Sun, X., et al. (2003). Enhanced proteolysis of β-amyloid in APP transgenic mice prevents plaque formation, secondary pathology, and premature death. *Neuron* 40, 1087–1093. doi: 10.1016/S0896-6273(03)00787-6

Lester-Coll, N., Rivera, E. J., Soscia, S. J., Doiron, K., Wands, J. R., and de la Monte, S. M. (2006). Intracerebral streptozotocin model of type 3 diabetes: relevance to sporadic Alzheimer's disease. *J. Alzheimers. Dis.* 9, 13–33. doi: 10.3233/JAD-2006-9102

Lim, A. S. P., Ellison, B. A., Wang, J. L., Yu, L., Schneider, J. A., Buchman, A. S., et al. (2014). Sleep is related to neuron numbers in the ventrolateral preoptic/intermediate nucleus in older adults with and without Alzheimer's disease. *Brain* 137, 2847–2861. doi: 10.1093/brain/awu222

Liu, F., Day, M., Muñiz, L. C., Bitran, D., Arias, R., Revilla-Sanchez, R., et al. (2008). Activation of estrogen receptor-β regulates hippocampal synaptic plasticity and improves memory. *Nat. Neurosci.* 11, 334–343. doi: 10.1038/nn2057

Lourenco, M. V., Clarke, J. R., Frozza, R. L., Bomfim, T. R., Forny-Germano, L., Batista, A. F., et al. (2013). TNF-α mediates PKR-dependent memory impairment and brain IRS-1 inhibition induced by Alzheimer's β-amyloid oligomers in mice and monkeys. *Cell Metab.* 18, 831–843. doi: 10.1016/j.cmet.2013.11.002

Lourenco, M. V., Ferreira, S. T., and De Felice, F. G. (2015). Neuronal stress signaling and eIF2α phosphorylation as molecular links between Alzheimer's disease and diabetes. *Prog. Neurobiol.* 129, 37–57. doi: 10.1016/j.pneurobio.2015.03.003

Lyketsos, C. G., and Olin, J. (2002). Depression in Alzheimer's disease: overview and treatment. *Biol. Psychiatry* 52, 243–252. doi: 10.1016/S0006-3223(02)01348-3

Ma, Q.-L., Yang, F., Rosario, E. R., Ubeda, O. J., Beech, W., Gant, D. J., et al. (2009). Beta-amyloid oligomers induce phosphorylation of tau and inactivation of insulin receptor substrate via c-jun n-terminal kinase signaling: suppression by omega-3 fatty acids and curcumin. *J. Neurosci.* 9, 9078–9089. doi: 10.1523/JNEUROSCI.1071-09.2009

Ma, T., Trinh, M. A., Wexler, A. J., Bourbon, C., Gatti, E., Pierre, P., et al. (2013). Suppression of eIF2α kinases alleviates Alzheimer's disease–related plasticity and memory deficits. *Nat. Neurosci.* 16, 1299–1305. doi: 10.1038/nn.3486

Mandrekar-Colucci, S., Karlo, J. C., and Landreth, G. E. (2012). Mechanisms underlying the rapid peroxisome proliferator-activated receptor- -mediated amyloid clearance and reversal of cognitive deficits in a murine model of alzheimer's disease. *J. Neurosci.* 32, 10117–10128. doi: 10.1523/JNEUROSCI.5268-11.2012

Masliah, E., Ellisman, M., Carragher, B., Mallory, M., Young, S., Hansen, L., et al. (1992). Three-dimensional analysis of the relationship between synaptic

pathology and neuropil threads in Alzheimer disease. *J. Neuropathol. Exp. Neurol.* 51, 404–414. doi: 10.1097/00005072-199207000-00003

Masters, M. C., Morris, J. C., and Roe, C. M. (2015). "Noncognitive" symptoms of early Alzheimer disease : a longitudinal analysis. *Neurology* 84, 617–622. doi: 10.1212/WNL.0000000000001238

Matsuzaki, T., Sasaki, K., Tanizaki, Y., Hata, J., Fujimi, K., Matsui, Y., et al. (2010). Insulin resistance is associated with the pathology of Alzheimer disease: the Hisayama study. *Neurology* 75, 764–770. doi: 10.1212/WNL.0b013e3181eee25f

Mattson, M. P. (2010). ER calcium and Alzheimer's disease: in a state of flux. *Sci. Signal.* 3:pe10. doi: 10.1126/scisignal.3114pe10

McNamara, C. G., Tejero-Cantero, Á., Trouche, S., Campo-Urriza, N., and Dupret, D. (2014). Dopaminergic neurons promote hippocampal reactivation and spatial memory persistence. *Nat. Neurosci.* 17, 1658–1660. doi: 10.1038/nn.3843

Medeiros, R., Baglietto-Vargas, D., and Laferla, F. M. (2011). The role of Tau in Alzheimer's disease and related disorders. *CNS Neurosci. Ther.* 17, 514–524. doi: 10.1111/j.1755-5949.2010.00177.x

Milanski, M., Degasperi, G., Coope, A., Morari, J., Denis, R., Cintra, D. E., et al. (2009). Saturated fatty acids produce an inflammatory response predominantly through the activation of TLR4 signaling in hypothalamus: implications for the pathogenesis of obesity. *J. Neurosci.* 29, 359–370. doi: 10.1523/JNEUROSCI.2760-08.2009

Miñano-Molina, A. J., España, J., Martín, E., Barneda-Zahonero, B., Fadó, R., Solé, M., et al. (2011). Soluble oligomers of amyloid-β peptide disrupt membrane trafficking of α-amino-3-hydroxy-5-methylisoxazole-4-propionic acid receptor contributing to early synapse dysfunction. *J. Biol. Chem.* 286, 27311–27321. doi: 10.1074/jbc.M111.227504

Moloney, A. M., Griffin, R. J., Timmons, S., O'Connor, R., Ravid, R., and O'Neill, C. (2010). Defects in IGF-1 receptor, insulin receptor and IRS-1/2 in Alzheimer's disease indicate possible resistance to IGF-1 and insulin signalling. *Neurobiol. Aging* 31, 224–243. doi: 10.1016/j.neurobiolaging.2008.04.002

Morales, I., GuzmÃ¡n-MartÃ-nez, L., Cerda-Troncoso, C., FarÃ-as, G. A., and Maccioni, R. B. (2014). Neuroinflammation in the pathogenesis of Alzheimer's disease. A rational framework for the search of novel therapeutic approaches. *Front. Cell. Neurosci.* 8:112. doi: 10.3389/fncel.2014.00112

Morris, M., Maeda, S., Vossel, K., and Mucke, L. (2011). The many faces of Tau. *Neuron* 70, 410–426. doi: 10.1016/j.neuron.2011.04.009

Mosconi, L., Berti, V., Guyara-Quinn, C., McHugh, P., Petrongolo, G., Osorio, R. S., et al. (2017a). Perimenopause and emergence of an Alzheimer's bioenergetic phenotype in brain and periphery. *PLoS ONE* 12:e0185926. doi: 10.1371/journal.pone.0185926

Mosconi, L., Berti, V., Quinn, C., McHugh, P., Petrongolo, G., Varsavsky, I., et al. (2017b). Sex differences in Alzheimer risk. *Neurology* 89, 1382–1390. doi: 10.1212/WNL.0000000000004425

Murakami, K., Tokuda, M., Suzuki, T., Irie, Y., Hanaki, M., Izuo, N., et al. (2016). Monoclonal antibody with conformational specificity for a toxic conformer of amyloid β42 and its application toward the Alzheimer's disease diagnosis. *Sci. Rep.* 6:29038. doi: 10.1038/srep29038

Musiek, E. S., and Holtzman, D. M. (2015). Three dimensions of the amyloid hypothesis: time, space and "wingmen." *Nat. Neurosci.* 18, 800–806. doi: 10.1038/nn.4018

Musiek, E. S., and Holtzman, D. M. (2016). Mechanisms linking circadian clocks, sleep, and neurodegeneration. *Science* 354, 1004–1008. doi: 10.1126/science.aah4968

Musiek, E. S., Xiong, D. D., and Holtzman, D. M. (2015). Sleep, circadian rhythms, and the pathogenesis of Alzheimer Disease. *Exp. Mol. Med.* 47, e148. doi: 10.1038/emm.2014.121

Nobili, A., Latagliata, E. C., Viscomi, M. T., Cavallucci, V., Cutuli, D., Giacovazzo, G., et al. (2017). Dopamine neuronal loss contributes to memory and reward dysfunction in a model of Alzheimer's disease. *Nat. Commun.* 8:14727. doi: 10.1038/ncomms14727

Ogomori, K., Kitamoto, T., Tateishi, J., Sato, Y., Suetsugu, M., and Abe, M. (1989). Beta-protein amyloid is widely distributed in the central nervous system of patients with Alzheimer's disease. *Am. J. Pathol.* 134, 243–251.

Ott, A., Stolk, R. P., Hofman, A., Van Harskamp, F., Grobbee, D. E., and Breteler, M. M. B. (1996). Association of diabetes mellitus and dementia: the Rotterdam Study. *Diabetologia* 39, 1392–1397. doi: 10.1007/s001250050588

Ott, A., Stolk, R. P., van Harskamp, F., Pols, H. A. P., Hofman, A., and Breteler, M. M. B. (1999). Diabetes mellitus and the risk of dementia: the Rotterdam Study. *Neurology* 53, 1937–1937. doi: 10.1212/WNL.53.9.1937

Ownby, R. L., Crocco, E., Acevedo, A., John, V., and Loewenstein, D. (2006). Depression and risk for Alzheimer disease. *Arch. Gen. Psychiatry* 63, 530. doi: 10.1001/archpsyc.63.5.530

Perez-Nievas, B. G., Stein, T. D., Tai, H. C., Dols-Icardo, O., Scotton, T. C., Barroeta-Espar, I., et al. (2013). Dissecting phenotypic traits linked to human resilience to Alzheimer's pathology. *Brain* 136, 2510–2526. doi: 10.1093/brain/awt171

Perry, D., Sperling, R., Katz, R., Berry, D., Dilts, D., Hanna, D., et al. (2014). Building a roadmap for developing combination therapies for Alzheimer's disease. *Expert Rev. Neurother.* 15, 327–333. doi: 10.1586/14737175.2015.996551

Perry, G., Cash, A. D., and Smith, M. A. (2002). Alzheimer disease and oxidative stress. *J. Biomed. Biotechnol.* 23, 120–123. doi: 10.1155/S1110724302203010

Perry, V. H., Nicoll, J. A. R., and Holmes, C. (2010). Microglia in neurodegenerative disease. *Nat. Rev. Neurol.* 6, 193–201. doi: 10.1038/nrneurol.2010.17

Piacentini, R., Li Puma, D. D., Mainardi, M., Lazzarino, G., Tavazzi, B., Arancio, O., et al. (2017). Reduced gliotransmitter release from astrocytes mediates tau-induced synaptic dysfunction in cultured hippocampal neurons. *Glia* 65, 1302–1316. doi: 10.1002/glia.23163

Prince, M., Bryce, R., Albanese, E., Wimo, A., Ribeiro, W., and Ferri, C. P. (2013). The global prevalence of dementia: a systematic review and metaanalysis. *Alzheimer's Dement.* 9, 63–75. doi: 10.1016/j.jalz.2012.11.007

Prince, M., Comas-Herrera, A., Knapp, M., Guerchet, M., and Karagiannidou, M. (2016). *World Alzheimer Report 2016 Improving Healthcare for People Living with Dementia. Coverage, Quality and Costs Now and in the Future.* Available online at: https://www.alz.co.uk/research/world-report-2016

Prinz, P., Vitaliano, P. P., Vitiello, M. V., Bokan, J., Raskind, M., Peskind, E., et al. (1982). Sleep, EEG and mental function changes in senile dementia of the Alzheimer's type. *Neurobiol. Aging* 3, 361–370.

Puzzo, D., Piacentini, R., Fá, M., Gulisano, W., Li Puma, D. D., Staniszewski, A., et al. (2017). LTP and memory impairment caused by extracellular Aβ and tau oligomers is APP- dependent. *Elife* 6:e26991. doi: 10.7554/eLife.26991

Qiu, W. Q., Walsh, D. M., Ye, Z., Vekrellis, K., Zhang, J., Podlisny, M. B., et al. (1998). Insulin-degrading enzyme regulates extracellular levels of amyloid β- protein by degradation. *J. Biol. Chem.* 273, 32730–32738. doi: 10.1074/jbc.273.49.32730

Querfurth, H. W., and LaFerla, F. M. (2010). Alzheimer's disease. *N. Engl. J. Med.* 362, 329–344. doi: 10.1056/NEJMra0909142

Reilly, P., Winston, C. N., Baron, K. R., Trejo, M., Rockenstein, E. M., Akers, J. C., et al. (2017). Novel human neuronal tau model exhibiting neurofibrillary tangles and transcellular propagation. *Neurobiol. Dis.* 106, 222–234. doi: 10.1016/j.nbd.2017.06.005

Rivera, E. J., Goldin, A., Fulmer, N., Tavares, R., Wands, J. R., and de la Monte, S. M. (2005). Insulin and insulin-like growth factor expression and function deteriorate with progression of Alzheimer's disease: link to brain reductions in acetylcholine. *J. Alzheimers Dis.* 8, 247–268. doi: 10.3233/JAD-2005-8304

Romano, A., Pace, L., Tempesta, B., Lavecchia, A. M., Macheda, T., Bedse, G., et al. (2014). Depressive-like behavior is paired to monoaminergic alteration in a murine model of Alzheimer's disease. *Int. J. Neuropsychopharmacol.* 18, 1–12. doi: 10.1093/ijnp/pyu020

Roselli, F., Tirard, M., Lu, J., Hutzler, P., Lamberti, P., Livrea, P., et al. (2005). Soluble β-amyloid 1-40 induces NMDA-dependent degradation of postsynaptic density-95 at glutamatergic synapses. *J. Neurosci.* 25, 11061–11070. doi: 10.1523/JNEUROSCI.3034-05.2005

Rossato, J. I., Bevilaqua, L. R. M., Izquierdo, I., Medina, J. H., and Cammarota, M. (2009). Dopamine controls persistence of long-term memory storage. *Science* 325, 1017–1020. doi: 10.1126/science.1172545

Rowan, M. J., Klyubin, I., Wang, Q., and Anwyl, R. (2005). Synaptic plasticity disruption by amyloid beta protein: modulation by potential Alzheimer's disease modifying therapies. *Biochem. Soc. Trans.* 33, 563–567. doi: 10.1042/BST0330563

Russo, S. J., and Nestler, E. J. (2013). The brain reward circuitry in mood disorders. *Nat. Rev. Neurosci.* 14, 609–625. doi: 10.1038/nrn3381

Salter, M. W., and Stevens, B. (2017). Microglia emerge as central players in brain disease. *Nat. Med.* 23, 1018–1027. doi: 10.1038/nm.4397

Santos, L. E., Beckman, D., and Ferreira, S. T. (2016). Microglial dysfunction connects depression and Alzheimer's disease. *Brain. Behav. Immun.* 55, 151–165. doi: 10.1016/j.bbi.2015.11.011

Scheltens, P., Blennow, K., Breteler, M. M. B., de Strooper, B., Frisoni, G. B., Salloway, S., et al. (2016). Alzheimer's disease. *Lancet* 388, 505–517. doi: 10.1016/S0140-6736(15)01124-1

Selkoe, D. J. (2002). Alzheimer's disease is a synaptic failure. *Science* 298, 789–791. doi: 10.1126/science.1074069

Selkoe, D. J. (2008). Soluble oligomers of the amyloid β-protein impair synaptic plasticity and behavior. *Behav. Brain Res.* 192, 106–113. doi: 10.1007/978-3-540-76330-7_8

Selkoe, D. J., and Hardy, J. (2016). The amyloid hypothesis of Alzheimer's disease at 25 years. *EMBO Mol. Med.* 8, 1–14. doi: 10.15252/emmm.201606210

Shankar, G. M., Bloodgood, B. L., Townsend, M., Walsh, D. M., Selkoe, D. J., and Sabatini, B. L. (2007). Natural oligomers of the alzheimer amyloid- protein induce reversible synapse loss by modulating an NMDA-type glutamate receptor-dependent signaling pathway. *J. Neurosci.* 27, 2866-75. doi: 10.1523/JNEUROSCI.4970-06.2007

Shankar, G. M., Li, S., Mehta, T. H., Garcia-Munoz, A., Shepardson, N. E., Smith, I., et al. (2008). Amyloid-β protein dimers isolated directly from Alzheimer's brains impair synaptic plasticity and memory. *Nat. Med.* 14, 837–842. doi: 10.1038/nm1782

Small, S. A., and Duff, K. (2008). Linking Aβ and Tau in late-onset Alzheimer's disease: a dual pathway hypothesis. *Neuron* 60, 534–542. doi: 10.1016/j.neuron.2008.11.007

Smith, M. A., Hirai, K., Hsiao, K., Pappolla, M. A., Harris, P. L., Siedlak, S. L., et al. (1998). Amyloid-beta deposition in Alzheimer transgenic mice is associated with oxidative stress. *J. Neurochem.* 70, 2212–2215. doi: 10.1046/j.1471-4159.1998.70052212.x

Snyder, E. M., Nong, Y., Almeida, C. G., Paul, S., Moran, T., Choi, E. Y., et al. (2005). Regulation of NMDA receptor trafficking by amyloid-β. *Nat. Neurosci.* 8, 1051–1058. doi: 10.1038/nn1503

Snyder, H. M., Asthana, S., Bain, L., Brinton, R., Craft, S., Dubal, D. B., et al. (2016). Sex biology contributions to vulnerability to Alzheimer's disease: a think tank convened by the Women's Alzheimer's Research Initiative. *Alzheimer's Dement.* 12, 1186–1196. doi: 10.1016/j.jalz.2016.08.004

Sperling, R. A., Aisen, P. S., Beckett, L. A., Bennett, D. A., Craft, S., Fagan, A. M., et al. (2011a). Toward defining the preclinical stages of Alzheimer's disease: recommendations from the National Institute on Aging-Alzheimer's Association workgroups on diagnostic guidelines for Alzheimer's disease. *Alzheimer's Dement.* 7, 280–292. doi: 10.1016/j.jalz.2011.03.003

Sperling, R. A., Jack, C. R., and Aisen, P. S. (2011b). Testing the right target and right drug at the right stage. *Sci. Transl. Med.* 3:111cm33. doi: 10.1126/scitranslmed.3002609

Spires-Jones, T. L., and Hyman, B. T. (2014). The intersection of amyloid beta and tau at synapses in Alzheimer's disease. *Neuron* 82, 756–771. doi: 10.1016/j.neuron.2014.05.004

Standaert, D. G., Lee, V. M., Greenberg, B. D., Lowery, D. E., and Trojanowski, J. Q. (1991). Molecular features of hypothalamic plaques in Alzheimer's disease. *Am. J. Pathol.* 139, 681–691.

Stanley, M., Macauley, S. L., Caesar, E. E., Koscal, L. J., Moritz, W., Robinson, G. O., et al. (2016). The effects of peripheral and central high insulin on brain insulin signaling and amyloid-β in young and old APP/PS1 mice. *J. Neurosci.* 36, 11704–11715. doi: 10.1523/JNEUROSCI.2119-16.2016

Starkstein, S. E., and Mizrahi, R. (2006). Depression in Alzheimer's disease. *Exp. Rev. Neurother.* 6, 887–895. doi: 10.1586/14737175.6.6.887

Steen, E., Terry, B. M., Rivera, E. J., Cannon, J. L., Neely, T. R., Tavares, R., et al. (2005). Impaired insulin and insulin-like growth factor expression and signaling mechanisms in Alzheimer's disease–is this type 3 diabetes? *J. Alzheimers. Dis.* 7, 63–80. doi: 10.3233/JAD-2005-7107

Stephenson, D., Perry, D., Bens, C., Bain, L. J., Berry, D., Krams, M., et al. (2014). Charting a path toward combination therapy for Alzheimer's disease. *Exp. Rev. Neurother.* 15, 1–7. doi: 10.1586/14737175.2015.1002173

Stevanovic, K., Yunus, A., Joly-Amado, A., Gordon, M., Morgan, D., Gulick, D., et al. (2017). Disruption of normal circadian clock function in a mouse model of tauopathy. *Exp. Neurol.* 294, 58–67. doi: 10.1016/j.expneurol.2017.04.015

Stine, W. B., Dahlgren, K. N., Krafft, G. A., and LaDu, M. J. (2003). *In vitro* characterization of conditions for amyloid-β peptide oligomerization and fibrillogenesis. *J. Biol. Chem.* 278, 11612–11622. doi: 10.1074/jbc.M210207200

Storga, D., Vrecko, K., Birkmayer, J. G. D., and Reibnegger, G. (1996). Monoaminergic neurotransmitters, their precursors and metabolites in brains of Alzheimer patients. *Neurosci. Lett.* 203, 29–32. doi: 10.1016/0304-3940(95)12256-7

Swardfager, W., Lanctt, K., Rothenburg, L., Wong, A., Cappell, J., and Herrmann, N. (2010). A meta-analysis of cytokines in Alzheimer's disease. *Biol. Psychiatry* 68, 930–941. doi: 10.1016/j.biopsych.2010.06.012

Takeda, S., Sato, N., Uchio-Yamada, K., Sawada, K., Kunieda, T., Takeuchi, D., et al. (2010). Diabetes-accelerated memory dysfunction via cerebrovascular inflammation and A deposition in an Alzheimer mouse model with diabetes. *Proc. Natl. Acad. Sci. U.S.A.* 107, 7036–7041. doi: 10.1073/pnas.1000645107

Talbot, K., Wang, H. Y., Kazi, H., Han, L. Y., Bakshi, K. P., Stucky, A., et al. (2012). Demonstrated brain insulin resistance in Alzheimer's disease patients is associated with IGF-1 resistance, IRS-1 dysregulation, and cognitive decline. *J. Clin. Invest.* 122, 1316–1338. doi: 10.1172/JCI59903

Tarasoff-Conway, J. M., Carare, R. O., Osorio, R. S., Glodzik, L., Butler, T., Fieremans, E., et al. (2015). Clearance systems in the brain—implications for Alzheimer disease. *Nat. Rev. Neurol.* 11, 457–470. doi: 10.1038/nrneurol.2015.119

Terry, R. D., Masliah, E., Salmon, D. P., Butters, N., DeTeresa, R., Hill, R., et al. (1991). Physical basis of cognitive alterations in alzheimer's disease: synapse loss is the major correlate of cognitive impairment. *Ann. Neurol.* 30, 572–580.

Thaler, J. P., Yi, C. X., Schur, E. A., Guyenet, S. J., Hwang, B. H., Dietrich, M. O., et al. (2012). Obesity is associated with hypothalamic injury in rodents and humans. *J. Clin. Invest.* 122, 153–162. doi: 10.1172/JCI59660

Valdearcos, M., Xu, A. W., and Koliwad, S. K. (2015). Hypothalamic inflammation in the control of metabolic function. *Annu. Rev. Physiol.* 77, 131–160. doi: 10.1146/annurev-physiol-021014-071656

Vandal, M., White, P., Chevrier, G., Tremblay, C., St-Amour, I., Planel, E., et al. (2015). Age-dependent impairment of glucose tolerance in the 3xTg-AD mouse model of Alzheimer's disease. *FASEB J.* 29, 4273–4284. doi: 10.1096/fj.14-268482

van Maurik, I. S., Zwan, M. D., Tijms, B. M., Bouwman, F. H., Teunissen, C. E., Scheltens, P., et al. (2017). Interpreting biomarker results in individual patients with mild cognitive impairment in the Alzheimer's biomarkers in daily Practice (ABIDE) Project. *JAMA Neurol.* 74, 1481–1491. doi: 10.1001/jamaneurol.2017.2712

Villemagne, V. L., Burnham, S., Bourgeat, P., Brown, B., Ellis, K. A., Salvado, O., et al. (2013). Amyloid β deposition, neurodegeneration, and cognitive decline in sporadic Alzheimer's disease: a prospective cohort study. *Lancet Neurol.* 12, 357–367. doi: 10.1016/S1474-4422(13)70044-9

Viña, J., and Lloret, A. (2010). Why women have more Alzheimer's disease than men: gender and mitochondrial toxicity of amyloid-beta peptide. *J. Alzheimers. Dis.* 20(Suppl. 2), S527–S533. doi: 10.3233/JAD-2010-100501

Viola, K. L., and Klein, W. L. (2015). Amyloid β oligomers in Alzheimer's disease pathogenesis, treatment, and diagnosis. *Acta Neuropathol.* 129, 183–206. doi: 10.1007/s00401-015-1386-3

Viola, K. L., Sbarboro, J., Sureka, R., De, M., Bicca, M. A., Wang, J., et al. (2014). Towards non-invasive diagnostic imaging of early-stage Alzheimer's disease. *Nat. Nanotechnol.* 10, 91–98. doi: 10.1038/nnano.2014.254

Walsh, D. M., and Selkoe, D. J. (2007). Aβ oligomers - A decade of discovery. *J. Neurochem.* 101, 1172–1184 doi: 10.1111/j.1471-4159.2006.04426.x

Wang, J., Tan, L., Wang, H.-F., Tan, C.-C., Meng, X.-F., Wang, C., et al. (2015). Anti-inflammatory drugs and risk of Alzheimer's disease: an updated systematic review and meta-analysis. *J. Alzheimers Dis.* 44, 385–396. doi: 10.3233/JAD-141506

Wang, W.-Y., Tan, M.-S., Yu, J.-T., and Tan, L. (2015). Role of pro-inflammatory cytokines released from microglia in Alzheimer's disease. *Ann. Transl. Med.* 3, 136. doi: 10.3978/j.issn.2305-5839.2015.03.49

White, H., Pieper, C., Schmader, K., and Fillenbaum, G. (1996). Weight change in Alzheimer's disease. *J. Am. Geriatr. Soc.* 44, 265–272. doi: 10.1111/j.1532-5415.1996.tb00912.x

Xia, W., Yang, T., Shankar, G., Smith, I. M., Shen, Y., Walsh, D. M., et al. (2009). A specific enzyme-linked immunosorbent assay for measuring β-amyloid protein

oligomers in human plasma and brain tissue of patients with alzheimer disease. *Arch. Neurol.* 66, 190–199. doi: 10.1001/archneurol.2008.565

Yang, T., Li, S., Xu, H., Walsh, D. M., and Selkoe, D. J. (2017). Large soluble oligomers of amyloid β-protein from alzheimer brain are far less neuroactive than the smaller oligomers to which they dissociate. *J. Neurosci.* 37, 152–163. doi: 10.1523/JNEUROSCI.1698-16.2016

Yao, J., and Brinton, R. D. (2012). Estrogen regulation of mitochondrial bioenergetics. *Adv. Pharmacol.* 64, 327–371. doi: 10.1016/B978-0-12-394816-8.00010-6

Yirmiya, R., Rimmerman, N., and Reshef, R. (2015). Depression as a microglial disease. *Trends Neurosci.* 38, 637–658. doi: 10.1016/j.tins.2015.08.001

Zenaro, E., Pietronigro, E., Della Bianca, V., Piacentino, G., Marongiu, L., Budui, S., et al. (2015). Neutrophils promote Alzheimer's disease-like pathology and cognitive decline via LFA-1 integrin. *Nat. Med.* 21, 880–886. doi: 10.1038/nm.3913

Zhang, J., Ke, K. F., Liu, Z., Qiu, Y. H., and Peng, Y. P. (2013). Th17 Cell-mediated neuroinflammation is involved in neurodegeneration of Aβ1-42-Induced Alzheimer's disease model rats. *PLoS ONE* 8:e75786. doi: 10.1371/journal.pone.0075786

Zhang, X., Zhang, G., Zhang, H., Karin, M., Bai, H., and Cai, D. (2008). Hypothalamic β/NF-κB and ER stress link overnutrition to energy imbalance and obesity. *Cell* 135, 61–73. doi: 10.1016/j.cell.2008.07.043

Zhao, L., Mao, Z., Woody, S. K., and Brinton, R. D. (2016). Sex differences in metabolic aging of the brain: insights into female susceptibility to Alzheimer's disease. *Neurobiol. Aging* 42, 69–79. doi: 10.1016/j.neurobiolaging.2016.02.011

Conflict of Interest Statement: The authors declare that the research was conducted in the absence of any commercial or financial relationships that could be construed as a potential conflict of interest.

Copyright © 2018 Frozza, Lourenco and De Felice. This is an open-access article distributed under the terms of the Creative Commons Attribution License (CC BY). The use, distribution or reproduction in other forums is permitted, provided the original author(s) and the copyright owner are credited and that the original publication in this journal is cited, in accordance with accepted academic practice. No use, distribution or reproduction is permitted which does not comply with these terms.

frontiers in Aging Neuroscience

ORIGINAL RESEARCH
published: 02 February 2018
doi: 10.3389/fnagi.2018.00005

Auditory Memory Decay as Reflected by a New Mismatch Negativity Score Is Associated with Episodic Memory in Older Adults at Risk of Dementia

Daria Laptinskaya[1,2], Franka Thurm[2,3], Olivia C. Küster[1,4], Patrick Fissler[1,4], Winfried Schlee[5], Stephan Kolassa[6], Christine A. F. von Arnim[4] and Iris-Tatjana Kolassa[1,2]*

[1]Clinical and Biological Psychology, Institute of Psychology and Education, Ulm University, Ulm, Germany, [2]Department of Psychology, University of Konstanz, Konstanz, Germany, [3]Faculty of Psychology, TU Dresden, Dresden, Germany, [4]Department of Neurology, Ulm University, Ulm, Germany, [5]Department for Psychiatry and Psychotherapy, University Hospital Regensburg, Regensburg, Germany, [6]SAP (Switzerland) AG, Tägerwilen, Switzerland

The auditory mismatch negativity (MMN) is an event-related potential (ERP) peaking about 100–250 ms after the onset of a deviant tone in a sequence of identical (standard) tones. Depending on the interstimulus interval (ISI) between standard and deviant tones, the MMN is suitable to investigate the pre-attentive auditory discrimination ability (short ISIs, $\leq$ 2 s) as well as the pre-attentive auditory memory trace (long ISIs, >2 s). However, current results regarding the MMN as an index for mild cognitive impairment (MCI) and dementia are mixed, especially after short ISIs: while the majority of studies report positive associations between the MMN and cognition, others fail to find such relationships. To elucidate these so far inconsistent results, we investigated the validity of the MMN as an index for cognitive impairment exploring the associations between different MMN indices and cognitive performance, more specifically with episodic memory performance which is among the most affected cognitive domains in the course of Alzheimer's dementia (AD), at baseline and at a 5-year-follow-up. We assessed the amplitude of the MMN for short ISI (stimulus onset asynchrony, SOA = 0.05 s) and for long ISI (3 s) in a neuropsychologically well-characterized cohort of older adults at risk of dementia (subjective memory impairment, amnestic and non-amnestic MCI; n = 57). Furthermore, we created a novel difference score (ΔMMN), defined as the difference between MMNs to short and to long ISI, as a measure to assess the decay of the auditory memory trace, higher values indicating less decay. ΔMMN and MMN amplitude after long ISI, but not the MMN amplitude after short ISI, was associated with episodic memory at baseline (β = 0.38, p = 0.003; β = −0.27, p = 0.047, respectively). ΔMMN, but not the MMN for long ISIs, was positively associated with episodic memory performance at the

OPEN ACCESS

Edited by:
Mohammad Amjad Kamal, King Fahad Medical Research Center, King Abdulaziz University, Saudi Arabia

Reviewed by:
Adriana Mihai, University of Medicine and Pharmacy of Târgu Mureş, Romania
Márk Molnár, Institute of Cognitive Neuroscience and Psychology, Centre of Natural Sciences, Hungarian Academy of Sciences, Hungary

***Correspondence:**
Daria Laptinskaya
daria.laptinskaya@uni-ulm.de

Received: 26 September 2017
Accepted: 08 January 2018
Published: 02 February 2018

Citation:
Laptinskaya D, Thurm F, Küster OC, Fissler P, Schlee W, Kolassa S, von Arnim CAF and Kolassa I-T (2018) Auditory Memory Decay as Reflected by a New Mismatch Negativity Score Is Associated with Episodic Memory in Older Adults at Risk of Dementia. Front. Aging Neurosci. 10:5. doi: 10.3389/fnagi.2018.00005

Abbreviations: AD, Alzheimer's dementia; aMCI, amnestic mild cognitive impairment; MCI, mild cognitive impairment; MemTra, Memory Trace; MMN, mismatch negativity; MMN–Dur, mismatch negativity after duration deviants; MMSE, Mini-Mental State Examination; MVGT, Münchner Verbaler Gedächtnistest; naMCI, non-amnestic mild cognitive impairment; NMDA, N-methyl-D-aspartate; Opt1, Optimum–1; SMI, subjective memory impairment; TMT, Trail Making Test; ΔMMN, difference score between MMNs to short and to long ISIs; ΔMMN–Dur, index for auditory memory trace decay, amplitude difference between the MMN after duration deviant in the Optimum–1 paradigm and the Memory Trace paradigm, higher values indicating less auditory memory trace decay.

5-year-follow-up (β = 0.57, p = 0.013). The results suggest that the MMN after long ISI might be suitable as an indicator for the decline in episodic memory and indicate ΔMMN as a potential biomarker for memory impairment in older adults at risk of dementia.

Keywords: mismatch negativity, auditory memory, cognition, episodic memory, mild cognitive impairment, subjective memory impairment, Alzheimer's disease, event-related potentials

INTRODUCTION

The global number of people aged 50 years and older is constantly increasing (e.g., Gerland et al., 2014; United Nations, 2015). Age is the major risk factor of Alzheimer's dementia (AD). Until 2050 about three million older adults will be affected by AD in Germany (Bickel, 2016) and 132 million worldwide (Prince et al., 2015). Alzheimer's pathology is characterized by amyloid-beta and tau deposition in the entorhinal cortex, hippocampus, neocortex and other brain regions (for a review see Ballard et al., 2011). Furthermore, Alzheimer's pathology is associated with deficiencies in neuronal signal transmission and neuronal death and precedes the manifestation of cognitive symptoms by many years or even decades (for a review see Bateman et al., 2012).

Mild cognitive impairment (MCI) can be a prodromal syndrome of AD and is therefore intensively studied in the context of early diagnosis of the disease. Individuals with MCI show cognitive decline in at least one cognitive domain, while overall daily functioning is still intact (Petersen, 2016). MCI is associated with an increased risk of dementia, particularly AD, compared to the general population with a conversion rate to dementia of about 8%–15% per year (Petersen, 2016). Amnestic MCI (aMCI) has a higher progression rate than non-amnestic MCI (naMCI; Petersen, 2016). Furthermore, recent research indicates that subjective memory impairment (SMI) that cannot be confirmed during objective testing is associated with an increased risk for AD up to 6 years later (Jessen et al., 2014).

Event-related potentials (ERPs) can provide further insights into neurophysiological correlates of cognitive decline and neuropathology in old age (e.g., Papaliagkas et al., 2008; Lai et al., 2010; Vecchio and Määttä, 2011; Thurm et al., 2013), with the advantages of being non-invasive and cost-efficient. One of the most widely investigated ERP components in EEG research is the mismatch negativity (MMN; Näätänen et al., 1978). The MMN is elicited when a presentation that has been automatically predicted by the central nervous system is violated (for a review see Näätänen et al., 2011), i.e., when a deviant tone is presented in a sequence of standard tones. It peaks at about 100–250 ms after the onset of the deviant (for a review see e.g., Fishman, 2014). The MMN indicates a generally pre-attentive process, but can be modulated by attention (e.g., Erickson et al., 2016). Previous studies suggest an association between MMN in a passive paradigm and the active deviant tone detection (e.g., Todd et al., 2012). Nevertheless, the MMN elucidation does not depend on the subject's active involvement and can be observed even in the fetus in the womb (e.g., Draganova et al., 2007) or in coma patients (see Morlet and Fischer, 2014 for a recent review). Because of its pre-attentive character the MMN is independent of fluctuations in vigilance and motivation which may be of special importance at long EEG recordings or in older and/or clinical populations (Näätänen et al., 2004).

Depending on the interval length between the standard and deviant tones (interstimulus interval, ISI), the MMN is suitable to determine two different, but strongly interrelated, processes. In case of a short ISI of 2 s or less (see Cheng et al., 2013), the MMN primarily reflects the detection of a mismatch between a stored auditory regularity and the current presentation of the environment and can therefore be considered as an index of the pre-attentive auditory discrimination ability (for a review see Näätänen et al., 2012). With increasing ISI, the MMN provides information on the duration of the pre-attentive auditory memory trace for the standard tone (for a review see Bartha-Doering et al., 2015). In young, healthy adults the auditory memory trace approximates 10 s (Böttcher-Gandor and Ullsperger, 1992; Sams et al., 1993; see Bartha-Doering et al., 2015 for a recent review on MMN in healthy and clinical populations).

A limited number of studies so far investigated the MMN in normal compared to pathological aging, specifically in AD, with equivocal results. While some studies report an attenuated MMN in AD for short (e.g., Schroeder et al., 1995) as well as for long ISIs (e.g., Pekkonen et al., 1994; Papadaniil et al., 2016), others failed to find MMN differences between AD and healthy controls (e.g., Kazmerski et al., 1997; Engeland et al., 2002; Brønnick et al., 2010; Hsiao et al., 2014). Studies investigating MMN in older adults with MCI are even scarcer. The majority of studies report an altered MMN in MCI in comparison to matched controls (e.g., Lindín et al., 2013; Ji et al., 2015; Papadaniil et al., 2016; but see Tsolaki et al., 2017 for contrary results). However, the results vary in MMN parameter (i.e., amplitude, latency), MMN localization (i.e., frontal, temporal), and the applied ISI length (i.e., short, long).

In sum, previous studies suggest that MMN after short as well as after long ISIs has the potential to be a biomarker for cognition, where the results for MMN after long ISIs are more consistent than for short ISIs. On the other hand, the MMN after short ISIs is the most often investigated one in AD research so far. Since the impact of pre-attentive auditory memory processes increases with ISI length, auditory memory processes seem to be an important factor that is responsible for the MMN-cognition relationship. We assumed that the difference score between MMN after short and long ISI (ΔMMN) might be a better and more reliable biomarker for cognitive (especially episodic memory) decline, compared to the simple MMN after long or short ISI, since ΔMMN takes individual differences in auditory discrimination ability as well as auditory memory into account. The difference between MMN after short and

after long ISI is strongly determined by the pre-attentive maintenance of the memory trace for the standard tone. On the one hand ΔMMN would be 0 if the MMN amplitude after the short and long ISI is the same and thus the standard tone is well remembered independent of the ISI. On the other hand, the ΔMMN would become higher as the MMN amplitude attenuates as a function of the ISI. Thus, the ΔMMN could constitute a biomarker for automatic auditory memory decay, which in turn seems to be the key index for cognitive decline.

The main aim of the present study was to evaluate the validity of pre-attentive auditory memory decay as well as the MMN after short and long ISI as biomarkers for cognitive decline in an at risk population for AD (i.e., aMCI, naMCI, SMI). MMN after short ISI was assessed using the Optimum–1 (Opt1, stimulus onset asynchrony [SOA] = 0.5 s) paradigm (see Näätänen et al., 2004), whereas the MMN after long ISI (3 s) was investigated using the Memory Trace (MemTra) paradigm (in accordance with Grau et al., 1998). Pre-attentive memory trace decay was assessed by the difference score between the MMN after short and long ISIs (ΔMMN).

We hypothesized that pre-attentive auditory memory decay, reflected by the ΔMMN at baseline, is positively associated with episodic memory performance assessed at baseline as well as episodic memory 5 years later (5-year-follow-up). Further, we expected a smaller MMN in the MemTra paradigm in comparison to the Opt1 paradigm and a more pronounced decay of the pre-attentive auditory memory trace in aMCI compared to naMCI/SMI subjects.

MATERIALS AND METHODS

Participants

The inclusion and exclusion criteria for study participation have previously been described in detail (Küster et al., 2016). In brief, subjects were recruited in the Memory Clinic of the University Hospital Ulm, Germany and the Center for Psychiatry Reichenau, Germany or via public advertisements. Inclusion criteria were: 55 years of age or older, fluency in the German language, subjective memory complaints or MCI, stable antidementive and/or antidepressive medication, normal or adjusted-to-normal hearing, and independent living. Exclusion criteria were: probable moderate or severe dementia (Mini-Mental State Examination, MMSE [Folstein et al., 1975] < 20), a history of other neurological or psychiatric disorders, except mild to moderate depression). Depressive symptoms were assessed with the 15-item short version of the Geriatric Depression Scale (Yesavage et al., 1983). Participants without contraindication were offered structural magnetic resonance imaging (MRI) to exclude other brain abnormalities such as major strokes and brain tumors.

SMI was assessed with the question "Do you feel like your memory is getting worse?" (according to Geerlings et al., 1999; Jessen et al., 2010). The evaluation of objective cognitive impairment was based on encoding (sum of words of the five learning trials) and long-delay free recall scores of the adapted German version of the California Verbal Learning Test (German: Münchner Verbaler Gedächtnistest [MVGT, Munich Vebal Memory Test]; Ilmberger, 1988) for memory functions. For non-memory cognitive functions the following subtests from the Consortium to Establish a Registry for Alzheimer's Disease–plus (Welsh et al., 1994) were used: Trail Making Test (TMT) part A and B, phonematic and semantic word fluency, and Boston Naming Test. Objective cognitive impairment was defined as 1.0 *SD* below the age- and education-adjusted norm; aMCI was assigned if at least one of the memory tests was below average; naMCI was assigned if performance in the memory tests was average while one of the test scores of the other cognitive domains was below average. Subjects with severe objective impairment (≤ 2 *SD* below the norm) in memory and non-memory, indicating probable dementia, were excluded from further analysis ($n = 6$), even if they reached the critical MMSE score ≥ 20.

From altogether 122 subjects who were screened for eligibility, 59 met the inclusion criteria. For 14 participants no MRI scan was available. No participant had to be excluded because of abnormalities in the MRI scan. According to the classification criteria 16 subjects were classified as SMI, 19 as naMCI and 24 as aMCI. Demographic and cognitive characteristics of the groups are listed in **Table 1**. Groups did not differ with regard to distribution of gender or crystallized (premorbid) intelligence as indicated by a Verbal Knowledge Test (German: Wortschatztest; Schmidt and Metzler, 1992; all $ps > 0.05$). However, aMCI subjects showed lower education ($p = 0.041$) and tended to be older than naMCI and SMI which was, however, not significant ($p = 0.098$).

Procedure

The study was approved by the ethics committees of both study centers, University of Konstanz and Ulm University, Germany. The study was part of a controlled clinical trial investigating the effect of physical exercise and cognitive training on cognition as well as on biological and electrophysiological parameters (Küster et al., 2016, 2017; Fissler et al., 2017). All participants provided written informed consent in accordance with the Declaration of Helsinki prior to study participation. The neuropsychological assessment and the EEG examination were carried out by intensively trained assessors (i.e., doctorial and psychology students). Both MMN paradigms were carried out at the same session. Prior to the beginning of the EEG recordings, individual hearing thresholds were assessed using in-house software PyTuneSounds (Hartmann, 2009).

Five years ($M = 5.23$, $SD = 0.19$) after baseline assessment, a telephone interview-based follow-up was obtained for participants of the Konstanz sample. Out of the 32 potential follow-up participants, 28 subjects could be contacted again, five subjects refused participation and another two subjects had to be excluded since they were no longer able to attend the telephone interview due to severe progression of cognitive and functional decline. As a result, 21 complete data sets were available for follow-up analysis with four subjects classified as SMI, 11 as naMCI and six as aMCI at the baseline assessment.

TABLE 1 | Demographic and cognitive data within groups.

Variable	Group values			aMCI vs. naMCI/SMI	
	SMI (n = 14)	naMCI (n = 19)	aMCI (n = 24)	$F_{(1,55)}$	p
Age (y.)	71.9 ± 5.4	68.1 ± 6.1	72.5 ± 6.2	2.83	0.098
Education (y.)	11.1 ± 1.9	10.5 ± 1.8	9.7 ± 1.8	4.37[a]	0.041
WST (z)	1.1 ± 0.8	0.6 ± 0.9	0.6 ± 0.7	0.89	0.349
MMSE (0–30)	28.9 ± 0.9	28.7 ± 1.2	27.5 ± 1.8	10.46	0.002
Episodic memory (cs)	0.6 ± 0.4	0.6 ± 0.7	−0.8 ± 0.5	92.15	<0.001
Attention/EF (cs)	0.6 ± 0.8	−0.1 ± 0.9	−0.3 ± 0.9	4.96	0.030
ADAS free rec. (0–10, error rate)	4.1 ± 1.4	4.8 ± 1.8	5.7 ± 1.4	8.29	0.006
Digit span (0–28)	15.0 ± 3.6	14.4 ± 3.6	13.6 ± 2.5	1.52	0.223
ECB (0–28)	14.7 ± 4.6	16.0 ± 5.0	10.9 ± 5.4	10.20[b]	0.002
MVGT enc. (0–80)	50.5 ± 5.4	52.4 ± 8.1	36.2 ± 5.1	81.57	<0.001
MVGT rec. (0–16)	10.9 ± 2.3	11.0 ± 2.5	4.6 ± 2.8	84.11[a]	<0.001
TMT A (s)	38.0 ± 8.4	53.8 ± 14.7	54.0 ± 19.7	2.32	0.134
TMT B (s)	92.2 ± 22.0	121.3 ± 46.2	129.8 ± 48.5	3.14	0.082
Word fluency (w.)	40.1 ± 7.8	31.3 ± 6.7	32.0 ± 7.8	1.65[a]	0.204

Values are means (M) ± standard deviations (SD). aMCI, amnestic MCI; naMCI, non-amnestic MCI; SMI, subjective memory impairment; WST, Wortschatztest [Verbal Knowledge Test]; MMSE, Mini-Mental State Examination; ADAS free rec., Alzheimer's Diseases Assessment Scale–free recall; Digit span, total value from the forward and backward part; ECB, Everyday Cognition Battery–computation span; MVGT enc., Münchner Verbaler Gedächtnistest [Munich Verbal Memory Test]–encoding (sum of words of the five learning trials); MVGT rec., Münchner Verbaler Gedächtnistest [Munich Verbal Memory Test]–long-delay free recall; TMT, Trail Making Test; Word fluency, total value of the episodic and phonemic word fluency; EF, executive functions; y., years; cs, composite score; w., words. Distribution of gender–aMCI vs. naMCI/SMI: $\chi^2_{(1)} = 3.18$, $p = 0.074$. [a]$F_{(1,54)}$; [b]$F_{(1,50)}$.

Because of the limited neuropsychological assessment no renewed classification was carried out at the 5-year-follow-up. All participants were asked if they had received an AD diagnosis during the past 5 years, which was not the case for the final $n = 21$.

Neuropsychological Assessment

All participants completed the following assessments: the Alzheimer's Disease Assessment Scale–cognitive subscale (Ihl and Weyer, 1993), phonemic and semantic word fluency as well as TMT part A and B of the Consortium to Establish a Registry for Alzheimer's Disease–plus test battery, the subtests digit span and digit-symbol coding of the Wechsler Adult Intelligence Scale (Tewes, 1991), and the MVGT. Additionally, everyday cognition in an ecologically valid task was assessed using the working-memory subtest of the Everyday Cognition Battery (Allaire and Marsiske, 1999). Crystallized abilities were assessed using the Verbal Knowledge Test (German: Wortschatztest).

In order to assess latent cognitive function scores, a principal component analysis was performed across all participants (n = 59) to reduce multiple testing and thus α-inflation. An oblique rotation technique was chosen for the assumption of correlations between the extracted components. The following test scores were entered: MVGT encoding, MVGT free long-delay recall, free recall of the Alzheimer's Disease Assessment Scale, TMT part A and B (time in sec), Everyday Cognition Battery–computation span, digit span forward and backward (total value), digit-symbol coding, and semantic and phonemic word fluency (total value as indicator for verbal word fluency). Using the Kaiser criterion (eigenvalues $\geq$ 1.0) two components were extracted, the first one showing high loadings of episodic memory scores (MVGT encoding, MVGT long-delay free recall, and free recall of the Alzheimer's Disease Assessment Scale) and the second one showing high loadings of attention and executive functions scores (TMT part A and B, digit span, digit-symbol and verbal word fluency). All variables were z-standardized and two component scores were built, representing the weighted average of those z-standardized variables with loadings of at least a_{ij} = 0.50 on the respective component. Only the Everyday Cognition Battery–computation span did not reach the critical threshold (a_{ij} = 0.48) and was excluded from further component calculation.

For the follow-up investigation we selected tests from the baseline investigation, which were suitable for assessments via telephone (for telephone tools for cognitive assessment see e.g., Castanho et al., 2014; Duff et al., 2015), namely the MVGT, the digit span forward and backward, and the Consortium to Establish a Registry for Alzheimer's Disease–plus subtests phonemic and semantic word fluency. The composite scores were built in the same manner as at baseline using the same weights from the available variables, i.e., MVGT encoding and MVGT long-delay free recall for the memory domain score; and digit span (total value for forward and backward) and verbal word fluency (total value for phonemic and semantic word fluency) for the attention/executive domain score.

MMN Stimuli and Task Procedure

Two passive mismatch-negativity paradigms were applied: the Opt1 paradigm (see, Näätänen et al., 2004) to assess auditory discrimination ability and the newly developed MemTra paradigm (in accordance with Grau et al., 1998) to investigate auditory memory trace. The standard tone, duration and frequency deviant were further used in the MemTra paradigm (see below). The standard tone was a harmonic tone of three sinusoidal partials of 500, 1000 and 1500 Hz with the second partial being 3 dB and the third being 6 dB lower in intensity then the first partial. The standard tone was 75 ms in duration

including 5 ms rise and fall times. In comparison to the standard tone, the duration deviant was 50 ms shorter and the gap deviant comprised a 7 ms silent gap (including 1 ms fall and rise times) in the middle of the tone. One half of all frequency deviants were 10% higher (partials: 550, 1100, 1650 Hz) and the other half 10% lower in frequency than the standard tone (partials: 450, 900, 1350 Hz). Intensity deviants were 10 dB louder or lower than the standard tone (50% each). The location deviants had an interaural time difference of 800 μs to the left or to the right ear (50% each).

Optimum–1 Paradigm

In the Opt1 paradigm (Näätänen et al., 2004; **Figure 1**) a total number of 1845 auditory stimuli were presented in three blocks of 5 min each. Every second tone was a standard tone, resulting in a probability of 50% for standard and deviant stimuli and a probability of 10% for each deviant type. A sequence of 15 standard tones was presented at the beginning of each block to allow the formation of the standard tone as such. Stimuli were presented with a constant SOA of 0.5 s. Thus, the Opt1 paradigm is suitable to investigate the MMN after short ISI for five deviant types in a very short administration time.

Memory Trace Paradigm

The MemTra paradigm (Grau et al., 1998; **Figure 1**) was developed to investigate the effect of longer ISIs on the MMN-related memory trace. The paradigm presented 462 auditory stimuli within three blocks of 6 min each. As in the Opt1 paradigm, 15 standard tones were presented consecutively at the beginning of each block. Duration and frequency deviants were presented with one to three standard tones between two deviants. The ISI between standard tone and consecutive deviant was constantly 3 s. The number of standard stimuli between the deviants and the ISI (0.5 s, 1.5 s and 3 s) between standard tones were assigned pseudorandomly. Standard stimuli were presented with 66.2% probability; deviants (duration, frequency) with the probability of 16.9% each. Only MMNs elicited to deviants following a standard tone (ISI = 3 s) were included into MMN analysis.

EEG Recording

EEG was recorded using a high-density 256-channel HydroGel™ Geodesic Sensor Net (HCGSN; Electrical Geodesics, Inc., Eugene, OR, USA) with Cz (vertex) as reference during data acquisition. Continuous data were sampled with 1000 Hz and hardware filters were set to 0.1 Hz high-pass and 100 Hz low-pass. After recording, the data were imported into MATLAB (version 2015b; The MathWorks, 2015) and preprocessed using the FieldTrip toolbox (version 20151012; Oostenveld et al., 2011). During EEG recordings, participants were sitting comfortably in an electrically shielded and sound-attenuated room watching silent Charlie Chaplin videos. All auditory stimuli were presented binaurally through stereo headphones with 50 dB above the individual hearing threshold. All participants were instructed to watch the video carefully and not to pay attention to the delivered tones. The paradigm order was counter-balanced between subjects.

MMN Analysis

For both the Opt1 and the MemTra paradigm, EEG data were band-pass filtered in the range of 1–35 Hz (24 dB/octave) and noisy channels were interpolated using the average method before rereferencing the data to the linked mastoids. Continuous data were further down-sampled to 250 Hz, segmented into epochs starting 100 ms before and ending 350 ms after stimulus onset and baseline-corrected (100-ms pre-stimulus time window). After manually rejecting artifact contaminated epochs, the remaining epochs were averaged for the standard tone and for each deviant type separately. On average, no more than 20% of the trials were excluded. Consequently, the following number of trials was left for averaging in the Opt1 paradigm (values are means ± standard deviations): 753 ± 53 for the standard stimulus, 152 ± 11 for the duration deviant, 151 ± 11 for the frequency deviant, 150 ± 11 for the intensity deviant, 150 ± 11 for the location deviant, and 149 ± 13 for the gap deviant. In the MemTra paradigm the reaction to standard stimulus was averaged over 83 ± 6 trials, for the duration deviant over 65 ± 5 trials, and for the frequency deviant over 65 ± 5 trials. Difference

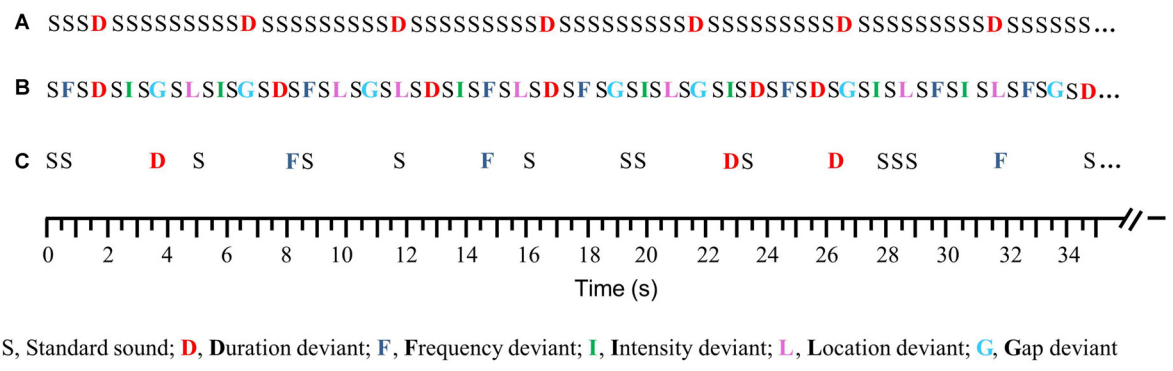


FIGURE 1 | Schematic illustration of the auditory paradigms, compared to the traditional oddball paradigm, which was not used in the study. **(A)** Traditional oddball paradigm (SOA = 0.5 s), **(B)** Optimum–1 (Opt–1) paradigm (SOA = 0.5 s), and **(C)** Memory Trace (MemTra) paradigm (ISI = 0.5, 1.5, and 3 s; $ISI_{standard-deviant}$ = 3 s).

waveforms between the ERPs to the standard and to the deviant stimuli were carried out for each paradigm and deviant type, respectively. The MMN search window was determined within 100–250 ms, corresponding to previous studies on older adults with MCI (see Mowszowski et al., 2012, 2014; Ji et al., 2015). The MMN amplitude was defined as the mean voltage in a 40 ms time window centered at the peak of the grand-average waveform of each group (SMI, aMCI and naMCI). The MMN latency was defined at the most negative peak within the MMN search window after deviant onset (100–250 ms for frequency, intensity, and location deviants; 125–275 for duration deviant, and 134–284 ms for gap deviant). As the largest MMN is often assessed at fronto-central EEG electrodes and the averaging of electrodes with similar activity has been demonstrated to show more reliable results than the measure of single separate electrodes (Huffmeijer et al., 2014), the average voltage at FCz, Fz, and Cz was computed as mean MMN amplitude for all further analyses. The mean MMN latency was computed accordingly.

In two subjects (both SMI) the MMN amplitude extracted from the difference between standard and deviant tone showed a value above mean (−0.68 for duration and −0.17 frequency deviant) + 1.5 × interquartile range and >2 μV for both deviant types (duration and frequency) in the MemTra paradigm. Because of this abnormally high positive value (the difference score should be negative or around zero), we assumed that the paradigm did not work for them properly. To avoid any inaccuracies we excluded their datasets from all further analyses.

Statistical Analyses

All statistical analyses were performed using R (version 3.2.3; R Core Team, 2016) in RStudio (RStudio Team, 2015). Statistical analyses of the baseline sample were performed with 57 subjects (24 classified as aMCI, 19 as naMCI and 14 as SMI). For one SMI subject only data for the Opt1 paradigm and for one aMCI subject only the MemTra paradigm data were available. All contrasts for group comparisons were set to aMCI vs. naMCI/SMI. Since all model residuals were normally distributed, parametric tests were applied for group comparisons. Comparisons for age, years of education, and cognitive function were conducted with univariate analysis of variance (ANOVA) models. Group differences in gender distribution were assessed by Pearson's Chi-square (χ^2)-test.

As a first step of the statistical ERP analysis, one-tailed *t*-tests for dependent samples for normally distributed data and Wilcoxon signed-rank tests for non-normally distributed data were conducted to determine whether mean MMN amplitudes significantly differed from zero within groups. Second, since both MMN paradigms applied a different number of deviants (five in the Opt1 and two in the MemTra paradigm), we explored differences in mean MMN amplitudes and latencies depending on group and deviant type for each paradigm separately.

The statistical models were carried out as follows: (1) for the MMN after short ISI (i.e., Opt1 paradigm) we conducted Group (aMCI vs. naMCI/SMI) × Deviant Type (duration, frequency, intensity, location, gap) linear mixed effect models with Subject as random intercept (lme4 package in R version 1.1-12; Bates et al., 2015) separately for mean MMN amplitude and mean MMN latency as dependent variable. (2) For the MMN after long ISI, statistical analyses focused only on the duration deviant, since there was no significant MMN component elicited by the frequency deviant in the MemTra paradigm. In order to investigate differences in the mean MMN amplitude for the duration deviant between paradigms (and thus ISIs), we carried out a Paradigm (Opt1/SOA = 0.5 s vs. MemTra/ISI = 3 s) × Group (aMCI vs. naMCI/SMI) linear mixed effects model including Subject as random intercept. (3) Second level (*post hoc*) analyses were conducted using univariate ANOVA models and pairwise *t*-tests with Bonferroni correction for multiple comparisons (multcomp package for R version 1.4-6; Hothorn et al., 2008).

As a final step, hierarchical linear regression models were carried out to investigate associations between MMN after short ISI, MMN after long ISI and pre-attentive auditory memory trace decay (i.e., ΔMMN for the duration deviant; ΔMMN–Dur) and neuropsychological composite scores for episodic memory and attention/executive functions at baseline (n = 57) and follow-up assessment (n = 21) as dependent variables, respectively. Based on previous research indicating higher age as a risk factor and education as a protective factor for cognitive decline (e.g., Ardila et al., 2000; Cansino, 2009; Salthouse, 2009, 2012), we statistically accounted for age and education by entering them into the model first (reduced models), followed by ΔMMN–Dur and MemTra MMN after duration deviants (MemTra MMN–Dur) as predictors in two separate models (full models). To explore the effect of Opt1 MMN we entered an Opt1 MMN × Deviant Type (duration, frequency, intensity, location, gap) term into the model instead of calculating models for each deviant type separately which would increase multiple testing and thus α-inflation. Using ANOVA, the full regression models were then compared to the reduced regression models without MMN indices as additional predictor. Collinearity between predictors was examined by computing the variance inflation factor (VIF) for each predictor's beta score and for the mean beta score as well as the VIF tolerance score (1/VIF). Individual VIF scores > 10, a mean VIF score > 1, and a VIF tolerance score < 0.1 indicated beta score inflation by collinearity in the models (Bowerman and O'Connell, 1990; Myers, 1990; Menard, 1995). For illustration purposes significant associations between auditory memory and cognition are depicted as Pearson's product-moment correlation coefficients (r).

Normal distribution of all models' residuals was confirmed using the Shapiro-Wilk test (W statistic) and visual inspection (Q-Q plots). The statistical significance level (α) was set to 0.05 for all analyses.

The stability of significant associations between MMN indices and cognition was evaluated by the inclusion of the participants who were excluded before because of probable AD (see section "Participants").

RESULTS

ERP Analysis of the MMN

In order to examine whether all deviants elicited a MMN, one-tailed *t*-tests for dependent samples for normally distributed variables and Wilcoxon signed-rank tests for non-normally distributed data were conducted. **Figure 2** shows the difference waveforms for the Opt1 and MemTra paradigm, respectively. The mean MMN difference waveform in the Opt1 condition significantly differed from zero for all deviant types in all groups (see Supplementary Table S1). In the MemTra paradigm only the difference waveform for the duration deviant significantly differed from zero in all groups (see Supplementary Table S1). Therefore, all further statistical analyses regarding the MemTra paradigm were restricted to the duration deviant (MMN–Dur).

Group Differences between MMN Parameters

MMN after Short ISI

Analysis of the MMN after short ISI focused on the Opt1 paradigm and was conducted with linear mixed-effects models. The mixed-effects models with Group (aMCI vs. naMCI/SMI) as between-subject factor and Deviant Type (duration, frequency, intensity, location, gap) as within-subject factor showed a main effect of Deviant Type for both the mean MMN amplitude, $F_{(4,216)} = 11.65$, $p < 0.001$, and the mean MMN latency, $F_{(4,216)} = 14.49$, $p < 0.001$. Mean MMN amplitudes were largest for the duration deviant ($ps \leq 0.029$) and mean MMN latencies were shortest for the duration and gap deviants ($ps \leq 0.131$; $ps \leq 0.002$, respectively).

Neither a main effect of Group nor a Group × Deviant Type interaction was found in both models (amplitude and latency; see **Table 2** for MMN amplitudes and latencies for each group and see Supplementary Table S2 for pairwise comparison of the deviant types).

MMN after Long ISI and ISI Duration Effect

Comparing the MMN amplitudes for the duration deviant between both paradigms, a mixed-effects model of Paradigm (Opt1 vs. MemTra) as within-subject factor × Group (aMCI vs. naMCI/SMI) as between-subject factor revealed a main effect of Paradigm, $F_{(1,55)} = 61.88$, $p < 0.001$, indicating smaller mean MMN–Dur amplitudes in the MemTra compared to the Opt1 paradigm (**Figure 3**), i.e., a stronger pre-attentive auditory memory decay in the long ISI condition. Subjects with aMCI showed a more pronounced pre-attentive auditory memory decay in comparison to naMCI and SMI, even though the Paradigm × Group interaction was only significant at a trend level, $F_{(1,55)} = 3.21$, $p = 0.079$ (see also **Table 2**). No main effect or interaction was found for the mean MMN–Dur latency.

Associations between the MMN Parameters and Baseline Cognition

To investigate the associations between baseline MMN indices and baseline cognitive performance, linear hierarchical regression models were conducted across groups. The models were carried out separately for the episodic memory and the attention/executive functions composite scores as dependent variables, including age and education at baseline (reduced models) and additionally ΔMMN–Dur, MemTra MMN–Dur, or Opt1 MMN × Deviant Type term as predictors (full models; see **Table 3**). In the reduced models, age, but not education was a significant predictor of both episodic memory, $\beta = -0.38$, $t_{(50)} = -2.94$, $p = 0.005$, and attention/executive functions, $\beta = -0.41$, $t_{(50)} = -3.30$, $p = 0.002$, at baseline assessment; indicating worse performance in older participants. According to our hypothesis adding ΔMMN–Dur as predictor to the reduced model explained an additional 14% of the variance in the episodic memory score, $F_{(49,1)} = 10.16$, $p = 0.002$; $\beta_{\Delta MMN-Dur} = 0.38$, $t_{(49)} = 3.19$, $p = 0.002$ (see also **Figure 4** for correlative association). MemTra MMN–Dur

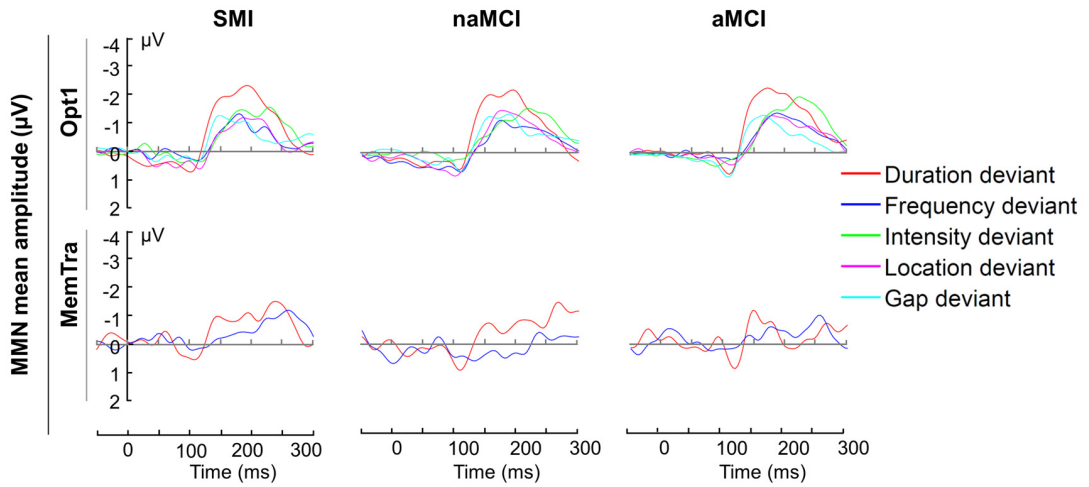


FIGURE 2 | Mean MMN amplitudes for the Opt1 paradigm and MemTra paradigm within groups. Mean values are the averaged signal of the fronto-central electrodes Fz, FCz, and Cz. Opt1, Optimum–1; MemTra, Memory Trace; aMCI, amnestic MCI; naMCI, non-amnestic MCI; SMI, subjective memory impairment.

TABLE 2 | Mean MMN amplitudes and latencies within groups.

MMN parameter	Group values			aMCI vs. naMCI/SMI	
	SMI	naMCI	aMCI	$F_{(1,54)}$	*p*
		Amplitudes			
Opt–Dur	−2.2 ± 1.1	−2.1 ± 1.2	−2.1 ± 1.1	0.01	0.910
Opt–Freq	−1.1 ± 0.7	−1.1 ± 1.0	−1.3 ± 1.0	1.02	0.317
Opt–Intens	−1.4 ± 1.0	−1.4 ± 1.3	−1.9 ± 1.4	1.76	0.191
Opt–Loc	−1.1 ± 0.8	−1.4 ± 1.6	−1.2 ± 1.1	0.01	0.935
Opt–Gap	−1.1 ± 1.3	−1.2 ± 1.0	−1.2 ± 1.0	0.02	0.880
MemTra–Dur	−1.1 ± 1.2	−1.0 ± 1.4	−0.5 ± 1.2	3.06	0.086
ΔMMN–Dur	−1.0 ± 1.3	−1.1 ± 1.4	−1.7 ± 1.2	3.03[a]	0.087
		Latencies			
Opt–Dur	183.5 ± 23.5	184.5 ± 21.2	190.4 ± 29.8	0.74	0.394
Opt–Freq	191.7 ± 20.5	198.7 ± 21.7	199.0 ± 26.4	0.21	0.651
Opt–Intens	213.0 ± 23.9	208.5 ± 25.4	210.5 ± 29.7	0.50	0.483
Opt–Loc	195.0 ± 28.7	200.4 ± 27.7	199.6 ± 27.4	0.01	0.940
Opt–Gap	174.2 ± 20.6	184.9 ± 24.2	177.2 ± 28.0	0.01	0.913
MemTra–Dur	203.7 ± 34.1	184.4 ± 31.3	187.3 ± 31.9	1.92	0.172

aMCI, amnestic MCI; naMCI, non-amnestic MCI; SMI, subjective memory impairment; Opt–Dur, MMN after duration deviants in the Optimum–1 paradigm; Opt–Freq, MMN after frequency deviants in the Optimum–1 paradigm; Opt–Intens, MMN after intensity deviants in the Optimum–1 paradigm; Opt–Loc, MMN after location deviants in the Optimum–1 paradigm; Opt–Gap, MMN after gap deviants in the Optimum–1 paradigm; MemTra–Dur, MMN after duration deviants in the Memory Trace paradigm; ΔMMN–Dur, difference score between MMN amplitude after duration deviant in the Optimum–1 paradigm and the Memory Trace paradigm, higher values indicating less auditory memory trace decay. [a]$F_{(1,53)}$.

as predictor explained an additional 7% of the variance in the episodic memory score, $F_{(50,1)} = 4.14$, $p = 0.047$; $\beta_{\text{MemTraMMN–Dur}} = -0.27$, $t_{(50)} = -2.04$, $p = 0.047$. There was no additive effect in predicting individual differences in the attention/executive functions score. No additive effect was found for the model including the Opt1 MMN × Deviant Type interaction.

Even when the analysis was repeated with $n = 6$ subjects who were excluded because of probable AD the additive effect of ΔMMN–Dur remained significant, $F_{(54,1)} = 13.93$, $p < 0.001$; $\beta_{\Delta\text{MMN–Dur}} = 0.41$, $t_{(54)} = 3.73$, $p < 0.001$.

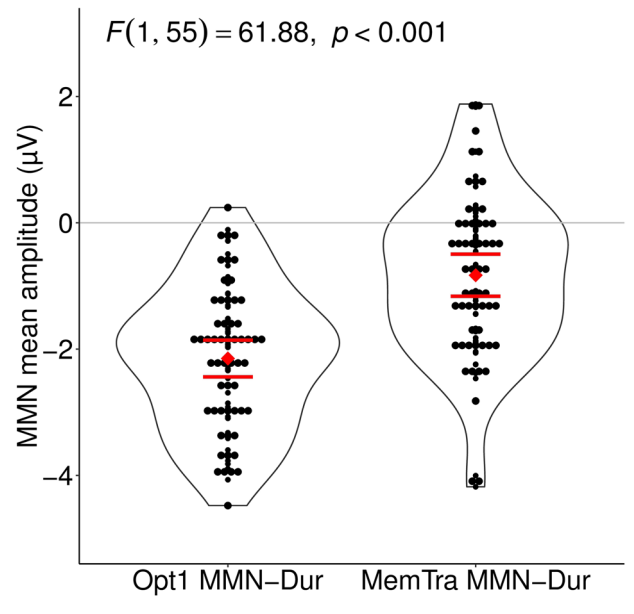


FIGURE 3 | Mean MMN after duration deviants in comparison between the Opt1 and the MemTra paradigm. Mean values build from the averaged signal of the fronto-central electrodes Fz, FCz, and Cz. The depicted *F*-value is accounted for Group main effect and Group × Paradigm interaction. 95% confidence intervals for the average MMN amplitude are shown as horizontal bars, red dot representing the mean value. Opt1, Optimum–1; MemTra, Memory Trace; MMN Opt–Dur, MMN after duration deviants in the Optimum–1 paradigm; MMN Memtra–Dur, MMN after duration deviants in the Memory Trace paradigm.

Associations between MMN Parameters and Cognition at the 5-Year-Follow-up

To investigate the prognostic effect of baseline auditory memory on cognition, linear hierarchical regression models were carried out across groups, separately for the episodic memory and the attention/executive functions composite score assessed 5 years later (see **Table 4**). In the reduced models including only age and education at baseline as predictors, neither age nor education was a significant predictor for episodic memory or attention/executive functions at the 5-year follow-up. Corroborating our hypothesis, including ΔMMN–Dur as additional predictor explained an additional 36% of the variance in the episodic memory (but not in the attention/executive functions) composite score compared to age and education entered alone, $F_{(16,1)} = 7.91$, $p = 0.013$; $\beta_{\Delta\text{MMN–Dur}} = 0.57$, $t_{(16)} = 2.81$, $p = 0.013$ (see also **Figure 5** for correlative association). No additive effects were found for MemTra MMN–Dur or the model including the Opt1 MMN × Deviant Type interaction. The additive effect of ΔMMN–Dur remained significant after inclusion of one subject ($n = 6$ at baseline) with probable AD, $F_{(17,1)} = 8.63$, $p = 0.009$; $\beta_{\Delta\text{MMN–Dur}} = 0.55$, $t_{(17)} = 2.94$, $p = 0.009$.

DISCUSSION

We investigated the auditory MMN after short and after long ISI as well as a novel pre-attentive auditory memory trace decay index in older adults with SMI, aMCI and naMCI as

TABLE 3 | Baseline associations between auditory memory trace decay and episodic memory as well as executive functions accounting for age and education.

	Episodic memory				Attention/EF			
Predictor	**ΔR^2**	***B***	**β**	***p***	**ΔR^2**	***B***	**β**	***p***
Model 1	0.17			0.010	0.21			0.002
Age		−0.06	−0.38	0.005		−0.07	−0.41	0.002
Education		0.08	0.17	0.187		0.12	0.23	0.073
Model 2	0.14			0.002	0.02			0.214
Age		−0.05	−0.32	0.011		−0.06	−0.39	0.003
Education		0.07	0.16	0.183		0.11	0.22	0.078
ΔMMN–Dur		0.26	0.38	0.002		0.12	0.16	0.214

EF, executive functions. ΔMMN–Dur, difference score between MMN amplitude after duration deviant in the Optimum–1 paradigm and the Memory Trace paradigm, higher values indicating less auditory memory trace decay.

an at risk population of AD. The MMN after short ISI was investigated using the Opt1 paradigm (applying short ISI), with respect to five deviants (duration, frequency, intensity, location, gap). The MMN after long ISI was investigated using the MemTra paradigm (with long ISI) with respect to two different auditory deviant types (duration, frequency). Pre-attentive auditory memory trace decay was assessed by the difference score between the MMN after short and long ISI (ΔMMN). In line with the majority of studies (Verleger et al., 1992; Kazmerski et al., 1997; Gaeta et al., 1999; Brønnick et al., 2010; Cheng et al., 2012; Hsiao et al., 2014), we found no group differences in MMN after short ISI (see Pekkonen et al., 1994; Ruzzoli et al., 2016; but see also Engeland et al., 2002 for contrary results) suggesting preserved pre-attentive auditory encoding in MCI (aMCI and naMCI) in comparison to SMI. As a proof of concept, all groups showed an attenuated MMN in the MemTra (ISI = 3 s) in comparison to the Opt1 paradigm (SOA = 0.5 s) for the duration deviant.

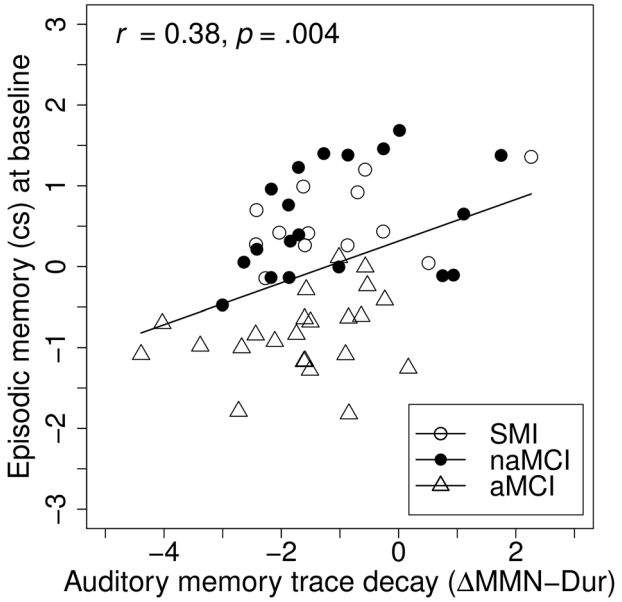


FIGURE 4 | Baseline associations between auditory memory decay and episodic memory. Auditory memory reflected by the difference score between MMN amplitude after duration deviant in the Opt1 paradigm and the MemTra paradigm (ΔMMN–Dur), higher scores indicating less auditory memory trace decay. Opt1, Optimum–1; MemTra, Memory Trace, cs, composite score.

In line with our main hypothesis, the ΔMMN–Dur (indicative of the pre-attentive auditory memory trace decay for the duration deviant) was positively associated with episodic memory performance across groups at baseline and 5 years later even after accounting for age and education. In contrast, no such relation was found for attention/executive functions, which is in line with previous work by Ruzzoli et al. (2012). The authors investigated the MMN for duration deviants in an auditory oddball paradigm with 4 s ISI in a healthy adult sample aged 21–60 years. In this, the frontal MMN for duration deviants was positively correlated with memory performance but not with executive functions. Foster et al. (2013) reported a positive association between MMN employing different ISIs as standard and deviants and verbal memory assessed with the Rey Auditory Verbal Learning Test in older healthy adults.

TABLE 4 | Associations between baseline auditory memory trace decay and follow-up episodic memory as well as executive functions accounting for age and education.

	Episodic memory				Attention/EF			
Predictor	**ΔR^2**	***B***	**β**	***p***	**ΔR^2**	***B***	**β**	***p***
Model 1	0.07			0.556	0.19			0.164
Age		−0.04	−0.25	0.294		−0.05	−0.39	0.090
Education		0.02	0.03	0.885		0.08	0.18	0.431
Model 2	0.31			0.013	0.01			0.592
Age		−0.03	−0.18	0.391		−0.04	−0.38	0.115
Education		0.07	0.11	0.596		0.09	0.19	0.405
ΔMMN–Dur		0.40	0.57	0.013		0.06	0.12	0.592

EF, executive functions. ΔMMN–Dur, difference score between MMN amplitude after duration deviant in the Optimum–1 paradigm and the Memory Trace paradigm, higher values indicating less auditory memory trace decay.

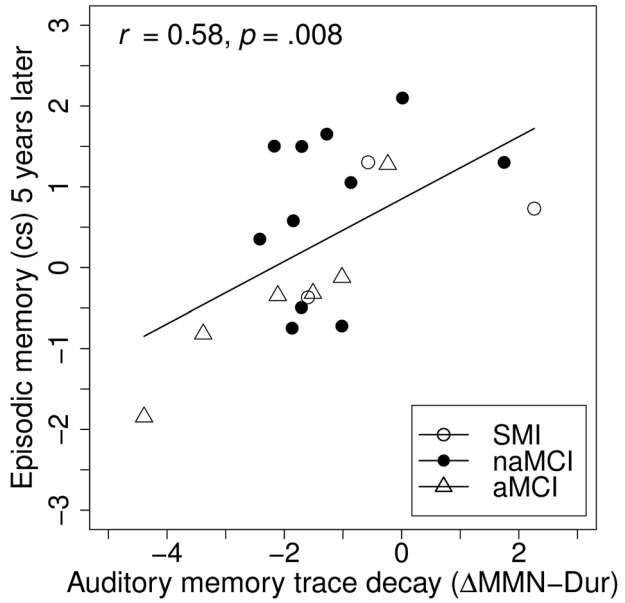


FIGURE 5 | Associations between baseline auditory memory decay and follow-up episodic memory. Auditory memory reflected by the difference score between MMN amplitude after duration deviant in the Opt1 paradigm and the MemTra paradigm (ΔMMN–Dur), higher scores indicating less auditory memory trace decay. Opt1, Optimum–1; MemTra, Memory Trace, cs, composite score.

Shared underlying neurobiological mechanisms might be responsible for the association between pre-attentive auditory memory trace decay and episodic memory. Interestingly, the pre-attentive auditory memory trace, measured with the MMN, especially after long ISIs, and episodic memory are both related to N-methyl-D-aspartate (NMDA) receptor functioning. It is well known that the NMDA receptor is highly involved in neuronal plasticity, long-term-potentiation, as well as learning and episodic memory (for a review see Newcomer et al., 2000). A distorted NMDA receptor-subunit expression and functionality has been reported for healthy older adults and in AD (Mishizen-Eberz et al., 2004; Amada et al., 2005; for a review see Magnusson et al., 2010) and is thought to be involved in age-associated cognitive impairment (for a review see Kumar, 2015). Recently, the decay in the pre-attentive auditory memory trace has also been discussed in the context of NMDA receptor modulation of plasticity, and predictive coding theory (Friston, 2005; Garrido et al., 2009; Näätänen et al., 2014), an integrative model to explain the formation of the MMN within the fronto-temporal network (Friston, 2005; Baldeweg, 2006). Predictive coding considers neuronal activity as a reflection of matches or mismatches between internal predictions based on previous experiences stored in short-term memory and current external events (Heekeren et al., 2008). The theory of predictive coding is well studied in the visual domain (see Stefanics et al., 2014 for a recent review) and has also been increasingly discussed for auditory processing in recent years (e.g., Friston, 2005; Garrido et al., 2009). Regarding the auditory paradigms used in this study, this can be a form of a detection error, indexed by the MMN, whenever the incoming information (deviant tone) does not match the prediction (standard tone). The memory trace formation for the standard tone as well as its changes demand short-term synaptic plasticity which is codetermined by an intact NMDA receptor activity (e.g., Garrido et al., 2009).

The MMN after the duration deviant was significantly larger than the one after the other four deviant types (see also **Figure 2**) in the Opt1 paradigm. Näätänen et al. (2004) report the same finding in healthy young adults. Thus, it seems as if the fronto-temporal network described above is more sensitive to deviations in duration in comparison to deviations in frequency, intensity, location, or a gap in the middle of the tone.

No MMN was detectable in the MemTra paradigm for the frequency deviant, which might indicate that the slope of memory trace decay varies for different tone characteristics (in case of the MemTra paradigm duration and frequency), with the memory trace for frequency deviants fading faster with time compared to duration deviants. Consequently, our results regarding the applicability of ΔMMN are restricted to MMN for duration deviants. To our best knowledge, no study exists to date which investigated MMN after different deviant types and for different ISI lengths within one AD or MCI sample. Contrary to our results, two studies investigating the MMN after duration and frequency deviants for short as well as long ISIs in healthy older adults indicate a faster decay of the pre-attentive auditory memory trace for duration in comparison to frequency deviants (Schroeder et al., 1995; Pekkonen et al., 1996). However, Cooper et al. (2006) failed to find such differences in healthy aging. Interestingly, MMN for duration deviants suggests the best prognostic value in the prediction of psychosis in at risk individuals in comparison to frequency and intensity deviants (see Näätänen et al., 2015 for a recent review and Erickson et al., 2016 for a recent meta-analysis). Notably, the vast majority of studies of MMN in schizophrenia use short ISIs only.

Regarding the fact that subjects with aMCI have the highest risk to develop AD, we expected a more pronounced pre-attentive auditory memory trace decay reflected by the ΔMMN–Dur in aMCI in comparison to naMCI/SMI. This effect was only present at the trend level (p = 0.079). Nevertheless, visual inspections indicate a smaller MMN after long ISIs in aMCI compared to the other two groups (**Figure 2**).

It needs to be mentioned that aMCI subjects had a significantly lower education (p = 0.041; **Table 1**) in comparison to SMI and naMCI. This finding is in line with the well-studied findings of education as a protective factor against cognitive decline (e.g., Salthouse, 2009).

The following limitations need to be considered for this study: as all participants investigated in this study showed subjective or objective cognitive impairment, our results are restricted to this at risk of developing AD group only. Thus, we cannot draw any conclusion about the prognostic value of ΔMMN–Dur in healthy aging. The sample size of the study, especially in the follow-up investigation, was rather small. Nevertheless, we found hypothesis-confirming significant positive associations between auditory memory trace decay and episodic memory.

As all tests included in the episodic memory composite score were verbal in nature (Alzheimer's Disease Assessment Scale free recall, MVGT), it remains open whether the association between auditory memory and episodic memory is restricted to verbal memory only or if it can be generalized to other memory modalities.

Due to logistic reasons, we had two dropouts from the 5-year-follow-up due to severe cognitive and functional decline, a group of especially great interest. Larger sample sizes in future studies would help to handle dropout analyses. Future studies with larger sample sizes are needed to replicate the effects (including e.g., survival analyses).

CONCLUSION

The strong significant association between ΔMMN–Dur and episodic memory at baseline and at the 5-year-follow-up provides an additional insight into neurobiological processes associated with pathological aging and may help in developing new tools for early diagnosis as well as for treatment monitoring. Since EEG recording is a non-invasive and cost-efficient tool, ΔMMN–Dur might become a useful extension to complement neuropsychological assessment in older populations at risk of developing AD. Further research and longitudinal studies with larger sample sizes and healthy age-matched as well as younger healthy controls are needed to evaluate possible clinical implications.

AUTHOR CONTRIBUTIONS

DL contributed to study conception and design, organized study procedures and acquired data, analyzed and interpreted the data, and wrote the first draft of the manuscript. FT contributed to study conception and design, organized study procedures, acquired data, contributed to data analysis, and critically revised the first draft of the manuscript and the article. PF and OCK contributed to study conception and design, organized study procedures and acquired data, contributed to data interpretation and critically revised the manuscript. SK supervised the statistical analysis of the data and critically revised the manuscript. WS provided support in data analyses and data interpretation and critically revised the manuscript. CAFA and I-TK conceptualized the study, obtained funding, supervised all phases of the study as principal investigators and critically revised the manuscript. All authors read and approved the final manuscript.

FUNDING

This research was funded by the Heidelberg Academy of Sciences and Humanities, Germany. During the data collection, I-TK was a fellow (now alumna) of the Zukunftskolleg of the University of Konstanz, Germany.

ACKNOWLEDGMENTS

DL, FT and I-TK were at University of Konstanz at the time of baseline data acquisition. We thank Thomas Elbert for general advice and support in study conception and implementation as well as Anne Korzowski for her support in data acquisition. We further thank Risto Näätänen and colleagues (University of Helsinki, Finland) who kindly provided all stimuli of the Opt1 paradigm (standard tone and deviants in the types of duration, frequency, intensity, location and gap).

SUPPLEMENTARY MATERIAL

The Supplementary Material for this article can be found online at: https://www.frontiersin.org/articles/10.3389/fnagi.2018.00005/full#supplementary-material

REFERENCES

Allaire, J. C., and Marsiske, M. (1999). Everyday cognition: age and intellectual ability correlates. *Psychol. Aging* 14, 627–644. doi: 10.1037/0882-7974.14.4.627

Amada, N., Aihara, K., Ravid, R., and Horie, M. (2005). Reduction of NR1 and phosphorylated Ca^{2+}/calmodulin-dependent protein kinase II levels in Alzheimer's disease. *Neuroreport* 16, 1809–1813. doi: 10.1097/01.WNR.0000185015.44563.5d

Ardila, A., Ostrosky-Solis, F., Rosselli, M., and Gómez, C. (2000). Age-related cognitive decline during normal aging: the complex effect of education. *Arch. Clin. Neuropsychol.* 15, 495–513. doi: 10.1093/arclin/15.6.495

Baldeweg, T. (2006). Repetition effects to sounds: evidence for predictive coding in the auditory system. *Trends Cogn. Sci.* 10, 93–94. doi: 10.1016/j.tics.2006.01.010

Ballard, C., Gauthier, S., Corbett, A., Brayne, C., Aarsland, D., and Jones, E. (2011). Alzheimer's disease. *Lancet* 377, 1019–1031. doi: 10.1016/S0140-6736(10)61349-9

Bartha-Doering, L., Deuster, D., Giordano, V., am Zehnhoff-Dinnesen, A., and Dobel, C. (2015). A systematic review of the mismatch negativity as an index for auditory sensory memory: from basic research to clinical and developmental perspectives. *Psychophysiology* 52, 1115–1130. doi: 10.1111/psyp.12459

Bateman, R. J., Xiong, C., Benzinger, T. L. S., Fagan, A. M., Goate, A., Fox, N. C., et al. (2012). Clinical and biomarker changes in dominantly inherited Alzheimer's disease. *N. Engl. J. Med.* 367, 795–804. doi: 10.1056/NEJMoa1202753

Bates, D., Mächler, M., Bolker, B., and Walker, S. (2015). Fitting linear mixed-effects models using lme4. *J. Stat. Softw.* 67, 1–48. doi: 10.18637/jss.v067.i01

Bickel, H. (2016). *Die Häufigkeit Von Demenzerkrankungen [The Prevalence of Dementia]*. Berlin, Germany: Deutsche Alzheimer Gesellschaft e.V. Available online at: https://www.deutsche-alzheimer.de/

Böttcher-Gandor, C., and Ullsperger, P. (1992). Mismatch negativity in event-related potentials to auditory stimuli as a function of varying interstimulus interval. *Psychophysiology* 29, 546–550. doi: 10.1111/j.1469-8986.1992.tb02028.x

Bowerman, B. L., and O'Connell, R. T. (1990). *Linear Statistical Models: An Applied Approach.* 2nd Edn. Belmont: CA: Duxbury.

Brønnick, K. S., Nordby, H., Larsen, J. P., and Aarsland, D. (2010). Disturbance of automatic auditory change detection in dementia associated with Parkinson's disease: a mismatch negativity study. *Neurobiol. Aging* 31, 104–113. doi: 10.1016/j.neurobiolaging.2008.02.021

Cansino, S. (2009). Episodic memory decay along the adult lifespan: a review of behavioral and neurophysiological evidence. *Int. J. Psychophysiol.* 71, 64–69. doi: 10.1016/j.ijpsycho.2008.07.005

Castanho, T. C., Amorim, L., Zihl, J., Palha, J. A., Sousa, N., and Santos, N. C. (2014). Telephone-based screening tools for mild cognitive impairment and dementia in aging studies: a review of validated instruments. *Front. Aging Neurosci.* 6:16. doi: 10.3389/fnagi.2014.00016

Cheng, C.-H., Hsu, W.-Y., and Lin, Y.-Y. (2013). Effects of physiological aging on mismatch negativity: a meta-analysis. *Int. J. Psychophysiol.* 90, 165–171. doi: 10.1016/j.ijpsycho.2013.06.026

Cheng, C.-H., Wang, P.-N., Hsu, W.-Y., and Lin, Y.-Y. (2012). Inadequate inhibition of redundant auditory inputs in Alzheimer's disease: an MEG study. *Biol. Psychol.* 89, 365–373. doi: 10.1016/j.biopsycho.2011.11.010

Cooper, R. J., Todd, J., McGill, K., and Michie, P. T. (2006). Auditory sensory memory and the aging brain: a mismatch negativity study. *Neurobiol. Aging* 27, 752–762. doi: 10.1016/j.neurobiolaging.2005.03.012

Draganova, R., Eswaran, H., Murphy, P., Lowery, C., and Preissl, H. (2007). Serial magnetoencephalographic study of fetal and newborn auditory discriminative evoked responses. *Early Hum. Dev.* 83, 199–207. doi: 10.1016/j.earlhumdev.2006.05.018

Duff, K., Tometich, D., and Dennett, K. (2015). The modified Telephone Interview for Cognitive Status is more predictive of memory abilities than the Mini-Mental State examination. *J. Geriatr. Psychiatry Neurol.* 28, 193–197. doi: 10.1177/0891988715573532

Engeland, C., Mahoney, C., Mohr, E., Ilivitsky, V., and Knott, V. J. (2002). Acute nicotine effects on auditory sensory memory in tacrine-treated and nontreated patients with Alzheimer's disease: an event-related potential study. *Pharmacol. Biochem. Behav.* 72, 457–464. doi: 10.1016/s0091-3057(02)00711-6

Erickson, M. A., Ruffle, A., and Gold, J. M. (2016). A meta-analysis of mismatch negativity in schizophrenia: from clinical risk to disease specificity and progression. *Biol. Psychiatry* 79, 980–987. doi: 10.1016/j.biopsych.2015.08.025

Fishman, Y. I. (2014). The mechanisms and meaning of the mismatch negativity. *Brain Topogr.* 27, 500–526. doi: 10.1007/s10548-013-0337-3

Fissler, P., Müller, H.-P., Küster, O. C., Laptinskaya, D., Thurm, F., Woll, A., et al. (2017). No evidence that short-term cognitive or physical training programs or lifestyles are related to changes in white matter integrity in older adults at risk of dementia. *Front. Hum. Neurosci.* 11:110. doi: 10.3389/fnhum.2017.00110

Folstein, M. F., Folstein, S. E., and McHugh, P. R. (1975). "Mini-mental state". A practical method for grading the cognitive state of patients for the clinician. *J. Psychiatr. Res.* 12, 189–198. doi: 10.1016/0022-3956(75)90026-6

Foster, S. M., Kisley, M. A., Davis, H. P., Diede, N. T., Campbell, A. M., and Davalos, D. B. (2013). Cognitive function predicts neural activity associated with pre-attentive temporal processing. *Neuropsychologia* 51, 211–219. doi: 10.1016/j.neuropsychologia.2012.09.017

Friston, K. (2005). A theory of cortical responses. *Philos. Trans. R. Soc. Lond. B Biol. Sci.* 360, 815–836. doi: 10.1098/rstb.2005.1622

Gaeta, H., Friedman, D., Ritter, W., and Cheng, J. (1999). Changes in sensitivity to stimulus deviance in Alzheimer's disease: an ERP perspective. *Neuroreport* 10, 281–287. doi: 10.1097/00001756-199902050-00014

Garrido, M. I., Kilner, J. M., Stephan, K. E., and Friston, K. J. (2009). The mismatch negativity: a review of underlying mechanisms. *Clin. Neurophysiol.* 120, 453–463. doi: 10.1016/j.clinph.2008.11.029

Geerlings, M. I., Jonker, C., Bouter, L. M., Adèr, H. J., and Schmand, B. (1999). Association between memory complaints and incident Alzheimer's disease in elderly people with normal baseline cognition. *Am. J. Psychiatry* 156, 531–537.

Gerland, P., Raftery, A. E., Sevčíková, H., Li, N., Gu, D., Spoorenberg, T., et al. (2014). World population stabilization unlikely this century. *Science* 346, 234–237. doi: 10.1126/science.1257469

Grau, C., Escera, C., Yago, E., and Polo, M. D. (1998). Mismatch negativity and auditory sensory memory evaluation: a new faster paradigm. *Neuroreport* 9, 2451–2456. doi: 10.1097/00001756-199808030-00005

Hartmann, T. (2009). *PyTuneSounds*. Konstanz, San Diego, CA: Slashdot Media. Available online at: https://sourceforge.net

Heekeren, H. R., Marrett, S., and Ungerleider, L. G. (2008). The neural systems that mediate human perceptual decision making. *Nat. Rev. Neurosci.* 9, 467–479. doi: 10.1038/nrn2374

Hothorn, T., Bretz, F., and Westfall, P. (2008). Simultaneous inference in general parametric models. *Biom. J.* 50, 346–363. doi: 10.1002/bimj.200810425

Hsiao, F.-J., Chen, W.-T., Wang, P.-N., Cheng, C.-H., and Lin, Y.-Y. (2014). Temporo-frontal functional connectivity during auditory change detection is altered in Alzheimer's disease. *Hum. Brain Mapp.* 35, 5565–5577. doi: 10.1002/hbm.22570

Huffmeijer, R., Bakermans-Kranenburg, M. J., Alink, L. R. A., and van Ijzendoorn, M. H. (2014). Reliability of event-related potentials: the influence of number of trials and electrodes. *Physiol. Behav.* 130, 13–22. doi: 10.1016/j.physbeh.2014.03.008

Ihl, R., and Weyer, G. (1993). *Die Alzheimer Disease Assessment Scale (ADAS)*. Weinheim, Germany: Beltz Test.

Ilmberger, J. (1988). *Münchner Verbaler Gedächtnistest (MVGT) [Munich Verbal Memory Test, Unpublished Manuscript]*. München: Institut für Medizinische Psychologie, Universität München.

Jessen, F., Wiese, B., Bachmann, C., Eifflaender-Gorfer, S., Haller, F., Kölsch, H., et al. (2010). Prediction of dementia by subjective memory impairment: effects of severity and temporal association with cognitive impairment. *Arch. Gen. Psychiatry* 67, 414–422. doi: 10.1001/archgenpsychiatry.2010.30

Jessen, F., Wolfsgruber, S., Wiese, B., Bickel, H., Mösch, E., Kaduszkiewicz, H., et al. (2014). AD dementia risk in late MCI, in early MCI, and in subjective memory impairment. *Alzheimers Dement.* 10, 76–83. doi: 10.1016/j.jalz.2012.09.017

Ji, L.-L., Zhang, Y.-Y., Zhang, L., He, B., and Lu, G.-H. (2015). Mismatch negativity latency as a biomarker of amnestic mild cognitive impairment in chinese rural elders. *Front. Aging Neurosci.* 7:22. doi: 10.3389/fnagi.2015.00022

Kazmerski, V. A., Friedman, D., and Ritter, W. (1997). Mismatch negativity during attend and ignore conditions in Alzheimer's disease. *Biol. Psychiatry* 42, 382–402. doi: 10.1016/s0006-3223(96)00344-7

Kumar, A. (2015). NMDA receptor function during senescence: implication on cognitive performance. *Front. Neurosci.* 9:473. doi: 10.3389/fnins.2015.00473

Küster, O. C., Fissler, P., Laptinskaya, D., Thurm, F., Scharpf, A., Woll, A., et al. (2016). Cognitive change is more positively associated with an active lifestyle than with training interventions in older adults at risk of dementia: a controlled interventional clinical trial. *BMC Psychiatry* 16:315. doi: 10.1186/s12888-016-1018-z

Küster, O. C., Laptinskaya, D., Fissler, P., Schnack, C., Zügel, M., Nold, V., et al. (2017). Novel blood-based biomarkers of cognition, stress, and physical or cognitive training in older adults at risk of dementia: preliminary evidence for a role of BDNF, irisin and the kynurenine pathway. *J. Alzheimers Dis.* 59, 1097–1111. doi: 10.3233/JAD-170447

Lai, C. L., Lin, R. T., Liou, L. M., and Liu, C. K. (2010). The role of event-related potentials in cognitive decline in Alzheimer's disease. *Clin. Neurophysiol.* 121, 194–199. doi: 10.1016/j.clinph.2009.11.001

Lindín, M., Correa, K., Zurrón, M., and Díaz, F. (2013). Mismatch negativity (MMN) amplitude as a biomarker of sensory memory deficit in amnestic mild cognitive impairment. *Front. Aging Neurosci.* 5:79. doi: 10.3389/fnagi.2013.00079

Magnusson, K. R., Brim, B. L., and Das, S. R. (2010). Selective vulnerabilities of N-methyl-D-aspartate (NMDA) receptors during brain aging. *Front. Aging Neurosci.* 2:11. doi: 10.3389/fnagi.2010.00011

Menard, S. (1995). *Applied Logistic Regression Analysis. Sage University Series on Quantitative Applications in the Social Sciences*. Thousand Oaks, CA: Sage.

Mishizen-Eberz, A. J., Rissman, R. A., Carter, T. L., Ikonomovic, M. D., Wolfe, B. B., and Armstrong, D. M. (2004). Biochemical and molecular studies of NMDA receptor subunits NR1/2A/2B in hippocampal subregions throughout progression of Alzheimer's disease pathology. *Neurobiol. Dis.* 15, 80–92. doi: 10.1016/j.nbd.2003.09.016

Morlet, D., and Fischer, C. (2014). MMN and novelty P3 in coma and other altered states of consciousness: a review. *Brain Topogr.* 27, 467–479. doi: 10.1007/s10548-013-0335-5

Mowszowski, L., Hermens, D. F., Diamond, K., Norrie, L., Cockayne, N., Ward, P. B., et al. (2014). Cognitive training enhances pre-attentive neurophysiological responses in older adults "at risk" of dementia. *J. Alzheimers Dis.* 41, 1095–1108. doi: 10.3233/JAD-131985

Mowszowski, L., Hermens, D. F., Diamond, K., Norrie, L., Hickie, I. B., Lewis, S. J. G., et al. (2012). Reduced mismatch negativity in mild cognitive impairment: associations with neuropsychological performance. *J. Alzheimers Dis.* 30, 209–219. doi: 10.3233/JAD-2012-111868

Myers, R. H. (1990). *Classical and Modern Regression with Applications.* 2nd Edn. Boston: PWS and Kent Publishing Company.

Näätänen, R., Gaillard, A., and Mäntysalo, S. (1978). Early selective-attention effect on evoked potential reinterpreted. *Acta Psychol.* 42, 313–329. doi: 10.1016/0001-6918(78)90006-9

Näätänen, R., Kujala, T., and Winkler, I. (2011). Auditory processing that leads to conscious perception: a unique window to central auditory processing opened by the mismatch negativity and related responses. *Psychophysiology* 48, 4–22. doi: 10.1111/j.1469-8986.2010.01114.x

Näätänen, R., Kujala, T., Escera, C., Baldeweg, T., Kreegipuu, K., Carlson, S., et al. (2012). The mismatch negativity (MMN)—a unique window to disturbed central auditory processing in ageing and different clinical conditions. *Clin. Neurophysiol.* 123, 424–458. doi: 10.1016/j.clinph.2011.09.020

Näätänen, R., Pakarinen, S., Rinne, T., and Takegata, R. (2004). The mismatch negativity (MMN): towards the optimal paradigm. *Clin. Neurophysiol.* 115, 140–144. doi: 10.1016/j.clinph.2003.04.001

Näätänen, R., Shiga, T., Asano, S., and Yabe, H. (2015). Mismatch negativity (MMN) deficiency: a break-through biomarker in predicting psychosis onset. *Int. J. Psychophysiol.* 95, 338–344. doi: 10.1016/j.ijpsycho.2014.12.012

Näätänen, R., Sussman, E. S., Salisbury, D., and Shafer, V. L. (2014). Mismatch negativity (MMN) as an index of cognitive dysfunction. *Brain Topogr.* 27, 451–466. doi: 10.1007/s10548-014-0374-6

Newcomer, J. W., Farber, N. B., and Olney, J. W. (2000). NMDA receptor function, memory, and brain aging. *Dialogues Clin. Neurosci.* 2, 219–232.

Oostenveld, R., Fries, P., Maris, E., and Schoffelen, J.-M. (2011). FieldTrip: open source software for advanced analysis of MEG, EEG, and invasive electrophysiological data. *Comput. Intell. Neurosci.* 2011:156869. doi: 10.1155/2011/156869

Papadaniil, C. D., Kosmidou, V. E., Tsolaki, A., Tsolaki, M., Kompatsiaris, I. Y., and Hadjileontiadis, L. J. (2016). Cognitive MMN and P300 in mild cognitive impairment and Alzheimer's disease: a high density EEG-3D vector field tomography approach. *Brain Res.* 1648, 425–433. doi: 10.1016/j.brainres.2016.07.043

Papaliagkas, V., Kimiskidis, V., Tsolaki, M., and Anogianakis, G. (2008). Usefulness of event-related potentials in the assessment of mild cognitive impairment. *BMC Neurosci.* 9:107. doi: 10.1186/1471-2202-9-107

Pekkonen, E., Jousmäki, V., Könönen, M., Reinikainen, K., and Partanen, J. (1994). Auditory sensory memory impairment in Alzheimer's disease: an event-related potential study. *Neuroreport* 5, 2537–2540. doi: 10.1097/00001756-199412000-00033

Pekkonen, E., Rinne, T., Reinikainen, K., Kujala, T., Alho, K., and Näätänen, R. (1996). Aging effects on auditory processing: an event-related potential study. *Exp. Aging Res.* 22, 171–184. doi: 10.1080/03610739608254005

Petersen, R. C. (2016). Mild cognitive impairment. *Continuum (Minneap Minn)* 22, 404–418. doi: 10.1212/CON.0000000000000313

Prince, M., Wimo, A., Guerchet, M., Ali, G.-C., Wu, Y.-T., and Prina, M. (2015). *World Alzheimer Report 2015.* London: Alzheimer's Disease International. Available online at: https://www.alz.co.uk/research/world-report-2015

R Core Team. (2016). *R: A Language and Environment for Statistical Computing.* Vienna: R Foundation for Statistical Computing. Available online at: http://www.r-project.org

RStudio Team. (2015). *R Studio: Integrated Development for R.* Boston, MA: R Studio, Inc. Available online at: https://www.rstudio.com/

Ruzzoli, M., Pirulli, C., Brignani, D., Maioli, C., and Miniussi, C. (2012). Sensory memory during physiological aging indexed by mismatch negativity (MMN). *Neurobiol. Aging* 33, 625.e21–625.e30. doi: 10.1016/j.neurobiolaging.2011.03.021

Ruzzoli, M., Pirulli, C., Mazza, V., Miniussi, C., and Brignani, D. (2016). The mismatch negativity as an index of cognitive decline for the early detection of Alzheimer's disease. *Sci. Rep.* 6:33167. doi: 10.1038/srep33167

Salthouse, T. A. (2009). When does age-related cognitive decline begin? *Neurobiol. Aging* 30, 507–514. doi: 10.1016/j.neurobiolaging.2008.09.023

Salthouse, T. A. (2012). Consequences of age-related cognitive declines. *Annu. Rev. Psychol.* 63, 201–226. doi: 10.1146/annurev-psych-120710-100328

Sams, M., Hari, R., Rif, J., and Knuutila, J. (1993). The human auditory sensory memory trace persists about 10 sec: neuromagnetic evidence. *J. Cogn. Neurosci.* 5, 363–370. doi: 10.1162/jocn.1993.5.3.363

Schmidt, K.-H., and Metzler, P. (1992). *Wortschatztest [WST, Verbal Knowledge Test].* Weinheim, Germany: Beltz Test.

Schroeder, M. M., Ritter, W., and Vaughan, H. G. Jr. (1995). The mismatch negativity to novel stimuli reflects cognitive decline. *Ann. N Y Acad. Sci.* 769, 399–401. doi: 10.1111/j.1749-6632.1995.tb38155.x

Stefanics, G., Kremláček, J., and Czigler, I. (2014). Visual mismatch negativity: a predictive coding view. *Front. Hum. Neurosci.* 8:666. doi: 10.3389/fnhum.2014.00666

Tewes, U. (1991). *Hamburg-Wechsler-Intelligenztest für Erwachsene [HAWIE-R, Hamburg-Wechsler-Intelligence Test for Adults].* Bern, Stuttgart, Toronto: Huber.

The MathWorks. (2015). *MATLAB and Statistics Toolbox Release 2015b.* Natick, MA: The MathWorks, Inc. Available online at: https://de.mathworks.com

Thurm, F., Antonenko, D., Schlee, W., Kolassa, S., Elbert, T., and Kolassa, I.-T. (2013). Effects of aging and mild cognitive impairment on electrophysiological correlates of performance monitoring. *J. Alzheimers Dis.* 35, 575–587. doi: 10.3233/JAD-121348

Todd, J., Michie, P. T., Schall, U., Ward, P. B., and Catts, S. V. (2012). Mismatch negativity (MMN) reduction in schizophrenia-impaired prediction-error generation, estimation or salience? *Int. J. Psychophysiol.* 83, 222–231. doi: 10.1016/j.ijpsycho.2011.10.003

Tsolaki, A. C., Kosmidou, V., Kompatsiaris, I. Y., Papadaniil, C., Hadjileontiadis, L., Adam, A., et al. (2017). Brain source localization of MMN and P300 ERPs in mild cognitive impairment and Alzheimer's disease: a high-density EEG approach. *Neurobiol. Aging* 55, 190–201. doi: 10.1016/j.neurobiolaging.2017.03.025

United Nations (2015). *World Population Ageing. 1950–2050.* New York, NY: United Nations Publications.

Vecchio, F., and Määttä, S. (2011). The use of auditory event-related potentials in Alzheimer's disease diagnosis. *Int. J. Alzheimers Dis.* 2011:653173. doi: 10.4061/2011/653173

Verleger, R., Kömpf, D., and Neukäter, W. (1992). Event-related EEG potentials in mild dementia of the Alzheimer type. *Electroencephalogr. Clin. Neurophysiol.* 84, 332–343. doi: 10.1016/0168-5597(92)90086-q

Welsh, K. A., Butters, N., Mohs, R. C., Beekly, D., Edland, S., Fillenbaum, G., et al. (1994). The consortium to establish a registry for Alzheimer's disease (CERAD). Part V. A normative study of the neuropsychological battery. *Neurology* 44, 609–614. doi: 10.1212/WNL.44.4.609

Yesavage, J. A., Brink, T. L., Rose, T. L., Lum, O., Huang, V., Adey, M., et al. (1983). Development and validation of a geriatric depression screening scale: a preliminary report. *J. Psychiatr. Res.* 17, 37–49. doi: 10.1016/0022-3956(82)90033-4

Conflict of Interest Statement: The authors declare that the research was conducted in the absence of any commercial or financial relationships that could be construed as a potential conflict of interest.

Copyright © 2018 Laptinskaya, Thurm, Küster, Fissler, Schlee, Kolassa, von Arnim and Kolassa. This is an open-access article distributed under the terms of the Creative Commons Attribution License (CC BY). The use, distribution or reproduction in other forums is permitted, provided the original author(s) and the copyright owner are credited and that the original publication in this journal is cited, in accordance with accepted academic practice. No use, distribution or reproduction is permitted which does not comply with these terms.

frontiers in Neuroscience

REVIEW
published: 05 January 2018
doi: 10.3389/fnins.2017.00728

Metabolic Abnormalities of Erythrocytes as a Risk Factor for Alzheimer's Disease

Elena A. Kosenko[1], Lyudmila A. Tikhonova[1], Carmina Montoliu[2], George E. Barreto[3,4], Gjumrakch Aliev[5]* and Yury G. Kaminsky[1]*

[1] Institute of Theoretical and Experimental Biophysics, Russian Academy of Sciences, Pushchino, Russia, [2] Fundación Investigación Hospital Clínico, INCLIVA Instituto Investigación Sanitaria, Valencia, Spain, [3] Departamento de Nutrición y Bioquímica, Facultad de Ciencias, Pontificia Universidad Javeriana, Bogotá, Colombia, [4] Instituto de Ciencias Biomédicas, Universidad Autónoma de Chile, Santiago, Chile, [5] GALLY International Biomedical Research Institute Inc., San Antonio, TX, United States

OPEN ACCESS

Edited by:
Ghulam Md Ashraf, King Abdulaziz University, Saudi Arabia

Reviewed by:
Etheresia Pretorius, Stellenbosch University, South Africa
Zemin Wang, Harvard Medical School, United States

***Correspondence:**
Elena A. Kosenko
eakos@rambler.ru
Gjumrakch Aliev
aliev03@gmail.com

Specialty section:
This article was submitted to Neurodegeneration, a section of the journal Frontiers in Neuroscience

Received: *24 October 2017*
Accepted: *13 December 2017*
Published: *05 January 2018*

Citation:
Kosenko EA, Tikhonova LA, Montoliu C, Barreto GE, Aliev G and Kaminsky YG (2018) Metabolic Abnormalities of Erythrocytes as a Risk Factor for Alzheimer's Disease. Front. Neurosci. 11:728. doi: 10.3389/fnins.2017.00728

Alzheimer's disease (AD) is a slowly progressive, neurodegenerative disorder of uncertain etiology. According to the amyloid cascade hypothesis, accumulation of non-soluble amyloid β peptides (Aβ) in the Central Nervous System (CNS) is the primary cause initiating a pathogenic cascade leading to the complex multilayered pathology and clinical manifestation of the disease. It is, therefore, not surprising that the search for mechanisms underlying cognitive changes observed in AD has focused exclusively on the brain and Aβ-inducing synaptic and dendritic loss, oxidative stress, and neuronal death. However, since Aβ depositions were found in normal non-demented elderly people and in many other pathological conditions, the amyloid cascade hypothesis was modified to claim that intraneuronal accumulation of soluble Aβ oligomers, rather than monomer or insoluble amyloid fibrils, is the first step of a fatal cascade in AD. Since a characteristic reduction of cerebral perfusion and energy metabolism occurs in patients with AD it is suggested that capillary distortions commonly found in AD brain elicit hemodynamic changes that alter the delivery and transport of essential nutrients, particularly glucose and oxygen to neuronal and glial cells. Another important factor in tissue oxygenation is the ability of erythrocytes (red blood cells, RBC) to transport and deliver oxygen to tissues, which are first of all dependent on the RBC antioxidant and energy metabolism, which finally regulates the oxygen affinity of hemoglobin. In the present review, we consider the possibility that metabolic and antioxidant defense alterations in the circulating erythrocyte population can influence oxygen delivery to the brain, and that these changes might be a primary mechanism triggering the glucose metabolism disturbance resulting in neurobiological changes observed in the AD brain, possibly related to impaired cognitive function. We also discuss the possibility of using erythrocyte biochemical aberrations as potential tools that will help identify a risk factor for AD.

Keywords: Alzheimer's disease, amyloid β, erythrocytes, metabolic dysfunction, multilayered pathology, clinical manifestation

INTRODUCTION

Alzheimer's disease (AD) is a slowly progressing, systemic neurodegenerative disorder of uncertain etiology. Clinical manifestation of this disorder usually consists of cognitive deficits in memory in the elderly. Some estimates suggest that 50% of the population over the age of 80 years suffers from this type of dementia. With increases in life expectancy of our population, AD is already approaching epidemic proportions with no cure or preventative therapy yet available. Now, AD affects ∼24 million people worldwide with 4.6 million new cases of dementia every year (one new case every 7 s), and if existing trends continue, 115 million individuals worldwide will have Alzheimer's disease (AD) by 2050 (Wimo and Prince, 2010; Fita et al., 2011).

AD develops sporadically in 95–98% of the AD population (Bird, 2005; Reddy, 2006; Kaminsky et al., 2010). However, the genetic-linked cases have provided a great deal of biochemical insights in the disease process. The research field has been focused on the role of Aβ in the brain stemming from the fact that accumulation of these peptides results in aggregation and formation of insoluble plaques, which trigger a cascade of deleterious changes, leading to neuronal death and thus causing AD. This train of events has been called the amyloid-cascade hypothesis of AD (Hardy and Higgins, 1992). It is significant that accumulation of aggregated Aβ is the primary abnormality in AD and that its deposition is required for postmortem diagnosis. Now, however, a large body of evidence exists, and new data continues to accumulate indicating that the number of Aβ deposits in the brain does not correlate well with the degree of cognitive impairment (Braak and Braak, 1991; Terry et al., 1991; Giannakopoulos et al., 2003; Guillozet et al., 2003). Indeed, Aβ deposition may occur in normal non-demented elderly people (Joachim et al., 1989; Mann et al., 1992; Lue et al., 1999; Schmitt et al., 2000; Pike et al., 2007), that is in agree with the fact that virtually all humans start to accumulate Aβ in the brain upon aging (Funato et al., 1998; Wang et al., 1999; Morishima-Kawashima et al., 2000). Besides, amyloid plaques are not specific for Alzheimer's disease and have been found in many other pathological conditions, including transmissible spongiform encephalopathies (Liberski, 2004), Down's syndrome (Glenner and Wong, 1984), Lewy body in Parkinson's disease (Arai et al., 1992), acute traumatic brain injury with diffuse axonal damage (Smith et al., 2003) and chronic traumatic brain injury associated with boxing (Roberts et al., 1990; Jordan, 2000) and football (Omalu et al., 2005). What is clear from these studies is that the presence of brain plaques alone is insufficient to produce cognitive decline in AD (Jack et al., 2009) and that such studies support the basis for the formation of a new hypothesis.

Recently, a modified Aβ-cascade hypothesis has been formulated that predicts intraneuronal accumulation of soluble Aβ oligomers, but not monomer or insoluble amyloid fibrils, as the first step of a fatal cascade in AD (McLean et al., 1999; Wirths et al., 2004; Selkoe, 2007). The amyloid oligomerization is observed to occur intracellularly (Connolly and Volpe, 1990) and $A\beta_{1-42}$ oligomers turn out to be potent neurotoxins in animal brain and neuronal cultures where they are able to disrupt glutamatergic synaptic function (Lambert et al., 1998; Hsia et al., 1999; Klein et al., 2001; Hardy and Selkoe, 2002; Kamenetz et al., 2003; Walsh and Selkoe, 2004; Roselli et al., 2005) and neuronal calcium homeostasis (Bapat et al., 1983; Mattson et al., 1992; Demuro et al., 2005), promote abnormal release of glutamate in hippocampal neurons (Brito-Moreira et al., 2011), induce oxidative stress (De Felice et al., 2007), incite tau hyperphosphorylation (De Felice et al., 2008), and synapse loss (Lue et al., 1999; Selkoe, 2008), inhibit long-term potentiation in the hippocampus (Walsh et al., 2002), which is required for memory formation, and in turn leads to the cognitive deficits in the animal. Using oligomer-sensitive immunoassay, the soluble Aβ oligomers have been found in brains of AD patients (Kuo et al., 1996; Lue et al., 1999; Gong et al., 2003). This confirms the prediction that soluble oligomeric Aβ-forms are characteristic of AD pathology. However, the soluble Aβ burden displayed considerable individual variation in the brain of AD patients. Thus, the mean level of soluble Aβ can increase 3-fold (McLean et al., 1999), 6-fold, 12-fold (Kuo et al., 1996), and 70-fold (Gong et al., 2003) in brain of AD patients compared to age-matched control, at that, the majority of soluble peptides was $A\beta_{1-42}$ (Kuo et al., 1996). On the other hand, it was found that the levels of soluble $A\beta_{1-42}$ were smallest in the AD brain (0.7%) and that the soluble pools of $A\beta_{1-40}$ and $A\beta_{1-42}$ were the largest fractions of total Aβ in the normal brain (50 and 23% respectively, Wang et al., 1999). Other authors also showed that the $A\beta_{1-42}$ levels were found in the brains of normal elderly subjects (Tabaton and Piccini, 2005) and that in subjects with AD these concentrations increased slightly compared with the age-matched control (Lue et al., 1999). These studies suggest that within individual AD subjects, the areas with greater numbers of soluble Aβ oligomers did not, as a rule, and whether the levels of these "concentration-jumping" oligomers correlate with the memory decline in AD remains to be determined. Indeed, previous studies have shown that these Aβ forms were observed in the brains of patients with Down's syndrome (DS) (Teller et al., 1996; Gyure et al., 2001; Tabaton and Gambetti, 2006) indicating that the accumulation of soluble oligomers are not specific for AD. Moreover, in brains of patients with DS, increased levels of oxidative damage occur prior to the onset of Aβ deposition (Nunomura et al., 2000). Hence, the formation of diffuse amyloid plaques may be considered as the message talking about the disruption of brain homeostasis or as a compensatory response to remove reactive oxygen species (Atwood et al., 2003). Thus, these facts provide the opportunity to investigate the pathological conditions that precede the formation of the Aβ deposits in the human brain.

It is well known that a characteristic reduction of cerebral perfusion and metabolism occurs in patients with AD (de la Torre, 2000b; Aliev et al., 2003a). It was suggested that capillary distortions commonly found in the AD brain elicit hemorheological changes that altered the delivery and transport of essential nutrients, particularly glucose, and oxygen required for its aerobic oxidation in brain cells (de la Torre and Mussivand, 1993; de la Torre, 2002a; Chang et al., 2007; Aliev, 2011) resulting in an energy metabolic breakdown of the biosynthetic and synaptic pathways, subsequently leading to the death of

neurons as a consequence of cognitive deterioration. In fact, it was proposed that AD may originate as a vascular disorder with the resultant impairment of oxygen delivery to the brain with the plaques and tangles found in the brain secondary to the effects of the vascular pathology (de la Torre, 2002a). Another important factor in tissue oxygenation is the ability of red blood cells (RBC) to the binding, transport and delivery of oxygen to tissues that depends, first of all, on RBC energy metabolism and antioxidant status (Brewer et al., 1974) that is extremely important for the functioning and regulation of oxygen affinity to hemoglobin (van Wijk and van Solinge, 2005).

Surprisingly, despite the main role of RBC metabolism in the delivery of oxygen to the tissues, no systematic programs of research have examined the relationship between the breach of the energy metabolism of these cells in destabilization of glucose metabolism in the brain pathology and this relationship is still not sufficiently discussed in the literature. Therefore, our current hypothesis is that RBC metabolism plays a key role in AD brain disorders. We propose that the long-term lack of sufficient energy, disturbance of glycolytic, antioxidant RBSs pathways, and sodium potassium pump in oldest subjects [caused by different reasons and also in contact with Aβ, which is located on the luminal surfaces of cerebral microvessels (Grammas et al., 2002; Michaud et al., 2013)] can cause a decrease in the ability of RBC to transfer oxygen to tissue, leading to inadequate oxygenation and can result in abnormal glucose/energy metabolism, oxidative stress and, thereby, increase the susceptibility of neurons to damage, and reduce mental capacity as a consequence thereof. We have called this chain of events as "*the erythrocytic hypothesis of Alzheimer disease*" (Kosenko et al., 2016). In support of this hypothesis we also believe that erythrocyte biochemical aberrations might be used as potential tools in the early detection of the brain pathology development. This hypothesis provides ideas for the development of innovative personalized medical technologies allowing recovering the energy metabolism and the system of antioxidant defense in erythrocytes.

BRAIN GLUCOSE METABOLISM, GLUTAMATE TOXICITY, AND Aβ ACCUMULATION: CAUSE OR EFFECT?

The brain is normally dependent on glucose for oxidative metabolism and function, therefore it is extremely sensitive to fluctuation in the blood glucose concentration, and since no satisfactory brain endogenous substitute exists. In spite of the fact that under certain conditions such as starvation or diabetes the ketone bodies can supply up to 50% of the brain's energy needs, the rest of the energy anyway must come from glucose. Therefore, within even just a few minutes glucose and oxygen deprivation induces significant dysfunction, and a longer time period can ultimately result in cell death (Blass, 2002). In addition to ATP production, the oxidation of glucose can produce other important intermediate such as lactate, which does not enter necessarily in the tricarboxylic acid cycle, but rather can be released and transported by the circulation into the liver for glucose synthesis de novo. Glucose also can be incorporated into lipids, proteins, and glycogen, and it is also the precursor of certain neurotransmitters such as γ-aminobutyric acid (GABA) (Plum and Posner, 1972), glutamate (Hamberger et al., 1979), and acetylcholine (Gibson et al., 1975). Thus, circulating glucose regulates many brain functions, including brain vitality, activity, learning, and memory (Korol and Gold, 1998).

Whereas the cerebral energy status is only slightly decreased during the normal aging process, glucose metabolism, and cellular ATP production are severely reduced in sporadic AD (Kyles et al., 1993; Hoyer, 1996). Certain neuronal populations are especially vulnerable to cut glucose oxidation, specifically neurons in the CA1, subiculum, and dentate gyrus of the hippocampus, and neurons in the outer layers of the cortex (Auer and Siesjö, 1993). A substantial proportion of neurons in these regions is glutamatergic and evidence suggests that hypoglycemic injury in these neurons is initiated almost entirely by hyperactivation of glutamate receptor (Auer et al., 1985), followed by the glutamate cascade and oxidative stress. The numerous studies have provided conclusive proof that glutamate becomes neurotoxic via the NMDA receptor when intracellular energy levels are reduced (Novelli et al., 1988; Beal et al., 1991; Albin and Greenamyre, 1992; Beal, 1992; Storey et al., 1992; Kosenko et al., 1994; Gonzalez et al., 2015). On the other hand, there is a direct relationship between disturbances in energy metabolism and mental disorder. For example, in 1932 Quastel J. first put forward a general suggestion that disturbances in energy metabolism would impair the neurological function, including particularly cognition (Quastel, 1932). During the past decades, a lot of work has proved Quastel's theory to be prescient and showed that the cause-effect relation is nonspecific as impairing cerebral energy metabolism can induce mental disorders to varying degrees (confusion, mental fatigue, agnosia, or dementia) in different pathological situations. Thus, impaired mental function has been reported in association with hypoglycemia (Bruce et al., 2009), inadequate transportation of glucose across the blood-brain barrier (Klepper and Voit, 2002; Pascual et al., 2004), defective astroglial glutamate transportation (Rönnbäck and Hansson, 2004), hypoxia (Gibson et al., 1981), diabetes (Richardson, 1990), heart failure (Riegel et al., 2002), reduced glucose tolerance (Vanhanen et al., 1997), bradycardia, hypotension (Ackerman, 1974), high intracranial pressure (Yoshida et al., 1996), stroke (van der Zwaluw et al., 2011), hypothermia, alcohol intoxication, thiamine and vitamin C deficiency, sedative-hypnotic drugs, opioids consumption (Martindale et al., 2010), general anesthesia (Parikh and Chung, 1995; Xie et al., 2006b), hypocapnia (Dodds and Allison, 1998), chronic stress (Conrad et al., 1996; Conrad, 2006), chronic noise stress (Arnsten and Goldman-Rakic, 1998; Manikandan et al., 2006), mixed brain pathologies (Schneider et al., 2007), hepatic encephalopathy (Butterworth, 2003), hyperammonemia (Llansola et al., 2007), trauma (Brooks et al., 2000), and so forth. Interestingly, after trauma, a large number of Aβ positive neurons appeared in human (Chen et al., 2004; Uryu et al., 2007) and animal brain (Kamal et al., 2001; Kasa et al., 2001; Papp et al., 2002; Hamberger et al., 2003). APP (amyloid precursor protein) accumulation is also observed following rat (Li et al., 1995) and human spinal cord injury (Ahlgren et al., 1996; Cornish et al.,

2000). Long-term presence of APP and accumulation of Aβ in the rat thalamus were observed after middle cerebral artery occlusion (van Groen et al., 2005) and in cultured cells that had been treated with spirochetes or bacterial lipopolysaccharide (LPS) (Miklossy et al., 2006) and other infectious agents (Balin and Appelt, 2001).

A number of studies have also demonstrated that abnormal activation of β-adrenergic receptors (β-ARs), which mediate the effect of stress, might contribute to Aβ peptides production resulting in accelerating amyloid plaque formation *in vitro* and *in vivo* by enhancing γ-secretase activity (Ni et al., 2006) and that blocking β-ARs attenuates acute stress-induced Aβ peptide production (Yu et al., 2010). Indeed, the common inhalation anesthetic isoflurane has been reported to increase brain Aβ protein levels *in vitro* (Xie et al., 2006a) and *in vivo* (Xie et al., 2008; Zhang et al., 2008; Dong et al., 2009). Hypocapnia can also increase Aβ production in H4 human neuroglioma cells (Xie et al., 2004). Nanoscale particulates, a major component airborne pollution, inducing the blood-brain barrier disruption and neuroinflammation (Murr et al., 2006), result in AD-associated $A\beta_{1-42}$, accumulation in the brains of children living in the high-pollution area (Calderón-Garcidueñas et al., 2008a,b). Upon careful analysis of these pathologies, one can see that there is a steady disruption of brain aerobic metabolism and the subsequent increase in APP processing and the formation of amyloids (Gabuzda et al., 1994; Webster et al., 1998; Velliquette et al., 2005). Thus, according to positron emission tomography (PET), isoflurane anesthesia can cause a 50% decrease in the rate of glucose uptake by the brain (Alkire et al., 1995, 1997), which leads to a sharp inhibition of aerobic oxidation in the cells and development of severe hypoxia, decreased neuronal activity (Hodes et al., 1985), and the appearance of amyloid in the brain 6-24 h after application of the anesthetic (Xie et al., 2006a, 2008). In ischemia-reperfusion, in addition to increasing oxidative stress, there is a decrease in the rate of blood flow, since migration of neutrophils to the site damaged by hypoxia can cause blockage of capillaries (Simpson et al., 1988), which impairs the entry of glucose and oxygen into the brain and promotes the formation of amyloids in damaged brain structures (van Groen et al., 2005; Tesco et al., 2007). In hypoglycemia, the limited supply of glucose from the blood to the brain also contributes to the accumulation of amyloids in the brain (Shi et al., 1997).

Altogether, these findings suggest that a transient insult, e.g., trauma, ischemia, neuroinflammation, anesthesia, or infectious agents could lead to secondary and persistent brain injuries and that the initial production of Aβ and its precursor, perhaps, are associated with physiological compensatory mechanisms for repair or protection of neurons exposed to significant disturbances in homeostasis (Smith et al., 2000; Lee et al., 2004). These facts are consistent with the numerous data showing that amyloid exhibits trophic and neuroprotective (Whitson et al., 1989; Koo et al., 1993; Singh et al., 1994; Luo et al., 1996), antioxidant (Smith et al., 1998, 2002a; Kontush et al., 2001; Atwood et al., 2002) properties and accumulates in the tissue after impairment of the energy metabolism with non-specific stimulus (Gabuzda et al., 1994; Webster et al., 1998; Velliquette et al., 2005), while under physiological conditions the diurnal fluctuation of brain Aβ levels is strictly regulated (Kang et al., 2009). Additionally, scores obtained on mini-mental state examination in AD subjects correlate highly with reductions of glucose metabolism (Blass, 2003), suggesting that the metabolic lesion precedes the development of neuropsychological abnormalities (Gibson and Huang, 2002) and support the conclusion that sporadic AD is a hypometabolic disorder which is provoked by a dysfunctional cerebral energy metabolism (Hoyer et al., 1988; Blass and Gibson, 1991; Meier-Ruge and Bertoni-Freddari, 1996; Perry et al., 1998; Smith et al., 2002b; Aliev et al., 2003b, 2004; Zhu et al., 2007). Obviously, the detection of mechanisms of disturbance of aerobic glucose metabolism in the brain is one of the most pressing tasks which will facilitate further progress on to determine not only to the midlife AD risk factor, but also on the lifespan of the older persons. Therefore, any pharmacological intervention, directed at correcting the chronic hypoperfusion state would possibly change the natural course of development of dementing neurodegeneration (Aliev et al., 2003a).

THE POSSIBLE ROLE OF RBC IN PATHOGENESIS OF AD

The pathologic causes of brain glucose metabolism disorders in AD may vary in signs and symptoms, which are as follows: desensitization of the neuronal insulin receptor (Hoyer, 2000), a decrease in the enzymes of the tricarbonic acid cycle activities (Meier-Ruge et al., 1984; Marcus et al., 1989; Marcus and Freedman, 1997; Bubber et al., 2005), impaired glucose transporter at the blood-brain barrier (Kalaria and Harik, 1989), depressed glucose transport into neurons (Simpson and Davies, 1994; Simpson et al., 1994), hippocampal region atrophy (Jobst et al., 1992; Villain et al., 2008) neuronal loss in the affected areas (McGeer et al., 1990), NO-dependent endothelial dysfunction and degeneration (De Jong et al., 1999; de la Torre, 2000a, 2002b) in brain capillaries that affect the capillary blood flow and optimal delivery of glucose and oxygen to neuronal cells (de la Torre, 2000b; Aliev et al., 2003a).

Another important factor in tissue oxygenation is the ability of RBC to bind, transport and release oxygen to tissues. For this, the RBC requires several essential metabolic pathways such as (i) anaerobic glycolysis, which is the only source of energy (ATP production) for sustaining cell structure and function; (ii) maintenance of the electrolyte gradient between plasma and red cell cytoplasm through the activity of adenosine triphosphate (ATP)-driven membrane pumps; (iii) pentose phosphate shunt (PPS) that controls the anti-oxidant pathways by produced NADPH, which plays an important role in maintaining glutathione in the reduced state; (iv) antioxidant pathways necessary for the protection of RBC proteins and hemoglobin against oxidation; and (v) nucleotide metabolism for the maintenance of the purine and pyrimidine homeostasis. Moreover, erythrocytes possess a unique glycolytic bypass, Rapoport-Luebering shunt to produce 2,3-diphosphoglycerate (2,3-DPG), a crucial metabolite in the regulation of hemoglobin affinity for oxygen (Cho et al., 2008). Thus, the mature erythrocyte retains a strictly regulated system

of soluble enzymes, structural proteins, carbohydrates, lipids, anions, cations, cofactors, metabolites, antioxidants all of which are required in balance for effective metabolism and functioning of the cell. A change of at least one component of this system will lead to an imbalance and loss of RBC functional capacity. Indeed, a significant loss in ATP (Rabini et al., 1997), Mg^{2+}, Na^{+}, and ATP-ase activity (Ajmani and Rifkind, 1998) all of which may decrease erythrocyte deformability (Sakuta, 1981; Kucukatay et al., 2009), changes morphology (Gov and Safran, 2005) and increases RBC volume (Kowluru et al., 1989; Kucukatay et al., 2009). Extensive diminution of intracellular antioxidant GSH promotes oxidative damage of protein and lipids and compromises structural integrity of the RBC (Morris et al., 2008). Decreased 2,3-DPG, operating as a regulator of the oxygen affinity of RBC (Duhm, 1971) reduces the ability of RBC to release oxygen, resulting in tissue hypoxia (MacDonald, 1977; Nakamura et al., 1995; **Figure 1**). Considering the cause-effect relationship between various intracellular metabolic pathways and RBC function, it may be inferred that intact biochemical intracellular pathways are a major factor controlling the paramount RBC function associated with the ability to bind, transport, and release oxygen to tissues.

Recently, we measured some parameters of adenine nucleotide metabolism, glycolysis, pentose phosphate pathway, 2,3-DPG shunt (Kaminsky et al., 2013), oxidant and antioxidant enzymes and metabolites (Kosenko et al., 2012) in RBCs samples from Alzheimer's subjects (AD) and non-Alzheimer's dementia (NA) patients. We found that activities of all glycolytic, pentose phosphate pathway and 2,3-DPG shunt enzymes, Na^{+}, K^{+}-ATPase, as well as NAD/NADH ratio, pyruvate and lactate levels evidently decreased in aging and increased equally in AD and NA to levels or above levels of the YC (young controls) group indicating an increase in RBC glycolysis and ion fluxes. Elevated Na^{+}, K^{+}-ATPase activity and decreased ATP levels imply that ATP loss was mostly based on energy-expending redistribution of Na^{+} and K^{+} across the plasma membrane in erythrocytes from AD patients. These results confirm the fact that in AD, as in certain other diseases the balance between ATP formation and ion pumping may be disordered resulting in a decrease in intercellular energy charge, and an increase in lactate formation and catabolism of adenylates (Ronquist and Waldenström, 2003). These defects were accompanied by a significant decrease [relatively to both age-matched controls (AMC) and young adult controls (YC)] in the 2,3-DPG concentration that was accompanied by increases in the activity of diphosphoglycerate phosphatase (DPGP-ase), an enzyme that converts 2,3-DPG to 3PG (Kosenko et al., 2016). Of course, other factors besides of 2,3-DPG may affect the affinity of oxygen to hemoglobin (Samaja et al., 2003), but the relationship between the 2,3-DPG concentration in RBC as a biological indicator of tissue hypoxia in diabetic neuropathy (Nakamura et al., 1995), as well as in preterm infants with perinatal problems (Tsirka et al., 1990; Cholevas et al., 2008), in patients with the nondeletion genotype of hemoglobinopathy (Papassotiriou et al., 1998), with hypertension (Resnick et al., 1994), in experimental endotoxin shock (Matsumoto, 1995), severe hypophosphatemia (Larsen et al., 1996), and some types of glycolytic enzymes disturbances (McCully et al., 1999) was well established. Thus, the results generated the hypothesis that chronic enhancement in the rate of active transport in AD (Ronquist and Waldenström, 2003) leading to the increase in ATP and 2,3-DPG hydrolysis and can increase in Hb affinity to oxygen, loss of adequate oxygen delivery to tissues that may be one of the factors contributing to brain hypoxia (Aliev et al., 2004), glucose hypometabolism, and memory dysfunction in AD. It should be noted, however, that RBC of even cognitively stable aging persons (AMC) was characterized by a slight but significant decrease in 2,3-DPG when compared with the young adult control group. The tendency for the ATP production, adenylate energy charge, adenine nucleotide pool size, and ATP/ADP ratio (Kosenko et al., 2016) was a decrease in aging with no notable changes in dementia. There were no differences between AMC, AD, and NA groups in GSH levels, as well as in GSSG levels and the GSH/GSSG ratio in RBCs (Kosenko et al., 2012). Activities of calpain and caspase-3 in RBCs from aged subjects, on the contrary, were three times higher than those in young controls and were equally high in both dementia types (Kaminsky et al., 2012). The trend for the hydroperoxide generation was an increase in aging with no dramatic changes in dementia. There were no significant differences between AC, AD, and NA subjects in H_2O_2, organic hydroperoxide and the sum of H_2O_2 plus organic hydroperoxides content of RBC (Kaminsky et al., 2013). The results suggest that oxidative stress to some extent is already present in the RBC of the AMC subjects (Kosenko et al., 2012) and that together with the disturbances of glycolytic and transport processes and proteolysis increasing are a general feature of aging and not a feature of dementia. This view is supported by data comparing AD with normal aging, where was documented the same profile of damage (Smith et al., 1991; Moreira et al., 2006) suggesting that RBC oxidative damage is no longer an end stage but rather a signal of underlying changes of state (Moreira et al., 2006).

Although endogenous oxidative stress may damage the RBC itself the mass effect of large quantities of free radicals leaving the red cell has a prodigious potential to damage other components of the circulation (Johnson et al., 2005) including endothelial cells resulting in the microvascular pathology (Kiefmann et al., 2008). The combined effects of these damages most likely contribute to the morphological changes in oldster subjects (Richards et al., 2007), which may result in decreased erythrocyte deformability (Kuypers et al., 1990) and alter rheology and reduce the threshold for the development of neuropathology (Ajmani et al., 2003). We propose that the long-term lack of sufficient energy, disturbances of glycolytic pathway and sodium/potassium pump in aged subjects can decrease the ability of RBC to transfer oxygen, leading to inadequate tissue oxygenation and abnormal glucose metabolism in the brain and thereby reducing mental capacity and cognition. Thus, the reduced mental capacity may be, to a large extent, due to the imbalance in the metabolic processes in RBC. Obviously, other factors may be operative, but the role of RBC biochemical alterations as possible preclinical indicator of mental disorders must be critically examined. During the last 10 years, numerous biochemical abnormalities in RBC of subjects suffering from various mental disturbances have been detected

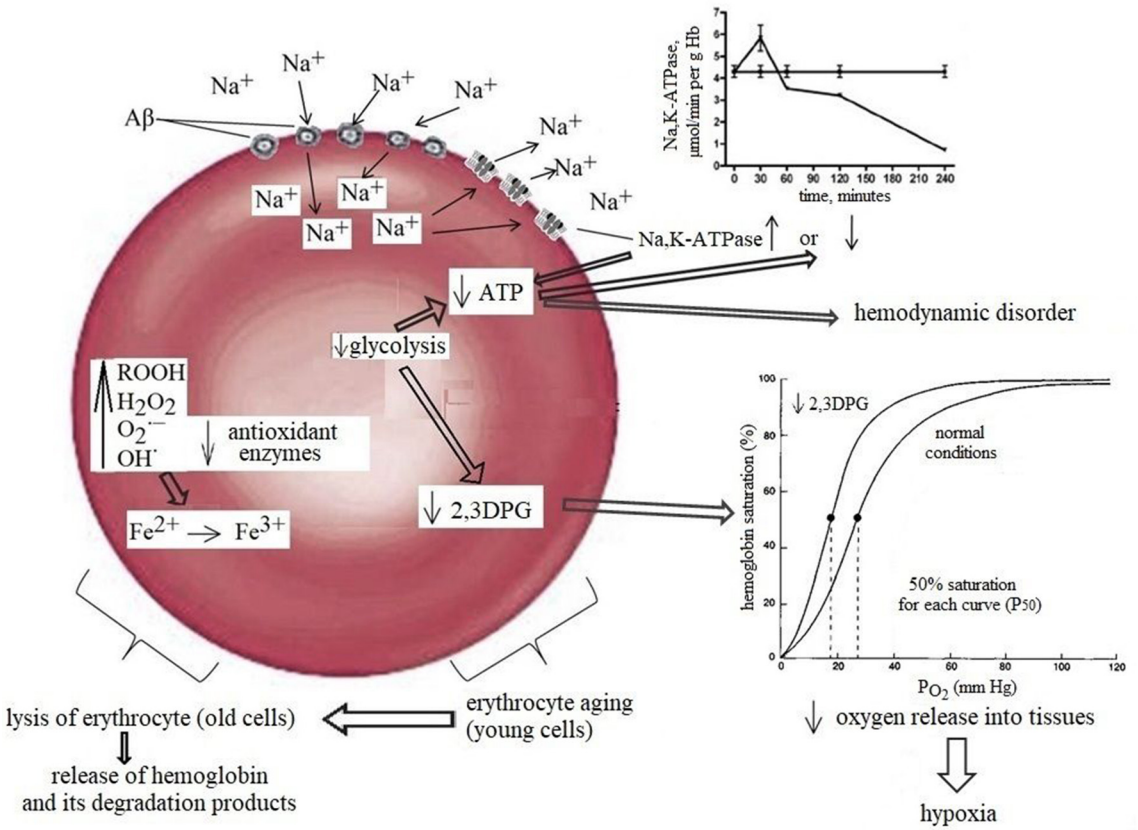


FIGURE 1 | Normal aging diminishes RBC functions, including a detectable decrease in the activity of glycolytic and antioxidant enzymes. The combined effects of these damage together with a slight but significant decrease in 2,3-DPG are most likely contributor to the morphological changes in oldster subject which may result in decreased erythrocyte deformability, alter rheology, loss of adequate oxygen delivery and reduce the threshold for the development of neuropathology. The left part of the scheme: Amyloids possess gramicidin D-like action and upon contact with erythrocytes rapidly increase the concentration of sodium in the cells causing rapid activation of the Na^+, K^+-ATPase leading to the increase in ATP and 2,3DPG hydrolysis and can increase in Hb affinity to oxygen, that may be one of the factors contributing to brain hypoxia which lead to glucose hypometabolism and memory dysfunction in AD. The right part of the scheme: Prolonged contact with erythrocytes depletes ATP stores, causing Na^+, K^+-ATPase pumps and Na^+- dependent ion channels to stop working and, consequently, the erythrocytes to swell and lyse. RBCs release hemoglobin, which is a source of iron. In turn, this metal catalyses the formation of toxic reactive oxygen species that mediate neuronal injury.

(Danon et al., 1992; Rifkind et al., 1999; Ponizovsky et al., 2003; Pankowska et al., 2005; Lang et al., 2015; Pretorius et al., 2016). We believe that obligatory measurement of RBC biochemical parameters in peoples older than 50 years in the dynamics will help identify the risk factor for AD.

The problem is clear, but a number of questions arise in connection with the above-mentioned. If oxidative stress is more or less present in the erythrocytes of all elderly people and is a risk factor for dementia, why does this risk factor "work" for some people, while others, with the same risk factor, live to a very old age, maintaining "bright mind" and working capacity? The same question arises with regard to the concentration of 2,3-DPG reduction and the energy metabolism rate in the erythrocytes in general. It is obvious that the answers to these questions can only be obtained after identification of the reasons causing a global energy metabolism disorder, an increase of oxidative stress that are the basis of quick aging, affection of erythrocytes and that lead to a disruption of their functional capacity and early death. In other words, it is necessary to find out, under what influence factors (endogenous and exogenous) the reserve capacity of erythrocytes to withstand the stress that they are constantly exposed to, which circulate from the lungs to the tissues, decreases too soon.

Another problem is the lack of absolute knowledge of the hemopoiesis status in older people and especially in stressful situations that require intensification of the formation of blood cells. Numerous data indicate that the functions of basal hemopoiesis, which maintains the number of blood cells within the norm, changes insignificantly with age (Sansoni et al., 1993; Bagnara et al., 2000), whereas the reserve capacity of the bone marrow to resist stressful situations requiring its activation, even in healthy elderly people, reduces significantly with age (Williams et al., 1986; Globerson, 1999). For example, during bacterial infection or other periods of high hematopoietic demand, the formation of blood becomes "flaccid" and badly regulated, paradoxically (Rothstein, 1993), which makes it possible to

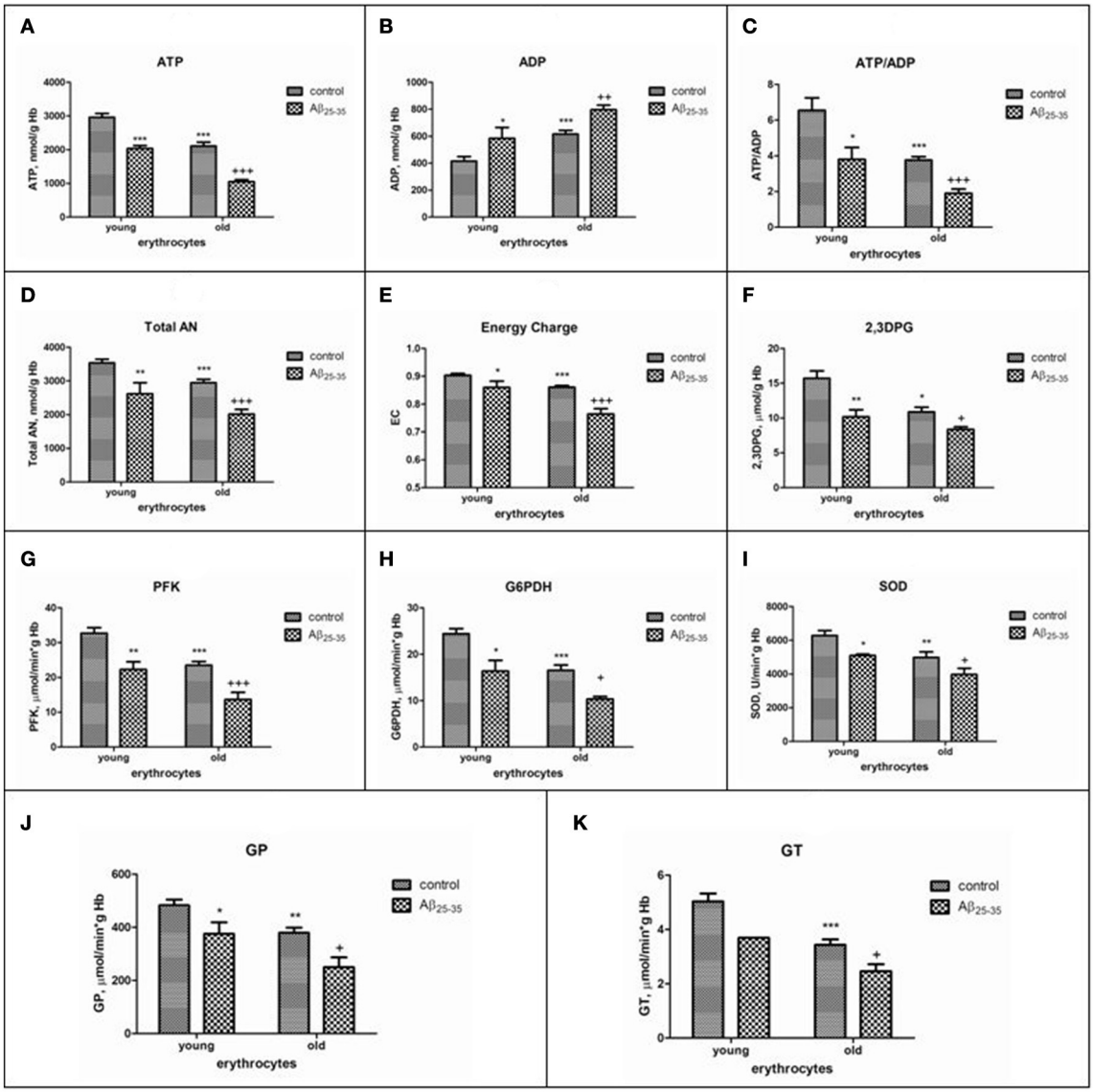


FIGURE 2 | The effects of Aβ25-35 on the parameters of the adenylate system, concentration of 2,3–DPG and activities of some glycolytic and antioxidant enzymes activities in young and old erythrocytes (RBCs). **(A)** ATP, **(B)** ADP, **(C)** ratio ATP/ADP, **(D)** total adenine nucleotide pool size, **(E)** energy charge, **(F)** 2,3DPG, **(G–K)** activities of phosphofructokinase, glucose-6-phosphate dehydrogenase, superoxide dismutase, glutathione peroxidase, glutathione transferase, respectively. ATP and AN are expressed as micromol/g Hb, ADP as nmol/g Hb. AN, total adenine nucleotide pool size; EC, adenylate energy charge [EC = (ATP + 1/2ADP)/AN]; phosphofructokinase (PFK), glucose-6-phosphate dehydrogenase (G-6PDH), glutathione peroxidase (GP), glutathione transferase (GT) activities are expressed as IU/g hemoglobin (Hb); superoxide dismutase (SOD) is expressed as units/min per g Hb. One unit of SOD activity is defined as the amount of enzyme required to produce a 50% inhibition of the rate of p-nitrotetrazolium blue reduction. The results are the mean±SEM of 16 rats. Cells were incubated at 25°C for 30 min in 10 mmol/L potassium phosphate buffer, pH 7.4, containing 0.9% NaCl, 5 mmol/L KCl, and 10 μmol/L $A\beta_{25\text{-}35}$. Control was incubated with nontoxic $A\beta_{35\text{-}25}$. Significant differences are indicated: $^{*}P < 0.05$, $^{**}P < 0.01$, and $^{***}P < 0.001$ as compared to young cells; $^{+}P < 0.05$, $^{++}P < 0.01$, and $^{+++}P < 0.001$ as compared to the old control (one-way analysis of variance [ANOVA] with Bonferroni's multiple comparison test). Aβ indicates amyloid β.

assume that there is a hidden defect in the achievement of hematopoietic equilibrium in older people. Hence, the main question arises. Is such a hidden bone marrow defect typical for people with dementia? And does this defect lead only to the disruption of cellular equilibrium, or does it also cause the appearance of defective cells in the circulation that have not received adequate "strength reserve" in the bone marrow, and therefore they quickly age and get damaged in the bloodstream? It is clear that without the answers to these questions, it is impossible to evaluate the contribution of the impaired functional capacity of erythrocytes to the clinical symptoms of AD and other types of dementia. However, when dementia is exclusively referred to brain diseases, the attention of scientists is concentrated only on neurological symptoms, whereas all

possible "defects" of erythrocytes, which cause pathological consequences for the brain, remain unexplored. We found only a few literature sources discussing the role of morphological changes that characterize the violation of the architecture of the erythrocyte membranes in the development of neurological symptoms characteristic of dementia (Mohanty et al., 2008). In particular, it has been shown that the appearance of atypical cells with altered morphological features, that is giant elongated erythrocytes with a nonhomogeneous membrane (acanthocytes or erythrocytes with numerous random spur-like cytoplasmic outgrowths) (Brecher and Bessis, 1972; Lan et al., 2015), occurs in advance (for several years) before the onset of memory disorders (Goodall et al., 1994). The mechanism of the acanthocytes emergence in the bloodstream is unknown, but since atypical cells are only a small part of the general population of normal erythrocytes, it has been suggested that the cause of their formation is related to a disruption in the synthesis of membrane structural proteins that occurs in the stage of erythrocyte formation in the bone marrow, although the possibility of the cell damage under the influence of unknown factors immediately after they come out from the bone marrow into the blood is not ruled out. Soluble amyloid peptides that are found in various cerebral vessels of the patients with AD [cerebral amyloid angiopathy (CAA)] and which, on the one hand, are capable to contact the cellular elements of blood, on the other—to damage the walls of blood vessels and cause a hemorrhage in the brain (Thanvi and Robinson, 2006), have recently been recognized as one of these factors. However, it is possible that the appearance of erythrocytes of the atypical form is associated with amyloids that circulate in the bloodstream and bind to the cell membrane (Kuo et al., 2000; Kiko et al., 2012) leading to its damage.

THE ROLE OF AMYLOID ANGIOPATHY IN ERYTHROCYTE DAMAGE

The fact that AD is a systemic disease has been known for a long time, dating back to the last century, when amyloid peptides were first detected in small vessels of the brains of patients with AD (Scholz, 1938). For the sake of justice, it is worth mentioning that the existence of amyloid peptides was known back in 1878 when Atkins discovered amyloids in the brain and blood vessels of the brain in a young patient with dementia caused by a head injury (Atkins, 1878). At that time, it has been also identified that amyloids accumulate in the brain vessels in patients with syphilis (Atkins, 1875), and epilepsy (Blocq and Marinesco, 1892) indicating that cerebral amyloidosis and CAA are accompanying a number of diseases.

As it is now well known, in patients with DA, amyloids (mainly $A\beta_{1-40}$) are found in the capillaries (Attems and Jellinger, 2004), arteries, arterioles, veins, and venules (Thal et al., 2002), which penetrate the leptomeningeal, cortical and subcortical areas of the brain (Weller et al., 2009), as well as in blood vessels supplying the hippocampus (Masuda et al., 1988). Localized in various structures of blood vessels (Wisniewski and Wegiel, 1994) and in contact with numerous cells (myocytes, pericytes), amyloids cause their damage (Vonsattel et al., 1991; Dalkara et al., 2011), as a result of which the membrane of the vessels seems to loosen, becoming unstable, which can eventually lead to the formation of an aneurysms, its rupture and cerebral hemorrhage (Thanvi and Robinson, 2006), that is, a condition that usually occurs with strokes and which irrespective of AD causes the formation of hematoma, lysis of erythrocytes, brain edema (Xi et al., 2006), local cell death, and memory damage (Pfeifer et al., 2002). Interestingly, the multiple microvascular pathology, mediated by the presence of amyloids in different structures of the blood vessels, was confirmed not only at postmortem examination, but also in life in virtually all patients with AD (Kalaria and Hedera, 1995; Farkas and Luiten, 2001; Bailey et al., 2004; Smith and Greenberg, 2009) regardless of the presence of atherosclerotic changes in the vessels. It should be noted, however, that CAA in AD patients is observed in 90–100% of cases, while brain zones with hemorrhage are detected only in 20–25% of patients with AD (Urbach, 2011). This means that brain damage in AD can occur for reasons not associated with CAA-induced hemorrhage. Indeed, a significant accumulation of amyloids in the brain vessels can cause their occlusion, thereby blocking blood flow, supplying the brain with oxygen and glucose (de la Torre and Stefano, 2000), and causing neurodegeneration of neurons and memory impairment (Thal et al., 2008, 2009). In addition, localized in endothelial cells lining the lumen of blood vessels (Michaud et al., 2013), amyloids are constantly in contact with erythrocytes circulating in the bloodstream, causing, on the one hand, their adhesion to endothelial cells, thereby violating the blood flow (Ravi et al., 2004), on the other—interacting with the membrane of erythrocytes, cause its modification and damage (Nicolay et al., 2007).

It was true that some studies have demonstrated that AD patients have increased RBC membrane injury suggesting the increased capability for erythrocyte lysis *in vivo* (Bosman et al., 1991; Goodall et al., 1994; Mattson et al., 1997; Solerte et al., 2000; Kosenko et al., 2009), as evidenced by the accumulation of free hemoglobin and iron in the brain of AD patients (Wu et al., 2004; Perry et al., 2008). The consequences of RBC lysis for the brain are well known (Xi et al., 1998). It has been shown that the appearance of free hemoglobin in the brain leads to rapid destruction of the hemato-encephalic barrier, DNA fragmentation, increased lipid peroxidation and global oxidative stress, development of the inflammatory process, vasoconstriction, hypoperfusion, brain atrophy (Alexander and LoVerme, 1980), memory impairment and death (Hackett and Anderson, 2000).

The lytic effect of amyloids was confirmed on the general population of erythrocytes. *In vitro* Aβ induces rapid lysis of human and rat erythrocytes that can be either attenuated by antioxidants (Mattson et al., 1997) or amplified in the presence of inhibitors of glycolytic and antioxidant enzymes or Na^+, K^+-ATPase (Kosenko et al., 2008a), and suggested the role of RBC glycolysis, ion pumping capacity and antioxidant status in the bioactivity and erythrotoxicity of amyloids. Given the above, we assumed that the constant contact of erythrocytes with amyloids can cause not only the change and damage on the membrane structures, but also the metabolic/energy metabolism in the erythrocytes underlying the aging, integrity,

and functional ability of the cells. This assumption does not contradict the known pathological consequence of chronic brain hypoperfusion, leading to reducing oxygen delivery to the brain (de la Torre, 2017). On the contrary, it clearly points to the possible existence of additional unspecified mechanisms, restricting the oxygen supply to the brain and, therefore, participating in the development of hypoxia and neurodegenerative processes specific to AD (Thal et al., 2009). However, the population of erythrocytes is not homogeneous, and the facts that the least resistance of old erythrocytes to endogenous and exogenous pathological factors caused by a reduced rate of energy metabolism, antioxidant defense, and strengthening of catabolic processes (Bonsignore et al., 1964; Shinozuka et al., 1994) are well established.

Data on the effect of amyloid peptides on erythrocytes of different ages at present are currently not available and are of special interest, since patients with AD are characterized by accelerated aging of erythrocytes in the bloodstream (Bosman et al., 1991). We have recently showed that sensibility of RBC to βA-induced hemolysis was in proportion to both cell age and βA concentration (Tikhonova et al., 2014). The inhibition of glucose consumption and lactate production by βA was found to occur in both cells type. However, greater demand for ATP of the Na^+, K^+ -ATPase, in combination with a more reduced capacity of the glycolytic pathway and 2,3-DPG levels in old cells lead to more pronounced imbalance between ATP and 2,3-DPG formation, total nucleotide changes and ion pumping in aging erythrocytes exposed to the amyloid. Interestingly, the decline in the levels of antioxidative, glycolytic enzymes, 2,3DPG, ATP, adenine nucleotide pool and the adenylate energy charge in young cells treated with amyloid were similar to that we found as occurring during *in vivo* red cell aging (control old erythrocytes). Thus, our data obtained show that even a limited contact of amyloid with erythrocytes is sufficient to transform young erythrocytes into old ones and that similar biochemical mechanisms can underlie the accelerated aging of cells in the bloodstream of patients with AD (Bosman et al., 1991) (**Figure 2**), that may be one of the main reasons of both inadequate supply of oxygen to the brain, and lysis of cells in circulation.

NOVEL THERAPEUTIC STRATEGY: PROBLEMS AND POSSIBLE SOLUTIONS

At present there are no medical drugs which are able to increase and improve perfusion of the brain of AD patients, since due to the absence of early diagnostics the use of any drug therapy, when the brain tissue is irreparably damaged, is late and inefficient (Hachinski and Munoz, 1997). Thus, it is very problematic "to repair" chronically damaged blood vessels of the brain and to restore their functional state with the preparations available, as well as it is hard "to cure diseased erythrocytes." This is connected, first of all, with the fact that real causes of "chronic disease" of erythrocytes during natural aging of the organism are unknown. One of the important problems, as noted above, is the absence of total knowledge on the hematopoietic status of the elderly, especially during long bed rest, accompanied by undernourishment, leads to a decrease in metabolism rate.

It is interesting to note that the problems in relation to the "disease" of erythrocytes arise during transfusion of the whole donor blood or packed RBC to the patients with different diseases in order to restore oxygen transport to the tissues and release carbonic acid from them. The main challenge is that all intracellular indices of erythrocytes change very quickly during the storage period of the donated blood leading to rapid cell aging (Lang et al., 2016). And if these indices are not corrected before blood transfusion this may result in irreparable consequences (Beutler et al., 1969). It has been shown, for example, that if during red blood cell transfusion intracellular ATP concentration of erythrocytes was lower by 40% compared to the normal cells, these erythrocytes were lysed to an excessive degree in blood flow of the recipient (Hamasaki et al., 1981). Transfusion of erythrocytes with low intracellular content of 2,3-DPG did not allow for quick restoration of adequate delivery of oxygen to the tissues. Taken together, these observations require development of the ways to increase the concentrations of ATP and 2,3-DPG in erythrocytes immediately before RBC transfusion to the patient (Beutler et al., 1969). Further studies in this field are actively undertaken, and multiple developments directed toward restoration of energy exchange in the stored erythrocytes are successively utilized by the physicians to save the patients life (Valeri and Hirsch, 1969). The main components restoring energy exchange in erythrocytes are glucose, adenine, ascorbate-2-phosphate, phosphoenolpyruvat or the cations and activators of glycolysis, which can penetrate into erythrocytes (Moore et al., 1981). It has been shown that different activators of enzymes introduced into the medium, where erythrocytes are stored, maintain normal concentration of ATP and 2,3-DPG for 1,5 months (Vora, 1987). However, although the scientists have made a considerable progress in solving the problems with regard to restoration of energy exchange disturbed during storage of erythrocytes, all the developments use modulators and activators, which are able to quickly and easily pass through the cell membrane of erythrocytes. This is a limitation for the use of the wider class of active compounds that are unable to be transported into the cells. We tried to circumvent this problem and developed a technology of the encapsulation of substrates and high molecular enzymes in erythrocytes under hypotonic conditions leading to the formation of pores in the membranes of erythrocytes (Seeman et al., 1973), enabling the enzymes with great molecular mass (Baker, 1967; Kosenko et al., 2008b; Godfrin et al., 2012; Kaminsky and Kosenko, 2012; Alexandrovich et al., 2017) to pass through the cells. For instance, we developed an approach on how to introduce regulatory glycolytic enzymes into erythrocytes, where the activity of these enzymes in erythrocytes of old animals and in the elderly decreased by 30–50% (Kaminsky et al., 2013). The data obtained showed that the encapsulation of even one regulatory enzyme in erythrocytes stimulated glycolysis to considerable extent. The signs of it were the increased rate of glucose consumption and the formation of lactate. Moreover, the erythrocytes obtained circulated in the animal's blood flow within many days, sustaining the activity of encapsulated enzymes, the

normal level of ATP, 2,3-DPG and other metabolites of energy exchange and antioxidant defense (data not shown). These results obtained are important by two reasons. First, such technology can be applied to restore ATP, 2,3-DPG and other metabolites of energy exchange, the concentration of which is decreased sharply in erythrocytes in aging of the organism. Transfusion of own erythrocytes, possessing encapsulated enzymes, should theoretically reduce the risk of the onset of inadequate oxygen supply to the brain both in the elderly and in patients with AD. Secondly, investigations make the basis for further development of innovative personalized therapeutic strategy.

CONCLUSIONS

Presently, non-genetic Alzheimer's disease is classified as a neurodegenerative disorder. However, there is an impressive body of evidence indicating that AD is a systemic metabolic disease (Perry et al., 2003), and it has originated as a vascular disorder with the resultant impairment of the delivery and transport of essential nutrients, particularly glucose and oxygen resulting in an energy metabolic breakdown with the plaques and tangles found in the brain secondary to the effects of the vascular pathology (de la Torre, 2002a). Since erythrocyte serve as the only oxygen carrier and their ability to the binding, transport, and delivery of oxygen to tissues depends, first of all, on the energy metabolism and antioxidant status there is therefore a strong possibility that the disturbance of energy metabolism and oxidative enhancement in these cells may have a dramatic impact on destabilization of aerobic glucose metabolism in the brain and AD development. With regard to RBC-controlled brain vital activity there is incontrovertible evidence that even just a few minutes of oxygen deprivation (together with glucose) initiate significant brain dysfunction and chronic effect can ultimately result in the irreversible brain damage and permanent impairment of cognition. This implies that the cerebrometabolic abnormalities are the most common form of dementia (Chibber et al., 2016; Gonzalez-Reyes et al., 2016). However, although major mechanisms involved in brain damage due to metabolic abnormalities resulting from the oxygen deprivation including alterations in neurotransmission, defect of mitochondrial oxidative phosphorylation, disturbance of Ca^{2+} homeostasis, oxidative stress and eventually apoptotic or necrotic cell death are profound and obvious (Barreto et al., 2011; Cabezas et al., 2012, 2015; Avila Rodriguez et al., 2014; Toro-Urrego et al., 2016; Baez et al., 2017; Baez-Jurado et al., 2017a,b; Martin-Jiménez et al., 2017a,b; Shevtsova et al., 2017), no systematic programs of research have examined the relationship between the breach of the energy metabolism of erythrocytes in the causing of leading to cerebrometabolic abnormalities and dementia. One of the reasons of this paradox is the large number of reports stating that brain atrophy and degeneration of nerve cells, observed with dementia, can occur without cerebrovascular pathology, but only through the amyloid fault, leading to the struggle with amyloids, and not with the causes that "gave birth to them," and made the AD a permanently incurable disease with unknown etiology. In our view, a careful examination and reversing age-related metabolic/energetic changes in erythrocytes is an achievable goal and will provide these cells as a marker of a risk of inadequate brain oxygen supply, resulting the irreversible brain damage and permanent impairment of cognition. We also strongly believe that biochemical erythrocyte indicators (ATP, 2,3DPG, glucose, lactate and others), as well as the enzymes of glycolysis, pentose phosphate and Rapoport-Luebering shunt, antioxidant pathways all of which are responsible for interrelated metabolism and functional capacity of RBC should be studied (especially in people over 50 years, and in the dynamics) not only in research laboratories, but also in clinical settings that may provide a basis for innovative personalized therapeutic strategies.

The development of technologies to assist in restoration of erythrocyte energy metabolism must form an integral part of new therapeutic strategies in the treatment of a great variety of disorders accompanied by inadequate oxygen delivery. Similar studies just are gathering pace but have already marked a turning-point in our knowledge regarding AD and amyloid peptides that cannot be the only pharmacological target in the struggle against this devastating illness of human beings.

AUTHOR CONTRIBUTIONS

All of authors (EK, LT, CM, GB, GA, and YK) write manuscript, created figures, and proof final version of this manuscript.

ACKNOWLEDGMENTS

The reported study was funded by RFBR and Moscow region according to the research project No 17-44-500561.

REFERENCES

Ackerman, W. J. (1974). Stupor, bradycardia, hypotension and hypothermia. A presentation of Wernicke's encephalopathy with rapid response to thiamine. *West. J. Med*. 121, 428–429.

Ahlgren, S., Li, G. L., and Olsson, Y. (1996). Accumulation of beta-amyloid precursor protein and ubiquitin in axons after spinal cord trauma in humans: immunohistochemical observations on autopsy material. *Acta Neuropathol.* 92, 49–55. doi: 10.1007/s0040100 50488

Ajmani, R. S., and Rifkind, J. M. (1998). Hemorheological changes during human aging. *Gerontology* 44, 111–120. doi: 10.1159/000021993

Ajmani, R. S., Fleg, J. L., Demehin, A. A., Wright, J. G., O'Connor, F., Heim, J. M., et al. (2003). Oxidative stress and hemorheological changes induced by acute treadmill exercise. *Clin. Hemorheol. Microcirc*. 28, 29–40.

Albin, R. L., and Greenamyre, J. T. (1992). Alternative excitotoxic hypotheses. *Neurology* 42, 733–738. doi: 10.1212/WNL.42.4.733

Alexander, M. P., and LoVerme, S. R. (1980). Aphasia after left hemispheric intracerebral hemorrhage. *Neurology* 30, 1193–1202. doi: 10.1212/WNL.30.11.1193

Alexandrovich, Y. G., Kosenko, E. A., Sinauridze, E. I., Obydennyi, S. I., Kireev, I. I., Ataullakhanov, F. I., et al. (2017). Rapid elimination of blood alcohol using erythrocytes: mathematical modeling and *in vitro* study. *BioMed Res. Int*. 2017:5849593. doi: 10.1155/2017/5849593

Aliev, G. (2011). Oxidative stress induced-metabolic imbalance, mitochondrial failure, and cellular hypoperfusion as primary pathogenetic factors for the development of Alzheimer disease which can be used as a alternate and successful drug treatment strategy: past, present and future. *CNS Neurol. Disord. Drug Targets* 10, 147–148. doi: 10.2174/187152711794480492

Aliev, G., Obrenovich, M. E., Smith, M. A., and Perry, G. (2003a). Hypoperfusion, mitochondria failure, oxidative stress, and Alzheimer disease. *J. Biomed. Biotechnol.* 2003, 162–163. doi: 10.1155/S1110724303305029

Aliev, G., Smith, M. A., de la Torre, J. C., and Perry, G. (2004). Mitochondria as a primary target for vascular hypoperfusion and oxidative stress in Alzheimer's disease. *Mitochondrion* 4, 649–663. doi: 10.1016/j.mito.2004.07.018

Aliev, G., Smith, M. A., Obrenovich, M. E., de la Torre, J. C., and Perry, G. (2003b). Role of vascular hypoperfusion-induced oxidative stress and mitochondria failure in the pathogenesis of Azheimer disease. *Neurotox. Res.* 5, 491–504. doi: 10.1007/BF03033159

Alkire, M. T., Haier, R. J., Barker, S. J., Shah, N. K., Wu, J. C., and Kao, Y. J. (1995). Cerebral metabolism during propofol anesthesia in humans studied with positron emission tomography. *Anesthesiology* 82, 393–403. discussion: 27A. doi: 10.1097/00000542-199502000-00010

Alkire, M. T., Haier, R. J., Shah, N. K., and Anderson, C. T. (1997). Positron emission tomography study of regional cerebral metabolism in humans during isoflurane anesthesia. *Anesthesiology* 86, 549–557. doi: 10.1097/00000542-199703000-00006

Arai, H., Lee, V. M., Hill, W. D., Greenberg, B. D., and Trojanowski, J. Q. (1992). Lewy bodies contain beta-amyloid precursor proteins of Alzheimer's disease. *Brain Res.* 585, 386–390. doi: 10.1016/0006-8993(92)91242-7

Arnsten, A. F., and Goldman-Rakic, P. S. (1998). Noise stress impairs prefrontal cortical cognitive function in monkeys: evidence for a hyperdopaminergic mechanism. *Arch. Gen. Psychiatry* 55, 362–368. doi: 10.1001/archpsyc.55.4.362

Atkins, R. (1875). Half-yearly report on mental disease. *Dublin J. Med. Sci.* 314–331. doi: 10.1007/BF02975691

Atkins, R. (1878). On the morbid histology of the spinal cord in five cases of insanity. *Br. Med. J.* 2, 96–99. doi: 10.1136/bmj.2.916.96

Attems, J., and Jellinger, K. A. (2004). Only cerebral capillary amyloid angiopathy correlates with Alzheimer pathology–a pilot study. *Acta Neuropathol.* 107, 83–90. doi: 10.1007/s00401-003-0796-9

Atwood, C. S., Obrenovich, M. E., Liu, T., Chan, H., Perry, G., Smith, M. A., et al. (2003). Amyloid-beta: a chameleon walking in two worlds: a review of the trophic and toxic properties of amyloid-beta. *Brain Res. Brain Res. Rev.* 43, 1–16. doi: 10.1016/S0165-0173(03)00174-7

Atwood, C. S., Robinson, S. R., and Smith, M. A. (2002). Amyloid-β: redox-metal chelator and antioxidant. *J. Alzheimers Dis.* 4, 203–214. doi: 10.3233/JAD-2002-4310

Auer, R. N., and Siesjö, B. K. (1993). Hypoglycaemia: brain neurochemistry and neuropathology. *Baillieres Clin. Endocrinol. Metab.* 7, 611–625. doi: 10.1016/S0950-351X(05)80210-1

Auer, R., Kalimo, H., Olsson, Y., and Wieloch, T. (1985). The dentate gyrus in hypoglycemia: pathology implicating excitotoxin-mediated neuronal necrosis. *Acta Neuropathol.* 67, 279–288. doi: 10.1007/BF00687813

Avila Rodriguez, M., Garcia-Segura, L. M., Cabezas, R., Torrente, D., Capani, F., Gonzalez, J., et al. (2014). Tibolone protects T98G cells from glucose deprivation. *J. Steroid Biochem. Mol. Biol.* 144(Pt B), 294–303. doi: 10.1016/j.jsbmb.2014.07.009

Baez, E., Guio-Vega, G. P., Echeverria, V., Sandoval-Rueda, D. A., and Barreto, G. E. (2017). 4'-Chlorodiazepam protects mitochondria in T98G astrocyte cell line from glucose deprivation. *Neurotox. Res.* 32, 163–171. doi: 10.1007/s12640-017-9733-x

Baez-Jurado, E., Hidalgo-Lanussa, O., Guio-Vega, G., Ashraf, G. M., Echeverria, V., Aliev, G., et al. (2017a). Conditioned medium of human adipose mesenchymal stem cells increases wound closure and protects human astrocytes following scratch assay *in vitro*. *Mol. Neurobiol.* doi: 10.1007/s12035-017-0771-4. [Epub ahead of print].

Baez-Jurado, E., Vega, G. G., Aliev, G., Tarasov, V. V., Esquinas, P., Echeverria, V., et al. (2017b). Blockade of neuroglobin reduces protection of conditioned medium from human mesenchymal stem cells in human astrocyte model (T98G) under a *scratch* assay. *Mol. Neurobiol.* doi: 10.1007/s12035-017-0481-y. [Epub ahead of print].

Bagnara, G. P., Bonsi, L., Strippoli, P., Bonifazi, F., Tonelli, R., D'Addato, S., et al. (2000). Hemopoiesis in healthy old people and centenarians: well-maintained responsiveness of $CD34^+$ cells to hemopoietic growth factors and remodeling of cytokine network. *J. Gerontol. A Biol. Sci. Med. Sci.* 55, B61–B66. discussion: B67–B70. doi: 10.1093/gerona/55.2.B61

Bailey, T. L., Rivara, C. B., Rocher, A. B., and Hof, P. R. (2004). The nature and effects of cortical microvascular pathology in aging and Alzheimer's disease. *Neurol. Res.* 26, 573–578. doi: 10.1179/016164104225016272

Baker, R. F. (1967). Entry of ferritin into human red cells during hypotonic haemolysis. *Nature* 215, 424–425. doi: 10.1038/215424a0

Balin, B. J., and Appelt, D. M. (2001). Role of infection in Alzheimer's disease. *J. Am. Osteopath. Assoc.* 101, S1–S6.

Bapat, R. D., Supe, A. N., and Sathe, M. J. (1983). Management of small bowel perforation with intra- and post-operative lavages with povidone iodine. (A prospective study). *J. Postgrad. Med.* 29, 29–33.

Barreto, G., White, R. E., Ouyang, Y., Xu, L., and Giffard, R. G. (2011). Astrocytes: targets for neuroprotection in stroke. *Cent. Nerv. Syst. Agents Med. Chem.* 11, 164–173. doi: 10.2174/187152411796011303

Beal, M. F. (1992). Does impairment of energy metabolism result in excitotoxic neuronal death in neurodegenerative illnesses? *Ann. Neurol.* 31, 119–130. doi: 10.1002/ana.410310202

Beal, M. F., Swartz, K. J., Hyman, B. T., Storey, E., Finn, S. F., and Koroshetz, W. (1991). Aminooxyacetic acid results in excitotoxin lesions by a novel indirect mechanism. *J. Neurochem.* 57, 1068–1073. doi: 10.1111/j.1471-4159.1991.tb08258.x

Beutler, E., Meul, A., and Wood, L. A. (1969). Depletion and regeneration of 2,3-diphosphoglyceric acid in stored red blood cells. *Transfusion* 9, 109–115. doi: 10.1111/j.1537-2995.1969.tb05527.x

Bird, T. D. (2005). Genetic factors in Alzheimer's disease. *N. Engl. J. Med.* 352, 862–864. doi: 10.1056/NEJMp058027

Blass, J. P. (2002). Glucose/mitochondria in neurological conditions. *Int. Rev. Neurobiol.* 51, 325–376. doi: 10.1016/S0074-7742(02)51010-2

Blass, J. P. (2003). Cerebrometabolic abnormalities in Alzheimer's disease. *Neurol. Res.* 25, 556–566. doi: 10.1179/016164103101201995

Blass, J. P., and Gibson, G. E. (1991). The role of oxidative abnormalities in the pathophysiology of Alzheimer's disease. *Rev. Neurol.* 147, 513–525.

Blocq, P., and Marinesco, G. (1892). Sur les le'sions et la pathoge'nie del 'epilepsie dite essentielle. *Sem. Me'dical* 12, 445–446.

Bonsignore, A., Fornaini, G., Fantoni, A., Leoncini, G., and Segni, P. (1964). Relationship between age and enzymatic activities in human erythrocytes from normal and fava bean-sensitive subjects. *J. Clin. Invest.* 43, 834–842. doi: 10.1172/JCI104969

Bosman, G. J., Bartholomeus, I. G., de Man, A. J., van Kalmthout, P. J., and de Grip, W. J. (1991). Erythrocyte membrane characteristics indicate abnormal cellular aging in patients with Alzheimer's disease. *Neurobiol. Aging* 12, 13–18. doi: 10.1016/0197-4580(91)90033-G

Braak, H., and Braak, E. (1991). Neuropathological stageing of Alzheimer-related changes. *Acta Neuropathol.* 82, 239–259. doi: 10.1007/BF00308809

Brecher, G., and Bessis, M. (1972). Present status of spiculed red cells and their relationship to the discocyte-echinocyte transformation: a critical review. *Blood* 40, 333–344.

Brewer, G. J., Oelshlegel, F. J., Moore, L. G., and Noble, N. A. (1974). *In vivo* red cell glycolytic control and DPG-ATP levels. *Ann. N. Y. Acad. Sci.* 241, 513–523. doi: 10.1111/j.1749-6632.1974.tb21907.x

Brito-Moreira, J., Paula-Lima, A. C., Bomfim, T. R., Oliveira, F. B., Sepúlveda, F. J., De Mello, F. G., et al. (2011). Aβ oligomers induce glutamate release from hippocampal neurons. *Curr. Alzheimer Res.* 8, 552–562. doi: 10.2174/156720511796391917

Brooks, W. M., Stidley, C. A., Petropoulos, H., Jung, R. E., Weers, D. C., Friedman, S. D., et al. (2000). Metabolic and cognitive response to human traumatic brain injury: a quantitative proton magnetic resonance study. *J. Neurotrauma* 17, 629–640. doi: 10.1089/089771500415382

Bruce, D. G., Davis, W. A., Casey, G. P., Clarnette, R. M., Brown, S. G. A., Jacobs, I. G., et al. (2009). Severe hypoglycaemia and cognitive impairment in older patients with diabetes: the Fremantle diabetes study. *Diabetologia* 52, 1808–1815. doi: 10.1007/s00125-009-1437-1

Bubber, P., Haroutunian, V., Fisch, G., Blass, J. P., and Gibson, G. E. (2005). Mitochondrial abnormalities in Alzheimer brain: mechanistic implications. *Ann. Neurol*. 57, 695–703. doi: 10.1002/ana.20474

Butterworth, R. F. (2003). Hepatic encephalopathy–a serious complication of alcoholic liver disease. *Alcohol Res. Health* 27, 143–145.

Cabezas, R., Avila, M. F., Gonzalez, J., El-Bacha, R. S., and Barreto, G. E. (2015). PDGF-BB protects mitochondria from rotenone in T98G cells. *Neurotox. Res*. 27, 355–367. doi: 10.1007/s12640-014-9509-5

Cabezas, R., El-Bacha, R. S., Gonzalez, J., and Barreto, G. E. (2012). Mitochondrial functions in astrocytes: neuroprotective implications from oxidative damage by rotenone. *Neurosci. Res*. 74, 80–90 doi: 10.1016/j.neures.2012.07.008

Calderón-Garcidueñas, L., Mora-Tiscare-o, A., Ontiveros, E., Gómez-Garza, G., Barragán-Mejía, G., Broadway, J., et al. (2008a). Air pollution, cognitive deficits and brain abnormalities: a pilot study with children and dogs. *Brain Cogn*. 68, 117–127. doi: 10.1016/j.bandc.2008.04.008

Calderón-Garcidueñas, L., Solt, A. C., Henríquez-Roldán, C., Torres-Jardón, R., Nuse, B., Herritt, L., et al. (2008b). Long-term air pollution exposure is associated with neuroinflammation, an altered innate immune response, disruption of the blood-brain barrier, ultrafine particulate deposition, and accumulation of amyloid beta-42 and alpha-synuclein in children and young adults. *Toxicol. Pathol*. 36, 289–310. doi: 10.1177/0192623307313011

Chang, C.-Y., Liang, H.-J., Chow, S.-Y., Chen, S.-M., and Liu, D.-Z. (2007). Hemorheological mechanisms in Alzheimer's disease. *Microcirculation* 14, 627–634. doi: 10.1080/10739680701411056

Chen, X.-H., Siman, R., Iwata, A., Meaney, D. F., Trojanowski, J. Q., and Smith, D. H. (2004). Long-term accumulation of amyloid-β, β-secretase, presenilin-1, and caspase-3 in damaged axons following brain trauma. *Am. J. Pathol*. 165, 357–371. doi: 10.1016/S0002-9440(10)63303-2

Chibber, S., Alexiou, A., Alama, M. N., Barreto, G. E., Aliev, G., and Ashraf, G. M. (2016). A synopsis on the linkage between age-related dementias and vascular disorders. *CNS Neurol. Disord. Drug Targets* 15, 250–258. doi: 10.2174/1871527315666160202121809

Cho, J., King, J. S., Qian, X., Harwood, A. J., and Shears, S. B. (2008). Dephosphorylation of 2,3-bisphosphoglycerate by MIPP expands the regulatory capacity of the Rapoport-Luebering glycolytic shunt. *Proc. Natl. Acad. Sci. U.S.A*. 105, 5998–6003. doi: 10.1073/pnas.0710980105

Cholevas, V., Challa, A., Lapatsanis, P. D., and Andronikou, S. (2008). Changes in red cell phosphate metabolism of preterm and fullterm infants with perinatal problems during their first month of life. *Eur. J. Pediatr*. 167, 211–218. doi: 10.1007/s00431-007-0464-5

Connolly, A. M., and Volpe, J. J. (1990). Clinical features of bilirubin encephalopathy. *Clin. Perinatol*. 17, 371–379.

Conrad, C. D. (2006). What is the functional significance of chronic stress-induced CA3 dendritic retraction within the hippocampus? *Behav. Cogn. Neurosci. Rev*. 5, 41–60. doi: 10.1177/1534582306289043

Conrad, C. D., Galea, L. A., Kuroda, Y., and McEwen, B. S. (1996). Chronic stress impairs rat spatial memory on the Y maze, and this effect is blocked by tianeptine pretreatment. *Behav. Neurosci*. 110, 1321–1334. doi: 10.1037/0735-7044.110.6.1321

Cornish, R., Blumbergs, P. C., Manavis, J., Scott, G., Jones, N. R., and Reilly, P. L. (2000). Topography and severity of axonal injury in human spinal cord trauma using amyloid precursor protein as a marker of axonal injury. *Spine* 25, 1227–1233. doi: 10.1097/00007632-200005150-00005

Dalkara, T., Gursoy-Ozdemir, Y., and Yemisci, M. (2011). Brain microvascular pericytes in health and disease. *Acta Neuropathol*. 122, 1–9. doi: 10.1007/s00401-011-0847-6

Danon, D., Bologna, N. B., and Gavendo, S. (1992). Memory performance of young and old subjects related to their erythrocyte characteristics. *Exp. Gerontol*. 27, 275–285. doi: 10.1016/0531-5565(92)90055-5

De Felice, F. G., Velasco, P. T., Lambert, M. P., Viola, K., Fernandez, S. J., Ferreira, S. T., et al. (2007). Aβ oligomers induce neuronal oxidative stress through an N-methyl-D-aspartate receptor-dependent mechanism that is blocked by the Alzheimer drug memantine. *J. Biol. Chem*. 282, 11590–11601. doi: 10.1074/jbc.M607483200

De Felice, F. G., Wu, D., Lambert, M. P., Fernandez, S. J., Velasco, P. T., Lacor, P. N., et al. (2008). Alzheimer's disease-type neuronal tau hyperphosphorylation induced by Aβ oligomers. *Neurobiol. Aging* 29, 1334–1347. doi: 10.1016/j.neurobiolaging.2007.02.029

De Jong, G. I., Farkas, E., Stienstra, C. M., Plass, J. R., Keijser, J. N., de la Torre, J. C., et al. (1999). Cerebral hypoperfusion yields capillary damage in the hippocampal CA1 area that correlates with spatial memory impairment. *Neuroscience* 91, 203–210. doi: 10.1016/S0306-4522(98)00659-9

de la Torre, J. C. (2000a). Cerebral hypoperfusion, capillary degeneration, and development of Alzheimer disease. *Alzheimer Dis. Assoc. Disord*. 14(Suppl. 1), S72–S81. doi: 10.1097/00002093-200000001-00012

de la Torre, J. C. (2000b). Impaired cerebromicrovascular perfusion. Summary of evidence in support of its causality in Alzheimer's disease. *Ann. N. Y. Acad. Sci*. 924, 136–152. doi: 10.1111/j.1749-6632.2000.tb05572.x

de la Torre, J. C. (2002a). Alzheimer disease as a vascular disorder: nosological evidence. *Stroke* 33, 1152–1162. doi: 10.1161/01.STR.0000014421.15948.67

de la Torre, J. C. (2002b). Alzheimer's disease: how does it start? *J. Alzheimers Dis*. 4, 497–512. doi: 10.3233/JAD-2002-4606

de la Torre, J. C. (2017). Are major dementias triggered by poor blood flow to the brain? Theoretical considerations. *J. Alzheimers Dis*. 57, 353–371. doi: 10.3233/JAD-161266

de la Torre, J. C., and Mussivand, T. (1993). Can disturbed brain microcirculation cause Alzheimer's disease? *Neurol. Res*. 15, 146–153. doi: 10.1080/01616412.1993.11740127

de la Torre, J. C., and Stefano, G. B. (2000). Evidence that Alzheimer's disease is a microvascular disorder: the role of constitutive nitric oxide. *Brain Res. Brain Res. Rev*. 34, 119–136. doi: 10.1016/S0165-0173(00)00043-6

Demuro, A., Mina, E., Kayed, R., Milton, S. C., Parker, I., and Glabe, C. G. (2005). Calcium dysregulation and membrane disruption as a ubiquitous neurotoxic mechanism of soluble amyloid oligomers. *J. Biol. Chem*. 280, 17294–17300. doi: 10.1074/jbc.M500997200

Dodds, C., and Allison, J. (1998). Postoperative cognitive deficit in the elderly surgical patient. *Br. J. Anaesth*. 81, 449–462.

Dong, Y., Zhang, G., Zhang, B., Moir, R. D., Xia, W., Marcantonio, E. R., et al. (2009). The common inhalational anesthetic sevoflurane induces apoptosis and increases beta-amyloid protein levels. *Arch. Neurol*. 66, 620–631. doi: 10.1001/archneurol.2009.48

Duhm, J. (1971). Effects of 2,3-diphosphoglycerate and other organic phosphate compounds on oxygen affinity and intracellular pH of human erythrocytes. *Pflugers Arch*. 326, 341–356. doi: 10.1007/BF00586998

Farkas, E., and Luiten, P. G. (2001). Cerebral microvascular pathology in aging and Alzheimer's disease. *Prog. Neurobiol*. 64, 575–611. doi: 10.1016/S0301-0082(00)00068-X

Fita, I. G., Enciu, A. M., and Stanoiu, B. P. (2011). New insights on Alzheimer's disease diagnostic. *Rom. J. Morphol. Embryol*. 52, 975–979.

Funato, H., Yoshimura, M., Kusui, K., Tamaoka, A., Ishikawa, K., Ohkoshi, N., et al. (1998). Quantitation of amyloid beta-protein (A beta) in the cortex during aging and in Alzheimer's disease. *Am. J. Pathol*. 152, 1633–1640.

Gabuzda, D., Busciglio, J., Chen, L. B., Matsudaira, P., and Yankner, B. A. (1994). Inhibition of energy metabolism alters the processing of amyloid precursor protein and induces a potentially amyloidogenic derivative. *J. Biol. Chem*. 269, 13623–13628.

Giannakopoulos, P., Herrmann, F. R., Bussière, T., Bouras, C., Kövari, E., Perl, D. P., et al. (2003). Tangle and neuron numbers, but not amyloid load, predict cognitive status in Alzheimer's disease. *Neurology* 60, 1495–1500. doi: 10.1212/01.WNL.0000063311.58879.01

Gibson, G. E., and Huang, H.-M. (2002). Oxidative processes in the brain and non-neuronal tissues as biomarkers of Alzheimer's disease. *Front. Biosci. J. Virtual Libr*. 7, d1007–d1015. doi: 10.2741/gibson

Gibson, G. E., Jope, R., and Blass, J. P. (1975). Decreased synthesis of acetylcholine accompanying impaired oxidation of pyruvic acid in rat brain minces. *Biochem. J*. 148, 17–23. doi: 10.1042/bj1480017

Gibson, G. E., Pulsinelli, W., Blass, J. P., and Duffy, T. E. (1981). Brain dysfunction in mild to moderate hypoxia. *Am. J. Med*. 70, 1247–1254. doi: 10.1016/0002-9343(81)90834-2

Glenner, G. G., and Wong, C. W. (1984). Alzheimer's disease and Down's syndrome: sharing of a unique cerebrovascular amyloid fibril protein. *Biochem. Biophys. Res. Commun*. 122, 1131–1135. doi: 10.1016/0006-291X(84)91209-9

Globerson, A. (1999). Hematopoietic stem cells and aging. *Exp. Gerontol*. 34, 137–146. doi: 10.1016/S0531-5565(98)00069-2

Godfrin, Y., Horand, F., Franco, R., Dufour, E., Kosenko, E., Bax, B. E., et al. (2012). International seminar on the red blood cells as vehicles for drugs. *Expert Opin. Biol. Ther.* 12, 127–133. doi: 10.1517/14712598.2012.631909

Gong, Y., Chang, L., Viola, K. L., Lacor, P. N., Lambert, M. P., Finch, C. E., et al. (2003). Alzheimer's disease-affected brain: presence of oligomeric Aβ ligands (ADDLs) suggests a molecular basis for reversible memory loss. *Proc. Natl. Acad. Sci. U.S.A.* 100, 10417–10422. doi: 10.1073/pnas.1834302100

Gonzalez, J., Jurado-Coronel, J. C., Avila, M. F., Sabogal, A., Capani, F., and Barreto, G. E. (2015). NMDARs in neurological diseases: a potential therapeutic target. *Int. J. Neurosci.* 125, 315–327. doi: 10.3109/00207454.2014.940941

Gonzalez-Reyes, R. E., Aliev, G., Avila-Rodrigues, M., and Barreto, G. E. (2016). Alterations in glucose metabolism on cognition: a possible link between diabetes and dementia. *Curr. Pharm. Des.* 22, 812–818. doi: 10.2174/1381612822666151209152013

Goodall, H. B., Reid, A. H., Findlay, D. J., Hind, C., Kay, J., and Coghill, G. (1994). Irregular distortion of the erythrocytes (acanthocytes, spur cells) in senile dementia. *Dis. Markers* 12, 23–41. doi: 10.1155/1994/493810

Gov, N. S., and Safran, S. A. (2005). Red blood cell membrane fluctuations and shape controlled by ATP-induced cytoskeletal defects. *Biophys. J.* 88, 1859–1874. doi: 10.1529/biophysj.104.045328

Grammas, P., Yamada, M., and Zlokovic, B. (2002). The cerebromicrovasculature: a key player in the pathogenesis of Alzheimer's disease. *J. Alzheimers Dis.* 4, 217–223. doi: 10.3233/JAD-2002-4311

Guillozet, A. L., Weintraub, S., Mash, D. C., and Mesulam, M. M. (2003). Neurofibrillary tangles, amyloid, and memory in aging and mild cognitive impairment. *Arch. Neurol.* 60, 729–736. doi: 10.1001/archneur.60.5.729

Gyure, K. A., Durham, R., Stewart, W. F., Smialek, J. E., and Troncoso, J. C. (2001). Intraneuronal abeta-amyloid precedes development of amyloid plaques in down syndrome. *Arch. Pathol. Lab. Med.* 125, 489–492. doi: 10.1043/0003-9985(2001)125<0489:IAAPDO>2.0.CO;2

Hachinski, V., and Munoz, D. G. (1997). Cerebrovascular pathology in Alzheimer's disease: cause, effect or epiphenomenon? *Ann. N. Y. Acad. Sci.* 826, 1–6. doi: 10.1111/j.1749-6632.1997.tb48456.x

Hackett, M. L., and Anderson, C. S. (2000). Health outcomes 1 year after subarachnoid hemorrhage: an international population-based study. The Australian cooperative research on subarachnoid hemorrhage study Group. *Neurology* 55, 658–662. doi: 10.1212/WNL.55.5.658

Hamasaki, N., Ideguchi, H., and Ikehara, Y. (1981). Regeneration of 2,3-bisphosphoglycerate and ATP in stored erythrocytes by phosphoenolpyruvate: a new preservative for blood storage. *Transfusion* 21, 391–396. doi: 10.1046/j.1537-2995.1981.21481275994.x

Hamberger, A. C., Chiang, G. H., Nylén, E. S., Scheff, S. W., and Cotman, C. W. (1979). Glutamate as a CNS transmitter. I. Evaluation of glucose and glutamine as precursors for the synthesis of preferentially released glutamate. *Brain Res.* 168, 513–530. doi: 10.1016/0006-8993(79)90306-8

Hamberger, A., Huang, Y.-L., Zhu, H., Bao, F., Ding, M., Blennow, K., et al. (2003). Redistribution of neurofilaments and accumulation of β-amyloid protein after brain injury by rotational acceleration of the head. *J. Neurotrauma* 20, 169–178. doi: 10.1089/08977150360547080

Hardy, J., and Selkoe, D. J. (2002). The amyloid hypothesis of Alzheimer's disease: progress and problems on the road to therapeutics. *Science* 297, 353–356. doi: 10.1126/science.1072994

Hardy, J. A., and Higgins, G. A. (1992). Alzheimer's disease: the amyloid cascade hypothesis. *Science* 256, 184–185. doi: 10.1126/science.1566067

Hodes, J. E., Soncrant, T. T., Larson, D. M., Carlson, S. G., and Rapoport, S. I. (1985). Selective changes in local cerebral glucose utilization induced by phenobarbital in the rat. *Anesthesiology* 63, 633–639. doi: 10.1097/00000542-198512000-00013

Hoyer, S. (1996). Oxidative metabolism deficiencies in brains of patients with Alzheimer's disease. *Acta Neurol. Scand. Suppl.* 165, 18–24. doi: 10.1111/j.1600-0404.1996.tb05868.x

Hoyer, S. (2000). Brain glucose and energy metabolism abnormalities in sporadic Alzheimer disease. Causes and consequences: an update. *Exp. Gerontol.* 35, 1363–1372. doi: 10.1016/S0531-5565(00)00156-X

Hoyer, S., Oesterreich, K., and Wagner, O. (1988). Glucose metabolism as the site of the primary abnormality in early-onset dementia of Alzheimer type? *J. Neurol.* 235, 143–148. doi: 10.1007/BF00314304

Hsia, A. Y., Masliah, E., McConlogue, L., Yu, G. Q., Tatsuno, G., Hu, K., et al. (1999). Plaque-independent disruption of neural circuits in Alzheimer's disease mouse models. *Proc. Natl. Acad. Sci. U.S.A.* 96, 3228–3233. doi: 10.1073/pnas.96.6.3228

Jack, C. R., Lowe, V. J., Weigand, S. D., Wiste, H. J., Senjem, M. L., Knopman, D. S., et al. (2009). Serial PIB and MRI in normal, mild cognitive impairment and Alzheimer's disease: implications for sequence of pathological events in Alzheimer's disease. *Brain J. Neurol.* 132, 1355–1365. doi: 10.1093/brain/awp062

Joachim, C. L., Mori, H., and Selkoe, D. J. (1989). Amyloid beta-protein deposition in tissues other than brain in Alzheimer's disease. *Nature* 341, 226–230. doi: 10.1038/341226a0

Jobst, K. A., Smith, A. D., Barker, C. S., Wear, A., King, E. M., Smith, A., et al. (1992). Association of atrophy of the medial temporal lobe with reduced blood flow in the posterior parietotemporal cortex in patients with a clinical and pathological diagnosis of Alzheimer's disease. *J. Neurol. Neurosurg. Psychiatry* 55, 190–194. doi: 10.1136/jnnp.55.3.190

Johnson, R. M., Goyette, G., Ravindranath, Y., and Ho, Y.-S. (2005). Hemoglobin autoxidation and regulation of endogenous H_2O_2 levels in erythrocytes. *Free Radic. Biol. Med.* 39, 1407–1417. doi: 10.1016/j.freeradbiomed.2005.07.002

Jordan, B. D. (2000). Chronic traumatic brain injury associated with boxing. *Semin. Neurol.* 20, 179–185. doi: 10.1055/s-2000-9826

Kalaria, R. N., and Harik, S. I. (1989). Reduced glucose transporter at the blood-brain barrier and in cerebral cortex in Alzheimer disease. *J. Neurochem.* 53, 1083–1088. doi: 10.1111/j.1471-4159.1989.tb07399.x

Kalaria, R. N., and Hedera, P. (1995). Differential degeneration of the cerebral microvasculature in Alzheimer's disease. *Neuroreport* 6, 477–480. doi: 10.1097/00001756-199502000-00018

Kamal, A., Almenar-Queralt, A., LeBlanc, J. F., Roberts, E. A., and Goldstein, L. S. (2001). Kinesin-mediated axonal transport of a membrane compartment containing beta-secretase and presenilin-1 requires APP. *Nature* 414, 643–648. doi: 10.1038/414643a

Kamenetz, F., Tomita, T., Hsieh, H., Seabrook, G., Borchelt, D., Iwatsubo, T., et al. (2003). APP processing and synaptic function. *Neuron* 37, 925–937. doi: 10.1016/S0896-6273(03)00124-7

Kaminsky, Y., Poghosyan, A., Tikhonova, L., Palacios, H. H., Kamal, M. A., Kosenko, E., et al. (2012). Glycolytic and proteolytic metabolism in erythrocytes from elderly and demented patients. *Am. J. Neuroprotect. Neuroregeneration* 4, 1–5. doi: 10.1166/ajnn.2012.1039

Kaminsky, Y. G., and Kosenko, E. A. (2012). Argocytes containing enzyme nanoparticles reduce toxic concentrations of arginine in the blood. *Bull. Exp. Biol. Med.* 153, 406–408. doi: 10.1007/s10517-012-1727-3

Kaminsky, Y. G., Marlatt, M. W., Smith, M. A., and Kosenko, E. A. (2010). Subcellular and metabolic examination of amyloid-β peptides in Alzheimer disease pathogenesis: evidence for Aβ (25-35). *Exp. Neurol.* 221, 26–37. doi: 10.1016/j.expneurol.2009.09.005

Kaminsky, Y. G., Reddy, V. P., Ashraf, G. M., Ahmad, A., Benberin, V. V., Kosenko, E. A., et al. (2013). Age-related defects in erythrocyte 2,3-diphosphoglycerate metabolism in dementia. *Aging Dis.* 4, 244–255. doi: 10.14336/AD.2013.0400244

Kang, J.-E., Lim, M. M., Bateman, R. J., Lee, J. J., Smyth, L. P., Cirrito, J. R., et al. (2009). Amyloid-β dynamics are regulated by orexin and the sleep-wake cycle. *Science* 326, 1005–1007. doi: 10.1126/science.1180962

Kasa, P., Papp, H., and Pakaski, M. (2001). Presenilin-1 and its N-terminal and C-terminal fragments are transported in the sciatic nerve of rat. *Brain Res.* 909, 159–169. doi: 10.1016/S0006-8993(01)02679-8

Kiefmann, R., Rifkind, J. M., Nagababu, E., and Bhattacharya, J. (2008). Red blood cells induce hypoxic lung inflammation. *Blood* 111, 5205–5214. doi: 10.1182/blood-2007-09-113902

Kiko, T., Nakagawa, K., Satoh, A., Tsuduki, T., Furukawa, K., Arai, H., et al. (2012). Amyloid β levels in human red blood cells. *PLoS ONE* 7:e49620. doi: 10.1371/journal.pone.0049620

Klein, W. L., Krafft, G. A., and Finch, C. E. (2001). Targeting small Abeta oligomers: the solution to an Alzheimer's disease conundrum? *Trends Neurosci.* 24, 219–224. doi: 10.1016/S0166-2236(00)01749-5

Klepper, J., and Voit, T. (2002). Facilitated glucose transporter protein type 1 (GLUT1) deficiency syndrome: impaired glucose transport into brain– a review. *Eur. J. Pediatr.* 161, 295–304. doi: 10.1007/s00431-002-0939-3

Kontush, A., Berndt, C., Weber, W., Akopyan, V., Arlt, S., Schippling, S., et al. (2001). Amyloid-β is an antioxidant for lipoproteins in cerebrospinal fluid and plasma. *Free Radic. Biol. Med.* 30, 119–128. doi: 10.1016/S0891-5849(00)00458-5

Koo, E. H., Park, L., and Selkoe, D. J. (1993). Amyloid beta-protein as a substrate interacts with extracellular matrix to promote neurite outgrowth. *Proc. Natl. Acad. Sci. U.S.A.* 90, 4748–4752. doi: 10.1073/pnas.90.10.4748

Korol, D. L., and Gold, P. E. (1998). Glucose, memory, and aging. *Am. J. Clin. Nutr.* 67, 764S—771S.

Kosenko, E., Kaminsky, Y., Grau, E., Miñana„ M. D., Marcaida, G., Grisolía, S., et al. (1994). Brain ATP depletion induced by acute ammonia intoxication in rats is mediated by activation of the NMDA receptor and Na^+,K^+-ATPase. *J. Neurochem.* 63, 2172–2178. doi: 10.1046/j.1471-4159.1994.63062172.x

Kosenko, E. A., Aliev, G., and Kaminsky, Y. G. (2016). Relationship between chronic disturbance of 2,3-diphosphoglycerate metabolism in erythrocytes and Alzheimer disease. *CNS Neurol. Disord. Drug Targets* 15, 113–123. doi: 10.2174/1871527314666150821103444

Kosenko, E. A., Aliev, G., Tikhonova, L. A., Li, Y., Poghosyan, A. C., and Kaminsky, Y. G. (2012). Antioxidant status and energy state of erythrocytes in Alzheimer dementia: probing for markers. *CNS Neurol. Disord. Drug Targets* 11, 926–932. doi: 10.2174/1871527311201070926

Kosenko, E. A., Solomadin, I. N., and Kaminskii, I. G. (2009). Effect of the beta-amyloid peptide Abeta25-35 and fullerene C60 on the activity of enzymes in erythrocytes. *Bioorg. Khim.* 35, 172–177.

Kosenko, E. A., Solomadin, I. N., Marov, N. V., Venediktova, N. I., Pogosian, A. S., and Kaminskĭ, I. G. (2008a). [Role of glycolysis and antioxidant enzymes in the toxicity of amyloid beta peptide Aβ25-35 to erythrocytes]. *Bioorg. Khim.* 34, 654–660.

Kosenko, E. A., Venediktova, N. I., Kudryavtsev, A. A., Ataullakhanov, F. I., Kaminsky, Y. G., Felipo, V., et al. (2008b). Encapsulation of glutamine synthetase in mouse erythrocytes: a new procedure for ammonia detoxification. *Biochem. Cell Biol. Biochim. Biol. Cell.* 86, 469–476. doi: 10.1139/O08-134

Kowluru, R., Bitensky, M. W., Kowluru, A., Dembo, M., Keaton, P. A., and Buican, T. (1989). Reversible sodium pump defect and swelling in the diabetic rat erythrocyte: effects on filterability and implications for microangiopathy. *Proc. Natl. Acad. Sci. U.S.A.* 86, 3327–3331. doi: 10.1073/pnas.86.9.3327

Kucukatay, V., Erken, G., Bor-Kucukatay, M., and Kocamaz, E. (2009). Effect of sulfite treatment on erythrocyte deformability in young and aged rats. *Toxicol. Mech. Methods* 19, 19–23. doi: 10.1080/15376510802175788

Kuo, Y. M., Emmerling, M. R., Vigo-Pelfrey, C., Kasunic, T. C., Kirkpatrick, J. B., Murdoch, G. H., et al. (1996). Water-soluble Aβ (N-40, N-42) oligomers in normal and Alzheimer disease brains. *J. Biol. Chem.* 271, 4077–4081. doi: 10.1074/jbc.271.8.4077

Kuo, Y. M., Kokjohn, T. A., Kalback, W., Luehrs, D., Galasko, D. R., Chevallier, N., et al. (2000). Amyloid-β peptides interact with plasma proteins and erythrocytes: implications for their quantitation in plasma. *Biochem. Biophys. Res. Commun.* 268, 750–756. doi: 10.1006/bbrc.2000.2222

Kuypers, F. A., Scott, M. D., Schott, M. A., Lubin, B., and Chiu, D. T. (1990). Use of ektacytometry to determine red cell susceptibility to oxidative stress. *J. Lab. Clin. Med.* 116, 535–545.

Kyles, A. E., Waterman, A. E., Livingston, A., and Vetmed, B. (1993). Antinociceptive effects of combining low doses of neuroleptic drugs and fentanyl in sheep. *Am. J. Vet. Res.* 54, 1483–1488.

Lambert, M. P., Barlow, A. K., Chromy, B. A., Edwards, C., Freed, R., Liosatos, M., et al. (1998). Diffusible, nonfibrillar ligands derived from Aβ1-42 are potent central nervous system neurotoxins. *Proc. Natl. Acad. Sci. U.S.A.* 95, 6448–6453. doi: 10.1073/pnas.95.11.6448

Lan, J., Liu, J., Zhao, Z., Xue, R., Zhang, N., Zhang, P., et al. (2015). The peripheral blood of Aβ binding RBC as a biomarker for diagnosis of Alzheimer's disease. *Age Ageing* 44, 458–464. doi: 10.1093/ageing/afv009

Lang, E., Pozdeev, V. I., Xu, H. C., Shinde, P. V., Behnke, K., Hamdam, J. M., et al. (2016). Storage of erythrocytes induces suicidal erythrocyte death. *Cell. Physiol. Biochem.* 39, 668–676. doi: 10.1159/000445657

Lang, F., Jilani, K., and Lang, E. (2015). Therapeutic potential of manipulating suicidal erythrocyte death. *Expert Opin. Ther. Targets* 19, 1219–1227. doi: 10.1517/14728222.2015.1051306

Larsen, V. H., Waldau, T., Gravesen, H., and Siggaard-Andersen, O. (1996). Erythrocyte 2,3-diphosphoglycerate depletion associated with hypophosphatemia detected by routine arterial blood gas analysis. *Scand. J. Clin. Lab. Investig. Suppl.* 224, 83–87. doi: 10.3109/00365519609088626

Lee, H.-G., Casadesus, G., Zhu, X., Takeda, A., Perry, G., and Smith, M. A. (2004). Challenging the amyloid cascade hypothesis: senile plaques and amyloid-beta as protective adaptations to Alzheimer disease. *Ann. N.Y. Acad. Sci.* 1019, 1–4. doi: 10.1196/annals.1297.001

Li, G. L., Farooque, M., Holtz, A., and Olsson, Y. (1995). Changes of β-amyloid precursor protein after compression trauma to the spinal cord: an experimental study in the rat using immunohistochemistry. *J. Neurotrauma* 12, 269–277. doi: 10.1089/neu.1995.12.269

Liberski, P. P. (2004). Amyloid plaques in transmissible spongiform encephalopathies (prion diseases). *Folia Neuropathol.* 42(Suppl. B), 109–119.

Llansola, M., Rodrigo, R., Monfort, P., Montoliu, C., Kosenko, E., Cauli, O., et al. (2007). NMDA receptors in hyperammonemia and hepatic encephalopathy. *Metab. Brain Dis.* 22, 321–335. doi: 10.1007/s11011-007-9067-0

Lue, L. F., Kuo, Y. M., Roher, A. E., Brachova, L., Shen, Y., Sue, L., et al. (1999). Soluble amyloid β peptide concentration as a predictor of synaptic change in Alzheimer's disease. *Am. J. Pathol.* 155, 853–862. doi: 10.1016/S0002-9440(10)65184-X

Luo, Y., Sunderland, T., Roth, G. S., and Wolozin, B. (1996). Physiological levels of β-amyloid peptide promote PC12 cell proliferation. *Neurosci. Lett.* 217, 125–128. doi: 10.1016/0304-3940(96)13087-1

MacDonald, R. (1977). Red cell 2,3-diphosphoglycerate and oxygen affinity. *Anaesthesia* 32, 544–553. doi: 10.1111/j.1365-2044.1977.tb10002.x

Manikandan, S., Padma, M. K., Srikumar, R., Jeya Parthasarathy, N., Muthuvel, A., and Sheela Devi, R. (2006). Effects of chronic noise stress on spatial memory of rats in relation to neuronal dendritic alteration and free radical-imbalance in hippocampus and medial prefrontal cortex. *Neurosci. Lett.* 399, 17–22. doi: 10.1016/j.neulet.2006.01.037

Mann, D. M., Jones, D., South, P. W., Snowden, J. S., and Neary, D. (1992). Deposition of amyloid beta protein in non-Alzheimer dementias: evidence for a neuronal origin of parenchymal deposits of β protein in neurodegenerative disease. *Acta Neuropathol.* 83, 415–419. doi: 10.1007/BF00713534

Marcus, D. L., and Freedman, M. L. (1997). Decreased brain glucose metabolism in microvessels from patients with Alzheimer's disease. *Ann. N. Y. Acad. Sci.* 826, 248–253. doi: 10.1111/j.1749-6632.1997.tb48476.x

Marcus, D. L., de Leon, M. J., Goldman, J., Logan, J., Christman, D. R., Wolf, A. P., et al. (1989). Altered glucose metabolism in microvessels from patients with Alzheimer's disease. *Ann. Neurol.* 26, 91–94. doi: 10.1002/ana.410260114

Martindale, J. L., Senecal, E. L., Obermeyer, Z., Nadel, E. S., and Brown, D. F. M. (2010). Altered mental status and hypothermia. *J. Emerg. Med.* 39, 491–496. doi: 10.1016/j.jemermed.2010.03.021

Martin-Jiménez, C. A., Gáitan-Vaca, D. M., Echeverria, V., González, J., and Barreto, G. E. (2017a). Relationship between obesity, alzheimer's disease, and Parkinson's disease: an astrocentric view. *Mol. Neurobiol.* 54, 7096–7115. doi: 10.1007/s12035-016-0193-8

Martin-Jiménez, C. A., García-Vega, Á., Cabezas, R., Aliev, G., Echeverria, V., González, J., et al. (2017b). Astrocytes and endoplasmic reticulum stress: a bridge between obesity and neurodegenerative diseases. *Prog. Neurobiol.* 158, 45–68. doi: 10.1016/j.pneurobio.2017.08.001

Masuda, J., Tanaka, K., Ueda, K., and Omae, T. (1988). Autopsy study of incidence and distribution of cerebral amyloid angiopathy in Hisayama, Japan. *Stroke* 19, 205–210. doi: 10.1161/01.STR.19.2.205

Matsumoto, Y. (1995). [The function of red blood cells during experimental hemorrhagic and endotoxic shock]. *Masui* 44, 342–348.

Mattson, M. P., Begley, J. G., Mark, R. J., and Furukawa, K. (1997). Aβ25-35 induces rapid lysis of red blood cells: contrast with Abeta1-42 and examination of underlying mechanisms. *Brain Res.* 771, 147–153. doi: 10.1016/S0006-8993(97)00824-X

Mattson, M. P., Cheng, B., Davis, D., Bryant, K., Lieberburg, I., and Rydel, R. E. (1992). beta-Amyloid peptides destabilize calcium homeostasis and render human cortical neurons vulnerable to excitotoxicity. *J. Neurosci. Off. J. Soc. Neurosci.* 12, 376–389.

McCully, K., Chance, B., and Giger, U. (1999). *In vivo* determination of altered hemoglobin saturation in dogs with M-type phosphofructokinase deficiency. *Muscle Nerve* 22, 621–627. doi: 10.1002/(SICI)1097-4598(199905)22:5<621::AID-MUS11>3.0.CO;2-D

McGeer, E. G., McGeer, P. L., Harrop, R., Akiyama, H., and Kamo, H. (1990). Correlations of regional postmortem enzyme activities with premortem local glucose metabolic rates in Alzheimer's disease. *J. Neurosci. Res.* 27, 612–619. doi: 10.1002/jnr.490270422

McLean, C. A., Cherny, R. A., Fraser, F. W., Fuller, S. J., Smith, M. J., Vbeyreuther, K., et al. (1999). Soluble pool of Aβ amyloid as a determinant of severity of neurodegeneration in Alzheimer's disease. *Ann. Neurol.* 46, 860–866. doi: 10.1002/1531-8249(199912)46:6<860::AID-ANA8>3.0.CO;2-M

Meier-Ruge, W., and Bertoni-Freddari, C. (1996). The significance of glucose turnover in the brain in the pathogenetic mechanisms of Alzheimer's disease. *Rev. Neurosci.* 7, 1–19. doi: 10.1515/REVNEURO.1996.7.1.1

Meier-Ruge, W., Iwangoff, P., and Reichlmeier, K. (1984). Neurochemical enzyme changes in Alzheimer's and Pick's disease. *Arch. Gerontol. Geriatr.* 3, 161–165. doi: 10.1016/0167-4943(84)90007-4

Michaud, J.-P., Bellavance, M.-A., Préfontaine, P., and Rivest, S. (2013). Real-time *in vivo* imaging reveals the ability of monocytes to clear vascular amyloid β. *Cell Rep.* 5, 646–653. doi: 10.1016/j.celrep.2013.10.010

Miklossy, J., Kis, A., Radenovic, A., Miller, L., Forro, L., Martins, R., et al. (2006). Beta-amyloid deposition and Alzheimer's type changes induced by Borrelia spirochetes. *Neurobiol. Aging* 27, 228–236. doi: 10.1016/j.neurobiolaging.2005.01.018

Mohanty, J. G., Eckley, D. M., Williamson, J. D., Launer, L. J., and Rifkind, J. M. (2008). Do red blood cell-beta-amyloid interactions alter oxygen delivery in Alzheimer's disease? *Adv. Exp. Med. Biol.* 614, 29–35. doi: 10.1007/978-0-387-74911-2_4

Moore, G. L., Ledford, M. E., and Brummell, M. R. (1981). Improved red blood cell storage using optional additive systems (OAS) containing adenine, glucose and ascorbate-2-phosphate. *Transfusion* 21, 723–731. doi: 10.1046/j.1537-2995.1981.21682085764.x

Moreira, P. I., Zhu, X., Liu, Q., Honda, K., Siedlak, S. L., Harris, P. L., et al. (2006). Compensatory responses induced by oxidative stress in Alzheimer disease. *Biol. Res.* 39, 7–13. doi: 10.4067/S0716-97602006000100002

Morishima-Kawashima, M., Oshima, N., Ogata, H., Yamaguchi, H., Yoshimura, M., Sugihara, S., et al. (2000). Effect of apolipoprotein E allele epsilon4 on the initial phase of amyloid β-protein accumulation in the human brain. *Am. J. Pathol.* 157, 2093–2099. doi: 10.1016/S0002-9440(10)64847-X

Morris, C. R., Suh, J. H., Hagar, W., Larkin, S., Bland, D. A., Steinberg, M. H., et al. (2008). Erythrocyte glutamine depletion, altered redox environment, and pulmonary hypertension in sickle cell disease. *Blood* 111, 402–410. doi: 10.1182/blood-2007-04-081703

Murr, L. E., Soto, K. F., Garza, K. M., Guerrero, P. A., Martinez, F., Esquivel, E. V., et al. (2006). Combustion-generated nanoparticulates in the El Paso, TX, USA/Juarez, Mexico Metroplex: their comparative characterization and potential for adverse health effects. *Int. J. Environ. Res. Public. Health* 3, 48–66. doi: 10.3390/ijerph2006030007

Nakamura, J., Koh, N., Sakakibara, F., Hamada, Y., Wakao, T., Hara, T., et al. (1995). Polyol pathway, 2,3-diphosphoglycerate in erythrocytes and diabetic neuropathy in rats. *Eur. J. Pharmacol.* 294, 207–214. doi: 10.1016/0014-2999(95)00531-5

Ni, Y., Zhao, X., Bao, G., Zou, L., Teng, L., Wang, Z., et al. (2006). Activation of β2-adrenergic receptor stimulates gamma-secretase activity and accelerates amyloid plaque formation. *Nat. Med.* 12, 1390–1396. doi: 10.1038/nm1485

Nicolay, J. P., Gatz, S., Liebig, G., Gulbins, E., and Lang, F. (2007). Amyloid induced suicidal erythrocyte death. *Cell. Physiol. Biochem.* 19, 175–184. doi: 10.1159/000099205

Novelli, A., Reilly, J. A., Lysko, P. G., and Henneberry, R. C. (1988). Glutamate becomes neurotoxic via the N-methyl-D-aspartate receptor when intracellular energy levels are reduced. *Brain Res.* 451, 205–212. doi: 10.1016/0006-8993(88)90765-2

Nunomura, A., Perry, G., Pappolla, M. A., Friedland, R. P., Hirai, K., Chiba, S., et al. (2000). Neuronal oxidative stress precedes amyloid-β deposition in down syndrome. *J. Neuropathol. Exp. Neurol.* 59, 1011–1017. doi: 10.1093/jnen/59.11.1011

Omalu, B. I., DeKosky, S. T., Minster, R. L., Kamboh, M. I., Hamilton, R. L., and Wecht, C. H. (2005). Chronic traumatic encephalopathy in a National Football League player. *Neurosurgery* 57, 128–134. discussion: 128–134. doi: 10.1227/01.NEU.0000163407.92769.ED

Pankowska, E., Szypowska, A., Wysocka, M., and Lipka, M. (2005). [The role of 2,3-DPG in nerve conduction of children with type 1 diabetes]. *Endokrynol. Diabetol. Chor. Przemiany Materii Wieku Rozw.* 11, 207–210.

Papassotiriou, I., Kister, J., Griffon, N., Abraham, D. J., Kanavakis, E., Traeger-Synodinos, J., et al. (1998). Synthesized allosteric effectors of the hemoglobin molecule: a possible mechanism for improved erythrocyte oxygen release capability in hemoglobinopathy H disease. *Exp. Hematol.* 26, 922–926.

Papp, H., Pakaski, M., and Kasa, P. (2002). Presenilin-1 and the amyloid precursor protein are transported bidirectionally in the sciatic nerve of adult rat. *Neurochem. Int.* 41, 429–435. doi: 10.1016/S0197-0186(02)00014-1

Parikh, S. S., and Chung, F. (1995). Postoperative delirium in the elderly. *Anesth. Analg.* 80, 1223–1232.

Pascual, J. M., Wang, D., Lecumberri, B., Yang, H., Mao, X., Yang, R., et al. (2004). GLUT1 deficiency and other glucose transporter diseases. *Eur. J. Endocrinol.* 150, 627–633. doi: 10.1530/eje.0.1500627

Perry, G., Nunomura, A., Raina, A. K., Aliev, G., Siedlak, S. L., Harris, P. L. R., et al. (2003). A metabolic basis for Alzheimer disease. *Neurochem. Res.* 28, 1549–1552. doi: 10.1023/A:1025678510480

Perry, G., Smith, M. A., McCann, C. E., Siedlak, S. L., Jones, P. K., and Friedland, R. P. (1998). Cerebrovascular muscle atrophy is a feature of Alzheimer's disease. *Brain Res.* 791, 63–66. doi: 10.1016/S0006-8993(98)00006-7

Perry, R. T., Gearhart, D. A., Wiener, H. W., Harrell, L. E., Barton, J. C., Kutlar, A., et al. (2008). Hemoglobin binding to A β and HBG2 SNP association suggest a role in Alzheimer's disease. *Neurobiol. Aging* 29, 185–193. doi: 10.1016/j.neurobiolaging.2006.10.017

Pfeifer, L. A., White, L. R., Ross, G. W., Petrovitch, H., and Launer, L. J. (2002). Cerebral amyloid angiopathy and cognitive function: the HAAS autopsy study. *Neurology* 58, 1629–1634. doi: 10.1212/WNL.58.11.1629

Pike, K. E., Savage, G., Villemagne, V. L., Ng, S., Moss, S. A., Maruff, P., et al. (2007). β-amyloid imaging and memory in non-demented individuals: evidence for preclinical Alzheimer's disease. *Brain J. Neurol.* 130, 2837–2844. doi: 10.1093/brain/awm238

Plum, F., and Posner, J. B. (1972). The diagnosis of stupor and coma. *Contemp. Neurol. Ser.* 10, 1–286.

Ponizovsky, A. M., Barshtein, G., and Bergelson, L. D. (2003). Biochemical alterations of erythrocytes as an indicator of mental disorders: an overview. *Harv. Rev. Psychiatry* 11, 317–332. doi: 10.1080/10673220390264258

Pretorius, E., Olumuyiwa-Akeredolu, O.-O. O., Mbotwe, S., and Bester, J. (2016). Erythrocytes and their role as health indicator: using structure in a patient-orientated precision medicine approach. *Blood Rev.* 30, 263–274. doi: 10.1016/j.blre.2016.01.001

Quastel, J. H. (1932). Biochemistry and mental disorder. *Lancet* 220, 1417–1419. doi: 10.1016/S0140-6736(00)97278-7

Rabini, R. A., Petruzzi, E., Staffolani, R., Tesei, M., Fumelli, P., Pazzagli, M., et al. (1997). Diabetes mellitus and subjects' ageing: a study on the ATP content and ATP-related enzyme activities in human erythrocytes. *Eur. J. Clin. Invest.* 27, 327–332. doi: 10.1046/j.1365-2362.1997.1130652.x

Ravi, L. B., Mohanty, J. G., Chrest, F. J., Jayakumar, R., Nagababu, E., Usatyuk, P. V., et al. (2004). Influence of beta-amyloid fibrils on the interactions between red blood cells and endothelial cells. *Neurol. Res.* 26, 579–585. doi: 10.1179/016164104225016227

Reddy, P. H. (2006). Amyloid precursor protein-mediated free radicals and oxidative damage: implications for the development and progression of Alzheimer's disease. *J. Neurochem.* 96, 1–13. doi: 10.1111/j.1471-4159.2005.03530.x

Resnick, L. M., Gupta, R. K., Barbagallo, M., and Laragh, J. H. (1994). Is the higher incidence of ischemic disease in patients with hypertension and diabetes related to intracellular depletion of high energy metabolites? *Am. J. Med. Sci.* 307(Suppl. 1), S66–S69.

Richards, R. S., Wang, L., and Jelinek, H. (2007). Erythrocyte oxidative damage in chronic fatigue syndrome. *Arch. Med. Res.* 38, 94–98. doi: 10.1016/j.arcmed.2006.06.008

Richardson, J. T. (1990). Cognitive function in diabetes mellitus. *Neurosci. Biobehav. Rev.* 14, 385–388. doi: 10.1016/S0149-7634(05)80060-0

Riegel, B., Bennett, J. A., Davis, A., Carlson, B., Montague, J., Robin, H., et al. (2002). Cognitive impairment in heart failure: issues of measurement and etiology. *Am. J. Crit. Care Off. Publ. Am. Assoc. Crit. Care Nurses* 11, 520–528.

Rifkind, J. M., Abugo, O. O., Peddada, R. R., Patel, N., Speer, D., Balagopalakrishna, C., et al. (1999). Maze learning impairment is associated with stress hemopoiesis induced by chronic treatment of aged rats with human recombinant erythropoietin. *Life Sci*. 64, 237–247. doi: 10.1016/S0024-3205(98)00559-1

Roberts, G. W., Allsop, D., and Bruton, C. (1990). The occult aftermath of boxing. *J. Neurol. Neurosurg. Psychiatry* 53, 373–378. doi: 10.1136/jnnp.53.5.373

Rönnbäck, L., and Hansson, E. (2004). On the potential role of glutamate transport in mental fatigue. *J. Neuroinflammation* 1:22. doi: 10.1186/1742-2094-1-22

Ronquist, G., and Waldenström, A. (2003). Imbalance of plasma membrane ion leak and pump relationship as a new aetiological basis of certain disease states. *J. Intern. Med*. 254, 517–526. doi: 10.1111/j.1365-2796.2003.01235.x

Roselli, F., Tirard, M., Lu, J., Hutzler, P., Lamberti, P., Livrea, P., et al. (2005). Soluble β-amyloid1-40 induces NMDA-dependent degradation of postsynaptic density-95 at glutamatergic synapses. *J. Neurosci. Off. J. Soc. Neurosci*. 25, 11061–11070. doi: 10.1523/JNEUROSCI.3034-05.2005

Rothstein, G. (1993). Hematopoiesis in the aged: a model of hematopoietic dysregulation? *Blood* 82, 2601–2604.

Sakuta, S. (1981). Blood filtrability in cerebrovascular disorders, with special reference to erythrocyte deformability and ATP content. *Stroke* 12, 824–828. doi: 10.1161/01.STR.12.6.824

Samaja, M., Crespi, T., Guazzi, M., and Vandegriff, K. D. (2003). Oxygen transport in blood at high altitude: role of the hemoglobin-oxygen affinity and impact of the phenomena related to hemoglobin allosterism and red cell function. *Eur. J. Appl. Physiol*. 90, 351–359. doi: 10.1007/s00421-003-0954-8

Sansoni, P., Cossarizza, A., Brianti, V., Fagnoni, F., Snelli, G., Monti, D., et al. (1993). Lymphocyte subsets and natural killer cell activity in healthy old people and centenarians. *Blood* 82, 2767–2773.

Schmitt, F. A., Davis, D. G., Wekstein, D. R., Smith, C. D., Ashford, J. W., and Markesbery, W. R. (2000). "Preclinical" AD revisited: neuropathology of cognitively normal older adults. *Neurology* 55, 370–376. doi: 10.1212/WNL.55.3.370

Schneider, J. A., Arvanitakis, Z., Bang, W., and Bennett, D. A. (2007). Mixed brain pathologies account for most dementia cases in community-dwelling older persons. *Neurology* 69, 2197–2204. doi: 10.1212/01.wnl.0000271090.28148.24

Scholz, W. (1938). Studien zur Pathologie der Hirngefasse II. Die drusige Entartung der Hirnarterien und capillarien. *Z Ges Neurol. Psychiat*. 162, 694–715. doi: 10.1007/BF02890989

Seeman, P., Cheng, D., and Iles, G. H. (1973). Structure of membrane holes in osmotic and saponin hemolysis. *J. Cell Biol*. 56, 519–527. doi: 10.1083/jcb.56.2.519

Selkoe, D. J. (2007). Developing preventive therapies for chronic diseases: lessons learned from Alzheimer's disease. *Nutr. Rev*. 65, S239–S243. doi: 10.1301/nr.2007.dec.S239-S243

Selkoe, D. J. (2008). Soluble oligomers of the amyloid β-protein impair synaptic plasticity and behavior. *Behav. Brain Res*. 192, 106–113. doi: 10.1016/j.bbr.2008.02.016

Shevtsova, E. F., Vinogradova, D. V., Neganova, M. E., Avila-Rodriguez, M., Ashraf, G. M., Barreto, G. E., et al. (2017). Mitochondrial permeability transition pore as a suitable target for neuroprotective agents against Alzheimer's Disease. *CNS Neurol. Disord. Drug Targets* 16, 677–685. doi: 10.2174/1871527316666170424114444

Shi, J., Xiang, Y., and Simpkins, J. W. (1997). Hypoglycemia enhances the expression of mRNA encoding β-amyloid precursor protein in rat primary cortical astroglial cells. *Brain Res*. 772, 247–251. doi: 10.1016/S0006-8993(97)00827-5

Shinozuka, T., Miyamoto, T., Hirazono, K., Ebisawa, K., Murakami, M., Kuroshima, Y., et al. (1994). Follow-up laparoscopy in patients with ovarian cancer. *Tokai J. Exp. Clin. Med*. 19, 53–59.

Simpson, I. A., Chundu, K. R., Davies-Hill, T., Honer, W. G., and Davies, P. (1994). Decreased concentrations of GLUT1 and GLUT3 glucose transporters in the brains of patients with Alzheimer's disease. *Ann. Neurol*. 35, 546–551. doi: 10.1002/ana.410350507

Simpson, I. A., and Davies, P. (1994). Reduced glucose transporter concentrations in brains of patients with Alzheimer's disease. *Ann. Neurol*. 36, 800–801. doi: 10.1002/ana.410360522

Simpson, P. J., Mickelson, J., Fantone, J. C., Gallagher, K. P., and Lucchesi, B. R. (1988). Reduction of experimental canine myocardial infarct size with prostaglandin E1: inhibition of neutrophil migration and activation. *J. Pharmacol. Exp. Ther*. 244, 619–624.

Singh, V. K., Cheng, J. F., and Leu, S. J. (1994). Effect of substance P and protein kinase inhibitors on beta-amyloid peptide-induced proliferation of cultured brain cells. *Brain Res*. 660, 353–356. doi: 10.1016/0006-8993(94)91313-7

Smith, C. D., Carney, J. M., Starke-Reed, P. E., Oliver, C. N., Stadtman, E. R., Floyd, R. A., et al. (1991). Excess brain protein oxidation and enzyme dysfunction in normal aging and in Alzheimer disease. *Proc. Natl. Acad. Sci. U.S.A*. 88, 10540–10543. doi: 10.1073/pnas.88.23.10540

Smith, D. H., Chen, X.-H., Iwata, A., and Graham, D. I. (2003). Amyloid β accumulation in axons after traumatic brain injury in humans. *J. Neurosurg*. 98, 1072–1077. doi: 10.3171/jns.2003.98.5.1072

Smith, E. E., and Greenberg, S. M. (2009). β-amyloid, blood vessels, and brain function. *Stroke* 40, 2601–2606. doi: 10.1161/STROKEAHA.108.536839

Smith, M. A., Casadesus, G., Joseph, J. A., and Perry, G. (2002a). Amyloid-β and tau serve antioxidant functions in the aging and Alzheimer brain. *Free Radic. Biol. Med*. 33, 1194–1199. doi: 10.1016/S0891-5849(02)01021-3

Smith, M. A., Drew, K. L., Nunomura, A., Takeda, A., Hirai, K., Zhu, X., et al. (2002b). Amyloid-β, tau alterations and mitochondrial dysfunction in Alzheimer disease: the chickens or the eggs? *Neurochem. Int*. 40, 527–531. doi: 10.1016/S0197-0186(01)00123-1

Smith, M. A., Hirai, K., Hsiao, K., Pappolla, M. A., Harris, P. L., Siedlak, S. L., et al. (1998). Amyloid-β deposition in Alzheimer transgenic mice is associated with oxidative stress. *J. Neurochem*. 70, 2212–2215. doi: 10.1046/j.1471-4159.1998.70052212.x

Smith, M. A., Joseph, J. A., and Perry, G. (2000). Arson. Tracking the culprit in Alzheimer's disease. *Ann. N. Y. Acad. Sci*. 924, 35–38. doi: 10.1111/j.1749-6632.2000.tb05557.x

Solerte, S. B., Ceresini, G., Ferrari, E., and Fioravanti, M. (2000). Hemorheological changes and overproduction of cytokines from immune cells in mild to moderate dementia of the Alzheimer's type: adverse effects on cerebromicrovascular system. *Neurobiol. Aging* 21, 271–281. doi: 10.1016/S0197-4580(00)00105-6

Storey, E., Hyman, B. T., Jenkins, B., Brouillet, E., Miller, J. M., Rosen, B. R., et al. (1992). 1-Methyl-4-phenylpyridinium produces excitotoxic lesions in rat striatum as a result of impairment of oxidative metabolism. *J. Neurochem*. 58, 1975–1978. doi: 10.1111/j.1471-4159.1992.tb10080.x

Tabaton, M., and Gambetti, P. (2006). Soluble amyloid-β in the brain: the scarlet pimpernel. *J. Alzheimers Dis*. 9, 127–132. doi: 10.3233/JAD-2006-9S315

Tabaton, M., and Piccini, A. (2005). Role of water-soluble amyloid-β in the pathogenesis of Alzheimer's disease. *Int. J. Exp. Pathol*. 86, 139–145. doi: 10.1111/j.0959-9673.2005.00428.x

Teller, J. K., Russo, C., DeBusk, L. M., Angelini, G., Zaccheo, D., Dagna-Bricarelli, F., et al. (1996). Presence of soluble amyloid beta-peptide precedes amyloid plaque formation in Down's syndrome. *Nat. Med*. 2, 93–95. doi: 10.1038/nm0196-93

Terry, R. D., Masliah, E., Salmon, D. P., Butters, N., DeTeresa, R., Hill, R., et al. (1991). Physical basis of cognitive alterations in Alzheimer's disease: synapse loss is the major correlate of cognitive impairment. *Ann. Neurol*. 30, 572–580. doi: 10.1002/ana.410300410

Tesco, G., Koh, Y. H., Kang, E. L., Cameron, A. N., Das, S., Sena-Esteves, M., et al. (2007). Depletion of GGA3 stabilizes BACE and enhances beta-secretase activity. *Neuron* 54, 721–737. doi: 10.1016/j.neuron.2007.05.012

Thal, D. R., Capetillo-Zarate, E., Larionov, S., Staufenbiel, M., Zurbruegg, S., and Beckmann, N. (2009). Capillary cerebral amyloid angiopathy is associated with vessel occlusion and cerebral blood flow disturbances. *Neurobiol. Aging* 30, 1936–1948. doi: 10.1016/j.neurobiolaging.2008.01.017

Thal, D. R., Ghebremedhin, E., Rüb, U., Yamaguchi, H., Del Tredici, K., and Braak, H. (2002). Two types of sporadic cerebral amyloid angiopathy. *J. Neuropathol. Exp. Neurol*. 61, 282–293. doi: 10.1093/jnen/61.3.282

Thal, D. R., Griffin, W. S. T., and Braak, H. (2008). Parenchymal and vascular Aβ-deposition and its effects on the degeneration of neurons and cognition in Alzheimer's disease. *J. Cell. Mol. Med*. 12, 1848–1862. doi: 10.1111/j.1582-4934.2008.00411.x

Thanvi, B., and Robinson, T. (2006). Sporadic cerebral amyloid angiopathy–an important cause of cerebral haemorrhage in older people. *Age Ageing* 35, 565–571. doi: 10.1093/ageing/afl108

Tikhonova, L. A., Kaminsky, Y. G., Reddy, V. P., Li, Y., Solomadin, I. N., Kosenko, E. A., et al. (2014). Impact of amyloid β25-35 on membrane stability, energy metabolism, and antioxidant enzymes in erythrocytes. *Am. J. Alzheimers Dis. Other Demen*. 29, 685–695. doi: 10.1177/1533317514534757

Toro-Urrego, N., Garcia-Segura, L. M., Echeverria, V., and Barreto, G. E. (2016). Testosterone protects mitochondrial function and regulates neuroglobin expression in astrocytic cells exposed to glucose deprivation. *Front. Aging Neurosci.* 8:152. doi: 10.3389/fnagi.2016.00152

Tsirka, A., Challa, A., and Lapatsanis, P. D. (1990). Red cell phosphate metabolism in preterm infants with idiopathic respiratory distress syndrome. *Acta Paediatr. Scand.* 79, 763–768. doi: 10.1111/j.1651-2227.1990.tb11552.x

Urbach, H. (2011). Comment on: Brain Microbleeds and Alzheimer's disease: innocent observation or key player?: Cordonnier C, van der Flier WM. Brain. 2011;134:335-44. *Clin. Neuroradiol.* 21, 43–44. doi: 10.1007/s00062-011-0063-8

Uryu, K., Chen, X.-H., Martinez, D., Browne, K. D., Johnson, V. E., Graham, D. I., et al. (2007). Multiple proteins implicated in neurodegenerative diseases accumulate in axons after brain trauma in humans. *Exp. Neurol.* 208, 185–192. doi: 10.1016/j.expneurol.2007.06.018

Valeri, C. R., and Hirsch, N. M. (1969). Restoration *in vivo* of erythrocyte adenosine triphosphate, 2,3-diphosphoglycerate, potassium ion, and sodium ion concentrations following the transfusion of acid-citrate-dextrose-stored human red blood cells. *J. Lab. Clin. Med.* 73, 722–733.

van der Zwaluw, C. S., Valentijn, S. A. M., Nieuwenhuis-Mark, R., Rasquin, S. M. C., and van Heugten, C. M. (2011). Cognitive functioning in the acute phase poststroke: a predictor of discharge destination? *J. Stroke Cerebrovasc. Dis.* 20, 549–555. doi: 10.1016/j.jstrokecerebrovasdis.2010.03.009

van Groen, T., Puurunen, K., Mäki, H.-M., Sivenius, J., and Jolkkonen, J. (2005). Transformation of diffuse beta-amyloid precursor protein and beta-amyloid deposits to plaques in the thalamus after transient occlusion of the middle cerebral artery in rats. *Stroke* 36, 1551–1556. doi: 10.1161/01.STR.0000169933.88903.cf

Vanhanen, M., Koivisto, K., Karjalainen, L., Helkala, E. L., Laakso, M., Soininen, H., et al. (1997). Risk for non-insulin-dependent diabetes in the normoglycaemic elderly is associated with impaired cognitive function. *Neuroreport* 8, 1527–1530. doi: 10.1097/00001756-199704140-00041

van Wijk, R., and van Solinge, W. W. (2005). The energy-less red blood cell is lost: erythrocyte enzyme abnormalities of glycolysis. *Blood* 106, 4034–4042. doi: 10.1182/blood-2005-04-1622

Velliquette, R. A., O'Connor, T., and Vassar, R. (2005). Energy inhibition elevates β-secretase levels and activity and is potentially amyloidogenic in APP transgenic mice: possible early events in Alzheimer's disease pathogenesis. *J. Neurosci.* 25, 10874–10883. doi: 10.1523/JNEUROSCI.2350-05.2005

Villain, N., Desgranges, B., Viader, F., de la Sayette, V., Mézenge, F., Landeau, B., et al. (2008). Relationships between hippocampal atrophy, white matter disruption, and gray matter hypometabolism in Alzheimer's disease. *J. Neurosci.* 28, 6174–6181. doi: 10.1523/JNEUROSCI.1392-08.2008

Vonsattel, J. P., Myers, R. H., Hedley-Whyte, E. T., Ropper, A. H., Bird, E. D., and Richardson, E. P. (1991). Cerebral amyloid angiopathy without and with cerebral hemorrhages: a comparative histological study. *Ann. Neurol.* 30, 637–649. doi: 10.1002/ana.410300503

Vora, S. (1987). Metabolic manipulation of key glycolytic enzymes: a novel proposal for the maintenance of red cell 2,3-DPG and ATP levels during storage. *Biomed. Biochim. Acta* 46, S285–S289.

Walsh, D. M., Klyubin, I., Fadeeva, J. V., Cullen, W. K., Anwyl, R., Wolfe, M. S., et al. (2002). Naturally secreted oligomers of amyloid β protein potently inhibit hippocampal long-term potentiation *in vivo*. *Nature* 416, 535–539. doi: 10.1038/416535a

Walsh, D. M., and Selkoe, D. J. (2004). Deciphering the molecular basis of memory failure in Alzheimer's disease. *Neuron* 44, 181–193. doi: 10.1016/j.neuron.2004.09.010

Wang, J., Dickson, D. W., Trojanowski, J. Q., and Lee, V. M. (1999). The levels of soluble versus insoluble brain Aβ distinguish Alzheimer's disease from normal and pathologic aging. *Exp. Neurol.* 158, 328–337. doi: 10.1006/exnr.1999.7085

Webster, M. T., Pearce, B. R., Bowen, D. M., and Francis, P. T. (1998). The effects of perturbed energy metabolism on the processing of amyloid precursor protein in PC12 cells. *J. Neural Transm.* 105, 839–853. doi: 10.1007/s007020050098

Weller, R. O., Boche, D., and Nicoll, J. A. R. (2009). Microvasculature changes and cerebral amyloid angiopathy in Alzheimer's disease and their potential impact on therapy. *Acta Neuropathol.* 118, 87–102. doi: 10.1007/s00401-009-0498-z

Whitson, J. S., Selkoe, D. J., and Cotman, C. W. (1989). Amyloid β protein enhances the survival of hippocampal neurons *in vitro*. *Science* 243, 1488–1490. doi: 10.1126/science.2928783

Williams, L. H., Udupa, K. B., and Lipshitz, D. A. (1986). Evaluation of the effect of age on hematopoiesis in the C57BL/6 mouse. *Exp. Hematol.* 14, 827–832.

Wimo, A., and Prince, M. (2010). *World Alzheimer Report 2010: The Global Economic Impact of Dementia*. Alzheimer's Disease International, London.

Wirths, O., Multhaup, G., and Bayer, T. A. (2004). A modified β-amyloid hypothesis: intraneuronal accumulation of the β-amyloid peptide–the first step of a fatal cascade. *J. Neurochem.* 91, 513–520. doi: 10.1111/j.1471-4159.2004.02737.x

Wisniewski, H. M., and Wegiel, J. (1994). Beta-amyloid formation by myocytes of leptomeningeal vessels. *Acta Neuropathol.* 87, 233–241. doi: 10.1007/BF00296738

Wu, C.-W., Liao, P.-C., Yu, L., Wang, S.-T., Chen, S.-T., Wu, C.-M., et al. (2004). Hemoglobin promotes Aβ oligomer formation and localizes in neurons and amyloid deposits. *Neurobiol. Dis.* 17, 367–377. doi: 10.1016/j.nbd.2004.08.014

Xi, G., Keep, R. F., and Hoff, J. T. (1998). Erythrocytes and delayed brain edema formation following intracerebral hemorrhage in rats. *J. Neurosurg.* 89, 991–996. doi: 10.3171/jns.1998.89.6.0991

Xi, G., Keep, R. F., and Hoff, J. T. (2006). Mechanisms of brain injury after intracerebral haemorrhage. *Lancet Neurol.* 5, 53–63. doi: 10.1016/S1474-4422(05)70283-0

Xie, Z., Culley, D. J., Dong, Y., Zhang, G., Zhang, B., Moir, R. D., et al. (2008). The common inhalation anesthetic isoflurane induces caspase activation and increases amyloid β-protein level *in vivo*. *Ann. Neurol.* 64, 618–627. doi: 10.1002/ana.21548

Xie, Z., Dong, Y., Maeda, U., Alfille, P., Culley, D. J., Crosby, G., et al. (2006a). The common inhalation anesthetic isoflurane induces apoptosis and increases amyloid β protein levels. *Anesthesiology* 104, 988–994. doi: 10.1097/00000542-200605000-00015

Xie, Z., Dong, Y., Maeda, U., Moir, R., Inouye, S. K., Culley, D. J., et al. (2006b). Isoflurane-induced apoptosis: a potential pathogenic link between delirium and dementia. *J. Gerontol. A. Biol. Sci. Med. Sci.* 61, 1300–1306. doi: 10.1093/gerona/61.12.1300

Xie, Z., Moir, R. D., Romano, D. M., Tesco, G., Kovacs, D. M., and Tanzi, R. E. (2004). Hypocapnia induces caspase-3 activation and increases Aβ production. *Neurodegener. Dis.* 1, 29–37. doi: 10.1159/000076667

Yoshida, K., Furuse, M., Izawa, A., Iizima, N., Kuchiwaki, H., and Inao, S. (1996). Dynamics of cerebral blood flow and metabolism in patients with cranioplasty as evaluated by 133Xe CT and 31P magnetic resonance spectroscopy. *J. Neurol. Neurosurg. Psychiatry* 61, 166–171. doi: 10.1136/jnnp.61.2.166

Yu, N.-N., Wang, X.-X., Yu, J.-T., Wang, N.-D., Lu, R.-C., Miao, D., et al. (2010). Blocking β2-adrenergic receptor attenuates acute stress-induced amyloid β peptides production. *Brain Res.* 1317, 305–310. doi: 10.1016/j.brainres.2009.12.087

Zhang, B., Dong, Y., Zhang, G., Moir, R. D., Xia, W., Yue, Y., et al. (2008). The inhalation anesthetic desflurane induces caspase activation and increases amyloid β-protein levels under hypoxic conditions. *J. Biol. Chem.* 283, 11866–11875. doi: 10.1074/jbc.M800199200

Zhu, X., Smith, M. A., Honda, K., Aliev, G., Moreira, P. I., Nunomura, A., et al. (2007). Vascular oxidative stress in Alzheimer disease. *J. Neurol. Sci.* 257, 240–246. doi: 10.1016/j.jns.2007.01.039

Conflict of Interest Statement: The authors declare that the research was conducted in the absence of any commercial or financial relationships that could be construed as a potential conflict of interest.

Copyright © 2018 Kosenko, Tikhonova, Montoliu, Barreto, Aliev and Kaminsky. This is an open-access article distributed under the terms of the Creative Commons Attribution License (CC BY). The use, distribution or reproduction in other forums is permitted, provided the original author(s) or licensor are credited and that the original publication in this journal is cited, in accordance with accepted academic practice. No use, distribution or reproduction is permitted which does not comply with these terms.

frontiers in Neuroscience

REVIEW
published: 15 October 2018
doi: 10.3389/fnins.2018.00669

Fighting the Cause of Alzheimer's and GNE Myopathy

*Shreedarshanee Devi, Rashmi Yadav, Pratibha Chanana and Ranjana Arya**

School of Biotechnology, Jawaharlal Nehru University, New Delhi, India

Age is the common risk factor for both neurodegenerative and neuromuscular diseases. Alzheimer disease (AD), a neurodegenerative disorder, causes dementia with age progression while GNE myopathy (GNEM), a neuromuscular disorder, causes muscle degeneration and loss of muscle motor movement with age. Individuals with mutations in presenilin or amyloid precursor protein (APP) gene develop AD while mutations in GNE (UDP *N*-acetylglucosamine 2 epimerase/*N*-acetyl Mannosamine kinase), key sialic acid biosynthesis enzyme, cause GNEM. Although GNEM is characterized with degeneration of muscle cells, it is shown to have similar disease hallmarks like aggregation of Aβ and accumulation of phosphorylated tau and other misfolded proteins in muscle cell similar to AD. Similar impairment in cellular functions have been reported in both disorders such as disruption of cytoskeletal network, changes in glycosylation pattern, mitochondrial dysfunction, oxidative stress, upregulation of chaperones, unfolded protein response in ER, autophagic vacuoles, cell death, and apoptosis. Interestingly, AD and GNEM are the two diseases with similar phenotypic condition affecting neuron and muscle, respectively, resulting in entirely different pathology. This review represents a comparative outlook of AD and GNEM that could lead to target common mechanism to find a plausible therapeutic for both the diseases.

Keywords: amyloid β, NFT, GNE, hyposialylation, sialic acid, ER stress, apoptosis, autophagy

OPEN ACCESS

Edited by:
Mohammad Amjad Kamal, King Abdulaziz University, Saudi Arabia

Reviewed by:
Petr A. Slominsky, Institute of Molecular Genetics (RAS), Russia
Chaoyang Li, Wuhan Institute of Virology (CAS), China

***Correspondence:**
Ranjana Arya
arya.ranjana24@gmail.com; ranjanaa@jnu.ac.in

Specialty section:
This article was submitted to Neurodegeneration, a section of the journal Frontiers in Neuroscience

Received: *28 February 2018*
Accepted: *06 September 2018*
Published: *15 October 2018*

Citation:
Devi S, Yadav R, Chanana P and Arya R (2018) Fighting the Cause of Alzheimer's and GNE Myopathy. Front. Neurosci. 12:669. doi: 10.3389/fnins.2018.00669

INTRODUCTION

Aging is the process, which initiates with subclinical changes at molecular level including accumulation of mutations, telomere attrition, epigenetic alterations resulting in genome instability (López-Otín et al., 2013). These changes multiply at a very fast rate, ultimately leading to the morphological and functional deterioration of brain by progressive loss of the neurons, reduction in the levels of neurotransmitters at the synaptic junction and disruption of integrity of the brain (Sibille, 2013). In addition to neurons, muscle cells are also affected with age. Loss of muscle mass, reduction in muscle fiber size and number is observed in muscles with age that decreases muscle strength (Narici and Maffulli, 2010; Siparsky et al., 2014). Thus, age is a common risk factor for both neurodegenerative and neuromuscular diseases, that progress with time.

The neurodegenerative disorders like Alzheimer's disease (AD), Parkinson's disease, Huntington's disease and amyotrophic lateral sclerosis (ALS) share similar pattern of brain alterations and relate to each other at sub-cellular levels in numerous studies (Garden and La Spada, 2012; Montie and Durcan, 2013). Oxidative stress and altered Ca^{2+} and mitochondrial

Abbreviations: Aβ, β amyloid; AD, Alzheimer's disease; GNE, UDP-GlcNAc 2-epimerase/ManNAc kinase; GNEM, GNE myopathy; NFT, neurofibrillary tangles.

dysfunctions cause neuronal damage with age (Thibault et al., 1998, 2001). Further, neurons do not divide (with rare exceptions), thus cellular damage tend to accumulate with age (Sibille, 2013). Similarly neuromuscular disorders such as multiple sclerosis, muscular dystrophy, GNE related myopathy, Myasthenia gravis, Spinal muscular atrophy and ALS show subcellular damage in muscle cells where oxidative stress and altered calcium/mitochondrial, and ER stress are observed (Kanekura et al., 2009; Roussel et al., 2013; Stone and Lin, 2015; Xiang et al., 2017). Muscle cells are also among the least dividing cells with average lifespan of 15 years or sometimes reaching four decades. Due to its long life span like neurons, the cellular damage in muscle also accumulates in due course of time. As the age progresses, the satellite cells of muscle decline reducing the regeneration capacity of healthy muscle in place of affected cells (Narici and Maffulli, 2010). Whether there is any correlation of cellular damage in neurons versus muscle cells that can be a common therapeutic target is not known.

Indeed some disorders such as ALS can be placed in either of the two disorders as it affects both neurons and muscle cells. Several neuromuscular disorders, which include muscular dystrophies have reported degeneration of neurons in brain and affect the cognitive function leading to memory loss (Anderson et al., 2002; Ricotti et al., 2011). In ALS, loss of motor neurons affect the movement of various muscles of body leading to muscle wasting and paralysis, along with cognitive impairment (Taylor et al., 2016). Interestingly, a novel missense mutation (histidine to arginine at 705 amino acid) in GNE gene (UDP *N*-acetylglucosamine 2 epimerase/*N*-acetyl Mannosamine kinase) was observed in familial ALS patient (Köroğlu et al., 2017). Mutation in GNE gene causes GNEM, a rare neuromuscular disorder with completely different pathology compared to ALS (Huizing and Krasnewich, 2009). This raises a possibility of a missing link between the two disorders where the pathomechanisms might merge at a common target.

In this review, we have correlated and compared Alzheimer's disease, a neurodegenerative disorder with GNEM, a neuromuscular disorder and put forth how these diseases share common pathological events like aggregation of misfolded proteins, oxidative stress, mitochondrial dysfunction, autophagy and cellular death. This will help us to find a common therapeutic approach for the treatment of these diseases.

EPIDEMIOLOGY

Among various neurological disorders, Alzheimer's disease is the most common form of dementia accounting for 60–80% of all the cases of dementia, with worldwide prevalence above 45 million[1]. It is more prevalent in the Western European and North American population. On the other hand, GNEM is a rare genetic neuromuscular disorder with worldwide prevalence of 1–9 in a millionth population (Orphanet[2]). GNEM has been reported in the Irish, Jewish, Japanese and Indian populations. Also, there are reports of GNEM from North America, European (United Kingdom and Scotland) and other Asian country like Thailand (Bhattacharya et al., 2018).

CAUSES, CHARACTERISTICS AND GENETIC PREDISPOSITION

AD is a multifactorial disease without any single cause. The main characteristic features of AD are senile plaques, composed mainly of extracellular amyloid-β (Aβ) peptides, and Neurofibrillary Tangles (NFTs) formed after accumulation of intracellular hyperphosphorylated tau (Serrano-Pozo et al., 2011). GNEM is caused by autosomal recessive mutation in GNE gene responsible for sialic acid biosynthesis. The characteristic features for GNEM involves weakness in the distal muscles, sparing the quadriceps, presence of rimmed vacuoles in muscle fibers and tubulofilamentous inclusions of aggregated proteins such as Aβ and phosphorylated tau (Jay et al., 2009). Despite the differences in tissues that are affected in the two diseases, accumulation of aggregates of amyloid-β and tau are common characteristics of both the diseases.

Initial symptom of AD is gradual loss in ability of the person to remember new information (Souchay and Moulin, 2009). The greatest risk factor for the development of AD is age as its pathological features increase exponentially with age (doubling every 5 years after the attainment of 65 years of age) (Querfurth and LaFerla, 2010). In GNEM, the initial symptoms include foot drop and weakness in the distal muscles, which gradually worsen with age toward wheel-chair dependence of patients. In GNEM, unlike AD, the brain function has been reported as normal (Anada et al., 2014). The onset of AD is late adulthood while GNEM onset is early adulthood during the second or third decade of life. How aging leads to sudden onset of GNEM is not known.

Beside aging, AD is caused due to mutation in either the presenilin genes or in Amyloid Precursor Protein (APP) gene (Goate et al., 1991; Hutton and Hardy, 1997; Holtzman et al., 2011). There is also an increased risk of AD in individuals suffering from Down's syndrome because chromosome 21 includes a gene encoding the production of APP (Wiseman et al., 2015). The epsilon four allele of the apolipoprotein E gene (APOE) located on chromosome 19 is found to be a risk factor for AD (Reiman et al., 2005). People with a history of diabetes, hypertension, obesity, smoking, head injury leading to memory loss and a family history of AD in close relatives are at a greater risk of AD (Barnes and Yaffe, 2011). The prevalence of AD is higher in women and less educated masses (Letenneur et al., 2000).

On the other hand, GNEM is caused due to mutation in GNE (UDP-GlcNAc 2-epimerase/ManNAc kinase) gene that catalyzes the first two rate limiting steps in the biosynthesis of sialic acid (Jay et al., 2009). Whether hyposialylation is the only cause of GNEM is still unknown. GNEM is a genetic disorder and not known to be associated with lifestyle disease. No gender bias has been reported for GNEM. A complete comparison of

[1] www.alzheimers.net

[2] http://www.orpha.net/

characteristics of both AD and GNEM has been described in **Table 1**.

DISEASE PATHOLOGY

In normal condition, neuronal cells release soluble Aβ after cleavage of a cell surface receptor called APP. In case of AD, the cleavage is abnormal leading to the precipitation of Aβ into dense beta sheets and formation of senile plaques (Zhang et al., 2011). To clear the amyloid aggregates, an inflammatory response is generated by astrocytes and microglia leading to the destruction of adjacent neurons and their neuritis (Norfray and Provenzale, 2004; Querfurth and LaFerla, 2010).

The tau protein is a microtubule stabilizing protein and has a role in intracellular transport (both axonal and vesicular). In its abnormally hyper-phosphorylated form, tau form intracellular aggregates called the NFTs or senile plaques, interfering with normal axonal transport of molecules along microtubules (Norfray and Provenzale, 2004).

In GNEM, main pathological feature includes formation of rimmed vacuoles, which is comprised of aggregated proteins such as Aβ and tau (Nalini et al., 2010). Cytoplasmic and nuclear inclusion bodies have also been observed by electron microscopy in muscle biopsies, which contain degradative products from the membrane, cytoplasmic tubulofilaments and mitochondria with irregular size and shape (Huizing and Krasnewich, 2009). However, since GNE is a key sialic acid biosynthetic enzyme, mutation in GNE affects the sialylation of proteins (Noguchi et al., 2004). The immunohistochemistry of GNEM muscle samples revealed upregulation of αβ-crystallin, NCAM, MHC-1, and iNOS levels (Fischer et al., 2013). NCAM was hyposialylated in GNEM and proposed as diagnostic marker for GNEM (Ricci et al., 2006). In aging brain and AD, the expression and function of NCAM and MHC-1 was altered that may result in synaptic and cognitive loss (Aisa et al., 2010). Also, reduced polysialated-NCAM load was reported in entorhinal cortex causing AD (Murray et al., 2016). Thus, NCAM sialylation can be a common target in the pathology of AD and GNEM in addition to Aβ and tau accumulation.

DIAGNOSIS

Medical and family history of individuals, which include psychiatric history, changes in behavior and cognitive functions, help in the diagnosis of AD. Amyloid plaques, presence of NFT's and distribution in the brain are used to establish the disease by an autopsy based pathological evaluation. The clinical diagnosis of AD is about 70–90% accurate relative to the pathological diagnosis (Beach et al., 2012).

GNEM is clinically characterized by weakness in tibialis anterior muscles with a unique sparing of the quadriceps leading to foot drop, gait abnormalities, mild or no elevation in serum creatine kinase levels with no involvement of cardiac muscles, usually in the second or third decade of life (Nalini et al., 2013). Pathologically, GNEM is characterized by presence of rimmed vacuoles in muscle biopsies, without inflammation (Argov and Yarom, 1984). The confirmation of GNEM mainly relies on identification of bi-allelic mutation in GNE gene. As more than 190 mutations in GNE have been identified worldwide, complete

TABLE 1 | Comparison of the characteristics of AD and GNEM.

	Characteristics of AD and GNEM	
	AD	**GNEM**
Disease type	Neurodegenerative	Neuromuscular
Onset of the disease	Early (5%) and late onset (>95%)	Early adulthood
Age	Mainly above 65 years of age	20–30 years of age
Prevalence	45 Million and above	∼1–9 in one Million
Demographics	Worldwide but common in Western Europe and North American population	Jewish, Japanese and Indian population
Initial signs	Loss in memory	Foot drop
Gender biasness	Higher in women	Not found
Mutation	FAD-autosomally dominant	Autosomal recessive
Genetic defects	Mutations in Presenilin genes, APOE gene	Mutations in GNE gene
Symptoms	Memory loss, agitation, sleeplessness, and delusions	Foot drop, weakness in distal muscles, and difficulty in walking
Progressiveness	Fast	Slow
Brain function	Affected	Not affected
Pathological effect	Damage to limbic system and neocortical region, Senile plaques and NFTs, aggregation of proteins	Rimmed vacuole of aggregated proteins tubulofilaments and small fibers, cytoplasmic and nuclear inclusion bodies, aggregation of proteins
Diagnosis	Medical history, pathological diagnosis of plaques and NFTs, MRI and CT scan of brain lesions, levels of serum B12, TSH, T4 etc.	Time of disease onset, Gait study, walking pattern, pathological study of rimmed vacuoles and other factors, biallelic mutations in GNE gene through sequencing
Treatment	Acetylcholinesterase (Ach esterase) inhibitors, drugs targeting Aβ and tau protein accumulation	Supplementation with sialic acid and its precursor molecules, IVIG administration, gene therapy

sequencing of the GNE is necessary for diagnosis of GNE myopathy.

COMPARATIVE ANALYSIS OF MOLECULAR MECHANISMS AFFECTING AD AND GNEM

Effect of Glycosylation, Particularly Sialylation, in AD and GNEM

Glycosylation is the process of incorporation of glycan, either monosaccharides or oligosaccharides, unit to proteins and lipid moieties (Spiro, 2002). The role of glycosylation in case of AD was first reported when impaired glucose metabolism increased toxicity from Aβ and affected glycosylation pattern (Ott et al., 1999; Peila et al., 2002; Chornenkyy et al., 2018). Several key proteins involved in Aβ deposition cascade such as APP, BACE-1 (β secretase), γ-secretase, nicastrin, neprisilin (NEP) undergo altered glycosylation in AD (Kizuka et al., 2017). Deletion of N-glycosylation of APP protein results in its reduced secretion (Schedin-Weiss et al., 2014). APP trafficking from trans-Golgi network to plasma membrane and non-amyloidogenic processing is enhanced by *O*-GlcNAcylation of APP (Chun et al., 2015). Interestingly, enhanced sialylation of APP increased APP secretion and Aβ production (Nakagawa et al., 2006). Defect in sialic acid biosynthesis due to mutation in GNE affects sialylation of glycoproteins in GNEM. Several proteins such as neural cell adhesion molecule (NCAM), α-dystroglycan, integrin, IGF-1R, and other proteins have been found with altered sialylation in absence of functional GNE (Huizing et al., 2004; Ricci et al., 2006; Grover and Arya, 2014; Singh et al., 2018). However, changes in glycosylation pattern of APP or Aβ are not studied in GNEM despite elevated levels of APP reported in ALS and GNEM (Koistinen et al., 2006; Fischer et al., 2013). Thus, there is a need to investigate whether hyposialylation of muscle cells, as effect of mutation in GNE, affects the glycosylation pattern and sialylation of accumulated glycoproteins and proteins like Aβ, presenilin-1 etc.

Proper glycosylation of nicastrin (a subunit of γ-secretase) affects its trafficking to Golgi apparatus and proper binding to presenilin-1, thereby, inhibiting APP processing and γ-secretase substrate preference (Yang et al., 2002; Xie et al., 2014; Moniruzzaman et al., 2018). Expression of glycosylated NEP, protein involved in Aβ clearance, is also reduced in AD (Reilly, 2001). Interestingly, in GNEM also, the glycosylation and sialylation of neprilysin is dramatically reduced, affecting its expression and normal enzymatic activity (Broccolini et al., 2008). The effect of reduced activity in NEP in GNEM may lead to its failure of clearance of Aβ from muscle. Additionally, it has also been reported that enzyme GNE undergoes *O*-GlcNAcylation thereby, modulating its enzymatic activity (Bennmann et al., 2016). Thus, it would be of interest to study effect of altered sialylation due to GNE mutation on glycosylation pattern of aggregating proteins.

Several reports indicate alteration of protein sialylation to be a leading cause of AD (Wang, 2009; Schnaar et al., 2014). Binding of Aβ to cells is sialic acid dependent as its binding to surface is mediated through sialylated gangliosides, glycolipids, and glycoproteins (Ariga et al., 2001). The levels of sialyltransferase reduce with age that may contribute to altered sialic acid levels (Maguire et al., 1994; Maguire and Breen, 1995). In addition, clearance of Aβ by microglia is enhanced in absence of sialylated immunoglobulin, CD33 (siglec-33) (Jiang et al., 2014; Siddiqui et al., 2017). This suggests that sialylation is important for Aβ uptake and accumulation.

Interestingly, altered levels of sialyltransferases ST3Gal5 and ST8Sia1 were reported in HEKAD293 cells overexpressing wild type recombinant GNE resulting in increased levels of gangliosides GM3 and GD3 (Wang et al., 2006). Thus, GNE may affect sialyltransferases with an unknown mechanism. Molecules affecting sialyltransferase levels may influence Aβ uptake in both GNEM as well as AD. Thus, changes in the sialylation pattern of Aβ deposition cascade proteins in muscle cells may affect rimmed vacuole formation in GNEM and offer new therapeutic approach.

Role of Cytoskeleton Network in AD and GNEM

Cytoskeletal proteins are important functional proteins in both neuronal and muscle cells. In muscle, they help in conducting contraction and movement, while in neurons, they have a vital role in neuronal plasticity that is important for learning and memory process. Cytoskeletal proteins include different proteins like actin, tubulin, and lamin that provide mechanical support to the cell and modulate their dynamics inside the cell.

Tau, the first microtubule associated protein to be identified, was found to be one of the important hallmarks of AD along with Aβ. Tau directly helps in self-assembly of microtubule from tubulin. In AD, tau is found to be hyperphosphorylated at different site than normal (Gong et al., 2005; Hanger et al., 2007). The extent of tau aggregation is correlated with amount of phosphorylation at different sites (Iqbal et al., 2008). Also increased auto-antibodies of tubulin and tau were found in the serum of AD patients indicating a robust target for disease diagnosis (Salama et al., 2018). In GNEM, phosphorylated tau has been observed to accumulate in rimmed vacuoles (Nogalska et al., 2015), but whether aggregated tau is hyperphosphorylated from the normal form is not yet studied.

Actin dynamics and modulation of G-actin and F-actin is an important feature for neuronal plasticity and memory developments (Penzes and Rafalovich, 2012). Impaired cognitive function has been reported in AD pathology where cofilin-1, an actin depolymerizer, was found to be inactive (Barone et al., 2014). Inactivation of cofilin 1 contributes to actin dependent impairment of synaptic plasticity and thus, learning (Rust, 2015). Further, cofilin-1 inactivation is γ-secretase dependent, which controls Aβ peptide production. Also, cofilin-actin rods result in synaptic loss in AD (Bamburg et al., 2010). Small GTPases like RhoA, Rac1, and Cdc42 regulate APP, formation of Aβ and neurotoxicity (Boo et al., 2008; Wang et al., 2009). Phosphorylation of collapsin mediator response

protein-2 (CRMP-2) in AD disrupts its binding with kinesin hampering axonal transport and resulting in neuronal defect (Mokhtar et al., 2018). RhoGTPases also play important role in muscle differentiation and muscle contraction (DeHart and Jones, 2004; Zhang et al., 2012). Interestingly, GNE has been shown to interact with CRMP-1, α-actinin-1, and α-actinin-2, key cytoskeletal regulatory proteins (Weidemann et al., 2006; Amsili et al., 2008; Harazi et al., 2017). Being an actin binding protein, binding of α-actinin-1 and α-actinin-2 with GNE raises a possibility of impaired actin function in GNEM. Differential cytoskeletal protein expression was observed in muscle biopsy samples of GNEM patients (Sela et al., 2011). Upstream of actin, FAK (focal adhesion complex) and integrin (extracellular matrix protein) function was affected in mutant GNE cells (Grover and Arya, 2014). It has also been reported that induction of Aβ led to the increased expression of FAK and autophosphorylation at Tyr397 (Han et al., 2013). However, role of RhoA, actin, cofilin needs to be further elucidated in GNEM. Taken together these studies indicate cytoskeletal proteins to be a common target that regulate Aβ production and need therapeutic intervention to explore effective molecules.

Mitochondrial Dysfunction in AD and GNEM

Mitochondria are self-dividing organelles undergoing fission and fusion inside a cell. It is the power house of a cell that provides energy by oxidative phosphorylation during TCA cycle. Neurons and muscle cells have higher demand for mitochondria for their neuronal processes and muscle contraction, respectively. It has been reported that different cytoskeletal proteins help in motility of mitochondria in the cytoplasm (Lackner, 2013). Accumulation of Aβ and increased cellular death has been reported upon dissection of brains of AD patients (Cha et al., 2012). Further, Aβ accumulation in mitochondria precedes amyloid plaque, indicative of an early stage AD (Ankarcrona et al., 2010). In the early stages of AD, the number of mitochondria in the affected neurons is highly reduced leading to decreased glucose metabolism and impaired TCA cycle enzyme activity (Bubber et al., 2005; Mosconi, 2005). Additionally, elevated level of oxidative damage and significant increase in mutation of mtDNA and cytochrome c oxidase has been reported in AD patients (Castellani et al., 2002). Further, impaired mitochondrial trafficking has been observed in rat hippocampal neurons upon exposure to sub-cytotoxic levels of Aβ (Rui et al., 2006). Altered calcium homeostasis affects ATP generation and cause mitochondrial dysfunction (Supnet and Bezprozvanny, 2010; Swerdlow, 2018).

In GNEM, upregulation of a number of mitochondrial genes and transcript encoding mitochondrial proteins like COX, Cytochrome C Oxidase, ATPases, NADH dehydrogenase etc., have been reported in GNEM patient muscle biopsies (Eisenberg et al., 2008). Vacuolar and swollen mitochondria indicative of structure and functional dysfunction have been observed in HEK cells with mutated GNE (Eisenberg et al., 2008). Since function of mitochondria is dependent on its structure, increased branching of mitochondria observed in cells of GNEM patients could lead to oxidative stress (Eisenberg et al., 2008). Thus, both GNEM and AD show mitochondrial dysfunction. It would be of interest to determine the stage at which mitochondria are affected in GNEM and whether any Aβ accumulation occurs in mitochondria besides rimmed vacuoles.

In AD mouse study, COX gene knock out reduced oxidative stress by reducing Aβ plaque formation (Fukui et al., 2007). Inhibition of COX2 function results in protection of neurons and reduces the accumulation of Aβ in neurons of AD transgenic mice (Woodling et al., 2016). In GNEM, COX7A protein is reported to be upregulated (Eisenberg et al., 2008). Thus, inhibiting COX gene in GNEM may reduce mitochondrial oxidative stress and inhibit Aβ aggregate formation in GNE deficient cells and could serve as an important therapeutic target.

Effect of Oxidative Stress in AD and GNEM

Oxidative stress is a key player in many neurodegenerative diseases. With age, oxidative stress in brain elevates due to imbalance of redox potential leading to generation of reactive oxygen species (ROS) (Andreyev et al., 2005; Wang and Michaelis, 2010). When the amount of ROS species produced is greater than scavenged by ROS defense mechanisms, it leads to oxidative stress leading to cell damage (Feng and Wang, 2012). Reports suggest that Aβ(1-42) accumulation is associated with oxidative stress in hippocampal neuron of *C. elegans* (Yatin et al., 1999). Phosphorylation of tau is also reported to be increased during oxidative stress via activation of glycogen synthase kinase 3-β (Lovell et al., 2004). Aberrant S-nitrosylation of proteins at cysteine residue of ApoE, Cdk5, and PDI leads to oxidative stress and neurodestruction (Zhao et al., 2014). In fact, oxidation of proteins in neurons that control Aβ solubilization and tau hyperphosphorylation severely affect progression of AD.

In GNEM, upregulation of cell stress molecules, such as Aβ oligomers, αβ-crystallin that signals to elevate APP protein was reported (Fischer et al., 2013). Upregulation of iNOS enzyme suggested that cell stress in GNE myopathy is mainly due to NO-related free radicals (Fischer et al., 2013). In GNEM patients and mouse model, proteins were found to be highly modified with S-nitrosylation (Cho et al., 2017). In AD, generation of NO correlates with the activation of iNOS in glial cells. Generation of NO by iNOS is robust and render neurotoxicity, contributing to neuronal death and injury (Zhao et al., 2014). Atrogenes and oxidative stress response proteins are highly upregulated in hyposialylated condition and supplementation with sialic acid restores ROS levels in muscle cells (Cho et al., 2017). Additionally, in HEK293 cell based model system for GNEM overexpressing pathologically relevant GNE mutation, PrdxIV, an ER resident Peroxiredoxin was found to be downregulated. The downregulation of Prdx IV may disturb the redox state of ER, affecting proper folding of proteins eventually leading to ER stress (Chanana et al., 2017). Also expression level of Prdx I and Prdx IV was substantially decreased in post-mortem brain of AD with higher level of protein oxidation (Majd and Power, 2018). These studies suggest that oxidative stress may be common to both the

disorders. ER based peroxiredoxins may play an important role in the pathology of both the diseases.

Role of Endoplasmic Reticulum and Chaperones in Protein Aggregation

Endoplasmic reticulum is an important cellular organelle involved in proper folding and processing of proteins. Perturbation in functioning of ER leads to misfolding of proteins and eventually protein aggregation, which is the key feature in several neurodegenerative diseases. Accumulation of misfolded proteins in ER elicits ER stress and unfolded protein response (UPR) that triggers cell death by apoptosis to eliminate cell toxicity (Tabas and Ron, 2011). Misfolded proteins that are retained in ER undergo proteosomal degradation via ER-associated degradation or ERAD (Smith et al., 2011). Activation of UPR proteins such as IRE1 and chaperone, GRP78, have been reported in the cortex and hippocampal tissue of AD brain (Hoozemans et al., 2005; Lee et al., 2010a). Activation of UPR proteins such as IRE1α, PERK, and ATF6 have been reported in AD by Xiang et al. (2017). Even GNEM muscle biopsies revealed upregulation of different UPR proteins including GRP78/BiP, GRP94, calnexin, and calreticulin, which are ER resident chaperones. The same study showed localization of GRP78/BiP and GRP94 with Aβ in the ER (Li et al., 2013). Upregulation of chaperone GRP94 is reported in HEK cell based model of GNEM (Grover and Arya, 2014). Since upregulation of chaperones is also observed in GNEM, they may play an important role in protein aggregate and subsequently rimmed vacuole formation. Thus, small molecules affecting chaperone activity to enhance proper protein folding and inhibition of protein aggregation offer a promising therapeutic approach for GNEM.

Interestingly, calreticulin, molecular chaperone that modulates Ca^{2+} homeostasis, is downregulated in cortical neurons of AD patients and used as negative biomarker for AD progression (Lin et al., 2014). Another study reported that calreticulin co-localizes with both Aβ and APP and helps in proper folding of Aβ (Johnson et al., 2001). Stemmer et al have showed that calreticulin bound directly with Presenilin and Nicastrin molecular component of γ-secretase, along with Aβ (Stemmer et al., 2013). The binding of calreticulin with γ-secretase may direct the proper binding and cleavage of APP to Aβ. Due to the downregulation of calreticulin in neurons, serum γ-secretase losses its proper cleaving activity leading to misfolded Aβ and accumulation in neurons. Altered calreticulin levels could affect protein folding in GNEM as calreticulin interact with phosphodiisomerase (PDI) to serve chaperone function in ER. PDI interacts with peroxiredoxin IV, which is downregulated in GNE deficient cells (Chanana et al., 2017). Thus, calreticulin may need further investigation towards its role as molecular chaperones in GNEM.

Heat Shock Proteins (HSPs) present in the cytosol also help protein to achieve native structure and avoid aggregation (Franklin et al., 2005; Paul and Mahanta, 2014). Elevated levels of HSP70 and HSP27 were found in brain tissues of AD patients (Perez et al., 1991; Renkawek et al., 1993). HSP70 has been reported to interfere with the secretory pathway of APP by binding to APP and reducing Aβ production. Along with HSP70, HSP90 has been shown to degrade Aβ oligomers and tau via the proteasome degradation pathway (Lu et al., 2014). Overexpression of HSP70 and HSP90 helps to maintain tau homeostasis and increases its solubility, thereby preventing aggregation (Petrucelli et al., 2004). Overexpression of the chaperones also prevents the activation of Caspases, which may lead to neuronal death due to accumulation of aggregated proteins (Sabirzhanov et al., 2012). Proteomic study on GNEM patient biopsies also indicates an increase in HSP70, Crystallin and HSPB1 levels (Sela et al., 2011). Thus, more intensive research is demanded to explore chaperones as therapeutic drug targets for GNEM that can reduce protein aggregation and inhibit rimmed vacuole formation.

Autophagy in AD and GNEM

Autophagy is the major degradative pathway for recycling of various proteins and organelles inside the cell, as it is essential for maintaining a balance between protein synthesis and degradation (Yang et al., 2009). Autophagy has been reported to be elevated when cells sense any kind of stress (Kwang et al., 2008). In AD, number of autophagosomes increase indicative of impaired recycling of cellular constituents (Funderburk et al., 2010). Mutation in Presenilin-1 gene affects lysosome mediated autophagy, reduces p62 protein levels leading to imbalance in tau proteostasis (Chui et al., 1999; Lee et al., 2010b; Tung et al., 2014). Many genes common to autophagy and AD pathology have been identified such as autophagy-related 7 (ATG7), BCL2, Beclin 1 (BECN1/ATG6), cyclin dependent kinase 5 (CDK5), Cathepsin D (CTSD), microtubule associated protein tau (MAPT/TAU), Presenilin-1, α-Synuclein (SNCA/PARK1/NACP), Ubiquitin 1 etc., (Uddin et al., 2018). Aβ accumulated intracellularly also regulates autophagy (Son et al., 2012). Tau pro-aggregates act as targets for macrophagy and chaperone mediated autophagy (Zare-Shahabadi et al., 2015).

Rimmed vacuoles observed in GNEM pathology are also defined as clusters of autophagic vacuoles and multi-lamellar bodies, which contain congophilic amyloid proteins, ubiquitin and tau proteins (Nonaka et al., 2005). Higher expression of lysosomal-associated membrane proteins (LAMPs), LC3 and various other lysosomal proteins involved in autophagic pathway were observed in the skeletal muscle of the mice model for GNEM (Malicdan et al., 2007). Differential regulation of BCL2 in GNEM also supports that some common proteins of autophagy pathway in AD may play a role in GNEM autophagic vacuole formation. A comparison of the autophagic mechanisms in AD vs. GNEM is shown in **Figure 1**. Thus, it would be of interest to study and identify novel targets causing autophagy in GNEM and several autophagy stimulating drugs for AD may serve as therapeutic option for myopathy.

Cell Death and Apoptosis

Cell death is the most common feature of the neurodegenerative diseases and occurs massively. In AD, neuronal loss is mainly in cerebral cortex and limbic lobe (Alzheimer's Association, 2017). There are two major pathways for apoptosis, extrinsic pathway and intrinsic pathway. The extrinsic pathway involves

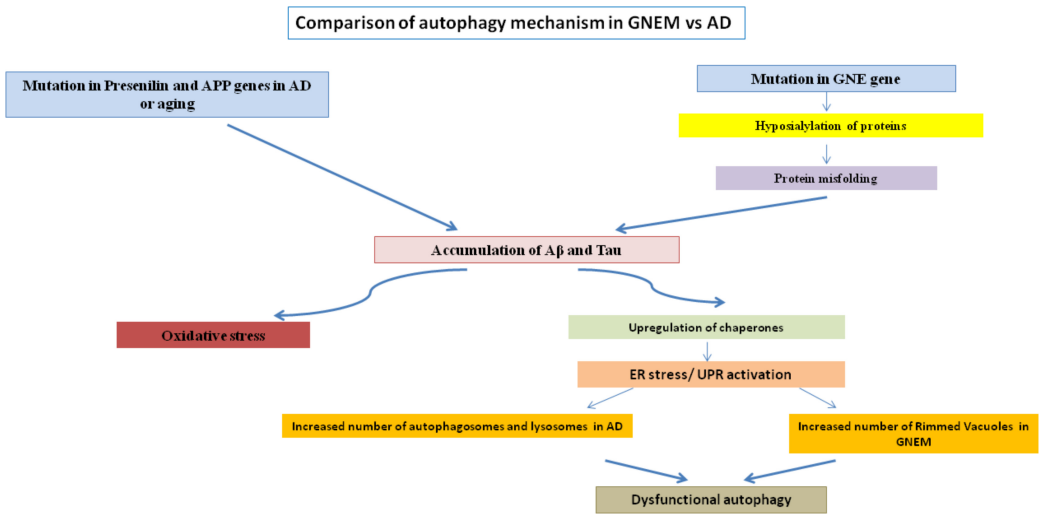


FIGURE 1 | Comparison of autophagy mechanism in AD and GNEM. Mutation in genes of Presenilin and APP for AD and GNE for GNEM leads to the accumulation of various proteins like Aβ and tau. This accumulation causes oxidative stress and ER stress/UPR activation due to upregulation of chaperones, ultimately leading to dysfunctional autophagy as the number of autophagosomes, lysosomes, and rimmed vacuoles increases.

cell surface receptors like TNF in which the binding of Aβ or Aβ oligomers to these receptors remains to be established but the pattern of activation of downstream Caspases (e.g., Caspases 2 and 8) involved in the extrinsic pathway is mediated by Aβ (Ghavami et al., 2014). In the intrinsic pathway, Aβ plays an important role as its intracellular accumulation in the ER cause ER stress and when it binding to a mitochondrial alcohol dehydrogenase leads to mitochondrial stress followed by activation of the downstream apoptotic markers (Lustbader et al., 2004). The upstream mediators of the apoptotic processes are yet to be determined, but the Caspases are activated in the process, which cleaves the tau protein leading to NFT formation (Dickson, 2004). Therefore, in AD, proteolysis of both APP and tau takes place leading to abnormal proteins, which aggregate and form lesions of fibrils extracellularly and intracellularly. Thus, direct involvement of Caspases in apoptosis of neurons is not yet established but many Caspases have been found to play a role in regulation of neuronal death upon Aβ accumulation (Behl, 2000; Dickson, 2004). Aβ(1-42) exposure leads to down regulation of anti-apoptotic proteins like Bcl-2 and upregulation of pro-apoptotic proteins like Bax, cytochrome-c and cleaved caspases in PC12 cells (Chen et al., 2018). Altered levels of various microRNAs that target neuropathological mechanisms have been reported in AD (Ma et al., 2017; Dehghani et al., 2018). Activation of programmed necrosis leading to cell death is reported in the brain of AD patients (Caccamo et al., 2017). The suppression of apoptotic cell signaling pathway proteins such as p38 MAPK can rescue tau pathology in AD (Maphis et al., 2016). These study suggest that various effector molecules targeting signaling proteins in the apoptotic pathway can play a role is preventing cell apoptosis caused due to Aβ accumulation or tau dysfunction and hence potential drug molecules for AD.

In GNEM, degeneration is seen in the myofibrils of the patient muscle biopsies, which might lead to rimmed vacuole formation (Yan et al., 2001). Similar to AD, activation of Caspases 3 and 9 was observed in the myoblast cells of the GNEM patient with M743T kinase mutation (Amsili et al., 2007). Along with this, increased pAKT levels was observed which suggests impairment in the apoptotic event (Amsili et al., 2007). Mitochondrial dependent apoptosis and disruption in both the structure and function of the mitochondria was observed in HEK cell based model system of GNEM over-expressing pathologically relevant GNE mutation (Singh and Arya, 2016). Also, activation of PTEN and PDK1 was observed in the myoblasts which might lead to muscle loss and on stimulation with insulin, activates PI3K and downstream signaling through AKT causing the activation of cell survival pathway (Harazi et al., 2014). Increased Anoikis, apoptosis due to loss of anchorage to extracellular matrix, was observed in pancreatic carcinoma cells when the GNE gene was silenced. Additionally, the level of CHOP has been reported to increase in GNE deficient cells indicative of apoptosis through ATF4-ATF3-CHOP pathway (Kemmner et al., 2012). Increased apoptosis due to internalization of Aβ peptides in hyposialylated C2C12 myotubes and skeletal muscles was observed in the patients of GNEM (Bosch-Morató et al., 2016). This suggests that sialylation has a role in Aβ uptake and cell apoptosis and molecules involved in apoptotic pathway can be therapeutic targets. Thus, molecular and cellular phenomenon for apoptosis in AD and GNEM seem to overlap despite difference in cell types, neuron vs. muscle cell, respectively.

A comparison of the apoptotic mechanisms in AD vs. GNEM has been described in **Figure 2**. Interestingly, treatment of GNE deficient cells with Insulin Growth Factor seems to rescue the apoptotic phenotype and hence could be a potential therapeutic target that counters apoptotic cell toward cell survival (Singh et al., 2018). In summary, proteins and drug molecules that rescue cell death phenomenon in AD by targeting common proteins, can be explored for GNEM therapy.

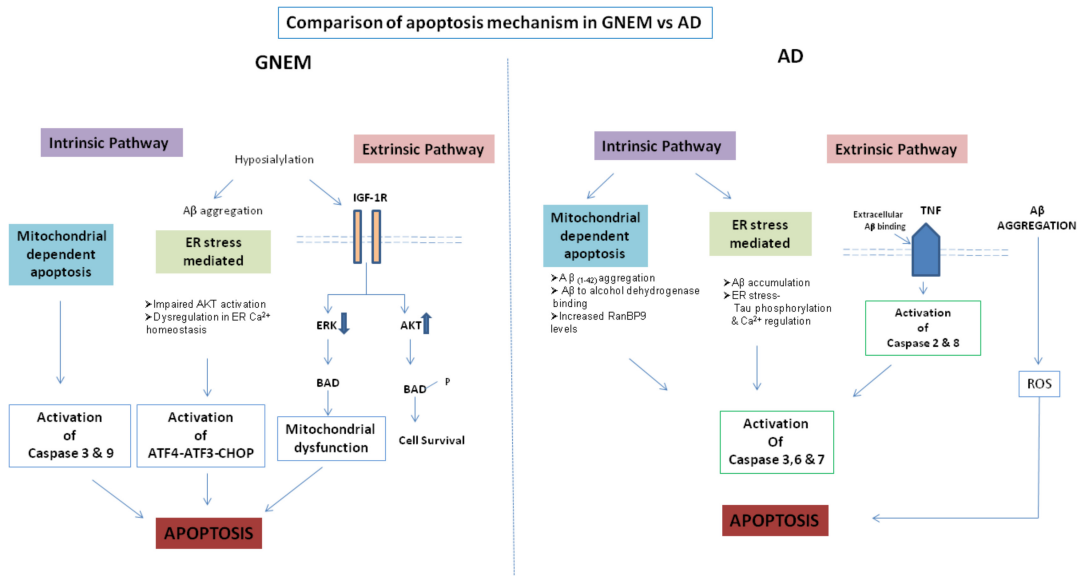


FIGURE 2 | Comparison of apoptosis mechanism in AD and GNEM. In GNEM, intrinsic pathway is mediated through mitochondria as a consequence of mitochondrial dysfunction and consequent release of cytochrome C and activation of executioner caspases-Caspase-3 and Caspase-9. Further, in the extrinsic pathway, mutation in GNE causes hyposialylation of Aβ leading to its aggregation progressing toward ER stress where AKT pathway is impaired and sarcoplasmic calcium is released into the cytoplasm, eventually leading to apoptosis. In the extrinsic pathway, hyposialylation of IGF1R receptor leads to impairment of ERK pathway and activation of BAD, inhibiting anti-apoptotic Bcl-2 and thus leading to apoptosis. Whereas in AD, in the intrinsic pathway, Aβ accumulation and tau phosphorylation in the ER leads to ER stress. In the mitochondria of AD patients, Aβ binds to Aβ binding-alcohol dehydrogenase (ABAD) leading to mitochondrial dysfunction. Both ER and mitochondrial stress lead to activation of effector caspases 3, 6, and 7, which might cleave tau leading to formation of NFTs. In the extrinsic pathway, accumulated Aβ binds to ligand TNF leading to activation of Caspase 2 and 8.

A complete comparison of molecular and cellular changes in AD and GNEM are listed in **Table 2**.

TREATMENT

There is no cure for AD till date as the medications available only help to control the symptoms of AD. The AD drug therapy includes drugs, which target neurotransmitter system of the brain such as Acetylcholinesterase (Ach esterase) inhibitors that increases neurotransmitter levels at synaptic junctions (Schenk et al., 2012). Three FDA approved acetylcholinesterase inhibitors are Rivastigmine, Galantamine (for mild AD), and Donepezil (for all stages of AD) are available (Schenk et al., 2012). Also Memantine, antagonist for *N*-methyl-D-aspartate (NMDA) receptor is used in combination with Ach esterase inhibitor. None of the pharmacological drugs are able to stop the damage and destruction of the neurons therefore, making the disease fatal.

Since, Aβ accumulation is one of the major causes leading to the disease; therefore drugs, which can lower the amount of Aβ accumulation in the brain are of prime importance. Secretase inhibitor drugs, inhibit the cleavage of APP into Aβ, therefore minimizing their accumulation (Imbimbo and Giardina, 2011). Another set of drugs used as a passive vaccination strategy in the form of antibodies, help in the clearance of Aβ species (Schenk et al., 2012). Several drugs were developed which completed Phase-III clinical trials but failed to demonstrate their efficacy in patients. The passive vaccination strategy in case of tau also proved to be ineffective (Wischik et al., 2014). A major limitation with respect to effectiveness of anti-amyloid drugs was thought to be late diagnosis of the disease. Thus, research focussing on the stage of initiation of amyloid formation could offer better drug targets. Indeed aducanumab, human monoclonal antibody, selective for aggregated form of Aβ showed reduced amyloid uptake and improved cognitive function in early AD patients (Scheltens et al., 2016).

In case of GNEM also, there is no treatment therapy available, which could reverse disease progression and stop muscle degeneration. Administration of *N*-acetylmannosamine, neuraminic acid, and sialyllactose in the mouse models of GNEM improved survival of the mouse by reduction in rimmed vacuole formation and β-amyloid deposition (Yonekawa et al., 2014). Gene therapy by administration of GNE gene lipoplex through intravenous infusion to the patients leads to an improvement in muscle strength and increased cell surface sialylation (Nemunaitis et al., 2010). An FDA approved molecular chaperone aiding in protein folding – 4-PBA (4-phenyl butyrate) has been proposed for GNEM (Krause, 2015). Anti-ActII activin antibody (bimagrumab or BYM338), an atrophic protein has been found to be helpful in preventing muscle atrophy in GNEM (Krause, 2015). Some of the compounds are under clinical trials such as sialic acid precursor, *N*-acetylmannosamine (ManNAc), and extended release sialic acid form, aceneuramic acid. However, due to lack of statistical significance in the cohort of patient study, the compound was discontinued by Ultragenyx (Mori-Yoshimura and Nishino, 2015; Argov et al., 2016).

TABLE 2 | Comparison of the molecular and cellular changes in AD and GNEM.

	Molecular and cellular changes in AD and GNEM	
	AD	**GNEM**
Glycosylation	• Impaired glucose metabolism • Glycosylation of proteins affected	• Glycosylation of NCAM, integrin, α-dystroglycan, IGF1R, neprilysin
Sialic acid involvement	Sialic acid dependent binding of Aβ to cells • Decrease Level sialyltransferases	Low Sialic acid production • Hyposialylation of glycoproteins.
Mitochondrial dysfunction	• Mitochondria number reduced • Aβ accumulation in mitochondria • Impaired TCA cycle • Mutation in mtDNA and cytochrome c oxidase • Impaired mitochondrial trafficking	• Vacuolar and swollen mitochondria • Increased branching of mitochondria • Upregulation of mitochondrial proteins like COX, Cytochrome C Oxidase, ATPases, NADH dehydrogenase
Oxidative stress	• Neurotoxicity and protein oxidation due to accumulated Aβ • Increased p-Tau • S-nitrosylation of different proteins like Cdk5, PDI, ApoE	• Upregulation of cell stress molecule • PrdxIV downregulated • Proteins found to be highly S-nitrosylated
ER stress	• XBP1 mRNA splicing leading to activation of IRE1α • GRP78/BiP, GRP94, calnexin and calreticulin upregulated • Co-localization of GRP78/BiP GRP94 and calreticulin with Aβ • Calreticulin binds with presenilin and neprisilin	• Upregulation of different UPR pathway proteins such as GRP78, GRP94, Calreticulin and Calnexin
Protein aggregation	• Aβ and p-tau proteins	• β-amyloid, phosphorylated Tau, TDP-43, α-synuclein
Chaperone involvement	• HSE (Heat Shock Element) associated with APP gene promoter • Elevated levels of HSP70 and HSP27 • HSP90 and HSP70 degrades Aβ oligomers and tau • Higher levels of HSP70 and HSP90 promotes the binding of tau to the microtubules	• Upregulation of various chaperones • The mutant protein preferentially retained in the ER
Apoptosis	• Activation of downstream caspases mediated by Aβ • Caspases cleaves the Tau protein • Nuclear chromatin clumping and apoptotic bodies	• Degeneration in myofibrils • Activation of Caspases 3 and 9 • Mitochondrial dependent apoptosis and disruption of mitochondria • Increased Anoikis • Increased levels of CHOP
Autophagy	• Failure of autophagy • Increased number of autophagosomes and lysosomes • Rab7 and LAMP proteins dysregulated	• Rimmed vacuoles-clusters of the autophagic vacuoles and multi-lamellar bodies • Higher expression of lysosomal-associated membrane proteins (LAMPs), LC3
Inflammation	**Occurs**	**Occurs rarely**
Cytoskeleton framework	• Aggregation of hyperphosphorylated tau • Inactivation of cofilin 1, SSH1 • Rac1 leads to APP accumulation • RhoA increases Aβ • Cofilin-actin rod results in synaptic loss	• GNE interact with Collapsin Response Mediator Protein-1 (CRMP-1), α-actinin-1 and α-actinin-2 • β-integrin mediated cell adhesion affected • Aβ induces FAK

Recent studies in GNEM indicate that sialic acid supplementation alone may not be sufficient to rescue disease phenotype. As discussed above several other cellular phenomena affect GNEM including accumulation of aggregated proteins such as β-amyloid and tau proteins. Sialic acid has been shown to affect β-amyloid uptake in C2C12 myoblast indicating role of sialic acid in β-amyloid uptake (Bosch-Morató et al., 2016). Thus, drug molecules affecting β-amyloid uptake and initiation of Aβ accumulation may serve as better therapeutic targets and offer common mechanism for AD as well as GNEM.

CONCLUSION

While much is known for AD, GNEM is poorly understood rare disease. Lack of number of patient samples for GNEM also limits the study. Also, absence of appropriate animal model system for GNEM, as $GNE^{-/-}$ mice are embryonically lethal at day E8.5, restricts the understanding for genotype to phenotype co-relation. There could be some interesting leads from AD studies that could help explore GNEM pathomechanism. While both diseases have lot of similarities at cellular level such as Aβ amyloid deposition, protein aggregation, autophagic vacuoles, major difference is that in AD, brain/neurons are affected while in GNEM, only muscles in particular anterior tibialis muscle cells are affected. No changes in the neurons of GNEM patients are reported. It would be of interest to study the stage of Aβ deposition in GNE deficient cells and whether protein aggregation could be prevented to slow the disease progression for GNEM. Also, whether there is any genetic predisposition of AD or GNEM in patient families would be important to understand epigenetics of these neurodegenerative disorders. Future studies could be planned toward deciphering common therapeutic targets for these disorders.

AUTHOR CONTRIBUTIONS

SD and RY have written the first draft of the manuscript. PC and RA revised and improved the first draft. RY prepared the tables and **Figure 2**. PC prepared **Figure 1**. RA edited and finalized the version. All authors have seen and agreed on the finally submitted version of the manuscript.

FUNDING

This work was supported by grants from the UPOE-II (Project ID:16), University Grants Commission, India, DST PURSE II (DST/SR/PURSE Phase II/11, Department of Science and Technology, Government of India and SERB (Science and Engineering Research Board) EMR/2015/001798, Government of India. We acknowledge Jawaharlal Nehru University, New Delhi for providing financial assistance towards publication and infrastructure.

ACKNOWLEDGMENTS

We thank Prof. M. A. Kamal, King Fahd Medical Research Center, King Abdulaziz University, Kingdom of Saudi Arabia for fruitful suggestions regarding conceptualizing the review. We also thank Dr. Kulvinder Singh Saini, Professor of Biotechnology, Department of Biology, King Abdulaziz University, Jeddah, Saudi Arabia for support and encouragement.

REFERENCES

Aisa, B., Gil-Bea, F. J., Solas, M., García-Alloza, M., Chen, C. P., Lai, M. K., et al. (2010). Altered NCAM expression associated with the cholinergic system in alzheimer's disease. *J. Alzheimers Dis.* 20, 659–668. doi: 10.3233/JAD-2010-1398

Alzheimer's Association (2017). Alzheimer's disease facts and figures. *Alzheimers Dement.* 13, 325–373. doi: 10.1016/j.jalz.2017.02.001

Amsili, S., Shlomai, Z., Levitzki, R., Krause, S., Lochmuller, H., Ben-Bassat, H., et al. (2007). Characterization of hereditary inclusion body myopathy myoblasts: possible primary impairment of apoptotic events. *Cell Death Differ.* 14, 1916–1924. doi: 10.1038/sj.cdd.4402208

Amsili, S., Zer, H., Hinderlich, S., Krause, S., Becker-Cohen, M., MacArthur, D. G., et al. (2008). UDP-N-acetylglucosamine-2-epimerase/N-acetylmannosamine kinase (GNE) binds to alpha-actinin 1: novel pathways in skeletal muscle? *PLoS One* 3:e2477. doi: 10.1371/journal.pone.0002477

Anada, R. P., Wong, K. T., Malicdan, M. C., Goh, K. J., Hayashi, Y., Nishino, I., et al. (2014). Absence of beta-amyloid deposition in the central nervous system of a transgenic mouse model of distal myopathy with rimmed vacuoles. *Amyloid* 21, 138–139. doi: 10.3109/13506129.2014.889675

Anderson, J. L., Head, S. I., Rae, C., and Morley, J. W. (2002). . Brain function in Duchenne muscular dystrophy. *Brain* 125(Pt 1), 4–13. doi: 10.1093/brain/awf012

Andreyev, A. Y., Kushnareva, Y. E., and Starkov, A. A. (2005). Mitochondrial metabolism of reactive oxygen species. *Biochemistry* 70, 200–214.

Ankarcrona, M., Mangialasche, F., and Winblad, B. (2010). Rethinking Alzheimer's disease therapy: Are mitochondria the key? *J. Alzheimers Dis.* 20, S579–S590. doi: 10.3233/JAD-2010-100327

Argov, Z., Caraco, Y., Lau, H., Pestronk, A., Shieh, P. B., Skrinar, A., et al. (2016). Aceneuramic acid extended release administration maintains upper limb muscle strength in a 48-week study of subjects with GNE myopathy: results from a phase 2, randomized, controlled study. *J. Neuromuscul. Dis.* 3, 49–66. doi: 10.3233/JND-159900

Argov, Z., and Yarom, R. (1984). "Rimmed vacuole myopathy" sparing the quadriceps. A unique disorder in iranian jews. *J. Neurol. Sci.* 64, 33–43. doi: 10.1016/0022-510X(84)90053-4

Ariga, T., Kobayashi, K., Hasegawa, A., Kiso, M., Ishida, H., and Miyatake, T. (2001). Characterization of high-affinity binding between gangliosides and amyloid beta-protein. *Arch Biochem. Biophys.* 388, 225–230. doi: 10.1006/abbi.2001.2304

Bamburg, J. R., Bernstein, B. W., Davis, R. C., Flynn, K. C., Goldsbury, C., Jensen, J. R., et al. (2010). ADF/Cofilin-actin rods in neurodegenerative diseases. *Curr. Alzheimers Res.* 7, 241–250. doi: 10.2174/156720510791050902

Barnes, D. E., and Yaffe, K. (2011). The projected effect of risk factor reduction on Alzheimer's disease prevalence. *Lancet Neurol.* 10, 819–828. doi: 10.1016/S1474-4422(11)70072-2

Barone, E., Mosser, S., and Fraering, P. C. (2014). Inactivation of brain Cofilin-1 by age, Alzheimer's disease and γ-secretase. *Biochim. Biophys. Acta* 1842(12 Pt A), 2500–2509. doi: 10.1016/j.bbadis.2014.10.004

Beach, T. G., Monsell, S. E., Phillips, L. E., and Kukull, W. (2012). Accuracy of the clinical diagnosis of Alzheimer disease at National Institute on Aging Alzheimer Disease Centers, 2005-2010. *J. Neuropathol. Exp. Neurol.* 71, 266–273. doi: 10.1097/NEN.0b013e31824b211b

Behl, C. (2000). Apoptosis and Alzheimer's disease. *J. Neural Transm.* 107, 1325–1344. doi: 10.1007/s007020070021

Bennmann, D., Weidemann, W., Thate, A., Kreuzmann, D., and Horstkorte, R. (2016). Aberrant O-GlcNAcylation disrupts GNE enzyme activity in GNE myopathy. *FEBS J.* 283, 2285–2294. doi: 10.1111/febs.13729

Bhattacharya, S., Khadilkar, S. V., Nalini, A., Ganapathy, A., Mannan, A. U., Majumder, P. P., et al. (2018). Mutation spectrum of GNE myopathy in the Indian sub-continent. *J Neuromuscul. Dis.* 5, 85–92. doi: 10.3233/JND-170270

Boo, J. H., Sohn, J. H., Kim, J. E., Song, H., and Mook-Jung, I. (2008). Rac1 changes the substrate specificity of gamma-secretase between amyloid precursor protein and Notch1. *Biochem. Biophys. Res. Commun.* 372, 913–917. doi: 10.1016/j.bbrc.2008.05.153

Bosch-Morató, M., Iriondo, C., Guivernau, B., Valls-Comamala, V., Vidal, N., Olivé, M., et al. (2016). Increased amyloid β-peptide uptake in skeletal muscle is induced by hyposialylation and may account for apoptosis in GNE myopathy. *Oncotarget* 7, 13354–13371. doi: 10.18632/oncotarget.7997

Broccolini, A., Gidaro, T., De Cristofaro, R., Morosetti, R., Gliubizzi, C., Ricci, E., et al. (2008). Hyposialylation of neprilysin possibly affects its expression and enzymatic activity in hereditary inclusion-body myopathy muscle. *J. Neurochem.* 105, 971–981. doi: 10.1111/j.1471-4159.2007.05208.x

Bubber, P., Haroutunian, V., Fisch, G., Blass, J. P., and Gibson, G. E. (2005). Mitochondrial abnormalities in Alzheimer brain: mechanistic implications. *Ann. Neurol.* 57, 695–703. doi: 10.1002/ana.20474

Caccamo, A., Branca, C., Piras, I. S., Ferreira, E., Huentelman, M. J., Liang, W. S., et al. (2017). Necroptosis activation in Alzheimer's disease. *Nat. Neurosci.* 20, 1236–1246. doi: 10.1038/nn.4608

Castellani, R., Hirai, K., Aliev, G., Drew, K. L., Nunomura, A., Takeda, A., et al. (2002). Role of mitochondrial dysfunction in Alzheimer's disease. *J. Neurosci. Res.* 70, 357–360. doi: 10.1002/jnr.10389

Cha, M. Y., Han, S. H., Son, S. M., Hong, H. S., Choi, Y. J., Byun, J., et al. (2012). Mitochondria-specific accumulation of amyloid β induces mitochondrial dysfunction leading to apoptotic cell death. *PLoS One* 7:e34929. doi: 10.1371/journal.pone.0034929

Chanana, P., Padhy, G., Bhargava, K., and Arya, R. (2017). Mutation in GNE downregulates peroxiredoxin IV altering ER redox homeostasis. *NeuroMolecular Med.* 19, 525–540. doi: 10.1007/s12017-017-8467-5

Chen, K., Lu, Y., Liu, C., Zhang, L., Fang, Z., and Yu, G. (2018). Morroniside prevents H2O2or Aβ1–42-induced apoptosis via attenuating JNK and p38 MAPK phosphorylation. *Eur. J. Pharmacol.* 834, 295–304. doi: 10.1016/j.ejphar.2018.07.047

Cho, A., Malicdan, M. C. V., Miyakawa, M., Nonaka, I., Nishino, I., and Noguchi, S. (2017). Sialic acid deficiency is associated with oxidative stress leading to

muscle atrophy and weakness in the GNE myopathy. *Hum. Mol. Genet.* 274, 19792–19798. doi: 10.1093/hmg/ddx192

Chornenkyy, Y., Wang, W.-X., Wei, A., and Nelson, P. T. (2018). Alzheimer's disease and Type 2 Diabetes mellitus are distinct diseases with potential overlapping metabolic dysfunction upstream of observed cognitive decline. *Brain Pathol.* doi: 10.1111/bpa.12655 [Epub ahead of print].

Chui, D. H., Tanahashi, H., Ozawa, K., Ikeda, S., Checler, F., Ueda, O., et al. (1999). Transgenic mice with Alzheimer presenilin 1 mutations show accelerated neurodegeneration without amyloid plaque formation. *Nat. Med.* 5, 560–564. doi: 10.1038/8438

Chun, Y. S., Park, Y., Oh, H. G., Kim, T. W., Yang, H. O., Park, M. K., et al. (2015). O-GlcNAcylation promotes non-amyloidogenic processing of amyloid-β protein precursor via inhibition of endocytosis from the plasma membrane. *J. Alzheimers Dis.* 44, 261–275. doi: 10.3233/JAD-140096

DeHart, G. W., and Jones, J. C. R. (2004). Myosin-mediated cytoskeleton contraction and Rho GTPases regulate laminin-5 matrix assembly. *Cell Motil. Cytoskeleton* 57, 107–117. doi: 10.1002/cm.10161

Dehghani, R., Rahmani, F., and Rezaei, N. (2018). MicroRNA in Alzheimer's disease revisited: implications for major neuropathological mechanisms. *Rev. Neurosci.* 29, 161–182. doi: 10.1515/revneuro-2017-0042

Dickson, D. W. (2004). Apoptotic mechanisms in Alzheimer neurofibrillary degeneration: cause or effect? *J. Clin. Investigat.* 114, 23–27. doi: 10.1172/JCI22317

Eisenberg, I., Novershtern, N., Itzhaki, Z., Becker-Cohen, M., Sadeh, M., Willems, P. H., et al. (2008). Mitochondrial processes are impaired in hereditary inclusion body myopathy. *Hum. Mol. Genet.* 17, 3663–3674. doi: 10.1093/hmg/ddn261

Feng, Y., and Wang, X. (2012). Antioxidant therapies for Alzheimer's disease. *Oxid. Med. Cell. Longev.* 2012:472932. doi: 10.1155/2012/472932

Fischer, C., Kleinschnitz, K., Wrede, A., Muth, I., Kruse, N., Nishino, I., et al. (2013). Cell stress molecules in the skeletal muscle of GNE myopathy. *BMC Neurol.* 13:24. doi: 10.1186/1471-2377-13-24

Franklin, T. B., Krueger-Naug, A. M., Clarke, D. B., Arrigo, A. P., and Currie, R. W. (2005). The role of heat shock proteins Hsp70 and Hsp27 in cellular protection of the central nervous system. *Int. J. Hyperthermia* 21, 379–392. doi: 10.1080/02656730500069955

Fukui, H., Diaz, F., Garcia, S., and Moraes, C. T. (2007). Cytochrome c oxidase deficiency in neurons decreases both oxidative stress and amyloid formation in a mouse model of Alzheimer's disease. *Proc. Natl. Acad. Sci. U.S.A.* 104, 14163–14168. doi: 10.1073/pnas.0705738104

Funderburk, S. F., Marcellino, B. K., and Yue, Z. (2010). Cell "self-eating" (autophagy) mechanism in Alzheimer's disease. *Mt. Sinai J. Med.* 77, 59–68. doi: 10.1002/msj.20161

Garden, G. A., and La Spada, A. R. (2012). Intercellular (Mis)communication in neurodegenerative disease. *Neuron* 73, 886–901. doi: 10.1016/j.neuron.2012.02.017

Ghavami, S., Shojaei, S., Yeganeh, B., Ande, S. R., Jangamreddy, J. R., Mehrpour, M., et al. (2014). Autophagy and apoptosis dysfunction in neurodegenerative disorders. *Prog. Neurobiol.* 112, 24–49. doi: 10.1016/j.pneurobio.2013.10.004

Goate, A., Chartier-Harlin, M. C., Mullan, M., Brown, J., Crawford, F., Fidani, L., et al. (1991). Segregation of a missense mutation in the amyloid precursor protein gene with familial Alzheimer's disease. *Nature* 349, 704–706. doi: 10.1038/349704a0

Gong, C. X., Liu, F., Grundke-Iqbal, I., and Iqbal, K. (2005). Post-translational modifications of tau protein in Alzheimer's disease. *J. Neural Transm.* 112, 813–838. doi: 10.1007/s00702-004-0221-0

Grover, S., and Arya, R. (2014). Role of UDP-N-acetylglucosamine2-epimerase/N-acetylmannosamine kinase (GNE) in ??1-integrin-mediated cell adhesion. *Mol. Neurobiol.* 50, 257–273. doi: 10.1007/s12035-013-8604-6

Han, H. Y., Zhang, J. P., Ji, S. Q., Liang, Q. M., Kang, H. C., Tang, R. H., et al. (2013). αv and β1 integrins mediate Aβ-induced neurotoxicity in hippocampal neurons via the FAK signaling pathway. *PLoS One* 8:e64839. doi: 10.1371/journal.pone.0064839

Hanger, D. P., Byers, H. L., Wray, S., Leung, K. Y., Saxton, M. J., Seereeram, A., et al. (2007). Novel phosphorylation sites in Tau from Alzheimer brain support a role for casein kinase 1 in disease pathogenesis. *J. Biol. Chem.* 282, 23645–23654. doi: 10.1074/jbc.M703269200

Harazi, A., Becker-Cohen, M., Zer, H., Moshel, O., Hinderlich, S., and Mitrani-Rosenbaum, S. (2017). The interaction of UDP-N-acetylglucosamine 2-Epimerase/N-Acetylmannosamine Kinase (GNE) and Alpha-actinin 2 is altered in GNE Myopathy M743T mutant. *Mol. Neurobiol.* 54, 2928–2938. doi: 10.1007/s12035-016-9862-x

Harazi, A., Chaouat, M., Shlomai, Z., Levitzki, R., Becker-Cohen, M., Sadeh, M., et al. (2014). Survival-apoptosis associated signaling in GNE myopathy-cultured myoblasts. *J. Recept Signal Transduct. Res.* 35, 249–257. doi: 10.3109/10799893.2014.956755

Holtzman, D. M., Morris, J. C., and Goate, A. M. (2011)). Alzheimer's disease: the challenge of the second century. *Sci. Transl. Med.* 3:77sr1. doi: 10.1126/scitranslmed.3002369

Hoozemans, J. J. M., Veerhuis, R., Van Haastert, E. S., Rozemuller, J. M., Baas, F., Eikelenboom, P., et al. (2005). The unfolded protein response is activated in Alzheimer's disease. *Acta Neuropathol.* 110, 165–172. doi: 10.1007/s00401-005-1038-0

Huizing, M., and Krasnewich, D. M. (2009). Hereditary inclusion body myopathy: a decade of progress. *Biochim. Biophys. Acta* 1792, 881–887. doi: 10.1016/j.bbadis.2009.07.001

Huizing, M., Rakocevic, G., Sparks, S. E., Mamali, I., Shatunov, A., Goldfarb, L., et al. (2004). Hypoglycosylation of α-dystroglycan in patients with hereditary IBM due to GNE mutations. *Mol. Genet. Metab.* 81, 196–202. doi: 10.1016/j.ymgme.2003.11.012

Hutton, M., and Hardy, J. (1997). The presenilins and Alzheimer's disease. *Hum. Mol. Genet.* 6, 1639–1646. doi: 10.1093/hmg/6.10.1639

Imbimbo, B. P., and Giardina, G. A. (2011). γ-Secretase Inhibitors and Modulators for the treatment of Alzheimer's disease: disappointments and hopes. *Curr. Top. Med. Chem.* 11, 1555–1570. doi: 10.2174/156802611795860942

Iqbal, K., Alonso, A. D. C., and Grundke-Iqbal, I. (2008). Cytosolic abnormally hyperphosphorylated tau but not paired helical filaments sequester normal MAPs and inhibit microtubule assembly. *J. Alzheimers Dis.* 14, 365–370. doi: 10.3233/JAD-2008-14402

Jay, C. M., Levonyak, N., Nemunaitis, G., Maples, P. B., and Nemunaitis, J. (2009). Hereditary inclusion body myopathy (HIBM2). *Gene Regul. Syst. Biol.* 3, 181–190. doi: 10.4137/GRSB.S2594

Jiang, T., Yu, J. T., Hu, N., Tan, M. S., Zhu, X. C., and Tan, L. (2014). CD33 in Alzheimer's disease. *Mol. Neurobiol.* 49, 529–535. doi: 10.1007/s12035-013-8536-1

Johnson, R. J., Xiao, G., Shanmugaratnam, J., and Fine, R. E. (2001). Calreticulin functions as a molecular chaperone for the beta-amyloid precursor protein. *Neurobiol. Aging* 22, 387–395. doi: 10.1016/S0197-4580(00)00247-5

Kanekura, K., Suzuki, H., Aiso, S., and Matsuoka, M. (2009). ER stress and unfolded protein response in amyotrophic lateral sclerosis. *Mol. Neurobiol.* 39, 81–89. doi: 10.1007/s12035-009-8054-3

Kemmner, W., Kessel, P., Sanchez-Ruderisch, H., Moller, H., Hinderlich, S., Schlag, P. M., et al. (2012). Loss of UDP-N-acetylglucosamine 2-epimerase/N-acetylmannosamine kinase (GNE) induces apoptotic processes in pancreatic carcinoma cells. *FASEB J.* 26, 938–946. doi: 10.1096/fj.11-186700

Kizuka, Y., Kitazume, S., and Taniguchi, N. (2017). N-glycan and Alzheimer's disease. *Biochim. Biophys. Acta* 1861, 2447–2454. doi: 10.1016/j.bbagen.2017.04.012

Koistinen, H., Prinjha, R., Soden, P., Harper, A., Banner, S. J., Pradat, P.-F., et al. (2006). Elevated levels of amyloid precursor protein in muscle of patients with amyotrophic lateral sclerosis and a mouse model of the disease. *Muscle Nerve* 34, 444–450. doi: 10.1002/mus.20612

Köroğlu, Ç, Yılmaz, R., Sorgun, M. H., Solakoğlu, S., and Şener, Ö (2017). GNE missense mutation in recessive familial amyotrophic lateral sclerosis. *Neurogenetics* 18, 237–243. doi: 10.1007/s10048-017-0527-3

Krause, S. (2015). Insights into muscle degeneration from heritable inclusion body myopathies. *Front. Aging Neurosci.* 7:13. doi: 10.3389/fnagi.2015.00013

Kwang, W. K., Hwang, M., Moretti, L., Jaboin, J. J., Cha, Y. I., and Lu, B. (2008). Autophagy upregulation by inhibitors of caspase-3 and mTOR enhances radiotherapy in a mouse model of lung cancer. *Autophagy* 4, 659–668. doi: 10.4161/auto.6058

Lackner, L. L. (2013). Determining the shape and cellular distribution of mitochondria: The integration of multiple activities. *Curr. Opin. Cell Biol.* 25, 471–476. doi: 10.1016/j.ceb.2013.02.011

Lee, J. H., Won, S. M., Suh, J., Son, S. J., Moon, G. J., Park, U. J., et al. (2010a). Induction of the unfolded protein response and cell death pathway in Alzheimer's disease, but not in aged Tg2576 mice. *Exp. Mol. Med.* 42, 386–394. doi: 10.3858/emm.2010.42.5.040

Lee, J. H., Yu, W. H., Kumar, A., Lee, S., Mohan, P. S., Peterhoff, C. M., et al. (2010b). Lysosomal proteolysis and autophagy require presenilin 1 and are disrupted by Alzheimer-related PS1 mutations. *Cell* 141, 1146–1158. doi: 10.1016/j.cell.2010.05.008

Letenneur, L., Launer, L. J., Andersen, K., Dewey, M. E., Ott, A., Copeland, J. R. M., et al. (2000). Education and the risk for Alzheimer's disease: sex makes a difference. EURODEM pooled analyses. *Am. J. Epidemiol.* 151, 1064–1071. doi: 10.1093/oxfordjournals.aje.a010149

Li, H., Chen, Q., Liu, F., Zhang, X., Li, W., Liu, S., et al. (2013). Unfolded Protein Response and activated degradative pathways regulation in GNE myopathy. *PLoS One* 8:e58116. doi: 10.1371/journal.pone.0058116

Lin, Q., Cao, Y., and Gao, J. (2014). Serum calreticulin is a negative biomarker in patients with Alzheimer's disease. *Int. J. Mol. Sci.* 15, 21740–21753. doi: 10.3390/ijms151221740

López-Otín, C., Blasco, M. A., Partridge, L., Serrano, M., and Kroemer, G. (2013). The hallmarks of aging. *Cell* 153, 1194–1217. doi: 10.1016/j.cell.2013.05.039

Lovell, M. A., Xiong, S., Xie, C., Davies, P., and Markesbery, W. R. (2004). Induction of hyperphosphorylated tau in primary rat cortical neuron cultures mediated by oxidative stress and glycogen synthase kinase-3. *J. Alzheimers Dis.* 6, 659–671. doi: 10.3233/JAD-2004-6610

Lu, R.-C., Tan, M.-S., Wang, H., Xie, A.-M., Yu, J.-T., and Tan, L. (2014). Heat shock protein 70 in Alzheimer's disease. *Biomed. Res. Int.* 2014, 1–8. doi: 10.1155/2014/435203

Lustbader, J. W., Cirilli, M., Lin, C., Xu, H. W., Takuma, K., Wang, N., et al. (2004). ABAD directly links Abeta to mitochondrial toxicity in Alzheimer's disease. *Science.* 304, 448–452. doi: 10.1126/science.1091230

Ma, X., Liu, L., and Meng, J. (2017). MicroRNA-125b promotes neurons cell apoptosis and Tau phosphorylation in Alzheimer's disease. *Neurosci. Lett.* 661, 57–62. doi: 10.1016/j.neulet.2017.09.043

Maguire, T. M., and Breen, K. C. (1995). A decrease in neural sialyltransferase activity in Alzheimer's disease. *Dement Geriatr. Cogn. Disord.* 6, 185–190. doi: 10.1159/000106944

Maguire, T. M., Gillian, A. M., O'Mahony, D., Coughlan, C. M., and Breen, K. C. (1994). A decrease in serum sialyltransferase levels in Alzheimer's disease. *Neurobiol. Aging* 15, 99–102. doi: 10.1016/0197-4580(94)90149-X

Majd, S., and Power, J. H. (2018). Oxidative stress and decreased mitochondrial superoxide dismutase 2 and Peroxiredoxin 1 and 4 based mechanism of concurrent activation of AMPK and mTOR in Alzheimer's disease. *Curr. Alzheimer Res.* 15, 764–776. doi: 10.2174/1567205015666180223093020

Malicdan, M. C. V., Noguchi, S., Nonaka, I., Hayashi, Y. K., and Nishino, I. (2007). A Gne knockout mouse expressing human GNE D176V mutation develops features similar to distal myopathy with rimmed vacuoles or hereditary inclusion body myopathy. *Hum. Mol. Genet.* 16, 2669–2682. doi: 10.1093/hmg/ddm220

Maphis, N., Jiang, S., Xu, G., Kokiko-Cochran, O. N., Roy, S. M., Van Eldik, L. J., et al. (2016). Selective suppression of the α isoform of p38 MAPK rescues late-stage tau pathology. *Alzheimers Res. Ther.* 8:54. doi: 10.1186/s13195-016-0221-y

Mokhtar, S. H., Kim, M. J., Magee, K. A., Aui, P. M., Thomas, S., Bakhuraysah, M. M., et al. (2018). Amyloid-beta-dependent phosphorylation of collapsin response mediator protein-2 dissociates kinesin in Alzheimer's disease. *Neural Regen. Res.* 13, 1066–1080. doi: 10.4103/1673-5374.233451

Moniruzzaman, M., Ishihara, S., Nobuhara, M., Higashide, H., and Funamoto, S. (2018). Glycosylation status of nicastrin influences catalytic activity and substrate preference of γ-secretase. *Biochem. Biophys. Res. Commun.* 502, 98–103. doi: 10.1016/j.bbrc.2018.05.126

Montie, H. L., and Durcan, T. M. (2013). The cell and molecular biology of neurodegenerative diseases: an overview. *Front. Neurol.* 4:194. doi: 10.3389/fneur.2013.00194

Mori-Yoshimura, M., and Nishino, I. (2015). Sialic acid replacement therapy for distal myopathy with rimmed vacuoles. *Brain Nerve* 67, 1115–1123.

Mosconi, L. (2005). Brain glucose metabolism in the early and specific diagnosis of Alzheimer's disease: FDG-PET studies in MCI and AD. *Eur. J. Nucl. Med. Mol. Imaging* 32, 486–510. doi: 10.1007/s00259-005-1762-7

Murray, H. C., Low, V. F., Swanson, M. E. V., Dieriks, B. V., Turner, C., Faull, R. L. M., et al. (2016). Distribution of PSA-NCAM in normal, Alzheimer's and Parkinson's disease human brain. *Neuroscience* 330, 359–375. doi: 10.1016/j.neuroscience.2016.06.003

Nakagawa, K., Kitazume, S., Oka, R., Maruyama, K., Saido, T. C., Sato, Y., et al. (2006). Sialylation enhances the secretion of neurotoxic amyloid-β peptides. *J. Neurochem.* 96, 924–933. doi: 10.1111/j.1471-4159.2005.03595.x

Nalini, A., Gayathri, N., and Dawn, R. (2010). Distal myopathy with rimmed vacuoles: report on clinical characteristics in 23 cases. *Neurol. India* 58, 235–241. doi: 10.4103/0028-3886.63804

Nalini, A., Nishino, I., Gayathri, N., and Hayashi, Y. (2013). GNE myopathy in India. *Neurol. India* 61:371. doi: 10.4103/0028-3886.117609

Narici, M. V., and Maffulli, N. (2010). Sarcopenia: characteristics, mechanisms and functional significance. *Br. Med. Bull.* 95, 139–159. doi: 10.1093/bmb/ldq008

Nemunaitis, G., Maples, P. B., Jay, C., Gahl, W. A., Huizing, M., Poling, J., et al. (2010). Hereditary inclusion body myopathy: single patient response to GNE gene Lipoplex therapy. *J. Gene. Med.* 12, 403–412. doi: 10.1002/jgm.1450

Nogalska, A., D'Agostino, C., Engel, W. K., Cacciottolo, M., Asada, S., Mori, K., et al. (2015). Activation of the unfolded protein response in sporadic inclusion-body myositis but not in hereditary GNE inclusion-body myopathy. *J. Neuropathol. Exp. Neurol.* 74, 538–546. doi: 10.1097/NEN.0000000000000196

Noguchi, S., Keira, Y., Murayama, K., Ogawa, M., Fujita, M., Kawahara, G., et al. (2004). Reduction of UDP-N-acetylglucosamine 2-Epimerase/N-Acetylmannosamine kinase activity and sialylation in distal Myopathy with rimmed vacuoles. *J. Biol. Chem.* 279, 11402–11407. doi: 10.1074/jbc.M313171200

Nonaka, I., Noguchi, S., and Nishino, I. (2005). Distal myopathy with rimmed vacuoles and hereditary inclusion body myopathy. *Curr. Neurol. Neurosci. Rep.* 5, 61–65. doi: 10.1007/s11910-005-0025-0

Norfray, J. F., and Provenzale, J. M. (2004). Alzheimer's disease: neuropathologic findings and recent advances in imaging. *Am. J. Roentgenol.* 182, 3–13. doi: 10.2214/ajr.182.1.1820003

Ott, A., Stolk, R. P., van Harskamp, F., Pols, H. A., Hofman, A., and Breteler, M. M. (1999). Diabetes mellitus and the risk of dementia: the rotterdam study. *Neurology* 53, 1937–1942. doi: 10.1212/WNL.53.9.1937

Paul, S., and Mahanta, S. (2014). Association of heat-shock proteins in various neurodegenerative disorders: Is it a master key to open the therapeutic door? *Mol. Cell. Biochem.* 386, 45–61. doi: 10.1007/s11010-013-1844-y

Peila, R., Rodriguez, B. L., and Launer, L. J. (2002). Type 2 diabetes, APOE gene, and the risk for dementia and related pathologies. *Diabetes* 51, 1256–1262. doi: 10.2337/diabetes.51.4.1256

Penzes, P., and Rafalovich, I. (2012). Regulation of the actin cytoskeleton in dendritic spines. *Adv. Exp. Med. Biol.* 970, 81–95. doi: 10.1007/978-3-7091-0932-8_4

Perez, N., Sugar, J., Charya, S., Johnson, G., Merril, C., Bierer, L., et al. (1991). Increased synthesis and accumulation of heat shock 70 proteins in Alzheimer's disease. *Mol. Brain Res.* 11, 249–254. doi: 10.1016/0169-328X(91)90033-T

Petrucelli, L., Dickson, D., Kehoe, K., Taylor, J., Snyder, H., Grover, A., et al. (2004). CHIP and Hsp70 regulate tau ubiquitination, degradation and aggregation. *Hum. Mol. Genet.* 13, 703–714. doi: 10.1093/hmg/ddh083

Querfurth, H. W., and LaFerla, F. M. (2010). Alzheimer's disease. *N. Engl. J. Med.* 362, 329–344. doi: 10.1056/NEJMra0909142

Reilly, C. E. (2001). Neprilysin content is reduced in Alzheimer brain areas. *J. Neurol.* 248, 159–160. doi: 10.1007/s004150170259

Reiman, E. M., Chen, K., Alexander, G. E., Caselli, R. J., Bandy, D., Osborne, D., et al. (2005). Correlations between apolipoprotein E epsilon4 gene dose and brain-imaging measurements of regional hypometabolism. *Proc. Natl. Acad. Sci. U.S.A.* 102, 8299–8302. doi: 10.1073/pnas.0500579102

Renkawek, K., Bosman, G. J., and Gaestel, M. (1993). Increased expression of heat-shock protein 27 kDa in Alzheimer disease: a preliminary study. *Neuroreport* 5, 14–16. doi: 10.1097/00001756-199310000-00003

Ricci, E., Broccolini, A., Gidaro, T., Morosetti, R., Gliubizzi, C., Frusciante, R., et al. (2006). NCAM is hyposialylated in hereditary inclusion body myopathy due to GNE mutations. *Neurology* 66, 755–758. doi: 10.1212/01.wnl.0000200956.76449.3f

Ricotti, V., Roberts, R. G., and Muntoni, F. (2011). Dystrophin and the brain. *Dev. Med. Child Neurol.* 53, 12–12. doi: 10.1111/j.1469-8749.2010.03836.x

Roussel, B. D., Kruppa, A. J., Miranda, E., Crowther, D. C., Lomas, D. A., and Marciniak, S. J. (2013). Endoplasmic reticulum dysfunction in neurological disease. *Lancet Neurol.* 12, 105–118. doi: 10.1016/S1474-4422(12)70238-7

Rui, Y., Tiwari, P., Xie, Z., and Zheng, J. Q. (2006). Acute impairment of mitochondrial trafficking by beta-amyloid peptides in hippocampal neurons. *J. Neurosci.* 26, 10480–10487. doi: 10.1523/JNEUROSCI.3231-06.2006

Rust, M. B. (2015). ADF/cofilin: a crucial regulator of synapse physiology and behavior. *Cell. Mol. Life Sci.* 72, 3521–3529. doi: 10.1007/s00018-015-1941-z

Sabirzhanov, B., Stoica, B. A., Hanscom, M., Piao, C. S., and Faden, A. I. (2012). Over-expression of HSP70 attenuates caspase-dependent and caspase-independent pathways and inhibits neuronal apoptosis. *J. Neurochem.* 123, 542–554. doi: 10.1111/j.1471-4159.2012.07927.x

Salama, M., Shalash, A., Magdy, A., Makar, M., Roushdy, T., Elbalkimy, M., et al. (2018). Tubulin and tau: possible targets for diagnosis of Parkinson's and Alzheimer's diseases. *PLoS One* 13:e0196436. doi: 10.1371/journal.pone.0196436

Schedin-Weiss, S., Winblad, B., and Tjernberg, L. O. (2014). The role of protein glycosylation in Alzheimer disease. *FEBS J.* 281, 46–62. doi: 10.1111/febs.12590

Scheltens, P., Blennow, K., Breteler, M. M. B., de Strooper, B., Frisoni, G. B., Salloway, S., et al. (2016). Alzheimer's disease. *Lancet* 388, 505–517. doi: 10.1016/S0140-6736(15)01124-1

Schenk, D., Basi, G. S., and Pangalos, M. N. (2012). Treatment strategies targeting amyloid β-protein. *Cold Spring Harb. Perspect. Med.* 2:a006387. doi: 10.1101/cshperspect.a006387

Schnaar, R. L., Gerardy-Schahn, R., and Hildebrandt, H. (2014). Sialic acids in the brain: gangliosides and polysialic acid in nervous system development, stability, disease, and regeneration. *Physiol. Rev.* 94, 461–518. doi: 10.1152/physrev.00033.2013

Sela, I., Krentsis, I. M., Shlomai, Z., Sadeh, M., Dabby, R., Argov, Z., et al. (2011). The proteomic profile of hereditary inclusion body myopathy. *PLoS One* 6:e16334. doi: 10.1371/journal.pone.0016334

Serrano-Pozo, A., Frosch, M. P., Masliah, E., and Hyman, B. T. (2011). Neuropathological alterations in Alzheimer disease. *Cold Spring Harb. Perspect. Med.* 1:a006189. doi: 10.1101/cshperspect.a006189

Sibille, E. (2013). Molecular aging of the brain, neuroplasticity, and vulnerability to depression and other brain-related disorders. *Dialogues Clin. Neurosci.* 15, 53–65.

Siddiqui, S. S., Springer, S. A., Verhagen, A., Sundaramurthy, V., Alisson-Silva, F., Jiang, W., et al. (2017). The Alzheimer's Disease-protective CD33 splice variant mediates adaptive loss of function via diversion to an intracellular pool. *J. Biol. Chem.* 292, 15312–15320. doi: 10.1074/jbc.M117.799346

Singh, R., and Arya, R. (2016). GNE Myopathy and cell apoptosis: a comparative mutation analysis. *Mol. Neurobiol.* 53, 3088–3101. doi: 10.1007/s12035-015-9191-5

Singh, R., Chaudhary, P., and Arya, R. (2018). Role of IGF-1R in ameliorating apoptosis of GNE deficient cells. *Sci. Rep.* 8:7323. doi: 10.1038/s41598-018-25510-9

Siparsky, P. N., Kirkendall, D. T., and Garrett, W. E. (2014). Muscle changes in aging: understanding sarcopenia. *Sports Health* 6, 36–40. doi: 10.1177/1941738113502296

Smith, M. H., Ploegh, H. L., and Weissman, J. S. (2011). Road to ruin: targeting proteins for degradation in the endoplasmic reticulum. *Science* 334, 1086–1090. doi: 10.1126/science.1209235

Son, S. M., Jung, E. S., Shin, H. J., Byun, J., and Mook-Jung, I. (2012). Aβ-induced formation of autophagosomes is mediated by RAGE-CaMKKβ-AMPK signaling. *Neurobiol. Aging* 33:1006.e11-23. doi: 10.1016/j.neurobiolaging.2011.09.039

Souchay, C., and Moulin, C. (2009). Memory and consciousness in Alzheimers disease. *Curr. Alzheimer Res.* 6, 186–195. doi: 10.2174/156720509788486545

Spiro, R. G. (2002). Protein glycosylation: nature, distribution, enzymatic formation, and disease implications of glycopeptide bonds. *Glycobiology* 12, 43R–56R. doi: 10.1093/glycob/12.4.43R

Stemmer, N., Strekalova, E., Djogo, N., Plöger, F., Loers, G., Lutz, D., et al. (2013). Generation of amyloid-β is reduced by the interaction of calreticulin with amyloid precursor protein, presenilin and Nicastrin. *PLoS One* 8:e61299. doi: 10.1371/journal.pone.0061299

Stone, S., and Lin, W. (2015). The unfolded protein response in multiple sclerosis. *Front. Neurosci.* 9:264. doi: 10.3389/fnins.2015.00264

Supnet, C., and Bezprozvanny, I. (2010). Neuronal calcium signaling, mitochondrial dysfunction, and Alzheimer's disease. *J. Alzheimers Dis.* 20(Suppl. 2), S487–S498. doi: 10.3233/JAD-2010-100306

Swerdlow, R. H. (2018). Mitochondria and mitochondrial cascades in Alzheimer's disease. *J. Alzheimers Dis.* 62, 1403–1416. doi: 10.3233/JAD-170585

Tabas, I., and Ron, D. (2011). Integrating the mechanisms of apoptosis induced by endoplasmic reticulum stress. *Nat. Cell Biol.* 13, 184–190. doi: 10.1038/ncb0311-184

Taylor, J. P., Brown, R. H., and Cleveland, D. W. (2016). Decoding ALS: from genes to mechanism. *Nature* 539, 197–206. doi: 10.1038/nature20413

Thibault, O., Hadley, R., and Landfield, P. W. (2001). Elevated postsynaptic [Ca2 +]i and L-type calcium channel activity in aged hippocampal neurons: relationship to impaired synaptic plasticity. *J. Neurosci.* 21, 9744–9756. doi: 10.1523/JNEUROSCI.21-24-09744.2001

Thibault, O., Porter, N. M., Chen, K. C., Blalock, E. M., Kaminker, P. G., Clodfelter, G. V., et al. (1998). Calcium dysregulation in neuronal aging and Alzheimer's disease: History and new directions. *Cell Calcium* 24, 417–433. doi: 10.1016/S0143-4160(98)90064-1

Tung, Y. T., Wang, B. J., Hsu, W. M., Hu, M. K., Her, G. M., Huang, W. P., et al. (2014). Presenilin-1 regulates the expression of p62 to govern p62-dependent tau degradation. *Mol. Neurobiol.* 49, 10–27. doi: 10.1007/s12035-013-8482-y

Uddin, M. S., Stachowiak, A., Al Mamun, A., Tzvetkov, N. T., Takeda, S., Atanasov, A. G., et al. (2018). Autophagy and Alzheimer's disease: from molecular mechanisms to therapeutic implications. *Front. Aging Neurosci.* 10:04. doi: 10.3389/fnagi.2018.00004

Wang, B. (2009). Sialic Aacid is an essential nutrient for brain development and cognition. *Annu. Rev. Nutr.* 29, 177–222. doi: 10.1146/annurev.nutr.28.061807.155515

Wang, P.-L., Niidome, T., Akaike, A., Kihara, T., and Sugimoto, H. (2009). Rac1 inhibition negatively regulates transcriptional activity of the amyloid precursor protein gene. *J. Neurosci. Res.* 87, 2105–2114. doi: 10.1002/jnr.22039

Wang, X., and Michaelis, E. K. (2010). Selective neuronal vulnerability to oxidative stress in the brain. *Front. Aging Neurosci.* 2:12. doi: 10.3389/fnagi.2010.00012

Wang, Z., Sun, Z., Li, A. V., and Yarema, K. J. (2006). Roles for UDP-GlcNAc 2-epimerase/ManNAc 6-kinase outside of sialic acid biosynthesis: modulation of sialyltransferase and BiP expression, GM3 and GD3 biosynthesis, proliferation, and apoptosis, and ERK1/2 phosphorylation. *J. Biol. Chem.* 281, 27016–27028. doi: 10.1074/jbc.M604903200

Weidemann, W., Stelzl, U., Lisewski, U., Bork, K., Wanker, E. E., Hinderlich, S., et al. (2006). The collapsin response mediator protein 1 (CRMP-1) and the promyelocytic leukemia zinc finger protein (PLZF) bind to UDP-N-acetylglucosamine 2-epimerase/N-acetylmannosamine kinase (GNE), the key enzyme of sialic acid biosynthesis. *FEBS Lett.* 580, 6649–6654. doi: 10.1016/j.febslet.2006.11.015

Wischik, C. M., Harrington, C. R., and Storey, J. M. D. (2014). Tau-aggregation inhibitor therapy for Alzheimer's disease. *Biochem. Pharmacol.* 88, 529–539. doi: 10.1016/j.bcp.2013.12.008

Wiseman, F. K., Al-Janabi, T., Hardy, J., Karmiloff-Smith, A., Nizetic, D., Tybulewicz, V. L. J., et al. (2015). A genetic cause of Alzheimer disease: Mechanistic insights from Down syndrome. *Nat. Rev. Neurosci.* 16, 564–574. doi: 10.1038/nrn3983

Woodling, N. S., Colas, D., Wang, Q., Minhas, P., Panchal, M., Liang, X., et al. (2016). Cyclooxygenase inhibition targets neurons to prevent early behavioural decline in Alzheimer's disease model mice. *Brain* 139(Pt 7), 2063–2081. doi: 10.1093/brain/aww117

Xiang, C., Wang, Y., Zhang, H., and Han, F. (2017). The role of endoplasmic reticulum stress in neurodegenerative disease. *Apoptosis* 22, 1–26. doi: 10.1007/s10495-016-1296-4

Xie, T., Yan, C., Zhou, R., Zhao, Y., Sun, L., Yang, G., et al. (2014). Crystal structure of the γ-secretase component nicastrin. *Proc. Natl. Acad. Sci. U.S.A.* 111, 13349–13354. doi: 10.1073/pnas.1414837111

Yan, C., Ikezoe, K., and Nonaka, I. (2001). Apoptotic muscle fiber degeneration in distal myopathy with rimmed vacuoles. *Acta Neuropathol.* 101, 9–16.

Yang, D.-S., Lee, J.-H., and Nixon, R. A. (2009). Monitoring autophagy in Alzheimer's disease and related neurodegenerative diseases. *Methods Enzymol.* 453, 111–144. doi: 10.1016/S0076-6879(08)04006-8

Yang, D. S., Tandon, A., Chen, F., Yu, G., Yu, H., Arawaka, S., et al. (2002). Mature glycosylation and trafficking of nicastrin modulate its binding to presenilins. *J. Biol. Chem.* 277, 28135–28142. doi: 10.1074/jbc.M110871200

Yatin, S. M., Varadarajan, S., Link, C. D., and Butterfield, D. A. (1999). In vitro and in vivo oxidative stress associated with Alzheimer's amyloid beta-peptide (1-42). *Neurobiol. Aging* 20, 325–330.

Yonekawa, T., Malicdan, M. C. V., Cho, A., Hayashi, Y. K., Nonaka, I., Mine, T., et al. (2014). Sialyllactose ameliorates myopathic phenotypes in symptomatic GNE myopathy model mice. *Brain* 137, 2670–2679. doi: 10.1093/brain/awu210

Zare-Shahabadi, A., Masliah, E., Johnson, G. V. W., and Rezaei, N. (2015). Autophagy in Alzheimer's disease. *Rev. Neurosci.* 26, 385–395. doi: 10.1515/revneuro-2014-0076

Zhang, W., Huang, Y., and Gunst, S. J. (2012). The small GTPase RhoA regulates the contraction of smooth muscle tissues by catalyzing the assembly of cytoskeletal signaling complexes at membrane adhesion sites. *J. Biol. Chem.* 287, 33996–34008. doi: 10.1074/jbc.M112.369603

Zhang, Y., Thompson, R., Zhang, H., and Xu, H. (2011). APP processing in Alzheimer's disease. *Mol. Brain* 4:3. doi: 10.1186/1756-6606-4-3

Zhao, Q. F., Yu, J. T., and Tan, L. (2014). S-Nitrosylation in Alzheimer's disease. *Mol. Neurobiol.* 51, 268–280. doi: 10.1007/s12035-014-8672-2

Conflict of Interest Statement: The authors declare that the research was conducted in the absence of any commercial or financial relationships that could be construed as a potential conflict of interest.

Copyright © 2018 Devi, Yadav, Chanana and Arya. This is an open-access article distributed under the terms of the Creative Commons Attribution License (CC BY). The use, distribution or reproduction in other forums is permitted, provided the original author(s) and the copyright owner(s) are credited and that the original publication in this journal is cited, in accordance with accepted academic practice. No use, distribution or reproduction is permitted which does not comply with these terms.

frontiers in Neuroscience

REVIEW
published: 08 June 2018
doi: 10.3389/fnins.2018.00383

Alzheimer's Disease and Type 2 Diabetes: A Critical Assessment of the Shared Pathological Traits

Shreyasi Chatterjee and Amritpal Mudher*

Centre of Biological Sciences, University of Southampton, Southampton, United Kingdom

Alzheimer's disease (AD) and Type 2 Diabetes Mellitus (T2DM) are two of the most prevalent diseases in the elderly population worldwide. A growing body of epidemiological studies suggest that people with T2DM are at a higher risk of developing AD. Likewise, AD brains are less capable of glucose uptake from the surroundings resembling a condition of brain insulin resistance. Pathologically AD is characterized by extracellular plaques of Aβ and intracellular neurofibrillary tangles of hyperphosphorylated tau. T2DM, on the other hand is a metabolic disorder characterized by hyperglycemia and insulin resistance. In this review we have discussed how Insulin resistance in T2DM directly exacerbates Aβ and tau pathologies and elucidated the pathophysiological traits of synaptic dysfunction, inflammation, and autophagic impairments that are common to both diseases and indirectly impact Aβ and tau functions in the neurons. Elucidation of the underlying pathways that connect these two diseases will be immensely valuable for designing novel drug targets for Alzheimer's disease.

Keywords: insulin resistance, tau proteins, abeta oligomers, synaptic dysfunction, autophagy, inflammation

OPEN ACCESS

Edited by:
Athanasios Alexiou, Novel Global Community Educational Foundation (NGCEF), Hebersham, Australia

Reviewed by:
Roland Brandt, University of Osnabrück, Germany
Subashchandrabose Chinnathambi, National Chemical Laboratory (CSIR), India

****Correspondence:***
Shreyasi Chatterjee
s.chatterjee@soton.ac.uk

Specialty section:
This article was submitted to Neurodegeneration, a section of the journal Frontiers in Neuroscience

Received: *31 January 2018*
Accepted: *22 May 2018*
Published: *08 June 2018*

Citation:
Chatterjee S and Mudher A (2018) Alzheimer's Disease and Type 2 Diabetes: A Critical Assessment of the Shared Pathological Traits. Front. Neurosci. 12:383. doi: 10.3389/fnins.2018.00383

INTRODUCTION

Alzheimer's Disease: Neuropathological Alterations and Metabolic Risk Factors

Diagnosed by the German psychiatrist and neuropathologist, Prof. Alois Alzheimer in 1906, Alzheimer's disease is the most prevalent form of dementia in the aging population (van der Flier and Scheltens, 2005). Recently declared as the sixth major cause of death in the world, patients affected with AD suffer a gradual decline of cognitive abilities and memory functions till the disease renders them incapable of performing daily functions (James et al., 2014). Statistical data reveals that over 30 million people are suffering from AD worldwide and this number is estimated to double every 20 years to reach 66 million in 2030 and about 115 million by 2050[1].

Clinically AD can be classified into two subtypes. About 95% 0f AD patients are aged 65 years or older and are diagnosed with "late-onset" or "sporadic AD" (sAD) while 5% of AD patients carry rare genetic mutations associated with "early-onset" or "familial AD" (fAD) that causes the onset of disease symptoms in a person's thirties, forties, or fifties (De Strooper, 2007). In early onset fAD, the disease pathology is caused by mutation in three known genes namely: amyloid precursor protein (APP), presenilin-1 (PS-1), and presenilin-2(PS-2). Although PS-1 mutations account for most of the fAD, there are mutations outside these three genes that are yet unknown. Unlike the fAD, the genetics of sAD is more complex (Dorszewska et al., 2016).

[1] Available online at: https://www.alz.co.uk/research/WorldAlzheimerReport2015.pdf.

Other than aging, which is the strongest risk factor for sAD, GWAS studies reveal that the epsilon four allele of the apolipoprotein E (ApoE4) gene is a significant risk factor for the development of this disease. Two copies of ApoE4 gene increases risk of AD by 12-fold, while one copy of this allele enhances the risk by 4-fold (Bertram and Tanzi, 2009). However, only 50–60% individuals are carriers of this gene suggesting that other factors also confer risk. Studies suggest that these include factors such as cerebrovascular infarction, family history of diabetes, hypertension, and obesity (Li et al., 2015a).

At a cellular level, AD is characterized by a progressive loss of pyramidal cells in the entorhinal cortex and CA1 region of the hippocampus that are responsible for maintenance of higher cognitive functions (Serrano-Pozo et al., 2011). Early symptoms of AD are also marked by synaptic dysfunction that disrupts connectivity between neural circuits, thereby initiating the gradual loss of memory.

Neuropathologically, AD is characterized by extracellular plaques of insoluble amyloid-β protein, and intracellular neurofibrillary tangles (NFTs) of hyperphosphorylated tau protein (Iqbal et al., 2010; Serrano-Pozo et al., 2011). In AD, abnormal cleavage of APP results in the formation of insoluble amyloid-β protein, densely packed with beta sheets, which form the core of the senile plaques (Serpell et al., 2000). Tau protein, in a physiological state serves as a microtubule binding protein and plays an important role in axonal and vesicular transport (Mandelkow and Mandelkow, 1995). Conversely, in the disease state tau protein is hyperphosphorylated and detached from the microtubules. In animal models this phospho-tau-mediated disruption of cytoskeletal integrity manifests in synaptic and behavioral impairments (Mudher et al., 2004; Quraishe et al., 2013; Gilley et al., 2016; Lathuilière et al., 2017). Although a large body of *in vitro* studies have investigated tau-microtubule binding interactions, most of these studies have been conducted *in silico* or in non-neural cellular models (Kadavath et al., 2015; Huda et al., 2017). In a series of elegant experiments involving single-molecule tracking of tau in axonal processes, Niewidok et al. and Janning et al. have shown that the interaction of tau with the microtubules follows a "kiss-and-hop" mechanism. Their studies show that a single tau molecule resides only 40 ms on a particular microtubule and then hops longitudinally and transversely on adjacent microtubules. This novel mechanism has been particularly effective in resolving the paradoxical observation that despite regulating microtubule dynamics, alterations in tau levels may not interfere with axonal transport (Janning et al., 2014; Niewidok et al., 2016). Using pseudo-hyperphosphorylated tau constructs they observed a considerable weakening of the tau-microtubule interactions that corroborated with previous *in vitro* studies.

A large body of evidence supports the idea that the formation of Aβ plaques occurs 15–20 years earlier before the cognitive functions decline, whereas the spatial and temporal spread of tau pathology correlates more strongly with the severity with disease progression (Serrano-Pozo et al., 2011; Vlassenko et al., 2012). Although Aβ and tau are the pathological hallmarks that characterize sAD, it is not yet clear whether these two factors trigger AD or if they are manifested as the effect of the disease.

The drug therapy of AD is still at a nascent stage providing symptomatic relief but not slowing down disease progression. Such treatments include FDA-approved choline esterase inhibitors and NMDA (glutamate) receptor agonists. Thus, from a public health perspective AD exerts a significant healthcare burden that is expected to escalate 5-fold in the coming decades. Hence, the need for early detection and effective treatment is an urgent priority (Yiannopoulou and Papageorgiou, 2013).

In recent times, it has been hypothesized that various risk factors promote Aβ and tau-related pathological changes before the onset of clinical symptoms in AD. One of the formidable challenges of the twenty-first century is to identify these risk factors and enable early detection of pathophysiological alterations at the cellular and biochemical level so that effective treatments can be designed against this devastating disease. A significant risk factor associated with sAD that has received a considerable attention in recent times is Type 2 Diabetes (T2D) (Li et al., 2015a).

Type 2 Diabetes

Diabetes mellitus is a chronic metabolic disorder that is increasing worldwide at an alarming rate. It is estimated that 387 million people are affected by Type1 and T2DM and this number is expected to reach 552 million by 2030 (American Diabetes, 2009). The financial costs for the treatment of diabetes and support for the patients presents a significant healthcare challenge for any country across the world.

The most prevalent subtype of diabetes is the Type 2 diabetes mellitus (T2DM) that comprises 95% of this disease. The salient features of T2DM are high levels of blood glucose (hyperglycaemia), hyper-insulinemia, and insulin resistance (Taylor, 2012). Insulin resistance arises due to decreased insulin sensitivity of muscle, liver, and fat cells to insulin. Another prominent feature of T2DM is the formation of human islet amyloid polypeptide that causes pancreatic β-cell dysfunction (Marzban et al., 2003). Both these features ultimately result in a reduced uptake of circulating blood glucose for glycogenesis eventually leading to chronic hyperglycemia as one of the pathological hallmarks of T2DM.

What is the evidence that there is a patho-physiological link between Diabetes and AD?

Evidence From Epidemiological Studies

Epidemiological studies show that T2DM increases the risk of AD by at least 2-fold (Barbagallo and Dominguez, 2014). In a study cohort recruited from Manhattan in 1992–1994 and then in 1999–2001 Cheng et al. demonstrated that T2DM is associated strongly with late-onset AD (LOAD) after adjustment of sex and age. Their findings also suggested that the link between T2DM and LOAD is partly mediated by cerebrovascular pathology (Cheng et al., 2011). Recent studies from Li et al. report that T2DM in an elderly Chinese population with mild cognitive impairment (MCI) influences the progression to AD, while no change is observed in age-matched controls (Li et al., 2016). These data are supported by longitudinal studies conducted by Leibson et al. and Huang et al. in which patients with adult onset

diabetes exhibited a significantly higher risk of developing AD than age-matched subjects without T2DM (Leibson et al., 1997; Huang et al., 2014). Epidemiological studies have also examined the association between ApoE4 genotype and diabetes or insulin resistance, although the reports are controversial. For instance, a longitudinal study in Japanese-American men demonstrated that ApoE4 increases the risk of LOAD in individuals with T2DM (Peila et al., 2002). In contrast, population-based studies conducted by Marseglia et al. show an association between T2DM and risk of dementia only in ApoE4 non-carriers (Marseglia et al., 2016).

Evidence From Neuroimaging Studies

The evidence from epidemiological studies has recently been corroborated by findings from neuroimaging studies (PET and MRI) that monitor the structural alterations in brains of patients affected by AD and T2DM. The data from the neuroimaging studies reveals a considerable overlap between the vulnerable brain regions in both patient groups.

AD is generally associated with widespread brain atrophy that initiates in the transentorhinal and entorhinal cortex in the early stages and then spreads to the remaining neocortical areas (Fjell et al., 2015). Neuroimaging studies show that the widespread pattern of neurodegeneration caused by AD in the limbic and neocortical regions correlates closely with cognitive deficits and behavioral patterns that AD patients exhibit. However, determining the early stages of AD pathophysiology still remains a challenge. Recently a comprehensive study based on high-resolution MRI on people with MCI and AD revealed that the earliest signs of AD pathology appeared in the cholinergic cells of the nucleus basalis of Meynert (NbM) in the basal forebrain (Schmitz et al., 2016).

Interestingly, neuroimaging studies of brains in individuals with T2DM also show structural alterations that resemble those seen in AD patients. In an elegant study conducted by Moran et al. 350 people with T2DM and 363 control individuals were assessed for cognitive functions with an MRI scan to identify the regional distribution of brain atrophy to identify the causes of cognitive impairment in T2DM patients (Beckett et al., 2015; Moran et al., 2015). The investigators found that T2DM was associated with more cerebral infarcts and reduced volumes of gray matter, white matter, and hippocampus compared to non-diabetic individuals. It was further observed that in people with T2DM, gray matter loss was most prominent in medial temporal, anterior, cingulate, and medial frontal lobes—the regions maximally vulnerable to AD. Moreover, cognitive functions, and in particular visuo-spatial skills, were markedly affected in the T2DM group. Another study by Roberts et al. examined the associations of T2DM with imaging biomarkers and cognitive abilities in 1,437 elderly individuals without dementia (Roberts et al., 2014). They found that midlife T2DM was associated with reduced hippocampal and whole brain volumes strongly indicating decline of cognitive functions later in life. Wennberg et al. conducted a study on 233 cognitively normal individuals who were assessed for fasting blood glucose and cortical thickness measurements by MRI (Wennberg et al., 2016). This study showed that higher blood glucose was associated with reduced average thickness in the AD vulnerable regions. Based on these observations, the authors conclude that the brain atrophy in T2DM, evident from imaging studies, bears striking resemblance to that seen in preclinical AD.

Shared Pathophysiology Between AD and T2DM

PET and MRI studies show marked impairment of glucose and energy metabolism in both T2DM and AD (Umegaki, 2014). In addition, amyloidogenesis remains a salient feature in both these diseases. Extracellular β-amyloid plaques form one of the characteristic features of AD. Likewise, deposits of amyloidogenic peptide (IAPP) are detected in the pancreatic islets of Langerhans of T2DM patients (Haataja et al., 2008). Interestingly, diabetic mice overexpressing IAPP develop oligomers and fibrils with more severe diabetic trait similar to AD mouse models that overexpress APP (Marzban et al., 2003). Advanced glycation end products (AGE) and their receptors (RAGE) accumulate in the sites of diabetic complications such as kidney, retina, and atherosclerotic plaques under conditions of ER and oxidative stress (Nowotny et al., 2015). Similarly, glycated products of Aβ and tau form in transgenic AD models as well as in post-mortem brains of AD patients under similar stress conditions and form an important component of neurofibrillary tangles (Schedin-Weiss et al., 2014). Moreover, additional traits of synaptic dysfunction, activation of the inflammatory response pathways and impairment of autophagy are pathological features common to both AD and T2DM (De Felice and Ferreira, 2014; Carvalho et al., 2015).

The first section of this review will discuss the impact of brain insulin resistance evident in T2DM on the two hallmarks of AD, Aβ, and tau and describe the possible mechanisms that interconnect AD and T2DM in the areas of synaptic dysfunction, inflammation, and autophagic impairment (**Figure 1**).

ALZHEIMER'S DISEASE: INSULIN RESISTANCE IN THE BRAIN

Brain insulin resistance is a significant, yet often over-looked feature of AD (De Felice et al., 2014). Insulin released from the pancreas is transported to the brain via the blood brain barrier using a receptor-mediated mechanism. While the crucial role of insulin response in the peripheral tissues is well documented, there are very few reports about the function of insulin in the central nervous system. The insulin levels in human and rodent brain tissue are relatively low compared to circulating levels (Talbot, 2014). There are some reports about reduced insulin levels in the AD brains; however, this finding was not significant compared to the age-matched controls (Stanley et al., 2016). Recently several studies have reported reductions of insulin mRNA in AD, however the results of *de novo* insulin synthesis have been controversial (Blázquez et al., 2014). Thus, it is hypothesized that majority of brain insulin comes from the peripheral tissues and the role of insulin produced in the CNS is still unclear.

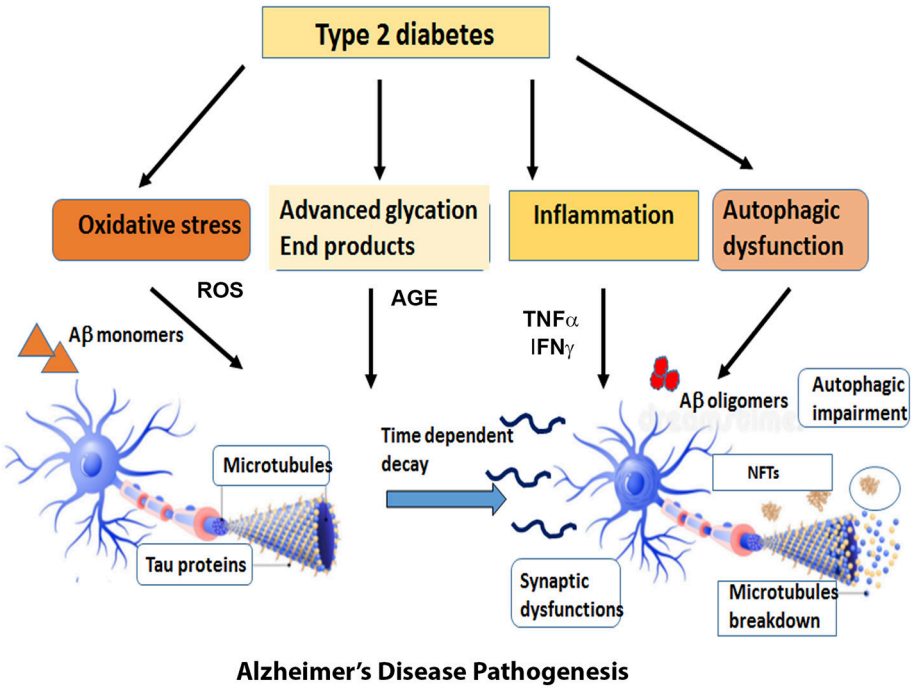


FIGURE 1 | Overview of the diverse mechanisms by which Type 2 Diabetes can cause AD pathogenesis. Type 2 Diabetes accompanied by insulin resistance and hyperglycemia gives rise to metabolic problems in the brain and other target tissues that sets off a cascade of pathogenic processes such as oxidative stress, inflammatory responses, advanced glycation products and autophagic dysfunction. The reactive oxygen species generated by these pathways expedite the process of neuronal death. At the same time, the insulin resistance impairs the downstream signaling pathways and exacerbates the formation of Aβ oligomers and aggregates of hyperphosphorylated tau. The cumulative effect of all these factors expose the neurons to a range of assaults and gradually result in the loss of synapses and neuronal death.

Although, the brain was initially considered a non-insulin target organ; several studies indicate the widespread distribution of insulin receptors (IR) in the brain particularly in the olfactory bulb, cortex, hippocampus, and hypothalamus indicating an intricate "neuroregulatory" role for insulin (Kim and Feldman, 2015). IRs in the brain are enriched in neurons compared to glia, and concentrated at the synapse. However, contrary to the IRs found in the peripheral tissues, the primary function of brain IRs is not glucose transport and metabolism. Instead, the brain IRs perform diverse functions including homeostatic regulation, modulation of synaptic plasticity, and neurotransmission and age related neurodegeneration (Plum et al., 2005).

The crucial function of glucose uptake and utilization in the brain is carried out by Glucose transporter 4 (GLUT4). Insulin activates GLUT4 gene expression and translocation from the cytosol to the plasma membrane to regulate glucose homeostasis in the brain and maintains energy requirements for a variety neuronal functions (Chiang et al., 2001; Reno et al., 2017).

Insulin Signaling in the Brain

A large number of recent studies provide compelling evidence that deficits in insulin signaling, arising due to insulin resistance, occurs in AD (Talbot et al., 2012; Mullins et al., 2017). FDG-PET studies of the brains of "early stage" AD patients have demonstrated reduced glucose uptake leading Suzanne de la Monte and colleagues to classify AD as "Type 3 Diabetes"(de la Monte and Wands, 2008).

In the brain, insulin and IGF signaling mechanisms are crucial for maintaining synaptic plasticity and cognitive functions (Boucher et al., 2014). Once insulin binds to the IR, it is activated by auto-phosphorylation of several tyrosine residues which in turn activates insulin receptor substrates 1 (IRS-1) and 2 that initiate a host of downstream signaling cascades through phosphatidylinositol-3-kinase (PI3K) (**Figure 2**). PI3K then activates AKT, which phosphorylates GSK-3β at serine 9 residue thereby inhibiting its activity and resulting in glycogen synthesis (Avila et al., 2012). There are numerous reports that GSK-3β is one of the key tau kinases playing a central role in AD pathogenesis (Chatterjee et al., 2009; Hernandez et al., 2013). Physiologically GSK-3β is involved in maintaining synaptic plasticity and regulates NMDA receptor-mediated long-term potentiation (LTP) and long-term depression (LTD) effects at the synapses (Bradley et al., 2012). In the disease state however, GSK-3β is hyperactive and phosphorylates tau at pathological epitopes. Hyperphosphorylated tau then aggregates to form neurofibrillary tangles (Avila et al., 2010). GSK-3β is also a key mediator of apoptosis suggesting that it might activate neuronal loss in degenerative diseases with increased production of Aβ (Qu et al., 2014). Emerging data also shows that PI3K/AKT pathway regulates synaptic plasticity by stimulating excitatory and

inhibitory cell membrane receptors, enhances neurotransmitter activities and increases cortical glucose metabolism in the brain regions that are important for learning and memory (Farrar et al., 2005). In parallel, insulin activates the MAPK pathways leading to Ras activation at the plasma membrane and the sequential activation of Raf, MEK, and ERK (Zhang et al., 2011) (**Figure 2**). Although a direct role of the components of the MAPK pathway in mediating AD pathology has not yet been deciphered, recent reports indicate that ERK plays a crucial role in synapse formation and learning/memory functions implying that it may have additional neuroprotective functions (Thiels and Klann, 2001). Apart from PI3K/AKT and Ras/Raf/MAPK pathways, less well-defined roles in AD pathogenesis are played by mammalian target of rapamycin (mTOR) and its downstream targets that regulate neuronal survival and nutrient sensing. mTOR regulates protein synthesis by phosphorylating the key substrates of the translational machinery namely the eukaryotic initiation factor 4E-binding protein (4E-BP1) and p70S6 kinase (S6K1). Rapamycin inhibits mTOR *in vivo* and halts cellular growth and proliferation (Showkat et al., 2014).

It is hypothesized that in an insulin-resistant state these downstream signaling pathways are compromised leading to increased levels of Aβ oligomers and hyperphosphorylated tau not only due to a dysregulation of the downstream kinases but also due to an impairment of autophagic clearance that arises as a result of imbalance of the mTOR and autophagy pathways. Autophagic dysfunction, which is an emerging feature of AD causes the progressive accumulation of toxic proteins and eventually leads to neuronal death (Orr and Oddo, 2013).

From the epidemiological and brain neuroimaging studies it is evident that insulin and IGF signaling pathways are important for preservation and maintenance of learning and memory processes that are compromised in AD. Supporting this, intranasal insulin administration improves learning and memory functions in AD patients, emphasizing the shared pathophysiology in both diseases (Benedict et al., 2007).

CROSSTALK OF T2DM AND Aβ PATHOLOGY IN AD

One of the hallmarks of AD pathology is the formation of extracellular amyloid plaques composed of insoluble deposits of amyloid-β protein aggregates. Aβ is generated from the proteolytic cleavage of amyloid precursor protein (APP) by a sequence of enzymatic reactions from BACE-1, β and γ-secretase complex (Vassar, 2004). It is hypothesized that lower concentration of Aβ remains in the soluble form and subject to clearance after degradation, while higher concentrations aggregate into insoluble plaques that are resistant to degradation (Esparza et al., 2016). While there is no evidence that AD brains secrete more soluble Aβ than normal brains, a recent body of evidence suggests that an increased accumulation of insoluble Aβ plaques arise due to impaired clearance of Aβ protein (Wildsmith et al., 2013).

Impact of Hyperinsulinemia on Aβ

Emerging studies indicate that hyperinsulinemia may confer risk of AD by modulating Aβ toxicity. The enzyme responsible for degrading the Aβ protein is Insulin Degrading Enzyme (IDE), which also degrades insulin (Qiu and Folstein, 2006). In T2DM, peripheral hyperinsulinemia increases the concentration of insulin which acts as a competitive substrate for IDE and inhibits the degradation of Aβ that gradually accumulates to form insoluble plaques. IDE has previously been identified as the primary regulator of Aβ in both neurons and glia (Son et al., 2016). In a recent study Farris et al. demonstrated that homozygous deletions of IDE gene (IDE–/–) in mice, resulted in 50% decrease in Aβ clearance in brain homogenates and primary neuronal cultures (Farris et al., 2003). The IDE depleted mice exhibited increased cerebral accumulation of endogenous Aβ, in addition to the hyperinsulinemia and glucose intolerance that characterize T2DM. Hyperinsulinemia also affects APP transport. *In vitro* studies by Gasparini et al. demonstrated that in βAPP overexpressing N2a cells and primary neuronal cultures, insulin decreases the intracellular accumulation of Aβ by promoting the transport of βAPP/Aβ from the trans-golgi network to the plasma membrane (Gasparini et al., 2001). Thus, in addition to inhibiting the degradation of Aβ by IDE, insulin increases the concentration of extracellular Aβ by modulating the trafficking of APP. The investigators also show the involvement of receptor tyrosine kinase/mitogen-activated protein (MAP) kinase pathway in regulating intracellular Aβ transport (Matos et al., 2008).

Impact of Insulin Resistance on Aβ

Studies by Cheignon et al. have shown that inhibition of PI3K leads to reduced Aβ production (Cheignon et al., 2018). When they crossed neuron specific IR knockout mice to APP overexpressing Tg2576 transgenic mice, this study found that loss of insulin signaling in the brain reduced production of Aβ and amyloid plaque deposits. However, the decrease of Aβ burden was not sufficient to rescue the mortality observed in these transgenic mice. Nevertheless, this data provides strong evidence that IRS signaling plays an important role in modulating the Aβ deposition.

Investigating the effect of diet-induced insulin resistance on amyloidosis in Tg2576 AD transgenic mouse models, Ho et al. found that the animals displayed the first signs of memory deficits only at 6 months of age. These animals also maintained normal circulating insulin levels and glucose metabolism till they were 13 months old when there was evidence of plasma hyperinsulinemia. Interestingly, despite high production of Aβ and senile plaques in the brain, these mice showed no evidence of neuronal death and neurofibrillary tangles. However when these mice were reared on a high fat diet they developed non-insulin dependent diabetes mellitus, that led to increased production of Aβ40 and Aβ42, higher activation of γ-secretase as well as GSK-3α and GSK-3β. Biochemical evidence has shown that these mice displayed lower PI3K and AKT activation signals denoting insulin resistance with impaired learning and memory functions (Ho et al., 2004; Chouliaras et al., 2010).

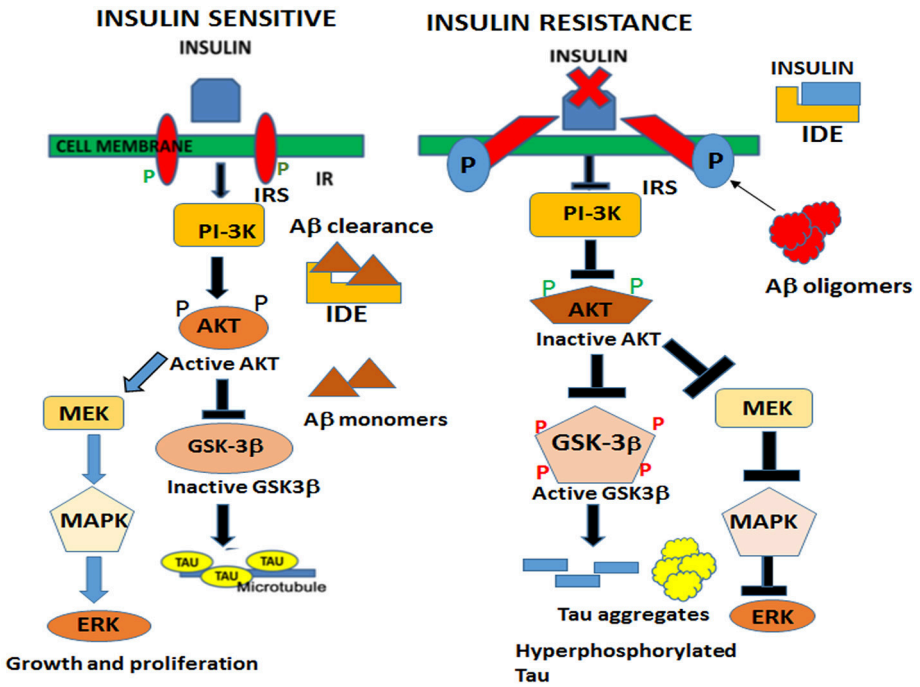


FIGURE 2 | Neuronal signaling mechanisms in a state of insulin sensitivity and insulin resistance. In the insulin sensitive state insulin binds to the receptor and activates the insulin receptor tyrosine kinase that initiates a cascade of phosphorylation events at the IRS/PI3K/AKT and Ras/Raf/ERK pathways. AKT phosphorylates GSK-3β at the inhibitory serine 9 residue and allows tau to maintain its physiological function of binding to microtubules and facilitates normal axonal transport of neuronal vesicles. In a state of insulin resistance, GSK-3β is activated by phosphorylation at Tyrosine 216 residue and hyperphosphorylates tau at pathological epitopes. Hyperphosphorylated tau then detaches from the microtubules and aggregates to form neurofibrillary tangles. Likewise, in the presence of excess insulin, the insulin degrading enzyme (IDE) is unable to degrade and facilitate clearance of Aβ oligomers that act as a competitive substrate for insulin. Thus, insulin resistance facilitates the formation of both Aβ and tau oligomers.

Impact of Hyperglycemia on Aβ

Elevated plasma glucose levels are a common pathological feature of T2DM affected individuals. A compelling link between glucose metabolism and AD was established in a study conducted in transgenic APP/PS1 murine models (Macauley et al., 2015). The researchers observed that the induction of acute hyperglycaemia in young mice increased the production of Aβ and lactate in hippocampal interstitial fluid and this was associated with an increase in neuronal activity (Minkeviciene et al., 2009). These effects worsened in aged AD mice with increased Aβ plaque pathology. These findings suggest that transient hyperglycemia associated with T2DM can initiate the formation of Aβ plaques. In this study, the authors also show that hippocampal ATP sensitive potassium (KATP) channels act as metabolic sensors of the alterations in glucose concentration with changes in electrical activity and extracellular Aβ deposition.

In addition, aberrant glucose metabolism activates glycation reactions that leads to the formation of advanced glycated end products (AGE). Elevated AGE levels in the circulation and in the brain have been associated with cognitive impairments in AD patients (Li et al., 2013). Numerous studies show that there is an increased accumulation of AGE in the brain of diabetic rats implying that AGE products impair the removal of Aβ42 and induce Aβ aggregation in the brain (Moreira et al., 2003).

AGEs enhance the expression of its receptor RAGE, which is also a presumed receptor for Aβ (Srikanth et al., 2011). Recent reports have shown increased RAGE expression in the astrocytes and microglia of AD brains (Solito and Sastre, 2012). Also, studies on triple transgenic model of AD (3xTg AD) expressing 3 dementia-related transgenes, namely APPSWE, PS1M146V, and tauP301L and raised on high-fat diet as well as STZ-induced diabetic APP/PS1 dual transgenic AD mice demonstrate increased RAGE expression in neurons and astrocytes with an activation of pro-inflammatory cytokines and enhanced decline of cognitive and memory functions (Choi et al., 2014). As a consequence of the damaging inflammatory responses, RAGE causes vascular complications in AD and T2DM. Neuron-specific overexpression of dominant negative RAGE results in restoration of cognitive functions and stops the progression of neuropathological changes in AD mice (Liu L. P. et al., 2009). Treatment of transgenic AD mice with RAGE inhibitor decreases microglial activation and Aβ production (Criscuolo et al., 2017). Interestingly, soluble form of RAGE (sRAGE) is neuroprotective (Deane et al., 2012; Lee and Park, 2013).

O-GlcNAcylation is a nucleocytoplasmic post-translational modification that occurs abundantly in neurons and protects against Aβ-mediated neuronal toxicity. Recent studies show that a moderate level of O-GlcNAcylation is neuroprotective

and decreases formation of Aβ production by inhibiting γ-secretase activity (Hanover and Wang, 2013). Insulin resistance and hyperglycemia increases the level of O-GlcNAcylation but the amelioration of γ-secretase activity is counterbalanced by the accumulation of glycated end products that are ultimately toxic to neurons.

Impact of Dyslipidemia on Aβ

Insulin plays a crucial role in lipid metabolism and impairments in insulin signaling lead to increased lipolysis and elevated synthesis of free fatty acids (FFA) (Wilson and Binder, 1997). Human brain produces approximately 30% of total body cholesterol, hence slight alterations in lipid metabolism can have profound effects on cognitive function. Recent studies show that the interaction between cholesterol and APP in the plasma membrane is necessary for Aβ synthesis and clearance. Tg2576 AD mice raised on a diet supplemented with high fat and high cholesterol displayed increased production of Aβ. When these animals were treated with cholesterol lowering drugs the brain amyloid levels were reduced by more than 2-fold (Nizari et al., 2016).

Impact of Aβ Oligomers on Insulin Resistance

Soluble oligomers of Aβ42 have been shown to be the most toxic species to the neurons. In the brains of AD patients with MCI, Aβ oligomers have been shown to correlate with rapid cognitive decline (Ferreira et al., 2015). Also, in the brain and CSF of AD patients the level of soluble oligomers ranging from trimer to 24-mer or higher is significantly elevated when compared to levels found in non-demented controls (Jimenez et al., 2014). Studies in human APP overexpressing Tg2576 AD mice show that the onset of memory deficits correlate with production of soluble Aβ oligomers. Small oligomers of Aβ, particularly dimers and trimers that are formed within the neurons *in vitro* are secreted into conditioned medium. The treatment of rat hippocampal slices or live animals with these oligomers showed potent LTP defects and cognitive deficits (Puzzo et al., 2017). Similarly, synaptotoxicity is observed when soluble Aβ oligomers isolated from the brains and CSF of AD patients are applied to brain tissue slices or live animals (Minkeviciene et al., 2009). These, inhibitory effects are blocked by Aβ antibodies and γ-secretase inhibitors (Goure et al., 2014). This LTP blockage is also restored by treatment with 1μM insulin (Sakono and Zako, 2010). These observations were confirmed by other investigators who demonstrated that Aβ42 oligomers were more potent in blocking LTP than monomers and this effect was rescued by insulin by preventing Aβ oligomerization (Selkoe, 2008; Mucke and Selkoe, 2012).

Recent evidence indicates an intimate connection between brain insulin resistance and the formation of Aβ oligomers. In a study by Zhao et al. the scientists found that the treatment of primary hippocampal neurons by soluble Aβ oligomers results in a profound loss of insulin receptors from the neuronal surface. In addition, Aβ oligomers were found to increase the AKT phosphorylation at Serine-473 residue which results in insulin resistance (Zhao and Townsend, 2009). In addition, Aβ oligomers inhibit insulin signaling by phosphorylating IRS1 at inhibitory serine residues via the JNK/TNF alpha pathway (De Felice et al., 2009). Conversely, treating AD patients and transgenic animals with intranasal insulin lowers the concentration of soluble Aβ and improves memory (De Felice et al., 2009). Aβ-induced insulin resistance was also observed in the Familial AD (5XFAD) transgenic mouse models that overexpress high levels of mutant APP and PS1 and display severe amyloid pathology since 2 months of age (Mosconi et al., 2008).

Overall these studies demonstrate a strong impact of insulin resistance, hyperglycemia, dyslipidemia, and other hallmarks of T2DM on the pathological effects of Aβ amyloidogenesis as observed in AD.

CROSSTALK OF T2DM AND TAU PATHOLOGY IN AD

The traditional physiological function of tau protein is to promote assembly and stabilization of microtubules, though newer, atypical functions are now being reported (Sotiropoulos et al., 2017). There are about 80 Ser/Thr and 5 Tyr phosphorylation sites on tau that are phosphorylated by the key tau kinases namely GSK-3β, MARK/PAR1, and CDK5 (Stoothoff and Johnson, 2005; Chatterjee et al., 2009). While in the normal brain, tau contains 2–3 moles of phosphate/mole of tau protein; in abnormal situations as seen in AD brains and other tauopathies, tau becomes hyperphosphorylated with 6–9 moles of phosphate/mole of tau and aggregates to form intracellular neurofibrillary tangles, one of the pathological hallmarks of AD (Iqbal et al., 2010).

A wealth of emerging studies in recent years indicate that the density of the neurofibrillary tau tangles deposited at the neocortex of the brains of MCI patients correlated more strongly with the severity of the disease (Bierer et al., 1995; Nelson et al., 2012). This study showed that learning and memory defects were more acute in patients with higher accumulation of the tangles in the temporal lobe which is the brain region associated with learning and memory. Thus, the post translational modifications of tau (hyperphosphorylation, truncation, acetylation, and glycation) and associated cellular and biochemical changes that cause these abnormal structural alterations are of potential interest for the development of tau targeted therapeutic studies.

Two of the important features of T2DM namely insulin resistance and hyperglycemia are able to influence post translational modifications of tau and exacerbate tau pathology, discussed below:

Impact of Insulin Resistance on Tau Kinases and Phosphatases

Under physiological conditions, a host of kinases and phosphatases regulate the intricate balance between tau phosphorylation and dephosphorylation to maintain neuronal homeostasis. Several protein kinases such as GSK-3β, CDK5, MARK, PKA, PKB/AKT, and MAPK including ERK1/2, c-JUN N terminal kinase (JNK) and p38 are the important kinases that phosphorylate tau (Avila, 2008; Gómez-Sintes et al., 2011).

Among these kinases, AKT and GSK-3β are located downstream of one arm of the insulin signaling pathway while components of the MAPK pathway lie downstream of the other arm (Fröjdö et al., 2009). AKT phosphorylates GSK-3β at the inhibitory Serine-9 residue and maintains GSK-3β in the inactive form. However, under conditions of insulin resistance, GSK-3β is converted to its active form by phosphorylation at Tyrosine-216 residue. Active GSK-3β then hyperphosphorylates tau to generate the pathological epitopes AT8, AT100, and PHF1 which make up the pre-tangles and NFTs in the AD brains (Clodfelder-Miller et al., 2005).

Several other studies have found that p70S6 ribosomal protein kinase—an AKT/mTOR substrate can directly phosphorylate tau and upregulate its synthesis through phosphorylation of S6 (Yoon, 2017).

These key pathways, namely PI3K/AKT, MAPK, and mTOR/p70S6K are regulated by insulin binding to the insulin receptor and trigger downstream phosphorylation events (Fröjdö et al., 2009). Thus, it is not surprising that in an insulin resistant state, insulin is unable to activate these pathways thereby disrupting physiological tau phosphorylation. Additionally, in diabetic brains p38 and JNK activation can cause insulin resistance by inhibiting the insulin receptor substrate and trigger tau hyperphosphorylation and pathological events (Wu et al., 2013).

Tau is also regulated by phosphatases especially PP2A that dephosphorylates it at crucial residues Thr205, Thr212, and Ser 262 that are phospho-epitopes of GSK-3β and MARK/PAR-1. In addition, PP2A dephosphorylates the kinases GSK-3β and p70S6K to maintain tau phosphorylation at a physiological level (Gratuze et al., 2017). Interestingly, several researchers have shown a downregulation of PP2A in both T1DM and T2DM mice suggesting that insulin resistance might exacerbate tau phosphorylation by downregulating PP2A (Qu et al., 2011; Jung et al., 2013).

The impact of isolated CNS-specific insulin resistance on tau phosphorylation was investigated *in vivo* by Schubert et al. using NIRKO mice where the brain/neuron specific IR gene was conditionally inactivated. They found that NIRKO mice displayed a complete loss of insulin-mediated PI3K/AKT signaling resulting in reduced phosphorylation of GSK-3β at Serine-9 and increased tau phosphorylation. However, these animals did not exhibit any change in survival or learning and memory defects or basal brain glucose metabolism (Schubert et al., 2004). In another study modeling peripheral insulin resistance in IRS2 knock out (KO) mice Schubert and colleagues show that neurofibrillary tangles composed of hyperphosphorylated tau aggregates accumulate in the hippocampus of IRS2 KO mice, revealing a direct molecular link between diabetes and Alzheimer's disease (Schubert et al., 2003). Likewise, Cheng et al. in IGF KO mouse brains displayed increased tau phosphorylation at Ser-396 and Ser-202 residues both of which are implicated in neurodegeneration (Cheng et al., 2005). In STZ-induced Type 1 diabetic mouse models, Planel and colleagues observed a robust increase in tau hyperphosphorylation that prevented tau from binding to microtubules (Planel et al., 2007). The scientists further observed that a downregulation in the activity of PP2A in these transgenic models exacerbated tau pathology. Similarly, Yazi and colleagues administered STZ to induce diabetes in pR5 mice expressing P301L mutation. Compared to non-transgenic controls, the pR5 mice displayed massive tau hyper-phosphorylation with the formation of neurofibrillary tangles by 6 months of age (Ke et al., 2009). In addition, other studies show that treatment of STZ-induced diabetic mice with GSK-3β inhibitors improves learning and memory functions (King et al., 2013). All these studies study provide compelling evidence that both Type 1 and Type 2 diabetes can accelerate onset and disease progression in individuals with a predisposition to developing tau pathology.

Impact of Insulin Resistance on Tau Cleavage

In addition to hyperphosphorylation, another abnormal post-translational modification of tau is truncation. Tau is cleaved by a host of proteolytic enzymes including caspases, calpains, thrombins, and puromycin-sensitive amino peptidase. These truncated tau fragments lack both N terminal and C terminal fragments and form the core component of NFTs (Karsten et al., 2006; Zilka et al., 2006).

In AD brains, caspases are activated causing tau protein to be cleaved at several residues. The C-terminal cleavage of tau by caspase-3 gives rise to Asp421 residue that has a higher propensity of aggregation and is found to be associated with neurofibrillary pathology in AD brains. The presence of Asp421 truncated tau in the neurofibrillary aggregates observed in the neurons of double transgenic mice (Tet/GSK-3β/VLW) and in P301S mouse models of tauopathy indicates that the formation of Asp421 cleavage product is an important step toward formation and maturation of tau aggregates (Basurto-Islas et al., 2008; Gendron and Petrucelli, 2009; Gómez-Sintes et al., 2011).

Diabetes has been known to stimulate apoptosis by the activation of caspase-3 in affected tissues (Savu et al., 2013). Using an animal model of T2DM, Kim et al. in their studies demonstrated an increased level of tau phosphorylation and cleavage in the brains of db/db mice which are models for diabetic dyslipidemia (Kim B. et al., 2013). Feldman and colleagues found that hyperglycemia promotes tau cleavage by activation of caspases (Kim et al., 2009). Thus, these studies demonstrate that T2DM enhances the formation of tau truncated fragments by caspase activation that contribute toward an increased risk of AD in diabetic patients.

Impact of Hyperglycemia on Other Posttranslational Modifications of Tau

Acetylation is a post translational modification in which the acetyl group from acetyl CoA is reversibly transferred to lysine ε amino group in the tau protein. This process is modulated by acetyltransferases and deacetylases (Cook et al., 2014). Cohen et al. observed that tau acetylation at the key lysine residues at K/163/280/281/369 was crucial for tau-microtubule binding interactions and microtubule stabilization. Using cellular and transgenic mouse models as well as human brains from a wide spectrum of tauopathies this group has demonstrated that tau

acetylation disrupts the tau-microtubule binding interactions and promotes pathological tau aggregation. This group further demonstrated that acetylated tau was associated with the formation of insoluble tau NFTs in tau transgenic mice and human tauopathies indicating "acetylation" as a pathogenic post-translational modification of tau (Cohen et al., 2011).

Protein acetylation plays an important role in intermediary metabolism and metabolic disorders including T2DM. Mass spectrometry on STZ-induced diabetic rats showed high levels of lysine-acetylated proteins in their kidney cells compared to control animals (Kosanam et al., 2014). Also, treatment of murine aorta cells with high glucose or FFA to induce short term diabetes causes increased levels of lysine acetylation (Samuel et al., 2017). Although, there are very few reports, aberrant acetylation of tau in T2DM may interfere with the physiological functions of microtubule binding and assembly predisposing cytoplasmic tau toward the formation of aggregates (Irwin et al., 2013; Trzeciakiewicz et al., 2017).

Glycosylation involves the attachment of oligosachharide moieties to proteins and lipids. O-glycosylation is the linkage of sugar residues to the hydroxyl groups of Serine or Threonine residues while N-glycosylation involves attaching the sugar moieties to the amine group of the aspargine residues in proteins (Wang et al., 1996). Impaired OGlcNAc cycling is implicated in AD. In *post-mortem* AD brains Zhu et al. have demonstrated a significant decrease of O-GlcNAc glycosylation of tau proteins compared to controls (Zhu et al., 2014). Other studies from AD patients show hyperphosphorylated but hypo-O-GlcNAc glycosylated tau implying that phosphorylation and O-glycosylation at Serine and Threonine residues act in opposition (Wang et al., 1996; Iqbal et al., 2010). *In vitro* studies in NMR and Mass spectrometry analysis by Smet-Nocca et al. demonstrated that tau hyper phosphorylation at residues Ser-396 and Ser-404 were reduced by O-glycosylation at Ser-400 (Smet-Nocca et al., 2011). Treatment of mouse models of AD with OGA inhibitor Thiamet-G (that increases the levels of O-GlcNAcylation of tau) was found to decrease the levels of NFT burden and pathological tau species and slow down disease progression (Robertson et al., 2004; Gong et al., 2005; Yuzwa et al., 2012). However, it is interesting that Thiamet-G decreases tau phosphorylation over a short period of time and prolonged OGA inhibition has no effect on phosphorylation. This is probably due to cellular adaptability over time. Compared to O-glycosylation, *in vitro* studies show that N-glycosylated tau isolated from AD brain promotes tau hyperphosphorylaton (Liu Y. et al., 2009). Taken together these studies demonstrate that glycosylation exerts varying effects on tau hyperphosphorylation.

Although it is still speculative, it has been hypothesized that abnormal glucose metabolism in the brain induced by T2DM may lead to decreased brain O-GlcNAc levels. This reflects a failure in the neuroprotective mechanism in the brain and triggers the cascade of tau pathology enabling disease progression.

Impact of Tau on Insulin Resistance

While insulin resistance stimulates tau hyperphosphorylation and aggregation, in a recent study Rodriguez-Rodriguez and colleagues have shown that pathological alterations in tau (hyperphosphorylation and aggregation) accumulates insulin. In this study, the researchers have shown that insulin accumulates in the sarcosyl-insoluble fractions of the AD brain. Moreover, the researchers found increased accumulation of insulin *in vivo* in the brains of tau overexpressing P301S mice and SHSY5Y cells as well as in okadoic acid treated primary neuronal cultures. Both the cells and primary neurons demonstrated increased insulin uptake from the surroundings that eventually led to insulin resistance (Rodriguez-Rodriguez et al., 2017). Another study shows impaired insulin sensitivity in hippocampal slices from tau KO mice compared to litter-mate controls (Marciniak et al., 2017).

These studies suggest a complex relationship between tau and insulin resistance as it is evident that not only insulin resistance can exacerbate tau pathology but pathological tau phosphorylation or absence of tau can affect neuronal insulin resistance.

SYNAPTIC DYSFUNCTIONS AT THE CROSSROADS OF AD AND T2DM

There is widespread neuronal loss and atrophy of the cortex and hippocampus in the brains of AD patients (Sheng et al., 2012). The cognitive failure in AD patients is accompanied by loss in synapses and neuronal cell death with a marked reduction in brain volumes particularly at the entorhinal cortex and hippocampus. Although plaques and tangles characterize the neuropathological features of AD, the closest correlation to the severity of disease progression is the synapse loss that occurs in the disease. There are conflicting reports as to whether the amyloid plaques or NFTs correlate more strongly with disease progression. Some scientists have reported that the spatiotemporal signature of NFTs of tau correlate more severely with the disease pathology (Nelson et al., 2012; Horvath et al., 2013). However, investigating the "neurodegenerative triad" Tackenberg et al. have shown that the loss of dendritic spines and LTP that occurs early in the disease is mediated by Aβ while the late stage cell death mediated by NMDAR requires tau phosphorylation (Tackenberg and Brandt, 2009).

Alterations in synaptic transmission and plasticity are also observed in the hippocampus of diabetic animal models including depletion of synaptic vesicles at presynaptic sites and changes of AMPA and NMDA receptors at the postsynaptic sites. Moreover, diabetes affected the synthesis and release of both inhibitory and excitatory neurotransmitters (Gaspar et al., 2016). All of these factors have the potential to activate synaptic dysfunction and widespread neuronal loss thereby predisposing the diabetic brain to AD. In this section the impact of T2DM on Aβ and tau mediated dysfunctions will be elaborated.

Synaptic Dysfunctions in AD

Recent studies indicate that cognitive ability in AD patients is closely related to the alterations of the density of the presynaptic glutamatergic boutons with an elevation of the glutamatergic synapses in MCI patients and a gradual depletion of the boutons with the progression of AD (Bell et al., 2007).

Aβ and Synaptic Dysfunction

There are numerous reports that show Aβ oligomers can cause synaptic dysfunction and toxicity (LaFerla and Oddo, 2005; Shankar and Walsh, 2009). Under physiological conditions, low concentration of monomeric Aβ is essential for maintaining synaptic plasticity and neuronal survival with the improvement of cognitive abilities. Conversely, in the disease state higher concentration of Aβ together with aging causes synaptic dysfunction followed by neuronal loss as seen in AD. Recent studies show that APP and BACE1 KO mice display pronounced defects in LTP and memory functions (Tyan et al., 2012). Puzzo et al. showed that the treatment of mouse brain hippocampal slices with low concentrations (200 picomoles) of synthetic Aβ42 monomers and oligomers increased the LTP. This study suggests that LTP is mediated by α7-nicotinic acetylcholine receptors indicating a presynaptic role of Aβ. Likewise, treatment with nanomolar concentration of Aβ produced synaptic depression. This indicates that an optimal level of Aβ is needed for synaptic transmission (Puzzo et al., 2017).

Elevated levels of Aβ impairs glutamatergic transmission by decreasing the number of AMPA and NMDA receptors on the surface of the neurons. Moreover, increased concentration of Aβ results in the internalization of NMDA receptors enhancing LTD at the synapses. LTD causes a significant loss of dendritic spines that is associated with early symptoms of AD and disease progression (Palop and Mucke, 2010). EEG recording from cortical and hippocampal networks In human APP overexpressing mouse models shows that high levels of Aβ oligomers elicits epileptic and nonconvulsive seizures (LaFerla and Oddo, 2005). Consistent with these findings, *in vivo* calcium imaging of cortical circuits shows that double transgenic (hAPP/PS1) mice have a greater proportion of hyperactive and hypoactive neurons than nontransgenic control (Palop and Mucke, 2010; Puzzo et al., 2017). AD transgenic mice showed an increased neuronal activity in the hippocampal regions before the formation of insoluble amyloid plaques. On treatment with a γ-secretase inhibitor, soluble Aβ levels were reduced and the neuronal activity decreased implying that this effect was a soluble Aβ-dependent effect (Busche et al., 2012). Although the mechanisms are not completely elucidated, these studies suggest that Aβ-dependent effects on synaptic plasticity and neurotransmission are tightly controlled by the activation of α7-nicotinic acetylcholine receptors or NMDARs and involves downstream effector components including p38 MAPK and GSK-3β (Baglietto-Vargas et al., 2016).

T2DM may trigger Aβ-mediated synaptic dysfunction in multiple ways. Hyperinsulinemia in T2DM promotes the formation of Aβ oligomers that cause synaptotoxicity. Investigators have shown that when Aβ oligomers are applied *in vitro* to rat hippocampal slices or *in vivo* to live animals they blocked LTP and inhibited memory formation (Busche et al., 2012). Interestingly, this effect is overcome by 1μm insulin. A similar result was reported by Li et al. who observed that Aβ monomers were more effective than Aβ oligomers in inhibiting LTP and that insulin prevented Aβ-induced LTP defects by blocking Aβ oligomerization (Balducci et al., 2010; Li et al., 2011). Previous studies have shown that Aβ oligomers are capable of binding to insulin receptors which causes an impairment of receptor functions (Bradley et al., 2012; Uranga et al., 2013). In addition, it has been shown that Aβ oligomers alter GSK-3β phosphorylation state and directly impacts the ERK pathway (Magrane et al., 2006; Reddy, 2013).

Tau and Synaptic Dysfunction

Recent research suggests an emerging role of tau at the synapse (Pooler et al., 2014). Physiologically tau is localized primarily in the axons where it binds and regulates microtubule dynamics in a phosphorylation dependent manner (Janning et al., 2014). However, recent isolation and analysis of AD brain-derived synaptoneurosomes indicate that tau is present in both pre-synaptic and post-synaptic compartments (Tai et al., 2012). There are multiple mechanisms by which tau could mediate synaptic function and neuronal excitability. Recent study has shown that tau binds to the post-synaptic protein complex which includes the PSD-95 through Fyn kinase. The interaction of tau and Fyn appears to be crucial for directing Fyn to the postsynaptic compartments where it can regulate the NMDA receptor by phosphorylating one of its subunits. Abnormal tau phosphorylation can disrupt the tau-Fyn interaction and affect postsynaptic receptor targeting (Haass and Mandelkow, 2010). Thus, neurons from conditionally overexpressing P301L tau mice display impaired targeting of excitatory glutamate receptors to dendritic spines. In addition, biochemical analysis of the synaptosomes from these mice display a marked decrease in the levels of synaptic markers (PSD95, Synapsin, NMDAR1, and GluR1) implying that the loss of functional synapses plays an important role in maintaining postsynaptic integrity (Katsuse et al., 2006; Spires-Jones and Hyman, 2014). Electron microscopy of NFT-carrying motor neurons in P301L mice revealed a significant decrease in the number and size of synaptic boutons compared to nontransgenic controls. These studies point out that loss of synapses occur during neurodegeneration. Evidence for tau involvement in regulating neuronal excitability comes from a study in which a reduction in tau levels reduced hyperexcitability in a mouse model of seizure (Holth et al., 2013; Guerrero-Muñoz et al., 2015). Other studies have found that neurons isolated from transgenic Tg4510 mice overexpressing 0N4R P301L mutation were more excitable than neurons from nontransgenic mice (Kopeikina et al., 2013). However, it is worth noting that the animal models mostly express mutant tau protein and therefore could be more representative of FTDP-17 cases than AD.

Although there are fewer reports, glucotoxicity in T1 and T2DM are capable of influencing tau-mediated synaptic impairments. Investigators have shown synaptic defects and cognitive impairments in STZ-induced diabetic models, where genetically ablating tau ameliorated cognitive defects. (Abbondante et al., 2014). Using a mouse model of tauopathy, scientists have observed that under glucose-deprived conditions as observed in hypometabolic AD brains, transgenic mice

had impaired memory and reduced LTP accompanied by tau hyperphosphorylation and apoptosis (Lauretti et al., 2017).

Synaptic Dysfunctions in Diabetes That Influence Neurodegeneration

Other than directly influencing Aβ and tau-mediated synaptic defects, diabetes also affects the synthesis and release of key neurotransmitters that may underlie cognitive defects. For instance under chronic hyperglycemia extracellular brain levels of GABA and glutamate were decreased in STZ-induced diabetic animal models (van Bussel et al., 2016). An imbalance between excitatory and inhibitory neurotransmission impaired the cognitive deficits observed in these animals. Diabetes also affects acetylcholine esterase that plays a crucial role in cognitive processes. Recent studies have shown a reduction of cholinergic transmission in the hippocampus of STZ-induced diabetic animals (Molina et al., 2014). Moreover, in the STZ-induced animals, treatment of hippocampal slices with insulin resulted in a significant decrease in the number of NMDA receptors that consequently affected LTP and decreased postsynaptic densities (van der Heide et al., 2005).

Taken together these results suggest that both Type 1 and Type 2 diabetes are able to directly influence Aβ and tau-mediated synaptic dysfunctions. In addition, both these subtypes cause an imbalance of neurotransmitter release and alterations in synaptic plasticity that ultimately leads to memory impairments. Hence, synaptic dysfunctions form a shared pathological trait between AD and T2DM.

INFLAMMATION: SHARED PATHOPHYSIOLOGY OF AD AND T2DM

Emerging evidence in recent times points toward a compelling link between inflammation and the pathogenesis of Alzheimer's disease since Aβ plaques and NFTs colocalize with glial cells (Serrano-Pozo et al., 2011). T2DM disease pathogenesis in particular involves high levels of ER and oxidative stress response that might trigger the inflammatory cascade (Back and Kaufman, 2012). Additionally, misfolded toxic protein species detected in AD and T2DM may generate oxidative stress and activate inflammatory pathways. In this section, we discuss the role of inflammation in AD and T2DM and how this impacts the shared pathophysiology in both these diseases.

Inflammation and AD Pathology

Recently preclinical, genetic, and bioinformatics studies have shown that the immune system activation accompanies AD pathology. The genome wide association studies (GWAS) between AD and rare mutations in the genes encoding triggering receptor expressed on myeloid cells 2 (TREM2) and myeloid cell surface antigen CD33 provide clear evidence that there is a strong linkage between alterations in the immune system and the progression of AD pathology (Griciuc et al., 2013; Ulrich et al., 2017).

Based on the amyloid cascade hypothesis, the Aβ deposition is followed by immune system activation mediated by glial cells such as microglia and astrocytes. This is supported by electron microscopy studies that show increased accumulation of glial cells surrounding the amyloid plaque deposits in AD brain (Wyss-Coray et al., 2003). However, recent data of cerebrospinal fluid analysis from patients with symptoms of MCI has demonstrated a marked alteration in the inflammatory markers implying their involvement early in the disease pathway (Zotova et al., 2010; Wyss-Coray, 2012). In another significant study, scientists showed that systemic immune challenge elicited by injecting viral mimics of polyriboinosinic-polyribocytidilic acid resulted in "sporadic AD" like features in wild-type mouse models accompanied by Aβ deposition, tau pathology, microglia activation, and reactive gliosis implying that alterations in the immune system can precede AD pathology and drive the disease itself (Michalovicz et al., 2015). In addition, tissue microarrays from patients with neurodegenerative diseases including AD revealed an upregulation of inflammatory components further suggesting an intimate linkage between inflammatory markers and AD, early in the pathogenic cascade (Sekar et al., 2015).

Aβ and Inflammation

In AD brains, microglia and astrocytes have been known to accumulate around neuritic plaques and are associated with the tissue damages that occur in AD. Aβ oligomers and fibrils are capable of binding to receptors expressed by microglia including CD14, CD36, CD47, a6β1 integrin, RAGE, and Toll-like receptors (TLRs) (Doens and Fernandez, 2014). *In vitro* studies have shown that binding of Aβ to RAGE receptors, helps guide microglia to Aβ deposits and this effect is inhibited by anti-RAGE antibodies (Wyss-Coray, 2012). Binding of Aβ to CD36 or TLR4, on the other hand, results in the production of inflammatory chemokines and cytokines that eventually lead to increased neuronal damage in vulnerable regions of the AD brain (Doens and Fernandez, 2014). Besides the secretion of inflammatory cytokines, microglia are found to phagocytose soluble Aβ oligomers via the extracellular proteases such as neprilysin and insulin-degrading enzyme (IDE). However, there are evidences of Aβ dependent impairment of microglial phagocytosis functions in AD mouse models (Koenigsknecht and Landreth, 2004). Recent studies have shown that microglia isolated from AD transgenic mouse models displayed a substantial reduction in the levels of Aβ-binding scavenger receptor and Aβ-degrading enzyme (Zhao et al., 2017). Interestingly, it has been shown that transient depletion of dysfunctional microglia has no impact on Aβ deposition in an animal model of AD (Morimoto et al., 2011). This is because microglial impairment maybe compensated by inflammatory cytokines such as TNF, IL-1, IL-12, and IL-23 suggesting a negative feedback loop, that might exacerbate the AD pathology (Rubio-Perez and Morillas-Ruiz, 2012). In addition, an upregulation in the levels of inflammatory markers has been demonstrated in animal models of AD or in the brains or CSF of AD patients (Moro et al., 2018).

Recently a huge repertoire of GWAS studies show that structural variants of genes encoding immune receptors TREM2, CD33, and CR1, all of which are expressed in the microglia confer higher risk of AD (Tosto and Reitz, 2013). However, the function of TREM2 deficiency in the progression of AD has been controversial. For instance, while TREM2 deficiency in APP/PS1 mice ameliorated hippocampal Aβ accumulation; the 5XFAD mice displayed an opposite result. In these mice the Aβ pathology was found to develop slower than APP/PS1 mice and increased accumulation of hippocampal Aβ was observed in the absence of TREM2 (Bemiller et al., 2017; Jay et al., 2017). Elevated levels of soluble TREM2 was detected in the CSF of early AD patients suggesting a change in microglial activation in response to neuronal death. Although the exact mechanism still remains to be deciphered, these findings show that impaired TREM2 function plays a vital role in Aβ-mediated AD pathogenesis.

The transmembrane protein CD33 is another microglial receptor the structural variants of which has led to increased risk of AD. A significant study from *post mortem* AD brains has shown the upregulation of CD33 compared to age-matched controls (Jiang et al., 2014). Conversely, the expression of a CD33 variant, namely the protective CD33 (SNP) rs3865444 was downregulated in AD brains and reduced insoluble Aβ deposits (Hu et al., 2014; Li et al., 2015b).

Astrocytes too respond to AD pathogenic stimuli by reactive gliosis. In transgenic AD mouse models exhibiting cerebral amyloidosis the activation of astrocytes occur in the early stages of pathogenesis. In these transgenic animals the astrocytes underwent severe atrophy which preceded the Aβ plaque mediated gliosis (Verkhratsky et al., 2010). Conversely, reducing astrocytes in a transgenic Aβ overexpressing mouse model ameliorated AD pathology (Garwood et al., 2017). The involvement of astrocytes in neuroinflammation entails increased production of cytokines that either affect the neurons directly or via microglial activation (Van Eldik et al., 2016). For instance, NFκβ-mediated activation of astrocytes release the complement protein C3 that can bind to neuronal C3aR and trigger neuronal damage. Another astrocyte signaling molecule is the soluble CD40 ligand that binds to microglial cell surface receptor. This binding interaction releases pro-inflammatory tumor necrosis alpha (TNF-α) that has been widely reported to contribute to tissue damage in AD (Van Eldik et al., 2016). Astrocytes also play a neuroprotective role. Recent studies have also shown that reactive astrocytes surrounding the Aβ plaques take up and degrade Aβ. For instance, in Tg2576 transgenic mice this has been shown to be linked to insulin degrading enzyme (IDE) which plays an important role in Aβ degradation. Reportedly, Aβ exposure of IDE enhanced the number of activated astrocytes surrounding the neuritic plaques (Wyss-Coray, 2012). Other studies have shown that treatment of astrocytes with *ex-vivo* Aβ extracts, increase the secretion of Aβ degrading enzymes (Wyss-Coray et al., 2003). Thus, the Aβ pathogenesis in AD may result in alterations of normal astrocyte functions which may be then trigger downstream inflammatory cascades prompting further neuronal damage in AD.

Tau and Inflammation

Although there are fewer reports, *in vitro* studies have shown that microglial cells stimulated by Aβ or LPS release pro-inflammatory cytokines such as interleukin-1β and activate tau phosphorylation at the pathological phospho-epitopes via MAPK pathway. This was confirmed by *in vivo* studies in 3xTg mouse model that displays both Aβ and tau pathologies. When these animals were subjected to high dose of LPS treatment, tau hyperphosphorylation was triggered at the pathological epitopes mediated by GSK-3β, CDK5, JNK, and MAP kinases (Barron et al., 2017). Several other studies have shown that the activation of the key kinases CDK5 and GSK-3β by themselves resulted in microglial activation and secretion of IL-1β implying a close link between tau hyperphosphorylation and pro-inflammatory markers. The gene expression profile analysis in a mouse model of tauopathy (rTg4510) which expresses the P301L mutation, revealed upregulation of pro-inflammatory markers such as complement 4B, glial fibrillary acidic protein (GFAP) and osteopontin (Spp1) on treatment with LPS. This result confirms that neuroinflammation modulates tau pathology in the absence of Aβ plaques (Wes et al., 2014). In addition, TREM2 levels were decreased in these transgenic mouse models indicating an alteration in microglial functions (Maphis et al., 2015). In this landmark study, Bhaskar et al. showed that LPS treatment of hTau mice expressing all 6 non-mutated tau isoforms enhanced microglial activation and accelerated tau pathology. These mice were deficient in microglia-specific fractalkine receptor (CX3CR1) that caused an exacerbation of tau hyperphosphorylation via p38/MAPK pathway. Further, studies in a P301S mutant human tau transgenic mice demonstrated that these animals displayed synaptic pathology and microgliosis before the onset of tangle formation confirming that microglial activation occurs early in the disease pathway. In this study, the researchers have shown that the immunosuppression of young P301S transgenic mice by FK506 significantly diminished tau pathology and increased their lifespan (Yoshiyama et al., 2007). These studies conclude that neuroinflammation accompanies early AD progression and blocking neuroinflammatory pathways might be beneficial in ameliorating tauopathies.

Hence, anti-inflammatory drugs have been used in clinical trials to prevent disease progression in AD. A study of nonsteroidal anti-inflammatory drugs (NSAIDS) in a Netherlands population (Rotterdam study) showed a significantly decreased risk of AD with increasing use of NSAIDS. In this study the short-term use of NSAID showed a relative risk of 0.95 while a long-term use of 24 months or more showed a relative risk of 0.2 with a confidence interval of 0.05–0.83 (In 't Veld et al., 1998). In a similar study reported in 2011 by Breitner et al. administration of NSAID Naproxen over a period of 2–3 years decreased the incidence of AD. These results were enhanced by measuring a marker of neurodegeneration, CSF ratios of tau to Aβ1-42 (Breitner et al., 2011). In contrast, a recent study by Marjerova et al. found that LPS treatment of immortalized microglial cells *in vitro* were capable of removing intracellular and extracellular tau

oligomers by phagocytosis. These observations were validated *in vivo* in C57BL/6 mice. When injected with soluble and insoluble human tau aggregates, these mice displayed active microglial phagocytosis of both tau species (Barron et al., 2017). Thus, the suppression of immune system by anti-inflammatory drugs may not prove beneficial to AD treatment in the long run as these might enhance the spread of tau oligomers across healthy neurons.

Inflammation in Type 2 Diabetes That Influence Neurodegeneration

Type 2 Diabetes has been associated with excess immune system activation, which increases the expression of proinflammatory cytokines especially microglia in the brain. It is noteworthy that Swaroop et al. observed elevated levels of TNFα, IL-1β, IL-2, and IL-6 in the hippocampus of diabetic animals (Swaroop et al., 2012). Previous studies have shown that incubation of cells with TNFα or high levels of FFA promotes inhibitory phosphorylation of the serine residues of IRS-1. This impairs the ability of IRS-1 to interact with the insulin receptor and generates an insulin-resistant condition capable of triggering Aβ and tau pathological cascades (Peraldi et al., 1996). It has also been demonstrated that obesity and hyperglycemia in T2DM contributes to ER and mitochondrial stress that generates reactive oxygen species (ROS). Elevated ROS then causes enhanced activation of inflammatory pathways (Kaneto et al., 2010; Back and Kaufman, 2012).

Along with evidences that relate oxidative stress and inflammation to the pathophysiology of diabetes, studies performed in various cellular and animal models suggest NFκβ activation is a key event early in the disease pathobiology and its complications. Several studies have shown that NF-κβ is induced by hyperglycemia and in conditions of neuronal damage (Romeo et al., 2002; Wellen and Hotamisligil, 2005). The activation of NF-κβ is followed by the expression of pro-inflammatory cytokines that jointly trigger brain inflammation and neuronal apoptosis eventually leading to cognitive decline. For instance, in the hippocampus of the STZ-treated rats there is a strong increase of ROS followed by NF-κβ activation (Locke and Anderson, 2011). Activated NF-κβ can induce cytotoxicity, trigger inflammation and promote apoptosis (Jaeschke et al., 2004). In STZ-induced retinopathy rat models, NF-κβ activation has been associated with enhanced expression of caspase 1 (Yin et al., 2017). Recent reports show that NF-κβ might be an important regulator of insulin sensitivity in T2DM by controlling the expression of GLUT2 receptor which is important for glucose secretion and transport in pancreatic beta cells (Patel and Santani, 2009).

Incidentally, the metabolic stresses that promote insulin resistance and T2DM also activate the inflammation and stress-induced kinases Ikβ kinase-β (IKKβ) and JUN N-terminal kinase (JNK) suggesting that these kinases play an important role in disease pathogenesis. Both JNK and IKκβ can phosphorylate the IRS-1 at the inhibitory Serine 307 thereby impairing insulin action (Jaeschke et al., 2004; Morel et al., 2010).

Oxidative stress in insulin resistance generates FFA and AGE products which result in glucotoxicity and impairment of insulin signaling. These ligands act through Toll-like receptors (TLRs) and receptors for advanced glycation end products (RAGE) that are also activated in neurodegenerative diseases (Ozcan et al., 2004). RAGE especially acts as a putative Aβ receptor and plays a significant role in AD pathogenesis. It is therefore predicted that the cumulative effect of these stress factors may lead to neuronal apoptosis and brain inflammation, both of which are prominent features of neurodegenerative diseases including AD.

To investigate whether inflammatory pathways act as a potential link between AD and T2DM, Takeda et al. generated a dual model of AD and T2DM by crossing an APP23 transgenic mice that overexpresses human APP to leptin-deficient ob/ob mice or polygenic NSY mice as a model for diabetes. The APP+/ob/ob dual transgenics showed increased levels of amyloid deposition around brain microvessels and enhanced cerebrovascular inflammation even before the manifestation of cerebral amyloid angiopathy. (Takeda et al., 2010). The authors also report an increased levels of RAGE in blood vessels as well as elevated levels of TNFα and IL-6 in the brain microvasculature of these animals. Progressive cognitive deficits and increased cerebrovascular inflammation were also noted in APP_{+}-NSY dual transgenics raised on high-fat diet compared to NSY mice raised on the same diet. In a study conducted by Knight et al. a similar impact of high-fat diet was observed in 3xTg AD mice that overexpress triple mutations in human APP/MAPT-P301L/PSEN1 and in nontransgenic mice. When raised on a high-fat diet both the transgenics and the control animals displayed considerable weight gain and memory impairments. However, the memory impairments were more severe in the 3xTg mice compared to the controls. It is also interesting that although no significant differences were observed in the amyloid plaques and tau-tangle loads, the brains of 3xTg animals were accompanied by severe microgliosis that was not observed in age-matched controls. This strongly implies the role of neuroinflammation in the development of AD pathogenesis especially when subjected to abnormal dietary conditions (Knight et al., 2014).

Emerging studies have shown that loss of inflammatory mediators prevents insulin resistance, therefore pharmacological targeting of inflammatory pathways improve insulin action. For instance, salicylates activate insulin signaling by inhibiting inflammatory kinases within the cell (Kim M. S. et al., 2013). Similarly, targeting JNK using a synthetic inhibitor has been reported to enhance insulin signaling in obese mice and reduce atherosclerosis in ApoE mutant rodent model (Lee et al., 2003). There are yet other studies which show that thiazolidinediones (TZDs), high-affinity ligands of PPARγ act as insulin sensitizing agents and improve insulin action by activating lipid metabolism as well as by reducing the production of inflammatory molecules like TNFα (Peraldi et al., 1996).

These studies support a significant correlation between hyperglycemia, impaired insulin resistance, oxidative stress, and inflammation. All these factors are capable of directly impacting Aβ and tau pathologies as well as triggering a chain of inflammatory stress responses that might eventually lead to neurodegeneration as observed in AD.

AUTOPHAGIC IMPAIRMENTS IN AD AND T2DM

Intracellular accumulation of misfolded protein aggregates is a salient feature of most neurodegenerative diseases (Frake et al., 2015). Autophagy is the process by which such protein aggregates are cleared from the neurons and is important for maintaining neuronal homeostasis. As neurons age they accumulate toxic intracellular protein aggregates and damaged organelles such as mitochondria that must be immediately cleared for the neuron to function at a physiological level (Lee, 2012; Son et al., 2012). Recent studies show that autophagic machinery is also involved in the pathophysiology of T2DM and it regulates the normal function of pancreatic beta cells. Insulin resistance generates oxidative stress on insulin-responsive tissues, enhanced autophagy in these cases acts as a protective factor (Masini et al., 2009). Other than indirect effects, there are studies that report direct impact of insulin resistance on autophagy by an inhibition of the downstream mTOR signaling pathway (Blagosklonny, 2013). Although, the connection between AD and T2DM pathogenesis in terms of autophagic dysfunction is not well documented, in this section we elaborate on the shared pathophysiologies of autophagy malfunctioning in these diseases and elaborate on the mechanisms by which insulin resistance might impact autophagy impairment and exacerbate AD pathogenesis.

Autophagy Malfunction in AD

Macroautophagy is the most prevalent form of neuronal autophagy (Frake et al., 2015). In this process, cytoplasmic proteins and organelles are sequestered into double membrane bound structures called autophagosomes (**Figure 3**). In the next step, the autophagosomes fuse with the lysosomes to form autolysosomes or alternatively with endosomes to form amphisomes before fusing with lysosomes and finally the contents are degraded.

There is a substantial evidence that autophagy is dysregulated in the brains of AD patients. In 2005, Nixon and colleagues used immunogold labeling and electron microscopy techniques on AD brain biopsies of neocortical regions and detected diverse formations of immature autophagic vacuoles (AVs) in the dystrophic neurites (Nixon, 2007). The same phenomenon was also observed in transgenic animal models of AD. A study in PS-1/APP double transgenic mice showed that AVs were formed in dendrites and soma before the appearance of Aβ plaques compared to age-matched control animals (Nixon et al., 2005). Chen et al. using LC3-EGFP overexpressing 5X FAD mouse models and age-matched controls, observed increased accumulation of autophagosomes in the neurons of FAD-mouse models compared to the controls. This was more prominent under conditions of starvation. Interestingly, the macroautophagy induced by starvation in the transgenic animals was not sufficient to degrade the endogenous Aβ levels which resulted due to increased cellular uptake of extracellular Aβ (Chen et al., 2015). The importance of autophagy in the brain was highlighted in a study demonstrating that neuron-specific loss of autophagy proteins (ATG7 and ATG5) in mice results in neurodegeneration even when other pathological factors are absent (Frake et al., 2015). However, actual mechanisms underlying autophagic dysfunctions in AD has not been fully elucidated. Till date it is a matter of debate as to whether autophagy is the cause or a result of AD.

Presenilins as Autophagy Modulators

Neely et al. has shown that Presenilins play an important role in mediating autophagy as PS-1 has been shown to facilitate N-glycosylation of V0a1 subunit of the lysosomal vacuolar ATPase (v-ATPase) (Neely et al., 2011). FAD-associated mutations in PS-1 and PS-2 leads to an impairment of lysosomal function due to failed acidification of the internal lysosomal contents. This causes an increased accumulation of autophagosomes and a failure to fuse with dysfunctional lysosomes. In their study, Wilson et al. found that in PS-1–/– neurons both α and β synuclein are mislocalized to the lysosomes of the neuronal cell body and not in the presynaptic regions. The increased accumulation of synuclein suggests that PS-1 deficiencies play a crucial role in developing α-syn lesions in neurodegenerative diseases as observed in familial AD and PD (Wilson et al., 2004). Interestingly, Tung et al. found that non-neuronal and neuronal cells lacking PS-1 displayed reduced levels of p62 protein which serves as a "cargo receptor" for tau degradation. Their study suggests a novel mechanism by which the reduction PS-1 or its mutation in FAD impairs p62-dependent tau clearance (Tung et al., 2014).

Aβ as an Autophagy Modulator

There is a complex interplay between Aβ and autophagy. Several studies have shown that autophagy plays a crucial role in Aβ metabolism including Aβ production, secretion, and degradation (Nilsson et al., 2015). Autophagy facilitates the degradation and clearance of APP and all APP cleavage products comprising Aβ and APP-C-terminal-fragments. Deficiency of autophagy protein beclin 1 in cultured neurons and human APP transgenic mice resulted in elevated intraneuronal Aβ and formation of extracellular amyloid plaques. Overexpression of beclin 1 promoted neuronal autophagy, reduced Aβ levels, and ameliorated neurodegeneration (Pickford et al., 2008). Autophagy may also play a role in the secretion of Aβ into extracellular environment where it causes plaque formation. For instance, deletion of ATG7 in APP transgenic mice resulted in less amount of Aβ secretion and plaque formation (Xiong, 2015).

Interestingly, Aβ by itself could also be a regulator of autophagy as intracellular Aβ can activate autophagy by an AKT-dependent pathway or RAGE-CAMκβ-AMPK pathway by induction of mitochondrial ROS generation (Kim et al., 2017). Thus rapamycin, an mTOR inhibitor that upregulates autophagy, is able to reduce both Aβ pathology in AD mouse models and improve cognition (Spilman et al., 2010).

Several studies indicate that insulin resistance in T2DM inhibits the downstream mTOR pathway and activates autophagy. Insulin resistance also causes ER and oxidative

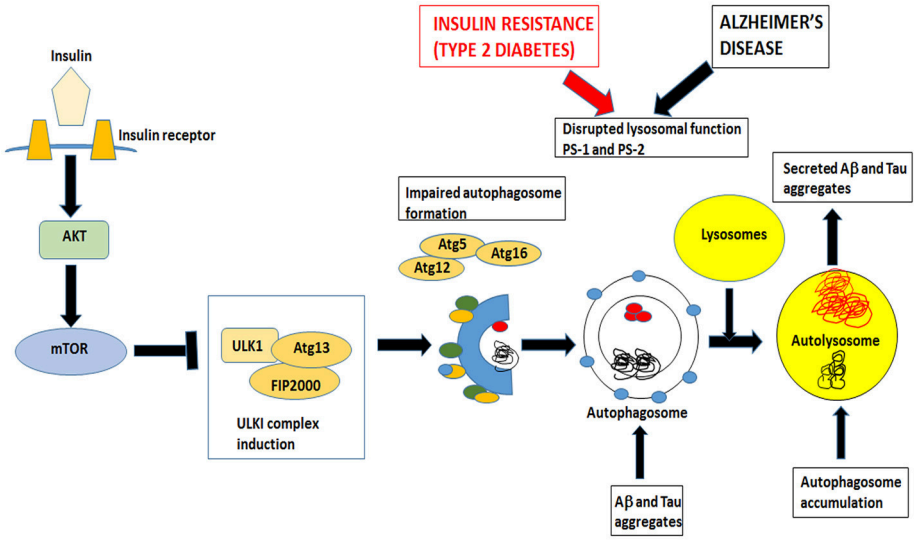


FIGURE 3 | Insulin signaling also controls mTOR pathway that inhibits autophagy. Both insulin resistance in Type 2 Diabetes and Alzheimer's disease impairs the formation of autophagosomes and disrupts lysosomal function. Autophagosomes fuse with lysosomes to form autolysosomes. These autolysosomes have impaired lysosomal function in AD and T2DM and accumulate Aβ and tau aggregates. Undigested toxic aggregates are secreted out of the neurons and propagate toxic oligomers in adjacent neurons.

stress that are capable of inducing autophagy (Quan et al., 2012). Ideally, enhanced autophagy should facilitate Aβ clearance; however, studies in ATG7 mouse models have shown that increased autophagy may also cause an increased secretion of Aβ in the extracellular matrix and enhance the deposition of Aβ plaques (Inoue et al., 2012). Thus, activation of autophagy under conditions of insulin resistance may worsen Aβ-mediated AD pathogenesis.

Tau and Autophagic Dysfunction

Recent studies suggest that autophagy plays a vital role in tau protein degradation and clearance (Inoue et al., 2012). A study in autophagy-impaired Nrf2 KO mice shows that the levels of phosphorylated and sarcosyl-insoluble tau increases (Jo et al., 2014). In ATG7 conditional KO mouse models the loss of ATG7 from the forebrains of transgenic mice leads to an accumulation of phospho-tau resembling pre-tangle formation within neurons (Inoue et al., 2012). On the restoration of autophagy, the levels of phospho-tau was found to be diminished. It has also been shown that the full-length tau (2N4R) and the caspase cleaved version (tauδC) are preferentially degraded by macroautophagy, while the truncated version of tau (taudelta280) is translocated to lysosomes by cell mediated autophagy (CMA) pathway (Dolan and Johnson, 2010).

Recent studies in primary neurons and transgenic P301S mouse models have demonstrated that treatment with autophagy-inducers trehalose and rapamycin reduced insoluble tau levels (Schaeffer et al., 2012; Ozcelik et al., 2013). Conversely, other studies have shown that mammalian target of rapamycin (mTOR) impairs tau clearance by inhibiting autophagy. The TSC1 and TSC2 are negative regulators of mTOR. Consequently, in TSC−/− transgenic mice the elevated levels of endogenous total and phosphorylated tau suggests an impairment of autophagy (Caccamo et al., 2013; Steele et al., 2013).

Under physiological conditions, tau promotes microtubule assembly and regulates microtubule dynamics (Janning et al., 2014). The microtubular arrays provide tracks for retrograde trafficking and maturation of autophagosomes before fusing with lysosomes in the soma (Kononenko, 2017). In the disease state, hyperphosphorylated tau is capable of disassembly and breakdown of microtubules that could subsequently inhibit retrograde trafficking causing the accumulation of immature autophagosomes within the axons (Rodríguez-Martín et al., 2013).

Autophagic Dysfunction in T2DM That Can Trigger AD Pathogenesis

Insulin resistance in T2DM effectively results in increased oxidative stress that causes the production of ROS leading to damage of intracellular organelles such as ER and mitochondria (Jung et al., 2011). These ER and mitochondrial stress factors are the critical upstream events for the induction of downstream autophagic pathways for the removal and clearance of misfolded proteins in the ER lumen and the dysfunctional ER and mitochondria (Quan et al., 2012). However, during prolonged periods of intracellular stress autophagy pathway becomes inefficient leading to increased accumulation of autophagosomes and impaired clearance. *In vivo* studies in pancreatic beta-cell specific ATG7 KO mice have shown a decrease in the number of pancreatic beta-cells, impaired glucose tolerance, and reduction in insulin secretion (Chen et al., 2011). In addition, these cells accumulate large ubiquitinated proteinaceous materials and p62 implying an autophagic impairment. Supporting these observations, Fujitani et al. demonstrated an increased

accumulation of autophagosomes in the pancreas of db/db mice (Fujitani et al., 2009). In addition, these ATG7-null beta-cells were found to be apoptotic leading to a decreased beta cell mass. When these ATG7 KO mice were crossed to ob/ob mice (a model for obesity with a mutation in the leptin gene) the progeny displayed severe diabetes suggesting that autophagic impairment in obese animals might make them more susceptible to diabetes (Quan et al., 2012). These studies suggest that autophagy acts as a neuroprotective factor in response to ER and mitochondrial stress generated in T2DM.

To elucidate the autophagic impairments underlying AD and T2DM, Jung et al. compared tau pathology and its associated signaling pathways in diabetic OLEF rats and age-matched non-diabetic controls (Jung et al., 2011). The scientists observed an increased accumulation of total and phospho-tau in the soluble fractions of brain extracts from OLEF rats. Interestingly, the increased accumulation of polyubiquitinated tau protein in the neurons of OLEF rats was accompanied by a decrease in p62 protein levels that is responsible for degradation of ubiquitinated tau by autophagy and proteasomal pathways In a similar study by Carvalho et al. using 3xTgAD and T2DM mouse models, a significant reduction was observed in the levels of autophagy markers ATG7 and LC3-II in the cerebral cortex and hippocampus of both these mice (Carvalho et al., 2015). Pronounced behavioral deficits were observed in these animals that correlated strongly with a reduction of the autophagy markers including the lysosomal marker LAMP1 suggesting an accumulation of autophagosomes and impaired protein clearance in both these models. It can be inferred that the impaired clearance of toxic, soluble aggregates of hyperphosphorylated tau protein is a critical mechanism underlying increased AD-like pathology in T2DM.

Taken together, these results show that firstly insulin resistance in T2DM is capable of inducing prolonged period of oxidative stress which leads to the failure of autophagic machinery and impaired autophagic clearance. This in turn may lead to the progressive build-up of toxic protein aggregates such as Aβ and tau oligomers and trigger AD pathogenesis. Secondly, under abnormal metabolic conditions or aging, autophagic impairment might be a crucial risk factor for T2DM. This could lead to a viscous cycle in which T2DM can promote tau hyperphosphorylation and induce the accumulation of autophagosomes within the neurons. Impaired autophagic clearance then triggers neurodegenerative events that lead to AD pathogenesis. The crucial role played by autophagy in AD and T2DM opens a new chapter in the development of pro-autophagy drugs that would be used as part of combinatorial therapy in targeting both diseases.

CONCLUSION

In this review we have attempted to summarize the growing body of research that depicts the shared pathophysiology of AD and T2DM and elaborated on the underlying mechanistic pathways at the crossroads of these two diseases. However, it should be noted that almost all the animal models of Aβ and tau that have been used for preclinical studies are based on FTDP-17 cases and not on sporadic AD models. Although the mechanistic uderpinnings that link AD and T2DM could be similar, there is a possibility of considerable variation in the development and propagation of the disease pathology in the familial vs. sporadic cases. This is particularly relevant when designing combinatorial therapies.

A growing body of evidence suggests that the structural and functional integrity of the CNS is compromised in T2DM in the presence of excess insulin or under a condition of insulin resistance. In addition, T2DM impairs glucose metabolism and generates oxidative stress in vital cell organelles. Insulin resistance which is a prominent feature of T2DM is capable of increasing the production and secretion of Aβ by decreasing proteolysis by IDE. Also, insulin resistance dysregulates the PI3K/AKT/GSK-3β signaling cascade and generates hyperphosphorylated tau. Insulin resistance leads to loss of synapses, impaired autophagy and increased neuronal apoptosis. These alterations might trigger a cascade of events leading to abnormal Aβ and tau accumulation culminating in Alzheimer's disease pathology. Hence, targeting brain insulin signaling with pharmacological therapies used for treating T2DM is a novel and compelling approach to treat AD (Morris and Burns, 2012). This has given way to "drug-repositioning" strategies in which pre-existing anti-diabetic drugs are subjected to clinical trials to test their efficacy in AD therapeutics (Watson et al., 2005; Chen et al., 2009; Miller et al., 2011; Moore et al., 2013; Yarchoan and Arnold, 2014; Luchsinger et al., 2016; Femminella et al., 2017).

AUTHOR CONTRIBUTIONS

SC researched articles and prepared the manuscript for the review. AM critically revised the draft before submission.

FUNDING

Funded by European Union's Horizon 2020 research and innovation programme under Marie Sklodowska-Curie grant agreement number 705417.

REFERENCES

Abbondante, S., Baglietto-Vargas, D., Rodriguez-Ortiz, C. J., Estrada-Hernandez, T., Medeiros, R., and Laferla, F. M. (2014). Genetic ablation of tau mitigates cognitive impairment induced by type 1 diabetes. *Am. J. Pathol.* 184, 819–826. doi: 10.1016/j.ajpath.2013.11.021

American Diabetes, A. (2009). Diagnosis and classification of diabetes mellitus. *Diabetes Care 32(Suppl.* 1), S62–S67. doi: 10.2337/dc09-S062

Avila, J. (2008). Tau kinases and phosphatases. *J. Cell. Mol. Med.* 12, 258–259. doi: 10.1111/j.1582-4934.2007.00214.x

Avila, J., Leon-Espinosa, G., García, E., García-Escudero, V., Hernández, F., and Defelipe, J. (2012). Tau phosphorylation by GSK3 in different

conditions. *Int. J. Alzheimers Dis.* 2012:578373. doi: 10.1155/2012/578373

Avila, J., Wandosell, F., and Hernández, F. (2010). Role of glycogen synthase kinase-3 in Alzheimer's disease pathogenesis and glycogen synthase kinase-3 inhibitors. *Expert. Rev. Neurother.* 10, 703–710. doi: 10.1586/ern.10.40

Back, S. H., and Kaufman, R. J. (2012). Endoplasmic reticulum stress and type 2 diabetes. *Annu. Rev. Biochem.* 81, 767–793. doi: 10.1146/annurev-biochem-072909-095555

Baglietto-Vargas, D., Shi, J., Yaeger, D. M., Ager, R., and LaFerla, F. M. (2016). Diabetes and Alzheimer's disease crosstalk. *Neurosci. Biobehav. Rev.* 64, 272–287. doi: 10.1016/j.neubiorev.2016.03.005

Balducci, C., Beeg, M., Stravalaci, M., Bastone, A., Sclip, A., Biasini, E., et al. (2010). Synthetic amyloid-β oligomers impair long-term memory independently of cellular prion protein. *Proc. Natl. Acad. Sci. U.S.A.* 107, 2295–2300. doi: 10.1073/pnas.0911829107

Barbagallo, M., and Dominguez, L. J. (2014). Type 2 diabetes mellitus and Alzheimer's disease. *World J. Diabetes* 5, 889–893. doi: 10.4239/wjd.v5.i6.889

Barron, H., Hafizi, S., Andreazza, A. C., and Mizrahi, R. (2017). Neuroinflammation and oxidative stress in psychosis and psychosis risk. *Int. J. Mol. Sci.* 18:651. doi: 10.3390/ijms18030651

Basurto-Islas, G., Luna-Munoz, J., Guillozet-Bongaarts, A. L., Binder, L. I., Mena, R., and Garcia-Sierra, F. (2008). Accumulation of aspartic acid421- and glutamic acid391-cleaved tau in neurofibrillary tangles correlates with progression in Alzheimer disease. *J. Neuropathol. Exp. Neurol.* 67, 470–483. doi: 10.1097/NEN.0b013e31817275c7

Beckett, L. A., Donohue, M. C., Wang, C., Aisen, P., Harvey, D. J., Saito, N., et al. (2015). The Alzheimer's disease neuroimaging initiative phase 2: increasing the length, breadth, and depth of our understanding. *Alzheimers Dement.* 11, 823–831. doi: 10.1016/j.jalz.2015.05.004

Bell, K. F., Bennett, D. A., and Cuello, A. C. (2007). Paradoxical upregulation of glutamatergic presynaptic boutons during mild cognitive impairment. *J. Neurosci.* 27, 10810–10817. doi: 10.1523/JNEUROSCI.3269-07.2007

Bemiller, S. M., McCray, T. J., Allan, K., Formica, S. V., Xu, G., Wilson, G., et al. (2017). TREM2 deficiency exacerbates tau pathology through dysregulated kinase signaling in a mouse model of tauopathy. *Mol. Neurodegener.* 12:74. doi: 10.1186/s13024-017-0216-6

Benedict, C., Hallschmid, M., Schultes, B., Born, J., and Kern, W. (2007). Intranasal insulin to improve memory function in humans. *Neuroendocrinology* 86, 136–142. doi: 10.1159/000106378

Bertram, L., and Tanzi, R. E. (2009). Genome-wide association studies in Alzheimer's disease. *Hum. Mol. Genet.* 18, R137–R145. doi: 10.1093/hmg/ddp406

Bierer, L. M., Hof, P. R., Purohit, D. P., Carlin, L., Schmeidler, J., Davis, K. L., et al. (1995). Neocortical neurofibrillary tangles correlate with dementia severity in Alzheimer's disease. *Arch. Neurol.* 52, 81–88. doi: 10.1001/archneur.1995.00540250089017

Blagosklonny, M. V. (2013). TOR-centric view on insulin resistance and diabetic complications: perspective for endocrinologists and gerontologists. *Cell Death Dis.* 4:e964. doi: 10.1038/cddis.2013.506

Blázquez, E., Velazquez, E., Hurtado-Carneiro, V., and Ruiz-Albusac, J. M. (2014). Insulin in the brain: its pathophysiological implications for States related with central insulin resistance, type 2 diabetes and Alzheimer's disease. *Front. Endocrinol.* 5:161. doi: 10.3389/fendo.2014.00161

Boucher, J., Kleinridders, A., and Kahn, C. R. (2014). Insulin receptor signaling in normal and insulin-resistant states. *Cold Spring Harb. Perspect. Biol.* 6:a009191. doi: 10.1101/cshperspect.a009191

Bradley, C. A., Peineau, S., Taghibiglou, C., Nicolas, C. S., Whitcomb, D. J., Bortolotto, Z. A., et al. (2012). A pivotal role of GSK-3 in synaptic plasticity. *Front. Mol. Neurosci.* 5:13. doi: 10.3389/fnmol.2012.00013

Breitner, J. C., Baker, L. D., Montine, T. J., Meinert, C. L., Lyketsos, C. G., Ashe, K. H., et al. (2011). Extended results of the Alzheimer's disease anti-inflammatory prevention trial. *Alzheimers Dement.* 7, 402–411. doi: 10.1016/j.jalz.2010.12.014

Busche, M. A., Chen, X., Henning, H. A., Reichwald, J., Staufenbiel, M., Sakmann, B., et al. (2012). Critical role of soluble amyloid-β for early hippocampal hyperactivity in a mouse model of Alzheimer's disease. *Proc. Natl. Acad. Sci. U.S.A.* 109, 8740–8745. doi: 10.1073/pnas.1206171109

Caccamo, A., Magri, A., Medina, D. X., Wisely, E. V., Lopez-Aranda, M. F., Silva, A. J., et al. (2013). mTOR regulates tau phosphorylation and degradation: implications for Alzheimer's disease and other tauopathies. *Aging Cell* 12, 370–380. doi: 10.1111/acel.12057

Carvalho, C., Santos, M. S., Oliveira, C. R., and Moreira, P. I. (2015). Alzheimer's disease and type 2 diabetes-related alterations in brain mitochondria, autophagy and synaptic markers. *Biochim. Biophys. Acta* 1852, 1665–1675. doi: 10.1016/j.bbadis.2015.05.001

Chatterjee, S., Sang, T. K., Lawless, G. M., and Jackson, G. R. (2009). Dissociation of tau toxicity and phosphorylation: role of GSK-3beta, MARK and Cdk5 in a Drosophila model. *Hum. Mol. Genet.* 18, 164–177. doi: 10.1093/hmg/ddn326

Cheignon, C., Tomas, M., Bonnefont-Rousselot, D., Faller, P., Hureau, C., and Collin, F. (2018). Oxidative stress and the amyloid beta peptide in Alzheimer's disease. *Redox. Biol.* 14, 450–464. doi: 10.1016/j.redox.2017.10.014

Chen, X., Kondo, K., Motoki, K., Homma, H., and Okazawa, H. (2015). Fasting activates macroautophagy in neurons of Alzheimer's disease mouse model but is insufficient to degrade amyloid-β. *Sci. Rep.* 5:12115. doi: 10.1038/srep12115

Chen, Y., Zhou, K., Wang, R., Liu, Y., Kwak, Y. D., Ma, T., et al. (2009). Antidiabetic drug metformin (GlucophageR) increases biogenesis of Alzheimer's amyloid peptides via up-regulating BACE1 transcription. *Proc. Natl. Acad. Sci. U.S.A.* 106, 3907–3912. doi: 10.1073/pnas.0807991106

Chen, Z. F., Li, Y. B., Han, J. Y., Wang, J., Yin, J. J., Li, J. B., et al. (2011). The double-edged effect of autophagy in pancreatic β cells and diabetes. *Autophagy* 7, 12–16. doi: 10.4161/auto.7.1.13607

Cheng, C. M., Tseng, V., Wang, J., Wang, D., Matyakhina, L., and Bondy, C. A. (2005). Tau is hyperphosphorylated in the insulin-like growth factor-I null brain. *Endocrinology* 146:508. doi: 10.1210/en.2005-0063

Cheng, D., Noble, J., Tang, M. X., Schupf, N., Mayeux, R., and Luchsinger, J. A. (2011). Type 2 diabetes and late-onset Alzheimer's disease. *Dement. Geriatr. Cogn. Disord.* 31, 424–430. doi: 10.1159/000324134

Chiang, S. H., Baumann, C. A., Kanzaki, M., Thurmond, D. C., Watson, R. T., Neudauer, C. L., et al. (2001). Insulin-stimulated GLUT4 translocation requires the CAP-dependent activation of TC10. *Nature* 410, 944–948. doi: 10.1038/35073608

Choi, B. R., Cho, W. H., Kim, J., Lee, H. J., Chung, C., Jeon, W. K., et al. (2014). Increased expression of the receptor for advanced glycation end products in neurons and astrocytes in a triple transgenic mouse model of Alzheimer's disease. *Exp. Mol. Med.* 46:e75. doi: 10.1038/emm.2013.147

Chouliaras, L., Sierksma, A. S., Kenis, G., Prickaerts, J., Lemmens, M. A., Brasnjevic, I., et al. (2010). Gene-environment interaction research and transgenic mouse models of Alzheimer's disease. *Int. J. Alzheimers Dis.* 2010:859101. doi: 10.4061/2010/859101

Clodfelder-Miller, B., De Sarno, P., Zmijewska, A. A., Song, L., and Jope, R. S. (2005). Physiological and pathological changes in glucose regulate brain Akt and glycogen synthase kinase-3. *J. Biol. Chem.* 280, 39723–39731. doi: 10.1074/jbc.M508824200

Cohen, T. J., Guo, J. L., Hurtado, D. E., Kwong, L. K., Mills, I. P., Trojanowski, J. Q., et al. (2011). The acetylation of tau inhibits its function and promotes pathological tau aggregation. *Nat. Commun.* 2:252. doi: 10.1038/ncomms1255

Cook, C., Stankowski, J. N., Carlomagno, Y., Stetler, C., and Petrucelli, L. (2014). Acetylation: a new key to unlock tau's role in neurodegeneration. *Alzheimers Res. Ther.* 6:29. doi: 10.1186/alzrt259

Criscuolo, C., Fontebasso, V., Middei, S., Stazi, M., Ammassari-Teule, M., Yan, S. S., et al. (2017). Entorhinal cortex dysfunction can be rescued by inhibition of microglial RAGE in an Alzheimer's disease mouse model. *Sci. Rep.* 7:42370. doi: 10.1038/srep42370

De Felice, F. G., and Ferreira, S. T. (2014). Inflammation, defective insulin signaling, and mitochondrial dysfunction as common molecular denominators connecting type 2 diabetes to Alzheimer disease. *Diabetes* 63, 2262–2272. doi: 10.2337/db13-1954

De Felice, F. G., Lourenco, M. V., and Ferreira, S. T. (2014). How does brain insulin resistance develop in Alzheimer's disease? *Alzheimers Dement.* 10, S26–S32. doi: 10.1016/j.jalz.2013.12.004

De Felice, F. G., Vieira, M. N., Bomfim, T. R., Decker, H., Velasco, P. T., Lambert, M. P., et al. (2009). Protection of synapses against Alzheimer's-linked toxins: insulin signaling prevents the pathogenic binding of Abeta oligomers. *Proc. Natl. Acad. Sci. U.S.A.* 106, 1971–1976. doi: 10.1073/pnas.0809158106

de la Monte, S. M., and Wands, J. R. (2008). Alzheimer's disease is type 3 diabetes-evidence reviewed. *J. Diabetes Sci. Technol.* 2, 1101–1113. doi: 10.1177/193229680800200619

De Strooper, B. (2007). Loss-of-function presenilin mutations in Alzheimer disease. *talking point on the role of presenilin mutations in Alzheimer disease. EMBO Rep.* 8, 141–146. doi: 10.1038/sj.embor.7400897

Deane, R., Singh, I., Sagare, A. P., Bell, R. D., Ross, N. T., LaRue, B., et al. (2012). A multimodal RAGE-specific inhibitor reduces amyloid beta-mediated brain disorder in a mouse model of Alzheimer disease. *J. Clin. Invest.* 122, 1377–1392. doi: 10.1172/JCI58642

Doens, D., and Fernandez, P. L. (2014). Microglia receptors and their implications in the response to amyloid β for Alzheimer's disease pathogenesis. *J. Neuroinflammation* 11:48. doi: 10.1186/1742-2094-11-48

Dolan, P. J., and Johnson, G. V. (2010). A caspase cleaved form of tau is preferentially degraded through the autophagy pathway. *J. Biol. Chem.* 285, 21978–21987. doi: 10.1074/jbc.M110.110940

Dorszewska, J., Prendecki, M., Oczkowska, A., Dezor, M., and Kozubski, W. (2016). Molecular basis of familial and sporadic Alzheimer's disease. *Curr. Alzheimer Res.* 13, 952–963. doi: 10.2174/1567205013666160314150501

Esparza, T. J., Wildburger, N. C., Jiang, H., Gangolli, M., Cairns, N. J., Bateman, R. J., et al. (2016). Soluble amyloid-beta aggregates from human Alzheimer's disease brains. *Sci. Rep.* 6:38187. doi: 10.1038/srep38187

Farrar, C., Houser, C. R., and Clarke, S. (2005). Activation of the PI3K/Akt signal transduction pathway and increased levels of insulin receptor in protein repair-deficient mice. *Aging Cell* 4, 1–12. doi: 10.1111/j.1474-9728.2004.00136.x

Farris, W., Mansourian, S., Chang, Y., Lindsley, L., Eckman, E. A., Frosch, M. P., et al. (2003). Insulin-degrading enzyme regulates the levels of insulin, amyloid beta-protein, and the beta-amyloid precursor protein intracellular domain *in vivo*. *Proc. Natl. Acad. Sci. U.S.A.* 100, 4162–4167. doi: 10.1073/pnas.0230450100

Femminella, G. D., Bencivenga, L., Petraglia, L., Visaggi, L., Gioia, L., Grieco, F. V., et al. (2017). Antidiabetic drugs in Alzheimer's Disease: mechanisms of action and future perspectives. *J. Diabetes Res.* 2017:7420796. doi: 10.1155/2017/7420796

Ferreira, S. T., Lourenco, M. V., Oliveira, M. M., and De Felice, F. G. (2015). Soluble amyloid-beta oligomers as synaptotoxins leading to cognitive impairment in Alzheimer's disease. *Front. Cell. Neurosci.* 9:191. doi: 10.3389/fncel.2015.00191

Fjell, A. M., Amlien, I. K., Sneve, M. H., Grydeland, H., Tamnes, C. K., Chaplin, T. A., et al. (2015). The roots of Alzheimer's disease: are high-expanding cortical areas preferentially targeted?dagger. *Cereb. Cortex* 25, 2556–2565. doi: 10.1093/cercor/bhu055

Frake, R. A., Ricketts, T., Menzies, F. M., and Rubinsztein, D. C. (2015). Autophagy and neurodegeneration. *J. Clin. Invest.* 125, 65–74. doi: 10.1172/JCI73944

Fröjdö, S., Vidal, H., and Pirola, L. (2009). Alterations of insulin signaling in type 2 diabetes: a review of the current evidence from humans. *Biochim. Biophys. Acta* 1792, 83–92. doi: 10.1016/j.bbadis.2008.10.019

Fujitani, Y., Kawamori, R., and Watada, H. (2009). The role of autophagy in pancreatic β-cell and diabetes. *Autophagy* 5, 280–282. doi: 10.4161/auto.5.2.7656

Garwood, C. J., Ratcliffe, L. E., Simpson, J. E., Heath, P. R., Ince, P. G., and Wharton, S. B. (2017). Review: Astrocytes in Alzheimer's disease and other age-associated dementias: a supporting player with a central role. *Neuropathol. Appl. Neurobiol.* 43, 281–298. doi: 10.1111/nan.12338

Gaspar, J. M., Baptista, F. I., Macedo, M. P., and Ambrosio, A. F. (2016). Inside the diabetic brain: role of different players involved in cognitive decline. *ACS Chem. Neurosci.* 7, 131–142. doi: 10.1021/acschemneuro.5b00240

Gasparini, L., Gouras, G. K., Wang, R., Gross, R. S., Beal, M. F., Greengard, P., et al. (2001). Stimulation of beta-amyloid precursor protein trafficking by insulin reduces intraneuronal beta-amyloid and requires mitogen-activated protein kinase signaling. *J. Neurosci.* 21, 2561–2570. doi: 10.1523/JNEUROSCI.21-08-02561.2001

Gendron, T. F., and Petrucelli, L. (2009). The role of tau in neurodegeneration. *Mol. Neurodegener.* 4:13. doi: 10.1186/1750-1326-4-13

Gilley, J., Ando, K., Seereeram, A., Rodriguez-Martin, T., Pooler, A. M., Sturdee, L., et al. (2016). Mislocalization of neuronal tau in the absence of tangle pathology in phosphomutant tau knockin mice. *Neurobiol. Aging* 39, 1–18. doi: 10.1016/j.neurobiolaging.2015.11.028

Gómez-Sintes, R., Hernandez, F., Lucas, J. J., and Avila, J. (2011). GSK-3 mouse models to study neuronal apoptosis and neurodegeneration. *Front. Mol. Neurosci.* 4:45. doi: 10.3389/fnmol.2011.00045

Gong, C. X., Liu, F., Grundke-Iqbal, I., and Iqbal, K. (2005). Post-translational modifications of tau protein in Alzheimer's disease. *J. Neural Transm.* 112, 813–838. doi: 10.1007/s00702-004-0221-0

Goure, W. F., Krafft, G. A., Jerecic, J., and Hefti, F. (2014). Targeting the proper amyloid-beta neuronal toxins: a path forward for Alzheimer's disease immunotherapeutics. *Alzheimers Res. Ther.* 6:42. doi: 10.1186/alzrt272

Gratuze, M., Julien, J., Petry, F. R., Morin, F., and Planel, E. (2017). Insulin deprivation induces PP2A inhibition and tau hyperphosphorylation in hTau mice, a model of Alzheimer's disease-like tau pathology. *Sci. Rep.* 7:46359. doi: 10.1038/srep46359

Griciuc, A., Serrano-Pozo, A., Parrado, A. R., Lesinski, A. N., Asselin, C. N., Mullin, K., et al. (2013). Alzheimer's disease risk gene CD33 inhibits microglial uptake of amyloid β. *Neuron* 78, 631–643. doi: 10.1016/j.neuron.2013.04.014

Guerrero-Muñoz, M. J., Gerson, J., and Castillo-Carranza, D. L. (2015). Tau oligomers: the toxic player at Synapses in Alzheimer's Disease. *Front. Cell. Neurosci.* 9:464. doi: 10.3389/fncel.2015.00464

Haass, C., and Mandelkow, E. (2010). Fyn-tau-amyloid: a toxic triad. *Cell* 142, 356–358. doi: 10.1016/j.cell.2010.07.032

Haataja, L., Gurlo, T., Huang, C. J., and Butler, P. C. (2008). Islet amyloid in type 2 diabetes, and the toxic oligomer hypothesis. *Endocr. Rev.* 29, 303–316. doi: 10.1210/er.2007-0037

Hanover, J. A., and Wang, P. (2013). O-GlcNAc cycling shows neuroprotective potential in C. *elegans models of neurodegenerative disease. Worm* 2:e27043. doi: 10.4161/worm.27043

Hernandez, F., Lucas, J. J., and Avila, J. (2013). GSK3 and tau: two convergence points in Alzheimer's disease. *J. Alzheimers Dis.* 33(Suppl. 1), S141–S144. doi: 10.3233/JAD-2012-129025

Ho, L., Qin, W., Pompl, P. N., Xiang, Z., Wang, J., Zhao, Z., et al. (2004). Diet-induced insulin resistance promotes amyloidosis in a transgenic mouse model of Alzheimer's disease. *FASEB J.* 18, 902–904. doi: 10.1096/fj.03-0978fje

Holth, J. K., Bomben, V. C., Reed, J. G., Inoue, T., Younkin, L., Younkin, S. G., et al. (2013). Tau loss attenuates neuronal network hyperexcitability in mouse and Drosophila genetic models of epilepsy. *J. Neurosci.* 33, 1651–1659. doi: 10.1523/JNEUROSCI.3191-12.2013

Horvath, J., Herrmann, F. R., Burkhard, P. R., Bouras, C., and Kovari, E. (2013). Neuropathology of dementia in a large cohort of patients with Parkinson's disease. *Parkinsonism Relat. Disord. 19*, 864–868. doi: 10.1016/j.parkreldis.2013.05.010

Hu, N., Tan, M. S., Sun, L., Jiang, T., Wang, Y. L., Tan, L., et al. (2014). Decreased expression of CD33 in peripheral mononuclear cells of Alzheimer's disease patients. *Neurosci. Lett.* 563, 51–54. doi: 10.1016/j.neulet.2014.01.004

Huang, C. C., Chung, C. M., Leu, H. B., Lin, L. Y., Chiu, C. C., Hsu, C. Y., et al. (2014). Diabetes mellitus and the risk of Alzheimer's disease: a nationwide population-based study. *PLoS ONE* 9:e87095. doi: 10.1371/journal.pone.0087095

Huda, M. N., Erdene-Ochir, E., and Pan, C. H. (2017). Assay for phosphorylation and microtubule binding along with localization of tau protein in colorectal cancer cells. *J. Vis. Exp.* doi: 10.3791/55932

In 't Veld, B. A., Launer, L. J., Hoes, A. W., Ott, A., Hofman, A., Breteler, M. M., et al. (1998). NSAIDs and incident Alzheimer's disease. *The Rotterdam Study. Neurobiol. Aging* 19, 607–611. doi: 10.1016/S0197-4580(98)00096-7

Inoue, K., Rispoli, J., Kaphzan, H., Klann, E., Chen, E. I., Kim, J., et al. (2012). Macroautophagy deficiency mediates age-dependent neurodegeneration through a phospho-tau pathway. *Mol. Neurodegener.* 7:48. doi: 10.1186/1750-1326-7-48

Iqbal, K., Liu, F., Gong, C. X., and Grundke-Iqbal, I. (2010). Tau in Alzheimer disease and related tauopathies. *Curr. Alzheimer Res.* 7, 656–664. doi: 10.2174/156720510793611592

Irwin, D. J., Cohen, T. J., Grossman, M., Arnold, S. E., McCarty-Wood, E., Van Deerlin, V. M., et al. (2013). Acetylated tau neuropathology in sporadic and hereditary tauopathies. *Am. J. Pathol.* 183, 344–351. doi: 10.1016/j.ajpath.2013.04.025

Jaeschke, A., Czech, M. P., and Davis, R. J. (2004). An essential role of the JIP1 scaffold protein for JNK activation in adipose tissue. *Genes Dev.* 18, 1976–1980. doi: 10.1101/gad.1216504

James, B. D., Leurgans, S. E., Hebert, L. E., Scherr, P. A., Yaffe, K., and Bennett, D. A. (2014). Contribution of Alzheimer disease to mortality in the United States. *Neurology* 82, 1045–1050. doi: 10.1212/WNL.0000000000000240

Janning, D., Igaev, M., Sundermann, F., Bruhmann, J., Beutel, O., Heinisch, J. J., et al. (2014). Single-molecule tracking of tau reveals fast kiss-and-hop interaction with microtubules in living neurons. *Mol. Biol. Cell* 25, 3541–3551. doi: 10.1091/mbc.e14-06-1099

Jay, T. R., Hirsch, A. M., Broihier, M. L., Miller, C. M., Neilson, L. E., Ransohoff, R. M., et al. (2017). Disease progression-dependent effects of TREM2 deficiency in a mouse model of Alzheimer's disease. *J. Neurosci.* 37, 637–647. doi: 10.1523/JNEUROSCI.2110-16.2016

Jiang, T., Yu, J. T., Hu, N., Tan, M. S., Zhu, X. C., and Tan, L. (2014). CD33 in Alzheimer's disease. *Mol. Neurobiol.* 49, 529–535. doi: 10.1007/s12035-013-8536-1

Jimenez, S., Navarro, V., Moyano, J., Sanchez-Mico, M., Torres, M., Davila, J. C., et al. (2014). Disruption of amyloid plaques integrity affects the soluble oligomers content from Alzheimer disease brains. *PLoS ONE* 9:e114041. doi: 10.1371/journal.pone.0114041

Jo, C., Gundemir, S., Pritchard, S., Jin, Y. N., Rahman, I., and Johnson, G. V. (2014). Nrf2 reduces levels of phosphorylated tau protein by inducing autophagy adaptor protein NDP52. *Nat. Commun.* 5:3496. doi: 10.1038/ncomms4496

Jung, H. J., Kim, Y. J., Eggert, S., Chung, K. C., Choi, K. S., and Park, S. A. (2013). Age-dependent increases in tau phosphorylation in the brains of type 2 diabetic rats correlate with a reduced expression of p62. *Exp. Neurol.* 248, 441–450. doi: 10.1016/j.expneurol.2013.07.013

Jung, H. J., Park, S. S., Mok, J. O., Lee, T. K., Park, C. S., and Park, S. A. (2011). Increased expression of three-repeat isoforms of tau contributes to tau pathology in a rat model of chronic type 2 diabetes. *Exp. Neurol.* 228, 232–241. doi: 10.1016/j.expneurol.2011.01.012

Kadavath, H., Hofele, R. V., Biernat, J., Kumar, S., Tepper, K., Urlaub, H., et al. (2015). Tau stabilizes microtubules by binding at the interface between tubulin heterodimers. *Proc. Natl. Acad. Sci. U.S.A.* 112, 7501–7506. doi: 10.1073/pnas.1504081112

Kaneto, H., Katakami, N., Matsuhisa, M., and Matsuoka, T. A. (2010). Role of reactive oxygen species in the progression of type 2 diabetes and atherosclerosis. *Mediators Inflamm.* 2010:453892. doi: 10.1155/2010/453892

Karsten, S. L., Sang, T. K., Gehman, L. T., Chatterjee, S., Liu, J., Lawless, G. M., et al. (2006). A genomic screen for modifiers of tauopathy identifies puromycin-sensitive aminopeptidase as an inhibitor of tau-induced neurodegeneration. *Neuron* 51, 549–560. doi: 10.1016/j.neuron.2006.07.019

Katsuse, O., Lin, W. L., Lewis, J., Hutton, M. L., and Dickson, D. W. (2006). Neurofibrillary tangle-related synaptic alterations of spinal motor neurons of P301L tau transgenic mice. *Neurosci. Lett.* 409, 95–99. doi: 10.1016/j.neulet.2006.09.021

Ke, Y. D., Delerue, F., Gladbach, A., Gotz, J., and Ittner, L. M. (2009). Experimental diabetes mellitus exacerbates tau pathology in a transgenic mouse model of Alzheimer's disease. *PLoS ONE* 4:e7917. doi: 10.1371/journal.pone.0007917

Kim, B., and Feldman, E. L. (2015). Insulin resistance as a key link for the increased risk of cognitive impairment in the metabolic syndrome. *Exp. Mol. Med.* 47:e149. doi: 10.1038/emm.2015.3

Kim, B., Backus, C., Oh, S., and Feldman, E. L. (2013). Hyperglycemia-induced tau cleavage *in vitro* and *in vivo*: a possible link between diabetes and Alzheimer's disease. *J. Alzheimers Dis.* 34, 727–739. doi: 10.3233/JAD-121669

Kim, B., Backus, C., Oh, S., Hayes, J. M., and Feldman, E. L. (2009). Increased tau phosphorylation and cleavage in mouse models of type 1 and type 2 diabetes. *Endocrinology* 150, 5294–5301. doi: 10.1210/en.2009-0695

Kim, I., Lee, K. O., Yun, Y. J., Jeong, J. Y., Kim, E. H., Cheong, H., et al. (2017). Biophysical characterization of $Ca^{(2+)}$-binding of S100A5 and Ca(2+)-induced interaction with RAGE. *Biochem. Biophys. Res. Commun.* 483, 332–338. doi: 10.1016/j.bbrc.2016.12.143

Kim, M. S., Yamamoto, Y., Kim, K., Kamei, N., Shimada, T., Liu, L., et al. (2013). Regulation of diet-induced adipose tissue and systemic inflammation by salicylates and pioglitazone. *PLoS ONE* 8:e82847. doi: 10.1371/journal.pone.0082847

King, M. R., Anderson, N. J., Guernsey, L. S., and Jolivalt, C. G. (2013). Glycogen synthase kinase-3 inhibition prevents learning deficits in diabetic mice. *J. Neurosci. Res.* 91, 506–514. doi: 10.1002/jnr.23192

Knight, E. M., Martins, I. V., Gumusgoz, S., Allan, S. M., and Lawrence, C. B. (2014). High-fat diet-induced memory impairment in triple-transgenic Alzheimer's disease (3xTgAD) mice is independent of changes in amyloid and tau pathology. *Neurobiol. Aging* 35, 1821–1832. doi: 10.1016/j.neurobiolaging.2014.02.010

Koenigsknecht, J., and Landreth, G. (2004). Microglial phagocytosis of fibrillar β-amyloid through a beta1 integrin-dependent mechanism. *J. Neurosci.* 24, 9838–9846. doi: 10.1523/JNEUROSCI.2557-04.2004

Kononenko, N. L. (2017). Lysosomes convene to keep the synapse clean. *J Cell Biol.* 216:2251. doi: 10.1083/jcb.201707070

Kopeikina, K. J., Polydoro, M., Tai, H. C., Yaeger, E., Carlson, G. A., Pitstick, R., et al. (2013). Synaptic alterations in the rTg4510 mouse model of tauopathy. *J. Comp. Neurol.* 521, 1334–1353. doi: 10.1002/cne.23234

Kosanam, H., Thai, K., Zhang, Y., Advani, A., Connelly, K. A., Diamandis, E. P., et al. (2014). Diabetes induces lysine acetylation of intermediary metabolism enzymes in the kidney. *Diabetes* 63, 2432–2439. doi: 10.2337/db12-1770

LaFerla, F. M., and Oddo, S. (2005). Alzheimer's disease: Aβ, tau and synaptic dysfunction. *Trends Mol. Med.* 11, 170–176. doi: 10.1016/j.molmed.2005.02.009

Lathuilière, A., Valdes, P., Papin, S., Cacquevel, M., Maclachlan, C., Knott, G. W., et al. (2017). Motifs in the tau protein that control binding to microtubules and aggregation determine pathological effects. *Sci. Rep.* 7:13556. doi: 10.1038/s41598-017-13786-2

Lauretti, E., Li, J. G., Di Meco, A., and Pratico, D. (2017). Glucose deficit triggers tau pathology and synaptic dysfunction in a tauopathy mouse model. *Transl. Psychiatry* 7:e1020. doi: 10.1038/tp.2016.296

Lee, E. J., and Park, J. H. (2013). Receptor for advanced glycation endproducts (RAGE), its ligands, and soluble RAGE: potential biomarkers for diagnosis and therapeutic targets for human renal diseases. *Genomics Inform.* 11, 224–229. doi: 10.5808/GI.2013.11.4.224

Lee, J. A. (2012). Neuronal autophagy: a housekeeper or a fighter in neuronal cell survival? *Exp. Neurobiol.* 21, 1–8. doi: 10.5607/en.2012.21.1.1

Lee, Y. H., Giraud, J., Davis, R. J., and White, M. F. (2003). c-Jun N-terminal kinase (JNK) mediates feedback inhibition of the insulin signaling cascade. *J. Biol. Chem.* 278, 2896–2902. doi: 10.1074/jbc.M208359200

Leibson, C. L., Rocca, W. A., Hanson, V. A., Cha, R., Kokmen, E., O'Brien, P. C., et al. (1997). The risk of dementia among persons with diabetes mellitus: a population-based cohort study. *Ann. N. Y. Acad. Sci.* 826, 422–427. doi: 10.1111/j.1749-6632.1997.tb48496.x

Li, S., Jin, M., Koeglsperger, T., Shepardson, N. E., Shankar, G. M., and Selkoe, D. J. (2011). Soluble Aβ oligomers inhibit long-term potentiation through a mechanism involving excessive activation of extrasynaptic NR2B-containing NMDA receptors. *J. Neurosci.* 31, 6627–6638. doi: 10.1523/JNEUROSCI.0203-11.2011

Li, W., Wang, T., and Xiao, S. (2016). Type 2 diabetes mellitus might be a risk factor for mild cognitive impairment progressing to Alzheimer's disease. *Neuropsychiatr. Dis. Treat.* 12, 2489–2495. doi: 10.2147/NDT.S111298

Li, X. H., Du, L. L., Cheng, X. S., Jiang, X., Zhang, Y., Lv, B. L., et al. (2013). Glycation exacerbates the neuronal toxicity of beta-amyloid. *Cell Death Dis.* 4:e673. doi: 10.1038/cddis.2013.180

Li, X., Shen, N., Zhang, S., Liu, J., Jiang, Q., Liao, M., et al. (2015b). CD33 rs3865444 polymorphism contributes to alzheimer's disease susceptibility in Chinese, European, and North American Populations. *Mol. Neurobiol.* 52, 414–421. doi: 10.1007/s12035-014-8880-9

Li, X., Song, D., and Leng, S. X. (2015a). Link between type 2 diabetes and Alzheimer's disease: from epidemiology to mechanism and treatment. *Clin. Interv. Aging* 10, 549–560. doi: 10.2147/CIA.S74042

Liu, L. P., Hong, H., Liao, J. M., Wang, T. S., Wu, J., Chen, S. S., et al. (2009). Upregulation of RAGE at the blood-brain barrier in streptozotocin-induced diabetic mice. *Synapse* 63, 636–642. doi: 10.1002/syn.20644

Liu, Y., Liu, F., Grundke-Iqbal, I., Iqbal, K., and Gong, C. X. (2009). Brain glucose transporters, O-GlcNAcylation and phosphorylation of tau in diabetes and Alzheimer's disease. *J. Neurochem.* 111, 242–249. doi: 10.1111/j.1471-4159.2009.06320.x

Locke, M., and Anderson, J. (2011). NF-kappaB activation in organs from STZ-treated rats. *Appl. Physiol. Nutr. Metab.* 36, 121–127. doi: 10.1139/H10-094

Luchsinger, J. A., Perez, T., Chang, H., Mehta, P., Steffener, J., Pradabhan, G., et al. (2016). Metformin in amnestic mild cognitive impairment: results of a pilot

randomized placebo controlled clinical trial. *J. Alzheimers Dis.* 51, 501–514. doi: 10.3233/JAD-150493

Macauley, S. L., Stanley, M., Caesar, E. E., Yamada, S. A., Raichle, M. E., Perez, R., et al. (2015). Hyperglycemia modulates extracellular amyloid-beta concentrations and neuronal activity *in vivo*. *J. Clin. Invest.* 125, 2463–2467. doi: 10.1172/JCI79742

Magrane, J., Christensen, R. A., Rosen, K. M., , Veereshwarayya, V., and Querfurth, H. W. (2006). Dissociation of ERK and Akt signaling in endothelial cell angiogenic responses to beta-amyloid. *Exp. Cell Res.* 312, 996–1010. doi: 10.1016/j.yexcr.2005.12.009

Mandelkow, E., and Mandelkow, E. M. (1995). Microtubules and microtubule-associated proteins. *Curr. Opin. Cell Biol.* 7, 72–81. doi: 10.1016/0955-0674(95)80047-6

Maphis, N., Xu, G., Kokiko-Cochran, O. N., Jiang, S., Cardona, A., Ransohoff, R. M., et al. (2015). Reactive microglia drive tau pathology and contribute to the spreading of pathological tau in the brain. *Brain 138*, 1738–1755. doi: 10.1093/brain/awv081

Marciniak, E., Leboucher, A., Caron, E., Ahmed, T., Tailleux, A., Dumont, J., et al. (2017). Tau deletion promotes brain insulin resistance. *J. Exp. Med.* 214, 2257–2269. doi: 10.1084/jem.20161731

Marseglia, A., Fratiglioni, L., Laukka, E. J., Santoni, G., Pedersen, N. L., Backman, L., et al. (2016). Early cognitive deficits in Type 2 Diabetes: a population-based study. *J. Alzheimers Dis.* 53, 1069–1078. doi: 10.3233/JAD-160266

Marzban, L., Park, K., and Verchere, C. B. (2003). Islet amyloid polypeptide and type 2 diabetes. *Exp. Gerontol.* 38, 347–351. doi: 10.1016/S0531-5565(03)00004-4

Masini, M., Bugliani, M., Lupi, R., del Guerra, S., Boggi, U., Filipponi, F., et al. (2009). Autophagy in human type 2 diabetes pancreatic β cells. *Diabetologia* 52, 1083–1086. doi: 10.1007/s00125-009-1347-2

Matos, M., Augusto, E., Oliveira, C. R., and Agostinho, P. (2008). Amyloid-beta peptide decreases glutamate uptake in cultured astrocytes: involvement of oxidative stress and mitogen-activated protein kinase cascades. *Neuroscience* 156, 898–910. doi: 10.1016/j.neuroscience.2008.08.022

Michalovicz, L. T., Lally, B., and Konat, G. W. (2015). Peripheral challenge with a viral mimic upregulates expression of the complement genes in the hippocampus. *J. Neuroimmunol.* 285, 137–142. doi: 10.1016/j.jneuroim.2015.06.003

Miller, B. W., Willett, K. C., and Desilets, A. R. (2011). Rosiglitazone and pioglitazone for the treatment of Alzheimer's disease. *Ann. Pharmacother.* 45, 1416–1424. doi: 10.1345/aph.1Q238

Minkeviciene, R., Rheims, S., Dobszay, M. B., Zilberter, M., Hartikainen, J., Fulop, L., et al. (2009). Amyloid β-induced neuronal hyperexcitability triggers progressive epilepsy. *J. Neurosci.* 29, 3453–3462. doi: 10.1523/JNEUROSCI.5215-08.2009

Molina, J., Rodriguez-Diaz, R., Fachado, A., Jacques-Silva, M. C., Berggren, P. O., and Caicedo, A. (2014). Control of insulin secretion by cholinergic signaling in the human pancreatic islet. *Diabetes* 63, 2714–2726. doi: 10.2337/db13-1371

Moore, E. M., Mander, A. G., Ames, D., Kotowicz, M. A., Carne, R. P., Brodaty, H., et al. (2013). Increased risk of cognitive impairment in patients with diabetes is associated with metformin. *Diabetes Care* 36, 2981–2987. doi: 10.2337/dc13-0229

Moro, M., Phillips, A. S., Gaimster, K., Paul, C., Mudher, A., Nicoll, J., et al. (2018). Pyroglutamate and isoaspartate modified amyloid-beta in ageing and Alzheimer's disease. *Acta Neuropathol. Commun.* 6:3. doi: 10.1186/s40478-017-0505-x

Moran, C., Beare, R., Phan, T. G., Bruce, D. G., Callisaya, M. L., Srikanth, V., et al. (2015). Type 2 diabetes mellitus and biomarkers of neurodegeneration. *Neurology* 85, 1123–1130. doi: 10.1212/WNL.0000000000001982

Moreira, P. I., Santos, M. S., Moreno, A. M., Seica, R., and Oliveira, C. R. (2003). Increased vulnerability of brain mitochondria in diabetic (Goto-Kakizaki) rats with aging and amyloid-beta exposure. *Diabetes* 52, 1449–1456. doi: 10.2337/diabetes.52.6.1449

Morel, C., Standen, C. L., Jung, D. Y., Gray, S., Ong, H., Flavell, R. A., et al. (2010). Requirement of JIP1-mediated c-Jun N-terminal kinase activation for obesity-induced insulin resistance. *Mol. Cell Biol.* 30, 4616–4625. doi: 10.1128/MCB.00585-10

Morimoto, K., Horio, J., Satoh, H., Sue, L., Beach, T., Arita, S., et al. (2011). Expression profiles of cytokines in the brains of Alzheimer's disease (AD) patients compared to the brains of non-demented patients with and without increasing AD pathology. *J. Alzheimers Dis.* 25, 59–76. doi: 10.3233/JAD-2011-101815

Morris, J. K., and Burns, J. M. (2012). Insulin: an emerging treatment for Alzheimer's disease dementia? *Curr. Neurol. Neurosci. Rep.* 12, 520–527. doi: 10.1007/s11910-012-0297-0

Mosconi, L., Pupi, A., and De Leon, M. J. (2008). Brain glucose hypometabolism and oxidative stress in preclinical Alzheimer's disease. *Ann. N. Y. Acad. Sci.* 1147, 180–195. doi: 10.1196/annals.1427.007

Mucke, L., and Selkoe, D. J. (2012). Neurotoxicity of amyloid beta-protein: synaptic and network dysfunction. *Cold Spring Harb. Perspect. Med.* 2:a006338. doi: 10.1101/cshperspect.a006338

Mudher, A., Shepherd, D., Newman, T. A., Mildren, P., Jukes, J. P., Squire, A., et al. (2004). GSK-3beta inhibition reverses axonal transport defects and behavioural phenotypes in Drosophila. *Mol. Psychiatry* 9, 522–530. doi: 10.1038/sj.mp.4001483

Mullins, R. J., Diehl, T. C., Chia, C. W., and Kapogiannis, D. (2017). Insulin resistance as a link between amyloid-beta and tau pathologies in Alzheimer's disease. *Front. Aging Neurosci.* 9:118. doi: 10.3389/fnagi.2017.00118

Neely, K. M., Green, K. N., and LaFerla, F. M. (2011). Presenilin is necessary for efficient proteolysis through the autophagy-lysosome system in a gamma-secretase-independent manner. *J. Neurosci.* 31, 2781–2791. doi: 10.1523/JNEUROSCI.5156-10.2010

Nelson, P. T., Alafuzoff, I., Bigio, E. H., Bouras, C., Braak, H., Cairns, N. J., et al. (2012). Correlation of Alzheimer disease neuropathologic changes with cognitive status: a review of the literature. *J. Neuropathol. Exp. Neurol.* 71, 362–381. doi: 10.1097/NEN.0b013e31825018f7

Niewidok, B., Igaev, M., Sundermann, F., Janning, D., Bakota, L., and Brandt, R. (2016). Presence of a carboxy-terminal pseudorepeat and disease-like pseudohyperphosphorylation critically influence tau's interaction with microtubules in axon-like processes. *Mol. Biol. Cell* 27, 3537–3549. doi: 10.1091/mbc.e16-06-0402

Nilsson, P., Sekiguchi, M., Akagi, T., Izumi, S., Komori, T., Hui, K., et al. (2015). Autophagy-related protein 7 deficiency in amyloid β (Abeta) precursor protein transgenic mice decreases Abeta in the multivesicular bodies and induces Abeta accumulation in the Golgi. *Am. J. Pathol.* 185, 305–313. doi: 10.1016/j.ajpath.2014.10.011

Nixon, R. A. (2007). Autophagy, amyloidogenesis and Alzheimer disease. *J. Cell. Sci. 120(Pt* 23), 4081–4091. doi: 10.1242/jcs.019265

Nixon, R. A., Wegiel, J., Kumar, A., Yu, W. H., Peterhoff, C., Cataldo, A., et al. (2005). Extensive involvement of autophagy in Alzheimer disease: an immuno-electron microscopy study. *J. Neuropathol. Exp. Neurol.* 64, 113–122. doi: 10.1093/jnen/64.2.113

Nizari, S., Carare, R. O., and Hawkes, C. A. (2016). Increased Abeta pathology in aged Tg2576 mice born to mothers fed a high fat diet. *Sci. Rep.* 6:21981. doi: 10.1038/srep21981

Nowotny, K., Jung, T., Hohn, A., Weber, D., and Grune, T. (2015). Advanced glycation end products and oxidative stress in type 2 diabetes mellitus. *Biomolecules* 5, 194–222. doi: 10.3390/biom5010194

Orr, M. E., and Oddo, S. (2013). Autophagic/lysosomal dysfunction in Alzheimer's disease. *Alzheimers Res. Ther.* 5:53. doi: 10.1186/alzrt217

Ozcan, U., Cao, Q., Yilmaz, E., Lee, A. H., Iwakoshi, N. N., Ozdelen, E., et al. (2004). Endoplasmic reticulum stress links obesity, insulin action, and type 2 diabetes. *Science* 306, 457–461. doi: 10.1126/science.1103160

Ozcelik, S., Fraser, G., Castets, P., Schaeffer, V., Skachokova, Z., Breu, K., et al. (2013). Rapamycin attenuates the progression of tau pathology in P301S tau transgenic mice. *PLoS ONE* 8:e62459. doi: 10.1371/journal.pone.0062459

Palop, J. J., and Mucke, L. (2010). Amyloid-β-induced neuronal dysfunction in Alzheimer's disease: from synapses toward neural networks. *Nat. Neurosci.* 13, 812–818. doi: 10.1038/nn.2583

Patel, S., and Santani, D. (2009). Role of NF-kappa B in the pathogenesis of diabetes and its associated complications. *Pharmacol. Rep.* 61, 595–603. doi: 10.1016/S1734-1140(09)70111-2

Peila, R., Rodriguez, B. L., Launer, L. J., and Honolulu-Asia Aging Study. (2002). Type 2 diabetes, APOE gene, and the risk for dementia and related pathologies: the honolulu-asia aging study. *Diabetes* 51, 1256–1262. doi: 10.2337/diabetes.51.4.1256

Peraldi, P., Hotamisligil, G. S., Buurman, W. A., White, M. F., and Spiegelman, B. M. (1996). Tumor necrosis factor (TNF)-α inhibits insulin signaling through stimulation of the p55 TNF receptor and activation of sphingomyelinase. *J. Biol. Chem.* 271, 13018–13022. doi: 10.1074/jbc.271.22.13018

Pickford, F., Masliah, E., Britschgi, M., Lucin, K., Narasimhan, R., Jaeger, P. A., et al. (2008). The autophagy-related protein beclin 1 shows reduced expression in early Alzheimer disease and regulates amyloid beta accumulation in mice. *J. Clin. Invest.* 118, 2190–2199. doi: 10.1172/JCI33585

Planel, E., Tatebayashi, Y., Miyasaka, T., Liu, L., Wang, L., Herman, M., et al. (2007). Insulin dysfunction induces *in vivo* tau hyperphosphorylation through distinct mechanisms. *J. Neurosci. 27*, 13635–13648. doi: 10.1523/JNEUROSCI.3949-07.2007

Plum, L., Schubert, M., and Bruning, J. C. (2005). The role of insulin receptor signaling in the brain. *Trends Endocrinol. Metab.* 16, 59–65. doi: 10.1016/j.tem.2005.01.008

Pooler, A. M., Noble, W., and Hanger, D. P. (2014). A role for tau at the synapse in Alzheimer's disease pathogenesis. Neuropharmacology 76(Pt A), 1–8. doi: 10.1016/j.neuropharm.2013.09.018

Puzzo, D., Piacentini, R., Fa, M., Gulisano, W., Li Puma, D. D., Staniszewski, A., et al. (2017). LTP and memory impairment caused by extracellular Aβ and Tau oligomers is APP-dependent. *Elife* 6:e26991. doi: 10.7554/eLife.26991

Qiu, W. Q., and Folstein, M. F. (2006). Insulin, insulin-degrading enzyme and amyloid-beta peptide in Alzheimer's disease: review and hypothesis. *Neurobiol. Aging* 27, 190–198. doi: 10.1016/j.neurobiolaging.2005.01.004

Qu, Z. S., Li, L., Sun, X. J., Zhao, Y. W., Zhang, J., Geng, Z., et al. (2014). Glycogen synthase kinase-3 regulates production of amyloid-β peptides and tau phosphorylation in diabetic rat brain. *ScientificWorldJournal* 2014:878123. doi: 10.1155/2014/878123

Qu, Z., Jiao, Z., Sun, X., Zhao, Y., Ren, J., and Xu, G. (2011). Effects of streptozotocin-induced diabetes on tau phosphorylation in the rat brain. *Brain Res.* 1383, 300–306. doi: 10.1016/j.brainres.2011.01.084

Quan, W., Lim, Y. M., and Lee, M. S. (2012). Role of autophagy in diabetes and endoplasmic reticulum stress of pancreatic β-cells. *Exp. Mol. Med.* 44, 81–88. doi: 10.3858/emm.2012.44.2.030

Quraishe, S., Cowan, C. M., and Mudher, A. (2013). NAP (davunetide) rescues neuronal dysfunction in a Drosophila model of tauopathy. *Mol. Psychiatry* 18, 834–842. doi: 10.1038/mp.2013.32

Reddy, P. H. (2013). Amyloid beta-induced glycogen synthase kinase 3β phosphorylated VDAC1 in Alzheimer's disease: implications for synaptic dysfunction and neuronal damage. *Biochim. Biophys. Acta* 1832, 1913–1921. doi: 10.1016/j.bbadis.2013.06.012

Reno, C. M., Puente, E. C., Sheng, Z., Daphna-Iken, D., Bree, A. J., Routh, V. H., et al. (2017). Brain GLUT4 knockout mice have impaired glucose tolerance, decreased insulin sensitivity, and impaired hypoglycemic counterregulation. *Diabetes* 66, 587–597. doi: 10.2337/db16-0917

Roberts, R. O., Knopman, D. S., Przybelski, S. A., Mielke, M. M., Kantarci, K., Preboske, G. M., et al. (2014). Association of type 2 diabetes with brain atrophy and cognitive impairment. *Neurology* 82, 1132–1141. doi: 10.1212/WNL.0000000000000269

Robertson, L. A., Moya, K. L., and Breen, K. C. (2004). The potential role of tau protein O-glycosylation in Alzheimer's disease. *J. Alzheimers Dis.* 6, 489–495. doi: 10.3233/JAD-2004-6505

Rodríguez-Martín, T., Cuchillo-Ibanez, I., Noble, W., Nyenya, F., Anderton, B. H., and Hanger, D. P. (2013). Tau phosphorylation affects its axonal transport and degradation. *Neurobiol. Aging* 34, 2146–2157. doi: 10.1016/j.neurobiolaging.2013.03.015

Rodriguez-Rodriguez, P., Sandebring-Matton, A., Merino-Serrais, P., Parrado-Fernandez, C., Rabano, A., Winblad, B., et al. (2017). Tau hyperphosphorylation induces oligomeric insulin accumulation and insulin resistance in neurons. *Brain* 140, 3269–3285. doi: 10.1093/brain/awx256

Romeo, G., Liu, W. H., Asnaghi, V., Kern, T. S., and Lorenzi, M. (2002). Activation of nuclear factor-kappaB induced by diabetes and high glucose regulates a proapoptotic program in retinal pericytes. *Diabetes* 51, 2241–2248. doi: 10.2337/diabetes.51.7.2241

Rubio-Perez, J. M., and Morillas-Ruiz, J. M. (2012). A review: inflammatory process in Alzheimer's disease, role of cytokines. *ScientificWorldJournal* 2012:756357. doi: 10.1100/2012/756357

Sakono, M., and Zako, T. (2010). Amyloid oligomers: formation and toxicity of Abeta oligomers. *FEBS J.* 277, 1348–1358. doi: 10.1111/j.1742-4658.2010.07568.x

Samuel, S., Zhang, K., Tang, Y. D., Gerdes, A. M., and Carrillo-Sepulveda, M. A. (2017). Triiodothyronine potentiates vasorelaxation via PKG/VASP signaling in vascular smooth muscle cells. *Cell. Physiol. Biochem.* 41, 1894–1904. doi: 10.1159/000471938

Savu, O., Bradescu, O. M., Serafinceanu, C., Iosif, L., Tirgoviste, C. I., and Stoian, I. (2013). Erythrocyte caspase-3 and antioxidant defense is activated in red blood cells and plasma of type 2 diabetes patients at first clinical onset. *Redox Rep.* 18, 56–62. doi: 10.1179/1351000213Y.0000000040

Schaeffer, V., Lavenir, I., Ozcelik, S., Tolnay, M., Winkler, D. T., and Goedert, M. (2012). Stimulation of autophagy reduces neurodegeneration in a mouse model of human tauopathy. *Brain* 135, 2169–2177. doi: 10.1093/brain/aws143

Schedin-Weiss, S., Winblad, B., and Tjernberg, L. O. (2014). The role of protein glycosylation in Alzheimer disease. *FEBS J.* 281, 46–62. doi: 10.1111/febs.12590

Schmitz, T. W., Nathan Spreng, R., and Alzheimer's Disease Neuroimaging Initiative. (2016). Basal forebrain degeneration precedes and predicts the cortical spread of Alzheimer's pathology. *Nat. Commun.* 7:13249. doi: 10.1038/ncomms13249

Schubert, M., Brazil, D. P., Burks, D. J., Kushner, J. A., Ye, J., Flint, C. L., et al. (2003). Insulin receptor substrate-2 deficiency impairs brain growth and promotes tau phosphorylation. *J. Neurosci.* 23, 7084–7092. doi: 10.1523/JNEUROSCI.23-18-07084.2003

Schubert, M., Gautam, D., Surjo, D., Ueki, K., Baudler, S., Schubert, D., et al. (2004). Role for neuronal insulin resistance in neurodegenerative diseases. *Proc. Natl. Acad. Sci. U.S.A.* 101, 3100–3105. doi: 10.1073/pnas.0308724101

Sekar, S., McDonald, J., Cuyugan, L., Aldrich, J., Kurdoglu, A., Adkins, J., et al. (2015). Alzheimer's disease is associated with altered expression of genes involved in immune response and mitochondrial processes in astrocytes. *Neurobiol. Aging* 36, 583–591. doi: 10.1016/j.neurobiolaging.2014.09.027

Selkoe, D. J. (2008). Soluble oligomers of the amyloid beta-protein impair synaptic plasticity and behavior. *Behav. Brain Res.* 192, 106–113. doi: 10.1016/j.bbr.2008.02.016

Serpell, L. C., Blake, C. C., and Fraser, P. E. (2000). Molecular structure of a fibrillar Alzheimer's A beta fragment. *Biochemistry* 39, 13269–13275. doi: 10.1021/bi000637v

Serrano-Pozo, A., Frosch, M. P., Masliah, E., and Hyman, B. T. (2011). Neuropathological alterations in Alzheimer disease. *Cold Spring Harb. Perspect. Med.* 1:a006189. doi: 10.1101/cshperspect.a006189

Shankar, G. M., and Walsh, D. M. (2009). Alzheimer's disease: synaptic dysfunction and Abeta. *Mol. Neurodegener.* 4:48. doi: 10.1186/1750-1326-4-48

Sheng, M., Sabatini, B. L., and Sudhof, T. C. (2012). Synapses and Alzheimer's disease. *Cold Spring Harb. Perspect. Biol.* 4:a005777 doi: 10.1101/cshperspect.a005777

Showkat, M., Beigh, M. A., and Andrabi, K. I. (2014). mTOR signaling in protein translation regulation: implications in cancer genesis and therapeutic interventions. *Mol. Biol. Int.* 2014:686984. doi: 10.1155/2014/686984

Smet-Nocca, C., Broncel, M., Wieruszeski, J. M., Tokarski, C., Hanoulle, X., Leroy, A., et al. (2011). Identification of O-GlcNAc sites within peptides of the Tau protein and their impact on phosphorylation. *Mol. Biosyst.* 7, 1420–1429. doi: 10.1039/c0mb00337a

Solito, E., and Sastre, M. (2012). Microglia function in Alzheimer's disease. *Front. Pharmacol.* 3:14. doi: 10.3389/fphar.2012.00014

Son, J. H., Shim, J. H., Kim, K. H., Ha, J. Y., and Han, J. Y. (2012). Neuronal autophagy and neurodegenerative diseases. *Exp. Mol. Med.* 44, 89–98. doi: 10.3858/emm.2012.44.2.031

Son, S. M., Cha, M. Y., Choi, H., Kang, S., Choi, H., Lee, M. S., et al. (2016). Insulin-degrading enzyme secretion from astrocytes is mediated by an autophagy-based unconventional secretory pathway in Alzheimer disease. *Autophagy* 12, 784–800. doi: 10.1080/15548627.2016.1159375

Sotiropoulos, I., Galas, M. C., Silva, J. M., Skoulakis, E., Wegmann, S., Maina, M. B., et al. (2017). Atypical, non-standard functions of the microtubule associated Tau protein. *Acta Neuropathol. Commun.* 5:91. doi: 10.1186/s40478-017-0489-6

Spilman, P., Podlutskaya, N., Hart, M. J., Debnath, J., Gorostiza, O., Bredesen, D., et al. (2010). Inhibition of mTOR by rapamycin abolishes cognitive deficits and reduces amyloid-β levels in a mouse model of Alzheimer's disease. *PLoS ONE* 5:e9979. doi: 10.1371/journal.pone.0009979

Spires-Jones, T. L., and Hyman, B. T. (2014). The intersection of amyloid beta and tau at synapses in Alzheimer's disease. *Neuron* 82, 756–771. doi: 10.1016/j.neuron.2014.05.004

Srikanth, V., Maczurek, A., Phan, T., Steele, M., Westcott, B., Juskiw, D., et al. (2011). Advanced glycation endproducts and their receptor RAGE in Alzheimer's disease. *Neurobiol. Aging* 32, 763–777. doi: 10.1016/j.neurobiolaging.2009.04.016

Stanley, M., Macauley, S. L., and Holtzman, D. M. (2016). Changes in insulin and insulin signaling in Alzheimer's disease: cause or consequence? *J. Exp. Med.* 213, 1375–1385. doi: 10.1084/jem.20160493

Steele, J. W., Fan, E., Kelahmetoglu, Y., Tian, Y., and Bustos, V. (2013). Modulation of Autophagy as a Therapeutic Target for Alzheimer's Disease. *Postdoc J* 1, 21–34.

Stoothoff, W. H., and Johnson, G. V. (2005). Tau phosphorylation, physiological and pathological consequences. *Biochim. Biophys. Acta* 1739, 280–297. doi: 10.1016/j.bbadis.2004.06.017

Swaroop, J. J., Rajarajeswari, D., and Naidu, J. N. (2012). Association of TNF-α with insulin resistance in type 2 diabetes mellitus. *Indian J. Med. Res.* 135, 127–130. doi: 10.4103/0971-5916.93435

Tackenberg, C., and Brandt, R. (2009). Divergent pathways mediate spine alterations and cell death induced by amyloid-β, wild-type tau, and R406W tau. *J. Neurosci.* 29, 14439–14450. doi: 10.1523/JNEUROSCI.3590-09.2009

Tai, H. C., Serrano-Pozo, A., Hashimoto, T., Frosch, M. P., Spires-Jones, T. L., and Hyman, B. T. (2012). The synaptic accumulation of hyperphosphorylated tau oligomers in Alzheimer disease is associated with dysfunction of the ubiquitin-proteasome system. *Am. J. Pathol.* 181, 1426–1435. doi: 10.1016/j.ajpath.2012.06.033

Takeda, S., Sato, N., Uchio-Yamada, K., Sawada, K., Kunieda, T., Takeuchi, D., et al. (2010). Diabetes-accelerated memory dysfunction via cerebrovascular inflammation and Abeta deposition in an Alzheimer mouse model with diabetes. *Proc. Natl. Acad. Sci. U.S.A.* 107, 7036–7041. doi: 10.1073/pnas.1000645107

Talbot, K. (2014). Brain insulin resistance in Alzheimer's disease and its potential treatment with GLP-1 analogs. *Neurodegener. Dis. Manag.* 4, 31–40. doi: 10.2217/nmt.13.73

Talbot, K., Wang, H. Y., Kazi, H., Han, L. Y., Bakshi, K. P., Stucky, A., et al. (2012). Demonstrated brain insulin resistance in Alzheimer's disease patients is associated with IGF-1 resistance, IRS-1 dysregulation, and cognitive decline. *J. Clin. Invest.* 122, 1316–1338. doi: 10.1172/JCI59903

Taylor, R. (2012). Insulin resistance and type 2 diabetes. *Diabetes* 61, 778–779. doi: 10.2337/db12-0073

Thiels, E., and Klann, E. (2001). Extracellular signal-regulated kinase, synaptic plasticity, and memory. *Rev. Neurosci.* 12, 327–345. doi: 10.1515/REVNEURO.2001.12.4.327

Tosto, G., and Reitz, C. (2013). Genome-wide association studies in Alzheimer's disease: a review. *Curr. Neurol. Neurosci. Rep.* 13:381. doi: 10.1007/s11910-013-0381-0

Trzeciakiewicz, H., Tseng, J. H., Wander, C. M., Madden, V., Tripathy, A., Yuan, C. X., et al. (2017). A dual pathogenic mechanism links tau acetylation to sporadic tauopathy. *Sci. Rep.* 7:44102. doi: 10.1038/srep44102

Tung, Y. T., Wang, B. J., Hsu, W. M., Hu, M. K., Her, G. M., Huang, W. P., et al. (2014). Presenilin-1 regulates the expression of p62 to govern p62-dependent tau degradation. *Mol. Neurobiol.* 49, 10–27. doi: 10.1007/s12035-013-8482-y

Tyan, S. H., Shih, A. Y., Walsh, J. J., Maruyama, H., Sarsoza, F., Ku, L., et al. (2012). Amyloid precursor protein (APP) regulates synaptic structure and function. *Mol. Cell Neurosci.* 51, 43–52. doi: 10.1016/j.mcn.2012.07.009

Ulrich, J. D., Ulland, T. K., Colonna, M., and Holtzman, D. M. (2017). Elucidating the role of TREM2 in Alzheimer's Disease. *Neuron* 94, 237–248. doi: 10.1016/j.neuron.2017.02.042

Umegaki, H. (2014). Type 2 diabetes as a risk factor for cognitive impairment: current insights. *Clin. Interv. Aging* 9, 1011–1019. doi: 10.2147/CIA.S48926

Uranga, R. M., Katz, S., and Salvador, G. A. (2013). Enhanced phosphatidylinositol 3-kinase (PI3K)/Akt signaling has pleiotropic targets in hippocampal neurons exposed to iron-induced oxidative stress. *J Biol Chem* 288, 19773–19784. doi: 10.1074/jbc.M113.457622

van Bussel, F. C., Backes, W. H., Hofman, P. A., Puts, N. A., Edden, R. A., van Boxtel, M. P., et al. (2016). Increased GABA concentrations in type 2 diabetes mellitus are related to lower cognitive functioning. *Medicine* 95:e4803. doi: 10.1097/MD.0000000000004803

van der Flier, W. M., and Scheltens, P. (2005). Epidemiology and risk factors of dementia. *J. Neurol. Neurosurg. Psychiatry. 76 (Suppl.* 5), v2–v7. doi: 10.1136/jnnp.2005.082867

van der Heide, L. P., Kamal, A., Artola, A., Gispen, W. H., and Ramakers, G. M. (2005). Insulin modulates hippocampal activity-dependent synaptic plasticity in a N-methyl-d-aspartate receptor and phosphatidylinositol-3-kinase-dependent manner. *J. Neurochem.* 94, 1158–1166. doi: 10.1111/j.1471-4159.2005.03269.x

Van Eldik, L. J., Carrillo, M. C., Cole, P. E., Feuerbach, D., Greenberg, B. D., Hendrix, J. A., et al. (2016). The roles of inflammation and immune mechanisms in Alzheimer's disease. *Alzheimers Dement.* 2, 99–109. doi: 10.1016/j.trci.2016.05.001

Vassar, R. (2004). BACE1: the beta-secretase enzyme in Alzheimer's disease. *J. Mol. Neurosci.* 23, 105–114. doi: 10.1385/JMN:23:1-2:105

Verkhratsky, A., Olabarria, M., Noristani, H. N., Yeh, C. Y., and Rodriguez, J. J. (2010). Astrocytes in Alzheimer's disease. *Neurotherapeutics* 7, 399–412. doi: 10.1016/j.nurt.2010.05.017

Vlassenko, A. G., Benzinger, T. L., and Morris, J. C. (2012). PET amyloid-beta imaging in preclinical Alzheimer's disease. *Biochim. Biophys. Acta* 1822, 370–379. doi: 10.1016/j.bbadis.2011.11.005

Wang, J. Z., Grundke-Iqbal, I., and Iqbal, K. (1996). Glycosylation of microtubule-associated protein tau: an abnormal posttranslational modification in Alzheimer's disease. *Nat. Med.* 2, 871–875. doi: 10.1038/nm0896-871

Watson, G. S., Cholerton, B. A., Reger, M. A., Baker, L. D., Plymate, S. R., Asthana, S., et al. (2005). Preserved cognition in patients with early Alzheimer disease and amnestic mild cognitive impairment during treatment with rosiglitazone: a preliminary study. *Am. J. Geriatr. Psychiatry* 13, 950–958. doi: 10.1176/appi.ajgp.13.11.950

Wellen, K. E., and Hotamisligil, G. S. (2005). Inflammation, stress, and diabetes. *J. Clin. Invest.* 115, 1111–1119. doi: 10.1172/JCI25102

Wennberg, A. M., Spira, A. P., Pettigrew, C., Soldan, A., Zipunnikov, V., Rebok, G. W., et al. (2016). Blood glucose levels and cortical thinning in cognitively normal, middle-aged adults. *J. Neurol. Sci.* 365, 89–95. doi: 10.1016/j.jns.2016.04.017

Wes, P. D., Easton, A., Corradi, J., Barten, D. M., Devidze, N., DeCarr, L. B., et al. (2014). Tau overexpression impacts a neuroinflammation gene expression network perturbed in Alzheimer's disease. *PLoS ONE* 9:e106050. doi: 10.1371/journal.pone.0106050

Wildsmith, K. R., Holley, M., Savage, J. C., Skerrett, R., and Landreth, G. E. (2013). Evidence for impaired amyloid beta clearance in Alzheimer's disease. *Alzheimers Res. Ther.* 5:33. doi: 10.1186/alzrt187

Wilson, C. A., Murphy, D. D., Giasson, B. I., Zhang, B., Trojanowski, J. Q., and Lee, V. M. (2004). Degradative organelles containing mislocalized α-and α-synuclein proliferate in presenilin-1 null neurons. *J. Cell Biol.* 165, 335–346. doi: 10.1083/jcb.200403061

Wilson, D. M., and Binder, L. I. (1997). Free fatty acids stimulate the polymerization of tau and amyloid beta peptides, *in vitro* evidence for a common effector of pathogenesis in Alzheimer's disease. *Am. J. Pathol.* 150, 2181–2195.

Wu, J., Nie, S. D., and Wang, S. (2013). Tau pathology in diabetes mellitus. *Pharmazie* 68, 649–652.

Wyss-Coray, T., Loike, J. D., Brionne, T. C., Lu, E., Anankov, R., Yan, F., et al. (2003). Adult mouse astrocytes degrade amyloid-β *in vitro* and *in situ*. *Nat. Med.* 9, 453–457. doi: 10.1038/nm838

Wyss-Coray, T., and Rogers, J. (2012). Inflammation in Alzheimer disease-a brief review of the basic science and clinical literature. *Cold Spring Harb. Perspect. Med.* 2:a006346. doi: 10.1101/cshperspect.a006346

Xiong, J. (2015). Atg7 in development and disease: panacea or Pandora's Box? *Protein Cell* 6, 722–734. doi: 10.1007/s13238-015-0195-8

Yarchoan, M., and Arnold, S. E. (2014). Repurposing diabetes drugs for brain insulin resistance in Alzheimer disease. *Diabetes* 63, 2253–2261. doi: 10.2337/db14-0287

Yiannopoulou, K. G., and Papageorgiou, S. G. (2013). Current and future treatments for Alzheimer's disease. *Ther. Adv. Neurol. Disord.* 6, 19–33. doi: 10.1177/1756285612461679

Yin, Y., Chen, F., Wang, W., Wang, H., and Zhang, X. (2017). Resolvin D1 inhibits inflammatory response in STZ-induced diabetic retinopathy rats: possible involvement of NLRP3 inflammasome and NF-kappaB signaling pathway. *Mol. Vis.* 23, 242–250.

Yoon, M. S. (2017). The role of mammalian target of rapamycin (mTOR) in insulin signaling. *Nutrients* 9:E1176. doi: 10.3390/nu9111176

Yoshiyama, Y., Higuchi, M., Zhang, B., Huang, S. M., Iwata, N., Saido, T. C., et al. (2007). Synapse loss and microglial activation precede tangles in a P301S tauopathy mouse model. *Neuron* 53, 337–351. doi: 10.1016/j.neuron.2007.01.010

Yuzwa, S. A., Shan, X., Macauley, M. S., Clark, T., Skorobogatko, Y., Vosseller, K., et al. (2012). Increasing O-GlcNAc slows neurodegeneration and stabilizes tau against aggregation. *Nat. Chem. Biol.* 8, 393–399. doi: 10.1038/nchembio.797

Zhang, W., Thompson, B. J., Hietakangas, V., and Cohen, S. M. (2011). MAPK/ERK signaling regulates insulin sensitivity to control glucose metabolism in Drosophila. *PLoS Genet.* 7:e1002429. doi: 10.1371/journal.pgen.1002429

Zhao, R., Hu, W., Tsai, J., Li, W., and Gan, W. B. (2017). Microglia limit the expansion of beta-amyloid plaques in a mouse model of Alzheimer's disease. *Mol. Neurodegener.* 12:47. doi: 10.1186/s13024-017-0188-6

Zhao, W. Q., and Townsend, M. (2009). Insulin resistance and amyloidogenesis as common molecular foundation for type 2 diabetes and Alzheimer's disease. *Biochim. Biophys. Acta* 1792, 482–496. doi: 10.1016/j.bbadis.2008.10.014

Zhu, Y., Shan, X., Yuzwa, S. A., and Vocadlo, D. J. (2014). The emerging link between O-GlcNAc and Alzheimer disease. *J. Biol. Chem.* 289, 34472–34481. doi: 10.1074/jbc.R114.601351

Zilka, N., Filipcik, P., Koson, P., Fialova, L., Skrabana, R., Zilkova, M., et al. (2006). Truncated tau from sporadic Alzheimer's disease suffices to drive neurofibrillary degeneration *in vivo*. *FEBS Lett.* 580, 3582–3588. doi: 10.1016/j.febslet.2006.05.029

Zotova, E., Nicoll, J. A., Kalaria, R., Holmes, C., and Boche, D. (2010). Inflammation in Alzheimer's disease: relevance to pathogenesis and therapy. *Alzheimers Res. Ther.* 2:1. doi: 10.1186/alzrt24

Conflict of Interest Statement: The authors declare that the research was conducted in the absence of any commercial or financial relationships that could be construed as a potential conflict of interest.

Copyright © 2018 Chatterjee and Mudher. This is an open-access article distributed under the terms of the Creative Commons Attribution License (CC BY). The use, distribution or reproduction in other forums is permitted, provided the original author(s) and the copyright owner are credited and that the original publication in this journal is cited, in accordance with accepted academic practice. No use, distribution or reproduction is permitted which does not comply with these terms.

frontiers in Neuroscience

MINI REVIEW
published: 31 May 2018
doi: 10.3389/fnins.2018.00330

Sleep Disorders Associated With Alzheimer's Disease: A Perspective

*Anna Brzecka[1], Jerzy Leszek[2], Ghulam Md Ashraf[3], Maria Ejma[4], Marco F. Ávila-Rodriguez[5], Nagendra S. Yarla[6], Vadim V. Tarasov[7], Vladimir N. Chubarev[7], Anna N. Samsonova[8], George E. Barreto[9,10] and Gjumrakch Aliev[8,11,12]**

[1] Department of Pulmonology and Lung Cancer, Wroclaw Medical University, Wroclaw, Poland, [2] Department of Psychiatry, Wroclaw Medical University, Wroclaw, Poland, [3] King Fahd Medical Research Center, King Abdulaziz University, Jeddah, Saudi Arabia, [4] Department of Neurology, Wroclaw Medical University, Wroclaw, Poland, [5] Facultad de Ciencias de la Salud, Universidad del Tolima, Ibagué, Colombia, [6] Department of Biochemistry and Bioinformatics, School of Life Sciences, Institute of Science, Gandhi Institute of Technology and Management University, Visakhapatnam, India, [7] Institute for Pharmaceutical Science and Translational Medicine, Sechenov First Moscow State Medical University, Moscow, Russia, [8] Institute of Physiologically Active Compounds of the Russian Academy of Sciences, Chernogolovka, Russia, [9] Departamento de Nutrición y Bioquímica, Facultad de Ciencias, Pontificia Universidad Javeriana, Bogotá, Colombia, [10] Instituto de Ciencias Biomédicas, Universidad Autónoma de Chile, Santiago, Chile, [11] GALLY International Biomedical Research and Consulting LLC, San Antonio, TX, United States, [12] School of Health Science and Healthcare Administration, University of Atlanta, Johns Creek, GA, United States

Sleep disturbances, as well as sleep-wake rhythm disturbances, are typical symptoms of Alzheimer's disease (AD) that may precede the other clinical signs of this neurodegenerative disease. Here, we describe clinical features of sleep disorders in AD and the relation between sleep disorders and both cognitive impairment and poor prognosis of the disease. There are difficulties of the diagnosis of sleep disorders based on sleep questionnaires, polysomnography or actigraphy in the AD patients. Typical disturbances of the neurophysiological sleep architecture in the course of the AD include deep sleep and paradoxical sleep deprivation. Among sleep disorders occurring in patients with AD, the most frequent disorders are sleep breathing disorders and restless legs syndrome. Sleep disorders may influence circadian fluctuations of the concentrations of amyloid-β in the interstitial brain fluid and in the cerebrovascular fluid related to the glymphatic brain system and production of the amyloid-β. There is accumulating evidence suggesting that disordered sleep contributes to cognitive decline and the development of AD pathology. In this mini-review, we highlight and discuss the association between sleep disorders and AD.

Keywords: AD, diagnosis, sleep disorders, disturbance, sleep-rhythm

OPEN ACCESS

Edited by:
Hamid R. Sohrabi, Macquarie University, Australia

Reviewed by:
Stephanie R. Rainey-Smith, Edith Cowan University, Australia
Akifumi Kishi, The University of Tokyo, Japan

***Correspondence:**
Gjumrakch Aliev
aliev03@gmail.com;
cobalt55@gallyinternational.com

Specialty section:
This article was submitted to Neurodegeneration, a section of the journal Frontiers in Neuroscience

Received: *26 October 2017*
Accepted: *30 April 2018*
Published: *31 May 2018*

Citation:
Brzecka A, Leszek J, Ashraf GM, Ejma M, Ávila-Rodriguez MF, Yarla NS, Tarasov VV, Chubarev VN, Samsonova AN, Barreto GE and Aliev G (2018) Sleep Disorders Associated With Alzheimer's Disease: A Perspective. Front. Neurosci. 12:330. doi: 10.3389/fnins.2018.00330

INTRODUCTION

Alzheimer's disease (AD) is the most common cause of dementia, and its etiology is multifactorial (Chibber et al., 2016). The primary event in AD is the accumulation of amyloid-β (Aβ) in the brain (Karran et al., 2011). Abnormal deposition of Aβ triggers a cascade of events leading to neuroinflammation and neuronal cell death (Wyss-Coray and Mucke, 2002; Selkoe and Hardy, 2016). As a consequence, clinical manifestations of AD, mainly impaired cognitive function, develop progressively over 15 years since the beginning of accumulation of Aβ (Sen et al., 2017). Neuropathological modifications may develop progressively for several decades and during this preclinical period of AD, mild cognitive impairment (MCI) may occur (Drago et al., 2011; Bhat et al., 2017). In over 90% of cases, AD begins

after the age of 65 as a sporadic form of dementia (Prince et al., 2013; Ashraf et al., 2016). Of late, AD has been found to coexist with other chronic diseases like cancer, diabetes, and cardiovascular diseases (Aliev et al., 2014; Jabir et al., 2015; Rizvi et al., 2015; Ashraf et al., 2016). This has opened up new dimensions of AD diagnosis and therapy based on proteomics (Ashraf et al., 2014, 2015) and nanotechnology (Soursou et al., 2015; Ansari et al., 2017).

In AD, and likely in other neurodegenerative diseases, sleep disorders appear early (Dos Santos et al., 2014, 2015). Although the time meant for sleeping extend during the day, sleeping and waking rhythms are disturbed (McCurry et al., 1999). Common symptoms include difficulties in falling asleep, arousal at night, repeated awakenings and waking up too early in the morning, and sleepiness and frequent naps during the day (McCurry and Ancoli-Israel, 2003; Most et al., 2012). Sleep disorders can be an important diagnostic indication that foreruns development of AD's pathological disorders in the form of Aβ deposition in the brain and during dementia onset (Lim et al., 2013; Spira et al., 2013). Sleep disorders worsen as the disease progresses (Bliwise et al., 1995), and their considerable intensification in the late stage of the disease is a strong predictive factor for mortality (Spalletta et al., 2015). In the present mini-review, we discuss the association of sleep disorders in AD (**Figure 1**).

Night-Time Sleep Duration and AD

Results of clinical and epidemiological studies regarding a connection between night-time sleep duration and risk of AD are not equivocal. Although a prospective, 2-years self-reporting study in 1,844 community-dwelling women in the age ≥70 has shown that women sleeping ≤5 h per night had poorer cognitive abilities than women sleeping longer, though the difference was small (Tworoger et al., 2006). Similar results were found in the Spanish study in 3,212 people at the age of ≥60, where no correlation was found between shortened (<7 h) sleep time (according to self reported data) and cognitive disorders, determined by Mini-Mental State Examination (MMSE) questionnaire (Faubel et al., 2009). However, among persons sleeping longer than 7 h, a statistically significant ($p < 0.001$) trend was proved, indicating that the longer the sleep (more than 7, 8, 9, 10, or 11 h), the worse the cognitive abilities are (Faubel et al., 2009). A progressive study based on the Pittsburgh Sleep Quality Index and encompassing 1,664 persons at the age of 65 years without cognitive disorders during a 1-year observation found that extended sleep time (>9 h) among women and shortened sleep time (<5 h) among men correlated with cognitive impairment (OR 3.70; 95% CI 1.49–9.17 and OR 4.95; 95% CI 1.72–14.27, respectively) (Potvin et al., 2012). Further, in a study in 298 women without dementia at the age of 82.3 ± 3.2 years, a total sleep time (TST) during polysomnography (PSG) did not show correlation with the degree of cognitive impairment (Yaffe et al., 2011).

Based on results obtained in empirical study conducted among healthy men in middle age, it has been hypothesized that $A\beta_{42}$ increases with chronic sleep deprivation (Ooms et al., 2014). In this study, encompassing men, aged 40–60 years, without cognitive impairments, 13 persons have not been allowed to fall asleep at night, while the other 13 persons were permitted to unlimitedly long sleep. In both groups, a concentration of $A\beta_{42}$ was measured in cerebrospinal fluid (CSF) collected in the evening and in the morning. In persons who slept at night, a 6% decrease of $A\beta_{42}$ level in the morning compared to evening hours had been observed (95% CI [0.94, 49.6], $p = 0.04$). However, among those who did not sleep, the physiological decrease of $A\beta_{42}$ level in the morning hours had not been noticed. Thus, observed increased levels of $A\beta_{42}$ in CSF after sleep deprivation might indicate a higher risk of development of AD. Moreover, there was a correlation between total sleep duration and maximal decrease of $A\beta_{42}$ ($r = -0.5$, $p = 0.04$).

Diagnostics of Sleep Disorders Based on Questionnaires in AD Patients

In patients with AD, the diagnostics of sleep disorders based on specific questionnaires is difficult due to cognitive impairment affecting reliability of self-report measures of sleep. It may happen that patients who suffer from severe difficulties in falling asleep and frequent awakenings at night do not complain of insomnia at all (Most et al., 2012). The study comparing results of sleep questionnaires, such as Pittsburgh Sleep Quality Index, the Sleep Disorders Questionnaire, and the Athens Insomnia Scale, with the results of actigraphy in 55 patients with AD and 26 controls revealed limited value of those sleep questionnaires in early and moderate AD stage (Most et al., 2012). Based on the results obtained in the questionnaires, it has been found that sleep disorders occurred in 24.5% of patients with mild to moderate form of AD (Moran et al., 2005). However, it appears that sleep disorders occur much more frequently in the course of this disease (Zhao et al., 2016).

PSG in the Diagnostics of Sleep Disorders in AD Patients

PSG is a basic and objective method of diagnosing sleep disorders. In the patients with AD, PSG usually shows prolonged sleep latency, i.e., time taken to fall asleep (McCurry and Ancoli-Israel, 2003). Indeed, increased number of awakenings and lengthened time of wakefulness after sleep onset causes reduced sleep efficiency (Bliwise, 1993; Rauchs et al., 2008).

The number of sleep cycles remains unchanged (Petit et al., 2004), but duration of both rapid eye movement (REM) sleep and deep sleep (N3) is usually shortened (Maestri et al., 2015). However, in AD, recognition of sleep stages—especially stage N3—is frequently difficult, because usually in electroencephalogram (EEG) recordings there are generalized slow waves (0.5–2 Hz) of low amplitude during both sleep and wakefulness (Petit et al., 2004; Peter-Derex et al., 2015). Also, during REM sleep, an increased amount of delta and theta waves and reduced number of faster α and β waves can be observed (Hassainia et al., 1997). Reduced activity of EEG is

Abbreviations: AD, Alzheimer's disease; CSF, Cerebrospinal fluid; EEG, Electroencephalogram; PSG, Polysomnography; MCI, Mild cognitive impairment; PLM, Periodic leg movements; REM, Rapid eye movement; RLS, Restless leg syndrome; TST, Total sleep time.

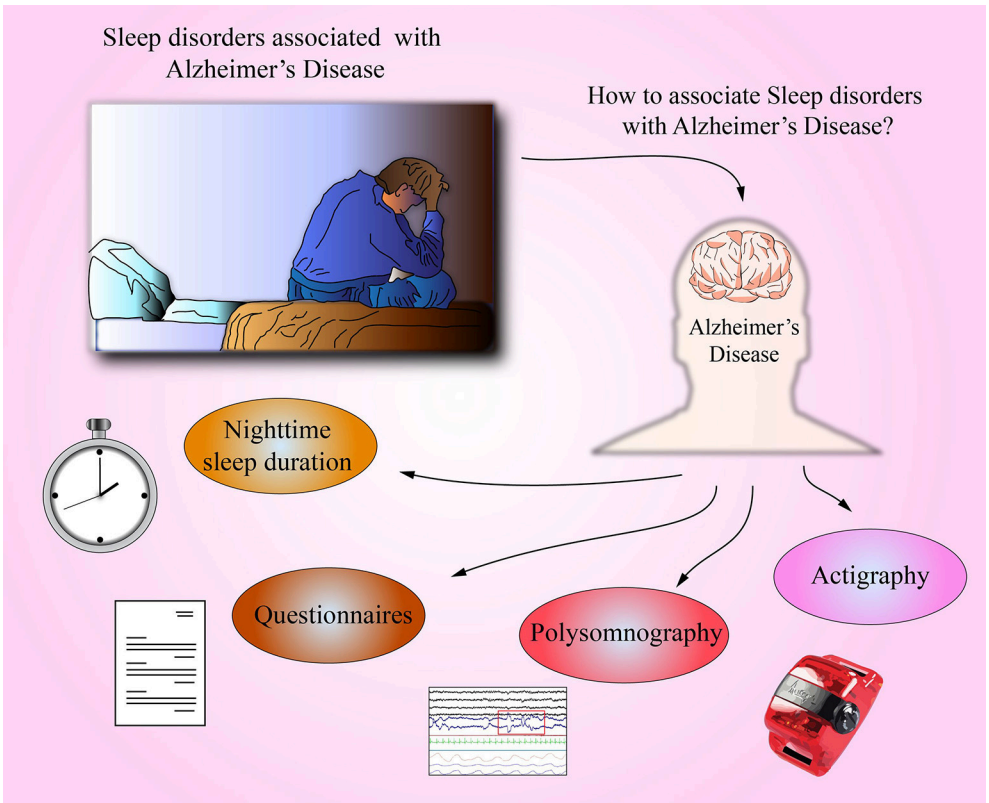


FIGURE 1 | Identification of sleep disorders and possible relationship with AD. Several sleep conditions may indicate the risk of undergo AD; for example, nighttime sleep (<5 h) is linked in many epidemiological studies as a risk factor for AD. Additionally, it is possible to qualitatively survey for sleep quality by means of questionnaires i.e., Athens Insomnia Scale or Pittsburg Sleep Quality Index. Polysomnography is a procedure to diagnose sleep disorders, and in AD patients, it is observed prolonged sleep latency and increased number of arousals. Finally, some portable equipment like Actigraph can provide key data of sleep quality by measuring the wakefulness and sleep activity in several days (10 days registration).

considered as a biological marker of AD (Prinz et al., 1982). Based on the measurements of the cyclic alternating pattern (CAP) in the PSG recordings, sleep instability was found both in the subjects with MCI (age 68.5 ± 7.0 years) and—to a greater extent—in patients with mild AD (age 72.7 ± 5.9 years) as compared to healthy persons without cognitive impairment (age 69.2 ± 12.6 years) (Maestri et al., 2015). In this study, encompassing 33 subjects in the three equally numerous groups, PSG revealed abnormalities in the microstructure of sleep, as indicated by decreased CAP rate and slow components of CAP. Thus, PSG abnormalities could serve as a potentially useful marker of neurodegeneration in subjects with cognitive impairments. Disordered sleep structure correlates with a degree of cognitive abilities impairment, including those assessed by MMSE. The correlations of cognitive impairments and sleep structure abnormalities in PSG recordings were found in a study of 48 patients with AD (21 patients with mild AD and 27 patients with moderate to severe AD) (Liguori et al., 2014). In this study, abnormalities of macrostructural sleep variables in PSG were more pronounced in patients with poorer cognitive function (MMSE score < 21).

Abnormalities in the PSG recordings were also noted in patients with preclinical AD. In a previous study of 25 subjects with MCI (age 70.5 ± 6.8 years, MMSE score 26.7 ± 2.4), higher density of arousals during slow wave sleep and decreased percentage of REM sleep during total sleep time as compared with healthy subjects in similar age were found (0.09 ± 0.11 vs. 0.19 ± 0.10; $p < 0.01$ and 14.7 ± 3.7 vs. 10.1 ± 5.4; $p < 0.007$, respectively) (Hita-Yañez et al., 2013).

In patients with amnestic MCI—who constitute a group of increased risk of progression to AD—abnormalities in the sleep structure were also observed. In a study of 8 amnestic MCI patients (age 72.1 ± 5.1), as compared with 16 age-matched healthy adults, there were fewer sleep spindles, shortened SWS and lower delta and theta power (Westerberg et al., 2012). However, PSG has limited usage for patients with AD. Its limitations rely in the fact that most patients with AD—especially in advanced stage—are not able to cooperate during the examination and do not tolerate any electrodes and sensors on the skin (Peter-Derex et al., 2015).

Actigraphy to Examine Sleep Disorders in Patients With AD

Actigraphy turned out to be appropriate method to examine sleep disorders in AD (Ancoli-Israel et al., 1997; Most et al., 2012). Prospective study based on actigraphy (10 days registration)

conducted in 737 men and women at the age of 81.6 ± 7.2 has shown that after an average 3.3 years, risk of symptoms of AD was 1.5 times higher in subjects with high sleep fragmentation as compared to subjects with slight sleep fragmentation (Lim et al., 2013). Sleep studies on the basis of actigraphy (2 weeks registration) have been conducted in 142 persons without cognitive disorders at the age of ≥45 years (Ju et al., 2013). In this group, more than half of the persons (54.2%) were at the age >65 years, including 18 persons (12.7%) at the age over 75 years. TST (i.e., the amount of sleep) and the percentage of sleep in the time spent in bed (i.e., efficiency of sleep) have been determined. In this study, it has been arbitrarily stated that sleep efficiency <75% showed worse sleep quality, and correlation of quantity and quality of sleep and the level of $A\beta_{42}$ in CSF have been evaluated. No differences in TST have been found in persons with decreased and normal levels of $A\beta_{42}$ in CSF. In 32 persons (22.5%) on the basis of lowered level of $A\beta_{42}$ in CSF (≤ 500 pg/ml), pre-clinical form of AD was diagnosed. In this group, quality of sleep was worse than among other persons (80.4 vs. 83.7%, $p = 0.04$) (Ju et al., 2013). High proportions of the persons studied were at the age > 65 years, indicating possible influence of this factor on the obtained results. Additionally, it should be stated that $A\beta_{42}$ thresholds in CSF are not clearly defined in cognitively healthy persons. For persons in pre-clinical stage of AD, as defined on the basis of decreased $A\beta_{42}$ levels in the CSF, at least 3 naps in a week have been noted, i.e., more than for persons without signs of amyloid deposition (31.2 vs. 14.7%; $p = 0.03$). The results of the study have confirmed that the most important sleep disorder in AD is sleep fragmentation, causing worsening of the sleep quality (Ju et al., 2013). However, there might be bidirectional influence of amyloid deposition on sleep, and the authors indicate both the possibilities that $A\beta_{42}$ interferes with neuronal function related to sleep-wake cycle and that sleep disturbances contribute to amyloid deposition.

Breathing Disorders During Sleep in AD Patients

Sleep disorders in AD can be caused by breathing disorders during sleep and among them by repetitive obstructive sleep apnea (OSA). However, a correlation between breathing disorders during sleep and AD is not well explained. OSA syndrome occurs—similarly to AD—more often in older patients (Ancoli-Israel et al., 1991). The main risk factor of OSA syndrome is overweight or obesity. Obesity is diagnosed when body mass index (BMI) exceeds 30 kg/m^2. In the population of obese persons, with BMI >30 kg/m^2, OSA risk is about 20–40% (Saint Martin et al., 2015). A connection of AD with obesity is complex. High BMI in the middle of life relates with increased risk of AD in later life, while high BMI in later life is associated with lower risk (Whitmer et al., 2005; Emmerzaal et al., 2015). In a prospective study, where correlation between AD and body weight was analyzed, it has been stated that among patients who were obese at 50 years old, risk of AD was higher (HR 1.39; 95% CI 1.03–1.87) in comparison to patients with normal weight. A reversed correlation has been found by analyzing BMI in later life (i.e., in 65 years of age): among obese patients, the risk of AD was lower (HR 0.63, 95%CI 0.44–0.91) when compared to patients with normal BMI (Fitzpatrick et al., 2009). In the other prospective study comprising 1,394 persons, who at the age of 50 did not show any cognitive disorders, were followed-up for 14 years, and results showed that 142 of them had developed AD. It has been stated that among persons who were obese, upon the beginning of trial, AD developed, on the average, 6.7 months earlier (Chuang et al., 2016). Decrease of BMI before AD (about 0.21 kg/m^2 annually, otherwise about 0.6 kg annually for a person being 1.7 m tall) and stabilization or increase in BMI after the appearance of clinical symptoms of the disease were observed (Gu et al., 2014). Unfortunately, in the above cited studies on the link between obesity and AD risk, sleep breathing disorders have not been assessed. However, as there is increasing incidence of sleep apneas and hypopneas with increasing weight and sleep breathing disorders, and these variables should be taken into the consideration. According to some reports, breathing disorders during sleep occur more often in AD than among persons without dementia (Hoch et al., 1986; Gehrman et al., 2003; Janssens et al., 2009; Kinugawa et al., 2014). In other studies, differences in the frequency of sleep breathing disorders in PSG studies in AD, in comparison to control groups, were minor (Bliwise, 2002; Moraes et al., 2008); while in some studies these differences have not been noticed at all (Bliwise et al., 1989). A possibility of participation of breathing disorders during sleep in etiology of AD is considered by inflammation states, oxidative stress and hypoxemia being caused by them (Dyken et al., 2004; Daulatzai, 2012, 2013). Moreover, breathing disorders during sleep may contribute to progress of AD-related vascular changes. For example, in the study of Buratti et al. (2014) the intima-media thickness (IMT) and cerebrovascular reactivity to hypercapnia based on a breath-holding index (BHI) have been compared in groups of patients with and without OSA syndrome in the course of AD (Buratti et al., 2014). It has been stated that incorrect values of examined parameters (IMT > 1.0 mm, BHI < 0.69) occurred more often in patients with OSA syndrome than in patients without breathing disorders during sleep (HR respectively, 2.98; 95% CI: 1.37–6.46, $p < 0.05$ and 5.25; 95% CI: 2.35–11.74, $p < 0.05$). Indirectly, a correlation between sleep fragmentation and appearance of cognitive disorders was found in the observations conducted in 298 women at the age of 82.3 ± 3.2 years, who were diagnosed with OSA syndrome. Repeated breathing disorders in this syndrome caused sleep fragmentation, because arousals finish the periods of apneas and hypopneas. A prospective study revealed that after 5 years, the risk of mild cognitive disorders or dementi clearly grows (OR 2.04; 95% CI 1.10–3.78) together with increase of apneas and hypopneas frequency (Yaffe et al., 2011).

In a previous study encompassing 59 patients with dementia (MMSE 20.1 ± 6.6), who underwent PSG, OSA syndrome (moderate or severe form) was diagnosed in almost half of the patients (49%). It has been stated at the same time that risk of excitation at night was the smallest in the patients with high apnoe/hypopnoe index (AHI), i.e., with more severe OSA syndrome (Rose et al., 2011). It has been also proved that for some patients with mild or moderate form of AD, prevention of obstructive breathing disorders during sleep with continuous

positive airway pressure (CPAP) can slow down development of dementia (Cooke et al., 2009). For instance, in the group of 23 patients with mild and moderate form of AD (MMSE > 15), as well as with severe form of OSA syndrome (AHI ≥ 30), cognitive disorders were compared after 3 years among patients who used or did not use CPAP and a reduction in the rate of cognitive disorders decline has been stated—measured in MMSE scale—in the group using CPAP [−0.7 (90% CI −1.7; +0.8 vs. −2.2 (90% CI 3.3–1.9); $p = 0.013$] (Troussière et al., 2014).

There is evidence indicating a link between OSA and AD (**Figure 2**). In a recently published study, it has been shown that OSA might induce early changes in CSF Aß 42 concentrations (Liguori et al., 2017). In this study, CSF $Aß_{42}$ concentrations were measured in 25 moderate or severe OSA patients with apnea and hypopnea index > 15/h, in 10 OSA patients treated with continuous positive airway pressure (CPAP, method of choice eliminating sleep apneas) and in 15 controls. In untreated OSA patients, CSF $Aß_{42}$ concentrations were lower than in controls and lower than in CPAP treated OSA patients. Additionally, in OSA patients, a correlation between CSF $Aß_{42}$ concentrations and arterial oxygen saturation during sleep was found, thus confirming the influence of the sleep disordered breathing on AD biomarkers. In another recent study, cognitively normal elderly persons (aged 55–90 years) were prospectively observed for 2 years (Sharma et al., 2017). After adjusting for age, sex and BMI, the association between severity of OSA, as indicated by apnea/hypopnea index, an annual rate change of CSF $Aß_{42}$ concentrations was found. These findings indicate that in cognitively normal older persons, OSA is associated with increased amyloid brain deposition. Repetitive arterial oxygen desaturations and/or sleep fragmentation, and known direct consequences of sleep apneas and hypopneas (Brzecka and Davies, 1993) are likely mechanisms linking OSA with MCI and AD. In a study of 38 cognitively normal persons −19 OSA patients (apnea/hypopnea index > 15/h, mean 21.2 ± 5.1/h, age 58.5 ± 4.1 years) and 19 controls of similar age—amyloid deposition in the brain was studied with Pittsburgh Compound B PET imaging (Yun et al., 2017). Higher amyloid deposition in the areas of right posterior cingulated gyrus and right temporal cortex was found in OSA patients as compared with controls, indicating the possibility of development or progression of AD as a consequence of sleep disordered breathing. Another confirmation of the link between OSA and AD was provided by a longitudinal 15-years long study of 1,667 participants (Lutsey et al., 2018). In the patients with severe OSA (with apnea/hypopnea index > 30/h)—but not in all OSA patients—there was higher risk ratio of AD dementia (1.66, 95% CI 1.06–5.18).

Periodic Limb Movements During Sleep and Restless Legs Syndrome

Periodic leg movements (PLM) can also lead to sleep fragmentation. In the study cited above (Rose et al., 2011), among 37% older people with dementia, PLM index (PLMI) was ≥15/h, indicating moderate to severe form of the disease. In comparison to results of the study conducted in 455 women at the age of 82.9 years, where PLMI ≥15/h has been found in 52% of patients (Claman et al., 2006), the percentage was smaller. In the other study, including 28 patients at the age of 67.8 ± 8.7 years with AD of moderate severity (MMSE 17.8 ± 6.8 points), not receiving any treatment possibly interfering with sleeps, and examined with PSG, more frequent occurrence of PLM was not observed in comparison to healthy people at similar age (Bliwise et al., 2012). PLM is usually accompanied by restless leg syndrome (RLS). This syndrome is diagnosed on the basis of medical history. However, it has been proved that patients with AD, even in the time of mild cognitive disorders, were not able to describe the symptoms of RLS properly (Tractenberg et al., 2005). On the other hand, based on the observations of the patients, it has been stated that symptoms indicating RLS (probable diagnosis of RLS) in the course of AD occur among about 4%–5.5% of patients (Ohayon and Roth, 2002; Talarico et al., 2013). In a study of 339 patients with AD, there were 14 patients meeting the criteria of RLS (Talarico et al., 2013). The patients with concomitant RLS were younger and more apathetic than AD patients without RLS ($p = 0.029$ and $p = 0.001$, respectively). This clinical observation suggested a dysfunction of dopaminergic system in the patients with RLS in the course of AD disease. The problem of RLS in AD may be important, as there are observations from other patients' groups that up to 90% of patients with RLS have sleep disruption caused by concomitant PLM syndrome (Skalski, 2017).

Sleep and Brain Glymphatic System in AD

Recent reports indicate an important relation between disrupted sleep, brain glymphatic system and AD (Mendelsohn and Larrick, 2013; Lee et al., 2015; O'Donnell et al., 2015; Krueger et al., 2016). For instance, glymphatic system consists of para-vascular channels located around blood vessels of the brain. CSF flows along para-arterial space, reaches the capillary bed and penetrates into the brain parenchyma, where it gets mixed with interstitial fluid and after collecting metabolic waste it is moved to para-venous space and then to cervical lymphatic vessels (Ratner et al., 2015). Thus, it can be stated that glymphatic system acts like the lymphatic system in the other body organs.

One of the glymphatic system functions is the removal of metabolites and neurotoxic compounds, including soluble Aβ from the CNS parenchyma (Kyrtsos and Baras, 2015; Bakker et al., 2016; Simon and Iliff, 2016). It has been demonstrated that more than half of Aβ could be removed from the brain through the glymphatic system (Iliff et al., 2012). It seems that sleep may influence glymphatic system function. During natural sleep, there is a marked increase of the brain's interstitial space as compared with wakefulness, possibly resulting from the shrinkage of astroglial cells (Mendelsohn and Larrick, 2013; Xie et al., 2013; Kress et al., 2014; O'Donnell et al., 2015). The enlargement of the extracellular space accelerates clearance processes. It has been found that in mice, the clearance of the Aβ during sleep was two-fold faster than during wakefulness (Xie et al., 2013). In the other animal study, it has been demonstrated that the speed of clearance through the glymphatic system depends also on the body posture (Lee et al., 2015). The glymphatic transport was the

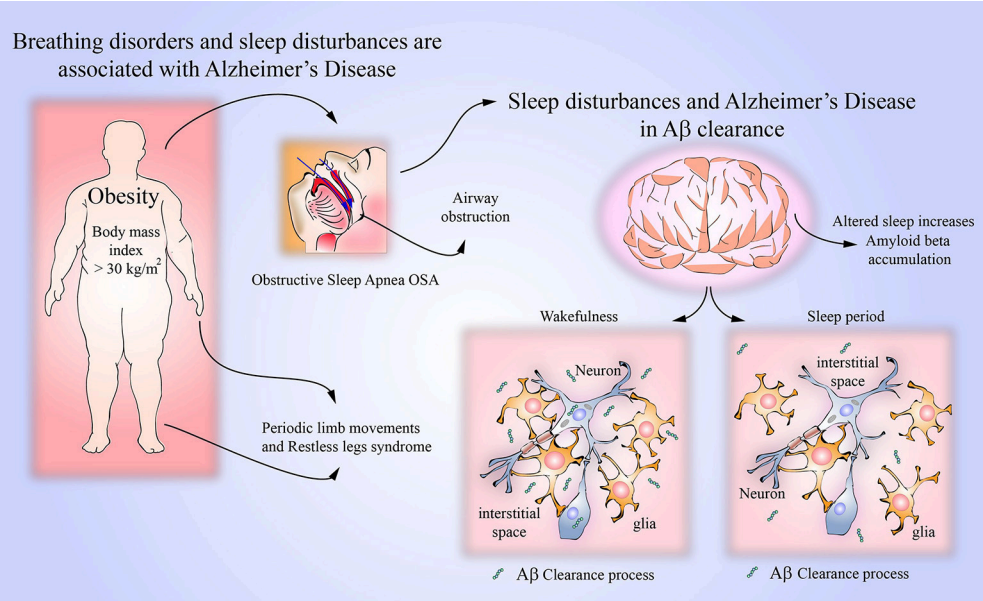


FIGURE 2 | Breathing disorders and amyloid beta clearance. It has been observed that sleep disorders in AD can be caused by obstructive sleep apnea (OSA). OSA is caused by an obstruction of respiratory airways, and its main risk overweight in obesity. Prospective studies have shown that patients with OSA may develop AD by several mechanisms such as neuroinflammation, oxidative stress and hypoxemia. Interestingly, clinical conditions like periodic limb movements and restless legs syndrome, which also lead to sleep disturbances, may be associated to AD. The removal of metabolites and neurotoxic compounds via glymphatic system is a function regulated by sleep and wakefulness activity. It is known that soluble amyloid beta can be cleared from the CNS parenchyma using the glymphatic system. Sleep may influence the clearance of amyloid beta due to the increased brain's interstitial space possibly by the shrinkage of astroglial cells.

most efficient in the lateral position, which is the most common during sleep.

As Aβ clearance is impaired in both early and late forms of AD (Tarasoff-Conway et al., 2015), it can be assumed that there is a link between impaired glymphatic system function and AD. Experiments in animal and humans revealed diurnal oscillation of the Aβ level in the brain interstitial fluid (Musiek, 2015). Indeed, as endogenous neuronal activity influences the regional concentration of the Aβ in the interstitial fluid (Bero et al., 2011), decreased neuronal activity in some stages of sleep may cause the oscillations of the Aβ concentrations. Slow wave sleep with periodic neuronal hyperpolarization and diminished neuronal firing in some brain regions can be associated with decreased Aβ production (Musiek, 2015). Thus, altered sleep quality might contribute to the onset and progression of the AD both through impaired glymphatic clearance and disturbances in the Aβ production in case of disordered slow wave sleep.

Although the presence of glymphatic system has been proved in animal studies, there is also evidence indicating its function in humans (Kiviniemi et al., 2016). The diffusion-based MR technique called diffusion tensor image analysis along the perivascular space has been used to reflect impairment of the glymphatic system in AD patients (Taoka et al., 2017). The usefulness of diffusion tensor imaging measurements has been also shown in distinguishing patients with early-stage AD from those with subcortical ischemic vascular disease (Tu et al., 2017).

Among sleep stages, specifically slow wave sleep, exert the influence on $A\beta_{42}$ level in the CSF. In a study encompassing 36 cognitively normal and elderly subjects, CSF $A\beta_{42}$ levels inversely correlated with slow wave sleep duration ($r = -0.35$, $p < 0.05$), slow wave sleep % of total sleep time ($r = -0.36$, $p < 0.05$) and slow wave activity in frontal EEG leads during sleep time ($r = -0.45$, $p < 0.01$) (Varga et al., 2016). Additionally, local Aβ accumulation was found to be associated specifically with diminished slow wave activity during sleep in the low frequency range (0.6–1 Hz) (Mander et al., 2015). These findings may indicate the association between decreased clearance and/or production of Aβ and slow wave sleep deficiency.

Final Remarks

The above listed clinical and experimental observations strongly suggest bidirectional relationship between sleep and AD. Sleep disorders, such as difficulties in falling asleep, sleep disruption and altered circadian sleep-wake cycle, are typical symptoms of AD and usually escalate with progression of the disease (Bliwise et al., 1995; McCurry et al., 1999; McCurry and Ancoli-Israel, 2003; Most et al., 2012; Lim et al., 2013; Spira et al., 2013; Dos Santos et al., 2014, 2015; Spalletta et al., 2015). PSG studies reveal macro- and micro-structure sleep abnormalities in both clinical and preclinical AD (Prinz et al., 1982; Bliwise, 1993; Rauchs et al., 2008; Westerberg et al., 2012; Hita-Yañez et al., 2013; Liguori et al., 2014; Maestri et al., 2015). There is a correlation between sleep-wake rhythm disturbance and signs of cerebral Aβ deposition (Lim et al., 2013). On the other hand, sleep abnormalities may increase the risk of AD development. There are empirical data showing increased levels

of $A\beta_{42}$ in CSF after sleep deprivation (Ooms et al., 2014). There is also growing evidence showing that severe sleep disturbances caused by breathing disorders during sleep may influence AD development and progression (Dyken et al., 2004; Cooke et al., 2009; Rose et al., 2011; Daulatzai, 2013; Buratti et al., 2014; Troussière et al., 2014; Liguori et al., 2017; Sharma et al., 2017; Yun et al., 2017; Lutsey et al., 2018). In OSA patients the signs of increased amyloid deposition in the brain were observed (Sharma et al., 2017; Yun et al., 2017).

The key to understanding the link between sleep disturbances and AD development may be the function of glymphatic system. The activity of glymphatic system augments during sleep (Pistollato et al., 2016) and —to some extent —Aβ is cleared through the glymphatic system (Boespflug and Iliff, 2018). Thus, disrupted sleep may lead to glymphatic system function impairment and Aβ accumulation. Possible mechanisms of bidirectional relationship between sleep disturbances and Aβ clearance should be taken into consideration.

CONCLUSION

Clinical observations indicate the likelihood of a bidirectional relationship between abnormalities of sleep and AD. Changes in sleep structure, worse sleep quality in both preclinical and symptomatic AD, correlation of cognitive impairments with sleep structure abnormalities, changes in CSF Aß concentrations induced by sleep apneas and correlating with severity of sleep disordered breathing, the influence of physiological sleep on clearance of Aβ through the glymphatic system, possible influence of impaired glymphatic system on Aβ level, and observations with the use of the newest technical equipment reflecting impairment of the glymphatic system in AD patients allow to conclude that disordered sleep may contribute to the development of AD pathology.

Future Direction of the Research

1. Electrophysiologic sleep studies aimed to find early signs of risk of development of AD in target populations.
2. Development of specific procedures leading to improvement of sleep structure and quality.
3. The studies on glymphatic system in sleep breathing disorders in relation to the risk of $A\beta_{42}$ accumulation.
4. Testing possible relationship between worsening of cognitive abilities and inflammatory state, oxidative stress, hypoxemia or vascular pathology and other neuropathological signs in AD, and TAU protein production.
5. Based on the analysis of sleep and its disorders, identify new directions of AD therapy, especially at its pre-symptomatic stages.

AUTHOR CONTRIBUTIONS

All authors listed, have made substantial, direct and intellectual contribution to the work, and approved it for publication.

ACKNOWLEDGMENTS

This research was supported in part by RSF project #14-23-00160P and the scientific projects of IPAC (topics 48.8. and 48.9). Authors' also very grateful for the animal facilities were provided by Center for preclinical trials of IPAC RAS.

REFERENCES

Aliev, G., Priyadarshini, M., Reddy, V. P., Grieg, N. H., Kaminsky, Y., Cacabelos, R., et al. (2014). Oxidative stress mediated mitochondrial and vascular lesions as markers in the pathogenesis of Alzheimer disease. *Curr. Med. Chem.* 21, 2208–2217. doi: 10.2174/09298673216661312271613 03

Ancoli-Israel, S., Clopton, P., Klauber, M. R., Fell, R., and Mason, W. (1997). Use of wrist activity for monitoring sleep/wake in demented nursing-home patients. *Sleep* 20, 24–27. doi: 10.1093/sleep/20.1.24

Ancoli-Israel, S., Kripke, D. F., Klauber, M. R., Mason, W. J., Fell, R., and Kaplan, O., et al. (1991). Sleep-disordered breathing in community-dwelling elderly. *Sleep* 14, 486–495. doi: 10.1093/sleep/14.6.486

Ansari, S. A., Satar, R., Perveen, A., and Ashraf, G. M. (2017). Current opinion in Alzheimer's disease therapy by nanotechnology-based approaches. *Curr. Opin. Psychiatry* 30, 128–135. doi: 10.1097/YCO.0000000000000310

Ashraf, G. M., Chibber, S., Mohammad, Zaidi, S. K., Tabrez, S., Ahmad, A., et al. (2016). Recent updates on the association between Alzheimer's disease and vascular dementia. *Med. Chem.* 12, 226–237. doi: 10.2174/1573406411666151030111820

Ashraf, G. M., Greig, N. H., Khan, T. A., Hassan, I., Tabrez, S., and Shakil, S. (2014). Protein misfolding and aggregation in Alzheimer's disease and type 2 diabetes mellitus. *CNS Neurol. Disord. Drug Targets* 13, 1280–1293. doi: 10.2174/1871527313666140917095514

Ashraf, G. M., Tabrez, S., Jabir, N. R., Firoz, C. K., Ahmad, S., Hassan, I., et al. (2015). An overview on global trends in nanotechnological approaches for Alzheimer therapy. *Curr. Drug Metab.* 16, 719–727. doi: 10.2174/1389200216081511071257 57

Bakker, E. N., Bacska, B. J., Arbel-Ornath, M., Aldea, R., Bedussi, B., Morris, A. W., et al. (2016). Lymphatic clearance of the brain: perivascular, paravascular and significance for neurodegenerative diseases. *Cell Mol. Neurobiol.* 36, 181–194. doi: 10.1007/s10571-015-0273-8

Bero, A. W., Yan, P., Roh, J. H., Cirrito, J. R., Stewart, F. R., Raichle, M. E., et al. (2011). Neuronal activity regulates the regional vulnerability to amyloid-beta deposition. *Nat. Neurosci.* 14, 750–756. doi: 10.1038/nn.2801

Bhat, S. A., Kamal, M. A., Yarla, N. S., and Ashraf, G. M. (2017). Synopsis on managment strategies for neurodegenerative disorders: challenges from bench to bedside in successful drug discovery and development. *Curr. Top. Med. Chem.* 17, 1371–1378. doi: 10.2174/1568026616666161222121229

Bliwise, D. L. (1993). Sleep in normal aging and dementia. *Sleep* 16, 40–81. doi: 10.1093/sleep/16.1.40

Bliwise, D. L. (2002). Sleep apnea, APOE4 and Alzheimer's disease 20 years and counting? *J. Psychosom. Res.* 53, 539–546. doi: 10.1016/S0022-3999(02)00436-1

Bliwise, D. L., Hughes, M., McMahon, P. M., and Kutner, N. (1995). Observed sleep/wakefulness and severity of dementia in an Alzheimer's disease special care unit. *J. Gerontol. A Biol. Sci. Med. Sci.* 50, M303–M306. doi: 10.1093/gerona/50A.6.M303

Bliwise, D. L., Trotti, L. M., Yesavage, J. A., and Rye, D. B. (2012). Periodic leg movements in sleep in elderly patients with Parkinsonism and Alzheimer's disease. *Eur. J. Neurol.* 19, 918–923. doi: 10.1111/j.1468-1331.2012.03673.x

Bliwise, D. L., Yesavage, J. A., Tinklenberg, J. R., and Dement, W. C. (1989). Sleep apnea in Alzheimer's disease. *Neurobiol. Aging* 10, 343–346. doi: 10.1016/0197-4580(89)90046-8

Boespflug, E. L., and Iliff, J. J. (2018). The emerging relationship between interstitial fluid-cerebrospinal fluid exchange, amyloid-β, and sleep. *Biol. Psychiatry* 83, 328–336. doi: 10.1016/j.biopsych.2017.11.031

Brzecka, A., and Davies, S. F. (1993). Profound sleep hypoxia in morbidly obese hypercapnic patients with obstructive sleep apnea. *Mater. Med. Pol.* 25, 63–71.

Buratti, L., Viticchi, G., Falsetti, L., Cagnetti, C., Luzzi, S., and Bartolini, M. (2014). Vascular impairment in Alzheimer's disease: the role of obstructive sleep apnea. *J. Alzheimers Dis*. 38, 445–453. doi: 10.3233/JAD-131046

Chibber, S., Alexiou, A., Alama, M. N., Barreto, G. E., Aliev, G., and Ashraf, G. M. (2016). A synopsis on the linkage between age-related dementias and vascular disorders. *CNS Neurol. Disord. Drug Targets*. 15, f250–f258. doi: 10.2174/1871527315666160202121809

Chuang, Y. F., An, Y., Bilgel, M., Wong, D. F., Troncoso, J. C., O'Brien, R. J., et al. (2016). Midlife adiposity predicts earlier onset of Alzheimer's dementia, neuropathology and presymptomatic cerebral amyloid accumulation. *Mol. Psychiatry* 21, 910–915. doi: 10.1038/mp.2015.129

Claman, D. M., Redline, S., Blackwell, T., Ancoli-Israel, S., Surovec, S., Scott, N., et al. (2006). Prevalence and correlates of periodic limb movements in older women. *J. Clin. Sleep Med*. 2, 438–445.

Cooke, J. R., Ayalon, L., Palmer, B. W., Loredo, J. S., Corey-Bloom, J., Natarajan, L., et al. (2009). Sustained use of CPAP slows deterioration of cognition, sleep, and mood in patients with Alzheimer's disease and obstructive sleep apnea: a preliminary study. *J. Clin. Sleep Med*. 5, 305–309. doi: 10.1016/j.sleep.2008.12.016

Daulatzai, M. A. (2012). Pathogenesis of cognitive dysfunction in patients with obstructive sleep apnea: a hypothesis with emphasis on the nucleus tractus solitarius. *Sleep Disord*. 2012:251096. doi: 10.1155/2012/251096

Daulatzai, M. A. (2013). Death by a thousand cuts in Alzheimer's disease: hypoxia–the prodrome. *Neurotox. Res.* 24, 216–243. doi: 10.1007/s12640-013-9379-2

Dos Santos, A. B., Barreto, G. E., and Kohlmeier, K. A. (2014). Treatment of sleeping disorders should be considered in clinical management of Parkinson's disease. *Front. Aging Neurosci*. 6:273. doi: 10.3389/fnagi.2014.00273

Dos Santos, A. B., Kohlmeier, K. A., and Barreto, G. E. (2015). Are sleep disturbances preclinical markers of Parkinson's disease? *Neurochem. Res*. 40, 421–427. doi: 10.1007/s11064-014-1488-7

Drago, V., Babiloni, C., Bartrés-Faz, D., Caroli, A., Bosch, B., Hensch, T., et al. (2011). Disease tracking markers for Alzheimer's disease at the prodromal (MCI) stage. *J. Alzheimers Dis*. 26, 159–199. doi: 10.3233/JAD-2011-0043

Dyken, M. E., Yamada, T., Glenn, C. L., and Berger, H. A. (2004). Obstructive sleep apnea associated with cerebral hypoxemia and death. *Neurology* 62, 491–493. doi: 10.1212/01.WNL.0000106952.84223.F3

Emmerzaal, T. L., Kiliaan, A. J., and Gustafson, D. R. (2015). 2003–2013: a decade of body mass index, Alzheimer's disease, and dementia. *J. Alzheimers Dis*. 43, 739–755. doi: 10.3233/JAD-141086

Faubel, R., López-García, E., Guallar-Castillón, P., Graciani, A., Banegas, J. R., and Rodríguez-Artalejo, F. (2009). Usual sleep duration and cognitive function in older adults in Spain. *J. Sleep Res*. 18, 427–435. doi: 10.1111/j.1365-2869.2009.00759.x

Fitzpatrick, A. L., Kuller, L. H., Lopez, O. L., Diehr, P., O'Meara, E. S., and Longstreth, W. T. Jr. (2009). Midlife and late-life obesity and the risk of dementia: cardiovascular health study. *Arch. Neurol*. 66, 336–342. doi: 10.1001/archneurol.2008.582

Gehrman, P. R., Martin, J. L., Shochat, T., Nolan, S., Corey-Bloom, J., and Ancoli-Israel, S. (2003). Sleep-disordered breathing and agitation in institutionalized adults with Alzheimer disease. *Am. J. Geriatr. Psychiatry* 11, 426–433. doi: 10.1097/00019442-200307000-00005

Gu, Y., Scarmeas, N., Cosentino, S., Brandt, J., Albert, M., Blacker, D., et al. (2014). Change in body mass index before and after Alzheimer's disease onset. *Curr. Alzheimer Res*. 11, 349–356. doi: 10.2174/1567205010666131120110930

Hassainia, F., Petit, D., Nielsen, T., Gauthier, S., and Montplaisir, J. (1997). Quantitative EEG and statistical mapping of wakefulness and REM sleep in the evaluation of mild to moderate Alzheimer's disease. *Eur. Neurol*. 37, 219–224. doi: 10.1159/000117446

Hita-Yañez, E., Atienza, M., and Cantero, J. L. (2013). Polysomnographic and subjective sleep markers of mild cognitive impairment. *Sleep* 36, 1327–1334. doi: 10.5665/sleep.2956

Hoch, C. C., Reynolds, C. F. III., Kupfer, D. J., Houck, P. R., Berman, S. R., and Stack, J. A. (1986). Sleep-disordered breathing in normal and pathologic aging. *J. Clin. Psychiatry* 47, 499–503.

Iliff, J. J., Wang, M., Liao, Y., Plogg, B. A., Peng, W., Gundersen, G. A., et al. (2012). A paravascular pathway facilitates CSF flow through the brain parenchyma and the clearance of interstitial solutes, including amyloid β. *Sci. Transl. Med*. 4:147ra111. doi: 10.1126/scitranslmed.3003748

Jabir, N. R., Firoz, C. K., Baeesa, S. S., Ashraf, G. M., Akhtar, S., Kamal, W., et al. (2015). Synopsis on the linkage of Alzheimer's and Parkinson's disease with chronic diseases. *CNS Neurosci. Ther*. 21, 1–7. doi: 10.1111/cns.12344

Janssens, J. P., Metzger, M., and Sforza, E. (2009). Impact of volume targeting on efficacy of bi-level non-invasive ventilation and sleep in obesity-hypoventilation. *Respir. Med*. 103, 165–172. doi: 10.1016/j.rmed.2008.03.013

Ju, Y. E., McLeland, J. S., Toedebusch, C. D., Xiong, C., Fagan, A. M., Duntley, S. P., et al. (2013). Sleep quality and preclinical Alzheimer disease. *JAMA Neurol*. 70, 587–593. doi: 10.1001/jamaneurol.2013.2334

Karran, E., Mercken, M., and De Strooper, B. (2011). The amyloid cascade hypothesis for Alzheimer's disease: an appraisal for the development of therapeutics. *Nat. Rev. Drug Discov*. 10, f698–f712. doi: 10.1038/nrd3505

Kinugawa, K., Nguyen-Michel, V. H., and Mariani, J. (2014). [Obstructive sleep apnea syndrome: a cause of cognitive disorders in the elderly?]. *Rev. Med. Interne*. 35, 664–669. doi: 10.1016/j.revmed.2014.02.005

Kiviniemi, V., Wang, X., Korhonen, V., Keinänen, T., Tuovinen, T., Autio, J., et al. (2016). Ultra-fast magnetic resonance encephalography of physiological brain activity-Glymphatic pulsationmechanisms? *J. Cereb. Blood Flow Metab*. 36, 1033–1045. doi: 10.1177/0271678X15622047

Kress, B. T., Iliff, J. J., Xia, M., Wang, M., Wei, H. S., Zeppenfeld, D., et al. (2014). Impairment of paravascular clearance pathways in the aging brain. *Ann. Neurol*. 76, 845–861. doi: 10.1002/ana.24271

Krueger, J. M., Frank, M. G., Wisor, J. P., and Roy, S. (2016). Sleep function: toward elucidating an enigma. *Sleep Med. Rev*. 28, 46–54. doi: 10.1016/j.smrv.2015.08.005

Kyrtsos, C. R., and Baras, J. S. (2015). Modeling the role of the glymphatic pathway and cerebral blood vessel properties in Alzheimer's disease pathogenesis. *PLoS ONE* 10:e0139574. doi: 10.1371/journal.pone.0139574

Lee, H., Xie, L., Yu, M., Kang, H., Feng, T., Deane, R., et al. (2015). The effect of body posture on brain glymphatic transport. *J. Neurosci*. 35, 11034–11044. doi: 10.1523/JNEUROSCI.1625-15.2015

Liguori, C., Mercuri, N. B., Izzi, F., Romigi, A., Cordella, A., Sancesario, G., et al. (2017). Obstructive sleep apnea is associated with early but possibly modifiable Alzheimer's disease biomarkers changes. *Sleep* 40:zsx011. doi: 10.1093/sleep/zsx011

Liguori, C., Romigi, A., Nuccetelli, M., Zannino, S., Sancesario, G., Martorana, A., et al. (2014). Orexinergic system dysregulation, sleep impairment, and cognitive decline in Alzheimer disease. *JAMA Neurol*. 71, 1498–1505. doi: 10.1001/jamaneurol.2014.2510

Lim, A. S., Kowgier, M., Yu, L., Buchman, A. S., and Bennett, D. A. (2013). Sleep fragmentation and the risk of incident Alzheimer's disease and cognitive decline in older persons. *Sleep* 36, 1027–1032. doi: 10.5665/sleep.2802

Lutsey, P. L., Misialek, J. R., Mosley, T. H., Gottesman, R. F., Punjabi, N. M., Shahar, E., et al. (2018). Sleep characteristics and risk of dementia and Alzheimer's disease: the atherosclerosis risk in communities study. *Alzheimers Dement*. 14, 157–166. doi: 10.1016/j.jalz.2017.06.2269

Maestri, M., Carnicelli, L., Tognoni, G., Di Coscio, E., Giorgi, F. S., Volpi, L., et al. (2015). Non-rapid eye movement sleep instability in mild cognitive impairment: a pilot study. *Sleep Med*. 16, 1139–1145. doi: 10.1016/j.sleep.2015.04.027

Mander, B. A., Marks, S. M., Vogel, J. W., Rao, V., Lu, B., Saletin, J. M., et al. (2015). β-amyloid disrupts human NREM slow waves and related hippocampus-dependent memory consolidation. *Nat. Neurosci*. 18, 1051–1057. doi: 10.1038/nn.4035

McCurry, S. M., and Ancoli-Israel, S. (2003). Sleep dysfunction in Alzheimer's disease and other dementias. *Curr. Treat. Options Neurol*. 5, 261–272. doi: 10.1007/s11940-003-0017-9

McCurry, S. M., Logsdon, R. G., Teri, L., Gibbons, L. E., Kukull, W. A., Bowen, J. D., et al. (1999). Characteristics of sleep disturbance in community-dwelling Alzheimer's disease patients. *J. Geriatr. Psychiatry Neurol*. 12, 53–59. doi: 10.1177/089198879901200203

Mendelsohn, A. R., and Larrick, J. W. (2013). Sleep facilitates clearance of metabolites from the brain: glymphatic function in aging and neurodegenerative diseases. *Rejuvenation Res.* 16, 518–523. doi: 10.1089/rej.2013.1530

Moraes, W., Poyares, D., Sukys-Claudino, L., Guilleminault, C., and Tufik, S. (2008). Donepezil improves obstructive sleep apnea in Alzheimer disease: a double-blind, placebo-controlled study. *Chest* 133, 677–683. doi: 10.1378/chest.07-1446

Moran, M., Lynch, C. A., Walsh, C., Coen, R., Coakley, D., and Lawlor, B. A. (2005). Sleep disturbance in mild to moderate Alzheimer's disease. *Sleep Med.* 6, 347–352. doi: 10.1016/j.sleep.2004.12.005

Most, E. I., Aboudan, S., Scheltens, P., and Van Someren, E. J. (2012). Discrepancy between subjective and objective sleep disturbances in early- and moderate-stage Alzheimer disease. *Am. J. Geriatr. Psychiatry* 20, 460–467. doi: 10.1097/JGP.0b013e318252e3ff

Musiek, E. S. (2015). Circadian clock disruption in neurodegenerative diseases: cause and effect? *Front. Pharmacol.* 6:29. doi:10.3389/fphar.2015.00029

O'Donnell, J., Ding, F., and Nedergaard, M. (2015). Distinct functional states of astrocytes during sleep and wakefulness: is norepinephrine the master regulator? *Curr. Sleep Med. Rep.* 1, 1–8. doi: 10.1007/s40675-014-0004-6

Ohayon, M. M., and Roth, T. (2002). Prevalence of restless legs syndrome and periodic limb movement disorder in the general population. *J. Psychosom. Res.* 53, 547–554. doi: 10.1016/S0022-3999(02)00443-9

Ooms, S., Overeem, S., Besse, K., Rikkert, M. O., Verbeek, M., and Claassen, J. A. (2014). Effect of 1 night of total sleep deprivation on cerebrospinal fluid beta-amyloid 42 in healthy middle-aged men: a randomized clinical trial. *JAMA Neurol.* 71, 971–977. doi: 10.1001/jamaneurol.2014.1173

Peter-Derex, L., Yammine, P., Bastuji, H., and Croisile, B. (2015). Sleep and Alzheimer's disease. *Sleep Med. Rev.* 19, 29–38. doi: 10.1016/j.smrv.2014.03.007

Petit, D., Gagnon, J. F., Fantini, M. L., Ferini-Strambi, L., and Montplaisir, J. (2004). Sleep and quantitative EEG in neurodegenerative disorders. *J. Psychosom. Res.* 56, 487–496. doi: 10.1016/j.jpsychores.2004.02.001

Pistollato, F., Sumalla Cano, S., Elio, I., Masias Vergara, M., Giampieri, F., and Battino, M. (2016). Associations between sleep, cortisol regulation, and diet: possible implications for the risk of Alzheimer disease. *Adv. Nutr.* 7, 679–689. doi: 10.3945/an.115.011775

Potvin, O., Lorrain, D., Forget, H., Dubé, M., Grenier, S., Préville, M., et al. (2012). Sleep quality and 1-year incident cognitive impairment in community-dwelling older adults. *Sleep* 35, f491–f499. doi: 10.5665/sleep.1732

Prince, M., Bryce, R., Albanese, E., Wimo, A., Ribeiro, W., and Ferri, C. P. (2013). The global prevalence of dementia: a systematic review and metaanalysis. *Alzheimers. Dement.* 9, 63.e2–75.e2. doi: 10.1016/j.jalz.2012.11.007

Prinz, P. N., Peskind, E. R., Vitaliano, P. P., Raskind, M. A., Eisdorfer, C., Zemcuznikov, N., et al. (1982). Changes in the sleep and waking EEGs of nondemented and demented elderly subjects. *J. Am. Geriatr. Soc.* 30, 86–93. doi: 10.1111/j.1532-5415.1982.tb01279.x

Ratner, V., Zhu, L., Kolesov, I., Nedergaard, M., Benveniste, H., and Tannenbaum, A. (2015). Optimal-mass-transfer-based estimation of glymphatic transport in living brain. *Proc. SPIE Int. Soc. Opt. Eng.* 9413:94131J. doi: 10.1117/12.2076289

Rauchs, G., Schabus, M., Parapatics, S., Bertran, F., Clochon, P., Hot, P., et al. (2008). Is there a link between sleep changes and memory in Alzheimer's disease? *Neuroreport* 19, 1159–1162. doi: 10.1097/WNR.0b013e32830867c4

Rizvi, S. M., Shaikh, S., Waseem, S. M., Shakil, S., Abuzenadah, A. M., Biswas, D., et al. (2015). Role of anti-diabetic drugs as therapeutic agents in Alzheimer's disease. *EXCLI J.* 14, 684–696. doi: 10.17179/excli2015-252

Rose, K. M., Beck, C., Tsai, P. F., Liem, P. H., Davila, D. G., Kleban, M., et al. (2011). Sleep disturbances and nocturnal agitation behaviors in older adults with dementia. *Sleep* 34, 779–786. doi: 10.5665/SLEEP.1048

Saint Martin, M., Roche, F., Thomas, T., Collet, P., Barthélémy, J. C., and Sforza, E. (2015). Association of body fat composition and obstructive sleep apnea in the elderly: a longitudinal study. *Obesity* 23, 1511–1516. doi: 10.1002/oby.21121

Selkoe, D., and Hardy, J. (2016). The amyloid hypothesis of Alzheimer's disease at 25 years. *EMBO Mol. Med.* 8, 595–608. doi: 10.15252/emmm.201606210

Sen, D., Majumder, A., Arora, V., Yadu, N., and Chakrabarti, R. (2017). Taming Alzheimer's disease: new perspectives, newer horizons. *Iran J. Neurol.* 16, 146–155.

Sharma, R. A., Varga, A. W., Bubu, O. M., Pirraglia, E., Kam, K., Parekh, A., et al. (2017). Obstructive sleep apnea severity affects amyloid burden in cognitively normal elderly: a longitudinal study. *Am. J. Respir. Crit. Care Med.* 197, 933–943. doi: 10.1164/rccm.201704-0704OC

Simon, M. J., and Iliff, J. J. (2016). Regulation of cerebrospinal fluid (CSF) flow in neurodegenerative, neurovascular and neuroinflammatory disease. *Biochim. Biophys. Acta.* 1862, 442–451. doi: 10.1016/j.bbadis.2015.10.014

Skalski, M. (2017). *[Sleep-Wake Disorders; DSM-5 Selections]*, Wroclaw: Edra, Urban and Partner.

Soursou, G., Alexiou, A., Ashraf, G. M., Siyal, A. A., Mushtaq, G., and Kamal, M. A. (2015). Applications of nanotechnology in diagnostics and therapeutics of Alzheimer's and Parkinson's disease. *Curr. Drug Metab.* 16, 705–712. doi: 10.2174/1389200216081511071250 49

Spalletta, G., Long, J. D., Robinson, R. G., Trequattrini, A., Pizzoli, S., Caltagirone, C., et al. (2015). Longitudinal neuropsychiatric predictors of death in Alzheimer's disease. *J. Alzheimers Dis.* 48, 627–636. doi: 10.3233/JAD-150391

Spira, A. P., Gamaldo, A. A., An, Y., Wu, M. N., Simonsick, E. M., and Bilgel, M. (2013). Self-reported sleep and beta-amyloid deposition in community-dwelling older adults. *JAMA Neurol.* 70, 1537–1543. doi: 10.1001/jamaneurol.2013.4258

Talarico, G., Canevelli, M., Tosto, G., Vanacore, N., Letteri, F., Prastaro, M., et al. (2013). Restless legs syndrome in a group of patients with Alzheimer's disease. *Am. J. Alzheimers Dis. Other Demen.* 28, 165–170. doi: 10.1177/1533317512470208

Taoka, T., Masutani, Y., Kawai, H., Nakane, T., Matsuoka, K., Yasuno, F., et al. (2017). Evaluation of glymphatic system activity with the diffusion MR technique: diffusion tensor image analysis along the perivascular space (DTI-ALPS) in Alzheimer's disease cases. *Jpn. J. Radiol.* 35, 172–178. doi: 10.1007/s11604-017-0617-z

Tarasoff-Conway, J. M., Carare, R. O., Osorio, R. S., Glodzik, L., Butler, T., Fieremans, E., et al. (2015). Clearance systems in the brain-implications for Alzheimer disease. *Nat. Rev. Neurol.* 11, 457–470. doi: 10.1038/nrneurol.2015.119

Tractenberg, R. E., Singer, C. M., and Kaye, J. A. (2005). Symptoms of sleep disturbance in persons with Alzheimer's disease and normal elderly. *J. Sleep Res.* 14, 177–185. doi: 10.1111/j.1365-2869.2005.00445.x

Troussière, A. C., Charley, C. M., Salleron, J., Richard, F., Delbeuck, X., Derambure, P., et al. (2014). Treatment of sleep apnoea syndrome decreases cognitive decline in patients with Alzheimer's disease. *J. Neurol. Neurosurg. Psychiatr.* 85, 1405–1408. doi: 10.1136/jnnp-2013-307544

Tu, M. C., Lo, C. P., Huang, C. F., Hsu, Y. H., Huang, W. H., Deng, J. F., et al. (2017). Effectiveness of diffusion tensor imaging in differentiating early-stage subcortical ischemic vascular disease, Alzheimer's disease and normal ageing. *PLoS ONE* 12:e0175143. doi: 10.1371/journal.pone.0175143

Tworoger, S. S., Lee, S., Schernhammer, E. S., and Grodstein, F. (2006). The association of self-reported sleep duration, difficulty sleeping, and snoring with cognitive function in older women. *Alzheimer Dis. Assoc. Disord.* 20, 41–48. doi: 10.1097/01.wad.0000201850.52707.80

Varga, A. W., Wohlleber, M. E., Giménez, S., Romero, S., Alonso, J. F., Ducca, E. L., et al. (2016). Reduced slow-wave sleep is associated with high cerebrospinal fluid Aβ42 levels in cognitively normal elderly. *Sleep* 39, 2041–2048. doi: 10.5665/sleep.6240

Westerberg, C. E., Mander, B. A., Florczak, S. M., Weintraub, S., Mesulam, M. M., Zee, P. C., et al. (2012). Concurrent impairments in sleep and memory in amnestic mild cognitive impairment. *J. Int. Neuropsychol. Soc.* 18, 490–500. doi: 10.1017/S135561771200001X

Whitmer, R. A., Gunderson, E. P., Barrett-Connor, E., Quesenberry, C. P. Jr, and Yaffe, K. (2005). Obesity in middle age and future risk of dementia: a 27 year longitudinal population based study. *BMJ* 330:1360. doi: 10.1136/bmj.38446.466238.E0

Wyss-Coray, T., and Mucke, L. (2002). Inflammation in neurodegenerative disease–a double-edged sword. *Neuron* 35, f419–f432. doi: 10.1016/S0896-6273(02)00794-8

Xie, L., Kang, H., Xu, Q., Chen, M. J., Liao, Y., Thiyagarajan, M., et al. (2013). Sleep drives metabolite clearance from the adult brain. *Science* 342, 373–377. doi: 10.1126/science.1241224

Yaffe, K., Laffan, A. M., Harrison, S. L., Redline, S., Spira, A. P., Ensrud, K. E., et al. (2011). Sleep-disordered breathing, hypoxia, and risk of mild cognitive impairment and dementia in older women. *JAMA* 306, 613–619. doi: 10.1001/jama.2011.1115

Yun, C. H., Lee, H. Y., Lee, S. K., Kim, H., Seo, H. S., Bang, S. A., et al. (2017). Amyloid burden in obstructive sleep apnea. *J. Alzheimers Dis.* 59, 21–29. doi: 10.3233/JAD-161047

Zhao, Q. F., Tan, L., Wang, H. F., Jiang, T., Tan, M. S., Tan, L., et al. (2016). The prevalence of neuropsychiatric symptoms in Alzheimer's disease: systematic review and meta-analysis. *J. Affect. Disord.* 190, 264–271. doi: 10.1016/j.jad.2015.09.069

Conflict of Interest Statement: GA was employed by GALLY International Biomedical Research Consulting LLC, San Antonio, Texas, USA.

The other authors declare that the research was conducted in the absence of any commercial or financial relationships that could be construed as a potential conflict of interest.

Copyright © 2018 Brzecka, Leszek, Ashraf, Ejma, Ávila-Rodriguez, Yarla, Tarasov, Chubarev, Samsonova, Barreto and Aliev. This is an open-access article distributed under the terms of the Creative Commons Attribution License (CC BY). The use, distribution or reproduction in other forums is permitted, provided the original author(s) and the copyright owner are credited and that the original publication in this journal is cited, in accordance with accepted academic practice. No use, distribution or reproduction is permitted which does not comply with these terms.

frontiers in Aging Neuroscience

ORIGINAL RESEARCH
published: 17 October 2017
doi: 10.3389/fnagi.2017.00334

Repetitive Transcranial Magnetic Stimulation (rTMS) Modulates Lipid Metabolism in Aging Adults

Weicong Ren[1,2,3†], *Jiang Ma*[4†], *Juan Li*[3], *Zhijie Zhang*[1,2*] *and Mingwei Wang*[2,5*]

[1]*Department of Psychology, Hebei Normal University, Shijiazhuang, China,* [2]*Key Laboratory of Brain Aging and Cognitive Neuroscience of Hebei Province, Hebei Medical University, Shijiazhuang, China,* [3]*Center on Aging Psychology, Key Laboratory of Mental Health, Institute of Psychology, Chinese Academy of Sciences, Beijing, China,* [4]*Department of Rehabilitation, First Hospital of Shijiazhuang, Shijiazhuang, China,* [5]*Department of Neurology, First Hospital of Hebei Medical University, Shijiazhuang, China*

Hyperlipidemia, one of the cardiovascular (CV) risk factors, is associated with an increase in the risk for dementia. Repetitive transcranial magnetic stimulation (rTMS) was applied over the right dorsolateral prefrontal cortex (DLPFC) to modulate serum lipid levels in older adults. Participants received 10 sessions of rTMS or sham stimulation intervention within 2 weeks. The serum lipid and thyroid hormone-related endocrine levels were assessed before and after the treatment. We found that rTMS significantly decreased serum lipid levels, including the total cholesterol (CHO) and triglyceride (TG); meanwhile, it also increased the thyroid-stimulating hormone (TSH) as well as thyroxine (T4) levels. This suggests that rTMS modulated the serum lipid metabolism by altering activity in the hypothalamo-pituitary-thyroid (HPT) axis. The trial was registered on the website of Chinese Clinical Trial Registry (http://www.chictr.org.cn).

Keywords: rTMS, older adults, cardiovascular disease, lipid metabolism, HPT axis

OPEN ACCESS

Edited by:
Athanasios Alexiou, Novel Global Community Educational Foundation (NGCEF), Hebersham, Australia

Reviewed by:
Giovanni Messina, University of Foggia, Italy
Marco Carotenuto, Università degli Studi della Campania "Luigi Vanvitelli" Caserta, Italy

***Correspondence:**
Zhijie Zhang
zhangzhj2002@sina.com
Mingwei Wang
mwei99@yahoo.com

†These authors have contributed equally to this work.

Received: *05 June 2017*
Accepted: *29 September 2017*
Published: *17 October 2017*

Citation:
Ren W, Ma J, Li J, Zhang Z and Wang M (2017) Repetitive Transcranial Magnetic Stimulation (rTMS) Modulates Lipid Metabolism in Aging Adults. Front. Aging Neurosci. 9:334. doi: 10.3389/fnagi.2017.00334

INTRODUCTION

Cardiovascular (CV) risk factors, such as hyperlipidemia, diabetes and hypertension, are associated with increased risk of dementia in older adults (Chuang et al., 2014). Longitudinal population-based studies have been used to assess the incidence of dementia in relation to CV diseases (CVD). Kloppenborg et al. (2008) reviewed the evidence for the association of CVD risk factors, including dyslipidemia, obesity, diabetes and hypertension with dementia. They found that these risk factors were indeed associated with an increased risk of dementia. Notably, for older adults, dyslipidemia appears to convey high risk of dementia.

Previous studies showed that cholesterol plays an important role in Alzheimer's disease (AD) as it forms the core of neuritic plaques that characterize AD (Puglielli et al., 2003). Moreover, it has been suggested that blood lipids are promising AD biomarkers. For example, epidemiological studies proposed that high total serum cholesterol in midlife is linked to sporadic AD in old age (Notkola et al., 1998). Lipid measures, such as high-density lipoproteins (HDL) and total cholesterol (Kivipelto et al., 2006; Reitz et al., 2010), are currently used as assessment tools to evaluate the risk of AD and dementia (Wang H. L. et al., 2016). This suggests that vascular risk factors, especially blood lipids, should be regarded as a major target for preventive measures later in life.

It has been suggested that non-invasive brain stimulation (NIBS) is a promising therapeutic tool for CVD (Cogiamanian et al., 2010; Makovac et al., 2017). In a series of meta-analyses, it was demonstrated that NIBS, especially repetitive transcranial magnetic stimulation (rTMS), was effective in reducing the heart rate (HR) and enhancing the HR variability (HRV; Makovac et al., 2017), which are the risk factors for CVD.

George et al. (1996) applied rTMS over the prefrontal cortex (PFC) and found that stimulation of PFC was associated with increases in serum thyroid-stimulating hormone (TSH). Furthermore, in a case study, Trojak et al. (2011) applied rTMS to a patient with depression and demonstrated that serum TSH remained increased during the whole rTMS period. This suggests that rTMS may influence the hypothalamo-pituitary-thyroid (HPT) axis. In cross-sectional studies, serum TSH levels in the upper part of the reference range have been associated with low levels of HDL cholesterol (Boekholdt et al., 2010; Ittermann et al., 2012, 2013). In an 11-year prospective population-based study, it was demonstrated that high TSH levels within the reference range might be associated with decreased serum lipids (Åsvold et al., 2013). In animal studies, it was found that rTMS applied to aged mice could reverse the metabolic abnormalities of cholesterol levels (Wang et al., 2013). It can be speculated, from the above studies, that rTMS might alter the serum lipid level by modulating the HPT axis.

In the present study, we aimed to directly examine the aforementioned hypothesis. Specifically, we investigated the effect of rTMS on the serum lipid level, with rTMS applied over the right PFC. The total cholesterol (CHO), triglyceride (TG), high density lipoprotein cholesterol (HDL-C) and low density lipoprotein cholesterol (LDL-C) were measured as indexes of lipid level. Additionally, TSH, as well as thyroxine (T4), and triiodothyronine (T3), were assessed before and after the treatment. It is expected that lipid levels would be decreased after the session of rTMS treatment, along with alterations of thyroid-related hormones.

MATERIALS AND METHODS

Participants

The participants met the following inclusion criteria: (1) age $\geq$60 years; (2) education $\geq$8 years; (3) a score of $\geq$21 on the Beijing Version of the Montreal cognitive assessment (MoCA; Yu et al., 2012); (4) right-handed; (5) a score of $\geq$2 on the Chinese memory symptoms scale (CMSS; Lam et al., 2005); (6) eligible for TMS procedures (Rossi et al., 2009). The exclusion criteria were: (1) history of neurological or psychiatric diseases; (2) history of brain damage; (3) history of thyroid disease; (4) dropout from the experiment because of bodily discomfort. All 30 elderly subjects, who were recruited and screened were randomly assigned into the rTMS group (n = 14) or the control (sham) group (n = 16) according to the random number table method.

This research is registered in the Chinese Clinical Trial Registry (ChiCTR-IOR-15006731). This study was carried out in accordance with the recommendations of the institutional review board of the Institute of Psychology, Chinese Academy of Sciences with written informed consent from all subjects. All subjects gave written informed consent in accordance with the Declaration of Helsinki. The protocol was approved by the review board of the First Hospital of Hebei Medical University, as well as the institutional review board of the Institute of Psychology, Chinese Academy of Sciences.

Procedure

Participants were randomly assigned into the rTMS or control group. Both groups participated in rTMS or sham stimulation protocol for 2 weeks, including five sessions every week. The baseline assessment occurred the day before the first stimulation session. The post-intervention assessment occurred 1 day after the final stimulation session. All participants had blood drawn at 8:00 am. Blood samples were collected to detect blood lipids and thyroid hormones. Participants were kept blind to the study hypothesis.

rTMS Protocol

The rTMS was applied with the MagPro X100 stimulator (MagVenture) and figure-of-eight coil (MFC-B65). The right dorsolateral PFC (DLPFC) was the target site, which was defined as the F4 region of the international 10-20 system for electroencephalography. The motor threshold was determined before the stimulation. It was defined as the minimum stimulator output value required to generate contraction of the abductor pollicis brevis for at least 5 of 10 consecutive pulses, and was measured via EMG by means of the Biopac MP100, using a contraction threshold of 50 mV (Moscatelli et al., 2016a,b,c). In each session, 10 Hz of rTMS was applied at 90% motor threshold to the stimulation location. In each stimulation block, rTMS pulses were present for 2 s and absent for 28 s; there were 40 blocks in total. Subjects in the sham stimulation group received the same stimulation protocol applied in the same manner, except that the coil was held at an angle of 90° (Kim et al., 2012).

Output Measures

Hematological Examination

All subjects fasted prior to having blood drawn at 8:00 am before receiving rTMS intervention and the day after the intervention. Blood was drawn using right elbow flexion, routine disinfection and at about 10 ml for each patient. The venous blood was extracted into the coagulation vacuum tube and left at about 25°C for 1 h. The serum was separated with 3000 rotations/min centrifugal force (LODZ-1.2, Beijing centrifuge factory) for 10 min and was kept in a −70°C refrigerator. Before the experiment, serum samples were removed from the refrigerator and were re-dissolved in a water-bath at 37°C water. After the second centrifugation, supernatant was used to measure the indexes. Throughout the whole process, the instrument maintained a good working state, and the quality was controlled in strict accordance with the reagent manual for testing.

Blood Lipids

CHO, TG, HDL-C and LDL-C were measured using the enzyme method. The reagents were sealed away from light, stored at 2–8°C, and could not be inverted.

Thyroid-Related Hormones

T3, T4 and TSH were measured using the electrochemical luminescence method (Roche company cobas e601 automatic immunoassay). The reagents we used were: roche reagents T3 detection kit, Roche reagent T4 detection kit, and Roche reagent thyrotropin detection kit. Reagents were stored at 2–8°C away from light and not inverted.

T3 measurement steps (competition law principle)

1. Take 30 μl of the specimen; mix it with anti-T3 antibody (ruthenium mark) and 8-Anilino-1-naphthalenesulfonic acid (ANS) following the instructions; the ANS release combined T3.
2. Add streptavidin-coated microparticles and biotinylated T3. Biotinylated T3 occupies the relevant binding site on the labeled antibody (still in a free state).
3. Add the mixture to the measurement cell (immune complex), and adsorb the particles to the electrode through the magnet. Form the electrochemical luminescence by adding voltage to the electrode. Use the photomultiplier to detect T3 content.

T4 measurement steps (competition law principle)

1. Take 15 μl of the specimen; mix it with anti-T4 antibody (ruthenium) and ANS following the instructions; the ANS release combined T4.
2. Add streptavidin-coated microparticles and biotinylated T4. Biotinylated T4 occupies the relevant binding site on the labeled antibody (still in a free state).
3. Add the mixture to the measurement cell (immune complex), and adsorb the particles to the electrode through the magnet. Form the electrochemical luminescence by adding voltage to the electrode. Use the photomultiplier to detect T4 content.

TSH assay procedure (double antibody sandwich principle)

1. Take 50 μl of the sample; mix the anti-TSH monoclonal antibody (biotinylated antibody) and anti-TSH monoclonal antibody (ruthenium).
2. Add streptavidin-coated particles to the microparticles, and combine the mixture in step 1 with the microparticles. This combination uses the reaction between biotin and streptavidin.
3. Add the mixture to the measurement cell (immune complex), and adsorb the particles to the electrode through the magnet. Form the electrochemical luminescence by adding voltage to the electrode. Use the photomultiplier to detect TSH content.

Data Analysis

The two-sample two-tailed Student's *t*-test was used to assess the baseline characteristics (age, years of education, scores of CMSS and MoCA) of participants in both groups, and the Chi-squared test was used to assess the gender difference between group. Paired sample *t*-test was used to examine the effect of rTMS/sham stimulation on the serum lipid metabolism activity, as well as on the endocrine activity related to the thyroid. All statistical analyses were conducted using SPSS 19.0 (IBM Corporation, Somers, NY, USA). The absolute effect size, Cohen's d (Cohen, 1988), were calculated to assess the effect of the rTMS intervention.

RESULTS

Demographic Characteristics

No significant differences at baseline were found between the two groups in age, gender, education, memory complaint and MoCA ($p > 0.05$), as shown in **Table 1**.

Effect of rTMS on Lipid Levels

The blood lipid levels between the two groups had no statistical difference at baseline ($p > 0.05$). As shown in **Table 2**, the CHO and TG levels were significantly lower after rTMS intervention ($p < 0.05$). Cohen's d for CHO was 0.54, and that for TG was 0.31. While in the sham group, no significant differences were found between baseline and post-treatment assessments ($p > 0.05$).

Effect of rTMS on Endocrine Activity Related to the Thyroid Gland

Serum thyroid hormone levels between the two groups had no statistical differences at baseline assessment ($p > 0.05$). As shown in **Table 3**, after rTMS intervention, the TSH and T4 levels were found to be significantly higher than those at baseline ($p < 0.05$). Cohen's d for T4 was 0.40, and that for TSH was 0.27. In the sham group, no significant differences were found between pre- and post-assessments ($p > 0.05$).

DISCUSSION

In this study, 10 Hz of rTMS was applied to healthy older adults with normal baseline lipid levels. After 10 sessions of stimulation, CHO and TG levels were significantly decreased, accompanied by increased TSH and T4, compared with the baseline condition, while no significant differences were found in the control group.

TABLE 1 | Characteristics of repetitive transcranial magnetic stimulation (rTMS) and sham groups.

Group	Age (years)	Gender		Education (years)	CMSS	MoCA
		M	F			
rTMS group (n = 14)	65.71 ± 5.08	3	11	12.21 ± 2.75	3.79 ± 1.81	28.07 ± 1.49
Sham group (n = 16)	66.62 ± 5.19	5	11	11.94 ± 3.04	4.25 ± 1.61	28 ± 2.07
p	>0.05[a]	>0.05[b]		>0.05[a]	>0.05[a]	>0.05[a]

Note: CMSS, the Chinese Memory Symptoms Scale; MoCA, the Beijing Version of the Montreal cognitive assessment. [a]The p value was obtained using a two-sample two-tailed t test. [b]The p value was obtained using a two-tailed Pearson chi-square test. Data are shown as mean ± SD.

TABLE 2 | Comparison of lipid levels (mmol/L) between rTMS and sham groups.

Group	Test	CHO	TG	HDL-C	LDL-C
rTMS (n = 14)	Pre	6.23 ± 1.82	1.94 ± 1.49	1.43 ± 0.80	3.68 ± 0.79
	Post	5.37 ± 1.33	1.54 ± 1.10	1.19 ± 0.40	3.15 ± 1.28
	t	2.682*	2.513*	1.552	1.636
Sham (n = 16)	Pre	5.26 ± 1.25	1.45 ± 1.06	1.17 ± 0.33	3.25 ± 0.89
	Post	5.76 ± 1.70	1.68 ± 1.03	1.3 ± 0.52	3.48 ± 0.97
	t	−1.704	−1.706	−1.273	−1.519

*Note: CHO, the total cholesterol; TG, triglyceride; HDL-C, high density lipoprotein cholesterol; LDL-C, low density lipoprotein cholesterol. *$p < 0.05$, two-tailed. Data are shown as mean ± SD.*

TABLE 3 | Comparison of thyroid hormone levels (nmol/L) between rTMS and sham groups.

Test	rTMS (n = 14)			Sham (n = 16)		
	T3	T4	TSH	T3	T4	TSH
Pre	1.65 ± 0.19	93.63 ± 14.24	3.45 ± 2.76	1.79 ± 0.25	102.53 ± 12.23	3.45 ± 2.35
Post	1.70 ± 0.25	99.14 ± 13.18	4.31 ± 3.56	1.75 ± 0.26	102.05 ± 10.55	3.32 ± 2.24
t	1.744	3.248**	2.379*	−0.428	−0.099	−0.181

*Note: T3, triiodothyronine; T4, thyroxine; TSH, the thyroid-stimulating hormone. *$p < 0.05$, **$p < 0.01$, two-tailed. Data are shown as mean ± SD.*

Our results indicate that rTMS may be effective for CVD risk factors. Previous studies confirmed the effect of rTMS on CV systems indexed by HR and HRV. In this study, we investigated the effect of rTMS on endocrine activity related to CVD risk factors and found that decreased serum lipid levels resulted from rTMS, suggesting rTMS influence on endocrine activity. In an animal study, Wang et al. (2013) explored the metabolic mechanism underlying the effects of rTMS. They observed that in mature mice, rTMS could reverse the metabolic abnormalities of cholesterol levels, to a degree similar to the young mice, showing that the rTMS could improve the metabolic profiles in PFC. Combining the present study with previous studies shows that rTMS could modulate the lipid metabolic activity associated with CVD.

The effect of rTMS on the serum lipid metabolic activity might result from its influence on the HPT axis. George et al. (1996) found that rTMS, applied over regions within the PFC, was associated with increases in serum TSH. Furthermore, Trojak et al. (2011) reported a significant increase in plasma TSH, above normal range, during low frequency rTMS (1 Hz) treatment. In addition, Osuch et al. (2009) demonstrated an increase in plasma T4 during treatment of anxiety disorders using low frequency rTMS. Thus, it can be inferred that rTMS may have significant effects on the pituitary-thyroid axis, which may potentially induce hyperthyroidism. Similar to previous studies, our study found significantly elevated TSH after rTMS, along with increased T4. Furthermore, in this study, we directly observed the alteration of serum lipid levels, suggesting that rTMS may influence the HPT axis and then affect the serum lipid levels.

Based on animal studies, we had confirmed that both normal aging (Wang et al., 2014) and pathological aging (Han et al., 2016; Wang J. et al., 2016; Shen et al., 2017) lead to metabolic abnormalities and that rTMS treatment could ameliorate metabolic abnormalities (Wang H. L. et al., 2016). For example, rTMS normalized prefrontal dysfunctions and cognitive-related metabolic profiling in aged mice (Wang H. L. et al., 2016). Besides, Lee et al. (2012) found that the effects of rTMS are related to changes in the brain lipids. In human studies, it also has been found that rTMS affects cortical metabolism (Bohning et al., 1999; Kimbrell et al., 2002). In the present study, we found that rTMS applied over the right DLPFC could alter the endocrine activity in normal aging adults. Combined evidence suggested that there is a pathway between the PFC and the hypothalamus, through which the PFC could modulate the endocrine activity.

As a non-invasive tool for the electrical stimulation of neural tissue (Barker et al., 1985), rTMS has the potential to modify excitability of the cerebral cortex at the stimulated site and at remote areas along functional anatomical connections (for a review, see Rossini et al., 2010). The PFC is linked to the thalamus (Alexander et al., 1986; Jones, 2007; Bolkan et al., 2017), and as a result, rTMS applied to the DLPFC might modulate the neural activity in the thalamus, which would then have an effect on the activity of the hypothalamus. The hypothalamus links the nervous system to the endocrine system, via the pituitary gland, in order to modulate the serum metabolic activity. It can be speculated that the PFC-thalamus pathway might play an important role in the present study to influence the HPT axis, and finally to modulate the serum metabolic activity of lipid levels.

Previous studies showed that CVD risk factors could be reduced with aerobic exercises. In a meta-analysis, Kodama et al. (2007) demonstrated that regular aerobic exercise could increase HDL-C level, which is associated with decreased risk of CVD (Maron, 2000). Alternative to physical exercise, in this study, the non-invasive rTMS is demonstrated as another promising tool for modulating CVD risk factors, specifically lipid levels, suggesting that rTMS is effective in minimizing CVD prevalence. Aerobic exercise may influence CV fitness, which results in changes to endocrine activity. While the effect of rTMS on endocrine activity might result from the altered excitability of the neuron, which may influence the signaling pathway of the HPT axis. This suggests that there is a pathway that underlies the transmission between electric signal and

chemical signal. Future research on this issue is of great importance.

CONCLUSION

rTMS of the PFC is associated with increases in the TSH and T4 levels and decreases in the serum CHO and TG levels. rTMS might alter the serum lipid levels by modulating the activity of the HPT axis. It is a promising tool for the modulation of lipid metabolism in older adults, and it reduces the risk for AD. In future studies, more indexes related to lipid metabolism and the activity of the HPT axis need to be assessed to clarify the effect of rTMS on the risk for CVD and to examine the direct relationship between lipid metabolism and the activity of the HPT axis following rTMS.

AUTHOR CONTRIBUTIONS

WR designed the work and drafted the manuscript. JM collected and analyzed the data. JL guided the research project. ZZ and MW revised the work and agreed to be accountable for all aspects of the work.

REFERENCES

Alexander, G. E., DeLong, M. R., and Strick, P. L. (1986). Parallel organization of functionally segregated circuits linking basal ganglia and cortex. *Annu. Rev. Neurosci.* 9, 357–381. doi: 10.1146/annurev.neuro.9.1.357

Åsvold, B. O., Bjøro, T., and Vatten, L. J. (2013). Associations of TSH levels within the reference range with future blood pressure and lipid concentrations: 11-year follow-up of the HUNT study. *Eur. J. Endocrinol.* 169, 73–82. doi: 10.1530/EJE-13-0087

Barker, A. T., Jalinous, R., and Freeston, I. L. (1985). Non-invasive magnetic stimulation of human motor cortex. *Lancet* 325, 1106–1107. doi: 10.1016/s0140-6736(85)92413-4

Boekholdt, S. M., Titan, S. M., Wiersinga, W. M., Chatterjee, K., Basart, D. C., Luben, R., et al. (2010). Initial thyroid status and cardiovascular risk factors: the EPIC-Norfolk prospective population study. *Clin. Endocrinol.* 72, 404–410. doi: 10.1111/j.1365-2265.2009.03640.x

Bohning, D., Shastri, A., McConnell, K., Nahas, Z., Lorberbaum, J., Roberts, D., et al. (1999). A combined TMS/fMRI study of intensity-dependent TMS over motor cortex. *Biol. Psychiatry* 45, 385–394. doi: 10.1016/s0006-3223(98)00368-0

Bolkan, S. S., Stujenske, J. M., Parnaudeau, S., Spellman, T. J., Rauffenbart, C., Abbas, A. I., et al. (2017). Thalamic projections sustain prefrontal activity during working memory maintenance. *Nat. Neurosci.* 20, 987–996. doi: 10.1038/nn.4568

Chuang, Y. F., Eldreth, D., Erickson, K. I., Varma, V., Harris, G., Fried, L. P., et al. (2014). Cardiovascular risks and brain function: a functional magnetic resonance imaging study of executive function in older adults. *Neurobiol. Aging* 35, 1396–1403. doi: 10.1016/j.neurobiolaging.2013.12.008

Cogiamanian, F., Brunoni, A. R., Boggio, P. S., Fregni, F., Ciocca, M., and Priori, A. (2010). Non-invasive brain stimulation for the management of arterial hypertension. *Med. Hypotheses* 74, 332–336. doi: 10.1016/j.mehy.2009.08.037

Cohen, J. (1988). *Statistical Power Analysis for the Behavioral Sciences.* 2nd Edn. Hillsdale, NJ: Lawrence Earlbam Associates.

George, M. S., Wassermann, E. M., Williams, W. A., Steppel, J., Pascual-Leone, A., Basser, P., et al. (1996). Changes in mood and hormone levels after rapid-rate transcranial magnetic stimulation (rTMS) of the prefrontal cortex. *J. Neuropsychiatry Clin. Neurosci.* 8, 172–180. doi: 10.1176/jnp.8.2.172

Han, B., Yu, L., Geng, Y., Shen, L., Wang, H., Wang, Y., et al. (2016). Chronic stress aggravates cognitive impairment and suppresses insulin associated signaling pathway in APP/PS1 mice. *J. Alzheimers Dis.* 53, 1539–1552. doi: 10.3233/JAD-160189

Ittermann, T., Thamm, M., Wallaschofski, H., Rettig, R., and Völzke, H. (2012). Serum thyroid-stimulating hormone levels are associated with blood pressure in children and adolescents. *J. Clin. Endocrinol. Metab.* 97, 828–834. doi: 10.1210/jc.2011-2768

Ittermann, T., Tiller, D., Meisinger, C., Agger, C., Nauck, M., Rettig, R., et al. (2013). High serum thyrotropin levels are associated with current but not with incident hypertension. *Thyroid* 23, 955–963. doi: 10.1089/thy.2012.0626

Jones, E. G. (2007). *The Thalamus.* 2nd Edn. Cambridge, MA: Cambridge University Press.

Kim, S. H., Han, H. J., Ahn, H. M., Kim, S. A., and Kim, S. E. (2012). Effects of five daily high-frequency rTMS on Stroop task performance in aging individuals. *Neurosci. Res.* 74, 256–260. doi: 10.1016/j.neures.2012.08.008

Kimbrell, T. A., Dunn, R. T., George, M. S., Danielson, A. L., Willis, M. W., Repella, J. D., et al. (2002). Left prefrontal-repetitive transcranial magnetic stimulation (rTMS) and regional cerebral glucose metabolism in normal volunteers. *Psychiatry Res.* 115, 101–113. doi: 10.1016/s0925-4927(02)00041-0

Kivipelto, M., Ngandu, T., Laatikainen, T., Winblad, B., Soininen, H., and Tuomilehto, J. (2006). Risk score for the prediction of dementia risk in 20 years among middle aged people: a longitudinal, population-based study. *Lancet Neurol.* 5, 735–741. doi: 10.1016/s1474-4422(06)70537-3

Kloppenborg, R. P., van den Berg, E., Kappelle, L. J., and Biessels, G. J. (2008). Diabetes and other vascular risk factors for dementia: which factor matters most? A systematic review. *Eur. J. Pharmacol.* 585, 97–108. doi: 10.1016/j.ejphar.2008.02.049

Kodama, S., Tanaka, S., Saito, K., Shu, M., Sone, Y., Onitake, F., et al. (2007). Effect of aerobic exercise training on serum levels of high-density lipoprotein cholesterol: a meta-analysis. *Arch. Int. Med.* 167, 999–1008. doi: 10.1001/archinte.167.10.999

Lam, L. C. W., Lui, V. W. C., Tam, C. W. C., and Chiu, H. F. K. (2005). Subjective memory complaints in Chinese subjects with mild cognitive impairment and early Alzheimer's disease. *Int. J. Geriatr. Psychiatry* 20, 876–882. doi: 10.1002/gps.1370

Lee, L. H. W., Tan, C. H., Lo, Y. L., Farooqui, A. A., Shui, G., Wenk, M. R., et al. (2012). Brain lipid changes after repetitive transcranial magnetic stimulation: potential links to therapeutic effects? *Metabolomics* 8, 19–33. doi: 10.1007/s11306-011-0285-4

Makovac, E., Thayer, J. F., and Ottaviani, C. (2017). A meta-analysis of non-invasive brain stimulation and autonomic functioning: implications for brain-heart pathways to cardiovascular disease. *Neurosci. Biobehav. Rev.* 74, 330–341. doi: 10.1016/j.neubiorev.2016.05.001

Maron, D. J. (2000). The epidemiology of low levels of high-density lipoprotein cholesterol in patients with and without coronary artery disease. *Am. J. Cardiol.* 86, 11L–14L. doi: 10.1016/s0002-9149(00)01462-4

Moscatelli, F., Messina, G., Valenzano, A., Monda, V., Viggiano, A., Messina, A., et al. (2016a). Functional assessment of corticospinal system excitability in karate athletes. *PLoS One* 11:e0155998. doi: 10.1371/journal.pone.0155998

Moscatelli, F., Messina, G., Valenzano, A., Petito, A., Triggiani, A. I., Messina, A., et al. (2016b). Differences in corticospinal system activity and reaction response between karate athletes and non-athletes. *Neurol. Sci.* 37, 1947–1953. doi: 10.1007/s10072-016-2693-8

Moscatelli, F., Valenzano, A., Petito, A., Triggiani, A. I., Ciliberti, M. A. P., Luongo, L., et al. (2016c). Relationship between blood lactate and cortical excitability between taekwondo athletes and non-athletes after hand-grip exercise. *Somatosensory Mot. Res.* 33, 137–144. doi: 10.1080/08990220.2016.1203305

Notkola, I. L., Sulkava, R., Pekkanen, J., Erkinjuntti, T., Ehnholm, C., Kivinen, P., et al. (1998). Serum total cholesterol, apolipoprotein E {FC12}e4 allele, and Alzheimer's disease. *Neuroepidemiology* 17, 14–20. doi: 10.1159/000026149

Osuch, E. A., Benson, B. E., Luckenbaugh, D. A., Geraci, M., Post, R. M., and McCann, U. (2009). Repetitive TMS combined with exposure therapy for

PTSD: a preliminary study. *J. Anxiety Disord.* 23, 54–59. doi: 10.1016/j.janxdis.2008.03.015

Puglielli, L., Tanzi, R. E., and Kovacs, D. M. (2003). Alzheimer's disease: the cholesterol connection. *Nat. Neurosci.* 6, 345–351. doi: 10.1038/nn0403-345

Reitz, C., Tang, M., Schupf, N., Manly, J. J., Mayeux, R., and Luchsinger, J. A. (2010). A summary risk score for the prediction of alzheimer disease in elderly persons. *Arch. Neurol.* 67, 835–841. doi: 10.1001/archneurol.2010.136

Rossi, S., Hallett, M., Rossini, P. M., and Pascual-Leone, A. (2009). Safety, ethical considerations, and application guidelines for the use of transcranial magnetic stimulation in clinical practice and research. *Clin. Neurophysiol.* 120, 2008–2039. doi: 10.1016/j.clinph.2009.08.016

Rossini, P. M., Rossini, L., and Ferreri, F. (2010). Brain-behavior relations: transcranial magnetic stimulation: a review. *IEEE Eng. Med. Biol. Mag.* 29, 84–96. doi: 10.1109/MEMB.2009.935474

Shen, L., Han, B., Geng, Y., Wang, J., Wang, Z., and Wang, M. (2017). Amelioration of cognitive impairments in APPswe/PS1dE9 mice is associated with metabolites alteration induced by total salvianolic acid. *PLoS One* 12:e0174763. doi: 10.1371/journal.pone.0174763

Trojak, B., Chauvet-Gelinier, J.-C., Vergès, B., and Bonin, B. (2011). Significant increase in plasma thyroid-stimulating hormone during low-frequency repetitive transcranial magnetic stimulation. *J. Neuropsychiatry Clin. Neurosci.* 23:E12. doi: 10.1176/appi.neuropsych.23.1.e12

Wang, H., Geng, Y., Han, B., Qiang, J., Li, X., Sun, M., et al. (2013). Repetitive transcranial magnetic stimulation applications normalized prefrontal dysfunctions and cognitive-related metabolic profiling in aged mice. *PLoS One* 8:e81482. doi: 10.1371/journal.pone.0081482

Wang, H., Lian, K., Han, B., Wang, Y., Kuo, S. H., Geng, Y., et al. (2014). Age-related alterations in the metabolic profile in the hippocampus of the senescence-accelerated mouse prone 8: a spontaneous Alzheimer's disease mouse model. *J. Alzheimers Dis.* 39, 841–848. doi: 10.3233/JAD-131463

Wang, H. L., Wang, Y. Y., Liu, X. G., Kuo, S. H., Liu, N., Song, Q. Y., et al. (2016). Cholesterol, 24-hydroxycholesterol, and 27-hydroxycholesterol as surrogate biomarkers in cerebrospinal fluid in mild cognitive impairment and Alzheimer's disease: a meta-analysis. *J. Alzheimers Dis.* 51, 45–55. doi: 10.3233/JAD-150734

Wang, J., Yuan, J., Pang, J., Ma, J., Han, B., Geng, Y., et al. (2016). Effects of chronic stress on cognition in male SAMP8 mice. *Cell. Physiol. Biochem.* 39, 1078–1086. doi: 10.1159/000447816

Yu, J., Li, J., and Huang, X. (2012). The Beijing version of the montreal cognitive assessment as a brief screening tool for mild cognitive impairment: a community-based study. *BMC Psychiatry* 12:156. doi: 10.1186/1471-244X-12-156

Conflict of Interest Statement: The authors declare that the research was conducted in the absence of any commercial or financial relationships that could be construed as a potential conflict of interest.

Copyright © 2017 Ren, Ma, Li, Zhang and Wang. This is an open-access article distributed under the terms of the Creative Commons Attribution License (CC BY). The use, distribution or reproduction in other forums is permitted, provided the original author(s) or licensor are credited and that the original publication in this journal is cited, in accordance with accepted academic practice. No use, distribution or reproduction is permitted which does not comply with these terms.

frontiers in Aging Neuroscience

ORIGINAL RESEARCH
published: 01 September 2017
doi: 10.3389/fnagi.2017.00288

Divergent Roles of Vascular Burden and Neurodegeneration in the Cognitive Decline of Geriatric Depression Patients and Mild Cognitive Impairment Patients

*Qing Ye, Fan Su, Liang Gong, Hao Shu, Wenxiang Liao, Chunming Xie, Hong Zhou, Zhijun Zhang and Feng Bai**

Department of Neurology, Affiliated ZhongDa Hospital, School of Medicine, Southeast University, Nanjing, China

Both geriatric depression and mild cognitive impairment (MCI) confer an increased risk for the development of dementia. The mechanisms underlying the development of cognitive impairment in geriatric depression patients remain controversial. The present study aimed to explore the association of cognitive decline with vascular risk, white matter hyperintensity (WMH) burden and hippocampal volume in both remitted geriatric depression (RGD) subjects and amnestic mild cognitive impairment (aMCI) subjects. Forty-one RGD subjects, 51 aMCI subjects, and 64 healthy elderly subjects underwent multimodal MRI scans and neuropsychological tests at both baseline and a 35-month follow-up. According to the changing patterns (declining or stable) of global cognitive function during the follow-up period, each group was further divided into a declining subgroup and a stable subgroup. The Framingham 10-year cardiovascular risk, WMH volume and hippocampal volume were measured to assess vascular pathology and neurodegeneration, respectively. The RGD declining group displayed a higher vascular risk and greater WMH volume than the RGD stable group, whereas no such difference was found in the aMCI subjects. In contrast, the aMCI declining group displayed a smaller left hippocampal volume than the aMCI stable group, whereas no such difference was found in the RGD subjects. Furthermore, greater increases in the WHM volume correlated with greater decreases in global cognitive function in the RGD declining group, and greater decreases in the left hippocampal volume correlated with greater decreases in global cognitive function in the aMCI declining group. In conclusion, the cognitive decline in RGD patients is associated with vascular burden, whereas the cognitive decline in aMCI patients is associated with neurodegeneration. These findings could contribute to a better understanding of the specific mechanisms of the development of dementia in each condition.

Keywords: cognitive decline, geriatric depression, hippocampal volume, mild cognitive impairment, vascular risk, white matter hyperintensity

OPEN ACCESS

Edited by:
Mohammad Amjad Kamal, King Abdulaziz University, Saudi Arabia

Reviewed by:
Christos Frantzidis, Aristotle University of Thessaloniki, Greece
Panteleimon Giannakopoulos, Université de Genève, Switzerland

***Correspondence:**
Feng Bai
baifeng515@126.com

Received: *20 June 2017*
Accepted: *17 August 2017*
Published: *01 September 2017*

Citation:
Ye Q, Su F, Gong L, Shu H, Liao W, Xie C, Zhou H, Zhang Z and Bai F (2017) Divergent Roles of Vascular Burden and Neurodegeneration in the Cognitive Decline of Geriatric Depression Patients and Mild Cognitive Impairment Patients. Front. Aging Neurosci. 9:288. doi: 10.3389/fnagi.2017.00288

INTRODUCTION

Geriatric depression refers to a major depressive episode that develops in adults older than 60 years and is frequently accompanied by general impairments in physical health, global functioning, and quality of life. Geriatric depression often presents with cognitive deficits and confers an up to 50% increased risk for the development of dementia (Ownby et al., 2006; Diniz et al., 2013). Mild cognitive impairment (MCI) has been considered as a transitional state between normal aging and early Alzheimer's disease (AD), which is the most common form of dementia characterized by progressive cognitive impairment and behavioral deficits. MCI confers a high conversion rate to AD of 10–15% per year (Petersen et al., 1999). Interestingly, 11–63% of elderly MCI patients exhibit accompanying depressive symptoms, and 18–55% of depressed patients develop cognitive deficits (Panza et al., 2010). The co-existence of MCI and depression confers over twice the risk for AD as MCI alone (Modrego and Ferrandez, 2004). In view of the distinct clinical link between geriatric depression and MCI, increasing attention has been paid to the convergence and divergence of the pathogeneses of geriatric depression and MCI.

While the amyloid beta (Aβ) pathology and subsequent neurodegeneration due to tau pathology play a major role in MCI and AD pathogenesis (Albert et al., 2011), a controversy has arisen over the mechanisms underlying the cognitive impairment in geriatric depression patients. Several studies have found that the cognitive impairment in geriatric depression patients is associated with the AD-related pathology, including Aβ deposition and hippocampal atrophy (O'Brien et al., 2004; Hou et al., 2012; Byun et al., 2016). Other findings suggest that the cognitive impairment in geriatric depression patients is due to vascular pathology that is frequently represented by the white matter hyperintensity (WMH) burden in the brain (Hickie et al., 1997; Murata et al., 2001). However, these studies only explored single biomarkers in isolation and lacked an overall view of AD-related pathology and vascular pathology. Interestingly, two recent studies measured both AD-related pathology and vascular burden in geriatric depression patients with and without MCI (Diniz et al., 2015; Byun et al., 2016). However, one study found that geriatric depression subjects with MCI display greater WMH burden than geriatric depression subjects with normal cognition, suggesting that vascular pathology is related to the cognitive impairment in geriatric depression subjects (Diniz et al., 2015). The other study demonstrated that AD processes contribute to the co-existence of geriatric depression and MCI (Byun et al., 2016). Both of these studies employed cross-sectional data. A great deal of studies have revealed that cognitive impairment is improved following the remission of depressive symptoms in a significant proportion of geriatric depression patients but not in all patients (Barch et al., 2012). Thus, measuring cognitive impairment in geriatric depression patients using cross-sectional data may have increased the heterogeneity and contributed to the divergence. However, few studies have explored and compared the relationships of cognitive impairment, AD-related pathology, and vascular pathology in both geriatric depression subjects and MCI subjects despite the close link between geriatric depression and MCI. The investigation of the convergence and divergence between the two conditions could deepen the understanding of the mechanisms underlying the development of dementia in each condition.

The present 35-month longitudinal study recruited remitted geriatric depression (RGD) subjects, amnestic mild cognitive impairment (aMCI, a subtype of MCI characterized by episodic memory deficits) subjects and healthy elderly subjects. Neuropsychological tests and multimodal MRI scans were performed at both baseline and a 35-month follow-up. According to the changing patterns (declining or stable) of global cognitive function during the follow-up period, the subjects were further divided into an RGD declining group, an RGD stable group, an aMCI declining group, an aMCI stable group, a control declining group, and a control stable group. Vascular risk, WMH volume, and hippocampal volume were explored to assess vascular pathology and neurodegeneration, respectively. The present study aimed to (i) explore and compare the associations of cognitive decline with vascular risk, WMH burden and hippocampal volume in RGD subjects and aMCI subjects and (ii) determine the behavioral significance of WMH burden and hippocampal atrophy.

MATERIALS AND METHODS

Participants

As described in our previous study (Ye et al., 2017), 72 RGD patients, 87 aMCI patients, and 135 healthy elderly controls were recruited at the Affiliated ZhongDa Hospital, Southeast University. This study was performed in accordance with the recommendations of the Affiliated ZhongDa Hospital of Southeast University Research Ethics Committee with written informed consent from all subjects. All subjects provided written informed consent in accordance with the Declaration of Helsinki. The protocol was approved by the Affiliated ZhongDa Hospital of Southeast University Research Ethics Committee. The participants were followed up for 35 months on average. A total of 41 RGD subjects, 51 aMCI subjects, and 64 controls were included in the present study. All of these subjects underwent multimodal MRI scans and neuropsychological tests at both baseline and follow-up. The reasons for the loss to follow-up of the other subjects included the development of neurological or other psychiatric diseases, relocation to other cities, death, and subjective unwillingness. According to the changing patterns (declining or stable) of global cognitive function during the follow-up period, the included subjects were further divided into the following six groups: RGD declining group ($n = 18$), RGD stable group ($n = 23$), aMCI declining group ($n = 33$), aMCI stable group ($n = 18$), control declining group ($n = 21$), and control stable group ($n = 43$).

Neuropsychological Assessments

Each subject underwent a standardized diagnostic evaluation that included demographic information, medical history, and examinations of the neurological and mental statuses. Global cognitive function was assessed with the Mini Mental State Examination (MMSE), a Clinical Dementia Rating (CDR) and

a Mattis Dementia Rating Scale-2 (MDRS-2). The MDRS-2 is a reliable and valid psychometric instrument for detecting and staging dementia (Vitaliano et al., 1984; Smith et al., 1994; Green et al., 1995; Monsch et al., 1995). The MDRS is also effective for tracking cognitive decline over time (Salmon et al., 1990; Galasko et al., 2000; Gould et al., 2001). Subjects with an MDRS-2 score below 130 or a loss of more than five points during the follow-up period were defined as the "declining group" (Schmidt et al., 1994; Tard et al., 2015). Other subjects were defined as the "stable group." The mental statuses were assessed with the *Structured Clinical Interview for Diagnostic and Statistical Manual of Mental Disorders*, Fourth Edition (DSM-IV) Axis I Disorders (SCID-I), the Hamilton Depression Scale (HAMD), and the Self-Rating Depression Scale. All subjects underwent a neuropsychological battery test that included the Auditory-Verbal Learning Test-Delayed Recall (AVLT-DR), Rey-Osterrieth Complex Figure Test (CFT) with its 20-min Delayed Recall (CFT-DR), Trail Making Tests (TMT)-A and B, Stroop Color and Word Tests A, B, and C (Stroop A, B, and C), Verbal Fluency Test (VFT), Digital Span Test (DST), Semantic Similarity Test (Similarity), Digital Symbol Substitution Test (DSST), and Clock Drawing Test (CDT).

Inclusion and Exclusion Criteria

The inclusion and exclusion assessments were performed by two experienced neuropsychiatric physicians who administered a structured interview to subjects and their informants. The inclusion criteria for RGD subjects were as follows: (1) the age was >60 years; (2) all subjects had previously met the DSM-IV criteria for major depression disorder and had remitted for >6 months before enrollment; (3) the duration of illness was <5 years and the period of remaining anti-depressant medication-free was >3 months before the assessment; and (4) the HAMD scores were <7 and MMSE scores were >24. The exclusion criteria were as follows: (1) primary neurological illness, including stroke or dementia; (2) another major psychiatric illness, including substance abuse or dependence; (3) history of electroconvulsive therapy; and (4) a medical illness that impaired cognitive function.

aMCI subjects were included according to the diagnostic criteria proposed by Petersen (2004) and others (Winblad et al., 2004), which was also described in our prior study (Ye et al., 2016). The inclusion criteria for the aMCI subjects were as follows: (1) subjective memory impairment corroborated by the subject and an informant; (2) objective memory performances documented by an AVLT-DR score ≤1.5 standard deviations from the age-adjusted and education-adjusted norms (the cutoff was ≤4 correct responses on 12 items for ≥8 years of education); (3) normal general cognitive function evaluated by an MMSE score ≥24; (4) a CDR of 0.5, with at least a 0.5 in the memory domain; (5) minimal or no impairment of routine daily life activities; and (6) the absence of dementia or insufficiency in meeting the National Institute of Neurological and Communicative Disorders and Stroke and the AD and Related Disorders Association (NINCDS-ADRDA) and DSM-IV criteria for AD. The exclusion criteria were as follows: (1) a history of stroke (modified Hachinski score of >4), head injury, alcoholism, epilepsy, Parkinson's disease, major depression (excluded by a self-rating depression scale), or other psychiatric or neurological illness (excluded by case history and clinical assessment); (2) major medical illness (e.g., anemia, cancer, or thyroid dysfunction); (3) severe visual or hearing loss; and (4) T2-weighted MRI showing major infarction or other lesions (two experienced radiologists executed the scans).

Control subjects were required to have a CDR of 0, an MMSE score ≥26, and a delayed recall score >4 for those with ≥8 years of education. These participants also met the aforementioned exclusion criteria for aMCI.

Apolipoprotein E (*ApoE*) Genotyping

To control for possible differences in hippocampal volume related to the *ApoE* ε4 allele (*ApoE* ε4), the most important genetic risk factor for sporadic AD, the status of *ApoE* ε4 was also assessed. Genomic DNA was extracted from 250 μL of EDTA-anticoagulated blood collected from each subject using a DNA direct kit (Tiangen, China). A polymerase chain reaction-based restriction fragment length polymorphism (PCR-RFLP) assay was employed to detect the rs7412 and rs429358 alleles, the haplotypes of which ultimately determine the *ApoE* genotype.

Framingham 10-Year Cardiovascular Risk

The Framingham 10-year risk for developing general cardiovascular disease (including myocardial infarction, coronary death, heart failure, angina, stroke, transient ischemic attack, and peripheral artery disease) was calculated using gender, age, systolic blood pressure, treatment for hypertension, smoking, diabetes, and body mass index (D'Agostino et al., 2008). The Framingham 10-year cardiovascular risk was assessed for each subject at baseline.

Magnetic Resonance Imaging Procedures

The subjects were scanned using a Siemens Verio 3.0-T scanner (Siemens, Erlangen, Germany) with a 12-channel head coil at the Affiliated ZhongDa Hospital of Southeast University. A belt and foam pads were used to immobilize their heads to minimize head motion. High-resolution T1-weighted axial images covering the whole brain were obtained by a 3D-magnetization prepared rapid gradient-echo sequence: repetition time (TR) = 1,900 ms; echo time (TE) = 2.48 ms; flip angle (FA) = 9°; acquisition matrix = 256 × 256; field of view (FOV) = 250 × 250 mm; thickness = 1.0 mm; gap = 0 mm, number of slices = 176. The T2 FLAIR axial images were obtained with the following parameters: TR = 8,000 ms; TE = 94 ms; FA = 150°; acquisition matrix = 256 × 162; thickness = 5.0 mm; gap = 0 mm, number of slices = 20.

WMH Segmentation and Quantification

Lesions were segmented by the lesion growth algorithm (Schmidt et al., 2012) as implemented in the LST toolbox version 2.0.15 (www.statistical-modelling.de/lst.html) for Statistical Parametric Mapping software (SPM12, http://www.fil.ion.ucl.ac.uk/spm). The algorithm first segments the T1 images into the three main tissue classes (cerebrospinal fluid, gray matter, and white matter). This information is then combined with the coregistered T2 FLAIR intensities to calculate lesion belief maps. By thresholding these maps with a pre-chosen initial threshold (κ = 0.30) an initial binary lesion map is obtained and is subsequently grown along voxels that appear hyperintense on the T2 FLAIR image.

The result is a lesion probability map. It should be noted that the κ-value was determined by the visual inspection of the results by three experienced raters.

Hippocampal Volume Assessment

As described in our previous study (Bai et al., 2009), hippocampal volume analysis was performed using the VBM8 toolbox for SPM12. First, the T1 images were normalized to the Montreal Neurological Institute (MNI) template using an affine and non-linear spatial normalization and re-sampled to a voxel size of 1.5 × 1.5 × 1.5 mm. Second, the normalized images were segmented into cerebrospinal fluid, gray matter, and white matter segments according to MNI prior probability maps. Then, Jacobian modulation was applied to the segmented gray matter image, which could be incorporated to compensate for the effect of spatial normalization. Finally, the extracted gray matter set was smoothed with an 8-mm full width at half maximum Gaussian filter to reduce the effects of individual variation in gyral anatomy and to increase the signal-to-noise ratio. The hippocampus (left and right separately) was isolated using automated anatomical labeling implemented through the Resting State fMRI Data Analysis Toolkit 1.7 software (http://restfmri.net/forum/index.php). Next, the hippocampal regions were interpolated to the same dimension, sizes, and origins with individual images. Finally, a mean volume index of all of the voxels of the hippocampal region (left and right) was computed for each subject. The hippocampal volume was obtained by multiplying the mean volume index by the number of voxels and the size of each voxel (1.5 × 1.5 × 1.5 mm).

Statistical Analysis

Demographic and Neuropsychological Data

Mixed analysis of variance (ANOVA; with disease, cognitive change and time as fixed factors) and χ^2-tests (applied for the comparisons of gender and *ApoE* ε4 status) were used to analyse the demographic data and neuropsychological data for statistically significant differences ($P < 0.05$). The individual raw scores of each cognitive test (except the MMSE and MDRS-2) were transformed into Z scores according to the following equation: $Z_i = \frac{r_i - m}{S}$. Z_i indicates the Z scores for the ith subject, r_i indicates the raw score for the ith subject, m indicates the average score for each test for each group, and S indicates the standard deviation of the test scores for each group. The neuropsychological tests were grouped into four cognitive domains, including episodic memory, executive function, visuospatial function, and information processing speed. The composite Z score for each cognitive domain was obtained by averaging the Z scores of the relevant neuropsychological tests according to the following divisions: episodic memory (two tests, including the AVLT-DR and CFT-DR), executive function (five tests, including the TMT-B, Stroop C, VFT, DST-backward, and Similarity tests), visuospatial function (two tests, including the CFT and CDT), and information processing speed (four tests, including the DSST, TMT-A, Stroop A, and Stroop B). All statistical procedures were performed with the SPSS 19.0 software (SPSS, Inc., Chicago, IL, USA).

Vascular Risk, WMH Volume, and Hippocampal Volume Data

To improve the normal distribution of the Framingham 10-year cardiovascular risk data, a $\log_{10}$-transformation was applied to the raw data. Mixed ANOVA (with disease and cognitive change as fixed factors) was used to analyse the Framingham 10-year cardiovascular risk. Mixed analysis of covariance (ANCOVA; with disease, cognitive change, and time as fixed factors) was used to analyse the WMH volume and hippocampal volume, controlling for age, gender, and years of education. *ApoE* status was also treated as a covariate in the analysis of hippocampal volume. *Post-hoc* tests were performed to explore group differences in the ANOVA or ANCOVA. All statistical procedures utilized SPSS 19.0 software (SPSS, Inc., Chicago, IL, USA) with significance set at $P < 0.05$.

Correlative Analysis between Cognitive Impairment and WMH Volume or Hippocampal Volume

Correlation analyses were performed between the longitudinal changes of global cognitive function (MMSE and MDRS-2) and the longitudinal changes of WMH volume and hippocampal volume in RGD declining group and aMCI declining group. All statistical procedures for correlation analysis utilized SPSS 19.0 software (SPSS, Inc., Chicago, IL, USA) with significance of $P < 0.05$.

RESULTS

Demographic and Neuropsychological Data

As shown in **Table 1**, no significant differences in age or years of education were noted between the six groups. There were more females in the RGD stable group. A greater percentage of *ApoE* ε4 carriers were shown in the aMCI declining group. Significant main effects of disease were found on all cognitive tests. Compared with the control subjects, both the RGD subjects and aMCI subjects displayed poorer performances in all cognitive tests with the exception of the information processing speed for the RGD subjects. Significant main effects of cognitive change were found on the MDRS-2 scores and episodic memory scores. Subjects with declining cognitive function displayed poorer performances in these two tests than the subjects with stable cognitive function. Furthermore, a main effect of time revealed longitudinal decreases in the MDRS-2 scores and executive function scores in the whole sample during the follow-up period. Finally, there was no significant interaction of disease, cognitive change and time on the neuropsychological data (data on the interactions of any two factors are not shown).

Framingham 10-year Cardiovascular Risk

As presented in **Table 2**, a significant interaction of disease and cognitive change was found in the Framingham 10-year cardiovascular risk. *Post-hoc* tests revealed that the RGD declining group displayed a higher risk than the RGD stable group, whereas no such difference was found within the control subjects or aMCI subjects (**Figure 1A**).

TABLE 1 | Demographic and neuropsychological data.

Items	Control		RGD		aMCI		*P*-value			
	Declining ($n = 21$)	Stable ($n = 43$)	Declining ($n = 18$)	Stable ($n = 23$)	Declining ($n = 33$)	Stable ($n = 18$)	Disease	Cognitive change	Time	Disease × cognitive change × time or χ^2
Age (years)	70.14 ± 6.92	69.35 ± 5.27	68.33 ± 5.97	67.13 ± 6.21	69.06 ± 7.57	67.67 ± 5.66	0.271	0.289	–	–
Education (years)	12.07 ± 3.16	13.17 ± 2.87	10.86 ± 3.03	11.35 ± 2.94	12.17 ± 3.57	11.97 ± 3.47	0.069	0.385	–	–
Gender (male: female)	10 : 11	19 : 24	8 : 10	4 : 19	23 : 10	10 : 8	–	–	–	0.008*
ApoE status (ε4 +: −)	4 : 17	6 : 37	1 : 17	2 : 21	13 : 20	5 : 13	–	–	–	0.019*
MMSE										
Baseline	28.29 ± 1.15	28.26 ± 1.45	27.56 ± 1.89	27.52 ± 1.73	26.82 ± 2.44	27.17 ± 1.69	< 0.001*a,b	0.057	0.167	0.129
Follow-up	27.95 ± 1.56	28.19 ± 1.56	26.67 ± 2.28	27.30 ± 1.58	25.36 ± 3.83	28.00 ± 1.20				
MDRS-2										
Baseline	139.10 ± 2.26	137.44 ± 3.80	134.11 ± 5.39	136.35 ± 3.26	133.03 ± 6.56	133.28 ± 5.96	< 0.001*a,b,c	< 0.001*	< 0.001*	0.074
Follow-up	131.52 ± 3.47	137.58 ± 3.73	129.28 ± 4.51	135.55 ± 2.42	124.16 ± 10.38	135.13 ± 2.64				
EPISODIC MEMORY										
Baseline	0.63 ± 0.44	0.46 ± 0.55	−0.33 ± 0.72	0.10 ± 0.64	−0.81 ± 0.57	−0.34 ± 0.62	< 0.001*a,b,c	0.004*	0.913	0.718
Follow-up	0.46 ± 0.46	0.50 ± 0.65	−0.30 ± 0.70	0.07 ± 0.75	−0.77 ± 0.75	−0.32 ± 0.82				
EXECUTIVE FUNCTION										
Baseline	0.31 ± 0.57	0.41 ± 0.61	−0.06 ± 0.57	0.13 ± 0.47	−0.31 ± 0.56	−0.20 ± 0.64	< 0.001*a,b,c	0.158	0.020*	0.167
Follow-up	0.14 ± 0.59	0.17 ± 0.63	−0.13 ± 0.66	−0.05 ± 0.56	−0.64 ± 0.63	−0.14 ± 0.57				
VISUOSPATIAL FUNCTION										
Baseline	0.37 ± 0.59	0.26 ± 0.71	−0.26 ± 0.81	−0.15 ± 0.76	−0.31 ± 0.93	−0.18 ± 0.82	0.001*a,b	0.336	0.563	0.570
Follow-up	0.27 ± 0.95	0.16 ± 0.90	−0.15 ± 0.84	−0.07 ± 1.07	−0.33 ± 1.38	0.19 ± 0.52				
INFORMATION PROCESSING SPEED										
Baseline	0.35 ± 0.71	0.27 ± 0.85	0.12 ± 0.75	0.32 ± 0.76	−0.46 ± 0.64	−0.24 ± 0.62	0.001*b,c	0.900	0.089	0.964
Follow-up	0.12 ± 0.64	0.12 ± 0.88	0.05 ± 0.80	0.30 ± 0.86	−0.67 ± 0.71	−0.35 ± 0.64				

Values are presented as the means ± the standard deviations (SD). ANOVAs (with disease, cognitive change, and time as fixed factors) were applied in the comparisons of age, years of education, and neuropsychological data. χ^2-tests were applied in the comparisons of gender and ApoE status.

**$P < 0.05$. [a]$P < 0.05$, RGD subjects differ from control subjects; [b]$P < 0.05$, aMCI subjects differ from control subjects; [c]$P < 0.05$, RGD subjects differ from aMCI subjects.*

Apolipoprotein E, ApoE; ANOVA, analysis of variance; MDRS-2, Mattis Dementia Rating Scale-2.

TABLE 2 | Vascular risk, white matter hyperintensity volume, and hippocampal volume data.

Items	Control	RGD		aMCI		*P*-value					
	Declining ($n = 21$)	Stable ($n = 43$)	Declining ($n = 18$)	Stable ($n = 23$)	Declining ($n = 33$)	Stable ($n = 18$)	Disease	Cognitive change	Time	Disease × cognitive change	Disease × time	Cognitive change × time	Disease × cognitive change × time
FRAMINGHAM 10-YEAR CV RISK [log_{10}(%)]													
Baseline	1.28 ± 0.24	1.32 ± 0.27	1.41 ± 0.25	1.17 ± 0.24	1.37 ± 0.26	1.31 ± 0.24	0.581	0.061	–	0.040*	–	–	–
WHITE MATTER HYPERINTENSITY VOLUME (ml)													
Baseline	2.62 ± 3.03	3.53 ± 5.14	6.55 ± 8.60	2.52 ± 3.50	4.19 ± 5.91	3.11 ± 3.57	0.030*	0.172	0.036*	0.003*	0.936	0.861	0.760
Follow-up	3.44 ± 3.75	5.09 ± 7.14	8.79 ± 9.05	3.06 ± 3.94	5.85 ± 7.73	5.01 ± 6.22							
LEFT HIPPOCAMPAL VOLUME (ml)													
Baseline	2.99 ± 0.27	2.95 ± 0.31	2.91 ± 0.37	2.93 ± 0.24	2.79 ± 0.45	2.99 ± 0.44	0.031*	0.328	0.109	0.016*	0.797	0.689	0.837
Follow-up	2.93 ± 0.29	2.79 ± 0.56	2.90 ± 0.44	2.89 ± 0.26	2.69 ± 0.56	2.91 ± 0.57							
RIGHT HIPPOCAMPAL VOLUME (ml)													
Baseline	3.15 ± 0.37	3.09 ± 0.31	3.13 ± 0.42	3.10 ± 0.24	3.00 ± 0.49	3.16 ± 0.51	0.063	0.838	0.116	0.017*	0.915	0.817	0.699
Follow-up	3.13 ± 0.37	2.94 ± 0.57	3.07 ± 0.48	3.06 ± 0.26	2.88 ± 0.57	3.08 ± 0.63							

*Values are presented as the means ± the standard deviations (SD). ANOVA (with disease, cognitive change, and time as fixed factors) was applied in the comparison of the Framingham 10-year CV risk. ANCOVAs (with disease, cognitive change, and time as fixed factors) were applied in the comparisons of white matter hyperintensity volume and hippocampal volume, controlling for ApoE status (only for hippocampal volume), age, gender and years of education. *P < 0.05.*

ANCOVA, Analysis of covariance; ANOVA, analysis of variance; CV, cardiovascular.

WMH Volume

WMH lesions were segmented from T2 FLAIR images and T1 images in each subject (**Figure 1B**). As presented in **Table 2**, a significant main effect of disease on WMH volume was found. The RGD subjects exhibited greater WMH volume than the control subjects, whereas no significant difference was found between the aMCI subjects and the control subjects or between the aMCI subjects and the RGD subjects (**Figure 1C**). A significant main effect of time revealed that the whole sample displayed greater WMH volume at follow-up than at baseline (**Figure 1D**).

Notably, a significant interaction of disease and cognitive change was also demonstrated. *Post-hoc* tests as illustrated in **Figure 1E**, revealed the following: first, in the comparisons according to the cognitive change patterns (declining vs. stable), the RGD declining group displayed greater WMH volume than did the RGD stable group, whereas no such difference was found in the control subjects or aMCI subjects; and second, in the comparisons according to disease status (control vs. RGD vs. aMCI), the RGD declining group displayed greater WMH volume than did the control declining group.

Hippocampal Volume

Left Hippocampal Volume

The mean volume index for the hippocampal region in each group was calculated by interpolating the hippocampus to the individual gray matter images segmented from the T1 images (**Figure 2A**). As presented in **Table 2**, a significant main effect of disease was found on the left hippocampal volume. The aMCI subjects had smaller left hippocampal volumes than did the control subjects, whereas no significant difference was found between the RGD subjects and the control subjects (**Figure 2B**). Furthermore, a significant interaction of disease and cognitive change was identified. *Post-hoc* tests revealed the following: first, in the comparisons according to cognitive change patterns (declining vs. stable), the aMCI declining group displayed smaller hippocampal volumes than did the aMCI stable group, whereas no such difference was found in the control subjects or RGD subjects; second, in the comparisons according to disease status (control vs. RGD vs. aMCI), the aMCI declining group had smaller hippocampal volumes than did the control declining group (**Figure 2C**).

Right Hippocampal Volume

As presented in **Table 2**, a significant interaction of disease and cognitive change was found in the right hippocampal volume. *Post-hoc* tests revealed the following, as illustrated in **Figure 2D**: first, in the comparisons according to cognitive change patterns (declining vs. stable), no significant difference was found in the control subjects, RGD subjects or aMCI subjects; second, in the comparisons according to disease status (control vs. RGD vs. aMCI), the aMCI declining group had smaller right hippocampal volumes than did the control declining group.

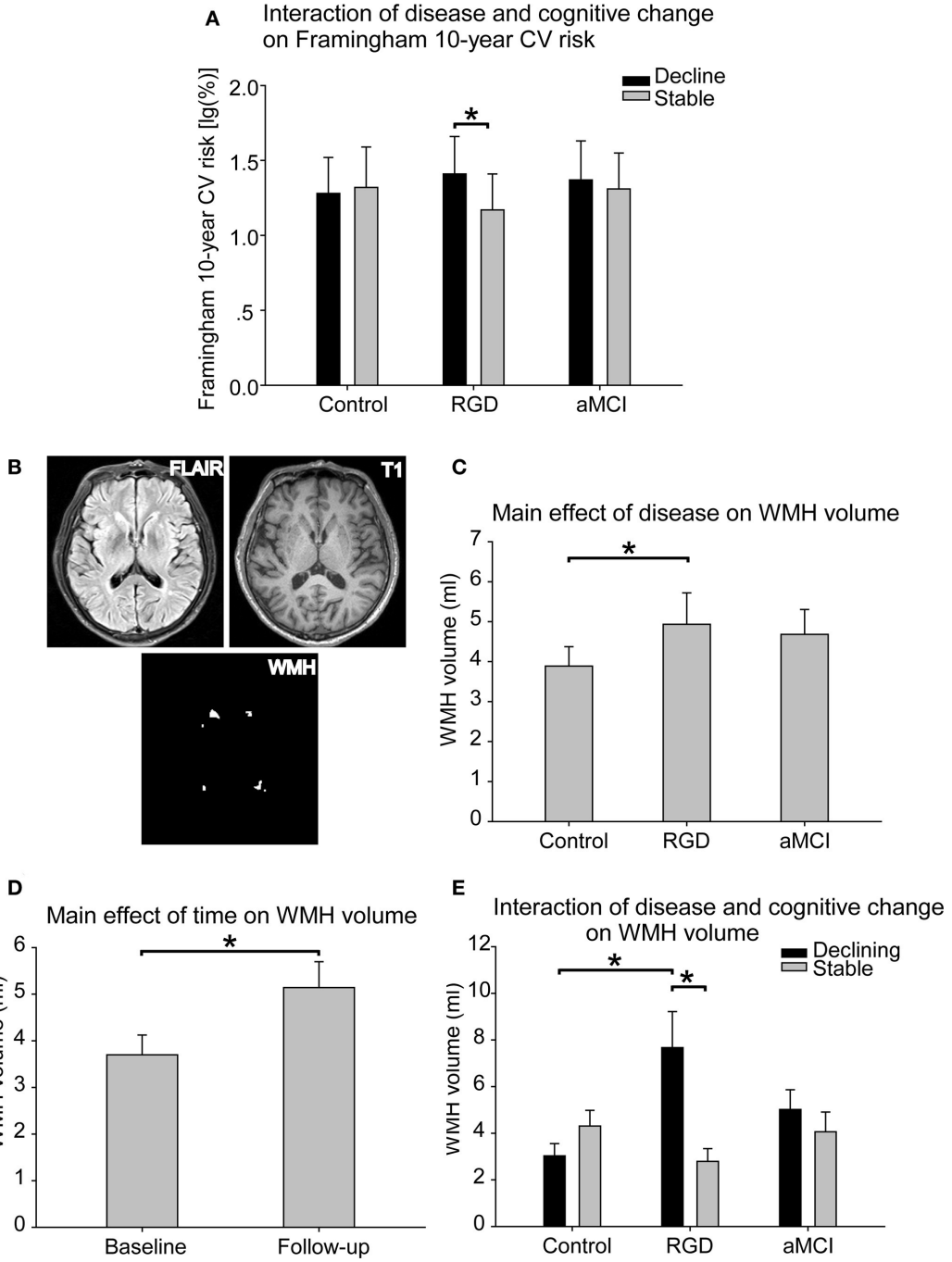


FIGURE 1 | (A) The interaction of disease and cognitive change on the Framingham 10-year cardiovascular risk. The RGD declining group displayed a higher risk than the RGD stable group, whereas no such difference was found within the control subjects or aMCI subjects. The bars are presented with the risk values [$\log_{10}$(%)]. The error bars represent the standard errors of the means of the risk values. **(B)** The segmentation of the WMH. The WMH lesions were segmented and quantified from T2 FLAIR images and T1 images. **(C)** The main effect of disease on WMH volume. The RGD subjects had greater WMH volumes than the control subjects. **(D)** The main effect of time on WMH volume. The whole sample displayed greater WMH volume at follow-up than at baseline. **(E)** The interaction of disease and cognitive change on WMH volume. The RGD declining group displayed greater WMH volume than the RGD stable group. The RGD declining group displayed greater WMH volume than the control declining group. The bars are presented with the WMH volumes. The error bars represent the standard errors of the means of the WMH volumes. *$P < 0.05$. aMCI, Amnestic mild cognitive impairment; CV, cardiovascular; RGD, remitted geriatric depression; WMH, white matter hyperintensities.

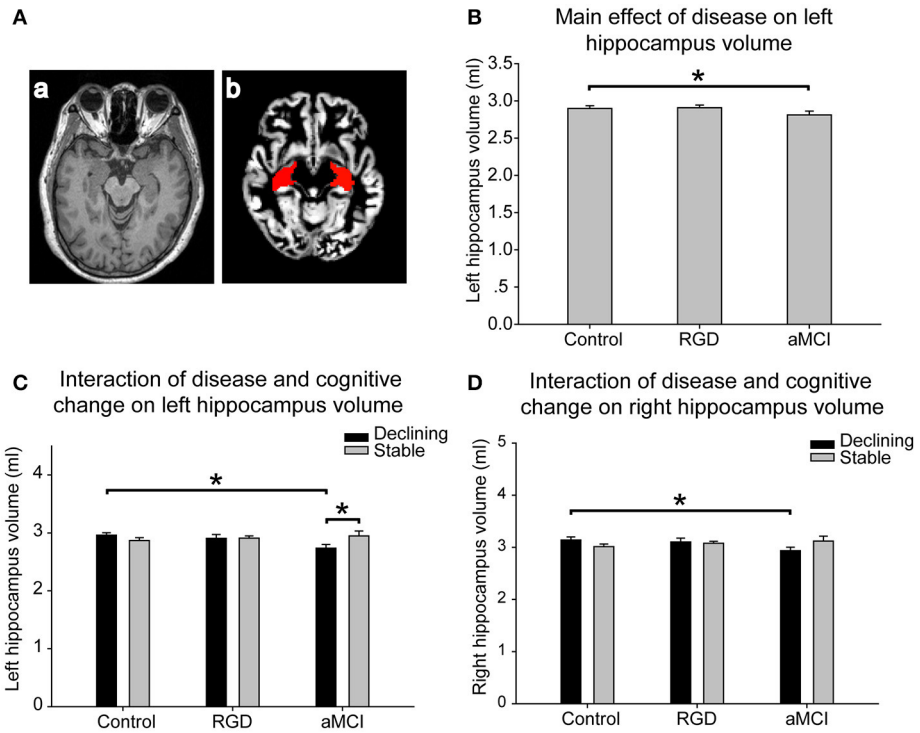


FIGURE 2 | (A) Hippocampal volume assessment. The gray matter was segmented from T1 images **(a)**. The hippocampus, isolated using automated anatomical labeling, was interpolated to individual gray matter images **(b)**. A mean volume index of all voxels of the hippocampal regions was computed for each subject. **(B)** The main effect of disease on the left hippocampal volume. The aMCI subjects had smaller left hippocampal volumes than the control subjects. **(C)** The interaction of disease and cognitive change on the left hippocampal volume. The aMCI declining group displayed smaller hippocampal volumes than the aMCI stable group. The aMCI declining group had smaller hippocampal volumes than the control declining group. **(D)** The interaction of disease and cognitive change on the right hippocampal volume. The aMCI declining group had smaller right hippocampal volumes than the control declining group. The bars are presented with the hippocampal volumes. The error bars represent the standard errors of the means of the hippocampal volumes. *$P < 0.05$. aMCI, Amnestic mild cognitive impairment; RGD, remitted geriatric depression.

Behavioral Significance of WHM Volume Changes and Hippocampal Volume Changes

As illustrated in **Figure 3**, in the RGD declining group, greater increases in WHM volume correlated with greater decreases in MMSE scores ($r = -0.457$, $P = 0.049$, two-tailed; **Figure 3A**). In the aMCI declining group, greater decreases in the left hippocampal volume correlated with greater decreases in the MDRS-2 scores ($r = 0.362$, $P = 0.042$, two-tailed; **Figure 3B**).

DISCUSSION

From the integrated perspective of vascular pathology and neurodegeneration, the present longitudinal study is the first to explore the association of cognitive decline with vascular risk, WMH burden and hippocampal volume in both RGD subjects and aMCI subjects. The findings revealed that the cognitive decline in RGD subjects was associated with high vascular risk and high WMH burden, whereas the cognitive decline in aMCI subjects was associated with small hippocampal volume. These findings suggest that different pathogeneses may underline the cognitive decline in RGD patients and aMCI patients.

A strength of the present study is that the 35-month longitudinal data were used to define "cognitive decline" in RGD patients and aMCI patients. As mentioned above, cognitive impairment may be improved following the remission of depressive symptoms in a portion of the population (Barch et al., 2012). Similarly, there was also a great heterogeneity in the MCI patients, although MCI has been proposed as an intermediate state between normal aging and early AD. While many MCI subjects eventually develop dementia, others remain cognitively stable, and a small proportion may actually convert to cognitively normal subjects (McKhann et al., 2011; Villemagne et al., 2011). Thus, assessing cognitive impairment using cross-sectional data may display high heterogeneity, and the definition of "cognitive decline" based on the present 35-month longitudinal data could be more reliable. RGD or aMCI subjects with cognitive decline would have a much higher risk for dementia than subjects with stable cognition.

The other strength is that the present study provided an overall view of AD-related pathology and vascular pathology in both RGD patients and aMCI patients. Studies assessing a single biomarker could show a significant association of the biomarker with cognitive impairment more easily than those that

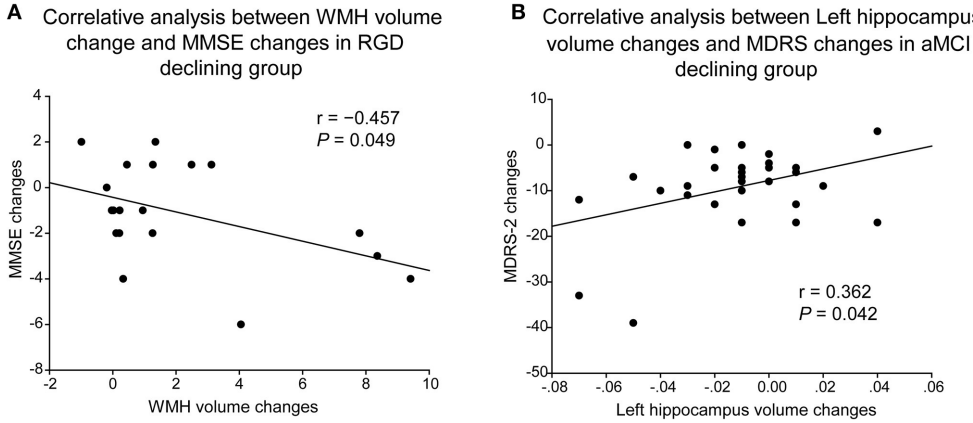


FIGURE 3 | Correlative analyses of cognitive impairment with WMH volume or hippocampal volume. **(A)** Greater increases of WHM volume correlated with greater decreases of MMSE scores in the RGD declining group. **(B)** Greater decreases of the left hippocampal volume correlated with greater decreases of the MDRS-2 scores in the aMCI declining group. aMCI, Amnestic mild cognitive impairment; MDRS-2, Mattis Dementia Rating Scale-2; RGD, remitted geriatric depression.

assess multiple biomarkers. As described above, previous studies that have assessed a single biomarker have demonstrated wide divergences of the association of cognitive decline with vascular burden and AD-related pathology in geriatric depression patients. A single biomarker may be associated with cognitive impairment; however, which biomarker has a major role has not been revealed by these studies. The present study explored vascular risk, WMH burden and hippocampal volume in both geriatric depression patients and aMCI patients. This overall view of AD-related pathology and vascular pathology could help to identify which pathology plays a major role in cognitive decline in each disorder.

The Framingham 10-year risk score provides an integrative perspective of multiple vascular risk factors (D'Agostino et al., 2008). In the present study, the RGD declining group had a much higher risk than did the RGD stable group. This is consentient with a previous study that demonstrated that a high score on the Framingham stroke risk scale is associated with cognitive impairment in elderly patients with major depressive disorder (Yeh et al., 2011). In contrast, the aMCI declining group and the aMCI stable group did not differ significantly in Framingham 10-year risk scores. Similarly, a 2.4-year follow-up study investigated the contribution of vascular burden to the progression of MCI to dementia and found no association between the Framingham Stroke Risk Profile scores and the progression to dementia (Clerici et al., 2012). A recent study explored the association between a vascular risk index and cognitive outcomes among MCI subjects and cognitively normal elderly subjects using linear regression models. Increased Framingham Stroke Risk Profile scores for MCI subjects only correlated with worse longitudinal episodic memory and not with the global cognition or other cognitive domains (Jefferson et al., 2015). Together with these findings, the present study highlighted the association of cognitive decline with vascular risk in geriatric depression by investigating the link in both RGD subjects and aMCI subjects.

The burden of small vessel cerebrovascular disease is well represented by WMH lesions on T2 FLAIR images. In the present study, greater WMH volume was found in the RGD subjects than in the control subjects. These findings support the vascular depression hypothesis in which cerebrovascular disease may predispose, precipitate, or perpetuate geriatric depression; this hypothesis is also known as "vascular depression" (Alexopoulos et al., 1997). In addition to geriatric depression, the cognitive decline in the RGD subjects was also related to WMH burden as suggested by the difference between the RGD declining group and the RGD stable group. The RGD declining group displayed greater WMH volume than did the RGD stable group, and greater increases in the WHM volume correlated with greater decreases of global function in the RGD declining group. This is consistent with previous findings that greater WMH burden is associated with cognitive deficits in geriatric depression patients (Hickie et al., 1997; Murata et al., 2001; Diniz et al., 2015). A significant advance of the present study is that the vascular burden was represented by both vascular risk and WMH volume. The present consistent findings in vascular risk and WMH volume convincingly relate the vascular burden to cognitive decline in geriatric depression patients. Indeed, increasing attention has been given to the concept of "disconnection syndromes" in which extensive ischemia and white matter lesions result in depression and cognitive deficits by disrupting cortical-subcortical or cortical-cortical connections (Alexopoulos, 2002).

However, the present study did not find a significant difference in WMH volume between the aMCI declining group and the aMCI stable group. A previous study also demonstrated that WMH is not associated with cognition in MCI subjects (Chen et al., 2006). However, other studies have demonstrated that greater WMH is associated with poor episodic memory and slow processing speed in MCI subjects (Fujishima et al., 2014; Lorius et al., 2015). Greater WMH is related to rapid cognitive decline in MCI subjects (Tosto et al., 2014). Furthermore, severe WMH also predicts the progression from MCI to dementia (Prasad

et al., 2011; Kim et al., 2015). The divergences may be due to two reasons. First, the present follow-up period may not have been long enough to generate significant differences in WMH volume between the aMCI declining group and the aMCI stable group, although the aMCI declining group had moderately, but not significantly, greater WMH volumes than did the aMCI stable group. We will continue to follow up these subjects. Second, the analysis of WMH volume was performed in RGD subjects, aMCI subjects, and control subjects using an ANCOVA, with which it was more difficult to show differences than with the analyses used for the aMCI subjects alone or in the comparison between the aMCI subjects and the control subjects. Nevertheless, the present findings highlight a major role of vascular burden in the mechanisms underlying cognitive decline in RGD patients and suggest a secondary role of vascular burden in cognitive decline in aMCI patients.

Atrophy of the hippocampus, which is one of the earliest brain areas developing AD-related pathology, indicates the degree of neurodegeneration in MCI patients and serves as a well-established indicator for the early diagnosis of AD (Aisen et al., 2010; Jack et al., 2010). The present study revealed that the aMCI subjects had smaller hippocampal volumes than the controls, and the aMCI declining group had smaller hippocampal volumes than the aMCI stable group and/or control group. Furthermore, greater decreases in the left hippocampal volume correlated with greater decreases of global cognitive function in the aMCI declining group. In contrast, no significant difference in hippocampal volume was found between the RGD declining group and the RGD stable group. A handful of studies have explored the relationship between hippocampal volume and cognitive impairment in geriatric depression patients. Smaller hippocampal volumes are associated with impairments in global cognitive function (Sachs-Erisson et al., 2011), memory (O'Brien et al., 2004), and executive function (Hou et al., 2012) in geriatric depression patients. A recent study demonstrated that hippocampal volume is not associated with executive dysfunction, i.e., the common cognitive deficit in geriatric depression, although both smaller hippocampal volume and poor cognitive performance are displayed in depressed patients. The study suggested that the link between hippocampal volume and executive dysfunction may be indirect (Khan et al., 2015). The present data did not support the association between hippocampal volume and global cognitive function in RGD patients. These divergences may come from the heterogeneities of geriatric depression populations and methodologies, including statistical methods and the assessment and definition of cognitive impairment/decline.

Several limitations should be addressed. First, the present study did not measure Aβ deposition, which is a major hallmark of the pathological changes in AD. Increasing evidence suggests that vascular pathology interacts with Aβ pathology. Cerebral ischaemia promotes the accumulation of Aβ, and Aβ deposition in turn results in further decreases in cerebral blood flow (Popa-Wagner et al., 2015). The coexistence of vascular pathology and Aβ pathology is very common in dementia (Saito and Murayama, 2007; Schneider et al., 2009). Thus, although the present study demonstrated that different pathologies were associated with the cognitive decline in RGD patients and aMCI patients, there may also be convergent pathologies contributing to the cognitive decline in both conditions. Indeed, our previous study found both convergent and divergent patterns of microstructural integrity of white matter between RGD and aMCI subjects (Bai et al., 2012). Second, the range of the declines in the MDRS-2 scores in the RGD declining group, aMCI declining group and control declining group were not matched. Thus, the results of comparisons of WMH volume and hippocampal volume between these three groups should be treated with caution. Finally, the present study did not measure the Aβ pathology and tau pathology using PET imaging or cerebrospinal fluid analyses of Aβ and Tau. Some control subjects, especially those with cognitive decline, might also have AD-related pathology and could not serve as a control group. Some control declining subjects may improve their performance later on. Similarity, not all of aMCI subjects with cognitive decline would display AD-related pathology and ultimately develop dementia.

In conclusion, the present findings suggest that cognitive decline in RGD patients is associated with vascular burden, whereas the cognitive decline in aMCI patients is associated with neurodegeneration. These findings could contribute to a better understanding of specific mechanisms involved in the development of dementia in each condition, which may further provide novel strategies for the prevention and treatment of dementia.

ETHICS STATEMENT

This study was carried out in accordance with the recommendations of the Affiliated ZhongDa Hospital of Southeast University Research Ethics Committee with written informed consent from all subjects. All subjects gave written informed consent in accordance with the Declaration of Helsinki. The protocol was approved by the Affiliated ZhongDa Hospital of Southeast University Research Ethics Committee.

AUTHOR CONTRIBUTIONS

FB: Study design, interpretation, data analysis, and manuscript writing. ZZ, HZ, and CX: Study design and interpretation. QY: Study design, data collection, analysis, and manuscript writing. FS, LG, HS, and WL: Data collection and analysis.

FUNDING

This research was supported by the National Natural Science Foundation of China (No. 81671665); Jiangsu Provincial Key Medical Talents (No.ZDRCA2016085); Natural Science Foundation of Jiangsu Province (No. BK20160071); Six talent peaks project in Jiangsu Province (No. 2015-WSN-003); National High-tech R.D Program (863 Program) (No.2015AA020508).

ACKNOWLEDGMENTS

We thank Haifeng Chen, Qin Xu, and Ying Cheng for their help in fMRI scanning.

REFERENCES

Aisen, P. S., Petersen, R. C., Donohue, M. C., Gamst, A., Raman, R., Thomas, R. G., et al. (2010). Clinical core of the Alzheimer's disease neuroimaging initiative: progress and plans. *Alzheimers. Dement.* 6, 239–246. doi: 10.1016/j.jalz.2010.03.006

Albert, M. S., DeKosky, S. T., Dickson, D., Dubois, B., Feldman, H. H., Fox, N. C., et al. (2011). The diagnosis of mild cognitive impairment due to Alzheimer's disease: recommendations from the National Institute on Aging-Alzheimer's Association workgroups on diagnostic guidelines for Alzheimer's disease. *Alzheimers. Dement.* 7, 270–279. doi: 10.1016/j.jalz.2011.03.008

Alexopoulos, G. S. (2002). Frontostriatal and limbic dysfunction in late-life depression. *Am. J. Geriatr. Psychiatry* 10, 687–695. doi: 10.1097/00019442-200211000-00007

Alexopoulos, G. S., Meyers, B. S., Young, R. C., Campbell, S., Silbersweig, D., and Charlson, M. (1997). 'Vascular depression' hypothesis. *Arch. Gen. Psychiatry* 54, 915–922. doi: 10.1001/archpsyc.1997.01830220033006

Bai, F., Shu, N., Yuan, Y., Shi, Y., Yu, H., Wu, D., et al. (2012). Topologically convergent and divergent structural connectivity patterns between patients with remitted geriatric depression and amnestic mild cognitive impairment. *J. Neurosci.* 32, 4307–4318. doi: 10.1523/JNEUROSCI.5061-11.2012

Bai, F., Zhang, Z., Watson, D. R., Yu, H., Shi, Y., and Yuan, Y. (2009). Abnormal white matter independent of hippocampal atrophy in amnestic type mild cognitive impairment. *Neurosci. Lett.* 462, 147–151. doi: 10.1016/j.neulet.2009.07.009

Barch, D. M., D'Angelo, G., Pieper, C., Wilkins, C. H., Welsh-Bohmer, K., Taylor, W., et al. (2012). Cognitive improvement following treatment in late-life depression: relationship to vascular risk and age of onset. *Am. J. Geriatr. Psychiatry* 20, 682–690. doi: 10.1097/JGP.0b013e318246b6cb

Byun, M. S., Choe, Y. M., Sohn, B. K., Yi, D., Han, J. Y., Park, J., et al. (2016). Association of cerebral amyloidosis, blood pressure, and neuronal injury with late-life onset depression. *Front. Aging Neurosci.* 8:236. doi: 10.3389/fnagi.2016.00236

Chen, Y. F., Wang, H., Chu, Y., Huang, Y. C., and Su, M. Y. (2006). Regional quantification of white matter hyperintensity in normal aging, mild cognitive impairment, and Alzheimer's disease. *Dement. Geriatr. Cogn. Disord.* 22, 177–184. doi: 10.1159/000094785

Clerici, F., Caracciolo, B., Cova, I., Fusari Imperatori, S., Maggiore, L., Galimberti, D., et al. (2012). Does vascular burden contribute to the progression of mild cognitive impairment to dementia? *Dement. Geriatr. Cogn. Disord.* 34, 235–243. doi: 10.1159/000343776

D'Agostino, R. B. Sr., Vasan, R. S., Pencina, M. J., Wolf, P. A., Cobain, M., Massaro, J. M., et al. (2008). General cardiovascular risk profile for use in primary care: the Framingham heart study. *Circulation* 117, 743–753. doi: 10.1161/CIRCULATIONAHA.107.699579

Diniz, B. S., Butters, M. A., Albert, S. M., Dew, M. A., and Reynolds, C. F. III. (2013). Late-life depression and risk of vascular dementia and Alzheimer's disease: systematic review and meta-analysis of community-based cohort studies. *Br. J. Psychiatry* 202, 329–335. doi: 10.1192/bjp.bp.112.118307

Diniz, B. S., Sibille, E., Ding, Y., Tseng, G., Aizenstein, H. J., Lotrich, F., et al. (2015). Plasma biosignature and brain pathology related to persistent cognitive impairment in late-life depression. *Mol. Psychiatry* 20, 594–601. doi: 10.1038/mp.2014.76

Fujishima, M., Maikusa, N., Nakamura, K., Nakatsuka, M., Matsuda, H., and Meguro, K. (2014). Mild cognitive impairment, poor episodic memory, and late-life depression are associated with cerebral cortical thinning and increased white matter hyperintensities. *Front. Aging Neurosci.* 6:306. doi: 10.3389/fnagi.2014.00306

Galasko, D. R., Gould, R. L., Abramson, I. S., and Salmon, D. P. (2000). Measuring cognitive change in a cohort of patients with Alzheimer's disease. *Stat. Med.* 19, 1421–1432. doi: 10.1002/(SICI)1097-0258(20000615/30)19:11/12<1421::AID-SIM434>3.0.CO;2-P

Gould, R., Abramson, I., Galasko, D., and Salmon, D. (2001). Rate of cognitive change in Alzheimer's disease: methodological approaches using random effects models. *J. Int. Neuropsychol. Soc.* 7, 813–824.

Green, R. C., Woodard, J. L., and Green, J. (1995). Validity of the mattis dementia rating scale for detection of cognitive impairment in the elderly. *J. Neuropsychiatry Clin. Neurosci.* 7, 357–360. doi: 10.1176/jnp.7.3.357

Hickie, I., Scott, E., Wilhelm, K., and Brodaty, H. (1997). Subcortical hyperintensities on magnetic resonance imaging in patients with severe depression–a longitudinal evaluation. *Biol. Psychiatry* 42, 367–374. doi: 10.1016/S0006-3223(96)00363-0

Hou, Z., Yuan, Y., Zhang, Z., Bai, F., Hou, G., and You, J. (2012). Longitudinal changes in hippocampal volumes and cognition in remitted geriatric depressive disorder. *Behav. Brain Res.* 227, 30–35. doi: 10.1016/j.bbr.2011.10.025

Jack, C. R. Jr., Wiste, H. J., Vemuri, P., Weigand, S. D., Senjem, M. L., Zeng, G., et al. (2010). Brain beta-amyloid measures and magnetic resonance imaging atrophy both predict time-to-progression from mild cognitive impairment to Alzheimer's disease. *Brain* 133, 3336–3348. doi: 10.1093/brain/awq277

Jefferson, A. L., Hohman, T. J., Liu, D., Haj-Hassan, S., Gifford, K. A., Benson, E. M., et al. (2015). Adverse vascular risk is related to cognitive decline in older adults. *J. Alzheimers. Dis.* 44, 1361–1373. doi: 10.3233/JAD-141812

Khan, S. A., Ryali, V., Bhat, P. S., Prakash, J., Srivastava, K., and Khanam, S. (2015). The hippocampus and executive functions in depression. *Ind. Psychiatry J.* 24, 18–22. doi: 10.4103/0972-6748.160920

Kim, S., Choi, S. H., Lee, Y. M., Kim, M. J., Kim, Y. D., Kim, J. Y., et al. (2015). Periventricular white matter hyperintensities and the risk of dementia: a CREDOS study. *Int. Psychogeriatr.* 27, 2069–2077. doi: 10.1017/S1041610215001076

Lorius, N., Locascio, J. J., Rentz, D. M., Johnson, K. A., Sperling, R. A., Viswanathan, A., et al. (2015). Vascular disease and risk factors are associated with cognitive decline in the Alzheimer disease spectrum. *Alzheimer Dis. Assoc. Disord.* 29, 18–25. doi: 10.1097/WAD.0000000000000043

McKhann, G. M., Knopman, D. S., Chertkow, H., Hyman, B. T., Jack, C. R. Jr., Kawas, C. H., et al. (2011). The diagnosis of dementia due to Alzheimer's disease: recommendations from the National Institute on Aging-Alzheimer's Association workgroups on diagnostic guidelines for Alzheimer's disease. *Alzheimers. Dement.* 7, 263–269. doi: 10.1016/j.jalz.2011.03.005

Modrego, P. J., and Ferrandez, J. (2004). Depression in patients with mild cognitive impairment increases the risk of developing dementia of Alzheimer type: a prospective cohort study. *Arch. Neurol.* 61, 1290–1293. doi: 10.1001/archneur.61.8.1290

Monsch, A. U., Bondi, M. W., Salmon, D. P., Butters, N., Thal, L. J., Hansen, L. A., et al. (1995). Clinical validity of the mattis dementia rating scale in detecting Dementia of the Alzheimer type. A double cross-validation and application to a community-dwelling sample. *Arch. Neurol.* 52, 899–904. doi: 10.1001/archneur.1995.00540330081018

Murata, T., Kimura, H., Omori, M., Kado, H., Kosaka, H., Iidaka, T., et al. (2001). MRI white matter hyperintensities, (1)H-MR spectroscopy and cognitive function in geriatric depression: a comparison of early- and late-onset cases. *Int. J. Geriatr. Psychiatry* 16, 1129–1135. doi: 10.1002/gps.501

O'Brien, J. T., Lloyd, A., McKeith, I., Gholkar, A., and Ferrier, N. (2004). A longitudinal study of hippocampal volume, cortisol levels, and cognition in older depressed subjects. *Am. J. Psychiatry* 161, 2081–2090. doi: 10.1176/appi.ajp.161.11.2081

Ownby, R. L., Crocco, E., Acevedo, A., John, V., and Loewenstein, D. (2006). Depression and risk for Alzheimer disease: systematic review, meta-analysis, and metaregression analysis. *Arch. Gen. Psychiatry* 63, 530–538. doi: 10.1001/archpsyc.63.5.530

Panza, F., Frisardi, V., Capurso, C., D'Introno, A., Colacicco, A. M., Imbimbo, B. P., et al. (2010). Late-life depression, mild cognitive impairment, and dementia: possible continuum? *Am. J. Geriatr. Psychiatry* 18, 98–116. doi: 10.1097/JGP.0b013e3181b0fa13

Petersen, R. C. (2004). Mild cognitive impairment as a diagnostic entity. *J. Intern. Med.* 256, 183–194. doi: 10.1111/j.1365-2796.2004.01388.x

Petersen, R. C., Smith, G. E., Waring, S. C., Ivnik, R. J., Tangalos, E. G., and Kokmen, E. (1999). Mild cognitive impairment: clinical characterization and outcome. *Arch. Neurol.* 56, 303–308. doi: 10.1001/archneur.56.3.303

Popa-Wagner, A., Buga, A. M., Popescu, B., and Muresanu, D. (2015). Vascular cognitive impairment, dementia, aging and energy demand. A vicious cycle. *J. Neural Transm.* 122(Suppl. 1), S47–S54. doi: 10.1007/s00702-013-1129-3

Prasad, K., Wiryasaputra, L., Ng, A., and Kandiah, N. (2011). White matter disease independently predicts progression from mild cognitive impairment to Alzheimer's disease in a clinic cohort. *Dement. Geriatr. Cogn. Disord.* 31, 431–434. doi: 10.1159/000330019

Sachs-Erisson, N., Sawyer, K., Corsentino, E., Collins, N., and Steffens, D. C. (2011). The moderating effect of the APOE [small element of] 4 allele on the relationship between hippocampal volume and cognitive decline in older depressed patients. *Am. J. Geriatr. Psychiatry* 19, 23–32. doi: 10.1097/JGP.0b013e3181f61ae8

Saito, Y., and Murayama, S. (2007). Neuropathology of mild cognitive impairment. *Neuropathology* 27, 578–584. doi: 10.1111/j.1440-1789.2007.00806.x

Salmon, D. P., Thal, L. J., Butters, N., and Heindel, W. C. (1990). Longitudinal evaluation of dementia of the Alzheimer type: a comparison of 3 standardized mental status examinations. *Neurology* 40, 1225–1230. doi: 10.1212/WNL.40.8.1225

Schmidt, P., Gaser, C., Arsic, M., Buck, D., Forschler, A., Berthele, A., et al. (2012). An automated tool for detection of FLAIR-hyperintense white-matter lesions in multiple sclerosis. *Neuroimage* 59, 3774–3783. doi: 10.1016/j.neuroimage.2011.11.032

Schmidt, R., Freidl, W., Fazekas, F., Reinhart, B., Grieshofer, P., Koch, M., et al. (1994). The Mattis Dementia Rating Scale: normative data from 1,001 healthy volunteers. *Neurology* 44, 964–966. doi: 10.1212/WNL.44.5.964

Schneider, J. A., Arvanitakis, Z., Leurgans, S. E., and Bennett, D. A. (2009). The neuropathology of probable Alzheimer disease and mild cognitive impairment. *Ann. Neurol.* 66, 200–208. doi: 10.1002/ana.21706

Smith, G. E., Ivnik, R. J., Malec, J. F., Kokmen, E., Tangalos, E., and Petersen, R. C. (1994). Psychometric properties of the mattis dementia rating scale. *Assessment* 1, 123–132. doi: 10.1177/1073191194001002002

Tard, C., Demailly, F., Delval, A., Semah, F., Defebvre, L., Dujardin, K., et al. (2015). Hypometabolism in posterior and temporal areas of the brain is associated with cognitive decline in Parkinson's disease. *J. Parkinsons. Dis.* 5, 569–574. doi: 10.3233/JPD-150583

Tosto, G., Zimmerman, M. E., Carmichael, O. T., and Brickman, A. M. (2014). Predicting aggressive decline in mild cognitive impairment: the importance of white matter hyperintensities. *JAMA Neurol.* 71, 872–877. doi: 10.1001/jamaneurol.2014.667

Villemagne, V. L., Pike, K. E., Chetelat, G., Ellis, K. A., Mulligan, R. S., Bourgeat, P., et al. (2011). Longitudinal assessment of Aβ and cognition in aging and Alzheimer disease. *Ann. Neurol.* 69, 181–192. doi: 10.1002/ana.22248

Vitaliano, P. P., Breen, A. R., Russo, J., Albert, M., Vitiello, M. V., and Prinz, P. N. (1984). The clinical utility of the dementia rating scale for assessing Alzheimer patients. *J. Chronic Dis.* 37, 743–753. doi: 10.1016/0021-9681(84)90043-2

Winblad, B., Palmer, K., Kivipelto, M., Jelic, V., Fratiglioni, L., Wahlund, L. O., et al. (2004). Mild cognitive impairment–beyond controversies, towards a consensus: report of the International Working Group on Mild Cognitive Impairment. *J. Intern. Med.* 256, 240–246. doi: 10.1111/j.1365-2796.2004.01380.x

Ye, Q., Su, F., Shu, H., Gong, L., Xie, C. M., Zhou, H., et al. (2017). Shared effects of the clusterin gene on the default mode network among individuals at risk for Alzheimer's disease. *CNS Neurosci. Ther.* 23, 395–404. doi: 10.1111/cns.12682

Ye, Q., Su, F., Shu, H., Gong, L., Xie, C., Zhang, Z., et al. (2016). The apolipoprotein E gene affects the three-year trajectories of compensatory neural processes in the left-lateralized hippocampal network. *Brain Imaging Behav.* doi: 10.1007/s11682-016-9623-5. [Epub ahead of print].

Yeh, Y. C., Tsang, H. Y., Lin, P. Y., Kuo, Y. T., Yen, C. F., Chen, C. C., et al. (2011). Subtypes of mild cognitive impairment among the elderly with major depressive disorder in remission. *Am. J. Geriatr. Psychiatry* 19, 923–931. doi: 10.1097/JGP.0b013e318202clc6

Conflict of Interest Statement: The authors declare that the research was conducted in the absence of any commercial or financial relationships that could be construed as a potential conflict of interest.

Copyright © 2017 Ye, Su, Gong, Shu, Liao, Xie, Zhou, Zhang and Bai. This is an open-access article distributed under the terms of the Creative Commons Attribution License (CC BY). The use, distribution or reproduction in other forums is permitted, provided the original author(s) or licensor are credited and that the original publication in this journal is cited, in accordance with accepted academic practice. No use, distribution or reproduction is permitted which does not comply with these terms.

frontiers in Neurology

ORIGINAL RESEARCH
published: 15 August 2017
doi: 10.3389/fneur.2017.00399

Subregional Structural Alterations in Hippocampus and Nucleus Accumbens Correlate with the Clinical Impairment in Patients with Alzheimer's Disease Clinical Spectrum: Parallel Combining Volume and Vertex-Based Approach

*Xiuling Nie[1†], Yu Sun[1,2†], Suiren Wan[1†], Hui Zhao[3], Renyuan Liu[4], Xueping Li[4], Sichu Wu[4], Zuzana Nedelska[5,6], Jakub Hort[5,6], Zhao Qing[4], Yun Xu[3] and Bing Zhang[4]**

[1]State Key laboratory of Bioelectronics, School of Biological Sciences and Medical Engineering, Southeast University, Nanjing, China, [2]Institute of Cancer and Genetic Science, University of Birmingham, Birmingham, United Kingdom, [3]Department of Neurology, Affiliated Drum Tower Hospital of Nanjing University Medical School, Nanjing, China, [4]Department of Radiology, Affiliated Drum Tower Hospital of Nanjing University Medical School, Nanjing, China, [5]Department of Neurology, Memory Clinic, 2nd Faculty of Medicine, Charles University in Prague, Motol University Hospital, Prague, Czechia, [6]International Clinical Research Center, St. Anne's University Hospital Brno, Brno, Czech Republic

Deep gray matter structures are associated with memory and other important functions that are impaired in Alzheimer's disease (AD) and mild cognitive impairment (MCI). However, systematic characterization of the subregional atrophy and deformations in these structures in AD and MCI still need more investigations. In this article, we combined complex volumetry- and vertex-based analysis to investigate the pattern of subregional structural alterations in deep gray matter structures and its association with global clinical scores in AD (n = 30) and MCI patients (n = 30), compared to normal controls (NCs, n = 30). Among all seven pairs of structures, the bilateral hippocampi and nucleus accumbens showed significant atrophy in AD compared with NCs ($p < 0.05$). But only the subregional atrophy in the dorsal–medial part of the left hippocampus, the ventral part of right hippocampus, and the left nucleus accumbens, the posterior part of the right nucleus accumbens correlated with the worse clinical scores of MMSE and MOCA ($p < 0.05$). Furthermore, the medial–ventral part of right thalamus significantly shrank and correlated with clinical scores without decreasing in its whole volume ($p > 0.05$). In conclusion, the atrophy of these four subregions in bilateral hippocampi and nucleus accumbens was associated with cognitive impairment of patients, which might be potential target regions of treatment in AD. The surface analysis could provide additional information to volume comparison in finding the early pathological progress in deep gray matter structures.

Keywords: Alzheimer's disease, mild cognitive impairment, deep gray matter structures, surface alteration, vertex analysis

OPEN ACCESS

Edited by:
Mohammad Amjad Kamal, King Abdulaziz University, Saudi Arabia

Reviewed by:
Bo Zhou, Stanford University, United States
Gianfranco Spalletta, Fondazione Santa Lucia (IRCCS), Italy

***Correspondence:**
Bing Zhang
zhangbing_nanjing@vip.163.com

†Cofirst author: these authors have contributed equally to this work.

Specialty section:
This article was submitted to Neurodegeneration, a section of the journal Frontiers in Neurology

Received: *06 June 2017*
Accepted: *25 July 2017*
Published: *15 August 2017*

Citation:
Nie XL, Sun Y, Wan SR, Zhao H, Liu RY, Li XP, Wu SC, Nedelska Z, Hort J, Qing Z, Xu Y and Zhang B (2017) Subregional Structural Alterations in Hippocampus and Nucleus Accumbens Correlate with the Clinical Impairment in Patients with Alzheimer's Disease Clinical Spectrum: Parallel Combining Volume and Vertex-Based Approach. Front. Neurol. 8:399. doi: 10.3389/fneur.2017.00399

INTRODUCTION

Alzheimer's disease (AD) is the most prevalent form of age-related dementia (1, 2) and is usually preceded by a stage of cognitive decline. This clinical state of cognitive decline is conceptualized as mild cognitive impairment (MCI) (3, 4). Previous studies showed that MRI-based assessments of brain volume, such as hippocampal atrophy, can provided additional information for diagnosis of AD (5). Specifically deep gray matter structures, including bilateral nucleus accumbens (NAc), amygdala, caudate nucleus, hippocampus, pallidum, putamen, and thalamus, are associated with memory, emotional learning, shifting attention, and spatial working memory (6, 7), which were typically impaired in AD stage. Previous studies have focused on these regions and reported that there was atrophy on hippocampus and entorhinal cortex (8–12). Besides, it also suggested that other deep gray matter structures, like amygdala, putamen, and thalamus also showed significantly reduced volume, even in MCI (10, 13–15).

However, the subregions of deep gray matter structures may have different function and their impairment in AD may also have subregional specificity (9, 15–17). Therefore, it is very informative to explore the changes of deep gray matter structures on the subregional level in the AD and MCI. Previous studies have reported shape abnormalities in multiple deep gray matter structures, such as the dorsal–medial part of thalamus (15), the anterior hippocampus (9, 17), and the basolateral complex of amygdala (16, 17) in AD patients compared to controls. However, there is still lack of a systematic investigation of all deep gray matter structures.

In the current study, we unitized the automated software package, FMRIB's Integrated Registration and Segmentation Tool (FIRST) (16, 18, 19), which provided a powerful tool to analyze subregional atrophy and shape alterations within seven pairs of deep gray matter structures. The volumes of each deep gray matter structure and the vertex-wised distortion were compared among clinically normal controls (NCs) as well as MCI and AD patients. We hypothesized that the pattern of atrophy on subregional level would differ among the three mentioned groups, and the specific pattern of more profound atrophy or shape alterations would correlate with poorer scores of global clinical scores.

MATERIALS AND METHODS

Subjects

Ninety consecutive subjects were recruited from the memory clinic of Affiliated Drum Tower Hospital of Nanjing University Medical School. All subjects underwent a clinical evaluation using Mini-Mental State Examination (MMSE) (20) and Montreal Cognitive Assessment (MOCA) (21). Written consent was obtained from all subjects or their proxies after a detailed explanation of the study procedures, which was approved by the local Ethics Committee.

The MCI patients ($n = 30$) were diagnosed based on the following criteria (22): (a) memory complaint, preferably confirmed by an informant; (b) objective memory impairment, adjusted for age, and education; (c) normal or near-normal performance on general cognitive functioning and no or minimum impairment of daily life activities; and (d) not meeting the criteria for dementia. AD patients ($n = 30$) met NINCDS-ADRDA criteria (23). For comparison, we included NC ($n = 30$) who (a) had no cognitive complaints, (b) scored normally on global cognitive scales such as MMSE and MOCA, and (c) had no evidence of any structural abnormality on a conventional MRI scan.

Exclusion criteria were history of any significant medical, psychiatric, or neurological illness other than MCI or AD; history of brain injury; alcohol or drug abuse of alcohol; and missing clinical assessments.

MRI Acquisition

Images were acquired on a 3.0-T MR scanner (Achieva 3.0T TX dual Medical Systems; Philips Medical Systems, Eindhoven, Netherlands) using a three-dimensional turbo fast echo (3D-TFE) T_1-weighted pulse sequence with TR = 9.7 ms, TE = 4.6 ms, flip angle = 8°, slice thickness = 1 mm, slice gap = 1 mm, FOV = 256 mm × 256 mm, and matrix = 192.

Image Processing

The flowchart of image processing is shown in **Figure 1**. MRI volume were processed using FMRIB Software Library (FSL, Version 5.0, http://www.fmrib.ox.ac.uk/fsl) (18, 24). Briefly, brain extraction was performed on 3D T1-weighted MR images using Brain Extraction Tool (25), which uses a deformable model that evolves to fit the brain's surface by the application of a set of locally adaptive model forces (25).

FMRIB's Integrated Registration and Segmentation Tool (16) was applied to perform the segmentation and to measure volumes and vertexes in seven deep gray matter structures bilaterally, including NAc, amygdala, caudate nucleus, hippocampus, pallidum, putamen, and thalamus. FIRST initially performed a two-stage linear registration using 12 degrees of freedom, and the registration was performed by FLIRT (26). In the first stage, an affine registration of the whole-head to a standard space template (MNI template), with 1 mm × 1 mm × 1 mm resolution, was implemented. In the second stage, a subcortical mask was used to exclude regions outside the deep gray matter structures. Finally, a boundary correction was used to determine whether boundary voxels belong to this structure or not.

Based on this deep gray matter segmentation, the volume of each region was first extracted. The boundary of each region was reconstructed into a vertex-based surface, and the vertex locations from each subject (at a corresponding anatomical point) were projected onto the surface normal of the average shape of all

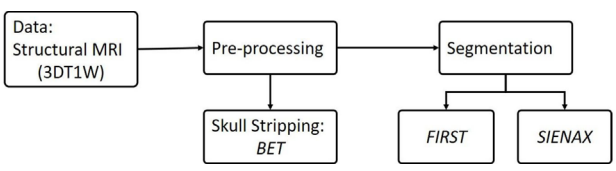


FIGURE 1 | Flowchart of structural MR image processing.

the subjects. The projections were scalar values representing the signed, perpendicular distance from the average surface, where a positive value was outside the surface and a negative value was inside. Therefore, these scalar values of the vertex-based projection represented the shape information of each subjects and were used in the analysis of vertex-level group difference and to evaluate the shape deformation.

To reduce the influence of variation in head size, all volumes were scaled by normalized brain volume (NBV) estimated using SIENAX-FSL tool (24, 27). The segmentation result of each subject was visually checked and no error was observed. In the following statistical analysis, the volumes of each structure for each individual subject were corrected for NBV.

Statistical Analysis

Volume-Based Analysis

After calculating the volumes, we used SPSS v 21.0 to analyze the data, including two statistical methods: analysis of covariance (ANCOVA) and linear regression. To correct the differences in head size among individual participants, volumes of each structure were scaled by NBV using the following equation:

$$V_{\text{standard}} = \left(V_{\text{roi}} / V_{\text{NBV}}\right) \times 10^6$$

where V_{standard} means the standardized volume corrected with NBV, V_{roi} means the absolute volume of each segmented structure, and V_{NBV} means NBV.

Analysis of covariance model was used to evaluate group-wise differences in volume measures between AD, MCI and NC, with controlling for age and gender. In this model, volumes of deep gray matter structures were included as dependent factors and diagnosis as independent factors. A correction for multiple comparisons was carried out using the false discovery rate (FDR) correction at $p < 0.05$. Subsequently, *post hoc* pair-wise comparisons were applied to identify between-group differences with p-value $\leq$0.05, which is considered as significant. Second, a linear regression model was applied to measure the associations between global clinical scores (MMSE and MOCA score) and volumes of each structure among all of the subjects. In the linear regression model, global clinical scores were included as the dependent variables and the volumes of deep gray matter structure were included as independent variables. Age, gender and NBV were included as covariates. A collinearity test was also performed to rule out multicollinearity between age and the volumes of deep gray matter structure.

Vertex-Based Analysis

To carry out the vertex analysis, we used FSL dedicated tools, generalized linear model (18) to design the statistical matrix and Randomize (28) to perform permutation inference. Two statistical models were also designed in the vertex analysis.

First, ANCOVA was applied to determine the subregional changes within the deep gray matter structures across AD, MCI, and NC groups. Second, we correlated local subregional changes with global clinical scores at p-value $\leq$0.05 across all subjects. Age and gender were taken into as covariates in both of the ANCOVA and correlational analyses. We applied the FDR ($q = 0.05$) to correct for the multiple comparisons. The MNI coordinates of the center of gravity (COG) (18) at subregional alterations were also calculated for a better awareness of the locations where subregional changes occurred.

RESULTS

Group Characteristics

Demographic and clinical characteristics of three groups are listed in **Table 1**. The AD, MCI, and NC groups did not differ in NBV ($p = 0.052$) and gender ($p = 0.194$), but differ in age ($p = 0.028$). As expected, the pathological alteration among groups led to the significant difference in the scores of MMSE and MOCA among patients with AD, MCI, and NC ($p < 0.001$).

Deep Gray Matter Structures Volumes in AD and MCI Groups

Group-wise differences in volumes of the deep gray matter structure are displayed in **Table 2**. Volumes of bilateral NAc and bilateral hippocampi (Hipp) were smaller in AD, compared to NC group (L_Hipp: $p = 0.001$, R_Hipp: $p = 0.001$, L_NAc: $p = 0.003$, R_NAc: $p = 0.003$). MCI had smaller left hippocampus ($p = 0.020$), right NAc ($p = 0.010$), and left putamen ($p = 0.038$) volumes, compared to the NC group. Only right hippocampus showed a smaller volume in AD, compared to MCI group ($p = 0.012$).

Associations between Volumes and Clinical Rating Scales

We did not find a multicollinearity among the selected variables: age and volumes of deep gray matter structures. After controlling age, gender, and NBV, the p-values and β-regression coefficient of the correlations between volumes of deep gray matter structures and the global clinical scores across all subjects are displayed in **Table 3**. The volumes of bilateral NAc, bilateral hippocampi, which also showed significant atrophy in AD, compared to NC, were significantly correlated with MMSE and MOCA scores ($p \leq 0.05$). The volumes of other deep gray matter structures did not show significant correlations with clinical scores ($p > 0.05$).

TABLE 1 | Study sample characteristics.

Group	AD ($n = 30$)	MCI ($n = 30$)	NC ($n = 30$)	p-Value
Age (years; SD)	74.1 ± 10.5	74.6 ± 9.6	68.0 ± 11.0	0.028*
Gender (M/F)	13:17	17:13	20:10	0.194
NBV (cm^3; SD)	1,154.6 ± 114.9	1,225.6 ± 116.6	1,183.5 ± 102.9	0.052
MMSE (SD)	16.5 ± 5.5	25.4 ± 2.1	29.0 ± 1.2	<0.001**
MOCA (SD)	11.9 ± 4.7	21.9 ± 2.1	26.9 ± 2.1	<0.001**

*$p \leq 0.05$.
**$p \leq 0.01$.
Demographic data are presented as means ± SDs for continuous and proportions for categorical variables.
AD, Alzheimer's disease; MCI, mild cognitive impairment; NC, normal controls; NBV, normalized brain volume; MMSE, Mini-Mental State Examination; MOCA, Montreal Cognitive Assessment; M, male; F, female.

TABLE 2 | Group-wise differences in the deep gray matter structures.

Structure	AD, mean ± SD	MCI, mean ± SD	NC, mean ± SD	*t*-Test (*p*-value)		
				AD-MCI	AD-NC	MCI-NC
L_NAc	316.5 ± 135.0	355.9 ± 126.2	443.3 ± 89.2	0.171	**0.003****	0.078
R_ NAc	215.7 ± 104.5	228.1 ± 105.0	322.6 ± 83.2	0.585	**0.003****	**0.010****
L_Hipp	2,583.5 ± 591.0	2,724.7 ± 544.9	3,166.8 ± 374.9	0.283	**0.001****	**0.020***
R_Hipp	2,652.4 ± 625.7	2,988.9 ± 493.7	3,283.6 ± 386.3	**0.012***	**0.001****	0.240
L_Put	3,395.1 ± 804.1	3,409.9 ± 466.9	3,923.5 ± 618.7	0.853	0.062	**0.038***
R_Put	3,415.8 ± 770.5	3,461.3 ± 591.0	3,847.9 ± 604.6	0.981	0.276	0.277
L_Thal	5,100.6 ± 650.5	5,033.1 ± 773.1	5,466.3 ± 534.6	0.592	0.352	0.145
R_Thal	4,833.0 ± 570.8	4,754.2 ± 687.0	5,152.1 ± 516.8	0.515	0.367	0.125

**p ≤ 0.05; ***p ≤ 0.01 using ANCOVA; FDR corrected for t-test and adjusted for normalized brain volume, age, and gender.*
Significant across and between-group differences are in bold.
L, left; R, right; NAc, nucleus accumbens; Hipp, hippocampus; Put, putamen; Thal, thalamus.

TABLE 3 | Association between volumes in deep gray matter structures and global clinical scores.

Structure	MMSE	MOCA
L_NAc	0.359 (0.002**)	0.382 (0.001**)
R_NAc	0.277 (0.024*)	0.324 (0.007**)
L_Hipp	0.389 (0.001**)	0.359 (0.001**)
R_Hipp	0.383 (0.001**)	0.369 (0.001**)
L_Put	0.103 (0.377)	0.078 (0.493)
R_Put	0.174 (0.139)	0.139 (0.232)
L_Thal	0.074 (0.522)	0.008 (0.945)
R_Thal	0.016 (0.888)	0.000 (0.998)

Results are presented as β-coefficient (p-values) based on linear regression model.
**p ≤ 0.05.*
***p ≤ 0.01.*

Vertex Analysis of Deep Gray Matter Structures

The results from vertex analysis are illustrated as probabilistic images that show the significant shape abnormalities within deep gray matter structures with $1 - p \geq 0.95$ ($p \leq 0.05$) in **Figure 2**. After controlling for age and gender, the surface abnormalities were located within bilateral hippocampi and NAc in AD, compared to NC group, and only shape alterations in the right hippocampus were found in AD, compared to MCI group. Specifically, significant shape differences were detected in the ventral part of left NAc (left ventral NAc) and right hippocampus (right ventral hippocampus), posterior part of right NAc (right posterior NAc), the dorsal–medial part of left hippocampus (left dorsal–medial hippocampus), and medial–ventral part of right thalamus (right medial–ventral thalamus) in AD when compared to NC. Less surface alterations were found in left hippocampus, right NAc, and left putamen in MCI, compared to NC without correction for the multiple comparisons, while these alterations did not survive under FDR correction. **Figure 3** shows the location of shape abnormalities using MNI coordinates of COG (colored in yellow).

Relationship between Regional Shape Alterations and Clinical Measures

Figure 4 shows correlations between shape alterations of deep gray matter structures and clinical measures of MMSE and MOCA within the whole sample. MMSE scores were associated with shape abnormalities in bilateral hippocampi, left NAc, and right thalamus, whereas MOCA scores were associated with shape abnormalities in bilateral hippocampi, NAc, and thalami. The localization of subregional alterations and their correlation with MMSE and MOCA scores is shown in **Table 4**. It can be observed that the left dorsal–medial hippocampus, the right ventral hippocampus, the left ventral NAc, and the right medial–ventral thalamus significantly correlated with MMSE and MOCA, while the right posterior NAc and the medial–ventral part of the left thalamus only correlated with MOCA. Notably, compared with NC, these results are quite consistent with the atrophy regions found in AD groups, which are shown in **Figures 2** and **3**.

DISCUSSION

In this study, we assessed the pattern of subregional structural alterations in deep gray matter structures in AD and MCI patients. Compared with NC, we found that among all seven pairs of structures, the bilateral hippocampi and NAc showed significant atrophy in AD. But only the atrophy in the left dorsal-medial hippocampus, the right ventral hippocampus, the left ventral NAc and the right posterior NAc correlated with the worse global clinical scores. These results suggested that the atrophy of these four subregions in bilateral hippocampi and NAc was associated with clinical impairment in MCI and AD patients, which might be useful in diagnosis, evaluation and management of AD. Furthermore, compared with NC, the volume of bilateral thalami did not significantly decrease in AD patients, but the significant atrophy was observed in the right medial-ventral thalamus and correlated with global clinical scores by using surface analysis. These results implied that the surface analysis could provide additional information for volume comparison in finding the early pathological progress.

It is well known that hippocampus plays an important role in spatial, semantic, and episodic memory, which are generally impaired in AD and MCI patients (29–32). Numerous studies indicated that hippocampal atrophy contributes to memory impairment in patients with AD (33–38). Recent studies in AD found that obvious atrophy in hippocampal CA1, especially in MCI patients who converted to AD over time (37, 38). In the current study, we found that hippocampal atrophy and its

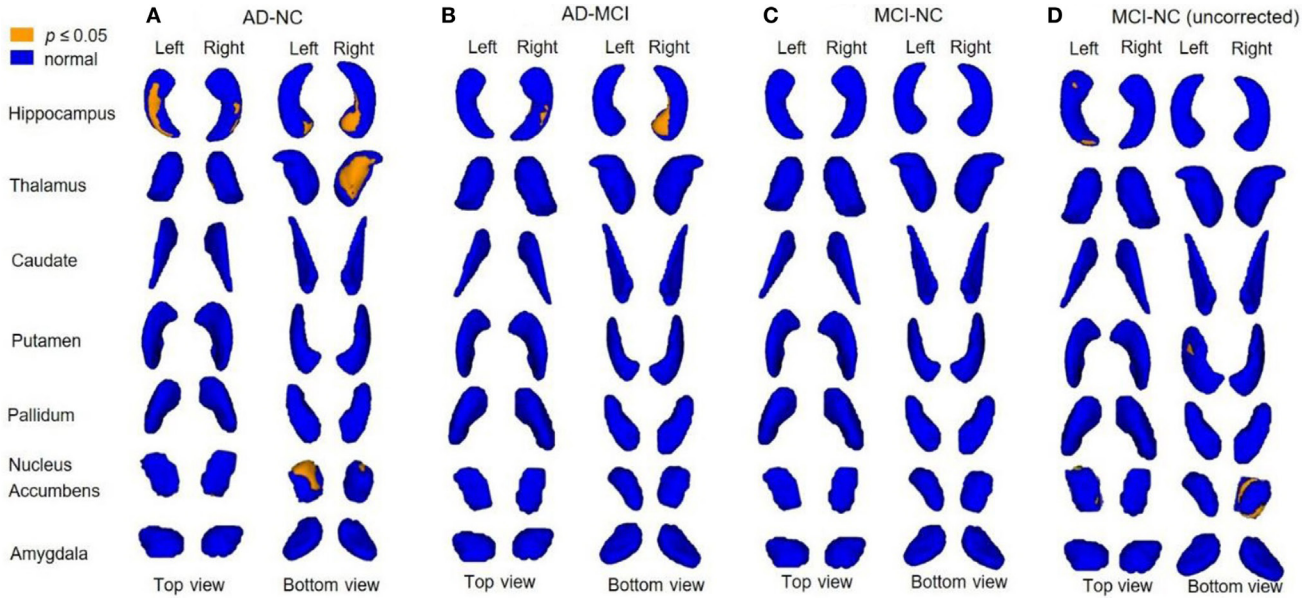


FIGURE 2 | Analysis of covariance (ANCOVA) of between-group shape differences. 3D rendering of 1 – *p* value images with vertex analysis between-group comparisons showing the subregional changes (yellow color coded) of deep gray matter structures [adjusted for age and gender; *p*-value corrected for multiple comparisons using false discovery rate (FDR)]. Shape alterations are seen in Alzheimer's disease (AD) compared to normal control (NC) **(A)** in bilateral hippocampi, bilateral nucleus accumbens (NAc), right thalamus; AD compared to mild cognitive impairment (MCI) **(B)** in right hippocampus; MCI showed no significant alteration compared to NC after FDR corrected **(C)**, while there are alterations found in left hippocampus, right NAc, and left putamen before FDR corrected **(D)**.

correlation with global clinical scores. Moreover, vertex analysis showed a alteration in the right ventral hippocampus and the left dorsal-medial hippocampus. This result is in line with a previous report that hippocampal atrophy is not homogeneous across the various hippocampal subregions during the progression of AD (5, 39). The dorsal hippocampus has been studied extensively for its significant role in spatial working memory, especially when processing the short-term spatial memory (40). Fanselow and Dong reported that the dorsal hippocampus performs primarily cognitive functions, while the ventral hippocampus relates to stress, emotion, and affect (41). Other studies also indicated that loss of neurogenesis in the dorsal and ventral hippocampus was associated with the impaired cognitive function (42), and the ventral hippocampus supported working memory for odor information (43). Experiments in rats showed that dorsal-medial hippocampus plays a role in flexible, adaptive behavior, and cognitive processing, and rats with dorsal-medial hippocampus lesions suffered significant working memory deficits (44). In line with the previous studies, the significant correlation between the dorsal/ventral hippocampal shape distortion and the global clinical scores in our study also emphasized the critical role of these two hippocampal subregions in cognitive impairment in AD process. Besides, the subregional level atrophy in hippocampi, which is slightly in MCI patients, but dramatically deteriorated in AD, further supporting the concept that AD is generally converted from MCI. Therefore, treatment on dorsal/ventral hippocampus may be effective to prevent the progression of AD. Drug treatment upon reduction of memory consolidation in rats with impaired dorsal hippocampus indicated that morphine may prevent impairment of memory consolidation (45). Yiu et al. also reported that targeting CREB in the CA1 region of dorsal hippocampus may be a useful therapeutic strategy in treating humans with AD (46). The role of the ventral hippocampus in AD is still not clear. Since the stress management related to the ventral hippocampus is suggested as a useful intervention in early AD and MCI (47), the treatment on ventral hippocampus for AD still need to be explored. The measurement in hippocampal subregion might be useful in monitoring the effect of treatment or intervention on subregional level.

In addition to hippocampus, NAc participates in integrating the information involved in learning and executive function and is also related to the cognitive processing of aversion, motivation, pleasure, reward, and reinforcement learning (48, 49). NAc is part of the striatum and has close connections with both limbic structures of the hippocampus, the amygdala, and the prefrontal cortex. One previous research about late-onset Alzheimer's disease patients showed the significant reductions in NAc volumes (50). Some previous studies have shown that atrophy of NAc occurred in patients with AD (51, 52), while they failed to reveal its function in cognitive decline. In our study, our results were on par with these previous studies that the bilateral NAc were more atrophied in AD and MCI patients compared to NCs. Furthermore, we found the atrophy in NAc was correlated with MMSE and MOCA scores. These results suggested that in addition to hippocampus, the atrophy in bilateral NAc may also play an important role in clinical impairment in AD and MCI. The localized atrophy in NAc has been confirmed to be associated with apathy in Parkinson's disease, and the severity of apathy was correlated with morphological changes in this region (53). Comparably, the vertex analyses in our study found

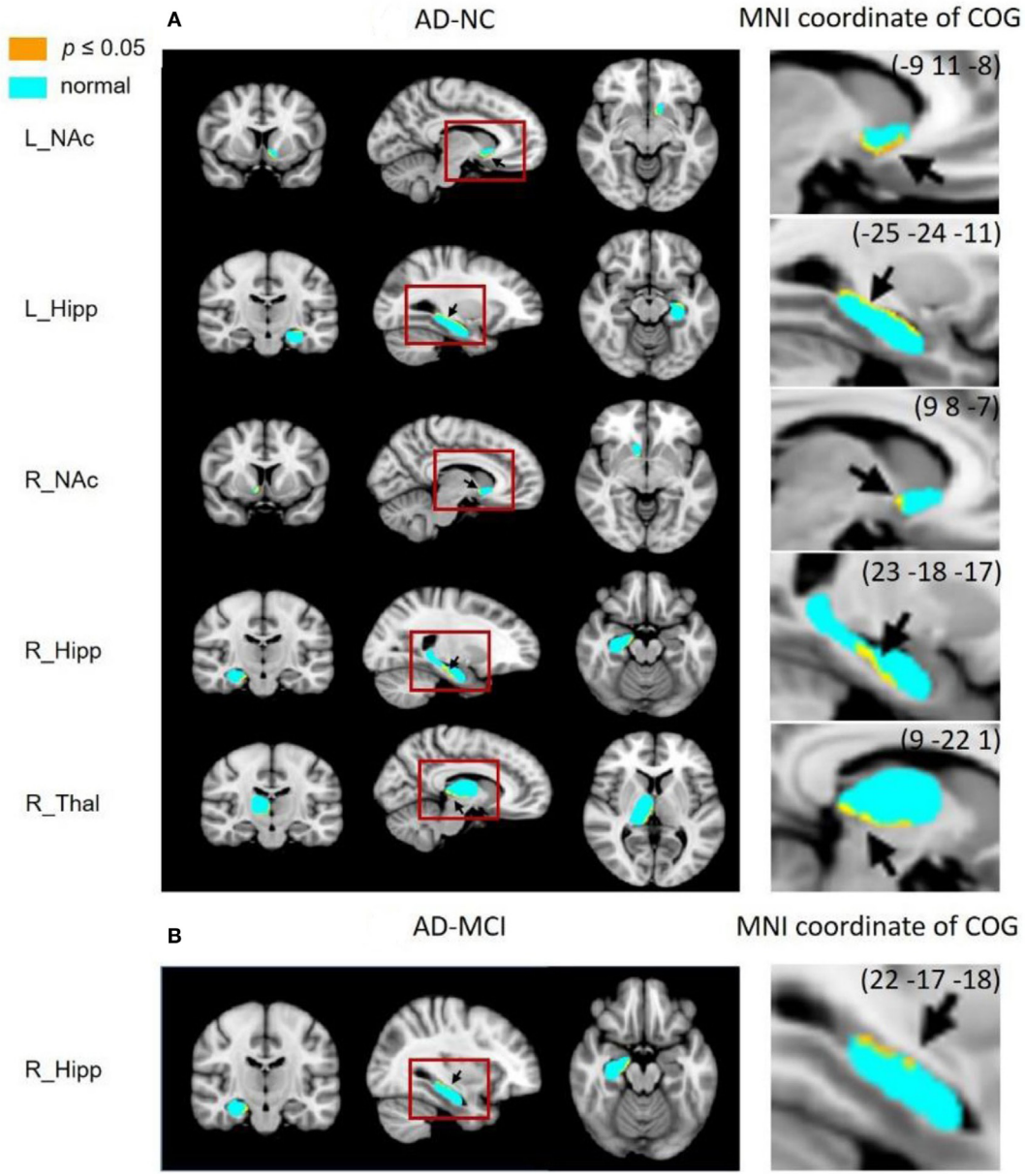


FIGURE 3 | Subregional surface alterations in hippocampus, nucleus accumbens (NAc), and thalamus, indicating the MNI coordinates of subregions where shape changes occurred (marked with an arrow). COG, center of gravity. **(A)** AD-NC and **(B)** AD-MCI.

that the atrophy of NAc and its association with clinical scores were both constrained within the ventral and posterior aspects in AD. Our results suggested that the ventral/posterior parts of NAc may involve in AD progression. However, few studies have explored the function of NAc in subregional level, especially its functions in AD or MCI, which need to be investigated in the future. A previous study reported that the deep brain stimulation of NAc could be a new treatment strategies to addiction (54). In the future, treatment like deep brain stimulation on subregional level of NAc may be considered for intervention in AD patients.

Some studies have revealed that other deep gray matter structures, such as amygdala, basal nuclei, and thalamus, also suffer atrophy in AD patients (55). Shape changes of ventricle system were reported in ventricular regions adjacent to amygdala, caudate nucleus, and thalamus in AD patients (56). MRI study showed strongly reduced volumes of putamen and thalamus in AD patients and this atrophy may contribute to cognitive impairment (10). Volumes of caudate and thalamus in familial AD reduced at a presymptomatic stage (57). It is well recognized that thalamus is essential for generating attention (58) and is involved as a subcortical hub in many different neuronal pathways related to emotional, motivational and cognitive abilities that are impaired in AD (6). To our knowledge, few studies have investigated the subregional atrophy and its relationship with

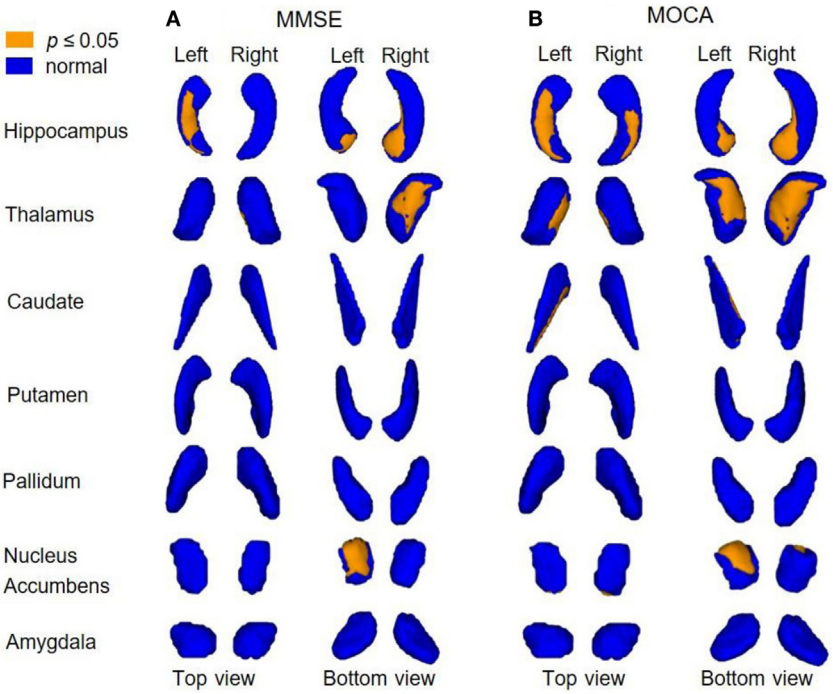


FIGURE 4 | Correlations between subregional shape alterations and global clinical scores. This 3D rendering of 1 – *p* value images shows the correlations (yellow color coded) between subregional atrophy and clinical scores (adjusted for age and gender; FDR corrected). Across the whole data cohort, correlations were observed **(A)** in hippocampi, left NAc, and right thalamus and MMSE scores; **(B)** in hippocampi, NAc, and thalami and MOCA scores.

TABLE 4 | Associations between subregional shape alterations and clinical measures (corresponding to the yellow areas in **Figure 4**).

Structure	L_NAc	R_NAc	L_Hipp	R_Hipp	L_Thal	R_Thal
MMSE	Ventral	–	Dorsal–medial	Ventral	–	Medial–ventral
MOCA	Ventral	Posterior	Dorsal–medial	Ventral	Medial–ventral	Medial–ventral

global clinical scores in thalami. Significant bilateral volumetric and subregional atrophy in the dorsal–medial part of the thalamus in AD patients has already been reported (10, 15). Another study found the subregional atrophy in the medial part of bilateral thalami (59), but not explored the relationship with clinical scores. Our study revealed significant shape abnormalities in the right medial-ventral thalamus in AD patients, but not found smaller volumes in bilateral thalami. Furthermore, the atrophy in right medial-ventral thalamus significantly correlated with MMSE and MOCA, suggesting that some parts of thalamus may be more vulnerable in AD and MCI. Our results suggest a specific atrophy pattern of the thalamus in AD and MCI, and also indicated that vertex-based (shape) analysis may provide additional and valuable information to popular volumetric analysis.

The main limitation of our study is that, although we adjusted our analysis for age, gender, and NBV, relatively small group samples may have reduced the statistical power. Therefore, some counterintuitive results were also need to be further validated in the future. For example, the putamen volume was significantly different between MCI and NC, but not between AD and NC. Furthermore, this was a cross-sectional study, and so it was difficult to judge whether atrophy of specific deep gray matter structures was a primary or secondary phenomenon to the hippocampal or entorhinal cortex. Therefore, further and preferable longitudinal investigations are needed to confirm the relationship between clinical and cognitive decline and the subregional atrophy patterns.

CONCLUSION

Based both on volumetric and vertex-based (shape) analysis of deep gray matter structures, this study showed that atrophy of deep gray matter structures in AD and MCI patients occurs at subregional level even when the volume of the whole given structure is not reduced. And this subregional atrophy within hippocampi and NAc correlates with worse global clinical scores. Atrophy measurement on subregional level may be useful in early diagnosis and management of AD patients or in evaluation of the treatment strategies.

AUTHOR CONTRIBUTIONS

XLN, YS, and SRW contributed to this article equally, being responsible for the image procession, data analysis, and writing the article. HZ, RYL, XPL, and SCW are responsible for the MRI acquisition and data collection; ZN, JH, ZQ, and YX give advice on how to do the data analysis and modify the article. BZ put forward the research ideas and guide the whole study.

ACKNOWLEDGMENTS

This work was supported by the National Natural Science Foundation of China (91649116, 81571040, and 81471643), Jiangsu province key medical talents, "13th Five-Year" health promotion project of Jiangsu province (BZ.2016-2020), Social development project of science and technology project in Jiangsu Province (BE2016605), the National and Provincial postdoctoral project (BE179 and 1501076A, BZ), the key project of Nanjing Health Bureau (ZKX14027, BZ), Nanjing science and technology development program (NE179, BZ), Jiangsu Provincial Key Medical Discipline (Laboratory) (ZDXKA2016020, XY), and Jiangsu Provincial KeyMedical Discipline (Laboratory) (ZDXKA2016020). ZN and JH are supported by the project no. LQ1605 from the National Program of Sustainability II (MEYS CR) and ZN is supported by "Nadani" Foundation and Czech Alzheimer Foundation. The funders had no role in study design, data collection and analysis, decision to publish, or preparation of the manuscript.

REFERENCES

1. Schott J, Kennedy J, Fox N. New developments in mild cognitive impairment and Alzheimer's disease. *Curr Opin Neurol* (2006) 19:552–8. doi:10.1097/01.wco.0000247611.44106.76
2. Yaari R, Corey-Bloom J. Alzheimer's disease. *Semin Neurol* (2007) 27:32–41. doi:10.1055/s-2006-956753
3. Petersen RC, Doody R, Kurz A, Mohs R, Morris J, Rabins P, et al. Current concepts in mild cognitive impairment. *Arch Neurol* (2001) 58:1985–92. doi:10.1001/archneur.58.12.1985
4. Peterson RC. Mild cognitive impairment: current research and clinical implications. *Semin Neurol* (2007) 27:22–31. doi:10.1055/s-2006-956752
5. Carlesimo GA, Piras F, Orfei MD, Iorio M, Caltagirone C, Spalletta G. Atrophy of presubiculum and subiculum is the earliest hippocampal anatomical marker of Alzheimer's disease. *Alzheimers Dement* (2015) 1:24–32. doi:10.1016/j.dadm.2014.12.001
6. Herrero MT, Barcia C, Navarro JM. Functional anatomy of thalamus and basal ganglia. *Childs Nerv Syst* (2002) 18:386–404. doi:10.1007/s00381-002-0604-1
7. Rugg MD, Yonelinas AP. Human recognition memory: a cognitive neuroscience perspective. *Trends Cogn Sci* (2003) 7:313–9. doi:10.1016/S1364-6613(03)00131-1
8. Fox NC, Freeboroug PA. Brain atrophy progression measured from registered serial MRI: validation and application to Alzheimer's disease. *J Magn Reson Imaging* (1997) 7:1069–75. doi:10.1002/jmri.1880070620
9. Gerardin E, Chételat G, Chupin M, Cuingnet R, Desgranges B, Kim H, et al. Multidimensional classification of hippocampal shape features discriminates Alzheimer's disease and mild cognitive impairment from normal aging. *Neuroimage* (2009) 47:1476–86. doi:10.1016/j.neuroimage.2009.05.036
10. de Jong LW, van der Hiele K, Veer IM, Houwing JJ, Westendorp RG, Bollen EL, et al. Strongly reduced volumes of putamen and thalamus in Alzheimer's disease: an MRI study. *Brain* (2008) 131:3277–85. doi:10.1093/brain/awn278
11. Scheltens P, Leys D, Barkhof F, Huglo D, Weinstein H, Vermersch P, et al. Atrophy of medial temporal lobes on MRI in "probable" Alzheimer's disease and normal ageing: diagnostic value and neuropsychological correlates. *J Neurol Neurosurg Psychiatry* (1992) 55:967–72. doi:10.1136/jnnp.55.10.967
12. Stoub TR, Bulgakova M, Leurqans S, Bennett DA, Fleischman D, Turner DA, et al. MRI predictors of risk of incident Alzheimer disease: a longitudinal study. *Neurology* (2005) 64:1520–4. doi:10.1212/01.WNL.0000160089.43264.1A
13. Alves GS, O'Dwyer L, Jurcoane A, Oertel-Knöchel V, Knöchel C, Prvulovic D, et al. Different patterns of white matter degeneration using multiple diffusion indices and volumetric data in mild cognitive impairment and Alzheimer patients. *PLoS One* (2012) 7:e52859. doi:10.1371/journal.pone.0052859
14. Cheng WC, Cheng PE, Liou M. Group factor analysis for Alzheimer's disease. *Comput Math Methods Med* (2013) 2013:1–8. doi:10.1155/2013/830237
15. Zarei M, Patenaude B, Damoiseaux J, Morgese C, Smith S, Matthews PM, et al. Combining shape and connectivity analysis: an MRI study of thalamic degeneration in Alzheimer's disease. *Neuroimage* (2010) 49:1–8. doi:10.1016/j.neuroimage.2009.09.001
16. Patenaude B, Smith SM, Kennedy DN, Jenkinson M. A Bayesian model of shape and appearance for subcortical brain segmentation. *Neuroimage* (2011) 56:907–22. doi:10.1016/j.neuroimage.2011.02.046
17. Qiu A, Fennema-Notestine C, Dale AM, Miller MI. Regional shape abnormalities in mild cognitive impairment and Alzheimer's disease. *Neuroimage* (2009) 45:656–61. doi:10.1016/j.neuroimage.2009.01.013
18. Jenkinson M, Beckmann CF, Behrens TEJ, Woolrich MW, Smith SM. FSL. *Neuroimage* (2012) 62:782–90. doi:10.1016/j.neuroimage.2011.09.015
19. Nugent AC, Luckenbaugh DA, Wood SE, Bogers W, Zarate CA, Drevets WC. Automated subcortical segmentation using FIRST: test-retest reliability, interscanner reliability, and comparison to manual segmentation. *Hum Brain Mapp* (2013) 34:2313–29. doi:10.1002/hbm.22068
20. Folstein MF, Folstein SE, McHugh PR. Mini-mental state: a practical method for grading the cognitive state of patients for the clinician. *J Psychiatr Res* (1975) 12:189–98. doi:10.1016/0022-3956(75)90026-6
21. Smith T, Gildeh N, Holmes C. The Montreal Cognitive Assessment: validity and utility in a memory clinic setting. *Can J Psychiatry* (2007) 52:329–32. doi:10.1177/070674370705200508
22. Winblad B, Palmer K, Kivipelto M, Jelic V, Fratiglioni L, Wahlund LO, et al. Mild cognitive impairment-beyond controversies, towards a consensus: report of the International Working Group on mild cognitive impairment. *J Intern Med* (2004) 256:240–6. doi:10.1111/j.1365-2796.2004.01380.x
23. McKhann G, Drachman D, Folstein M, Katzman R, Price D, Stadlan EM. Clinical diagnosis of Alzheimer's disease: report of the NINCDS–ADRDA work group under the auspices of department of health and human services task force on Alzheimer's disease. *Neurology* (1984) 34:939–44. doi:10.1212/WNL.34.7.939
24. Smith SM, Jenkinson M, Woolrich MW, Beckmann CF, Behrens TEJ, Johansen-Berg H, et al. Advances in functional and structural MR image analysis and implementation as FSL. *Neuroimage* (2004) 23:S208–19. doi:10.1016/j.neuroimage.2004.07.051
25. Smith SM. Fast robust automated brain extraction. *Hum Brain Mapp* (2002) 17:143–55. doi:10.1002/hbm.10062
26. Jenkinson MBP, Brady M, Smith S. Improved optimization for the robust and accurate linear registration and motion correction of brain images. *Neuroimage* (2002) 17:825–41. doi:10.1006/nimg.2002.1132
27. Smith SM, Zhang Y, Jenkinson M, Chen J. Accurate, robust and automated longitudinal and cross-sectional brain change analysis. *Neuroimage* (2002) 17:479–89. doi:10.1006/nimg.2002.1040
28. Winkler AM, Ridgway GR, Webster MA, Smith SM, Nichols TE. Permutation inference for the general linear model. *Neuroimage* (2014) 92:381–97. doi:10.1016/j.neuroimage.2014.01.060
29. Cohen NJ, Eichenbaum H. *Memory, Amnesia, and the Hippocampal System*. Massachusetts: MIT Press (1993).
30. Squire LR, Schacter DL. *The Neuropsychology of Memory*. New York: Guilford Press (2002).
31. Mavrogiorgou P, Gertz HJ, Ferszt R, Wolf R, Bär KJ, Juckel G. Are routine methods good enough to stain senile plaques and neurofibrillary tangles in different brain regions of demented patients. *Psychiatr Danub* (2011) 23:334–9.
32. Wood R, Chan D. The hippocampus, spatial memory and Alzheimer's disease. *ACNR* (2015) 15:5–7.
33. Dubois B, Feldman HH, Jacova C, Dekosky ST, Barberger-Gateau P, Cummings J, et al. Research criteria for the diagnosis of Alzheimer's disease: revising the NINCDS-ADRDA criteria. *Lancet Neurol* (2007) 6:734–46. doi:10.1016/S1474-4422(07)70178-3
34. Chetelat G, Baron JC. Early diagnosis of Alzheimer's disease: contribution of structural neuroimaging. *Neuroimage* (2003) 18:525–41. doi:10.1016/S1053-8119(02)00026-5
35. de Leon MJ, Convit A, DeSanti S, Golomb J, Tarshish C, Rusinek H, et al. The hippocampus in aging and Alzheimer's disease. *Neuroimag Clin N Am* (1995) 5:1–17.

36. Laakso MP, Soininen H, Partanen K, Helkala EL, Hartikainen P, Vainio P, et al. Volumes of hippocampus, amygdala and frontal lobes in the MRI-based diagnosis of early Alzheimer's disease: correlation with memory functions. *J Neural Transm Park Dis Dement Sect* (1995) 9:73–86. doi:10.1007/BF02252964
37. Tang X, Holland D, Dale AM, Younes L, MI M. The diffeomorphometry of regional shape change rates and its relevance to cognitive deterioration in mild cognitive impairment and Alzheimer's disease. *Hum Brain Mapp* (2015) 36:2093–117. doi:10.1002/hbm.22758
38. Tang X, Holland D, Dale AM, Younes L, Miller M. Shape abnormalities of subcortical and ventricular structures in mild cognitive impairment and Alzheimer's disease: detecting, quantifying, and predicting. *Hum Brain Mapp* (2014) 35:3701–25. doi:10.1002/hbm.22431
39. Wachinger C, Salat DH, Weiner M, Reuter M. Whole-brain analysis reveals increased neuroanatomical asymmetries in dementia for hippocampus and amygdala. *Brain* (2016) 139:3253–66. doi:10.1093/brain/aww243
40. Lee I, Kesner RP. Time-dependent relationship between the dorsal hippocampus and the prefrontal cortex in spatial memory. *J Neurosci* (2003) 23:1517–23.
41. Fanselow MS, Dong HW. Are the dorsal and ventral hippocampus functionally distinct structures. *Neuron* (2010) 65:7–19. doi:10.1016/j.neuron.2009.11.031
42. Vetreno RP, Crews FT. Binge ethanol exposure during adolescence leads to a persistent loss of neurogenesis in the dorsal and ventral hippocampus that is associated with impaired adult cognitive functioning. *Front Neurosci* (2015) 9:35. doi:10.3389/fnins.2015.00035
43. Kesner R, Hunsaker M, Ziegler W. The role of the dorsal and ventral hippocampus in olfactory working memory. *Neurobiol Learn Mem* (2011) 96:361–6. doi:10.1016/j.nlm.2011.06.011
44. Sahina H. *Lesions of the Dorsal Medial Hippocampus Induce Different Forms of Repetitive Behaviour in the Rat*. New Zealand: University of Canterbury (2015).
45. Zarrindast MR, Navaeian M, Nasehi M. Influence of three-day morphine-treatment upon impairment of memory consolidation induced by cannabinoid infused into the dorsal hippocampus in rats. *Neurosci Res* (2011) 69:51–9. doi:10.1016/j.neures.2010.09.007
46. Yiu AP, Rashid AJ, Josselyn SA. Increasing CREB function in the CA1 region of dorsal hippocampus rescues the spatial memory deficits in a mouse model of Alzheimer's disease. *Neuropsychopharmacology* (2011) 36:2169–86. doi:10.1038/npp.2011.107
47. Lombardo NBE, Wu B, Volicer L, Martin A, Serper LL, Zhang XW. Evidence based nutrition, exercise, cognitive rehabilitation & stress management interventions for Alzheimer's disease: treatment or prevention? *Neurobiol Aging* (2004) 25:S206–7. doi:10.1016/S0197-4580(04)80692-4
48. Nestler E, Hyman S, Malenka R. *Molecular Neuropharmacology: A Foundation for Clinical Neuroscience*. 2nd ed. New York, NY: McGraw-Hill Professional (2015).
49. Wenzel JM, Rauscher NA, Cheer JF, Oleson EB. A role for phasic dopamine release within the nucleus accumbens in encoding aversion: a review of the neurochemical literature. *ACS Chem Neurosci* (2015) 6:16–26. doi:10.1021/cn500255p
50. Pievani M, Bocchetta M, Boccardi M, Cavedo E, Bonetti M, Thompson PM, et al. Striatal morphology in early-onset and late-onset Alzheimer's disease: a preliminary study. *Neurobiol Aging* (2013) 34:1728–39. doi:10.1016/j.neurobiolaging.2013.01.016
51. Hilal S, Amin SM, Venketasubramanian N, Niessen WJ, Vrooman H, Wong TY, et al. Subcortical atrophy in cognitive impairment and dementia. *J Alzheimer Dis* (2015) 48:813–23. doi:10.3233/JAD-150473
52. Möller C, Dieleman N, van der Flier WM, Versteeg A, Pijnenburg Y, Scheltens P, et al. More atrophy of deep gray matter structures in frontotemporal dementia compared to Alzheimer's disease. *J Alzheimers Dis* (2015) 44(2):635–47. doi:10.3233/JAD-141230
53. Carriere N, Besson P, Dujardin K, Duhamel A, Defebvre L, Delmaire C, et al. Apathy in Parkinson's disease is associated with nucleus accumbens atrophy: a magnetic resonance imaging shape analysis. *Mov Disord* (2014) 29:897–903. doi:10.1002/mds.25904
54. de Leon MJ, George AE, Stylopoulos LA, Smith G, Miller DC. Early marker for Alzheimer's disease: the atrophic hippocampus. *Lancet* (1989) 2:672–3. doi:10.1016/S0140-6736(89)90911-2
55. Cherubini A, Péran P, Spoletini I, Di Paola M, Di Iulio F, Hagberg GE, et al. Combined volumetry and DTI in subcortical structures of mild cognitive impairment and Alzheimer's disease patients. *J Alzheimers Dis* (2010) 19:1273–82. doi:10.3233/JAD-2010-091186
56. Ferrarini L, Palm WM, Olofsen H, van Buchem MA, Reiber JH, Admiraal-Behloul F. Shape differences of the brain ventricles in Alzheimer's disease. *Neuroimage* (2006) 32:1060–9. doi:10.1016/j.neuroimage.2006.05.048
57. Ryan NS, Keihaninejad S, Shakespeare TJ, Lehmann M, Crutch SJ, Malone IB, et al. Magnetic resonance imaging evidence for presymptomatic change in thalamus and caudate in familial Alzheimer's disease. *Brain* (2013) 136:1399–414. doi:10.1093/brain/awt065
58. Newman J. Thalamic contributions to attention and consciousness. *Conscious Cogn* (1995) 4:172–93. doi:10.1006/ccog.1995.1024
59. Cho H, Kim J, Kim C, Ye B, Kim H, Yoon C, et al. Shape changes of the basal ganglia and thalamus in Alzheimer's disease: a three-year longitudinal study. *J Alzheimers Dis* (2014) 40:285–95. doi:10.3233/JAD-132072

Conflict of Interest Statement: The authors declare that the research was conducted in the absence of any commercial or financial relationships that could be construed as a potential conflict of interest.

Copyright © 2017 Nie, Sun, Wan, Zhao, Liu, Li, Wu, Nedelska, Hort, Qing, Xu and Zhang. This is an open-access article distributed under the terms of the Creative Commons Attribution License (CC BY). The use, distribution or reproduction in other forums is permitted, provided the original author(s) or licensor are credited and that the original publication in this journal is cited, in accordance with accepted academic practice. No use, distribution or reproduction is permitted which does not comply with these terms.

frontiers in Aging Neuroscience

MINI REVIEW
published: 01 November 2017
doi: 10.3389/fnagi.2017.00356

Perspective Insights into Disease Progression, Diagnostics, and Therapeutic Approaches in Alzheimer's Disease: A Judicious Update

Arif Tasleem Jan[1†‡], Mudsser Azam[2‡], Safikur Rahman[1], Angham M. S. Almigeiti[1], Duk Hwan Choi[1], Eun Ju Lee[1], Qazi Mohd Rizwanul Haq[2] and Inho Choi[1]*

[1] Department of Medical Biotechnology, Yeungnam University, Gyeongsan, South Korea, [2] Department of Biosciences, Jamia Millia Islamia, New Delhi, India

Alzheimer's disease (AD) is a neurodegenerative disorder characterized by the progressive accumulation of β-amyloid fibrils and abnormal tau proteins in and outside of neurons. Representing a common form of dementia, aggravation of AD with age increases the morbidity rate among the elderly. Although, mutations in the ApoE4 act as potent risk factors for sporadic AD, familial AD arises through malfunctioning of APP, PSEN-1, and−2 genes. AD progresses through accumulation of amyloid plaques (Aβ) and neurofibrillary tangles (NFTs) in brain, which interfere with neuronal communication. Cellular stress that arises through mitochondrial dysfunction, endoplasmic reticulum malfunction, and autophagy contributes significantly to the pathogenesis of AD. With high accuracy in disease diagnostics, Aβ deposition and phosphorylated tau (p-tau) are useful core biomarkers in the cerebrospinal fluid (CSF) of AD patients. Although five drugs are approved for treatment in AD, their failures in achieving complete disease cure has shifted studies toward a series of molecules capable of acting against Aβ and p-tau. Failure of biologics or compounds to cross the blood-brain barrier (BBB) in most cases advocates development of an efficient drug delivery system. Though liposomes and polymeric nanoparticles are widely adopted for drug delivery modules, their use in delivering drugs across the BBB has been overtaken by exosomes, owing to their promising results in reducing disease progression.

Keywords: Alzheimer's disease, diagnostics, drugs, neurodegeneration, therapeutics

OPEN ACCESS

Edited by:
Ghulam Md Ashraf, King Abdulaziz University, Saudi Arabia

Reviewed by:
Cláudia Fragão Pereira, University of Coimbra, Portugal
Victoria Campos-Peña, Instituto Nacional de Neurología y Neurocirugía, Mexico

***Correspondence:**
Inho Choi
inhochoi@ynu.ac.kr

***Present Address:**
Arif Tasleem Jan, School of Biosciences and Biotechnology, Baba Ghulam Shah Badshah University, Rajouri, India

These authors have contributed equally to this work.

Received: *19 June 2017*
Accepted: *18 October 2017*
Published: *01 November 2017*

Citation:
Jan AT, Azam M, Rahman S, Almigeiti AMS, Choi DH, Lee EJ, Haq QMR and Choi I (2017) Perspective Insights into Disease Progression, Diagnostics, and Therapeutic Approaches in Alzheimer's Disease: A Judicious Update. Front. Aging Neurosci. 9:356. doi: 10.3389/fnagi.2017.00356

INTRODUCTION

Alzheimer's disease (AD) is recognized as a disease of neurons and neuronal circuits. It arises as a result of progressive accumulation of β-amyloid fibrils (β-amyloid plaques) and abnormal forms of tau (tau tangles) within and outside of neurons (Jucker and Walker, 2013; Jaunmuktane et al., 2015). Approximately 46.8 million people over the age of 60 years have been diagnosed with AD worldwide (Prince et al., 2016). Though occurrence of the early onset of dementia is <1% per 4,000 individuals, the projected figure is estimated to be 131.5 million in 2050 (Prince et al., 2016). The projected increase in the prevalence of dementia is substantially higher in developing countries

than in the USA and Europe, which already have a high proportion of older individuals in their populations. The Alzheimer's Association presented an estimate of 5.5 million people suffering from AD in the USA, and the incidence of AD in the USA is projected to be 7.7 millions in 2030 and 11–16 millions in 2050 (ADFF, 2016).

The pathology of AD begins well before symptom manifestation, with intracellular accumulation of neurofibrillary tangles that arise via abnormal tau protein phosphorylation and extracellular deposition of Aβ-plaques (Selkoe, 1994, 2001a,b). Interfering with neuronal communication, deposition of β-amyloid plaques causes neuronal death, while tau tangles Blocks transport of essentials into interior of the neurons. Characterized by progressive memory loss and cognitive impairment, advanced stage AD patients show symptoms ranging from neuron inflammation to neuron death. Various risk factors promote pathological changes well before the onset of clinical symptoms of AD. In addition to cardiovascular risk, studies suggest a significant contribution of lifestyle related factors such as obesity, diabetes, depression, smoking, and insufficient diet in dementia. This review presents an overview of AD with recent updates on epidemiology, factors that aggravate the disease, and a prospective insight into diagnostic markers and therapeutic options for disease treatment.

GENETIC SUSCEPTIBILITY

AD represents one of the greatest health-care challenges of the twenty-first century. Its dependence on age and genetic background has resulted in its classification as either familial (FAD; showing early onset), which is observed in 5% of AD cases, or sporadic (SAD; showing late disease onset), which shows a high disease incidence rate. Though ApoE4 is a well-characterized risk factor in SAD, disease etiology in FAD is attributed to mutations of *amyloid precursor protein* (APP), *presenilin*1 (PS1), and *presenilin* 2 (PS2) genes (Goate et al., 1991; Levy-Lahad et al., 1995; Rogaev et al., 1995; Sherrington et al., 1996; Selkoe, 2001b). Accounting for 15% of total ApoE, APOE4 interferes with the clearance of Aβ from brain. Differing in amino acid substitutions at 112 and 158 positions, ApoE4 carries two arginines, while ApoE3 have two cysteines and ApoE2 has arginine and cysteine at these positions (Mahley and Huang, 2009). Attribution of APOE4 to AD is 50% in homozygous (Apo E4/E4) and 20–30% in heterozygous condition with APOE3 (Genin et al., 2011).

Over the time, substantial evidences regarding accumulation of misfolded Aβ and tau tangles (so-called seeds of pathological consequences) in the brain of patients suffering from AD have been established (Karran et al., 2011). Evidential support of Aβ and tau involvement comes from FAD studies that report mutations in APP (Aβ precursor) and PS1&2 (catalytic γ-secretase subunit; Karch and Goate, 2015; Ahmad et al., 2016). Having a critical role in the multi-causality of dementia (Boyle et al., 2013), mutations in APP enhance aggregation, while PSEN1&2 mutations cause less efficient APP processing, leading to longer and more hydrophobic Aβs (Scheuner et al., 1996; Chávez-Gutiérrez et al., 2012; Wong et al., 2013; **Table 1**). Though mutations in APP and PS1&2 accelerate generation of disease seeds, decreased Aβ clearance (Mawuenyega et al., 2010) and increased Aβ accumulation (Wahlster et al., 2013) enhances SAD.

MITOCHONDRIAL STRESS IN AD

Performing vital biochemical functions, mitochondrial dysfunction significantly affects progression in the pathogenesis of AD (Swerdlow et al., 2014). Associated with the regulation of cellular metabolism, functional impairment of metabolic enzymes, in particular enzymes of the TCA cycle, causes reduction in the energy metabolism in brain (Huang et al., 2003; Bubber et al., 2005). Studies of the AD brain have revealed significant impairment in the functioning of pyruvate dehydrogenase complex (PDHC) and α-ketoglutarate dehydrogenase complex (KGDHC) enzymes, followed by impairment of isocitrate dehydrogenase (Huang et al., 2003; Bubber et al., 2005). Although, increased activity of succinate and malate dehydrogenases was observed, activities of the remaining four enzymes remains unaltered. Considering the high energy demand of neurons, a role of mitochondrial oxidative stress leading to energy imbalance appears to have a considerable effect on neurodegeneration.

Mitochondrial dysfunction, observed as altered mitochondrial DNA and increased cytochrome oxidase (COX) levels, indicates oxidative damage to the neurons of AD patients (Hirai et al., 2001; Nunomura et al., 2001; Moreira et al., 2006, 2007, 2009; Su et al., 2008). In concert with the amyloid hypothesis, altered APP processing increases Aβ deposition (Furukawa et al., 1996), whose aggregation causes oxidative stress through an increase in the production of H_2O_2 (Readnower et al., 2011). Inhibition of the mitochondrial electron transport chain (ETC) causes increased ROS production, which damages proteins, lipids, and nucleic acids, observed as increases in 8-hydroxy-2-deoxyguanosine (8-OHdG) and nitrotyrosine levels (Wang et al., 2005). Accumulation of Aβ in the synaptic mitochondria makes them susceptible to changes in synaptic Ca^{2+} as they have high levels of cyclophilin D (CypD; Sayre et al., 2005). Being a component of the mitochondrial permeability transition pore (mPTP), CypD translocation from matrix to mPTP increases interaction of CypD-mPTP with adenine nucleotide translocase resulting in opening of the pore and as such collapse of membrane potential, which ultimately leads to neuronal death (Juhaszova et al., 2004). An increase in the oxidative burden of mitochondria mediates activation of FoxO transcription factor (Kops et al., 2002; Fu and Tindall, 2008), which is associated with induction of SOD and catalase activity, as well as causing cell cycle arrest and cell death (Castellani et al., 2002). Increased ROS attenuation of the antioxidant arsenal of mitochondria alters the cellular redox state. Increased ROS levels act as an autophagy trigger and subjects mitochondria to mitophagy (Scherz-Shouval and Elazar, 2011).

TABLE 1 | Summary of mutations predicted in genes that have been associated with the occurrence of AD.

S. No	Gene	No. of mutations	Mutation type	Representation	Location	Effect
1.	APP	52	Point, Missense, Silent, Deletion	Both coding & non-coding	Exon 5 = 1 Exon 6 = 3 Exon 7 = 2 Exon 11 = 2 Exon 12 = 2 Exon 13 = 2 Exon 14 = 4 Exon 16 = 10 Exon 17 = 25 Non-coding = 1	Pathogenic = 1 Not-pathogenic = 15 Unclear pathogenicity = 9 Protective = 1
2.	MAPT	15	Point, Missense, Deletion	Both coding & non-coding	Exon 1 = 2 Exon 3 = 1 Exon 4a = 5 Exon 6 = 1 Exon 7 = 1 Exon 8 = 1 Exon 10 = 2 Non-coding = 1 *In silico* = 1	Pathogenic = 0 Not-pathogenic = 5 Unclear pathogenicity = 10 Risk modifier = 1
3.	PSEN1	241	Point, Missense, Insertion, Deletion, Complex	Both coding & non-coding (Intron)	Exon 4 = 22 Exon 5 = 46 Exon 6 = 27 Exon 7 = 56 Exon 8 = 36 Exon 9 = 7 Exon 10 = 7 Exon 11 = 22 Exon 12 = 17 Intron = 1	Pathogenic = 223 Not-pathogenic = 3 Unclear pathogenicity = 16
4.	PSEN 2	45	Point, Missense, Insertion, Deletion	Coding	Exon 3 = 2 Exon 4 = 8 Exon 5 = 12 Exon 6 = 3 Exon 7 = 11 Exon 8 = 1 Exon 9 = 1 Exon 10 = 3 Exon 11 = 2 Exon 12 = 2	Pathogenic = 18 Not-pathogenic = 12 Unclear pathogenicity = 15

ENDOPLASMIC RETICULUM (ER) STRESS IN AD

Acting as a site of protein synthesis, disruption in the proteostasis causes accumulation of unfolded proteins in the ER lumen (Wu and Kaufman, 2006; Ron and Walter, 2007). To reduce abnormal protein aggregation, unfolded proteins are translocated to cytoplasm for degradation; a process referred as ER-associated protein degradation (ERAD; Hetz et al., 2011; Walter and Ron, 2011). Attainment of saturation in the ER's protein-folding capacity elicits a dynamic signaling response referred as unfolded protein response (UPR; Lee, 2001; Ledoux et al., 2003). Recognition of unfolded proteins by stress sensors such as inositol requiring protein 1 (IRE1), protein kinase RNA (PKR) like ER kinase (PERK), and activating transcription factor 6 (ATF6) triggers downstream signaling via transcription factors (Hetz and Mollereau, 2014). PERK induces rapid translational attenuation by inhibition of the eukaryotic translational initiation factor 2α (eIF2α). PERK-mediated phosphorylation of eIF2α also favors translation of transcription factor ATF4, which is capable of controlling expression of genes related to amino acid metabolism, autophagy, and apoptosis. Increased phosphorylation of eIF2α in PS1 mutant knockout mice confirmed the inhibition of eIF2α phosphorylation by PS1 (Milhavet et al., 2002). Additionally, PS1-mediated abnormal processing of IRE1 disturbs UPR by interfering with the ER stress. Activation of IRE1 signaling induces splicing of X-box binding protein 1 (XBP-1), which controls the expression of lipid synthesis, ER protein translocation, protein folding, and ERAD genes (Hetz et al., 2011; Walter and Ron, 2011). Polymorphism in the promoter region of XBP-1, which reduces its transcription, is considered as a risk factor for AD (Liu

et al., 2013). Expression of GPR78 and GPR94 associated with the refolding of unfolded proteins attenuated in PS2-expressed cells is attributed to impaired IRE1 phosphorylation. Though protection against Aβ toxicity through enforced *Xbp1* expression in a *Drosophila melanogaster* AD model is attributed to reduction in the release of Ca^{2+} from ER (Casas-Tinto et al., 2011), a similar effect in *Caenorhabditis elegans* AD model is correlated with augmented stress levels and enhanced autophagy (Safra et al., 2013). Nuclear translocation of ATF6 following protease cleavage activates ERAD genes and XBP-1. Moreover, ATF4, ATF6, and XBP-1 stimulate C/EBP homologous protein (CHOP) and its target growth arrest and DNA damage inducible 34 (GADD34), as well as pro-apoptotic components of the B cell lymphoma-2 (BCL2) family of proteins (Xu et al., 2005). Neurons expressing p-tau show enhanced UPR activation (Hoozemans et al., 2009; Abisambra et al., 2013). Excessive adaptive capacity of UPR triggers pro-apoptotic events through upregulation of the cell death genes such as caspase-12 (Szegezdi et al., 2003).

AUTOPHAGY IN AD

Degradation of non-essential cellular components, such as misfolded and aggregated proteins, occurs through the autophagy-lysosomal system (ALS; Li et al., 2010; Murrow and Debnath, 2013). Activated by oxidative stress, nutrient starvation, etc., clearance of unwanted entities helps in restoring substrates for cellular remodeling (Ichimura and Komatsu, 2010; Li et al., 2010; Murrow and Debnath, 2013). Abundance of growth factors and cellular nutrients activates mTOR kinase, whereas a starvation state exerts inhibitory effect on mTOR kinase activity. The mTOR kinase-mediated phosphorylation of ATG13 prevents its association to Unc-51 like kinase (ULK), and recruitment of focal adhesion kinase family interacting protein of 200 kD (FIP200) inhibits autophagy, whereas inhibition of mTOR activates phosphatases that cause dephosphorylation of ATG13 (Kundu, 2011; Lee et al., 2012), thereby promotes autophagy. Although mTOR-dependent autophagy is prominent, there are reports of mTOR-independent autophagy mediated by (1) ATG5 and ATG7 via microtubule associated light chain 3-II (LC3-II; Nishida et al., 2009); (2) autophagic proteins Beclin1, Bcl-2, and ULK1 (Nishida et al., 2009; Shimizu et al., 2010); and (3) non-canonical signaling events involving Ca^{2+}. In addition, Ca^{2+} has a prominent role in both canonical and non-canonical mTOR-independent autophagy (Cárdenas and Foskett, 2012; Decuypere et al., 2013). Deletion of Beclin-1 in AD mouse models has resulted in increased Aβ accumulation, while its overexpression leads to reduction in amyloid pathology (Pickford et al., 2008; Jaeger and Wyss-Coray, 2010). Though IP3 receptor-mediated Ca^{2+} signaling inhibits autophagy, an increase in the cytosolic Ca^{2+} level promotes autophagy (Criollo et al., 2007; Wang et al., 2008; Khan and Joseph, 2010; Vingtdeux et al., 2010). Some studies have linked PS mutation in FAD with neuronal dysfunction and apoptosis via Ca^{2+} dysfunction (Del Prete et al., 2014; Duggan and McCarthy, 2016).

Despite entrapping non-selective molecules, selective trapping of various molecules occurs through interaction of LC3-II with cargo-receptors such as nuclear dot protein-52 (NDP52), p62, and neighbor of BRAC1 (NRB1; Bjørkøy et al., 2005; Kirkin et al., 2009; Jo et al., 2014). Acting as an autophagic adaptor for degradation of toll/IL-1 receptor homology domain containing adaptor including IFN-β (TRIF) and tumor receptor associated factor-6 (TRAF6), a role of NDP-52 in docking of autophagosomes to T6BP, myosin VI, and optineurin for maturation has been reported (Inomata et al., 2012; Tumbarello et al., 2012). Interaction of NBR1 and p62 with ubiquitinated misfolded proteins and members of the ATG8 family makes them critical for autophagosome formation (Kabeya et al., 2000; Bjørkøy et al., 2005; Pankiv et al., 2007; Kirkin et al., 2009). PS1 mutations that cause a loss of lysosomal acidification ultimately lead to loss of lysosomal proteolytic activity (Lee et al., 2010). Disruption in the lysosomal function causes accumulation of autophagosomes containing protein aggregates, as observed in the AD brain. Studies indicate involvement of NDP-52 as a downstream facilitator of nuclear factor erythroid-2 related factor 2 (Nrf2)-mediated tau (phosphorylated) degradation (Jo et al., 2014). Reduction in the autophagy-aggravated AD pathology underlines the critical role of autophagy in the removal of Aβ aggregates (Cai et al., 2012; Di Domenico et al., 2014).

BIOMARKERS OF AD

Cortical amyloid deposition of Aβ and phosphorylated tau (p-tau) are core biomarkers of AD in CSF (Blennow et al., 2010). With high accuracy diagnostics, specificity of the core repertoire of biomarkers is in the 80–90% range in the mild cognitive impairment stage of AD (Shaw et al., 2009; Visser et al., 2009). Despite this, assessment of the sensitivity of disease biomarkers reflects an imperfect criterion in the gold standard of clinical diagnosis of the disease because it fails to distinguish pathological changes such as plaque count between cognitively normal elderly persons and those with AD (Coart et al., 2015; Curtis et al., 2015). Changes in α-synuclein (α-syn), TDP43, and several vascular indicators, are other pathological markers in patients suffering from AD (Kovacs et al., 2013).

A step to increase the specificity and sensitivity of biomarkers has led to the screening of several different entities for use in the diagnosis of AD. One such biomarker involves Aβ oligomers (toxic forms of Aβ), which are associated with synaptic dysfunction (Overk and Masliah, 2014). Though increases in the Aβ oligomers are observed in AD, their limited occurrence in the CSF hinders their reliability in the diagnosis of AD (Hölttä et al., 2013; Yang et al., 2013). Neurogranin, a dendritic protein, is another synaptic biomarker candidate (Díez-Guerra, 2010). Increased amount of neurogranin in CSF of AD patients is correlated with the progression of mild cognitive impairment (Kvartsberg et al., 2015). Additionally, an increase in the level of presynaptic protein SNAP25 might indicate AD diagnosis (Brinkmalm et al., 2014). Of the other biomarkers, screening of CNS-specific protein candidates in blood also seems suitable; when sampling populations for AD. Combinations of proteins, lipids, and other molecules have been used in the assessment of AD (Henriksen et al., 2014; Mapstone et al., 2014). However,

as they may be secreted in low amounts and are prone to degradation by plasma proteases, their suitability as biomarkers for AD is uncertain. Similarly, tau-imaging, which is commonly employed in drug trials to determine delay in the progression of AD may be another potentially suitable option for AD diagnosis.

THERAPEUTIC APPROACHES TO COMBAT AD

The fact that critical care provides patients a better quality of life family care is considered as the mainstay in the treatment of AD. At present, efforts are being made on two fronts; toward developing disease modifying therapies that can uphold progression of the disease, and; developing drugs that can act as disease pathway blockers. As Aβ and tau hyper-phosphorylation are well-recognized hallmarks of AD (Lee et al., 2005; Querfurth and Laferla, 2010; Ahmad et al., 2017), current drug approaches are aimed at:

Improved APP Processing via Inhibition and/or Activation of Enzymatic Machinery

To date, only five drugs have been approved by the USA FDA for treatment of cognitive manifestations of AD (**Table 2**). Of the different drug regimes, glutamate agonist memantine, and acetylcholine esterase (AchE) inhibitors such as rivastigmine, donepezil, and galantamine are employed in the treatment of the dementia phase of AD (Raina et al., 2008). Blocking the pathological stimulation of NMDA receptors, memantine protects neural cells from glutamate-mediated excitoxicity. AchE inhibitors cause temporary slowdown in cognitive function by decreasing activity of cholinesterase, leading to enhanced acetylcholine (Ach) levels and, thereby, brain functions (Godyn et al., 2016). As disruption of AchE has a direct correlation with NFT and Aβ deposits (Tavitian et al., 1993), AchE inhibitors stabilize cognitive performance and daily functioning in early dementia stages, whereas application of memantine provides benefits to patients suffering from moderate to severe dementia (Godyn et al., 2016). The fifth drug, tacrine is less prescribed due to its hepatotoxicity. Although these drugs provide symptomatic improvement in AD, benefits are generally short lived and with no effect on the pathogenic mechanism or on disease progression. Research into potential strategies is currently directed at screening bioactive compounds for their effect on enzyme inhibition, aggregation, prevention of Aβ formation, and upregulation in the removal of toxic Aβ.

Immunotherapeutic Approaches to Existing Amyloids

Currently, the most attractive Aβ-directed approach, immunotherapy enlists both active (immune stimulation by vaccine for antibody production) and passive (injection of pre-prepared antibodies) immunization. Engaging both the cellular and humoral immune systems, active immunization is cost effective and ensures long-term high antibody titers. An active vaccination journey begins with AN1792, a full-length $A\beta_{1-42}$ peptide injected with the immune stimulant adjuvant QS21 (Panza et al., 2014). However, on observing meningoencephalitis among 6% of the enrolled AD patients, the phase II AN1792 trial was halted in 2002. Taking strong cognizance of AN1792 trials, larger studies were directed at testing passive immunotherapy by using human anti-Aβ monoclonal antibodies. At present various 2nd generation active Aβ vaccines are undergoing clinical trials; of particular note are CAD106 ($A\beta_{1-6}$; Novartis), ACC001 ($A\beta_{1-6}$; Janssen and Pfizer), ACI-24, V-950, and AD-02 ($A\beta_{1-6}$; Alzforum, 2016). Compared to active immunization that leads to a polyclonal antibody response, target specificity (specific against monomeric Aβ, Aβ fibrils, and their carrier and transport proteins) in passive immunization has advantages both in preventing Aβ-aggregation and in promoting Aβ-clearance in anti-Aβ immunotherapy. The first monoclonal antibody was bapineuzumab directed against $A\beta_{1-5}$ (Abushouk et al., 2017; Xing et al., 2017). Although it reduced Aβ in brain during phase II trials, it failed to achieve significant benefit in a phase III trial, leading to its termination in 2012. This was followed by trials of mAb m266, which showed enhanced Aβ clearance from brain to blood (Demattos et al., 2001; Dodart et al., 2002). Using am266 precursor, Solanezumab directed against mid-domain $A\beta_{16-24}$ revealed dose-dependent increases in plasma Aβ, suggesting cleavage of insoluble species from senile plaques (Farlow et al., 2012; Han and Mook-Jung, 2014). Other Abs undergoing clinical trials include gantenerumab (showing binding specificity for Aβ plaques), crenezumab IgG4 mAb (showing binding specificity for Aβ oligomers, plaques, and fibrils that inhibit aggregation), GSK933766, and BAN2401 mAb (Alzforum, 2016). Reduction in Aβ production is also achieved by using inhibitors against secretases such as NIC5-15, Bryostatin-1, AZD3293, MK8931, and E2609 (Alzforum, 2016).

Tau Centric Therapies

Tau centric therapies include the use of putative tau kinase inhibitors, microtubule stabilizers, and tau immunotherapy. Glycogen synthase kinase-3β (GSK-3β), the primary enzyme involved in tau phosphorylation, is considered the primary target for disease modification (Jaworski et al., 2011). As Aβ promotes GSK-3β activity, studies of GSK-3β inhibitors such as tideglusib and AZD1080 were pursued (King et al., 2014; Lovestone et al., 2015). Clinical trials of AZD1080 revealed nephrotoxicity (Eldar-Finkelman and Martinez, 2011), while the trials for tideglusib showed diminished clinical benefits. Microtubule stabilizers inhibit tau aggregation (Bulic et al., 2010). LMTC, a methylthionium chloride (MTC) derivative prevents tau interactions, thereby facilitating its clearance from the brain (Wischik et al., 2015). Other microtubule stabilizers include TPI207 and BMS241027 (epothilone-D). Immunotherapy for tau protein is directed toward prevention of NFT formation. Both AADvac1 (a synthetic tau derived peptide) and ACI-35 (liposome formulated based tau protein) are currently being evaluated for their effects on avoiding tau aggregation (Alzforum, 2016).

TABLE 2 | Summary of therapeutic options available in the treatment of AD.

S. No	Therapy type (categorization)	Phase 1/2	Phase 3	Phase 4		Approval for treatment			
		Number	Name	Name (synonyms)	Target	Name	Synonyms	Target	Approved for
1.	Small molecules	50	LMTM, AGB101, ALZT-OP1, AVP-786, AZD3293, Aripiprazole, Azeliragon, Brexpiprazole, Elenbecestat, ITI-007, Idalopirdine, Intepirdine, Masitinib, Nilvadipine, Pioglitazone, Verubecestat	AVP-923 (Nuedexta, Zenvia)	Other Neurotransmitters	Donepezil	Aricept™, Donepezil hydrochloride, Eranz®, E 2020	Cholinergic system	Alzheimer's disease
				Carvedilol (Coreg, Artist, Aucardic, Dilatrend, Kredex)	Unknown	Galantamine	Razadyne™, Reminyl™, Nivalin®	Cholinergic system	Mild to Moderate Alzheimer's disease
				Prazosin (Prazosin hydrochloride, Minipress, VasoflexHypovase,)	Other Neurotransmitters	Memantine	Ebixa™, Memary®, Axura®, Akatinol®, Namenda™,	Other neurotransmitters	Alzheimer's disease
				Resveratrol (trans-3,4′,5-trihydroxystilbene)	Other	Rivastigmine	Exelon™, Rivastigmine tartrate, Rivastach® Patch, Prometax®, SDZ ENA 713	Cholinergic system	Mild to moderate Alzheimer's disease
				Simvastatin (Zocor®, Denan®, Lipovas® Lipex®)	Cholesterol	Tacrine	Cognex™	Cholinergic system	Alzheimer's disease
2.	Dietary Supplement	4	Alpha-Tocopherol (Vitamin E)	Docosahexaenoic acid (DHA; Omega 3 fatty acid)	Others (reduction of amyloid, tau)	–	–	–	–
				Ketasyn (Axona, Caprylic Acid, AC-1202)	Others	–	–	–	–
				Resveratrol (trans-3,4′,5-trihydroxystilbene)	Others (prevention of amyloid deposition, induction of sirtuin-1 gene)	–	–	–	–
3.	Immunotherapy (active)	8	–	–	–	–	–	–	–
4.	Immunotherapy (passive)	11	Aducanumab (BIIB037), Crenezumab (MABT5102A, RG7412), Gantenerumab (RO4909832, RG1450), Solanezumab (LY2062430)	–	–	–	–	–	–
5.	Procedural intervention	2	Continuous Positive Airway Pressure (CPAP)	–	–	–	–	–	–

http://www.alzforum.org/therapeutics

Therapies to Combat Oxidative Stress

Oxidative stress due to reactive oxygen species (ROS), being a major player in neurodegeneration strategies, are currently being devised to combat its emergence at mitochondria (Federico et al., 2012; Yan et al., 2013; Kim et al., 2015). On the forefront, ferulic acid (FA), epigallocatechin-3-gallate, and nano formulation of naturally occurring curcumin were found exerting strong antioxidant, anti-inflammatory and amyloid disintegration properties (Rezai-Zadeh et al., 2005; Yang et al., 2005; Cheng et al., 2013; Sgarbossa et al., 2015; Cascella et al., 2017). Alleviating mitochondrial dysfunction under diseased conditions, peptide based strategies complemented with different drug molecules have shown positive results in overcoming the inefficiency of low antioxidant levels (Kumar and Singh, 2015). Of them, Szeto-Schiller (SS) peptides displaying a sequence motif that directs its accumulation inside mitochondria inhibit lipid peroxidation. Accumulation of SS31 on inner mitochondrial membrane prevents release of cyt-C (Szeto, 2008; Kumar and Singh, 2015). Similarly, accumulation of drugs such as MitoQ inside mitochondria increases its potential to neutralize free radicals several 100-folds than that attributed by natural antioxidants (Tauskela, 2007; Ross et al., 2008). Probucol, a drug that helps establishment of balance of mitochondal fission-fusion processes, also maintains AD mitochondria induced extracellular signal regulated kinase (ERK) activation (Champagne et al., 2003; Gan et al., 2014).

Autophagy Enhancer Therapy

As accumulation of the aggregated proteins enhances neurodegeneration, enhancement in the degenerative capacity via, autophagy inducers seems a good therapeutic approach. Their mode of action involves prevention in the accumulation of Aβ plaques and tau tangles via degradation of the aggregates. Of the available drugs, rapamycin acting as mTOR inhibitor was found ameliorating Aβ and tau pathies in AD mouse model (Caccamo et al., 2010; Rubinsztein et al., 2012). Latrepirdine stimulation of autophagy reduces Aβ neuropathy in mouse brain (Steele and Gandy, 2013). Metformin, a PP2A agonist, inhibition of TORC1 prevents hyperphosphorylation of tau protein (Kickstein et al., 2010). Other authophagy enhancers include reservatol and its analogs, RSVA314 and RSVA405, virally packaged BECN1 and its mimetics, nicotinamide, etc (Vingtdeux et al., 2010; Shoji-Kawata et al., 2013). Though, Beclin1 deficiency increases APP and Aβ levels, its over-expression in cultured neurons cause significant reduction in Aβ accumulation (Pickford et al., 2008). Additionally, PS1 and PS2 serving as a catalytic subunit of γ-secretase was found acting as autophagy modulators (Lee et al., 2010). Associated with the substrate cleavage, their knockdown was found exhibiting inefficiency in the clearance of protein aggregates. Cells deficient in PS1 was found having reduced levels of cargo shuttle protein p62, associated with the degradation of abnormal tau (Tung et al., 2014; Caccamo et al., 2017).

Failure of biologics that target amyloids to cross the blood-brain barrier (BBB) indicates the necessity of development of an efficient drug delivery system. Liposomes and polymeric nanoparticles have shown promising results in delivering drugs and other therapeutic molecules (Ha et al., 2016); however, their use as a means to deliver drugs across the BBB has encountered roadblocks associated with biocompatibility and long-term safety. Persistent problems with low biocompatibility, restricted immune escape, circulation stability, and toxicity have led to a gradual shift of research toward the use of exosomes. Their long circulatory half-life, host biocompatibility, target-specific drug delivery ability, and low toxicity have increased the interest in using exosomes to deliver drugs in several neurodegenerative diseases (Lai and Breakefield, 2012; Liu et al., 2016). As drug delivery through exosomes has shown promising results in the ongoing studies, their utilization in reducing disease progression may indicate their suitability in reducing progression of AD.

CONCLUSION

AD progresses via aggregation and accumulation in the extracellular milieu of amyloid plaques and intraneuronal neurofibrillary tangles produced by p-tau. Although malfunctioning APP, PS-1 &-2 genes are considered the main culprits behind AD, mitochondrial dysfunction, ER stress and mitophagy significantly increase progression of the disease. Current research provides useful information on new targets and their utilization in designing novel inhibitors or drugs as part of attempts to achieve successful treatment of AD. It also studies different entities for employment as potent biomarkers in disease diagnosis and provides information on therapeutic suitability in the treatment of AD. Further studies on the use of exosomes as drug delivery vehicles are needed in order to reveal and reduce safety and ethical concerns. With increases in newly identified targets, studies pertaining to the design of drugs and other potent therapeutic molecules are needed in order to combat the progression of AD.

AUTHOR CONTRIBUTIONS

IC, QH, and AJ: conceived the idea; AJ and MA: contributed to writing of the manuscript; AJ, SR, AA, DC, and EL: contributed to upgrading the contents and preparing the tables.

ACKNOWLEDGMENTS

Authors extend their thanks to colleagues for their criticism, which helped to improve the quality of this paper's contents and broaden its perspective to reach a broader audience. This work was supported by the Creative Economy Leading Technology Development Program through the Gyeongsangbuk-Do and Gyeongbuk Science & Technology Promotion Center of Korea (SF316001A).

REFERENCES

Abisambra, J. F., Jinwal, U. K., Blair, L. J., O'leary, J. C., Li, Q., Brady, S., et al. (2013). Tau accumulation activates the unfolded protein response by impairing endoplasmic reticulum-associated degradation. *J. Neurosci.* 33, 9498–9507. doi: 10.1523/JNEUROSCI.5397-12.2013

Abushouk, A. I., Elmaraezy, A., Aglan, A., Salama, R., Fouda, S., Fouda, R., et al. (2017). Bapineuzumab for mild to moderate Alzheimer's disease: a meta-analysis of randomized controlled trials. *BMC Neurol* 17:66. doi: 10.1186/s12883-017-0850-1

ADFF (2016). Alzheimer's disease facts and figures. *Alzheimers Dement.* 12, 459–509. doi: 10.1016/j.jalz.2016.03.001

Ahmad, K., Baig, M. H., Gupta, G. K., Kamal, M. A., Pathak, N., and Choi, I. (2016). Identification of common therapeutic targets for selected neurodegenerative disorders: an *in silico* approach. *J. Comput. Sci.* 17, 292–306. doi: 10.1016/j.jocs.2016.03.007

Ahmad, K., Baig, M. H., Mushtaq, G., Kamal, M. A., Greig, N. H., and Choi, I. (2017). Commonalities in biological pathways, genetics, and cellular mechanism between Alzheimer Disease and other neurodegenerative diseases: an *in silico*-updated overview. *Curr Alzheimer Res.* 14, 1190–1197. doi: 10.2174/1567205014666170203141151

Alzforum (2016). *Therapeutics for Alzheimers Disease.* Available online at: http://www.alzforum.org/therapeutics.

Bjørkøy, G., Lamark, T., Brech, A., Outzen, H., Perander, M., Overvatn, A., et al. (2005). p62/SQSTM1 forms protein aggregates degraded by autophagy and has a protective effect on huntingtin-induced cell death. *J. Cell. Biol.* 171, 603–614. doi: 10.1083/jcb.200507002

Blennow, K., Hampel, H., Weiner, M., and Zetterberg, H. (2010). Cerebrospinal fluid and plasma biomarkers in Alzheimer disease. *Nat. Rev. Neurol.* 6, 131–144. doi: 10.1038/nrneurol.2010.4

Boyle, P. A., Wilson, R. S., Yu, L., Barr, A. M., Honer, W. G., Schneider, J. A., et al. (2013). Much of late life cognitive decline is not due to common neurodegenerative pathologies. *Ann. Neurol.* 74, 478–489. doi: 10.1002/ana.23964

Brinkmalm, A., Brinkmalm, G., Honer, W. G., Frölich, L., Hausner, L., Minthon, L., et al. (2014). SNAP-25 is a promising novel cerebrospinal fluid biomarker for synapse degeneration in Alzheimer's disease. *Mol. Neurodegener.* 9:53. doi: 10.1186/1750-1326-9-53

Bubber, P., Haroutunian, V., Fisch, G., Blass, J. P., and Gibson, G. E. (2005). Mitochondrial abnormalities in Alzheimer brain: mechanistic implications. *Ann. Neurol.* 57, 695–703. doi: 10.1002/ana.20474

Bulic, B., Pickhardt, M., Mandelkow, E. M., and Mandelkow, E. (2010). Tau protein and tau aggregation inhibitors. *Neuropharmacology* 59, 276–289. doi: 10.1016/j.neuropharm.2010.01.016

Caccamo, A., Ferreira, E., Branca, C., and Oddo, S. (2017). p62 improves AD-like pathology by increasing autophagy. *Mol. Psychiatry* 22, 865–873. doi: 10.1038/mp.2016.139

Caccamo, A., Majumder, S., Richardson, A., Strong, R., and Oddo, S. (2010). Molecular interplay between mammalian target of rapamycin (mTOR), amyloid-beta, and Tau: effects on cognitive impairments. *J. Biol. Chem.* 285, 13107–13120. doi: 10.1074/jbc.M110.100420

Cai, Z., Zhao, B., Li, K., Zhang, L., Li, C., Quazi, S. H., et al. (2012). Mammalian target of rapamycin: a valid therapeutic target through the autophagy pathway for Alzheimer's disease? *J. Neurosci. Res.* 90, 1105–1118. doi: 10.1002/jnr.23011

Cárdenas, C., and Foskett, J. K. (2012). Mitochondrial Ca(2+) signals in autophagy. *Cell Calcium* 52, 44–51. doi: 10.1016/j.ceca.2012.03.001

Casas-Tinto, S., Zhang, Y., Sanchez-Garcia, J., Gomez-Velazquez, M., Rincon-Limas, D. E., and Fernandez-Funez, P. (2011). The ER stress factor XBP1s prevents amyloid-beta neurotoxicity. *Hum. Mol. Genet.* 20, 2144–2160. doi: 10.1093/hmg/ddr100

Cascella, M., Bimonte, S., Muzio, M. R., Schiavone, V., and Cuomo, A. (2017). The efficacy of Epigallocatechin-3-gallate (green tea) in the treatment of Alzheimer's disease: an overview of pre-clinical studies and translational perspectives in clinical practice. *Infect. Agent Cancer* 12:36. doi: 10.1186/s13027-017-0145-6

Castellani, R., Hirai, K., Aliev, G., Drew, K. L., Nunomura, A., Takeda, A., et al. (2002). Role of mitochondrial dysfunction in Alzheimer's disease. *J. Neurosci. Res.* 70, 357–360. doi: 10.1002/jnr.10389

Champagne, D., Pearson, D., Dea, D., Rochford, J., and Poirier, J. (2003). The cholesterol-lowering drug Probucol increases apolipoprotein e production in the hippocampus of aged rats: implications for Alzheimer's disease. *Neuroscience* 121, 99–110. doi: 10.1016/S0306-4522(03)00361-0

Chávez-Gutiérrez, L., Bammens, L., Benilova, I., Vandersteen, A., Benurwar, M., Borgers, M., et al. (2012). The mechanism of gamma-Secretase dysfunction in familial Alzheimer disease. *EMBO J.* 31, 2261–2274. doi: 10.1038/emboj.2012.79

Cheng, K. K., Yeung, C. F., Ho, S. W., Chow, S. F., Chow, A. H., and Baum, L. (2013). Highly stabilized curcumin nanoparticles tested in an *in vitro* blood-brain barrier model and in Alzheimer's disease Tg2576 mice. *AAPS J.* 15, 324–336. doi: 10.1208/s12248-012-9444-4

Coart, E., Barrado, L. G., Duits, F. H., Scheltens, P., van der Flier, W. M., Teunissen, C. E., et al. (2015). Correcting for the absence of a gold standard improves diagnostic accuracy of biomarkers in Alzheimer's Disease. *J Alzheimers Dis.* 46, 889–899. doi: 10.3233/JAD-142886

Criollo, A., Maiuri, M. C., Tasdemir, E., Vitale, I., Fiebig, A. A., Andrews, D., et al. (2007). Regulation of autophagy by the inositol trisphosphate receptor. *Cell Death Differ* 14, 1029–1039. doi: 10.1038/sj.cdd.4402099

Curtis, C., Gamez, J. E., Singh, U., Sadowsky, C. H., Villena, T., Sabbagh, M. N., et al. (2015). Phase 3 trial of flutemetamol labeled with radioactive fluorine 18 imaging and neuritic plaque density. *JAMA Neurol.* 72, 287–294. doi: 10.1001/jamaneurol.2014.4144

Decuypere, J. P., Kindt, D., Luyten, T., Welkenhuyzen, K., Missiaen, L., De Smedt, H., et al. (2013). mTOR-controlled autophagy requires intracellular Ca(2+) signaling. *PLoS ONE* 8:e61020. doi: 10.1371/journal.pone.0061020

Del Prete, D., Checler, F., and Chami, M. (2014). Ryanodine receptors: physiological function and deregulation in Alzheimer disease. *Mol. Neurodegener.* 9, 21–29. doi: 10.1186/1750-1326-9-21

Demattos, R. B., Bales, K. R., Cummins, D. J., Dodart, J. C., Paul, S. M., and Holtzman, D. M. (2001). Peripheral anti-A beta antibody alters CNS and plasma A beta clearance and decreases brain A beta burden in a mouse model of Alzheimer's disease. *Proc. Natl. Acad. Sci. U.S.A.* 98, 8850–8855. doi: 10.1073/pnas.151261398

Di Domenico, F., Head, E., Butterfield, D. A., and Perluigi, M. (2014). Oxidative stress and proteostasis network: culprit and casualty of Alzheimer's- like Neurodegeneration. *Adv. Geriatr.* 2014:14. doi: 10.1155/2014/527518

Díez-Guerra, F. J. (2010). Neurogranin, a link between calcium/calmodulin and protein kinase C signaling in synaptic plasticity. *IUBMB Life* 62, 597–606. doi: 10.1002/iub.357

Dodart, J. C., Bales, K. R., Gannon, K. S., Greene, S. J., Demattos, R. B., Mathis, C., et al. (2002). Immunization reverses memory deficits without reducing brain Abeta burden in Alzheimer's disease model. *Nat. Neurosci.* 5, 452–457. doi: 10.1038/nn842

Duggan, S. P., and McCarthy, J. V. (2016). Beyond gamma-secretase activity: the multifunctional nature of presenilins in cell signalling pathways. *Cell Signal* 28, 1–11. doi: 10.1016/j.cellsig.2015.10.006

Eldar-Finkelman, H., and Martinez, A. (2011). GSK-3 Inhibitors: preclinical and clinical focus on CNS. *Front. Mol. Neurosci.* 4:32. doi: 10.3389/fnmol.2011.00032

Farlow, M., Arnold, S. E., Van Dyck, C. H., Aisen, P. S., Snider, B. J., Porsteinsson, A. P., et al. (2012). Safety and biomarker effects of solanezumab in patients with Alzheimer's disease. *Alzheimers Dement.* 8, 261–271. doi: 10.1016/j.jalz.2011.09.224

Federico, A., Cardaioli, E., Da Pozzo, P., Formichi, P., Gallus, G. N., and Radi, E. (2012). Mitochondria, oxidative stress and neurodegeneration. *J. Neurol. Sci.* 322, 254–262. doi: 10.1016/j.jns.2012.05.030

Fu, Z., and Tindall, D. J. (2008). FOXOs, cancer and regulation of apoptosis. *Oncogene* 27, 2312–2319. doi: 10.1038/onc.2008.24

Furukawa, K., Sopher, B. L., Rydel, R. E., Begley, J. G., Pham, D. G., Martin, G. M., et al. (1996). Increased activity-regulating and neuroprotective efficacy of alpha-secretase-derived secreted amyloid precursor protein conferred by a C-terminal heparin-binding domain. *J. Neurochem.* 67, 1882–1896. doi: 10.1046/j.1471-4159.1996.67051882.x

Gan, X., Huang, S., Wu, L., Wang, Y., Hu, G., Li, G., et al. (2014). Inhibition of ERK-DLP1 signaling and mitochondrial division alleviates mitochondrial dysfunction in Alzheimer's disease cybrid cell. *Biochim. Biophys. Acta* 1842, 220–231. doi: 10.1016/j.bbadis.2013.11.009

Genin, E., Hannequin, D., Wallon, D., Sleegers, K., Hiltunen, M., Combarros, O., et al. (2011). APOE and Alzheimer disease: a major gene with semi-dominant inheritance. *Mol. Psychiatry* 16, 903–907. doi: 10.1038/mp.2011.52

Goate, A., Chartier-Harlin, M. C., Mullan, M., Brown, J., Crawford, F., Fidani, L., et al. (1991). Segregation of a missense mutation in the amyloid precursor protein gene with familial Alzheimer's disease. *Nature* 349, 704–706. doi: 10.1038/349704a0

Godyn, J., Jonczyk, J., Panek, D., and Malawska, B. (2016). Therapeutic strategies for Alzheimer's disease in clinical trials. *Pharmacol. Rep.* 68, 127–138. doi: 10.1016/j.pharep.2015.07.006

Ha, D., Yang, N., and Nadithe, V. (2016). Exosomes as therapeutic drug carriers and delivery vehicles across biological membranes: current perspectives and future challenges. *Acta Pharm. Sin. B* 6, 287–296. doi: 10.1016/j.apsb.2016.02.001

Han, S. H., and Mook-Jung, I. (2014). Diverse molecular targets for therapeutic strategies in Alzheimer's disease. *J. Korean Med. Sci.* 29, 893–902. doi: 10.3346/jkms.2014.29.7.893

Henriksen, K., O'Bryant, S. E., Hampel, H., Trojanowski, J. Q., Montine, T. J., Jeromin, A., et al. (2014). The future of blood-based biomarkers for Alzheimer's disease. *Alzheimers Dement.* 10, 115–131. doi: 10.1016/j.jalz.2013.01.013

Hetz, C., and Mollereau, B. (2014). Disturbance of endoplasmic reticulum proteostasis in neurodegenerative diseases. *Nat. Rev. Neurosci.* 15, 233–249. doi: 10.1038/nrn3689

Hetz, C., Martinon, F., Rodriguez, D., and Glimcher, L. H. (2011). The unfolded protein response: integrating stress signals through the stress sensor IRE1alpha. *Physiol. Rev.* 91, 1219–1243. doi: 10.1152/physrev.00001.2011

Hirai, K., Aliev, G., Nunomura, A., Fujioka, H., Russell, R. L., Atwood, C. S., et al. (2001). Mitochondrial abnormalities in Alzheimer's disease. *J. Neurosci.* 21, 3017–3023.

Hölttä, M., Hansson, O., Andreasson, U., Hertze, J., Minthon, L., Nägga, K., et al. (2013). Evaluating amyloid-beta oligomers in cerebrospinal fluid as a biomarker for Alzheimer's disease. *PLoS ONE* 8:e66381. doi: 10.1371/journal.pone.0066381

Hoozemans, J. J., Van Haastert, E. S., Nijholt, D. A., Rozemuller, A. J., Eikelenboom, P., and Scheper, W. (2009). The unfolded protein response is activated in pretangle neurons in Alzheimer's disease hippocampus. *Am. J. Pathol.* 174, 1241–1251. doi: 10.2353/ajpath.2009.080814

Huang, H. M., Ou, H. C., Xu, H., Chen, H. L., Fowler, C., and Gibson, G. E. (2003). Inhibition of alpha-ketoglutarate dehydrogenase complex promotes cytochrome c release from mitochondria, caspase-3 activation, and necrotic cell death. *J. Neurosci. Res.* 74, 309–317. doi: 10.1002/jnr.10756

Ichimura, Y., and Komatsu, M. (2010). Selective degradation of p62 by autophagy. *Semin. Immunopathol.* 32, 431–436. doi: 10.1007/s00281-010-0220-1

Inomata, M., Niida, S., Shibata, K., and Into, T. (2012). Regulation of Toll-like receptor signaling by NDP52-mediated selective autophagy is normally inactivated by A20. *Cell. Mol. Life Sci.* 69, 963–979. doi: 10.1007/s00018-011-0819-y

Jaeger, P. A., and Wyss-Coray, T. (2010). Beclin 1 complex in autophagy and Alzheimer disease. *Arch. Neurol.* 67, 1181–1184. doi: 10.1001/archneurol.2010.258

Jaunmuktane, Z., Mead, S., Ellis, M., Wadsworth, J. D., Nicoll, A. J., Kenny, J., et al. (2015). Evidence for human transmission of amyloid-beta pathology and cerebral amyloid angiopathy. *Nature* 525, 247–250. doi: 10.1038/nature15369

Jaworski, T., Dewachter, I., Lechat, B., Gees, M., Kremer, A., Demedts, D., et al. (2011). GSK-3alpha/beta kinases and amyloid production *in vivo*. *Nature* 480, E4–E5; discussion: E6. doi: 10.1038/nature10615

Jo, C., Gundemir, S., Pritchard, S., Jin, Y. N., Rahman, I., and Johnson, G. V. (2014). Nrf2 reduces levels of phosphorylated tau protein by inducing autophagy adaptor protein NDP52. *Nat. Commun.* 5:3496. doi: 10.1038/ncomms4496

Jucker, M., and Walker, L. C. (2013). Self-propagation of pathogenic protein aggregates in neurodegenerative diseases. *Nature* 501, 45–51. doi: 10.1038/nature12481

Juhaszova, M., Zorov, D. B., Kim, S. H., Pepe, S., Fu, Q., Fishbein, K. W., et al. (2004). Glycogen synthase kinase-3beta mediates convergence of protection signaling to inhibit the mitochondrial permeability transition pore. *J. Clin. Invest.* 113, 1535–1549. doi: 10.1172/JCI19906

Kabeya, Y., Mizushima, N., Ueno, T., Yamamoto, A., Kirisako, T., Noda, T., et al. (2000). LC3, a mammalian homologue of yeast Apg8p, is localized in autophagosome membranes after processing. *EMBO J.* 19, 5720–5728. doi: 10.1093/emboj/19.21.5720

Karch, C. M., and Goate, A. M. (2015). Alzheimer's disease risk genes and mechanisms of disease pathogenesis. *Biol. Psychiatry* 77, 43–51. doi: 10.1016/j.biopsych.2014.05.006

Karran, E., Mercken, M., and De Strooper, B. (2011). The amyloid cascade hypothesis for Alzheimer's disease: an appraisal for the development of therapeutics. *Nat. Rev. Drug Discov.* 10, 698–712. doi: 10.1038/nrd3505

Khan, M. T., and Joseph, S. K. (2010). Role of inositol trisphosphate receptors in autophagy in DT40 cells. *J. Biol. Chem.* 285, 16912–16920. doi: 10.1074/jbc.M110.114207

Kickstein, E., Krauss, S., Thornhill, P., Rutschow, D., Zeller, R., Sharkey, J., et al. (2010). Biguanide metformin acts on tau phosphorylation via mTOR/protein phosphatase 2A (PP2A) signaling. *Proc. Natl. Acad. Sci. U.S.A.* 107, 21830–21835. doi: 10.1073/pnas.0912793107

Kim, G. H., Kim, J. E., Rhie, S. J., and Yoon, S. (2015). The role of oxidative stress in neurodegenerative diseases. *Exp. Neurobiol.* 24, 325–340. doi: 10.5607/en.2015.24.4.325

King, M. K., Pardo, M., Cheng, Y., Downey, K., Jope, R. S., and Beurel, E. (2014). Glycogen synthase kinase-3 inhibitors: rescuers of cognitive impairments. *Pharmacol. Ther.* 141, 1–12. doi: 10.1016/j.pharmthera.2013.07.010

Kirkin, V., Lamark, T., Sou, Y. S., Bjørkøy, G., Nunn, J. L., Bruun, J. A., et al. (2009). A role for NBR1 in autophagosomal degradation of ubiquitinated substrates. *Mol. Cell* 33, 505–516. doi: 10.1016/j.molcel.2009.01.020

Kops, G. J., Dansen, T. B., Polderman, P. E., Saarloos, I., Wirtz, K. W., Coffer, P. J., et al. (2002). Forkhead transcription factor FOXO3a protects quiescent cells from oxidative stress. *Nature* 419, 316–321. doi: 10.1038/nature01036

Kovacs, G. G., Milenkovic, I., Wöhrer, A., Höftberger, R., Gelpi, E., Haberler, C., et al. (2013). Non-Alzheimer neurodegenerative pathologies and their combinations are more frequent than commonly believed in the elderly brain: a community-based autopsy series. *Acta Neuropathol.* 126, 365–384. doi: 10.1007/s00401-013-1157-y

Kumar, A., and Singh, A. (2015). A review on mitochondrial restorative mechanism of antioxidants in Alzheimer's disease and other neurological conditions. *Front. Pharmacol.* 6:206. doi: 10.3389/fphar.2015.00206

Kundu, M. (2011). ULK1, mammalian target of rapamycin, and mitochondria: linking nutrient availability and autophagy. *Antioxid. Redox Signal.* 14, 1953–1958. doi: 10.1089/ars.2010.3809

Kvartsberg, H., Duits, F. H., Ingelsson, M., Andreasen, N., Ohrfelt, A., Andersson, K., et al. (2015). Cerebrospinal fluid levels of the synaptic protein neurogranin correlates with cognitive decline in prodromal Alzheimer's disease. *Alzheimers Dement.* 11, 1180–1190. doi: 10.1016/j.jalz.2014.10.009

Lai, C., and Breakefield, X. (2012). Role of exosomes/microvesicles in the nervous system and use in emerging therapies. *Front. Physiol.* 3:228. doi: 10.3389/fphys.2012.00228

Ledoux, S., Yang, R., Friedlander, G., and Laouari, D. (2003). Glucose depletion enhances P-glycoprotein expression in hepatoma cells: role of endoplasmic reticulum stress response. *Cancer Res.* 63, 7284–7290.

Lee, A. S. (2001). The glucose-regulated proteins: stress induction and clinical applications. *Trends Biochem. Sci.* 26, 504–510. doi: 10.1016/S0968-0004(01)01908-9

Lee, H. G., Perry, G., Moreira, P. I., Garrett, M. R., Liu, Q., Zhu, X., et al. (2005). Tau phosphorylation in Alzheimer's disease: pathogen or protector? *Trends Mol. Med.* 11, 164–169. doi: 10.1016/j.molmed.2005.02.008

Lee, J. H., Yu, W. H., Kumar, A., Lee, S., Mohan, P. S., Peterhoff, C. M., et al. (2010). Lysosomal proteolysis and autophagy require presenilin 1 and are disrupted by Alzheimer-related PS1 mutations. *Cell* 141, 1146–1158. doi: 10.1016/j.cell.2010.05.008

Lee, J., Giordano, S., and Zhang, J. (2012). Autophagy, mitochondria and oxidative stress: cross-talk and redox signalling. *Biochem. J.* 441, 523–540. doi: 10.1042/BJ20111451

Levy-Lahad, E., Wasco, W., Poorkaj, P., Romano, D. M., Oshima, J., Pettingell, W. H., et al. (1995). Candidate gene for the chromosome 1 familial Alzheimer's disease locus. *Science* 269, 973–977. doi: 10.1126/science.7638622

Li, L., Zhang, X., and Le, W. (2010). Autophagy dysfunction in Alzheimer's disease. *Neurodegener. Dis.* 7, 265–271. doi: 10.1159/000276710

Liu, D., Yang, F., Xiong, F., and Gu, N. (2016). The smart drug delivery system and its clinical potential. *Theranostics* 6, 1306–1323. doi: 10.7150/thno.14858

Liu, S. Y., Wang, W., Cai, Z. Y., Yao, L. F., Chen, Z. W., Wang, C. Y., et al. (2013). Polymorphism−116C/G of human X-box-binding protein 1 promoter is associated with risk of Alzheimer's disease. *CNS Neurosci. Ther.* 19, 229–234. doi: 10.1111/cns.12064

Lovestone, S., Boada, M., Dubois, B., Hull, M., Rinne, J. O., Huppertz, H. J., et al. (2015). A phase II trial of tideglusib in Alzheimer's disease. *J. Alzheimers Dis.* 45, 75–88. doi: 10.3233/JAD-141959

Mahley, R. W., and Huang, Y. (2009). Alzheimer disease: multiple causes, multiple effects of apolipoprotein E4, and multiple therapeutic approaches. *Ann. Neurol.* 65, 623–625. doi: 10.1002/ana.21736

Mapstone, M., Cheema, A. K., Fiandaca, M. S., Zhong, X., Mhyre, T. R., Macarthur, L. H., et al. (2014). Plasma phospholipids identify antecedent memory impairment in older adults. *Nat. Med.* 20, 415–418. doi: 10.1038/nm.3466

Mawuenyega, K. G., Sigurdson, W., Ovod, V., Munsell, L., Kasten, T., Morris, J. C., et al. (2010). Decreased clearance of CNS beta-amyloid in Alzheimer's disease. *Science* 330:1774. doi: 10.1126/science.1197623

Milhavet, O., Martindale, J. L., Camandola, S., Chan, S. L., Gary, D. S., Cheng, A., et al. (2002). Involvement of Gadd153 in the pathogenic action of presenilin-1 mutations. *J. Neurochem.* 83, 673–681. doi: 10.1046/j.1471-4159.2002.01165.x

Moreira, P. I., Cardoso, S. M., Santos, M. S., and Oliveira, C. R. (2006). The key role of mitochondria in Alzheimer's disease. *J. Alzheimers Dis.* 9, 101–110. doi: 10.3233/JAD-2006-9202

Moreira, P. I., Duarte, A. I., Santos, M. S., Rego, A. C., and Oliveira, C. R. (2009). An integrative view of the role of oxidative stress, mitochondria and insulin in Alzheimer's disease. *J. Alzheimers Dis.* 16, 741–761. doi: 10.3233/JAD-2009-0972

Moreira, P. I., Santos, M. S., and Oliveira, C. R. (2007). Alzheimer's disease: a lesson from mitochondrial dysfunction. *Antioxid. Redox Signal.* 9, 1621–1630. doi: 10.1089/ars.2007.1703

Murrow, L., and Debnath, J. (2013). Autophagy as a stress-response and quality-control mechanism: implications for cell injury and human disease. *Annu. Rev. Pathol.* 8, 105–137. doi: 10.1146/annurev-pathol-020712-163918

Nishida, Y., Arakawa, S., Fujitani, K., Yamaguchi, H., Mizuta, T., Kanaseki, T., et al. (2009). Discovery of Atg5/Atg7-independent alternative macroautophagy. *Nature* 461, 654–658. doi: 10.1038/nature08455

Nunomura, A., Perry, G., Aliev, G., Hirai, K., Takeda, A., Balraj, E. K., et al. (2001). Oxidative damage is the earliest event in Alzheimer disease. *J. Neuropathol. Exp. Neurol.* 60, 759–767. doi: 10.1093/jnen/60.8.759

Overk, C. R., and Masliah, E. (2014). Pathogenesis of synaptic degeneration in Alzheimer's disease and Lewy body disease. *Biochem. Pharmacol.* 88, 508–516. doi: 10.1016/j.bcp.2014.01.015

Pankiv, S., Clausen, T. H., Lamark, T., Brech, A., Bruun, J. A., Outzen, H., et al. (2007). p62/SQSTM1 binds directly to Atg8/LC3 to facilitate degradation of ubiquitinated protein aggregates by autophagy. *J. Biol. Chem.* 282, 24131–24145. doi: 10.1074/jbc.M702824200

Panza, F., Logroscino, G., Imbimbo, B. P., and Solfrizzi, V. (2014). Is there still any hope for amyloid-based immunotherapy for Alzheimer's disease? *Curr. Opin. Psychiatry* 27, 128–137. doi: 10.1097/YCO.0000000000000041

Pickford, F., Masliah, E., Britschgi, M., Lucin, K., Narasimhan, R., Jaeger, P. A., et al. (2008). The autophagy-related protein beclin 1 shows reduced expression in early Alzheimer disease and regulates amyloid beta accumulation in mice. *J. Clin. Invest.* 118, 2190–2199. doi: 10.1172/JCI33585

Prince, M., Comas-Herrera, A., Knapp, M., Guerchet, M., and Karagiannidou, M. (2016). *World Alzheimer Report*. Alzheimers Disease International.

Querfurth, H. W., and Laferla, F. M. (2010). Alzheimer's disease. *N. Engl. J. Med.* 362, 329–344. doi: 10.1056/NEJMra0909142

Raina, P., Santaguida, P., Ismaila, A., Patterson, C., Cowan, D., Levine, M., et al. (2008). Effectiveness of cholinesterase inhibitors and memantine for treating dementia: evidence review for a clinical practice guideline. *Ann. Intern. Med.* 148, 379–397. doi: 10.7326/0003-4819-148-5-200803040-00009

Readnower, R. D., Sauerbeck, A. D., and Sullivan, P. G. (2011). Mitochondria, amyloid beta, and Alzheimer's Disease. *Int. J. Alzheimers Dis.* 2011:104545. doi: 10.4061/2011/104545

Rezai-Zadeh, K., Shytle, D., Sun, N., Mori, T., Hou, H., Jeanniton, D., et al. (2005). Green Tea Epigallocatechin-3-Gallate (EGCG) modulates amyloid precursor protein cleavage and reduces cerebral amyloidosis in alzheimer transgenic mice. *J. Neurosci.* 25:8807. doi: 10.1523/JNEUROSCI.1521-05.2005

Rogaev, E. I., Sherrington, R., Rogaeva, E. A., Levesque, G., Ikeda, M., Liang, Y., et al. (1995). Familial Alzheimer's disease in kindreds with missense mutations in a gene on chromosome 1 related to the Alzheimer's disease type 3 gene. *Nature* 376, 775–778. doi: 10.1038/376775a0

Ron, D., and Walter, P. (2007). Signal integration in the endoplasmic reticulum unfolded protein response. *Nat. Rev. Mol. Cell Biol.* 8, 519–529. doi: 10.1038/nrm2199

Ross, M. F., Prime, T. A., Abakumova, I., James, A. M., Porteous, C. M., Smith, R. A., et al. (2008). Rapid and extensive uptake and activation of hydrophobic triphenylphosphonium cations within cells. *Biochem. J.* 411, 633–645. doi: 10.1042/BJ20080063

Rubinsztein, D. C., Codogno, P., and Levine, B. (2012). Autophagy modulation as a potential therapeutic target for diverse diseases. *Nat. Rev. Drug Discov.* 11, 709–730. doi: 10.1038/nrd3802

Safra, M., Ben-Hamo, S., Kenyon, C., and Henis-Korenblit, S. (2013). The ire-1 ER stress-response pathway is required for normal secretory-protein metabolism in *C. elegans*. *J. Cell. Sci.* 126, 4136–4146. doi: 10.1242/jcs.123000

Sayre, L. M., Moreira, P. I., Smith, M. A., and Perry, G. (2005). Metal ions and oxidative protein modification in neurological disease. *Ann. Ist. Super. Sanita* 41, 143–164.

Scherz-Shouval, R., and Elazar, Z. (2011). Regulation of autophagy by ROS: physiology and pathology. *Trends Biochem. Sci.* 36, 30–38. doi: 10.1016/j.tibs.2010.07.007

Scheuner, D., Eckman, C., Jensen, M., Song, X., Citron, M., Suzuki, N., et al. (1996). Secreted amyloid beta-protein similar to that in the senile plaques of Alzheimer's disease is increased *in vivo* by the presenilin 1 and 2 and APP mutations linked to familial Alzheimer's disease. *Nat. Med.* 2, 864–870. doi: 10.1038/nm0896-864

Selkoe, D. J. (1994). Amyloid beta-protein precursor: new clues to the genesis of Alzheimer's disease. *Curr. Opin. Neurobiol.* 4, 708–716. doi: 10.1016/0959-4388(94)90014-0

Selkoe, D. J. (2001a). Alzheimer's disease results from the cerebral accumulation and cytotoxicity of amyloid beta-protein. *J. Alzheimers Dis.* 3, 75–80. doi: 10.3233/JAD-2001-3111

Selkoe, D. J. (2001b). Presenilin, Notch, and the genesis and treatment of Alzheimer's disease. *Proc. Natl. Acad. Sci. U.S.A.* 98, 11039–11041. doi: 10.1073/pnas.211352598

Sgarbossa, A., Giacomazza, D., and Di Carlo, M. (2015). Ferulic acid: a hope for Alzheimer's Disease therapy from plants. *Nutrients* 7, 5764–5782. doi: 10.3390/nu7075246

Shaw, L. M., Vanderstichele, H., Knapik-Czajka, M., Clark, C. M., Aisen, P. S., Petersen, R. C., et al. (2009). Cerebrospinal fluid biomarker signature in Alzheimer's disease neuroimaging initiative subjects. *Ann. Neurol.* 65, 403–413. doi: 10.1002/ana.21610

Sherrington, R., Froelich, S., Sorbi, S., Campion, D., Chi, H., Rogaeva, E. A., et al. (1996). Alzheimer's disease associated with mutations in presenilin 2 is rare and variably penetrant. *Hum. Mol. Genet.* 5, 985–988. doi: 10.1093/hmg/5.7.985

Shimizu, S., Arakawa, S., and Nishida, Y. (2010). Autophagy takes an alternative pathway. *Autophagy* 6, 290–291. doi: 10.4161/auto.6.2.11127

Shoji-Kawata, S., Sumpter, R., Leveno, M., Campbell, G. R., Zou, Z., Kinch, L., et al. (2013). Identification of a candidate therapeutic autophagy-inducing peptide. *Nature* 494, 201–206. doi: 10.1038/nature11866

Steele, J. W., and Gandy, S. (2013). Latrepirdine (Dimebon®), a potential Alzheimer therapeutic, regulates autophagy and neuropathology in an Alzheimer mouse model. *Autophagy* 9, 617–618. doi: 10.4161/auto.23487

Su, B., Wang, X., Nunomura, A., Moreira, P. I., Lee, H. G., Perry, G., et al. (2008). Oxidative stress signaling in Alzheimer's disease. *Curr. Alzheimer Res.* 5, 525–532. doi: 10.2174/156720508786898451

Swerdlow, R. H., Burns, J. M., and Khan, S. M. (2014). The Alzheimer's disease mitochondrial cascade hypothesis: progress and perspectives. *Biochim. Biophys. Acta* 1842, 1219–1231. doi: 10.1016/j.bbadis.2013.09.010

Szegezdi, E., Fitzgerald, U., and Samali, A. (2003). Caspase-12 and ER-stress-mediated apoptosis: the story so far. *Ann. N.Y. Acad. Sci.* 1010, 186–194. doi: 10.1196/annals.1299.032

Szeto, H. H. (2008). Mitochondria-targeted cytoprotective peptides for ischemia-reperfusion injury. *Antioxid. Redox Signal.* 10, 601–619. doi: 10.1089/ars.2007.1892

Tauskela, J. S. (2007). MitoQ–a mitochondria-targeted antioxidant. *IDrugs* 10, 399–412.

Tavitian, B., Pappata, S., Bonnot-Lours, S., Prenant, C., Jobert, A., Crouzel, C., et al. (1993). Positron emission tomography study of [11C]methyl-tetrahydroaminoacridine (methyl-tacrine) in baboon brain. *Eur. J. Pharmacol.* 236, 229–238. doi: 10.1016/0014-2999(93)90593-7

Tumbarello, D. A., Waxse, B. J., Arden, S. D., Bright, N. A., Kendrick-Jones, J., and Buss, F. (2012). Autophagy receptors link myosin VI to autophagosomes to mediate Tom1-dependent autophagosome maturation and fusion with the lysosome. *Nat. Cell Biol.* 14, 1024–1035. doi: 10.1038/ncb2589

Tung, Y. T., Wang, B. J., Hsu, W. M., Hu, M. K., Her, G. M., Huang, W. P., et al. (2014). Presenilin-1 regulates the expression of p62 to govern p62-dependent tau degradation. *Mol. Neurobiol.* 49, 10–27. doi: 10.1007/s12035-013-8482-y

Vingtdeux, V., Giliberto, L., Zhao, H., Chandakkar, P., Wu, Q., Simon, J. E., et al. (2010). AMP-activated protein kinase signaling activation by resveratrol modulates amyloid-beta peptide metabolism. *J. Biol. Chem.* 285, 9100–9113. doi: 10.1074/jbc.M109.060061

Visser, P. J., Verhey, F., Knol, D. L., Scheltens, P., Wahlund, L. O., Freund-Levi, Y., et al. (2009). Prevalence and prognostic value of CSF markers of Alzheimer's disease pathology in patients with subjective cognitive impairment or mild cognitive impairment in the DESCRIPA study: a prospective cohort study. *Lancet Neurol.* 8, 619–627. doi: 10.1016/S1474-4422(09)70139-5

Wahlster, L., Arimon, M., Nasser-Ghodsi, N., Post, K. L., Serrano-Pozo, A., Uemura, K., et al. (2013). Presenilin-1 adopts pathogenic conformation in normal aging and in sporadic Alzheimer's disease. *Acta Neuropathol.* 125, 187–199. doi: 10.1007/s00401-012-1065-6

Walter, P., and Ron, D. (2011). The unfolded protein response: from stress pathway to homeostatic regulation. *Science* 334, 1081–1086. doi: 10.1126/science.1209038

Wang, J., Xiong, S., Xie, C., Markesbery, W. R., and Lovell, M. A. (2005). Increased oxidative damage in nuclear and mitochondrial DNA in Alzheimer's disease. *J. Neurochem.* 93, 953–962. doi: 10.1111/j.1471-4159.2005.03053.x

Wang, S. H., Shih, Y. L., Ko, W. C., Wei, Y. H., and Shih, C. M. (2008). Cadmium-induced autophagy and apoptosis are mediated by a calcium signaling pathway. *Cell Mol. Life Sci.* 65, 3640–3652. doi: 10.1007/s00018-008-8383-9

Wischik, C. M., Staff, R. T., Wischik, D. J., Bentham, P., Murray, A. D., Storey, J. M., et al. (2015). Tau aggregation inhibitor therapy: an exploratory phase 2 study in mild or moderate Alzheimer's disease. *J. Alzheimers Dis.* 44, 705–720. doi: 10.3233/JAD-142874

Wong, H. K., Veremeyko, T., Patel, N., Lemere, C. A., Walsh, D. M., Esau, C., et al. (2013). De-repression of FOXO3a death axis by microRNA-132 and−212 causes neuronal apoptosis in Alzheimer's disease. *Hum. Mol. Genet.* 22, 3077–3092. doi: 10.1093/hmg/ddt164

Wu, J., and Kaufman, R. J. (2006). From acute ER stress to physiological roles of the unfolded protein response. *Cell Death Differ.* 13, 374–384. doi: 10.1038/sj.cdd.4401840

Xing, H. Y., Li, B., Peng, D., Wang, C. Y., Wang, G. Y., Li, P., et al. (2017). A novel monoclonal antibody against the N-terminus of Abeta1-42 reduces plaques and improves cognition in a mouse model of Alzheimer's disease. *PLoS ONE* 12:e0180076. doi: 10.1371/journal.pone.0180076

Xu, C., Bailly-Maitre, B., and Reed, J. C. (2005). Endoplasmic reticulum stress: cell life and death decisions. *J. Clin. Invest.* 115, 2656–2664. doi: 10.1172/JCI26373

Yan, J. J., Jung, J. S., Kim, T. K., Hasan, A., Hong, C. W., Nam, J. S., et al. (2013). Protective effects of ferulic acid in amyloid precursor protein plus presenilin-1 transgenic mouse model of Alzheimer disease. *Biol. Pharm. Bull.* 36, 140–143. doi: 10.1248/bpb.b12-00798

Yang, F., Lim, G. P., Begum, A. N., Ubeda, O. J., Simmons, M. R., Ambegaokar, S. S., et al. (2005). Curcumin inhibits formation of amyloid beta oligomers and fibrils, binds plaques, and reduces amyloid *in vivo*. *J. Biol. Chem.* 280, 5892–5901. doi: 10.1074/jbc.M404751200

Yang, T., Hong, S., O'malley, T., Sperling, R. A., Walsh, D. M., and Selkoe, D. J. (2013). New ELISAs with high specificity for soluble oligomers of amyloid beta-protein detect natural Abeta oligomers in human brain but not CSF. *Alzheimers Dement.* 9, 99–112. doi: 10.1016/j.jalz.2012.11.005

Conflict of Interest Statement: The authors declare that the research was conducted in the absence of any commercial or financial relationships that could be construed as a potential conflict of interest.

Copyright © 2017 Jan, Azam, Rahman, Almigeiti, Choi, Lee, Haq and Choi. This is an open-access article distributed under the terms of the Creative Commons Attribution License (CC BY). The use, distribution or reproduction in other forums is permitted, provided the original author(s) or licensor are credited and that the original publication in this journal is cited, in accordance with accepted academic practice. No use, distribution or reproduction is permitted which does not comply with these terms.

frontiers in Neuroinformatics

ORIGINAL RESEARCH
published: 29 May 2018
doi: 10.3389/fninf.2018.00031

Application of Ferulic Acid for Alzheimer's Disease: Combination of Text Mining and Experimental Validation

Guilin Meng[1,2†], Xiulin Meng[3†], Xiaoye Ma[1], Gengping Zhang[4], Xiaolin Hu[5], Aiping Jin[1], Yanxin Zhao[1] and Xueyuan Liu[1*]*

[1]*Shanghai Tenth People's Hospital, Tongji University School of Medicine, Shanghai, China,* [2]*School of Computer Science and Informatics, Indiana University, Bloomington, IN, United States,* [3]*Houma People's Hospital, Linfen, China,* [4]*Library of Tongji University, Shanghai, China,* [5]*School of Life Sciences, Tsinghua University, Beijing, China*

Alzheimer's disease (AD) is an increasing concern in human health. Despite significant research, highly effective drugs to treat AD are lacking. The present study describes the text mining process to identify drug candidates from a traditional Chinese medicine (TCM) database, along with associated protein target mechanisms. We carried out text mining to identify literatures that referenced both AD and TCM and focused on identifying compounds and protein targets of interest. After targeting one potential TCM candidate, corresponding protein-protein interaction (PPI) networks were assembled in STRING to decipher the most possible mechanism of action. This was followed by validation using Western blot and co-immunoprecipitation in an AD cell model. The text mining strategy using a vast amount of AD-related literature and the TCM database identified curcumin, whose major component was ferulic acid (FA). This was used as a key candidate compound for further study. Using the top calculated interaction score in STRING, BACE1 and MMP2 were implicated in the activity of FA in AD. Exposure of SHSY5Y-APP cells to FA resulted in the decrease in expression levels of BACE-1 and APP, while the expression of MMP-2 and MMP-9 increased in a dose-dependent manner. This suggests that FA induced BACE1 and MMP2 pathways maybe novel potential mechanisms involved in AD. The text mining of literature and TCM database related to AD suggested FA as a promising TCM ingredient for the treatment of AD. Potential mechanisms interconnected and integrated with Aβ aggregation inhibition and extracellular matrix remodeling underlying the activity of FA were identified using *in vitro* studies.

Keywords: Alzheimer disease, BACE1, curcumin, ferulic acid, MMP2, STRING, text mining

OPEN ACCESS

Edited by:
Ghulam Md Ashraf,
King Abdulaziz University,
Saudi Arabia

Reviewed by:
Tarique Khan,
Buck Institute for Research on Aging,
United States
Luigia Trabace,
University of Foggia, Italy

***Correspondence:**
Yanxin Zhao
287594350@qq.com
Xueyuan Liu
1510922@tongji.edu.cn

†Co-first authors.

Received: *02 February 2018*
Accepted: *11 May 2018*
Published: *29 May 2018*

Citation:
Meng G, Meng X, Ma X, Zhang G, Hu X, Jin A, Zhao Y and Liu X (2018) Application of Ferulic Acid for Alzheimer's Disease: Combination of Text Mining and Experimental Validation. Front. Neuroinform. 12:31. doi: 10.3389/fninf.2018.00031

INTRODUCTION

Alzheimer's disease (AD) is a chronic neurodegenerative disease that usually progresses from short memory loss to dementia, and accounts for 50%–70% of dementia cases (Burns and Iliffe, 2009). According to the World Alzheimer Report (Prince, 2015), 46.8 million people worldwide are living with dementia, and this number is estimated to reach 131.5 million by 2050, which will result in an

increasing burden on society and families. In addition, the cost of long-term care, home services, and non-professional caregivers is greater than the cost of direct medical care (Bullock, 2004; Winblad et al., 2016; Yokoyama et al., 2016).

Despite enormous financial and research investments, appropriate interventions to prevent the progress of AD are lacking (Iqbal and Grundke-Iqbal, 2011; Selkoe, 2013). Based on the failure of a number of novel AD drugs, investigators are increasingly convinced that AD is not a single but rather a multifactorial disease (Iqbal et al., 2013), and hence, drugs that target one node on the classical pathway have little effect on the AD disease network. Since AD is a multifactorial disease, drugs that modulate systemic or multiple targets are of interest.

Traditional Chinese medicine (TCM) compositions usually exert systemic impact and can be a source of drug repositioning efforts (Wang et al., 2011). TCM treatments are natural herbs discovered by the ancient Chinese and evolved through at least 3000 years of clinical practice. TCM is gaining increasing attention with the emergence of integrative and personalized medicine, characterized by pattern differentiation on individual variance and treatments based on natural herbal synergism (Wang and Wei, 2009). With the growing popularity and promising approach of TCM applicability, the ever-increasing demand for understanding the pharmacological mechanisms and potential drug efficacy are the major issues that need to be addressed.

In this study, we sought to shed light on TCM for AD. What typical TCM treatments could be effective for AD, and what are the underlying target-based mechanisms? How can we integrate systemic and target-based understandings of the disease and treatments (Cho et al., 2006)? With the overwhelming amount of biomedical knowledge recorded in texts, text mining is essential for identifying, extracting, managing, integrating and exploiting this information to discover new, hidden, or unsuspected information. Text mining is a computer-based discovery of new, previously unknown information, which automatically extracts information from different written resources (Ding et al., 2013), drawing on information retrieval, statistics, and computational linguistics. It has considerable potential for drug target discovery and re-labeling of existing drugs. Some typical proven drug repositioning cases are available for text mining, such as the beneficial effect of estrogen on human memory discovered by Smalheiser and Swanson (1996), thalidomide for treating acute pancreatitis extracted by Weeber et al. (2003), and the association of migraine with AMPA receptors identified using Litlinker (Yetisgen-Yildiz and Pratt, 2006).

Herein, we report an approach for finding an appropriate TCM for AD through the utilization of text-mining from literature database, exploring the underlying therapeutic mechanisms followed by searching for protein-protein interactions (PPI) using the STRING platform, and finally using the SHSY5Y-APP AD cell line model for validation.

MATERIALS AND METHODS

Our first aim was to select a TCM candidate from the extensive literature collection. The study workflow is shown in **Figure 1**.

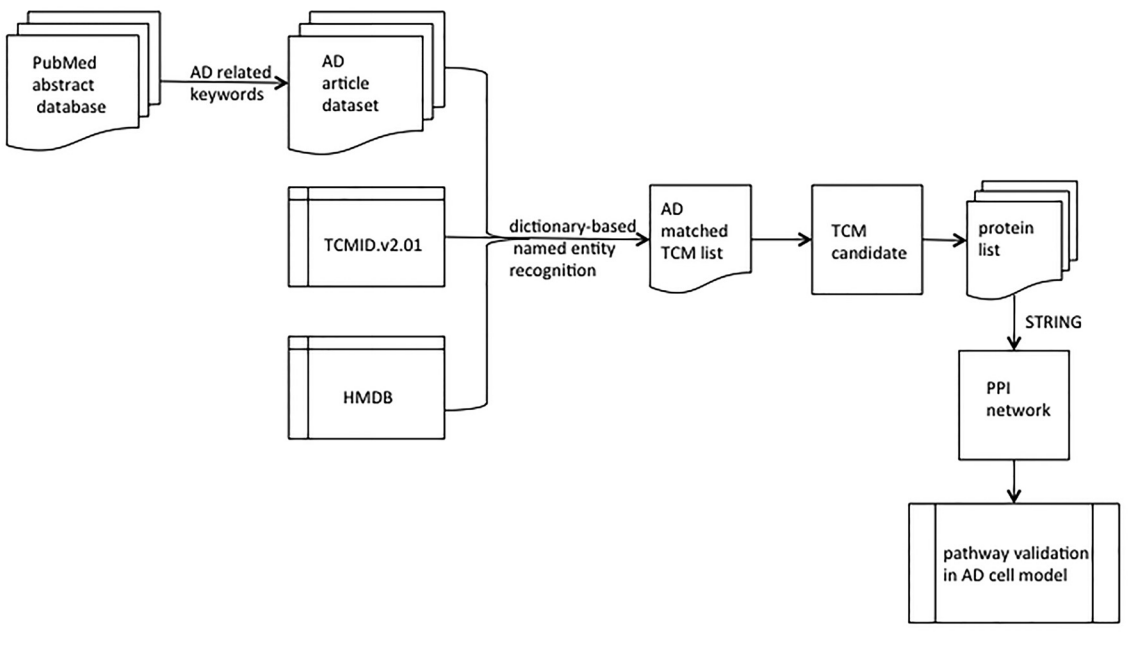


FIGURE 1 | Flowchart for selecting TCM candidates for validation. AD, Alzheimer's disease; TCM, traditional Chinese medicine; TCMID.v2.01, a TCM database; HMDB, human metabolomics database; STRING, a platform of protein-protein interaction (PPI).

Data Collection and Extraction to Find a TCM Candidate for AD

First, we assembled an AD literature dataset by retrieving articles from PubMed using AD-related keywords: "Alzheimer or Mild cognitive impairment or Dementia or Significant memory concern or Subjective memory complaint," a resource for extracting and defining TCM candidates. The TCM database, TCMID.v2.01 (Chen et al., 2006), was then utilized, which included names, stitch_id, PubChem_id, synonyms, formula, SMILES strings, and the source of the involved chemicals. The TCM terminologies, mentioned in the abstracts of the retrieved articles were then extracted using dictionary-based named entity recognition (i.e., simple word matching) provided by LingPipe[1]. Using this method, the selection of the TCM for AD was retrieved in a relatively short duration.

Furthermore, we matched the PubChem ID of TCM and the origin ontology in the human metabolome database (HMDB; Southan et al., 2013) to determine the optimal TCM candidates. After focusing on a possible lead TCM candidate, we retrieved articles in the AD dataset, and extracted protein names that co-occurred with the candidate TCM using the dictionary-based entity recognition from NCBI protein list[2]. This gave us with a list of possible proteins affected by the TCM candidate.

Inferring Possible PPI (Li et al., 2017) Networks of the TCM Candidate Using STRING

STRING presents a specific and productive functional relationship between two proteins into a combined interaction confidence score, which is derived from the co-expression score, experimentally determined interaction score, and the automated text mining score. In this system, the automated text mining score is higher than or approximately equal to the experimentally determined interaction score since it is integrated from these scores. However, if the text mining score was lower than the experimentally determined interaction, there were two possibilities: (1) the experimentally determined interaction score was a false positive; (2) only a few studies are available related to these two proteins; however, experimental validation could be conducted.

We deposited the protein list mentioned above in the multiple protein column in the search webpage of STRING[3] and acquired the PPI network after deleting results with co-expression scores >0 (already validated PPI), or experimentally determined interaction score × automated text mining score = 0 (little relevance). In the next step, we rearranged the PPI network according to text mining scores and obtained the top proteins in the network, which were most likely related to candidate mechanisms in AD.

[1]http://alias-i.com/lingpipe/index.html
[2]https://www.ncbi.nlm.nih.gov/protein/
[3]https://string-db.org/

Validation of Protein Expression and PPI in an AD Cell Line Model

In order to generate strong evidence not only in the data level, we validated the possible mechanisms mined from STRING using AD cell lines.

Cell Culture and Treatment With TCM Candidate for AD

SHSY5Y-APP cells, a classic cell line for AD research, were a kind gift from Shanghai Jiao Tong University. The cells were cultured in MEM supplemented with 10% heat-inactivated fetal bovine serum (FBS), 100 units/mL penicillin, and 100 μg/mL streptomycin (Invitrogen, Carlsbad, CA, USA) at 95% humidity, 37°C, and 5% CO_2 in an incubator. The cells were passaged by trypsinization every 2–3 days. The SHSY5Y-APP cells were treated with different doses of the TCM candidate for 24 h. In the existing researches, the effective ferulic acid (FA) concentrations vary from 10 nM to 1 mM without toxic reactions in a variety of cell lines, in accordance with the point that FA is highly safe for daily and long-term consumption (Thakkar et al., 2015; Sompong et al., 2017; Zhang et al., 2017). In line with a previous study using the same cell line (Cui et al., 2013), micromolar (μM) was chosen as the unit for FA concentration and upgraded in steps of 0 μM, 15 μM, 30 μM and 60 μM.

Co-immunoprecipitation Assays (co-IP)

Cell lysates were centrifuged (10,000× *g*) at 4°C for 15 min. Proteins were then immunoprecipitated with the relevant antibodies to determine interactions. The precleared Protein A/G Plus-Agarose beads (Merck KGaA, Darmstadt, Germany) were incubated with the immunocomplexes for 2 h and washed four times with phosphate-buffered saline. The immunoprecipitates were subjected to sodium dodecyl sulfate-polyacrylamide gel electrophoresis (SDS-PAGE; Merck KGaA, Darmstadt, Germany), followed by transfer to polyvinylidene difluoride (PVDF) membrane (Amresco, OH, USA). The antibody-antigen complexes were visualized using the UPV software according to the manufacturer's instructions. The immunoreactive bands were quantified to confirm the appropriate levels of proteins.

Western Blot

Preparation of Protein Samples

After TCM candidate exposure for 24 h, SHSY5Y-APP cells were washed with pre-cooled 4°C PBS, and then the wash solution was discarded. The above procedure was repeated twice. PMSF was added to lyse the cells on ice with frequent shaking for 30 min. After lysis, the cells were scraped with a clean scraper, and then the cell debris and lysate were transferred and centrifuged at 12,000 rpm for 5 min at 4°C. The supernatant after centrifugation was stored at −20°C.

Determination of Protein Concentration

The standard BCA assay procedure was done as previously described (Huang et al., 2010). After blocking, the membranes were probed with the following primary antibodies (Cell

Signaling, Beverly, MA, USA) using different dilutions: rabbit anti-MMP2 (92 kDa, Abcam ab92539, 1:2000), rabbit anti-MMP9 (92 kDa, Abcam ab38898, 1:2000), rabbit anti-BACE1 (68 kDa, Abcam ab183612, 1:1000), rabbit anti-APP (87 kDa, Abcam ab15272, 1:600), and mouse anti-beta-actin (42 kDa, Boster, BM0627, 1:200). All experiments were performed at least three times.

Electrophoresis

We prepared the 12% separation gel, 10% separation gel and 5% concentration gel. The prepared protein sample and the maker were added to 40 μg. After the sample was added, constant 80 V electrophoresis was performed until the bromophenol blue indicator was linear at the junction of the concentrated gel and the separation gel, and the pressure was changed to constant 120 V. This process took about 1.5 h. Next, we removed the gel and the target band according to the Marker. The PVDF membrane was soaked in methanol for several seconds and soaked in the electroporation buffer together with the filter paper. The transfer membrane conditions were as below: β-actin 200 mA 90 min, BACE1 200 mA 120 min, APP, MMP2 and MMP9 250 mA 120 min.

Immunoblotting and Analysis

The PVDF membrane was soaked in TBST containing 5% skimmed milk powder and shaken at room temperature for 2 h. We mixed the ECL reagent with the stable peroxidase solution in a ratio of 1:1, added the solution onto the PVDF membrane. X-ray film was placed in the solution, flushed, dried, scanned, and finally analyzed grayscale value with BandScan 5.0 software (NIH, USA). Statistical analysis was performed using SPSS 20.0 software (SPSS, Chicago, IL, USA). Quantitative data are presented as mean ± standard deviation (SD) of triplicates in an independent experiment that was repeated three times. Data were compared using Student's unpaired *t*-test for direct comparison between two-groups and the Tukey-Kramer test after a significant one-way analysis of variance (ANOVA), and *F*-test for multiple-group comparisons. $P < 0.05$ was considered as statistically significant.

RESULTS

Text Mining Using AD Literature and the TCM Database

We retrieved 195,882 articles from PubMed using AD-related keywords and assembled an AD article dataset.

After matching TCMID.v2.01 ingredients to the AD article database, we extracted a list of AD-related TCM ingredients with PubChem IDs, which was checked for origin ontology in HMDB.

We ranked the TCM ingredients by the number of mentions and focused on the top 20 frequent terms after deleting common words, such as "protein," "glucose," "amino acid," and others (**Table 1**).

Next, we checked the origin ontology of all the 20 components. In **Table 1**, a total of 12 endogenous ingredients, including Tau, Acetylcholine, Dopamine, Melatonin, Glutathione, Aspartate, Serotonin, Tyrosine, Serine, Levodopa, Estradiol and Creatine were selected. These endogenous ingredients could not only be absorbed from the environment but also produced and synthesized within the organism or system. Cholinesterase does not have an origin result in HMDB, and hence, our list was narrowed down to Glutamate, Choline, Nicotine, Scopolamine, Curcumin, Methionine and Physostigmine, of which Glutamate, Choline, Methionine and Physostigmine could be extracted from a broad list of drug and food options, in which includes Nicotine, Scopolamine and Curcumin. Literature suggested that Scopolamine induced retrograde amnesia, or an inability to recall events prior to its administration (Colettis et al., 2014), and hence, it was

TABLE 1 | TCM ingredients' AD-matched list in PubMed.

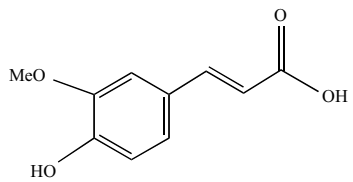
No.	Frequency	TCM ingredients	PubChem ID	Origin ontology in HMDB
1	41288	Tau	156615	Endogenous
2	5431	Glutamate	5128032	Bacteria and beans
3	3609	Cholinesterase	4460501	Not available
4	3557	Acetylcholine	5315629	Endogenous
5	3453	Dopamine	681	Endogenous
6	2824	Choline	305	Many plants and animal organs
7	1999	Nicotine	89594	Tobacco
8	1973	Melatonin	896	Endogenous
9	1898	Glutathione	124886	Drug metabolite and Endogenous
10	1722	Aspartate	5460541	Endogenous
11	1718	Serotonin	5202	Endogenous
12	1593	Tyrosine	6057	Endogenous
13	1534	Scopolamine	5184	Solanaceae
14	1432	Serine	5951	Endogenous
15	1372	*Curcumin*	969516	*Curcuma longa*
16	1089	Levodopa	6047	Endogenous
17	939	Estradiol	5757	Drug, Endogenous, Food
18	931	Methionine	6137	Drug metabolite and Food
19	788	Creatine	586	Endogenous
20	785	Physostigmine	5983	Drug

TCM, traditional Chinese medicine; HMDB, human metabolome database.

deleted from our list. Compared to the double-edged function of Nicotine, Curcumin has not been shown to cause any toxicity despite its daily consumption for centuries in Asian countries (Maheshwari et al., 2006). Thus, we first focused on Curcumin in the candidate list, an obvious TCM component that is extracted from Curcuma longa, a common plant in China.

In order to confirm its effect, we extracted all the sentences that contained "curcumin" from the AD article database. From the 107 retrieved sentences, one sentence inferred that Curcumin was suitable for treating AD; whereas, FA appeared in the same sentence with Curcumin at a high frequency. Three representative sentences are shown in **Table 2**.

Curcumin and FA share some similarities, and as a major metabolite of curcumin, FA has better bioavailability and metabolic stability than curcumin, thus rendering it as a better candidate (Badavath et al., 2016). Thus, we re-assigned our TCM target from curcumin to FA. FA also denoted as 3-(4-hydroxy-3-methoxyphenyl)-2-propenoic acid, has the following chemical structure:



After selecting FA as our TCM target, the next step was to understand the possible mechanism of FA in AD. Given the apparent complexity of the FA mechanism network, understanding its involvement in the underlying AD pathological pathways was a challenge.

We retrieved 178,725 articles using FA-related keywords "Curcumin, or FA, or Sodium Ferulate" in PubMed. From these articles, we extracted a list of proteins that was co-mentioned with FA, using the dictionary-based entity recognition. This resulted in 178 proteins that were ranked by the number of times mentioned with links to sentence sources in PubMed. After deleting a large number of false positives using the auto stop list (Fenner, 2008) of drug abbreviations, experimental test abbreviations, cell lines, synonyms of other genes, and common serum proteins, we reduced the list of proteins to 20, which are listed below:

APOB, BACE1, BCL2, CCNB1, CCND1, ERBB2, GAPDH, GSR, HMOX1, MMP2, MYB, NOS1, PCNA, PEA15, PIK3CA, PPARA, PTGS2, RAF1, TXN and VEGFA.

Potential PPI Network in STRING

Next, we entered these proteins into STRING in order to obtain direct as well as indirect protein associations (**Figure 2**).

The PPI scores were also exported into **Table 3**. The BACE1 and MMP2 combined score ranked on top among the interactions, however it had a lower automated text mining score than in the experimentally determined interaction score. We selected BACE1-MMP2 interaction as the target PPI. The edges connecting BACE1 and MMP2 (**Figure 1**) are and , which indicates that BACE1 and MMP2 may interact with each other. However, when we searched for *in-silico* evidence, the two words occurred in the full-text of some experimental articles, albeit without any direct correlation, such that the experimentally determined interaction was a false positive with a high validation possibility.

Novel Hypothesis for the FA Related Mechanism in AD

Based on the above results, we hypothesized that BACE1 and MMP2 were closely linked to the mechanism of FA. The two possibilities are as follows: these two proteins interacted directly, which could be validated by co-IP; in addition to proteolytic cleaving of the amyloid precursor protein (APP), the extracellular matrix proteins may also have a role in the AD pathological pathways, and these two pathways were always concurrent in AD.

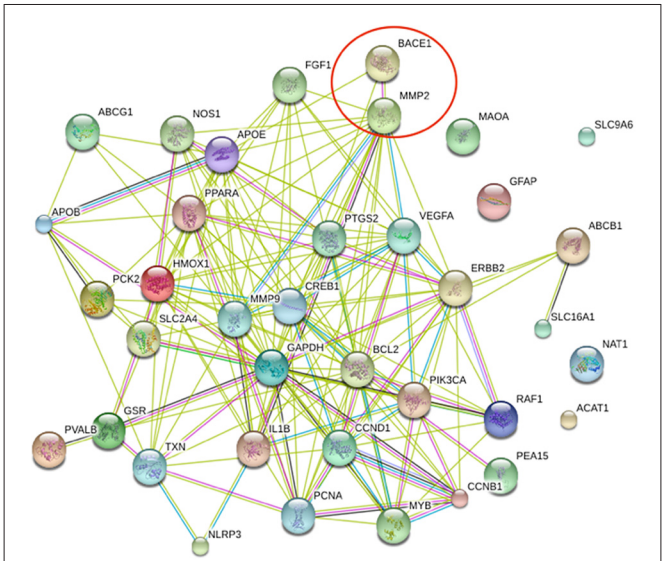


FIGURE 2 | PP1 map generated by STRING showing the interactions of the selected 20 proteins Edges represent protein-protein associations, interactions from experimentally determined, text mining, known interactions from curated databases, gene fusions, gene co-occurrence, co-expression and protein homology.

TABLE 2 | Sentences retrieved from the literature based on the entities' biomedical researches.

PMID	Sentences retrieved from literature
16387689	Because it can modulate the expression of these targets, curcumin is now being used to treat cancer, arthritis, diabetes, Crohn's disease, cardiovascular diseases, osteoporosis, Alzheimer's disease, psoriasis and other pathologies.
17127365	Food supplementation with curcumin and ferulic acid is considered a nutritional approach to reduce oxidative damage and amyloid pathology in Alzheimer's disease.
26592858	Ferulic acid has structural similarity with curcumin, which is known for its monoamine oxidase (MAO) inhibitory activity.

TABLE 3 | Ranking scores of protein interactions in STRING.

Node 1	Node 2	Co-expression	Experimentally determined interaction	Automated text mining	Combined score
BACE1	MMP2	0	0.534	0.149	0.586
PPARA	APOB	0.053	0	0.578	0.583
CCND1	MMP2	0	0	0.575	0.575
NOS1	BCL2	0.048	0	0.566	0.569
APOB	GAPDH	0	0.179	0.491	0.564
BCL2	PPARA	0	0.377	0.304	0.548
MYB	GAPDH	0.061	0	0.517	0.527
RAF1	GAPDH	0.059	0	0.503	0.512
TXN	BCL2	0	0	0.507	0.507
PCNA	PTGS2	0	0	0.507	0.507
PCNA	TXN	0.2	0.102	0.367	0.506
PCNA	MMP2	0	0	0.506	0.506
PPARA	GAPDH	0	0.042	0.501	0.501
NOS1	GAPDH	0.084	0	0.476	0.5
ERBB2	RAF1	0	0.292	0.76	0.487
BACE1	GAPDH	0.053	0	0.465	0.472
ERBB2	CCNB1	0	0	0.454	0.454
BCL2	GSR	0.048	0	0.446	0.45
NOS1	MMP2	0.055	0	0.442	0.45
TXN	VEGFA	0	0	0.442	0.442
PCNA	MYB	0.058	0	0.426	0.436
VEGFA	CCNB1	0	0	0.432	0.432
TXN	APOB	0	0	0.417	0.416
MYB	PIK3CA	0.055	0.104	0.349	0.401

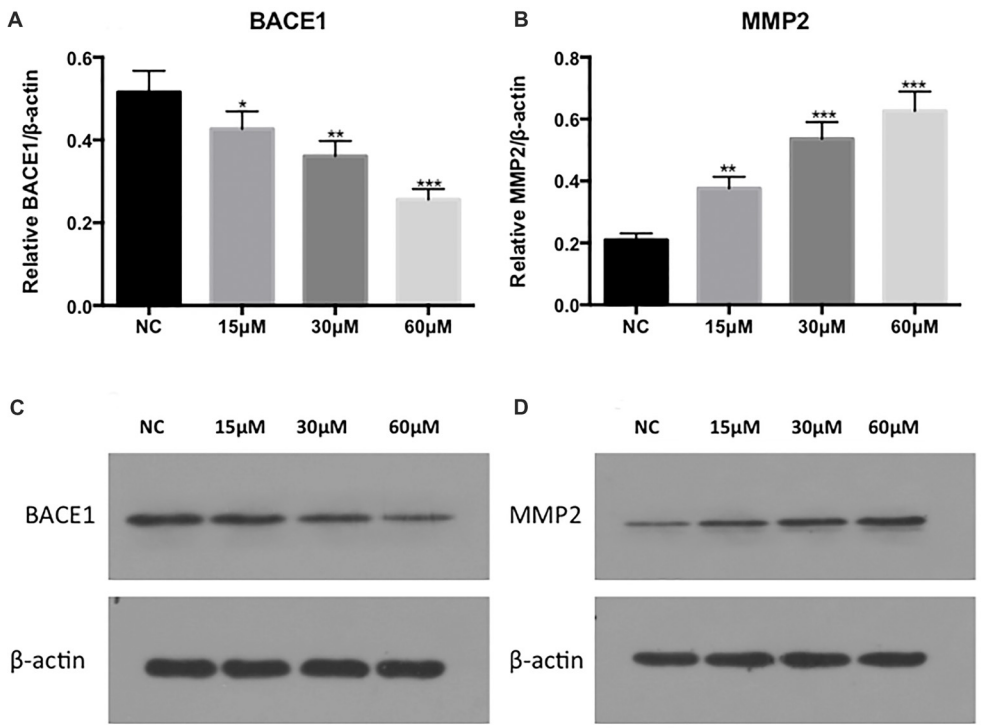


FIGURE 3 | Protein expression of BACE-1 and MMP-2 after exposure to 0, 15, 30 and 60 μM ferulic acid (FA). **(A,B)** are the expression analysis results of **(C,D)**. Statistical significance is denoted by $^{*}p < 0.05$, $^{**}p < 0.01$, $^{***}p < 0.001$ (one-way ANOVA; N = NC).

The SHSY5Y-APP cell lines were passaged every 2–3 days by trypsinization, and treated with 0, 15, 30 and 60 μM FA (Yuanmu Tech, China) for 24 h. After FA exposure for 24 h, the BACE-1 expression decreased and MMP-2 expression increased in a dose-dependent manner (**Figure 3**).

We next tested the expression of APP, another dominant protein in the Aβ aggregation pathway, which is positively correlated with BACE1. After exposure to FA, the proteolytic cleavage of APP and APP enzymolysis is decreased, thereby improving the AD process. In addition, we tested MMP9, another protein in the extracellular matrix pathway. We observed that extracellular matrix protein expression was increased after FA exposure and contributes to the pathological process of AD (**Figure 4**).

DISCUSSION

TCM Candidate Selection for AD Using Data Mining

In this study, we used text mining to select a TCM candidate for subsequent validation. FA was selected and *in vitro* validation was performed to understand the potential mechanisms involved in AD. Furthermore, the current study used the information-medicine integrated system to map TCM for AD research. In addition, text mining was coupled to the experimental validation to assess the drug selection outcomes. This offset the information gap and maximized the utilization of existing knowledge to select the optimal TCM candidate to study.

Drug discovery for AD is no longer a game of chance or just limited to the availability of new technology. Societal expectations about drug efficacy are rising; thus, early-stage drug discovery necessitates accessible, standardized data sets to generate a complete scenario of the physiological function and disease relevance. Some pioneering studies have focused on drug repurposing, such as systematic "omics" data mining of genome-wide association studies (GWAS), HMDB, epigenomics and proteomics data (Zhang et al., 2016; Pimplikar, 2017). These studies suggested drugs that were applicable for other diseases having novel anti-AD indications. These attempts were very logical however these studies did not consider TCM as a source of information for AD research. TCM is a good source for drug discovery. The uniqueness of the TCM system is based on the philosophical logic underlying daily practices (Ho et al., 2011), which was accumulated over thousands of years of empirical studies and provides a unique view of the relationships between the human body and the universe (Gu and Chen, 2014). Therefore, a better understanding of TCM and key learning from the past with appropriate strategies for the future is essential to make a significant difference. These theories render the proposed approach useful in identifying novel relationships between diseases and drugs that have a high probability of being physiologically effective. On the other hand, existing TCM drug mining primarily focuses on the assessment of ancient classic literature, with less analysis of herbal components (May et al., 2014; Pae et al., 2016), and thus may affect knowledge dissemination. Our study is the first to combine well-known TCM database with text mining approaches. This led us to select FA as a lead candidate for experimental validation for AD.

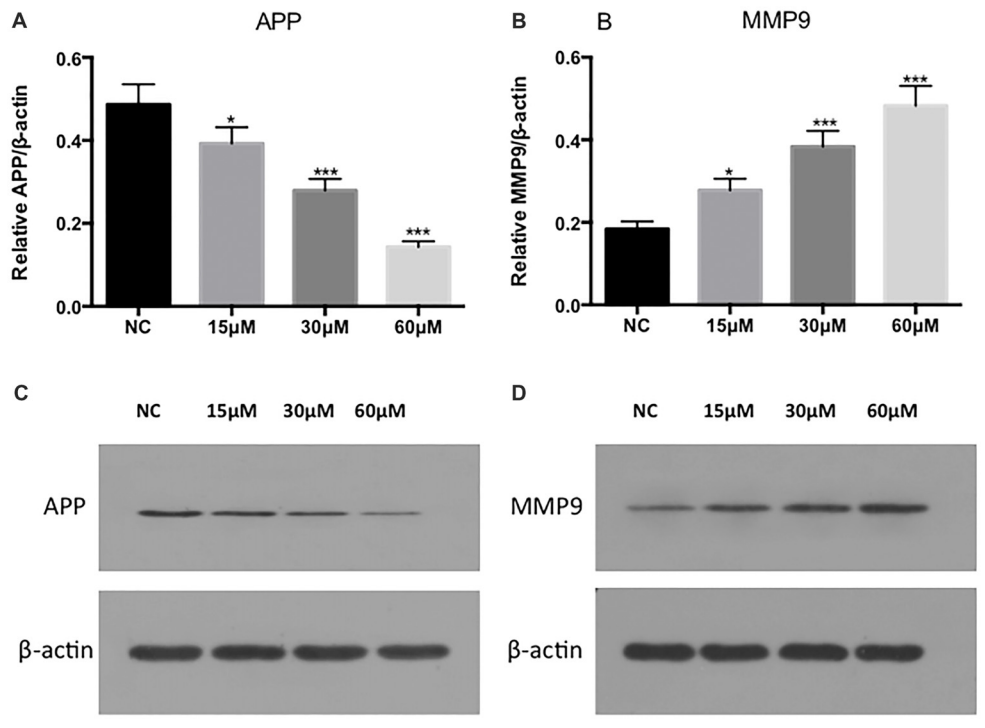


FIGURE 4 | Protein expression of APP and MMP9 after exposure to 0, 15, 30 and 60 μM FA. **(A,B)** are the expression analysis results of **(C,D)**. Statistical significance is denoted by $^{*}p < 0.05$, $^{***}p < 0.001$ (one-way ANOVA; N = NC).

MMP2-BACE1 Mechanisms of FA in AD

Our findings suggested that FA might be a promising multi-targeted TCM with a therapeutic potential for AD (Jung et al., 2016). We evaluated the APP and BACE1 inhibitory activities, which inhibit Ab aggregation; in addition, the matrix clearance properties of MMP-2 and MMP-9 implicated FA was actively involved in the alteration of matrix proteins and that it played a major role in *in vitro* extracellular matrix remodeling. As shown in a previous *in situ* proximity ligation assay (*in situ* PLA), which is a new technique to monitor PPI with high specificity and sensitivity, it was found that APP, MMP2 and MMP9 all interacted with TGFB1, and the interaction of MMP2 and BACE1 was also positive (Chen et al., 2014). Furthermore, from the Human Protein Reference Database (HPRD) in the STRING platform (Higashi and Miyazaki, 2003), the COOH-terminal parts of APP were found to interact with the extracellular matrix and highly selectively inhibit MMP2, in which the decapeptide region of APP was likely an active site-directed inhibitor toward MMP2.

The pathways of PPI at the molecular level include cellular transduction and biological function. Hence, the two pathways of Aβ aggregation inhibition and extracellular matrix remodeling were interconnected and integrated to the biological function-signaling map for AD. The results of these analyses might have potential application in exploring FA mechanism because they can be used as rational targets to inhibit the function of pathways essential to AD. In the multi-targeted AD model, APP cleavage, inhibition of Aβ deposition, and extracellular matrix remodeling are co-operative interactions involved in AD pathology, which could be attractive therapeutics with respect to pharmacokinetics and pharmacodynamics when compared to a specific highly specific single target molecule. These results highlight the prospective beneficial effects of FA as a therapeutic agent against AD pathology.

One limitation of this study was that no animal model was validated, and the experimental validation in the AD cell model was not sufficient to make a conclusive statement regarding the potential efficacy and benefit of FA. However, we found evidence in previous study of FA's protective effects on different animal models of intra-cerebroventricular (i.c.v.) injection of Aß1–42 in mice and APP/PS1 mutant transgenic mice (Jung et al., 2016), which shows potent anti-oxidant and anti-inflammatory activities. Future studies should discuss the in-depth mechanisms of FA together with the physiological data to evaluate FA efficacy and involvement in an AD animal model. These include: What are the safety implications of the different doses of FA for AD? What biomarkers exist for FA metabolites? In addition, understanding the role of FA within the system, the pathways and networks of the different protein interactions are invaluable.

CONCLUSION

In summary, we demonstrate that the combination of text mining and professional medical knowledge is an effective approach for finding new mechanisms underlying the clinical therapeutics for AD. Equipped with this data, the clinical scientist can obtain information in a short period of time without searching large volumes of articles. Moreover, using *in vitro* studies for validation, the data-driven results were based on not only a hypothesis but also true novel findings of potential mechanisms interconnected and integrated by Aβ aggregation inhibition and extracellular matrix remodeling underlying the activity of FA. The present study strongly supported text mining of the ever-increasing volume of literature and TCM database as a drug repositioning approach for elucidating FA as a promising TCM ingredient for treating AD.

AUTHOR CONTRIBUTIONS

GM, YZ and XMeng designed the study. XMa and AJ performed experiments and prepared figures. XMa, GZ and XH analyzed the data. GM and XMeng wrote and discussed all sections of the manuscript. All authors reviewed and approved the manuscript.

FUNDING

This study was supported by the International Exchange Program for Graduate Students, Tongji University (2016020033), the National Natural Science Foundation of China (81571033, 81771131) and the Shanghai Science and Technology Committee (17411950100, 17411950101).

REFERENCES

Badavath, V. N., Baysal, I., Uçar, G., Mondal, S. K., Sinha, B. N., and Jayaprakash, V. (2016). Monoamine oxidase inhibitory activity of ferulic acid amides: curcumin-based design and synthesis. *Arch. Pharm.* 349, 9–19. doi: 10.1002/ardp.201500317

Bullock, R. (2004). The needs of the caregiver in the long-term treatment of Alzheimer disease. *Alzheimer Dis. Assoc. Disord.* 18, S17–S23. doi: 10.1097/01.wad.0000127493.65032.9a

Burns, A., and Iliffe, S. (2009). Alzheimer's disease. *BMJ* 338:b158. doi: 10.1136/bmj.b158

Chen, T. C., Lin, K. T., Chen, C. H., Lee, S. A., Lee, P. Y., Liu, Y. W., et al. (2014). Using an in situ proximity ligation assay to systematically profile endogenous protein-protein interactions in a pathway network. *J. Proteome Res.* 13, 5339–5346. doi: 10.1021/pr5002737

Chen, X., Zhou, H., Liu, Y. B., Wang, J. F., Li, H., Ung, C. Y., et al. (2006). Database of traditional Chinese medicine and its application to studies of mechanism and to prescription validation. *Br. J. Pharmacol.* 149, 1092–1103. doi: 10.1038/sj.bjp.0706945

Cho, C. R., Labow, M., Reinhardt, M., van Oostrum, J., and Peitsch, M. C. (2006). The application of systems biology to drug discovery. *Curr. Opin. Chem. Biol.* 10, 294–302. doi: 10.1016/j.cbpa.2006.06.025

Colettis, N. C., Snitcofsky, M., Kornisiuk, E. E., Gonzalez, E. N., Quillfeldt, J. A., and Jerusalinsky, D. A. (2014). Amnesia of inhibitory avoidance by scopolamine is overcome by previous open-field exposure. *Learn. Mem.* 21, 634–645. doi: 10.1101/lm.036210.114

Cui, L., Zhang, Y., Cao, H., Wang, Y., Teng, T., Ma, G., et al. (2013). Ferulic acid inhibits the transition of amyloid-β42 monomers to oligomers but accelerates the transition from oligomers to fibrils. *J. Alzheimers Dis.* 37, 19–28. doi: 10.3233/JAD-130164

Ding, Y., Song, M., Han, J., Yu, Q., Yan, E., Lin, L., et al. (2013). Entitymetrics: measuring the impact of entities. *PLoS One* 8:e71416. doi: 10.1371/journal.pone.0071416

Fenner, M. (2008). Duplication: stop favouring applicant with longest list. *Nature* 452:29. doi: 10.1038/452029a

Gu, P., and Chen, H. (2014). Modern bioinformatics meets traditional Chinese medicine. *Brief. Bioinform.* 15, 984–1003. doi: 10.1093/bib/bbt063

Higashi, S., and Miyazaki, K. (2003). Identification of a region of β-amyloid precursor protein essential for its gelatinase A inhibitory activity. *J. Biol. Chem.* 278, 14020–14028. doi: 10.1074/jbc.M212264200

Ho, Y. S., So, K. F., and Chang, R. C. (2011). Drug discovery from Chinese medicine against neurodegeneration in Alzheimer's and vascular dementia. *Chin. Med.* 6:15. doi: 10.1186/1749-8546-6-15

Huang, T., Long, M., and Huo, B. (2010). Competitive binding to cuprous ions of protein and BCA in the bicinchoninic acid protein assay. *Open Biomed. Eng. J.* 4, 271–278. doi: 10.2174/1874120701004010271

Iqbal, K., Flory, M., and Soininen, H. (2013). Clinical symptoms and symptom signatures of Alzheimer's disease subgroups. *J. Alzheimers Dis.* 37, 475–481. doi: 10.3233/JAD-130899

Iqbal, K., and Grundke-Iqbal, I. (2011). Opportunities and challenges in developing Alzheimer disease therapeutics. *Acta Neuropathol.* 122, 543–549. doi: 10.1007/s00401-011-0878-z

Jung, J. S., Yan, J. J., Li, H. M., Sultan, M. T., Yu, J., Lee, H. S., et al. (2016). Protective effects of a dimeric derivative of ferulic acid in animal models of Alzheimer's disease. *Eur. J. Pharmacol.* 782, 30–34. doi: 10.1016/j.ejphar.2016.04.047

Li, T., Wernersson, R., Hansen, R. B., Horn, H., Mercer, J., Slodkowicz, G., et al. (2017). A scored human protein-protein interaction network to catalyze genomic interpretation. *Nat. Methods* 14, 61–64. doi: 10.1038/nmeth.4083

Maheshwari, R. K., Singh, A. K., Gaddipati, J., and Srimal, R. C. (2006). Multiple biological activities of curcumin: a short review. *Life Sci.* 78, 2081–2087. doi: 10.1016/j.lfs.2005.12.007

May, B. H., Zhang, A., Lu, Y., Lu, C., and Xue, C. C. (2014). The systematic assessment of traditional evidence from the premodern Chinese medical literature: a text-mining approach. *J. Altern. Complement. Med.* 20, 937–942. doi: 10.1089/acm.2013.0372

Pae, S. B., Yun, B. C., Han, Y. K., Choi, B. T., Shin, H. K., and Baek, J. U. (2016). Cognitive-enhancing herbal formulae in korean medicine: identification of candidates by text mining and literature review. *J. Altern. Complement. Med.* 22, 413–418. doi: 10.1089/acm.2015.0257

Pimplikar, S. W. (2017). Multi-omics and Alzheimer's disease: a slower but surer path to an efficacious therapy? *Am. J. Physiol. Cell Physiol.* 313, C1–C2. doi: 10.1152/ajpcell.00109.2017

Prince, M. J. (2015). World Alzheimer Report 2015: the global impact of dementia: an analysis of prevalence, incidence, cost and trends. Available online at: http://www.alz.co.uk/research/world-report-2015

Selkoe, D. J. (2013). The therapeutics of Alzheimer's disease: where we stand where we are heading. *Ann. Neurol.* 74, 328–336. doi: 10.1002/ana.24001

Smalheiser, N. R., and Swanson, D. R. (1996). Linking estrogen to Alzheimer's disease: an informatics approach. *Neurology* 47, 809–810. doi: 10.1212/WNL.47.3.809

Sompong, W., Cheng, H., and Adisakwattana, S. (2017). Ferulic acid prevents methylglyoxal-induced protein glycation, DNA damage, and apoptosis in pancreatic β-cells. *J. Physiol. Biochem.* 73, 121–131. doi: 10.1007/s13105-016-0531-3

Southan, C., Sitzmann, M., and Muresan, S. (2013). Comparing the chemical structure and protein content of ChEMBL, DrugBank, human metabolome database and the therapeutic target database. *Mol. Inform.* 32, 881–897. doi: 10.1002/minf.201300103

Thakkar, A., Chenreddy, S., Wang, J., and Prabhu, S. (2015). Ferulic acid combined with aspirin demonstrates chemopreventive potential towards pancreatic cancer when delivered using chitosan-coated solid-lipid nanoparticles. *Cell Biosci.* 5:46. doi: 10.1186/s13578-015-0041-y

Wang, H., Ding, Y., Tang, J., Dong, X., He, B., Qiu, J., et al. (2011). Finding complex biological relationships in recent PubMed articles using Bio-LDA. *PLoS One* 6:e17243. doi: 10.1371/journal.pone.0017243

Wang, J. F., and Wei, D. Q. (2009). Role of structural bioinformatics and traditional Chinese medicine databases in pharmacogenomics. *Pharmacogenomics* 10, 1213–1215. doi: 10.2217/pgs.09.81

Weeber, M., Vos, R., Klein, H., De Jong-Van Den Berg, L. T., Aronson, A. R., and Molema, G. (2003). Generating hypotheses by discovering implicit associations in the literature: a case report of a search for new potential therapeutic uses for thalidomide. *J. Am. Med. Inform. Assoc.* 10, 252–259. doi: 10.1197/jamia.m1158

Winblad, B., Amouyel, P., Andrieu, S., Ballard, C., Brayne, C., Brodaty, H., et al. (2016). Defeating Alzheimer's disease and other dementias: a priority for European science and society. *Lancet Neurol.* 15, 455–532. doi: 10.1016/S1474-4422(16)00062-4

Yetisgen-Yildiz, M., and Pratt, W. (2006). Using statistical and knowledge-based approaches for literature-based discovery. *J. Biomed. Inform.* 39, 600–611. doi: 10.1016/j.jbi.2005.11.010

Yokoyama, J. S., Wang, Y., Schork, A. J., Thompson, W. K., Karch, C. M., Cruchaga, C., et al. (2016). Association between genetic traits for immune-mediated diseases and Alzheimer disease. *JAMA Neurol* 73, 691–697. doi: 10.1001/jamaneurol.2016.0150

Zhang, M., Schmitt-Ulms, G., Sato, C., Xi, Z., Zhang, Y., Zhou, Y., et al. (2016). Drug repositioning for Alzheimer's disease based on systematic 'omics' data mining. *PLoS One* 11:e0168812. doi: 10.1371/journal.pone.0168812

Zhang, X. D., Wu, Q., and Yang, S. H. (2017). Ferulic acid promoting apoptosis in human osteosarcoma cell lines. *Pak. J. Med. Sci.* 33, 127–131. doi: 10.12669/pjms.331.12066

Conflict of Interest Statement: The authors declare that the research was conducted in the absence of any commercial or financial relationships that could be construed as a potential conflict of interest.

Copyright © 2018 Meng, Meng, Ma, Zhang, Hu, Jin, Zhao and Liu. This is an open-access article distributed under the terms of the Creative Commons Attribution License (CC BY). The use, distribution or reproduction in other forums is permitted, provided the original author(s) and the copyright owner are credited and that the original publication in this journal is cited, in accordance with accepted academic practice. No use, distribution or reproduction is permitted which does not comply with these terms.

frontiers in Aging Neuroscience

HYPOTHESIS AND THEORY
published: 16 April 2018
doi: 10.3389/fnagi.2018.00100

Targeting Beta-Amyloid at the CSF: A New Therapeutic Strategy in Alzheimer's Disease

Manuel Menendez-Gonzalez[1,2,3], Huber S. Padilla-Zambrano[4], Gabriel Alvarez[5], Estibaliz Capetillo-Zarate[6,7,8,9], Cristina Tomas-Zapico[3,10] and Agustin Costa[11]*

[1] Servicio de Neurologia, Hospital Universitario Central de Asturias, Oviedo, Spain, [2] Department of Cellular Morphology and Biology, University of Oviedo, Oviedo, Spain, [3] Instituto de Investigacion Sanitaria del Principado de Asturias, Oviedo, Spain, [4] Centro de Investigaciones Biomedicas (CIB), University of Cartagena, Cartagena, Colombia, [5] HealthSens, S.L., Oviedo, Spain, [6] Departamento de Neurociencias, Universidad del Pais Vasco (UPV/EHU), Leioa, Spain, [7] El Centro de Investigación Biomédica en Red sobre Enfermedades Neurodegenerativas, Madrid, Spain, [8] Achucarro Basque Center for Neuroscience, Leioa, Spain, [9] Ikerbasque, Basque Foundation for Science, Bilbao, Spain, [10] Department of Functional Biology, University of Oviedo, Oviedo, Spain, [11] Department of Physical and Analytical Chemistry, University of Oviedo, Oviedo, Spain

Although immunotherapies against the amyloid-β (Aβ) peptide tried so date failed to prove sufficient clinical benefit, Aβ still remains the main target in Alzheimer's disease (AD). This article aims to show the rationale of a new therapeutic strategy: clearing Aβ from the CSF continuously (the "CSF-sink" therapeutic strategy). First, we describe the physiologic mechanisms of Aβ clearance and the resulting AD pathology when these mechanisms are altered. Then, we review the experiences with peripheral Aβ-immunotherapy and discuss the related hypothesis of the mechanism of action of "peripheral sink." We also present Aβ-immunotherapies acting on the CNS directly. Finally, we introduce alternative methods of removing Aβ including the "CSF-sink" therapeutic strategy. As soluble peptides are in constant equilibrium between the ISF and the CSF, altering the levels of Aβ oligomers in the CSF would also alter the levels of such proteins in the brain parenchyma. We conclude that interventions based in a "CSF-sink" of Aβ will probably produce a steady clearance of Aβ in the ISF and therefore it may represent a new therapeutic strategy in AD.

Keywords: Alzheimer disease, amyloid beta-peptides, cerebrospinal fluid, immunotherapy, "CSF sink hypothesis"

OPEN ACCESS

Edited by:
Mohammad Amjad Kamal, King Abdulaziz University, Saudi Arabia

Reviewed by:
Fabrizio Piazza, Università degli Studi di Milano Bicocca, Italy
Alessandro Stefani, Università degli Studi di Roma Tor Vergata, Italy

****Correspondence:***
Manuel Menendez-Gonzalez
manuelmenendezgonzalez@gmail.com

Received: *31 October 2017*
Accepted: *26 March 2018*
Published: *16 April 2018*

Citation:
Menendez-Gonzalez M, Padilla-Zambrano HS, Alvarez G, Capetillo-Zarate E, Tomas-Zapico C and Costa A (2018) Targeting Beta-Amyloid at the CSF: A New Therapeutic Strategy in Alzheimer's Disease. Front. Aging Neurosci. 10:100. doi: 10.3389/fnagi.2018.00100

PHYSIOLOGICAL CLEARANCE OF Aβ

Amyloid beta (Aβ) denotes peptides of 36–43 amino acids that are intrinsically unstructured, meaning that in solution it does not acquire a unique tertiary fold but rather populates a set of structures. These peptides derive from the amyloid precursor protein (APP), which is cleaved by beta- (BACE) and gamma-secretases to yield Aβ (Menendez-Gonzalez et al., 2005; O'Nuallain et al., 2010).

Amyloid beta is cleared from the brain by several independent mechanisms (Malm et al., 2010; Diem et al., 2017; Zuroff et al., 2017), including drainage to the vascular and glymphatic systems (DeMattos et al., 2001; Iliff et al., 2012, 2013; Tarasoff-Conway et al., 2015; Bakker et al., 2016; Zuroff et al., 2017), and *in situ* degradation by glial cells (Ries and Sastre, 2016; Zuroff et al., 2017). Astrocytes and microglia can produce Aβ degrading proteases like neprilysin, as well as chaperones involved in the clearance of Aβ. There is also a receptor mediated

endocytosis, where receptors located in the surface of glial cells are involved in the uptake and clearance of Aβ, like lipoprotein receptor-related protein 1 (LRP), receptor for advanced glycation end products (RAGE) and others (Ries and Sastre, 2016). In transcytosis, Aβ is removed from ISF across the blood brain barrier (BBB) by LRP (Yamada et al., 2009). LRP binds Aβ in the brain and then transports it across the BBB into the systemic blood. The LRP extracellular domain is cleaved allowing the LRP bound to Aβ. RAGE protein brings unbound Aβ back into the CNS. The whole process is regulated by PICALM (Zhao et al., 2015). A perivascular pathway facilitates CSF flow through the brain parenchyma and the clearance of interstitial solutes, including Aβ (Iliff et al., 2012, 2013). It was thought that changes in arterial pulsatility may contribute to accumulation and deposition of toxic solutes, including Aβ, in the aging brain (Iliff et al., 2012, 2013). However, mathematical simulation showed that arterial pulsations are not strong enough to produce drainage velocities comparable to experimental observations and that a valve mechanism such as directional permeability of the intramural periarterial drainage pathway is necessary to achieve a net reverse flow (Diem et al., 2017).

ALTERED CLEARANCE OF Aβ IN ALZHEIMER'S DISEASE

The pathophysiology of Alzheimer's disease (AD) is characterized by the accumulation of Aβ and phospho-tau protein in the form of neuritic plaques and neurofibrillary tangles, respectively (Braak and Braak, 1991; Atwood et al., 2002). Aβ molecules can aggregate to form flexible soluble oligomers, which exist in several forms and are toxic to neurons (Haass and Selkoe, 2007), and finally into diffuse and dense plaques. Moreover, variable amounts of misfolded oligomers (known as "seeds") are taken up by neurons then transmitted from neuron to neuron via the extracellular milieu and can propagate aggregates by a 'seeding' or "prion like" mechanism (Walker et al., 2016; Lei et al., 2017). Tau also forms such prion-like misfolded oligomers, and there is some evidence that misfolded Aβ can induce tau misfolding (Pulawski et al., 2012; Nussbaum et al., 2013).

Amyloid-β accumulation has been hypothesized to result from an imbalance between Aβ production and clearance. An overproduction is probably the main cause of the disease in the familial AD where a mutation in the *APP, PSEN1,* or *PSEN2* genes is present (presenilins are postulated to regulate APP processing through their effects on gamma-secretase) while altered clearance is probably the main cause of the disease in sporadic AD. A good amount of studies reporting altered clearance of Aβ in AD have been published in recent years (Atwood et al., 2002; Mawuenyega et al., 2010; Tarasoff-Conway et al., 2015; Ries and Sastre, 2016; de Leon et al., 2017; Zuroff et al., 2017), becoming one of the "hot-topics" in AD research today.

The different clearance systems probably contribute to varying extents on Aβ homeostasis. Any alteration to their function may trigger the progressive accumulation of Aβ (Morrone et al., 2015; Tarasoff-Conway et al., 2015; de Leon et al., 2017), which is the fundamental step in the hypothesis of the amyloid cascade (Lambert et al., 1998; Quan and Banks, 2007; Mawuenyega et al., 2010; Bateman et al., 2012; Fagan et al., 2014; Fleisher et al., 2015). There is a relationship between the decrease in the rate of turnover of amyloid peptides and the probability of aggregation due to incorrect protein misfolding (Patterson et al., 2015) resulting in its accumulation. As soluble molecules can move in constant equilibrium between the ISF and the CSF, Aβ monomers and oligomers can be detected in the CSF. The AP42, and Aβ oligomer/protofibril levels in cortical biopsy samples are higher in subjects with insoluble cortical Aβ aggregates than in subjects without aggregates, and brain tissue levels of AP42 are negatively correlated with CSF AP42 (Patel et al., 2012; Cesarini and Marklund, 2018). Indeed, measuring the levels of Aβ in the CSF is one of the main proposed biomarkers already accepted in the diagnostic criteria of AD (McKhann et al., 2011). It has been reported that levels of Aβ in the CSF vary with time. Results from cross-sectional analysis in familial AD demonstrate higher levels of Aβ in the CSF from mutation carriers compared to controls very early in the disease process (∼20–30 years prior to estimated symptom onset), which then drop with disease progression, becoming significantly lower than controls ∼10–20 years prior to symptom onset (Morrone et al., 2015; Tarasoff-Conway et al., 2015). These low levels then begin to plateau with the development of cognitive symptoms (Iliff et al., 2013). In sporadic AD at very early preclinical stage (transitional stage) there might be either elevations or reductions in CSF AP42 (Clark et al., 2018; de Leon et al., 2018).

THERAPEUTIC CLEARANCE OF Aβ

Different approaches have been investigated with the aim of removing brain Aβ. Decreasing Aβ production might be the first approach that one can think of to reduce ISF Aβ. For instance, the inhibition BACE is one of the first therapeutic strategies formulated after the amyloid cascade hypothesis, and it is still being explored today. Alternatively, increasing the elimination of Aβ by enzymatic degradation or by clearance enhancement may be able to slow down both the aggregation and the spread processes of the disease given the relevance of Aβ as a substrate in AD (Ryan et al., 2010). Among all strategies to enhance the clearance of Aβ, immunotherapy is the most explored approach so far.

Aβ Immunotherapy

Peripheral Aβ Immunotherapy and the Mechanism of Action of "Peripheral-Sink"

The Aβ immunotherapy consist on activating the immune system against Aβ through the induction (active immunotherapy) or administration (passive immunotherapy) of Aβ-antibodies (Menendez-Gonzalez et al., 2011). Passive immunotherapy can be either monoclonal (mAbs) or polyclonal (immunoglobulins). Active immunization activates the immune system to produce specific antigen antibodies. In AD, Aβ or fragments of Aβ can be used as an antigen, conjugated to a T-cell epitope-bearing protein, together with a booster of the immune system (adjuvant). Passive immunization avoids the need to activate and initiate

an immune response to produce antigen-specific antibodies. In both active and passive immunization, Aβ-antibodies bind to Aβ, potentially promoting the clearance of the peptide (Georgievska et al., 2015).

Some interventions have been shown to produce some positive changes on brain Aβ, both in animal models and in human subjects. Unfortunately, these neuropathological benefits were not accompanied by sufficient clinical benefit; therefore, none of these therapies have been transferred to the clinic. One of the reasons may be that effective development of AD therapeutic strategies targeting Aβ require very early administration (before amyloid-plaques are in place) and consideration of the age- and ApoE-specific changes to endogenous Aβ clearance mechanisms in order to optimize efficacy (Morrone et al., 2015).

Understanding how Aβ-antibodies remove Aβ from the brain is a key in the design of Aβ immunotherapies for AD. Two distinct but not mutually exclusive mechanisms have been proposed: The "microglial phagocytosis" would require the antibodies to enter the brain, where they mediate the uptake of Aβ into local microglia. The "peripheral sink" mechanism of action relies only on peripheral antibodies to sequester Aβ in the systemic blood, lowering the level of free Aβ and inducing the brain to release its store of the peptide. This sequestration of circulating Aβ produces a shift in the concentration gradient of Aβ between the brain and the blood causing an efflux of Aβ out of the brain. Thus, it has been hypothesized that reducing Aβ peptides in the periphery would be a way to diminish Aβ levels and plaque load in the brain (Xiang et al., 2015). However, controversy still remains, with evidence both in favor and against the peripheral sink mechanism (Deane et al., 2009; Yamada et al., 2009). Studies with transgenic AD mice seem to validate the hypothesis of the peripheral sink as the main mechanism of Aβ removal after immunization. Some others showed that little or no antibody enters the brain (Vasilevko et al., 2007) and that peripheral anti-Aβ antibody alters CNS and plasma Aβ clearance decreasing brain Aβ burden (DeMattos et al., 2001). Additionally, mice with the Dutch and Iowa mutations have an Aβ peptide that is a poor substrate for the efflux transporter LRP, and so accumulates to high levels in the brain. Indeed, these mice have no peripheral sink effect, and despite a massive buildup of vascular amyloid and parenchymal plaque in brain, Aβ remains undetectable in their blood (Deane et al., 2004; Davis et al., 2006). Direct measurements of brain extracts revealed that little or no antibody was able to enter the brain from the periphery (Ryan et al., 2010). Sagare et al. (2007) showed that infusing in the blood a recombinant version of LRP (sLRP) binding Aβ lowers plaque burden in these mice, producing the peripheral sink effect. Authors also proved that Aβ shifted out of the CNS into the blood (Sagare et al., 2007).

On the other hand, sustained peripheral depletion of Aβ with a new form of neprilysin, which fuses with albumin to prolong plasma half-life, is designed to confer increased Aβ degradation activity and does not affect central Aβ levels in transgenic mice, rats and monkeys (Henderson et al., 2014). In other report (Deane et al., 2009), authors tested the peripheral sink hypothesis by investigating how selective inhibition of Aβ production in the periphery, using a BACE inhibitor or reducing BACE gene dosage, affects Aβ load in the brain. Selective inhibition of peripheral BACE activity in wildtype or transgenic mice reduced Aβ levels in the periphery but not in the brain, even after chronic treatment over several months. In contrast, a BACE inhibitor with improved brain disposition reduced Aβ levels in both brain and periphery already after acute dosing. BACE heterozygous mice displayed an important reduction in plasma Aβ, whereas Aβ reduction in the brain was much lower. These data suggest that reduction of Aβ in the periphery is not sufficient to reduce brain Aβ levels and that BACE is not the rate-limiting enzyme for Aβ processing in the brain (Georgievska et al., 2015). Recent research suggests that CSF naturally occurring antibodies against Aβ seem to have a protective effect for AD, while serum naturally occurring antibodies against Aβ do not seem to have any effect (Kimura et al., 2017; Menendez Gonzalez, 2017a). In line with this, Piazza et al. (2013) reported the first evidence about the participation of natural anti-Aβ autoantibodies in cerebral amyloid-related angiopathy (CAA) and the possible elimination mechanism of soluble Aβ in the CSF by antibodies. Today, CSF anti-Aβ autoantibodies are known to play a key role in the development of amyloid-related imaging abnormalities (ARIA) (DiFrancesco et al., 2015; Chen et al., 2016; Piazza and Winblad, 2016), which are MRI signal changes representing vasogenic edema (VE) and microhemorrhages (mH). VE and mH share some common underlying pathophysiological mechanisms, both in the natural history of AD and in immunotherapies (Sperling et al., 2011). Furthermore, this ARIA has been associated with a massive release of soluble Aβ, plaques and vascular deposits during the acute inflammatory phase (DiFrancesco et al., 2015; Chen et al., 2016; Piazza and Winblad, 2016).

Administered monoclonal antibodies also showed molecular effect, but clinical benefit in humans was not significant. For instance, Solanezumab increases the elimination of soluble Aβ and decreases the deposition of cerebral amyloid plaque in AD mice. In clinical trials, the administration of Solanezumab in patients with mild to moderate AD generated an increase of unbound Aβ in CSF, suggesting that the antibody has a direct peripheral effect with central indirect effect. However, clinical trials showed not improvement of the cognitive and functional capacities of patients (Doody et al., 2014; Chen et al., 2016; Siemers et al., 2016). Similarly, Bapineuzumab modifies Aβ accumulation and CSF biomarkers, but none of the trials showed a significant clinical benefit (Salloway et al., 2014).

Aβ-Immunotherapy Into the CNS

Many investigators have indicated that peripheral clearance through the BBB is not recommended in elderly people, in whom the normal transport of Aβ may present alterations. In addition, the risk of antibody-mediated hemorrhage in sites of cerebral amyloid angiopathy decreases the authors' interest in peripheral passive as well as in active reduction mediated by CNS Aβ antibodies. Due to this, it has been considered that the direct administration of immunotherapy to the CNS is more efficient than the peripheral one, but the intrinsic characteristics of the BBB make the pharmacological approach difficult. This has led to the search for strategies to overcome

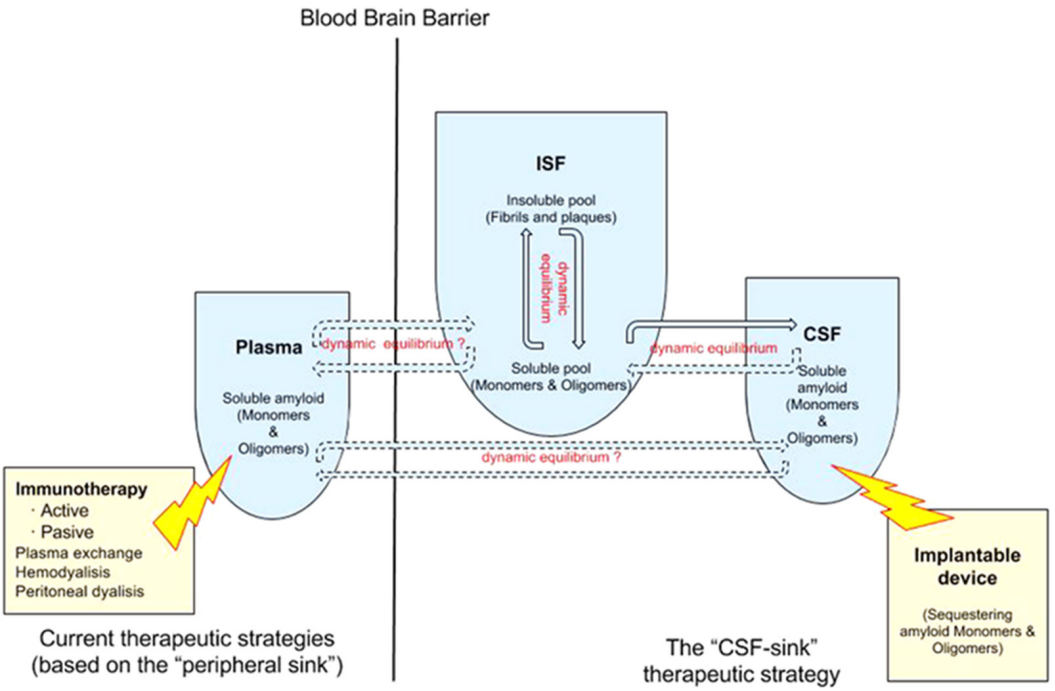


FIGURE 1 | Double dynamic equilibrium of Aβ: there is a bidirectional equilibrium between insoluble and soluble pools of Aβ in the ISF and there is a second equilibrium, also probably bidirectional, of soluble Aβ between the ISF and the CSF. The "CSF-sink therapeutic strategy" consists on sequestering target proteins from the CSF with implantable devices, thus inducing changes in the levels of these proteins in the ISF. Current therapeutic strategies rely on the "peripheral sink" hypothesis mostly. There is some controversy about the existence of a equilibrium of Aβ between plasma and the ISF/CSF.

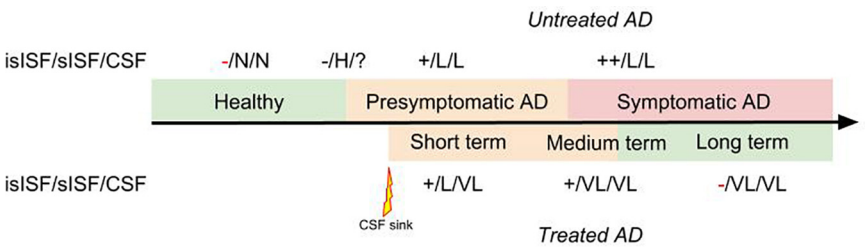


FIGURE 2 | Diagram representing the therapeutic effect of a "CSF-sink" intervention on the predicted levels of Aβ in the insoluble ISF (isISF), soluble ISF (sISF) and CSF pools in a patient with AD treated at presymptomatic stage. Legend: +, positive deposits; −, negative deposits; N, normal; H, high; VH, very high; L, low; VL, very low.

the BBB. These approaches were divided into two categories: the first comprises techniques that facilitate the passage of drugs through the BBB (for example, molecular "Trojan horses," oligopeptides transporters coupled to protons, exosomes, liposomes, nanoparticles, chimeric peptides, prodrugs); and the second consists on techniques that avoid BBB through direct delivery to the SNC. In this last category, the techniques have been investigated include the interruption of BBB (for example, with ultrasound and microbubbles) and intrathecal, intracerebroventricular and intranasal administration (Wilcock et al., 2003; Carty et al., 2006). Although much less explored, passive Aβ-immunotherapy into the CNS has been tested on animal models. Several groups have reported to have achieved clearance of brain Aβ after intracerebral or intraventricular injection of either Aβ antibodies (Wilcock et al., 2003, 2004; Oddo et al., 2004; Carty et al., 2006; Levites et al., 2006), antibodies to oligomeric assemblies of Aβ (Chauhan, 2007) or promoting cellular expression of Aβ-specific antibodies, delivered using viral vectors (Ryan et al., 2010). In most cases, the clearance was rapid (within a few days), but the benefits of the injections were transient because the decrease in amyloid plaques approached reversion at 30 days (Sevigny et al., 2016). Authors also observed a decrease in tau hyperphosphorylation, an increase in the number of microglia counts and an improved learning behavior (Doody et al., 2014). In different reports, the level of clearance achieved by this method varies significantly and ranges from what appears to be elimination throughout the CNS (Sakai et al., 2016) to the limited elimination of diffuse

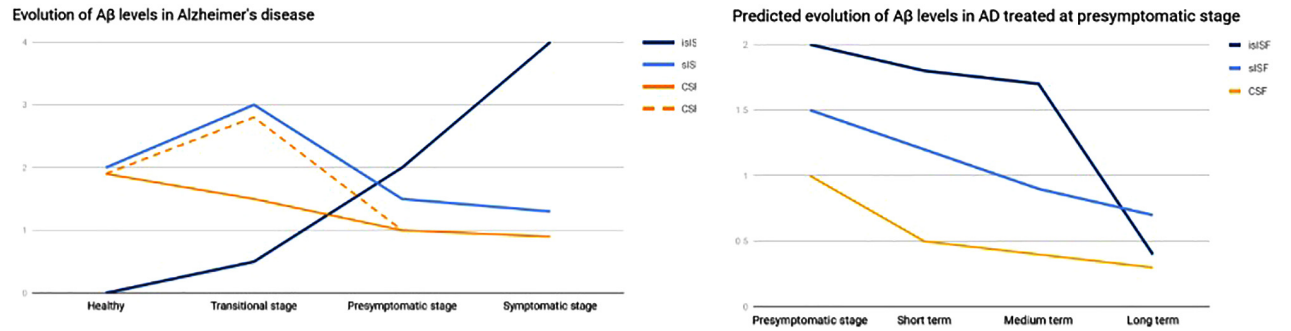


FIGURE 3 | Graph representing the evolution of Aβ in the different pools. On the left, evolution of Aβ levels across the different stages of a AD. On the right, predicted evolution of Aβ levels in a case of AD treated at presymptomatic stage. isISF, insoluble pool in the ISF; sISF, soluble pool in the ISF.

amyloid around the site of antibody injection (Ostrowitzki et al., 2012).

Some human monoclonal antibodies have been shown to enter the brain even when administered peripherally. In a transgenic mouse model of AD, Aducanumab is shown to enter the brain, bind parenchymal Aβ, and reduce soluble and insoluble Aβ in a dose-dependent manner. In patients with prodromal or mild AD, 1 year of monthly intravenous infusions of Aducanumab reduces brain Aβ in a dose- and time-dependent manner. This is accompanied by a slowing of clinical decline. The main safety issues are amyloid-related imaging abnormalities (Sevigny et al., 2016). Phase 3 clinical trials are ongoing. Gantenerumab preferentially interacts with aggregated brain Aβ, both parenchymal and vascular. This antibody acts centrally to disassemble and degrade amyloid plaques by recruiting microglia and activating phagocytosis (Ostrowitzki et al., 2012) but it does not alter plasma Aβ (Bohrmann et al., 2012). As with Adenacumab, trials showed positive trends in clinical scales, main safety worries are amyloid-related imaging abnormalities and clinical trials in different phases are ongoing.

In conclusion, no Aβ immunotherapy has demonstrated significant efficacy in humans to date. A meta-analysis of immunotherapies (Penninkilampi et al., 2017) found no significant treatment differences for typical primary outcome measures. Clinical benefits of peripheral immunotherapy in humans are limited, while the benefits of central immunotherapy in animal models are transient.

Alternative Therapeutic Strategies

Despite Aβ immunotherapy showed not conclusive results to date, Aβ remains the main target in AD. A study using an image biomarker determined that a 15% decrease in Aβ is related to a cognitive improvement of 15–20% (Liu et al., 2015). For all that, there is an urgent need to find alternative methods to achieve a depletion of Aβ in the brain.

A number of studies showed that blood dialysis and plasmapheresis reduces Aβ levels in plasma and CSF in humans and attenuates AD symptoms and pathology in AD mouse models (58,6165), suggesting that removing Aβ from the plasma seems to be an effective -albeit indirect- way of removing Aβ. Different methodologies, from peritoneal dialysis (Jin et al., 2017) to hemodialysis (Kitaguchi et al., 2015; Sakai et al., 2016; Tholen et al., 2016) and plasma exchange (Boada et al., 2009), reported some extent of success removing Aβ from the plasma, which in turn reduces Aβ in the CSF and in the ISF -this last compartment has been confirmed in animals only-. Again, the "peripheral-sink hypothesis" adds new sources of support from these alternative strategies (**Figure 1**).

However, there might be a much more direct way of removing Aβ from the ISF than clearing it from the plasma: clearing it from the CSF. A starting rationale is that there is an equilibrium of Aβ levels between the ISF and plasma in AD transgenic mice before developing Aβ deposits (DeMattos et al., 2002; Cirrito et al., 2003; Hong et al., 2011; Nag et al., 2011). However, this equilibrium is lost once Aβ deposits are in place while the equilibrium of Aβ between the ISF and the CSF still persists (DeMattos et al., 2002). Some studies also found a relationship between the load of cortical deposits and levels in the CSF in humans who underwent neurosurgery (ventriculo-peritoneal shunt) (Seppala et al., 2012; Pyykko et al., 2014; Herukka et al., 2015; Abu Hamdeh et al., 2018). At equilibrium, Aβ remains predominantly monomeric up to 3 pM, above which forms large aggregates (Nag et al., 2011). Once aggregated are in place, amyloid deposits can rapidly sequester soluble A from the ISF (Cirrito et al., 2003; Hong et al., 2011). Aβ in the ISF in plaque-rich mice is thought to be derived not from new A biosynthesis but rather from the large reservoir of less soluble Aβ in brain parenchyma (Cirrito et al., 2003). Moreover, a portion of the insoluble Amyloid pool is in dynamic equilibrium with ISF Amyloid. *In vitro* studies have shown that A aggregates contain a readily dissociable pool of Aβ, or "docked Aβ" as well as a long-lasting or stable "locked" pool of Aβ (Maggio et al., 1992; Esler et al., 2000). *In vitro*, as the concentration of Aβ in solution decreases, this docked pool can quickly dissociate from fibrils. *In vivo*, when Aβ production is inhibited and ISF Aβ levels begin to decrease, it is likely that this associated docked pool can return to solution over a finite period of time, as occurs *in vitro*, causing this pool of Aβ to dissociate from fibrils and become soluble. This results in a prolonged apparent half-life of ISF Aβ in animals with Aβ deposition (Cirrito et al., 2003).

We previously posed the hypothesis that soluble proteins can be cleared from the brain with interventions where soluble proteins are continuously removed from the CSF (Liu et al., 2015;

Menendez Gonzalez, 2017c). This is since soluble proteins are in constant equilibrium between the ISF and the CSF. Therefore, clearing Aβ from the CSF continuously will probably promote the efflux of Aβ from the ISF to the CSF (**Figure 2**).

The "CSF-sink" therapeutic strategy consists on sequestering Aβ from the CSF (**Figure 2**). Today, we can conceive several ways of accessing the CSF with implantable devices (Menendez Gonzalez, 2017b). These devices can be endowed with different technologies able to capture target molecules, such as Aβ, from the CSF. Thus, these interventions would work as a central sink of Aβ, reducing the levels of CSF Aβ, and by means of the CSF-ISF equilibrium would promote the efflux of Aβ from the ISF to the CSF (**Figure 2**).

A study on the Aβ clearance kinetics suggests that the speed and efficiency of Aβ clearance pathways may influence the effect on Aβ deposits (Yuede et al., 2016). A therapeutic strategy aimed at rapid clearance at only high concentrations may be different from a strategy that is designed for a sustained, possibly larger, suppression of Aβ. The "CSF-sink" therapeutic strategy is expected to provide an intense and sustained depletion of Aβ in the CSF and, in turn, a steady decrease Aβ in the ISF, preventing the formation of new aggregates and deposits in the short term and potentially reversing the already existing deposits in the medium and long terms (**Figure 3**).

Albeit AD is a complex disease, and targeting one single molecule might not be enough to hinder the whole neurodegenerative process, we consider this strategy is worth trying, since it is feasible and potentially efficient.

Finally, we would like to mention this strategy might also be valid for other neurodegenerative and neuroimmune diseases where target molecules are well identified and present in the CSF in equilibrium with the ISF. A series of studies in cellular and animal models are needed to prove this hypothesis.

CONCLUSION

We introduce the rationale basis for the "CSF-sink" hypothesis and conclude that continuous depletion of Aβ in the CSF will probably produce a steady clearance of Aβ in the ISF. Implantable devices aimed at sequestering Aβ from the CSF may represent a new therapeutic strategy in AD.

AUTHOR CONTRIBUTIONS

MM-G is the author of the hypothesis and wrote the whole manuscript. All the other authors revised the existing literature and critically reviewed the manuscript.

REFERENCES

Abu Hamdeh, S., Virhammar, J., Sehlin, D., Alafuzoff, I., Cesarini, K. G., and Marklund, N. (2018). Brain tissue Abeta42 levels are linked to shunt response in idiopathic normal pressure hydrocephalus. *J. Neurosurg.* doi: 10.3171/2017.7.JNS171005 [Epub ahead of print].

Atwood, C. S., Martins, R. N., Smith, M. A., and Perry, G. (2002). Senile plaque composition and posttranslational modification of amyloid-beta peptide and associated proteins. *Peptides* 23, 1343–1350. doi: 10.1016/S0196-9781(02)00070-0

Bakker, E. N., Bacskai, B. J., Arbel-Ornath, M., Aldea, R., Bedussi, B., Morris, A. W. J., et al. (2016). Lymphatic clearance of the brain: perivascular, paravascular and significance for neurodegenerative diseases. *Cell Mol. Neurobiol.* 36, 181–194. doi: 10.1007/s10571-015-0273-8

Bateman, R. J., Xiong, C., Benzinger, T. L. S., Fagan, A. M., Goate, A., Fox, N. C., et al. (2012). Clinical and biomarker changes in dominantly inherited Alzheimer's disease. *N. Engl. J. Med.* 367, 795–804. doi: 10.1056/NEJMoa1202753

Boada, M., Ortiz, P., Anaya, F., Hernandez, I., Munoz, J., Nunez, L., et al. (2009). Amyloid-targeted therapeutics in Alzheimer's disease: use of human albumin in plasma exchange as a novel approach for Abeta mobilization. *Drug News Perspect.* 22, 325–339. doi: 10.1358/dnp.2009.22.6.1395256

Bohrmann, B., Baumann, K., Benz, J., Gerber, F., Huber, W., Knoflach, F., et al. (2012). Gantenerumab: a novel human anti-Abeta antibody demonstrates sustained cerebral amyloid-beta binding and elicits cell-mediated removal of human amyloid-beta. *J. Alzheimers Dis.* 28, 49–69. doi: 10.3233/JAD-2011-110977

Braak, H., and Braak, E. (1991). Neuropathological stageing of Alzheimer-related changes. *Acta Neuropathol.* 82, 239–259. doi: 10.1007/BF00308809

Carty, N. C., Wilcock, D. M., Rosenthal, A., Grimm, J., Pons, J., Ronan, V., et al. (2006). Intracranial administration of deglycosylated C-terminal-specific anti-Aβ antibody efficiently clears amyloid plaques without activating microglia in amyloid-depositing transgenic mice. *J. Neuroinflammation* 3:11. doi: 10.1186/1742-2094-3-11

Cesarini, K. G., and Marklund, N. (2018). Brain tissue Aβ42 levels are linked to shunt response in idiopathic normal pressure hydrocephalus. *J. Neurosurg.* doi: 10.3171/2017.7.JNS171005 [Epub ahead of print].

Chauhan, N. B. (2007). Intracerebroventricular passive immunization with anti-oligoAbeta antibody in TgCRND8. *J. Neurosci. Res.* 85, 451–463. doi: 10.1002/jnr.21110

Chen, Y. F., Ma, X., Sundell, K., Alaka, K., Schuh, K., Raskin, J., et al. (2016). Quantile regression to characterize solanezumab effects in Alzheimer's disease trials. *Alzheimers Dement.* 2, 192–198. doi: 10.1016/j.trci.2016.07.005

Cirrito, J. R., May, P. C., O'Dell, M. A., Taylor, J. W., Parsadanian, M., Cramer, J. W., et al. (2003). In vivo assessment of brain interstitial fluid with microdialysis reveals plaque-associated changes in amyloid-beta metabolism and half-life. *J. Neurosci.* 23, 8844–8853.

Clark, L. R., Berman, S. E., Norton, D. L., Koscik, R., Jonaitis, E., Blennow, K., et al. (2018). Age-accelerated cognitive decline in asymptomatic adults with CSF β-amyloid. *Neurology*. doi: 10.1212/WNL.0000000000005291

Davis, J., Xu, F., Miao, J., Previti, M. L., Romanov, G., Ziegler, K., et al. (2006). Deficient cerebral clearance of vasculotropic mutant Dutch/Iowa Double A beta in human A betaPP transgenic mice. *Neurobiol. Aging* 27, 946–954. doi: 10.1016/j.neurobiolaging.2005.05.031

de Leon, M. J., Li, Y., Okamura, N., Tsui, W. H., Saint-Louis, L. A., Glodzik, L., et al. (2017). Cerebrospinal fluid clearance in Alzheimer disease measured with dynamic PET. *J. Nucl. Med.* 58, 1471–1476. doi: 10.2967/jnumed.116.187211

de Leon, M. J., Pirraglia, E., Osorio, R. S., Glodzik, L., Saint-Louis, L., Kim, H.-J., et al. (2018). The nonlinear relationship between cerebrospinal fluid Abeta42 and tau in preclinical Alzheimer's disease. *PLoS One* 13:e0191240. doi: 10.1371/journal.pone.0191240

Deane, R., Bell, R. D., Sagare, A., and Zlokovic, B. V. (2009). Clearance of amyloid-beta peptide across the blood-brain barrier: implication for therapies in Alzheimer's disease. *CNS Neurol. Disord. Drug Targets* 8, 16–30. doi: 10.2174/187152709787601867

Deane, R., Wu, Z., Sagare, A., Davis, J., Du Yan, S., Hamm, K., et al. (2004). LRP/amyloid beta-peptide interaction mediates differential brain efflux of Abeta isoforms. *Neuron* 43, 333–344. doi: 10.1016/j.neuron.2004.07.017

DeMattos, R. B., Bales, K. R., Cummins, D. J., Dodart, J. C., Paul, S. M., and Holtzman, D. M. (2001). Peripheral anti-A beta antibody alters CNS and plasma

A beta clearance and decreases brain A beta burden in a mouse model of Alzheimer's disease. *Proc. Natl. Acad. Sci. U.S.A.* 98, 8850–8855. doi: 10.1073/pnas.151261398

DeMattos, R. B., Bales, K. R., Parsadanian, M., O'Dell, M. A., Foss, E. M., Paul, S. M., et al. (2002). Plaque-associated disruption of CSF and plasma amyloid-beta (Abeta) equilibrium in a mouse model of Alzheimer's disease. *J. Neurochem.* 81, 229–236. doi: 10.1046/j.1471-4159.2002.00889.x

Diem, A. K., MacGregor Sharp, M., Gatherer, M., Bressloff, N. W., Carare, R. O., and Richardson, G. (2017). Arterial pulsations cannot drive intramural periarterial drainage: significance for Aβ drainage. *Front. Neurosci.* 11:475. doi: 10.3389/fnins.2017.00475

DiFrancesco, J. C., Longoni, M., and Piazza, F. (2015). Anti-Abeta autoantibodies in amyloid related imaging abnormalities (ARIA): candidate biomarker for immunotherapy in Alzheimer's disease and cerebral amyloid angiopathy. *Front. Neurol.* 6:207. doi: 10.3389/fneur.2015.00207

Doody, R. S., Thomas, R. G., Farlow, M., Iwatsubo, T., Vellas, B., Joffe, S., et al. (2014). Phase 3 trials of solanezumab for mild-to-moderate Alzheimer's disease. *N. Engl. J. Med.* 370, 311–321. doi: 10.1056/NEJMoa1312889

Esler, W. P., Stimson, E. R., Jennings, J. M., Vinters, H. V., Ghilardi, J. R., Lee, J. P., et al. (2000). Alzheimer's disease amyloid propagation by a template-dependent dock-lock mechanism. *Biochemistry* 39, 6288–6295. doi: 10.1021/bi992933h

Fagan, A. M., Xiong, C., Jasielec, M. S., Bateman, R. J., Goate, A. M., Benzinger, T. L. S., et al. (2014). Longitudinal change in CSF biomarkers in autosomal-dominant Alzheimer's disease. *Sci. Transl. Med.* 6:226ra30. doi: 10.1126/scitranslmed.3007901

Fleisher, A. S., Chen, K., Quiroz, Y. T., Jakimovich, L. J., Gutierrez Gomez, M., Langois, C. M., et al. (2015). Associations between biomarkers and age in the presenilin 1 E280A autosomal dominant Alzheimer disease kindred: a cross-sectional study. *JAMA Neurol.* 72, 316–324. doi: 10.1001/jamaneurol.2014.3314

Georgievska, B., Gustavsson, S., Lundkvist, J., Neelissen, J., Eketjall, S., Ramberg, V., et al. (2015). Revisiting the peripheral sink hypothesis: inhibiting BACE1 activity in the periphery does not alter beta-amyloid levels in the CNS. *J. Neurochem.* 132, 477–486. doi: 10.1111/jnc.12937

Haass, C., and Selkoe, D. J. (2007). Soluble protein oligomers in neurodegeneration: lessons from the Alzheimer's amyloid beta-peptide. *Nat. Rev. Mol. Cell Biol.* 8, 101–112. doi: 10.1038/nrm2101

Henderson, S. J., Andersson, C., Narwal, R., Janson, J., Goldschmidt, T. J., Appelkvist, P., et al. (2014). Sustained peripheral depletion of amyloid-β with a novel form of neprilysin does not affect central levels of amyloid-β. *Brain* 137, 553–564. doi: 10.1093/brain/awt308

Herukka, S.-K., Rummukainen, J., Ihalainen, J., von Und Zu Fraunberg, M., Koivisto, A. M., Nerg, O., et al. (2015). Amyloid-beta and tau dynamics in human brain interstitial fluid in patients with suspected normal pressure hydrocephalus. *J. Alzheimers Dis.* 46, 261–269. doi: 10.3233/JAD-142862

Hong, S., Quintero-Monzon, O., Ostaszewski, B. L., Podlisny, D. R., Cavanaugh, W. T., Yang, T., et al. (2011). Dynamic analysis of amyloid beta-protein in behaving mice reveals opposing changes in ISF versus parenchymal Abeta during age-related plaque formation. *J. Neurosci.* 31, 15861–15869. doi: 10.1523/JNEUROSCI.3272-11.2011

Iliff, J. J., Wang, M., Liao, Y., Plogg, B. A., Peng, W., Gundersen, G. A., et al. (2012). A paravascular pathway facilitates CSF flow through the brain parenchyma and the clearance of interstitial solutes, including amyloid beta. *Sci. Transl. Med.* 4:147ra111. doi: 10.1126/scitranslmed.3003748

Iliff, J. J., Wang, M., Zeppenfeld, D. M., Venkataraman, A., Plog, B. A., Liao, Y., et al. (2013). Cerebral arterial pulsation drives paravascular CSF-interstitial fluid exchange in the murine brain. *J. Neurosci.* 33, 18190–18199. doi: 10.1523/JNEUROSCI.1592-13.2013

Jin, W.-S., Shen, L.-L., Bu, X.-L., Zhang, W.-W., Chen, S.-H., Huang, Z.-L., et al. (2017). Peritoneal dialysis reduces amyloid-beta plasma levels in humans and attenuates Alzheimer-associated phenotypes in an APP/PS1 mouse model. *Acta Neuropathol.* 134, 207–220. doi: 10.1007/s00401-017-1721-y

Kimura, A., Takemura, M., Saito, K., Yoshikura, N., Hayashi, Y., and Inuzuka, T. (2017). Association between naturally occurring anti-amyloid β autoantibodies and medial temporal lobe atrophy in Alzheimer's disease. *J. Neurol. Neurosurg. Psychiatry* 88, 126L–131. doi: 10.1136/jnnp-2016-313476

Kitaguchi, N., Hasegawa, M., Ito, S., Kawaguchi, K., Hiki, Y., Nakai, S., et al. (2015). A prospective study on blood Abeta levels and the cognitive function of patients with hemodialysis: a potential therapeutic strategy for Alzheimer's disease. *J. Neural. Transm.* 122, 1593–1607. doi: 10.1007/s00702-015-1431-3

Lambert, M. P., Barlow, A. K., Chromy, B. A., Edwards, C., Freed, R., Liosatos, M., et al. (1998). Diffusible, nonfibrillar ligands derived from Abeta1-42 are potent central nervous system neurotoxins. *Proc. Natl. Acad. Sci. U.S.A.* 95, 6448–6453. doi: 10.1073/pnas.95.11.6448

Lei, Y., Han, H., Yuan, F., Javeed, A., and Zhao, Y. (2017). The brain interstitial system: anatomy, modeling, in vivo measurement, and applications. *Prog Neurobiol* 157, 230–246. doi: 10.1016/j.pneurobio.2015.12.007

Levites, Y., Das, P., Price, R. W., Rochette, M. J., Kostura, L. A., McGowan, E. M., et al. (2006). Anti-Abeta42- and anti-Abeta40-specific mAbs attenuate amyloid deposition in an Alzheimer disease mouse model. *J. Clin. Invest.* 116, 193–201. doi: 10.1172/JCI25410

Liu, Y.-H., Xiang, Y., Wang, Y.-R., Jiao, S.-S., Wang, Q.-H., Bu, X.-L., et al. (2015). Association between serum amyloid-beta and renal functions: implications for roles of kidney in amyloid-beta clearance. *Mol. Neurobiol.* 52, 115–119. doi: 10.1007/s12035-014-8854-y

Maggio, J. E., Stimson, E. R., Ghilardi, J. R., Allen, C. J., Dahl, C. E., Whitcomb, D. C., et al. (1992). Reversible in vitro growth of Alzheimer disease beta-amyloid plaques by deposition of labeled amyloid peptide. *Proc. Natl. Acad. Sci. U.S.A.* 89, 5462–5466. doi: 10.1073/pnas.89.12.5462

Malm, T., Koistinaho, M., Muona, A., Magga, J., and Koistinaho, J. (2010). The role and therapeutic potential of monocytic cells in Alzheimer's disease. *Glia* 58, 889–900. doi: 10.1002/glia.20973

Mawuenyega, K. G., Sigurdson, W., Ovod, V., Munsell, L., Kasten, T., Morris, J. C., et al. (2010). Decreased clearance of CNS beta-amyloid in Alzheimer's disease. *Science* 330:1774. doi: 10.1126/science.1197623

McKhann, G. M., Knopman, D. S., Chertkow, H., Hyman, B. T., Jack, C. R. J., Kawas, C. H., et al. (2011). The diagnosis of dementia due to Alzheimer's disease: recommendations from the National Institute on Aging-Alzheimer's Association workgroups on diagnostic guidelines for Alzheimer's disease. *Alzheimers Dement.* 7, 263–269. doi: 10.1016/j.jalz.2011.03.005

Menendez Gonzalez, M. (2017a). Association between naturally occurring antiamyloid β autoantibodies and medial temporal lobe atrophy in Alzheimer's disease. *J. Neurol. Neurosurg. Psychiatry* 88, 96–97. doi: 10.1136/jnnp-2016-314136

Menendez Gonzalez, M. (2017b). Implantable systems for continuous liquorpheresis and CSF replacement. *Cureus* 9:e1022. doi: 10.7759/cureus.1022

Menendez Gonzalez, M. (2017c). Mechanical dilution of beta-amyloid peptide and phosphorylated tau protein in Alzheimer's disease: too simple to be true? *Cureus* 9:e1062. doi: 10.7759/cureus.1062

Menendez-Gonzalez, M., Perez-Pinera, P., Martinez-Rivera, M., Calatayud, M. T., and Blazquez Menes, B. (2005). APP processing and the APP-KPI domain involvement in the amyloid cascade. *Neurodegener. Dis.* 2, 277–283. doi: 10.1159/000092315

Menendez-Gonzalez, M., Perez-Pinera, P., Martinez-Rivera, M., Muniz, A. L., and Vega, J. A. (2011). Immunotherapy for Alzheimer's disease: rational basis in ongoing clinical trials. *Curr. Pharm. Des.* 17, 508–520. doi: 10.2174/138161211795164112

Morrone, C. D., Liu, M., Black, S. E., and McLaurin, J. (2015). Interaction between therapeutic interventions for Alzheimer's disease and physiological Aβ clearance mechanisms. *Front. Aging Neurosci.* 7:64. doi: 10.3389/fnagi.2015.00064

Nag, S., Sarkar, B., Bandyopadhyay, A., Sahoo, B., Sreenivasan, V. K. A., Kombrabail, M., et al. (2011). Nature of the amyloid-beta monomer and the monomer-oligomer equilibrium. *J. Biol. Chem.* 286, 13827–13833. doi: 10.1074/jbc.M110.199885

Nussbaum, J. M., Seward, M. E., and Bloom, G. S. (2013). Alzheimer disease: a tale of two prions. *Prion* 7, 14–19. doi: 10.4161/pri.22118

Oddo, S., Billings, L., Kesslak, J. P., Cribbs, D. H., and LaFerla, F. M. (2004). Abeta immunotherapy leads to clearance of early, but not late, hyperphosphorylated tau aggregates via the proteasome. *Neuron* 43, 321–332. doi: 10.1016/j.neuron.2004.07.003

O'Nuallain, B., Freir, D. B., Nicoll, A. J., Risse, E., Ferguson, N., Herron, C. E., et al. (2010). Amyloid beta-protein dimers rapidly form stable synaptotoxic protofibrils. *J. Neurosci.* 30, 14411–14419. doi: 10.1523/JNEUROSCI.3537-10.2010

Ostrowitzki, S., Deptula, D., Thurfjell, L., Barkhof, F., Bohrmann, B., Brooks, D. J., et al. (2012). Mechanism of amyloid removal in patients with Alzheimer disease treated with gantenerumab. *Arch. Neurol.* 69, 198–207. doi: 10.1001/archneurol.2011.1538

Patel, S., Lee, E. B., Xie, S. X., Law, A., Jackson, E. M., Arnold, S. E., et al. (2012). Phosphorylated tau/amyloid beta 1-42 ratio in ventricular cerebrospinal fluid reflects outcome in idiopathic normal pressure hydrocephalus. *Fluids Barriers CNS* 9:7. doi: 10.1186/2045-8118-9-7

Patterson, B. W., Elbert, D. L., Mawuenyega, K. G., Kasten, T., Ovod, V., Ma, S., et al. (2015). Age and amyloid effects on human central nervous system amyloid-beta kinetics. *Ann. Neurol.* 78, 439–453. doi: 10.1002/ana.24454

Penninkilampi, R., Brothers, H. M., and Eslick, G. D. (2017). Safety and efficacy of anti-amyloid-beta immunotherapy in Alzheimer's disease: a systematic review and meta-analysis. *J. Neuroimmune Pharmacol.* 12, 194–203. doi: 10.1007/s11481-016-9722-5

Piazza, F., Greenberg, S. M., Savoiardo, M., Gardinetti, M., Chiapparini, L., Raicher, I., et al. (2013). Anti-amyloid β autoantibodies in cerebral amyloid angiopathy-related inflammation: implications for amyloid-modifying therapies. *Ann. Neurol.* 73, 449–458. doi: 10.1002/ana.23857

Piazza, F., and Winblad, B. (2016). Amyloid-related imaging abnormalities (ARIA) in immunotherapy trials for Alzheimer's disease: need for prognostic biomarkers? *J. Alzheimer's Dis.* 52, 417–420. doi: 10.3233/JAD-160122

Pulawski, W., Ghoshdastider, U., Andrisano, V., and Filipek, S. (2012). Ubiquitous amyloids. *Appl. Biochem. Biotechnol.* 166, 1626–1643. doi: 10.1007/s12010-012-9549-3

Pyykko, O. T., Lumela, M., Rummukainen, J., Nerg, O., Seppala, T. T., Herukka, S.-K., et al. (2014). Cerebrospinal fluid biomarker and brain biopsy findings in idiopathic normal pressure hydrocephalus. *PLoS One* 9:e91974. doi: 10.1371/journal.pone.0091974

Quan, N., and Banks, W. A. (2007). Brain-immune communication pathways. *Brain Behav. Immun.* 21, 727–735. doi: 10.1016/j.bbi.2007.05.005

Ries, M., and Sastre, M. (2016). Mechanisms of Aβ clearance and degradation by glial cells. *Front. Aging Neurosci.* 8:160. doi: 10.3389/fnagi.2016.00160

Ryan, D. A., Mastrangelo, M. A., Narrow, W. C., Sullivan, M. A., Federoff, H. J., and Bowers, W. J. (2010). Aβ-directed single-chain antibody delivery via a serotype-1 AAV vector improves learning behavior and pathology in Alzheimer's disease mice. *Mol. Ther.* 18, 1471–1481. doi: 10.1038/mt.2010.111

Sagare, A., Deane, R., Bell, R. D., Johnson, B., Hamm, K., Pendu, R., et al. (2007). Clearance of amyloid-beta by circulating lipoprotein receptors. *Nat. Med.* 13, 1029–1031. doi: 10.1038/nm1635

Sakai, K., Senda, T., Hata, R., Kuroda, M., Hasegawa, M., Kato, M., et al. (2016). Patients that have undergone hemodialysis exhibit lower amyloid deposition in the brain: evidence supporting a therapeutic strategy for Alzheimer's disease by removal of blood amyloid. *J. Alzheimers Dis.* 51, 997–1002. doi: 10.3233/JAD-151139

Salloway, S., Sperling, R., Fox, N. C., Blennow, K., Klunk, W., Raskind, M., et al. (2014). Two phase 3 trials of bapineuzumab in mild-to-moderate Alzheimer's disease. *N. Engl. J. Med.* 370, 322–333. doi: 10.1056/NEJMoa1304839

Seppala, T. T., Nerg, O., Koivisto, A. M., Rummukainen, J., Puli, L., Zetterberg, H., et al. (2012). CSF biomarkers for Alzheimer disease correlate with cortical brain biopsy findings. *Neurology* 78, 1568–1575. doi: 10.1212/WNL.0b013e3182563bd0

Sevigny, J., Chiao, P., Bussiere, T., Weinreb, P. H., Williams, L., Maier, M., et al. (2016). The antibody aducanumab reduces Aβ plaques in Alzheimer's disease. *Nature* 537, 50–56. doi: 10.1038/nature19323

Siemers, E. R., Sundell, K. L., Carlson, C., Case, M., Sethuraman, G., Liu-Seifert, H., et al. (2016). Phase 3 solanezumab trials: secondary outcomes in mild Alzheimer's disease patients. *Alzheimers Dement.* 12, 110–120. doi: 10.1016/j.jalz.2015.06.1893

Sperling, R. A., Jack, C. R. J., Black, S. E., Frosch, M. P., Greenberg, S. M., Hyman, B. T., et al. (2011). Amyloid-related imaging abnormalities in amyloid-modifying therapeutic trials: recommendations from the Alzheimer's association research roundtable workgroup. *Alzheimers Dement.* 7, 367–385. doi: 10.1016/j.jalz.2011.05.2351

Tarasoff-Conway, J. M., Carare, R. O., Osorio, R. S., Glodzik, L., Butler, T., Fieremans, E., et al. (2015). Clearance systems in the brain—implications for Alzheimer disease. *Nat. Rev. Neurol.* 11, 457–470. doi: 10.1038/nrneurol.2015.119

Tholen, S., Schmaderer, C., Chmielewski, S., Forstl, H., Heemann, U., Baumann, M., et al. (2016). Reduction of amyloid-beta plasma levels by hemodialysis: an anti-amyloid treatment strategy? *J. Alzheimers Dis.* 50, 791–796. doi: 10.3233/JAD-150662

Vasilevko, V., Xu, F., Previti, M. L., Van Nostrand, W. E., and Cribbs, D. H. (2007). Experimental investigation of antibody-mediated clearance mechanisms of amyloid-beta in CNS of Tg-SwDI transgenic mice. *J. Neurosci.* 27, 13376–13383. doi: 10.1523/JNEUROSCI.2788-07.2007

Walker, L. C., Schelle, J., and Jucker, M. (2016). The prion-like properties of amyloid-beta assemblies: implications for Alzheimer's disease. *Cold Spring Harb. Perspect. Med.* 6:a024398. doi: 10.1101/cshperspect.a024398

Wilcock, D. M., DiCarlo, G., Henderson, D., Jackson, J., Clarke, K., Ugen, K. E., et al. (2003). Intracranially administered anti-Abeta antibodies reduce beta-amyloid deposition by mechanisms both independent of and associated with microglial activation. *J. Neurosci.* 23, 3745–3751.

Wilcock, D. M., Munireddy, S. K., Rosenthal, A., Ugen, K. E., Gordon, M. N., and Morgan, D. (2004). Microglial activation facilitates Abeta plaque removal following intracranial anti-Abeta antibody administration. *Neurobiol. Dis.* 15, 11–20. doi: 10.1016/j.nbd.2003.09.015

Xiang, Y., Bu, X.-L., Liu, Y.-H., Zhu, C., Shen, L.-L., Jiao, S.-S., et al. (2015). Physiological amyloid-beta clearance in the periphery and its therapeutic potential for Alzheimer's disease. *Acta Neuropathol.* 130, 487–499. doi: 10.1007/s00401-015-1477-1

Yamada, K., Yabuki, C., Seubert, P., Schenk, D., Hori, Y., Ohtsuki, S., et al. (2009). Abeta immunotherapy: intracerebral sequestration of Abeta by an anti-Abeta monoclonal antibody 266 with high affinity to soluble Abeta. *J. Neurosci.* 29, 11393–11398. doi: 10.1523/JNEUROSCI.2021-09.2009

Yuede, C. M., Lee, H., Restivo, J. L., Davis, T. A., Hettinger, J. C., Wallace, C. E., et al. (2016). Rapid in vivo measurement of β-amyloid reveals biphasic clearance kinetics in an Alzheimer's mouse model. *J. Exp. Med.* 213, 677–685. doi: 10.1084/jem.20151428

Zhao, Z., Sagare, A. P., Ma, Q., Halliday, M. R., Kong, P., Kisler, K., et al. (2015). Central role for PICALM in amyloid-beta blood-brain barrier transcytosis and clearance. *Nat. Neurosci.* 18, 978–987. doi: 10.1038/nn.4025

Zuroff, L., Daley, D., Black, K. L., and Koronyo-Hamaoui, M. (2017). Clearance of cerebral Abeta in Alzheimer's disease: reassessing the role of microglia and monocytes. *Cell Mol. Life Sci.* 74, 2167–2201. doi: 10.1007/s00018-017-2463-7

Conflict of Interest Statement: GA is employed by HealthSens, S.L.

The other authors declare that the research was conducted in the absence of any commercial or financial relationships that could be construed as a potential conflict of interest.

Copyright © 2018 Menendez-Gonzalez, Padilla-Zambrano, Alvarez, Capetillo-Zarate, Tomas-Zapico and Costa. This is an open-access article distributed under the terms of the Creative Commons Attribution License (CC BY). The use, distribution or reproduction in other forums is permitted, provided the original author(s) and the copyright owner are credited and that the original publication in this journal is cited, in accordance with accepted academic practice. No use, distribution or reproduction is permitted which does not comply with these terms.

frontiers in Neuroscience

REVIEW
published: 10 April 2018
doi: 10.3389/fnins.2018.00215

Insulin Resistance as a Therapeutic Target in the Treatment of Alzheimer's Disease: A State-of-the-Art Review

Christian Benedict[1] *and Claudia A. Grillo*[2]*

[1] Department of Neuroscience, Uppsala University, Uppsala, Sweden, [2] Department of Pharmacology, Physiology and Neuroscience, University of South Carolina-School of Medicine, Columbia, SC, United States

Research in animals and humans has shown that type 2 diabetes and its prodromal state, insulin resistance, promote major pathological hallmarks of Alzheimer's disease (AD), such as the formation of amyloid plaques and neurofibrillary tangles (NFT). Worrisomely, dysregulated amyloid beta (Aβ) metabolism has also been shown to promote central nervous system insulin resistance; although the role of tau metabolism remains controversial. Collectively, as proposed in this review, these findings suggest the existence of a mechanistic interplay between AD pathogenesis and disrupted insulin signaling. They also provide strong support for the hypothesis that pharmacologically restoring brain insulin signaling could represent a promising strategy to curb the development and progression of AD. In this context, great hopes have been attached to the use of intranasal insulin. This drug delivery method increases cerebrospinal fluid concentrations of insulin in the absence of peripheral side effects, such as hypoglycemia. With this in mind, the present review will also summarize current knowledge on the efficacy of intranasal insulin to mitigate major pathological symptoms of AD, i.e., cognitive impairment and deregulation of Aβ and tau metabolism.

Keywords: intranasal insulin, diabetes, mild cognitive impairment, amyloid beta, neurofibrillary tangles

OPEN ACCESS

Edited by:
Athanasios Alexiou,
Novel Global Community Educational Foundation (NGCEF), Australia

Reviewed by:
Claire J. Garwood,
University of Sheffield, United Kingdom
Marzia Perluigi,
Sapienza Università di Roma, Italy

***Correspondence:**
Claudia A. Grillo
cgrillo@uscmed.sc.edu

Specialty section:
This article was submitted to Neurodegeneration, a section of the journal Frontiers in Neuroscience

Received: *15 December 2017*
Accepted: *19 March 2018*
Published: *10 April 2018*

Citation:
Benedict C and Grillo CA (2018) Insulin Resistance as a Therapeutic Target in the Treatment of Alzheimer's Disease: A State-of-the-Art Review. Front. Neurosci. 12:215. doi: 10.3389/fnins.2018.00215

BACKGROUND

Alzheimer's disease (AD) is a devastating disease characterized by a loss or decline in memory and other intellectual functions that can lead to impairments in everyday performance. AD affects 1 in 10 people ages 65 or older, and represents 60–70% of cases of dementia (Barker et al., 2002). At the macroscopic level, brain atrophy is the key neuropathological element of AD; at the microscopic level, the hallmarks of the disease are amyloid plaques, neurofibrillary tangles (NFT), and extensive neuronal loss. The principal proteinaceous component of amyloid plaques is the amyloid beta (Aβ) peptide, a 38–43 amino acid peptide produced from the cleavage of the transmembrane amyloid precursor protein (APP) by 2 enzymes: β-secretase and γ-secretase (Golde et al., 2000; Hardy and Selkoe, 2002). The active enzymatic component of the γ-secretase complex, presenilin, cleaves APP at several sites within the membrane to produce Aβ peptides of different lengths such as Aβ38, Aβ40, and Aβ42. The Aβ aggregation process is affected by the interaction of Aβ with the Aβ binding molecules such as apolipoprotein E (apoE) in the extracellular space (Kim et al., 2009). Human apoE has three common alleles (ε2, ε3, and ε4). The ε4 allele confers a genetic risk factor

for AD; conversely, ε2 allele plays a protective role (Corder et al., 1993; Strittmatter et al., 1993). Aβ clearance from the interstitial fluid (ISF) depends on molecules such as neprilysin and insulin-degrading enzyme (IDE), as well as CSF and ISF bulk flow (Qiu et al., 1998; Jiang et al., 2017). The other hallmark of AD, the NFTs, are intracellular structures composed predominantly by hyperphosphorylated tau (Grundke-Iqbal et al., 1986; Goedert et al., 1988; Wischik et al., 1988). Tau is synthesized in all neurons and is also present in glial cells. Tau is a microtubule-associated protein that binds to tubulin and stabilizes microtubules. Under physiological conditions tau phosphorylation/dephosphorylation is a dynamic process essential for tau functionality. Phosphorylation of tau induces its release from microtubules and facilitates axonal vesicle transport, when tau is dephosphorylated it binds again to tubulin (Mandelkow et al., 2004). Hyperphosphorylation of tau can be a consequence of an imbalance of tau kinase and phosphatase activity. When tau suffers a hyperphosphorylation process, the protein dissociates from microtubules and self-aggregates forming NFTs observed in cell bodies and dystrophic neurites of the patients with AD. There is strong evidence that neurofibrillary pathology contributes to neuronal dysfunction and correlates with the clinical progression of AD. It has been suggested this is likely partly through pathways downstream of Aβ. However, Aβ is not the only factor that stimulates tau deposition. Other factors such as tau levels, its sequence and its phosphorylation state also contribute to tau aggregation and toxicity (Holtzman et al., 2012). Moreover, tau-related brain damage in AD might progress independently of Aβ (Small and Duff, 2008). Recent studies of Aβ plaques and tau-related neurodegeneration showed that they progress gradually in a sequential but temporally overlapping profile (Jack and Holtzman, 2013). The presence of Aβ plaques in the brain is the first detectable biomarker, followed by CSF tau proteins; whereas the cognitive deficit is the last event in the progression of AD (Jack et al., 2013). Taking into account these parameters, it is estimated that AD pathology probably begins 10–15 years prior to cognitive decline. In other words, it takes more than one decade of protein misfolding and aggregation until substantial neurodegeneration is developed and cognitive decline shows as the main symptom of this progressing disease (Perrin et al., 2009; Jack et al., 2010). Remarkably, this gradual evolvement of the AD provides a window for early intervention.

The brain utilizes ∼20% of all glucose in a process that is mainly insulin independent. However, insulin receptors are widely distributed throughout the brain, with high concentrations in the olfactory bulb, hypothalamus and hippocampus (Fernandez and Torres-Alemán, 2012). The central function of insulin receptors ranges from regulation of whole-body energy metabolism in the hypothalamus (Woods et al., 1979; Brief and Davis, 1984; Hallschmid et al., 2004; Grillo et al., 2007; Benedict et al., 2011; Thienel et al., 2017) to modulation of memory at hippocampal level (Park et al., 2000; McNay et al., 2010; Grillo et al., 2015). Similarly to AD, reductions in insulin sensitivity (i.e., insulin resistance) occur years before the patients start to experience the symptoms and are diagnosed with diabetes (Dankner et al., 2009). Insulin resistance increases AD risk by at least two-fold (Sims-Robinson et al., 2010), and this deleterious effect can be due to the disruption of the function of the brain vasculature (Biessels and Reijmer, 2014; Frosch et al., 2017), and/or direct effects on Aβ aggregation or tau phosphorylation.

In recent years, type 2 diabetes and its prodromal state, insulin resistance (a pathological condition in which cells fail to respond normally to the hormone insulin), have been identified as risk factors for developing sporadic AD. For instance, a recent meta-analysis of longitudinal population-based studies (involving 1,746,777 individuals) has shown that the risk of AD is increased by about 50% in diabetic people compared to the general population (Zhang et al., 2017). The mechanistic pathways that might link impaired insulin signaling, particularly that of the brain and AD have been subject of intensive research in recent years, and will be comprehensively reviewed herein. These findings provide strong support for the hypothesis that pharmacologically restoring brain insulin signaling could be a promising novel strategy to curb the development and progression of AD. In this context, intranasal insulin administration has emerged as a very promising therapy for AD. With this in mind, one of the objectives of the current review is to summarize clinical trials and discuss the efficacy of intranasal insulin to improve major pathological symptoms of AD, i.e., cognitive dysfunction and deregulation of Aβ and tau metabolism. Additionally, we discuss some pre-clinical and clinical studies using drugs that enhance insulin sensitivity to ameliorate AD symptoms.

INSULIN RESISTANCE, BRAIN STRUCTURE, AND COGNITIVE FUNCTIONS

Clinical and pre-clinical studies consistently show an association between type 2 diabetes (and its prodromal state insulin resistance) and cognitive dysfunction. Additionally, the literature shows numerous examples of cognitive improvements due to insulin treatment.

Preclinical Studies

AD Models and Insulin Resistance

Insulin administration has been shown to ameliorate memory deficits and reverse diet-induced increases of Aβ levels in the brain of 3xTg-AD mice (Vandal et al., 2014). In the hippocampi of another AD mice model (APP/PS1 Tg), impairments in the insulin signaling were also reported (Bomfim et al., 2012). In addition, *in vivo* and *in vitro* experiments show that Aβ induces serine phosphorylation of insulin receptor substrate 1 (IRS-1) instead of tyrosine phosphorylation (Bomfim et al., 2012); this switch has been described as a major mechanism that triggers peripheral insulin resistance (Hirosumi et al., 2002). On the other hand, acute intrahippocampal administration of Aβ (1–42) impairs insulin signaling, decreasing phosphorylation of Akt and plasma membrane translocation of the insulin-sensitive glucose transporter 4, and these molecular effects were accompanied by deficits in spatial memory (Pearson-Leary and McNay, 2012).

Although it takes from 10 to 15 years after Aβ starts to aggregate to observe cognitive impairments in AD patients, an acute effect of Aβ upon cognition cannot be ruled out, especially taking into account the disruption in insulin signaling. Whether the same mechanism applies to human brains remains to be elucidated.

Diabetes Models and Cognitive Function

Experimental animal models of type 2 diabetes show impairments in hippocampal-based memory performance (Li et al., 2002; Winocur et al., 2005), deficits in hippocampal neuroplasticity including decreases in neuronal spine density and neurogenesis (Stranahan et al., 2008) and decreases in synaptic transmission (Kamal et al., 2013), whereas bolstering insulin signaling mitigates Aβ-induced synapse loss in mature cultures of hippocampal neurons (De Felice et al., 2009). Ultimately, the long-term consequences of diabetes-induced neuroplasticity deficits are reflected in cognitive impairments (Biessels and Reagan, 2015). Indeed, insulin resistance is a crucial contributor to the adverse effects on hippocampal cognitive function (de la Monte, 2012), and the literature consistently shows many examples that support the positive effects of insulin on cognitive function in rodent models. In this regard, central insulin administration improves spatial memory in a dose-dependent fashion in male rats (Haj-ali et al., 2009), whereas intrahippocampal insulin microinjections enhanced memory consolidation and retrieval (Moosavi et al., 2007). Acute delivery of insulin into the rat hippocampus also promotes spatial memory in the alternation test (McNay et al., 2010), and transiently enhances hippocampal-dependent memory in the inhibitory avoidance test (Stern et al., 2014). Nisticó et al. reported that mice with haploinsufficiency of insulin receptor β-subunit showed reduced hippocampal LTP and deficits in recognition memory (Nisticò et al., 2012). Concurrently, in a model of hippocampal-specific insulin resistance, rats showed deficits in LTP and spatial memory especially in long-term memory (Grillo et al., 2015).

Clinical Studies

AD and Insulin Resistance

Similar to preclinical studies, clinical studies show that disturbed insulin metabolism is a risk factor for cognitive dysfunction, brain atrophy, and dementia. There is evidence that insulin receptor density decreases in aging, and insulin signaling is impaired in AD (Frölich et al., 1998, 1999). In addition, post-mortem brain tissue from AD patients shows decreased insulin mRNA (Steen et al., 2005), suggesting a deficit in brain insulin signaling. Furthermore, brain tissue from AD patients without diabetes show insulin signaling impairments (Bruehl et al., 2010; De Felice and Ferreira, 2014; Yarchoan and Arnold, 2014).

Interestingly, a seminal work of Convit et al. describes memory deficits and hippocampal atrophy in individuals with impaired glucose metabolism (Convit et al., 2003). Conversion from mild cognitive impairment (MCI) to AD is higher in individuals with impaired glycemia compared to normoglycemic patients (Morris et al., 2014), suggesting that baseline glycemia and insulin resistance play key roles on cognitive decline and AD progression. Cognitive impairment is accompanied by whole-brain volume loss, although no difference was observed in hippocampal volume. In another study performed in healthy adults at risk for AD, the individuals that are strongly positive for Aβ (determined by Pittsburgh compound B tomography) show increased glucose metabolism in specific brain areas but not atrophy or cognitive loss compared to Aβ negative or Aβ indeterminate (Johnson et al., 2014). This potentially opens the opportunity to start an early intervention to prevent AD progression even in individuals that do not manifest abnormalities in peripheral glucose metabolism.

In a cross sectional study performed in cognitively healthy elderly individuals, it was shown that insulin resistance negatively correlates with verbal fluency performance and brain volume, especially in areas related to speech production (Benedict et al., 2012). However, there was no correlation when diabetic or cognitively impaired subjects were examined in an 11-year follow-up study carried out to examine a nationally representative adult population in Finland (Ekblad et al., 2017). Both studies concur that insulin resistance even in healthy individuals has a deleterious effect on verbal fluency performance. A recent cross-sectional study in late middle-aged participants at risk for AD showed that insulin resistance in normoglycemia has a positive correlation with Aβ deposition in frontal and temporal areas (Willette et al., 2015). It is important to note that these individuals are at risk for AD, whereas in previous studies in which type 2 diabetes was not associated with Aβ deposition or NFT, the brains were from patients without risk of AD (Nelson et al., 2009; Ahtiluoto et al., 2010). Furthermore, when cognitively asymptomatic middle-aged adults with a parental family history of AD were assessed, insulin resistance was associated with higher Aβ42 and long-term memory impairments (Hoscheidt et al., 2016).

When the other hallmark feature of AD, NFT, was considered, some studies suggest a link between insulin resistance and abnormal phosphorylation of tau protein (Liu et al., 2009). Insulin resistance is associated with higher P-Tau 181 and Total Tau in the CSF of asymptomatic late-middle-aged adults with risk factors for AD (APOEε4 carriers) and the association is negative for the APOEε4 non-carriers; whereas there is no effect on CSF Aβ42 levels (Starks et al., 2015). This suggests that insulin resistance may increase the susceptibility for tau pathology especially in the APOEε4 carriers.

Diabetic Patients and AD Hallmarks

Diabetes increases the odds of cognitive decline 1.2- to 1.5-fold compared to non-diabetic patients (Cukierman et al., 2005). Initial imaging studies in type 2 diabetic patients showed cortical and subcortical atrophy involving several brain regions accompanied by deficits in regional cerebral perfusion and vasoreactivity (Last et al., 2007) that ultimately may contribute to the cognitive dysfunction observed in elderly subjects with diabetes. In this regard, Crane et al. showed that higher glucose levels represent a risk factor for dementia in patients with or without diabetes. Unfortunately although hyperglycemia could result from decreases in insulin sensitivity, insulin levels were not reported (Crane et al., 2013). In a subsequent study, using glucose

and hemoglobin A1c levels to characterize glucose exposure over 5 years before death, the same group did not find an association between glucose levels and NFT and dementia in people without diabetes treatment history (Crane et al., 2016). In spite of the effort to find the hallmark features of AD in the brain of type 2 diabetes patient, post-mortem studies were not able to show increased Aβ deposition or neurofibrillary tangles (Nelson et al., 2009; Ahtiluoto et al., 2010). More recent studies using Pittsburgh compound B to detect amyloid plaques mainly consisting of insoluble fibrils of Aβ—also failed to associate type 2 diabetes and Aβ aggregation (Thambisetty et al., 2013; Roberts et al., 2014). However, it must be noted that the load of insoluble Aβ does not correlate well with disease progression (Engler et al., 2006). Clinical evidence confirms that diabetes accelerates cognitive function decline, although, the mechanism still remains to be elucidated and it does not necessarily include the hallmark features of AD.

In a study performed in adults with prediabetes or early type 2 diabetes without cognitive impairment, insulin resistance was associated with reduced cerebral glucose metabolic rate (CMRglu) in frontal, parietotemporal and cingulate regions. During a memory task, individuals with diabetes showed a different pattern of CMRglu (more diffuse and extensive activation) and more difficulties in recalling items compared to healthy adults (Baker et al., 2011). This pattern is similar to that observed in prodromal or early AD as well as in non-symptomatic APOEε4 carriers; possibly these changes in CMRglu may try to compensate the disruption in the neuroarchitectural network that normally supports the cognitive task (Bookheimer et al., 2000; Sperling et al., 2010).

LINKING INSULIN RESISTANCE AND AD: POSSIBLE MOLECULAR MECHANISMS

Insulin Signaling Pathway

Although it is not clear how insulin resistance manifests in the central nervous system (CNS), many evidences suggest that different steps of the insulin signaling pathway might be altered (Biessels and Reagan, 2015). Importantly, changes in the insulin receptor expression cannot be ruled out especially in the brains of AD patients (Steen et al., 2005; Moloney et al., 2010). The first step in the insulin pathway activation, the receptor autophosphorylation, is followed by the Tyr phosphorylation of IRS1; however, in AD brains many groups reported increases in p(Ser)-IRS1, a marker of insulin resistance, instead of p(Tyr)-IRS1 (Steen et al., 2005; Moloney et al., 2010; Bomfim et al., 2012; Talbot et al., 2012; **Figure 1**). In addition, higher levels of p-JNK which can stimulate Ser-phosphorylation of IRS1 have been also reported in AD brains (Bomfim et al., 2012; Talbot et al., 2012; **Figure 1**). What leads to this switch in the insulin pathway observed in insulin resistance and AD remains to be elucidated. Recent studies from the Kapogiannis lab. show that plasma exosomes from AD patients exhibit higher pSer-IRS-1 levels and lower pTyr-IRS-1 compared to control subjects, suggesting that these biomarkers might be associated with the brain atrophy observed in AD. In fact, using neural-origin exosomes isolated by immunoprecipitation for L1 CAM, a positive correlation was observed between brain volume and pTyr-IRS-1; while the correlation was negative for pSer-IRS-1 (Mullins et al., 2017). This innovative methodology supports the hypothesis that central insulin resistance could be developed by changes in insulin signaling similarly to the changes described in the periphery and at the same time provides a potential brain-specific insulin resistance biomarker to study brain atrophy with a non-invasive and relatively simple procedure.

Clearance and Degradation of Aβ

Another possible mechanism that could explain why insulin resistance increases the risk of AD is through the clearance and degradation of Aβ. Insulin degrading enzyme (IDE) not only breaks down insulin but also degrades Aβ. In insulin resistance with high levels of insulin, IDE is saturated by insulin and it is less effective at Aβ degradation (Qiu et al., 1998; **Figure 1**). Clearance of Aβ is significantly decreased in rats treated with high doses of insulin (Shiiki et al., 2004). Conversely, inhibition of PI3K, a key step in the insulin pathway, suppresses APP cleavage and secretase activity, leading to decreases in Aβ production (Stöhr et al., 2013). In a mouse model of AD with neuron specific knockout of insulin receptor, Stöhr et al. (2013) observed reduction in Aβ levels and amyloid aggregation, suggesting that insulin signaling has an important effect upon Aβ deposition. In humans in a hyperinsulinemic-euglycemic clamp, insulin improved declarative memory, and increased CSF Aβ in older participants (Watson et al., 2003). In other studies using the same type of clamp, plasma and CSF Aβ was increased along with markers of inflammation (Fishel et al., 2005). These data suggest that hyperinsulinemia can regulate levels of Aβ. However, we have to take into account that these are acute effects observed after transient increases of insulin, whereas in type 2 diabetes hyperinsulinemia is chronic and therefore the long-term effect on Aβ degradation, cognitive function and AD progression could be different.

Glymphatic Clearance

An alternative mechanism by which insulin resistance exacerbates AD progression could include the clearance of the extracellular amyloid plaques. Decreases in the clearance of interstitial fluid in the hippocampus was observed in an experimental model of diabetes, and the cognitive deficits observed in the diabetic rats were inversely correlated to the retention of the contrast agent used to determine glymphatic clearance (Jiang et al., 2017). This is one of the first demonstrations that the system responsible for clearing brain extracellular solutes is affected by diabetes and might explain how insulin resistance may contribute to the initiation and progress of AD.

Fasting Insulin Levels

The two extremes of fasting insulin levels (lower and upper 15th percentiles) increase the risk of dementia in a longitudinal study performed in Japanese-American elderly men (Peila et al., 2004). In both cases, lack of insulin or excess of insulin due to insulin

resistance lead to the convergent development of dementia. This finding is supported by studies in rodent models in which low levels of brain insulin and impaired insulin signaling preceded Aβ aggregation in a mouse model of AD (Chua et al., 2012). In other mouse model of AD, damaging the pancreatic cells that synthesize insulin leads to increases in Aβ levels (Wang et al., 2010). However, the lack of insulin resulting from the damage of the insulin-producing cells produces hyperglycemia that can also increase Aβ aggregation (MacAuley et al., 2015; Chao et al., 2016), making it difficult to elucidate if the increases in extracellular Aβ are due to the hypoinsulinemia and/or the glucotoxicity. Interestingly, lower levels of insulin produces decreases in IDE levels with the consequent increment in Aβ deposition.

Although the majority of the studies show that central insulin resistance in AD individuals has a deleterious effect, some studies in rodents have shown that deficiency in insulin receptor signaling in the brain can have a protective effect against Aβ deposition and even can extend lifespan (Freude et al., 2009; Stöhr et al., 2013). Deletion of insulin-like growth factor-1 receptor (IGF-1R) or insulin receptor in a mouse model of AD decreases APP processing delaying Aβ aggregation. However, only IGF-1R deficiency reduces premature mortality. According to cell based experiments inhibition of the PI3-kinase suppresses APP cleavage and decreases the secretases activity. This can explain the reduction in Aβ aggregation, but the differential effect on mortality remains still unknown.

Another question that remains unresolved is the time course of potential pre-diabetes relative to AD pathology and cognitive impairment. Recent studies from MacKlin et al. (2017) showed that APP/PS1 transgenic mice exhibit glucose intolerance at 2 months of age whereas Aβ accumulation and cognitive decline are not evident until 8–9 months of age. The metabolic deficit appears earlier and persists until the AD pathology and cognitive symptoms occur, indicating that at least in this model peripheral metabolic dysregulation precedes AD pathology (MacKlin et al., 2017).

Tau Hyperphosphorylation

The hypothesis that diabetes can facilitate tau pathology through induction of hyperphosphorylation of tau is supported

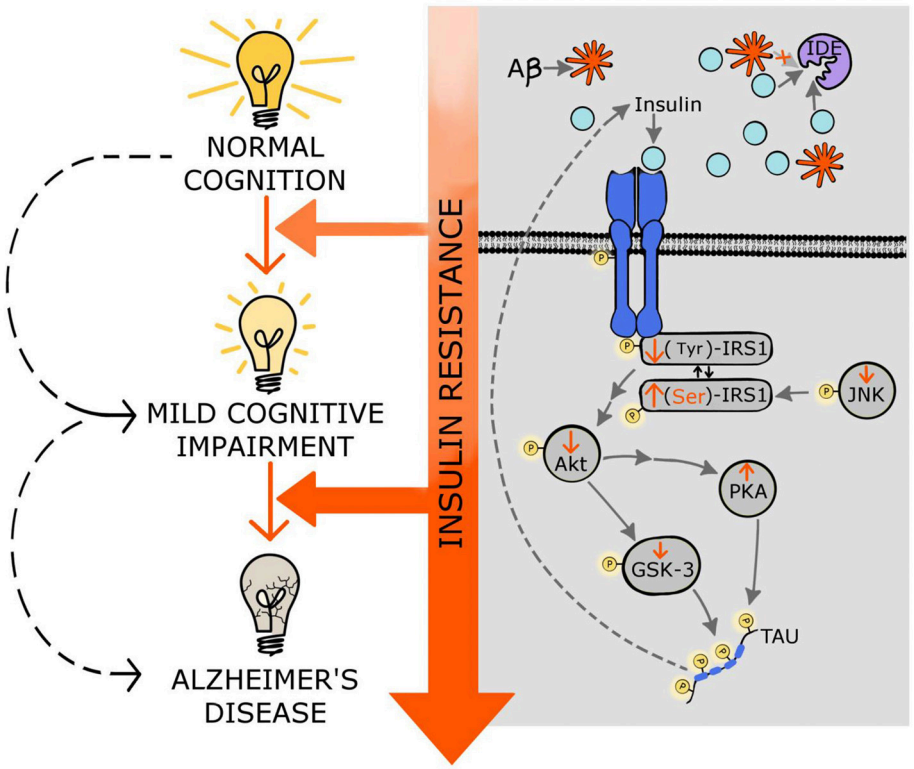


FIGURE 1 | Molecular mechanisms linking insulin resistance and Alzheimer's disease. Central insulin receptors are activated similarly to peripheral insulin receptors. This activation includes the autophosphorylation of the receptor followed by phosphorylation of other components of the cascade such as IRS1, Akt, and GSK-3. Insulin resistance results in stimulation of Ser-phosphorylation of IRS1 instead of normal Tyr-phosphorylation. Additionally, insulin resistance decreases p-JNK favoring the p(Ser)-IRS1. Insulin resistance also results in decreased phosphorylation of Akt affecting several downstream components of the insulin pathway, including GSK-3; this increment of the dephosphorylated form of GSK-3 (active state) stimulates tau hyperphosphorylation and NFT formation. Moreover, decreased activity of Akt induces PKA which also contributes to tau phosphorylation. Hyperphosphorylated tau further impairs insulin signaling. Additionally, the high levels of insulin, exhibited in insulin resistance states, compete with the Aβ for the insulin degrading enzyme (IDE) that is in charge of degrading both insulin and Aβ, affecting the clearance of Aβ. Through these multiple molecular mechanisms, insulin resistance might accelerate mild cognitive impairment as well as AD development and progression. See text for details.

by different molecular mechanisms. Under physiological conditions, insulin stimulates Akt phosphorylation that subsequently leads to Ser-phosphorylation of glycogen synthase kinase 3 (GSK3) and inactivates this enzyme. The active form of GSK3 stimulates tau phosphorylation and NFT formation (**Figure 1**). Hyperphosphorylation of tau may induce tau missorting which can lead to synaptic dysfunction and cognitive impairments (Wang and Mandelkow, 2016). Therefore, insulin resistance reduces p-Akt and p(Ser)-GSK3, and these decreases have also been described in postmortem brain tissue from patients with AD (Steen et al., 2005; Liu et al., 2011). Conversely, other groups reported the opposite: they observed increases in p-Akt and p(Ser)-GSK3 in AD brain samples (Pei et al., 2003; Griffin et al., 2005; Yarchoan et al., 2014). Therefore, there is no consensus about the participation of the phosphorylation/dephosphorylation processes of Akt and GSK3 upon the development of tau pathologies.

The impact of insulin resistance upon tau phosphorylation and cognition remains controversial. For instance, neuron-specific insulin receptor KO mice show higher levels of phosphorylated tau due to activation of GSK3 (Schubert et al., 2004). However, these mice have no memory impairments in spite of the higher levels of p-tau. Conversely, peripheral insulin administration increased abnormal phosphorylation of tau at Ser202 in a dose-dependent fashion in the CNS (Freude et al., 2005). On the other hand, in a model of obesity-associated hyperinsulinemia without changes in glucose homeostasis, no differences were observed in tau phosphorylation, the expression of the tau-kinases and tau-phosphatases (Becker et al., 2012). Although epidemiological studies show that diabetes is a risk factor for AD, there are still discrepancies about how insulin sensitivity modulates hyperphosphorylation of tau. A recent study in mice and monkeys demonstrates that chronic hyperinsulinemia leads to hyperphosphorylation of tau (Sajan et al., 2016; **Figure 1**). It is important to notice that in this last study the animal models exhibit hyperglycemia whereas in the Becker's study the animals were normoglycemic. Even though insulin sensitivity plays a crucial role on AD progress; the impact of glucotoxicity upon the neurodegenerative development cannot be ruled out.

Central insulin signaling dysregulation precedes the onset of peripheral insulin resistance in two mice models of AD, Tg2576 and 3xTg-AD. However, phosphorylation of several components of the insulin signaling cascade was differentially altered in both mouse models. Whereas phosphorylation of Akt and GSK3β showed the same trend in both models, p(Ser)-IRS1 and pPI3K were increased in Tg2576 and decreased in 3xTg-AD. These differences might be due to the tau pathology developed in 3xTg-AD mice (Velazquez et al., 2017).

Recently, a new contributor to the association between insulin signaling and tau pathology has been identified. In an animal model of insulin deficiency protein kinase A (PKA), a potent tau kinase, was activated. These effects on PKA and tau phosphorylation were confirmed by *in vitro* studies (van der Harg et al., 2017; **Figure 1**). Interestingly, insulin administration to diabetic rats was able to reverse both effects, emphasizing the potential of insulin treatment to ameliorate taupathies including AD.

Modulation of Insulin Signaling by Tau

Although the effects of insulin resistance upon tau pathogenesis has been studied (for review see El Khoury et al., 2014) the effects of tau pathology upon insulin signaling has been less explored. Marcianik et al. recently proposed a new function for tau by suggesting that tau might regulate brain insulin signaling (**Figure 1**). This concept was based on the observation that deletion of tau impairs insulin signaling in the hippocampus. In addition the anorexigenic effect of insulin acting on the hypothalamus is disrupted in these tau knockout mice. These new findings suggest a bidirectional effect between insulin resistance and tau loss-of-function, which ultimately might impair cognitive function in AD individuals (Marciniak et al., 2017). However, it would be interesting to discern between central and peripheral insulin sensitivity since tau is also expressed in pancreatic cells and its phosphorylation/dephosphorylation play an important role in insulin trafficking and release (Maj et al., 2016).

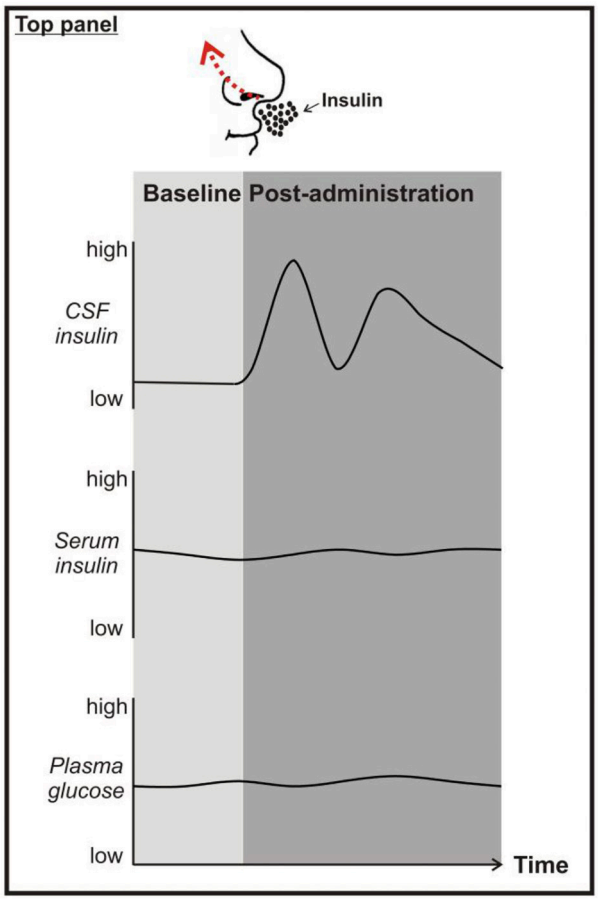
Figure 1 depicts some of the possible molecular mechanisms that link insulin resistance with MCI and AD, and shows how the progression of insulin resistance parallels the impairments in cognitive function.

INTRANASAL INSULIN AS A TREATMENT FOR ALZHEIMER'S DISEASE

Enhancing brain insulin function has recently emerged as a possible approach to mitigate AD symptoms and pathophysiology. An effective way to centrally administer insulin is via intranasal delivery. Using this route of administration insulin travels via convective bulk flow along perivascular pathways following the olfactory and trigeminal nerves and importantly bypassing the BBB. In this way, insulin can reach the hippocampus and the cortex in 15–30 mins (Chapman et al., 2013; Lochhead et al., 2015). Importantly, intranasal insulin does not reach the peripheral circulation (Born et al., 2002), thereby avoiding peripheral hypoglycemia (for advantages and disadvantages/possible side effects of intranasal insulin administration, see **Panel 1**). Clinical and preclinical studies have shown beneficial effects of intranasal insulin upon Aβ aggregation, NFT and cognitive function.

Intranasal Insulin in Diabetic and Healthy Individuals

In a recent study, acute intranasal insulin improved visuospatial memory in type 2 diabetic subjects as well as in the control individuals and this positive effect was due to regional vasoreactivity, especially vasodilatation in the anterior brain regions, such as insular cortex that regulates attention-related task performance (Novak et al., 2014). The same group of investigators demonstrated that intranasal insulin increases resting-state connectivity between the hippocampus and the medial frontal cortex compared to placebo and other default



Bottom panel

Therapeutic benefits of intranasal insulin therapy: Non-invasive; can be self-administered; no risk of hypoglycemia; little or no effect on plasma insulin concentration.

Possible side effects/disadvantages of intranasal insulin therapy: Mild rhinitis; nosebleeds; the optimal treatment schedule has not yet been established and long-term safety data are scarce; preferential affinity of insulin-degrading enzyme (IDE) for insulin results in insulin-mediated inhibition of the degradation of beta-amyloid; possibility of brain insulin receptor desensitization as a result of chronic treatment with intranasal insulin; current evidence suggests that intranasal insulin is less effective in improving cognitive functions in APOE4-positive patients; there is no assessment of how effective intranasal insulin is, in comparison with current 'gold standard' treatment (e.g. Donepezil).

Panel 1 | Top: Proposed effects of intranasal insulin on cerebrospinal fluid (CSF) insulin, serum insulin, and plasma glucose concentrations. **Bottom**: Therapeutic benefits and possible side effects of intranasal insulin.

mode network (DMN) regions in type 2 diabetic patients. Moreover, the lower connectivity between the hippocampus and the medial frontal cortex observed in diabetic subjects was increased by intranasal insulin to a level comparable to control individuals (Zhang et al., 2015). Intranasal insulin administration was also tested in healthy individuals showing beneficial effects on cognitive function. Chronic intranasal insulin improved declarative memory (word recall) and enhanced mood (less anger and more self-confidence) in healthy male and female subjects (Benedict et al., 2004). Interestingly, these positive effects can be enhanced by using a rapid—acting insulin analog (Benedict et al., 2007). In addition to these chronic effects, transient increase of brain insulin levels improved delayed (10 min) but not immediate odor-cued recall of spatial memory in young men (Brünner et al., 2015). Interestingly, single dose intranasal insulin reduces food intake in healthy normal-weight males but not in females; conversely, hippocampus-dependent memory and working memory were improved in females, but not in males (Benedict et al., 2008). These findings could be seen as support for the hypothesis that women are more sensitive to

the enhancement of hippocampus-dependent memory, whereas men are more susceptible to the anorexigenic effect of insulin. However, when obese men were long-term treated (8 weeks) with intranasal insulin although no changes were observed in body weight and adiposity, declarative memory and mood were improved similarly to normal-weight men (Hallschmid et al., 2008). It has moreover been demonstrated that intranasal insulin may normalize stress axis activity in humans by reducing cortisol levels (Benedict et al., 2004; Bohringer et al., 2008; Thienel et al., 2017). This inhibitory effect may also contribute to the positive impact on cognitive function. Finally, intranasal insulin administration has been shown to increase electroencephalogram delta power during non-rapid-eye-movement sleep in young adults (Feld et al., 2016). Sleep is a time period during which newly acquired memories are consolidated (Diekelmann and Born, 2010; Cedernaes et al., 2016) and cellular waste products accumulating in the ISF of the brain during wakefulness (such as soluble Aβ) are removed (Xie et al., 2013; Cedernaes et al., 2017). With these beneficial effects of sleep in mind, it could be speculated that intranasal insulin administration timed before sleep onset may have the strongest memory-improving and brain health-promoting therapeutic potential in humans.

Intranasal Insulin in Individuals With MCI or AD

Chronic intranasal insulin administration (4 months) in patients with MCI or mild to moderate AD improved delayed memory, preserved general cognition and functional abilities and these changes were associated with changes in Aβ42 level and tau/Aβ42 ratio in CSF. In addition, insulin impaired progression avoiding decreases in cerebral glucose metabolic rate in the parietotemporal, frontal, precuneus, and cuneus regions (Craft et al., 2012). Since no deleterious side effects were observed with this prolonged treatment, intranasal insulin emerges as an effective therapeutic approach for patients with MCI or AD. In a recent study aimed to compare regular insulin with long acting insulin (detemir) in adults with MCI or AD, the regular insulin showed improvements in memory after 2 and 4 months compared with placebo, whereas no significant effects were observed for the detemir-assigned group compared with the placebo group. Moreover, regular insulin treatment was associated with preserved volume on MRI and with reduction in the tau-P181/Aβ42 ratio (Craft et al., 2017).

APOE Status and Intranasal Insulin in Individuals With MCI or AD

Acute intranasal insulin improved verbal memory in ApoE ε4 negative subjects with MCI compared to ApoE ε4 positive or normal individuals (Reger et al., 2006). Interestingly and unexpectedly ApoE ε4 positive patients worsen their memory performance after insulin administration, suggesting differences in insulin metabolism due to the expression of ApoE ε4. Although both sexes were tested, gender differences were not analyzed. In a different study the same group found that repeated intranasal insulin improved verbal memory, attention and functional status compared to placebo-treated group in patients with MCI or early AD that was accompanied by increases in the short form of the beta-amyloid peptide (Reger et al., 2008b). This investigative group also found differential dose-response curves for intranasal insulin administration depending on ApoE ε4 allele: ApoE ε4 negative had a peak in verbal memory performance at 20 IU whereas ApoE ε4 positive patients showed memory decline after insulin treatment (Reger et al., 2008a). Interestingly, higher dose (60 IU) had a detrimental effect on memory in both groups (ApoE ε4 positive and negative).

A chronic study of 4 months of daily administration of intranasal insulin showed that men and women improved their cognitive function with 20 IU insulin, but just men benefited with higher dose (40 IU). When ApoE ε4 carriage was evaluated, the results showed that whereas ApoE ε4 negative men improved ApoE ε4 negative women worsened and the ApoE ε4 positive counterparts remained cognitively stable (Claxton et al., 2013). Conversely, using a long-lasting insulin analog (detemir), the results were also influenced by ApoE status; in ApoE ε4 carriers memory improvements were observed whereas non-carriers showed impairments (Claxton et al., 2015). The mechanistic basis of APOE-related treatment differences remains unknown. Collectively, these data highlight the importance of the APOE status upon the changes observed in cognition after intranasal insulin treatment. Since the treatment status can lead to beneficial or detrimental effects, it is crucial to take into account the APOE status when assessing the eligibility of the patients to participate in theses therapeutic approaches.

Insulin Sensitizer Agents and AD

Since insulin has beneficial effects upon memory in individuals with or without MCI or AD, it is logical to hypothesize that drugs that increase insulin sensitivity might also have a positive effect. In this regard, members of the incretin family were considered as prime candidates to ameliorate the MCI and AD symptoms. Within the incretin family, Glucagon-like peptide-1 (GLP-1) was one of the first to be tested. GLP-1 and its receptors (GLP-1Rs) are not just expressed in the pancreas and in the vascular endothelium, they are also found in the CNS, especially in the hypothalamus, hippocampus, cerebral cortex, and olfactory bulb (Lockie, 2013). Several studies have shown the importance of GLP-1 signaling on cognitive function, and many preclinical studies have been performed to evaluate the potential protective role of GLP-1 on the brain (Calsolaro and Edison, 2015). *In vitro* Aβ oligomers impaired axonal transport and this effect was prevented by treatment with a GLP-1R agonist that is used to treat diabetes; moreover this anti-diabetes agent decreases the serine phosphorylation of IRS-1 in hippocampus improving the cognitive function in a mice model of AD (Bomfim et al., 2012). This preclinical study establishes the molecular basis to investigate the potential therapeutic effect of GLP-1 agonists to prevent or treat AD in the clinical setting.

GLP-1 analogs have a dual role: in the periphery they modulate insulin release and centrally they enhance synaptic plasticity and even are able to reverse impairments induced by Aβ oligomers (McClean et al., 2010). In addition to facilitate insulin signaling, GLP-1 analogs have neuroprotective effects *per se*. Chronic treatment with liraglutide, a long-acting GLP-1R agonist, prevented memory decline, synapse loss, synaptic plasticity impairments, decreased the Aβ aggregation, and

neuroinflammation, and increased the expression of young neurons in APP/PS1 mice, suggesting that liraglutide has preventive effects at the early stage of AD (McClean et al., 2011). Interestingly, liraglutide also showed restorative effects in the later stages of the disease in 14 months-old APP/PS1 mice (McClean and Hölscher, 2014). Since liraglutide has preventive and restorative effects upon pathological hallmarks of AD, this incretin hormone has been tested in clinical trials in AD patients. Six months of liraglutide treatment did not have any effect on Aβ deposition in the temporal and occipital lobes compared to placebo-treated patients; glucose metabolism (CMRglu) decreased in placebo patients, whereas liraglutide-treated patients exhibited a trend to increase it; and cognitive function was not improved (Gejl et al., 2016). Although preclinical data were very promising in the clinical setting liraglutide failed to reverse the hallmarks of AD.

The insulin-sensitizing drug metformin, used to treat insulin resistance, was thought as a possible alternative to ameliorate the AD symptomatology. In a placebo-controlled crossover study conducted in non-diabetic patients with MCI or early AD, metformin was able to improve executive function without changes in cerebral blood flow (Koenig et al., 2017). The beneficial effects of metformin are also supported by other study that showed that 1 year of treatment improved total recall compare to baseline in overweight/obese patients with MCI (Luchsinger et al., 2016).

It is important to note that so far these insulin sensitizer agents have not been administered via intranasal route. Therefore, the efficacy of these drugs depends on the peripheral effects and the ability to cross the BBB; and these could explain the differences when compared to the intranasal insulin.

CONCLUDING REMARKS

Available evidence, as reviewed herein, suggests that central nervous system insulin resistance is frequently found in patients with AD (Freiherr et al., 2013). Worrisomely, central insulin resistance promotes major pathological hallmarks of AD that can be found in the brain long before the clinical onset of this devastating disease, such as the formation of Aβ plaques and neurofibrillary tangles (Jack and Holtzman, 2013). On the other hand, deregulated Aβ and tau metabolism has also been shown to promote central insulin resistance (Bruehl et al., 2010; De Felice and Ferreira, 2014; Yarchoan and Arnold, 2014). This suggests the existence of a mechanistic interplay between AD pathogenesis and insulin resistance. In an attempt to interrupt this vicious cycle, in recent years particular attention has been devoted to clinical trials testing effects of intranasal insulin on cognition, daily function, and AD biomarkers. This drug delivery method increases CSF concentrations of insulin in the absence of peripheral side effects such as hypoglycemia (Born et al., 2002). Collectively, results deriving from these clinical trials so far are promising in that they demonstrated beneficial effects on cognition, mood, and metabolic integrity of the brain in patients with MCI or early AD (Reger et al., 2008a,b; Craft et al., 2012, 2017; Claxton et al., 2015). However, many unanswered questions remain, such as which dose of intranasal insulin is optimal to improve cognition, preserve brain metabolism, and reduce possible side effects in AD patients? Are effects of intranasal insulin on cognition and brain health augmented when combined with insulin sensitivity-increasing interventions, such as GLP-1 infusions or exercise programs? Does the time of the day modulate central nervous system effects of intranasal insulin (e.g., morning vs. evening)? Does a chronic treatment with intranasal insulin lead to desensitization of brain insulin signaling, as seen in peripheral tissues (Kupila et al., 2003)? Notwithstanding these questions, the currently available scientific evidence provides a sufficiently strong basis for the hypothesis that counteracting insulin resistance represents a promising therapeutic target in the treatment of AD. Whether intranasal insulin represents such candidate therapy remains to be elucidated in future trials.

AUTHOR CONTRIBUTIONS

All authors listed have made a substantial, direct, and intellectual contribution to the work, and approved it for publication.

ACKNOWLEDGMENTS

The authors would like to thank Victoria Macht for design and preparation of **Figure 1**. The work of CB is supported by the Novo Nordisk Foundation (NNF14OC0009349), the Swedish Brain Foundation, and the Swedish Research Council (2015-03100). The work of CG is supported by the National Science Foundation, NSF IOS-1656626 (USA), and the National Institutes of Health CTT COBRE, P20 GM109091-03 (USA). The funders did not have any role in design of the review, interpretation of the discussed literature, or in the writing process. We apologize to the many researchers who have contributed to the field and who because of space constraints have not been cited herein.

REFERENCES

Ahtiluoto, S., Polvikoski, T., Peltonen, M., Solomon, A., Tuomilehto, J., Winblad, B., et al. (2010). Diabetes, Alzheimer disease, and vascular dementia: a population-based neuropathologic study. *Neurology* 75, 1195–1202. doi: 10.1212/WNL.0b013e3181f4d7f8

Baker, L. D., Cross, D. J., Minoshima, S., Belongia, D., Watson, G. S., and Craft, S. (2011). Insulin resistance and Alzheimer-like reductions in regional cerebral glucose metabolism for cognitively normal adults with prediabetes or early type 2 diabetes. *Arch. Neurol.* 68, 51–57. doi: 10.1001/archneurol.2010.225

Barker, W. W., Luis, C. A., Kashuba, A., Luis, M., Harwood, D. G., Loewenstein, D., et al. (2002). Relative frequencies of Alzheimer disease, Lewy body, vascular and frontotemporal dementia, and hippocampal sclerosis in the State of Florida Brain Bank. *Alzheimer Dis. Assoc. Disord.* 16, 203–212. doi: 10.1097/00002093-200210000-00001

Becker, K., Freude, S., Zemva, J., Stöhr, O., Krone, W., and Schubert, M. (2012). Chronic peripheral hyperinsulinemia has no substantial influence on tau phosphorylation *in vivo*. *Neurosci. Lett.* 516, 306–310. doi: 10.1016/j.neulet.2012.04.022

Benedict, C., Brede, S., Schiöth, H. B., Lehnert, H., Schultes, B., Born, J., et al. (2011). Intranasal insulin enhances postprandial thermogenesis and lowers postprandial serum insulin levels in healthy men. *Diabetes* 60, 114–118. doi: 10.2337/db10-0329

Benedict, C., Brooks, S. J., Kullberg, J., Burgos, J., Kempton, M. J., Nordenskjöld, R., et al. (2012). Impaired insulin sensitivity as indexed by the HOMA score is associated with deficits in verbal fluency and temporal lobe gray matter volume in the elderly. *Diabetes Care* 35, 488–494. doi: 10.2337/dc11-2075

Benedict, C., Hallschmid, M., Hatke, A., Schultes, B., Fehm, H. L., Born, J., et al. (2004). Intranasal insulin improves memory in humans. *Psychoneuroendocrinology* 29, 1326–1334. doi: 10.1016/j.psyneuen.2004.04.003

Benedict, C., Hallschmid, M., Schmitz, K., Schultes, B., Ratter, F., Fehm, H. L., et al. (2007). Intranasal insulin improves memory in humans: superiority of insulin aspart. *Neuropsychopharmacology* 32, 239–243. doi: 10.1038/sj.npp.1301193

Benedict, C., Kern, W., Schultes, B., Born, J., and Hallschmid, M. (2008). Differential sensitivity of men and women to anorexigenic and memory-improving effects of intranasal insulin. *J. Clin. Endocrinol. Metab.* 93, 1339–1344. doi: 10.1210/jc.2007-2606

Biessels, G. J., and Reagan, L. P. (2015). Hippocampal insulin resistance and cognitive dysfunction. *Nat. Rev. Neurosci.* 16, 660–671. doi: 10.1038/nrn4019

Biessels, G. J., and Reijmer, Y. D. (2014). Brain changes underlying cognitive dysfunction in diabetes: what can we learn from MRI? *Diabetes* 63, 2244–2252. doi: 10.2337/db14-0348

Bohringer, A., Schwabe, L., Richter, S., and Schachinger, H. (2008). Intranasal insulin attenuates the hypothalamic–pituitary–adrenal axis response to psychosocial stress. *Psychoneuroendocrinology* 33, 1394–1400. doi: 10.1016/j.psyneuen.2008.08.002

Bomfim, T. R., Forny-Germano, L., Sathler, L. B., Brito-Moreira, J., Houzel, J.-C., Decker, H., et al. (2012). An anti-diabetes agent protects the mouse brain from defective insulin signaling caused by Alzheimer's disease–associated Aβ oligomers. *J. Clin. Invest.* 122, 1339–1353. doi: 10.1172/JCI57256

Bookheimer, S. Y., Strojwas, M. H., Cohen, M. S., Saunders, A. M., Pericak-Vance, M. A., Mazziotta, J. C., et al. (2000). Patterns of brain activation in people at risk for Alzheimer's disease. *N. Engl. J. Med.* 343, 450–456. doi: 10.1056/NEJM200008173430701

Born, J., Lange, T., Kern, W., McGregor, G. P., Bickel, U., and Fehm, H. L. (2002). Sniffing neuropeptides: a transnasal approach to the human brain. *Nat. Neurosci.* 5, 514–516. doi: 10.1038/nn849

Brief, D. J., and Davis, J. D. (1984). Reduction of food intake and body weight by chronic intraventricular insulin infusion. *Brain Res. Bull.* 12, 571–575.

Bruehl, H., Sweat, V., Hassenstab, J., Polyakov, V., and Convit, A. (2010). Cognitive impairment in nondiabetic middle-aged and older adults is associated with insulin resistance. *J. Clin. Exp. Neuropsychol.* 32, 487–493. doi: 10.1080/13803390903224928

Brünner, Y. F., Kofoet, A., Benedict, C., and Freiherr, J. (2015). Central insulin administration improves odor-cued reactivation of spatial memory in young men. *J. Clin. Endocrinol. Metab.* 100, 212–219. doi: 10.1210/jc.2014-3018

Calsolaro, V., and Edison, P. (2015). Novel GLP-1 (glucagon-like peptide-1) analogues and insulin in the treatment for Alzheimer's disease and other neurodegenerative diseases. *CNS Drugs* 29, 1023–1039. doi: 10.1007/s40263-015-0301-8

Cedernaes, J., Osorio, R. S., Varga, A. W., Kam, K., Schiöth, H. B., and Benedict, C. (2017). Candidate mechanisms underlying the association between sleep-wake disruptions and Alzheimer's disease. *Sleep Med. Rev.* 31, 102–111. doi: 10.1016/j.smrv.2016.02.002

Cedernaes, J., Sand, F., Liethof, L., Lampola, L., Hassanzadeh, S., Axelsson, E. K., et al. (2016). Learning and sleep-dependent consolidation of spatial and procedural memories are unaltered in young men under a fixed short sleep schedule. *Neurobiol. Learn. Mem.* 131, 87–94. doi: 10.1016/j.nlm.2016.03.012

Chao, A.-C., Lee, T.-C., Juo, S.-H. H., and Yang, D.-I. (2016). Hyperglycemia increases the production of amyloid beta-peptide leading to decreased endothelial tight junction. *CNS Neurosci. Ther.* 22, 291–297. doi: 10.1111/cns.12503

Chapman, C. D., Frey, W. H., Craft, S., Danielyan, L., Hallschmid, M., Schiöth, H. B., et al. (2013). Intranasal treatment of central nervous system dysfunction in humans. *Pharm. Res.* 30, 2475–2484. doi: 10.1007/s11095-012-0915-1

Chua, L.-M., Lim, M.-L., Chong, P.-R., Hu, Z. P., Cheung, N. S., and Wong, B.-S. (2012). Impaired neuronal insulin signaling precedes Aβ42 accumulation in female AβPPsw/PS1ΔE9 mice. *J. Alzheimers Dis.* 29, 783–791. doi: 10.3233/JAD-2012-111880

Claxton, A., Baker, L. D., Hanson, A., Trittschuh, E. H., Cholerton, B., Morgan, A., et al. (2015). Long-acting intranasal insulin detemir improves cognition for adults with mild cognitive impairment or early-stage Alzheimer's disease dementia. *J. Alzheimers Dis.* 44, 897–906. doi: 10.3233/JAD-141791

Claxton, A., Baker, L. D., Wilkinson, C. W., Trittschuh, E. H., Chapman, D., Watson, G. S., et al. (2013). Sex and ApoE genotype differences in treatment response to two doses of intranasal insulin in adults with mild cognitive impairment or Alzheimer's disease. *J. Alzheimers. Dis.* 35, 789–797. doi: 10.3233/JAD-122308

Convit, A., Wolf, O. T., Tarshish, C., and de Leon, M. J. (2003). Reduced glucose tolerance is associated with poor memory performance and hippocampal atrophy among normal elderly. *Proc. Natl. Acad. Sci. U.S.A.* 100, 2019–2022. doi: 10.1073/pnas.0336073100

Corder, E. H., Saunders, A. M., Strittmatter, W. J., Schmechel, D. E., Gaskell, P. C., Small, G. W., et al. (1993). Gene dose of apolipoprotein E type 4 allele and the risk of Alzheimer's disease in late onset families. *Science* 261, 921–923.

Craft, S., Baker, L. D., Montine, T. J., Minoshima, S., Watson, G. S., Claxton, A., et al. (2012). Intranasal insulin therapy for Alzheimer disease and amnestic mild cognitive impairment. *Arch. Neurol.* 69:29. doi: 10.1001/archneurol.2011.233

Craft, S., Claxton, A., Baker, L. D., Hanson, A. J., Cholerton, B., Trittschuh, E. H., et al. (2017). Effects of regular and long-acting insulin on cognition and Alzheimer's disease biomarkers: a pilot clinical trial. *J. Alzheimers Dis.* 57, 1325–1334. doi: 10.3233/JAD-161256

Crane, P. K., Walker, R. L., Sonnen, J., Gibbons, L. E., Melrose, R., Hassenstab, J., et al. (2016). Glucose levels during life and neuropathologic findings at autopsy among people never treated for diabetes. *Neurobiol. Aging* 48, 72–82. doi: 10.1016/j.neurobiolaging.2016.07.021

Crane, P. K., Walker, R., Hubbard, R. A., Li, G., Nathan, D. M., Zheng, H., et al. (2013). Glucose levels and risk of dementia. *N. Engl. J. Med.* 369, 540–548. doi: 10.1056/NEJMoa1215740

Cukierman, T., Gerstein, H. C., and Williamson, J. D. (2005). Cognitive decline and dementia in diabetes–systematic overview of prospective observational studies. *Diabetologia* 48, 2460–2469. doi: 10.1007/s00125-005-0023-4

Dankner, R., Chetrit, A., Shanik, M. H., Raz, I., and Roth, J. (2009). Basal-state hyperinsulinemia in healthy normoglycemic adults is predictive of type 2 diabetes over a 24-year follow-up: a preliminary report. *Diabetes Care* 32, 1464–1466. doi: 10.2337/dc09-0153

De Felice, F. G., and Ferreira, S. T. (2014). Inflammation, defective insulin signaling, and mitochondrial dysfunction as common molecular denominators connecting type 2 diabetes to Alzheimer disease. *Diabetes* 63, 2262–2272. doi: 10.2337/db13-1954

De Felice, F. G., Vieira, M. N. N., Bomfim, T. R., Decker, H., Velasco, P. T., Lambert, M. P., et al. (2009). Protection of synapses against Alzheimer's-linked toxins: insulin signaling prevents the pathogenic binding of Abeta oligomers. *Proc. Natl. Acad. Sci. U.S.A.* 106, 1971–1976. doi: 10.1073/pnas.0809158106

de la Monte, S. M. (2012). Brain insulin resistance and deficiency as therapeutic targets in Alzheimer's disease. *Curr. Alzheimer Res.* 9, 35–66. doi: 10.2174/156720512799015037

Diekelmann, S., and Born, J. (2010). The memory function of sleep. *Nat. Rev. Neurosci.* 11, 114–126. doi: 10.1038/nrn2762

Ekblad, L. L., Rinne, J. O., Puukka, P., Laine, H., Ahtiluoto, S., Sulkava, R., et al. (2017). Insulin resistance predicts cognitive decline: an 11-year follow-up of a nationally representative adult population sample. *Diabetes Care* 40, 751–758. doi: 10.2337/dc16-2001

El Khoury, N. B., Gratuze, M., Papon, M.-A., Bretteville, A., and Planel, E. (2014). Insulin dysfunction and Tau pathology. *Front. Cell. Neurosci.* 8:22. doi: 10.3389/fncel.2014.00022

Engler, H., Forsberg, A., Almkvist, O., Blomquist, G., Larsson, E., Savitcheva, I., et al. (2006). Two-year follow-up of amyloid deposition in patients with Alzheimer's disease. *Brain* 129, 2856–2866. doi: 10.1093/brain/awl178

Feld, G. B., Wilhem, I., Benedict, C., Rüdel, B., Klameth, C., Born, J., et al. (2016). Central nervous insulin signaling in sleep-associated memory formation

and neuroendocrine regulation. *Neuropsychopharmacology* 41, 1540–1550. doi: 10.1038/npp.2015.312

Fernandez, A. M., and Torres-Alemán, I. (2012). The many faces of insulin-like peptide signalling in the brain. *Nat. Rev. Neurosci.* 13, 225–239. doi: 10.1038/nrn3209

Fishel, M. A., Watson, G. S., Montine, T. J., Wang, Q., Green, P. S., Kulstad, J. J., et al. (2005). Hyperinsulinemia provokes synchronous increases in central inflammation and β-amyloid in normal adults. *Arch. Neurol.* 62, 1539–1544. doi: 10.1001/archneur.62.10.noc50112

Freiherr, J., Hallschmid, M., Frey, W. H., Brünner, Y. F., Chapman, C. D., Hölscher, C., et al. (2013). Intranasal insulin as a treatment for Alzheimer's disease: a review of basic research and clinical evidence. *CNS Drugs* 27, 505–514. doi: 10.1007/s40263-013-0076-8

Freude, S., Hettich, M. M., Schumann, C., Stohr, O., Koch, L., Kohler, C., et al. (2009). Neuronal IGF-1 resistance reduces A accumulation and protects against premature death in a model of Alzheimer's disease. *FASEB J.* 23, 3315–3324. doi: 10.1096/fj.09-132043

Freude, S., Plum, L., Schnitker, J., Leeser, U., Udelhoven, M., Krone, W., et al. (2005). Peripheral hyperinsulinemia promotes tau phosphorylation *in vivo*. *Diabetes* 54, 3343–3348. doi: 10.2337/diabetes.54.12.3343

Frölich, L., Blum-Degen, D., Bernstein, H.-G., Engelsberger, S., Humrich, J., Laufer, S., et al. (1998). Brain insulin and insulin receptors in aging and sporadic Alzheimer's disease. *J Neural Transm*. 105:423. doi: 10.1007/s007020050068

Frölich, L., Blum-Degen, D., Riederer, P., and Hoyer, S. (1999). A disturbance in the neuronal insulin receptor signal transduction in sporadic Alzheimer's disease. *Ann. N. Y. Acad. Sci.* 893, 290–293.

Frosch, O. H., Yau, P. L., Osorio, R. S., Rusinek, H., Storey, P., and Convit, A. (2017). Insulin resistance among obese middle-aged is associated with decreased cerebrovascular reactivity. *Neurology* 89, 249–255. doi: 10.1212/WNL.0000000000004110

Gejl, M., Gjedde, A., Egefjord, L., Møller, A., Hansen, S. B., Vang, K., et al. (2016). In Alzheimer's disease, 6-month treatment with GLP-1 analog prevents decline of brain glucose metabolism: randomized, placebo-controlled, double-blind clinical trial. *Front. Aging Neurosci.* 8:108. doi: 10.3389/fnagi.2016.00108

Goedert, M., Wischik, C. M., Crowther, R. A., Walker, J. E., and Klug, A. (1988). Cloning and sequencing of the cDNA encoding a core protein of the paired helical filament of Alzheimer disease: identification as the microtubule-associated protein tau. *Proc. Natl. Acad. Sci. U.S.A.* 85, 4051–4055.

Golde, T. E., Eckman, C. B., and Younkin, S. G. (2000). Biochemical detection of Aβ isoforms: implications for pathogenesis, diagnosis, and treatment of Alzheimer's disease. *Biochim. Biophys. Acta* 1502, 172–187. doi: 10.1016/S0925-4439(00)00043-0

Griffin, R. J., Moloney, A., Kelliher, M., Johnston, J. A., Ravid, R., Dockery, P., et al. (2005). Activation of Akt/PKB, increased phosphorylation of Akt substrates and loss and altered distribution of Akt and PTEN are features of Alzheimer's disease pathology. *J. Neurochem.* 93, 105–117. doi: 10.1111/j.1471-4159.2004.02949.x

Grillo, C. A., Piroli, G. G., Lawrence, R. C., Wrighten, S. A., Green, A. J., Wilson, S. P., et al. (2015). Hippocampal insulin resistance impairs spatial learning and synaptic plasticity. *Diabetes* 64, 3927–3936. doi: 10.2337/db15-0596

Grillo, C. A., Tamashiro, K. L., Piroli, G. G., Melhorn, S., Gass, J. T., Newsom, R. J., et al. (2007). Lentivirus-mediated downregulation of hypothalamic insulin receptor expression. *Physiol. Behav.* 92, 691–701. doi: 10.1016/j.physbeh.2007.05.043

Grundke-Iqbal, I., Iqbal, K., Tung, Y. C., Quinlan, M., Wisniewski, H. M., and Binder, L. I. (1986). Abnormal phosphorylation of the microtubule-associated protein tau (tau) in Alzheimer cytoskeletal pathology. *Proc. Natl. Acad. Sci. U.S.A.* 83, 4913–4917.

Haj-ali, V., Mohaddes, G., and Babri, S. H. (2009). Intracerebroventricular insulin improves spatial learning and memory in male Wistar rats. *Behav. Neurosci.* 123, 1309–1314. doi: 10.1037/a0017722

Hallschmid, M., Benedict, C., Schultes, B., Born, J., and Kern, W. (2008). Obese men respond to cognitive but not to catabolic brain insulin signaling. *Int. J. Obes.* 32, 275–282. doi: 10.1038/sj.ijo.0803722

Hallschmid, M., Benedict, C., Schultes, B., Fehm, H.-L., Born, J., and Kern, W. (2004). Intranasal insulin reduces body fat in men but not in women. *Diabetes* 53, 3024–3029. doi: 10.2337/diabetes.53.11.3024

Hardy, J., and Selkoe, D. J. (2002). The amyloid hypothesis of Alzheimer's disease: progress and problems on the road to therapeutics. *Science* 297, 353–356. doi: 10.1126/science.1072994

Hirosumi, J., Tuncman, G., Chang, L., Görgün, C. Z., Uysal, K. T., Maeda, K., et al. (2002). A central role for JNK in obesity and insulin resistance. *Nature* 420, 333–336. doi: 10.1038/nature01137

Holtzman, D. M., Mandelkow, E., and Selkoe, D. J. (2012). Alzheimer Disease in 2020. *Cold Spring Harb. Perspect. Med.* 2:a011585. doi: 10.1101/cshperspect.a011585

Hoscheidt, S. M., Starks, E. J., Oh, J. M., Zetterberg, H., Blennow, K., Krause, R. A., et al. (2016). Insulin resistance is associated with increased levels of cerebrospinal fluid biomarkers of Alzheimer's disease and reduced memory function in at-risk healthy middle-aged adults. *J. Alzheimers Dis.* 52, 1373–1383. doi: 10.3233/JAD-160110

Jack, C. R., and Holtzman, D. M. (2013). Biomarker modeling of Alzheimer's disease. *Neuron* 80, 1347–1358. doi: 10.1016/j.neuron.2013.12.003

Jack, C. R., Knopman, D. S., Jagust, W. J., Petersen, R. C., Weiner, M. W., Aisen, P. S., et al. (2013). Tracking pathophysiological processes in Alzheimer's disease: an updated hypothetical model of dynamic biomarkers. *Lancet Neurol.* 12, 207–216. doi: 10.1016/S1474-4422(12)70291-0

Jack, C. R., Knopman, D. S., Jagust, W. J., Shaw, L. M., Aisen, P. S., Weiner, M. W., et al. (2010). Hypothetical model of dynamic biomarkers of the Alzheimer's pathological cascade. *Lancet Neurol.* 9, 119–128. doi: 10.1016/S1474-4422(09)70299-6

Jiang, Q., Zhang, L., Ding, G., Davoodi-Bojd, E., Li, Q., Li, L., et al. (2017). Impairment of the glymphatic system after diabetes. *J. Cereb. Blood Flow Metab.* 37, 1326–1337. doi: 10.1177/0271678X16654702

Johnson, S. C., Christian, B. T., Okonkwo, O. C., Oh, J. M., Harding, S., Xu, G., et al. (2014). Amyloid burden and neural function in people at risk for Alzheimer's disease. *Neurobiol. Aging* 35, 576–584. doi: 10.1016/j.neurobiolaging.2013.09.028

Kamal, A., Ramakers, G. M. J., Gispen, W. H., Biessels, G. J., and Al Ansari, A. (2013). Hyperinsulinemia in rats causes impairment of spatial memory and learning with defects in hippocampal synaptic plasticity by involvement of postsynaptic mechanisms. *Exp. Brain Res.* 226, 45–51. doi: 10.1007/s00221-013-3409-4

Kim, J., Basak, J. M., and Holtzman, D. M. (2009). The role of apolipoprotein E in Alzheimer's disease. *Neuron* 63, 287–303. doi: 10.1016/j.neuron.2009.06.026

Koenig, A. M., Mechanic-Hamilton, D., Xie, S. X., Combs, M. F., Cappola, A. R., Xie, L., et al. (2017). Effects of the insulin sensitizer metformin in alzheimer disease: pilot data from a randomized placebo-controlled crossover study. *Alzheimer Dis. Assoc. Disord.* 31, 107–113. doi: 10.1097/WAD.0000000000000202

Kupila, A., Sipilä, J., Keskinen, P., Simell, T., Knip, M., Pulkki, K., et al. (2003). Intranasally administered insulin intended for prevention of type 1 diabetes-a safety study in healthy adults. *Diabetes. Metab. Res. Rev.* 19, 415–420. doi: 10.1002/dmrr.397

Last, D., Alsop, D. C., Abduljalil, A. M., Marquis, R. P., de Bazelaire, C., Hu, K., et al. (2007). Global and regional effects of type 2 diabetes on brain tissue volumes and cerebral vasoreactivity. *Diabetes Care* 30, 1193–1199. doi: 10.2337/dc06-2052

Li, X. L., Aou, S., Hori, T., and Oomura, Y. (2002). Spatial memory deficit and emotional abnormality in OLETF rats. *Physiol. Behav.* 75, 15–23. doi: 10.1016/S0031-9384(01)00627-8

Liu, Y., Liu, F., Grundke-Iqbal, I., Iqbal, K., and Gong, C.-X. (2011). Deficient brain insulin signalling pathway in Alzheimer's disease and diabetes. *J. Pathol.* 225, 54–62. doi: 10.1002/path.2912

Liu, Y., Liu, F., Grundke-Iqbal, I., Iqbal, K., and Gong, C.-X. (2009). Brain glucose transporters, *O* -GlcNAcylation and phosphorylation of tau in diabetes and Alzheimer's disease. *J. Neurochem.* 111, 242–249. doi: 10.1111/j.1471-4159.2009.06320.x

Lochhead, J. J., Wolak, D. J., Pizzo, M. E., and Thorne, R. G. (2015). Rapid transport within cerebral perivascular spaces underlies widespread tracer distribution in the brain after intranasal administration. *J. Cereb. Blood Flow Metab.* 35, 371–381. doi: 10.1038/jcbfm.2014.215

Lockie, S. H. (2013). Glucagon-like peptide-1 receptor in the brain: role in neuroendocrine control of energy metabolism and treatment target for obesity. *J. Neuroendocrinol.* 25, 597–604. doi: 10.1111/jne.12039

Luchsinger, J. A., Perez, T., Chang, H., Mehta, P., Steffener, J., Pradabhan, G., et al. (2016). Metformin in amnestic mild cognitive impairment: results of a pilot randomized placebo controlled clinical trial. *J. Alzheimers. Dis.* 51, 501–514. doi: 10.3233/JAD-150493

MacAuley, S. L., Stanley, M., Caesar, E. E., Yamada, S. A., Raichle, M. E., Perez, R., et al. (2015). Hyperglycemia modulates extracellular amyloid-β concentrations and neuronal activity *in vivo*. *J. Clin. Invest*. 125, 2463–2467. doi: 10.1172/JCI79742

MacKlin, L., Griffith, C. M., Cai, Y., Rose, G. M., Yan, X.-X., and Patrylo, P. R. (2017). Glucose tolerance and insulin sensitivity are impaired in APP/PS1 transgenic mice prior to amyloid plaque pathogenesis and cognitive decline. *Exp. Gerontol*. 88, 9–18. doi: 10.1016/j.exger.2016.12.019

Maj, M., Hoermann, G., Rasul, S., Base, W., Wagner, L., and Attems, J. (2016). The microtubule-associated protein tau and its relevance for pancreatic beta cells. *J. Diabetes Res*. 2016:1964634. doi: 10.1155/2016/1964634

Mandelkow, E.-M., Thies, E., Trinczek, B., Biernat, J., and Mandelkow, E. (2004). MARK/PAR1 kinase is a regulator of microtubule-dependent transport in axons. *J. Cell Biol*. 167, 99–110. doi: 10.1083/jcb.200401085

Marciniak, E., Leboucher, A., Caron, E., Ahmed, T., Tailleux, A., Dumont, J., et al. (2017). Tau deletion promotes brain insulin resistance. *J. Exp. Med*. 214, 2257–2269. doi: 10.1084/jem.20161731

McClean, P. L., and Hölscher, C. (2014). Liraglutide can reverse memory impairment, synaptic loss and reduce plaque load in aged APP/PS1 mice, a model of Alzheimer's disease. *Neuropharmacology* 76, 57–67. doi: 10.1016/j.neuropharm.2013.08.005

McClean, P. L., Gault, V. A., Harriott, P., and Hölscher, C. (2010). Glucagon-like peptide-1 analogues enhance synaptic plasticity in the brain: a link between diabetes and Alzheimer's disease. *Eur. J. Pharmacol*. 630, 158–162. doi: 10.1016/j.ejphar.2009.12.023

McClean, P. L., Parthsarathy, V., Faivre, E., and Holscher, C. (2011). The diabetes drug liraglutide prevents degenerative processes in a mouse model of Alzheimer's disease. *J. Neurosci*. 31, 6587–6594. doi: 10.1523/JNEUROSCI.0529-11.2011

McNay, E. C., Ong, C. T., McCrimmon, R. J., Cresswell, J., Bogan, J. S., and Sherwin, R. S. (2010). Hippocampal memory processes are modulated by insulin and high-fat-induced insulin resistance. *Neurobiol. Learn. Mem*. 93, 546–553. doi: 10.1016/j.nlm.2010.02.002

Moloney, A. M., Griffin, R. J., Timmons, S., O'Connor, R., Ravid, R., and O'Neill, C. (2010). Defects in IGF-1 receptor, insulin receptor and IRS-1/2 in Alzheimer's disease indicate possible resistance to IGF-1 and insulin signalling. *Neurobiol. Aging* 31, 224–243. doi: 10.1016/j.neurobiolaging.2008.04.002

Moosavi, M., Naghdi, N., and Choopani, S. (2007). Intra CA1 insulin microinjection improves memory consolidation and retrieval. *Peptides* 28, 1029–1034. doi: 10.1016/j.peptides.2007.02.010

Morris, J. K., Vidoni, E. D., Honea, R. A., Burns, J. M., and Alzheimer's Disease Neuroimaging Initiative (2014). Impaired glycemia increases disease progression in mild cognitive impairment. *Neurobiol. Aging* 35, 585–589. doi: 10.1016/j.neurobiolaging.2013.09.033

Mullins, R. J., Mustapic, M., Goetzl, E. J., and Kapogiannis, D. (2017). Exosomal biomarkers of brain insulin resistance associated with regional atrophy in Alzheimer's disease. *Hum. Brain Mapp*. 38, 1933–1940. doi: 10.1002/hbm.23494

Nelson, P. T., Smith, C. D., Abner, E. A., Schmitt, F. A., Scheff, S. W., Davis, G. J., et al. (2009). Human cerebral neuropathology of Type 2 diabetes mellitus. *Biochim. Biophys. Acta* 1792, 454–469. doi: 10.1016/j.bbadis.2008.08.005

Nisticò, R., Cavallucci, V., Piccinin, S., Macrì, S., Pignatelli, M., Mehdawy, B., et al. (2012). Insulin receptor β-subunit haploinsufficiency impairs hippocampal late-phase, LTP, and recognition memory. *Neuromol. Med*. 14, 262–269. doi: 10.1007/s12017-012-8184-z

Novak, V., Milberg, W., Hao, Y., Munshi, M., Novak, P., Galica, A., et al. (2014). Enhancement of vasoreactivity and cognition by intranasal insulin in type 2 diabetes. *Diabetes Care* 37, 751–759. doi: 10.2337/dc13-1672

Park, C. R., Seeley, R. J., Craft, S., and Woods, S. C. (2000). Intracerebroventricular insulin enhances memory in a passive-avoidance task. *Physiol. Behav*. 68, 509–514. doi: 10.1016/S0031-9384(99)00220-6

Pearson-Leary, J., and McNay, E. C. (2012). Intrahippocampal administration of amyloid-β(1-42) oligomers acutely impairs spatial working memory, insulin signaling, and hippocampal metabolism. *J. Alzheimers Dis*. 30, 413–422. doi: 10.3233/JAD-2012-112192

Pei, J.-J., Khatoon, S., An, W.-L., Nordlinder, M., Tanaka, T., Braak, H., et al. (2003). Role of protein kinase B in Alzheimer's neurofibrillary pathology. *Acta Neuropathol*. 105, 381–392. doi: 10.1007/s00401-002-0657-y

Peila, R., Rodriguez, B. L., White, L. R., and Launer, L. J. (2004). Fasting insulin and incident dementia in an elderly population of Japanese-American men. *Neurology* 63, 228–233. doi: 10.1212/01.WNL.0000129989.28404.9B

Perrin, R. J., Fagan, A. M., and Holtzman, D. M. (2009). Multimodal techniques for diagnosis and prognosis of Alzheimer's disease. *Nature* 461, 916–922. doi: 10.1038/nature08538

Qiu, W. Q., Walsh, D. M., Ye, Z., Vekrellis, K., Zhang, J., Podlisny, M. B., et al. (1998). Insulin-degrading enzyme regulates extracellular levels of amyloid beta-protein by degradation. *J. Biol. Chem*. 273, 32730–32738.

Reger, M. A., Watson, G. S., Frey, W. H., Baker, L. D., Cholerton, B., Keeling, M. L., et al. (2006). Effects of intranasal insulin on cognition in memory-impaired older adults: modulation by APOE genotype. *Neurobiol. Aging* 27, 451–458. doi: 10.1016/j.neurobiolaging.2005.03.016

Reger, M. A., Watson, G. S., Green, P. S., Baker, L. D., Cholerton, B., Fishel, M. A., et al. (2008a). Intranasal insulin administration dose-dependently modulates verbal memory and plasma amyloid-beta in memory-impaired older adults. *J. Alzheimers Dis*. 13, 323–331. doi: 10.3233/JAD-2008-13309

Reger, M. A., Watson, G. S., Green, P. S., Wilkinson, C. W., Baker, L. D., Cholerton, B., et al. (2008b). Intranasal insulin improves cognition and modulates -amyloid in early AD. *Neurology* 70, 440–448. doi: 10.1212/01.WNL.0000265401.62434.36

Roberts, R. O., Knopman, D. S., Cha, R. H., Mielke, M. M., Pankratz, V. S., Boeve, B. F., et al. (2014). Diabetes and elevated hemoglobin A1c levels are associated with brain hypometabolism but not amyloid accumulation. *J. Nucl. Med*. 55, 759–764. doi: 10.2967/jnumed.113.132647

Sajan, M., Hansen, B., Ivey, R., Sajan, J., Ari, C., Song, S., et al. (2016). Brain insulin signaling is increased in insulin-resistant states and decreases in FOXOs and PGC-1α and increases in Aβ1-40/42 and phospho-tau may Abet Alzheimer development. *Diabetes* 65, 1892–1903. doi: 10.2337/db15-1428

Schubert, M., Gautam, D., Surjo, D., Ueki, K., Baudler, S., Schubert, D., et al. (2004). Role for neuronal insulin resistance in neurodegenerative diseases. *Proc. Natl. Acad. Sci. U.S.A*. 101, 3100–3105. doi: 10.1073/pnas.0308724101

Shiiki, T., Ohtsuki, S., Kurihara, A., Naganuma, H., Nishimura, K., Tachikawa, M., et al. (2004). Brain insulin impairs amyloid- (1-40) clearance from the brain. *J. Neurosci*. 24, 9632–9637. doi: 10.1523/JNEUROSCI.2236-04.2004

Sims-Robinson, C., Kim, B., Rosko, A., and Feldman, E. L. (2010). How does diabetes accelerate Alzheimer disease pathology? *Nat. Rev. Neurol*. 6, 551–559. doi: 10.1038/nrneurol.2010.130

Small, S. A., and Duff, K. (2008). Linking Aβ and tau in late-onset Alzheimer's disease: a dual pathway hypothesis. *Neuron* 60, 534–542. doi: 10.1016/j.neuron.2008.11.007

Sperling, R. A., Dickerson, B. C., Pihlajamaki, M., Vannini, P., LaViolette, P. S., Vitolo, O. V., et al. (2010). Functional alterations in memory networks in early Alzheimer's disease. *Neuromol. Med*. 12, 27–43. doi: 10.1007/s12017-009-8109-7

Starks, E. J., Patrick O'Grady, J., Hoscheidt, S. M., Racine, A. M., Carlsson, C. M., Zetterberg, H., et al. (2015). Insulin resistance is associated with higher cerebrospinal fluid tau levels in asymptomatic APOEε4 carriers. *J. Alzheimers. Dis*. 46, 525–533. doi: 10.3233/JAD-150072

Steen, E., Terry, B. M., Rivera, E. J., Cannon, J. L., Neely, T. R., Tavares, R., et al. (2005). Impaired insulin and insulin-like growth factor expression and signaling mechanisms in Alzheimer's disease–is this type 3 diabetes? *J. Alzheimers Dis*. 7, 63–80. doi: 10.3233/JAD-2005-7107

Stern, S. A., Chen, D. Y., and Alberini, C. M. (2014). The effect of insulin and insulin-like growth factors on hippocampus- and amygdala-dependent long-term memory formation. *Learn. Mem*. 21, 556–563. doi: 10.1101/lm.029348.112

Stöhr, O., Schilbach, K., Moll, L., Hettich, M. M., Freude, S., Wunderlich, F. T., et al. (2013). Insulin receptor signaling mediates APP processing and β-amyloid accumulation without altering survival in a transgenic mouse model of Alzheimer's disease. *Age* 35, 83–101. doi: 10.1007/s11357-011-9333-2

Stranahan, A. M., Arumugam, T. V., Cutler, R. G., Lee, K., Egan, J. M., and Mattson, M. P. (2008). Diabetes impairs hippocampal function through glucocorticoid-mediated effects on new and mature neurons. *Nat. Neurosci*. 11, 309–317. doi: 10.1038/nn2055

Strittmatter, W. J., Saunders, A. M., Schmechel, D., Pericak-Vance, M., Enghild, J., Salvesen, G. S., et al. (1993). Apolipoprotein E: high-avidity binding to beta-amyloid and increased frequency of type 4 allele in late-onset familial Alzheimer disease. *Proc. Natl. Acad. Sci. U.S.A.* 90, 1977–1981.

Talbot, K., Wang, H.-Y., Kazi, H., Han, L.-Y., Bakshi, K. P., Stucky, A., et al. (2012). Demonstrated brain insulin resistance in Alzheimer's disease patients is associated with IGF-1 resistance, IRS-1 dysregulation, and cognitive decline. *J. Clin. Invest*. 122, 1316–1338. doi: 10.1172/JCI59903

Thambisetty, M., Metter, E. J., Yang, A., Dolan, H., Marano, C., Zonderman, A. B., et al. (2013). Glucose intolerance, insulin resistance, and pathological features of alzheimer disease in the baltimore longitudinal study of aging. *JAMA Neurol*. 70 1167–1172. doi: 10.1001/jamaneurol.2013.284

Thienel, M., Wilhelm, I., Benedict, C., Born, J., and Hallschmid, M. (2017). Intranasal insulin decreases circulating cortisol concentrations during early sleep in elderly humans. *Neurobiol. Aging* 54, 170–174. doi: 10.1016/j.neurobiolaging.2017.03.006

van der Harg, J. M., Eggels, L., Bangel, F. N., Ruigrok, S. R., Zwart, R., Hoozemans, J. J. M., et al. (2017). Insulin deficiency results in reversible protein kinase A activation and tau phosphorylation. *Neurobiol. Dis*. 103, 163–173. doi: 10.1016/j.nbd.2017.04.005

Vandal, M., White, P. J., Tremblay, C., St-Amour, I., Chevrier, G., Emond, V., et al. (2014). Insulin reverses the high-fat diet-induced increase in brain a and improves memory in an animal model of Alzheimer disease. *Diabetes* 63, 4291–4301. doi: 10.2337/db14-0375

Velazquez, R., Tran, A., Ishimwe, E., Denner, L., Dave, N., Oddo, S., et al. (2017). Central insulin dysregulation and energy dyshomeostasis in two mouse models of Alzheimer's disease. *Neurobiol. Aging* 58, 1–13. doi: 10.1016/j.neurobiolaging.2017.06.003

Wang, X., Zheng, W., Xie, J.-W., Wang, T., Wang, S.-L., Teng, W.-P., et al. (2010). Insulin deficiency exacerbates cerebral amyloidosis and behavioral deficits in an Alzheimer transgenic mouse model. *Mol. Neurodegener*. 5:46. doi: 10.1186/1750-1326-5-46

Wang, Y., and Mandelkow, E. (2016). Tau in physiology and pathology. *Nat. Rev. Neurosci*. 17, 5–21. doi: 10.1038/nrn.2015.1

Watson, J. M., Sherwin, R. S., Deary, I. J., Scott, L., and Kerr, D. (2003). Dissociation of augmented physiological, hormonal and cognitive responses to hypoglycaemia with sustained caffeine use. *Clin. Sci.* 104, 447–454. doi: 10.1042/cs1040447

Willette, A. A., Johnson, S. C., Birdsill, A. C., Sager, M. A., Christian, B., Baker, L. D., et al. (2015). Insulin resistance predicts brain amyloid deposition in late middle-aged adults. *Alzheimers Dement.* 11, 504.e1–510.e1. doi: 10.1016/j.jalz.2014.03.011

Winocur, G., Greenwood, C. E., Piroli, G. G., Grillo, C., a, Reznikov, L. R., Reagan, L. P., et al. (2005). Memory impairment in obese Zucker rats: an investigation of cognitive function in an animal model of insulin resistance and obesity. *Behav. Neurosci*. 119, 1389–1395. doi: 10.1037/0735-7044.119.5.1389

Wischik, C. M., Novak, M., Thøgersen, H. C., Edwards, P. C., Runswick, M. J., Jakes, R., et al. (1988). Isolation of a fragment of tau derived from the core of the paired helical filament of Alzheimer disease. *Proc. Natl. Acad. Sci. U.S.A*. 85, 4506–4510.

Woods, S. C., Lotter, E. C., McKay, L. D., and Porte, D. (1979). Chronic intracerebroventricular infusion of insulin reduces food intake and body weight of baboons. *Nature* 282, 503–505.

Xie, L., Kang, H., Xu, Q., Chen, M. J., Liao, Y., Thiyagarajan, M., et al. (2013). Sleep drives metabolite clearance from the adult brain. *Science* 342, 373–377. doi: 10.1126/science.1241224

Yarchoan, M., and Arnold, S. E. (2014). Repurposing diabetes drugs for brain insulin resistance in Alzheimer disease. *Diabetes* 63, 2253–2261. doi: 10.2337/db14-0287

Yarchoan, M., Toledo, J. B., Lee, E. B., Arvanitakis, Z., Kazi, H., Han, L.-Y., et al. (2014). Abnormal serine phosphorylation of insulin receptor substrate 1 is associated with tau pathology in Alzheimer's disease and tauopathies. *Acta Neuropathol*. 128, 679–689. doi: 10.1007/s00401-014-1328-5

Zhang, H., Hao, Y., Manor, B., Novak, P., Milberg, W., Zhang, J., et al. (2015). Intranasal insulin enhanced resting-state functional connectivity of hippocampal regions in type 2 diabetes. *Diabetes* 64, 1025–1034. doi: 10.2337/db14-1000

Zhang, J., Chen, C., Hua, S., Liao, H., Wang, M., Xiong, Y., et al. (2017). An updated meta-analysis of cohort studies: diabetes and risk of Alzheimer's disease. *Diabetes Res. Clin. Pract*. 124, 41–47. doi: 10.1016/j.diabres.2016.10.024

Conflict of Interest Statement: The authors declare that the research was conducted in the absence of any commercial or financial relationships that could be construed as a potential conflict of interest.

Copyright © 2018 Benedict and Grillo. This is an open-access article distributed under the terms of the Creative Commons Attribution License (CC BY). The use, distribution or reproduction in other forums is permitted, provided the original author(s) and the copyright owner are credited and that the original publication in this journal is cited, in accordance with accepted academic practice. No use, distribution or reproduction is permitted which does not comply with these terms.

frontiers in Aging Neuroscience

REVIEW
published: 12 February 2018
doi: 10.3389/fnagi.2018.00003

Ethnopharmacological Approaches for Dementia Therapy and Significance of Natural Products and Herbal Drugs

Devesh Tewari[1†], *Adrian M. Stankiewicz*[2†], *Andrei Mocan*[3,4], *Archana N. Sah*[1], *Nikolay T. Tzvetkov*[5], *Lukasz Huminiecki*[2], *Jarosław O. Horbańczuk*[2] *and Atanas G. Atanasov*[2,6*]

[1] *Department of Pharmaceutical Sciences, Faculty of Technology, Kumaun University, Nainital, India,* [2] *Institute of Genetics and Animal Breeding of the Polish Academy of Sciences, Jastrzebiec, Poland,* [3] *Department of Pharmaceutical Botany, Iuliu Haţieganu University of Medicine and Pharmacy, Cluj-Napoca, Romania,* [4] *ICHAT and Institute for Life Sciences, University of Agricultural Sciences and Veterinary Medicine, Cluj-Napoca, Romania,* [5] *Department of Molecular Biology and Biochemical Pharmacology, Institute of Molecular Biology Roumen Tsanev, Bulgarian Academy of Sciences, Sofia, Bulgaria,* [6] *Department of Pharmacognosy, University of Vienna, Vienna, Austria*

OPEN ACCESS

Edited by:
Athanasios Alexiou, Novel Global Community Educational Foundation (NGCEF), Hebersham, Australia

Reviewed by:
Gjumrakch Aliev, GALLY International Biomedical Research, United States
Mohammad Hassan Baig, Yeungnam University, South Korea

***Correspondence:**
Atanas G. Atanasov
a.atanasov.mailbox@gmail.com

[†] *These authors have contributed equally to this study.*

Received: *29 October 2017*
Accepted: *08 January 2018*
Published: *12 February 2018*

Citation:
Tewari D, Stankiewicz AM, Mocan A, Sah AN, Tzvetkov NT, Huminiecki L, Horbańczuk JO and Atanasov AG (2018) Ethnopharmacological Approaches for Dementia Therapy and Significance of Natural Products and Herbal Drugs. Front. Aging Neurosci. 10:3. doi: 10.3389/fnagi.2018.00003

Dementia is a clinical syndrome wherein gradual decline of mental and cognitive capabilities of an afflicted person takes place. Dementia is associated with various risk factors and conditions such as insufficient cerebral blood supply, toxin exposure, mitochondrial dysfunction, oxidative damage, and often coexisting with some neurodegenerative disorders such as Alzheimer's disease (AD), Huntington's disease (HD), and Parkinson's disease (PD). Although there are well-established (semi-)synthetic drugs currently used for the management of AD and AD-associated dementia, most of them have several adverse effects. Thus, traditional medicine provides various plant-derived lead molecules that may be useful for further medical research. Herein we review the worldwide use of ethnomedicinal plants in dementia treatment. We have explored a number of recognized databases by using keywords and phrases such as "dementia", "Alzheimer's," "traditional medicine," "ethnopharmacology," "ethnobotany," "herbs," "medicinal plants" or other relevant terms, and summarized 90 medicinal plants that are traditionally used to treat dementia. Moreover, we highlight five medicinal plants or plant genera of prime importance and discuss the physiological effects, as well as the mechanism of action of their major bioactive compounds. Furthermore, the link between mitochondrial dysfunction and dementia is also discussed. We conclude that several drugs of plant origin may serve as promising therapeutics for the treatment of dementia, however, pivotal evidence for their therapeutic efficacy in advanced clinical studies is still lacking.

Keywords: Alzheimer's disease, amyloid fibrils, β-amyloid, dementia, ethnopharmacology, herbal drugs

INTRODUCTION

Dementia is a clinical syndrome wherein gradual decline of mental and cognitive capabilities of an afflicted person takes place. As the disease progresses, the ability to function independently of an affected individual deteriorates due to memory loss (Burgess et al., 2002; Damasio and Gabrowski, 2004; Grand et al., 2011). The causes of dementia can be either reversible or irreversible. The reversible causes include, for example, substance abuse, subdural hematoma, removable tumors, and central nervous system (CNS) infections (Tripathi and Vibha, 2009). Some of the irreversible causes of dementia are neurodegenerative diseases such as Alzheimer's disease (AD), Parkinson's disease (PD), and Huntington's disease (HD) (Mehan et al., 2012).

Thus, dementia is associated with multiple predisposing conditions and risk factors, among which aging is the greatest and most obvious one (Blennow et al., 2006; Corrada et al., 2010). The most widespread group of dementias is related to neurodegenerative disorders, including AD, PD, and HD, or amyotrophic lateral sclerosis (ALS). Another important group of dementias are vascular cognitive impairments. These pathologies often coexist with neurodegenerative dementias (Iadecola, 2013). Vascular cognitive impairments arise due to various cerebrovascular pathologies, such as hypoperfusions or hemorrhages causing disruption of the blood-brain barrier (BBB) and neurovascular units, usually in hemispheric white matter (Iadecola, 2013). Other diseases may also contribute to development of dementia. Such diseases include metabolic disorders, which participate in the pathology via dysregulation of energy management (Cai et al., 2012), AIDS, which causes indirect damage to the brain through immune activated macrophages (Navia and Rostasy, 2005), or even systemic infections (Lim et al., 2015). Various environmental factors also increase the risk of developing dementia. For example toxins contained in abused substances (Ridley et al., 2013), pesticides (Yan et al., 2016), or air pollution (Rivas-Arancibia et al., 2013; Power et al., 2016) may cause oxidative stress and subsequent neuronal cell death. In addition to the above factors, the etiology of dementia includes a genetic component. The occurrence of dementia is connected with numerous gene polymorphisms and other mutations (Weksler et al., 2013). For example, mutations in three deterministic autosomal dominant genes, i.e., presenilin 1 (PSEN1) on chromosome 14q, presenilin 2 (PSEN2) on 1q, and amyloid precursor protein (APP) on 21q, are associated with early-onset AD (EOAD) (Giri et al., 2016). The apolipoprotein E (APOE) gene, located at locus 19q13.2, is the strongest genetic risk factor for sporadic lead-onset AD (LOAD) (Corder et al., 1993; Giri et al., 2016; Swerdlow et al., 2017). There are three common APOE alleles, namely APOE ε2, ε3, and ε4 alleles, among which the APOE ε4 genotype is mainly associated with the higher risk of AD development (Mahley and Rall, 2000; Giri et al., 2016; Swerdlow et al., 2017). The link between the APOE ε4 genotype and development of AD pathology is complex (Giri et al., 2016). Studies suggest that APOE ε4 is associated with 3- up to 12-fold increased risk of LOAD and earlier onset of dementia in individuals with PSEN1 mutation, whereas APOE ε2 decreases the risk of LOAD (Pastor et al., 2003; Giri et al., 2016). In addition, APOE ε4 contributes to AD pathogenesis by Aβ-independent mechanisms involving neurovascular functions, synaptic plasticity, cholesterol homeostasis, and neuroinflammation (Giri et al., 2016). Thus, the presence of APOE4 ε4 allele is considered one of the risk factors for AD; more specifically, it is associated with increased risk of cerebral amyloid angiopathy and age-related cognitive decline during aging (Liu et al., 2013).

Dementia is a highly prevalent syndrome. Despite its prevalence, some evidence suggest that only 10% (low-middle-income countries) to 50% (high-income countries) of all dementia cases are diagnosed (Prince et al., 2016). In addition, the number of dementia cases will grow in consecutive years, as dementia mostly affects the elderly, and the number of people with advanced age is rising rapidly due to the global increase in life expectancy. Quaglio et al. (2016) approximate, that 1.5–2% of the Europeans are currently affected by dementia. On a similar note, Prince et al. (2016) estimated that in 2015 around 47 million people globally suffered from dementia. This number may reach roughly 131 million in 2050 (Prince et al., 2016). In the year 2021, one million people will be affected by dementia in the UK alone (Knapp et al., 2007). The importance of developing novel dementia treatments was recognized by the G7 summit in December 2014. The forum participants recommended that dementia should be treated as a global priority with the main objective to introduce effective therapy by 2025 (Cummings et al., 2016).

Dementia is a significant burden on society both by eliciting human suffering and financially. Dementia is the fifth most frequent cause of death in high-income countries (Dolgin, 2016). Their caregivers were also negatively affected by the health conditions of the patients and showed moderately high levels of depressive symptoms (Schulz et al., 2008). According to the World Alzheimer Report 2016 (Prince et al., 2016), not only in the low-income countries, but also in the high-income countries people with dementia have poor access to healthcare due to its high cost and ineffective diagnostic systems. Dementia management is very expensive due to long-lasting and costly care that the patients receive (Hurd et al., 2013). Various costs related to dementia, including health services, social services, unpaid careers, and others reach around €23 billion per year alone in the UK (Luengo-Fernandez et al., 2010). This economic burden can be further illustrated by the fact that, in the UK, the current annual cost of dementia is higher than current annual costs of heart disease and cancer combined (Luengo-Fernandez et al., 2010). Another prediction suggests that by 2050 dementia and Alzheimer's disease may cost the United States alone around USD 1 trillion (Dolgin, 2016).

In this review, we present a global overview on the worldwide use of ethnomedicine for the management of dementia. Moreover, we also focus on five prominent plants traditionally used for dementia treatment and highlight the constituents, which may be responsible for plant's bioactivity.

Currently, there is no highly effective medicine that stops the progressive course of dementia (Abbott, 2011). We propose that learning about the active substances produced by some plants and

TABLE 1 | Most common forms of dementia (according to Abbott, 2011).

Dementia form	Neuropathology	Symptoms	Dementia cases (%)
AD-related dementia	Aβ plaques, neurofibrillary tangles	Memory deficits, depression, poor judgment or evidence of mental confusion	50–80
Vascular dementia	Decreased or interrupted blood flow to the brain, hypoperfusion, oxidative stress	Similar to AD, but less affected memory	20–30
Dementia with Lewy bodies	α-Synuclein aggregates in neurons and glial cells (cortical Lewy bodies)	Similar to AD and less to PD, hallucinations, tremors, impaired attention	<5
Frontotemporal dementia	Accumulation of MAP tau, atrophy of frontal and temporal lobes	Changes in social behavior, difficulties with language	5–10

their mechanism of action may lead to the development of novel therapies for dementia. The natural products pool represents a continuous major source for drug discovery (Atanasov et al., 2015). In this context, the present review could serve as a useful resource for the development of ethnomedicine-derived pharmaceuticals for the dementia therapy.

FREQUENT FORMS OF DEMENTIA

The most common types of dementia are AD-related dementia (approximately 50–80% of all dementia cases) (Qiu et al., 2009; Abbott, 2011), vascular dementia (approximately 20–30%) (Abbott, 2011; Iadecola, 2013), dementia with Lewy bodies (between 15 and 35% according to Zupancic et al., 2011, or less than 5% according to Abbott, 2011) and the frontotemporal dementia (FTD), which is the fourth most frequent form of presenile dementia (between 5 and 10%) (Abbott, 2011; **Table 1**).

Common to these dysfunctions is a presence of abnormal accumulated proteins in the brains of patients. For example, in AD amyloid beta (Aβ) peptides aggregate into amyloid plaques (Hardy and Higgins, 1992), while TDP-43 protein accumulates in the human brain during the course of FTD (Baloh, 2011). Brains of FTD patients show gross atrophy of frontal and anterior temporal lobes (Brun, 1987; McKhann et al., 2001), and their histopathology reveals microvacuolar degeneration and loss of pyramidal neurons in the frontal and temporal cortex (Rabinovici and Miller, 2010). Furthermore, pathologic accumulation of microtubule-associated protein (MAP) tau is a process also common for AD and FTD (Iqbal et al., 2016). Abnormal hyperphosphorylation of tau protein leads to its aggregation into intraneuronal neurofibrillary tangles (Iqbal et al., 2010). Vascular dementia is a heterogeneous group of brain disorders associated with a cognitive impairment that is attributed to multifactorial cerebrovascular pathologies, such as hypoperfusion, oxidative stress, and inflammation (Iadecola, 2013). Dementia with Lewy bodies is characterized by the presence of α-synuclein aggregates in neurons and glial cells (Zupancic et al., 2011), and also associated with cholinergic as well as glutamate transmission deficiencies (Zupancic et al., 2011). It may also be concluded, that there is a great deal of overlap between the symptoms of different types of dementia (Abbott, 2011).

Naturally, the pathology of these diseases is more complicated (Blennow et al., 2006). Various markers of AD can be found in the brains of afflicted patients (Blennow et al., 2006). These markers include, e.g., dysregulation of signaling of memory-related neurotransmitter acetylcholine (ACh) (Kihara and Shimohama, 2004), vascular damage (Franzblau et al., 2013), loss of neurons (Niikura et al., 2006) and synapses (Shankar and Walsh, 2009). Mitochondrial dysfunction is another pathology, which was recognized as an important early event in the AD progression and, therefore, may be considered as promising target for the treatment of AD and AD-related dementia (Kumar and Singh, 2015). We briefly describe the mitochondrial dysfunction in the context of dementia in section Mitochondrial Dysfunction and Neurodegeneration.

MITOCHONDRIAL DYSFUNCTION AND NEURODEGENERATION

Mitochondria are double membrane-enclosed organelles that are responsible to exert a broad range of cellular functions that include the most important adenosine triphosphate (ATP) production (energy conversion), but also involvement in several homeostatic processes, such as regulation of cell cycle and cell growth, calcium handling, and apoptosis-programmed cell death (van Horssen et al., 2017). Moreover, mitochondria play a crucial role in many other essential metabolic processes (van Horssen et al., 2017). Thus, mitochondrial diseases often have an associated metabolic component and, therefore, mitochondrial defects are predictable in energy-dependent disturbances, inflammation, and aging (Chan, 2006; Banasch et al., 2011). Hence, mitochondrial dysfunction is one of the key pathological features in various age-related neurodegenerative diseases including AD-associated dementia due to the pivotal role of mitochondria in neuronal cell survival or death (Moreira et al., 2010). For example, it has been proposed that mitochondrial network remodeling plays a prominent role in neurodegeneration (Zhu et al., 2013; Burte et al., 2015). The mitochondrial cascade hypothesis proposed the mitochondrial dysfunction as a principal episode in AD pathology (Moreira et al., 2010; Swerdlow et al., 2010). Moreover, mitochondrial dysfunction, which is also described as an impairment of electron transport chain, is responsible to increase the production of reactive oxagen species (ROS) and change mitochondrial dynamics (Beal, 2005; Lin and Beal, 2006; Hung et al., 2018). A recent study has shown the reciprocal relationship between ROS and mitochondrial dynamics during early stages

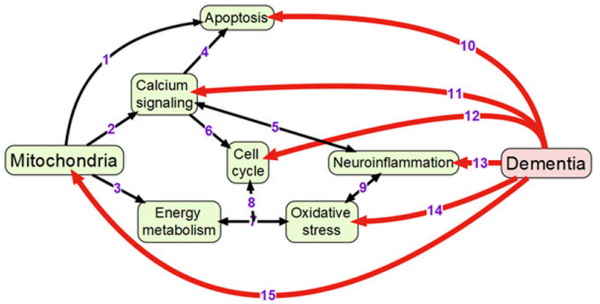


FIGURE 1 | Overview of mechanisms linking mitochondrial activity with dementia: (1) Mitochondria are crucially important for activating apoptosis (Wang and Youle, 2009); (2) Mitochondria regulate calcium signaling pathway (Walsh et al., 2009); (3) Oxidative phosphorylation occurs in electron transport chain of mitochondria; (4) Calcium signaling induces apoptosis (Hajnoczky et al., 2003); (5) Calcium and neuroinflammatory signaling pathways interact with each other (Sama and Norris, 2013); (6) Cell cycle requires calcium signaling (Berridge, 1995); (7) Mitochondrial oxidative phosphorylation is one of the main sources of reactive oxygen species (Dai et al., 2014); (8) Oxidative phosphorylation and reactive oxygen species regulate cell cycle (Antico Arciuch et al., 2012); (9) Oxidative stress and neuroinflammation are highly interconnected processes (Gao et al., 2014); (10) Neuronal apoptosis (LeBlanc, 2005; Favaloro et al., 2012); (11) Impaired calcium signaling (Berridge, 2011; Nimmrich and Eckert, 2013); (12) Changes in cell cycle (Raina et al., 2000; Katsel et al., 2013); (13) Presence of neuroinflammation (Pasqualetti et al., 2015); (14) Increased oxidative stress (Bennett et al., 2009; Kumar and Singh, 2015); (15) Changes in mitochondrial morphology and functions (Spano et al., 2015; Hung et al., 2018).

of neurodegeneration (Hung et al., 2018). It has also been found that the cause for mitochondria-mediated toxicity is the progressive accumulation of Aβ in mitochondria (Chen and Yan, 2010). Recent studies provided the crucial role of mitochondrial dysfunction in regulating the ROS and intracellular calcium levels in neuronal cells (Aminzadeh et al., 2018). In addition, Lee et al. investigated the relationship between the NAD-dependent deacetylase sirtuin-3 (SIRT3) protein and mitochondrial function using AD human brain samples, demonstrating that dysfunction of SIRT3 leads to mitochondrial and neuronal damage, and may improve the mitochondrial pathology and neurodegeneration in AD (Lee et al., 2017). Therefore, mitochondrial dysfunction is considered as a cardinal pathological hallmark for neurodegenerative diseases including AD and AD-related dementia (Lin and Beal, 2006; van Horssen et al., 2017). Detailed information of mitochondrial activities that may be associated with dementia is presented in **Figure 1**.

Summarizing the above, the oxidative stress and mitochondrial dysfunction are of high importance in the pathology and pathogenesis of AD and dementia. Therefore, natural antioxidants and mitochondria targeting molecules can be important strategies to treat elderly individuals with AD (Reddy and Reddy, 2017). Several naturally occurring antioxidants, such as *Ginkgo biloba* (Gb) and curcumin, showed blocking effect on the age-dependent spatial cognitive behavior and also increased the Aβ-degrading enzymes in transgenic mouse models (Stackman et al., 2003; Wang et al., 2014). Moreover, several other antioxidants, including ferulic acid, α-lipoic acid, R-lipoic acid, vitamin E, vitamin C, melatonin, CoQ10, *N*-acetyl-L-cysteine, pyrrolyl-alpha-nitronyl nitroxide, and zeolite supplementation, also showed beneficial effects on AD in different transgenic mouse models (Reddy and Reddy, 2017). Most of these naturally occurring compounds revealed reduction in Aβ levels, mitochondrial dysfunction, phosphorylated tau, and microglial activation, and also increased the synaptic activity (Reddy and Reddy, 2017). Therefore, many of them are available as supplements or can be used as alternative treatment strategies that may help certain neurological conditions, such as PD, AD, some dementia types, and other clinical conditions.

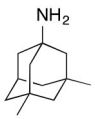
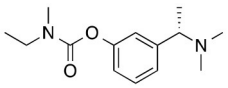
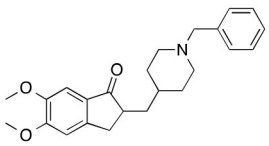
CURRENT PHARMACEUTICAL TREATMENTS OF DEMENTIA

Approved (Semi-)Synthetic Drugs

Several (semi-)synthetic drugs are available worldwide for the treatment of AD and some dementia types. The selective, reversible acetylcholinesterase (AChE) inhibitor donepezil, the non-selective butyrylcholinetserase (BuChE) and AChE inhibitor rivastigmine, as well as the *N*-methyl-D-aspartate (NMDA) receptor antagonist memantine are some of the most widely used therapeutics for AD-associated dementia (Blennow et al., 2006; Winblad et al., 2016). Some of these drugs, like the (semi-)synthetic drug rivastigmine, are also approved for treating other dementia types like PD-related dementia (Winblad et al., 2016). Most prominent drugs approved for clinical use in AD and different forms of dementia are present in **Table 2**. A combined donepezil–memantine drug with the brand name Namzaric® was approved by the FDA in 2014 for the treatment of moderate-to-severe AD in people who are taking donepezil hydrochloride at the recommended clinically efficient dose of 10 mg/day (http://www.alz.org AD report). However, this combinative medicine may cause various side effects, including muscle problems, slow heartbeat and fainting, increased stomach acid levels, nausea, vomiting, and seizures. In addition, some findings suggest that abovementioned drugs do not provide therapeutic benefits for agitation present in patients with severe behavioral symptoms (Howard et al., 2007; Fox et al., 2012). Some neuroleptic/antipsychotic drugs, such as haloperidol, risperidone, and olanzapine, are currently being used to treat behavioral and psychological symptoms of dementia (BPSD), however, their use is controversial (Ballard and Howard, 2006). Therefore, such drugs are not approved by FDA for the treatment of BPSD. Nevertheless, they are still often prescribed off-label as no better treatment for BPSD exists currently (Ibrahim et al., 2012).

The (semi-)synthetic drugs that are currently used for the treatment of dementia have an impact on several symptoms in different disease stages, but do not stop the progressive course of the disease (Tzvetkov and Antonov, 2017). Therefore, the investigation of naturally occurring compounds with potential therapeutic properties for the treatment of different dementia forms is of great medical and socioeconomic importance.

TABLE 2 | Approved (semi-)synthetic drugs used for the treatment of dementia.

	Memantine	**Rivastigmine**	**Donepezil**
Brand name	Namenda® (USA) Axura® (Europe) Ebixa® (Europe) Memando® (Ger)	Exelon® (USA, Europe)	Aricept® (USA, Europe)
Chemical structure	 Chem. formula: $C_{12}H_{21}N$ Mol. wt.: 179.3 g/mol	 Chem. formula: $C_{14}H_{22}N_2O_2$ Mol. wt.: 250.3	 Chem. formula: $C_{24}H_{29}NO_3$ Mol. wt.: 379.5 g/mol
Indications	Moderate-to-severe AD, AD-related dementia	Mild-to-moderate AD, AD-related dementia	Mild-to-moderate AD, early-to-mid AD dementia
Mode of action	Non-competitive NMDA-receptor antagonist	Slowly reversible, non-selective AChE and BuChE inhibitor	Reversible, selective AChE inhibitor
Side effects (http://www.alz.org)	Confusion, dizziness, constipation, and headache	Nausea, vomiting, loss of appetite, increased frequency of bowel movements	Nausea, vomiting, loss of appetite, increased frequency of bowel movements
Half-life (Blennow et al., 2006)	60–100 h (long)	1 h (very short)	70 h (long)
Doses per day (Blennow et al., 2006)	One (first week)	Two	One
Initial dose (Blennow et al., 2006)	5 mg/day	3 mg/day (2 × 1.5 mg)	5 mg/day
Recommended clinically efficient dose (Blennow et al., 2006)	20 mg/day	6–12 mg/day	10 mg/day

Galantamine—the Only Current Drug of Plant Origin against Dementia

Galantamine is an important drug of plant origin that is widely prescribed for the treatment of mild-to-moderate AD and AD-related dementia (Lilienfeld, 2002). Efficacy of galantamine has been confirmed in several clinical trials (Olin and Schneider, 2002). Galantamine, also known as galanthamine (for structure, see **Figure 2**), is an isoquinoline alkaloid produced by plants from *Amaryllidaceae* family. It was first discovered and isolated from bulbs of *Galanthus nivalis* (common snowdrop) by the Bulgarian chemist D. Paskov and his team in 1956 (Paskov, 1958). The original industrial phytopreparation of the pure galantamine extract (named Nivalin®) was prepared in late 1950s by the same research group (Chrusciel and Varagić, 1966). Galantamine was first applied to treat poliomyelitis and later, for the treatment of neuropathic pain and as an anesthetic (Ng et al., 2015). Today, galantamine is mainly obtained from *Galanthus woronowi* Losinsk and *Galanthus alpines* Sosn. (Caucasian snowdrop) daffodil bulbs and also synthesized artificially (Loy and Schneider, 2006).

Galantamine has a unique dual mode of action affecting the brain's cholinergic system (**Figure 2**). It is a reversible, competitive inhibitor of the AChE enzyme and an allosteric enhancer of the nicotinic acetylcholine receptor (nAChR) (Albuquerque et al., 2001).

Galantamine also prevents mitochondrial dysfunction, as shown by its capability to rescue changes in mitochondrial membrane potential (MMP) and morphology induced by Aβ25/35 or hydrogen peroxide treatment (Ezoulin et al., 2008; Liu et al., 2010). Oxidative stress is caused by toxic reactive oxygen species (ROS), which are generated mainly during the electron transport in mitochondria. By protecting the mitochondria and inhibiting AChE activity galantamine decreases oxidative damage to cells and thus mediates neuroprotection (Tsvetkova et al., 2013).

Furthermore, galantamine may interact with other brain-targeted drugs by decreasing activity of P-glycoprotein, a multi-drug resistance transporter present in brain's vascular endothelium (Namanja et al., 2009). It is responsible for actively effluxing drugs back into the bloodstream, thus preventing them from crossing into the brain (Namanja et al., 2009). Hence, galantamine may allow drugs that were co-administered with it to reach the brain more easily. Galantamine also enhances the protective effect of rofecoxib (an anti-inflammatory COX-2 inhibitor) and caffeic acid (a plant-derived phenol) against neurotoxicity-induced mitochondrial dysfunction, oxidative damage, and cognitive impairment in rats (Kumar et al., 2011). Similarly, galantamine potentiates antioxidative activity of melatonin, a brain sleep hormone (Romero et al., 2010). Combined galantamine and memantine treatment is also hypothesized to be a potential novel therapy for schizophrenia (Koola et al., 2014).

Treatment with galantamine has shown to consistently delay the onset of different behavioral symptoms of dementia, such as anxiety, euphoria, depression, irritability, delusions, and unusual motor behavior (Monsch and Giannakopoulos, 2004). A review by Loy and Schneider (2006) described in detail 10 clinical trials comprising the total of 6,805 demented patients, who were submitted to galantamine treatment. The results revealed that the galantamine is well-tolerated by the majority of patients. Some

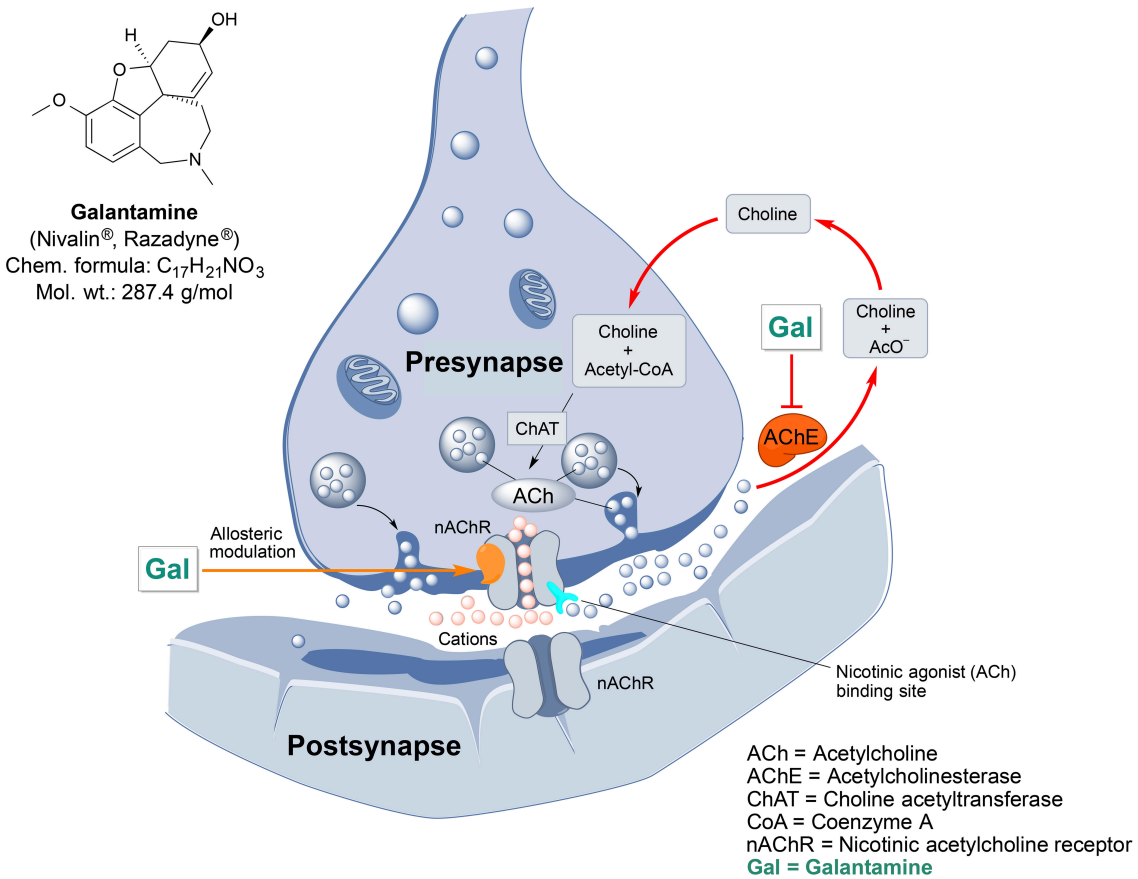


FIGURE 2 | Chemical structure and targeted mechanisms of galantamine (Gal) against AD and dementia. The major biological effects of Gal lead to significant neuroprotection via dual AChE inhibition and allosteric stimulation of nAChRs.

common side effects were observed in the treatment groups in a dose-dependent manner (Loy and Schneider, 2006).

Because of its efficacy, the drug is recommended by Alzheimer's disease/dementia treatment guidelines of the USA and Europe (Doody et al., 2001; Waldemar et al., 2007). The drug is also approved for use in roughly 29 countries including Canada, in the European Union (except for The Netherlands, under the name Nivalin® in 2000), Japan, Korea, Mexico, Singapore, South Africa, Thailand, etc. The FDA approved galantamine in the United States under the brand name Razadyne® in 2001 for the treatment of AD and AD-related dementia. In summary, the plant-derived galantamine is a well-established medicine for dementia treatment, which acts via modulation of acetylcholine signaling and inhibition of oxidative damage.

GENERAL OVERVIEW OF THE DIVERSITY OF PLANTS USED IN DEMENTIA TREATMENT

Modern research on dementias showed that they are complex diseases with multiple molecular mechanisms involved in their pathogenesis. With this realization emerged the new paradigm for treating these pathologies: therapies for dementia should target multiple underling molecular targets, instead of concentrating on any single one. Correspondingly, plant and plant extracts are composed of many substances that are hypothesized to act on multiple molecular targets in an additive or even synergistic manner (Long et al., 2015). Many herbal medicines are already being used for dementia treatment. Unfortunately, active ingredients of these herbs are poorly described. Similarly, we still know very little on how this myriad of substances interact with each other and with prescription medications (Zhou et al., 2016b). The research on these topics will be essential for developing therapeutics, comprised of substances that amplify each other activity and which are devoid of harmful side effects.

In this work, we attempted to collect and document scattered information from various ethnopharmacological reports. We searched several web databases namely, ScienceDirect, Pubmed, Scopus, and Google Scholar using keywords such as "dementia," "Alzheimer's," "traditional medicine," "ethnopharmacology," and "ethnobotany." Web hits from Google scholar were gathered through Boolean information retrieval method using plant name with "AND" operator (Pohl et al., 2010) followed by "dementia"

or "Alzheimer's." An overview of the identified medicinal plants used for treating dementia or AD is presented in **Table 3.**

SELECTED PROMINENT MEDICINAL PLANTS AND PLANT GENERA USED FOR THE TREATMENT OF DEMENTIA

After the extensive web-search for medicinal plants used for dementia treatment in various regions worldwide, the following five plants or plant genera described below were selected for detailed discussion according to the highest observed number of web hits.

Ginkgo biloba L.

Ginkgo is among the most unique plants on earth and belongs to world's oldest tree species (IARC Working Group, 2016). It is a living fossil which gross morphology did not change for around 200 million years (Guan et al., 2016). Gingko is the last living member of the *Ginkgoaceae* family, which appeared during the Mesozoic era. Gb was cultivated in ancient China due to its diverse medicinal properties. Extracts from this plant were utilized for the treatment of various ailments and symptoms viz. poor circulation, fatigue, vertigo, and tinnitus (Sun et al., 2013). Gingko extract is available on market in some countries (e.g., China) as a herbal supplement named Gingium. It is intended for use in certain age-related cognitive disorders including memory impairment and it alleviates the symptoms of dementias and AD (Zhou et al., 2016a). There are two main categories of chemical phytoconstituents likely responsible for the neuro-therapeutic potential of Gingko: terpene lactones (ginkgolides and bilobalide) and flavonoids (flavonols and flavone glycosides) (**Figure 3**; Solfrizzi and Panza, 2015; IARC Working Group, 2016).

The triterpene ginkgolides A, B, and C are unique to Gb (Solfrizzi and Panza, 2015). However, there are some other constituents such as the ginkgotoxin (found in Gb seeds) and the phenolic type lipid bilobol (found in Gb fruits) that possess some specific biological effects (IARC Working Group, 2016). For example, ginkgotoxin exhibit neurotoxic activity (induce the epileptic seizures) (IARC Working Group, 2016), whereas bilobol and its derivatives show cytotoxic and antibacterial activity (Tanaka et al., 2011).

Ginkgo leaf extract was first developed for therapeutic purposes in Germany in 1965 (Isah, 2015). The first commercially available extract was registered in France in 1974 under the name EGb761; it contains about 24% flavonoids and 6% terpene lactones (Isah, 2015). The standardized Gb extract (EGb761) belongs to the most widely tested in clinical trials herbal medications worldwide for cognitive impairment, AD, and AD-related dementia (Solfrizzi and Panza, 2015). EGb761 affects a multitude of mechanisms associated with proper brain functions (Zhou et al., 2016a; **Figure 4**).

It was reported to mediate neuroprotection by modulating circulating glucocorticoid levels, as well as Aβ aggregation, ion homeostasis and growth factors synthesis (Amri et al., 1996; Ahlemeyer and Krieglstein, 2003). These processes are likely involved in regulation of oxidative stress (Butterfield et al., 2013; Ruttkay-Nedecky et al., 2013; Dávila et al., 2016; Alam et al., 2017; Gómez-Sámano et al., 2017) which is in agreement with various reports showing antioxidative activity of Gb extract (Bridi et al., 2001; Chandrasekaran et al., 2003). Moreover, the influence of Ginkgo constituents on mitochondrial function is well recognized. Multiple *in vitro* studies show that Ginkgo constituents protect MMP from various toxicants and oxidative stress (Eckert et al., 2005; Abdel-Kader et al., 2007; Wang and Wang, 2016). Gingko extract affects many aspects of mitochondrial morphology such as fission (Zhou et al., 2017), swelling (Schwarzkopf et al., 2013), and coupling (Rhein et al., 2010). Gingko extract also interacts with mitochondrial electron transport chain (Abdel-Kader et al., 2007). Interestingly, it was found that improvement of the oxidative phosphorylation efficiency was more pronounced in cells overexpressing APP than in control cells (Rhein et al., 2010). This suggests that Ginkgo extract may be effective specifically in AD therapy. The extract also protected rodent neurons and glial cells against cerebral ischemia/reperfusion or scopolamine-induced toxicity (Chandrasekaran et al., 2003; Domoráková et al., 2006; Paganelli et al., 2006; Jahanshahi et al., 2012, 2013). Moreover, EGb761 enhanced the functional integrity and protected cerebral microvascular endothelial cells cultured *in vitro* from damage (Yan et al., 2008; Wan et al., 2014). These effects may be related to a known antiplatelet activity of Gingko extract (Kim et al., 2011). Antiplatelet agents are proposed as a possible therapeutics for vascular syndromes (Geeganage et al., 2010; Heim et al., 2017). Thus, EGb761 may counteract dysfunction of neurovascular unit, which is one of the pathologies associated with AD (Farkas and Luiten, 2001; Zlokovic, 2011).

The use of Ginkgo for the treatment of several cerebral dysfunctions connected to neurodegenerative dementia and brain aging has a long history (Abdou et al., 2016). Studies performed on several animal models suggest that Gingko extract may enhance the cognitive and behavioral functions in aged individuals and Parkinson's disease patients (Kim et al., 2004; Takuma et al., 2007; Ribeiro et al., 2016). Apart from the animal studies, several clinical trials also reported the lack of significant adverse effects and effectiveness of EGb 761 in the therapy of AD and vascular dementia (Kanowski et al., 1996; Napryeyenko et al., 2009; Ihl et al., 2012). Although the gingko extract seems to be beneficial for the treatment of cognitive impairments, further studies are required to assess its possible interaction with other drugs. Such studies may translate to better efficacy and safety of gingko extract therapy. Few important interactions between Ginkgo constituents and drugs are currently known (Izzo, 2012). Nevertheless, there are reports of single patients, which suffered serious neurological side effects after administering Ginkgo herb along with risperidone, valproic acid/phenytoin or trazodone (Izzo, 2012). In summary, Ginkgo extract shows neuroprotective effect, which may be underlined by its antioxidative and/or antiplatelet activities. Clinical studies confirm the effectiveness of Ginkgo extract for dementia treatment. Thus, we speculate that some Ginkgo-based drugs may reach the market in near future.

TABLE 3 | Overview of medicinal plants used to treat dementia worldwide.

Plant (Plant family)	References for the use of the plants for dementia treatment in ethnomedicine	Number of google scholar hits for keyword "dementia"	Number of google scholar hits for keyword "Alzheimer's"
Acorus calamus L. (Acoraceae)	Howes and Houghton, 2003	492	730
Aframomum melegueta (Roskoe) K. Schum. (Zingiberaceae)	Fatumbi, 1995	46	104
Agapanthus africanus (Agapanthaceae)	Stafford et al., 2008	06	06
Ammocharis coranica (Ker-Gawl.) Herb. (Amaryllidaceae)	Stafford et al., 2008	13	26
Ananas comosus (Bromeliaceae)	Wolters, 1994; Adams et al., 2007	129	414
Angelica sinensis (Oliv.) Diels (Apiaceae)	Mantle et al., 2000	1,010	1,660
Angelica archangelica (Apiaceae)	Ross, 2001; Howes and Houghton, 2003	196	318
Angelica species (Apiaceae)	Perry and Howes, 2011	4,670	3,140
Annona senegalensis Pers. (Annonaceae)	Stafford et al., 2008	139	80
Artemisia absinthium L. (Asteraceae)	Howes and Houghton, 2003; Adams et al., 2007	242	439
Asparagus africanus Lam. (Asparagaceae)	Stafford et al., 2008	26	34
Asparagus concinnus (Baker) Kies (Asparagaceae)	Stafford et al., 2008	01	01
Bacopa monnieri (L.) Wettst. (Plantaginaceae)	Manyam, 1999	1,370	1,990
Barbieria pinnata (Pers.) Baill. (Fabacea)	Schultes, 1993, 1994; Adams et al., 2007	04	06
Platycladus orientalis (L.) Franco (Syn. *Biota orientalis* (L.)Endl.) (Cupressaceae)	Nishiyama et al., 1995; Howes et al., 2003	150	236
Boophone disticha (L.f.) Herb. (Amaryllidaceae)	Stafford et al., 2008	39	78
Brugmansia ×candida Pers. (Solanaceae)	González Ayala, 1994; Adams et al., 2007	12	55
Bupleurum species (Apiaceae)	Perry and Howes, 2011	518	717
Camellia sinensis Kuntze (Theaceae)	Perry and Howes, 2011	1,420	3,910
Cannabis sativa L. (Cannabaceae)	Perry and Howes, 2011	1,740	3,260
Carum carvi L. (Apiaceae)	Adsersen et al., 2006	163	340
Caryophyllus spp. (Caryophyllaceae)	Tabernaemontanus, 1987; Adams et al., 2007	161	292
Cassia lucens Vog. (Fabaceae)	Schultes, 1993, 1994; Adams et al., 2007	28	93
Celastrus paniculatus Willd. (Celastraceae)	Howes and Houghton, 2003	189	274
Centella asiatica (L.) Urb (Apiaceae)	Stafford et al., 2008	1,060	1,970
Dysphania ambrosioides (L.) Mosyakin&Clemants (Amaranthaceae) {Syn. *Chenopodium ambrosioides* L.(Chenopodiaceae)}	de Barradas, 1957; CESA, 1992, 1993; Adams et al., 2007	94	154
Clitoria ternatea L. (Fabaceae)	Howes and Houghton, 2003	185	294
Codonopsis pilulosa (Franch.) Nannf. (Campanulaceae)	Howes and Houghton, 2003	198	245
Coffea arabica L. (Rubiaceae)	Perry and Howes, 2011	484	1,180
Convallaria majalis L. (Convallariaceae)	Tabernaemontanus, 1987; Adams et al., 2007	82	95
Coriandrum sativum L. (Apiaceae)	Tabernaemontanus, 1987; Adams et al., 2007	310	765
Corydalis cava (L.) Schw. et K. (Papaveraceae)	Adsersen et al., 2006; Adams et al., 2007	65	86
Corydalis intermedia (L.) M'erat (Papaveraceae)	Adsersen et al., 2006; Adams et al., 2007	71	141
Corydalis solida (L.) Swartz ssp. *laxa* (Papaveraceae)	Adsersen et al., 2006; Adams et al., 2007	21	30
Corydalis solida (L.) Swartz ssp. *slivenensis* (Papaveraceae)	Adsersen et al., 2006; Adams et al., 2007	04	04
Crinum bulbispermum (Burm.f.) Milne-Redh. & Schweick. (Amaryllidaceae)	Stafford et al., 2008	47	97
Crinum moorei Hook.f (Syn.*Crinum imbricatum* Baker) (Amaryllidaceae)	Stafford et al., 2008	20	54
Crinum macowanii Baker (Amaryllidaceae)	Stafford et al., 2008	41	93
Crocus sativus L. (Iridaceae)	Perry and Howes, 2011	678	1,310
Curcuma longa L. (Zingiberaceae)	Howes and Houghton, 2003; Perry and Howes, 2011	2,130	6,270
Euphrasia nemorosa (Pers.) Wallr. (Scrophulariaceae)	Adsersen et al., 2006	09	16

(Continued)

TABLE 3 | Continued

Plant (Plant family)	References for the use of the plants for dementia treatment in ethnomedicine	Number of google scholar hits for keyword "dementia"	Number of google scholar hits for keyword "Alzheimer's"
Tetradium ruticarpum (A.Juss.) T.G.Hartley (Syn. *Evodia rutaecarpa* Hook.f.&Thoms.) (Rutaceae)	Mantle et al., 2000; Howes and Perry, 2011	366	367
Ferula gummosa Boiss. (Apiaceae)	Tabernaemontanus, 1987; Adams et al., 2007	22	32
Galanthus woronowii Losinsk. (Amaryllidaceae)	Perry and Howes, 2011	155	286
Galanthus alpinus Sosn. (Syn. *Galanthus caucasicus*) (Amaryllidaceae)	Perry and Howes, 2011	27	55
Ginkgo biloba L. (Ginkgoaceae)	Gurib-Fakim, 2006; Perry and Howes, 2011	14,000	17,300
Glycyrrhiza species (Leguminosae)	Perry and Howes, 2011	2,410	4,050
Huperzia serrate (Thunb.) Trevis. (Lycopodiaceae)	Howes et al., 2003; Adams et al., 2007; Perry and Howes, 2011	1,130	1,710
Hydrolea glabra Schum. and Thonn. (Hydrophilaceae)	Fatumbi, 1995; Adams et al., 2007	01	03
Hypericum perforatum L. (Clusiaceae)	Perry and Howes, 2011	2,500	3,180
Lactuca sativa L. (Asteraceae)	Schweitzer de Palacios, 1994; Adams et al., 2007	287	895
Lannea schweinfurthii Engl. (Anacardiaceae)	Stafford et al., 2008	12	22
Lantana camara L. (Verbenaceae)	Müller-Ebeling and Rätsch, 1989; Adams et al., 2007	97	262
Lavandula angustifolia Miller (Lamiaceae)	Adsersen et al., 2006; Perry and Howes, 2011	800	981
Leucojum aestivum L. (Amaryllidaceae)	Perry and Howes, 2011	133	447
Lycoris radiata Herb. (Amaryllidaceae)	Howes and Houghton, 2003	227	273
Magnolia officinalis Rehder and Wilson (Magnoliaceae)	Howes and Houghton, 2003	389	715
Matricaria recutita L. (Asteraceae)	Tabernaemontanus, 1987; Adams et al., 2007	575	1,150
Medicago sativa L. (Fabaceae)	Finkler, 1985; Adams et al., 2007	390	1,180
Melissa officinalis L. (Lamiaceae)	Lonicerus, 1679; Mills, 1991; Perry et al., 1998; Mantle et al., 2000; Adsersen et al., 2006; Adams et al., 2007; Perry and Howes, 2011	1,140	1,920
Mentha spicata L. (Lamiaceae)	Adsersen et al., 2006	223	537
Narcissus spp. (Amaryllidaceae)	Perry and Howes, 2011	1,480	745
Nicotiana species (Solanaceae)	Perry and Howes, 2011	900	3,060
Ocimum basilicum L. (Lamiaceae)	Fuchs, 1543; Sfikas, 1980; Adams et al., 2007	407	997
Origanum majorana Moench (Lamiaceae)	Fuchs, 1543; Adams et al., 2007	675	1,550
Origanum vulgare L. (Lamiaceae)	Adsersen et al., 2006	358	978
Paeonia ×suffruticosa Andrews (Paeoniaceae)	Mantle et al., 2000	189	345
Panax ginseng C.A.Mey. (Araliaceae)	Perry and Howes, 2011	4,790	6,950
Paullinia cupana Kunth ex. H. B. K (Sapindaceae)	Taylor, 1998; Adams et al., 2007	248	515
Petroselinum crispum (Mil.) Nym.exA.W.Hill. (Apiaceae)	Adsersen et al., 2006	308	562
Physostigma venenosa Balf.f. (Leguminosae)	Mantle et al., 2000	08	11
Pimpinella anisum L. (Apiaceae)	Adsersen et al., 2006	214	493
Piper methysticum G.Forst. (Piperaceae)	Perry and Howes, 2011	768	953
Polygala tenuifolia Willd. (Polygalaceae)	Duke and Ayensu, 1985; Chang et al., 1986; Howes and Houghton, 2003	549	679
Pteroselinum vulgare (Mill.) Nym. and A.W. Hill (Apiaceae)	Adams et al., 2007	82	221
Rosmarinus officinalis L. (Lamiaceae)	Price and Price, 1995; Chevallier, 1996; Perry et al., 1998; Mantle et al., 2000; Adams et al., 2007	1,140	2,440
Rosmarinus officinalis L. (Lamiaceae)	Adsersen et al., 2006	1,140	2,440
Ruta graveolens L. (Rutaceae)	Adsersen et al., 2006	351	420
Salvia lavandulifolia Vahl. (Lamiaceae)	Perry and Howes, 2011	103	190
Salvia miltiorrhiza Bung. (Lamiaceae)	Howes and Houghton, 2003	1,430	2,090

(Continued)

TABLE 3 | Continued

Plant (Plant family)	References for the use of the plants for dementia treatment in ethnomedicine	Number of google scholar hits for keyword "dementia"	Number of google scholar hits for keyword "Alzheimer's"
Salvia officinalis L. (Lamiaceae)	Sfikas 1980; Tabernaemontanus, 1987; Akhondzadeh et al., 2003; Howes et al., 2003; Savelev et al., 2004; Adams et al., 2007	1,610	2,960
Scadoxus multiflorus (Martyn) Raf. (Amaryllidaceae)	Stafford et al., 2008	06	31
Syzygium aromaticum (L.) Merrill and Perry (Myrtaceae)	Tabernaemontanus, 1987; Adams et al., 2007	248	647
Tagetes lucida Cav. (Asteraceae)	Ortiz de Montellano, 1990; Adams et al., 2007	25	54
Terminalia chebula Retz. (Combretaceae)	Misra, 1998; Manyam, 1999; Howes and Houghton, 2003	545	938
Theobroma cacao L. (Sterculiaceae)	Roeder, 1988; Adams et al., 2007	535	1,400
Thymus vulgaris L. (Lamiaceae)	Adsersen et al., 2006	1,440	2,760
Valeriana officinalis L. (Valerianaceae)	Perry and Howes, 2011	973	1,340
Vinca minor L. (Apocynaceae)	Perry and Howes, 2011	1,520	2,070
Vitis vinifera L. (Vitaceae)	Perry and Howes, 2011	994	3,010

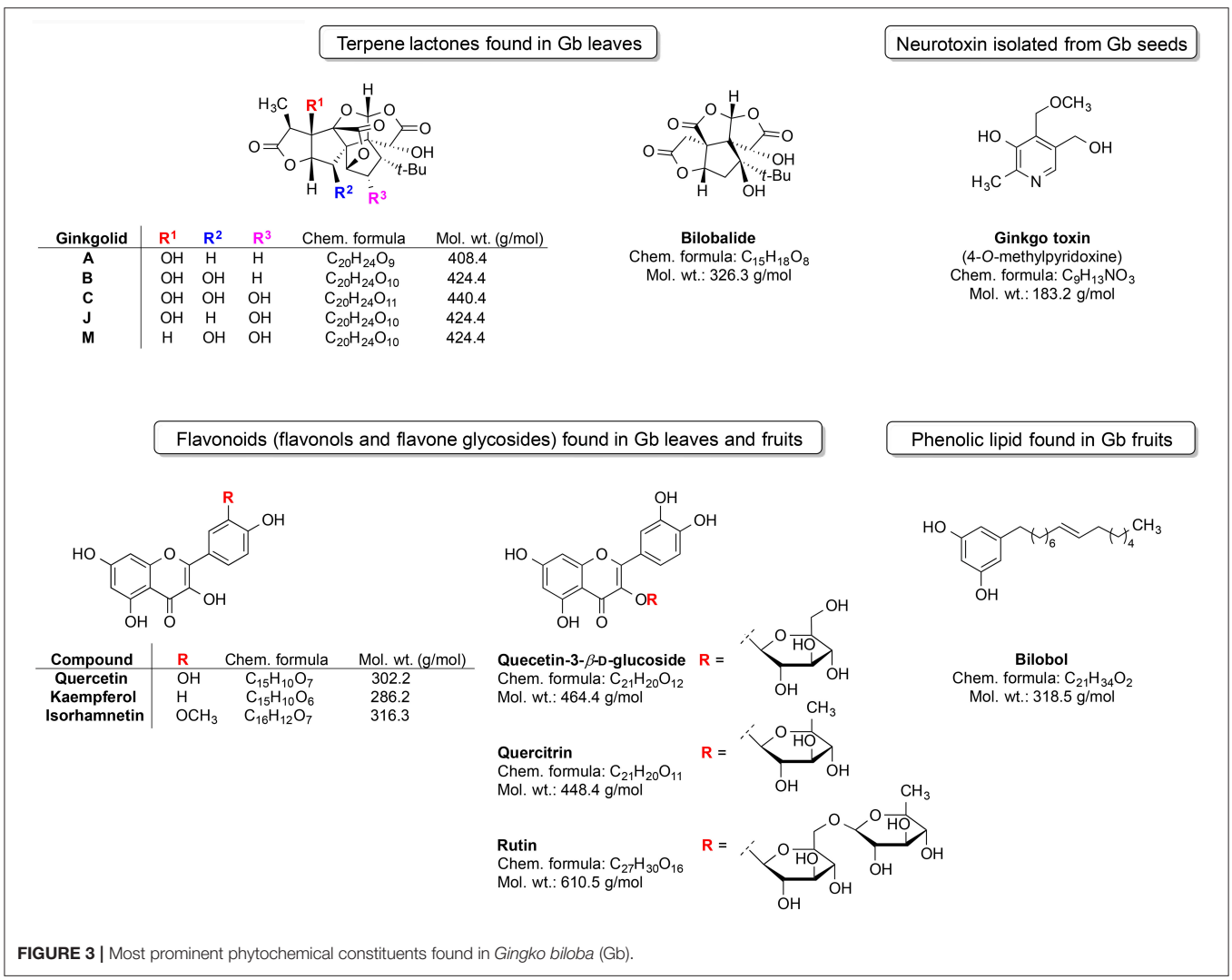


FIGURE 3 | Most prominent phytochemical constituents found in *Gingko biloba* (Gb).

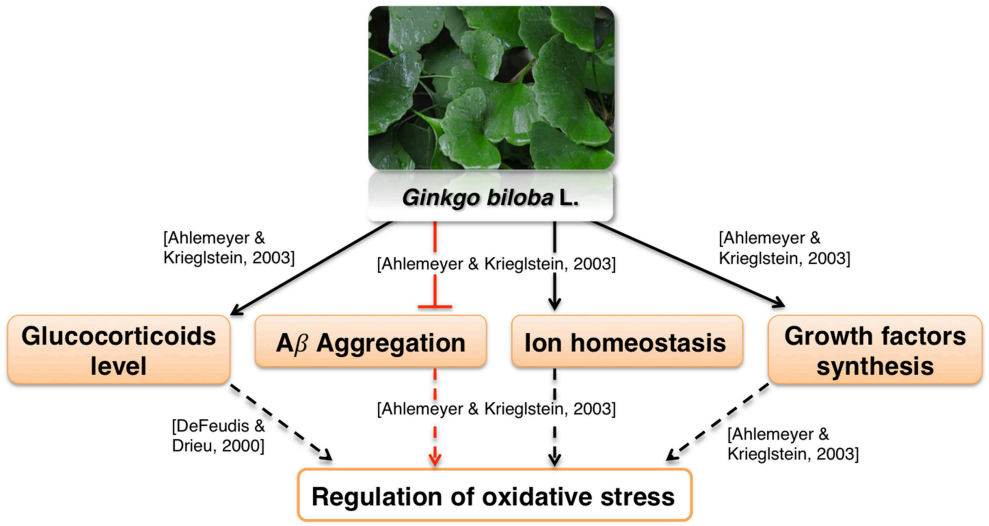


FIGURE 4 | Neuroprotective effects of *Gingko biloba* L.

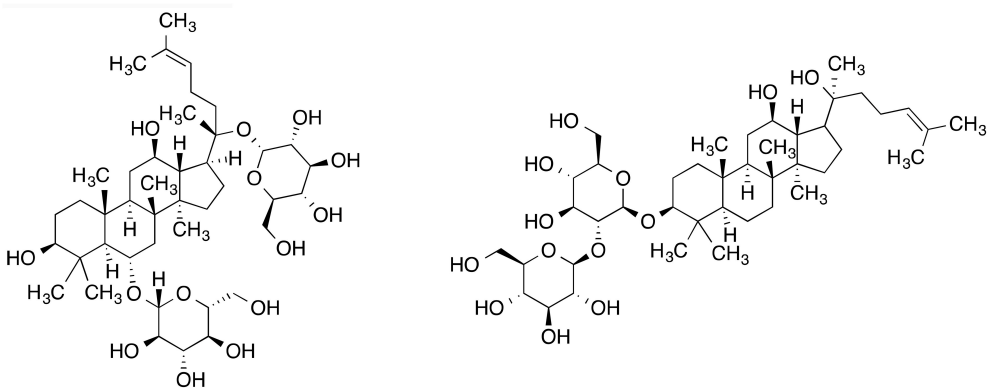


FIGURE 5 | Phytochemical constituents of ginseng.

Panax ginseng C.A. Meyer (Ginseng)

Ginseng is broadly used as an additive for dietary supplements or medicines. It serves as an adaptogen, which is a substance promoting homeostasis and protecting against various biological stressors. The dried root of this plant was used in the traditional medicine mainly in China and Korea (Yun, 2001).There are several species of *Panax* including *P. ginseng* (Oriental ginseng), *P. japonicus* (Japanese ginseng), *P. quinquefolius* (American ginseng), *P. trifolius*, *P. notoginseng* (Burkill), and *P. major* (Ngan et al., 1999). *Panax ginseng* CA Meyer is the most frequently used and extensively researched species of ginseng (Lee et al., 2005). The species is widely distributed in the northeastern part of China. The plant has been used in traditional Chinese medicine for a more than 2000 years as a tonic for fatigue, weakness and aging (Wang et al., 2010). Some constituents of this plant, such as ginsenosides Rg1 and Rg3 (**Figure 5**) and ginseng polysaccharides, have been investigated for their therapeutic potential (Yin et al., 2013; Song et al., 2017; Sun et al., 2017). The neuroprotective effect of ginseng is mainly attributed to the 20(*S*)-ginsenoside Rg3 (**Figure 5**), which has a steroidal backbone structure with carbohydrate part and aliphatic side chain (Yang et al., 2009). Rg3 is generated by heating the roots at high temperature (Popovich and Kitts, 2004; Sun et al., 2010).

A significant reduction of the amyloid-β40 and amyloid-β42 levels was reported after the ginsenoside Rg3 treatment in the brains of transgenic mice (Tg2576 line), as well as in

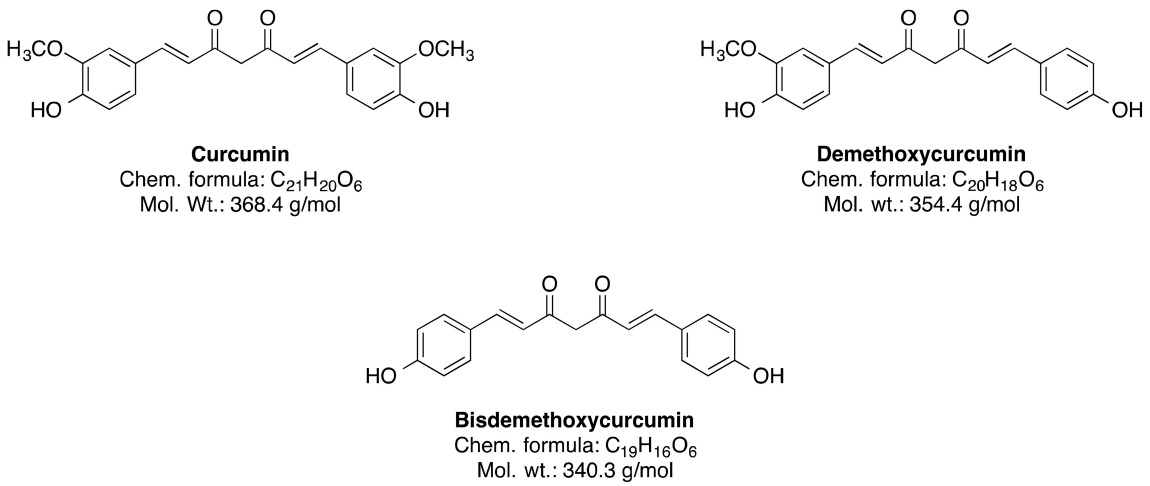


FIGURE 6 | Chemical structures of curcuminoids.

cultured cells (Chen et al., 2006). Ginsenoside Rg3 also protects against glutamate-induced neurotoxicity in cultured cortical neurons (Kim et al., 1998). Similarly, another ginseng constituent ginsenoside Rg1 (GRg1) suppressed Aβ-induced neurotoxicity, likely through p38 pathway activation in neuroblastoma cells (Li et al., 2012). Ginsenosides also regulate nicotinic acetylcholine receptor channel activity (Nah, 2014). As acetylcholine signaling mediates learning and memory, modulation of acetylcholine receptor activity may be involved in the compound effectiveness against dementia (Bartus et al., 1982; Giacobini, 2004). The ginseng extract specifically enriched with ginsenoside Rg3 rescues scopolamine-induced memory impairment possibly through modulation of the AChE activity and the NF-κB signaling pathway in the hippocampus of mice (Kim et al., 2016). NF-κB is a protein complex, which regulates neuroinflammation and is activated by ROS (Kaur et al., 2015). On a similar note, GRg1 reduces the Aβ-associated generation of ROS and cell death (Wang and Du, 2009). Correspondingly, many publications show protective effect of ginseng constituents on brain mitochondrial activity under multiple toxic conditions, including ischemia (Ye et al., 2011), calcium treatment (Tian et al., 2009; Zhou et al., 2014), hydrogen peroxide treatment (Tian et al., 2009), and even incubation of cells with Aβ *in vitro* (Ma et al., 2014).

A recent meta-analysis of randomized clinical trials showed inconsistent effect of ginseng on AD (Wang et al., 2016). Generally, the trials suffered from small sample size and poor design, including lack of placebo groups (Wang et al., 2016). Thus, there is a need of larger trials to determine the efficacy of ginseng in AD.

In summary, ginseng constituents are suggested to modulate a number of dementia-related mechanisms, such as amyloid-β metabolism, oxidative stress, neuroinflammation, and acetylcholine signaling. Unfortunately, the effect of gingseng on dementia patients remains poorly understood despite some efforts.

Curcuminoids from Genus Curcuma

The genus Curcuma (commonly termed as Turmeric) comprises around 80 species and is considered as one of the biggest genera of the *Zingiberaceae* family (Sirirugsa et al., 2007). Curcumin and its curcuminoid analogs, demethoxycurcumin and bisdemethoxycurcumin, are responsible for the typically yellow color of turmeric (Chin et al., 2013). However, the main bioactive phytoconstituent of Curcuma genus is curcumin (**Figure 6**).

It is an approved natural food colorant (E100) and can be easily obtained from turmeric through solvent extraction and crystallization (Chin et al., 2013). Furthermore, curcumin is widely used in traditional Indian medicine for the treatment of anorexia, hepatic diseases, cold, cough, and other disorders (Chin et al., 2013; Huminiecki et al., 2017). Nowadays, *in vivo* studies suggest that curcumin has potential neuroprotective properties including antioxidant, anti-neuroinflammatory, antiproliferative, anti-amyloidogenic, and neuro-regulative effects (Chin et al., 2013). A large epidemiological Indo-US Cross National Dementia study showed that the peasant Indian population has a low prevalence of AD and AD-associated dementia compared to the US population, and that may be linked to the high curcumin consumption in the Indian population (Chin et al., 2013), although such correlation does not necessarily imply causative connection.

Curcumin is comprised of two feruloyl moieties with 3-methoxy-4-hydroxy substituents (**Figure 7A**; Sahne et al., 2017). Both side units are linked together by an unsaturated seven-carbon spacer that includes a β-diketo function so that the molecule of curcumin is almost symmetric. Depending on pH of the environment, curcumin can exist in two possible tautomeric forms: enol and diketo (Sahne et al., 2017). The keto form is predominant in acidic and neutral media (pH $\leq$ 7.4) as well as in solid state, while in non-polar and basic milieu (pH $\geq$ 8.0) the enol form is occurring (Sahne et al., 2017). Moreover, the enol form co-exists in two equivalent tautomers that undergo

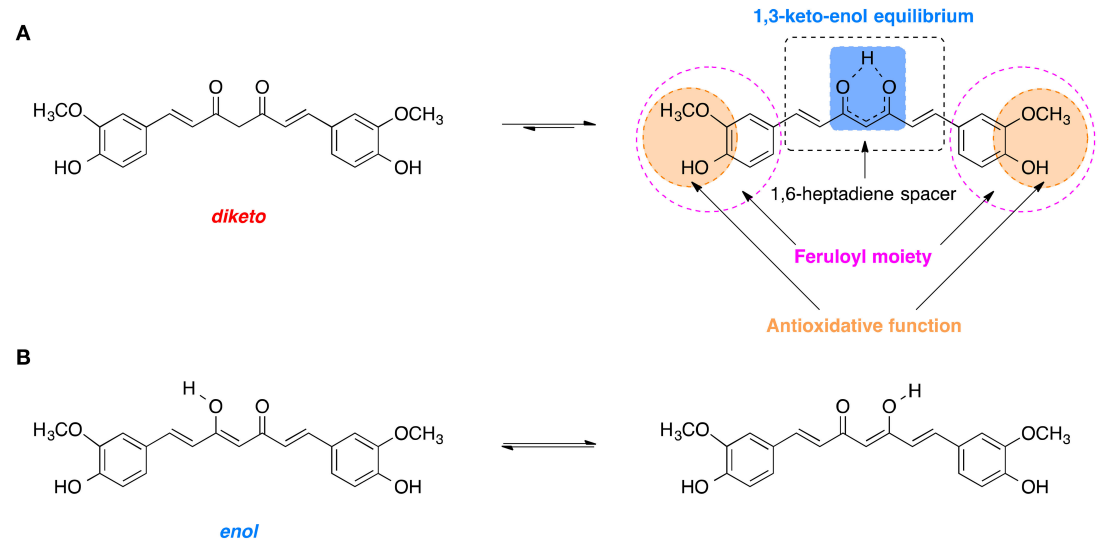


FIGURE 7 | Tautomerism of curcumin: **(A)** Diketo and 1,3-keto-enol equilibrium form of curcumin with its biologically relevant structural units. **(B)** Hydrogen transfer in the most stable enol form.

intramolecular hydrogen transfer (**Figure 7B**; Anjomshoa et al., 2016). Under physiological conditions (pH ∼7.4) curcumin can reach its 1,3-keto-enol equilibrium state. Some of the most important antioxidant properties of curcumin and its ability to scavenge ROS are associated with the stability and the antioxidative capability of the methoxy phenolic type groups that are present. The structural features of curcumin including its tautomeric forms and pharmacophores are present in **Figure 7**.

Curcumin suppresses tumor necrosis factor (TNF) activity, formation of Aβ plaques and protects brain cells from noxious agents (Belkacemi et al., 2011). In recent years, the natural polyphenols are being implemented in the treatment of different neurological disorders (Pathak et al., 2013; Hügel and Jackson, 2015).

Curcumin-enriched diet enhances memory and hippocampal neurogenesis in aged rats (Dong et al., 2012). This effect may be mediated by curcumin-induced modulation of expression of genes involved in cell growth and synaptic plasticity (Dong et al., 2012). Neuroprotective properties of curcumin are often attributed to its anti-inflammatory, antioxidant and lipophilic potential (Mishra and Palanivelu, 2008). For example, enhanced hippocampal expression of pro-inflammatory proteins TNF-α and IL-1 beta, which was caused by intracerebroventricular infusion of Aβ42 peptide solution, was at least partially normalized by infusion with curcumin-loaded lipid-core nanocapsules (but not free curcumin) (Hoppe et al., 2013a). Similarly, in neuroblastoma cells, curcumin suppressed the radiation-induced increase in activity of the pro-neuroinflammatory complex NF-κB (Aravindan et al., 2008). Activity of the neuroinflammation- and oxidative damage-related proteins NF-κB, Nrf2, and Sirt1 was also regulated in presence of curcumin in human neuroblastoma cells (Doggui et al., 2013). Curcumin treatment reduces ROS level in neuroblastoma cell lines treated with the noxious agent acrolein and in rat primary neurons with induced Ab42 hyper-expression (Ye and Zhang, 2012; Doggui et al., 2013). Curcumin protects mitochondria from noxious factors such as oxidative stress and rotenone (inhibitor of electron transport chain) *in vitro* (Daverey and Agrawal, 2016; Ramkumar et al., 2017). It also alleviates the age-associated loss of mitochondrial and oxidative activity in rodent brains (Dkhar and Sharma, 2010; Eckert et al., 2013; Rastogi et al., 2014). Curcumin also was shown to stimulate Sirt1 and Bcl-2 expression and to decrease brain cell death in experimental stroke (Miao et al., 2016). Reports also show that curcumin increases cell viability at low dosages (Ye and Zhang, 2012) and binds Aβ peptides, thus preventing them from aggregation into Aβ plaques (Yanagisawa et al., 2011). Due to its lipophillic properties, the curcumin can cross the BBB, bind to the plaques and decrease the β-amyloid plaques in AD by inducing phagocytosis of Aβ (Mishra and Palanivelu, 2008). Some of the curcumin derived pyrazoles and isoxazoles also bind to Aβ42 (**Figure 8**; Narlawar et al., 2008).

Curcumin treatment decreases Aβ40/42 and PSEN1 protein and mRNA levels in APP-overexpressing neuroblastoma cells (Xiong et al., 2011). Curcumin derivatives also increased the uptake of Aβ by macrophages, which were isolated from blood of AD patients and cultivated *in vitro* (Zhang et al., 2006). This is a relevant information, because peripheral macrophages are known to infiltrate brains of AD patients and participate in clearance of amyloid plaques (Gate et al., 2010). Moreover, in human neuroblastoma cells curcumin inhibits Aβ-induced tau phosphorylation likely via PTEN/Akt/GSK-3β pathway (Huang et al., 2014). Other researchers report, that Akt/GSK-3β and ERK pathways mediate the protective effect of curcumin on Aβ induced memory impairments (Hoppe et al., 2013b; Zhang et al., 2015). Curcumin treatment also improved hippocampal-dependent memory of Aβ-infused rats (Hoppe et al., 2013b).

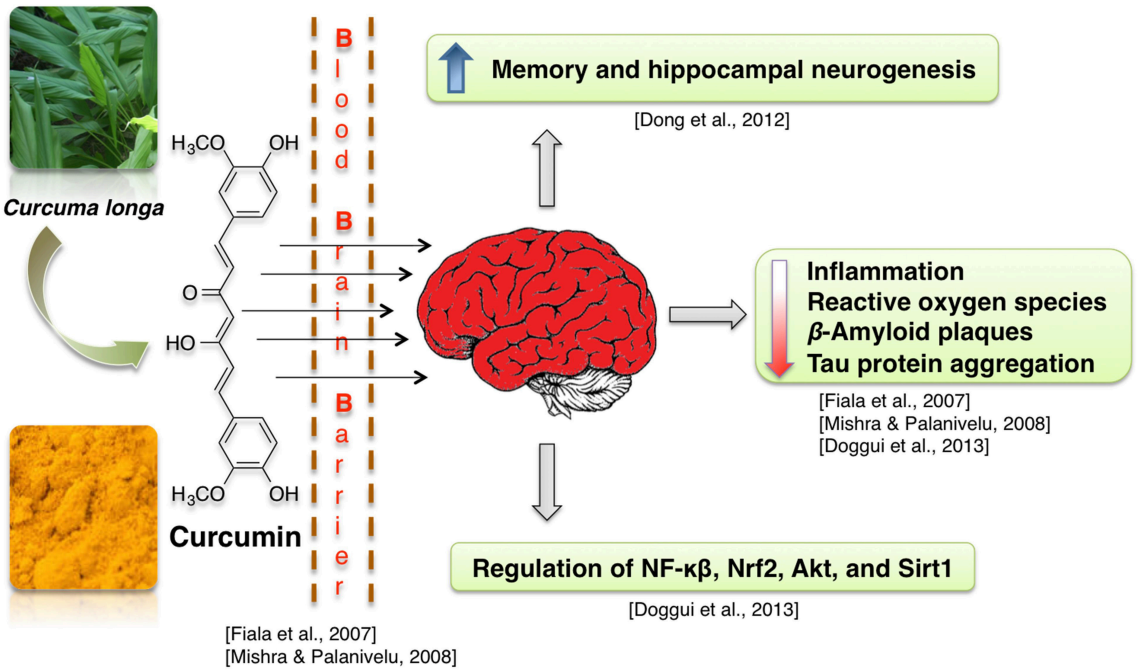


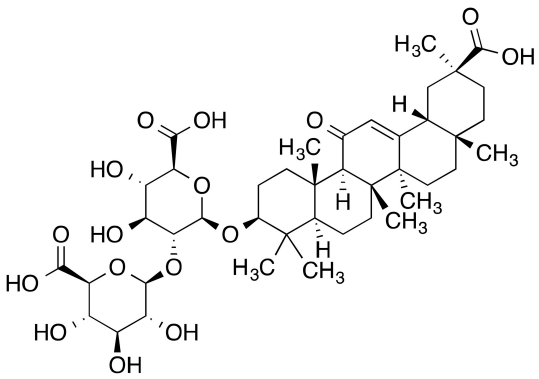
FIGURE 8 | Neuroprotective effects of curcumin.

A systematic review by Brondino et al. showed, that the few clinical trials studying the effect of curcumin on AD yielded inconclusive results (Brondino et al., 2014). Although curcumin was found to be safe during short-term use, future clinical studies need to determine its long-term safety and efficacy on human subjects (Brondino et al., 2014). Since the systematic review arrival, another clinical study was published on the topic, showing improvement of working memory and mood after curcumin treatment in a fairly small group of elderly participants (Cox et al., 2015). There is also a study showing correlation between consumption of curcumin-containing spice—curry—with cognitive performance in elderly (Ng et al., 2006). This finding should be taken with a grain of salt in context of curcumin-dementia research, as curcumin concentration in curry is fairly low (Tayyem et al., 2006) and the extent of biologically available curcumin ingested with curry is disputed. Co-administration of curcumin and donepezil (reversible cholinesterase inhibitor) had synergistic effect on cognition and oxidative stress (Akinyemi et al., 2017). Combined donepezil/curcumin therapeutic also showed good BBB permeability (Yan et al., 2017). Concluding, curcumin protects brain cells against damage induced by oxidative stress and Aβ pathology. These properties may underlie beneficial effects of curcumin for treatment of dementia symptoms, as seen in animal model studies. The data suggest, that curcumin may be a promising candidate for novel dementia medication, but conclusive clinical research that could verify this hypothesis is still lacking. Moreover, to date, researchers analyzed the efficacy of curcumin exclusively against AD-associated dementia, leaving out other dementias.

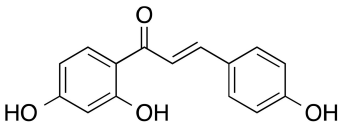
Glycyrrhiza Genus

Genus *Glycyrrhiza*, also known as licorice (liquorice), is a member of Fabaceae family and consists of about 30 species. Most of the plants of this genus are perennial herbs native to Mediterranean region, Asia, Southern Russia, and Iran (Asl and Hosseinzadeh, 2008). The *Glycyrrhiza* species are cultivated all throughout Europe and Asia (Blumenthal et al., 2000; Asl and Hosseinzadeh, 2008). The licorice roots and rhizomes are used worldwide as natural sweetener and a herbal medicine mainly for the therapy of autoimmune hepatitis C, jaundice, peptic ulcer, and skin diseases such as atopic dermatitis and inflammation-induced hyperpigmentation (Asl and Hosseinzadeh, 2008; Callender et al., 2011; Tewari et al., 2017); further studies suggest that licorice roots may also have pharmacologically useful properties such as anticancer, antioxidative, anti-inflammatory, antiviral, antimicrobial, hepato- and cardioprotectitve effects (Asl and Hosseinzadeh, 2008; Waltenberger et al., 2016). The main bioactive phytoconstituents of *Glycyrrhiza glabra* (liquorice) root are the sweet-tasting triterpene saponin glycyrrhizin (glycyrrhizic acid) and the phenolic type compound isoliquiritigenin (**Figure 9**). Other important constituents also include several isoflavonoid derivatives such as shinpterocarpin, glabrone, glabridin, galbrene, lico-isoflavones A and B (Asl and Hosseinzadeh, 2008).

Due to their antioxidative properties, several species of *Glycyrrhiza* were investigated for possible therapeutic effects as neuroprotectants against neurodegenerative disorders such as PD, AD, and dementia. For example, extract from *Glycyrrhiza inflata* prevents tau misfolding *in vitro* (Chang et al., 2016). Thus, the extract of this plant may be effective against various



Glycyrrhizin (Epigen™, Glycyron™)
(glycyrrhizic acid or glycyrrhizinic acid)
Chem. formula: $C_{42}H_{62}O_{16}$
Mol. wt.: 822.9 g/mol



Isoliquiritigenin
Chem. formula: $C_{15}H_{12}O_4$
Mol. wt.: 256.3

FIGURE 9 | Chemical structures of the major phytoconstituents of *Glycyrrhiza glabra*.

taupathies and AD. *G. inflata* extract decreased oxidative stress in cell models of spinocerebellar ataxia type 3 (SCA3), also known as Machado-Joseph disease (MJD), by upregulating the activity of PPARGC1A and the NFE2L2-ARE pathway (Chen et al., 2014). Glycyrrhizin prevents cytotoxicity, ROS generation and downregulation of glutathione (GSH), which are elicited by 1-methyl-4-phenylpyridinium (MPP^+) (Yim et al., 2007). MPP+ is a neurotoxic substance acting via interference with the mitochondrial oxidative phosphorylation (Yim et al., 2007). The GSH downregulation is noteworthy, because it is a crucial element of the antioxidative system of the brain (Dringen, 2000). Increased oxidative stress in dementia is attributed to dwindled levels of GSH (Yim et al., 2007; Saharan and Mandal, 2014). Similarly, *G. inflata* extract was shown to inhibit oxidative stress *in vitro* (Chang et al., 2016). The brain cells are susceptible to the oxidative stress. The effect of licorice extract on the oxidative stress may be connected to the beneficial effect of isoliquiritigenin on mitochondrial function (Yang et al., 2012). Licorice may reduce the damage to the brain cells, improve the neuronal function and prevent the memory impairment by diminishing oxidative stress associated with several dementia types (Ju et al., 1989; Dhingra et al., 2004).

Figure 10 summarizes the valuable effects of licorice root extract that may be useful for the treatment of dementia and/or AD-related dementia. Some authors suggest that memory-enhancing activity of the licorice root extract may be connected to its anti-inflammatory effect (Yokota et al., 1998; Dhingra et al., 2004). This data is in agreement with the known tight relationship between inflammation and oxidative stress (Dandekar et al., 2015). *Glycyrrhiza* is used in various polyherbal formulations. One of such formulations used in traditional Japanese Kampo medicine is yokukansan, which is composed of seven different plants including *Glycyrrhiza uralensis* Fisher. *Glycyrrhiza* extract antagonizes α2A adrenoceptors (Ikarashi and Mizoguchi, 2016). Several phytoconstituents of *Glycyrrhiza*: glycyrrhizin, glycycoumarin, liquiritin and isoliquiritigenin show neuroprotective effects when applied as a component of the yokukansan (Ikarashi and Mizoguchi, 2016). Isoliquiritigenin inhibited the activity of the NMDA receptors (Ikarashi and Mizoguchi, 2016). Noteworthy, memantine, an important synthetic drug against dementia, also shows antagonism for NMDA receptors (Danysz and Parsons, 2003). Moreover, the neuroprotective effect of glycycoumarin may be due to its ability to suppress the pro-apoptotic activity of caspase-3 (Kanno et al., 2015; Ikarashi and Mizoguchi, 2016).

Extract from another *Glycyrrhiza* species—*Glycyrrhiza glabra*—improved the learning ability of mice after 7 days of oral administration (Parle et al., 2004). However, another study reported the paradoxical sedative properties of the extract (Hikino, 1985). This shows that the *G. glabra* extract is useful for the improvement of the learning ability but its dose should be established carefully to prevent the sedative effects. A glycyrrhizin salt, diammonium-glycyrrhizinate, prevented the mitochondrial and cognitive dysfunctions induced by Aβ42 in mice (Zhu et al., 2012). Although not yet proven in context of brain function, licorice constituents have a potential to interact with other drugs because of its modulating activity of P450 proteins, which belong to the main regulators of xenobiotic metabolism (Qiao et al., 2014). In summary, glycyrrhiza extracts show anti-inflammatory and antioxidative properties and modulate glutamate signaling and apoptosis. Similarly to above described herbal medicines curcumin and ginseng, despite animal model-based evidence for glycyrrhiza effectiveness in regulating cognitive deficits, there are currently no studies on effectiveness of this plant for dementia therapy in patients.

Camellia sinensis Kuntze

Camellia sinensis Kuntze (green tea) brew is one of the most extensively consumed beverages in the world (Goenka et al., 2013). Several beneficial effects of green tea consumption

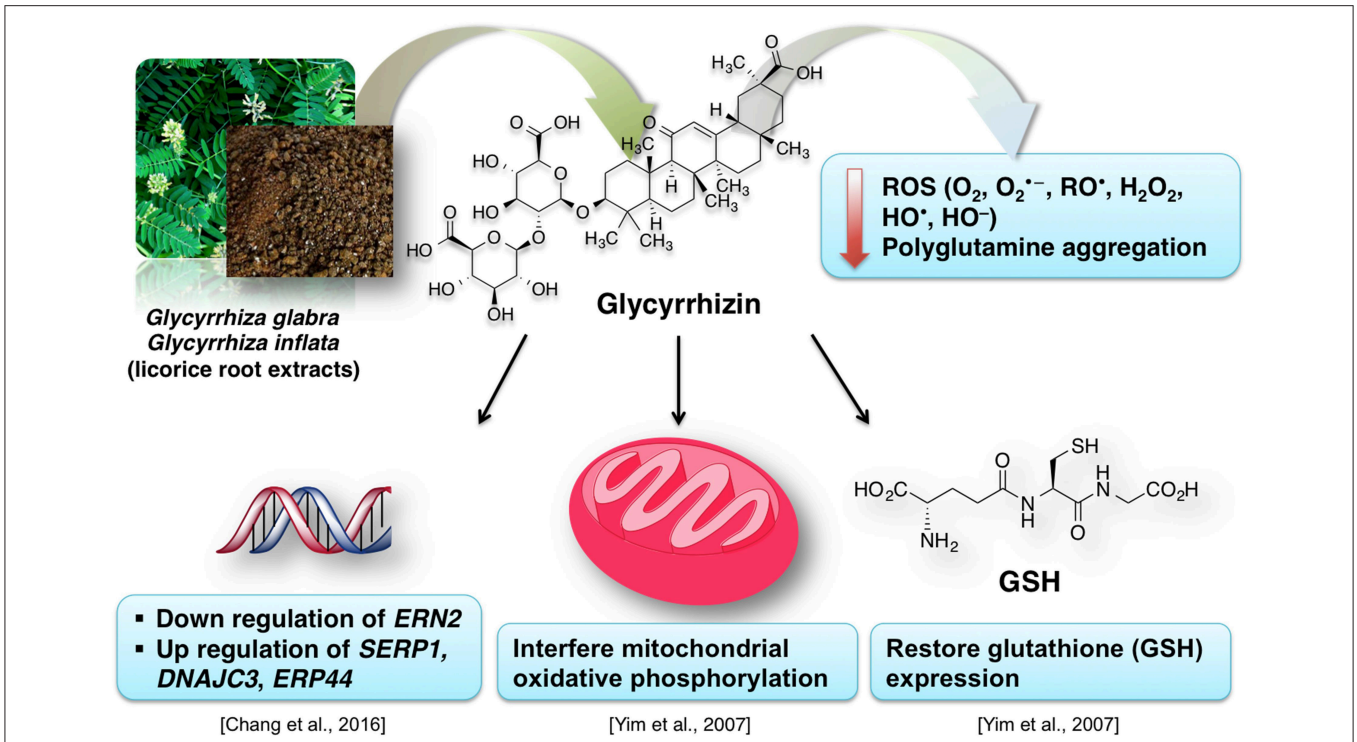


FIGURE 10 | A simplified representation of the neuroprotective effects of licorice for dementia treatment.

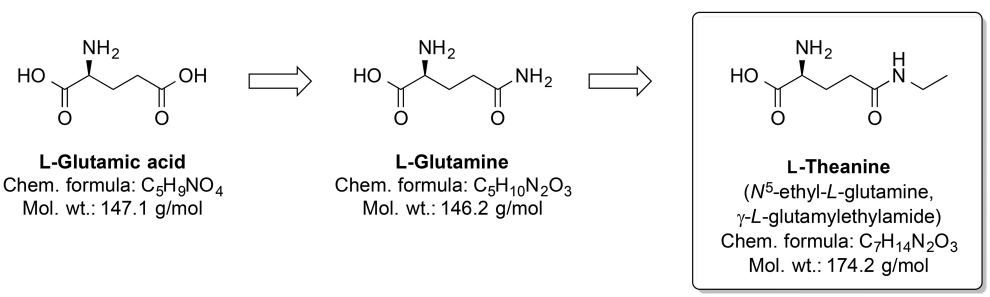


FIGURE 11 | Chemical structures of the nootropic drug L-Theanine and its proteinogenic amino acid analogs.

are reported for various conditions like obesity, diabetes, inflammation, coronary artery disease, stroke and some malignancies (de Mejia et al., 2009; Chacko et al., 2010). Consumption of green tea-related compounds [e.g., (-)-epigallocatechin-3-gallate] improves cognitive functions and prevents memory impairment in animals and humans (Rezai-Zadeh et al., 2008; de Mejia et al., 2009; Mandel et al., 2011).

Around one-third out of 4,000 bioactive compounds of *C. sinensis* are polyphenols (Mahmood et al., 2010). The gene expression and activity of the membrane metalloendopeptidase (MME) were enhanced by green tea extract. Several MME are capable of degrading Aβ peptides (Wang et al., 2006). Pretreatment by infusion with extract of green tea leaves into the left hippocampus of a rat prevented cognitive impairments and superoxide dismutase activity changes, and corrected deregulated activity of pro-inflammatory enzyme COX and AChE, which were induced by injecting $AlCl_3$ into the same brain area (Jelenkovic et al., 2014). When injected i.p. L-theanine, one of the amino acid components of *C. sinensis*, protects against memory impairment and cell death caused by ischemia (Egashira et al., 2007, 2008). Interestingly, chronic ingestion of L-theanine in rats also caused improvement in cognitive functions (Yamada et al., 2008) and decreased oxidation levels in the brain of the rats (Nishida et al., 2008). Similarly, in transgenic mouse AD model, the green tea constituent epigallocatechin-3-gallate normalized the dysregulated ROS production, as well as mitochondrial respiration and MMP (Dragicevic et al., 2011). Generally,

L-theanine is an *N*-amino-ethylated analog of the proteinogenic neurotransmitter L-glutamic acid and its precursor L-glutamine (**Figure 11**). L-theanine protects against Aβ42-induced memory deficits and death of cortical and hippocampal cells, possibly by suppressing the ERK/p38 and NF-κB signaling pathways and reducing the oxidative damage (Kim et al., 2009).

Daily consumption of green tea is hypothesized to reduce the risk of AD and age-related dementia (Ayoub and Melzig, 2006). In some clinical studies, L-theanine improved the cognitive functions and mood in combination with caffeine in healthy human subjects (Haskell et al., 2008; Owen et al., 2008). On the other hand, the results of studies on the effects of L-theanine alone on mood are inconclusive (Kimura et al., 2007; Haskell et al., 2008). Green tea catechins can regulate activity of P-glycoprotein (Zhou et al., 2004), which may influence brain availability of co-administered substances. Summarizing, green tea extract shows antiapoptotic and antioxidative activities and may even directly inhibit Aβ plaque formation. Moreover, several human studies provide credibility to the hypothesis that green tea constituents may be effective for modulation of human cognition and perhaps in dementia treatment.

CONCLUSIONS

In this work, we discuss that a large number of plants have been used for dementia treatment worldwide. The mechanisms of action of the reviewed five prominent representative plants generally involve anti-inflammatory, antioxidative, and antiapoptotic activity that are mainly associated with the neuroprotective effects of these plants or their bioactive constituents. Some of such naturally occurring compounds exhibit promising potential as alternative therapeutic strategies. For example, curcumin showed remarkable synergetic effects on cognition and oxidative stress, as well as good BBB permeability, when co-administrated with the approved reversible ChE inhibitor donepezil. Moreover, such combined donepezil/curcumin application may be useful for treatment of dementia symptoms, as seen in animal model studies. Furthermore, combined supplement treatment with some mitochondrial antioxidants, such as α-lipoic acid and acetyl-L-carnitine has been shown to reduce both physical and mental weariness or even to restore memory function in age-related diseases, including AD and different types of dementia, as provided in transgenic mouse model of AD. However, there are still many unknowns in this research area that need to be clarified by planning future studies. The scientific community needs more comprehensive research focused on identifying active ingredients of plants and investigating their mechanism of action. Such research will facilitate clinical studies evaluating the potential of the featured herbal products in dementia treatment. We conclude that further research on plants used in different ethnomedicinal practices and the traditional medicine could lead to the development of novel therapeutics for dementia and, therefore, is of a very high interest.

AUTHOR CONTRIBUTIONS

DT, AMS, and AA have written the first draft of the manuscript. AM, ANS, LH, JH, and NT revised and improved the first draft. All authors have seen and agreed on the finally submitted version of the manuscript.

ACKNOWLEDGMENTS

The authors acknowledge the support by the Polish KNOW (Leading National Research Centre) Scientific Consortium "Healthy Animal—Safe Food," decision of Ministry of Science and Higher Education No. 05-1/KNOW2/2015.

REFERENCES

Abbott, A. (2011). Dementia: a problem for our age. *Nature* 475, S2–S4. doi: 10.1038/475S2a

Abdel-Kader, R., Hauptmann, S., Keil, U., Scherping, I., Leuner, K., Eckert, A., et al. (2007). Stabilization of mitochondrial function by *Ginkgo biloba* extract (EGb 761). *Pharmacol. Res.* 56, 493–502. doi: 10.1016/j.phrs.2007.09.011

Abdou, H. M., Yousef, M. I., El Mekkawy, D. A., and Al-Shami, A. S. (2016). Prophylactic neuroprotective efficiency of co-administration of *Ginkgo biloba* and Trifolium pretense against sodium arsenite-induced neurotoxicity and dementia in different regions of brain and spinal cord of rats. *Food Chem. Toxicol.* 94, 112–127. doi: 10.1016/j.fct.2016.05.015

Adams, M., Gmünder, F., and Hamburger, M. (2007). Plants traditionally used in age related brain disorders—a survey of ethnobotanical literature. *J. Ethnopharmacol.* 113, 363–381. doi: 10.1016/j.jep.2007.07.016

Adsersen, A., Gauguin, B., Gudiksen, L., and Jäger, A. K. (2006). Screening of plants used in Danish folk medicine to treat memory dysfunction for acetylcholinesterase inhibitory activity. *J. Ethnopharmacol.* 104, 418–422. doi: 10.1016/j.jep.2005.09.032

Ahlemeyer, B., and Krieglstein, J. (2003). Neuroprotective effects of *Ginkgo biloba* extract. *Cell. Mol. Life Sci. C.* 60, 1779–1792. doi: 10.1007/s00018-003-3080-1

Akhondzadeh, S., Noroozian, M., Mohammadi, M., Ohadinia, S., Jamshidi, A. H., and Khani, M. (2003). Salvia officinalis extract in the treatment of patients with mild to moderate Alzheimer's disease: a double blind, randomized and placebo-controlled trial. *J. Clin. Pharm. Ther.* 28, 53–59. doi: 10.1046/j.1365-2710.2003.00463.x

Akinyemi, A. J., Oboh, G., Oyeleye, S. I., and Ogunsuyi, O. (2017). Anti-amnestic effect of curcumin in combination with donepezil, an anticholinesterase drug: involvement of cholinergic system. *Neurotox. Res.* 31, 560–569. doi: 10.1007/s12640-017-9701-5

Alam, M. M., Okazaki, K., Nguyen, L. T. T., Ota, N., Kitamura, H., Murakami, S., et al. (2017). Glucocorticoid receptor signaling represses the antioxidant response by inhibiting histone acetylation mediated by the transcriptional activator NRF2. *J. Biol. Chem.* 292, 7519–7530. doi: 10.1074/jbc.M116.773960

Albuquerque, E. X., Santos, M. D., Alkondon, M., Pereira, E. F., and Maelicke, A. (2001). Modulation of nicotinic receptor activity in the central nervous system: a novel approach to the treatment of Alzheimer disease. *Alzheimer Dis. Assoc. Disord.* 15(Suppl. 1), S19–25. doi: 10.1097/00002093-200108001-00004

Aminzadeh, M., Roghani, M., Sarfallah, A., and Riazi, G. H. (2018). TRPM2 dependence of ROS-induced NLRP3 activation in Alzheimer's disease. *Int. Immunopharmacol.* 54, 78–85. doi: 10.1016/j.intimp.2017.10.024

Amri, H., Ogwuegbu, S. O., Boujrad, N., Drieu, K., and Papadopoulos, V. (1996). *In vivo* regulation of peripheral-type benzodiazepine receptor and glucocorticoid synthesis by *Ginkgo biloba* extract EGb 761 and isolated ginkgolides. *Endocrinology* 137, 5707–5718. doi: 10.1210/endo.137.12.8940403

Anjomshoa, S., Namazian, M., and Noorbala, M. R. (2016). The effect of solvent on tautomerism, acidity and radical stability of curcumin and its derivatives

based on thermodynamic quantities. *J. Solution Chem.* 45, 1021–1030. doi: 10.1007/s10953-016-0481-y

Antico Arciuch, V. G., Elguero, M. E., Poderoso, J. J., and Carreras, M. C. (2012). Mitochondrial regulation of cell cycle and proliferation. *Antioxid. Redox Signal.* 16, 1150–1180. doi: 10.1089/ars.2011.4085

Aravindan, N., Madhusoodhanan, R., Ahmad, S., Johnson, D., and Herman, T. S. (2008). Curcumin inhibits NFκB mediated radioprotection and modulate apoptosis related genes in human neuroblastoma cells. *Cancer Biol. Ther.* 7, 569–576. doi: 10.4161/cbt.7.4.5534

Asl, M. N., and Hosseinzadeh, H. (2008). Review of pharmacological effects of *Glycyrrhiza* sp. and its bioactive compounds. *Phyther. Res.* 22, 709–724. doi: 10.1002/ptr.2362

Atanasov, A. G., Waltenberger, B., Pferschy-Wenzig, E.-M., Linder, T., Wawrosch, C., Uhrin, P., et al. (2015). Discovery and resupply of pharmacologically active plant-derived natural products: a review. *Biotechnol. Adv.* 33, 1582–1614. doi: 10.1016/j.biotechadv.2015.08.001

Ayoub, S., and Melzig, M. F. (2006). Induction of neutral endopeptidase (NEP) activity of SK-N-SH cells by natural compounds from green tea. *J. Pharm. Pharmacol.* 58, 495–501. doi: 10.1211/jpp.58.4.0009

Ballard, C., and Howard, R. (2006). Neuroleptic drugs in dementia: benefits and harm. *Nat. Rev. Neurosci.* 7, 492–500. doi: 10.1038/nrn1926

Baloh, R. H. (2011). TDP-43: the relationship between protein aggregation and neurodegeneration in amyotrophic lateral sclerosis and frontotemporal lobar degeneration. *FEBS J.* 278, 3539–3549. doi: 10.1111/j.1742-4658.2011.08256.x

Banasch, M., Ellrichmann, M., Tannapfel, A., Schmidt, W. E., and Goetze, O. (2011). The non-invasive (13)C-methionine breath test detects hepatic mitochondrial dysfunction as a marker of disease activity in non-alcoholic steatohepatitis. *Eur. J. Med. Res.* 16:258. doi: 10.1186/2047-783X-16-6-258

Bartus, R. T., Dean, R. L. III., Beer, B., and Lippa, A. S. (1982). The cholinergic hypothesis of geriatric memory dysfunction. *Science* 217, 408–414. doi: 10.1126/science.7046051

Beal, M. F. (2005). Mitochondria take center stage in aging and neurodegeneration. *Ann. Neurol.* 58, 495–505. doi: 10.1002/ana.20624

Belkacemi, A., Doggui, S., Dao, L., and Ramassamy, C. (2011). Challenges associated with curcumin therapy in Alzheimer disease. *Expert Rev. Mol. Med.* 13, e34. doi: 10.1017/S1462399411002055

Bennett, S., Grant, M. M., and Aldred, S. (2009). Oxidative stress in vascular dementia and Alzheimer's disease: a common pathology. *J. Alzheimers. Dis.* 17, 245–257. doi: 10.3233/JAD-2009-1041

Berridge, M. J. (1995). Calcium signalling and cell proliferation. *Bioessays* 17, 491–500. doi: 10.1002/bies.950170605

Berridge, M. J. (2011). Calcium signalling and Alzheimer's disease. *Neurochem. Res.* 36, 1149–1156. doi: 10.1007/s11064-010-0371-4

Blennow, K., de Leon, M. J., and Zetterberg, H. (2006). Alzheimer's disease. *Lancet (London, England)* 368, 387–403. doi: 10.1016/S0140-6736(06)69113-7

Blumenthal, M., Goldberg, A., and Brinkmann, J. (2000). *Herbal Medicine, Expanded Commission E Monographs Cd-Rom.* Austin, TX: American Botanical Council/Integrative Medical.

Bridi, R., Crossetti, F. P., Steffen, V. M., and Henriques, A. T. (2001). The antioxidant activity of standardized extract of *Ginkgo biloba* (EGb 761) in rats. *Phytother. Res.* 15, 449–451. doi: 10.1002/ptr.814

Brondino, N., Re, S., Boldrini, A., Cuccomarino, A., Lanati, N., Barale, F., et al. (2014). Curcumin as a therapeutic agent in dementia: a mini systematic review of human studies. *Sci. World J.* 2014:174282. doi: 10.1155/2014/174282

Brun, A. (1987). Frontal lobe degeneration of non-Alzheimer type. *I. Neuropathology. Arch. Gerontol. Geriatr.* 6, 193–208. doi: 10.1016/0167-4943(87)90021-5

Burgess, L., Page, S., and Hardman, P. (2002). Changing attitudes in dementia care and the role of nurses. *Nurs. Times* 99, 18–19.

Burte, F., Carelli, V., Chinnery, P. F., and Yu-Wai-Man, P. (2015). Disturbed mitochondrial dynamics and neurodegenerative disorders. *Nat. Rev. Neurol.* 11, 11–24. doi: 10.1038/nrneurol.2014.228

Butterfield, D. A., Swomley, A. M., and Sultana, R. (2013). Amyloid beta-peptide (1-42)-induced oxidative stress in Alzheimer disease: importance in disease pathogenesis and progression. *Antioxid. Redox Signal.* 19, 823–835. doi: 10.1089/ars.2012.5027

Cai, H., Cong, W., Ji, S., Rothman, S., Maudsley, S., and Martin, B. (2012). Metabolic dysfunction in Alzheimer's disease and related neurodegenerative disorders. *Curr. Alzheimer Res.* 9, 5–17. doi: 10.2174/156720512799015064

Callender, V. D., St Surin-Lord, S., Davis, E. C., and Maclin, M. (2011). Postinflammatory hyperpigmentation: etiologic and therapeutic considerations. *Am. J. Clin. Dermatol.* 12, 87–99. doi: 10.2165/11536930-000000000-00000

CESA (1992). *Usos Tradicionales de las Especies Forestales Nativas en el Ecuador*. Tomo II. CESA: Central Ecuatoriana de Servicios Agrícolas.

CESA (1993). *Usos Tradicionales de las Especies Forestales Nativas en el Ecuador*. Tomo III. CESA: Central Ecuatoriana de Servicios Agrícolas.

Chacko, S. M., Thambi, P. T., Kuttan, R., and Nishigaki, I. (2010). Beneficial effects of green tea: a literature review. *Chin. Med.* 5:13. doi: 10.1186/1749-8546-5-13

Chan, D. C. (2006). Mitochondria: dynamic organelles in disease, aging, and development. *Cell* 125, 1241–1252. doi: 10.1016/j.cell.2006.06.010

Chandrasekaran, K., Mehrabian, Z., Spinnewyn, B., Chinopoulos, C., Drieu, K., and Fiskum, G. (2003). Neuroprotective effects of bilobalide, a component of *Ginkgo biloba* extract (EGb 761®) in global brain ischemia and in excitotoxicity-induced neuronal death. *Pharmacopsychiatry* 36, 89–94. doi: 10.1055/s-2003-40447

Chang, H.-M., But, P. P. H., and Yao, S.-C. (1986). *Pharmacology and Applications of Chinese Materia Medica*. Singapore: World Scientific.

Chang, K.-H., Chen, I.-C., Lin, H.-Y., Chen, H.-C., Lin, C.-H., Lin, T.-H., et al. (2016). The aqueous extract of Glycyrrhiza inflata can upregulate unfolded protein response-mediated chaperones to reduce tau misfolding in cell models of Alzheimer's disease. *Drug Des. Devel. Ther.* 10, 885–896. doi: 10.2147/DDDT.S96454

Chen, C.-M., Weng, Y.-T., Chen, W.-L., Lin, T.-H., Chao, C.-Y., Lin, C.-H., et al. (2014). Aqueous extract of Glycyrrhiza inflata inhibits aggregation by upregulating PPARGC1A and NFE2L2-ARE pathways in cell models of spinocerebellar ataxia 3. *Free Radic. Biol. Med.* 71, 339–350. doi: 10.1016/j.freeradbiomed.2014.03.023

Chen, F., Eckman, E. A., and Eckman, C. B. (2006). Reductions in levels of the Alzheimer's amyloid beta peptide after oral administration of ginsenosides. *FASEB J. Off. Publ. Fed. Am. Soc. Exp. Biol.* 20, 1269–1271. doi: 10.1096/fj.05-5530fje

Chen, J. X., and Yan, S. S. (2010). Role of mitochondrial amyloid-beta in Alzheimer's disease. *J. Alzheimers. Dis.* 20(Suppl. 2), S569–S578. doi: 10.3233/JAD-2010-100357

Chevallier, A. (1996). *The Encyclopedia of Medicinal Plants*. London: Dorling Kindersley publishers.

Chin, D., Huebbe, P., Pallauf, K., and Rimbach, G. (2013). Neuroprotective properties of curcumin in Alzheimer's disease–merits and limitations. *Curr. Med. Chem.* 20, 3955–3985. doi: 10.2174/09298673113209990210

Chrusciel, M., and Varagić, V. (1966). The effect of galantamine on the blood pressure of the rat. *Br. J. Pharmacol.* 26, 295–301. doi: 10.1111/j.1476-5381.1966.tb01908.x

Corder, E. H., Saunders, A. M., Strittmatter, W. J., Schmechel, D. E., Gaskell, P. C., Small, G. W., et al. (1993). Gene dose of apolipoprotein E type 4 allele and the risk of Alzheimer's disease in late onset families. *Science* 261, 921–923.

Corrada, M. M., Brookmeyer, R., Paganini-Hill, A., Berlau, D., and Kawas, C. H. (2010). Dementia incidence continues to increase with age in the oldest old: the 90+ study. *Ann. Neurol.* 67, 114–121. doi: 10.1002/ana.21915

Cox, K. H. M., Pipingas, A., and Scholey, A. B. (2015). Investigation of the effects of solid lipid curcumin on cognition and mood in a healthy older population. *J. Psychopharmacol.* 29, 642–651. doi: 10.1177/0269881114552744

Cummings, J., Aisen, P. S., DuBois, B., Frölich, L., Jack, C. R., Jones, R. W., et al. (2016). Drug development in Alzheimer's disease: the path to 2025. *Alzheimer's Res. Ther.* 8:39. doi: 10.1186/s13195-016-0207-9

Dai, D.-F., Chiao, Y. A., Marcinek, D. J., Szeto, H. H., and Rabinovitch, P. S. (2014). Mitochondrial oxidative stress in aging and healthspan. *Longev. Heal.* 3:6. doi: 10.1186/2046-2395-3-6

Damasio, A. R., and Gabrowski, T. J. (2004). "Definition, clinical features and neuroanatomical basis of dementia," in *The Neuropathology of Dementia*, eds M. M. Esiri, V. M.-Y. Lee, and J. Q. Trojanowski (Cambridge: Cambridge University Press), 1–34.

Dandekar, A., Mendez, R., and Zhang, K. (2015). Cross talk between ER stress, oxidative stress, and inflammation in health and disease. *Methods Mol. Biol.* 1292, 205–214. doi: 10.1007/978-1-4939-2522-3_15

Danysz, W., and Parsons, C. G. (2003). The NMDA receptor antagonist memantine as a symptomatological and neuroprotective treatment for Alzheimer's disease: preclinical evidence. *Int. J. Geriatr. Psychiatry* 18, S23–S32. doi: 10.1002/gps.938

Daverey, A., and Agrawal, S. K. (2016). Curcumin alleviates oxidative stress and mitochondrial dysfunction in astrocytes. *Neuroscience* 333, 92–103. doi: 10.1016/j.neuroscience.2016.07.012

Dávila, D., Fernández, S., and Torres-Alemán, I. (2016). Astrocyte resilience to oxidative stress induced by insulin-like growth factor I (IGF-I) involves preserved AKT (protein kinase B) activity. *J. Biol. Chem.* 291, 12039. doi: 10.1074/jbc.A115.695478

de Barradas, J. P. (1957). *Plantas Mágicas Americanas*. Consejo Superior de Investigaciones Científicas, Instituto "Bernardino de Sahagún."

de Mejia, E. G., Ramirez-Mares, M. V., and Puangpraphant, S. (2009). Bioactive components of tea: cancer, inflammation and behavior. *Brain. Behav. Immun.* 23, 721–731. doi: 10.1016/j.bbi.2009.02.013

Dhingra, D., Parle, M., and Kulkarni, S. K. (2004). Memory enhancing activity of Glycyrrhiza glabra in mice. *J. Ethnopharmacol.* 91, 361–365. doi: 10.1016/j.jep.2004.01.016

Dkhar, P., and Sharma, R. (2010). Effect of dimethylsulphoxide and curcumin on protein carbonyls and reactive oxygen species of cerebral hemispheres of mice as a function of age. *Int. J. Dev. Neurosci.* 28, 351–357. doi: 10.1016/j.ijdevneu.2010.04.005

Doggui, S., Belkacemi, A., Paka, G. D., Perrotte, M., Pi, R., and Ramassamy, C. (2013). Curcumin protects neuronal-like cells against acrolein by restoring Akt and redox signaling pathways. *Mol. Nutr. Food Res.* 57, 1660–1670. doi: 10.1002/mnfr.201300130

Dolgin, E. (2016). How to defeat dementia. *Nature* 539, 156–158. doi: 10.1038/539156a

Domoráková, I., Burda, J., Mechírová, E., and Feriková, M. (2006). Mapping of rat hippocampal neurons with NeuN after ischemia/reperfusion and *Ginkgo biloba* extract (EGb 761) pretreatment. *Cell. Mol. Neurobiol.* 26, 1191–1202. doi: 10.1007/s10571-006-9080-6

Dong, S., Zeng, Q., Mitchell, E. S., Xiu, J., Duan, Y., Li, C., et al. (2012). Curcumin enhances neurogenesis and cognition in aged rats: implications for transcriptional interactions related to growth and synaptic plasticity. *PLoS ONE* 7:e31211. doi: 10.1371/journal.pone.0031211

Doody, R. S., Stevens, J. C., Beck, C., Dubinsky, R. M., Kaye, J. A., Gwyther, L., et al. (2001). Practice parameter: management of dementia (an evidence-based review) Report of the Quality Standards Subcommittee of the American Academy of Neurology. *Neurology* 56, 1154–1166. doi: 10.1212/WNL.56.9.1154

Dragicevic, N., Smith, A., Lin, X., Yuan, F., Copes, N., Delic, V., et al. (2011). Green tea epigallocatechin-3-gallate (EGCG) and other flavonoids reduce Alzheimer's amyloid-induced mitochondrial dysfunction. *J. Alzheimers. Dis.* 26, 507–521. doi: 10.3233/JAD-2011-101629

Dringen, R. (2000). Metabolism and functions of glutathione in brain. *Prog. Neurobiol.* 62, 649–671. doi: 10.1016/S0301-0082(99)00060-X

Duke, J. A., and Ayensu, E. S. (1985). *Medicinal Plants of China*. Algonac: Reference Publications.

Eckert, A., Keil, U., Scherping, I., Hauptmann, S., and Muller, W. E. (2005). Stabilization of mitochondrial membrane potential and improvement of neuronal energy metabolism by *Ginkgo biloba* extract EGb 761. *Ann. N.Y. Acad. Sci.* 1056, 474–485. doi: 10.1196/annals.1352.023

Eckert, G. P., Schiborr, C., Hagl, S., Abdel-Kader, R., Muller, W. E., Rimbach, G., et al. (2013). Curcumin prevents mitochondrial dysfunction in the brain of the senescence-accelerated mouse-prone 8. *Neurochem. Int.* 62, 595–602. doi: 10.1016/j.neuint.2013.02.014

Egashira, N., Hayakawa, K., Osajima, M., Mishima, K., Iwasaki, K., Oishi, R., et al. (2007). Involvement of GABA(A) receptors in the neuroprotective effect of theanine on focal cerebral ischemia in mice. *J. Pharmacol. Sci.* 105, 211–214. doi: 10.1254/jphs.SCZ070901

Egashira, N., Ishigami, N., Pu, F., Mishima, K., Iwasaki, K., Orito, K., et al. (2008). Theanine prevents memory impairment induced by repeated cerebral ischemia in rats. *Phytother. Res.* 22, 65–68. doi: 10.1002/ptr.2261

Ezoulin, M. J. M., Ombetta, J.-E., Dutertre-Catella, H., Warnet, J.-M., and Massicot, F. (2008). Antioxidative properties of galantamine on neuronal damage induced by hydrogen peroxide in SK-N-SH cells. *Neurotoxicology* 29, 270–277. doi: 10.1016/j.neuro.2007.11.004

Farkas, E., and Luiten, P. G. (2001). Cerebral microvascular pathology in aging and Alzheimer's disease. *Prog. Neurobiol.* 64, 575–611. doi: 10.1016/S0301-0082(00)00068-X

Fatumbi, P. V. P. (1995). *Ewé: The Use of Plants in Yoruba Society*. Salvador: Oderbrecht.

Favaloro, B., Allocati, N., Graziano, V., Di Ilio, C., and De Laurenzi, V. (2012). Role of Apoptosis in disease. *Aging (Albany NY)* 4, 330–349. doi: 10.18632/aging.100459

Finkler, K. (1985). *Spiritualist Healers in Mexico: Successes and Failures of Alternative Therapeutics*. Salem, WI: Praeger Publishers.

Fox, C., Crugel, M., Maidment, I., Auestad, B. H., Coulton, S., Treloar, A., et al. (2012). Efficacy of memantine for agitation in Alzheimer's dementia: a randomised double-blind placebo controlled trial. *PLoS ONE* 7:e35185. doi: 10.1371/journal.pone.0035185

Franzblau, M., Gonzales-Portillo, C., Gonzales-Portillo, G. S., Diamandis, T., Borlongan, M. C., Tajiri, N., et al. (2013). Vascular damage: a persisting pathology common to Alzheimer's disease and traumatic brain injury. *Med. Hypotheses* 81, 842–845. doi: 10.1016/j.mehy.2013.09.012

Fuchs, L. (1543). *Kräuterbuch. Michael Isingrin*. Basel.

Gao, H.-M., Zhou, H., and Hong, J.-S. (2014). "Oxidative stress, neuroinflammation, and neurodegeneration," in *Neuroinflammation, and Neurodegeneration*, eds P. K. Peterson and M. Toborek (New York, NY: Springer New York), 81–104.

Gate, D., Rezai-Zadeh, K., Jodry, D., Rentsendorj, A., and Town, T. (2010). Macrophages in Alzheimer's disease: the blood-borne identity. *J. Neural Transm.* 117, 961–970. doi: 10.1007/s00702-010-0422-7

Geeganage, C., Wilcox, R., and Bath, P. M. W. (2010). Triple antiplatelet therapy for preventing vascular events: a systematic review and meta-analysis. *BMC Med.* 8:36. doi: 10.1186/1741-7015-8-36

Giacobini, E. (2004). Cholinesterase inhibitors: new roles and therapeutic alternatives. *Pharmacol. Res.* 50, 433–440. doi: 10.1016/j.phrs.2003.11.017

Giri, M., Zhang, M., and Lu, Y. (2016). Genes associated with Alzheimer's disease: an overview and current status. *Clin. Interv. Aging* 11, 665–681. doi: 10.2147/CIA.S105769

Goenka, P., Sarawgi, A., Karun, V., Nigam, A. G., Dutta, S., and Marwah, N. (2013). Camellia sinensis (Tea): implications and role in preventing dental decay. *Pharmacogn. Rev.* 7, 152–156. doi: 10.4103/0973-7847.120515

Gómez-Sámano, M. Á., Grajales-Gómez, M., Zuarth-Vázquez, J. M., Navarro-Flores, M. F., Martínez-Saavedra, M., Juárez-León, Ó. A., et al. (2017). Fibroblast growth factor 21 and its novel association with oxidative stress. *Redox Biol.* 11, 335–341. doi: 10.1016/j.redox.2016.12.024

González Ayala, J. C. (1994). *Botánica Medicinal Popular: Etnobotánica Medicinal de El Salvador*. Jardín Botànico La Laguna.

Grand, J. H., Caspar, S., and Macdonald, S. W. (2011). Clinical features and multidisciplinary approaches to dementia care. *J Multidiscip Heal.* 2011, 125–147. doi: 10.2147/JMDH.S17773

Guan, R., Zhao, Y., Zhang, H., Fan, G., Liu, X., Zhou, W., et al. (2016). Draft genome of the living fossil *Ginkgo biloba*. *Gigascience* 5, 49. doi: 10.1186/s13742-016-0154-1

Gurib-Fakim, A. (2006). Medicinal plants: traditions of yesterday and drugs of tomorrow. *Mol. Aspects Med.* 27, 1–93. doi: 10.1016/j.mam.2005.07.008

Hajnoczky, G., Davies, E., and Madesh, M. (2003). Calcium signaling and apoptosis. *Biochem. Biophys. Res. Commun.* 304, 445–454. doi: 10.1016/S0006-291X(03)00616-8

Hardy, J. A., and Higgins, G. A. (1992). Alzheimer's disease: the amyloid cascade hypothesis. *Science (*256, 184.

Haskell, C. F., Kennedy, D. O., Milne, A. L., Wesnes, K. A., and Scholey, A. B. (2008). The effects of L-theanine, caffeine and their combination on cognition and mood. *Biol. Psychol.* 77, 113–122. doi: 10.1016/j.biopsycho.2007.09.008

Heim, C., Khan, M. A., Motsch, B., Gocht, A., Ramsperger-Gleixner, M., Stamminger, T., et al. (2017). microvascular integrity can be preserved by anti-platelet therapy and in combination with mTOR inhibitor. *J. Hear. Lung Transplant.* 36, S376. doi: 10.1016/j.healun.2017.01.1069

Hikino, H. (1985). Recent research on oriental medicinal plants. *Econ. Med. Plant. Res.* 1, 53–85.

Hoppe, J. B., Coradini, K., Frozza, R. L., Oliveira, C. M., Meneghetti, A. B., Bernardi, A., et al. (2013a). Free and nanoencapsulated curcumin suppress

beta-amyloid-induced cognitive impairments in rats: involvement of BDNF and Akt/GSK-3beta signaling pathway. *Neurobiol. Learn. Mem.* 106, 134–144. doi: 10.1016/j.nlm.2013.08.001

Hoppe, J. B., Haag, M., Whalley, B. J., Salbego, C. G., and Cimarosti, H. (2013b). Curcumin protects organotypic hippocampal slice cultures from Abeta1-42-induced synaptic toxicity. *Toxicol. In Vitro* 27, 2325–2330. doi: 10.1016/j.tiv.2013.10.002

Howard, R. J., Juszczak, E., Ballard, C. G., Bentham, P., Brown, R. G., Bullock, R., et al. (2007). Donepezil for the treatment of agitation in Alzheimer's disease. *N. Engl. J. Med.* 357, 1382–1392. doi: 10.1056/NEJMoa066583

Howes, M.-J. R., and Houghton, P. J. (2003). Plants used in Chinese and Indian traditional medicine for improvement of memory and cognitive function. *Pharmacol. Biochem. Behav.* 75, 513–527. doi: 10.1016/S0091-3057(03)00128-X

Howes, M.-J. R., and Perry, E. (2011). The role of phytochemicals in the treatment and prevention of dementia. *Drugs Aging* 28, 439–468. doi: 10.2165/11591310-000000000-00000

Howes, M. R., Perry, N. S. L., and Houghton, P. J. (2003). Plants with traditional uses and activities, relevant to the management of Alzheimer's disease and other cognitive disorders. *Phyther. Res.* 17, 1–18. doi: 10.1002/ptr.1280

Huang, H.-C., Tang, D., Xu, K., and Jiang, Z.-F. (2014). Curcumin attenuates amyloid-beta-induced tau hyperphosphorylation in human neuroblastoma SH-SY5Y cells involving PTEN/Akt/GSK-3beta signaling pathway. *J. Recept. Signal Transduct. Res.* 34, 26–37. doi: 10.3109/10799893.2013.848891

Hügel, H. M., and Jackson, N. (2015). Polyphenols for the prevention and treatment of dementia diseases. *Neural Regen. Res.* 10, 1756–1758. doi: 10.4103/1673-5374.169609

Huminiecki, L., Horbanczuk, J., and Atanasov, A. G. (2017). The functional genomic studies of curcumin. *Semin. Cancer Biol.* 46, 107–118. doi: 10.1016/j.semcancer.2017.04.002

Hung, C. H.-L., Cheng, S. S.-Y., Cheung, Y.-T., Wuwongse, S., Zhang, N. Q., Ho, Y.-S., et al. (2018). A reciprocal relationship between reactive oxygen species and mitochondrial dynamics in neurodegeneration. *Redox Biol.* 14, 7–19. doi: 10.1016/j.redox.2017.08.010

Hurd, M. D., Martorell, P., and Langa, K. M. (2013). Monetary costs of dementia in the United States. *N. Engl. J. Med.* 369, 489–490. doi: 10.1056/NEJMc1305541

Iadecola, C. (2013). The pathobiology of vascular dementia. *Neuron* 80, 844–866. doi: 10.1016/j.neuron.2013.10.008

IARC Working Group (2016). *Some Drugs and Herbal Products*. Lyon: Ginkgo Biloba. International Agency for Research and Cancer (IARC) Monographs, WHO.

Ibrahim, F., Knight, S. R., and Cramer, R. L. (2012). Addressing the controversial use of antipsychotic drugs for behavioral and psychological symptoms of dementia. *J. Pharm. Technol.* 28, 3–9. doi: 10.1177/875512251202800102

Ihl, R., Tribanek, M., and Bachinskaya, N. (2012). Efficacy and tolerability of a once daily formulation of *Ginkgo biloba* extract EGb 761(R) in Alzheimer's disease and vascular dementia: results from a randomised controlled trial. *Pharmacopsychiatry* 45, 41–46. doi: 10.1055/s-0031-1291217

Ikarashi, Y., and Mizoguchi, K. (2016). Neuropharmacological efficacy of the traditional Japanese Kampo medicine yokukansan and its active ingredients. *Pharmacol. Ther.* 166, 84–95. doi: 10.1016/j.pharmthera.2016.06.018

Iqbal, K., Liu, F., and Gong, C.-X. (2016). Tau and neurodegenerative disease: the story so far. *Nat. Rev. Neurol.* 12, 15–27. doi: 10.1038/nrneurol.2015.225

Iqbal, K., Liu, F., Gong, C.-X., and Grundke-Iqbal, I. (2010). Tau in Alzheimer disease and related tauopathies. *Curr. Alzheimer Res.* 7, 656–664. doi: 10.2174/156720510793611592

Isah, T. (2015). Rethinking *Ginkgo biloba* L.: medicinal uses and conservation. *Pharmacogn. Rev.* 9, 140–148. doi: 10.4103/0973-7847.162137

Izzo, A. A. (2012). Interactions between herbs and conventional drugs: overview of the clinical data. *Med. Princ. Pract.* 21, 404–428. doi: 10.1159/000334488

Jahanshahi, M., Nickmahzar, E. G., and Babakordi, F. (2013). Effect of Gingko biloba extract on scopolamine-induced apoptosis in the hippocampus of rats. *Anat. Sci. Int.* 88, 217–222. doi: 10.1007/s12565-013-0188-8

Jahanshahi, M., Nikmahzar, E., Yadollahi, N., and Ramazani, K. (2012). Protective effects of *Ginkgo biloba* extract (EGB 761) on astrocytes of rat hippocampus after exposure with scopolamine. *Anat. Cell Biol.* 45, 92–96. doi: 10.5115/acb.2012.45.2.92

Jelenkovic, A., Jovanovic, M. D., Stevanovic, I., Petronijevic, N., Bokonjic, D., Zivkovic, J., et al. (2014). Influence of the green tea leaf extract on neurotoxicity of aluminium chloride in rats. *Phytother. Res.* 28, 82–87. doi: 10.1002/ptr.4962

Ju, H. S., Li, X. J., Zhao, B. L., Han, Z. W., and Xin, W. J. (1989). Effects of glycyrrhiza flavonoid on lipid peroxidation and active oxygen radicals. *Yao Xue Xue Bao* 24, 807–812.

Kanno, H., Kawakami, Z., Tabuchi, M., Mizoguchi, K., Ikarashi, Y., and Kase, Y. (2015). Protective effects of glycycoumarin and procyanidin B1, active components of traditional Japanese medicine yokukansan, on amyloid beta oligomer-induced neuronal death. *J. Ethnopharmacol.* 159, 122–128. doi: 10.1016/j.jep.2014.10.058

Kanowski, S., Herrmann, W. M., Stephan, K., Wierich, W., and Horr, R. (1996). Proof of efficacy of the *Ginkgo biloba* special extract EGb 761 in outpatients suffering from mild to moderate primary degenerative dementia of the Alzheimer type or multi-infarct dementia. *Pharmacopsychiatry* 29, 47–56. doi: 10.1055/s-2007-979544

Katsel, P., Tan, W., Fam, P., Purohit, D. P., and Haroutunian, V. (2013). Cell cycle checkpoint abnormalities during dementia: a plausible association with the loss of protection against oxidative stress in Alzheimer's disease [corrected]. *PLoS ONE* 8:e68361. doi: 10.1371/journal.pone.0068361

Kaur, U., Banerjee, P., Bir, A., Sinha, M., Biswas, A., and Chakrabarti, S. (2015). Reactive oxygen species, redox signaling and neuroinflammation in Alzheimer's disease: the NF-kappaB connection. *Curr. Top. Med. Chem.* 15, 446–457. doi: 10.2174/1568026615666150114160543

Kihara, T., and Shimohama, S. (2004). Alzheimer's disease and acetylcholine receptors. *Acta Neurobiol. Exp. (Wars).* 64, 99–105.

Kim, J. M., Ryou, S. H., Kang, Y. H., and Kang, J. S. (2011). Effect of *Ginkgo biloba* leaf powder and extract on plasma and liver lipids, platelet aggregation and erythrocyte Na+ efflux in rats fed hypercholesterolemic diet. *FASEB J.* 25, 980–988.

Kim, J., Shim, J., Lee, S., Cho, W.-H., Hong, E., Lee, J. H., et al. (2016). Rg3-enriched ginseng extract ameliorates scopolamine-induced learning deficits in mice. *BMC Complement. Altern. Med.* 16:66. doi: 10.1186/s12906-016-1050-z

Kim, M.-S., Lee, J.-I., Lee, W.-Y., and Kim, S.-E. (2004). Neuroprotective effect of *Ginkgo biloba* L. extract in a rat model of Parkinson's disease. *Phytother. Res.* 18, 663–666. doi: 10.1002/ptr.1486

Kim, T. I., Lee, Y. K., Park, S. G., Choi, I. S., Ban, J. O., Park, H. K., et al. (2009). l-Theanine, an amino acid in green tea, attenuates beta-amyloid-induced cognitive dysfunction and neurotoxicity: reduction in oxidative damage and inactivation of ERK/p38 kinase and NF-kappaB pathways. *Free Radic. Biol. Med.* 47, 1601–1610. doi: 10.1016/j.freeradbiomed.2009.09.008

Kim, Y. C., Kim, S. R., Markelonis, G. J., and Oh, T. H. (1998). Ginsenosides Rb1 and Rg3 protect cultured rat cortical cells from glutamate-induced neurodegeneration. *J. Neurosci. Res.* 53, 426–432.

Kimura, K., Ozeki, M., Juneja, L. R., and Ohira, H. (2007). L-Theanine reduces psychological and physiological stress responses. *Biol. Psychol.* 74, 39–45. doi: 10.1016/j.biopsycho.2006.06.006

Knapp, M., Prince, M., Albanese, E., Banerjee, S., Dhanasiri, S., and Fernandez, J. L. (2007). *Dementia UK: The Full Report*. London: Alzheimer's Society.

Koola, M. M., Buchanan, R. W., Pillai, A., Aitchison, K. J., Weinberger, D. R., Aaronson, S. T., et al. (2014). Potential role of the combination of galantamine and memantine to improve cognition in schizophrenia. *Schizophr. Res.* 157, 84–89. doi: 10.1016/j.schres.2014.04.037

Kumar, A., Prakash, A., and Pahwa, D. (2011). Galantamine potentiates the protective effect of rofecoxib and caffeic acid against intrahippocampal Kainic acid-induced cognitive dysfunction in rat. *Brain Res. Bull.* 85, 158–168. doi: 10.1016/j.brainresbull.2011.03.010

Kumar, A., and Singh, A. (2015). A review on mitochondrial restorative mechanism of antioxidants in Alzheimer's disease and other neurological conditions. *Front. Pharmacol.* 6:206. doi: 10.3389/fphar.2015.00206

LeBlanc, A. C. (2005). The role of apoptotic pathways in Alzheimer's disease neurodegeneration and cell death. *Curr. Alzheimer Res.* 2, 389–402. doi: 10.2174/156720505774330573

Lee, J., Kim, Y., Liu, T., Hwang, Y. J., Hyeon, S. J., Im, H., et al. (2017). SIRT3 deregulation is linked to mitochondrial dysfunction in Alzheimer's disease. *Aging Cell*. doi: 10.1111/acel.12679. [Epub ahead of print].

Lee, T.-K., Johnke, R. M., Allison, R. R., O'Brien, K. F., and Dobbs, L. J. J. (2005). Radioprotective potential of ginseng. *Mutagenesis* 20, 237–243. doi: 10.1093/mutage/gei041

Li, W., Chu, Y., Zhang, L., Yin, L., and Li, L. (2012). Ginsenoside Rg1 attenuates tau phosphorylation in SK-N-SH induced by Abeta-stimulated THP-1 supernatant and the involvement of p38 pathway activation. *Life Sci.* 91, 809–815. doi: 10.1016/j.lfs.2012.08.028

Lilienfeld, S. (2002). Galantamine–a novel cholinergic drug with a unique dual mode of action for the treatment of patients with Alzheimer's disease. *CNS Drug Rev.* 8, 159–176. doi: 10.1111/j.1527-3458.2002.tb00221.x

Lim, S. L., Rodriguez-Ortiz, C. J., and Kitazawa, M. (2015). Infection, systemic inflammation, and Alzheimer's disease. *Microbes Infect.* 17, 549–556. doi: 10.1016/j.micinf.2015.04.004

Lin, M. T., and Beal, M. F. (2006). Mitochondrial dysfunction and oxidative stress in neurodegenerative diseases. *Nature* 443, 787–795. doi: 10.1038/nature05292

Liu, C.-C., Liu, C.-C., Kanekiyo, T., Xu, H., and Bu, G. (2013). Apolipoprotein E and Alzheimer disease: risk, mechanisms and therapy. *Nat. Rev. Neurol.* 9, 106–118. doi: 10.1038/nrneurol.2012.263

Liu, X., Xu, K., Yan, M., Wang, Y., and Zheng, X. (2010). Protective effects of galantamine against Aβ-induced PC12 cell apoptosis by preventing mitochondrial dysfunction and endoplasmic reticulum stress. *Neurochem. Int.* 57, 588–599. doi: 10.1016/j.neuint.2010.07.007

Long, F., Yang, H., Xu, Y., Hao, H., and Li, P. (2015). A strategy for the identification of combinatorial bioactive compounds contributing to the holistic effect of herbal medicines. *Sci. Rep.* 5:12361. doi: 10.1038/srep12361

Lonicerus, A. (1679). *Kräuterbuch, Matthias Wagner*. Ulm.

Loy, C., and Schneider, L. (2006). Galantamine for Alzheimer's disease and mild cognitive impairment. *Cochrane database Syst. Rev.* 25:CD001747. doi: 10.1002/14651858.CD001747.pub3

Luengo-Fernandez, R., Leal, J., and Gray, A. (2010). *Dementia 2010: The Economic Burden of Dementia and Associated Research Funding in the United Kingdom*. Oxford: Cambridge Alzheimer's Research Trust.

Ma, B., Meng, X., Wang, J., Sun, J., Ren, X., Qin, M., et al. (2014). Notoginsenoside R1 attenuates amyloid-beta-induced damage in neurons by inhibiting reactive oxygen species and modulating MAPK activation. *Int. Immunopharmacol.* 22, 151–159. doi: 10.1016/j.intimp.2014.06.018

Mahley, R. W., and Rall, S. C. Jr. (2000). Apolipoprotein E: far more than a lipid transport protein. *Annu. Rev. Genomics Hum. Genet.* 1, 507–537. doi: 10.1146/annurev.genom.1.1.507

Mahmood, T., Akhtar, N., and Khan, B. A. (2010). The morphology, characteristics, and medicinal properties of Camellia sinensis tea. *J. Med. Plants Res.* 4, 2028–2033. doi: 10.5897/JMPR10.010

Mandel, S. A., Amit, T., Weinreb, O., and Youdim, M. B. H. (2011). Understanding the broad-spectrum neuroprotective action profile of green tea polyphenols in aging and neurodegenerative diseases. *J. Alzheimers. Dis.* 25, 187–208. doi: 10.3233/JAD-2011-101803

Mantle, D., Pickering, A. T., and Perry, E. K. (2000). Medicinal plant extracts for the treatment of dementia. *CNS Drugs* 13, 201–213. doi: 10.2165/00023210-200013030-00006

Manyam, B., V (1999). Dementia in ayurveda. *J. Altern. Complement. Med.* 5, 81–88. doi: 10.1089/acm.1999.5.81

McKhann, G. M., Albert, M. S., Grossman, M., Miller, B., Dickson, D., and Trojanowski, J. Q. (2001). Clinical and pathological diagnosis of frontotemporal dementia: report of the Work Group on Frontotemporal Dementia and Pick's Disease. *Arch. Neurol.* 58, 1803–1809. doi: 10.1001/archneur.58.11.1803

Mehan, S., Sharma, D., Sharma, G., Arora, R., and Sehgal, V. (2012). *Dementia-A Complete Literature Review on Various Mechanisms Involves in Pathogenesis and an Intracerebroventricular Streptozotocin Induced Alzheimer's Disease*. INTECH Open Access Publisher. Available online at: http://www.intechopen.com/books/inflammatory-diseases-immunopathology-clinical-and-pharmacologicalbases/alzheimer-s-disease-an-updated-review-on-pathogenesis-and-intracerebroventricular-streptozotocin-ind

Miao, Y., Zhao, S., Gao, Y., Wang, R., Wu, Q., Wu, H., et al. (2016). Curcumin pretreatment attenuates inflammation and mitochondrial dysfunction in experimental stroke: the possible role of Sirt1 signaling. *Brain Res. Bull.* 121, 9–15. doi: 10.1016/j.brainresbull.2015.11.019

Mills, S. Y. (1991). *Out of the Earth: The Essential Book of Herbal Medicine*. London: Viking.

Mishra, S., and Palanivelu, K. (2008). The effect of curcumin (turmeric) on Alzheimer's disease: an overview. *Ann. Indian Acad. Neurol.* 11, 13–19. doi: 10.4103/0972-2327.40220

Misra, R. (1998). Modern drug development from traditional medicinal plants using radioligand receptor-binding assays. *Med. Res. Rev.* 18, 383–402.

Monsch, A. U., and Giannakopoulos, P. (2004). Effects of galantamine on behavioural and psychological disturbances and caregiver burden in patients with Alzheimer's disease. *Curr. Med. Res. Opin.* 20, 931–938. doi: 10.1185/030079904125003890

Moreira, P. I., Carvalho, C., Zhu, X., Smith, M. A., and Perry, G. (2010). Mitochondrial dysfunction is a trigger of Alzheimer's disease pathophysiology. *Biochim. Biophys. Acta* 1802, 2–10. doi: 10.1016/j.bbadis.2009.10.006

Müller-Ebeling, C., and Rätsch, C. (1989). *Heilpflanzen der Seychellen.VWB-Verlag für Wissenschaft und Bildung*. Berlin.

Nah, S.-Y. (2014). Ginseng ginsenoside pharmacology in the nervous system: involvement in the regulation of ion channels and receptors. *Front. Physiol.* 5:98. doi: 10.3389/fphys.2014.00098

Namanja, H. A., Emmert, D., Pires, M. M., Hrycyna, C. A., and Chmielewski, J. (2009). Inhibition of human P-glycoprotein transport and substrate binding using a galantamine dimer. *Biochem. Biophys. Res. Commun.* 388, 672–676. doi: 10.1016/j.bbrc.2009.08.056

Napryeyenko, O., Sonnik, G., and Tartakovsky, I. (2009). Efficacy and tolerability of *Ginkgo biloba* extract EGb 761 by type of dementia: analyses of a randomised controlled trial. *J. Neurol. Sci.* 283, 224–229. doi: 10.1016/j.jns.2009.02.353

Narlawar, R., Pickhardt, M., Leuchtenberger, S., Baumann, K., Krause, S., Dyrks, T., et al. (2008). Curcumin-derived pyrazoles and isoxazoles: swiss army knives or blunt tools for Alzheimer's disease? *ChemMedChem* 3, 165–172. doi: 10.1002/cmdc.200700218

Navia, B. A., and Rostasy, K. (2005). The AIDS dementia complex: clinical and basic neuroscience with implications for novel molecular therapies. *Neurotox. Res.* 8, 3–24. doi: 10.1007/BF03033817

Ng, T.-P., Chiam, P.-C., Lee, T., Chua, H.-C., Lim, L., and Kua, E.-H. (2006). Curry consumption and cognitive function in the elderly. *Am. J. Epidemiol.* 164, 898–906. doi: 10.1093/aje/kwj267

Ng, Y. P., Or, T. C. T., and Ip, N. Y. (2015). Plant alkaloids as drug leads for Alzheimer's disease. *Neurochem. Int.* 89, 260–270. doi: 10.1016/j.neuint.2015.07.018

Ngan, F., Shaw, P., But, P., and Wang, J. (1999). Molecular authentication of Panax species. *Phytochemistry* 50, 787–791. doi: 10.1016/S0031-9422(98)00606-2

Niikura, T., Tajima, H., and Kita, Y. (2006). Neuronal cell death in Alzheimer's disease and a neuroprotective factor, humanin. *Curr. Neuropharmacol.* 4, 139–147. doi: 10.2174/157015906776359577

Nimmrich, V., and Eckert, A. (2013). Calcium channel blockers and dementia. *Br. J. Pharmacol.* 169, 1203–1210. doi: 10.1111/bph.12240

Nishida, K., Yasuda, E., Nagasawa, K., and Fujimoto, S. (2008). Altered levels of oxidation and phospholipase C isozyme expression in the brains of theanine-administered rats. *Biol. Pharm. Bull.* 31, 857–860. doi: 10.1248/bpb.31.857

Nishiyama, N., Chu, P. J., and Saito, H. (1995). Beneficial effects of Biota, a traditional Chinese herbal medicine on learning impairment induced by basal forebrain-lesion in mice. *Biol. Pharm. Bull.* 28, 1513–1517.

Olin, J., and Schneider, L. (2002). Galantamine for Alzheimer's disease. *Cochrane database Syst. Rev.* 3:CD001747. doi: 10.1002/14651858.CD001747

Ortiz de Montellano, B. R. (1990). *Aztec Medicine, Health and Nutrition*. New Brunswick: Rutgers University Press.

Owen, G. N., Parnell, H., De Bruin, E. A., and Rycroft, J. A. (2008). The combined effects of L-theanine and caffeine on cognitive performance and mood. *Nutr. Neurosci.* 11, 193–198. doi: 10.1179/147683008X301513

Paganelli, R. A., Benetoli, A., and Milani, H. (2006). Sustained neuroprotection and facilitation of behavioral recovery by the *Ginkgo biloba* extract, EGb 761, after transient forebrain ischemia in rats. *Behav. Brain Res.* 174, 70–77. doi: 10.1016/j.bbr.2006.07.005

Parle, M., Dhingra, D., and Kulkarni, S. K. (2004). Memory-strengthening activity of Glycyrrhiza glabra in exteroceptive and interoceptive behavioral models. *J. Med. Food* 7, 462–466. doi: 10.1089/jmf.2004.7.462

Pasqualetti, G., Brooks, D. J., and Edison, P. (2015). The role of neuroinflammation in dementias. *Curr. Neurol. Neurosci. Rep.* 15:17. doi: 10.1007/s11910-015-0531-7

Pastor, P., Roe, C. M., Villegas, A., Bedoya, G., Chakraverty, S., Garcia, G., et al. (2003). Apolipoprotein Eepsilon4 modifies Alzheimer's disease onset in an E280A PS1 kindred. *Ann. Neurol.* 54, 163–169. doi: 10.1002/ana.10636

Pathak, L., Agrawal, Y., and Dhir, A. (2013). Natural polyphenols in the management of major depression. *Expert Opin. Investig. Drugs* 22, 863–880. doi: 10.1517/13543784.2013.794783

Perry, E., and Howes, M. R. (2011). Medicinal plants and dementia therapy: herbal hopes for brain aging? *CNS Neurosci. Ther.* 17, 683–698. doi: 10.1111/j.1755-5949.2010.00202.x

Perry, E. K., Pickering, A. T., Wang, W. W., Houghton, P., and Perry, N. S. L. (1998). Medicinal plants and Alzheimer's disease: integrating ethnobotanical and contemporary scientific evidence. *J. Altern. Complement. Med.* 4, 419–428.

Pohl, S., Zobel, J., and Moffat, A. (2010). "Extended boolean retrieval for systematic biomedical reviews," in *Proceedings of the Thirty-Third Australasian Conferenc on Computer Science - Volume 102* ACSC'10. (Darlinghurst, NSW: Australian Computer Society, Inc.), 117–126. Available online at: http://dl.acm.org/citation.cfm?id=1862199.1862212

Popovich, D. G., and Kitts, D. D. (2004). Generation of ginsenosides Rg3 and Rh2 from North American ginseng. *Phytochemistry* 65, 337–344. doi: 10.1016/j.phytochem.2003.11.020

Power, M. C., Adar, S. D., Yanosky, J. D., and Weuve, J. (2016). Exposure to air pollution as a potential contributor to cognitive function, cognitive decline, brain imaging, and dementia: a systematic review of epidemiologic research. *Neurotoxicology* 56, 235–253. doi: 10.1016/j.neuro.2016.06.004

Price, S., and Price, L. (1995). *Aromatherapy for Health Professionals*. Edinburgh: Churchill Livingston.

Prince, M., Comas-Herrera, A., Knapp, M., Guerchet, M., and Karagiannidou, M. (2016). *World Alzheimer Report 2016: Improving Healthcare for People Living with Dementia: Coverage, Quality and Costs Now and in the Future*. London: Personal Social Services Research Unit; London School of Economics and Political Science.

Qiao, X., Ji, S., Yu, S.-W., Lin, X.-H., Jin, H.-W., Duan, Y.-K., et al. (2014). Identification of key licorice constituents which interact with cytochrome P450: evaluation by LC/MS/MS cocktail assay and metabolic profiling. *AAPS J.* 16, 101–113. doi: 10.1208/s12248-013-9544-9

Qiu, C., Kivipelto, M., and von Strauss, E. (2009). Epidemiology of Alzheimer's disease: occurrence, determinants, and strategies toward intervention. *Dialogues Clin. Neurosci.* 11, 111–128.

Quaglio, G., Brand, H., and Dario, C. (2016). Fighting dementia in Europe: the time to act is now. *Lancet Neurol.* 15, 452–454. doi: 10.1016/S1474-4422(16)00079-X

Rabinovici, G. D., and Miller, B. L. (2010). Frontotemporal lobar degeneration: epidemiology, pathophysiology, diagnosis and management. *CNS Drugs* 24, 375–398. doi: 10.2165/11533100-000000000-00000

Raina, A. K., Zhu, X., Rottkamp, C. A., Monteiro, M., Takeda, A., and Smith, M. A. (2000). Cyclin' toward dementia: cell cycle abnormalities and abortive oncogenesis in Alzheimer disease. *J. Neurosci. Res.* 61, 128–133. doi: 10.1002/1097-4547(20000715)61:2<128::AID-JNR2>3.0.CO;2-H

Ramkumar, M., Rajasankar, S., Gobi, V. V., Dhanalakshmi, C., Manivasagam, T., Justin Thenmozhi, A., et al. (2017). Neuroprotective effect of Demethoxycurcumin, a natural derivative of Curcumin on rotenone induced neurotoxicity in SH-SY 5Y Neuroblastoma cells. *BMC Complement. Altern. Med.* 17, 217. doi: 10.1186/s12906-017-1720-5

Rastogi, M., Ojha, R. P., Sagar, C., Agrawal, A., and Dubey, G. P. (2014). Protective effect of curcuminoids on age-related mitochondrial impairment in female Wistar rat brain. *Biogerontology* 15, 21–31. doi: 10.1007/s10522-013-9466-z

Reddy, A. P., and Reddy, P. H. (2017). mitochondria-targeted molecules as potential drugs to treat patients with Alzheimer's disease. *Prog. Mol. Biol. Transl. Sci.* 146, 173–201. doi: 10.1016/bs.pmbts.2016.12.010

Rezai-Zadeh, K., Arendash, G. W., Hou, H., Fernandez, F., Jensen, M., Runfeldt, M., et al. (2008). Green tea epigallocatechin-3-gallate (EGCG) reduces beta-amyloid mediated cognitive impairment and modulates tau pathology in Alzheimer transgenic mice. *Brain Res.* 1214, 177–187. doi: 10.1016/j.brainres.2008.02.107

Rhein, V., Giese, M., Baysang, G., Meier, F., Rao, S., Schulz, K. L., et al. (2010). *Ginkgo biloba* extract ameliorates oxidative phosphorylation performance and rescues abeta-induced failure. *PLoS ONE* 5:e12359. doi: 10.1371/journal.pone.0012359

Ribeiro, M. L., Moreira, L. M., Arcari, D. P., Dos Santos, L. F., Marques, A. C., Pedrazzoli, J. J., et al. (2016). Protective effects of chronic treatment with a standardized extract of *Ginkgo biloba* L. in the prefrontal cortex and dorsal hippocampus of middle-aged rats. *Behav. Brain Res.* 313, 144–150. doi: 10.1016/j.bbr.2016.06.029

Ridley, N. J., Draper, B., and Withall, A. (2013). Alcohol-related dementia: an update of the evidence. *Alzheimers. Res. Ther.* 5, 3. doi: 10.1186/alzrt157

Rivas-Arancibia, S., Hernández-Zimbrón, L. F., Rodríguez-Martínez, E., Borgonio-Pérez, G., Velumani, V., and Durán-Bedolla, J. (2013). Chronic exposure to low doses of ozone produces a state of oxidative stress and blood-brain barrier damage in the hippocampus of rat. *Adv. Biosci. Biotechnol.* 4:24. doi: 10.4236/abb.2013.411A2004

Roeder, B.A. (1988). *Chicano Folk Medicine from Los Angeles*. Berkeley; Los Angeles: CA: University of California Press.

Romero, A., Egea, J., Garcia, A. G., and Lopez, M. G. (2010). Synergistic neuroprotective effect of combined low concentrations of galantamine and melatonin against oxidative stress in SH-SY5Y neuroblastoma cells. *J. Pineal Res.* 49, 141–148. doi: 10.1111/j.1600-079X.2010.00778.x

Ross, I. A. (2001). *Medicinal Plants of the World: Chemical Constituents, Traditional and Modern Medicinal Uses*. New York, NY: Humana Press.

Ruttkay-Nedecky, B., Nejdl, L., Gumulec, J., Zitka, O., Masarik, M., Eckschlager, T., et al. (2013). The role of metallothionein in oxidative stress. *Int. J. Mol. Sci.* 14, 6044–6066. doi: 10.3390/ijms14036044

Saharan, S., and Mandal, P. K. (2014). The emerging role of glutathione in Alzheimer's disease. *J. Alzheimers. Dis.* 40, 519–529. doi: 10.3233/JAD-132483

Sahne, F., Mohammadi, M., Najafpour, G. D., and Moghadamnia, A. A. (2017). Enzyme-assisted ionic liquid extraction of bioactive compound from turmeric (*Curcuma longa* L.): isolation, purification and analysis of curcumin. *Ind. Crops Prod.* 95, 686–694. doi: 10.1016/j.indcrop.2016.11.037

Sama, D. M., and Norris, C. M. (2013). Calcium dysregulation and neuroinflammation: discrete and integrated mechanisms for age-related synaptic dysfunction. *Ageing Res. Rev.* 12, 982–995. doi: 10.1016/j.arr.2013.05.008

Savelev, S. U., Okello, E. J., and Perry, E. K. (2004). Butyryl-and acetyl-cholinesterase inhibitory activities in essential oils of Salvia species and their constituents. *Phyther. Res.* 18, 315–324. doi: 10.1002/ptr.1451

Schultes, R. E. (1993). Plants in treating senile dementia in the Northwest Amazon. *J. Ethnopharmacol.* 38, 121–128. doi: 10.1016/0378-8741(93)90007-R

Schultes, R. E. (1994). *Amazonian Ethnobotany and the Search for New Drugs BT - Ciba Foundation Symposium 185*. Chichester: Wiley.

Schulz, R., McGinnis, K. A., Zhang, S., Martire, L. M., Hebert, R. S., Beach, S. R., et al. (2008). Dementia patient suffering and caregiver depression. *Alzheimer Dis. Assoc. Disord.* 22, 170–176. doi: 10.1097/WAD.0b013e31816653cc

Schwarzkopf, T. M., Koch, K. A., and Klein, J. (2013). Neurodegeneration after transient brain ischemia in aged mice: beneficial effects of bilobalide. *Brain Res.* 1529, 178–187. doi: 10.1016/j.brainres.2013.07.003

Schweitzer de Palacios, D. (1994). *Cambiashun. Las prácticas médicas tradicionales y sus expertos en San Miguel del Común, una comuna indígena en los alrededores de Quito*. Berlin: Holos-Verlag; Free University of Berlin.

Sfikas, G. (1980). *Heilpflanzen Griechenlands. P. Efstathiadis & Söhne AG*. Athen.

Shankar, G. M., and Walsh, D. M. (2009). Alzheimer's disease: synaptic dysfunction and Aβ. *Mol. Neurodegener.* 4:48. doi: 10.1186/1750-1326-4-48

Sirirugsa, P., Larsen, K., and Maknoi, C. (2007). The genus *Curcuma* L.(zingiberaceae): distribution and classification with reference to species diversity in Thailand. *Gard. Bull. Singapore* 59, 203–320.

Solfrizzi, V., and Panza, F. (2015). Plant-based nutraceutical interventions against cognitive impairment and dementia: meta-analytic evidence of efficacy of a standardized Gingko biloba extract. *J. Alzheimers. Dis.* 43, 605–611. doi: 10.3233/JAD-141887

Song, L., Xu, M.-B., Zhou, X.-L., Zhang, D.-P., Zhang, S.-L., and Zheng, G.-Q. (2017). A Preclinical systematic review of ginsenoside-Rg1 in experimental Parkinson's disease. *Oxid. Med. Cell. Longev.* 2017:2163053. doi: 10.1155/2017/2163053

Spano, M., Signorelli, M., Vitaliani, R., Aguglia, E., and Giometto, B. (2015). The possible involvement of mitochondrial dysfunctions in

Lewy body dementia: a systematic review. *Funct. Neurol.* 30, 151–158. doi: 10.11138/FNeur/2015.30.3.151

Stackman, R. W., Eckenstein, F., Frei, B., Kulhanek, D., Nowlin, J., and Quinn, J. F. (2003). Prevention of age-related spatial memory deficits in a transgenic mouse model of Alzheimer's disease by chronic *Ginkgo biloba* treatment. *Exp. Neurol.* 184, 510–520. doi: 10.1016/S0014-4886(03)00399-6

Stafford, G. I., Pedersen, M. E., van Staden, J., and Jäger, A. K. (2008). Review on plants with CNS-effects used in traditional South African medicine against mental diseases. *J. Ethnopharmacol.* 119, 513–537. doi: 10.1016/j.jep.2008.08.010

Sun, M., Ye, Y., Xiao, L., Duan, X., Zhang, Y., and Zhang, H. (2017). Anticancer effects of ginsenoside Rg3 (Review). *Int. J. Mol. Med.* 39, 507–518. doi: 10.3892/ijmm.2017.2857

Sun, S., Wang, C.-Z., Tong, R., Li, X.-L., Fishbein, A., Wang, Q., et al. (2010). Effects of steaming the root of Panax notoginseng on chemical composition and anticancer activities. *Food Chem.* 118, 307–314. doi: 10.1016/j.foodchem.2009.04.122

Sun, Z.-K., Yang, H.-Q., and Chen, S.-D. (2013). Traditional Chinese medicine: a promising candidate for the treatment of Alzheimer's disease. *Transl. Neurodegener.* 2:6. doi: 10.1186/2047-9158-2-6

Swerdlow, R. H., Burns, J. M., and Khan, S. M. (2010). The Alzheimer's disease mitochondrial cascade hypothesis. *J. Alzheimers. Dis.* 20(Suppl. 2), S265–S279. doi: 10.3233/JAD-2010-100339

Swerdlow, R. H., Koppel, S., Weidling, I., Hayley, C., Ji, Y., and Wilkins, H. M. (2017). mitochondria, cybrids, aging, and Alzheimer's disease. *Prog. Mol. Biol. Transl. Sci.* 146, 259–302. doi: 10.1016/bs.pmbts.2016.12.017

Tabernaemontanus, D. I. T. (1987). *Kräuterbuch, Johann Ludwig König/Johann Brandmüller*. Basel.

Takuma, K., Hoshina, Y., Arai, S., Himeno, Y., Matsuo, A., Funatsu, Y., et al. (2007). *Ginkgo biloba* extract EGb 761 attenuates hippocampal neuronal loss and cognitive dysfunction resulting from chronic restraint stress in ovariectomized rats. *Neuroscience* 149, 256–262. doi: 10.1016/j.neuroscience.2007.07.042

Tanaka, A., Arai, Y., Kim, S.-N., Ham, J., and Usuki, T. (2011). Synthesis and biological evaluation of bilobol and adipostatin A. *J. Asian Nat. Prod. Res.* 13, 290–296. doi: 10.1080/10286020.2011.554828

Taylor, L. (1998). *Herbal Secrets of the Rainforest: The Healing Power of over 50 Medicinal Plants You Should Know About*. Rocklin, CA: Prima Publishing.

Tayyem, R. F., Heath, D. D., Al-Delaimy, W. K., and Rock, C. L. (2006). Curcumin content of turmeric and curry powders. *Nutr. Cancer* 55, 126–131. doi: 10.1207/s15327914nc5502_2

Tewari, D., Mocan, A., Parvanov, E. D., Sah, A. N., Nabavi, S. M., Huminiecki, L., et al. (2017). Ethnopharmacological approaches for therapy of jaundice: Part II. Highly used plant species from Acanthaceae, Euphorbiaceae, Asteraceae, Combretaceae, and Fabaceae families. *Front. Pharmacol.* 8:519. doi: 10.3389/fphar.2017.00518

Tian, J., Zhang, S., Li, G., Liu, Z., and Xu, B. (2009). 20(S)-ginsenoside Rg3, a neuroprotective agent, inhibits mitochondrial permeability transition pores in rat brain. *Phytother. Res.* 23, 486–491. doi: 10.1002/ptr.2653

Tripathi, M., and Vibha, D. (2009). Reversible dementias. *Indian J. Psychiatry* 51, S52.

Tsvetkova, D., Obreshkova, D., Zheleva-Dimitrova, D., and Saso, L. (2013). Antioxidant activity of galantamine and some of its derivatives. *Curr. Med. Chem.* 20, 4595–4608. doi: 10.2174/09298673113209990148

Tzvetkov, N. T., and Antonov, L. (2017). Subnanomolar indazole-5-carboxamide inhibitors of monoamine oxidase B (MAO-B) continued: indications of iron binding, experimental evidence for optimised solubility and brain penetration. *J. Enzyme Inhib. Med. Chem.* 32, 960–967. doi: 10.1080/14756366.2017.1344980

van Horssen, J., van Schaik, P., and Witte, M. (2017). Inflammation and mitochondrial dysfunction: a vicious circle in neurodegenerative disorders? *Neurosci. Lett.* doi: 10.1016/j.neulet.2017.06.050. [Epub ahead of print].

Waldemar, G., Dubois, B., Emre, M., Georges, J., McKeith, I. G., Rossor, M., et al. (2007). Recommendations for the diagnosis and management of Alzheimer's disease and other disorders associated with dementia: EFNS guideline. *Eur. J. Neurol.* 14, e1–e26. doi: 10.1111/j.1468-1331.2006.01605.x

Walsh, C., Barrow, S., Voronina, S., Chvanov, M., Petersen, O. H., and Tepikin, A. (2009). Modulation of calcium signalling by mitochondria. *Biochim. Biophys. Acta* 1787, 1374–1382. doi: 10.1016/j.bbabio.2009.01.007

Waltenberger, B., Mocan, A., Smejkal, K., Heiss, E. H., and Atanasov, A. G. (2016). Natural Products to counteract the epidemic of cardiovascular and metabolic disorders. *Molecules* 21, 1–33. doi: 10.3390/molecules21060807

Wan, W., Cao, L., Liu, L., Kalionis, B., Chen, C., Tai, X., et al. (2014). EGb761 provides a protective effect against Aβ(1-42) oligomer-induced cell damage and blood-brain barrier disruption in an *in vitro* bEnd.3 endothelial model. *PLoS ONE* 9:e113126. doi: 10.1371/journal.pone.0113126

Wang, C., and Wang, B. (2016). *Ginkgo biloba* extract attenuates oxidative stress and apoptosis in mouse cochlear neural stem cells. *Phytother. Res.* 30, 774–780. doi: 10.1002/ptr.5572

Wang, C., and Youle, R. J. (2009). The Role of Mitochondria in Apoptosis. *Annu. Rev. Genet.* 43, 95–118. doi: 10.1146/annurev-genet-102108-134850

Wang, D.-S., Dickson, D. W., and Malter, J. S. (2006). beta-Amyloid degradation and Alzheimer's disease. *J. Biomed. Biotechnol.* 2006:58406. doi: 10.1155/JBB/2006/58406

Wang, P., Su, C., Li, R., Wang, H., Ren, Y., Sun, H., et al. (2014). Mechanisms and effects of curcumin on spatial learning and memory improvement in APPswe/PS1dE9 mice. *J. Neurosci. Res.* 92, 218–231. doi: 10.1002/jnr.23322

Wang, Y.-H., and Du, G.-H. (2009). Ginsenoside Rg1 inhibits beta-secretase activity *in vitro* and protects against Abeta-induced cytotoxicity in PC12 cells. *J. Asian Nat. Prod. Res.* 11, 604–612. doi: 10.1080/10286020902843152

Wang, Y., Huang, L., Tang, X., and Zhang, H. (2010). Retrospect and prospect of active principles from Chinese herbs in the treatment of dementia. *Acta Pharmacol. Sin.* 31, 649–664. doi: 10.1038/aps.2010.46

Wang, Y., Yang, G., Gong, J., Lu, F., Diao, Q., Sun, J., et al. (2016). Ginseng for Alzheimer's disease: a systematic review and meta-analysis of randomized controlled trials. *Curr. Top. Med. Chem.* 16, 529–536. doi: 10.2174/1568026615666150813143753

Weksler, M. E., Szabo, P., Relkin, N. R., Reidenberg, M. M., Weksler, B. B., and Coppus, A. M. W. (2013). Alzheimer's disease and Down's syndrome: treating two paths to dementia. *Autoimmun. Rev.* 12, 670–673. doi: 10.1016/j.autrev.2012.10.013

Winblad, B., Amouyel, P., Andrieu, S., Ballard, C., Brayne, C., Brodaty, H., et al. (2016). Defeating Alzheimer's disease and other dementias: a priority for European science and society. *Lancet Neurol.* 15, 455. doi: 10.1016/S1474-4422(16)00062-4

Wolters, B. (1994). *Drogen, Pfeilgift und Indianermedizin: Arzneipflanzen aus Südamerika*. Greifenberg: Urs Freud Verlag GmbH.

Xiong, Z., Hongmei, Z., Lu, S., and Yu, L. (2011). Curcumin mediates presenilin-1 activity to reduce beta-amyloid production in a model of Alzheimer's Disease. *Pharmacol. Rep.* 63, 1101–1108. doi: 10.1016/S1734-1140(11)70629-6

Yamada, T., Terashima, T., Honma, H., Nagata, S., Okubo, T., Juneja, L. R., et al. (2008). Effects of theanine, a unique amino acid in tea leaves, on memory in a rat behavioral test. *Biosci. Biotechnol. Biochem.* 72, 1356–1359. doi: 10.1271/bbb.70669

Yan, D., Zhang, Y., Liu, L., and Yan, H. (2016). Pesticide exposure and risk of Alzheimer's disease: a systematic review and meta-analysis. *Sci. Rep.* 6:32222. doi: 10.1038/srep32222

Yan, F.-L., Zheng, Y., and Zhao, F.-D. (2008). Effects of *Ginkgo biloba* extract EGb761 on expression of RAGE and LRP-1 in cerebral microvascular endothelial cells under chronic hypoxia and hypoglycemia. *Acta Neuropathol.* 116, 529–535. doi: 10.1007/s00401-008-0435-6

Yan, J., Hu, J., Liu, A., He, L., Li, X., and Wei, H. (2017). Design, synthesis, and evaluation of multitarget-directed ligands against Alzheimer's disease based on the fusion of donepezil and curcumin. *Bioorg. Med. Chem.* 25, 2946–2955. doi: 10.1016/j.bmc.2017.02.048

Yanagisawa, D., Taguchi, H., Yamamoto, A., Shirai, N., Hirao, K., and Tooyama, I. (2011). Curcuminoid binds to amyloid-beta1-42 oligomer and fibril. *J. Alzheimers. Dis.* 24(Suppl. 2), 33–42. doi: 10.3233/JAD-2011-102100

Yang, E.-J., Min, J. S., Ku, H.-Y., Choi, H.-S., Park, M., Kim, M. K., et al. (2012). Isoliquiritigenin isolated from Glycyrrhiza uralensis protects neuronal cells against glutamate-induced mitochondrial dysfunction. *Biochem. Biophys. Res. Commun.* 421, 658–664. doi: 10.1016/j.bbrc.2012.04.053

Yang, L., Hao, J., Zhang, J., Xia, W., Dong, X., Hu, X., et al. (2009). Ginsenoside Rg3 promotes beta-amyloid peptide degradation by enhancing gene expression of neprilysin. *J. Pharm. Pharmacol.* 61, 375–380. doi: 10.1211/jpp.61.03.0013

Ye, J., and Zhang, Y. (2012). Curcumin protects against intracellular amyloid toxicity in rat primary neurons. *Int. J. Clin. Exp. Med.* 5, 44–49.

Ye, R., Zhang, X., Kong, X., Han, J., Yang, Q., Zhang, Y., et al. (2011). Ginsenoside Rd attenuates mitochondrial dysfunction and sequential apoptosis after transient focal ischemia. *Neuroscience* 178, 169–180. doi: 10.1016/j.neuroscience.2011.01.007

Yim, S. B., Park, S. E., and Lee, C. S. (2007). Protective effect of glycyrrhizin on 1-methyl-4-phenylpyridinium-induced mitochondrial damage and cell death in differentiated PC12 cells. *J. Pharmacol. Exp. Ther.* 321, 816–822. doi: 10.1124/jpet.107.119602

Yin, S. Y., Kim, H. J., and Kim, H.-J. (2013). A comparative study of the effects of whole red ginseng extract and polysaccharide and saponin fractions on influenza A (H1N1) virus infection. *Biol. Pharm. Bull.* 36, 1002–1007. doi: 10.1248/bpb.b13-00123

Yokota, T., Nishio, H., Kubota, Y., and Mizoguchi, M. (1998). The inhibitory effect of glabridin from licorice extracts on melanogenesis and inflammation. *Pigment cell Res.* 11, 355–361. doi: 10.1111/j.1600-0749.1998.tb00494.x

Yun, T. K. (2001). Brief introduction of Panax ginseng C.A. Meyer. *J. Korean Med. Sci.* 16(Suppl.) S3–S5. doi: 10.3346/jkms.2001.16.S.S3

Zhang, L., Fang, Y., Xu, Y., Lian, Y., Xie, N., Wu, T., et al. (2015). Curcumin improves amyloid beta-peptide (1-42) induced spatial memory deficits through BDNF-ERK signaling pathway. *PLoS ONE* 10:e0131525. doi: 10.1371/journal.pone.0131525

Zhang, L., Fiala, M., Cashman, J., Sayre, J., Espinosa, A., Mahanian, M., et al. (2006). Curcuminoids enhance amyloid-beta uptake by macrophages of Alzheimer's disease patients. *J. Alzheimers. Dis.* 10, 1–7. doi: 10.3233/JAD-2006-10101

Zhou, J.-S., Wang, J.-F., He, B.-R., Cui, Y.-S., Fang, X.-Y., Ni, J.-L., et al. (2014). Ginsenoside Rd attenuates mitochondrial permeability transition and cytochrome c release in isolated spinal cord mitochondria: involvement of kinase-mediated pathways. *Int. J. Mol. Sci.* 15, 9859–9877. doi: 10.3390/ijms15069859

Zhou, S., Lim, L. Y., and Chowbay, B. (2004). Herbal modulation of P-glycoprotein. *Drug Metab. Rev.* 36, 57–104. doi: 10.1081/DMR-120028427

Zhou, X., Cui, G., Tseng, H. H. L., Lee, S. M.-Y., Leung, G. P. H., Chan, S. W., et al. (2016a). Vascular contributions to cognitive impairment and treatments with traditional chinese medicine. *Evid. Based. Complement. Alternat. Med.* 2016, 9627258. doi: 10.1155/2016/9627258

Zhou, X., Seto, S. W., Chang, D., Kiat, H., Razmovski-Naumovski, V., Chan, K., et al. (2016b). Synergistic effects of chinese herbal medicine: a comprehensive review of methodology and current research. *Front. Pharmacol.* 7:201. doi: 10.3389/fphar.2016.00201

Zhou, X., Wang, H.-Y., Wu, B., Cheng, C.-Y., Xiao, W., Wang, Z.-Z., et al. (2017). Ginkgolide K attenuates neuronal injury after ischemic stroke by inhibiting mitochondrial fission and GSK-3beta-dependent increases in mitochondrial membrane permeability. *Oncotarget* 8, 44682–44693. doi: 10.18632/oncotarget.17967

Zhu, X., Chen, C., Ye, D., Guan, D., Ye, L., Jin, J., et al. (2012). Diammonium glycyrrhizinate upregulates PGC-1α and protects against Aβ 1–42-induced neurotoxicity. *PLoS ONE* 7:e35823. doi: 10.1371/journal.pone.0035823

Zhu, X., Perry, G., Smith, M. A., and Wang, X. (2013). Abnormal mitochondrial dynamics in the pathogenesis of Alzheimer's disease. *J. Alzheimers. Dis.* 33(Suppl. 1), S253–S262. doi: 10.3233/JAD-2012-129005

Zlokovic, B., V (2011). Neurovascular pathways to neurodegeneration in Alzheimer's disease and other disorders. *Nat. Rev. Neurosci.* 12, 723–738. doi: 10.1038/nrn3114

Zupancic, M., Mahajan, A., and Handa, K. (2011). Dementia with lewy bodies: diagnosis and management for primary care providers. *Prim. Care Companion CNS Disord.* 13:PCC.11r01190.

Conflict of Interest Statement: Author NT was employed by NTZ Lab ltd.

The other authors declare that the research was conducted in the absence of any commercial or financial relationships that could be construed as a potential conflict of interest.

Copyright © 2018 Tewari, Stankiewicz, Mocan, Sah, Tzvetkov, Huminiecki, Horbańczuk and Atanasov. This is an open-access article distributed under the terms of the Creative Commons Attribution License (CC BY). The use, distribution or reproduction in other forums is permitted, provided the original author(s) and the copyright owner are credited and that the original publication in this journal is cited, in accordance with accepted academic practice. No use, distribution or reproduction is permitted which does not comply with these terms.

frontiers in Aging Neuroscience

MINI REVIEW
published: 06 February 2018
doi: 10.3389/fnagi.2018.00030

Dissecting Endoplasmic Reticulum Unfolded Protein Response (UPR^{ER}) in Managing Clandestine Modus Operandi of Alzheimer's Disease

*Safikur Rahman[1], Ayyagari Archana[2], Arif Tasleem Jan[3] and Rinki Minakshi[4]**

[1]*Department of Medical Biotechnology, Yeungnam University, Gyeongsan, South Korea,* [2]*Department of Microbiology, Swami Shraddhanand College, University of Delhi, New Delhi, India,* [3]*School of Biosciences and Biotechnology, Baba Ghulam Shah Badshah University, Rajouri, India,* [4]*Institute of Home Economics, University of Delhi, New Delhi, India*

Alzheimer's disease (AD), a neurodegenerative disorder, is most common cause of dementia witnessed among aged people. The pathophysiology of AD develops as a consequence of neurofibrillary tangle formation which consists of hyperphosphorylated microtubule associated tau protein and senile plaques of amyloid-β (Aβ) peptide in specific brain regions that result in synaptic loss and neuronal death. The feeble buffering capacity of endoplasmic reticulum (ER) proteostasis in AD is evident through alteration in unfolded protein response (UPR), where UPR markers express invariably in AD patient's brain samples. Aging weakens UPR^{ER} causing neuropathology and memory loss in AD. This review highlights molecular signatures of UPR^{ER} and its key molecular alliance that are affected in aging leading to the development of intriguing neuropathologies in AD. We present a summary of recent studies reporting usage of small molecules as inhibitors or activators of UPR^{ER} sensors/effectors in AD that showcase avenues for therapeutic interventions.

Keywords: Alzheimer disease, neurodegenerative diseases, endoplasmic reticulum stress (ER), aging, UPR (unfolded protein response)

OPEN ACCESS

Edited by:
Ghulam Md. Ashraf, King Abdulaziz University, Saudi Arabia

Reviewed by:
Gulam M. Rather, Rutgers Cancer Institute of New Jersey, United States
Gjumrakch Aliev, GALLY International Biomedical Research, United States
Showkat Bhawani, UNIMAS Sarawak, Malaysia

****Correspondence:***
Rinki Minakshi
rinki.minakshi@hotmail.com; minakshi4050@gmail.com

Received: *31 October 2017*
Accepted: *24 January 2018*
Published: *06 February 2018*

Citation:
Rahman S, Archana A, Jan AT and Minakshi R (2018) Dissecting Endoplasmic Reticulum Unfolded Protein Response (UPR^{ER}) in Managing Clandestine Modus Operandi of Alzheimer's Disease. Front. Aging Neurosci. 10:30. doi: 10.3389/fnagi.2018.00030

INTRODUCTION

Alzheimer's disease (AD), the most common form of dementia faced by more than 40 million people worldwide, significantly affect morbidity and mortality in aged people (Alzheimer's Association, 2016; Fiest et al., 2016; Scheltens et al., 2016; Cass, 2017). The most vulnerable group falling as target is above 65 years, which puts aging as the crucial risk factor associated with development of the disease (Alzheimer's Association, 2016; Fiest et al., 2016; Scheltens et al., 2016; Cass, 2017). AD is a progressively neurodegenerative disorder, characterized by cognitive alterations and behavioral changes that owe to synaptic impairment and loss of neurons (Alzheimer's Association, 2016; Scheltens et al., 2016). Mutations in genes encoding APP (amyloid precursor protein), presenilin 1 and 2 (PS1 and PS2 respectively), as well as ε4 allele of Apolipoprotein E are reported to be linked to rare familial and early development of AD (Selkoe, 2001a,b; Scheltens et al., 2016). AD leads to the formation of neurofibrillary tangles having hyperphosphorylated microtubule associated tau protein and senile plaques of amyloid-β (Aβ) peptide in specific brain regions, result in brain inflammation, astrogliosis and microglial proliferation (Citron, 2002; Selkoe, 2004a,b; Cleary et al., 2005; Haass and Selkoe, 2007; Atwood and Bowen, 2015; Minter et al., 2016; Sami et al., 2017). Gradual

accumulation of Aβ peptide attributed to β- and γ-secretases action on the APP, results in synaptic loss and neuronal death (Chyung et al., 2005; Tatarnikova et al., 2015).

The expression pattern of neurodegenerative pathologies shows distinct molecular signatures, such as misfolded Aβ aggregation and tau protein hyperphosphorylation in the brain (Jiang et al., 2010; Atwood and Bowen, 2015; Sami et al., 2017). How this load of protein aggregates disrupt the neuronal function is still a mystery to medical science? In this review, we have tried to focus on the role of ER stress and the ensuing unfolded protein response (UPR^{ER}) imposed on the neuronal cell due to misfolded protein aggregates. Also, we have discussed various therapeutic interventions targeting the molecules involved in UPR pathways aiming at averting the neuropathologies of AD.

ER STRESS AND UPR^{ER}

Adversities in the endoplasmic reticulum (ER) microenvironment like nutrient deprivation, changes in redox potential, calcium homeostasis, hypoxia and accumulation of unfolded/misfolded protein triggers the UPR^{ER} (Schroder and Kaufman, 2005; Moneim, 2015). UPR^{ER} is a highly conserved signaling cascade in all eukaryotes involved in the cellular homeostasis (Ellgaard and Helenius, 2003; Mori, 2009; Walter and Ron, 2011) through transcriptional remodeling of ER proteostasis pathways (Lee et al., 2003; Yamamoto et al., 2007; Shoulders et al., 2013; Genereux et al., 2015). The ER lumen harbors various molecular chaperones like the Glucose Regulated Protein 78 kDa (GRP78) that are recruited to misfolded nascent peptides for aiding in their proper folding (Bertolotti et al., 2000; Shen et al., 2002). A plethora of studies have reported UPR^{ER} upregulation in the brain samples of Alzheimer's patients (Hamos et al., 1991; Hoozemans et al., 2005, 2009).

The UPR^{ER} embodies a complex network comprised of three stress-responsive transmembrane proteins, Protein Kinase RNA like ER kinase (PERK), Inositol Requiring Element 1 (IRE1) and Activating Transcription Factor 6 (ATF6; **Figure 1**; Schroder and Kaufman, 2005; Walter and Ron, 2011; Minakshi et al., 2017; Rahman et al., 2017). PERK, a type 1 transmembrane kinase protein, gets trans-autophosphorylated and homodimerized after activation, thereby promoting phosphorylation of serine residues on cytoplasmic eIF2α (eukaryotic initiation factor 2 alpha; Harding et al., 1999; Bertolotti et al., 2000; Ma et al., 2002; Marciniak et al., 2006). Despite the general translational halt induced by the phosphorylated eIF2α (eIF2α-P), certain specific mRNAs bearing internal ribosome entry site (IRES), like the Activating Transcription Factor 4 (ATF4) mRNAs continues to be translated (Harding et al., 2000a; Baumeister et al., 2005). ATF4 regulates genes for various foldases, chaperones, regulatory proteins of the redox and autophagy, cholesterol metabolism etc. (Harding et al., 2003; Fusakio et al., 2016). CCAAT enhancer-binding (C/EBP) protein homologous protein (CHOP) is also a direct target of ATF4 and represents the pro-apoptotic component of the UPR^{ER} (Han et al., 2013). In a study, wild type mice subjected to tunicamycin injection showed higher degrees of apoptosis in their renal epithelium as compared to CHOP knockout mice (Marciniak et al., 2004; Onuki et al., 2004). PERK also induces the activation of another transcription factor nuclear factor (erythroid derived 2)-like 2 (Nrf2) independent of eIF2α, which regulates the antioxidant response (Cullinan et al., 2003; Cullinan and Diehl, 2004).

IRE1 is the most evolutionarily conserved ER stress transducer (Tirasophon et al., 1998), which upon activation, undergoes dimerization and trans-autophosphorylation, leading to the activation of its cytosolic endoribonuclease activity that splices a 26-nucleotide intron from the mRNA encoding transcription factor X box binding protein 1 (XBP1) forming XBP1(S) (Yoshida et al., 2001, 2003). The XBP1(S) upregulates genes involved in ER protein maturation and ER-associated degradation (ERAD; Lee et al., 2003; Acosta-Alvear et al., 2007). Cells lacking XBP1 are more sensitive to hypoxia-induced apoptosis (Romero-Ramirez et al., 2004). Upon activation, IRE1 also activates c-Jun N-terminal kinase (JNK) through tumor necrosis factor receptor-associated factor 2 (TRAF2); Zeng et al., 2015). IRE1-mediated JNK activation has been demonstrated to trigger autophagy under ER-stress (Urano et al., 2000).

ATF6 is a type II transmembrane protein, with a basic leucine zipper (bZIP) domain (Yoshida et al., 1998). During the imposed stress, luminal domain of ATF6 loses its association with GRP78, triggering the translocation of ATF6 into the Golgi apparatus where two intramembrane Golgi specific proteases, site 1 protease (S1P) and site 2 protease (S2P), process it. The N-terminal cleaved product p50ATF6 of full length ATF6 (p90ATF), then acts as a transcription factor, which upregulates several genes, including GRP78, Protein Disulfide Isomerase (PDI), XBP1 and CHOP (Haze et al., 1999; Walter and Ron, 2011).

UPR^{ER} IN ALZHEIMER'S DISEASE

In neuronal pathophysiology, the activation of UPR^{ER} can have paradoxical affects. During stress condition, activation of UPR^{ER} could reactivate proteostasis; thereby rescuing the neurons by escalating the rate of protein folding through molecular chaperones, or may trigger neurodegeneration and neuronal collapse through the expression of apoptotic markers.

Evidences support the presence of abundant hyperphosphorylated tau protein and ER stress markers in the neurons of the cortex in postmortem brain samples of AD patients (Scheper and Hoozemans, 2015). It is presumed that ER stress is a cell death mechanism triggered by Aβ, and is linked to changes in ER calcium homeostasis (Cornejo and Hetz, 2013). Under the influence of Aβ imposed ER stress, Ca^{2+} leaching from ER is taken up by mitochondria leading to activation of apoptotic death of neurons (Fonseca et al., 2013). The presenilins are responsible for passive ER Ca^{2+} outflow. Documents support that aging neurons fail to maintain tight Ca^{2+} homeostasis across plasma membrane and ER

(Supnet and Bezprozvanny, 2010). Such effects paved the way for "calcium hypothesis of brain aging and AD" (Khachaturian, 1989). Rise in prolonged imbalanced Ca^{2+} invites ROS accumulation and mitochondrial dysfunction resulting in neuronal death (Supnet and Bezprozvanny, 2010). ER stress may display binary role in AD, firstly modulating the production kinetics of amyloid plaques and secondly altering the cognitive functions in a distinct way (Halliday and Mallucci, 2015). Neurons of AD patients were also characterized by GRP78 induction in temporal cortex and hippocampus and phosphorylation of PERK (p-PERK; Hoozemans et al., 2005).

Active protein synthesis is a hallmark feature of synaptic plasticity and consolidation of memory (Costa-Mattioli et al., 2009). PERK signaling and protein translation control was linked to the cognitive impairment observed in AD models (Devi and Ohno, 2013, 2014). Impairment of cognitive functions due to the reduction in synaptic protein synthesis is displayed during increased phosphorylation of eIF2α (Costa-Mattioli et al., 2005, 2009; Jiang et al., 2010). Mitigating the expression of PERK improves cognitive function and synaptic plasticity in an AD model (Devi and Ohno, 2014). Moreover, targeting other eIF2α kinases like General Control Nonderepressible-2 (GCN2) and dsRNA-dependent protein kinase R (PKR) was also witnessed not only to improve learning and memory processes (Devi and Ohno, 2013), but also reduced inflammation (Lourenco et al., 2013). These results significantly indicate that genetic manipulation of PERK improved cognitive ability of cells to survive under stress conditions induced by Aβ deposition.

The activation of UPR^{ER} in early stages of AD could be protective through activation of autophagy. However, sustained UPR^{ER} activation may be detrimental to the neurons (Hoozemans et al., 2005; Nijholt et al., 2011). The expression of XBP1 in *Drosophila* where the AD-associated Aβ peptide was expressed in neurons, led to reduced neurotoxicity, supporting the cytoprotective role of XBP1 (Casas-Tinto et al., 2011). In *Caenorhabditis elegans* (*C. elegans*) models expressing aggregation-prone mutant tau variants, XBP-1 was identified to be playing a similar protective role (Kraemer et al., 2006; Loewen and Feany, 2010). However, reports also suggest that IRE1 interacts with PS1 leading to activation of proapoptotic signaling by JNK (Shoji et al., 2000). The JNK3 (member of JNK family) localized in brain, is highly expressed in brain tissue and cerebrospinal fluid sample from AD patients (Gourmaud et al., 2015) and the activation of JNK3 exacerbates stress perpetuating AD pathology (Yoon and Jo, 2012).

AGING, UPR^{ER} AND ALZHEIMER'S DISEASE

Aging is the single most important risk factor for AD. Decline in the UPR^{ER} with advancing age marked by the oxidative damage of ER chaperones, leads to disempowering of protein folding capacity (Rabek et al., 2003; Nuss et al., 2008). Studies report that the levels of GRP78 were low in murine cortex, in rat hippocampus, cortex, cerebellum, as well as in a multitude of organs (Paz Gavilán et al., 2006; Hussain and Ramaiah, 2007; Naidoo et al., 2008). Transcription of PERK mRNA were lowered in the aging rat hippocampus, while an increment was reported in the expression of growth arrest and DNA damage protein 34 (GADD34), because it escapes the effect of eIF2α-P translational inhibition (Paz Gavilán et al., 2006). Studies on *C. elegans* revealed that the activation of IRE1 branch of the UPR^{ER} diminishes during the fertile period of adulthood, manifesting in lowered immunity against ER stress (Taylor and Dillin, 2013). The implication of IRE1/XBP1 tier in aging was proven in *C. elegans* where IRE1 defect reduced life span (Chen et al., 2009).

MITOCHONDRIA, OXIDATIVE STRESS AND ALZHEIMER'S DISEASE

Under the imposed stress, apart from UPR^{ER} coming to the rescue, the herald of mitochondrial UPR (UPR^{mt}) ensuing after accumulation of unfolded peptide load is well documented. The pathway focuses on invigorating folding and degradation of misfolded peptides in mitochondrial matrix through the execution of retrograde transcriptional activation (Arnould et al., 2015). AD being a multifactorial malady, the accumulation of Aβ not only affects ER but also mitochondria. There are accumulating evidences, which support deposition of Aβ in mitochondrial matrix disrupting signaling of the organelle thereby leading to neurodegeneration (Kawamata and Manfredi, 2017). Impairment in the production and functionalities of metabolic enzymes preferentially of TCA cycle disturbs energy metabolism of the brain. Mitochondrial dysfunction causes depletion of cellular ATP pool and enhanced ROS production, which is well implicated in the pathogenesis of AD (Swerdlow et al., 2014; Hoekstra et al., 2016). Besides, impairment of mitochondrial turnover and function in brain, aging potentiates oxidative stress, leading to significant decrease in the cytochrome C oxidase activity that is associated with rise in oxygen radicals in different regions of postmortem AD brain (**Figure 2**; Hirai et al., 2001; Mosconi et al., 2007; Krishnan et al., 2012). A strong correlation of the cognitive decline with increase in oxidative stress is observed in AD patients (Revel et al., 2015). Incidence of aberrant Aβ processing ensues after the oxidation of mitochondrial DNA (mtDNA) under stressful circumstances (Volgyi et al., 2015).

Aberrations in mtDNA have been well studied in AD. In an elegant study by Aliev et al. (2013) mtDNA-proliferation and deletion has been reported in AD tissues. Furthermore, the report also illustrates abnormal mitochondrial function in damaged hippocampal neurons in human AD as well as transgenic AD models. In another study using *in situ* hybridization, Aliev et al. (2008) detected a 5 kB deletion in mtDNA under oxidative stress in abnormal neurons. Such mitochondrial anomalies were also reported to help in AD pathogenesis in Aβ transgenic mice (Aliev et al., 2008).

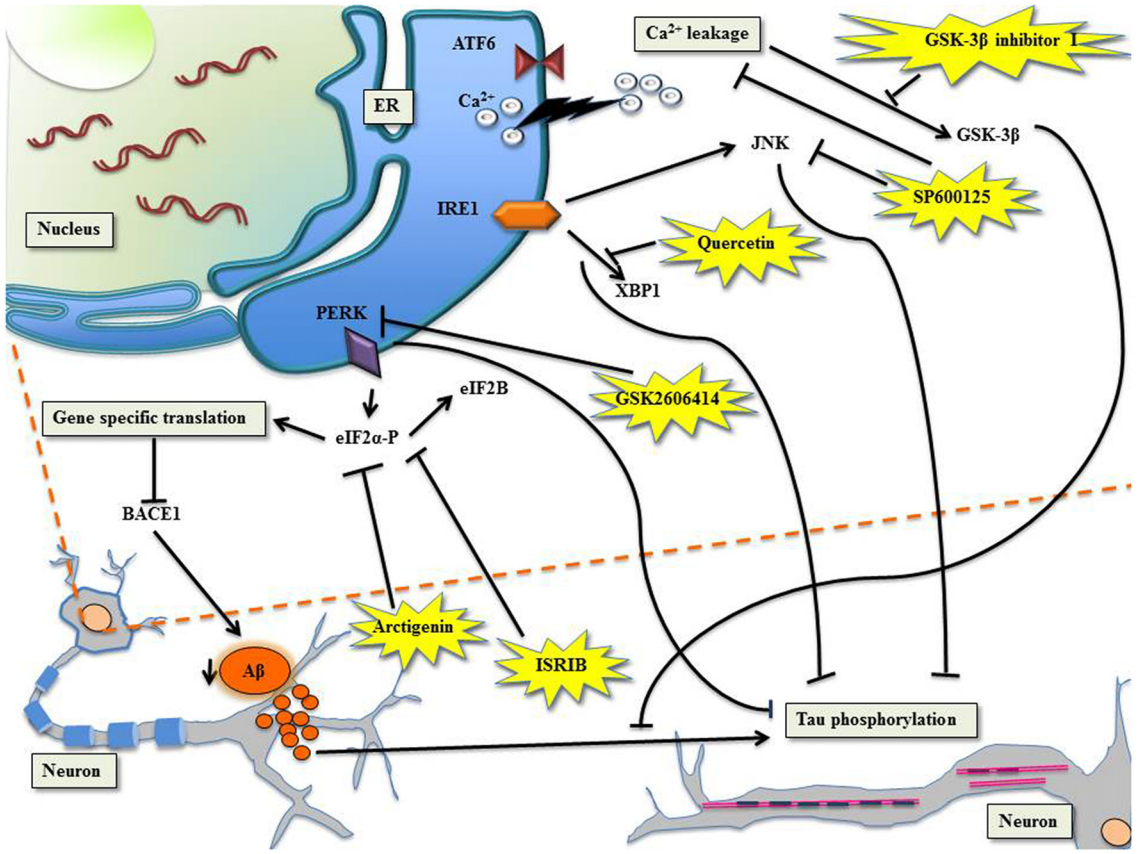


FIGURE 1 | Targeting unfolded protein response (UPR) to manage Alzheimer's disease (AD) with specific molecules. *PERK/eIF2α*: the phosphorylation of eIF2α shuts down global translation in the cell but for gene-specific translation upregulation of mRNA with internal ribosome entry site (IRES), for example β-site APP cleaving enzyme-1 (BACE1), the β-secretase enzyme (Ohno, 2014). Arctigenin, targets eIF2α-P thereby downregulating BACE1, consequently protects neurons from amyloid-β (Aβ) toxicity. ISRIB, affects eIF2B leading to inhibition of eIF2α-P, which comprehensively restores protein translation and hence enhances long term memory. PERK can be directly inhibited by GSK2606414, leading to halt in tau phosphorylation. Ca^{2+} leakage induced activation of glycogen synthase kinase-3β (GSK-3β) can be checked by GSK-3β inhibitor I, which prevents Aβ induced phosphorylation of tau. *IRE1/XBP1*: Quercetin, activates endoribonuclease activity of IRE1 inhibiting tau hyperphosphorylation. The c-Jun N-terminal kinase (JNK) inhibitor, SP600125, inhibits Ca^{2+} leakage and inhibits Aβ-induced c-Jun phosphorylation.

In a study proving the existence of interlink between mitochondrial dysfunction and AD, the pharmacological/genetic targeting of mitochondrial translation process not only increased life span of GMC101 (model of Aβ proteotoxicity), but also showed reduction in beta-amyloid aggregation in worms and transgenic mouse models of AD (Sorrentino et al., 2017). Treatment of the mitochondrial division inhibitor-1 (mdiv-1) that inhibits mitochondrial fragmentation, thereby rescuing mitochondrial distribution, improves mitochondrial function in CRND8 (AD mouse model) neurons (Reddy et al., 2017; Wang et al., 2017). Treatment with mdivi-1 also causes a decrease in extracellular amyloid deposition and Aβ1–42/Aβ1–40 ratio (Wang et al., 2017). Additionally, SIRT-3, a sirtuin localized to inner mitochondrial membrane, has been found associated with enhancement in the levels of glutathione (Onyango et al., 2002; Someya et al., 2010). As downregulation of SIRT-3 was found to be having a retrograde effect on p53 mediated mitochondrial and neuronal damage in AD, its modulation by therapeutics was found to ameliorate mitochondrial pathology and neurodegeneration in AD (Lee et al., 2018).

DERANGEMENT OF GLUCOSE METABOLISM IN ALZHEIMER'S DISEASE: THE FALLIBLE UPR^{ER}

Among the many observed hallmarks of AD, positron emission tomography (PET) revealed a deranged glucose metabolism in brain regions. Aging registers diminished brain glucose utilization that surges in AD (Ivançević et al., 2000). Various reports suggest that UPR^{ER} is linked to abnormal glucose metabolism and insulin resistance (Hetz et al., 2015). Type 2 diabetes mellitus (T2DM) has been mechanistically linked to AD pathogenesis, where higher insulin resistance poses a greater risk of AD with reduced glucose uptake in the brain

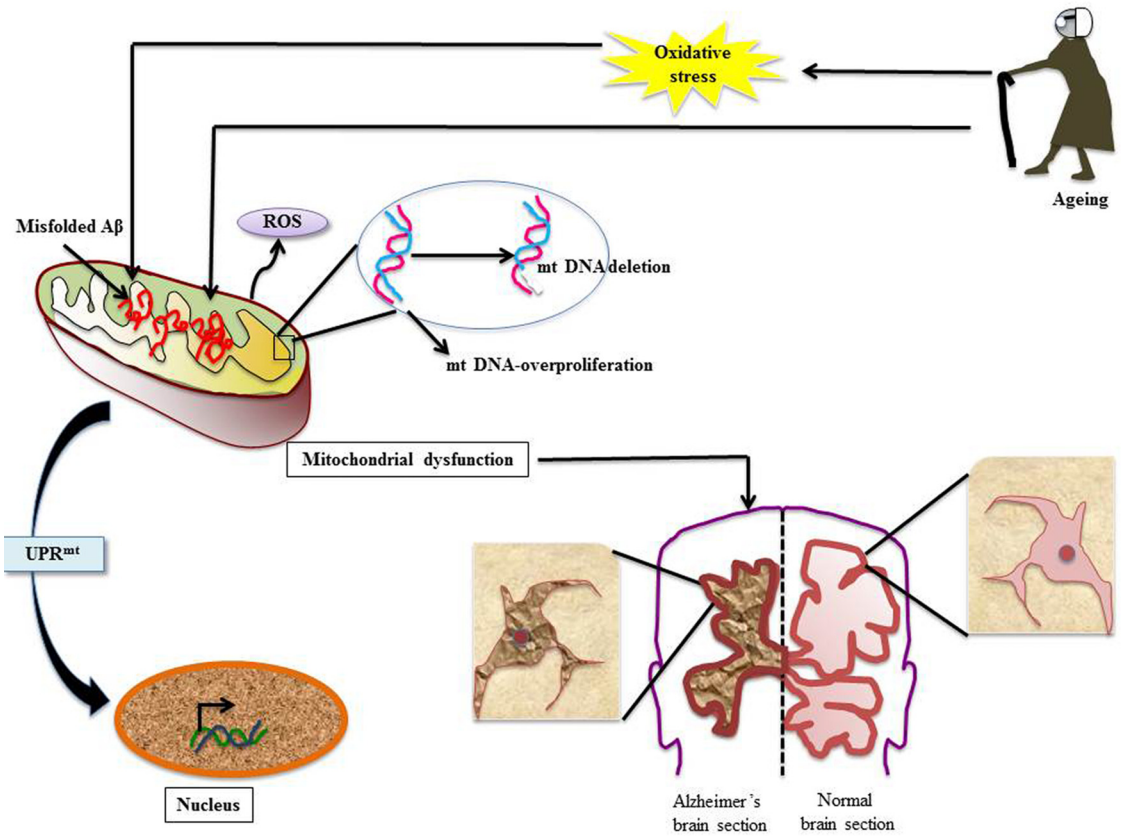


FIGURE 2 | Mitochondrial dysfunction in AD: various stress insults like aging and oxidative stress disrupt client protein folding in mitochondria thereby invoking mitochondrial UPR (UPR^{mt}). Numerous events line up; there is mitochondrial DNA (mtDNA) proliferation and deletion, misfolded Aβ overload and ROS generation. This leads to the condition of mitochondrial dysfunction and to rescue the ailing cell UPR^{mt} is stimulated. The effect of mitochondrial dysfunction leads to development of neuropathologies associated with AD (Aliev et al., 2008, 2013; Onyango et al., 2016).

as well as memory loss (Willette et al., 2015; Wijesekara et al., 2017). In addition, there is decline in key neuronal glucose transporters, GLUT1 and GLUT3, as shown in AD mouse models (Ding et al., 2013). The exact molecular mechanism underlying the effect of glucose uptake in AD model is not completely understood, but evidences suggest a close link between AD and insulin signaling. Apart from controlling glucose metabolism, insulin also regulates neural development with respect to learning and memory (Ying et al., 2017).

The lowering in glucose concentration due to lack of active transporters (GLUT1 and GLUT3) instates mitigating effect on hexosamine pathway (HBP), due to which O-GlcNAcylation is compromised with hyperphosphorylation on tau protein (Liu et al., 2009). XBP1(S) is shown to directly target the rate limiting enzyme of HBP, glutamine fructose-6-phosphate aminotransferase (GFAT1; Wang et al., 2014), as XBP1(S) transgenics showed rise in O-GlcNAcylation (Wang et al., 2014). The situation of insulin resistance established in aging has also been shown to increase HBP flux (Einstein et al., 2008). A gain-of-function mutation in GFAT1 of *C. elegans* showed significant induction of ERAD and autophagy favoring longevity (Denzel et al., 2014).

Protein aggregation is a consequence of AD which is a result of abnormal proteostasis in the cell (Kaushik and Cuervo, 2015). An increase in the UPR^{ER} driven protein homeostasis was observed with the overexpression of GLUT1 as this promoted downregulation of expression of GRP78. GRP78, being the negative regulator of the UPR^{ER}, binds ATF6 and IRE1 thereby continuing them in an inactive state. One interesting study showed that flies (with increased glucose transport) when fed with the drug metformin showed mitigated levels of GRP78 with ensuing gain in lifespan, additionally the expression of GLUT1 and its association with the beginning of UPR^{ER} exerted neuroprotective effect (Niccoli et al., 2016).

TARGETING UPR^{ER} TO MANAGE AD

The involvement of ER stress and hence the UPR^{ER} in neuropathologies exposes the molecules of the pathway as attractive targets for therapeutic interventions. Here, we have

compiled reports from studies that have targeted molecules of UPR^{ER} for managing the deterioration caused by AD (**Figure 1**).

eIF2α and PERK in AD

There are accumulating evidences that support increased phosphorylation of PERK and eIF2α in AD (Chang et al., 2002; Page et al., 2006; Kim et al., 2007). The processing of highly expressed single-pass transmembrane protein in brain, the amyloid precursor protein, leads to the generation of neurotoxic Aβ during neuropathogenesis. Reports suggest that the secretase β-site APP cleaving enzyme-1 (BACE1), increases APP cleavage as a result of eIF2α phosphorylation leading to the production of Aβ in neurons (O'Connor et al., 2008). The PERK tier of UPR when suppressed leads to the alleviation of synaptic plasticity and memory loss in AD (Ma et al., 2013). The administration of arctigenin, a bioactive product from *Arctium lappa* (L.), has been known to inhibit BACE1 translation through dephosphorylation of eIF2α-P (Zhu et al., 2013). The phosphorylation of eIF2α is central to integrated stress response (ISR) that modulates UPR (Harding et al., 2000b) and formation of memory proteins (Costa-Mattioli et al., 2005). ISR inhibitor (ISRIB) interferes with ISR by affecting eIF2B activity whose competitive inhibitor is eIF2α-P (Krishnamoorthy et al., 2001; Sekine et al., 2015; Bogorad et al., 2017). This comprehensively reverses the effect of eIF2α-P, which resulted in the restoration of translation and hence long term memory enhancement in rodents (Sidrauski et al., 2013, 2015). The genetic deletion of eIF2 kinases, PERK, GCN2 and dsRNA-dependent protein kinase (PKR) ameliorate synaptic plasticity and memory in AD models (Ma et al., 2013). The transient translational halt induced by PERK-P/eIF2α-P was challenged by GSK2606414, a PERK inhibitor, because of which tau phosphorylation could be checked, resulting in the amelioration of neurodegeneration (Axten et al., 2012; Radford et al., 2015). The development of AD manifested by Aβ accumulation forces tau hyper phosphorylation in sync with increased activity of glycogen synthase kinase-3β (GSK-3β) in the cortical neurons (Takashima et al., 1993, 1996; Tomidokoro et al., 2001; De Felice et al., 2008; Resende et al., 2008). Resende et al. (2008) showed that Aβ oligomers cause ER stress linked calcium leakage which in turn leads to GSK-3β activation, the later when inhibited by GSK-3β inhibitor I, led to the prevention of Aβ induced phosphorylation of tau.

IRE1/XBP1 in AD

The advantageous effects of XBP1 on memory was proven in neural-specific XBP1 knockout mice featuring impaired learning and synaptic plasticity deficit, where injections of adeno-associated viruses delivered XBP1(S) resulted in establishing long-term hippocampus memory (Martínez et al., 2016). In accordance with this finding, another study reinforced the neuro-protective role of XBP1 in AD mice (Casas-Tinto et al., 2011; Cisse et al., 2017). Nonetheless, a flavonol, called quercetin, activated endoribonuclease activity of IRE1 and inhibited tau hyperphosphorylation (de Boer et al., 2006; Suganthy et al., 2016). In cases of familial AD, deletions or mutations in presenilin genes accentuate ER Ca^{2+} leakage. The JNK inhibitor, SP600125, when challenged in PS1/PS2 double knockout mouse embryonic fibroblast, caused inhibition of Ca^{2+} leakage (Das et al., 2012). The neuroinflammation exhibited in AD through tau phosphorylation mediated by the kinase activity of JNK was inhibited by SP600125, consequently inhibiting Aβ-induced c-Jun phosphorylation (Vukic et al., 2009; Zhou et al., 2015).

FUTURE DIRECTIONS AND CONCLUDING REMARKS

ER, being a central organelle in nerve cells, coordinates with the cellular homeostasis by managing translation/modification of proteins and Ca^{2+} equilibrium, thereby maintains the proper signaling in brain. The disruption in neuronal physiology is quite evident in age-related AD where ER dysfunctions are prominently expressed in the form of imbalance in proteostasis. Advancements in studies based on AD models have clearly shown how we can intervene the molecular pillars of UPR^{ER} and its associated signaling cascades to manage neurodegeneration in age-related AD. The present review is an attempt to revise functional relevance of the studies conducted in the field of management of age-related AD through therapeutic interventions on the UPR^{ER} pathway and its associate's molecules. Studies reinforce that the strategies where intervening the molecules, which are involved in transposing effects of aging on neurodegeneration, will cause reduction in probability of AD pathology. The manifestation of ER proteostasis is a direct indication of healthy nervous system. Progression in AD witnesses glucose hypo-metabolism in brain, reduction in glucose transporters in neurons and endothelial cells of blood brain barrier in direct proportion with the amount of neurofibrillary tangles. Type 2 diabetics with higher insulin resistance are at a greater risk of AD. Recent reports elucidate that managing UPR^{ER} can exert neuroprotective effect in AD (Smith and Mallucci, 2016). Additionally, as evidenced in the study by Sorrentino et al. (2017), the recapitulation of mitochondrial function through activation of UPR^{mt} can impede plaque formation. Aliev et al., also demonstrated link between cancer and AD where mtDNA over-proliferation and deletion induces cell cycle dysregulation prompting oncogenic pathway (Aliev et al., 2013). We have supporting literature that underpins the reversal of AD pathology by anticancer drugs (Cramer et al., 2012). Aiming at therapeutic intervention, the ailing mitochondria can be challenged with specific antioxidants like MitoQ, acetyl-L-carnitine and R-alpha lipoic acid to alleviate AD (Aliev et al., 2011; Volgyi et al., 2015). One remarkable study on astrocytes underpins the protective role of conditioned medium of human mesenchymal stem cells (CM-hMSCA) sourced from adipose tissue against neuropathologies (Baez-Jurado et al., 2017). The state of astrocyte mitochondrial dysfunction has been proven to be a start point for neuronal death (Baez et al., 2016). Pharmacological targeting of astrocytes has been proposed to be a potential way in therapeutics of AD (Baez et al.,

2016). A transcriptomic analysis in astrocytes has put forward a conglomeration of various algorithms for strategic approaches in therapeutics of neuropathologies (Barreto et al., 2017).

We still need extensive and efficient model systems where the molecular intricacies of weakened UPR^{ER} in aging-induced neuropathology in AD can be ventured upon, so that pharmacological as well as genetic tools could underscore the significance of UPR^{ER} as well as UPR^{mt} in aged brain.

AUTHOR CONTRIBUTIONS

SR and RM conceived the idea. SR, ATJ, AA and RM contributed to writing of the manuscript.

ACKNOWLEDGMENTS

Authors extend their thanks to colleagues for their criticism that helped to improve the quality of contents in the perspective of broader audience. No funding was availed to carry out the study.

REFERENCES

Acosta-Alvear, D., Zhou, Y., Blais, A., Tsikitis, M., Lents, N. H., Arias, C., et al. (2007). XBP1 controls diverse cell type- and condition-specific transcriptional regulatory networks. *Mol. Cell* 27, 53–66. doi: 10.1016/j.molcel.2007.06.011

Aliev, G., Gasimov, E., Obrenovich, M. E., Fischbach, K., Shenk, J. C., Smith, M. A., et al. (2008). Atherosclerotic lesions and mitochondria DNA deletions in brain microvessels: implication in the pathogenesis of Alzheimer's disease. *Vasc. Health Risk Manag.* 4, 721–730. doi: 10.2147/vhrm.s2608

Aliev, G., Li, Y., Palacios, H. H., and Obrenovich, M. E. (2011). Oxidative stress induced mitochondrial DNA deletion as a hallmark for the drug development in the context of the cerebrovascular diseases. *Recent Pat. Cardiovasc. Drug Discov.* 6, 222–241. doi: 10.2174/157489011797376942

Aliev, G., Obrenovich, M. E., Tabrez, S., Jabir, N. R., Reddy, V. P., Li, Y., et al. (2013). Link between cancer and Alzheimer disease via oxidative stress induced by nitric oxide-dependent mitochondrial DNA overproliferation and deletion. *Oxid. Med. Cell. Longev.* 2013:962984. doi: 10.1155/2013/962984

Alzheimer's Association. (2016). 2016 Alzheimer's disease facts and figures. *Alzheimers Dement.* 12, 459–509. doi: 10.1016/j.jalz.2016.03.001

Arnould, T., Michel, S., and Renard, P. (2015). Mitochondria retrograde signaling and the UPR mt: where are we in mammals? *Int. J. Mol. Sci.* 16, 18224–18251. doi: 10.3390/ijms160818224

Atwood, C. S., and Bowen, R. L. (2015). A unified hypothesis of early- and late-onset Alzheimer's disease pathogenesis. *J. Alzheimers Dis.* 47, 33–47. doi: 10.3233/JAD-143210

Axten, J. M., Medina, J. R., Feng, Y., Shu, A., Romeril, S. P., Grant, S. W., et al. (2012). Discovery of 7-methyl-5-(1-[3-(trifluoromethyl)phenyl]acetyl-2,3-dihydro- 1*H*-indol-5-yl)-7H-p yrrolo[2,3-*d*]pyrimidin-4-amine (GSK2606414), a potent and selective first-in-class inhibitor of protein kinase R (PKR)-like endoplasmic reticulum kinase (PERK). *J. Med. Chem.* 55, 7193–7207. doi: 10.1021/jm300713s

Baez, E., Echeverria, V., Cabezas, R., Ávila-Rodriguez, M., Garcia-Segura, L. M., and Barreto, G. E. (2016). Protection by neuroglobin expression in brain pathologies. *Front. Neurol.* 7:146. doi: 10.3389/fneur.2016.00146

Baez-Jurado, E., Hidalgo-Lanussa, O., Guio-Vega, G., Ashraf, G. M., Echeverria, V., Aliev, G., et al. (2017). Conditioned medium of human adipose mesenchymal stem cells increases wound closure and protects human astrocytes following scratch assay *in vitro*. *Mol. Neurobiol.* doi: 10.1007/s12035-017-0771-4 [Epub ahead of print].

Barreto, G. E., Gomez, R. M., Bustos, R. H., Forero, D. A., Aliev, G., Tarasov, V. V., et al. (2017). Approaches of the transcriptomic analysis in astrocytes: potential pharmacological targets. *Curr. Pharm. Des.* 23, 4189–4197. doi: 10.2174/1381612823666170406113501

Baumeister, P., Luo, S., Skarnes, W. C., Sui, G., Seto, E., Shi, Y., et al. (2005). Endoplasmic reticulum stress induction of the Grp78/BiP promoter: activating mechanisms mediated by YY1 and its interactive chromatin modifiers. *Mol. Cell. Biol.* 25, 4529–4540. doi: 10.1128/mcb.25.11.4529-4540.2005

Bertolotti, A., Zhang, Y., Hendershot, L. M., Harding, H. P., and Ron, D. (2000). Dynamic interaction of BiP and ER stress transducers in the unfolded-protein response. *Nat. Cell Biol.* 2, 326–332. doi: 10.1038/35014014

Bogorad, A. M., Lin, K. Y., and Marintchev, A. (2017). Novel mechanisms of eIF2B action and regulation by eIF2α phosphorylation. *Nucleic Acids Res.* 45, 11962–11979. doi: 10.1093/nar/gkx845

Casas-Tinto, S., Zhang, Y., Sanchez-Garcia, J., Gomez-Velazquez, M., Rincon-Limas, D. E., and Fernandez-Funez, P. (2011). The ER stress factor XBP1s prevents amyloid-β neurotoxicity. *Hum. Mol. Genet.* 20, 2144–2160. doi: 10.1093/hmg/ddr100

Cass, S. P. (2017). Alzheimer's disease and exercise: a literature review. *Curr. Sports Med. Rep.* 16, 19–22. doi: 10.1249/JSR.0000000000000332

Chang, R. C., Wong, A. K., Ng, H. K., and Hugon, J. (2002). Phosphorylation of eukaryotic initiation factor-2α (eIF2α) is associated with neuronal degeneration in Alzheimer's disease. *Neuroreport* 13, 2429–2432. doi: 10.1097/00001756-200212200-00011

Chen, D., Thomas, E. L., and Kapahi, P. (2009). HIF-1 modulates dietary restriction-mediated lifespan extension via IRE-1 in Caenorhabditis elegans. *PLoS Genet.* 5:e1000486. doi: 10.1371/journal.pgen.1000486

Chyung, J. H., Raper, D. M., and Selkoe, D. J. (2005). γ-secretase exists on the plasma membrane as an intact complex that accepts substrates and effects intramembrane cleavage. *J. Biol. Chem.* 280, 4383–4392. doi: 10.1074/jbc.M409272200

Cisse, M., Duplan, E., Lorivel, T., Dunys, J., Bauer, C., Meckler, X., et al. (2017). The transcription factor XBP1s restores hippocampal synaptic plasticity and memory by control of the Kalirin-7 pathway in Alzheimer model. *Mol. Psychiatry* 22, 1562–1575. doi: 10.1038/mp.2016.152

Citron, M. (2002). Alzheimer's disease: treatments in discovery and development. *Nat. Neurosci.* 5, 1055–1057. doi: 10.1038/nn940

Cleary, J. P., Walsh, D. M., Hofmeister, J. J., Shankar, G. M., Kuskowski, M. A., Selkoe, D. J., et al. (2005). Natural oligomers of the amyloid-β protein specifically disrupt cognitive function. *Nat. Neurosci.* 8, 79–84. doi: 10.1038/nn1372

Cornejo, V. H., and Hetz, C. (2013). The unfolded protein response in Alzheimer's disease. *Semin. Immunopathol.* 35, 277–292. doi: 10.1007/s00281-013-0373-9

Costa-Mattioli, M., Gobert, D., Harding, H., Herdy, B., Azzi, M., Bruno, M., et al. (2005). Translational control of hippocampal synaptic plasticity and memory by the eIF2α kinase GCN2. *Nature* 436, 1166–1173. doi: 10.1038/nature03897

Costa-Mattioli, M., Sossin, W. S., Klann, E., and Sonenberg, N. (2009). Translational control of long-lasting synaptic plasticity and memory. *Neuron* 61, 10–26. doi: 10.1016/j.neuron.2008.10.055

Cramer, P. E., Cirrito, J. R., Wesson, D. W., Lee, C. Y., Karlo, J. C., Zinn, A. E., et al. (2012). ApoE-directed therapeutics rapidly clear β-amyloid and reverse deficits in AD mouse models. *Science* 335, 1503–1506. doi: 10.1126/science.1217697

Cullinan, S. B., and Diehl, J. A. (2004). PERK-dependent activation of Nrf2 contributes to redox homeostasis and cell survival following endoplasmic reticulum stress. *J. Biol. Chem.* 279, 20108–20117. doi: 10.1074/jbc.M314219200

Cullinan, S. B., Zhang, D., Hannink, M., Arvisais, E., Kaufman, R. J., and Diehl, J. A. (2003). Nrf2 is a direct PERK substrate and effector of PERK-dependent cell survival. *Mol. Cell. Biol.* 23, 7198–7209. doi: 10.1128/mcb.23.20.7198-7209.2003

Das, H. K., Tchedre, K., and Mueller, B. (2012). Repression of transcription of presenilin-1 inhibits γ-secretase independent ER Ca^{2+} leak that is impaired by FAD mutations. *J. Neurochem.* 122, 487–500. doi: 10.1111/j.1471-4159.2012.07794.x

de Boer, V. C., de Goffau, M. C., Arts, I. C., Hollman, P. C., and Keijer, J. (2006). SIRT1 stimulation by polyphenols is affected by their stability and metabolism. *Mech. Aging Dev.* 127, 618–627. doi: 10.1016/j.mad.2006.02.007

De Felice, F. G., Wu, D., Lambert, M. P., Fernandez, S. J., Velasco, P. T., Lacor, P. N., et al. (2008). Alzheimer's disease-type neuronal tau hyperphosphorylation induced by Aβ oligomers. *Neurobiol. Aging* 29, 1334–1347. doi: 10.1016/j.neurobiolaging.2007.02.029

Denzel, M. S., Storm, N. J., Gutschmidt, A., Baddi, R., Hinze, Y., Jarosch, E., et al. (2014). Hexosamine pathway metabolites enhance protein quality control and prolong life. *Cell* 156, 1167–1178. doi: 10.1016/j.cell.2014.01.061

Devi, L., and Ohno, M. (2013). Deletion of the eIF2α Kinase GCN2 fails to rescue the memory decline associated with Alzheimer's disease. *PLoS One* 8:e77335. doi: 10.1371/journal.pone.0077335

Devi, L., and Ohno, M. (2014). PERK mediates eIF2α phosphorylation responsible for BACE1 elevation, CREB dysfunction and neurodegeneration in a mouse model of Alzheimer's disease. *Neurobiol. Aging* 35, 2272–2281. doi: 10.1016/j.neurobiolaging.2014.04.031

Ding, F., Yao, J., Rettberg, J. R., Chen, S., and Brinton, R. D. (2013). Early decline in glucose transport and metabolism precedes shift to ketogenic system in female aging and Alzheimer's mouse brain: implication for bioenergetic intervention. *PLoS One* 8:e79977. doi: 10.1371/journal.pone.0079977

Einstein, F. H., Fishman, S., Bauman, J., Thompson, R. F., Huffman, D. M., Atzmon, G., et al. (2008). Enhanced activation of a "nutrient-sensing" pathway with age contributes to insulin resistance. *FASEB J.* 22, 3450–3457. doi: 10.1096/fj.08-109041

Ellgaard, L., and Helenius, A. (2003). Quality control in the endoplasmic reticulum. *Nat. Rev. Mol. Cell Biol.* 4, 181–191. doi: 10.1038/nrm1052

Fiest, K. M., Roberts, J. I., Maxwell, C. J., Hogan, D. B., Smith, E. E., Frolkis, A., et al. (2016). The prevalence and incidence of dementia due to Alzheimer's disease: a systematic review and meta-analysis. *Can. J. Neurol. Sci.* 43, S51–S82. doi: 10.1017/cjn.2016.36

Fonseca, A. C., Ferreiro, E., Oliveira, C. R., Cardoso, S. M., and Pereira, C. F. (2013). Activation of the endoplasmic reticulum stress response by the amyloid-β 1–40 peptide in brain endothelial cells. *Biochim. Biophys. Acta* 1832, 2191–2203. doi: 10.1016/j.bbadis.2013.08.007

Fusakio, M. E., Willy, J. A., Wang, Y., Mirek, E. T., Al Baghdadi, R. J., Adams, C. M., et al. (2016). Transcription factor ATF4 directs basal and stress-induced gene expression in the unfolded protein response and cholesterol metabolism in the liver. *Mol. Biol. Cell* 27, 1536–1551. doi: 10.1091/mbc.E16-01-0039

Genereux, J. C., Qu, S., Zhou, M., Ryno, L. M., Wang, S., Shoulders, M. D., et al. (2015). Unfolded protein response-induced ERdj3 secretion links ER stress to extracellular proteostasis. *EMBO J.* 34, 4–19. doi: 10.15252/embj.201488896

Gourmaud, S., Paquet, C., Dumurgier, J., Pace, C., Bouras, C., Gray, F., et al. (2015). Increased levels of cerebrospinal fluid JNK3 associated with amyloid pathology: links to cognitive decline. *J. Psychiatry Neurosci.* 40, 151–161. doi: 10.1503/jpn.140062

Haass, C., and Selkoe, D. J. (2007). Soluble protein oligomers in neurodegeneration: lessons from the Alzheimer's amyloid β-peptide. *Nat. Rev. Mol. Cell Biol.* 8, 101–112. doi: 10.1038/nrm2101

Halliday, M., and Mallucci, G. R. (2015). Modulating the unfolded protein response to prevent neurodegeneration and enhance memory. *Neuropathol. Appl. Neurobiol.* 41, 414–427. doi: 10.1111/nan.12211

Hamos, J. E., Oblas, B., Pulaski-Salo, D., Welch, W. J., Bole, D. G., and Drachman, D. A. (1991). Expression of heat shock proteins in Alzheimer's disease. *Neurology* 41, 345–350. doi: 10.1212/WNL.41.3.345

Han, J., Back, S. H., Hur, J., Lin, Y.-H., Gildersleeve, R., Shan, J., et al. (2013). ER-stress-induced transcriptional regulation increases protein synthesis leading to cell death. *Nat. Cell Biol.* 15, 481–490. doi: 10.1038/ncb2738

Harding, H. P., Novoa, I., Zhang, Y., Zeng, H., Wek, R., Schapira, M., et al. (2000a). Regulated translation initiation controls stress-induced gene expression in mammalian cells. *Mol. Cell* 6, 1099–1108. doi: 10.1016/s1097-2765(00)00108-8

Harding, H. P., Zhang, Y., Bertolotti, A., Zeng, H., and Ron, D. (2000b). Perk is essential for translational regulation and cell survival during the unfolded protein response. *Mol. Cell* 5, 897–904. doi: 10.1016/s1097-2765(00)80330-5

Harding, H. P., Zhang, Y., and Ron, D. (1999). Protein translation and folding are coupled by an endoplasmic-reticulum-resident kinase. *Nature* 397, 271–274. doi: 10.1038/16729

Harding, H. P., Zhang, Y., Zeng, H., Novoa, I., Lu, P. D., Calfon, M., et al. (2003). An integrated stress response regulates amino acid metabolism and resistance to oxidative stress. *Mol. Cell* 11, 619–633. doi: 10.1016/s1097-2765(03)00105-9

Haze, K., Yoshida, H., Yanagi, H., Yura, T., and Mori, K. (1999). Mammalian transcription factor ATF6 is synthesized as a transmembrane protein and activated by proteolysis in response to endoplasmic reticulum stress. *Mol. Biol. Cell* 10, 3787–3799. doi: 10.1091/mbc.10.11.3787

Hetz, C., Chevet, E., and Oakes, S. A. (2015). Proteostasis control by the unfolded protein response. *Nat. Cell Biol.* 17, 829–838. doi: 10.1038/ncb3184

Hirai, K., Aliev, G., Nunomura, A., Fujioka, H., Russell, R. L., Atwood, C. S., et al. (2001). Mitochondrial abnormalities in Alzheimer's disease. *J. Neurosci.* 21, 3017–3023.

Hoekstra, J. G., Hipp, M. J., Montine, T. J., and Kennedy, S. R. (2016). Mitochondrial DNA mutations increase in early stage Alzheimer disease and are inconsistent with oxidative damage. *Ann. Neurol.* 80, 301–306. doi: 10.1002/ana.24709

Hoozemans, J. J., van Haastert, E. S., Nijholt, D. A., Rozemuller, A. J., Eikelenboom, P., and Scheper, W. (2009). The unfolded protein response is activated in pretangle neurons in Alzheimer's disease hippocampus. *Am. J. Pathol.* 174, 1241–1251. doi: 10.2353/ajpath.2009.080814

Hoozemans, J. J., Veerhuis, R., Van Haastert, E. S., Rozemuller, J. M., Baas, F., Eikelenboom, P., et al. (2005). The unfolded protein response is activated in Alzheimer's disease. *Acta Neuropathol.* 110, 165–172. doi: 10.1007/s00401-005-1038-0

Hussain, S. G., and Ramaiah, K. V. (2007). Reduced eIF2α phosphorylation and increased proapoptotic proteins in aging. *Biochem. Biophys. Res. Commun.* 355, 365–370. doi: 10.1016/j.bbrc.2007.01.156

Ivançević, V., Alavi, A., Souder, E., Mozley, P. D., Gur, R. E., Bénard, F., et al. (2000). Regional cerebral glucose metabolism in healthy volunteers determined by fluordeoxyglucose positron emission tomography: appearance and variance in the transaxial, coronal, and sagittal planes. *Clin. Nucl. Med.* 25, 596–602. doi: 10.1097/00003072-200008000-00005

Jiang, X. Y., Litkowski, P. E., Taylor, A. A., Lin, Y., Snider, B. J., and Moulder, K. L. (2010). A role for the ubiquitin-proteasome system in activity-dependent presynaptic silencing. *J. Neurosci.* 30, 1798–1809. doi: 10.1523/JNEUROSCI.4965-09.2010

Kaushik, S., and Cuervo, A. M. (2015). Proteostasis and aging. *Nat. Med.* 21, 1406–1415. doi: 10.1038/nm.4001

Kawamata, H., and Manfredi, G. (2017). Proteinopathies and OXPHOS dysfunction in neurodegenerative diseases. *J. Cell Biol.* 216, 3917–3929. doi: 10.1083/jcb.201709172

Khachaturian, Z. S. (1989). Calcium, membranes, aging, and Alzheimer's disease. Introduction and overview. *Ann. N Y Acad. Sci.* 568, 1–4. doi: 10.1111/j.1749-6632.1989.tb12485.x

Kim, H. S., Choi, Y., Shin, K. Y., Joo, Y., Lee, Y. K., Jung, S. Y., et al. (2007). Swedish amyloid precursor protein mutation increases phosphorylation of eIF2α *in vitro* and *in vivo*. *J. Neurosci. Res.* 85, 1528–1537. doi: 10.1002/jnr.21267

Kraemer, B. C., Burgess, J. K., Chen, J. H., Thomas, J. H., and Schellenberg, G. D. (2006). Molecular pathways that influence human tau-induced pathology in Caenorhabditis elegans. *Hum. Mol. Genet.* 15, 1483–1496. doi: 10.1093/hmg/ddl067

Krishnamoorthy, T., Pavitt, G. D., Zhang, F., Dever, T. E., and Hinnebusch, A. G. (2001). Tight binding of the phosphorylated α subunit of initiation factor 2 (eIF2α) to the regulatory subunits of guanine nucleotide exchange factor eIF2B is required for inhibition of translation initiation. *Mol. Cell. Biol.* 21, 5018–5030. doi: 10.1128/mcb.21.15.5018-5030.2001

Krishnan, K. J., Ratnaike, T. E., De Gruyter, H. L., Jaros, E., and Turnbull, D. M. (2012). Mitochondrial DNA deletions cause the biochemical defect observed in Alzheimer's disease. *Neurobiol. Aging* 33, 2210–2214. doi: 10.1016/j.neurobiolaging.2011.08.009

Lee, A. H., Iwakoshi, N. N., and Glimcher, L. H. (2003). XBP-1 regulates a subset of endoplasmic reticulum resident chaperone genes in the unfolded protein response. *Mol. Cell. Biol.* 23, 7448–7459. doi: 10.1128/mcb.23.21.7448-7459.2003

Lee, J., Kim, Y., Liu, T., Hwang, Y. J., Hyeon, S. J., Im, H., et al. (2018). SIRT3 deregulation is linked to mitochondrial dysfunction in Alzheimer's disease. *Aging Cell* 17:e12679. doi: 10.1111/acel.12679

Liu, F., Shi, J., Tanimukai, H., Gu, J., Grundke-Iqbal, I., Iqbal, K., et al. (2009). Reduced O-GlcNAcylation links lower brain glucose metabolism

and tau pathology in Alzheimer's disease. *Brain* 132, 1820–1832. doi: 10.1093/brain/awp099

Loewen, C. A., and Feany, M. B. (2010). The unfolded protein response protects from tau neurotoxicity *in vivo*. *PLoS One* 5:e13084. doi: 10.1371/journal.pone.0013084

Lourenco, M. V., Clarke, J. R., Frozza, R. L., Bomfim, T. R., Forny-Germano, L., Batista, A. F., et al. (2013). TNF-α mediates PKR-dependent memory impairment and brain IRS-1 inhibition induced by Alzheimer's β-amyloid oligomers in mice and monkeys. *Cell Metab.* 18, 831–843. doi: 10.1016/j.cmet.2013.11.002

Ma, T., Trinh, M. A., Wexler, A. J., Bourbon, C., Gatti, E., Pierre, P., et al. (2013). Suppression of eIF2α kinases alleviates Alzheimer's disease-related plasticity and memory deficits. *Nat. Neurosci.* 16, 1299–1305. doi: 10.1038/nn.3486

Ma, K., Vattem, K. M., and Wek, R. C. (2002). Dimerization and release of molecular chaperone inhibition facilitate activation of eukaryotic initiation factor-2 kinase in response to endoplasmic reticulum stress. *J. Biol. Chem.* 277, 18728–18735. doi: 10.1074/jbc.M200903200

Marciniak, S. J., Garcia-Bonilla, L., Hu, J., Harding, H. P., and Ron, D. (2006). Activation-dependent substrate recruitment by the eukaryotic translation initiation factor 2 kinase PERK. *J. Cell Biol.* 172, 201–209. doi: 10.1083/jcb.200508099

Marciniak, S. J., Yun, C. Y., Oyadomari, S., Novoa, I., Zhang, Y., Jungreis, R., et al. (2004). CHOP induces death by promoting protein synthesis and oxidation in the stressed endoplasmic reticulum. *Genes Dev.* 18, 3066–3077. doi: 10.1101/gad.1250704

Martínez, G., Vidal, R. L., Mardones, P., Serrano, F. G., Ardiles, A. O., Wirth, C., et al. (2016). Regulation of memory formation by the transcription factor XBP1. *Cell Rep.* 14, 1382–1394. doi: 10.1016/j.celrep.2016.01.028

Minakshi, R., Rahman, S., Jan, A. T., Archana, A., and Kim, J. (2017). Implications of aging and the endoplasmic reticulum unfolded protein response on the molecular modality of breast cancer. *Exp. Mol. Med.* 49:e389. doi: 10.1038/emm.2017.215

Minter, M. R., Taylor, J. M., and Crack, P. J. (2016). The contribution of neuroinflammation to amyloid toxicity in Alzheimer's disease. *J. Neurochem.* 136, 457–474. doi: 10.1111/jnc.13411

Moneim, A. E. (2015). Oxidant/Antioxidant imbalance and the risk of Alzheimer's disease. *Curr. Alzheimer Res.* 12, 335–349. doi: 10.2174/1567205012666150325182702

Mori, K. (2009). Signalling pathways in the unfolded protein response: development from yeast to mammals. *J. Biochem.* 146, 743–750. doi: 10.1093/jb/mvp166

Mosconi, L., Brys, M., Switalski, R., Mistur, R., Glodzik, L., Pirraglia, E., et al. (2007). Maternal family history of Alzheimer's disease predisposes to reduced brain glucose metabolism. *Proc. Natl. Acad. Sci. U S A* 104, 19067–19072. doi: 10.1073/pnas.0705036104

Naidoo, N., Ferber, M., Master, M., Zhu, Y., and Pack, A. I. (2008). Aging impairs the unfolded protein response to sleep deprivation and leads to proapoptotic signaling. *J. Neurosci.* 28, 6539–6548. doi: 10.1523/JNEUROSCI.5685-07.2008

Niccoli, T., Cabecinha, M., Tillmann, A., Kerr, F., Wong, C. T., Cardenes, D., et al. (2016). Increased glucose transport into neurons rescues Aβ toxicity in Drosophila. *Curr. Biol.* 26, 2291–2300. doi: 10.1016/j.cub.2016.07.017

Nijholt, D. A., de Graaf, T. R., van Haastert, E. S., Oliveira, A. O., Berkers, C. R., Zwart, R., et al. (2011). Endoplasmic reticulum stress activates autophagy but not the proteasome in neuronal cells: implications for Alzheimer's disease. *Cell Death Differ.* 18, 1071–1081. doi: 10.1038/cdd.2010.176

Nuss, J. E., Choksi, K. B., Deford, J. H., and Papaconstantinou, J. (2008). Decreased enzyme activities of chaperones PDI and BiP in aged mouse livers. *Biochem. Biophys. Res. Commun.* 365, 355–361. doi: 10.1016/j.bbrc.2007.10.194

O'Connor, T., Sadleir, K. R., Maus, E., Velliquette, R. A., Zhao, J., Cole, S. L., et al. (2008). Phosphorylation of the translation initiation factor eIF2α increases BACE1 levels and promotes amyloidogenesis. *Neuron* 60, 988–1009. doi: 10.1016/j.neuron.2008.10.047

Ohno, M. (2014). Roles of eIF2α kinases in the pathogenesis of Alzheimer's disease. *Front. Mol. Neurosci.* 7:22. doi: 10.3389/fnmol.2014.00022

Onuki, R., Bando, Y., Suyama, E., Katayama, T., Kawasaki, H., Baba, T., et al. (2004). An RNA-dependent protein kinase is involved in tunicamycin-induced apoptosis and Alzheimer's disease. *EMBO J.* 23, 959–968. doi: 10.1038/sj.emboj.7600049

Onyango, P., Celic, I., McCaffery, J. M., Boeke, J. D., and Feinberg, A. P. (2002). SIRT3, a human SIR2 homologue, is an NAD-dependent deacetylase localized to mitochondria. *Proc. Natl. Acad. Sci. U S A* 99, 13653–13658. doi: 10.1073/pnas.222538099

Onyango, I. G., Dennis, J., and Khan, S. M. (2016). Mitochondrial dysfunction in Alzheimer's disease and the rationale for bioenergetics based therapies. *Aging Dis.* 7, 201–214. doi: 10.14336/AD.2015.1007

Page, G., Rioux Bilan, A., Ingrand, S., Lafay-Chebassier, C., Pain, S., Perault Pochat, M. C., et al. (2006). Activated double-stranded RNA-dependent protein kinase and neuronal death in models of Alzheimer's disease. *Neuroscience* 139, 1343–1354. doi: 10.1016/j.neuroscience.2006.01.047

Paz Gavilán, M., Vela, J., Castaño, A., Ramos, B., del Río, J. C., Vitorica, J., et al. (2006). Cellular environment facilitates protein accumulation in aged rat hippocampus. *Neurobiol. Aging* 27, 973–982. doi: 10.1016/j.neurobiolaging.2005.05.010

Rabek, J. P., Boylston, W. H. III., and Papaconstantinou, J. (2003). Carbonylation of ER chaperone proteins in aged mouse liver. *Biochem. Biophys. Res. Commun.* 305, 566–572. doi: 10.1016/s0006-291x(03)00826-x

Radford, H., Moreno, J. A., Verity, N., Halliday, M., and Mallucci, G. R. (2015). PERK inhibition prevents tau-mediated neurodegeneration in a mouse model of frontotemporal dementia. *Acta Neuropathol.* 130, 633–642. doi: 10.1007/s00401-015-1487-z

Rahman, S., Jan, A. T., Ayyagari, A., Kim, J., Kim, J., and Minakshi, R. (2017). Entanglement of UPRER in aging driven neurodegenerative diseases. *Front. Aging Neurosci.* 9:341. doi: 10.3389/fnagi.2017.00341

Reddy, P. H., Manczak, M., and Yin, X. (2017). Mitochondria-division inhibitor 1 protects against amyloid-β induced mitochondrial fragmentation and synaptic damage in Alzheimer's disease. *J. Alzheimers Dis.* 58, 147–162. doi: 10.3233/JAD-170051

Resende, R., Ferreiro, E., Pereira, C., and Oliveira, C. R. (2008). ER stress is involved in Aβ-induced GSK-3β activation and tau phosphorylation. *J. Neurosci. Res.* 86, 2091–2099. doi: 10.1002/jnr.21648

Revel, F., Gilbert, T., Roche, S., Drai, J., Blond, E., Ecochard, R., et al. (2015). Influence of oxidative stress biomarkers on cognitive decline. *J. Alzheimers Dis.* 45, 553–560. doi: 10.3233/JAD-141797

Romero-Ramirez, L., Cao, H., Nelson, D., Hammond, E., Lee, A. H., Yoshida, H., et al. (2004). XBP1 is essential for survival under hypoxic conditions and is required for tumor growth. *Cancer Res.* 64, 5943–5947. doi: 10.1158/0008-5472.can-04-1606

Sami, N., Rahman, S., Kumar, V., Zaidi, S., Islam, A., Ali, S., et al. (2017). Protein aggregation, misfolding and consequential human neurodegenerative diseases. *Int. J. Neurosci.* 127, 1047–1057. doi: 10.1080/00207454.2017.1286339

Scheltens, P., Blennow, K., Breteler, M. M., de Strooper, B., Frisoni, G. B., Salloway, S., et al. (2016). Alzheimer's disease. *Lancet* 388, 505–517. doi: 10.1016/S0140-6736(15)01124-1

Scheper, W., and Hoozemans, J. J. (2015). The unfolded protein response in neurodegenerative diseases: a neuropathological perspective. *Acta Neuropathol.* 130, 315–331. doi: 10.1007/s00401-015-1462-8

Schroder, M., and Kaufman, R. J. (2005). The mammalian unfolded protein response. *Annu. Rev. Biochem.* 74, 739–789. doi: 10.1146/annurev.biochem.73.011303.074134

Sekine, Y., Zyryanova, A., Crespillo-Casado, A., Fischer, P. M., Harding, H. P., and Ron, D. (2015). Stress responses. Mutations in a translation initiation factor identify the target of a memory-enhancing compound. *Science* 348, 1027–1030. doi: 10.1126/science.aaa6986

Selkoe, D. J. (2001a). Alzheimer's disease results from the cerebral accumulation and cytotoxicity of amyloid β-protein. *J. Alzheimers Dis.* 3, 75–80. doi: 10.3233/jad-2001-3111

Selkoe, D. J. (2001b). Alzheimer's disease: genes, proteins, and therapy. *Physiol. Rev.* 81, 741–766. doi: 10.1152/physrev.2001.81.2.741

Selkoe, D. J. (2004a). Alzheimer disease: mechanistic understanding predicts novel therapies. *Ann. Intern. Med.* 140, 627–638. doi: 10.7326/0003-4819-140-8-200404200-00047

Selkoe, D. J. (2004b). Cell biology of protein misfolding: the examples of Alzheimer's and Parkinson's diseases. *Nat. Cell Biol.* 6, 1054–1061. doi: 10.1038/ncb1104-1054

Shen, J., Chen, X., Hendershot, L., and Prywes, R. (2002). ER stress regulation of ATF6 localization by dissociation of BiP/GRP78 binding and unmasking

of Golgi localization signals. *Dev. Cell* 3, 99–111. doi: 10.1016/s1534-5807(02)00203-4

Shoji, M., Iwakami, N., Takeuchi, S., Waragai, M., Suzuki, M., Kanazawa, I., et al. (2000). JNK activation is associated with intracellular β-amyloid accumulation. *Brain Res. Mol. Brain Res.* 85, 221–233. doi: 10.1016/s0169-328x(00)00245-x

Shoulders, M. D., Ryno, L. M., Genereux, J. C., Moresco, J. J., Tu, P. G., Wu, C., et al. (2013). Stress-independent activation of XBP1s and/or ATF6 reveals three functionally diverse ER proteostasis environments. *Cell Rep.* 3, 1279–1292. doi: 10.1016/j.celrep.2013.03.024

Sidrauski, C., Acosta-Alvear, D., Khoutorsky, A., Vedantham, P., Hearn, B. R., Li, H., et al. (2013). Pharmacological brake-release of mRNA translation enhances cognitive memory. *Elife* 2:e00498. doi: 10.7554/eLife.00498

Sidrauski, C., McGeachy, A. M., Ingolia, N. T., and Walter, P. (2015). The small molecule ISRIB reverses the effects of eIF2α phosphorylation on translation and stress granule assembly. *Elife* 4:e05033. doi: 10.7554/eLife.05033

Smith, H. L., and Mallucci, G. R. (2016). The unfolded protein response: mechanisms and therapy of neurodegeneration. *Brain* 139, 2113–2121. doi: 10.1093/brain/aww101

Someya, S., Yu, W., Hallows, W. C., Xu, J., Vann, J. M., Leeuwenburgh, C., et al. (2010). Sirt3 mediates reduction of oxidative damage and prevention of age-related hearing loss under caloric restriction. *Cell* 143, 802–812. doi: 10.1016/j.cell.2010.10.002

Sorrentino, V., Romani, M., Mouchiroud, L., Beck, J. S., Zhang, H., D'Amico, D., et al. (2017). Enhancing mitochondrial proteostasis reduces amyloid-β proteotoxicity. *Nature* 552, 187–193. doi: 10.1038/nature25143

Suganthy, N., Devi, K. P., Nabavi, S. F., Braidy, N., and Nabavi, S. M. (2016). Bioactive effects of quercetin in the central nervous system: focusing on the mechanisms of actions. *Biomed. Pharmacother.* 84, 892–908. doi: 10.1016/j.biopha.2016.10.011

Supnet, C., and Bezprozvanny, I. (2010). The dysregulation of intracellular calcium in Alzheimer disease. *Cell Calcium* 47, 183–189. doi: 10.1016/j.ceca.2009.12.014

Swerdlow, R. H., Burns, J. M., and Khan, S. M. (2014). The Alzheimer's disease mitochondrial cascade hypothesis: progress and perspectives. *Biochim. Biophys. Acta* 1842, 1219–1231. doi: 10.1016/j.bbadis.2013.09.010

Takashima, A., Noguchi, K., Michel, G., Mercken, M., Hoshi, M., Ishiguro, K., et al. (1996). Exposure of rat hippocampal neurons to amyloid β peptide (25–35) induces the inactivation of phosphatidyl inositol-3 kinase and the activation of tau protein kinase I/glycogen synthase kinase-3 β. *Neurosci. Lett.* 203, 33–36. doi: 10.1016/s0006-3495(96)79570-x

Takashima, A., Noguchi, K., Sato, K., Hoshino, T., and Imahori, K. (1993). Tau protein kinase I is essential for amyloid β-protein-induced neurotoxicity. *Proc. Natl. Acad. Sci. U S A* 90, 7789–7793. doi: 10.1073/pnas.90.16.7789

Tatarnikova, O. G., Orlov, M. A., and Bobkova, N. V. (2015). β-amyloid and tau-protein: structure, interaction, and prion-like properties. *Biochemistry (Mosc)* 80, 1800–1819. doi: 10.1134/S000629791513012X

Taylor, R. C., and Dillin, A. (2013). XBP-1 is a cell-nonautonomous regulator of stress resistance and longevity. *Cell* 153, 1435–1447. doi: 10.1016/j.cell.2013.05.042

Tirasophon, W., Welihinda, A. A., and Kaufman, R. J. (1998). A stress response pathway from the endoplasmic reticulum to the nucleus requires a novel bifunctional protein kinase/endoribonuclease (Ire1p) in mammalian cells. *Genes Dev.* 12, 1812–1824. doi: 10.1101/gad.12.12.1812

Tomidokoro, Y., Ishiguro, K., Harigaya, Y., Matsubara, E., Ikeda, M., Park, J. M., et al. (2001). Aβ amyloidosis induces the initial stage of tau accumulation in APP(Sw) mice. *Neurosci. Lett.* 299, 169–172. doi: 10.1016/s0304-3940(00)01767-5

Urano, F., Wang, X., Bertolotti, A., Zhang, Y., Chung, P., Harding, H. P., et al. (2000). Coupling of stress in the ER to activation of JNK protein kinases by transmembrane protein kinase IRE1. *Science* 287, 664–666. doi: 10.1126/science.287.5453.664

Volgyi, K., Juhász, G., Kovacs, Z., and Penke, B. (2015). Dysfunction of endoplasmic reticulum (ER) and mitochondria (MT) in Alzheimer's disease: the role of the ER-MT cross-talk. *Curr. Alzheimer Res.* 12, 655–672. doi: 10.2174/1567205012666150710095035

Vukic, V., Callaghan, D., Walker, D., Lue, L. F., Liu, Q. Y., Couraud, P. O., et al. (2009). Expression of inflammatory genes induced by β-amyloid peptides in human brain endothelial cells and in Alzheimer's brain is mediated by the JNK-AP1 signaling pathway. *Neurobiol. Dis.* 34, 95–106. doi: 10.1016/j.nbd.2008.12.007

Walter, P., and Ron, D. (2011). The unfolded protein response: from stress pathway to homeostatic regulation. *Science* 334, 1081–1086. doi: 10.1126/science.1209038

Wang, Z. V., Deng, Y., Gao, N., Pedrozo, Z., Li, D. L., Morales, C. R., et al. (2014). Spliced X-box binding protein 1 couples the unfolded protein response to hexosamine biosynthetic pathway. *Cell* 156, 1179–1192. doi: 10.1016/j.cell.2014.01.014

Wang, W., Yin, J., Ma, X., Zhao, F., Siedlak, S. L., Wang, Z., et al. (2017). Inhibition of mitochondrial fragmentation protects against Alzheimer's disease in rodent model. *Hum. Mol. Genet.* 26, 4118–4131. doi: 10.1093/hmg/ddx299

Wijesekara, N., Ahrens, R., Sabale, M., Wu, L., Ha, K., Verdile, G., et al. (2017). Amyloid-β and islet amyloid pathologies link Alzheimer disease and type 2 diabetes in a transgenic model. *FASEB J.* 31, 5409–5418. doi: 10.1096/fj.201700431R

Willette, A. A., Bendlin, B. B., Starks, E. J., Birdsill, A. C., Johnson, S. C., Christian, B. T., et al. (2015). Association of insulin resistance with cerebral glucose uptake in late middle-aged adults at risk for Alzheimer disease. *JAMA Neurol.* 72, 1013–1020. doi: 10.1001/jamaneurol.2015.0613

Yamamoto, K., Sato, T., Matsui, T., Sato, M., Okada, T., Yoshida, H., et al. (2007). Transcriptional induction of mammalian ER quality control proteins is mediated by single or combined action of ATF6α and XBP1. *Dev. Cell* 13, 365–376. doi: 10.1016/j.devcel.2007.07.018

Ying, M., Sui, X., Zhang, Y., Sun, Q., Qu, Z., Luo, X., et al. (2017). Identification of novel key molecules involved in spatial memory impairment in triple transgenic mice of Alzheimer's disease. *Mol. Neurobiol.* 54, 3843–3858. doi: 10.1007/s12035-016-9959-2

Yoon, S. S., and Jo, S. A. (2012). Mechanisms of amyloid-β peptide clearance: potential therapeutic targets for Alzheimer's disease. *Biomol. Ther. (Seoul)* 20, 245–255. doi: 10.4062/biomolther.2012.20.3.245

Yoshida, H., Haze, K., Yanagi, H., Yura, T., and Mori, K. (1998). Identification of the cis-acting endoplasmic reticulum stress response element responsible for transcriptional induction of mammalian glucose-regulated proteins. Involvement of basic leucine zipper transcription factors. *J. Biol. Chem.* 273, 33741–33749. doi: 10.1074/jbc.273.50.33741

Yoshida, H., Matsui, T., Hosokawa, N., Kaufman, R. J., Nagata, K., and Mori, K. (2003). A time-dependent phase shift in the mammalian unfolded protein response. *Dev. Cell* 4, 265–271. doi: 10.1016/s1534-5807(03)00022-4

Yoshida, H., Matsui, T., Yamamoto, A., Okada, T., and Mori, K. (2001). XBP1 mRNA is induced by ATF6 and spliced by IRE1 in response to ER stress to produce a highly active transcription factor. *Cell* 107, 881–891. doi: 10.1016/s0092-8674(01)00611-0

Zeng, T., Peng, L., Chao, H., Xi, H., Fu, B., Wang, Y., et al. (2015). IRE1α-TRAF2-ASK1 complex-mediated endoplasmic reticulum stress and mitochondrial dysfunction contribute to CXC195-induced apoptosis in human bladder carcinoma T24 cells. *Biochem. Biophys. Res. Commun.* 460, 530–536. doi: 10.1016/j.bbrc.2015.03.064

Zhou, Q., Wang, M., Du, Y., Zhang, W., Bai, M., Zhang, Z., et al. (2015). Inhibition of c-Jun N-terminal kinase activation reverses Alzheimer disease phenotypes in APPswe/PS1dE9 mice. *Ann. Neurol.* 77, 637–654. doi: 10.1002/ana.24361

Zhu, Z., Yan, J., Jiang, W., Yao, X. G., Chen, J., Chen, L., et al. (2013). Arctigenin effectively ameliorates memory impairment in Alzheimer's disease model mice targeting both β-amyloid production and clearance. *J. Neurosci.* 33, 13138–13149. doi: 10.1523/JNEUROSCI.4790-12.2013

Conflict of Interest Statement: The authors declare that the research was conducted in the absence of any commercial or financial relationships that could be construed as a potential conflict of interest.

Copyright © 2018 Rahman, Archana, Jan and Minakshi. This is an open-access article distributed under the terms of the Creative Commons Attribution License (CC BY). The use, distribution or reproduction in other forums is permitted, provided the original author(s) and the copyright owner are credited and that the original publication in this journal is cited, in accordance with accepted academic practice. No use, distribution or reproduction is permitted which does not comply with these terms.

frontiers in Aging Neuroscience

REVIEW
published: 30 January 2018
doi: 10.3389/fnagi.2018.00004

Autophagy and Alzheimer's Disease: From Molecular Mechanisms to Therapeutic Implications

Md. Sahab Uddin[1], Anna Stachowiak[2], Abdullah Al Mamun[1], Nikolay T. Tzvetkov[3], Shinya Takeda[4], Atanas G. Atanasov[5,6], Leandro B. Bergantin[7], Mohamed M. Abdel-Daim[8,9] and Adrian M. Stankiewicz[5]**

[1] Department of Pharmacy, Southeast University, Dhaka, Bangladesh, [2] Department of Experimental Embryology, Institute of Genetics and Animal Breeding, Polish Academy of Sciences, Magdalenka, Poland, [3] Department of Molecular Biology and Biochemical Pharmacology, Institute of Molecular Biology "Roumen Tsanev", Bulgarian Academy of Sciences, Sofia, Bulgaria, [4] Department of Clinical Psychology, Tottori University Graduate School of Medical Sciences, Tottori, Japan, [5] Department of Molecular Biology, Institute of Genetics and Animal Breeding, Polish Academy of Sciences, Magdalenka, Poland, [6] Department of Pharmacognosy, University of Vienna, Vienna, Austria, [7] Department of Pharmacology, Federal University of São Paulo, São Paulo, Brazil, [8] Department of Pharmacology, Suez Canal University, Ismailia, Egypt, [9] Department of Ophthalmology and Micro-technology, Yokohama City University, Yokohama, Japan

OPEN ACCESS

Edited by:
Mohammad Amjad Kamal, King Abdulaziz University, Saudi Arabia

Reviewed by:
Charles Harrington, University of Aberdeen, United Kingdom
Caterina Scuderi, Sapienza Università di Roma, Italy
Agustina Alaimo, Universidad de Buenos Aires, Argentina

***Correspondence:**
Adrian M. Stankiewicz
adrianstankiewicz85@gmail.com
Atanas G. Atanasov
a.atanasov@ighz.pl

Received: *30 October 2017*
Accepted: *08 January 2018*
Published: *30 January 2018*

Citation:
Uddin MS, Stachowiak A, Mamun AA, Tzvetkov NT, Takeda S, Atanasov AG, Bergantin LB, Abdel-Daim MM and Stankiewicz AM (2018) Autophagy and Alzheimer's Disease: From Molecular Mechanisms to Therapeutic Implications. Front. Aging Neurosci. 10:4. doi: 10.3389/fnagi.2018.00004

Alzheimer's disease (AD) is the most common cause of progressive dementia in the elderly. It is characterized by a progressive and irreversible loss of cognitive abilities and formation of senile plaques, composed mainly of amyloid β (Aβ), and neurofibrillary tangles (NFTs), composed of tau protein, in the hippocampus and cortex of afflicted humans. In brains of AD patients the metabolism of Aβ is dysregulated, which leads to the accumulation and aggregation of Aβ. Metabolism of Aβ and tau proteins is crucially influenced by autophagy. Autophagy is a lysosome-dependent, homeostatic process, in which organelles and proteins are degraded and recycled into energy. Thus, dysfunction of autophagy is suggested to lead to the accretion of noxious proteins in the AD brain. In the present review, we describe the process of autophagy and its importance in AD. Additionally, we discuss mechanisms and genes linking autophagy and AD, i.e., the mTOR pathway, neuroinflammation, endocannabinoid system, *ATG7, BCL2, BECN1, CDK5, CLU, CTSD, FOXO1, GFAP, ITPR1, MAPT, PSEN1, SNCA, UBQLN1*, and *UCHL1*. We also present pharmacological agents acting via modulation of autophagy that may show promise in AD therapy. This review updates our knowledge on autophagy mechanisms proposing novel therapeutic targets for the treatment of AD.

Keywords: autophagy, Alzheimer's disease, amyloid beta, tau

INTRODUCTION

Introduced to biology in 1963 by Belgian biochemist Christian de Duve (De Duve and Wattiaux, 1966) autophagy (from Greek "self-eating") is an intracellular self-degradative process that is responsible for the systematic degradation and recycling of cellular components such as misfolded or accumulated proteins and damaged organelles (Glick et al., 2010). In 2016, the Japanese cell

Abbreviations: Aβ, Amyloid β; AD, Alzheimer's disease; CSF, cerebrospinal fluid; MAPT, microtubule-associated protein tau; NFTs, neurofibrillary tangles.

biologist Yoshinori Ohsumi was awarded Nobel Prize in Physiology or Medicine for identification of autophagy-related genes and the discovery of the mechanisms of autophagy (Nobelprize.org, 2017).

Autophagy has been classified into three categories based on the mechanism by which intracellular constituents are supplied into lysosome for degradation: microautophagy, chaperone-mediated autophagy, and macroautophagy. In microautophagy, the cytoplasmic material is absorbed into lysosome by direct invagination of the lysosomal membrane (Marzella et al., 1981). The chaperone-mediated autophagy facilitates the degradation of cytosolic proteins by directly targeting them to lysosomes and into the lysosomal lumen (Kaushik and Cuervo, 2012). In macroautophagy, degradable contents of cytoplasm are encapsulated in subcellular double-membrane structures named "autophagosomes". Autophagosomes transport the cell "waste" to the lysosomes for degradation (Settembre et al., 2013). Macroautophagy is the most predominant form of autophagy and will be denoted as such in this review.

Healthy mammalian cells show a low basal level of autophagy (Funderburk et al., 2010). This basal autophagic activity plays a dominant role in the intracellular homeostatic turnover of proteins and organelles (Funderburk et al., 2010). Basal activity of autophagy is essential in post-mitotic neuronal cells, possibly due to their inability to dilute noxious components through cell division (Funderburk et al., 2010). Autophagic activity is enhanced by diverse stresses such as nutrient starvation, hypoxia or inflammation (Melendez and Neufeld, 2008; Francois et al., 2013). Enhanced autophagy participates in various physiological processes and pathological conditions, including cell death, removal of microorganisms invading the cell, and tumor suppression (Glick et al., 2010). On the other hand, reduced autophagic potential is associated with aging (Rubinsztein et al., 2011). During autophagy, proteins are degraded into amino acids, which provide an energy source and are likely used as building blocks for protein synthesis (Onodera and Ohsumi, 2005; Meijer et al., 2015). Thus, dysregulated autophagy may result in accumulation of proteins inside the cell. Various autophagy dysfunctions may contribute to neurodegeneration or neurodegeneration-like symptoms, for example inhibition of the fusion of an autophagosome with a lysosome (Boland et al., 2008), reduction of lysosomal acidification (Shen and Mizushima, 2014) or accumulation of proteins in cells (Garcia-Arencibia et al., 2010).

Alzheimer's disease is the most predominant type of dementia diagnosed in the aged people (Uddin et al., 2016). It is characterized by a chronic, irreversible, and progressive neuronal degradation in the human brain caused by complex pathophysiological processes, including oxidative stress, neuroinflammation, excitotoxicity, mitochondrial dysfunction, proteolytic stress, and more (Jellinger, 2010). Formation of intracellular NFTs and extracellular senile plaques in the brain are two common hallmarks of AD (Armstrong, 2009). NFTs consist of aggregated, abnormally hyperphosphorylated MAPT (Iqbal et al., 2010). Senile plaques are primarily composed of insoluble and toxic amyloid-β (Aβ) peptides and of dysfunctional dystrophic neurites, which include abnormally large amounts of neurofilament, tau, or chromogranin A proteins (Dickson et al., 1999; Armstrong, 2009).

Despite the accumulated wealth of knowledge, AD remains incurable. The significance of autophagy in pathophysiology of AD is now appreciated due to the discoveries of molecular mechanisms for autophagy. The objective of this review is to introduce an outline of the discovery of autophagy and describe the relationship between autophagy and AD.

Please consider, that in the present review the names of genes are written in italic, while names of proteins are written in standard font. Names of human or *Saccharomyces* sp. genes/proteins are written in all capital letters. Names of rodent genes/proteins are written in capital letter followed by small letters.

HISTORY OF AUTOPHAGY RESEARCH

Lysosome

In the mid 1950's researchers explored a novel specialized cellular substructure (organelle), encapsulating enzymes that digest macromolecules such as proteins and lipids (Xu and Ren, 2015). This compartment was named "lysosome" (de Duve, 2005). The lysosome was discovered by the Belgian cytologist and biochemist Christian de Duve. For this achievement de Duve was awarded the 1974 Nobel Prize in Physiology or Medicine (Blobel, 2013).

The lysosome is generally 100–1500 nanometers in diameter and enclosed by a typical lipid bilayer membrane (Xu and Ren, 2015). Lysosomes contain more than 60 different hydrolase enzymes such as proteases and lipases (Xu and Ren, 2015). The lysosomal enzymes are the most active in acidic environment, such as this in the lumen of a lysosome (pH of approximately 4.6) (Xu and Ren, 2015). This characteristic of lysosomal enzymes provides protection against unrestrained, pathological digestion of the constituents of the cell, as cytosol pH is almost neutral (pH 7.2) (Alberts et al., 2002). Hence, even if lysosomal membrane would become damaged and the enzymes were to leak into the cytosol, harm to the cell itself would be minimal (Alberts et al., 2002).

Lysosomes serve as an intracellular digestive system protecting the cell from its unused and/or noxious constituents (Huber and Teis, 2016). Furthermore, lysosomes are involved in various cell processes, including secretion, cell membrane repair, cell signaling and energy metabolism (Settembre et al., 2013). Mutations in the genes involved in the synthesis of lysosomal proteins have been linked to over 40 human genetic diseases (lysosomal storage diseases) (Parenti et al., 2013).

Proteasome

Like autophagy, the ubiquitin-proteasome system is another degradation pathway for cellular proteins. During the 1970's

and 1980's, researchers began to study second system of cell protein degradation, namely the "proteasome". The significance of intracellular proteolytic degradation and the contribution of ubiquitin-proteasome system to the proteolytic pathways (i.e., discovery of ubiquitin-mediated proteolysis) was acknowledged with the award of the Nobel Prize in Chemistry in 2004 to the Israeli biologist Aaron Ciechanover; the Hungarian-born Israeli biochemist Avram Hershko and the American biologist Irwin Rose (Karigar and Murthy, 2005).

Proteasomes are large, multisubunit protease complexes that are responsible for the degradation of unnecessary or damaged proteins by proteolysis (Tanaka et al., 2004). Proteasomal degradation produces amino acids, which may be subsequently used in generation of new proteins (Rogel et al., 2010). Proteins are labeled for degradation with a 76-amino acid protein called "ubiquitin" (Weissman, 2001). Single labeling event leads to a cascade, resulting in the formation of polyubiquitin chain, which binds to the proteasome for proteolysis (Ciechanover and Schwartz, 1998; Li and Ye, 2008).

The proteasomal degradation pathway plays an important role in numerous cellular processes, for example cell cycle and immune response (Ciechanover and Schwartz, 1998). Improper ubiquitin-mediated protein degradation has been linked to several neurodegenerative disorders including AD, Parkinson's disease, Huntington's disease and amyotrophic lateral sclerosis (Atkin and Paulson, 2014).

Recent studies showed the existence of cross-talk between proteasomal and autophagy pathways (Lilienbaum, 2013). Both processes share protein degradation signaling network molecules, may be recruited by ubiquitinated substrates, and under specific conditions display compensatory functions to maintain cellular homeostasis (Lilienbaum, 2013).

Autophagosome

Additional biochemical and microscopic investigations identified a new type of vesicles carrying cellular cargo to the lysosome for degradation. Christian de Duve, the discoverer of the lysosome, introduced the term "autophagy" to define this process (Klionsky, 2008). The new vesicles were named autophagosomes (Klionsky, 2008). Autophagy research was kick-started in 1990s with studies performed by Yoshinori Ohsumi, for which he was awarded the 2016 Nobel Prize in Physiology or Medicine (Nobelprize.org, 2017).

He studied autophagy using as a model organism the budding yeast (Takeshige et al., 1992), whose vacuole is functionally similar to the mammalian lysosome (Li and Kane, 2009). His group has shown that starved yeast devoid of some of the functional vacuolar proteases developed spherical bodies inside the vacuoles (Takeshige et al., 1992). These bodies were encompassed by a membrane and contained constituents of cytosol such as cytoplasmic ribosomes, mitochondria, rough endoplasmic reticulum fragments, glycogen, etc. The constituents would be normally degraded in yeast cultured on the nutrient-poor medium to facilitate adaptation to adverse environment. Without functional proteases the degradation could not commence, and so the spherical bodies remained easily perceivable. These spherical structures were named "autophagic bodies".

In 1993, Ohsumi's group published research, in which they identified 15 genes (*APG1-15)* that are essential for the activation of autophagy in yeast cells (Tsukada and Ohsumi, 1993). Later, as a result of efforts of the scientific community to standardize the gene names, the *APG* genes were renamed to *ATG* (Klionsky et al., 2003). Afterward, Ohsumi's group cloned numerous *ATG* genes and identified the function of their protein products (e.g., Funakoshi et al., 1997; Matsuura et al., 1997). Further studies established the interactions between these products providing the basis for autophagy mechanisms (see **Figure 1**). They found that the ATG1 protein (now: ULK1) combines with the product of the *ATG13* gene to form autophagic complex (Kamada et al., 2000). This process is controlled by target of rapamycin (TOR) kinase (Kamada et al., 2000). Further, Ohsumi's group established that for proper activation the ATG1 protein needs to form complex not only with ATG13, but also with ATG17 (RB1CC1/FIP200) (**Figure 1**) (Ohsumi, 2014). As shown in **Figure 1**, the formation of this complex is the first stage in autophagosome genesis (The Nobel Assembly at Karolinska Institutet, 2016). The phosphatidylinositol-3 kinase (PI3K) complex that is composed of PIK3C3 (VPS34), PIK3R4 (VPS15), BECN1, and ATG14 (Barkor) proteins (Ohsumi, 2014), produces phosphatidylinositol-3 phosphate (PtdIns3P or PI3P), which facilitates binding of further effector proteins to the membrane of the autophagosome (Ohsumi, 2014).

In the late 1990', Ohsumi's group discovered two ubiquitin-like conjugation systems involved in the autophagosome formation (**Figure 1**) (Ohsumi, 2014). First conjugation system results in a formation of an ATG12-ATG5 complex, while the second one results in the formation of a conjugate of ATG8 (MAP1LC3A/GABARAPL2/LC3) with a membrane phospholipid, phosphatidylethanolamine (Ohsumi, 2014). The formation of both conjugates is mediated by the ATG7 protein (Ohsumi, 2014). ATG12-related system regulates ATG8 lipidation and lipidated ATG8 is a crucial participant in the processes of autophagosome elongation (Nakatogawa et al., 2007; Nakatogawa, 2013). These two conjugation systems are evolutionary conserved among yeast and mammals (Ohsumi, 2014). Actually, fluorescently labeled product of the mammalian homologue of yeast gene *ATG8* is used as an indicator of the formation of autophagosome in mammalian systems (Kabeya et al., 2000; Mizushima et al., 2004).

The *ATG* genes proved to play crucial roles in mammalian organisms. For example, mice with knock-out of *ATG5* gene die in the first days of life due to their inability to cope with the post-labor starvation period (Kuma et al., 2004). In this life period, functional autophagy allows the neonate to keep the steady energy supply before milk feeding starts (Kuma et al., 2004). Further studies on knockout mouse models lacking functional versions of autophagy-related genes have established the functions of the autophagy

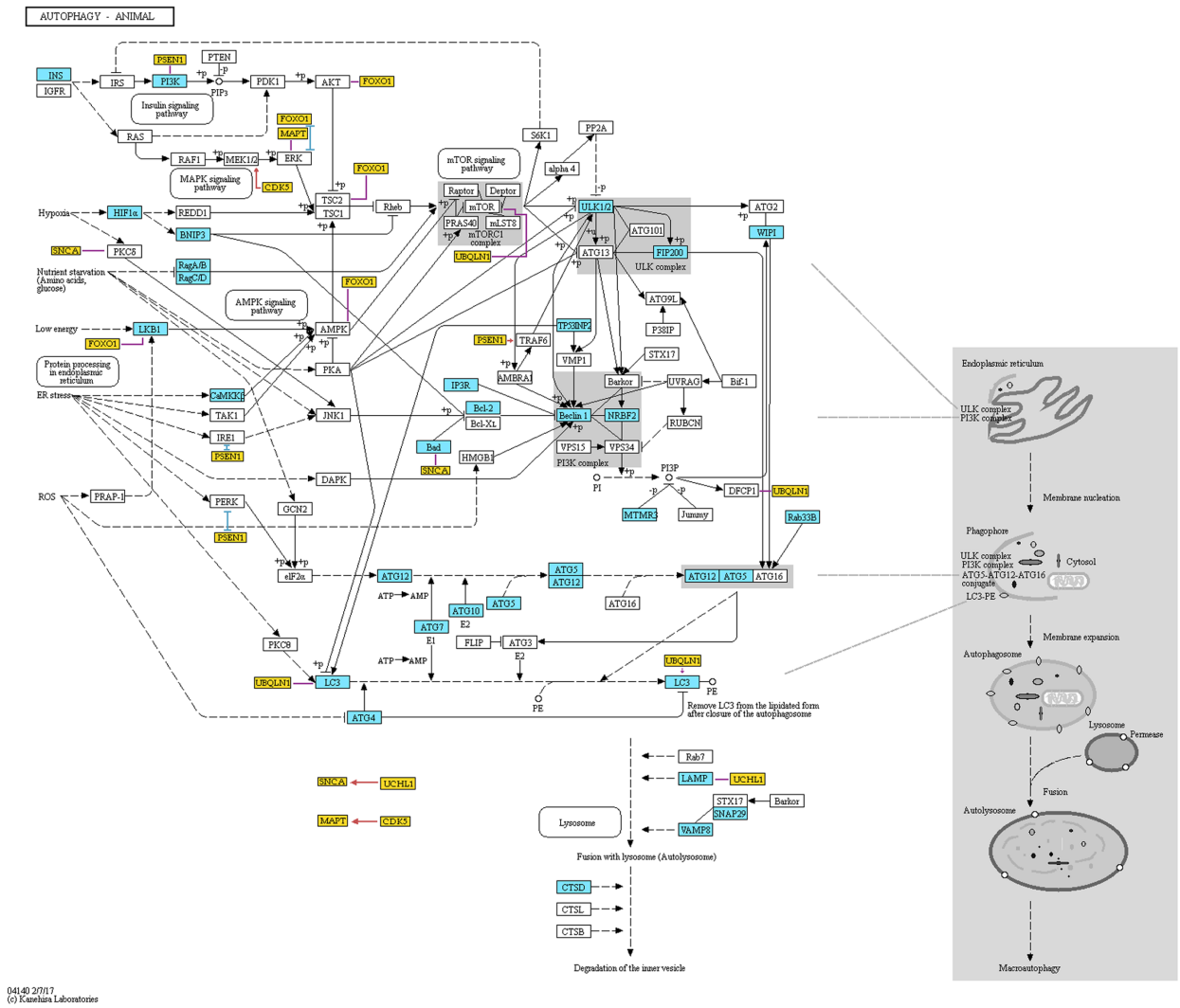


FIGURE 1 | Representation of proteins and protein complexes involved in the "Autophagy – animal" KEGG pathway. This figure was taken from the KEGG database (http://www.genome.jp/kegg-bin/show_pathway?ko04140) and modified. Blue boxes mark the proteins that are associated with AD. Orange boxes mark additional proteins that are not originally included in the pathway. These genes are associated with both AD and autophagy, and are discussed in the present review. Red, blue, and violet lines mark partners with which the additional proteins interact (red color means activation, blue color means inhibition, and violet color means unspecified or complex (e.g., both inhibitory and stimulatory effect) according to STRING database). The interactions data were extracted from the STRING database (http://string-db.org). To assure that the presented data is reliable, we have included only interactions that showed at least medium STRING confidence score and were either identified in an experiment or are annotated in manually curated databases. Additionally, we have added interaction between GFAP and LAMP, which was not included in STRING database but was found by manual literature search. Permission to use KEGG figure was granted.

in different mammalian tissues (Mizushima and Komatsu, 2011).

BIOLOGICAL MECHANISMS LINKING AUTOPHAGY AND AD

Aβ Metabolism and the Autophagy

Alzheimer's disease is a progressive neurodegenerative disorder, which pathophysiology includes formation of Aβ aggregates (Oddo et al., 2006). In a healthy human central nervous system the production rate of Aβ peptides is generally lower than their rate of clearance, at 7.6 and 8.3% per hour, respectively (Bateman et al., 2006).

Autophagy is a key regulator of Aβ generation and clearance (Nilsson and Saido, 2014). Aβ peptides are produced through cleavage of amyloid precursor protein (APP) in the autophagosomes during autophagic turnover of APP-rich organelles (Nixon, 2007; Steele et al., 2013). In AD the maturation of autophagolysosomes (i.e., autophagosomes that have undergone fusion with lysosomes) and their retrograde passage toward the neuronal body are hindered (Nixon, 2007). This contributes to an immense accretion of autophagic vacuoles in neurons. Such accretion may be related to dysfunction of

the ESCRT-III complex. This dysfunction is associated with neurodegeneration (Lee et al., 2007; Yamazaki et al., 2010) and may affect autophagosome maturation by disrupting fusion of autophagosomes with the endolysosomal system (Rusten and Stenmark, 2009).

There are two pathways for disposing Aβ peptides. Firstly, they can be simply degraded by various Aβ-degrading proteases, including BACE1 and CTSD (Saido and Leissring, 2012). Secondly, Aβ peptides can accumulate in autophagosomes of dystrophic neurites (i.e., main constituents of neuritic senile plaques in AD), thus being incorporated into primary intracellular reservoir of toxic peptides (Nixon et al., 2005; Yu et al., 2005). The second recycling path of Aβ peptides is especially prevalent in the brains of people suffering from AD (Nilsson et al., 2013; Nilsson and Saido, 2014).

A paper published by Nilsson et al. (2013) shows that Aβ peptides are released from neurons in an autophagy-dependent manner and suggests that the accumulation of intracellular Aβ plaques is toxic to brain cells leading to AD pathology. To explore the role of autophagy in Aβ pathology *in vivo*, Nilsson et al. (2013) crossed *App* transgenic mice, carrying Swedish mutation, with mice lacking functional autophagy mechanisms in the forebrain neurons due to conditional knockout of *Atg7*. They observed that the offspring had far fewer extracellular Aβ plaques than the mice with functional autophagy. The decrease of extracellular Aβ plaque content reported by Nilsson et al. (2013) was caused by inability of cells with disrupted autophagy to secrete Aβ peptides. Indeed, they report that in the autophagy deficient mice, reduction in Aβ peptides secretion co-occur with accumulation of Aβ inside the brain cells (Nilsson et al., 2013). Moreover, in the autophagy deficient mice, intracellular aggregation of Aβ likely caused neurodegeneration and, together with amyloidosis, memory impairment (Nilsson et al., 2013). These findings are in agreement with previous reports that intracellular Aβ is neurotoxic (Zhang et al., 2002).

Summing up, impaired autophagy is a well-established participating mechanism in the pathology of Aβ metabolism of AD.

Neuroinflammation

Present knowledge suggests that inflammation, autophagy and AD are connected processes. A study by Francois et al. (2013) provided an example of cross-talk between them. They showed that Aβ42 influences the expression and activation of some proteins involved in autophagy (p62, p70S6K) *in vitro* (Francois et al., 2013). They also showed that the processes of inflammation and autophagy interact within brain cells, as severe inflammation induced by IL-1β activated autophagy in microglia grown in tri- or mono-cultures (Francois et al., 2013). Although the role of IL-1β itself in AD is unclear, we do know how the neuroinflammation contributes to AD pathogenesis (Zhang and Jiang, 2015), and why IL-1β is a key mediator of neuroinflammation (Basu et al., 2004). Hence, one could speculate that IL-1β may play role in pathogenesis of AD by eliciting both neuroinflammation and autophagy. It seems viable that during the course of AD, immune signals induce autophagy. Indeed, it was shown that neuroinflammation might influence autophagy following stress-induced hypertension (Du et al., 2017). Correspondingly, another study reported that adult mice bearing mutations of *App* and *Psen1* genes showed higher brain levels of inflammatory mediators (including Il-1β) along with accumulation of autophagic vesicles within dystrophic neurons in the cortex and hippocampus (Francois et al., 2014). Moreover, the levels of inflammatory mediators correlated with expression of key autophagy regulators such as mTOR and Becn1 (Francois et al., 2014). On the other hand, Ye et al. (2017) suggest, that inhibition of autophagy may enhance microglia activity, including secretion of cytokines such as Il-1β and generation of toxic reactive oxygen species (ROS) *in vitro*.

Taken together, these studies suggest that AD and neuroinflammation feed autophagy (and each other), while autophagy decreases inflammation in the brain. Thus, the increase in autophagy may play some protective role during the course of AD via interaction with the immune system.

Mechanistic Target of Rapamycin (mTOR) Pathway

Mechanistic target of rapamycin signaling pathway is initiated by nutrients and growth factors and regulates autophagy (Jung et al., 2010). Human studies suggest participation of mTOR signaling in AD (Sun et al., 2014). It has been shown that mTOR signaling is inhibited in cortex and hippocampus of adult AD model mice (Francois et al., 2014). Decreased mTOR signaling leads to reduction in levels of Aβ (Spilman et al., 2010; Caccamo et al., 2014) and protects memory of AD model mice from deterioration (Caccamo et al., 2014). A study performed by Spilman et al. (2010) on mouse model of AD reported that blocking the mTOR signaling with rapamycin relieves cognitive deficits and reduces amyloid pathology, likely by activating autophagy in brain cells. Correspondingly, studies show that diet enriched with rapamycin prolongs lifespan of animals (Harrison et al., 2009). This may be relevant to AD research, because age is a major factor in the pathogenesis of AD (Guerreiro and Bras, 2015). Moreover, studies on human cells have shown that mTOR mediates intra- and extra-cellular distribution of tau (Tang et al., 2015), its phosphorylation and accumulation as well as resulting behavioral effects of tau pathology (Caccamo et al., 2013). Finally, multiple compounds tested for their efficacy as AD medication impose their beneficial effect by inducing mTOR-depending autophagy (see below).

Summarizing, mTOR pathway is currently one of the most promising targets for autophagy-related AD therapy.

Endocannabinoids

Recently published reports highlight the role of the endocannabinoid system in neurodegenerative diseases and autophagy (Maroof et al., 2013; Shao et al., 2014; Bedse et al., 2015). Endocannabinoids are lipophilic molecules that, when released, activate the cannabinoid receptors CNR1 and CNR2 (cannabinoid receptor 1 and 2) (Katona and Freund, 2012).

Mice with a *Cnr1* deletion have shown a pathological accumulation of some proteins, which are not degradable by lysosomal enzymes through autophagy (Piyanova et al., 2013).

Knockdown of CNR1 expression by siRNA results in both mTOR- and BECN1-independent increase of autophagic vesicle formation (Hiebel et al., 2014).

In a human AD frontal cortex, expression of the CNR1 receptor was significantly reduced (Ramirez et al., 2005; Solas et al., 2013). In an AD mouse model Cnr1 was decreased in dorsal hippocampus and basolateral amygdala complex (Bedse et al., 2014). It seems that in frontal cortex and hippocampus the activity of the CNR1 receptor depends on the progression of AD. While in early AD the activity is increased, it shifts to attenuation in later AD stages (Manuel et al., 2014). Additionally, the expression levels of the CNR2 receptor were increased in microglia cells of an AD patient's in the hippocampus, entorhinal cortex and frontal cortex (Benito et al., 2003; Solas et al., 2013). The high expression of CNR2 receptor was correlated with the Aβ42 levels and senile plaque burden (Solas et al., 2013).

All these findings suggest that there is a non-trivial connection between endocannabinoids, autophagy, and AD. A further investigation is required to fully understand the mechanisms involved.

Genes Common to Autophagy and AD

To identify the genes that may mediate cross-talk between molecular mechanisms of autophagy and AD, we have compared two groups of genes: (1) genes involved in autophagy, defined as being included either in Gene Ontology term "autophagy" (GO:0006914, *Homo sapiens*) or in KEGG Pathway (Kanehisa et al., 2017) "autophagy-animal" (ko04140), and (2) genes involved in AD, defined as being included either in databases AlzBase (Bai et al., 2016) or AlzGene (Bertram et al., 2007), or related to AD as shown by the text-mining tool GLAD4U (Jourquin et al., 2012). AlzBase provides data on "gene dysregulation in AD and closely related processes/diseases such as aging and neurological disorders" (Bai et al., 2016), while AlzGene provides data on "genetic association studies in the field of AD" (Bertram et al., 2007). AlzGene can be treated as a comprehensive database of genes that were associated with AD before year 2011, when it was last updated. Unfortunately, currently there is no other database that collects such information. Finally, GLAD4U is a prioritization tool querying PubMed for given phrase and returning associated genes (Jourquin et al., 2012). The genes that are common to both groups' are summarized in Supplementary Table S1. For detailed discussion we selected genes, which met following requirements: (1) reported to be involved in both autophagy and AD according to the PubMed database, AND (2) constituted top five results from either AlzBase, AlzGene or GLAD4U. Additionally, we arbitrarily selected five genes involved in KEGG Pathway "autophagy-animal" for further discussion. Gene hierarchy was established for AlzBase and AlzGene based on the total number of entries into database and for GLAD4U as a confidence score provided by the tool. Generally, selected genes showed strong (weight > 5) relationship with neuroinflammation, as detected by Chilibot (Chen and Sharp, 2004), especially BECN1, PSEN1, MAPT, GFAP, and CDK5 (see **Figure 2A**). Simultaneously, the genes were not significantly related to the endocannabinoid system (queried in Chilibot via keyword "cannabinoid"), with only BECN1 and GFAP showing strong interaction (see **Figure 2B**). The genes described below were also added to **Figure 1** along with their known interactions with other molecules of the pathway (see also Supplementary Table S2), as extracted from STRING database (organism: *Homo sapiens*) (Szklarczyk et al., 2017).

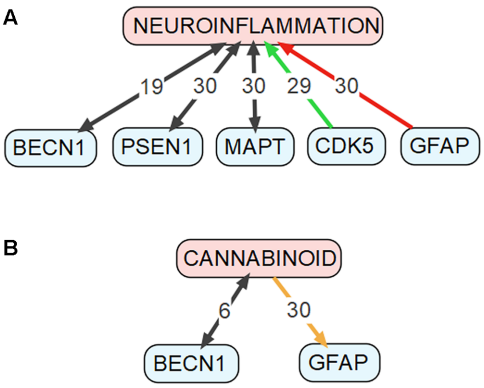


FIGURE 2 | Connections between genes discussed in the "Genes Common to Autophagy and AD" section and **(A)** neuroinflammation as well as **(B)** cannabinoids. This figure was drawn based on data obtained using the Chilibot tool. Black arrows mark relationships that are neither obviously stimulatory nor inhibitory. Orange arrow marks both stimulatory and inhibitory relationship. Red arrow marks inhibitory relationship. Green arrow mark stimulatory relationship. The respective numbers mark the weight of the relationship according to the Chilibot tool.

Autophagy-Related 7 (*ATG7*)

As stated previously, *ATG7* is a key gene regulating autophagic conjugation systems (Ohsumi, 2014). *ATG7* is involved in memory functions as evident from a study, in which forebrain-specific *Atg7* knockout mouse have shown memory deficits (Inoue et al., 2012). We have found two studies connecting dysregulated expression of ATG7 protein and AD-like pathology. Decreased levels of the Atg7 protein were found in cerebral cortex and hippocampus of mouse model of AD (Carvalho et al., 2015). On the other hand, no dysregulation of protein expression of ATG7 was found in temporal cortices of AD patients (Crews et al., 2010).

Atg7 mediates the transport of Aβ peptides to the multivesicular body and their secretion in mouse neurons (Nilsson et al., 2015). Inhibition of *ATG7* expression using siRNA partially protected against increase in production and secretion of Aβ40 *in vitro* (Cho et al., 2015). On the other hand, intra-hippocampal infusion of Aβ is able to increase the expression of the Atg7 protein in hippocampus of rats while reducing their memory performance (Mohammadi et al., 2016).

ATG7 seems to be involved in degradation of tau. Forebrain-specific *Atg7* knockout in mice resulted in an accumulation of phosphorylated tau protein in hippocampus and cerebral cortex, as well as neurodegeneration evident in loss of hippocampal neurons and memory dysfunction (Inoue et al., 2012).

BCL2

BCL2 is an anti-apoptotic factor that interacts with BECN1 to regulate autophagy (Decuypere et al., 2012).

Overexpression of neuronal *Bcl2* improved place recognition memory in mice (Rohn et al., 2008). Contrary, negative correlation between the cortical BLC2 protein expression and memory (immediate recall) was established in AD patients (Perez et al., 2015). Upregulation of the BCL2 protein was found in precuneus (cortex) of AD patients (Perez et al., 2015).

Aβ treatment decreases the BCL2 expression *in vitro* (Clementi et al., 2006), while *APP* mutation (Swedish) mediates similar effect *in vitro* during starvation (Yang et al., 2009). Overexpression of Bcl2 protects against Aβ-related death of neuronal cells *in vitro* (Ferreiro et al., 2007). Rohn et al. (2008) reported that AD model mice engineered to overexpress Bcl2 protein showed decreased processing of App and number of extracellular deposits of Aβ, as compared to base strain (3xTg-AD).

The overexpression of Bcl2 affects also tau processing, reducing the number of NFTs (Rohn et al., 2008).

Beclin 1 (*BECN1/ATG6*)

BECN1 protein mediates the initiation of autophagy and genesis of autophagosomes. Becn1 heterozygotic mice (Becn1+/−) show decreased autophagy in neurons (Pickford et al., 2008).

Several reports suggest, that BECN1 is involved in the pathophysiology of AD. Postmortem midfrontal cortex and isolated microglia of AD patients show reduced content of BECN1 protein (Pickford et al., 2008; Lucin et al., 2013). Similarly, reduced Becn1 expression was found in cortex and hippocampus of adult mouse model of AD (Francois et al., 2014). BECN1 may protect against AD-associated cellular death. Xue et al. (2013) report that expression of Becn1 correlates with viability of cells treated with toxic Aβ42. Interestingly, Becn1 activity seems to be regulated by Aβ42 (Nah et al., 2013).

A study performed on the frontoparietal cortex and the hippocampus of mice showed that decreasing of Becn1 expression leads to increased levels of Aβ (Pickford et al., 2008). Becn1-mediated decrease in autophagy leads to accretion of Aβ peptides and, finally, to neurodegeneration (Pickford et al., 2008).

BECN1 is also involved in neuroinflammation and cannabinoid system activity. Inhibition of Becn1 expression increases microglia inflammatory response (Zhou et al., 2011). Chronic LPS-induced inflammation decreases hippocampal Becn1 expression (Jiang et al., 2017). On the other hand, *Cb2r* deletion decreases Becn1 expression in the spinal cord of mice (Shao et al., 2014).

Cyclin Dependent Kinase 5 (CDK5)

CDK5 is an autophagy-regulating kinase (Wong et al., 2011), which expression is enriched in central nervous system as shown in Human Protein Atlas (HPA) (Uhlen et al., 2015).

Cdk5 modulates various cognition-related biological processes such as neurogenesis in adult hippocampus (Crews et al., 2011) and synaptic functions (Sheng et al., 2016). Silencing of hippocampal Cdk5 expression using RNAi resulted in improved memory performance in AD model mice (Posada-Duque et al., 2015). Study connected *CDK5*-associated polymorphisms with increased risk of AD (Rademakers et al., 2005). CDK5 protein expression is enhanced in frontal cortices of AD patients (Sadleir and Vassar, 2012). On the contrary, CDK5 protein expression is decreased in cerebrospinal fluid (CSF) of AD patients (Olah et al., 2015).

CDK5 influences the metabolism and effects of Aβ. CDK5 may regulate BACE1 protein expression (Sadleir and Vassar, 2012) as well as activity (Song W.J. et al., 2015). *BACE1* gene encodes β-secretase, which is a crucial enzyme involved in APP metabolism (Cai et al., 2015). Furthermore, Cdk5 participates in cytotoxic activity of Aβ42 in primary cortical neurons (Chang et al., 2012), mediates Aβ peptide-induced dendritic spine loss (Qu et al., 2011) and APP phosphorylation (Iijima et al., 2000). On the other hand, Aβ increases Cdk5 activity in primary cortical neurons (Seyb et al., 2007).

CDK5 is similarly involved in tau metabolism. Cdk5 binds to tau *in vitro* and is co-localized with it in rat cortex (Li et al., 2006). Cdk5 participates in tau phosphorylation (Noble et al., 2003), although whether this may lead to formation of NFTs is disputed (Bian et al., 2002; Noble et al., 2003). Prevention of Cdk5 hyperactivity in the mouse model of AD protects against tau hyperphosphorylation, Aβ accumulation, memory loss, and enhanced neuroinflammation (Shukla et al., 2013).

Clusterin (*CLU/APOJ*)

CLU is a chaperone protein that participates in autophagosome biogenesis via interaction with ATG8E (MAP1LC3A) (Zhang F. et al., 2014).

CLU is one of the top AD candidate genes with the third lowest *p*-value of the association ($p = 3.37E\text{-}23$) according to the meta-analysis included in AlzGene database (Bertram et al., 2007). Meta-analyses showed the involvement of *CLU*-related mutations in AD pathogenesis (Liu et al., 2014; Shuai et al., 2015). *CLU* mutations that are suggested as causal for AD affect hippocampal connectivity (Zhang et al., 2015), white matter integrity in several brain regions (Braskie et al., 2011), cortical gray matter volume (Stevens et al., 2014), as well as working memory (Stevens et al., 2014) and episodic memory performance (Barral et al., 2012). *CLU* mRNA is upregulated in hippocampi of AD patients (May et al., 1990). According to Miners et al. (2017) CLU protein rises in several brain regions, including frontal cortex, of AD patients in correlation with noxious Aβ40/42 levels. Results of study by Baig et al. (2012) did not confirm these findings. The CLU protein is upregulated in CSF of AD patients (Deming et al., 2016). The content of CLU protein in the blood plasma of AD patients was reported to be dysregulated in some studies (Mullan et al., 2013), while others did not confirm this finding (Deming et al., 2016).

Moreover, CLU protein interacts with Aβ, reduces its aggregation and protects against its toxic effects (Beeg et al., 2016). CLU decreases the Aβ intake by human primary glia cells (Mulder et al., 2014).

The interaction between tau and CLU is less studied (Zhou et al., 2014). However, Zhou et al. (2014) reported that the Clu

protein is upregulated in a tau-overexpressing mouse model of AD. Furthermore, the AD-associated *CLU* polymorphism rs11136000 regulates the levels of tau protein in CSF in AD patients (Zhou et al., 2014).

Cathepsin D (*CTSD*)

Cathepsin D is a lysosomal protease (Dean, 1975) that is involved in degradation of the APP protein (Letronne et al., 2016).

Two meta-analyses on the influence of *CTSD* mutation rs17571 on AD yielded contrary results (Schuur et al., 2011; Mo et al., 2014). Similar discrepancy is also reported for another *CTSD* mutation (Ala224Val) (Ntais et al., 2004; Paz-Y-Miño et al., 2015). Directionality of the change of *CTSD* gene expression seems to depend on studied tissue. CTSD level was decreased in bone marrow-derived monocytes isolated from AD patients (Tian et al., 2014). *CTSD* mRNA expression was upregulated in whole blood of AD patients (Bai et al., 2014). On the other hand, *CTSD* is downregulated on both mRNA and protein levels in skin fibroblasts from AD patients (Urbanelli et al., 2008).

Cathepsin D participates in processing of Aβ peptides (McDermott and Gibson, 1996) and clearance of amyloid plaques *in vitro* (Tian et al., 2014). Nevertheless, Aβ processing mechanisms are fairly resistant to modest (38%) changes in expression of *Ctsd*, at least in cerebral cortex of mouse model of AD (Cheng et al., 2017).

Cathepsin D also interacts with tau protein. Previously mentioned rs17571 mutation causes changes in processing of tau, but not of APP (Riemenschneider et al., 2006).

Forkhead Box O1 (*FOXO1*)

FOXO1 gene encodes transcription factor that plays a role in autophagy modulation in neurons (Xu et al., 2011). *FOXO1* mutation rs7981045 was associated with response of AD patients to a treatment based on acetylcholinesterase inhibitors (Paroni et al., 2014)

Glial Fibrillary Acidic Protein (*GFAP*)

GFAP is a cytoskeletal intermediate filament-III and a marker of astrocytes (Sofroniew and Vinters, 2010; Yang and Wang, 2015). GFAP binds with LAMP2A (**Figure 1**) (Bandyopadhyay et al., 2010). Multiple studies found increased levels of GFAP in tissues of AD patients. GFAP levels are increased in the frontal cortices, hippocampi (Korolainen et al., 2005; Kamphuis et al., 2014), and the CSF of AD patients (Ishiki et al., 2016). Moreover, *Gfap* expression is modulated by cannabinoid receptor 1 (Cnr1) in the hypothalamus of mice (Higuchi et al., 2010) and neuroinflammation regulates astrogliosis (abnormal increase in the number of astrocytes) (Carson et al., 2006).

Inositol 1,4,5-Trisphosphate Receptor Type 1 (*ITPR1/IP3R1*)

ITPR1 gene encodes intracellular receptor mediating calcium release from the endoplasmic reticulum (Santulli and Marks, 2015) and also plays a role in inducing autophagy (Messai et al., 2014). Engineered downregulation of *Itpr1* expression protected AD model mice from Aβ accumulation, tau hyperphosphorylation, as well as from dysfunction of memory and hippocampal LTP (Shilling et al., 2014).

Microtubule Associated Protein Tau (*MAPT/TAU*)

MAPT gene encodes tau protein, which pathology is one of the most well-recognized markers of AD. Autophagy is a main pathway of degradation of tauDeltaC, which is a form of the protein found in the brains of AD patients (Dolan and Johnson, 2010). Autophagy dysfunction plays important role in tau aggregation (Inoue et al., 2012). Tau may also regulate autophagy (Pacheco et al., 2009), likely via inhibition of HDAC6 activity (Perez et al., 2009). Finally, Mapt deficiency reduces neuroinflammation (Maphis et al., 2015), while neuroinflammation in turn induces Mapt phosphorylation (Bhaskar et al., 2010).

Presenilin 1 (*PSEN1*)

PSEN1 protein is a regulator of the APP-cleaving γ-secretase complex (De Strooper et al., 1998), and autophagic proteolysis (Neely and Green, 2011).

PSEN1 gene mutations contribute to the pathogenesis of early onset AD (Karch and Goate, 2015), and this effect may be mediated by loss of stability and hydrophobicity of the proteins encoded by the mutated variants (Somavarapu and Kepp, 2016). CSF of AD patients with *PSEN1* mutations showed lower levels of Aβ than AD patients without *PSEN1* mutation (Ikeda et al., 2013). This may suggest that the proteins are retained in the brain cells due to dysregulated autophagy. Cataldo et al. (2004) compared brains of AD patients with mutation of presenilin 1 with brains of sporadic AD patients. They concluded that *PSEN1* mutation is associated with higher prevalence of lysosomal pathology in neurons of AD patients (Cataldo et al., 2004). This corresponds to report by Lee et al. (2010), where the authors show that *Psen1* is crucial for modulating lysosome acidification and proteolysis during autophagy. Dysregulated lysosomal proteolysis may lead to accumulation of proteins and cell death (Lee et al., 2010). Additionally, PSEN1 is hypothesized to be involved in brain immune response as *Psen1/2* knock-out changes the expression of neuroinflammation-related genes (Mirnics et al., 2008).

Alpha-Synuclein (*SNCA/PARK1/NACP*)

Expression of *SNCA* is enriched in brain according to Human Protein Atlas (Uhlen et al., 2015). SNCA regulates autophagosome formation (Yan et al., 2014), but it is also negatively regulated by autophagy (Colasanti et al., 2014).

SNCA mutations are connected to the risk of AD (Matsubara et al., 2001; Wang et al., 2016). Changes in expression of SNCA proteins were also reported in some brain regions of AD patients (Quinn et al., 2012). Dysregulated levels of SNCA in CSF are associated with cognitive performance (Korff et al., 2013). Effect of Snca protein expression on memory was also reported in mice (Larson et al., 2012).

SNCA is an important component of Aβ plaques (Ueda et al., 1993). Snca induces expression of Aβ peptides and vice versa (Majd et al., 2013). SNCA also likely regulates APP processing by modulating the activity of BACE1 (Roberts et al., 2017), binds Aβ peptides and promotes their aggregation (Yoshimoto et al., 1995).

There are also reports of Snca inhibiting Aβ plaque formation (Bachhuber et al., 2015). On the other hand, Aβ40 decreases SNCA uptake by neurons (Chan et al., 2016).

Similarly to interaction of SNCA with Aβ peptides, SNCA and tau also induce each other fibrillization (Giasson et al., 2003). SNCA binds, phosphorylates, and inhibits microtubule assembly activity of tau (Oksman et al., 2013; Oikawa et al., 2016).

Ubiquilin 1 (*UBQLN1*)

UBQLN1 gene encodes ubiquitin-like protein involved in autophagosome–lysosome fusion (N'Diaye et al., 2009) likely by interacting with ATG8E (MAP1LC3A) (Rothenberg et al., 2010).

There is a strong evidence for involvement of *UBQLN1* in AD pathology. UBQ-8i polymorphism of *UBQLN1* was associated with increased risk of AD in two separate meta-analyses (Zhang and Jia, 2014; Yue et al., 2015). In hippocampi of AD patients UBQLN1 protein localizes to dystrophic neurites (Satoh et al., 2013). Expression of UBQLN1 protein is reduced in temporal and frontal cortices of AD patients (Stieren et al., 2011; Natunen et al., 2016). This decrease may cause enhanced processing and intracellular trafficking of APP (Hiltunen et al., 2006; Stieren et al., 2011), and secretion of Aβ40/42 (Hiltunen et al., 2006).

Moreover, UBQLN1 interacts with BACE1, which is a key APP processing protein. Ubqln1 overexpression causes an increase of Bace1 in neuron-microglia co-cultures, though this effect did not reach significance in the brains of mice (Natunen et al., 2016).

Ubiquitin C-Terminal Hydrolase L1 (*UCHL1*)

UCHL1 is a brain-enriched ubiquitin-specific hydrolase (Uhlen et al., 2015). It influences autophagy by interaction with LAMP2 (**Figure 1**), which modulates autophagosome-lysosome fusion (Costes et al., 2014; Hubert et al., 2016).

Uchl1 plays an important role in synaptic functions and memory as shown in mouse model of AD (Gong et al., 2006). This effect may be related to the Uchl1 ability to restore Bdnf signaling, which is disrupted by Aβ (Poon et al., 2013). BDNF is one of the most critical mediators of brain functions (Lu et al., 2014). Several publications have reported either effect or lack of effect of *UCHL1* mutations on AD (Xue and Jia, 2006; Shibata et al., 2012). Similarly, there is some discrepancy in the directionality of changes in expression of *UCHL1* gene between different studies performed on AD patients. In frontal cortices the UCHL1 protein was upregulated (Donovan et al., 2012). On the other hand, downregulation of UCHL1 was reported in hippocampi (Poon et al., 2013) and in unspecified brain area (Choi et al., 2004).

Co-immunoprecipitation assay showed that Uchl1 interacts with App (Zhang M. et al., 2014). The Uchl1 overexpression, induced by intracranial injection of *Uchl1*-expressing virus, decreases the Aβ production and protects AD model mice against memory impairment (Zhang M. et al., 2014). Decreased expression and activity of UCHL1 protein is associated with Aβ treatment *in vitro* (Guglielmotto et al., 2012). Similarly, decreased expression of UCHL1 protein is found in the cerebral cortex of AD patients (Guglielmotto et al., 2012). Additionally, the cortical UCHL1 protein levels seem to be inversely correlated to the number of NFT in AD patients (Chen et al., 2013). Moreover, UCHL1 is involved in lysosomal degradation of BACE1 (Guglielmotto et al., 2012).

UCHL1 protein co-localizes with NFTs in AD brains (Choi et al., 2004). The Uchl1 expression and activity negatively influence the levels of phosphorylated tau and aggregation of tau protein in mouse neuroblastoma cells (Xie et al., 2016). Tau induces mitochondrial degradation, synaptic deterioration, and cellular death by recruiting UCHL1 *in vitro* (Corsetti et al., 2015).

THERAPEUTIC IMPLICATIONS OF THE INTERPLAY OF ALZHEIMER'S DISEASE AND AUTOPHAGY

The protein aggregates, e.g., Aβ and tau proteins, participating in the pathology of neurodegenerative disorders cause neuronal damage and synaptic dysfunction (Irvine et al., 2008; Bloom, 2014). Their removal or inhibition of their formation are proposed as potential therapeutic approaches for the treatment of neurodegenerative disorders (Nowacek et al., 2009). Autophagy is one of the main mechanisms by which the cell degrades abnormal proteins. Thus, elimination of such protein aggregates may be achieved utilizing mechanisms of autophagy (Metcalf et al., 2012). Several autophagy-stimulating drugs have already demonstrated considerable therapeutic potential for AD treatment in clinical trials. We shortly discuss some of them below.

Carbamazepine (CBZ)

Carbamazepine was primarily developed as a drug used in the treatment of epilepsy (Okuma and Kishimoto, 1998). In the past, scientists studied therapeutic effect of CBZ on AD-related agitation (Xiao et al., 2010). Recently two publications have shown that carbamazepine-induced autophagy also protected against memory dysfunction and increase in Aβ content in brains of mouse model of AD (Li et al., 2013; Zhang et al., 2017).

Latrepirdine

Latrepirdine stimulates mTOR- and Atg5- dependent autophagy and reduces intracellular content of App metabolites, including Aβ peptides, in the brain of mouse (Steele and Gandy, 2013). Recent meta-analysis has shown no adverse effects and small improvement in dementia-related behaviors by latrepirdine in AD patients (Chau et al., 2015). Nevertheless, as Chau et al. (2015) themselves admit, the analyzed literature was not comprehensive enough to allow for more confident conclusions.

Lithium

Clinical trials have shown that lithium may ameliorate AD and this effect may be related to its mTOR-independent autophagy-inducing activity (Sarkar et al., 2005; Forlenza et al., 2012). In meta-analysis of clinical studies on AD, lithium significantly decreased cognitive decline compared to placebo, while showing no significant adverse effects (Matsunaga et al., 2015a).

Memantine

The NMDA (*N*-methyl-D-aspartate) receptors antagonist memantine is widely used for treatment of moderate-to-severe AD. According to recent meta-analysis it shows good tolerance and some efficacy in AD treatment (Matsunaga et al., 2015b). This effect may be in some extent mediated by memantine ability to influence autophagy in either mTOR-dependent or mTOR-independent manner (Song G. et al., 2015).

Nicotinamide

Liu et al. (2013) reported that long-term treatment with nicotinamide (Vitamin B3/PP) reduces Aβ and tau pathologies as well as cognitive decline in a mouse model of AD. The effect of nicotinamide is likely mediated by enhancement of the acidification of lysosome or autophagolysosome, leading to reduced autophagosome accretion (Liu et al., 2013). Gong et al. (2013) have shown that nicotinamide activity depends also on its ability to induce degradation of Bace1. Recently published clinical trials showed safety, but no effect of nicotinamide on cognitive function of AD patients (Phelan et al., 2017). Despite this, nicotinamide anti-AD activity is still studied and further trial is currently ongoing (Grill, 2017).

Protein Phosphatase 2A Agonists

Clinical trials have suggested that protein phosphatase 2A agonists, such as metformin, can inhibit the hyperphosphorylation of tau (Kickstein et al., 2010). Similar results were obtained from a study on mice (Li et al., 2012). Hyperphosphorylation of tau is a key step in generation of NFTs in AD patients (Iqbal et al., 2010). On the other hand, metformin did not protect diabetic mice from AD-like memory dysfunction (Li et al., 2012).

Rapamycin

Rapamycin, a selective inhibitor of target-of-rapamycin complex 1 (TORC1) and thus modulator of the mTOR pathway activity, improved learning and memory and reduced Aβ and tau pathology in the brains of AD mouse model (Caccamo et al., 2010; Spilman et al., 2010). Rapamycin also increased viability of cells treated with Aβ42 (Xue et al., 2013). Rapamycin prodrug, temsirolimus was shown to induce autophagy-dependent Aβ clearance and to improve memory in mouse model of AD (Jiang et al., 2014). Temsirolimus also lowered tau accumulation and rescued motor dysfunctions in tau mutant mice (Frederick et al., 2015). SMER28, a small molecule-based enhancer of rapamycin, increases autophagy via Atg5-dependent pathway while reducing the levels of Aβ peptide in a γ-secretase-independent manner (Tian et al., 2011). Recent rapamycin clinical trial showed non-significant decrease in expression of the cellular senescence marker beta galactosidase (Singh et al., 2016).

Resveratrol

Resveratrol, a grape-derived polyphenol, and its derivatives decreased extracellular Aβ peptide accumulation by activating autophagy via AMPK signaling pathway (**Figure 1**) (Vingtdeux et al., 2010). Recently published clinical trials studying the efficacy of resveratrol for AD treatment showed that resveratrol is well-tolerated but, surprisingly, AD biomarkers, such as plasma Aβ40 level, were present in treated group at even higher levels than in a placebo group (Turner et al., 2015). On the other hand, long-term resveratrol treatment rescued memory loss and Aβ levels in the brain of AD mouse model (Porquet et al., 2014). Hence, viability of this compound as a medication for AD is unclear.

Other Autophagy-Regulating Substances That Have Shown Relevant Results Only in Animal AD Models

Arctigenin

Arctigenin, a polyphenol extracted from *Arctium lappa*, was found to inhibit Aβ production and memory impairment in mouse model of AD (Zhu et al., 2013). The effect was mediated by mTOR- and AMPK-dependent autophagy (Zhu et al., 2013).

β-Asarone

β-asarone is an ether found, e.g., in *Acori graminei* (Liu et al., 2016). β-asarone treatment decreases Aβ42 levels in hippocampus and improves memory in a mouse model of AD, probably through mTOR-dependent autophagy (Deng et al., 2016).

GTM-1

It was shown that administration of GTM-1, a derivative of quinolone, rescues cognitive dysfunction and Aβ pathologies in mouse model of AD by activating mTOR-independent autophagy (Chu et al., 2013; Zhang et al., 2017).

Oleuropein Aglycone

Oleuropein aglycone is a polyphenol, which is present in plants of *Oleaceae* family and induces autophagy via mTOR pathway (Grossi et al., 2013; Luccarini et al., 2015). According to a recent review (Martorell et al., 2016), regulation of autophagy is one of the mechanisms via which oleuropein aglycone counteracts amyloid aggregation and toxicity.

Tetrahydrohyperforin

Tetrahydrohyperforin is a derivative of hyperforin, which is an active component of St. John's Wort plant (*Hypericum perforatum*). In AD model mice tetrahydrohyperforin prevented memory impairment and physiological dysfunctions such as tau hyperphosphorylation or turnover of amyloid plaques (Cerpa et al., 2010; Inestrosa et al., 2011). At least one of its beneficial effects is mediated by its autophagy-related activity, that is clearance of APP via ATG5-dependent pathway (Cavieres et al., 2015).

Trehalose

The disaccharide trehalose, an inducer of mTOR-independent autophagy (Sarkar et al., 2007), inhibits the aggregation of both Aβ40 and tau, and reduces their cytotoxicity *in vitro* (Liu et al., 2005; Kruger et al., 2012). Similarly, in two separate studies utilizing mouse models of AD, trehalose protected against cognitive dysfunction (Du et al., 2013; Portbury et al., 2017).

Interestingly, one of these studies also reported effect of trehalose on hippocampal Aβ levels (Du et al., 2013), while the other one reported a lack of this effect (Portbury et al., 2017).

Summarizing, scientific community puts a significant effort into developing autophagy-related therapeutics for AD. Several agents, such as rapamycin and latrepirdine, have already been tested on AD patients and show promising results. However, many more potential therapeutics showing efficacy for treatment of cognitive dysfunctions in animal models of AD await for more comprehensive studies and trials on humans.

CONCLUSION

Despite much of the data presented in the review being acquired in studies performed on animal models, we propose that properly functioning autophagy is crucial for the normal aging of neurons. Malfunction in neuronal autophagy is one of the key factors influencing the development of neurodegenerative disorders, including AD. The autophagy plays a key role in the metabolism of Aβ and tau protein, the mTOR pathway, neuroinflammation, and in the endocannabinoid system, all of which may mediate its effect on AD. Accordingly, autophagy-targeted therapeutic approaches may lead to the development of novel therapeutic strategies for the management of AD.

AUTHOR CONTRIBUTIONS

This work was carried out in collaboration between all authors. MU, AMS, AS, and AM have written the first draft of the manuscript. NT, ST, AA, LB, and MA-D revised and improved the first draft. All authors have seen and agreed on the finally submitted version of the manuscript.

FUNDING

The authors acknowledge the support by the Polish KNOW (Leading National Research Centre) Scientific Consortium "Healthy Animal—Safe Food" decision of Ministry of Science and Higher Education No. 05-1/KNOW2/2015.

ACKNOWLEDGMENTS

The authors are grateful to the Department of Pharmacy, Southeast University, Dhaka, Bangladesh.

SUPPLEMENTARY MATERIAL

The Supplementary Material for this article can be found online at: https://www.frontiersin.org/articles/10.3389/fnagi.2018.00004/full#supplementary-material

REFERENCES

Alberts, B., Johnson, A., Lewis, J., Raff, M., Roberts, K., and Walter, P. (2002). *Transport from the Trans Golgi Network to Lysosomes*. New York, NY: Garland Science.

Armstrong, R. A. (2009). The molecular biology of senile plaques and neurofibrillary tangles in Alzheimer's disease. *Folia Neuropathol.* 47, 289–299.

Atkin, G., and Paulson, H. (2014). Ubiquitin pathways in neurodegenerative disease. *Front. Mol. Neurosci.* 7:63. doi: 10.3389/fnmol.2014.00063

Bachhuber, T., Katzmarski, N., Mccarter, J. F., Loreth, D., Tahirovic, S., Kamp, F., et al. (2015). Inhibition of amyloid-beta plaque formation by alpha-synuclein. *Nat. Med.* 21, 802–807. doi: 10.1038/nm.3885

Bai, Z., Han, G., Xie, B., Wang, J., Song, F., Peng, X., et al. (2016). AlzBase: an integrative database for gene dysregulation in Alzheimer's disease. *Mol. Neurobiol.* 53, 310–319. doi: 10.1007/s12035-014-9011-3

Bai, Z., Stamova, B., Xu, H., Ander, B. P., Wang, J., Jickling, G. C., et al. (2014). Distinctive RNA expression profiles in blood associated with Alzheimer disease after accounting for white matter hyperintensities. *Alzheimer Dis. Assoc. Disord.* 28, 226–233. doi: 10.1097/WAD.0000000000000022

Baig, S., Palmer, L. E., Owen, M. J., Williams, J., Kehoe, P. G., and Love, S. (2012). Clusterin mRNA and protein in Alzheimer's disease. *J. Alzheimers Dis.* 28, 337–344. doi: 10.3233/JAD-2011-110473

Bandyopadhyay, U., Sridhar, S., Kaushik, S., Kiffin, R., and Cuervo, A. M. (2010). Identification of regulators of chaperone-mediated autophagy. *Mol. Cell* 39, 535–547. doi: 10.1016/j.molcel.2010.08.004

Barral, S., Bird, T., Goate, A., Farlow, M. R., Diaz-Arrastia, R., Bennett, D. A., et al. (2012). Genotype patterns at PICALM, CR1, BIN1, CLU, and APOE genes are associated with episodic memory. *Neurology* 78, 1464–1471. doi: 10.1212/WNL.0b013e3182553c48

Basu, A., Krady, J. K., and Levison, S. W. (2004). Interleukin-1: a master regulator of neuroinflammation. *J. Neurosci. Res.* 78, 151–156. doi: 10.1002/jnr.20266

Bateman, R. J., Munsell, L. Y., Morris, J. C., Swarm, R., Yarasheski, K. E., and Holtzman, D. M. (2006). Human amyloid-beta synthesis and clearance rates as measured in cerebrospinal fluid *in vivo*. *Nat. Med.* 12, 856–861. doi: 10.1038/nm1438

Bedse, G., Romano, A., Cianci, S., Lavecchia, A. M., Lorenzo, P., Elphick, M. R., et al. (2014). Altered expression of the CB1 cannabinoid receptor in the triple transgenic mouse model of Alzheimer's disease. *J. Alzheimers Dis.* 40, 701–712. doi: 10.3233/JAD-131910

Bedse, G., Romano, A., Lavecchia, A. M., Cassano, T., and Gaetani, S. (2015). The role of endocannabinoid signaling in the molecular mechanisms of neurodegeneration in Alzheimer's disease. *J. Alzheimers Dis.* 43, 1115–1136. doi: 10.3233/JAD-141635

Beeg, M., Stravalaci, M., Romeo, M., Carra, A. D., Cagnotto, A., Rossi, A., et al. (2016). Clusterin binds to Abeta1-42 oligomers with high affinity and interferes with peptide aggregation by inhibiting primary and secondary nucleation. *J. Biol. Chem.* 291, 6958–6966. doi: 10.1074/jbc.M115.689539

Benito, C., Nunez, E., Tolon, R. M., Carrier, E. J., Rabano, A., Hillard, C. J., et al. (2003). Cannabinoid CB2 receptors and fatty acid amide hydrolase are selectively overexpressed in neuritic plaque-associated glia in Alzheimer's disease brains. *J. Neurosci.* 23, 11136–11141.

Bertram, L., Mcqueen, M. B., Mullin, K., Blacker, D., and Tanzi, R. E. (2007). Systematic meta-analyses of Alzheimer disease genetic association studies: the AlzGene database. *Nat. Genet.* 39, 17–23. doi: 10.1038/ng1934

Bhaskar, K., Konerth, M., Kokiko-Cochran, O. N., Cardona, A., Ransohoff, R. M., and Lamb, B. T. (2010). Regulation of tau pathology by the microglial fractalkine receptor. *Neuron* 68, 19–31. doi: 10.1016/j.neuron.2010.08.023

Bian, F., Nath, R., Sobocinski, G., Booher, R. N., Lipinski, W. J., Callahan, M. J., et al. (2002). Axonopathy, tau abnormalities, and dyskinesia, but no neurofibrillary tangles in p25-transgenic mice. *J. Comp. Neurol.* 446, 257–266. doi: 10.1002/cne.10186

Blobel, G. (2013). Christian de Duve (1917-2013). *Nature* 498:300. doi: 10.1038/498300a

Bloom, G. S. (2014). Amyloid-beta and tau: the trigger and bullet in Alzheimer disease pathogenesis. *JAMA Neurol.* 71, 505–508. doi: 10.1001/jamaneurol.2013.5847

Boland, B., Kumar, A., Lee, S., Platt, F. M., Wegiel, J., Yu, W. H., et al. (2008). Autophagy induction and autophagosome clearance in neurons: relationship to autophagic pathology in Alzheimer's disease. *J. Neurosci.* 28, 6926–6937. doi: 10.1523/JNEUROSCI.0800-08.2008

Braskie, M. N., Jahanshad, N., Stein, J. L., Barysheva, M., Mcmahon, K. L., De Zubicaray, G. I., et al. (2011). Common Alzheimer's disease risk variant within the CLU gene affects white matter microstructure in young adults. *J. Neurosci.* 31, 6764–6770. doi: 10.1523/JNEUROSCI.5794-10.2011

Caccamo, A., De Pinto, V., Messina, A., Branca, C., and Oddo, S. (2014). Genetic reduction of mammalian target of rapamycin ameliorates Alzheimer's disease-like cognitive and pathological deficits by restoring hippocampal gene expression signature. *J. Neurosci.* 34, 7988–7998. doi: 10.1523/JNEUROSCI.0777-14.2014

Caccamo, A., Magri, A., Medina, D. X., Wisely, E. V., Lopez-Aranda, M. F., Silva, A. J., et al. (2013). mTOR regulates tau phosphorylation and degradation: implications for Alzheimer's disease and other tauopathies. *Aging Cell* 12, 370–380. doi: 10.1111/acel.12057

Caccamo, A., Majumder, S., Richardson, A., Strong, R., and Oddo, S. (2010). Molecular interplay between mammalian target of rapamycin (mTOR), amyloid-beta, and Tau: effects on cognitive impairments. *J. Biol. Chem.* 285, 13107–13120. doi: 10.1074/jbc.M110.100420

Cai, Z., Zhou, Y., Liu, Z., Ke, Z., and Zhao, B. (2015). Autophagy dysfunction upregulates beta-amyloid peptides via enhancing the activity of gamma-secretase complex. *Neuropsychiatr. Dis. Treat.* 11, 2091–2099. doi: 10.2147/NDT.S84755

Carson, M. J., Thrash, J. C., and Walter, B. (2006). The cellular response in neuroinflammation: the role of leukocytes, microglia and astrocytes in neuronal death and survival. *Clin. Neurosci. Res.* 6, 237–245. doi: 10.1016/j.cnr.2006.09.004

Carvalho, C., Santos, M. S., Oliveira, C. R., and Moreira, P. I. (2015). Alzheimer's disease and type 2 diabetes-related alterations in brain mitochondria, autophagy and synaptic markers. *Biochim. Biophys. Acta* 1852, 1665–1675. doi: 10.1016/j.bbadis.2015.05.001

Cataldo, A. M., Peterhoff, C. M., Schmidt, S. D., Terio, N. B., Duff, K., Beard, M., et al. (2004). Presenilin mutations in familial Alzheimer disease and transgenic mouse models accelerate neuronal lysosomal pathology. *J. Neuropathol. Exp. Neurol.* 63, 821–830. doi: 10.1093/jnen/63.8.821

Cavieres, V. A., Gonzalez, A., Munoz, V. C., Yefi, C. P., Bustamante, H. A., Barraza, R. R., et al. (2015). Tetrahydrohyperforin inhibits the proteolytic processing of amyloid precursor protein and enhances its degradation by Atg5-dependent autophagy. *PLOS ONE* 10:e0136313. doi: 10.1371/journal.pone.0136313

Cerpa, W., Hancke, J. L., Morazzoni, P., Bombardelli, E., Riva, A., Marin, P. P., et al. (2010). The hyperforin derivative IDN5706 occludes spatial memory impairments and neuropathological changes in a double transgenic Alzheimer's mouse model. *Curr. Alzheimer Res.* 7, 126–133. doi: 10.2174/156720510790691218

Chan, D. K., Braidy, N., Xu, Y. H., Chataway, T., Guo, F., Guillemin, G. J., et al. (2016). Interference of alpha-synuclein uptake by monomeric beta-Amyloid1-40 and potential core acting site of the interference. *Neurotox. Res.* 30, 479–485. doi: 10.1007/s12640-016-9644-2

Chang, K. H., Vincent, F., and Shah, K. (2012). Deregulated Cdk5 triggers aberrant activation of cell cycle kinases and phosphatases inducing neuronal death. *J. Cell Sci.* 125, 5124–5137. doi: 10.1242/jcs.108183

Chau, S., Herrmann, N., Ruthirakuhan, M. T., Chen, J. J., and Lanctot, K. L. (2015). Latrepirdine for Alzheimer's disease. *Cochrane Database Syst. Rev.* 4:CD009524. doi: 10.1002/14651858.CD009524.pub2

Chen, H., and Sharp, B. M. (2004). Content-rich biological network constructed by mining PubMed abstracts. *BMC Bioinformatics* 5:147. doi: 10.1186/1471-2105-5-147

Chen, J., Huang, R. Y., and Turko, I. V. (2013). Mass spectrometry assessment of ubiquitin carboxyl-terminal hydrolase L1 partitioning between soluble and particulate brain homogenate fractions. *Anal. Chem.* 85, 6011–6017. doi: 10.1021/ac400831z

Cheng, S., Wani, W. Y., Hottman, D. A., Jeong, A., Cao, D., Leblanc, K. J., et al. (2017). Haplodeficiency of Cathepsin D does not affect cerebral amyloidosis and autophagy in APP/PS1 transgenic mice. *J. Neurochem.* 142, 297–304. doi: 10.1111/jnc.14048

Cho, S. J., Yun, S. M., Jo, C., Lee, D. H., Choi, K. J., Song, J. C., et al. (2015). SUMO1 promotes Abeta production via the modulation of autophagy. *Autophagy* 11, 100–112. doi: 10.4161/15548627.2014.984283

Choi, J., Levey, A. I., Weintraub, S. T., Rees, H. D., Gearing, M., Chin, L. S., et al. (2004). Oxidative modifications and down-regulation of ubiquitin carboxyl-terminal hydrolase L1 associated with idiopathic Parkinson's and Alzheimer's diseases. *J. Biol. Chem.* 279, 13256–13264. doi: 10.1074/jbc.M314124200

Chu, C., Zhang, X., Ma, W., Li, L., Wang, W., Shang, L., et al. (2013). Induction of autophagy by a novel small molecule improves a beta pathology and ameliorates cognitive deficits. *PLOS ONE* 8:e65367. doi: 10.1371/journal.pone.0065367

Ciechanover, A., and Schwartz, A. L. (1998). The ubiquitin-proteasome pathway: the complexity and myriad functions of proteins death. *Proc. Natl. Acad. Sci. U.S.A.* 95, 2727–2730. doi: 10.1073/pnas.95.6.2727

Clementi, M. E., Pezzotti, M., Orsini, F., Sampaolese, B., Mezzogori, D., Grassi, C., et al. (2006). Alzheimer's amyloid beta-peptide (1-42) induces cell death in human neuroblastoma via bax/bcl-2 ratio increase: an intriguing role for methionine 35. *Biochem. Biophys. Res. Commun.* 342, 206–213. doi: 10.1016/j.bbrc.2006.01.137

Colasanti, T., Vomero, M., Alessandri, C., Barbati, C., Maselli, A., Camperio, C., et al. (2014). Role of alpha-synuclein in autophagy modulation of primary human T lymphocytes. *Cell Death Dis.* 5:e1265. doi: 10.1038/cddis.2014.211

Corsetti, V., Florenzano, F., Atlante, A., Bobba, A., Ciotti, M. T., Natale, F., et al. (2015). NH2-truncated human tau induces deregulated mitophagy in neurons by aberrant recruitment of Parkin and UCHL-1: implications in Alzheimer's disease. *Hum. Mol. Genet.* 24, 3058–3081. doi: 10.1093/hmg/ddv059

Costes, S., Gurlo, T., Rivera, J. F., and Butler, P. C. (2014). UCHL1 deficiency exacerbates human islet amyloid polypeptide toxicity in beta-cells: evidence of interplay between the ubiquitin/proteasome system and autophagy. *Autophagy* 10, 1004–1014. doi: 10.4161/auto.28478

Crews, L., Patrick, C., Adame, A., Rockenstein, E., and Masliah, E. (2011). Modulation of aberrant CDK5 signaling rescues impaired neurogenesis in models of Alzheimer's disease. *Cell Death Dis.* 2:e120. doi: 10.1038/cddis.2011.2

Crews, L., Spencer, B., Desplats, P., Patrick, C., Paulino, A., Rockenstein, E., et al. (2010). Selective molecular alterations in the autophagy pathway in patients with Lewy body disease and in models of alpha-synucleinopathy. *PLOS ONE* 5:e9313. doi: 10.1371/journal.pone.0009313

de Duve, C. (2005). The lysosome turns fifty. *Nat. Cell Biol.* 7, 847–849. doi: 10.1038/ncb0905-847

De Duve, C., and Wattiaux, R. (1966). Functions of lysosomes. *Annu. Rev. Physiol.* 28, 435–492. doi: 10.1146/annurev.ph.28.030166.002251

De Strooper, B., Saftig, P., Craessaerts, K., Vanderstichele, H., Guhde, G., Annaert, W., et al. (1998). Deficiency of presenilin-1 inhibits the normal cleavage of amyloid precursor protein. *Nature* 391, 387–390. doi: 10.1038/34910

Dean, R. T. (1975). Direct evidence of importance of lysosomes in degradation of intracellular proteins. *Nature* 257, 414–416. doi: 10.1038/257414a0

Decuypere, J. P., Parys, J. B., and Bultynck, G. (2012). Regulation of the autophagic bcl-2/beclin 1 interaction. *Cells* 1, 284–312. doi: 10.3390/cells1030284

Deming, Y., Xia, J., Cai, Y., Lord, J., Holmans, P., Bertelsen, S., et al. (2016). A potential endophenotype for Alzheimer's disease: cerebrospinal fluid clusterin. *Neurobiol. Aging* 37, 208.e1–208.e209. doi: 10.1016/j.neurobiolaging.2015.09.009

Deng, M., Huang, L., Ning, B., Wang, N., Zhang, Q., Zhu, C., et al. (2016). beta-asarone improves learning and memory and reduces Acetyl Cholinesterase and Beta-amyloid 42 levels in APP/PS1 transgenic mice by regulating Beclin-1-dependent autophagy. *Brain Res.* 1652, 188–194. doi: 10.1016/j.brainres.2016.10.008

Dickson, T. C., King, C. E., Mccormack, G. H., and Vickers, J. C. (1999). Neurochemical diversity of dystrophic neurites in the early and late stages of Alzheimer's disease. *Exp. Neurol.* 156, 100–110. doi: 10.1006/exnr.1998.7010

Dolan, P. J., and Johnson, G. V. (2010). A caspase cleaved form of tau is preferentially degraded through the autophagy pathway. *J. Biol. Chem.* 285, 21978–21987. doi: 10.1074/jbc.M110.110940

Donovan, L. E., Higginbotham, L., Dammer, E. B., Gearing, M., Rees, H. D., Xia, Q., et al. (2012). Analysis of a membrane-enriched proteome from postmortem

human brain tissue in Alzheimer's disease. *Proteomics Clin. Appl.* 6, 201–211. doi: 10.1002/prca.201100068

Du, D., Hu, L., Wu, J., Wu, Q., Cheng, W., Guo, Y., et al. (2017). Neuroinflammation contributes to autophagy flux blockage in the neurons of rostral ventrolateral medulla in stress-induced hypertension rats. *J. Neuroinflammation* 14:169. doi: 10.1186/s12974-017-0942-2

Du, J., Liang, Y., Xu, F., Sun, B., and Wang, Z. (2013). Trehalose rescues Alzheimer's disease phenotypes in APP/PS1 transgenic mice. *J. Pharm. Pharmacol.* 65, 1753–1756. doi: 10.1111/jphp.12108

Ferreiro, E., Eufrasio, A., Pereira, C., Oliveira, C. R., and Rego, A. C. (2007). Bcl-2 overexpression protects against amyloid-beta and prion toxicity in GT1-7 neural cells. *J. Alzheimers Dis.* 12, 223–228. doi: 10.3233/JAD-2007-12303

Forlenza, O. V., De Paula, V. J., Machado-Vieira, R., Diniz, B. S., and Gattaz, W. F. (2012). Does lithium prevent Alzheimer's disease? *Drugs Aging* 29, 335–342. doi: 10.2165/11599180-000000000-00000

Francois, A., Rioux Bilan, A., Quellard, N., Fernandez, B., Janet, T., Chassaing, D., et al. (2014). Longitudinal follow-up of autophagy and inflammation in brain of APPswePS1dE9 transgenic mice. *J. Neuroinflammation* 11:139. doi: 10.1186/s12974-014-0139-x

Francois, A., Terro, F., Janet, T., Rioux Bilan, A., Paccalin, M., and Page, G. (2013). Involvement of interleukin-1beta in the autophagic process of microglia: relevance to Alzheimer's disease. *J. Neuroinflammation* 10:151. doi: 10.1186/1742-2094-10-151

Frederick, C., Ando, K., Leroy, K., Heraud, C., Suain, V., Buee, L., et al. (2015). Rapamycin ester analog CCI-779/Temsirolimus alleviates tau pathology and improves motor deficit in mutant tau transgenic mice. *J. Alzheimers Dis.* 44, 1145–1156. doi: 10.3233/JAD-142097

Funakoshi, T., Matsuura, A., Noda, T., and Ohsumi, Y. (1997). Analyses of APG13 gene involved in autophagy in yeast, *Saccharomyces cerevisiae*. *Gene* 192, 207–213. doi: 10.1016/S0378-1119(97)00031-0

Funderburk, S. F., Marcellino, B. K., and Yue, Z. (2010). Cell "self-eating" (autophagy) mechanism in Alzheimer's disease. *Mt. Sinai J. Med.* 77, 59–68. doi: 10.1002/msj.20161

Garcia-Arencibia, M., Hochfeld, W. E., Toh, P. P., and Rubinsztein, D. C. (2010). Autophagy, a guardian against neurodegeneration. *Semin. Cell Dev. Biol.* 21, 691–698. doi: 10.1016/j.semcdb.2010.02.008

Giasson, B. I., Forman, M. S., Higuchi, M., Golbe, L. I., Graves, C. L., Kotzbauer, P. T., et al. (2003). Initiation and synergistic fibrillization of tau and alpha-synuclein. *Science* 300, 636–640. doi: 10.1126/science.1082324

Glick, D., Barth, S., and Macleod, K. F. (2010). Autophagy: cellular and molecular mechanisms. *J. Pathol.* 221, 3–12. doi: 10.1002/path.2697

Gong, B., Cao, Z., Zheng, P., Vitolo, O. V., Liu, S., Staniszewski, A., et al. (2006). Ubiquitin hydrolase Uch-L1 rescues beta-amyloid-induced decreases in synaptic function and contextual memory. *Cell* 126, 775–788. doi: 10.1016/j.cell.2006.06.046

Gong, B., Pan, Y., Vempati, P., Zhao, W., Knable, L., Ho, L., et al. (2013). Nicotinamide riboside restores cognition through an upregulation of proliferator-activated receptor-gamma coactivator 1alpha regulated beta-secretase 1 degradation and mitochondrial gene expression in Alzheimer's mouse models. *Neurobiol. Aging* 34, 1581–1588. doi: 10.1016/j.neurobiolaging.2012.12.005

Grill, J. (2017). *Nicotinamide as an Early Alzheimer's Disease Treatment (NEAT)*. Bethesda, MD: National Library of Medicine.

Grossi, C., Rigacci, S., Ambrosini, S., Dami, T., Luccarini, I., Traini, C., et al. (eds) (2013). The polyphenol oleuropein aglycone protects TgCRND8 mice against Ass plaque pathology. *PLOS ONE* 8:e71702. doi: 10.1371/journal.pone.0071702

Guerreiro, R., and Bras, J. (2015). The age factor in Alzheimer's disease. *Genome Med.* 7:106. doi: 10.1186/s13073-015-0232-5

Guglielmotto, M., Monteleone, D., Boido, M., Piras, A., Giliberto, L., Borghi, R., et al. (2012). Abeta1-42-mediated down-regulation of Uch-L1 is dependent on NF-kappaB activation and impaired BACE1 lysosomal degradation. *Aging Cell* 11, 834–844. doi: 10.1111/j.1474-9726.2012.00854.x

Harrison, D. E., Strong, R., Sharp, Z. D., Nelson, J. F., Astle, C. M., Flurkey, K., et al. (2009). Rapamycin fed late in life extends lifespan in genetically heterogeneous mice. *Nature* 460, 392–395. doi: 10.1038/nature08221

Hiebel, C., Kromm, T., Stark, M., and Behl, C. (2014). Cannabinoid receptor 1 modulates the autophagic flux independent of mTOR- and BECLIN1-complex. *J. Neurochem.* 131, 484–497. doi: 10.1111/jnc.12839

Higuchi, S., Irie, K., Mishima, S., Araki, M., Ohji, M., Shirakawa, A., et al. (2010). The cannabinoid 1-receptor silent antagonist O-2050 attenuates preference for high-fat diet and activated astrocytes in mice. *J. Pharmacol. Sci.* 112, 369–372. doi: 10.1254/jphs.09326SC

Hiltunen, M., Lu, A., Thomas, A. V., Romano, D. M., Kim, M., Jones, P. B., et al. (2006). Ubiquilin 1 modulates amyloid precursor protein trafficking and Abeta secretion. *J. Biol. Chem.* 281, 32240–32253. doi: 10.1074/jbc.M603106200

Huber, L. A., and Teis, D. (2016). Lysosomal signaling in control of degradation pathways. *Curr. Opin. Cell Biol.* 39, 8–14. doi: 10.1016/j.ceb.2016.01.006

Hubert, V., Peschel, A., Langer, B., Groger, M., Rees, A., and Kain, R. (2016). LAMP-2 is required for incorporating syntaxin-17 into autophagosomes and for their fusion with lysosomes. *Biol. Open* 5, 1516–1529. doi: 10.1242/bio.018648

Iijima, K., Ando, K., Takeda, S., Satoh, Y., Seki, T., Itohara, S., et al. (2000). Neuron-specific phosphorylation of Alzheimer's beta-amyloid precursor protein by cyclin-dependent kinase 5. *J. Neurochem.* 75, 1085–1091. doi: 10.1046/j.1471-4159.2000.0751085.x

Ikeda, M., Yonemura, K., Kakuda, S., Tashiro, Y., Fujita, Y., Takai, E., et al. (2013). Cerebrospinal fluid levels of phosphorylated tau and Abeta1-38/Abeta1-40/Abeta1-42 in Alzheimer's disease with PS1 mutations. *Amyloid* 20, 107–112. doi: 10.3109/13506129.2013.790810

Inestrosa, N. C., Tapia-Rojas, C., Griffith, T. N., Carvajal, F. J., Benito, M. J., Rivera-Dictter, A., et al. (2011). Tetrahydrohyperforin prevents cognitive deficit, A beta deposition, tau phosphorylation and synaptotoxicity in the APPswe/PSEN1DeltaE9 model of Alzheimer's disease: a possible effect on APP processing. *Transl. Psychiatry* 1:e20. doi: 10.1038/tp.2011.19

Inoue, K., Rispoli, J., Kaphzan, H., Klann, E., Chen, E. I., Kim, J., et al. (2012). Macroautophagy deficiency mediates age-dependent neurodegeneration through a phospho-tau pathway. *Mol. Neurodegener.* 7:48. doi: 10.1186/1750-1326-7-48

Iqbal, K., Liu, F., Gong, C. X., and Grundke-Iqbal, I. (2010). Tau in Alzheimer disease and related tauopathies. *Curr. Alzheimer Res.* 7, 656–664. doi: 10.2174/156720510793611592

Irvine, G. B., El-Agnaf, O. M., Shankar, G. M., and Walsh, D. M. (2008). Protein aggregation in the brain: the molecular basis for Alzheimer's and Parkinson's diseases. *Mol. Med.* 14, 451–464. doi: 10.2119/2007-00100.Irvine

Ishiki, A., Kamada, M., Kawamura, Y., Terao, C., Shimoda, F., Tomita, N., et al. (2016). Glial fibrillar acidic protein in the cerebrospinal fluid of Alzheimer's disease, dementia with Lewy bodies, and frontotemporal lobar degeneration. *J. Neurochem.* 136, 258–261. doi: 10.1111/jnc.13399

Jellinger, K. A. (2010). Basic mechanisms of neurodegeneration: a critical update. *J. Cell Mol. Med.* 14, 457–487. doi: 10.1111/j.1582-4934.2010.01010.x

Jiang, P., Guo, Y., Dang, R., Yang, M., Liao, D., Li, H., et al. (2017). Salvianolic acid B protects against lipopolysaccharide-induced behavioral deficits and neuroinflammatory response: involvement of autophagy and NLRP3 inflammasome. *J. Neuroinflammation* 14:239. doi: 10.1186/s12974-017-1013-4

Jiang, T., Yu, J. T., Zhu, X. C., Tan, M. S., Wang, H. F., Cao, L., et al. (2014). Temsirolimus promotes autophagic clearance of amyloid-beta and provides protective effects in cellular and animal models of Alzheimer's disease. *Pharmacol. Res.* 81, 54–63. doi: 10.1016/j.phrs.2014.02.008

Jourquin, J., Duncan, D., Shi, Z., and Zhang, B. (2012). GLAD4U: deriving and prioritizing gene lists from PubMed literature. *BMC Genomics* 13(Suppl. 8):S20. doi: 10.1186/1471-2164-13-S8-S20

Jung, C. H., Ro, S. H., Cao, J., Otto, N. M., and Kim, D. H. (2010). mTOR regulation of autophagy. *FEBS Lett.* 584, 1287–1295. doi: 10.1016/j.febslet.2010.01.017

Kabeya, Y., Mizushima, N., Ueno, T., Yamamoto, A., Kirisako, T., Noda, T., et al. (2000). LC3, a mammalian homologue of yeast Apg8p, is localized in autophagosome membranes after processing. *EMBO J.* 19, 5720–5728. doi: 10.1093/emboj/19.21.5720

Kamada, Y., Funakoshi, T., Shintani, T., Nagano, K., Ohsumi, M., and Ohsumi, Y. (2000). Tor-mediated induction of autophagy via an Apg1 protein kinase complex. *J. Cell Biol.* 150, 1507–1513. doi: 10.1083/jcb.150.6.1507

Kamphuis, W., Middeldorp, J., Kooijman, L., Sluijs, J. A., Kooi, E. J., Moeton, M., et al. (2014). Glial fibrillary acidic protein isoform expression in plaque related astrogliosis in Alzheimer's disease. *Neurobiol. Aging* 35, 492–510. doi: 10.1016/j.neurobiolaging.2013.09.035

Kanehisa, M., Furumichi, M., Tanabe, M., Sato, Y., and Morishima, K. (2017). KEGG: new perspectives on genomes, pathways, diseases and drugs. *Nucleic Acids Res.* 45, D353–D361. doi: 10.1093/nar/gkw1092

Karch, C. M., and Goate, A. M. (2015). Alzheimer's disease risk genes and mechanisms of disease pathogenesis. *Biol. Psychiatry* 77, 43–51. doi: 10.1016/j.biopsych.2014.05.006

Karigar, C., and Murthy, K. R. S. (2005). The Nobel Prize in Chemistry 2004. *Resonance* 10, 41–49. doi: 10.1007/BF02835891

Katona, I., and Freund, T. F. (2012). Multiple functions of endocannabinoid signaling in the brain. *Annu. Rev. Neurosci.* 35, 529–558. doi: 10.1146/annurev-neuro-062111-150420

Kaushik, S., and Cuervo, A. M. (2012). Chaperone-mediated autophagy: a unique way to enter the lysosome world. *Trends Cell Biol.* 22, 407–417. doi: 10.1016/j.tcb.2012.05.006

Kickstein, E., Krauss, S., Thornhill, P., Rutschow, D., Zeller, R., Sharkey, J., et al. (2010). Biguanide metformin acts on tau phosphorylation via mTOR/protein phosphatase 2A (PP2A) signaling. *Proc. Natl. Acad. Sci. U.S.A.* 107, 21830–21835. doi: 10.1073/pnas.0912793107

Klionsky, D. J. (2008). Autophagy revisited: a conversation with Christian de Duve. *Autophagy* 4, 740–743. doi: 10.4161/auto.6398

Klionsky, D. J., Cregg, J. M., Dunn, W. A. Jr., Emr, S. D., Sakai, Y., Sandoval, I. V., et al. (2003). A unified nomenclature for yeast autophagy-related genes. *Dev. Cell* 5, 539–545. doi: 10.1016/S1534-5807(03)00296-X

Korff, A., Liu, C., Ginghina, C., Shi, M., Zhang, J., and Alzheimer's Disease Neuroimaging Initiative. (2013). alpha-Synuclein in cerebrospinal fluid of Alzheimer's disease and mild cognitive impairment. *J. Alzheimers Dis.* 36, 679–688. doi: 10.3233/JAD-130458

Korolainen, M. A., Auriola, S., Nyman, T. A., Alafuzoff, I., and Pirttila, T. (2005). Proteomic analysis of glial fibrillary acidic protein in Alzheimer's disease and aging brain. *Neurobiol. Dis.* 20, 858–870. doi: 10.1016/j.nbd.2005.05.021

Kruger, U., Wang, Y., Kumar, S., and Mandelkow, E. M. (2012). Autophagic degradation of tau in primary neurons and its enhancement by trehalose. *Neurobiol. Aging* 33, 2291–2305. doi: 10.1016/j.neurobiolaging.2011.11.009

Kuma, A., Hatano, M., Matsui, M., Yamamoto, A., Nakaya, H., Yoshimori, T., et al. (2004). The role of autophagy during the early neonatal starvation period. *Nature* 432, 1032–1036. doi: 10.1038/nature03029

Larson, M. E., Sherman, M. A., Greimel, S., Kuskowski, M., Schneider, J. A., Bennett, D. A., et al. (2012). Soluble alpha-synuclein is a novel modulator of Alzheimer's disease pathophysiology. *J. Neurosci.* 32, 10253–10266. doi: 10.1523/JNEUROSCI.0581-12.2012

Lee, J. A., Beigneux, A., Ahmad, S. T., Young, S. G., and Gao, F. B. (2007). ESCRT-III dysfunction causes autophagosome accumulation and neurodegeneration. *Curr. Biol.* 17, 1561–1567. doi: 10.1016/j.cub.2007.07.029

Lee, J. H., Yu, W. H., Kumar, A., Lee, S., Mohan, P. S., Peterhoff, C. M., et al. (2010). Lysosomal proteolysis and autophagy require presenilin 1 and are disrupted by Alzheimer-related PS1 mutations. *Cell* 141, 1146–1158. doi: 10.1016/j.cell.2010.05.008

Letronne, F., Laumet, G., Ayral, A. M., Chapuis, J., Demiautte, F., Laga, M., et al. (2016). ADAM30 downregulates APP-linked defects through cathepsin D activation in Alzheimer's disease. *EBioMedicine* 9, 278–292. doi: 10.1016/j.ebiom.2016.06.002

Li, J., Deng, J., Sheng, W., and Zuo, Z. (2012). Metformin attenuates Alzheimer's disease-like neuropathology in obese, leptin-resistant mice. *Pharmacol. Biochem. Behav.* 101, 564–574. doi: 10.1016/j.pbb.2012.03.002

Li, L., Zhang, S., Zhang, X., Li, T., Tang, Y., Liu, H., et al. (2013). Autophagy enhancer carbamazepine alleviates memory deficits and cerebral amyloid-beta pathology in a mouse model of Alzheimer's disease. *Curr. Alzheimer Res.* 10, 433–441. doi: 10.2174/1567205011310040008

Li, S. C., and Kane, P. M. (2009). The yeast lysosome-like vacuole: endpoint and crossroads. *Biochim. Biophys. Acta* 1793, 650–663. doi: 10.1016/j.bbamcr.2008.08.003

Li, T., Hawkes, C., Qureshi, H. Y., Kar, S., and Paudel, H. K. (2006). Cyclin-dependent protein kinase 5 primes microtubule-associated protein tau site-specifically for glycogen synthase kinase 3beta. *Biochemistry* 45, 3134–3145. doi: 10.1021/bi051635j

Li, W., and Ye, Y. (2008). Polyubiquitin chains: functions, structures, and mechanisms. *Cell Mol. Life. Sci.* 65, 2397–2406. doi: 10.1007/s00018-008-8090-6

Lilienbaum, A. (2013). Relationship between the proteasomal system and autophagy. *Int. J. Biochem. Mol. Biol.* 4, 1–26.

Liu, D., Pitta, M., Jiang, H., Lee, J. H., Zhang, G., Chen, X., et al. (2013). Nicotinamide forestalls pathology and cognitive decline in Alzheimer mice: evidence for improved neuronal bioenergetics and autophagy procession. *Neurobiol. Aging* 34, 1564–1580. doi: 10.1016/j.neurobiolaging.2012.11.020

Liu, G., Wang, H., Liu, J., Li, J., Li, H., Ma, G., et al. (2014). The CLU gene rs11136000 variant is significantly associated with Alzheimer's disease in Caucasian and Asian populations. *Neuromolecular Med.* 16, 52–60. doi: 10.1007/s12017-013-8250-1

Liu, R., Barkhordarian, H., Emadi, S., Park, C. B., and Sierks, M. R. (2005). Trehalose differentially inhibits aggregation and neurotoxicity of beta-amyloid 40 and 42. *Neurobiol. Dis.* 20, 74–81. doi: 10.1016/j.nbd.2005.02.003

Liu, S. J., Yang, C., Zhang, Y., Su, R. Y., Chen, J. L., Jiao, M. M., et al. (2016). Neuroprotective effect of beta-asarone against Alzheimer's disease: regulation of synaptic plasticity by increased expression of SYP and GluR1. *Drug Des. Devel. Ther.* 10, 1461–1469. doi: 10.2147/DDDT.S93559

Lu, B., Nagappan, G., and Lu, Y. (2014). BDNF and synaptic plasticity, cognitive function, and dysfunction. *Handb. Exp. Pharmacol.* 220, 223–250. doi: 10.1007/978-3-642-45106-5_9

Luccarini, I., Grossi, C., Rigacci, S., Coppi, E., Pugliese, A. M., Pantano, D., et al. (2015). Oleuropein aglycone protects against pyroglutamylated-3 amyloid-ss toxicity: biochemical, epigenetic and functional correlates. *Neurobiol. Aging* 36, 648–663. doi: 10.1016/j.neurobiolaging.2014.08.029

Lucin, K. M., O'brien, C. E., Bieri, G., Czirr, E., Mosher, K. I., Abbey, R. J., et al. (2013). Microglial beclin 1 regulates retromer trafficking and phagocytosis and is impaired in Alzheimer's disease. *Neuron* 79, 873–886. doi: 10.1016/j.neuron.2013.06.046

Majd, S., Chegini, F., Chataway, T., Zhou, X. F., and Gai, W. (2013). Reciprocal induction between alpha-synuclein and beta-amyloid in adult rat neurons. *Neurotox. Res.* 23, 69–78. doi: 10.1007/s12640-012-9330-y

Manuel, I., Gonzalez De San Roman, E., Giralt, M. T., Ferrer, I., and Rodriguez-Puertas, R. (2014). Type-1 cannabinoid receptor activity during Alzheimer's disease progression. *J. Alzheimers Dis.* 42, 761–766. doi: 10.3233/JAD-140492

Maphis, N., Xu, G., Kokiko-Cochran, O. N., Cardona, A. E., Ransohoff, R. M., Lamb, B. T., et al. (2015). Loss of tau rescues inflammation-mediated neurodegeneration. *Front. Neurosci.* 9:196. doi: 10.3389/fnins.2015.00196

Maroof, N., Pardon, M. C., and Kendall, D. A. (2013). Endocannabinoid signalling in Alzheimer's disease. *Biochem. Soc. Trans.* 41, 1583–1587. doi: 10.1042/BST20130140

Martorell, M., Forman, K., Castro, N., Capo, X., Tejada, S., and Sureda, A. (2016). Potential therapeutic effects of oleuropein aglycone in Alzheimer's disease. *Curr. Pharm. Biotechnol.* 17, 994–1001. doi: 10.2174/1389201017666160725120656

Marzella, L., Ahlberg, J., and Glaumann, H. (1981). Autophagy, heterophagy, microautophagy and crinophagy as the means for intracellular degradation. *Virchows Arch. B Cell Pathol. Incl. Mol. Pathol.* 36, 219–234.

Matsubara, M., Yamagata, H., Kamino, K., Nomura, T., Kohara, K., Kondo, I., et al. (2001). Genetic association between Alzheimer disease and the alpha-synuclein gene. *Dement. Geriatr. Cogn. Disord.* 12, 106–109. doi: 10.1159/000051243

Matsunaga, S., Kishi, T., Annas, P., Basun, H., Hampel, H., and Iwata, N. (2015a). Lithium as a treatment for Alzheimer's disease: a systematic review and meta-analysis. *J. Alzheimers Dis.* 48, 403–410. doi: 10.3233/JAD-150437

Matsunaga, S., Kishi, T., and Iwata, N. (2015b). Memantine monotherapy for Alzheimer's disease: a systematic review and meta-analysis. *PLOS ONE* 10:e0123289. doi: 10.1371/journal.pone.0123289

Matsuura, A., Tsukada, M., Wada, Y., and Ohsumi, Y. (1997). Apg1p, a novel protein kinase required for the autophagic process in *Saccharomyces cerevisiae*. *Gene* 192, 245–250. doi: 10.1016/S0378-1119(97)00084-X

May, P. C., Lampert-Etchells, M., Johnson, S. A., Poirier, J., Masters, J. N., and Finch, C. E. (1990). Dynamics of gene expression for a hippocampal glycoprotein elevated in Alzheimer's disease and in response to experimental lesions in rat. *Neuron* 5, 831–839. doi: 10.1016/0896-6273(90)90342-D

McDermott, J. R., and Gibson, A. M. (1996). Degradation of Alzheimer's beta-amyloid protein by human cathepsin D. *Neuroreport* 7, 2163–2166. doi: 10.1097/00001756-199609020-00021

Meijer, A. J., Lorin, S., Blommaart, E. F., and Codogno, P. (2015). Regulation of autophagy by amino acids and MTOR-dependent signal transduction. *Amino Acids* 47, 2037–2063. doi: 10.1007/s00726-014-1765-4

Melendez, A., and Neufeld, T. P. (2008). The cell biology of autophagy in metazoans: a developing story. *Development* 135, 2347–2360. doi: 10.1242/dev.016105

Messai, Y., Noman, M. Z., Hasmim, M., Janji, B., Tittarelli, A., Boutet, M., et al. (2014). ITPR1 protects renal cancer cells against natural killer cells by inducing autophagy. *Cancer Res.* 74, 6820–6832. doi: 10.1158/0008-5472.CAN-14-0303

Metcalf, D. J., Garcia-Arencibia, M., Hochfeld, W. E., and Rubinsztein, D. C. (2012). Autophagy and misfolded proteins in neurodegeneration. *Exp. Neurol.* 238, 22–28. doi: 10.1016/j.expneurol.2010.11.003

Miners, J. S., Clarke, P., and Love, S. (2017). Clusterin levels are increased in Alzheimer's disease and influence the regional distribution of Abeta. *Brain Pathol.* 27, 305–313. doi: 10.1111/bpa.12392

Mirnics, K., Norstrom, E. M., Garbett, K., Choi, S. H., Zhang, X., Ebert, P., et al. (2008). Molecular signatures of neurodegeneration in the cortex of PS1/PS2 double knockout mice. *Mol. Neurodegener.* 3:14. doi: 10.1186/1750-1326-3-14

Mizushima, N., and Komatsu, M. (2011). Autophagy: renovation of cells and tissues. *Cell* 147, 728–741. doi: 10.1016/j.cell.2011.10.026

Mizushima, N., Yamamoto, A., Matsui, M., Yoshimori, T., and Ohsumi, Y. (2004). *In vivo* analysis of autophagy in response to nutrient starvation using transgenic mice expressing a fluorescent autophagosome marker. *Mol. Biol. Cell* 15, 1101–1111. doi: 10.1091/mbc.E03-09-0704

Mo, C., Peng, Q., Sui, J., Wang, J., Deng, Y., Xie, L., et al. (2014). Lack of association between cathepsin D C224T polymorphism and Alzheimer's disease risk: an update meta-analysis. *BMC Neurol.* 14:13. doi: 10.1186/1471-2377-14-13

Mohammadi, M., Guan, J., Khodagholi, F., Yans, A., Khalaj, S., Gholami, M., et al. (2016). Reduction of autophagy markers mediated protective effects of JNK inhibitor and bucladesine on memory deficit induced by A beta in rats. *Naunyn Schmiedebergs Arch. Pharmacol.* 389, 501–510. doi: 10.1007/s00210-016-1222-x

Mulder, S. D., Nielsen, H. M., Blankenstein, M. A., Eikelenboom, P., and Veerhuis, R. (2014). Apolipoproteins E and J interfere with amyloid-beta uptake by primary human astrocytes and microglia *in vitro*. *Glia* 62, 493–503. doi: 10.1002/glia.22619

Mullan, G. M., Mceneny, J., Fuchs, M., Mcmaster, C., Todd, S., Mcguinness, B., et al. (2013). Plasma clusterin levels and the rs11136000 genotype in individuals with mild cognitive impairment and Alzheimer's disease. *Curr. Alzheimer Res.* 10, 973–978. doi: 10.2174/15672050113106660162

Nah, J., Pyo, J. O., Jung, S., Yoo, S. M., Kam, T. I., Chang, J., et al. (2013). BECN1/Beclin 1 is recruited into lipid rafts by prion to activate autophagy in response to amyloid beta 42. *Autophagy* 9, 2009–2021. doi: 10.4161/auto.26118

Nakatogawa, H. (2013). Two ubiquitin-like conjugation systems that mediate membrane formation during autophagy. *Essays Biochem.* 55, 39–50. doi: 10.1042/bse0550039

Nakatogawa, H., Ichimura, Y., and Ohsumi, Y. (2007). Atg8, a ubiquitin-like protein required for autophagosome formation, mediates membrane tethering and hemifusion. *Cell* 130, 165–178. doi: 10.1016/j.cell.2007.05.021

Natunen, T., Takalo, M., Kemppainen, S., Leskela, S., Marttinen, M., Kurkinen, K. M. A., et al. (2016). Relationship between ubiquilin-1 and BACE1 in human Alzheimer's disease and APdE9 transgenic mouse brain and cell-based models. *Neurobiol. Dis.* 85, 187–205. doi: 10.1016/j.nbd.2015.11.005

N'Diaye, E. N., Kajihara, K. K., Hsieh, I., Morisaki, H., Debnath, J., and Brown, E. J. (2009). PLIC proteins or ubiquilins regulate autophagy-dependent cell survival during nutrient starvation. *EMBO Rep.* 10, 173–179. doi: 10.1038/embor.2008.238

Neely, K. M., and Green, K. N. (2011). Presenilins mediate efficient proteolysis via the autophagosome-lysosome system. *Autophagy* 7, 664–665. doi: 10.4161/auto.7.6.15448

Nilsson, P., Loganathan, K., Sekiguchi, M., Matsuba, Y., Hui, K., Tsubuki, S., et al. (2013). A beta secretion and plaque formation depend on autophagy. *Cell Rep.* 5, 61–69. doi: 10.1016/j.celrep.2013.08.042

Nilsson, P., and Saido, T. C. (2014). Dual roles for autophagy: degradation and secretion of Alzheimer's disease Abeta peptide. *Bioessays* 36, 570–578. doi: 10.1002/bies.201400002

Nilsson, P., Sekiguchi, M., Akagi, T., Izumi, S., Komori, T., Hui, K., et al. (2015). Autophagy-related protein 7 deficiency in amyloid beta (A beta) precursor protein transgenic mice decreases Abeta in the multivesicular bodies and induces Abeta accumulation in the Golgi. *Am. J. Pathol.* 185, 305–313. doi: 10.1016/j.ajpath.2014.10.011

Nixon, R. A. (2007). Autophagy, amyloidogenesis and Alzheimer disease. *J. Cell Sci.* 120, 4081–4091. doi: 10.1242/jcs.019265

Nixon, R. A., Wegiel, J., Kumar, A., Yu, W. H., Peterhoff, C., Cataldo, A., et al. (2005). Extensive involvement of autophagy in Alzheimer disease: an immuno-electron microscopy study. *J. Neuropathol. Exp. Neurol.* 64, 113–122. doi: 10.1093/jnen/64.2.113

Nobelprize.org (2017). *The Nobel Prize in Physiology or Medicine 2016 [Online]. Nobel Media AB 2014*. Available at: https://www.nobelprize.org/nobel_prizes/medicine/laureates/2016/

Noble, W., Olm, V., Takata, K., Casey, E., Mary, O., Meyerson, J., et al. (2003). Cdk5 is a key factor in tau aggregation and tangle formation *in vivo*. *Neuron* 38, 555–565. doi: 10.1016/S0896-6273(03)00259-9

Nowacek, A., Kosloski, L. M., and Gendelman, H. E. (2009). Neurodegenerative disorders and nanoformulated drug development. *Nanomedicine (Lond)* 4, 541–555. doi: 10.2217/nnm.09.37

Ntais, C., Polycarpou, A., and Ioannidis, J. P. (2004). Meta-analysis of the association of the cathepsin D Ala224Val gene polymorphism with the risk of Alzheimer's disease: a HuGE gene-disease association review. *Am. J. Epidemiol.* 159, 527–536. doi: 10.1093/aje/kwh069

Oddo, S., Caccamo, A., Smith, I. F., Green, K. N., and Laferla, F. M. (2006). A dynamic relationship between intracellular and extracellular pools of Abeta. *Am. J. Pathol.* 168, 184–194. doi: 10.2353/ajpath.2006.050593

Ohsumi, Y. (2014). Historical landmarks of autophagy research. *Cell Res.* 24, 9–23. doi: 10.1038/cr.2013.169

Oikawa, T., Nonaka, T., Terada, M., Tamaoka, A., Hisanaga, S., and Hasegawa, M. (2016). alpha-Synuclein fibrils exhibit gain of toxic function, promoting tau aggregation and inhibiting microtubule assembly. *J. Biol. Chem.* 291, 15046–15056. doi: 10.1074/jbc.M116.736355

Oksman, M., Wisman, L. A., Jiang, H., Miettinen, P., Kirik, D., and Tanila, H. (2013). Transduced wild-type but not P301S mutated human tau shows hyperphosphorylation in transgenic mice overexpressing A30P mutated human alpha-synuclein. *Neurodegener. Dis.* 12, 91–102. doi: 10.1159/000341596

Okuma, T., and Kishimoto, A. (1998). A history of investigation on the mood stabilizing effect of carbamazepine in Japan. *Psychiatry Clin. Neurosci.* 52, 3–12. doi: 10.1111/j.1440-1819.1998.tb00966.x

Olah, Z., Kalman, J., Toth, M. E., Zvara, A., Santha, M., Ivitz, E., et al. (2015). Proteomic analysis of cerebrospinal fluid in Alzheimer's disease: wanted dead or alive. *J. Alzheimers Dis.* 44, 1303–1312. doi: 10.3233/JAD-140141

Onodera, J., and Ohsumi, Y. (2005). Autophagy is required for maintenance of amino acid levels and protein synthesis under nitrogen starvation. *J. Biol. Chem.* 280, 31582–31586. doi: 10.1074/jbc.M506736200

Pacheco, C. D., Elrick, M. J., and Lieberman, A. P. (2009). Tau deletion exacerbates the phenotype of Niemann-Pick type C mice and implicates autophagy in pathogenesis. *Hum. Mol. Genet.* 18, 956–965. doi: 10.1093/hmg/ddn423

Parenti, G., Pignata, C., Vajro, P., and Salerno, M. (2013). New strategies for the treatment of lysosomal storage diseases (review). *Int. J. Mol. Med.* 31, 11–20. doi: 10.3892/ijmm.2012.1187

Paroni, G., Seripa, D., Fontana, A., D'onofrio, G., Gravina, C., Urbano, M., et al. (2014). FOXO1 locus and acetylcholinesterase inhibitors in elderly patients with Alzheimer's disease. *Clin. Interv. Aging* 9, 1783–1791. doi: 10.2147/CIA.S64758

Paz-Y-Miño, C. A., Garcia-Cardenas, J. M., Lopez-Cortes, A., Salazar, C., Serrano, M., and Leone, P. E. (2015). Positive association of the cathepsin D Ala224Val gene polymorphism with the risk of Alzheimer's disease. *Am. J. Med. Sci.* 350, 296–301. doi: 10.1097/MAJ.0000000000000555

Perez, M., Santa-Maria, I., Gomez De Barreda, E., Zhu, X., Cuadros, R., Cabrero, J. R., et al. (2009). Tau–an inhibitor of deacetylase HDAC6 function. *J. Neurochem.* 109, 1756–1766. doi: 10.1111/j.1471-4159.2009.06102.x

Perez, S. E., He, B., Nadeem, M., Wuu, J., Scheff, S. W., Abrahamson, E. E., et al. (2015). Resilience of precuneus neurotrophic signaling pathways despite amyloid pathology in prodromal Alzheimer's disease. *Biol. Psychiatry* 77, 693–703. doi: 10.1016/j.biopsych.2013.12.016

Phelan, M. J., Mulnard, R. A., Gillen, D. L., and Schreiber, S. S. (2017). Phase II clinical trial of nicotinamide for the treatment of mild to moderate Alzheimer's disease. *J. Geriatr. Med. Gerontol.* 3:021.

Pickford, F., Masliah, E., Britschgi, M., Lucin, K., Narasimhan, R., Jaeger, P. A., et al. (2008). The autophagy-related protein beclin 1 shows reduced expression in early Alzheimer disease and regulates amyloid beta accumulation in mice. *J. Clin. Invest.* 118, 2190–2199. doi: 10.1172/JCI33585

Piyanova, A., Albayram, O., Rossi, C. A., Farwanah, H., Michel, K., Nicotera, P., et al. (2013). Loss of CB1 receptors leads to decreased cathepsin D levels and accelerated lipofuscin accumulation in the hippocampus. *Mech. Ageing Dev.* 134, 391–399. doi: 10.1016/j.mad.2013.08.001

Poon, W. W., Carlos, A. J., Aguilar, B. L., Berchtold, N. C., Kawano, C. K., Zograbyan, V., et al. (2013). beta-Amyloid (A beta) oligomers impair brain-derived neurotrophic factor retrograde trafficking by down-regulating ubiquitin C-terminal hydrolase, UCH-L1. *J. Biol. Chem.* 288, 16937–16948. doi: 10.1074/jbc.M113.463711

Porquet, D., Grinan-Ferre, C., Ferrer, I., Camins, A., Sanfeliu, C., Del Valle, J., et al. (2014). Neuroprotective role of trans-resveratrol in a murine model of familial Alzheimer's disease. *J. Alzheimers Dis.* 42, 1209–1220. doi: 10.3233/JAD-140444

Portbury, S. D., Hare, D. J., Sgambelloni, C., Perronnes, K., Portbury, A. J., Finkelstein, D. I., et al. (2017). Trehalose improves cognition in the transgenic Tg2576 mouse model of Alzheimer's disease. *J. Alzheimers Dis.* 60, 549–560. doi: 10.3233/JAD-170322

Posada-Duque, R. A., Lopez-Tobon, A., Piedrahita, D., Gonzalez-Billault, C., and Cardona-Gomez, G. P. (2015). p35 and Rac1 underlie the neuroprotection and cognitive improvement induced by CDK5 silencing. *J. Neurochem.* 134, 354–370. doi: 10.1111/jnc.13127

Qu, J., Nakamura, T., Cao, G., Holland, E. A., Mckercher, S. R., and Lipton, S. A. (2011). S-Nitrosylation activates Cdk5 and contributes to synaptic spine loss induced by beta-amyloid peptide. *Proc. Natl. Acad. Sci. U.S.A.* 108, 14330–14335. doi: 10.1073/pnas.1105172108

Quinn, J. G., Coulson, D. T., Brockbank, S., Beyer, N., Ravid, R., Hellemans, J., et al. (2012). alpha-Synuclein mRNA and soluble alpha-synuclein protein levels in post-mortem brain from patients with Parkinson's disease, dementia with Lewy bodies, and Alzheimer's disease. *Brain Res.* 1459, 71–80. doi: 10.1016/j.brainres.2012.04.018

Rademakers, R., Sleegers, K., Theuns, J., Van Den Broeck, M., Bel Kacem, S., Nilsson, L. G., et al. (2005). Association of cyclin-dependent kinase 5 and neuronal activators p35 and p39 complex in early-onset Alzheimer's disease. *Neurobiol. Aging* 26, 1145–1151. doi: 10.1016/j.neurobiolaging.2004.10.003

Ramirez, B. G., Blazquez, C., Gomez Del Pulgar, T., Guzman, M., and De Ceballos, M. L. (2005). Prevention of Alzheimer's disease pathology by cannabinoids: neuroprotection mediated by blockade of microglial activation. *J. Neurosci.* 25, 1904–1913. doi: 10.1523/JNEUROSCI.4540-04.2005

Riemenschneider, M., Blennow, K., Wagenpfeil, S., Andreasen, N., Prince, J. A., Laws, S. M., et al. (2006). The cathepsin D rs17571 polymorphism: effects on CSF tau concentrations in Alzheimer disease. *Hum. Mutat.* 27, 532–537. doi: 10.1002/humu.20326

Roberts, H. L., Schneider, B. L., and Brown, D. R. (2017). alpha-Synuclein increases beta-amyloid secretion by promoting beta-/gamma-secretase processing of APP. *PLOS ONE* 12:e0171925. doi: 10.1371/journal.pone.0171925

Rogel, M. R., Jaitovich, A., and Ridge, K. M. (2010). The role of the ubiquitin proteasome pathway in keratin intermediate filament protein degradation. *Proc. Am. Thorac. Soc.* 7, 71–76. doi: 10.1513/pats.200908-089JS

Rohn, T. T., Vyas, V., Hernandez-Estrada, T., Nichol, K. E., Christie, L. A., and Head, E. (2008). Lack of pathology in a triple transgenic mouse model of Alzheimer's disease after overexpression of the anti-apoptotic protein Bcl-2. *J. Neurosci.* 28, 3051–3059. doi: 10.1523/JNEUROSCI.5620-07.2008

Rothenberg, C., Srinivasan, D., Mah, L., Kaushik, S., Peterhoff, C. M., Ugolino, J., et al. (2010). Ubiquilin functions in autophagy and is degraded by chaperone-mediated autophagy. *Hum. Mol. Genet.* 19, 3219–3232. doi: 10.1093/hmg/ddq231

Rubinsztein, D. C., Marino, G., and Kroemer, G. (2011). Autophagy and aging. *Cell* 146, 682–695. doi: 10.1016/j.cell.2011.07.030

Rusten, T. E., and Stenmark, H. (2009). How do ESCRT proteins control autophagy? *J. Cell Sci.* 122, 2179–2183. doi: 10.1242/jcs.050021

Sadleir, K. R., and Vassar, R. (2012). Cdk5 protein inhibition and Abeta42 increase BACE1 protein level in primary neurons by a post-transcriptional mechanism: implications of CDK5 as a therapeutic target for Alzheimer disease. *J. Biol. Chem.* 287, 7224–7235. doi: 10.1074/jbc.M111.333914

Saido, T., and Leissring, M. A. (2012). Proteolytic degradation of amyloid beta-protein. *Cold Spring Harb. Perspect. Med.* 2:a006379. doi: 10.1101/cshperspect.a006379

Santulli, G., and Marks, A. R. (2015). Essential roles of intracellular calcium release channels in muscle, brain, metabolism, and aging. *Curr. Mol. Pharmacol.* 8, 206–222. doi: 10.2174/1874467208666150507105105

Sarkar, S., Davies, J. E., Huang, Z., Tunnacliffe, A., and Rubinsztein, D. C. (2007). Trehalose, a novel mTOR-independent autophagy enhancer, accelerates the clearance of mutant huntingtin and alpha-synuclein. *J. Biol. Chem.* 282, 5641–5652. doi: 10.1074/jbc.M609532200

Sarkar, S., Floto, R. A., Berger, Z., Imarisio, S., Cordenier, A., Pasco, M., et al. (2005). Lithium induces autophagy by inhibiting inositol monophosphatase. *J. Cell Biol.* 170, 1101–1111. doi: 10.1083/jcb.200504035

Satoh, J., Tabunoki, H., Ishida, T., Saito, Y., and Arima, K. (2013). Ubiquilin-1 immunoreactivity is concentrated on Hirano bodies and dystrophic neurites in Alzheimer's disease brains. *Neuropathol. Appl. Neurobiol.* 39, 817–830. doi: 10.1111/nan.12036

Schuur, M., Ikram, M. A., Van Swieten, J. C., Isaacs, A., Vergeer-Drop, J. M., Hofman, A., et al. (2011). Cathepsin D gene and the risk of Alzheimer's disease: a population-based study and meta-analysis. *Neurobiol. Aging* 32, 1607–1614. doi: 10.1016/j.neurobiolaging.2009.10.011

Settembre, C., Fraldi, A., Medina, D. L., and Ballabio, A. (2013). Signals from the lysosome: a control centre for cellular clearance and energy metabolism. *Nat. Rev. Mol. Cell Biol.* 14, 283–296. doi: 10.1038/nrm3565

Seyb, K. I., Ansar, S., Li, G., Bean, J., Michaelis, M. L., and Dobrowsky, R. T. (2007). p35/Cyclin-dependent kinase 5 is required for protection against beta-amyloid-induced cell death but not tau phosphorylation by ceramide. *J. Mol. Neurosci.* 31, 23–35. doi: 10.1007/BF02686115

Shao, B. Z., Wei, W., Ke, P., Xu, Z. Q., Zhou, J. X., and Liu, C. (2014). Activating cannabinoid receptor 2 alleviates pathogenesis of experimental autoimmune encephalomyelitis via activation of autophagy and inhibiting NLRP3 inflammasome. *CNS Neurosci. Ther.* 20, 1021–1028. doi: 10.1111/cns.12349

Shen, H. M., and Mizushima, N. (2014). At the end of the autophagic road: an emerging understanding of lysosomal functions in autophagy. *Trends Biochem. Sci.* 39, 61–71. doi: 10.1016/j.tibs.2013.12.001

Sheng, Y., Zhang, L., Su, S. C., Tsai, L. H., and Julius Zhu, J. (2016). Cdk5 is a new rapid synaptic homeostasis regulator capable of initiating the early Alzheimer-like pathology. *Cereb. Cortex* 26, 2937–2951. doi: 10.1093/cercor/bhv032

Shibata, N., Motoi, Y., Tomiyama, H., Ohnuma, T., Kuerban, B., Tomson, K., et al. (2012). Lack of genetic association of the UCHL1 gene with Alzheimer's disease and Parkinson's disease with dementia. *Dement. Geriatr. Cogn. Disord.* 33, 250–254. doi: 10.1159/000339357

Shilling, D., Muller, M., Takano, H., Mak, D. O., Abel, T., Coulter, D. A., et al. (2014). Suppression of InsP3 receptor-mediated Ca2+ signaling alleviates mutant presenilin-linked familial Alzheimer's disease pathogenesis. *J. Neurosci.* 34, 6910–6923. doi: 10.1523/JNEUROSCI.5441-13.2014

Shuai, P., Liu, Y., Lu, W., Liu, Q., Li, T., and Gong, B. (2015). Genetic associations of CLU rs9331888 polymorphism with Alzheimer's disease: a meta-analysis. *Neurosci. Lett.* 591, 160–165. doi: 10.1016/j.neulet.2015.02.040

Shukla, V., Zheng, Y. L., Mishra, S. K., Amin, N. D., Steiner, J., Grant, P., et al. (2013). A truncated peptide from p35, a Cdk5 activator, prevents Alzheimer's disease phenotypes in model mice. *FASEB J.* 27, 174–186. doi: 10.1096/fj.12-217497

Singh, M., Jensen, M. D., Lerman, A., Kushwaha, S., Rihal, C. S., Gersh, B. J., et al. (2016). Effect of low-dose rapamycin on senescence markers and physical functioning in older adults with coronary artery disease: results of a pilot study. *J Frailty Aging* 5, 204–207.

Sofroniew, M. V., and Vinters, H. V. (2010). Astrocytes: biology and pathology. *Acta Neuropathol.* 119, 7–35. doi: 10.1007/s00401-009-0619-8

Solas, M., Francis, P. T., Franco, R., and Ramirez, M. J. (2013). CB2 receptor and amyloid pathology in frontal cortex of Alzheimer's disease patients. *Neurobiol. Aging* 34, 805–808. doi: 10.1016/j.neurobiolaging.2012.06.005

Somavarapu, A. K., and Kepp, K. P. (2016). Loss of stability and hydrophobicity of presenilin 1 mutations causing Alzheimer's disease. *J. Neurochem.* 137, 101–111. doi: 10.1111/jnc.13535

Song, G., Li, Y., Lin, L., and Cao, Y. (2015). Anti-autophagic and anti-apoptotic effects of memantine in a SH-SY5Y cell model of Alzheimer's disease via mammalian target of rapamycin-dependent and -independent pathways. *Mol. Med. Rep.* 12, 7615–7622. doi: 10.3892/mmr.2015.4382

Song, W. J., Son, M. Y., Lee, H. W., Seo, H., Kim, J. H., and Chung, S. H. (2015). Enhancement of BACE1 activity by p25/Cdk5-mediated phosphorylation in Alzheimer's disease. *PLOS ONE* 10:e0136950. doi: 10.1371/journal.pone.0136950

Spilman, P., Podlutskaya, N., Hart, M. J., Debnath, J., Gorostiza, O., Bredesen, D., et al. (2010). Inhibition of mTOR by rapamycin abolishes cognitive deficits and reduces amyloid-beta levels in a mouse model of Alzheimer's disease. *PLOS ONE* 5:e9979. doi: 10.1371/journal.pone.0009979

Steele, J. W., Fan, E., Kelahmetoglu, Y., Tian, Y., and Bustos, V. (2013). Modulation of autophagy as a therapeutic target for Alzheimer's disease. *Postdoc. J.* 1, 21–34. doi: 10.14304/SURYA.JPR.V1N2.3

Steele, J. W., and Gandy, S. (2013). Latrepirdine (Dimebon(R)), a potential Alzheimer therapeutic, regulates autophagy and neuropathology in an Alzheimer mouse model. *Autophagy* 9, 617–618. doi: 10.4161/auto.23487

Stevens, B. W., Dibattista, A. M., William Rebeck, G., and Green, A. E. (2014). A gene-brain-cognition pathway for the effect of an Alzheimers risk gene on working memory in young adults. *Neuropsychologia* 61, 143–149. doi: 10.1016/j.neuropsychologia.2014.06.021

Stieren, E. S., El Ayadi, A., Xiao, Y., Siller, E., Landsverk, M. L., Oberhauser, A. F., et al. (2011). Ubiquilin-1 is a molecular chaperone for the amyloid precursor protein. *J. Biol. Chem.* 286, 35689–35698. doi: 10.1074/jbc.M111.243147

Sun, Y. X., Ji, X., Mao, X., Xie, L., Jia, J., Galvan, V., et al. (2014). Differential activation of mTOR complex 1 signaling in human brain with mild to severe Alzheimer's disease. *J. Alzheimers Dis.* 38, 437–444. doi: 10.3233/JAD-131124

Szklarczyk, D., Morris, J. H., Cook, H., Kuhn, M., Wyder, S., Simonovic, M., et al. (2017). The STRING database in 2017: quality-controlled protein-protein association networks, made broadly accessible. *Nucleic Acids Res.* 45, D362–D368. doi: 10.1093/nar/gkw937

Takeshige, K., Baba, M., Tsuboi, S., Noda, T., and Ohsumi, Y. (1992). Autophagy in yeast demonstrated with proteinase-deficient mutants and conditions for its induction. *J. Cell Biol.* 119, 301–311. doi: 10.1083/jcb.119.2.301

Tanaka, K., Suzuki, T., Hattori, N., and Mizuno, Y. (2004). Ubiquitin, proteasome and parkin. *Biochim. Biophys. Acta* 1695, 235–247. doi: 10.1016/j.bbamcr.2004.09.026

Tang, Z., Ioja, E., Bereczki, E., Hultenby, K., Li, C., Guan, Z., et al. (2015). mTor mediates tau localization and secretion: Implication for Alzheimer's disease. *Biochim. Biophys. Acta* 1853, 1646–1657. doi: 10.1016/j.bbamcr.2015.03.003

The Nobel Assembly at Karolinska Institutet (2016). *Scientific Background Discoveries of Mechanisms for Autophagy*. Stockholm: The Nobel Assembly at Karolinska Institutet.

Tian, L., Zhang, K., Tian, Z. Y., Wang, T., Shang, D. S., Li, B., et al. (2014). Decreased expression of cathepsin D in monocytes is related to the defective degradation of amyloid-beta in Alzheimer's disease. *J. Alzheimers Dis.* 42, 511–520. doi: 10.3233/JAD-132192

Tian, Y., Bustos, V., Flajolet, M., and Greengard, P. (2011). A small-molecule enhancer of autophagy decreases levels of A beta and APP-CTF via Atg5-dependent autophagy pathway. *FASEB J.* 25, 1934–1942. doi: 10.1096/fj.10-175158

Tsukada, M., and Ohsumi, Y. (1993). Isolation and characterization of autophagy-defective mutants of *Saccharomyces cerevisiae*. *FEBS Lett.* 333, 169–174. doi: 10.1016/0014-5793(93)80398-E

Turner, R. S., Thomas, R. G., Craft, S., Van Dyck, C. H., Mintzer, J., Reynolds, B. A., et al. (2015). A randomized, double-blind, placebo-controlled trial of resveratrol for Alzheimer disease. *Neurology* 85, 1383–1391. doi: 10.1212/WNL.0000000000002035

Uddin, M. S., Mamun, A. A., Hossain, M. S., Asaduzzaman, M., Noor, M. A. A., Hossain, M. S., et al. (2016). Neuroprotective effect of *Phyllanthus acidus* L. on learning and memory impairment in a scopolamine-induced animal model of dementia and oxidative stress: natural wonder for regulating the development and progression of Alzheimer's disease. *Adv. Alzheimers Dis.* 5, 53–72. doi: 10.4236/aad.2016.52005

Ueda, K., Fukushima, H., Masliah, E., Xia, Y., Iwai, A., Yoshimoto, M., et al. (1993). Molecular cloning of cDNA encoding an unrecognized component of amyloid in Alzheimer disease. *Proc. Natl. Acad. Sci. U.S.A.* 90, 11282–11286. doi: 10.1073/pnas.90.23.11282

Uhlen, M., Fagerberg, L., Hallstrom, B. M., Lindskog, C., Oksvold, P., Mardinoglu, A., et al. (2015). Proteomics. Tissue-based map of the human proteome. *Science* 347:1260419. doi: 10.1126/science.1260419

Urbanelli, L., Emiliani, C., Massini, C., Persichetti, E., Orlacchio, A., Pelicci, G., et al. (2008). Cathepsin D expression is decreased in Alzheimer's disease fibroblasts. *Neurobiol. Aging* 29, 12–22. doi: 10.1016/j.neurobiolaging.2006.09.005

Vingtdeux, V., Giliberto, L., Zhao, H., Chandakkar, P., Wu, Q., Simon, J. E., et al. (2010). AMP-activated protein kinase signaling activation by resveratrol modulates amyloid-beta peptide metabolism. *J. Biol. Chem.* 285, 9100–9113. doi: 10.1074/jbc.M109.060061

Wang, Q., Tian, Q., Song, X., Liu, Y., and Li, W. (2016). SNCA gene polymorphism may contribute to an increased risk of Alzheimer's disease. *J. Clin. Lab. Anal.* 30, 1092–1099. doi: 10.1002/jcla.21986

Weissman, A. M. (2001). Themes and variations on ubiquitylation. *Nat. Rev. Mol. Cell Biol.* 2, 169–178. doi: 10.1038/35056563

Wong, A. S., Lee, R. H., Cheung, A. Y., Yeung, P. K., Chung, S. K., Cheung, Z. H., et al. (2011). Cdk5-mediated phosphorylation of endophilin B1 is required for induced autophagy in models of Parkinson's disease. *Nat. Cell Biol.* 13, 568–579. doi: 10.1038/ncb2217

Xiao, H., Su, Y., Cao, X., Sun, S., and Liang, Z. (2010). A meta-analysis of mood stabilizers for Alzheimer's disease. *J. Huazhong Univ. Sci. Technol. Med. Sci.* 30, 652–658. doi: 10.1007/s11596-010-0559-5

Xie, M., Han, Y., Yu, Q., Wang, X., Wang, S., and Liao, X. (2016). UCH-L1 inhibition decreases the microtubule-binding function of tau protein. *J. Alzheimers Dis.* 49, 353–363. doi: 10.3233/JAD-150032

Xu, H., and Ren, D. (2015). Lysosomal physiology. *Annu. Rev. Physiol.* 77, 57–80. doi: 10.1146/annurev-physiol-021014-071649

Xu, P., Das, M., Reilly, J., and Davis, R. J. (2011). JNK regulates FoxO-dependent autophagy in neurons. *Genes Dev.* 25, 310–322. doi: 10.1101/gad.1984311

Xue, S., and Jia, J. (2006). Genetic association between Ubiquitin Carboxy-terminal Hydrolase-L1 gene S18Y polymorphism and sporadic Alzheimer's disease in a Chinese Han population. *Brain Res.* 1087, 28–32. doi: 10.1016/j.brainres.2006.02.121

Xue, Z., Zhang, S., Huang, L., He, Y., Fang, R., and Fang, Y. (2013). Upexpression of Beclin-1-dependent autophagy protects against beta-amyloid-induced cell injury in PC12 cells. *J. Mol. Neurosci.* 51, 180–186. doi: 10.1007/s12031-013-9974-y

Yamazaki, Y., Takahashi, T., Hiji, M., Kurashige, T., Izumi, Y., Yamawaki, T., et al. (2010). Immunopositivity for ESCRT-III subunit CHMP2B in granulovacuolar degeneration of neurons in the Alzheimer's disease hippocampus. *Neurosci. Lett.* 477, 86–90. doi: 10.1016/j.neulet.2010.04.038

Yan, J. Q., Yuan, Y. H., Gao, Y. N., Huang, J. Y., Ma, K. L., Gao, Y., et al. (2014). Overexpression of human E46K mutant alpha-synuclein impairs macroautophagy via inactivation of JNK1-Bcl-2 pathway. *Mol. Neurobiol.* 50, 685–701. doi: 10.1007/s12035-014-8738-1

Yang, T. T., Hsu, C. T., and Kuo, Y. M. (2009). Amyloid precursor protein, heat-shock proteins, and Bcl-2 form a complex in mitochondria and modulate mitochondria function and apoptosis in N2a cells. *Mech. Ageing Dev.* 130, 592–601. doi: 10.1016/j.mad.2009.07.002

Yang, Z., and Wang, K. K. (2015). Glial fibrillary acidic protein: from intermediate filament assembly and gliosis to neurobiomarker. *Trends Neurosci.* 38, 364–374. doi: 10.1016/j.tins.2015.04.003

Ye, J., Jiang, Z., Chen, X., Liu, M., Li, J., and Liu, N. (2017). The role of autophagy in pro-inflammatory responses of microglia activation via mitochondrial reactive oxygen species *in vitro*. *J. Neurochem.* 142, 215–230. doi: 10.1111/jnc.14042

Yoshimoto, M., Iwai, A., Kang, D., Otero, D. A., Xia, Y., and Saitoh, T. (1995). NACP, the precursor protein of the non-amyloid beta/A4 protein (A beta)

component of Alzheimer disease amyloid, binds A beta and stimulates A beta aggregation. *Proc. Natl. Acad. Sci. U.S.A.* 92, 9141–9145. doi: 10.1073/pnas.92.20.9141

Yu, W. H., Cuervo, A. M., Kumar, A., Peterhoff, C. M., Schmidt, S. D., Lee, J. H., et al. (2005). Macroautophagy–a novel Beta-amyloid peptide-generating pathway activated in Alzheimer's disease. *J. Cell Biol.* 171, 87–98. doi: 10.1083/jcb.200505082

Yue, Z., Wang, S., Yan, W., and Zhu, F. (2015). Association of UBQ-8i polymorphism with Alzheimer's disease in Caucasians: a meta-analysis. *Int. J. Neurosci.* 125, 395–401. doi: 10.3109/00207454.2014.943369

Zhang, F., and Jiang, L. (2015). Neuroinflammation in Alzheimer's disease. *Neuropsychiatr. Dis. Treat.* 11, 243–256. doi: 10.2147/NDT.S75546

Zhang, F., Kumano, M., Beraldi, E., Fazli, L., Du, C., Moore, S., et al. (2014). Clusterin facilitates stress-induced lipidation of LC3 and autophagosome biogenesis to enhance cancer cell survival. *Nat. Commun.* 5:5775. doi: 10.1038/ncomms6775

Zhang, L., Wang, L., Wang, R., Gao, Y., Che, H., Pan, Y., et al. (2017). Evaluating the effectiveness of GTM-1, rapamycin, and carbamazepine on autophagy and Alzheimer disease. *Med. Sci. Monit.* 23, 801–808. doi: 10.12659/MSM.898679

Zhang, M., Cai, F., Zhang, S., and Song, W. (2014). Overexpression of ubiquitin carboxyl-terminal hydrolase L1 (UCHL1) delays Alzheimer's progression *in vivo*. *Sci. Rep.* 4:7298. doi: 10.1038/srep07298

Zhang, P., Qin, W., Wang, D., Liu, B., Zhang, Y., Jiang, T., et al. (2015). Impacts of PICALM and CLU variants associated with Alzheimer's disease on the functional connectivity of the hippocampus in healthy young adults. *Brain Struct. Funct.* 220, 1463–1475. doi: 10.1007/s00429-014-0738-4

Zhang, T., and Jia, Y. (2014). Meta-analysis of Ubiquilin1 gene polymorphism and Alzheimer's disease risk. *Med. Sci. Monit.* 20, 2250–2255. doi: 10.12659/MSM.891030

Zhang, Y., Mclaughlin, R., Goodyer, C., and Leblanc, A. (2002). Selective cytotoxicity of intracellular amyloid beta peptide1-42 through p53 and Bax in cultured primary human neurons. *J. Cell Biol.* 156, 519–529. doi: 10.1083/jcb.200110119

Zhou, X., Zhou, J., Li, X., Guo, C., Fang, T., and Chen, Z. (2011). GSK-3beta inhibitors suppressed neuroinflammation in rat cortex by activating autophagy in ischemic brain injury. *Biochem. Biophys. Res. Commun.* 411, 271–275. doi: 10.1016/j.bbrc.2011.06.117

Zhou, Y., Hayashi, I., Wong, J., Tugusheva, K., Renger, J. J., and Zerbinatti, C. (2014). Intracellular clusterin interacts with brain isoforms of the bridging integrator 1 and with the microtubule-associated protein Tau in Alzheimer's disease. *PLOS ONE* 9:e103187. doi: 10.1371/journal.pone.0103187

Zhu, Z., Yan, J., Jiang, W., Yao, X. G., Chen, J., Chen, L., et al. (2013). Arctigenin effectively ameliorates memory impairment in Alzheimer's disease model mice targeting both beta-amyloid production and clearance. *J. Neurosci.* 33, 13138–13149. doi: 10.1523/JNEUROSCI.4790-12.2013

Conflict of Interest Statement: The authors declare that the research was conducted in the absence of any commercial or financial relationships that could be construed as a potential conflict of interest.

Copyright © 2018 Uddin, Stachowiak, Mamun, Tzvetkov, Takeda, Atanasov, Bergantin, Abdel-Daim and Stankiewicz. This is an open-access article distributed under the terms of the Creative Commons Attribution License (CC BY). The use, distribution or reproduction in other forums is permitted, provided the original author(s) and the copyright owner are credited and that the original publication in this journal is cited, in accordance with accepted academic practice. No use, distribution or reproduction is permitted which does not comply with these terms.

frontiers in Human Neuroscience

ORIGINAL RESEARCH
published: 30 October 2017
doi: 10.3389/fnhum.2017.00514

Tai Chi Chuan and Baduanjin Mind-Body Training Changes Resting-State Low-Frequency Fluctuations in the Frontal Lobe of Older Adults: A Resting-State fMRI Study

Jing Tao[1,2,3], Xiangli Chen[4], Jiao Liu[1], Natalia Egorova[3], Xiehua Xue[5], Weilin Liu[1,2], Guohua Zheng[1], Ming Li[5], Jinsong Wu[1], Kun Hu[1], Zengjian Wang[3,6], Lidian Chen[1,2] and Jian Kong[3]**

[1]College of Rehabilitation Medicine, Fujian University of Traditional Chinese Medicine, Fuzhou, China, [2]Fujian Key Laboratory of Rehabilitation Technology, Fujian University of Traditional Chinese Medicine, Fuzhou, China, [3]Department of Psychiatry, Massachusetts General Hospital and Harvard Medical School, Charlestown, MA, United States, [4]Department of Rehabilitation Psychology and Special Education, University of Wisconsin-Madison, Madison, WI, United States, [5]Affiliated Rehabilitation Hospital, Fujian University of Traditional Chinese Medicine, Fuzhou, China, [6]Developmental and Educational Psychology, South China Normal University, Guangzhou, China

OPEN ACCESS

Edited by:
Athanasios Alexiou,
Novel Global Community Educational Foundation (NGCEF), Hebersham, Australia

Reviewed by:
Veena A. Nair,
University of Wisconsin-Madison, United States
Ruiwang Huang,
State Key Laboratory of Brain and Cognitive Science, Institute of Biophysics (CAS), China

***Correspondence:**
Lidian Chen
cld@fjtcm.edu.cn
Jian Kong
kongj@nmr.mgh.harvard.edu

Received: 11 May 2017
Accepted: 10 October 2017
Published: 30 October 2017

Citation:
Tao J, Chen X, Liu J, Egorova N, Xue X, Liu W, Zheng G, Li M, Wu J, Hu K, Wang Z, Chen L and Kong J (2017) Tai Chi Chuan and Baduanjin Mind-Body Training Changes Resting-State Low-Frequency Fluctuations in the Frontal Lobe of Older Adults: A Resting-State fMRI Study. Front. Hum. Neurosci. 11:514. doi: 10.3389/fnhum.2017.00514

Age-related cognitive decline is a significant public health concern. Recently, non-pharmacological methods, such as physical activity and mental training practices, have emerged as promising low-cost methods to slow the progression of age-related memory decline. In this study, we investigated if Tai Chi Chuan (TCC) and Baduanjin modulated the fractional amplitude of low-frequency fluctuations (fALFF) in different frequency bands (low-frequency: 0.01–0.08 Hz; slow-5: 0.01–0.027 Hz; slow-4: 0.027–0.073 Hz) and improved memory function. Older adults were recruited for the randomized study. Participants in the TCC and Baduanjin groups received 12 weeks of training (1 h/day for 5 days/week). Participants in the control group received basic health education. Each subject participated in memory tests and fMRI scans at the beginning and end of the experiment. We found that compared to the control group: (1) TCC and Baduanjin groups demonstrated significant improvements in memory function; (2) TCC increased fALFF in the dorsolateral prefrontal cortex (DLPFC) in the slow-5 and low-frequency bands; and (3) Baduanjin increased fALFF in the medial PFC in the slow-5 and low-frequency bands. This increase was positively associated with memory function improvement in the slow-5 and low-frequency bands across the TCC and Baduanjin groups.

Abbreviations: AD, Alzheimer's disease; ALFF, amplitude of low frequency fluctuations; aMCI, amnestic mild cognitive impairment; BDI, Beck depression inventory; CCN, cognitive control network; CSF, cerebrospinal fluid; DLPFC, dorsolateral prefrontal cortex; DPARSF, Data Processing Assistant for Resting-State fMRI; fALFF, fractional amplitude of low-frequency fluctuations; FWHM, full-width at half maximum; LFF, low frequency fluctuations; MCI, mild cognitive impairment; MDD, major depressive disorder; MMSE, Mini-Mental State Exam; mPFC, medial prefrontal cortex; MPRAGE, magnetization-prepared rapid gradient echo; PD, Parkinson's Disease; SAD, social anxiety disorder; TCC, Tai Chi Chuan; WMS-CR, Wechsler Memory Scale–Chinese Revision.

Our results suggest that TCC and Baduanjin may work through different brain mechanisms to prevent memory decline due to aging.

Keywords: mind-body exercise, memory, aging, fractional amplitude of low-frequency fluctuations (fALFF), resting-state functional magnetic resonance imaging (fMRI), frequency bands

INTRODUCTION

Age is the main risk factor for most common neurodegenerative diseases, such as mild cognitive impairment (MCI) and Alzheimer's disease (AD). Memory dysfunction is the primary cognitive symptom in MCI and AD and has a profound impact on those whom it affects (McKhann et al., 2011). Nevertheless, pharmaceutical treatments for age-related memory decline remain unsatisfactory.

Recently, non-pharmacological methods, such as physical activity and mental training practices, have emerged as promising low-cost methods to slow the progression of age-related memory decline (Hillman et al., 2008; Erickson et al., 2011, 2014; Killgore et al., 2013; Makizako et al., 2013; Voss et al., 2013; Kelly et al., 2014; Tang and Posner, 2014; Tamura et al., 2015). For instance, Ruscheweyh et al. (2011) found that a 6 months intervention of low-intensity physical activity can improve episodic memory performance in healthy elderly individuals, and this improvement is associated with increases in local gray matter volume in the prefrontal and cingulate cortex, and Brain-derived neurotrophic factor (BDNF) levels. Innes et al. (2017) also reported that 12 min/day for 3 months of Kirtan Kriya meditation training can significantly improve memory and cognitive performance. Unlike pharmaceutical treatments, these methods usually lack serious side effects.

Tai Chi Chuan (TCC) and Baduanjin are popular mind-body practices (Wang et al., 2010; Zheng et al., 2014; Tao et al., 2015). Both of these practices combine meditation with slow movements, deep breathing, and relaxation to smooth vital energy (or qi) flow in the body (Wang et al., 2010). However, these practices are also different from each other; TCC involves more complicated body movements and requires moving one's trunk and all four limbs (Wei et al., 2013), whereas the movement involved in Baduanjin is much simpler and is characterized by eight fixed movements (Xiong et al., 2015). Accumulating evidence has shown that TCC and Baduanjin practice improves cognitive performance and memory function (Wang, 2007; Chang et al., 2010; Lam et al., 2011; Tsai et al., 2013; Fong et al., 2014; Li F. et al., 2014; Wayne et al., 2014; Yin et al., 2014; Zheng et al., 2015). Nevertheless, the mechanisms underlying TCC and Baduanjin are still poorly understood.

In recent years, spontaneous fluctuations in brain activity during rest have drawn the attention of neuroimaging researchers. Investigators believe that these slow-frequency fluctuations may provide information about the intrinsic functional organization of the brain (Fox and Raichle, 2007). Furthermore, studies suggest that the human brain is a complex system that can generate a multitude of oscillatory waves, with different oscillatory classes carrying different dimensions of brain integration. The coupling of different bands of oscillators can provide enhanced combinatorial opportunities for storing complex temporal patterns to accomplish specific functions (Knyazev, 2007).

The low frequency fluctuations (LFF) between 0.01 Hz and 0.08 Hz are of particular relevance to resting state fMRI (rs-fMRI; Biswal et al., 1995). This low frequency range has been further divided into several distinct bands (Buzsáki and Draguhn, 2004), such as slow-4 (0.027–0.073 Hz) and slow-5 (0.01–0.027 Hz), which may indicate the modulation of cortical excitability and neuronal synchronization (Hoptman et al., 2010; Zuo et al., 2010). Recently, investigators have analyzed resting-state fMRI data filtered at the slow-4 and slow-5 bands separately to investigate AD (Liu et al., 2014), MCI (Han et al., 2012; Zhao et al., 2015), social anxiety disorder (SAD; Zhang et al., 2015), Parkinson's Disease (PD; Esposito et al., 2013), and schizophrenia (Hoptman et al., 2010). Studies have found characteristic differences between these specific bands, further endorsing the value of distinguishing the slow-4 and slow-5 bands.

There are many methods that can be used to investigate the brain's resting state spontaneous fluctuations. One such method is to characterize the regional spontaneous neuronal activity using the fractional amplitude of low frequency fluctuations (fALFF; Zang et al., 2007; Zou et al., 2008). As a normalized index of amplitude of low frequency fluctuations (ALFF), fALFF is defined as the total power within the low-frequency range divided by the total power in the entire detectable frequency range (Zuo et al., 2010). This method significantly suppresses non-specific signal components in resting state MRI and increases sensitivity to regional spontaneous brain activity (Zuo et al., 2010).

Alterations in fALFF have been found in several diseases. For instance, Sui et al. (2015) reported that in schizophrenic patients, increased cognitive performance was associated with higher fALFF in the striatum and decreased cognitive performance was associated with higher fALFF in the dorsolateral prefrontal cortex (DLPFC). McGill et al. (2014) reported decreased fALFF in the (PFC) and thalamus in patients with idiopathic generalized epilepsy. Additionally, Han et al. (2011) found that MCI is associated with decreased ALFF/fALFF values in the PCC/PCu, mPFC, hippocampus/PHG and prefrontal regions and increased ALFF/fALFF values in the occipital and temporal regions.

In this study, we investigated changes in spontaneous brain activity using fALFF in older adults following 3-months of TCC or Baduanjin practice. We hypothesized that 3-months of TCC and Baduanjin practice would improve memory function and modulate spontaneous brain activity in the brain regions associated with memory. In addition, we hypothesized that the modulatory effects of TCC and Baduanjin might vary in different low frequency bands.

MATERIALS AND METHODS

In this study, we applied a data driven method to investigate fALFF changes before and after TCC and Baduanjin as compared to a control group. Although, the data has been used previously to investigate the resting state functional connectivity changes of the hippocampus (Tao et al., 2016) and DLPFC (Tao et al., 2017a) and brain structure changes (Tao et al., 2017b) following TCC and Baduanjin practice, we have never reported the results published in this manuscript. Please also see these published studies for more details on the experimental procedure.

Participants

The study was approved by the Medical Ethics Committee of Affiliated Rehabilitation Hospital, Fujian University of Traditional Chinese Medicine and registered in the Chinese Clinical Trial Registry (ChiCTR[1], ChiCTR-IPR-15006131). All participants were informed and signed a written consent.

Two cohorts of older adults from one community were recruited independently and randomized into a TCC or control group in one cohort and a Baduanjin or control group in the other cohort. We recruited the two cohorts separately to avoid potential cross practicing between TCC and Baduanjin. The randomized treatment assignments were sealed in opaque envelopes and opened each time when new participants were included. Outcome raters were blind to the group allocation.

Inclusion criteria were: (1) 50–70 years old; (2) right-handed; and (3) no regular physical exercise for at least 1 year (the minimal standard for regular physical exercise was defined as 30 min 3–4 times per week for the past 3 months). Exclusion criteria were: (1) history of stroke; (2) suffered from severe cerebrovascular disease, musculoskeletal system disease, or other contraindications caused by sports injury; (3) a score of Beck depression inventory (BDI-II) $\geq$ 14 (Beck et al., 1996); and (4) a score on the Mini-Mental State Exam (MMSE) $<$ 24 (Zhang et al., 1990).

Intervention

Two professional instructors with more than 5 years of training experience from Fujian University of Traditional Chinese Medicine were responsible for TCC and Baduanjin exercise training. To guarantee research quality, two staff members monitored the whole training procedure.

Tai Chi Chuan Exercise Group

TCC exercise, which was based on Yang-style 24-form (China National Sports Commission, 1983), was conducted for 60 min per session, 5 days per week for 12 weeks. Each session consisted of a warm-up and review of Tai Chi principles, TCC exercises, breathing technique training, and relaxation.

[1]http://www.chictr.org.cn/index.aspx

Baduanjin Exercise Group

The Baduanjin training regimen was in accordance with "Health Qigong—Baduanjin", published by the General Administration of Sport of China. Each Baduanjin session consisted of a warm-up, eight fixed movements, and ending posture. The frequency of the Baduanjin exercise was the same as the TCC group, i.e. 60 min per session, one session per day, 5 days per week for 12 weeks.

Control Group

Participants in the control group received basic health education at the beginning of the experiment (Hughes et al., 2014). For the next 12 weeks, they were instructed to keep their original physical activity habits. At the end of the experiment (after the second MRI scan), free TCC or Baduanjin training was offered.

Behavioral Measurement

The Wechsler Memory Scale–Chinese Revision (WMS-CR) was used to assess the memory function of each participant. The WMS-CR is designed to assess memory function (Gong and Wang, 1989; Woodard and Axelrod, 1995) and is one of the most frequently used clinical assessments. It consists of ten subtests: information, orientation, mental control, picture, recognition, visual reproduction, associative learning, touch, comprehension memory, and digit span. It also provides an overall memory quotient (MQ). Two licensed WMS-CR raters who were blinded to the randomization distribution administered the WMS-CR.

MRI Acquisition

All MRI scans were acquired on a 3.0T magnetic resonance scanner (General Electric SignaHDxt, Milwaukee, WI, USA) with an 8-channel phased-array head coil. For the rs-fMRI, the scans were acquired with TR = 2100 ms, TE = 30 ms, flip angle = 90°, slice thickness = 3 mm, gap = 0.6 mm, acquisition matrix = 64 $\times$ 64, voxel size = 3.125 $\times$ 3.125 $\times$ 3.6 mm^3, 42 axial slices, FOV = 200 $\times$ 200 mm, phases per location = 160. The scan lasted for 5 min and 36 s, and participants were required to stay awake with their eyes closed and ears plugged during the rs-fMRI scanning. In addition, magnetization-prepared rapid gradient echo (MPRAGE) T1-weighted images were collected.

Statistical Analysis

Behavioral Analysis

Baseline characteristics were compared by one-way analysis of variance (ANOVA) and Chi square tests using SPSS 18.0 Software (SPSS Inc., Chicago, IL, USA). During the analysis, all control participants from the two cohorts were combined into one group to increase the power. In order to estimate the effects of TCC and Baduanjin, ANCOVA analysis was applied to compare the change of MQ and the subtests across the three groups with age (years), with gender and education (years) included as covariates in the model. *Post hoc* analysis (Sidak corrected) was applied to explore the between-group differences.

Resting State Data Analysis

The fMRI data preprocessing was performed using Data Processing Assistant for Resting-State fMRI (DPARSF) Software (available at: http://rfmri.org/DPARSF; Chao-Gan and Yu-Feng, 2010) in MATLAB (Mathworks Inc., Natick, MA, USA). The software is based on Statistical Parametric Mapping (SPM8)[2] and the Resting-State fMRI Data Analysis Toolkit[3] (Song et al., 2011).

The first 10 volumes of functional data for each subject were discarded for signal equilibrium and participants' adaptation to the imaging noise. The remaining volumes were slice timing corrected, within-subject spatially realigned, co-registered to the respective structural images for each subject, and then segmented. Subjects were excluded if head movement exceeded 3 mm on any axis or if head rotation was greater than 3°. To perform subject-level correction of head motion, the Friston 24-parameter model (6 head motion parameters, 6 head motion parameters one time point before, and the 12 corresponding squared items; Friston et al., 1996; Yan et al., 2013) was used. Images were normalized using structural image unified segmentation and then re-sampled to 3-mm cubic voxels. After smoothing with a 6 mm full-width at half maximum (FWHM) Gaussian kernel, the linear and quadric trends of the time courses were removed. Similar to previous studies (Han et al., 2011), no temporal filtering was implemented during preprocessing so that the entire frequency band could be calculated. In this study, we applied three frequency bands: slow-5 (0.01–0.027 Hz), slow-4 (0.027–0.073 Hz), and the traditionally used low-frequency (0.01–0.08 Hz) bands.

Group analysis was performed with a random effects model using SPM8. To explore the difference between TCC and Baduanjin after longitudinal treatment, we used a full factorial module in SPM8 with two factors for group analysis. The first factor had three levels (TCC, Baduanjin, control group) and the second factor had two levels (pre- and post-treatment). Age, gender and years of education were also included in the analysis as covariates of non-interest. A threshold of a voxel-wise $p < 0.001$ uncorrected and cluster-level $p < 0.05$ family-wise error corrected based on the random Gaussian field theory base (Lindquist et al., 2009) was applied.

[2]http://www.fil.ion.ucl.ac.uk/spm
[3]http://www.restfmri.net

RESULTS

102 older adults between 50–70 years old were screened for this study. Of the 90 participants who were qualified for the study and finished baseline scans, 62 participants completed all study procedures (21 in the TCC group, 16 in the Baduanjin group, and 25 in the control group). Four participants in the TCC group dropped out (1 due to relocation, 1 due to unwillingness to get the second MRI scan, and 2 due to scheduling conflicts). Nine participants in the Baduanjin group dropped out (8 due to scheduling conflicts and 1 due to unwillingness to participate in the MRI scan). Fifteen participants in the control group dropped out (11 due to scheduling conflicts and 4 due to inability to participate in post-treatment MRI scans). One subject in the Baduanjin group was excluded from fALFF analysis due to excessive head movement (exceeded 3.0 mm).

Behavioral Results

Group characteristics are shown in **Table 1**. Age, gender, handedness, average years of education, MMSE score, and BDI score did not significantly differ among the three groups ($P > 0.05$). Average attendance rates were 95% in the TCC group (ranging from 88% to 100%) and 97% in the Baduanjin group (ranging from 92% to 100%).

MQ scores before and after exercise are presented in **Table 1**. No significant differences were found among the three groups at baseline. ANCOVA analysis of change between the baseline and post-treatment MQ scores showed a significant difference among the three groups ($F = 25.45$, $p < 0.001$). *Post hoc* Sidak correction analysis showed that compared with the control group, MQ scores significantly increased in the TCC and Baduanjin groups (Baduanjin: $p < 0.001$, TCC: $p < 0.001$). There were no significant differences between the TCC and Baduanjin groups ($p = 0.233$). The comparisons of the subscores of WMS-CR showed TCC significantly increased visual reproduction subscores compared to controls. Baduanjin produced greater improvement in mental control, recognition, visual reproduction, touch and comprehension memory subscores compared to controls after bonferroni correction ($p < 0.0063$). Baduanjin also produced greater improvements in touch subscores compared to TCC after bonferroni correction ($p < 0.0063$). Please also see our previous

TABLE 1 | Demographics of study participants and clinical outcome measurements.

Characteristics	Control (n = 25) Mean (SD)	Tai Chi Chuan (n = 21) Mean (SD)	Baduanjin (n = 15) Mean (SD)	Between-group difference		
				Tai Chi Chuan vs. Control P value	Baduanjin vs. Control p value	Tai Chi Chuan vs. Baduanjin p value
Age†	59.76 (4.83)	62.38 (4.55)	62.33 (3.88)	0.055	0.087	0.975
Gender (female/male)‡	19/6	13/8	9/6		0.473	
Handedness (right/left)	25/0	21/0	15/0	-	-	-
Average years of education†	8.52 (3.65)	9.61 (3.02)	9.13 (2.69)	0.255	0.563	0.658
MQ_Pre treatment†	99.08 (14.59)	105.81 (10.24)	99.20 (9.30)	0.065	0.976	0.112
MQ_Post treatment†††	97.76 (13.92)	123.57 (11.42)	124.86 (11.21)	<0.001	<0.001	0.907

†p values were calculated with one-way analysis of variance, ‡p values were calculated with the chi-square test, †††p values were calculated with mixed-model regression.

publications on subscore changes across different treatment (Tao et al., 2017b).

Resting-State fMRI Data Analysis Results

fALFF in Low-Frequency Band (0.01–0.08 Hz)

Pre- and post-treatment comparison of fALFF in the low-frequency band (0.01–0.08 Hz) among the three groups showed that after 12 weeks, fALFF was significantly increased in the right DLPFC in the TCC group compared to the control group (**Table 2**, **Figure 1A**). In the Baduanjin group, there was a significant increase in fALFF in the bilateral medial prefrontal cortex (mPFC) compared to the control group (**Table 2**, **Figure 1B**). No significant difference was observed between the TCC and Baduanjin groups at the threshold we set.

To explore the difference between Tai Chi vs. Baduanjin intervention, we also applied a relatively less conservative threshold of voxel-wise $p < 0.005$ uncorrected with 10 continuous voxels. We found that compared to the Baduanjin group, there was a significant increase in fALFF in the periaqueductal gray, bilateral DLPFC, and temporoparietal junction in the TCC group. Compared with the TCC group, the Baduanjin group was associated with a significant fALFF increase in the left mPFC and left precuneus.

To explore the association between the fALFF changes observed above and behavioral outcomes, we also extracted the average fALFF values of the significant clusters (DLPFC and mPFC) and performed a multiple regression analysis including age, gender, and education as covariates. Results showed a significant association between the fALFF changes at mPFC and corresponding MQ ($r = 0.48$, $p = 0.005$ significant after Bonferroni correction (0.025 (0.05/2); **Figure 1C**), as well as a marginal association between the fALFF changes at DLPFC and corresponding MQ changes ($p = 0.048$, not significant after Bonferroni correction across the TCC and Baduanjin groups).

fALFF in Slow-5 Band

Pre- and post-treatment comparison of fALFF in the slow-5 band among the three groups is shown in **Table 2** and **Figure 1**. After 12 weeks, participants in the TCC group showed significant increases in the right DLPFC compared with participants in the control group (**Figure 1D**). Participants in the Baduanjin group showed significant increases in the bilateral mPFC compared with participants in the control group (**Figure 1E**). No significant difference was found between the TCC and Baduanjin groups at the threshold we set.

To further explore the difference between Tai Chi vs. Baduanjin comparisons, we applied a relatively less conservative threshold of voxel-wise $p < 0.005$ uncorrected with 10 continuous voxels. We found that compared to the Baduanjin group, there was a significant fALFF increase in the right lateral prefrontal cortex and periaqueductal gray/pon, and a significant fALFF decrease in the left DLPFC in the TCC group.

To explore the association between the fALFF changes observed above and behavioral outcomes, we also extracted the average fALFF values of the significant clusters and performed multiple regression analysis respectively including age, gender and education as covariates across the participants in TCC and Baduanjin group. Results showed a significant association between the mPFC fALFF changes and corresponding MQ changes ($r = 0.40$, $p = 0.02$, significant after after Bonferroni correction (0.025 (0.05/2; **Figure 1F**). There was no significant association between DLPFC fALFF changes and corresponding MQ changes ($p = 0.078$).

fALFF in Slow-4 Band

No significant differences among the three groups (two exercise groups and one control group) were observed. When we applied a relatively less conservative threshold of voxel-wise $p < 0.001$ uncorrected with 10 continuous voxels, we

TABLE 2 | Comparisons of fractional amplitude of low-frequency fluctuations (fALFF) at different bands between groups.

		MNI coordinates					
Contrast	**Brain regions**	**Cluster size**	**Peak *z*-value**	**Cluster effect size**	***X***	***Y***	***Z***
Low-frequency band							
TaiChiChuan > control	R DLPFC	60	5.45	3.02	51	18	39
Baduanjin > control	L mPFC	33	4.64	1.68	−12	12	66
	R mPFC	34	4.23	1.59	12	54	36
Control > Tai Chi Chuan			No brain region above the threshold				
Control > Baduanjin			No brain region above the threshold				
Tai Chi Chuan > Baduanjin			No brain region above the threshold				
Baduanjin > Tai Chi Chuan			No brain region above the threshold				
Slow-5 band							
Tai Chi Chuan > control	R DLPFC	65	5.1	2.17	48	15	42
Baduanjin > control	R mPFC	167	4.51	1.67	9	57	36
	L mPFC		4.41		−6	60	39
Control > Tai Chi Chuan			No brain region above the threshold				
Control > Baduanjin			No brain region above the threshold				
Tai Chi Chuan > Baduanjin			No brain region above the threshold				
Baduanjin > Tai Chi Chuan			No brain region above the threshold				

L, left; R, right; DLPFC, dorsolateral prefrontal cortex; mPFC, medial prefrontal cortex.

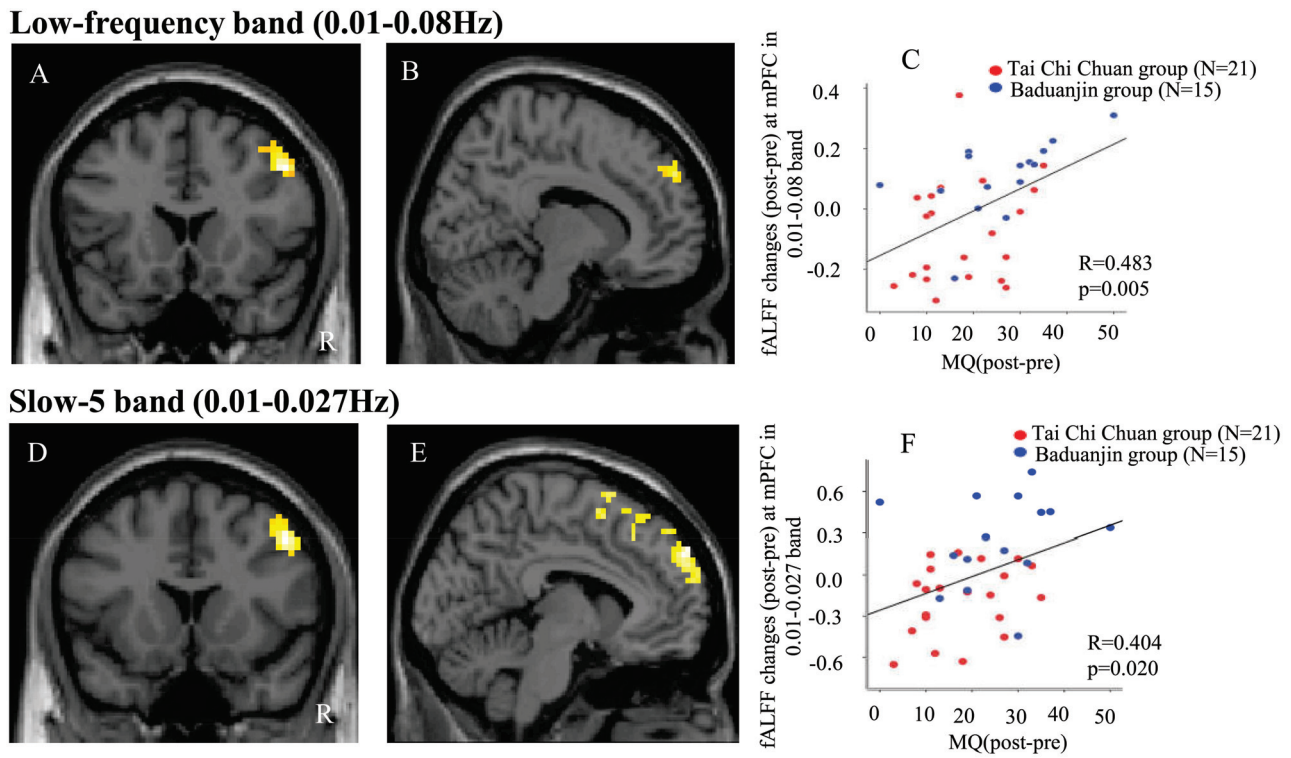


FIGURE 1 | (A) Increased fractional amplitude of low-frequency fluctuations (fALFF) in the 0.01–0.08 Hz band in the Tai Chi Chuan (TCC) group compared with the control group. **(B)** Increased fALFF in the 0.01–0.08 Hz band in the Baduanjin group compared with the control group. **(D)** Increased fALFF in the 0.01–0.027 Hz band in the TCC group compared with the control group. **(E)** Increased fALFF in the 0.01–0.027 Hz band in the Baduanjin group compared with the control group. **(C,F)** Scatter plots showing the association between the prefrontal cortex fALFF value of the significant cluster and improvements in memory across the TCC and Baduanjin groups, corrected for age, gender, years of education (**C**: $r = 0.483$, $p = 0.005$; **F**: $r = 0.404$, $p = 0.02$). R: right.

also did not find any significant results between the three groups.

DISCUSSION

In this study, we investigated the effects of 12 weeks of TCC and Baduanjin exercise on fALFF changes and clinical outcome measures in older adults. We found that: (1) MQ significantly increased in both TCC and Baduanjin groups compared with the control group; (2) TCC increased fALFF in the right DLPFC in the slow-5 band and the 0.01–0.08 Hz band; and (3) Baduanjin increased fALFF in the bilateral mPFC in the slow-5 band and the 0.01–0.08 Hz band following exercise. fALFF changes at the mPFC in the slow-5 and 0.01–0.08 Hz bands showed a significant positive association with corresponding MQ changes.

Both TCC and Baduanjin are mind-body exercises consisting of meditation, breathing, and gentle movements. From the viewpoint of physical exercise, both TCC and Baduanjin are safe aerobic activities (Li R. et al., 2014; Wayne et al., 2014). Aerobic exercise has been shown to improve memory function (Flöel et al., 2010; Erickson et al., 2011; Li L. et al., 2014; Seo et al., 2014). In addition to the physical component, TCC and Baduanjin also include sustained attention, focus, and multi-tasking. Thus, the mind-body exercise component may also have positive effects on cognitive function. Our finding of a significant improvement in general memory function after 3 months of TCC and Baduanjin practice is consistent with previous studies (Chang et al., 2010; Miller and Taylor-Piliae, 2014; Zheng et al., 2015) showing positive cognitive benefits of TCC in older adults. Our study demonstrates the power of TCC and Baduanjin practice in helping older adults improve memory.

We found that compared to controls, participants in the TCC group had increased fALFF in the right DLPFC, while the participants in the Baduanjin group had increased fALFF in the bilateral mPFC in the slow-5 band and the 0.01–0.08 Hz band. Although TCC and Baduanjin are associated with different patterns compared to controls, we did not find significant differences between the TCC and Baduanjin groups at this threshold we set. However, at a less conservative threshold of voxel-wise $p < 0.005$ uncorrected with 10 continuous voxels, there was a significant fALFF increase in the bilateral DLPFC, and decrease in the left mPFC and left precuneus in the TCC group compared to Baduanjin group in the 0.01–0.08 band. We also found that compared to the Baduanjin group, there was a significant fALFF increase in right lateral prefrontal cortex compared to the Baduanjin group in the

slow-5 band. These significant difference activity pattern between TCC and Baduanjin is consistent with the findings when comparing: (1) Tai Chi vs. Control; and (2) Baduanjin vs. Control. Furthermore, we also found that TCC and Baduanjin modulate the subtests of WMS-CR differently, Baduanjin can significantly increase the touch subscore compared to TCC, which further suggests that different mechanism may underlying Tai Chi Quan and Baduanjin. We speculate this difference may due to different exercise characteristics associated with the two mind-body interactions. TCC involves more complicated body movements and requires moving the trunk and all four limbs, whereas the movement involved in Baduanjin is much simpler.

In this study, we found that TCC exercise increased fALFF in the right DLPFC in the slow-5 band and the 0.01–0.08 Hz band compared to the control group. Previous studies have demonstrated that the DLPFC, a task positive region, is a key area in the cognitive control network (CCN; Miller and Cohen, 2001; Cieslik et al., 2013). The CCN is important in top-down modulation of attention–memory interactions (Corbetta and Shulman, 2002; Cole and Schneider, 2007; Chiu and Yantis, 2009; Spreng et al., 2010; Kong et al., 2013; Hwang et al., 2015; Rosen et al., 2016). Recent studies have shown that non-invasive brain stimulation techniques such as repetitive transcranial magnetic stimulation and transcranial direct current stimulation of the DLPFC enhanced memory-guided responses in a visuospatial working memory task (Balconi and Ferrari, 2012; Brunoni and Vanderhasselt, 2014; Giglia et al., 2014). These findings further confirm the DLPFC's role in memory function.

Previous studies (Baron Short et al., 2010) found significantly increased DLPFC activation during meditation in comparison to a control task. In a recent study, investigators found that compared with control participants, TCC experts show greater functional homogeneity in the right post-central gyrus and lower functional homogeneity in the right DLPFC and the left anterior cingulate cortex. The gain in functional integration was significantly correlated with cognitive performance in TCC experts (Wei et al., 2014). In another study, investigators found that multimodal intervention including TCC exercise enhanced the ALFF in the right middle frontal gyrus/DLPFC in older adults (Yin et al., 2014). In a more recent study, we found that TCC practice significantly modulates the rsFC between the CCN and the superior frontal gyrus and ACC, and that Baduanjin modulates the rsFC between the CCN and the putamen and insula (Tao et al., 2017a). Our results are partially consistent with these findings.

We also found fALFF increases in the slow-5 band and the 0.01–0.08 Hz band in the Baduanjin group at the mPFC. This change was significantly associated with memory function changes. The mPFC is associated with the highest baseline metabolic activity at rest (Gusnard et al., 2001) and is a key region in the default mode network (DMN; Li L. et al., 2014). The mPFC identified in the present study overlaps with the findings observed in previous studies on the impact of physical activity and meditation on cognitive functions (Flöel et al., 2010; Hasenkamp and Barsalou, 2012; Tang and Posner, 2014; Tamura et al., 2015).

The mPFC is known to undergo both structural and functional changes with aging (Gutchess et al., 2007; Hurtz et al., 2014; van de Vijver et al., 2014). Research suggests that the mPFC's function is related to different aspects of social cognitive processing (Amodio and Frith, 2006), which involves action monitoring (Barch et al., 2001), self-knowledge (Macrae et al., 2004), person perception, mentalization (Grèzes et al., 2004), and outcome monitoring (Camille et al., 2004). Studies also found the mPFC is involved in the encoding and retrieval of memory (van Kesteren et al., 2010, 2012; Brod et al., 2013). In a previous study based on the same data, we found that TCC and Baduanjin (at a less conservative threshold) can increase the rsFC between the hippocampus and mPFC (Tao et al., 2016). Taken together, our result suggests that Baduanjin may improve memory function through the mPFC and associated brain networks, such as the hippocampus.

In this study, we found that the slow-5 frequency band and the low-frequency band (0.01–0.08 Hz) showed fALFF changes after TCC and Baiduanjin practice, while no significant differences were observed in the slow-4 band. This suggests that the memory-relevant changes induced by 3 months of TCC and Baduanjin practice are specifically reflected difference low-frequency band. In a previous study, Han et al. (2011) investigated changes of ALFF and fALFF in patients with MCI between the slow-4 and slow-5 bands. They found significant differences in fALFF between MCI patients and controls only in the slow-5 band. The pattern of intrinsic functional connectivity is sensitive to specific frequency bands. Chao-Gan and Yu-Feng (2010) found that the low-frequency range (0.01–0.08 Hz) may better reveal the DMN. Zuo et al. (2010) also shown that Slow-5 (0.01–0.027 Hz) amplitudes at low frequency were more dominant within ventromedial prefrontal cortices. Consistent with these results, our findings also predominantly locate at the frontal area in Slow-5 band and low-frequency range. Further studies are needed to confirm and expand our findings.

The current study has several limitations. First, the sample size is relatively small. Second, both TCC and Baduanjin are considered mind-body exercises. Therefore, our design could not disentangle the effect of physical activity vs. mental exercise, and was unable to identify the crucial components of the exercise affecting memory improvement and brain functional fluctuation changes. Further research is needed to compare the effects of exercise, meditation, TCC and Baduanjin directly. Third, we did not record the participants' original physical activity habits, and only gave them an introduction to keep their original physical activity habits throughout the duration of the experiment. Further study should record the participants original physical activity habits for more accurate documentation of their activity intensity.

CONCLUSION

In this study, we found that 12 weeks of intensive group TCC/Baduanjin practice can significantly modulate fALFF in

different frequency bands and improve memory function. TCC increased fALFF in the slow-5 band and the 0.01–0.08 Hz band in the DLPFC, and Baduanjin increased fALFF in the slow-5 band and the 0.01–0.08 Hz band in the mPFC. fALFF changes in the mPFC in the slow-5 band and 0.01–0.08 Hz band were also correlated with general memory improvement. Our results imply that TCC and Baduanjin may work through different brain mechanisms due to differences in the characteristics and complexity of their respective regimens, but both exercises may hold the potential to prevent age-related memory decline.

ETHICS STATEMENT

The Medical Ethics Committee in the Affiliated Rehabilitation Hospital of Fujian University of Traditional Chinese Medicine approved all study procedures. The experiment was performed in accordance with approved guidelines. All participants signed a written consent. This study was registered on the Chinese Clinical Trial Registry (ChiCTR-IPR-15006131).

AUTHOR CONTRIBUTIONS

LC: experimental design; JK: analysis and manuscript preparation; JT: experimental design, data analysis and manuscript preparation; GZ: data analysis; JL and XX: data collection and data analysis; WL, JW, ML, ZW and KH: data collection; XC and NE: manuscript preparation. All authors contributed to manuscript draft and have read and approved the final manuscript.

FUNDING

This study is supported by the Special Scientific Research Fund of Public Welfare Profession of China (Grant No. 201307004), Ministry of Science and Technology and Ministry of Finance of the People's Republic of China. It is also supported by the National Rehabilitation Research Center of Traditional Chinese Medicine, Fujian rehabilitation industrial institution and Fujian Rehabilitation Tech Co-innovation Center (Grant No. X2012007-Collaboration). JK is supported by R01AT006364, R01AT008563, R61AT009310, R21AT008707 and P01 AT006663 from NIH/NCCIH.

ACKNOWLEDGMENTS

We thank two professional instructors from the Fujian University of Traditional Chinese Medicine Hongmei Yi and Tingjin Duan, for their training in Tai Chi Chuan and Baduanjin exercise. We thank Sharon Sun, Courtney Lang and Joel Park for editing the English.

REFERENCES

Amodio, D. M., and Frith, C. D. (2006). Meeting of minds: the medial frontal cortex and social cognition. *Nat. Rev. Neurosci.* 7, 268–277. doi: 10.1038/nrn1884

Balconi, M., and Ferrari, C. (2012). rTMS stimulation on left DLPFC increases the correct recognition of memories for emotional target and distractor words. *Cogn. Affect. Behav. Neurosci.* 12, 589–598. doi: 10.3758/s13415-012-0090-1

Barch, D. M., Braver, T. S., Akbudak, E., Conturo, T., Ollinger, J., and Snyder, A. (2001). Anterior cingulate cortex and response conflict: effects of response modality and processing domain. *Cereb. Cortex* 11, 837–848. doi: 10.1093/cercor/11.9.837

Baron Short, E., Kose, S., Mu, Q., Borckardt, J., Newberg, A., George, M. S., et al. (2010). Regional brain activation during meditation shows time and practice effects: an exploratory FMRI study. *Evid. Based Complement. Alternat. Med.* 7, 121–127. doi: 10.1093/ecam/nem163

Beck, A. T., Steer, R. A., and Brown, G. K. (1996). *Manual for the Beck Depression Inventory-II.* San Antonio, TX: Psychological Corporation.

Biswal, B., Yetkin, F. Z., Haughton, V. M., and Hyde, J. S. (1995). Functional connectivity in the motor cortex of resting human brain using echo-planar MRI. *Magn. Reson. Med.* 34, 537–541. doi: 10.1002/mrm.1910340409

Brod, G., Werkle-Bergner, M., and Shing, Y. L. (2013). The influence of prior knowledge on memory: a developmental cognitive neuroscience perspective. *Front. Behav. Neurosci.* 7:139. doi: 10.3389/fnbeh.2013.00139

Brunoni, A. R., and Vanderhasselt, M. A. (2014). Working memory improvement with non-invasive brain stimulation of the dorsolateral prefrontal cortex: a systematic review and meta-analysis. *Brain Cogn.* 86, 1–9. doi: 10.1016/j.bandc.2014.01.008

Buzsáki, G., and Draguhn, A. (2004). Neuronal oscillations in cortical networks. *Science* 304, 1926–1929. doi: 10.1126/science.1099745

Camille, N., Coricelli, G., Sallet, J., Pradat-Diehl, P., Duhamel, J. R., and Sirigu, A. (2004). The involvement of the orbitofrontal cortex in the experience of regret. *Science* 304, 1167–1170. doi: 10.1126/science.1094550

Chang, Y.-K., Nien, Y.-H., Tsai, C.-L., and Etnier, J. L. (2010). Physical activity and cognition in older adults: the potential of Tai Chi Chuan. *J. Aging Phys. Act.* 18, 451–472. doi: 10.1123/japa.18.4.451

Chao-Gan, Y., and Yu-Feng, Z. (2010). DPARSF: a MATLAB toolbox for 'Pipeline' data analysis of resting-state fMRI. *Front. Syst. Neurosci.* 4:13. doi: 10.3389/fnsys.2010.00013

China National Sports Commission. (1983). *Simplified Taijiquan.* Beijing: People's Sports Press.

Chiu, Y. C., and Yantis, S. (2009). A domain-independent source of cognitive control for task sets: shifting spatial attention and switching categorization rules. *J. Neurosci.* 29, 3930–3938. doi: 10.1523/jneurosci.5737-08.2009

Cieslik, E. C., Zilles, K., Caspers, S., Roski, C., Kellermann, T. S., Jakobs, O., et al. (2013). Is there "One" DLPFC in cognitive action control? Evidence for heterogeneity from co-activation-based parcellation. *Cereb. Cortex* 23, 2677–2689. doi: 10.1093/cercor/bhs256

Cole, M. W., and Schneider, W. (2007). The cognitive control network: integrated cortical regions with dissociable functions. *Neuroimage* 37, 343–360. doi: 10.1016/j.neuroimage.2007.03.071

Corbetta, M., and Shulman, G. L. (2002). Control of goal-directed and stimulus-driven attention in the brain. *Nat. Rev. Neurosci.* 3, 201–215. doi: 10.1038/nrn755

Erickson, K. I., Leckie, R. L., and Weinstein, A. M. (2014). Physical activity, fitness, and gray matter volume. *Neurobiol. Aging* 35, S20–S28. doi: 10.1016/j.neurobiolaging.2014.03.034

Erickson, K. I., Voss, M. W., Prakash, R. S., Basak, C., Szabo, A., Chaddock, L., et al. (2011). Exercise training increases size of hippocampus and improves memory. *Proc. Natl. Acad. Sci. U S A* 108, 3017–3022. doi: 10.1073/pnas.1015950108

Esposito, F., Tessitore, A., Giordano, A., De Micco, R., Paccone, A., Conforti, R., et al. (2013). Rhythm-specific modulation of the sensorimotor network in drug-naive patients with Parkinson's disease by levodopa. *Brain* 136, 710–725. doi: 10.1093/brain/awt007

Flöel, A., Ruscheweyh, R., Krüger, K., Willemer, C., Winter, B., Völker, K., et al. (2010). Physical activity and memory functions: are neurotrophins and cerebral gray matter volume the missing link? *Neuroimage* 49, 2756–2763. doi: 10.1016/j.neuroimage.2009.10.043

Fong, D.-Y., Chi, L.-K., Li, F., and Chang, Y.-K. (2014). The benefits of endurance exercise and Tai Chi Chuan for the task-switching aspect of executive function in older adults: an ERP study. *Front. Aging Neurosci.* 6:295. doi: 10.3389/fnagi.2014.00295

Fox, M. D., and Raichle, M. E. (2007). Spontaneous fluctuations in brain activity observed with functional magnetic resonance imaging. *Nat. Rev. Neurosci.* 8, 700–711. doi: 10.1038/nrn2201

Friston, K. J., Williams, S., Howard, R., Frackowiak, R. S., and Turner, R. (1996). Movement-related effects in fMRI time-series. *Magn. Reson. Med.* 35, 346–355. doi: 10.1002/mrm.1910350312

Giglia, G., Brighina, F., Rizzo, S., Puma, A., Indovino, S., Maccora, S., et al. (2014). Anodal transcranial direct current stimulation of the right dorsolateral prefrontal cortex enhances memory-guided responses in a visuospatial working memory task. *Funct. Neurol.* 29, 189–193. doi: 10.11138/FNeur/2014.29.3.189

Gong, Y., and Wang, D. J. (1989). *Handbook of Wechsler Memory Scale-Revised (WMS-RC), Chinese Version.* Changsha: Bulletin of Hunan Medical College.

Grèzes, J., Frith, C., and Passingham, R. E. (2004). Brain mechanisms for inferring deceit in the actions of others. *J. Neurosci.* 24, 5500–5505. doi: 10.1523/jneurosci.0219-04.2004

Gusnard, D. A., Akbudak, E., Shulman, G. L., and Raichle, M. E. (2001). Medial prefrontal cortex and self-referential mental activity: relation to a default mode of brain function. *Proc. Natl. Acad. Sci. U S A* 98, 4259–4264. doi: 10.1073/pnas.071043098

Gutchess, A. H., Kensinger, E. A., and Schacter, D. L. (2007). Aging, self-referencing, and medial prefrontal cortex. *Soc. Neurosci.* 2, 117–133. doi: 10.1080/17470910701399029

Han, Y., Lui, S., Kuang, W., Lang, Q., Zou, L., and Jia, J. (2012). Anatomical and functional deficits in patients with amnestic mild cognitive impairment. *PLoS One* 7:e28664. doi: 10.1371/journal.pone.0028664

Han, Y., Wang, J., Zhao, Z., Min, B., Lu, J., Li, K., et al. (2011). Frequency-dependent changes in the amplitude of low-frequency fluctuations in amnestic mild cognitive impairment: a resting-state fMRI study. *Neuroimage* 55, 287–295. doi: 10.1016/j.neuroimage.2010.11.059

Hasenkamp, W., and Barsalou, L. W. (2012). Effects of meditation experience on functional connectivity of distributed brain networks. *Front. Hum. Neurosci.* 6:38. doi: 10.3389/fnhum.2012.00038

Hillman, C. H., Erickson, K. I., and Kramer, A. F. (2008). Be smart, exercise your heart: exercise effects on brain and cognition. *Nat. Rev. Neurosci.* 9, 58–65. doi: 10.1038/nrn2298

Hoptman, M. J., Zuo, X. N., Butler, P. D., Javitt, D. C., D'Angelo, D., Mauro, C. J., et al. (2010). Amplitude of low-frequency oscillations in schizophrenia: a resting state fMRI study. *Schizophr. Res.* 117, 13–20. doi: 10.1016/j.schres.2009.09.030

Hughes, T. F., Flatt, J. D., Fu, B., Butters, M. A., Chang, C. C., and Ganguli, M. (2014). Interactive video gaming compared with health education in older adults with mild cognitive impairment: a feasibility study. *Int. J. Geriatr. Psychiatry* 29, 890–898. doi: 10.1002/gps.4075

Hurtz, S., Woo, E., Kebets, V., Green, A. E., Zoumalan, C., Wang, B., et al. (2014). Age effects on cortical thickness in cognitively normal elderly individuals. *Dement. Geriatr. Cogn. Dis. Extra* 4, 221–227. doi: 10.1159/000362872

Hwang, J. W., Egorova, N., Yang, X. Q., Zhang, W. Y., Chen, J., Yang, X. Y., et al. (2015). Subthreshold depression is associated with impaired resting-state functional connectivity of the cognitive control network. *Transl. Psychiatry* 5:e683. doi: 10.1038/tp.2015.174

Innes, K. E., Selfe, T. K., Khalsa, D. S., and Kandati, S. (2017). Meditation and music improve memory and cognitive function in adults with subjective cognitive decline: a pilot randomized controlled trial. *J. Alzheimers Dis.* 56, 899–916. doi: 10.3233/JAD-160867

Kelly, M. E., Loughrey, D., Lawlor, B. A., Robertson, I. H., Walsh, C., and Brennan, S. (2014). The impact of exercise on the cognitive functioning of healthy older adults: a systematic review and meta-analysis. *Ageing Res. Rev.* 16, 12–31. doi: 10.1016/j.arr.2014.05.002

Killgore, W. D., Olson, E. A., and Weber, M. (2013). Physical exercise habits correlate with gray matter volume of the hippocampus in healthy adult humans. *Sci. Rep.* 3:3457. doi: 10.1038/srep03457

Knyazev, G. G. (2007). Motivation, emotion, and their inhibitory control mirrored in brain oscillations. *Neurosci. Biobehav. Rev.* 31, 377–395. doi: 10.1016/j.neubiorev.2006.10.004

Kong, J., Jensen, K., Loiotile, R., Cheetham, A., Wey, H. Y., Tan, Y., et al. (2013). Functional connectivity of the frontoparietal network predicts cognitive modulation of pain. *Pain* 154, 459–467. doi: 10.1016/j.pain.2012.12.004

Lam, L. C., Chau, R. C., Wong, B. M., Fung, A. W., Lui, V. W., Tam, C. C., et al. (2011). Interim follow-up of a randomized controlled trial comparing chinese style mind body (Tai Chi) and stretching exercises on cognitive function in subjects at risk of progressive cognitive decline. *Int. J. Geriatr. Psychiatry* 26, 733–740. doi: 10.1002/gps.2602

Li, F., Harmer, P., Liu, Y., and Chou, L. S. (2014). Tai Ji Quan and global cognitive function in older adults with cognitive impairment: a pilot study. *Arch. Gerontol. Geriatr.* 58, 434–439. doi: 10.1016/j.archger.2013.12.003

Li, R., Jin, L., Hong, P., He, Z.-H., Huang, C.-Y., Zhao, J.-X., et al. (2014). The effect of baduanjin on promoting the physical fitness and health of adults. *Evid. Based Complement. Alternat. Med.* 2014:784059. doi: 10.1155/2014/784059

Li, L., Men, W. W., Chang, Y. K., Fan, M. X., Ji, L., and Wei, G. X. (2014). Acute aerobic exercise increases cortical activity during working memory: a functional MRI study in female college students. *PLoS One* 9:e99222. doi: 10.1371/journal.pone.0099222

Lindquist, M. A., Meng Loh, J., Atlas, L. Y., and Wager, T. D. (2009). Modeling the hemodynamic response function in fMRI: efficiency, bias and mis-modeling. *Neuroimage* 45, S187–S198. doi: 10.1016/j.neuroimage.2008.10.065

Liu, X., Wang, S., Zhang, X., Wang, Z., Tian, X., and He, Y. (2014). Abnormal amplitude of low-frequency fluctuations of intrinsic brain activity in Alzheimer's disease. *J. Alzheimers Dis.* 40, 387–397. doi: 10.3233/JAD-131322

Macrae, C. N., Moran, J. M., Heatherton, T. F., Banfield, J. F., and Kelley, W. M. (2004). Medial prefrontal activity predicts memory for self. *Cereb. Cortex* 14, 647–654. doi: 10.1093/cercor/bhh025

Makizako, H., Shimada, H., Doi, T., Park, H., Yoshida, D., and Suzuki, T. (2013). Six-minute walking distance correlated with memory and brain volume in older adults with mild cognitive impairment: a voxel-based morphometry study. *Dement. Geriatr. Cogn. Dis. Extra* 3, 223–232. doi: 10.1159/000354189

McGill, M. L., Devinsky, O., Wang, X., Quinn, B. T., Pardoe, H., Carlson, C., et al. (2014). Functional neuroimaging abnormalities in idiopathic generalized epilepsy. *Neuroimage Clin.* 6, 455–462. doi: 10.1016/j.nicl.2014.10.008

McKhann, G. M., Knopman, D. S., Chertkow, H., Hyman, B. T., Jack, C. R. Jr., Kawas, C. H., et al. (2011). The diagnosis of dementia due to Alzheimer's disease: recommendations from the national institute on aging- Alzheimer's association workgroups on diagnostic guidelines for Alzheimer's disease. *Alzheimers Dement.* 7, 263–269. doi: 10.1016/j.jalz.2011.03.005

Miller, E. K., and Cohen, J. D. (2001). An integrative theory of prefrontal cortex function. *Annu. Rev. Neurosci.* 24, 167–202. doi: 10.1146/annurev.neuro.24.1.167

Miller, S. M., and Taylor-Piliae, R. E. (2014). Effects of Tai Chi on cognitive function in community-dwelling older adults: a review. *Geriatr. Nurs.* 35, 9–19. doi: 10.1016/j.gerinurse.2013.10.013

Rosen, M. L., Stern, C. E., Michalka, S. W., Devaney, K. J., and Somers, D. C. (2016). Cognitive control network contributions to memory-guided visual attention. *Cereb. Cortex* 26, 2059–2073. doi: 10.1093/cercor/bhv028

Ruscheweyh, R., Willemer, C., Krüger, K., Duning, T., Warnecke, T., Sommer, J., et al. (2011). Physical activity and memory functions: an interventional study. *Neurobiol. Aging* 32, 1304–1319. doi: 10.1016/j.neurobiolaging.2009.08.001

Seo, T. B., Kim, T. W., Shin, M. S., Ji, E. S., Cho, H. S., Lee, J. M., et al. (2014). Aerobic exercise alleviates ischemia-induced memory impairment by enhancing cell proliferation and suppressing neuronal apoptosis in hippocampus. *Int. Neurourol. J.* 18, 187–197. doi: 10.5213/inj.2014.18.4.187

Song, X. W., Dong, Z. Y., Long, X. Y., Li, S. F., Zuo, X. N., Zhu, C. Z., et al. (2011). REST: a toolkit for resting-state functional magnetic resonance imaging data processing. *PLoS One* 6:e25031. doi: 10.1371/journal.pone.0025031

Spreng, R. N., Stevens, W. D., Chamberlain, J. P., Gilmore, A. W., and Schacter, D. L. (2010). Default network activity, coupled with the frontoparietal

control network, supports goal-directed cognition. *Neuroimage* 53, 303–317. doi: 10.1016/j.neuroimage.2010.06.016

Sui, J., Pearlson, G. D., Du, Y., Yu, Q., Jones, T. R., Chen, J., et al. (2015). In search of multimodal neuroimaging biomarkers of cognitive deficits in schizophrenia. *Biol. Psychiatry* 78, 794–804. doi: 10.1016/j.biopsych.2015.02.017

Tamura, M., Nemoto, K., Kawaguchi, A., Kato, M., Arai, T., Kakuma, T., et al. (2015). Long-term mild-intensity exercise regimen preserves prefrontal cortical volume against aging. *Int. J. Geriatr. Psychiatry* 30, 686–694. doi: 10.1002/gps.4205

Tang, Y.-Y., and Posner, M. I. (2014). Training brain networks and states. *Trends. Cogn. Sci.* 18, 345–350. doi: 10.1016/j.tics.2014.04.002

Tao, J., Chen, X., Egorova, N., Liu, J., Xue, X., Wang, Q., et al. (2017a). Tai Chi Chuan and baduanjin practice modulates functional connectivity of the cognitive control network in older adults. *Sci. Rep.* 7:41581. doi: 10.1038/srep41581

Tao, J., Liu, J., Liu, W., Huang, J., Xue, X., Chen, X., et al. (2017b). Tai Chi Chuan and baduanjin increase grey matter volume in older adults: a brain imaging study. *J. Alzheimers Dis.* 60, 389–400. doi: 10.3233/JAD-170477

Tao, J., Liu, J., Egorova, N., Chen, X., Sun, S., Xue, X., et al. (2016). Increased hippocampus–medial prefrontal cortex resting state functional connectivity and memory function after Tai Chi Chuan practice in elder adults. *Front. Aging Neurosci.* 8:25. doi: 10.3389/fnagi.2016.00025

Tao, J., Rao, T., Lin, L., Liu, W., Wu, Z., Zheng, G., et al. (2015). Evaluation of Tai Chi yunshou exercises on community-based stroke patients with balance dysfunction: a study protocol of a cluster randomized controlled trial. *BMC Complement. Altern. Med.* 15:31. doi: 10.1186/s12906-015-0555-1

Tsai, P. F., Chang, J. Y., Beck, C., Kuo, Y. F., and Keefe, F. J. (2013). A pilot cluster-randomized trial of a 20-week Tai Chi program in elders with cognitive impairment and osteoarthritic knee: effects on pain and other health outcomes. *J. Pain Symptom Manage.* 45, 660–669. doi: 10.1016/j.jpainsymman.2012.04.009

van de Vijver, I., Cohen, M. X., and Ridderinkhof, K. R. (2014). Aging affects medial but not anterior frontal learning-related theta oscillations. *Neurobiol. Aging* 35, 692–704. doi: 10.1016/j.neurobiolaging.2013.09.006

van Kesteren, M. T., Rijpkema, M., Ruiter, D. J., and Fernández, G. (2010). Retrieval of associative information congruent with prior knowledge is related to increased medial prefrontal activity and connectivity. *J. Neurosci.* 30, 15888–15894. doi: 10.1523/JNEUROSCI.2674-10.2010

van Kesteren, M. T., Ruiter, D. J., Fernández, G., and Henson, R. N. (2012). How schema and novelty augment memory formation. *Trends Neurosci.* 35, 211–219. doi: 10.1016/j.tins.2012.02.001

Voss, M. W., Heo, S., Prakash, R. S., Erickson, K. I., Alves, H., Chaddock, L., et al. (2013). The influence of aerobic fitness on cerebral white matter integrity and cognitive function in older adults: results of a one- year exercise intervention. *Hum. Brain Mapp.* 34, 2972–2985. doi: 10.1002/hbm.22119

Wang, S. T. (2007). Effect of baduanjin on physiological age of intelligence for old people. *J. Clin. Rehabil. Tissue Eng. Res.* 11, 7910–7913.

Wang, C., Schmid, C. H., Rones, R., Kalish, R., Yinh, J., Goldenberg, D. L., et al. (2010). A randomized trial of Tai Chi for fibromyalgia. *N. Engl. J. Med.* 363, 743–754. doi: 10.1056/NEJMoa0912611

Wayne, P. M., Walsh, J. N., Taylor-Piliae, R. E., Wells, R. E., Papp, K. V., Donovan, N. J., et al. (2014). Effect of Tai Chi on cognitive performance in older adults: systematic review and meta-analysis. *J. Am. Geriatr. Soc.* 62, 25–39. doi: 10.1111/jgs.12611

Wei, G. X., Dong, H. M., Yang, Z., Luo, J., and Zuo, X. N. (2014). Tai Chi Chuan optimizes the functional organization of the intrinsic human brain architecture in older adults. *Front. Aging Neurosci.* 6:74. doi: 10.3389/fnagi.2014.00074

Wei, G.-X., Xu, T., Fan, F.-M., Dong, H.-M., Jiang, L.-L., Li, H.-J., et al. (2013). Can taichi reshape the brain? a brain morphometry study. *PLoS One* 8:e61038. doi: 10.1371/journal.pone.0061038

Woodard, J. L., and Axelrod, B. N. (1995). Parsimonious prediction of wechsler memory scale—revised memory indices. *Psychol. Assess.* 7, 445–449. doi: 10.1037//1040-3590.7.4.445

Xiong, X., Wang, P., Li, S., Zhang, Y., and Li, X. (2015). Effect of baduanjin exercise for hypertension: a systematic review and meta-analysis of randomized controlled trials. *Maturitas* 80, 370–378. doi: 10.1016/j.maturitas.2015.01.002

Yan, C. G., Cheung, B., Kelly, C., Colcombe, S., Craddock, R. C., Di Martino, A., et al. (2013). A comprehensive assessment of regional variation in the impact of head micromovements on functional connectomics. *Neuroimage* 76, 183–201. doi: 10.1016/j.neuroimage.2013.03.004

Yin, S., Zhu, X., Li, R., Niu, Y., Wang, B., Zheng, Z., et al. (2014). Intervention-induced enhancement in intrinsic brain activity in healthy older adults. *Sci. Rep.* 4:7309. doi: 10.1038/srep07309

Zang, Y. F., He, Y., Zhu, C. Z., Cao, Q. J., Sui, M. Q., Liang, M., et al. (2007). Altered baseline brain activity in children with ADHD revealed by resting-state functional MRI. *Brain Dev.* 29, 83–91. doi: 10.1016/j.braindev.2006.07.002

Zhang, M. Y., Katzman, R., Salmon, D., Jin, H., Cai, G. J., Wang, Z. Y., et al. (1990). The prevalence of dementia and Alzheimer's disease in shanghai, china: impact of age, gender, and education. *Ann. Neurol.* 27, 428–437. doi: 10.1002/ana.410270412

Zhang, Y., Zhu, C., Chen, H., Duan, X., Lu, F., Li, M., et al. (2015). Frequency-dependent alterations in the amplitude of low-frequency fluctuations in social anxiety disorder. *J. Affect. Disord.* 174, 329–335. doi: 10.1016/j.jad.2014.12.001

Zhao, Z.-L., Fan, F.-M., Lu, J., Li, H.-J., Jia, L.-F., Han, Y., et al. (2015). Changes of gray matter volume and amplitude of low-frequency oscillations in amnestic MCI: an integrative multi-modal MRI study. *Acta Radiol.* 56, 614–621. doi: 10.1177/0284185114533329

Zheng, G., Chen, B., Fang, Q., Yi, H., Lin, Q., Chen, L., et al. (2014). Primary prevention for risk factors of ischemic stroke with baduanjin exercise intervention in the community elder population: study protocol for a randomized controlled trial. *Trials* 15:113. doi: 10.1186/1745-6215-15-113

Zheng, G., Liu, F., Li, S., Huang, M., Tao, J., and Chen, L. (2015). Tai Chi and the protection of cognitive ability. *Am. J. Prev. Med.* 49, 89–97. doi: 10.1016/j.amepre.2015.01.002

Zou, Q. H., Zhu, C. Z., Yang, Y., Zuo, X. N., Long, X. Y., Cao, Q. J., et al. (2008). An improved approach to detection of amplitude of low-frequency fluctuation (ALFF) for resting-state fMRI: fractional ALFF. *J. Neurosci. Methods* 172, 137–141. doi: 10.1016/j.jneumeth.2008.04.012

Zuo, X. N., Di Martino, A., Kelly, C., Shehzad, Z. E., Gee, D. G., Klein, D. F., et al. (2010). The oscillating brain: complex and reliable. *Neuroimage* 49, 1432–1445. doi: 10.1016/j.neuroimage.2009.09.037

Conflict of Interest Statement: JK has a disclosure to report; holding equity in the startup company MNT, but declares no conflict of interest.

The other authors declare that the research was conducted in the absence of any commercial or financial relationships that could be construed as a potential conflict of interest.

Copyright © 2017 Tao, Chen, Liu, Egorova, Xue, Liu, Zheng, Li, Wu, Hu, Wang, Chen and Kong. This is an open-access article distributed under the terms of the Creative Commons Attribution License (CC BY). The use, distribution or reproduction in other forums is permitted, provided the original author(s) or licensor are credited and that the original publication in this journal is cited, in accordance with accepted academic practice. No use, distribution or reproduction is permitted which does not comply with these terms.

frontiers in Neurology

ORIGINAL RESEARCH
published: 15 June 2018
doi: 10.3389/fneur.2018.00412

Effects of Oligosaccharides From *Morinda officinalis* on Gut Microbiota and Metabolome of APP/PS1 Transgenic Mice

Yang Xin[1,2†], Chen Diling[3†], Yang Jian[3], Liu Ting[2], Hu Guoyan[2], Liang Hualun[4], Tang Xiaocui[3], Lai Guoxiao[3,5], Shuai Ou[3], Zheng Chaoqun[3], Zhao Jun[6] and Xie Yizhen[3]*

[1] Department of Pharmacy, The Fifth Affiliated Hospital of Guangzhou Medical University, Guangzhou, China, [2] The Fifth Clinical School of Guangzhou Medical University, Guangzhou, China, [3] State Key Laboratory of Applied Microbiology Southern China, Guangdong Provincial Key Laboratory of Microbial Culture Collection and Application, Guangdong Open Laboratory of Applied Microbiology, Guangdong Institute of Microbiology, Guangzhou, China, [4] Department of Pharmacy, The Second Clinical Medical College of Guangzhou University of Chinese Medicine, Guangzhou, China, [5] College of Pharmacy, Guangxi University of Traditional Chinese Medicine, Nanning, China, [6] Department of Obstetrics, Guangdong Women and Children Hospital, Guangzhou, China

OPEN ACCESS

Edited by:
Ghulam Md Ashraf,
King Abdulaziz University, Saudi Arabia

Reviewed by:
Xin Qi,
Case Western Reserve University, United States
Robert Friedland,
University of Louisville, United States

***Correspondence:**
Chen Diling
diling1983@163.com

[†]These authors have contributed equally to this work.

Specialty section:
This article was submitted to Neurodegeneration, a section of the journal Frontiers in Neurology

Received: *14 December 2017*
Accepted: *18 May 2018*
Published: *15 June 2018*

Citation:
Xin Y, Diling C, Jian Y, Ting L, Guoyan H, Hualun L, Xiaocui T, Guoxiao L, Ou S, Chaoqun Z, Jun Z and Yizhen X (2018) Effects of Oligosaccharides From Morinda officinalis on Gut Microbiota and Metabolome of APP/PS1 Transgenic Mice. Front. Neurol. 9:412. doi: 10.3389/fneur.2018.00412

Alzheimer's disease (AD), a progressive neurodegenerative disorder, lacks preclinical diagnostic biomarkers and therapeutic drugs. Thus, earlier intervention in AD is a top priority. Studies have shown that the gut microbiota influences central nervous system disorders and that prebiotics can improve the cognition of hosts with AD, but these effects are not well understood. Preliminary research has shown that oligosaccharides from *Morinda officinalis* (OMO) are a useful prebiotic and cause substantial memory improvements in animal models of AD; however, the mechanism is still unclear. Therefore, this study was conducted to investigate whether OMO are clinically effective in alleviating AD by improving gut microbiota. OMO were administered to APP/PS1 transgenic mice, and potential clinical biomarkers of AD were identified with metabolomics and bioinformatics. Behavioral experiments demonstrated that OMO significantly ameliorated the memory of the AD animal model. Histological changes indicated that OMO ameliorated brain tissue swelling and neuronal apoptosis and downregulated the expression of the intracellular AD marker $A\beta_{1-42}$. 16S rRNA sequencing analyses indicated that OMO maintained the diversity and stability of the microbial community. The data also indicated that OMO are an efficacious prebiotic in an animal model of AD, regulating the composition and metabolism of the gut microbiota. A serum metabolomics assay was performed using UHPLC-LTQ Orbitrap mass spectrometry to delineate the metabolic changes and potential early biomarkers in APP/PS1 transgenic mice. Multivariate statistical analysis showed that 14 metabolites were significantly upregulated, and 8 metabolites were downregulated in the model animals compared to the normal controls. Thus, key metabolites represent early indicators of the development of AD. Overall, we report a drug and signaling pathway with therapeutic potential, including proteins associated with cognitive deficits in normal mice or gene mutations that cause AD.

Keywords: oligosaccharides of *Morinda officinalis*, Alzheimer's disease, gut microbiota, metabolomics, APP/PS1 transgenic mice, metabolites

INTRODUCTION

As an irreversible neurodegenerative disease that causes cognitive deficits, Alzheimer's disease (AD) accounts for 60–80% of all types of dementia (1). The typical neuropathological features of AD include the extracellular aggregation of amyloid-β (Aβ) peptide, the formation of tau protein aggregates inside neurons and the malfunction and/or loss of synapses and axons (2–4). Since ∼14 million people in the United States are predicted to be diagnosed with AD by 2050 (5), investigations of agents and reactions whose dysfunction causes AD are essential to provide insights into the etiology of the illness and to develop effective treatment strategies.

Some pathological features of AD, including cerebral atrophy, amyloid generation, altered gene expression, altered immune reactions, and cognitive deficits, have recently been linked to microbe infections (6–10). The brain and gut interact and modulate each other (11), and microbes in the gastrointestinal tract (GIT) are postulated to participate in AD development (12–14), although our understanding of the development and pathology of AD is insufficient and changing. Researchers have not determined how an imbalance in GIT microbes affects AD. The impact may be associated with the invasion of several pathogens, a decrease in the number of protective microbes, impaired immune tolerance, elevated membrane permeability and other defects in the immune system (15, 16). Probiotics have been shown to participate in the ability of the host to prevent and manage both chronic and acute conditions, such as AD (17). Alterations in the host physiology resulting from aging, genetics, diet, lifestyle and other factors might noticeably affect microbes (18–21). Metabolomics is a postgenomic field that offers new insights into the diagnostic and prognostic biomarkers of AD (22). Metabolomics has been used to identify metabolites and determine the expression of related genes in whole organisms, and it has recently been used in a wide range of applications in the clinic. Serum metabolites were discovered and considered potential biomarkers of AD (23), as retinoate has been used to help characterize and discriminate pathophysiological signatures of AD (24). According to recent reports, the gut microbiota and their metabolites influence the host metabolism (25). However, the roles of the gut microbiota and serum metabolites in AD are unclear.

Oligosaccharides from *Morinda officinalis* (OMO), a natural herbal extract used in traditional Chinese medicine, contain many active components. The saccharide content in the *M. officinalis* root is as high as 49.8–58.3%, mainly consisting of oligosaccharides with anti-dementia and memory-enhancing effects on many animal models (26–28). However, the mechanism underlying these beneficial effects has not been identified and will be elucidated in the present study. This study aims to provide a basis for the effective prediction and characterization of AD pathology by analyzing the gut microbiota and serum metabolite biomarkers.

Our research utilizes transgenic APPswe/PS1dE9 (APP/PS1) mouse models (29), which have been widely applied to investigations of the initial etiology of AD and evaluations of the efficacy of OMO treatments. Every specimen containing microbial 16S rRNA genes underwent concentration with the help of solid-phase reversible immobilization (SPRI) and subsequent quantification by electrophoresis utilizing an Agilent 2100 Bioanalyzer (Agilent, USA) prior to sequencing on an Illumina MiSeq sequencing system (30).

Whole-body blood specimens acquired from 8-month-old APP/PS1 and C57 mice were subjected to metabolomics evaluations using UHPLC-MS/MS. Subsequently, the entirety of the spectra were assessed using multivariate analysis to holistically investigate alterations in the levels of circulating metabolites. Fourteen metabolites were recognized that might contribute to the diagnosis and treatment of AD in the initial stage. Consequently, our research focused on assessing the therapeutic impact of OMO on AD by analyzing the diversity of microbes and performing metabolomics assays to provide insights into its etiology. Moreover, the results from this study will serve as the basis for the application of nutritional interventions and the AD-counteracting effects of OMO.

METHODS

Animal Model Preparation and Treatments

Adult male C57 mice and 2-month-old transgenic APP/PS1 mice weighing 18 to 22 grams were acquired from the Laboratory Animal Center of Guangdong Province (SCXK [Yue] 2008-0020, SYXK [Yue] 2008-0085) and were housed in pairs in the colony room on a 12/12-h light/dark cycle at 25°C in plastic cages and were allowed *ad libitum* access to food and water. Each procedure described in our study was approved by the Laboratory Animal Center of the Guangdong Institute of Microbiology. This study utilized as few mice as possible. 2-month-old APP/PS1 mice and age-matched C57 mice, which served as the control group ($n = 10$ animals), were utilized in the present study. Our research was approved by the Ethical Committee and complied with the Declaration of Helsinki.

Mice performed water maze tests (WMT) to identify adequate AD models before animals were randomized into the following 4 groups in this 6-month experiment: a C57 group (oral administration of distilled water), a transgenic APP/PS1 group [oral administration of distilled water], a high-dose transgenic APP/PS1 group [oral administration of 100 mg/(kg·d) OMO] and a low-dose transgenic APP/PS1 group (oral administration of 50 mg/(kg·d) OMO) ($n = 10$ animals per group).

WMTs

A Morris water maze (MWM, DMS-2, Chinese Academy of Medical Sciences Institute of Medicine) comprising a non-transparent circular fiberglass pool with a diameter of 20 cm that had been filled with water (25 ± 1°C) was used to examine murine spatial learning and memory. Wathet curtains tagged with three distal visual cues encircled the pool. Unified lighting of the examination room and pool was provided by four independent light sources of equivalent power. A CCD camera was placed over the center of the pool to record the swimming paths of each mouse. An EthoVision tracking system (Noldus, Leesburg, VA) was applied to digitize the video output. The

WMT consisted of three steps, as described in a previous study (31): primary spatial practice, reverse spatial practice and a probe examination.

Hematoxylin-Eosin (HE) and Immunohistochemical Staining

The look, activity and fur tint of each mouse were examined and recorded daily. The weight of each mouse was examined every 3 days when drugs were administered. Serum specimens were harvested, and murine cerebral samples were anatomically dissected after the WMT.

Three cerebral samples and three intestinum tenues were removed from randomly chosen mice in each experimental group, while the remaining tissues underwent fixation with four percent paraformaldehyde before processing into paraffin sections. Sections were stained with HE and immunohistochemistry before being examined under the light microscope (31, 32).

Microbiome Analysis

Fresh fecal specimens were acquired from murine nests and stored at −80°C. Microbe DNA specimens weighing from 1.2 to 20.0 ng were isolated from murine cecal specimens and stored at −20°C. The 16S rRNA genes of microbes were amplified with the following primers: forward 5′-ACTCCTACGGGAGGCAGCA-3′ and reverse 5′-GGACTACHVGGGTWTCTAAT-3′. Every amplified product was concentrated by SPRI and quantified by electrophoresis using an Agilent 2100 Bioanalyzer (Agilent). Every specimen was diluted to 1×10^9 molecules/μL in TE buffer and pooled into groups prior to the determination of DNA concentrations using a NanoDrop spectrophotometer. An Illumina MiSeq sequencing system was utilized to sequence 20 mL of the pooled admixture. The subsequent reads were analyzed as described in a previous study (30).

Serum Metabolomics Analysis

Eighty microliters of mouse serum was combined with 240 μL of a cold methanol-acetonitrile (2:1, v/v) mixture and 10 μL of an internal standard (0.3 mg/mL 2-chloro-L-phenylalanine in methanol). After vortexing for 2 min, the mixture was subjected to ultrasound disruption for 5 min, incubated in a −20°C freezer for 20 min, and centrifuged for 10 min at a low temperature (14,000 rpm at 4°C). Subsequently, 200 μL of the supernatant was loaded into the tube lining a sample vial and analyzed using LC-MS (33).

LC-MS Analysis Using an UHPLC-LTQ Orbitrap Spectrometer

An Ultimate 3000-Velos Pro system was utilized for LC-MS with the help of a binary solvent delivery manager and a specimen manager connected to an LTQ Orbitrap mass spectrometer equipped with an electrospray interface (Thermo Fisher Scientific, USA). LC settings are displayed below. The Acquity BEH C18 column (100 mm × 2.1 mm internal diameter, 1.7 μm; Waters, Milford, USA) was stored at 45°C. Isolation was performed with the following solvent gradient: 5% B−25% B from 0 to 1.5 min, 25% B−100% B from 1.5 to 10.0 min, 100% B−100% B from 10.0 to 13.0 min; 100% B−5% B from 13.0 to 13.5 min, and 13.5–14.5 min holding at 5% B at a flow rate of 0.40 mL/min. B represents acetonitrile (0.1% (v/v) acetonitrile), while A represents aqueous formic acid (0.1% (v/v) formic acid). The injection volume was 3 mL, and the column temperature was set to 45.0°C. Mass spectrometry data were recorded by the LTQ Orbitrap mass spectrometer in negative or positive electrospray ionization (ESI) mode. The capillary and source temperatures were 350°C, and the desolvation gas flow was maintained at 45 L/h. Centroid data were acquired from fifty to 1,000 m/z, with a 30,000 resolution.

Multivariate Statistical Analysis and Metabolite Identification

The XCMS program (https://xcmsonline.scripps.edu/landing_page.php?pgcontent=mainPage) was used for the non-linear alignment of data in the time domain and the spontaneous integration and isolation of peak intensities. The subsequent 3D matrix, including data such as retention time and m/z pairs (variable indices), specimen names (observations) and normalized ion intensities (variables), were integrated into the SIMCA program (version 14.0, Umetrics, Umeå, Sweden), in which a partial least squares discriminant analysis (PLS-DA), orthogonal partial least squares discriminant analysis (OPLS-DA) and principal component analysis (PCA) were conducted. Model quality was assessed using R^2X or R^2Y as well as Q^2-values. R^2X or R^2Y represent the percentage of variance in data interpreted using different models and suggested the goodness of fit, while Q^2 represented the prediction from the models detected using the cross-validation procedure. As a default, 7 rounds of cross-validation were conducted using SIMCA throughout the experiment to identify the most appropriate quantity of essential ingredients and prevent excessive model fitting. A permutation evaluation (200 times) was performed to confirm the OPLS-DA results.

Metabolomic Pathway Analysis

The web-based instrument Metabolomic Pathway Analysis (MetPA) (http://www.metaboanalyst.ca/faces/ModuleView.xhtml) was used to build and observe the metabolic pathways influenced by OMO by collecting information from databases such as the Kyoto Encyclopedia of Genes and Genomes (KEGG) and Human Metabolome Database (HMDB). The evaluation of KEGG pathways required Goatools (https://github.com/tanghaibao/Goatools) and KEGG (https://www.kegg.jp/) (34–37).

Statistical Analysis

The results are presented as the means ± SD from at least 3 independent experiments. ANOVA was employed to examine the significance of differences between groups using the Statistical Package for the Social Sciences software (SPSS, Abacus Concepts, Berkeley, CA) and Prism 5 (GraphPad Software, San Diego, USA) software. $P < 0.05$ indicated a significant difference.

RESULTS

OMO Administration Improved the AD Parameters in APP/PS1 Transgenic Mice

The average weight of the APP/PS1 group was increased compared with that of the control group ($p < 0.05$), and the former group exhibited abdominal swelling. The mice treated with OMO exhibited insignificant differences in weight compared with the control group ($p > 0.05$, **Figure 1A**).

The incubation time (IT) of every group treated with OMO was noticeably shorter than that of the APP/PS1 group. Mice that received a low dose of OMO displayed an IT of 86.49 ± 11.64 s, while mice receiving the high dose exhibited an IT of 82.06 ± 19.44 s on the 1st day; both values were noticeably different ($p < 0.01$) from the model group (113.75 ± 16.11). On the 4th day, the IT of mice treated with a low dose of OMO was reduced to 37.19 ± 5.36 s, while the IT of the high-dose group decreased to 28.27 ± 3.96 s, both of which differed remarkably from APP/PS1 mice (56.29 ± 9.69 s, $p < 0.01$, **Figure 1B**). Based on these findings, OMO reversed the learning and memory impairments observed in transgenic APP/PS1 mice.

According to the results of the probe trial, the differences in swimming distance and velocity were insignificant ($p > 0.05$). Mice in the control group swam for longer times in the northwest (target) quadrant (26.63 ± 3.83 s) than in the other quadrants ($p < 0.01$), while mice in the model group displayed a noticeably shorter swimming time (ST) of 20.77 ± 2.36 s ($p < 0.01$) in the aforementioned quadrant, indicating that mice in the control group recalled the position of the platform. The ST of mice receiving a low dose of OMO was 26.50 ± 3.59 s, while the ST of mice receiving the high dose was 27.36 ± 2.51 s, which was noticeably decreased compared with that of the control group. Mice receiving OMO exhibited noticeable differences in ST ($p < 0.01$) from mice in the control group, but the difference in swimming distance was not significant (**Figure 1C**).

HE staining did not reveal obvious alterations in hippocampal neurons in the control (**Figure 1D**). However, noticeable histopathological injury was observed in the hippocampus of APP/PS1 mice. Layered pyramidal neuron structure degeneration and neuronal loss (Nissl staining) were observed in the cortex and CA1 area. These alterations were ameliorated by the OMO supplement. Cells in mice receiving OMO displayed a better morphology, and the number of neurons was increased compared with that in mice that were not treated with OMO, particularly in mice receiving the high dose of OMO. The percentage of $A\beta_{1-42}$-positive cells exhibiting red IHC staining was substantially increased in the model group compared with that in the control group ($p < 0.05$). However, OMO administration decreased $A\beta_{1-42}$ expression (**Figure 1D**).

OMO Administration Improved the Gut Microbiota in APP/PS1 Transgenic Mice

The abundance of operational taxonomic units (OTUs) and the taxonomic profiles were evaluated (**Figure 2**).

Compared with the normal mice, the APP/PS1 transgenic mice exhibited a decrease in the microbial community diversity, as shown in **Figure 2A**, and all the APP/PS1 transgenic mice were clustered well using non-metric multidimensional scaling (NMDS) and PLS-DA (**Figures 2B,C**), indicating that the APP/PS1 transgenic mouse brain influenced the gut microbiota. After treatment with 50 mg/(kg·d) OMO, microbial diversity was improved to approximately the level of the normal control mice (**Figure 2B**).

Analysis revealed differences in the abundance of taxa between different groups, as displayed in **Figure 2D**. The abundance of some bacteria exhibited substantial changes at the genus and family levels in fecal samples from the APP/PS1 mice, while the OMO treatment changed those variations; in particular, obvious increases in the abundance of *Lactobacillus, Allobaculum, Lactobacillaceae,* and *Lachnospiraceae* were observed, indicating that OMO had a prebiotic role in protecting against intestinal dysbacteriosis in the AD model animals.

Moreover, at the genus level, the APP/PS1 transgenic mice exhibited an enrichment of some potential anti-AD microbes, such as *Lactobacillus, Akkermansia, Bacteroides, Adlercreutzia,* and *Desulfovibrio,* and reduced levels of other potential anti-AD microbes, such as *Ruminococcus, Bifidobacterium, Blautia, Oscillospira, Coprococcus, Sutterella,* and *Clostridium*, compared with the normal group (**Figure 4A**). At the family level, the APP/PS1 mice showed an enrichment of some potential anti-AD microbes, such as Lactobacillaceae, Lachnospiraceae, Bacteroidaceae, and Verrucomicrobiaceae, and reduced levels of other potential anti-AD microbes, such as S24–7, Ruminococcaceae, Coriobacteriaceae, Erysipelotrichaceae, and Bifidobacteriaceae, compared with the normal group (**Figure 4B**). Nevertheless, model mice treated with OMO displayed alterations in the quantity of microbes that counteracted AD. Based on these findings, OMO represents a promising treatment to modulate the community structure of GIT microbes.

GIT microbes have an obvious impact on the immune system of organisms. The differences in the gut microbiota among the APP/PS1 transgenic, OMO-treated and control mice are shown in **Figure 3**. A Venn diagram (**Figure 3A**) and a hierarchical tree (**Figure 3B**) revealed that Actinobacteria, Firmicutes, Coriobacterium, Lachnospiraceae, Bacilli, Clostridia, Bacteroidales, Clostridiales, Ruminococcaceae, Lactobacillales, Oscillospira, Bacteroidia, and Proteobacteria were the microbial types exhibiting increased levels after OMO administration and are thus promising candidates for future investigation. As shown in the heatmap (**Figure 3C**), OMO administration remarkably altered the composition of GIT microbes compared to the control group, as the relative abundance levels of the genera *Mucispirillum*, *Odoribacter*, *Rikenella*, *Faecalibacterium*, *Alistipes*, *Parabacteroides,* and *Anaerotruncus* were reduced, while the levels of *Arthrobacter*, *Phycicoccus*, *Streptococcus*, *Akkermansia*, *Blautia*, *Ruminococcus*, *Coprococcus*, *Allobaculum*, *Dehalobacterium*, *Methanolinea,* and *Candidatus Methanoregula* were increased. These findings indicate a relationship between the gut microbiota and AD.

According to the results of the KEGG pathway evaluation, categories of metabolic pathways such as the degeneration

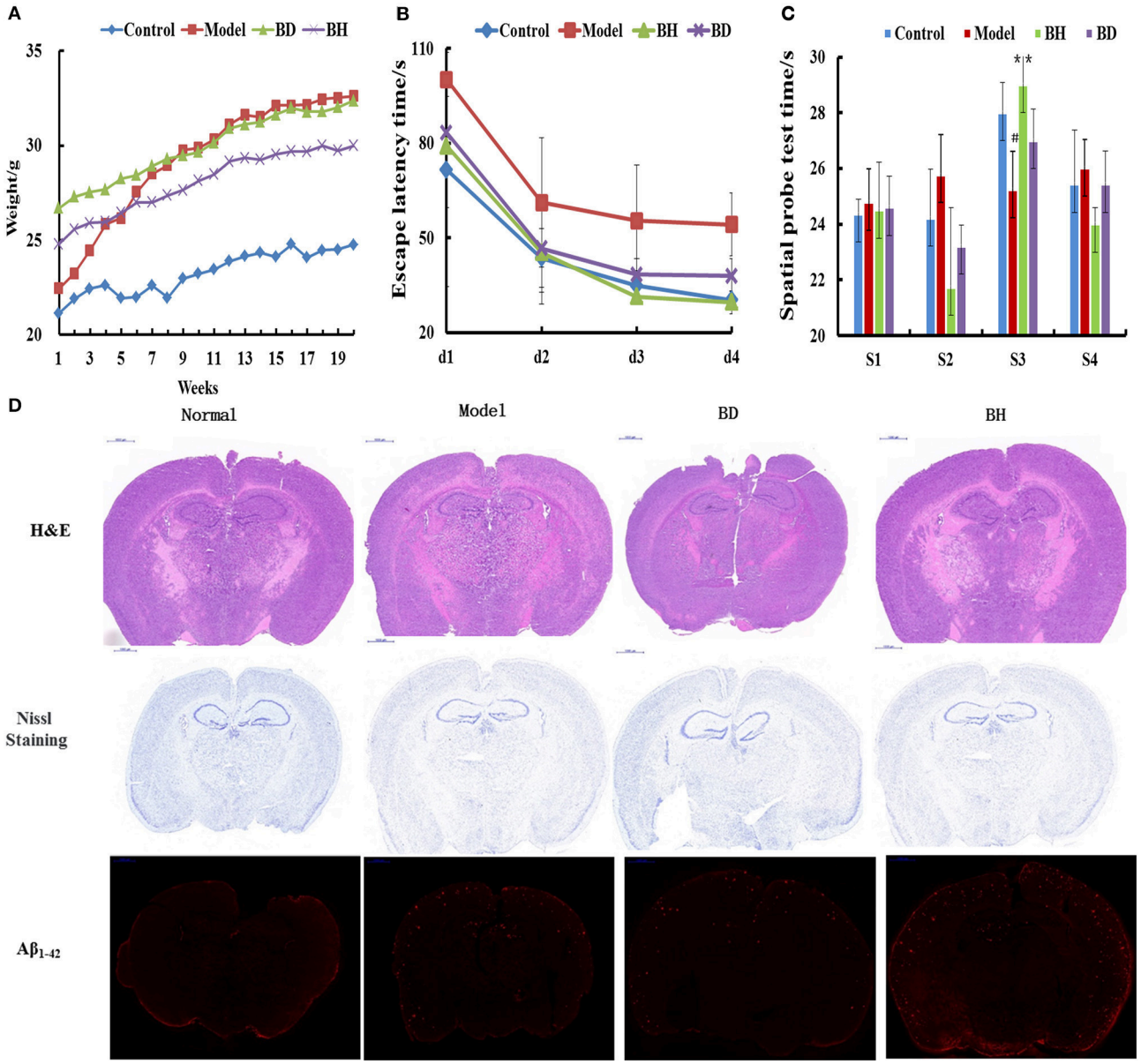


FIGURE 1 | Effect of OMO on APP/PS1 transgenic mice. Body weight changes were measured weekly **(A)**. Escape latencies in the H maze **(B)** and probe test results **(C)**, and histopathological changes in brain tissues **(D)** are shown. N represents the C57 group, M denotes the APP/PS1 transgenic group, BD indicates the group treated with 50 mg/kg OMO, and BH designates the group treated with 100 mg/kg OMO; the treatments were administered for 6 months ($n = 10$). Values are presented as the means ± SDs of six independent experiments. $^{\#}p < 0.05$ compared with the control group; $^{**}p < 0.01$ compared with the M group.

of xenobiotics, the generation and metabolism of glycan, the generation of secondary metabolic products, the enzyme families and metabolism of nucleotides, cofactors, terpenoids, amino acids, vitamins, polyketides, lipids, carbohydrate, and energy were altered in GIT microbes of APP/PS1 transgenic animals. Moreover, quite a few of these pathways were upregulated by the OMO supplement. Dynamic alterations in the 3 groups are displayed in **Figure 4C**, and the results suggested that OMO impacted the GIT microbial metabolism.

OMO Administration Changes On Metabolites in APP/PS1 Transgenic Mice

Multivariate Statistical Analysis

Typical negative and positive base peak APP/PS1 animals are displayed in **Figures 5A,B**, respectively. All the groups resembled one another in blood patterns of BPI chromatograms, with the exception of a few peaks. Multivariate statistical analysis was conducted with the aim of performing a more thorough investigation of the differences between complicated matrices.

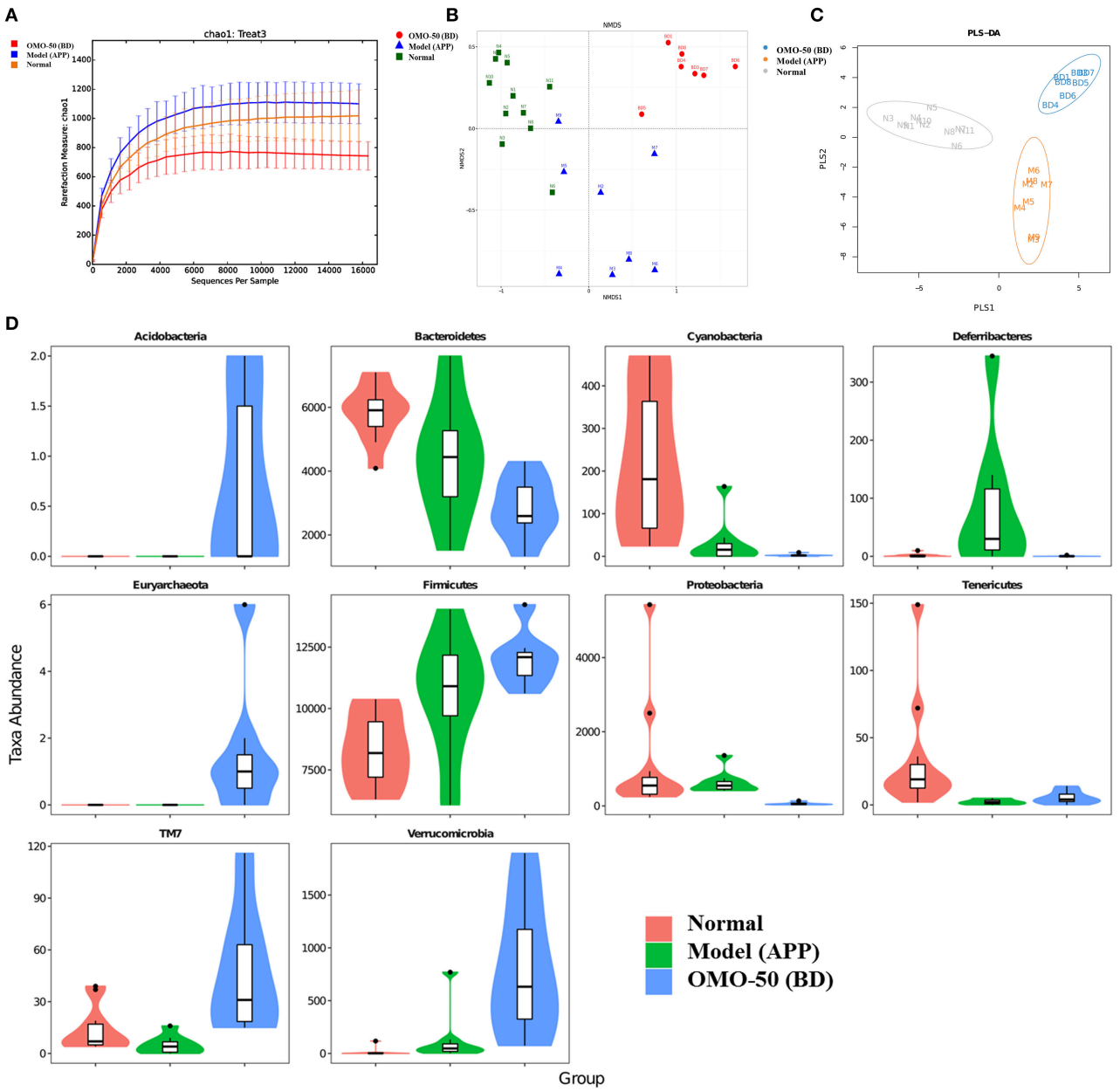


FIGURE 2 | Effects of OMO on the gut microbiota of the APP/PS1 transgenic mice, as determined from fecal samples. The rarefaction curve **(A)**, the results of the NMDS analysis **(B)**, PLS-DA results **(C)**, classification and abundance of fecal contents at the phylum level **(D)**, and the results of 16S rRNA sequencing of the gut microbiota using an Illumina MiSeq sequencing system are shown. N denotes the C57 group, M represents the APP/PS1 transgenic group, BD denotes the 50 mg/kg OMO-treated group, and BH indicates the 100 mg/kg OMO-treated group.

The loading plot showed a trend toward separation between any two groups (**Figure 6A**). Variables with higher loadings (positive and negative) exhibit greater contributions to the differences between the two groups of samples. The labeled metabolites may be relevant to the search for AD biomarkers. A supervised OPLS-DA was utilized to categorize the specimens into 2 blocks, aiming to differentiate between the two kinds of mice. Serum specimens from the two mouse strains were thoroughly isolated according to differences in metabolic patterns using the OPLS-DA loading plot assay. Furthermore, the categorized models were confirmed with the response permutation test (RPT) (38). A permutation plot assisted in the risk evaluation of obtaining a false result from the OPLS-DA. Every blue Q2 dot on the left side was elevated in comparison with primary dots on the right side, suggesting that the primary model was reliable and responsible for the differences observed between the two mouse strains (**Figure 6C**).

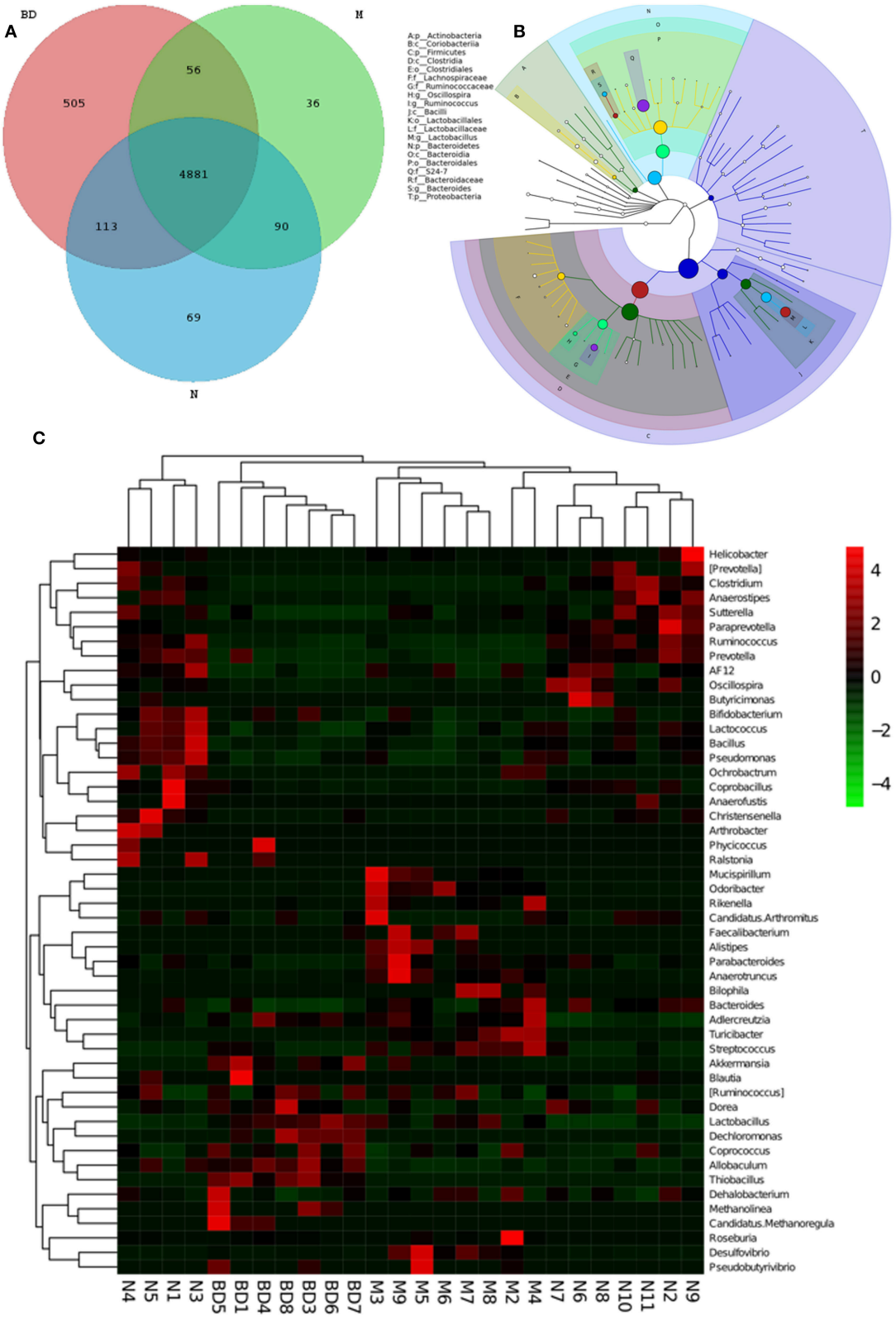


FIGURE 3 | Effects of OMO on the microbiota in fecal samples from the APP/PS1 transgenic mice. A Venn diagram of OTUs **(A)**, a sample species classification tree **(B)**, and the heatmap of 16S rRNA gene sequencing analysis of fecal contents at the genus level **(C)** are shown. N denotes the control group, M denotes the APP/PS1 transgenic group, and BD designates the 50 mg/kg OMO-treated group.

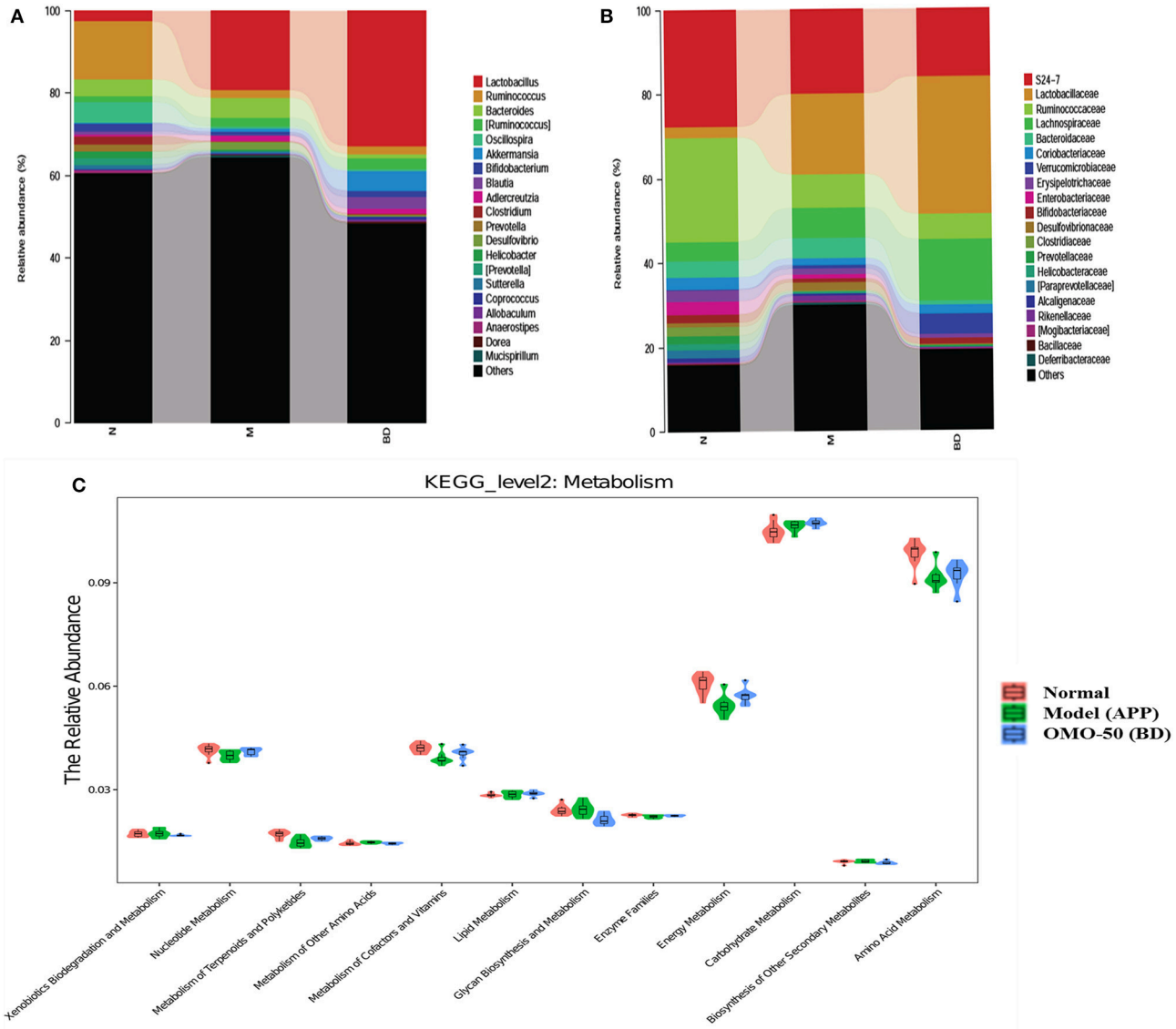


FIGURE 4 | Effects of OMO on the microbiota in fecal samples from the APP/PS1 transgenic mice. The graph in **(A)** shows the classification and abundance of fecal contents at the phylum level, **(B)** shows the classification and abundance of fecal contents at the family level, and **(C)** shows the results of the KEGG pathway enrichment analysis of the gut microbiota with respect to the metabolic systems. Values are presented as the means of six independent experiments. N denotes the control group, M represents the APP/PS1 transgenic group, and BD designates the 50 mg/kg OMO-treated group.

Identification of Candidate Metabolites

UHPLC-LTQ was used to evaluate metabolic pathways with the aim of investigating promising pathways that were influenced by APP/PS1 genes. The candidate metabolic products were identified from the MS/MS fragment data and subsequent searches of web-based databases, including KEGG, METLIN and HMDB. Twenty-two candidate markers were initially identified and featured in this way, a summary of which is displayed in **Figure 7A** (VIP $>$ 1 and $p < 0.05$). We compared the relative intensity of the markers among the APP/PS1 mice, the C57 mice, and the low- and high-dose OMO-treated mice to determine the degree to which those candidate markers were altered. Fourteen metabolites were upregulated, including PI (22:3(10Z, 13Z, 16Z)/16:0), linolelaidic acid, PI (16:0/22:2(13Z, 16Z)), PE (22:1(13Z)/22:5(7Z, 10Z, 13Z, 16Z, 19Z)), PC (18:4(6Z, 9Z, 12Z, 15Z)/20:0), PE (22:1(13Z)/P-18:1(11Z)), 10-methyltridecanoic acid, LysoPC (22:5(7Z, 10Z, 13Z, 16Z, 19Z)), PC (22:6(4Z, 7Z, 10Z, 13Z, 16Z, 19Z)/18:1(9Z)), PE (22:0/P-18:1(9Z)), LysoPE (22:0/0:0), MG (22:5(7Z, 10Z, 13Z, 16Z, 19Z)/0:0/0:0), LysoPC (18:1(11Z)) and 11-β-hydroxyandrosterone-3-glucuronide. The levels of nine metabolites were significantly reduced: PC(20:0/18:3(6Z, 9Z, 12Z)), PC(20:3(5Z, 8Z, 11Z)/20:3(8Z, 11Z, 14Z)), 15(S)-hydroxyeicosatrienoic acid, PC(22:5(7Z, 10Z, 13Z, 16Z, 19Z)/18:0), LysoPC(20:3(8Z, 11Z, 14Z)), diethylphosphate, LysoPE(20:0/0:0) and 9,13-cis-retinoate. Moreover, a clustering analysis of the heatmap of all metabolites

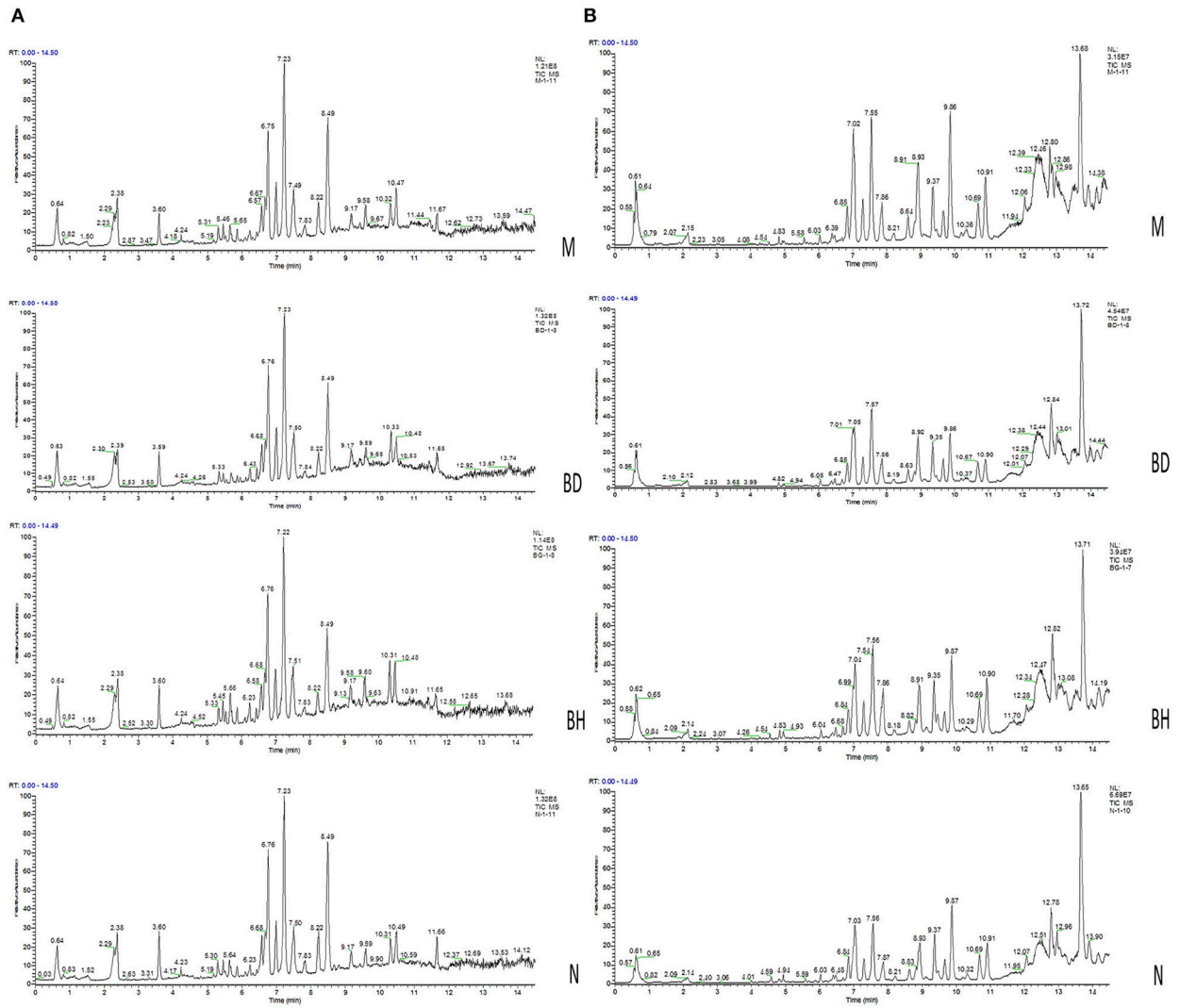


FIGURE 5 | Analysis of the metabolic profiles based on the UPLC/MS spectra of serum samples. Serum BPI chromatograms of APP/PS1 and wild-type mice collected in positive ion mode **(A)** and negative ion mode **(B)**. N denotes the control group, M represents the APP/PS1 transgenic group, BD denotes the 50 mg/kg OMO-treated group, and BH designates the 100 mg/kg OMO-treated group.

revealed the differences in relative levels between the four groups (**Figure 7B**). Furthermore, we obtained the KEGG pathway annotations of the metabolites (**Figure 7C**). In the figure, black indicates KEGG primary pathways, and colors represent KEGG secondary pathways; the number represents the counts of differentially produced metabolites in the metabolic pathway.

DISCUSSION

Pathological changes in AD are associated with microbial infections and gut microbes through four routes of interaction with the brain: direct effects on the vagus nerve, metabolites, direct production or alteration of neurotransmitters, and activation of immune signaling pathways (39). A study in *Nature* (14) also confirmed that the gut microbiota promotes neurodegenerative disease; the gut microbiota are closely associated with neurodegenerative disease in mouse models of Parkinson's disease, and the parkinsonian symptoms are relieved when the gut microbiota is altered. In the present study, OMO markedly modified behavior, regulated neurotransmitter secretion, and ameliorated brain tissue swelling. Moreover, OMO altered the diversity and steady-state composition of the microbial community, and the levels of metabolic products and AD biomarkers were altered. In addition, OMO was an efficacious prebiotic that regulated the composition and metabolism of the gut microbiota in an AD mouse model.

Mechanisms that regulate the GIT microbes have recently been shown to regulate cognition in the host, regardless of whether animals without germs, animals treated with antibiotics or probiotics administration or animals receiving a fecal microbial transplant (FMT) were used (40). The fecal microbial composition was noticeably altered by a 4-day treatment with

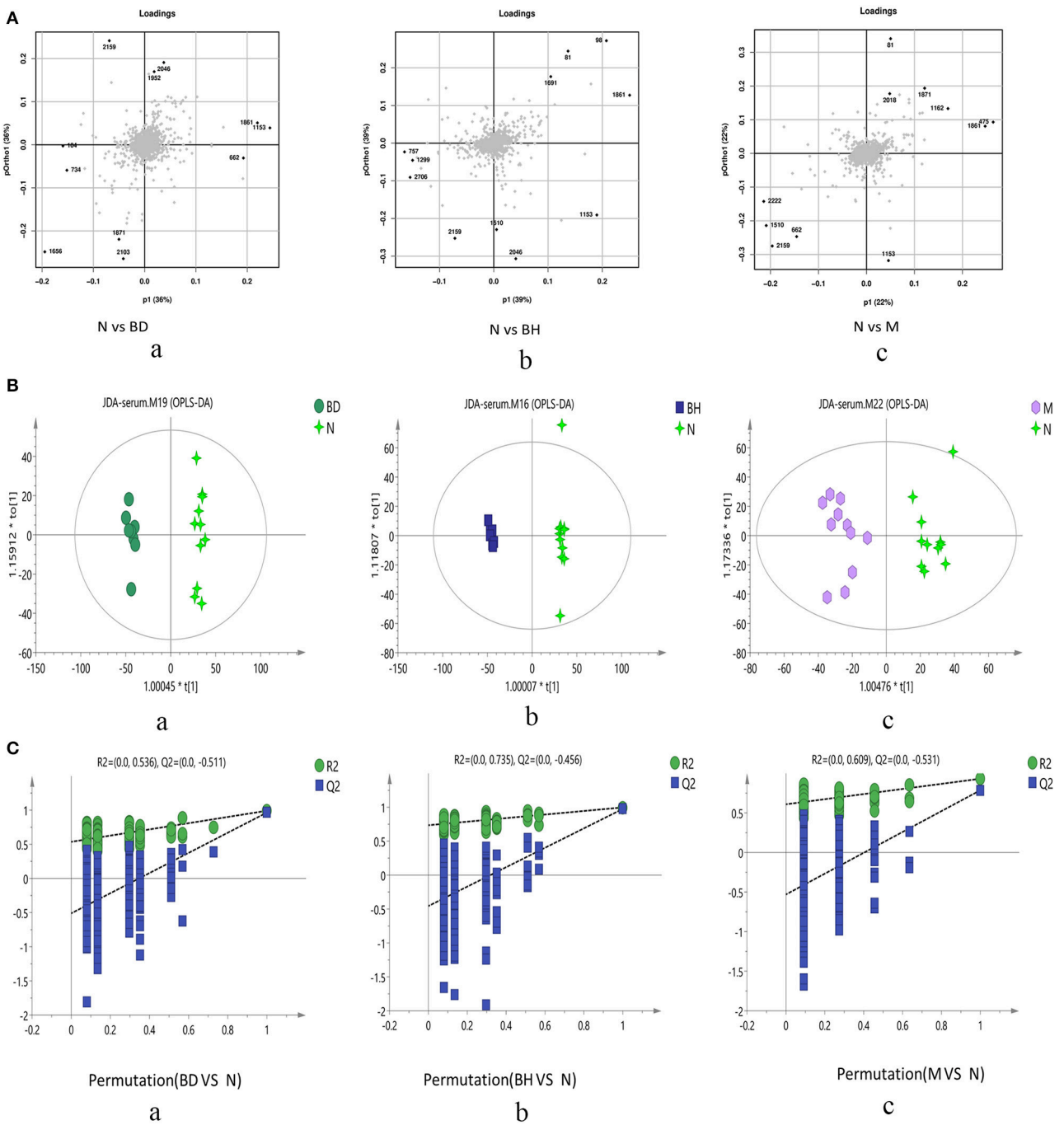


FIGURE 6 | Score plots of metabolite levels in a serum sample. OPLS-DA score plots of the serum metabolic profile **(A)**: (a) N vs. BD, (b) N vs. BH, and (c) N vs. M. Permutation score plots of serum metabolic profiles **(B)**: (a) N vs. BD, (b) N vs. BH, and (c) N vs. M. Loading score plot of the serum metabolic profile **(C)**: (a) N vs. BD, (b) N vs. BH, and (c) N vs. M. N denotes the control group, M represents the APP/PS1 transgenic group, BD denotes the 50 mg/kg OMO-treated group, and BH represents the 100 mg/kg OMO-treated group.

50 mg/(kg·day) OMO compared with that of the control group. Our data were consistent with findings from previous studies showing that alterations in the composition of the gut microbiota in APP/PS1 transgenic mice include a reduction in levels of *Bacteroidetes* and an increase in levels of *Firmicutes* ($p < 0.05$), while the OMO treatment reversed those changes ($p < 0.05$), as shown in **Figure 5** (Graphian), **Figure 6** (OUT and NMDS), indicating that GIT microbes are crucial contributors to host defense. Based on these findings, the gut microbiota acts as a barrier to protect the host from intestinal pathogen attacks (41).

Furthermore, through immunohistochemical staining of global brain tissues in the AD model mice, the present study

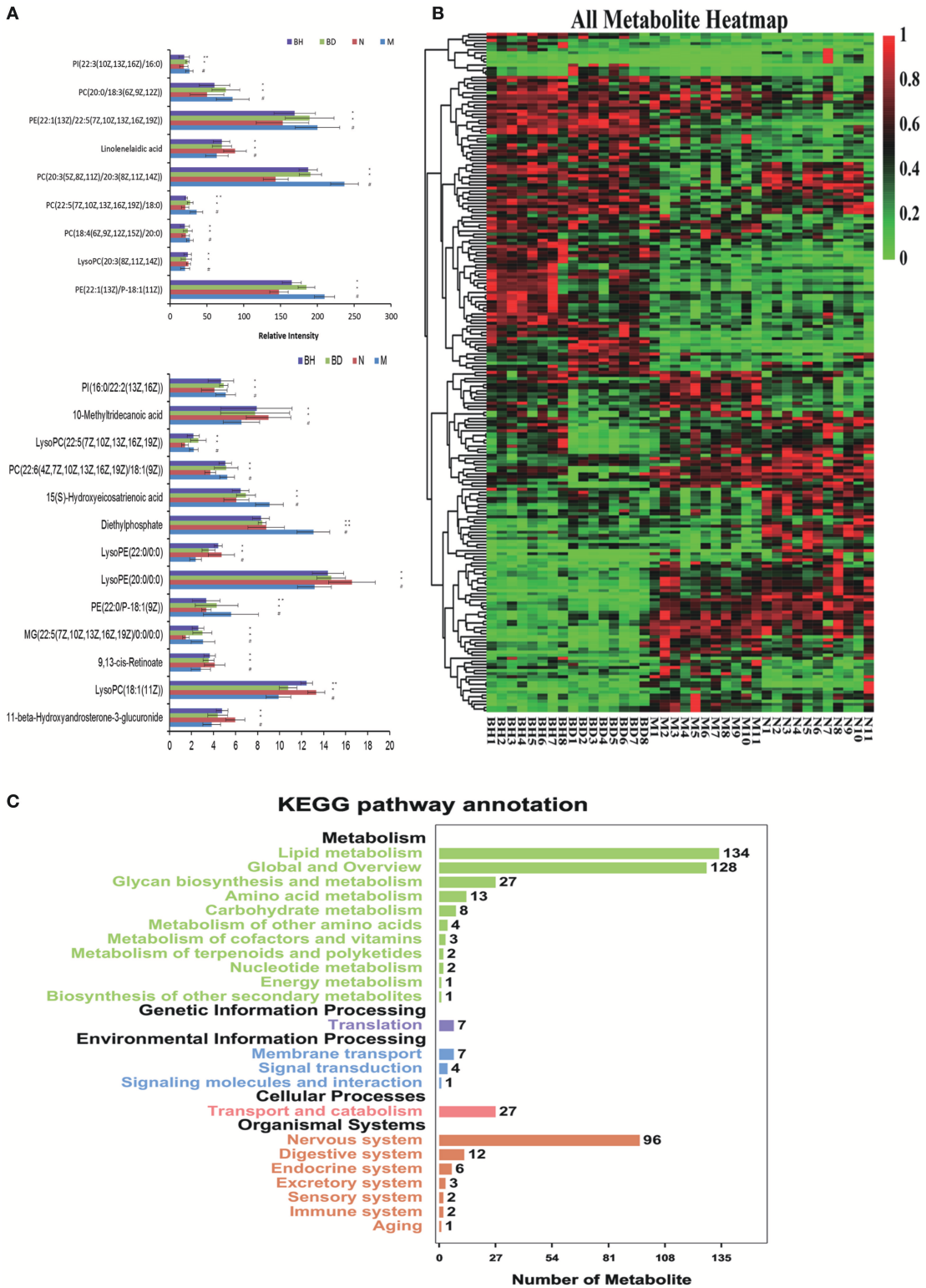


FIGURE 7 | Comparison of the relative intensities of the potential biomarkers **(A)**. KEGG pathway annotations of differentially expressed genes in serum samples **(B)**. Heatmap showing the levels of 24 different metabolites **(C)**. The degree of change is marked with different colors: red represents upregulation, and green indicates downregulation. Each row represents an individual sample, and each column represents a metabolite. N denotes the C57 mice, M represents the APP/PS1 transgenic mice, BD indicates the group treated with 50 mg/kg OMO, and BH denotes the group treated with 100 mg/kg OMO. Values are presented as the means ± SDs of six independent experiments. $^{\#}p < 0.05$ compared with the control group; $^{*}p < 0.05$ and $^{**}p < 0.01$ compared with the M group.

showed that weight, $A\beta_{1-42}$ levels and staining improved to near normal levels (**Figure 1C**), indicating that OMO might regulate protein expression and signaling pathways in cells through the help of the gut microbiota. However, additional studies are required to extend the current findings on the effects of the microbiota on mice to humans to provide a basis for gut microbiota-based therapeutic applications of OMO.

In addition, the OMO treatment had an impact on the quantities of some typical GIT microbes, such as Lactobacillus, Bifidobacterium, Bacteroides, Lachnospiraceae, Akkermansia, Ruminococcus, Blautia, S24–7, Lachnospiraceae, Bacteroidaceae and Ruminococcaceae, in APP/PS1 transgenic animals (**Figures 4A,B**). OMO also affected the gut morphology, mucin production, and gut permeability and reduced dysbacteriosis. According to the results of the 16S metagenome analysis, OMO administration altered the balance of Bacteroidetes and Firmicutes and reduced the abundance of a few beneficial bacterial genera, namely, Akkermansia, Bacteroides, Roseburia, Bifidobacterium, Lactobacillus, and Desulfovibrio, which corroborated previous reports of their roles in metabolic deregulation (42–44).

Importantly, emerging studies have confirmed pathogenic links between GIT microbes and various disorders, particularly the noticeable alteration in quantities of typical microbes in these disorders (45–51). Thus, OMO influences several microbes that affect the generation and secretion of some neurotransmitters and neuromodulators. Murine models of chronic stress displayed similar effects, in which the examined activities, genetic, neuroendocrine and neurochemical alterations observed after the administration of a prebiotic supplement (oligosaccharides and galacto-oligosaccharides) seemed to be regulated in part by short-chain fatty acids (52). Consequently, the therapeutic effects of OMO may be partially attributed to modulatory effects on GIT microbes.

The changes in behavior and the gut microbiota after the administration of OMO coincided with changes in gene expression in blood samples collected from the whole body. A metabolomic analysis of whole-body blood revealed significant changes in the expression of some genes (**Figure 7**).

We have implemented a metabolomic approach using UHPLC-LTQ Orbitrap mass spectrometry to study the metabolites present in mouse serum, with a special emphasis on revealing whole-body metabolic alterations that might indicate early-stage AD and its progression. Based on the results of the enrichment analysis, lipid metabolites might be related to AD (53). In the category of lipid metabolism, *glycerophospholipid metabolism* and *α-linolenic acid metabolism pathway* were prominently altered in AD. Lipid metabolism is affected by levels of glycerol, propylene glycol, and fatty acid compounds in AD (54). These findings were supported by previous studies reporting elevated levels of polyunsaturated fatty acids in the brain (55, 56). Those fatty acids cause lipid peroxidation and promote the generation of toxic products in response to oxidative stress, resulting in neural damage and promoting AD development.

In the present study, levels of endogenous metabolic products in murine blood differed among the normal, model and OMO-treated groups. These alterations correlate with metabolic diseases, such as monoaminergic neurotransmitters in the nervous system (NS) (57). Thus, blood metabolites represent primary predictors of AD generation.

Pathway enrichment analyses in the metabolomics study indicated that the KEGG pathways *Glutamatergic synapse, Calcium signaling pathway, GnRH signaling pathway, Long-term potentiation, Circadian entrainment,* and *Oxytocin signaling pathway* displayed the greatest alterations during disease pathogenesis. These pathways share mutual hub metabolites, such as pyruvate and oxaloacetate, which are the main compounds required for the TCA cycle, gluconeogenesis, and glyoxylate and dicarboxylate metabolism (58). Pyruvate and pyruvate-oxaloacetate protect NS metabolism by promoting brain-to-blood glutamate efflux (59–61).

Although our understanding of the complicated relationship networks between GIT microbes and the brain is insufficient, prebiotics are known to forcefully regulate the microbial ecology. The influences of the microbial composition, abundance, diversity and functions of all GIT microbes must be examined since they are associated with brain function. Data from our study offer stronger proof of the defensive effect of OMO (which contains prebiotics) and help characterize its effects on the microbiota-brain-gut axis in AD. Using the promising natural chemical product OMO, we were able to identify new therapeutic targets for AD and provide a basis for the further study of AD pathogenesis.

AUTHOR CONTRIBUTIONS

YX, CD, YJ, LH, LG, SO, ZC, ZJ, and XY conceived and esigned the experiments. YX, CD, YJ, TX, and ZC performed the experiments. YX, CD, LT, HG, and ZJ analyzed the data. YX and CD wrote the paper and edited the manuscript. All the authors read and approved the final manuscript.

FUNDING

The present work received financial support from the Guangdong Science and Technology Plan Projects (2015A020211021; 2016A050502032), the Guangzhou Science and Technology Plan Projects (201504281708257; 201604020009), the High-level Leading Talent Introduction Program of GDAS (2016GDASRC-0102), Guangzhou Medical University Research Projects (2016C28), National Natural Science Foundation of China (81701086), and the Nanyue Microbial Talents Cultivation Fund of Guangdong Institute of Microbiology.

REFERENCES

1. Owen JB, Di DF, Sultana R, Perluigi M, Cini C, Pierce WM, et al. Proteomics-determined diffences in the concanavalin-A-fractionated proteome of hippocampus and inferior parietal lobule in subjects with Alzheimer's disease and mild cognitive impairment: implications for progression of AD. *J Proteome Res.* (2009) 8:471–82. doi: 10.1021/pr800667a
2. Arendt T, Bigl V, Arendt A, Tennstedt A. Loss of neurons in the nucleus basalis of Meynert in Alzheimer's disease, paralysis agitans and Korsakoff's Disease. *Acta Neuropathol.* (1983) 61:101–8. doi: 10.1007/BF00697388
3. Tu S, Okamoto S, Lipton SA, Xu H. Oligomeric Aβ-induced synaptic dysfunction in Alzheimer's disease. *Mol Neurodegener.* (2014) 9:48. doi: 10.1186/1750-1326-9-48
4. Adams IM. Structural plasticity of synapses in Alzheimer's disease. *Mol Neurobiol.* (1991) 5:411–9. doi: 10.1007/BF02935562
5. Hebert LE, Weuve J, Scherr PA, Evans DA. Alzheimer disease in the United States (2010-2050) estimated using the 2010 census. *Neurology* (2013) 80:1778–83. doi: 10.1212/WNL.0b013e31828726f5
6. Heintz C, Mair W. You are what you host: microbiome modulation of the aging process. *Cell* (2014) 156:408–11. doi: 10.1016/j.cell.2014.01.025
7. Miklossy J. Emerging roles of pathogens in Alzheimer disease. *Expert Rev Mol Med.* (2011) 13:e30. doi: 10.1017/S1462399411002006
8. Bhattacharjee S, Lukiw WJ. Alzheimer's disease and the microbiome. *Front Cell Neurosci.* (2013) 7:153. doi: 10.3389/fncel.2013.00153
9. Huang WS, Yang TY, Shen WC, Lin CL, Lin MC, Kao CH. Association between Helicobacter pylori infection and dementia. *J Clin Neurosci.* (2014) 21:1355–8. doi: 10.1016/j.jocn.2013.11.018
10. Mancuso R, Baglio F, Cabinio M, Calabrese E, Hernis A, Nemni R, et al. Titers of herpes simplex virus type 1 antibodies positively correlate with grey matter volumes in Alzheimer's disease. *J Alzheimers Dis.* (2014) 38:741–5. doi: 10.3233/JAD-130977
11. Mayer EA. Gut feelings:the emerging biology of gut-braincommunication. *Nat Rev Neurosci.* (2011) 12:453–66. doi: 10.1038/nrn3071
12. Pistollato F, Sumalla CS, Elio I, Masias VM, Giampieri F, Battino M. Role of gut microbiota and nutrients in amyloid formation and pathogenesis of Alzheimer disease. *Nutr Rev.* (2016) 74:624–34. doi: 10.1093/nutrit/nuw023
13. Zhao Y, Jaber V, Lukiw WJ. Secretory products of the human GI tract microbiome and their potential impact on Alzheimer's Disease (AD): detection of lipopolysaccharide (LPS) in AD. *Front Cell Infect Microbiol.* (2017) 7:318. doi: 10.3389/fcimb.2017.00318
14. Daniel E, Marco P. Microbiology: gut microbes augment neurodegeneration.Nature (2017) 544:304–5. doi: 10.1038/nature21910
15. Walker AW, Sanderson JD, Churcher C, Parkes GC, Hudspith BN, Rayment N, et al. High-throughput clone library analysis of the mucosa-associated microbiota reveals dysbiosis and differences between inflamed and non-inflamed regions of the intestine in inflammatory bowel disease. *BMC Microbiol.* (2011) 11:7. doi: 10.1186/1471-2180-11-7
16. Round JL, Mazmanian SK. The gut microbiota shapes intestinal immune responses during health and disease. *Nat Rev Immunol.* (2009) 9:313–23. doi: 10.1038/nri2515
17. Hsiao EY, McBride SW, Hsien S, Sharon G, Hyde ER, McCue T, et al. Microbiota modulate behavioral and physiological abnormalities associated with neurodevelopmental disorders. *Cell* (2013) 155:1451–63. doi: 10.1016/j.cell.2013.11.024
18. De Filippo C, Cavalieri D, Di Paola M, Ramazzotti M, Poullet JB, Massart S, et al. Impact of diet in shaping gut microbiota revealed by a comparative study in children from Europe and rural Africa. *Proc Natl Acad Sci USA.* (2010) 107:14691–6. doi: 10.1073/pnas.1005963107
19. Maslowski KM, Vieira AT, Ng A, Kranich J, Sierro F, Yu D, et al. Regulation of inflammatory responses by gut microbiota and chemoattractant receptor GPR43. *Nature* (2009) 461:1282–6. doi: 10.1038/nature08530
20. Roca-Saavedra P, Mendez-Vilabrille V, Miranda JM, Nebot C, Cardelle-Cobas A, Franco CM, et al. Food additives contaminants and other minor components: effects on human gut microbiota-a review. *J Physiol Biochem.* (2017) 74:69–83. doi: 10.1007/s13105-017-0564-2
21. Neuman MG, Nanau RM. Inflammatory bowel disease: role of diet, microbiota, life style. *Transl Res.* (2012) 160:29–44. doi: 10.1016/j.trsl.2011.09.001
22. Kori M, Aydin B, Unal S, Arga KY, Kazan D. Metabolic biomarkers and neurodegeneration:a pathway enrichment analysis of Alzheimer's Disease, Parkinson's disease, and amyotrophic lateral sclerosis. *OMICS* (2016) 20:645–61. doi: 10.1089/omi.2016.0106
23. González-Domínguez R, Rupérez FJ, García-Barrera T, Barbas C, Gómez-Ariza JL. Metabolomic-driven elucidation of serum disturbances associated with Alzheimer's disease and mild cognitive impairment. *Curr Alzheimer Res.* (2016) 13:641–53. doi: 10.2174/1567205013666160129095138
24. Sahin M, Karauzum SB, Perry G, Smith MA, Aliciguzel Y. Retinoic acid isomers protect hippocampal neurons from amyloid-beta induced neurodegeneration. *Neurotox Res.* (2005) 7:243–50. doi: 10.1007/BF03036453
25. van de Wouw M, Schellekens H, Dinan TG, Cryan JF. Microbiota-gut-brain axis: modulator of host metabolism and appetite. *J Nutr.* (2017) 147:727–45. doi: 10.3945/jn.116.240481
26. Yang N, Wei Y, Xu Q, Tang B. Progress in epigenetic research on Alzheimer disease. *Chin J Med Genet.* (2016) 33:252–5. doi: 10.3760/cma.j.issn.1003-9406.2016.02.028
27. Chen DL, Zhang P, Lin L, Zhang HM, Liu SH. Protective effect of oligosaccharides from *Morinda officinalis* on β-amyloid-induced dementia rats. *China J Chin Mater Med.* (2013) 38:1306–9. doi: 10.4268/cjcmm20130908
28. Chen DL, Yang X, Yang J, Lai GX, Yong TQ, Tang XC, et al. Prebiotic effect of fructooligosaccharides from *Morinda officinalis* on Alzheimer's disease in rodent models by targeting the microbiota-gut-brain axis. *Front Aging Neurosci.* (2017) 9:403. doi: 10.3389/fnagi.2017.00403
29. Melnikova T, Savonenko A, Wang Q, Liang X, Hand T, Wu L, et al. Cycloxygenase-2 activity promotes cognitive deficits but not increased amyloid burden in a model of Alzheimer's disease in a sex-dimorphic pattern. *Neuroscience* (2006) 141:1149–62. doi: 10.1016/j.neuroscience.2006.05.001
30. Ling ZX, Xia L, Jia XY, Cheng YW, Luo YQ, Li Y, et al. Impacts of infection with different toxigenic Clostridium difficile strains on faecal microbiota in children. *Sci Rep.* (2014) 4:7485. doi: 10.1038/srep07485
31. Chen DL, Zhang P, Lin L, Zhang HM, Deng SD, Wu ZQ, et al. Protective effects of bajijiasu in a rat model of $A\beta_{25-35}$-induced neurotoxicity. *J Ethnopharmacol.* (2014) 154:206–17. doi: 10.1016/j.jep.2014.04.004
32. Zeng GF, Zhang ZY, Lu L, Xiao DQ, Zong SH, He JM. Protective effects of ginger root extract on Alzheimer disease-induced behavioral dysfunction in rats. *Rejuven Res.* (2013) 16:124–33. doi: 10.1089/rej.2012.1389
33. Tang Z, Liu LF, Li YL, Dong JY, Li M, Huang JD, et al. Urinary metabolomics reveals alterations of aromatic amino acid metabolism of Alzheimer's disease in the transgenic CRND8 mice. *Curr Alzheimer Res.* (2016) 13:764–76. doi: 10.2174/1567205013666160129095340
34. Wang L, Feng Z, Wang X, Wang X, Zhang X. DEGseq: an R package for identifying differentially expressed genes from RNA-seq data. *Bioinformatics* (2010) 26:136–8. doi: 10.1093/bioinformatics/btp612
35. Trapnell C, Hendrickson DG, Sauvageau M, Goff L, Rinn JL, Pachter L. Differential analysis of gene regulation at transcript resolution with RNA-seq. *Nat Biotech.* (2013) 31:46–53. doi: 10.1038/nbt.2450
36. Cabili MN, Trapnell C, Goff L, Koziol M, Tazon-Vega B, Regev A, et al. Integrative annotation of human large intergenic noncoding RNAs reveals global properties and specific subclasses. *Genes Dev.* (2011) 25:1915–27. doi: 10.1101/gad.17446611
37. Sun L, Luo H, Bu D, Zhao G, Yu K, Zhang C, et al. Utilizing sequence intrinsic composition to classify protein-coding and long non-coding transcripts. *Nucleic Acids Res.* (2013) 41:e166. doi: 10.1093/nar/gkt646
38. Golbraikh A, Tropsha A. Beware of q2!. *J Mol Graph Model.* (2002) 20:269–76. doi: 10.1016/S1093-3263(01)00123-1
39. Pochu H, David AR. More than a gut feeling: the implications of the gut microbiota in psychiatry. *Biol Psychiatry* (2017) 81:e35–7. doi: 10.1016/j.biopsych.2016.12.018
40. Hu X, Wang T, Jin F. Alzheimer's disease and gut microbiota. *Sci China Life Sci.* (2016) 59:1006–23. doi: 10.1007/s11427-016-5083-9
41. Vindigni SM, Zisman TL, Suskind DL, Damman CJ. The intestinal microbiome, barrier function, and immune system in inflammatory bowel disease: a tripartite pathophysiological circuit with implications

for new therapeutic directions. *Ther Adv Gastroenterol.* (2016) 9:606–25. doi: 10.1177/1756283X16644242
42. Dao MC, Everard A, Aron-Wisnewsky J, Sokolovska N, Prifti E, Verger EO, et al. *Akkermansia muciniphila* and improved metabolic health during a dietary intervention in obesity: relationship with gut microbiome richness and ecology. *Gut* (2016) 65:426–36. doi: 10.1136/gutjnl-2014-308778
43. Neyrinck AM, Possemiers S, Druart C, Van de WT, De Backer F, Cani PD, et al. Prebiotic effects of wheat arabinoxylan related to the increase in bifidobacteria, Roseburia and Bacteroides/Prevotella in diet-induced obese mice. *PLoS ONE* (2011) 6:e20944. doi: 10.1371/journal.pone.0020944
44. Wang J, Tang H, Zhang C, Zhao Y, Derrien M, Rocher E, et al. Modulation of gut microbiota during probiotic-mediated attenuation of metabolic syndrome in high fat diet-fed mice. *Isme J.* (2015) 9:1–15. doi: 10.1038/ismej.2014.99
45. Le CE, Nielsen T, Qin J, Prifti E, Hildebrand F, Falony G, et al. Richness of human gut microbiome correlates with metabolic markers. *Nature* (2013) 500:541–6. doi: 10.1038/nature12506
46. Cotillard A, Kennedy SP, Kong LC, Prifti E, Pons N, Le CE, et al. Dietary intervention impact on gut microbial gene richness. *Nature* (2013) 500:585–8. doi: 10.1038/nature12480
47. Arora T, Bäckhed F. The gut microbiota and metabolic disease: current understanding and future perspectives. *J Intern Med.* (2016) 280:339–49. doi: 10.1111/joim.12508
48. Ridaura VK, Faith JJ, Rey F, Cheng J, Duncan AE, Kau AL, et al. Gut microbiota from twins discordant for obesity modulate metabolism in mice. *Science* (2013) 341:1241214. doi: 10.1126/science.1241214
49. Turnbaugh PJ, Hamady M, Yatsunenko T. A core gut microbiome in obese and lean twins. *Nature* (2009) 457:480–4. doi: 10.1038/nature07540
50. Ott SJ, Musfeldt M, Wenderoth DF, Hampe J, Brant O, Fölsch UR, et al. Reduction in diversity of the colonic mucosa associated bacterial microflora in patients with active inflammatory bowel disease. *Gut* (2004) 53:685–93. doi: 10.1136/gut.2003.025403
51. Larsen N, Vogensen FK, van den Berg FW, Nielsen DS, Andreasen AS, Pedersen BK, et al. Gut microbiota in human adults with type 2 diabetes differsfrom non-diabetic adults. *PLoS ONE* (2010) 5:e9085. doi: 10.1371/journal.pone.0009085
52. Burokas A, Arboleya S, Moloney RD, Peterson VL, Murphy K, Clarke G, et al. Targeting the microbiota-gut-brain axis: prebiotics have anxiolytic and antidepressant-like effects and reverse the impact of chronic stress in mice. *Biol Psychiatry* (2017) 82:472–87. doi: 10.1016/j.biopsych.2016.12.031
53. González-Domínguez R, García-Barrera T, Vitorica J, Gómez-Ariza JL. Deciphering metabolic abnormalities associated with Alzheimer's disease in the APP/PS1 mouse model using integrated metabolomics approaches. *Biochimie* (2015) 110:119–28. doi: 10.1016/j.biochi.2015.01.005
54. Drolle E, Negoda A, Hammond K, Pavlov E, Leonenko Z. Changes in lipid membranes may trigger amyloid toxicity in Alzheimer's disease. *PLoS ONE* (2017) 12:e0182194. doi: 10.1371/journal.pone.0182194
55. Dias V, Junn E, Mouradian MM. The role of oxidative stress in Parkinson's disease. *J Parkinsons Dis.* (2013) 3:461–91. doi: 10.3233/JPD-130230
56. Liu X, Yamada N, Maruyama W, Osawa T. Formation of dopamine adducts derived from brain polyunsaturated fatty acids: mechanism for Parkinson disease. *J Biol Chem.* (2008) 283:34887–95. doi: 10.1074/jbc.M805682200
57. Yu J, Kong L, Zhang A, Han Y, Liu Z, Sun H, et al. High-throughput metabolomics for discovering potential metabolite biomarkers and metabolic mechanism from the APPswe/PS1dE9 transgenic model of Alzheimer's disease. *J Proteome Res.* (2017) 16:3219–28. doi: 10.1021/acs.jproteome.7b00206
58. Garrett RH, Grisham CM. *Principles of Biochemistry With a Human Focus*. Brooks/Cole; Thomson Learning (2002). p. 578–85.
59. Carvalho AS, Torres LB, Persike DS, Fernandes MJ, Amado D, Naffah-Mazzacoratti, MG, et al. Neuroprotective effect of pyruvate and oxaloacetate during pilocarpine induced status epilepticus in rats. *Neurochem Int.* (2011) 58:385–90. doi: 10.1016/j.neuint.2010.12.014
60. Zilberter Y, Gubkina O, Ivanov AI. A unique array of neuroprotective effects of pyruvate in neuropathology. *Front Neurosci.* (2015) 9:17. doi: 10.3389/fnins.2015.00017
61. Zlotnik A, Gurevich B, Tkachov S, Maoz I, Shapira Y, Teichberg VI. Brain neuroprotection by scavenging blood glutamate. *Exp Neurol.* (2007) 203:213–20. doi: 10.1016/j.expneurol.2006.08.021

Conflict of Interest Statement: The authors declare that the research was conducted in the absence of any commercial or financial relationships that could be construed as a potential conflict of interest.

Copyright © 2018 Xin, Diling, Jian, Ting, Guoyan, Hualun, Xiaocui, Guoxiao, Ou, Chaoqun, Jun and Yizhen. This is an open-access article distributed under the terms of the Creative Commons Attribution License (CC BY). The use, distribution or reproduction in other forums is permitted, provided the original author(s) and the copyright owner are credited and that the original publication in this journal is cited, in accordance with accepted academic practice. No use, distribution or reproduction is permitted which does not comply with these terms.

frontiers in Aging Neuroscience

ORIGINAL RESEARCH
published: 08 December 2017
doi: 10.3389/fnagi.2017.00403

Prebiotic Effect of Fructooligosaccharides from *Morinda officinalis* on Alzheimer's Disease in Rodent Models by Targeting the Microbiota-Gut-Brain Axis

Diling Chen[1], Xin Yang[2], Jian Yang[1], Guoxiao Lai[1,3], Tianqiao Yong[1], Xiaocui Tang[1], Ou Shuai[1,4], Gailian Zhou[3], Yizhen Xie[1,4]* and Qingping Wu[1]*

[1] State Key Laboratory of Applied Microbiology Southern China, Guangdong Provincial Key Laboratory of Microbial Culture Collection and Application, Guangdong Open Laboratory of Applied Microbiology, Guangdong Institute of Microbiology, Chinese Academy of Sciences, Guangzhou, China, [2] Department of Pharmacy, The Fifth Affiliated Hospital of Guangzhou Medical University, Guangzhou, China, [3] Guangxi University of Chinese Medicine, Nanning, China, [4] Guangdong Yuewei Edible Fungi Technology Co., Ltd., Guangzhou, China

OPEN ACCESS

Edited by:
Ghulam Md Ashraf,
King Abdulaziz University,
Saudi Arabia

Reviewed by:
Rongqiao He,
Institute of Biophysics (CAS), China
Tarique Khan,
Buck Institute for Research on Aging, United States

***Correspondence:**
Diling Chen
diling1983@163.com
Yizhen Xie
xieyizhen@126.com

Received: *08 September 2017*
Accepted: *22 November 2017*
Published: *08 December 2017*

Citation:
Chen D, Yang X, Yang J, Lai G, Yong T, Tang X, Shuai O, Zhou G, Xie Y and Wu Q (2017) Prebiotic Effect of Fructooligosaccharides from Morinda officinalis on Alzheimer's Disease in Rodent Models by Targeting the Microbiota-Gut-Brain Axis. Front. Aging Neurosci. 9:403. doi: 10.3389/fnagi.2017.00403

Gut microbiota influences the central nervous system disorders such as Alzheimer's disease (AD). The prebiotics and probiotics can improve the host cognition. A previous study demonstrated that fructooligosaccharides from *Morinda officinalis* (OMO) exert effective memory improvements in AD-like animals, thereby considered as potential prebiotics; however, the underlying mechanism still remains enigma. Thus, the present study investigated whether OMO is effective in alleviating AD by targeting the microbiota-gut-brain axis. OMO was administered in rats with AD-like symptoms (D-galactose- and $A\beta_{1-42}$-induced deficient rats). Significant and systematic deterioration in AD-like animals were identified, including learning and memory abilities, histological changes, production of cytokines, and microbial community shifts. Behavioral experiments demonstrated that OMO administration can ameliorate the learning and memory abilities in both AD-like animals significantly. AD parameters showed that OMO administration cannot only improve oxidative stress and inflammation disorder, but also regulate the synthesis and secretion of neurotransmitter. Histological changes indicated that OMO administration ameliorates the swelling of brain tissues, neuronal apoptosis, and down-regulation of the expression of AD intracellular markers (Tau and $A\beta_{1-42}$). 16S rRNA sequencing of gut microbiota indicated that OMO administration maintains the diversity and stability of the microbial community. In addition, OMO regulated the composition and metabolism of gut microbiota in inflammatory bowel disease (IBD) mice model treated by overdosed antibiotics and thus showed the prebiotic potential. Moreover, gut microbiota plays a major role in neurodevelopment, leading to alterations in gene expression in critical brain and intestinal regions, thereby resulting in perturbation to the programming of normal cognitive behaviors. Taken together, our findings suggest that

the therapeutic effect of the traditional medicine, *M. officinalis*, on various neurological diseases such as AD, is at least partially contributed by its naturally occurring chemical constituent, OMO, via modulating the interaction between gut ecology and brain physiology.

Keywords: fructooligosaccharides, prebiotics, Alzheimer's disease, behavior, microbiota-gut-brain axis

INTRODUCTION

Gut microbiota is associated with several diseases, including neurodegenerative diseases such as Parkinson's disease (PD) and Alzheimer's disease (AD) (Petra et al., 2015; Jiang et al., 2017). Notably, the microbiota-gut-brain axis is a bi-directional communication system that is not fully understood; however, it is known to include neural, immune, endocrine, and metabolic pathways. Studies in germ-free animals and those exposed to pathogenic microbial infections, antibiotics, probiotics, or fecal microbiota transplantation suggest the link of gut microbiota with host cognition or AD-related pathogenesis (Pistollato et al., 2016; Harach et al., 2017; Liu et al., 2017; Rieder et al., 2017; Russo et al., 2017).

Several studies have supported the theory of the occurrence of a pathway of communication between the gut and the brain, modulated by gut microbiota (Gareau, 2014; Mayer et al., 2014). It has been speculated that targeting the microbiota can affect the behavior and modulate brain plasticity and cognitive functions while aging (Leung and Thuret, 2015). Some studies demonstrated that gut-targeted intervention by consuming *lactic acid bacteria* such as those in yogurt, could improve or delay the onset of cognitive decline associated with aging (Jung et al., 2012; Choi et al., 2015; Scott et al., 2017). Therefore, using probiotics for ameliorating the cognitive and behavioral disorders could be a potential treatment.

The hypothesis that the microbiota-gut-brain axis (Rhee et al., 2009) plays a critical role in health and disease, including neuropsychiatric disorders (Liu et al., 2017), is rapidly progressing. Nurturing a beneficial gut microbiome with prebiotics, such as fructooligosaccharides and inulin, is an appealing but under-investigated microbiota-induced manipulation. A previous study showed that the prebiotic treatment could modify the behavior across domains relevant to anxiety, depression, cognition, stress response, and social behavior (Burokas et al., 2017). Previous findings strengthened the evidence supporting the therapeutic targeting of gut microbiota in brain-gut axis disorders, thereby opening new prospects in the field of nutritional neuropsychopharmacology. Thus, it is imperative to develop novel and effective drugs or foods with prebiotic effects from natural resources.

Morinda officinalis How. (*M. officinalis*), as a Chinese traditional natural herbal medicine, contains a number of active components. Reportedly, the content of saccharides in *M. officinalis* radix is 49.79–58.25%, which is highly composed of oligosaccharides, such as inulin-type hexasaccharide exerting antidepressant effects in the model systems (Cai et al., 1996; Li et al., 2001). This phenomenon can be effectuated by up-regulating the expression of neurotrophic factors and/or down-regulating the $[Ca^{2+}]_i$ overloading (Li et al., 2004). Bajijiasu, another oligosaccharide, protects PC12 cells from $A\beta_{25-35}$-induced neurotoxicity (Chen et al., 2013), ameliorates the cognitive deficits induced by D-galactose in mice, and protects against ischemia-induced neuronal damage or death (Tan et al., 2000a,b). Our previous study suggested that oligosaccharide extracted from *M. officinalis* (OMO) might inhibit the oxidative stress and neuronal apoptosis, restore normal energy metabolism, as well as, increase the cell viability and mitochondrial membrane potential in AD animal models significantly (Chen et al., 2014a). However, the underlying mechanism is yet to be elucidated.

Alzheimer's disease is the most common neurodegenerative disorder, affecting approximately >5% of the worldwide population aged >65 years, annually. AD is a chronic neurodegenerative disease that frequently exhibits a slow progression accompanied by a greater recession of the disease over a period. Although the cause of AD is poorly understood, among various biochemical and morphological events, the presence of neurofibrillary tangles, senile plaques, and neuronal and synaptic loss are considerably noted (Chen et al., 2017). Several pieces of evidence have confirmed that the accumulation of intracellular β-amyloid (Aβ) may be an early event in the development of AD. Aβ is a peptide comprised of 36–43 amino acids formed by a large transmembrane glycoprotein, such as amyloid precursor protein (APP), expressed on the cell. Aβ may activate the inflammatory and neurotoxic processes, including the excessive generation of free radicals and oxidative damage among intracellular proteins and other macromolecules (Abbott, 2011). D-galactose can form advanced glycation end products (AGEs). The administration of D-galactose to human populations can induce cognitive deficits and disruptions in the synaptic communication. Thus, D-galactose-treated rats with synaptic disruption and memory impairment have been extensively used as model rodents (Zhan et al., 2014; Gao et al., 2016; Huang et al., 2016; Li et al., 2016). In our previous, we have used these two models to screen the effective compounds for curing the AD (Chen et al., 2014b, 2017). Thus, in this study, the two AD-like models were induced by D-galactose and Aβ, respectively.

Herein, we investigated whether OMO is effective in alleviating AD by targeting the microbiota-gut-brain axis. OMO was administered in rats exhibiting AD-like symptoms induced by D-galactose and $A\beta_{1-42}$, respectively. Some indexes and histological deterioration, including learning and memory abilities, histological alterations, production of cytokines, microbial communities, and transcriptome in small intestine and brain, were identified in AD-like animals. And the prebiotics were directly evaluated in an overdose antibiotics-treated trinitro-benzene-sulfonic acid (TNBS)-induced mice model.

MATERIALS AND METHODS

Animal Models and Treatments

Adult male Sprague–Dawley rats (180–220 g) and C57 mice (18–22 g, 10-moth-old) obtained from the Center of Laboratory Animal of Guangdong Province, SCXK [Yue] 2008-0020, SYXK [Yue] 2008-0085) were pair-housed in plastic cages in a temperature-controlled (25°C) colony room at a 12/12 h light/dark cycle. Food and water were available *ad libitum*. All experimental protocols were approved by the Center of Laboratory Animals of the Guangdong Institute of Microbiology (GT-IACUC20160426). All efforts were made to minimize the number of animals used.

D-Galactose-Induced Deficient Rats and Treatment

The rats were randomly divided into four groups as follows: control group received distilled water orally, model group received intraperitoneal injection (i.p.) of 100 mg/kg/d D-galactose (Zhong et al., 2016; Chen et al., 2017; Liang et al., 2017), low-dose group was administered D-galactose (100 mg/kg/d) by i.p. and gavage at a dosage of 50 mg/[kg·d] OMO, and high-dose group received D-galactose (100 mg/kg/d) by i.p. and gavage at a dosage of 100 mg/[kg·d] OMO daily in the morning. Every group consisted of eight animals, and the duration of the procedure was 8 weeks.

$A\beta_{1-42}$-Induced Deficient Rats and Treatment

The procedures were similar to those described previously (Chen et al., 2014b). Rats were anesthetized using 30 g/L pentobarbital sodium (40 mg/kg, i.p.; Sigma–Aldrich) and placed in a stereotaxic frame (RWD Life Science Co., Ltd., Shenzhen, China). The hair was shaved, scalp opened, and holes drilled with an electric dental drill (brushless motor, 30,000 rpm) according to the mouse brain atlas (AP-3.6 mm, ML ± 2.5 mm, DV3.0 mm). Then, 5 μL (10 μg) $A\beta_{1-42}$ in a fibrillar state (Chen et al., 2013) was slowly injected into the CA1 region of the hippocampus over a 5-min period in one hole, and the needle was retained inside for an additional 5 min. Subsequently, the wound was sutured, and penicillin (30 U/kg) was injected intramuscularly to protect against infection. Finally, the rats were isolated in a warm box until consciousness was recovered.

After 15 days, the rats were screened with water maze tests to identify the animals that were appropriate models, followed by random categorization into four groups as follows: control group (received saline and distilled water orally), model group (received $A\beta_{1-42}$ and distilled water orally), low-dose group (received $A\beta_{1-42}$ and OMO 50 mg/[kg·d] orally), high-dose group (received $A\beta_{1-42}$ and OMO 100 mg/[kg·d] orally). Every group consisted of seven animals, and the duration of the experiments was 28 days.

Water Maze Tests

The spatial learning and memory abilities of the rats were tested using the Morris water maze (MWM, DMS-2, Chinese Academy of Medical Sciences Institute of Medicine). The MWM consisted of a circular opaque fiberglass pool (200 cm diameter) filled with water (25 ± 1°C). The pool was surrounded by light blue curtains, and three distal visual cues were fixed on the curtains. A total of four floor light sources of equal power provided uniform illumination to the pool and testing room. A CCD camera was placed above the center of the pool in order to record the swim paths of the animals. The video output was digitized by an EthoVision tracking system (Noldus, Leesburg, VA, United States). The tests included three periods: initial spatial training, spatial reversal training, and the probe test; the procedures were same as those described previously (Chen et al., 2014b).

Evaluation of AD Parameters

The appearance, behavior, and fur color of the animals were observed and documented daily. The weights of the animals were measured every 3 days during the period of drug administration. Following the MWM, the blood and serum were acquired, and the brains of the animals were dissected. Routine index and cytokines (Wang et al., 2016), including the production of cytokines interleukins [(1L)-1α, 1L-2, 1L-8, 1L-10, 1L-11, IL-12], tumor necrosis factor (TNF)-γ, TNF-α, vascular endothelial growth factor (VGEF), human macrophage inflammatory protein-1α (MIP-α), and macrophage colony-stimulating factor (M-CSF), activities of malondialdehyde (MDA), total superoxide dismutase (T-SOD), catalase (CAT), glutathione reductase (GSH-Px), and levels of acetylcholine (ACh), acetylcholinesterase (AChE), and Na^+/K^+-ATPase, and some monoamine neurotransmitters, were measured.

A total of three brains, small intestine, and other tissues from each group were fixed in 4% paraformaldehyde and prepared as paraffin sections that were stained with hematoxylin-eosin (H&E) and immunohistochemistry (IHC) before examining under light microscopy (Zeng et al., 2013; Chen et al., 2014b).

Evaluation of Prebiotic Effects of OMO in TNBS-Induced Mice

After 24 h fasting, the mice were anesthetized by intraperitoneal injection of 2% sodium pentobarbital (0.2 ml/100 g), followed by intubation (latex tubing of 2 mm diameter, lubricated with edible oil before usage) from the anus, gently inserted into the lumen about 4.0 cm. Subsequently, 150 mg/kg of TNBS (Sigma–Aldrich, St. Louis, MO, United States, solubilized in 50% ethanol) solution was injected through the latex tubing, the rats were hanged upside down for 30 s to ensure complete seepage of the mixture into the lumen without leakage (Wei et al., 2017). Then, the animals were randomly divided into nine groups ($n = 9$): control, model, model and high-dose antibiotics, OMO (100 mg/kg/d), *Bifidobacterium*, OMO and high-dose antibiotics, OMO and *Bifidobacterium*, *Bifidobacterium* and high-dose antibiotics, OMO and *Bifidobacterium* and high-dose antibiotics. All the antibiotics were administered for 4 days, then inflammatory bowel disease (IBD) was induced with TNBS, followed 7-day drug treatments and TNBS induction, followed by an additional 4-day drug treatments.

Consequently, the mice were anesthetized by intraperitoneal injection of 2% sodium pentobarbital (0.25 ml/100 g). The blood plasma was collected by abdominal aortic method and serum by centrifugation (1500 r/min, 10 min). Then, the serum was assessed for the production of cytokines GM-CSF (granulocyte-macrophage colony-stimulating factor), TNF-γ, 1L-10, IL-12, 1L-17α, 1L-4, TNF-α, and VGEF. The colon and spleen obtained from the rats were fixed in 4% paraformaldehyde at pH 7.4 for further pathological observations, and the cecum contents were collected for 16S rRNA gene-based analysis.

Microbiome Analysis

Fresh fecal samples were collected before fasting of the rats and stored at −80°C. Frozen microbial DNA was isolated from mice cecal sample with total mass ranging from 1.2 to 20.0 ng and preserved at −20°C. The microbial 16S rRNA genes were amplified using the forward primer 5′-CCTAYGGGRBGCASCAG-3′ and reverse primer 5′-GGACTACNNGGGTATCTAAT-3′ for rats. Each amplified product was concentrated via solid-phase reversible immobilization and quantified by electrophoresis using an Agilent 2100 Bioanalyzer (Agilent, United States). After quantification of DNA concentration by NanoDrop, each sample was diluted to 1×10^9 molecules/μL in TE buffer and pooled. Subsequently, 20 μL of the pooled mixture was used for sequencing on Illumina MiSeq sequencing platform according to the manufacturer's instructions. The resulting reads were analyzed as described previously (Ling et al., 2014).

Transcriptome Analysis

The RNA-seq transcriptome library was prepared using the TruSeq™ RNA Sample Preparation Kit (Illumina, San Diego, CA, United States). *De novo* assembly and annotation identified the differentially expressed genes (DEGs) between different treatments; the expression level of each transcript was measured according to the fragments/kb of exon per million mapped reads method. RSEM[1] was used to quantify the abundance of genes and isoforms. The R statistical package software EdgeR[2] was used for the analysis of differential expression. Functional enrichment analysis was performed to identify the DEGs enriched significantly in Gene Ontology (GO) and metabolic pathways at Bonferroni-corrected p-value ≤ 0.05 as compared to the whole- transcriptome background. GO functional enrichment and KEGG pathway analyses were performed using Goatools[3] and KOBAS[4], respectively (Wang et al., 2010; Cabili et al., 2011; Sun et al., 2013; Trapnell et al., 2013).

Statistical Analysis

All data are described as the means ± standard deviations (SD) of at least three independent experiments. The significant differences between treatments were analyzed by one-way analysis of variance (ANOVA) test at $p < 0.05$ using statistical package for the social sciences (SPSS, Abacus Concepts, Berkeley, CA, United States) and Prism5 (GraphPad, San Diego, CA, United States) software.

[1]http://deweylab.biostat.wisc.edu/rsem/

[2]http://www.bioconductor.org/packages/2.12/bioc/html/edgeR.html

[3]https://github.com/tanghaibao/Goatools

[4]http://kobas.cbi.pku.edu.cn

RESULTS

Effects of OMO in D-Galactose-Induced Deficient Rats

Antioxidative and Neuroprotective Effects, Activation of Energy Metabolism and Regulation of Acetylcholine Esterase by OMO in D-Galactose-Induced Deficient Rats

The fur of the treated animals was much smoother than that of the model group. The average weight between the treated and the model groups did not differ significantly ($p > 0.05$); the animals weighed approximately 320 g at the beginning and 500 g at the end of the experiment (**Figure 1A**).

Compared to the model group, the incubation period for each OMO-treated group was significantly shorter. The incubation period for the low-dose OMO group was (86.37 ± 11.46 s) and that for the high-dose group was (82.00 ± 19.44 s) on the 1st day. Compared to the model group, the differences were significant ($p < 0.01$). On the 4th day, the incubation period for the low-dose OMO group was (39.30 ± 5.63 s) and that for the high-dose group was 30.74 ± 3.69 s; the differences were significant as compared to the model group ($p < 0.01$; **Figure 1B**). These results demonstrated that OMO administration could ameliorate D-galactose-induced learning and memory dysfunction in rats.

Probe test results did not reveal any significant differences ($p > 0.05$) among the groups with respect to total swimming distance or speed. The swimming time of the control group in the NW quadrant (28.00 ± 0.81 s) was significantly longer than that in the other three quadrants (24.36 ± 0.40, 24.21 ± 1.33, and 25.43 ± 1.465 s; $p < 0.01$). The swimming time in the NW quadrant of the model group was 25.23 ± 1.04 s, which was significantly shorter than the control group ($p < 0.01$), suggesting that the rats remembered the location of the placement of the platform. The swimming durations of the low- and high-dose OMO groups were 27.13 ± 0.85 and 29.00 ± 1.08 s, respectively, which were significantly longer than the model group. Compared to the model group, the differences were significant ($p < 0.01$; **Figure 1C**).

As shown in **Figure 1D**, the SOD levels in the low- and high-dose OMO groups were 95.05 ± 1.21, and 97.70 ± 1.43 (% of control), respectively, as compared to 90.45 ± 2.17 in the model groups. The differences were significant as compared to the model group ($p < 0.05$). In addition, the levels of GSH-Px and CAT showed similar trends, while that of the MDA showed opposite trends, suggesting that OMO encouraged SOD, MDA, CAT, and inhibited MDA production, thereby indicating that OMO administration can enhance the antioxidative activities in the D-galactose-induced deficient rats.

To evaluate the protective efficacy of OMO on the energy metabolism in D-galactose-treated rats, we measured the

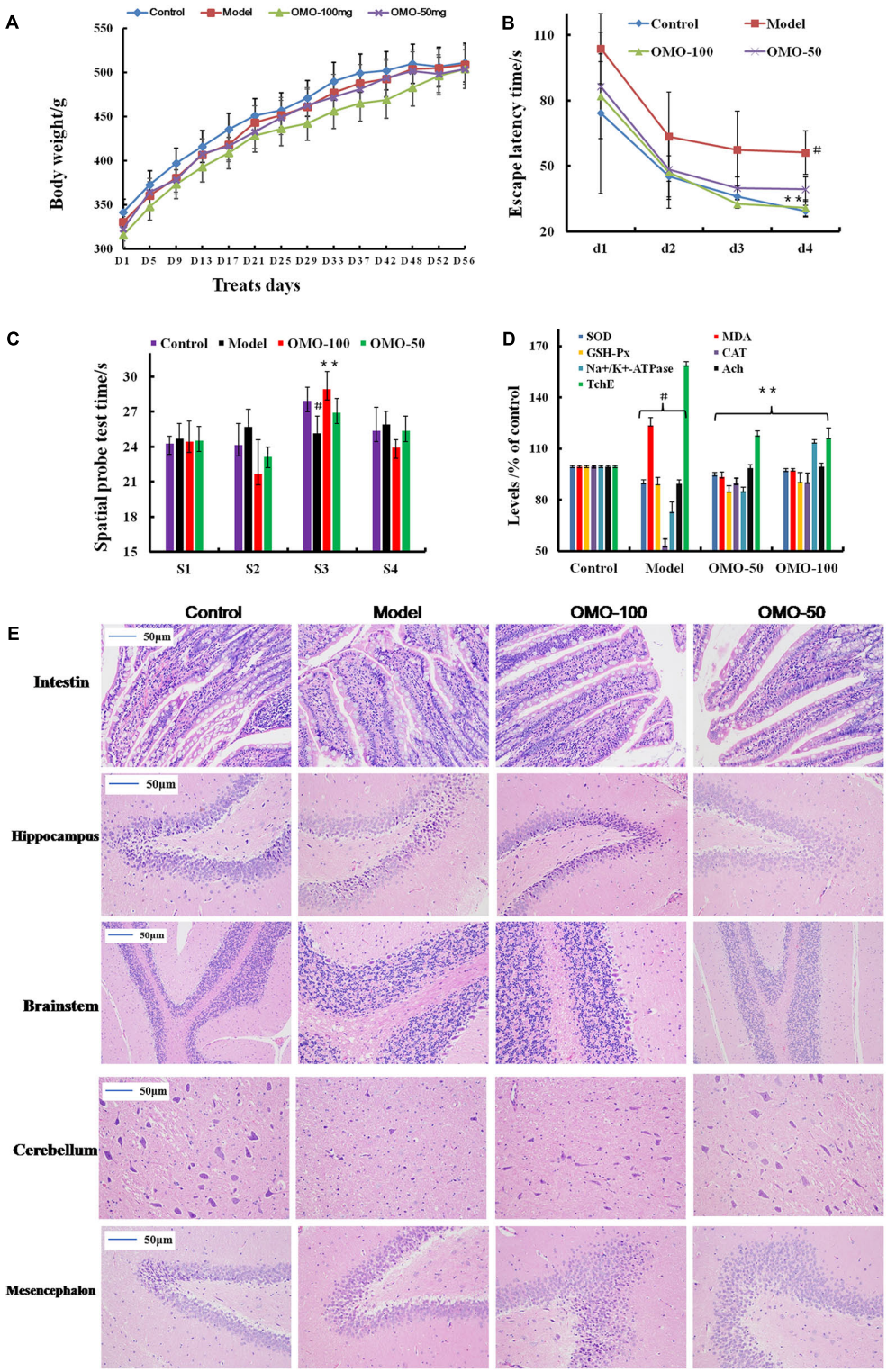


FIGURE 1 | Effect of OMO in D-galactose-induced deficient rats. **(A)** Body weight changes during the treatments time. **(B)** Escape latency in the MWM. **(C)** Swimming time in the platform quadrant during the spatial probe test. **(D)** Effect on SOD, MDA, CAT, GSH-Px TchE, Ach, and Na^+/K^+-ATPase levels. **(E)** Histopathological changes in the intestine and brain. The graph Control, control group; Model, model group; OMO-50 mg, low-dose group that received D-galactose (100 mg/kg/d) by i.p. and gavage at a dosage of 50 mg/[kg·d] in OMO; OMO-100 mg, high-dose group that received D-galactose (100 mg/kg/d) i.p. and gavage at a dosage of 100 mg/[kg·d] in OMO. Values are represented as mean ± SD ($n = 6$) and expressed as the percentage of the control group, $^{\#}p < 0.01$ vs. control group, $^{*}p < 0.05$ vs. model group, $^{**}p < 0.01$ vs. model group.

Na^+/K^+-ATPase levels in brain tissue. As shown in **Figure 1D**, the levels of Na^+/K^+-ATPase were significantly lower in the model group (73.53 ± 5.17% of control) as compared to the control group ($p < 0.05$). The levels of all the OMO-treated groups (90.15 ± 2.08 for low-dose, 90.83 ± 1.64 for high-dose) were increased significantly, and the differences were significantly different as compared to the model group ($p < 0.05$). These levels were based on the concentration-dependent activities; however, the specific underlying mechanism necessitates further studies.

Cholinergic system damage and abnormal ACh levels are observed in AD patients. The results are illustrated in **Figure 1D**. As compared to the model group (89.85 ± 1.93% of control), after treatment with different concentrations (50 and 100mg/[kg·d]) of OMO, the ACh levels of the model rats increased significantly to 99.22 ± 1.49 and 99.98 ± 1.52, respectively, ($p < 0.05$). The AchE decreased to 118.39 ± 1.93 and 116.70 ± 5.47, respectively. These differences were significant ($p < 0.05$) as compared to the model group (159.37 ± 4.15).

The HE staining of the small intestinal tissues revealed crypt atrophy, distortion, and surface irregularity in the model group D-galactose-induced deficient rats, while those changes in the OMO-treated groups were improved (**Figure 1E**, intestine). Moreover, the staining did not demonstrate any remarkable neuronal abnormalities in the hippocampus of the rats in the control group. The pyramidal cells in the CA1 region were arranged precisely and tightly, and no cell loss was observed. Additionally, in the control group, the cells were round and intact with stained clear, dark blue nuclei (**Figure 1E**). However, noticeable damage in the hippocampus was observed in the model groups by histopathology. The pyramidal layered structure was disintegrated, and the neuronal loss was found in the CA1 region. Neurons with pyknotic nuclei and shrunken or irregular shape were also observed. These abnormalities were attenuated by the treatment with OMO. The cells in the OMO-treated groups exhibited superior cell morphology and were more in number than those in the untreated groups, especially those in the OMO-100 treated group were superior to the control group. Together, these results demonstrated that the OMO administration could ameliorate the D-galactose-induced deficient rats.

Changes in Gut Microbiota after OMO Administration

Operational taxonomic unit (OTU) abundance and taxonomic profiles were analyzed as shown in **Figure 2**. The values of Chao1, ACE, Shannon, and npShannon were reduced, and that of Simpson was increased significantly in the D-galactose-induced group than the normal group ($p < 0.05$, **Figure 2A**). After treatment with 100 mg/kg/d OMO, the values of Chao1, ACE, Shannon, npShannon, and Simpson were improved to resemble the normal (**Figure 2A**). All the treated groups could be clustered using the principal component analysis (PCA) (**Figure 2B**); Bray–Curtis distance was shown at the phylum level in **Figure 2C** (*Verrucomicrotia*, *Proteobacteria*, *Firmicutes*, and *Bacteroidetes*), genus level in **Figure 2D** (left) (*Prevotella*, *Oscillospira*, *Lactobacillus*, *Bacteroides*, *Parabacteroides*, *Sutterella*, *Akkermansia*), and beta diversity at the genus level in **Figure 2D** (right). Our results indicated that OMO administration could maintain the abundance of gut microbiota in D-galactose-induced deficient rats, although additional studies are warranted.

Effects of OMO on $A\beta_{1-42}$-Induced Deficient Rats

Indexes Improvements by OMO Administration

The fur of the treated animals was much smoother than that of the model group. The average weight of model groups was found to be higher than that of the control group ($p < 0.05$), and we found that the rats in the model group present constipation and swollen belly. Moreover, the weight records of OMO-treated groups did not alter significantly ($p > 0.05$) as compared to the control group (**Figure 3A**).

Compared to the model group, the incubation period for each OMO-treated group was significantly shorter. The incubation period for the low-dose OMO group was 86.49 ± 11.64 s, while that for the high-dose group was 82.06 ± 19.44 s on the 1st day. Compared to the model group (113.75 ± 16.11 s), the differences were significant ($p < 0.01$). On the 4th day, the incubation period of the low-dose OMO group was 37.19 ± 5.36 s, and that for the high-dose group was 28.27 ± 3.96 s; the differences were significant as compared to the model group (56.29 ± 9.69 s, $p < 0.01$; **Figure 3Ba**). These results showed that OMO administration could ameliorate the $A\beta_{1-42}$-induced learning and memory dysfunction in rats.

Probe test results showed no significant differences ($p > 0.05$) among the groups with respect to the total swimming distance or speed. The swimming time of the control group in the NW quadrant (26.63 ± 3.83 s) was significantly longer than that in the other three quadrants ($p < 0.01$). The swimming time in the NW quadrant of the model group was 20.77 ± 2.36 s, which was significantly shorter than the control group ($p < 0.01$), suggesting that the rats remembered the location of the platform. The swimming time of the low- and high-dose OMO groups were 26.50 ± 3.59 and 27.36 ± 2.51 s, which were significantly longer than the model group. Compared to the model group, the differences were significant ($p < 0.01$), as shown in **Figure 3Bc**. The swimming distances did not differ among all groups (**Figure 3Bb**).

All the cytokines' levels in the serum of $A\beta_{1-42}$-induced group deviated from the normal; GM-CSF, TNF-γ, 1L-10, IL-12, 1L-17α, 1L-4, TNF-α, and VGEF were secreted significantly different ($p < 0.05$ or $p < 0.01$; **Figure 3C**). When treated with OMO, all these cytokines were strikingly recovered close to the baseline level (**Figure 3C**), thereby indicating that OMO administration can improve the inflammatory environment.

The monoamine neurotransmitter levels in right brain tissue were dissected from 4 rats in each group, according to the methods described previously (Chen et al., 2014b). **Figure 3D** showed that the levels of norepinephrine (NE), dopamine (DA), 5-hydroxytryptamine (5-HT), and 5-hydroxyindole acetic acid (5-HIAA) were reduced in $A\beta_{1-42}$-induced groups as compared to the control group, and the OMO administration can promote the secretion of some monoamine neurotransmitters (NE, DA,

A

Sequencing data summary at 97% similarity

Group	Label	Chao	Ace	Shannon	Npshannon	Simpson	Coverage
Model	0.03	12534 ± 2129#	22848 ± 4820	4.6015 ± 0.2331#	4.7236 ± 0.2399	0.0337 ± 0.0083#	0.9703 ± 0.0045
OMO-100	0.03	20851 ± 3266*	38967 ± 5280*	5.2774 ± 0.1225*	5.4313 ± 0.1441*	0.0197 ± 0.0035*	0.9565 ± 0.0072
Normal	0.03	23523 ± 2253	44079 ± 4056	5.6098 ± 0.2683	5.7747 ± 0.2074	0.0174 ± 0.0052	0.9472 ± 0.0192

The richness estimators (ACE and Chao), diversity indices (Shannon and Simpson), and Coverage were calculated using the Mothur software. Values given are the mean±SD, #$p<0.05$ *vs* normal, *$p<0.05$ *vs* model.

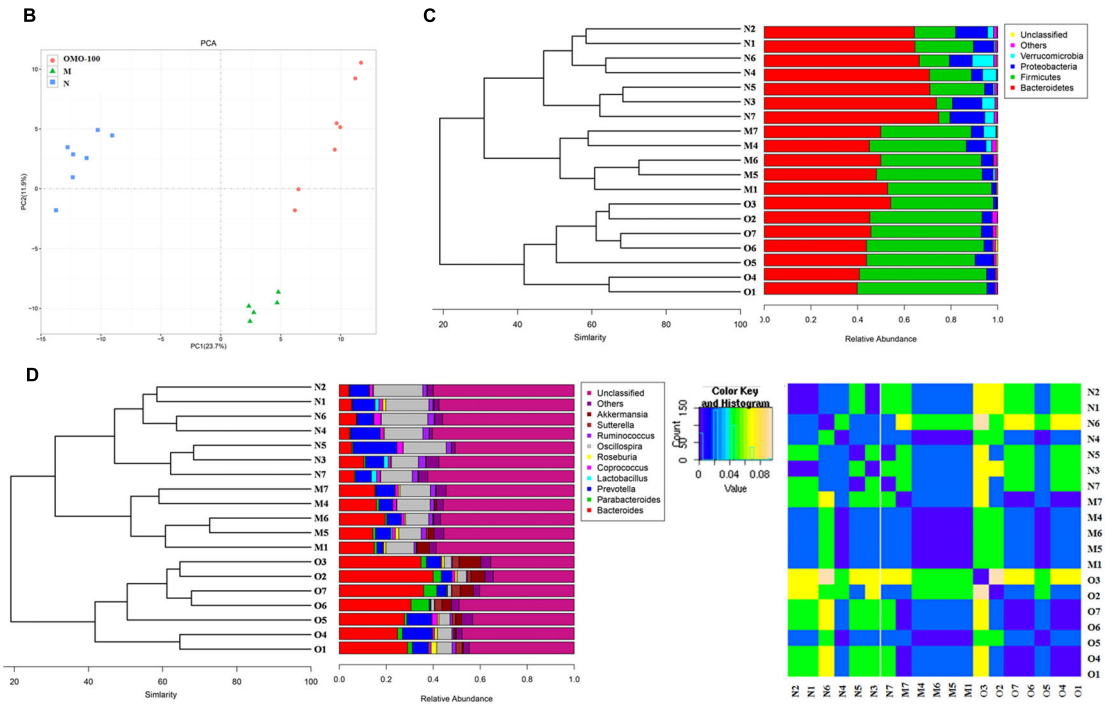


FIGURE 2 | Effects of OMO on gut microbiota in D-galactose-induced deficient rats. **(A)** Sequencing data summary at 97% similarity. **(B)** Results of PCA. **(C)** Classification and abundance of cecal contents at the phylum level. **(D)** Classification and abundance of cecal contents at the genus level, and the beta diversity. The graph N is normal group; M is model group; O is OMO-100 mg, high-dose group that received D-galactose (100 mg/kg/d) i.p., and gavage at a dosage of 100 mg/[kg·d] in OMO. Values are the means of six independent experiments ($n \geq 5$).

5-HT, and 5-HIAA) in a concentration-dependent manner (**Figure 3D**).

The HE staining of small intestinal tissues revealed crypt branching, atrophy, distortion, and surface irregularity in the model group $A\beta_{1-42}$-induced deficient rats, while those changes in the OMO-treated groups were improved (**Figure 3E**, intestine). The injury to the atrial tissues in the $A\beta_{1-42}$-induced group was more severe than that in the normal and OMO-treated groups. Furthermore, the HE staining did not reveal any remarkable neuronal abnormalities in the hippocampus of rats in the control group (**Figure 3E**). However, the obvious hippocampal histopathological damage was observed in the model groups. The pyramidal layered structure was disintegrated, and neuronal loss was found in the CA1 region. These abnormalities were attenuated by OMO treatment. The cells in OMO-treated groups exhibited better cell morphology and were more in number than those in the untreated groups, especially those in the OMO-100 treated group were superior to the control group. Compared to the normal group, the proportion of $A\beta_{1-42}$ and Tau-positive cells in rats in the model group was significantly higher than that in the normal group ($p < 0.05$), while the OMO administration down-regulated the expression of $A\beta_{1-42}$ and Tau proteins (**Figure 3E**).

The Gut Structure of the Microbiota Was Altered Significantly by OMO

OTU abundance and taxonomic profiles were analyzed as shown in **Figure 4**. Compared to the normal group, the diversity of the microbial communities in $A\beta_{1-42}$-induced (injected 10 or 20 μg fibrillar state of $A\beta_{1-42}$ into the CA1 region, **Figure 4D**) group was reduced and negatively related with the doses of $A\beta_{1-42}$ (**Figure 4A**); All the $A\beta_{1-42}$-induced groups were clustered as

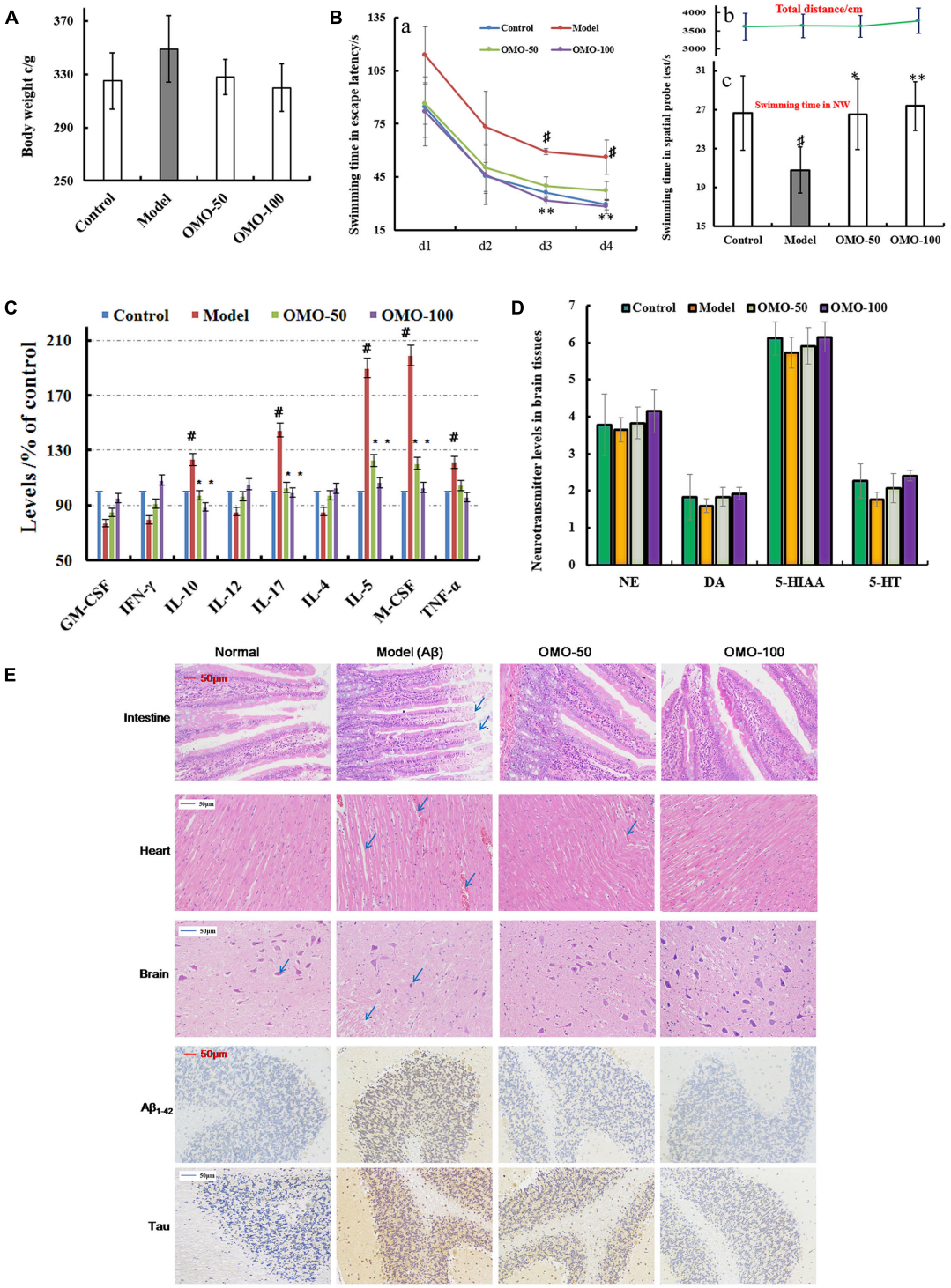


FIGURE 3 | Effect of OMO in $A\beta_{1-42}$-induced deficient rats. **(A)** Body weight changes during the treatments time. **(B-a)** Escape latency in the MWM. **(B-b)** Swimming distance. **(B-c)** Swimming time in the platform quadrant during the spatial probe test. **(C)** Level of cytokines GM-CSF, TNF-γ, 1L-10, IL-12, 1L-17α, 1L-4, TNF-α, and VGEF-α in the serum. **(D)** Levels of monoamine neurotransmitters (NE, DA, 5-HT, and 5-HIAA) in the brain tissue. **(E)** Histopathological changes in the intestine, heart, and brain, and the expressions of $A\beta_{1-42}$ and Tau proteins in brain tissues by immunohistochemistry. The graph Control, control group; Model, model group; OMO-50 mg, low-dose group that received D-galactose (100 mg/kg/d) i.p. and gavage at a dosage of 50 mg/[kg·d] in OMO; OMO-100 mg, high-dose group that received D-galactose (100 mg/kg/d) i.p. and gavage at a dosage of 100 mg/[kg·d] in OMO. Values are represented as mean ± SD ($n = 6$) and expressed as the percentage of the control group, $^{\#}p < 0.01$ vs. control group, $^{*}p < 0.05$ vs. model group, $^{**}p < 0.01$ vs. model group.

expected using PCA (**Figure 4B**), which indicated that the Aβ not only influences the brain but also changes the gut microbiota. After treatment with 50 mg/(kg·d) or 100 mg/(kg·d) OMO, the diversity of the microbial communities was improved similarly as that of the normal (**Figure 4C**).

Analysis revealed the difference of taxonomic abundance between different groups (**Figure 4E**). Some bacteria in the fecal samples changed considerably at the phylum level: for instance, *Verrucomicrotia*, *Proteobacteria*, *Firmicutes*, and *Bacteroidetes*. Moreover, at the genus level, the $A\beta_{1-42}$-induced rats exhibited the enrichment of potentially proinflammatory microbes, such as *Corynebacterium, Staphylococcus, Ruminococcus, Roseburia, Dorea,* and *Sutterella*, and the reduction of potentially anti-inflammatory microbes, such as *Bacteroides, Bifidobacterium, Prevotella, Parabacteroides, Coprococcus, Desulfovibrio,* and *Lactobacillus*, in comparison with the normal group (**Figure 4F**). However, the treatment with the OMO exhibited a reduction in proinflammatory microbes and enrichment of anti-inflammatory microbes. Thus, our results indicated that the OMO administration had the potential to regulate the structure of the gut microbiota.

We also constructed and visualized a taxonomic tree of the predominant taxa (**Figure 4G**), which showed that *Firmicutes*, *Bacteroidetes*, *Clostridia*, *Bacteroidia*, *Bacilli*, *Clostridiales*, *Lactobacillales*, *Bacteroidales*, *Lactobacillaceae*, and *Lactobacillus* were the predominant taxa. The altered details of the predominant taxa (**Figure 4H**) showed that the abundance of *Clostridia* and *Clostridiales* in $A\beta_{1-42}$-induced groups was increased sharply, while the aforementioned taxa as *Firmicutes*, *Bacteroidetes*, *Bacteroidia*, *Bacilli*, *Lactobacillales*, *Bacteroidales*, *Lactobacillaceae*, and *Lactobacillus* were reduced ($p < 0.05$ vs. normal group). On the other hand, the OMO-treated groups can reverse those changes, especially the probiotic *Lactobacillus* increased obviously, which indicated that OMO administration might have a prebiotic role in intestinal dysbacteriosis in AD animals as induced by $A\beta_{1-42}$.

Prebiotic Effect of OMO on TNBS-Induced Mice

The Tissue Damages and Inflammation Induced by TNBS Combined Antibiotics Were Relieved

In order to ensure the prebiotic role of OMO, we established an IBD mice model after a broad spectrum antibiotics treatment. Compared to the control group, post treatment with TNBS by enema, a majority of the mice presented diarrhea and the weight gain declined relatively (**Figure 5A**). All the cytokines' levels were deviated from the normal, as some anti-inflammatory cytokines of GM-CSF, TNF-γ, 1L-10, IL-12, 1L-17α, 1L-4, TNF-α, and VGEF were secreted differently ($p < 0.05$ or $p < 0.01$; **Figure 5C**). Simultaneously, we found that the content of lipopolysaccharide (LPS) (**Figure 5B**) was higher than that in the control group; the colon tissues (**Figure 5D**) and splenic tissues (**Figure 5E**) were severely damaged. Also, immunohistochemistry staining showed that the expressions of Foxp3 (**Figure 6A**), IL-17 (**Figure 6B**), NF-κB (**Figure 6C**), and TNF-α (**Figure 6D**) deviated from the control, especially the additional broad spectrum and overdose antibiotics groups. After treatment with OMO, all the deviated parameters returned to the baselines, especially the OMO + *Bifidobacterium*-treated group (**Figures 5**, **6**). Cumulatively, our results suggested that OMO and *Bifidobacterium* exert anti-inflammatory effects in IBD, synergistically; however, the underlying mechanism needs further studies.

Promotion of the Engraftment Ability of *Bifidobacterium*

To clarify the synergistical action between OMO and *Bifidobacterium*, OTU abundance and taxonomic profiles were analyzed as shown in **Figure 7**. Compared to the normal group, the diversity of the microbial community in TNBS and TNBS and antibiotics-induced groups was reduced (**Figure 7A**). OMO can ameliorate this dysbacteriosis; the bacterial compositions at the phylum (**Figure 7C**) and family level (**Figure 7D**) encompassed *Verrucomicrotia*, *Proteobacteria*, *Firmicutes*, *Bacteroidetes*, *Lactobacillaceae*, and *Lachnospiraceae*. Our results showed that the relative abundance of *Bifidobacterium* was increased remarkably ($p < 0.05$, **Figure 5**), and the other probiotics *Lactobacillaceae* were also abundant in the microbial community with stable structures. We also constructed and visualized a taxonomic tree of the predominant taxa (**Figure 7B**), which showed that the *Firmicutes*, *Bacteroidetes*, *Clostridia*, *Bacteroidia*, *Bacilli*, *Clostridiales*, *Lactobacillales*, *Bacteroidales*, *Lactobacillaceae,* and *Lactobacillus* were the predominant taxa.

Influence of Aβ Levels on Microbiota-Gut-Brain Axis

In order to explore whether Aβ can influence the gut microbiota by targeting the microbiota-gut-brain axis, we injected 10 and 20 μg $A\beta_{1-42}$ into the CA1 region, respectively. Then, the fecal samples were collected once a week and the last 4 weeks, followed by microbiome analysis using the 16S rRNA genes. We also monitored the transcriptome of the small intestine and brain tissues at the 5th week after injection of $A\beta_{1-42}$.

Dynamic Variations of Gut Microbiota and KEGG Pathway Analysis in the $A\beta_{1-42}$-Induced Deficient Rats

The dynamic variations of gut microbiota showed that the diversity in the $A\beta_{1-42}$-induced microbial community (injected 10 or 20 μg fibrillar state of $A\beta_{1-42}$ into the CA1 region) group was reduced in the 4th week (L3, H3) than that in the 2nd and 3rd week (L1, L2 and H1, H2), as shown in **Figures 8B,C**, thereby indicating that such a diversity was reduced with the progression of the disease. **Figures 8D–F** showed that the diversity of the microbial community changed with the levels of $A\beta_{1-42}$, which revealed that the levels of $A\beta_{1-42}$ in the brain influenced the composition of the gut microbiota significantly. We also constructed and visualized a taxonomic tree of the predominant taxa (**Figure 8G**), which displayed that the *Firmicutes*, *Bacteroidetes*, *Clostridia*, *Bacteroidia*, *Bacilli*, *Clostridiales*, *Lactobacillales*, *Bacteroidales*, *Lactobacillaceae*, and *Lactobacillus* were the predominant taxa. The changes in the details of predominant taxa (**Figure 8H**), along with the

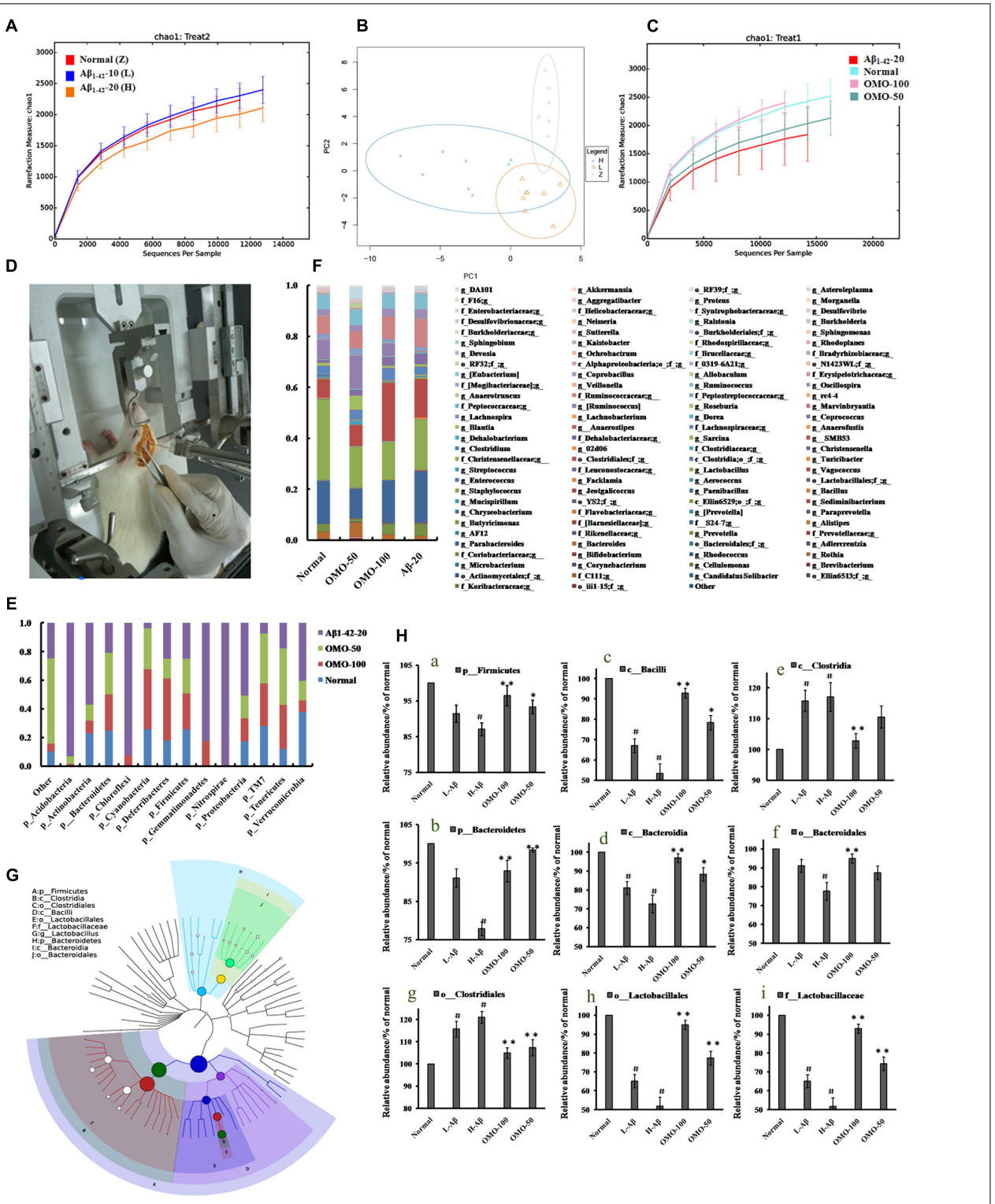


FIGURE 4 | Effects of OMO on gut microbiota in $A\beta_{1-42}$-induced deficient rats. **(A)** Rarefaction curve and **(B)** PCA results of different concentrations of $A\beta_{1-42}$-induced groups, H (20 μg of $A\beta_{1-42}$), L (20 μg of $A\beta_{1-42}$), Z (normal rats with vehicle). **(C)** Rarefaction curve. **(D)** Operation schematic diagram. **(E)** Classification and abundance of cecal contents at the phylum level. **(F)** Classification and abundance of cecal contents at the genus level. **(G)** The dominant species classification tree. **(H)** The relative abundance of the dominant microorganism. Values are the means of six independent experiments.

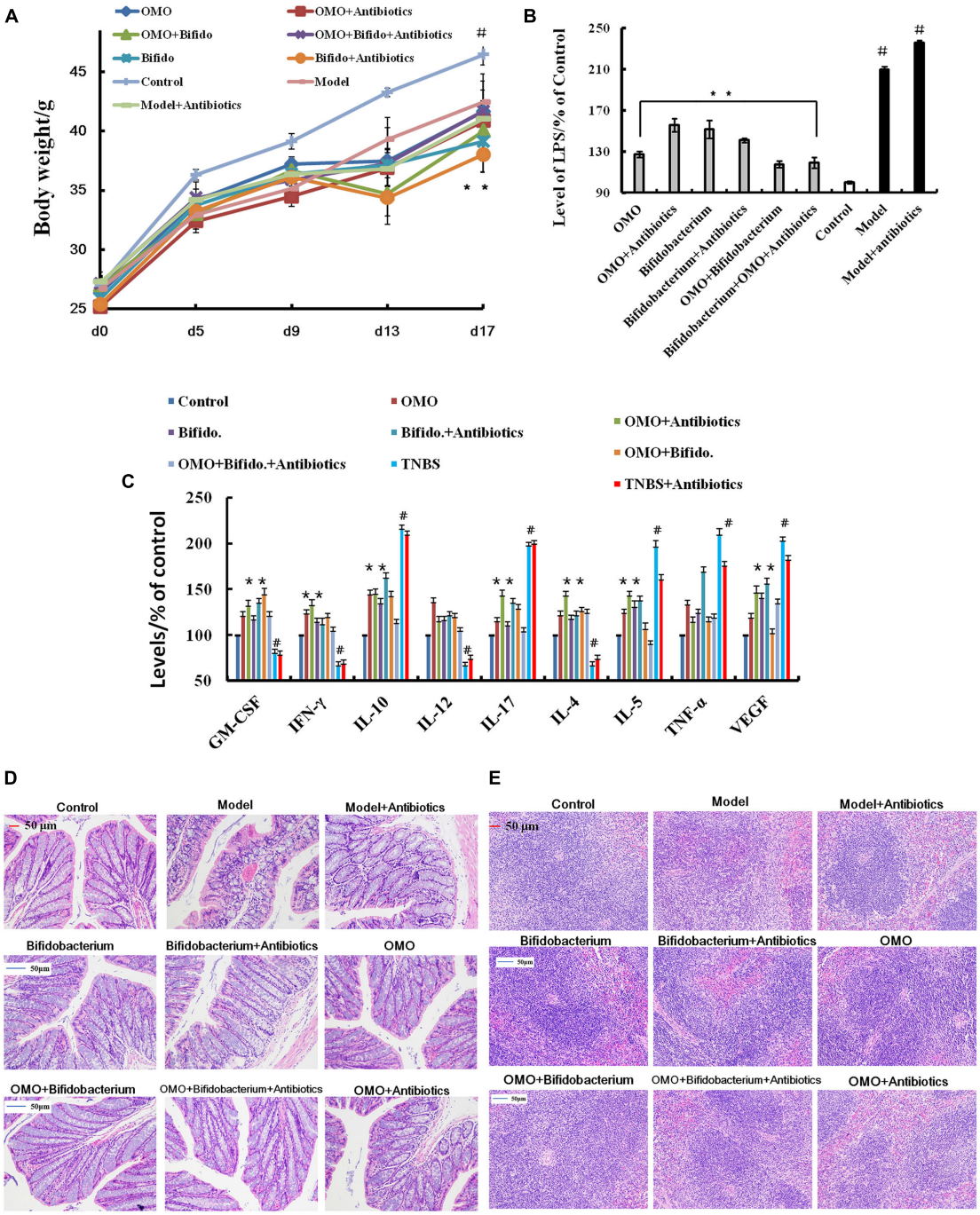


FIGURE 5 | OMO improves the pathological parameters of the high-dose broad spectrum antibiotics and TNBS-induced inflammatory bowel disease (IBD) mice. **(A)** Body weight changes. **(B)** Levels of LPS in serum. **(C)** The levels of cytokines (GM-CSF, TNF-γ, 1L-10, IL-12, 1L-17α, 1L-4, TNF-α, and VGEF-α) in serum. **(D)** The histopathological changes in colon. **(E)** The histopathological changes in spleen. Control is the normal group; model is the TNBS-induced group; model and high-dose antibiotics, HEP3 (100 mg/kg/d), *Bifidobacterium*, HEP3 and high-dose antibiotics, HEP3 and *Bifidobacterium*, *Bifidobacterium* and high-dose antibiotics, HEP3, *Bifidobacterium*, and high-dose antibiotics.

abundance of *Lactobacillaceae*, were negatively correlated with the dose of $A\beta_{1-42}$.

The KEGG pathway analysis showed that the metabolism of xenobiotics biodegradation, nucleotide metabolism, metabolism of terpenoids and polyketides, metabolism of other amino acids, metabolism of cofactors and vitamins, lipid metabolism, glycan biosynthesis and metabolism, enzyme families, energy metabolism, carbohydrate metabolism, biosynthesis of other

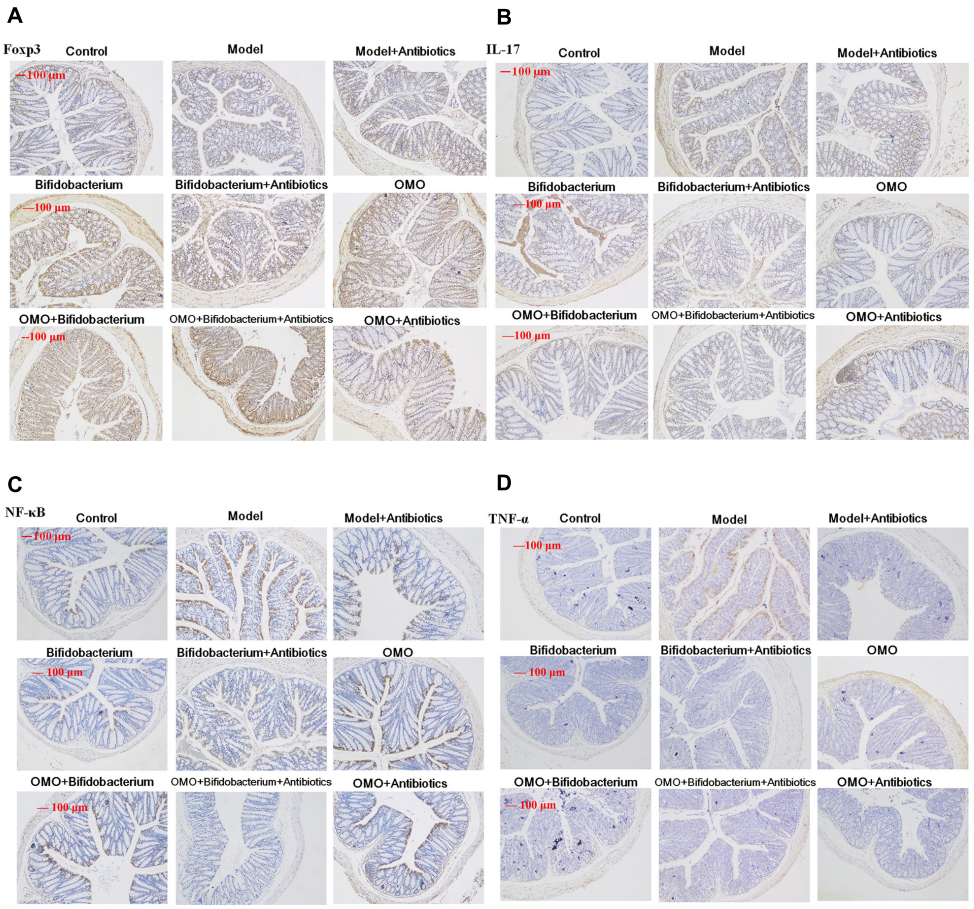


FIGURE 6 | Immunohistochemistry staining of Foxp3 **(A)**, IL-17 **(B)**, NF-κB p65 **(C)**, and TNF-α **(D)** in the colons of different experimental groups in high-dose broad spectrum antibiotics and TNBS-induced IBD mice after treatment with OMO.

secondary metabolites, and amino acid metabolism were altered according to the gut microbiota in the two AD-like rodent models. Additionally, many of these metabolisms were improved by the administration of OMO (**Figure 9A**) showed the dynamic variations in the 2nd, 3rd, and 4th week after injection of $A\beta_{1-42}$. **Figure 9B** represents the 5th week after injection of $A\beta_{1-42}$, all of which showed that the metabolism of gut microbiota was influenced by the levels of $A\beta_{1-42}$ in hippocampus.

Transcriptome Analysis in Small Intestine and Brain in Deficient Rats Post $A\beta_{1-42}$ Injection

Small intestine transcriptome analysis

After injection of $A\beta_{1-42}$ for 4 weeks, the rats were sacrificed, and the intestinal tissues were dissected and frozen in liquid nitrogen for RNA extraction and high-throughput RNA-sequencing. To obtain an overview of the gene expression profile of the intestine in AD model rats, three cDNA samples were generated from each group, mixed, and subjected to sequencing by the Illumina NextSeq 500 platform. Approximately 45,323,472, 55,358,634, and 45,134,740 raw reads with a length of 2 × 150 bp were generated for the $A\beta_{1-42}$-20, $A\beta_{1-42}$-10, and control group samples, respectively. After stringent quality assessment and data filtering, 44,973,944, 54,933,060, and 44,770,698 clean paired-end sequence reads with a Q20 percentage (those with a base quality >20) over 99% were obtained from the differently treated samples, respectively. Of all the reads, approximately 86.0% were mapped to the rat genome. Based on the normalized data, the expression of 21933 genes was detected (**Figure 10A**), and the relative expressions of DEGs in all the three treated groups ($A\beta_{1-42}$-10, $A\beta_{1-42}$-20, and control) were shown in **Table 1**.

The general chi-squared test was used for the selection of significant DEGs. Based on the criteria of twofold or greater change and Q of $p < 0.05$, 349 unigenes were identified as significant DEGs between $A\beta_{1-42}$-10 and control group samples and 420 unigenes between $A\beta_{1-42}$-20 and control group samples (**Figure 10B**). To elucidate the DEGs in different contents of $A\beta_{1-42}$-induced groups, we used the gene expression profiling. As illustrated in the Venn diagram (**Figure 10C**), the number of genes, as well as the relationships among the overlap between the different groups, were shown in **Figures 10B,D**, indicating that $A\beta_{1-42}$ level in the brain can influence the transcriptome of the intestine.

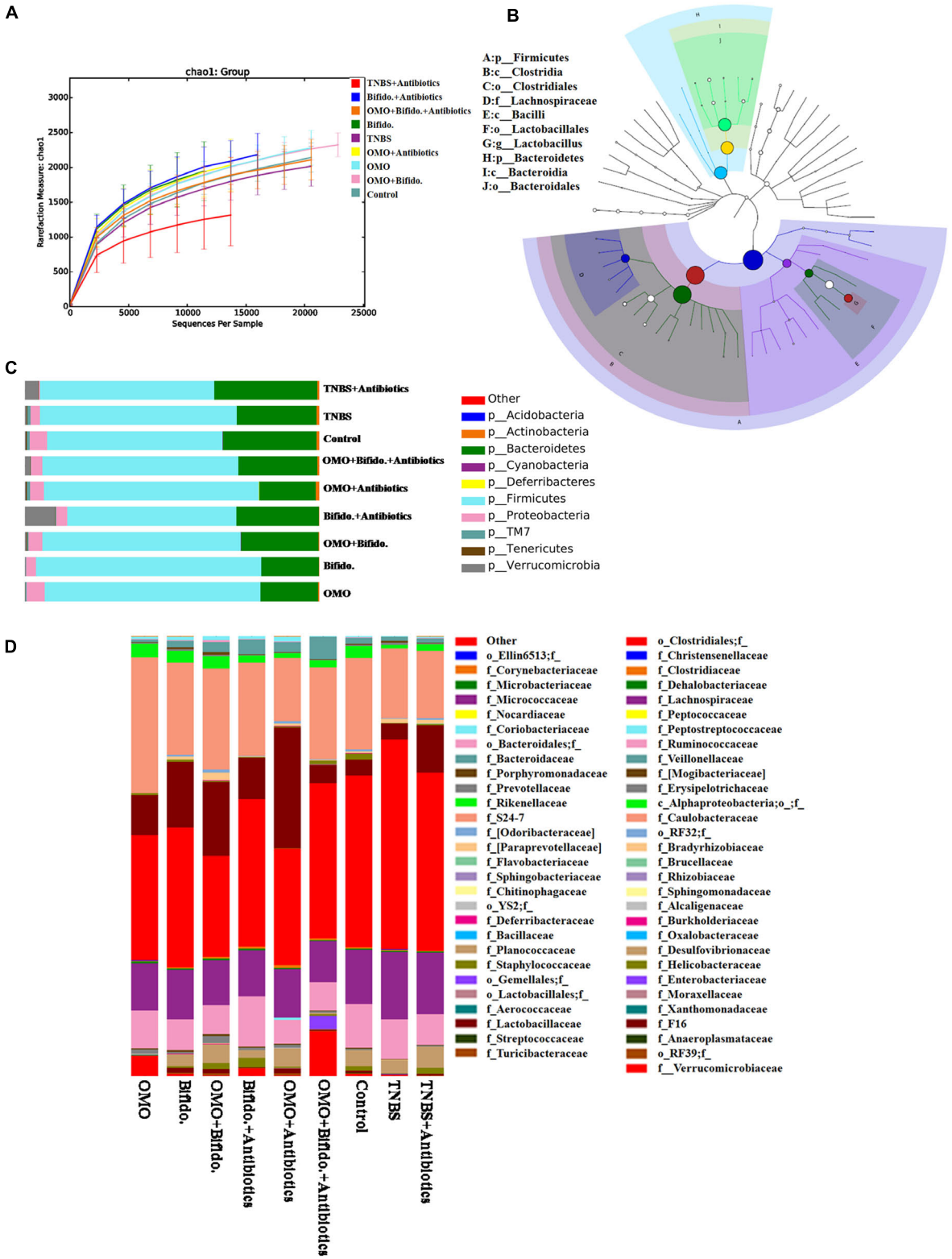


FIGURE 7 | Effects of OMO on the microbiota of cecal contents in high-dose broad spectrum antibiotics and TNBS-induced IBD mice. **(A)** The graph represents the rarefaction curve. **(B)** The dominant species classification tree. **(C)** The classification and abundance of cecal contents at the phylum level. **(D)** The classification and abundance of cecal contents at the family level. Values are the means of six independent experiments.

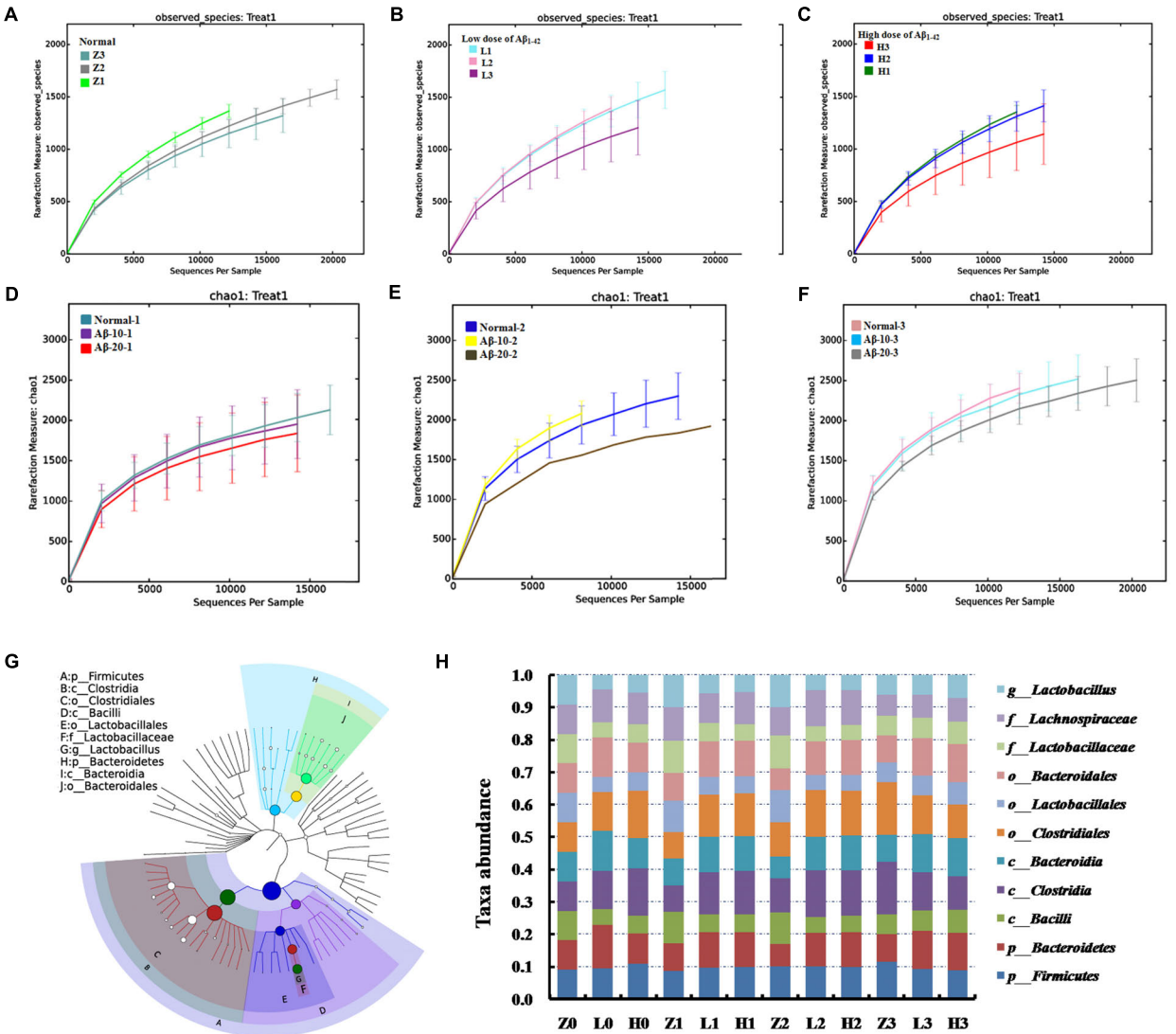


FIGURE 8 | Effects of $A\beta_{1-42}$ on gut microbiota in rats. **(A–F)** The rarefaction curve of different concentrations and durations in $A\beta_{1-42}$-induced groups, H (20 μg of $A\beta_{1-42}$), L (20 μg of $A\beta_{1-42}$), Z (normal rats with vehicle); H1, H2, and H3 (or L1, L2, L3) is the treatment time after injection of $A\beta_{1-42}$ at 2nd, 3rd, and 4th weeks; **(G)** is the dominant species classification tree; **(H)** is the relative abundance of the dominant microorganism. Values represent the means of six independent experiments.

To gain insights into the physiological processes regulated by the different $A\beta_{1-42}$ levels and identify the processes enriched in significant DEGs, we subjected significant DEGs to GO term enrichment analysis and KEGG pathway enrichment, a tool developed to represent the common and basic biological information in the annotation. The GO term enrichment results showed that the immune system, extracellular environment, and antigen reaction (Supplementary Tables S1-1–S1-3) altered in different $A\beta_{1-42}$ levels treated groups, which indicated that the inflammatory response of the gut is activated, the variations in the gut microbiota induced by $A\beta_{1-42}$ primarily influences the immune or inflammatory response in the gut.

The KEGG pathway results showed that the DEGs were mainly enriched in phagosome, antigen processing, and presentation, cell adhesion molecules (CAMs), PI3K-Akt signaling pathway, cytokine-cytokine receptor interaction, PPAR signaling pathway, ECM-receptor interaction, B cell receptor signaling pathway, and chemokine signaling pathway (**Figure 11**, and more details were showed in Supplementary Tables S2-1–S2-3), thereby indicating that $A\beta_{1-42}$ levels in the brain can influence the intestinal functions.

Brain transcriptome analysis

After injection of $A\beta_{1-42}$ for 4 weeks, the rats were sacrificed, and the brain tissues dissected and frozen in liquid nitrogen for RNA extraction and high-throughput RNA-sequencing. The overview of the brain gene expression profile in AD model rats was shown in **Figure 12**. The profiling analysis revealed the number

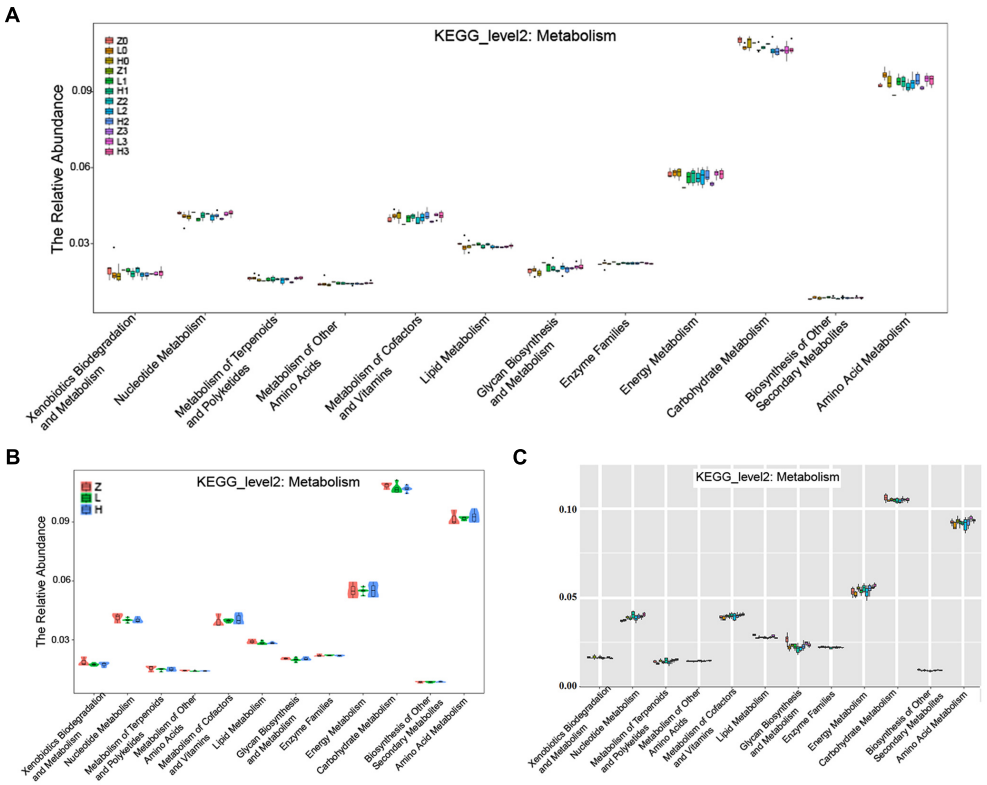


FIGURE 9 | The KEGG pathway enrichment of gut microbiota in the metabolism system. **(A)** The dynamic variations in the 2nd, 3rd, and 4th week after injection of $A\beta_{1-42}$ in rats. **(B)** The 4th week after injection of $A\beta_{1-42}$ in rats. **(C)** The high dose broad spectrum antibiotics and TNBS-induced IBD mice.

of genes (**Figures 12A-a,b**), the DEGs in **Figure 12B**, Venn diagram (**Figure 12C**), as well as, the relationships among the overlap between the different groups in **Figure 12D**; the relative expressions of DEGs in all the three treated groups ($A\beta_{1-42}$-10, $A\beta_{1-42}$-20, and control) were shown in **Table 2**, which indicated that the $A\beta_{1-42}$ levels could significantly influence the brain transcriptome.

The GO term enrichment results revealed that the single-multicellular organism process (GO:0044707), nervous system development (GO:0007399), system development (GO:0048731), single-organism developmental process (GO:0044767), multicellular organism development (GO:0007275), developmental process (GO:0032502), generation of neurons (GO:0048699), neurogenesis (GO:0022008), neuron differentiation (GO:0030182), and cell differentiation (GO:0030154) (Supplementary Tables S3-1–S3-3) were influenced after treatment with $A\beta_{1-42}$. In the $A\beta_{1-42}$-20 group, the synapse (GO:0045202), synaptic signaling (GO:0099536), synaptic transmission (GO:0007268), trans-synaptic signaling (GO:0099537), synapse part (GO:0044456), central nervous system development (GO:0007417), and behavior (GO:0007610) were changed more than that in the $A\beta_{1-42}$-10 group, which indicated that the occurrence of AD is dependent on the cumulative amount of $A\beta_{1-42}$. The KEGG pathway results showed that the DEGs were enriched mainly in neuroactive ligand-receptor interaction, cAMP signaling pathway, calcium signaling pathway, serotonergic synapse, PI3K-Akt signaling pathway, dopaminergic synapse, and ECM-receptor interaction (**Figure 13**, additional details were shown in Supplementary Tables S4-1–S4-3), all which indicated that the $A\beta_{1-42}$ levels can significantly influence the brain function.

DISCUSSION

Increasing evidence suggests that the microbiota-gut-brain axis plays a key role in regulating brain functions, and prebiotics are widely considered to have potential as modulators of brain dysfunctions; however, only limited studies are yet available. Herein, we reported that fructooligosaccharides from *M. officinalis* could markedly modify the behavior, improve oxidative stress and inflammation disorder, regulate the synthesis and secretion of neurotransmitter, ameliorate the swelling of brain tissues, and reduce neuronal apoptosis. We also reported that OMO administration alters the diversity and stability of the microbial community, the expression of the genes of AD intracellular markers such as Tau and $A\beta_{1-42}$. In addition, OMO administration exerted an adequate prebiotic role in regulating the composition and metabolism of gut microbiota in an overdose antibiotics-treated IBD mice model.

Gut microbiota plays a major role in maintaining normal physiological functions in the host. The changes in gut

A

A. Statistics of $A\beta_{1-42}$-induced deficits rat intestine transcriptome sequences

Sample	Useful Reads	Map events count	Total Mapped		Multiple Mapped		Uniquely Mapped	
			Reads	%	Reads	%	Reads	%
$A\beta_{1-42}$-20	54,933,060	55,788,025	47,162,606	85.85	3,019,287	6.40	44,143,319	93.60
$A\beta_{1-42}$-10	44,973,944	42,538,143	38,913,479	86.52	1,862,179	4.79	37,051,300	95.21
Control	44,770,698	43,515,860	38,469,828	85.93	2,078,474	5.40	36,391,354	94.60

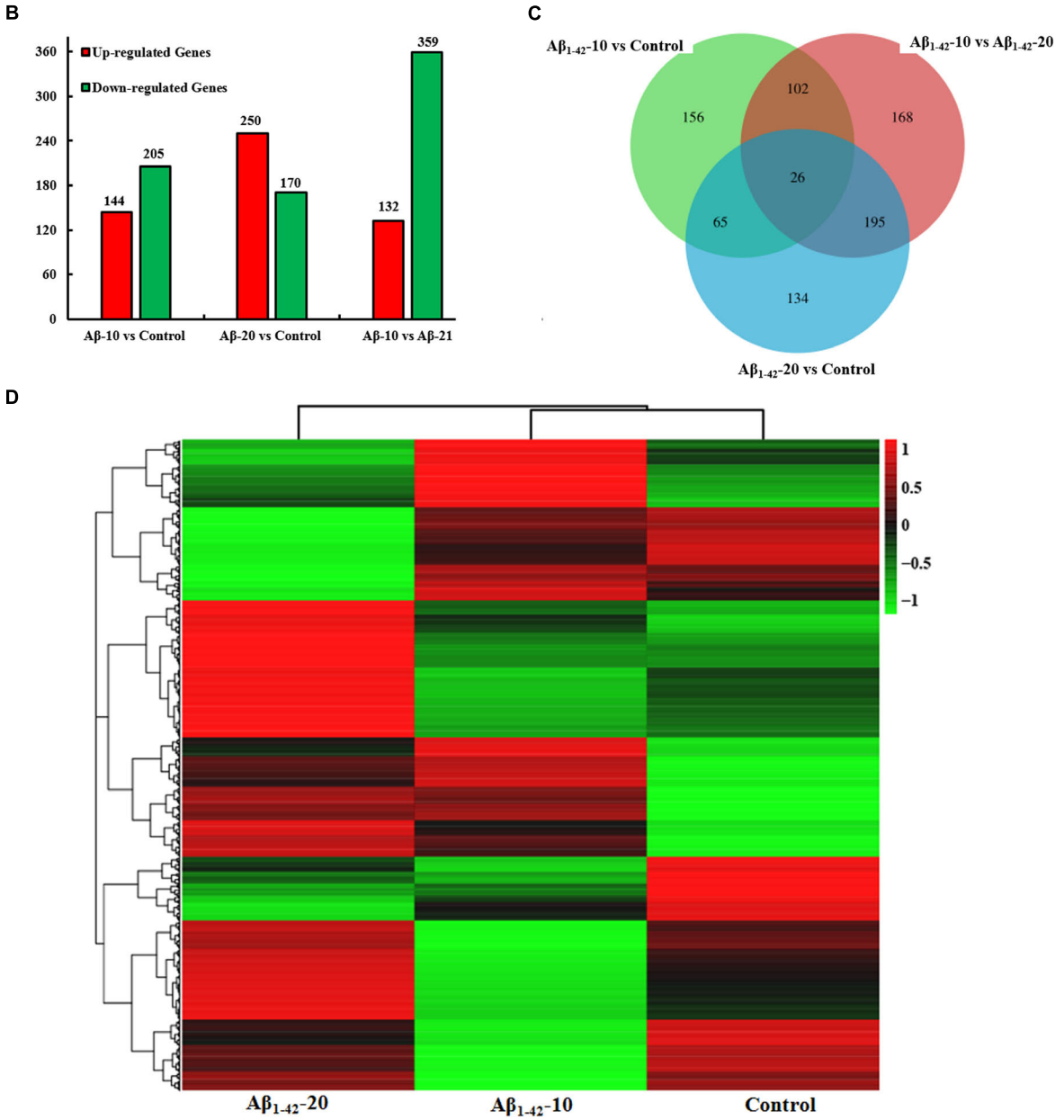


FIGURE 10 | Small intestine transcriptome analysis in the deficit rats by injected $A\beta_{1-42}$. **(A)** The statistics of transcriptome sequences. **(B)** DEGs in the small intestine at different concentrations of $A\beta_{1-42}$. **(C)** Venn diagram of DEGs. **(D)** The heat map of the relative expressions of DEGs in all three groups.

TABLE 1 | Differentially expressed genes (DEGs) in the small intestine of deficient rat injected at different concentration of $A\beta_{1-42}$.

Genes	FoldChange		log2FoldChange		Up–down	*p*-value	
	Normal/Aβ-10	Normal/Aβ-20	Normal/Aβ-10	Normal/Aβ-20		Normal/Aβ-10	Normal/Aβ-20
Slc5a4b	0.09	0.27	−3.47	−1.86	Down	0.000000	0.000494
Nts	0.41	4.57	−1.27	2.19	Down	0.002207	0.000056
Fkbp5	0.27	2.81	−1.90	1.49	Down	0.000004	0.000132
Cubn	0.40	2.81	−1.33	1.49	Down	0.000323	0.000132
Defa8	0.03	0.08	−5.11	−3.66	Down	0.000000	0.000000
AABR07000398.1	0.45	3.21	−1.17	1.68	Down	0.000995	0.000002
LOC257642	0.45	4.12	−1.15	2.04	Down	0.032226	0.012780
Hpse	5.37	0.39	2.43	−1.36	Up	0.000050	0.002196
Nop10	2.12	10.70	1.09	3.42	Down	0.032836	0.000000
Arhgdib	2.22	0.49	1.15	−1.03	Up	0.006915	0.007868
AABR07065789.1	2.13	7.85	1.09	2.97	Down	0.026618	0.000001
Reg3g	2.72	0.35	1.44	−1.52	Up	0.000232	0.000032
Rps24	4.88	66.16	2.29	6.05	Down	0.000000	0.000000
Pou2af1	2.14	0.36	1.10	−1.47	Up	0.048293	0.001217
Adh6	2.32	0.14	1.21	−2.88	Up	0.004548	0.000000
RGD1311933	2.24	5.12	1.16	2.36	Down	0.006467	0.000000
Rps27	2.08	19.07	1.05	4.25	Down	0.003563	0.000000
Wfdc21	2.46	0.45	1.30	−1.15	Up	0.002445	0.002823
Rps27a-ps1	3.22	6.84	1.69	2.77	Down	0.000020	0.000000
Ccl21	3.20	0.30	1.68	−1.73	Up	0.001820	0.000047
Pdx1	3.20	0.49	1.68	−1.03	Up	0.007298	0.037669
AABR07051670.1	7.56	0.36	2.92	−1.49	Up	0.000008	0.000992
Igkv5-48	30.08	0.32	4.91	−1.65	Up	0.000000	0.000302
AABR07051684.1	23.10	0.27	4.53	−1.91	Up	0.001867	0.003488
AABR07065768.3	23.64	0.11	4.56	−3.25	Up	0.032367	0.000002
Akp3	13.94	0.13	3.80	−2.93	Up	0.000000	0.000000

microbiota can lead to changes in brain function, thereby affecting the host behavior (Vuong et al., 2017). Recent studies showed a significant correlation between the changes in gut microbiota and cognitive behavior (Dinan and Cryan, 2017). The modulation of gut microbiota by germ-free animals, probiotics or antibiotics intervention, and fecal microbiota transplantation (FMT) can influence the cognitive behavior of the host (Hu et al., 2016). Our data were in agreement with previous studies, showing that the gut microbiota in two AD-like model rats was altered as compared to the normal rats, as the abundance of *Clostridia* and *Clostridiales* in $A\beta_{1-42}$-induced groups increased significantly ($p < 0.05$), while the groups administered OMO can reverse those changes, especially the probiotic *Lactobacillus* and *Akkermansia* increased distinctly ($p < 0.05$).

The probiotic administration had a marked effect on the cognitive behavior. The prototype probiotic bacterium has been found to up-regulate the hormone oxytocin and systemic immune responses in order to achieve a broad range of health benefits involving wound healing, mental health, metabolism, and myoskeletal maintenance (Servin, 2004; Erdman and Poutahidis, 2016). Studies showed that *Lactobacillus pentosus* var. plantarum C29 from kimchi, a traditional food manufactured by fermenting vegetables (Park et al., 2014), was beneficial to health. It can also protect the memory deficits by inducing the expressions of BDNF and p-CREB in scopolamine-induced memory-deficient mice (Jung et al., 2012), anti-inflammatory amelioration of age-dependent memory impairment in Fischer 344 rats (Jeong et al., 2015), and ameliorate memory impairment and inflammation in D-galactose-induced accelerated aging mouse (Woo et al., 2014). Another study also showed that *L. plantarum* could attenuate anxiety-related behavior and protect against stress-induced dysbiosis in adult zebrafish (Davis et al., 2016). *Lactobacilli* and *Bifidobacteria* exhibited antagonistic activities against microbial pathogens (Servin, 2004). Our data were in agreement with previous studies showing that *Lactobacillus* can ameliorate memory deficiencies (**Figure 4H**); the relative abundance of $A\beta_{1-42}$-induced *Lactobacillus* was reduced starkly, especially in the high-dose group. As a result of OMO administration, the relative abundance of *Lactobacillus* was increased significantly; also, the MWM tests showed that the learning and memory abilities were improved (**Figure 3B**). These results suggested that OMO can promote the abundance of *Lactobacillus* and ameliorate the memory deficiencies.

Fructo-oligosaccharides (FOS) are commonly regarded as a type of prebiotics, favorably stimulating the growth of *Bifidobacteria* and *Lactobacilli*. FOS from *Stevia rebaudiana* roots

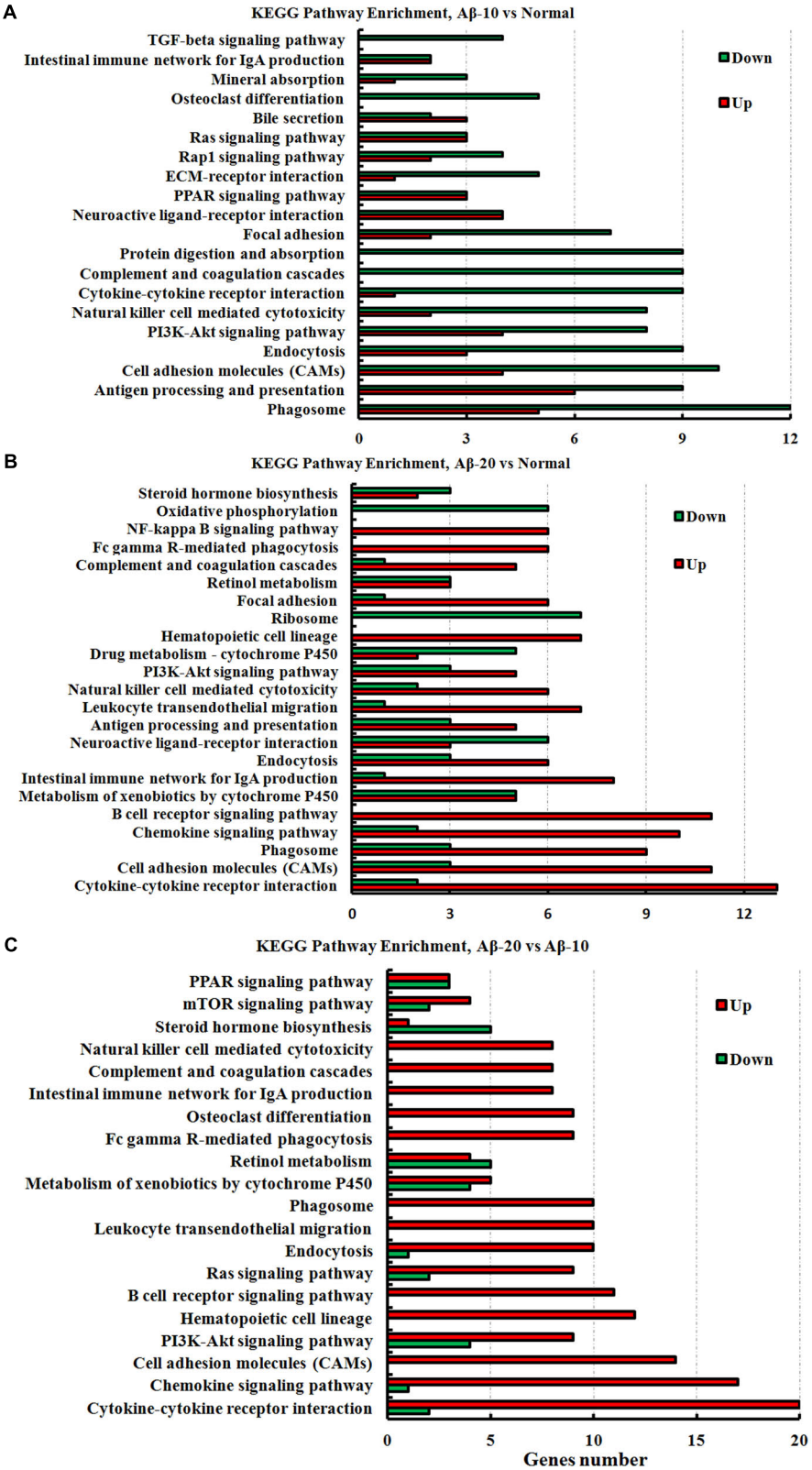


FIGURE 11 | The KEGG pathway enrichment of DEGs in the small intestine transcriptome in deficient rats induced by $A\beta_{1-42}$. **(A)** The group of Aβ-10 vs. the Normal; **(B)** the group of Aβ-20 vs. the Normal; **(C)** the group of Aβ-20 vs. the Aβ-10.

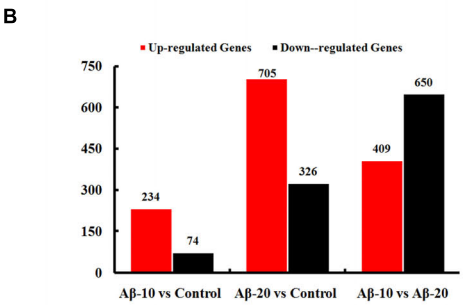
A

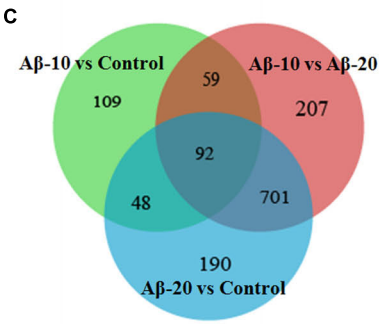
A-a. Statistics of $A\beta_{1-42}$-induced deficits rat brain RNA sequences mapped

Sample	Useful reads	Map event	Map reads	Map reads/%	Multiple reads	Multiple reads/%	Unique reads	Unique reads/%
$A\beta_{1-42}$-10	142490562	411476820	129291217	90.74	60113374	46.49	69177843	53.51
$A\beta_{1-42}$-20	143270656	444440717	131174213	91.56	63112535	48.11	68061678	51.89
Control	144332070	413610803	131924767	91.40	61196946	46.39	70727821	53.61

A-b. Statistics of $A\beta_{1-42}$-induced deficits rat brain RNA sequences mapped events

Sample	Map events count	Mapped to gene	Mapped to gene/%	Mapped to inter gene	Mapped to inter gene/%	Mapped to exon	Mapped to exon/%
$A\beta_{1-42}$-10	411476820	397038221	96.49	14438599	3.51	387464643	94.16
$A\beta_{1-42}$-20	444440717	431078830	96.99	13361887	3.01	418683541	94.20
Control	413610803	398932568	96.45	14678235	3.55	388408941	93.91





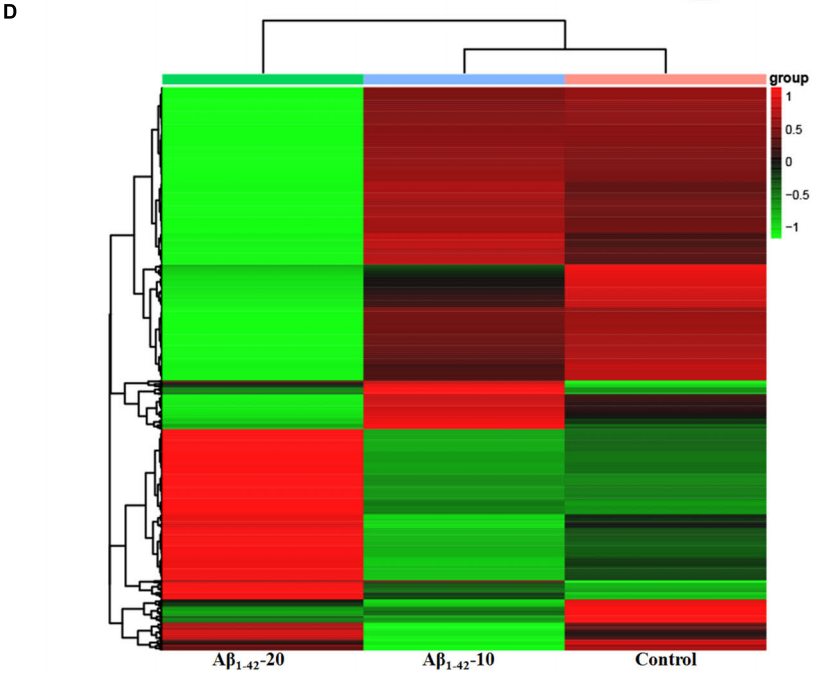


FIGURE 12 | Brain transcriptome analysis in the deficit rats by injected $A\beta_{1-42}$. **(A)** Statistics of the transcriptome sequences. **(B)** The differentially expressed genes in the brain at different concentration of $A\beta_{1-42}$. **(C)** Venn diagram of DEGs. **(D)** The heat map of the relative expressions of DEGs in all the three groups.

enhanced the growth of specific strains of both *Bifidobacteria* and *Lactobacilli*, especially, with respect to their fermentation ability (Sanches Lopes et al., 2016). FOS are reserve carbohydrates with important positive health effects and technological applications in the food industry. Another previous study indicated that short-chain fructooligosaccharides could be used optimally in combination with *Bifidobacterium animalis* or *B. longum* strains for the development of synbiotic foods or dietary supplements (Valdés-Varela et al., 2017). Our results showed that FOS from *M. officinalis* also enhances the growth

TABLE 2 | Differentially expressed genes in the brain of the deficient rats injected at different concentrations of $A\beta_{1-42}$.

Genes	Aβ-10		Aβ-20	
	Foldchange (Normal/Aβ-10)	*p*-value	Foldchange (Normal/Aβ-20)	*p*-value
Cbln1	10.94	0.000000	0.13	0.000105
Grm4	2.39	0.000030	0.21	0.002146
Pcp2	60.50	0.000000	0.09	0.000007
Uncx	36.00	0.000034	0.09	0.000041
Adora2a	2.31	0.000004	15.53	0.000001
Wdr66	3.13	0.000018	0.19	0.001367
Lhx5	Infinity	0.000034	0.20	0.007717
Barhl2	3.13	0.036893	0.09	0.000025
Lhx1	30.79	0.000182	0.10	0.000055
Slc6a4	10.61	0.004566	0.23	0.015495
Gabra6	107.05	0.000000	0.06	0.000000
Rgs9	2.88	0.000000	10.66	0.000012
Tph2	4.79	0.007662	0.21	0.006924
Arhgap6	2.00	0.001638	8.30	0.000186
Btg1	2.16	0.000475	0.34	0.034729
Rxrg	2.33	0.000179	15.69	0.000004
Neurod1	3.51	0.000000	0.11	0.000025
Car8	3.90	0.000000	0.12	0.000060
St14	2.78	0.017265	0.13	0.000206
Trim54	0.36	0.000003	11.11	0.000192
Grid2	2.34	0.000518	0.21	0.002420
Slc30a3	0.46	0.000006	5.77	0.000880
En2	191.37	0.000000	0.10	0.000026
Arhgef33	9.12	0.000000	0.11	0.000050
Tac1	4.23	0.000000	31.52	0.000000
Slc1a6	2.00	0.016579	0.11	0.000032
Crtam	2.24	0.000013	0.28	0.010983
Crtam	Infinity	0.000115	0.08	0.000020
Drd2	2.73	0.000002	10.76	0.000026
Cga	22.26	0.002718	0.08	0.000031
Kcnh5	0.37	0.000000	4.25	0.007422
Nyx	3.68	0.036361	0.13	0.000541
Fibcd1	2.76	0.000000	24.48	0.000000
Satb2	0.47	0.000200	43.65	0.000000
Hes3	7.22	0.008186	0.07	0.000006
Irx3	15.47	0.004015	0.14	0.001121
Adamts18	3.02	0.045565	0.11	0.000091
Il16	3.40	0.000000	0.10	0.000019
Tfap2b	3.39	0.022277	0.19	0.003907
Ppp1r17	17.05	0.000000	0.12	0.000083
Impg1	Infinity	0.009945	0.08	0.000060
Fat2	33.50	0.000000	0.10	0.000009
Irx2	9.63	0.003845	0.11	0.000157
Rgl3	3.76	0.000002	0.11	0.000045
Barhl1	21.79	0.003154	0.20	0.011641
Cdhr1	2.16	0.001501	18.13	0.000003
Glra1	3.33	0.005627	0.22	0.005136
Cbln2	0.43	0.000035	0.21	0.042611
Pax3	Infinity	0.035388	6.15	0.008361
Kcns1	0.12	0.000000	0.10	0.000187
Skor1	35.05	0.005526	0.16	0.000376
Zic1	3.08	0.000000	0.35	0.049800
Zic4	2.01	0.047534	14.65	0.000001
Cpne7	2.09	0.000020	77.78	0.000000
Emx1	0.46	0.001804	0.35	0.038103
Kcng4	2.18	0.000235	0.30	0.023002
Zfp521	3.24	0.000000	0.20	0.001811
Calb2	3.89	0.000000	0.17	0.000482
LOC688778	0.46	0.000054	51.87	0.000000
Atp2a3	4.19	0.000000	0.13	0.000074
Ptpn22	Infinity	0.035388	0.07	0.000080
Gng7	2.88	0.000000	24.88	0.000000
Asic4	2.15	0.000048	11.89	0.000008
Npas4	2.04	0.000529	13.37	0.000006
Cbln3	108.68	0.000000	0.08	0.000002
Adra1d	0.49	0.000370	4.54	0.006404
Ctxn3	3.24	0.006074	0.16	0.000811
Drd1	2.50	0.000005	35.19	0.000000
Syndig1l	3.07	0.000000	17.72	0.000001
Cdh15	2.20	0.000772	0.20	0.001638
Cnpy1	36.47	0.000030	0.11	0.000160
Robo3	0.22	0.000001	26.35	0.001324
Cyp11b2	0.23	0.000000	6.98	0.004899
Lrrc10b	2.40	0.000035	34.15	0.000000
Mab21l2	4.00	0.000280	0.17	0.000872
Slc6a5	4.53	0.003476	0.08	0.000009
Myom3	6.95	0.000135	0.33	0.049080
Svep1	2.27	0.000253	0.13	0.000107
Tll1	2.15	0.034882	0.20	0.003254
Irx1	5.63	0.001444	0.23	0.009492
Eomes	10.74	0.030867	0.07	0.000011
Tmem215	0.34	0.000002	10.90	0.000267
Spp1	3.32	0.000003	0.15	0.000348
Comp	6.67	0.000051	0.29	0.024367
Shisa8	3.49	0.000142	0.13	0.000128
Gpr6	2.45	0.000035	72.86	0.000000
Gdf10	4.42	0.001245	0.16	0.000964
Zic2	2.20	0.001201	0.21	0.002489
Dao	11.94	0.000011	0.12	0.000114
Lrp2	3.58	0.000003	0.28	0.013024
AABR07010944.1	Infinity	0.006930	0.12	0.001066
Sdc1	4.80	0.000003	0.11	0.000046

of some probiotics similar to that of *Bifidobacteria* and *Lactobacilli*.

The microbiota can modulate the changes in the gut barrier as well as metabolic and inflammatory responses. Gut barrier function is a key to maintaining a balanced response between the host and its microbiome. This highly complex system involves numerous microbiota-derived factors. *Akkermansia muciniphila*

is positively correlated with a lean phenotype, reduced body weight gain, amelioration of metabolic responses, and restoration of gut barrier function is effectuated by the modulation of mucus layer thickness (Bland, 2016; Derrien et al., 2016; Greer et al., 2016; Henning et al., 2017; Van Herreweghen et al., 2017). Our data in D-galactose-induced deficient rats showed that the *Akkermansia* were increased ($p < 0.05$, **Figure 2D**), and the intestinal pathological tissue changes (**Figure 1E**) were improved after administration of OMO, thereby indicating that OMO administration can improve the gut barrier function via targeting the abundance of *Akkermansia*, but need more studies.

Increased gut permeability (leaky gut) and alterations in gut microbiota are now widely accepted as an important link with the etiology, course, and treatment of several neuropsychiatric disorders (Anderson et al., 2016). Gut microbiota-released LPS contributes to chronic inflammation and oxidative stress (Le Sage et al., 2017). Moreover, inflammation was first implicated in AD pathology and development, with the neuropathological findings of activated inflammatory cells (microglia and astrocytes) and inflammatory proteins (for example, cytokines and complement), surrounding the amyloid plaques and the nerve fiber tangles (Alkasir et al., 2017). Our study showed that OMO administration could reduce the levels of LPS in TNBS-induced IBD mice and some pro-inflammatory cytokines in both $A\beta_{1-42}$ induced deficit rats (**Figure 3C**) and TNBS-induced IBD mice (**Figures 5C**, **6**). On the other hand, it can increase the levels of some anti-inflammatory cytokines, which suggested that the administration of OMO (prebiotics) can improve the host inflammatory immune response. The data also showed that OMO administration could enhance the oxidative stress, similar to elevated SOD, MDA, CAT, and inhibiting the MDA production in the D-galactose-induced deficit rats (**Figure 1D**). The gut microbiota is known to play a vital role in those responses (Vanegas et al., 2017), although not fully understood. Taken together, we can summarize that OMO administration influences the host inflammatory immune response and oxidative stress by regulating the gut microbiota.

Preliminary data suggested that FOS increases fecal *Bifidobacteria*, induce immunoregulatory dendritic cell (DC) responses, and reduce the disease activity in patients with Crohn's disease (Benjamin et al., 2011). Moreover, *Bifidobacteria* are predominant bacterial species in the human gut microbiota and have been considered to exert a beneficial effect on human health by maintaining the equilibrium of the resident organisms. *B. longum* with FOS reduces TNF-α, CRP, serum AST levels, HOMA-IR, serum endotoxin, steatosis, and the non-alcoholic steatohepatitis activity index significantly (Malaguarnera et al., 2012). Human milk contains *B. breve*, *Streptococcus thermophilus*, and short-chain galactooligosaccharides/long-chain fructooligosaccharides with pectin-derived acidic oligosaccharides conferring a protective role against gastrointestinal infections: ameliorating the AD symptoms, modulating the immune response, binding the viral particles, and protecting against rotavirus infection (Rigo-Adrover et al., 2017). The combination of fermented formula with short-chain galactooligosaccharides and long-chain fructooligosaccharides was well-tolerated showing a low overall crying time, low incidence of infantile colic infection, and a stool-softening effect in healthy term infants (Vandenplas et al., 2017). After a broad spectrum antibiotics treatment, the IBD mice model showed that FOS from *M. officinalis* also increases fecal *Bifidobacteria*, ameliorates the symptoms of IBD, and modulates the immune response; the $A\beta_{1-42}$ induced deficient rats showed a similar effect.

The gut microbiota can regulate the activity in the peripheral and central nervous system by various means of communication including vagal nerve and adrenergic nerve activation as well as producing several molecular candidates such as neurotransmitters, neuropeptides, endocrine hormones, and immunomodulators. Host stress hormones, such as noradrenaline, might affect the bacterial activities or signal between bacteria may change the microbial diversity and actions of the gut microbiota. However, these bacteria are capable of synthesizing and releasing several neurotransmitters and neuromodulators or eliciting the synthesis and release of neuropeptides from enteroendocrine cells. Previous studies showed that *Lactobacillus* and *Bifidobacterium* species could produce short-chain fatty acids; *Escherichia*, *Bacillus*, and *Saccharomyces* spp. can produce norepinephrine; spore-forming microbes can produce 5-HT; *Bacillus* can produce dopamine, and *Lactobacillus* can produce acetylcholine (Wall et al., 2014; Potgieter et al., 2015; Yano et al., 2015; Alkasir et al., 2017). In this study, the monoamine neurotransmitter (NE, DA, 5-HT, and 5-HIAA) levels in the brain tissue were reduced in $A\beta_{1-42}$ induced deficient rats, and the OMO administration can reverse this decreasing tendency. Thus, we can conclude that OMO influences some bacteria that affect the synthesis and release of some neurotransmitters and neuromodulators. Similar effects were observed in mice subjected to chronic stress, where the observed behavioral, neurochemical, genetic, and neuroendocrine changes after prebiotic (fructooligosaccharides and galactooligosaccharides) administration could be mediated partially by short chain fatty acids (SCFAs) (Burokas et al., 2017); the increased levels of acetate, propionate, and n-butyrate correlated with behavior and gene expression.

We also observed novel changes in microbiota composition, especially the increase in *Bifidobacterium*, immunological enhancement (**Figures 5**, **6**), and gut barrier impairment (**Figure 5**) in TNBS-induced IBD mice. Previous reports showed that *Bifidobacterium* combined with *L. acidophilus*, *L. casei*, and *L. fermentum* for 12 weeks can affect the cognitive function and some metabolic statuses in AD patients (Akbari et al., 2016), and *B. longum* 1714 reduced the stress and improved the memory in healthy volunteers (Allen et al., 2016). The abundance of *Bacteroides* was also increased with OMO administration in the two AD-like animal models (**Figures 3**, **5**). *Bacteroides* are strict anaerobes critical since the initiation of life (Arboleya et al., 2015), and some strains have been used as probiotics. Previous studies have shown that *Bacteroides fragilis* could reverse the autism-like behavior in mice (Hsiao et al., 2013).

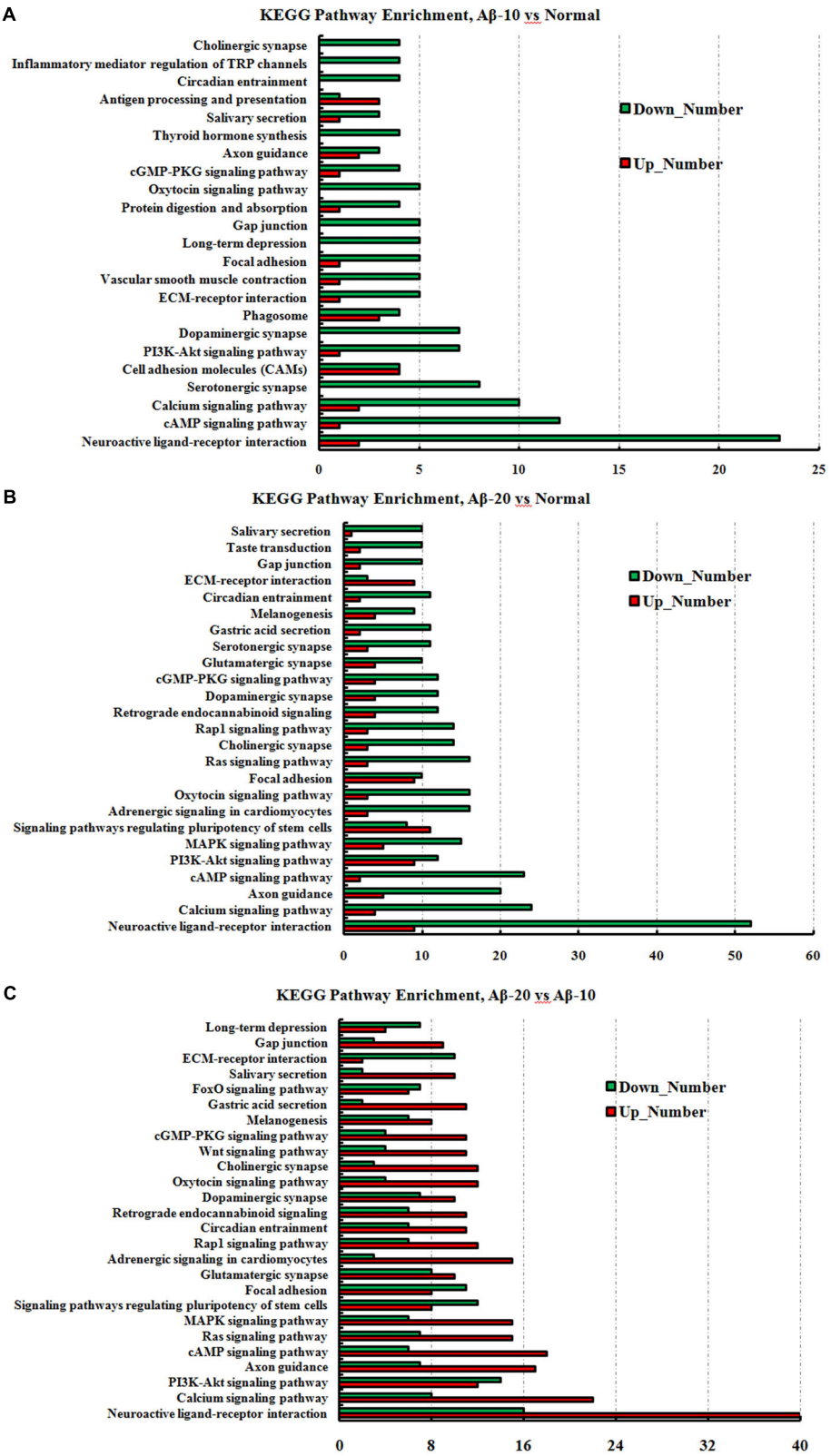


FIGURE 13 | The KEGG pathway enrichment of DEGs in brain transcriptome in the deficit rats induced by $A\beta_{1-42}$. **(A)** The group of Aβ-10 vs. the Normal; **(B)** the group of Aβ-20 vs. the Normal; **(C)** the group of Aβ-20 vs. the Aβ-10.

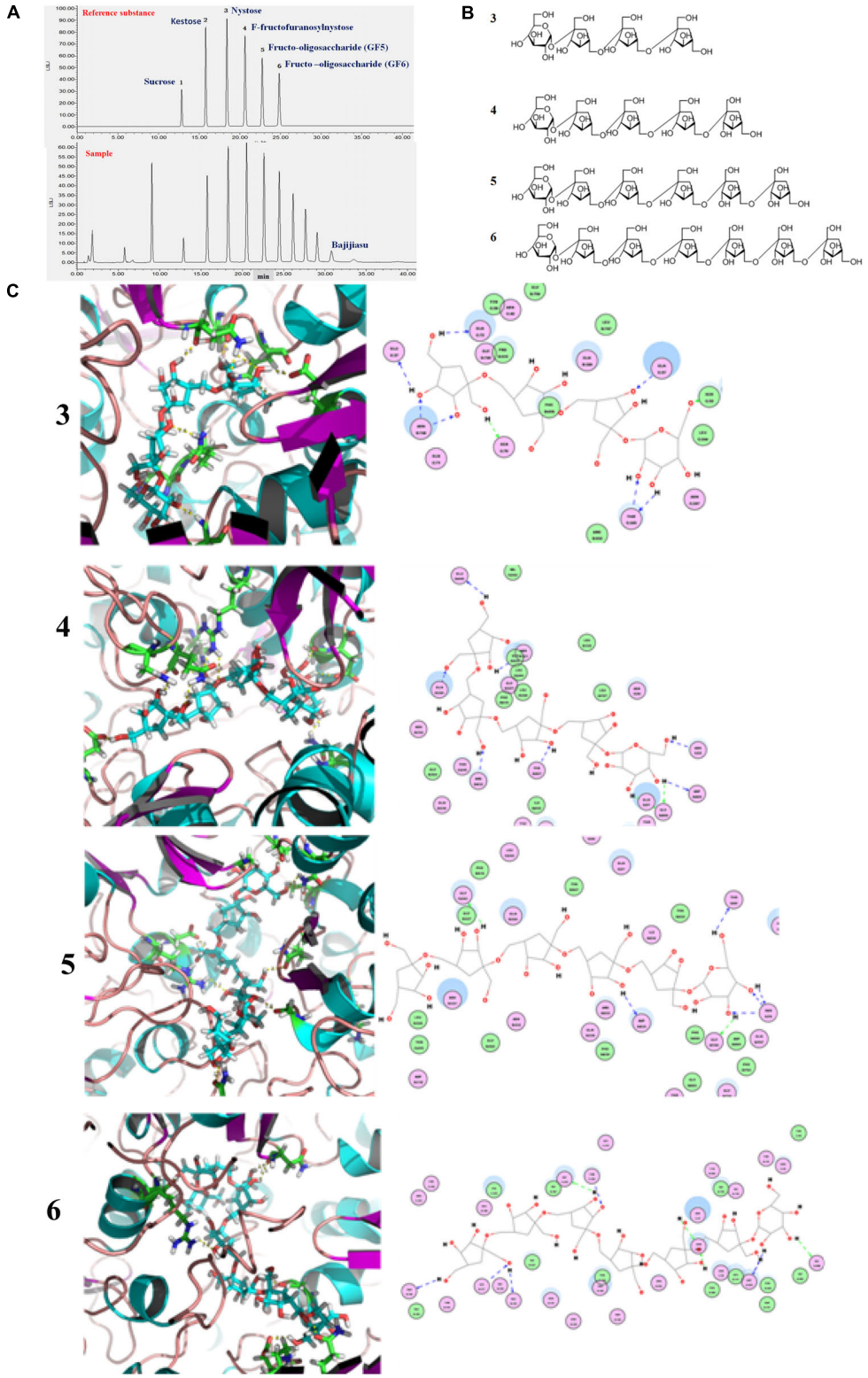


FIGURE 14 | Binding pattern of fructooligosaccharides from *Morinda officinalis*: **(A)** HPLC-ELSD analysis of fructooligosaccharides from *M. officinalis*. **(B)** The chemical structure of nystose (3), *F*-fructofuranose nystose (4), fructooligosaccharide (GF5, 5), fructooligosaccharide (GF6, 6); **(C)** The docked poses were ranked by CDOCKER- ENERGY and the top 10 poses with the co-crystal ligand for SusCD were retained. The data revealed compounds 3, 4, 5, and 6 with CDOCKER-ENERGY of –52.0244180, –75.5881, –101.88, and –110.387, respectively.



FIGURE 15 | The interactive information analysis of DEGs in brain and intestine in deficient rats by injected $A\beta_{1-42}$. **(A–C)** Wayne chart of DEGs in the brain and intestine transcriptome. **(D–F)** KEGG pathway enrichment of DEGs in the brain and intestine transcriptome.

The gut microbiota contains highly diverse microbial communities that play a critical role in the metabolic, immunological, and protective functions in health. This phenomenon is influenced by several factors including genetics, host physiology (age of the host, disease, and stress) and environmental factors such as living conditions and use of medications. Increasingly, diet has been recognized as a key environmental factor that mediates the composition and metabolic function of the gut microbiota. Furthermore, the consumption of specific dietary ingredients, such as oil, fibers,

and prebiotics, is an avenue that modulates the microbiota. Studies on pigs also suggests that the combination with fructooligosaccharides might represent a valuable symbiotic strategy to increase the probiotic levels of bacteria and survival in the gastrointestinal tracts for feed and food applications (Tanner et al., 2015). The administration of such oligosaccharides is attributable to high interindividual variation of the communities in fecal bacteria from pet cats and dogs (Garcia-Mazcorro et al., 2017). In this study, the fructooligosaccharides were extracted from *M. officinalis*, which was widely used in soup, wine, and sweetmeats in South China. Fructo-oligosaccharides are soluble fiber extensively used as prebiotics that is conventionally associated with the stimulation of beneficial bacteria such as *Bifidobacteria* and *Lactobacilli*, among other gut members. However, the mechanisms underlying the fructooligosaccharides stimulation of the beneficial bacteria are yet unknown. A previous study showed that the obtained nutrients process of bacteria require cell membrane protein machines called SusCD complexes (extracellular substrate binding proteins and SusC transporter) (Glenwright et al., 2017), in order to detect the binding capacities between SusCD and nutrients (as starch and other dietary polysaccharides) can evaluate the activity of prebiotics of nutritional ingredients. In this study, the molecular docking analysis was carried out for the evaluation of the binding capacities between SusCD and fructooligosaccharides from *M. officinalis*. The molecular docking study was conducted using the CDOCKER protocol for the four polysaccharides from *M. officinalis* using the Discovery Studio 2.5 (DS2.5) Provisional software. A total of four components (**Figures 14A,B**) from *M. officinalis* were assimilated by literature search, and 1048 poses were generated for all the compounds investigated. The docked poses were ranked by the CDOCKER-ENERGY, and the top 10 poses with the co-crystal ligand for SusCD were retained (**Figure 14**). The data revealed 4 hits namely, compounds 3 (Nystose), 4 (*F*-fructofuranosylnystose), 5 (fructooligosaccharide, GF5), and 6 (fructooligosaccharide, GF6) with CDOCKER-ENERGY -52.0244180, -75.5881, -101.88, and -110.387, respectively (**Figure 14C**). This indicated that the 4 polysaccharides might exert a potent binding activity on SusCD. The interaction between the SusCD protein and the four compounds was further analyzed using the receptor-ligand interaction module in DS. The analysis between SusCD and compound 3 revealed that 9 hydrogen bond interactions appeared in the docked pose. The analysis between SusCD and compound 5 revealed that 9 hydrogen bond interactions appeared in the docked pose. The analysis between SusCD and compound 5 revealed that 7 hydrogen bond interactions appeared in the docked pose. The analysis between SusCD and compound 6 revealed that 9 hydrogen bond interactions appeared in the docked pose. These results suggested that the fructooligosaccharides from *M. officinalis* could be absorbed sufficiently by bacteria with the help of SusCD, serving as optimal nutritional ingredients or prebiotics for bacteria.

The changes in behavior and gut microbiota, as a result of different concentrations of $A\beta_{1-42}$, coincided with the alterations in gene expression in critical brain and intestinal regions. The transcriptome analysis of intestine and brain tissues at the 5th week induced by $A\beta_{1-42}$ showed that the expression of some genes changed significantly (**Figures 10**, **12**). Furthermore, to understand the genetic pathways of the gut-brain axis, the significant DEGs both in the brain and intestine were analyzed to identify the gene elements by an interactive information using the Wayne chart (**Figures 15A–C**), which revealed that the interactive genes were increased by the $A\beta_{1-42}$ levels (14 for Aβ-10 vs. normal, while 25 for Aβ-20 vs. normal, $p < 0.05$). The KEGG pathway enrichment analysis showed that the DEGs were primarily enriched in protein digestion and absorption and platelet activation for Aβ-10 induced group (**Figure 15D**). This phenomenon might be attributed to the colonic bacteria that might not be able to run well or are lost, the non-digestible peptides and proteins (collagen) could not be fermented, and some short-chain fatty acids such as butyrate, propionate, and acetate are deficient, which resulted in platelet activation. Thus, the expressions of Col1a1, Col3a1, and Col14a1 mRNA were changed. With the altered mRNA expression of Lamc2, Sstr3, Nts, Spp1, Il6r, Vip, Kcnk3, and Nr4a1, the PI3K-Akt signaling pathway, neuroactive ligand-receptor interaction, focal adhesion, and ECM-receptor interaction were activated in the Aβ-20-induced group (**Figure 15E**). With the increased levels of $A\beta_{1-42}$ levels, the mRNA expressions of Igsf8, Kcnk3, and Mef2c were changed, and the KEGG pathway enrichment analysis showed that the aldosterone synthesis and secretion and MAPK signaling pathway were influenced (**Figure 15F**). Together with the changes in the gut microbiota community diversity shown in **Figure 8**, and the transcriptome analysis data of intestine and brain, we concluded that the $A\beta_{1-42}$ levels in hippocampus interact the gut and microbiota, although further studies are essential for substantiation.

Antibiotics intervention in APPSWE/PS1ΔE9 mouse model suggests that the diversity of the gut microbiota community can regulate the host innate immunity mechanisms that impact Aβ amyloidosis (Minter et al., 2016). The fecal microbiota transplantation implemented from Aβ precursor protein (APP) transgenic mice to non-transgenic wild-type mice showed a drastically increased level of cerebral Aβ levels, thereby indicating a microbial involvement in the development of Aβ pathology, and microbiota contributes to the development of neurodegenerative diseases (Harach et al., 2017; Liu et al., 2017). We also observed that the diversity in the gut microbiota community altered with the levels of Aβ and the induced time (**Figure 8**). Although the complex networks of communication between the gut microbiota and the brain are not yet fully elucidates, it is clear that prebiotics strongly modulates the ecology of the microbiota. However, the role of the microbial composition and the vast quantity, diversity, and functional capabilities of all these gut microorganisms on the brain and behavior are yet to be determined.

CONCLUSION

Taken together, these data provide further evidence for a beneficial role of fructooligosaccharides (prebiotics) from *M. officinalis* and the effects on microbiota-brain-gut axis in

AD, but need more studies. This study characterized OMO as a promising naturally occurring chemical constituent and suggested microbiota-brain-gut axis as a putative new therapeutic target for the treatment of various neurological diseases by using *M. officinalis* in conventional medicine.

ETHICS STATEMENT

The animal protocols used in this work were approved by the Institutional Animal Care and Use committee of the Center of Laboratory Animals of the Guangdong Institute of Microbiology (GT-IACUC20160426).

AUTHOR CONTRIBUTIONS

DC designed the study, carried out the computational analyses and wrote the manuscript. JY and GL collected animal physiological data and fecal samples and extracted ruminal DNA. XY and XT collected animal physiological data and brain samples. DC, TY, and OS collected data regarding the microbial metabolic networks and transcriptome analysis. YX and QW helped to design the study and to develop the metagenomic analysis tools and wrote the manuscript. GZ helped with computational tool development and statistical analyses (PCA). All authors read and approved the final manuscript.

FUNDING

The present work was supported by the financial support from the Guangdong Science and Technology Plan Projects (2015A020211021; 2016A050502032), the Guangzhou Science and Technology Plan Projects (201504281708257; 201604020009), the High-level Leading Talent Introduction Program of GDAS (2016GDASRC-0102), and the Nanyue Microbial Talents Cultivation Fund of Guangdong Institute of Microbiology and the Guangzhou Medical University Research Projects (2016C28).

ACKNOWLEDGMENTS

The authors would like to thank Zhang Heming, Burton B. Yang for helpful discussions in the preparation of this manuscript. Sequencing service was provided by Personal Biotechnology Co., Ltd., Shanghai, China.

SUPPLEMENTARY MATERIAL

The Supplementary Material for this article can be found online at: https://www.frontiersin.org/articles/10.3389/fnagi.2017.00403/full#supplementary-material

REFERENCES

Abbott, A. (2011). Dementia: a problem for our age. *Nature* 475, S2–S4. doi: 10.1038/475S2a

Akbari, E., Asemi, Z., Daneshvar Kakhaki, R., Bahmani, F., Kouchaki, E., Tamtaji, O. R., et al. (2016). Effect of probiotic supplementation on cognitive function and metabolic status in Alzheimer's disease: a randomized, double-blind and controlled trial. *Front. Aging Neurosci.* 8:256. doi: 10.3389/fnagi.2016.00256

Alkasir, R., Li, J., Li, X., Jin, M., and Zhu, B. (2017). Human gut microbiota: the links with dementia development. *Protein Cell.* 8, 90–102. doi: 10.1007/s13238-016-0338-6

Allen, A. P., Hutch, W., Borre, Y. E., Kennedy, P. J., Temko, A., Boylan, G., et al. (2016). *Bifidobacterium longum* 1714 as a translational psychobiotic: modulation of stress, electrophysiology and neurocognition in healthy volunteers. *Transl. Psychiatry* 6:e939. doi: 10.1038/tp.2016.191

Anderson, G., Seo, M., Berk, M., Carvalho, A. F., and Maes, M. (2016). Gut permeability and microbiota in Parkinson's disease: role of depression, tryptophan catabolites, oxidative and nitrosative stress and melatonergic pathways. *Curr. Pharm. Des.* 22, 6142–6151. doi: 10.2174/1381612822666160906161513

Arboleya, S., Sanchez, B., Milani, C., Duranti, S., Solis, G., Fernandez, N., et al. (2015). Intestinal microbiota development in preterm neonates and effect of perinatal antibiotics. *J. Pediatr.* 166, 538–544. doi: 10.1016/j.jpeds.2014.09.041

Benjamin, J. L., Hedin, C. R., Koutsoumpas, A., Ng, S. C., McCarthy, N. E., Hart, A. L., et al. (2011). Randomised, double-blind, placebo-controlled trial of fructo-oligosaccharides in active Crohn's disease. *Gut* 60, 923–929. doi: 10.1136/gut.2010.232025

Bland, J. (2016). Intestinal microbiome, *Akkermansia muciniphila*, and medical nutrition therapy. *Integr. Med.* 15, 14–16.

Burokas, A., Arboleya, S., Moloney, R. D., Peterson, V. L., Murphy, K., Clarke, G., et al. (2017). Targeting the microbiota-gut-brain axis: prebiotics have anxiolytic and antidepressant-like effects and reverse the impact of chronic stress in mice. *Biol. Psychiatry* 82, 472–487. doi: 10.1016/j.biopsych.2016.12.031

Cabili, M. N., Trapnell, C., Goff, L., Koziol, M., Tazon-Vega, B., Regev, A., et al. (2011). Integrative annotation of human large intergenic noncoding RNAs reveals global properties and specific subclasses. *Genes Dev.* 25, 1915–1927. doi: 10.1101/gad.17446611

Cai, B., Cui, C. B., Chen, Y. H., Luo, Z. P., Yang, M., and Yao, Z. W. (1996). Antidepressant effect of inulin- type oligosaccharides from *Morinda officinalis* How in mice. *Chin. J. Pharmacol. Toxicol.* 10, 109–112.

Chen, D. L., Li, N., Lin, L., Long, H. M., Lin, H., Chen, J., et al. (2014a). Confocal mirco-Raman spectroscopic analysis of the antioxidant protection mechanism of the oligosaccharides extracted from *Morinda officinalis* on human sperm DNA. *J. Ethnopharmacol.* 153, 119–124. doi: 10.1016/j.jep.2014.01.021

Chen, D. L., Yong, T. Q., Yang, J., Zheng, C. Q., Shuai, O., and Xie, Y. Z. (2017). Docking studies and biological evaluation of a potential β-secretase inhibitor of 3-hydroxyhericenone F from *Hericium erinaceus*. *Front. Pharmacol.* 8:219. doi: 10.3389/fphar.2017.00219

Chen, D. L., Zhang, P., Lin, L., Shuai, O., Zhang, H. M., Liu, S. H., et al. (2013). Protective effect of Bajijiasu against β-amyloid-induced neurotoxicity in PC12 cells. *Cell Mol. Neurobiol.* 33, 837–850. doi: 10.1007/s10571-013-9950-7

Chen, D. L., Zhang, P., Lin, L., Zhang, H. M., Deng, S. D., Wu, Z. Q., et al. (2014b). Protective effects of bajijiasu in a rat model of Aβ25-35-induced neurotoxicity. *J. Ethnopharmacol.* 154, 206–217. doi: 10.1016/j.jep.2014.04.004

Choi, Y. J., Yang, H. S., Jo, J. H., Lee, S. C., Park, T. Y., Choi, B. S., et al. (2015). Anti-amnesic effect of fermented Ganoderma lucidum water extracts by lactic acid bacteria on scopolamine-induced memory impairment in rats. *Prev. Nutr. Food Sci.* 20, 126–132. doi: 10.3746/pnf.2015.20.2.126

Davis, D. J., Doerr, H. M., Grzelak, A. K., Busi, S. B., Jasarevic, E., Ericsson, A. C., et al. (2016). *Lactobacillus plantarum* attenuates anxiety-related behavior and protects against stress-induced dysbiosis in adult zebrafish. *Sci. Rep.* 6:33726. doi: 10.1038/srep33726

Derrien, M., Belzer, C., and de Vos, W. M. (2016). *Akkermansia muciniphila* and its role in regulating host functions. *Microb. Pathog.* 106, 171–181. doi: 10.1016/j.micpath.2016.02.005

Dinan, T. G., and Cryan, J. F. (2017). The microbiome-gut-brain axis in health and disease. *Gastroenterol. Clin. North Am.* 46, 77–89. doi: 10.1016/j.gtc.2016.09.007

Erdman, S. E., and Poutahidis, T. (2016). Microbes and oxytocin: benefits for host physiology and behavior. *Int. Rev. Neurobiol.* 131, 91–126. doi: 10.1016/bs.irn.2016.07.004

Gao, J., Zhou, R., You, X., Luo, F., He, H., Chang, X., et al. (2016). Salidroside suppresses inflammation in a D-galactose-induced rat model of Alzheimer's disease via SIRT1/NF-κB pathway. *Metab. Brain Dis.* 31, 771–778. doi: 10.1007/s11011-016-9813-2

Garcia-Mazcorro, J. F., Barcenas-Walls, J. R., Suchodolski, J. S., and Steiner, J. M. (2017). Molecular assessment of the fecal microbiota in healthy cats and dogs before and during supplementation with fructo-oligosaccharides (FOS) and inulin using high-throughput 454-pyrosequencing. *PeerJ* 5:e3184. doi: 10.7717/peerj.3184

Gareau, M. G. (2014). Microbiota-gut-brain axis and cognitive function. *Adv. Exp. Med. Biol.* 817, 357–371. doi: 10.1007/978-1-4939-0897-4_16

Glenwright, A. J., Pothula, K. R., Bhamidimarri, S. P., Chorev, D. S., Baslé, A., Firbank, S. J., et al. (2017). Structural basis for nutrient acquisition by dominant members of the human gut microbiota. *Nature* 541, 407–411. doi: 10.1038/nature20828

Greer, R. L., Dong, X., Moraes, A. C., Zielke, R. A., Fernandes, G. R., Peremyslova, E., et al. (2016). *Akkermansia muciniphila* mediates negative effects of IFNγ on glucose metabolism. *Nat. Commun.* 7:13329. doi: 10.1038/ncomms13329

Harach, T., Marungruang, N., Duthilleul, N., Cheatham, V., Mc Coy, K. D., Frisoni, G., et al. (2017). Reduction of Abeta amyloid pathology in APP/PS1 transgenic mice in the absence of gut microbiota. *Sci. Rep.* 7:41802. doi: 10.1038/srep41802

Henning, S. M., Summanen, P. H., Lee, R. P., Yang, J., Finegold, S. M., Heber, D., et al. (2017). Pomegranate ellagitannins stimulate the growth of *Akkermansia muciniphila* in vivo. *Anaerobe* 43, 56–60. doi: 10.1016/j.anaerobe.2016.12.003

Hsiao, E. Y., McBride, S. W., Hsien, S., Sharon, G., Hyde, E. R., McCue, T., et al. (2013). Microbiota modulate behavioral and physiological abnormalities associated with neurodevelopmental disorders. *Cell* 155, 1451–1463. doi: 10.1016/j.cell.2013.11.024

Hu, X., Wang, T., and Jin, F. (2016). Alzheimer's disease and gut microbiota. *Sci. China Life Sci.* 59, 1006–1023. doi: 10.1007/s11427-016-5083-9

Huang, H. C., Zheng, B. W., Guo, Y., Zhao, J., Zhao, J. Y., Ma, X. W., et al. (2016). Antioxidative and neuroprotective effects of curcumin in an Alzheimer's disease rat model co-treated with intracerebroventricular streptozotocin and subcutaneous D-galactose. *J. Alzheimers Dis.* 52, 899–911. doi: 10.3233/JAD-150872

Jeong, J. J., Woo, J. Y., Kim, K. A., Han, M. J., and Kim, D. H. (2015). *Lactobacillus pentosus* var. *plantarum* C29 ameliorates age-dependent memory impairment in Fischer 344 rats. *Lett. Appl. Microbiol.* 60, 307–314. doi: 10.1111/lam.12393

Jiang, C., Li, G., Huang, P., Liu, Z., and Zhao, B. (2017). The gut microbiota and Alzheimer's disease. *J. Alzheimers Dis.* 58, 1–15. doi: 10.3233/JAD-161141

Jung, I. H., Jung, M. A., Kim, E. J., Han, M. J., and Kim, D. H. (2012). *Lactobacillus pentosus* var. *plantarum* C29 protects scopolamine-induced memory deficit in mice. *J. Appl. Microbiol.* 113, 1498–1506. doi: 10.1111/j.1365-2672.2012.05437.x

Le Sage, F., Meilhac, O., and Gonthier, M. P. (2017). *Porphyromonas gingivalis* lipopolysaccharide induces pro-inflammatory adipokine secretion and oxidative stress by regulating Toll-like receptor-mediated signaling pathways and redox enzymes in adipocytes. *Mol. Cell. Endocrinol.* 446, 102–110. doi: 10.1016/j.mce.2017.02.022

Leung, K., and Thuret, S. (2015). Gut microbiota: a modulator of brain plasticity and cognitive function in ageing. *Healthcare* 3, 898–916. doi: 10.3390/healthcare3040898

Li, X., Lu, F., Li, W., Xu, J., Sun, X. J., Qin, L. Z., et al. (2016). Minocycline ameliorates D-galactose- induced memory deficits and loss of Arc/Arg3.1 expression. *Mol. Biol. Rep.* 43, 1157–1163. doi: 10.1007/s11033-016-4051-6

Li, Y. F., Liu, Y. Q., Yang, M., Wang, H. L., Huang, W. C., Zhao, Y. M., et al. (2004). The cytoprotective effect of inulin-type hexasaccharide extracted from *Morinda officinalis* on PC12 cells against the lesion induced by corticosterone. *Life Sci.* 75, 1531–1538. doi: 10.1016/j.lfs.2004.02.029

Li, Y. F., Yuan, L., Xu, Y. K., Yang, M., Zhao, Y. M., and Luo, Z. P. (2001). Antistress effect of oligosaccharides extracted from *Morinda officinalis* in mice and rats. *Acta Pharmacol. Sin.* 22, 1084–1088.

Liang, C. Y., Liang, Y. M., Liu, H. Z., Zhu, D. M., Hou, S. Z., Wu, Y. Y., et al. (2017). Effect of *Dendrobium officinale* on D-galactose-induced aging mice. *Chin. J. Integr. Med.* doi: 10.1007/s11655-016-2631-x [Epub ahead of print].

Ling, Z. X., Xia, L., Jia, X. Y., Cheng, Y. W., Luo, Y. Q., Li, Y., et al. (2014). Impacts of infection with different toxigenic *Clostridium difficile* strains on faecal microbiota in children. *Sci. Rep.* 4:7485. doi: 10.1038/srep07485

Liu, K. L., He, Y. G., Yu, L. X., Chen, Y., and He, R. (2017). Elevated formaldehyde in the cecum of APP/PS1 mouse. *Microbiol. China* 44, 1761–1766.

Malaguarnera, M., Vacante, M., Antic, T., Giordano, M., Chisari, G., Acquaviva, R., et al. (2012). *Bifidobacterium longum* with fructo-oligosaccharides in patients with non alcoholic steatohepatitis. *Dig. Dis. Sci.* 57, 545–553. doi: 10.1007/s10620-011-1887-4

Mayer, E. A., Knight, R., Mazmanian, S. K., Cryan, J. F., and Tillisch, K. (2014). Gut microbes and the brain: paradigm shift in neuroscience. *J. Neurosci.* 34, 15490–15496. doi: 10.1523/JNEUROSCI.3299-14.2014

Minter, M. R., Zhang, C., Leone, V., Ringus, D. L., Zhang, X., Oyler-Castrillo, P., et al. (2016). Antibiotic-induced perturbations in gut microbial diversity influences neuro-inflammation and amyloidosis in a murine model of Alzheimer's disease. *Sci. Rep.* 6:30028. doi: 10.1038/srep30028

Park, K. Y., Jeong, J. K., Lee, Y. E., and Daily, J. W. III (2014). Health benefits of kimchi (Korean fermented vegetables) as a probiotic food. *J. Med. Food* 17, 6–20. doi: 10.1089/jmf.2013.3083

Petra, A. I., Panagiotidou, S., Hatziagelaki, E., Stewart, J. M., Conti, P., and Theoharides, T. C. (2015). Gut-microbiota-brain axis and its effect on neuropsychiatric disorders with suspected immune dysregulation. *Clin. Ther.* 37, 984–995. doi: 10.1016/j.clinthera.2015.04.002

Pistollato, F., Sumalla Cano, S., Elio, I., Masias Vergara, M., Giampieri, F., and Battino, M. (2016). Role of gut microbiota and nutrients in amyloid formation and pathogenesis of Alzheimer disease. *Nutr. Rev.* 74, 624–634. doi: 10.1093/nutrit/nuw023

Potgieter, M., Bester, J., Kell, D. B., and Pretorius, E. (2015). The dormant blood microbiome in chronic, inflammatory diseases. *FEMS Microbiol. Rev.* 39, 567–591. doi: 10.1093/femsre/fuv013

Rhee, S. H., Pothoulakis, C., and Mayer, E. A. (2009). Principles and clinical implications of the brain-gut-enteric microbiota axis. *Nat. Rev. Gastroenterol. Hepatol.* 6, 306–314. doi: 10.1038/nrgastro.2009.35

Rieder, R., Wisniewski, P. J., Alderman, B. L., and Campbell, S. C. (2017). Microbes and mental health: a review. *Brain Behav. Immun.* 66, 9–17. doi: 10.1016/j.bbi.2017.01.016

Rigo-Adrover, M., Pérez-Berezo, T., Ramos-Romero, S., van Limpt, K., Knipping, K., Garssen, J., et al. (2017). A fermented milk concentrate and a combination of short-chain galacto-oligosaccharides/long-chain fructo-oligosaccharides/pectin-derived acidic oligosaccharides protect suckling rats from rotavirus gastroenteritis. *Br. J. Nutr.* 117, 209–217. doi: 10.1017/S0007114516004566

Russo, R., Cristiano, C., Avagliano, C., De Caro, C., La Rana, G., Raso, G. M., et al. (2017). Gut-brain axis: role of lipids in the regulation of inflammation, pain and CNS diseases. *Curr. Med. Chem.* doi: 10.2174/0929867324666170216113756 [Epub ahead of print].

Sanches Lopes, S. M., Francisco, M. G., Higashi, B., de Almeida, R. T., Krausová, G., Pilau, E. J., et al. (2016). Chemical characterization and prebiotic activity of fructo-oligosaccharides from *Stevia rebaudiana* (Bertoni) roots and in vitro adventitious root cultures. *Carbohydr. Polym.* 152, 718–725. doi: 10.1016/j.carbpol.2016.07.043

Scott, K. A., Ida, M., Peterson, V. L., Prenderville, J. A., Moloney, G. M., Izumo, T., et al. (2017). Revisiting Metchnikoff: age-related alterations in microbiota-gut-brain axis in the mouse. *Brain Behav Immun.* 65, 20–32. doi: 10.1016/j.bbi.2017.02.004

Servin, A. L. (2004). Antagonistic activities of lactobacilli and bifidobacteria against microbial pathogens. *FEMS Microbiol. Rev.* 28, 405–440. doi: 10.1016/j.femsre.2004.01.003

Sun, L., Luo, H., Bu, D., Zhao, G., Yu, K., Zhang, C., et al. (2013). Utilizing sequence intrinsic composition to classify protein-coding and long non-coding transcripts. *Nucleic Acids Res.* 41:e166. doi: 10.1093/nar/gkt646

Tan, B. X., Chen, C. F., Chen, J. W., Su, W., Li, X. Y., Lin, R. S., et al. (2000a). Mechanism of BA-JI-SU in invigorating kidney to anti-aging. *J. New Chin. Med.* 32, 36–38.

Tan, B. X., Su, W., Chen, J. W., Chen, C. F., Wang, Y., and Li, X. Y. (2000b). improvement effect of bajiasu on spatial learning and memory ability of rats. *Tradit. Chin. Drugs Res. Clin. Pharmacol.* 11, 95–97.

Tanner, S. A., Lacroix, C., Del'Homme, C., Jans, C., Zihler Berner, A., Bernalier-Donadille, A., et al. (2015). Effect of *Bifidobacterium thermophilum* RBL67 and fructo-oligosaccharides on the gut microbiota in Göttingen minipigs. *Br. J. Nutr.* 114, 746–755. doi: 10.1017/S0007114515002263

Trapnell, C., Hendrickson, D. G., Sauvageau, M., Goff, L., Rinn, J. L., and Pachter, L. (2013). Differential analysis of gene regulation at transcript resolution with RNA-seq. *Nat. Biotechnol.* 31, 46–53. doi: 10.1038/nbt.2450

Valdés-Varela, L., Ruas-Madiedo, P., and Gueimonde, M. (2017). *In vitro* fermentation of different fructo-oligosaccharides by *Bifidobacterium* strains for the selection of synbiotic combinations. *Int. J. Food Microbiol.* 242, 19–23. doi: 10.1016/j.ijfoodmicro.2016.11.011

Van Herreweghen, F., Van den Abbeele, P., De Mulder, T., De Weirdt, R., Geirnaert, A., Hernandez-Sanabria, E., et al. (2017). In vitro colonisation of the distal colon by *Akkermansia muciniphila* is largely mucin and pH dependent. *Benef. Microbes* 8, 81–96. doi: 10.3920/BM2016.0013

Vandenplas, Y., Ludwig, T., Bouritius, H., Alliet, P., Forde, D., Peeters, S., et al. (2017). Randomised controlled trial demonstrates that fermented infant formula with short-chain galacto-oligosaccharides and long-chain fructo-oligosaccharides reduces the incidence of infantile colic. *Acta Paediatr.* 106, 1150–1158. doi: 10.1111/apa.13844

Vanegas, S. M., Meydani, M., Barnett, J. B., Goldin, B., Kane, A., Rasmussen, H., et al. (2017). Substituting whole grains for refined grains in a 6-wk randomized trial has a modest effect on gut microbiota and immune and inflammatory markers of healthy adults. *Am. J. Clin. Nutr.* 105, 635–650. doi: 10.3945/ajcn.116.146928

Vuong, H. E., Yano, J. M., Fung, T. C., and Hsiao, E. Y. (2017). The microbiome and host behavior. *Annu. Rev. Neurosci.* 40, 21–49. doi: 10.1146/annurev-neuro-072116-031347

Wall, R., Cryan, J. F., Ross, R. P., Fitzgerald, G. F., Dinan, T. G., and Stanton, C. (2014). Bacterial neuroactive compounds produced by psychobiotics. *Adv. Exp. Med. Biol.* 817, 221–239. doi: 10.1007/978-1-4939-0897-4_10

Wang, L., Feng, Z., Wang, X., Wang, X., and Zhang, X. (2010). DEGseq: an R package for identifying differentially expressed genes from RNA-seq data. *Bioinformatics* 26, 136–138. doi: 10.1093/bioinformatics/btp612

Wang, X., Li, G. J., Hu, H. X., Ma, C., Ma, D. H., Liu, X. L., et al. (2016). Cerebral mTOR signal and pro-inflammatory cytokines in Alzheimer's disease rats. *Transl. Neurosci.* 7, 151–157. doi: 10.1515/tnsci-2016-0022

Wei, Y., Lu, C., Chen, J., Cui, G., Wang, L., Yu, T., et al. (2017). High salt diet stimulates gut Th17 response and exacerbates TNBS-induced colitis in mice. *Oncotarget* 8, 70–82. doi: 10.18632/oncotarget.13783

Woo, J. Y., Gu, W., Kim, K. A., Jang, S. E., Han, M. J., and Kim, D. H. (2014). *Lactobacillus pentosus* var. *plantarum* C29 ameliorates memory impairment and inflammaging in a D-galactose-induced accelerated aging mouse model. *Anaerobe* 27, 22–26. doi: 10.1016/j.anaerobe.2014.03.003

Yano, J. M., Yu, K., Donaldson, G. P., Shastri, G. G., Ann, P., Ma, L., et al. (2015). Indigenous bacteria from the gut microbiota regulate host serotonin biosynthesis. *Cell* 161, 264–276. doi: 10.1016/j.cell.2015.02.047

Zeng, G. F., Zhang, Z. Y., Lu, L., Xiao, D. Q., Zong, S. H., and He, J. M. (2013). Protective effects of ginger root extract on Alzheimer disease-induced behavioral dysfunction in rats. *Rejuvenation Res.* 16, 124–133. doi: 10.1089/rej.2012.1389

Zhan, P. Y., Peng, C. X., and Zhang, L. H. (2014). Berberine rescues D-galactose-induced synaptic/memory impairment by regulating the levels of Arc. *Pharmacol. Biochem. Behav.* 117, 47–51. doi: 10.1016/j.pbb.2013.12.006

Zhong, L., Huang, F., Shi, H., Wu, H., Zhang, B., Wu, X., et al. (2016). Qing'E formula alleviates the aging process in D-galactose-induced aging mice. *Biomed. Rep.* 5, 101–106. doi: 10.3892/br.2016.667

Conflict of Interest Statement: The authors declare that the research was conducted in the absence of any commercial or financial relationships that could be construed as a potential conflict of interest.

Copyright © 2017 Chen, Yang, Yang, Lai, Yong, Tang, Shuai, Zhou, Xie and Wu. This is an open-access article distributed under the terms of the Creative Commons Attribution License (CC BY). The use, distribution or reproduction in other forums is permitted, provided the original author(s) or licensor are credited and that the original publication in this journal is cited, in accordance with accepted academic practice. No use, distribution or reproduction is permitted which does not comply with these terms.

frontiers in Aging Neuroscience

ORIGINAL RESEARCH
published: 01 June 2018
doi: 10.3389/fnagi.2018.00164

The Role of Fluoxetine in Activating Wnt/β-Catenin Signaling and Repressing β-Amyloid Production in an Alzheimer Mouse Model

Min Huang[1]†, Yubin Liang[2]†, Hongda Chen[3]†, Binchu Xu[1], Cuicui Chai[1] and Pengfei Xing[1]*

[1] Department of Neurology, The Seventh Affiliated Hospital, Sun Yat-sen University, Shenzhen, China, [2] Department of Neurology, The First Affiliated Hospital of Jinan University, Guangzhou, China, [3] Department of Traditional Chinese Medicine, The Seventh Affiliated Hospital, Sun Yat-sen University, Shenzhen, China

Fluoxetine (FLX) is one of the selective serotonin reuptake inhibitors (SSRIs) antidepressants, which could be used to relieve depression and anxiety among AD patients. This study was designed to search for new mechanisms by which fluoxetine could activate Wnt/β-catenin signaling pathway and reduce amyloidosis in AD brain. Fluoxetine was administered via intragastric injection to APP/tau/PS1 mouse model of Alzheimer's disease (3×Tg-AD) mice for 4 months. In the hippocampus of AD mouse model, there could be observed neuronal apoptosis, as well as an increase in Aβ (amyloid-β) production. Moreover, there is a strong association between down-regulation of Wnt/β-catenin signaling and the alteration of AD pathology. The activity of protein phosphatases of type 2A (PP2A) could be significantly enhanced by the treatment of fluoxetine. The activation of PP2A, caused by fluoxetine, could then play a positive role in raising the level of active β-catenin, and deliver a negative impact in GSK3β activity in the hippocampal tissue. Both the changes mentioned above would lead to the activation of Wnt/β-catenin signaling. Meanwhile, fluoxetine treatment would reduce APP cleavage and Aβ generation. It could also prevent apoptosis in 3×Tg-AD primary neuronal cell, and have protective effects on neuron synapse. These findings imply that Wnt/β-catenin signaling could be a potential target outcome for AD prevention, and fluoxetine has the potential to be a promising drug in both AD prevention and treatment.

Keywords: fluoxetine, Alzheimer's disease, Wnt/β-catenin signaling, protein phosphatases of type 2A (PP2A), amyloid-β

OPEN ACCESS

Edited by:
Ghulam Md Ashraf, King Abdulaziz University, Saudi Arabia

Reviewed by:
Gloria Patricia Cardona Gomez, Universidad de Antioquía, Colombia
Mahmood Ahmad Khan, University College of Medical Sciences, India

***Correspondence:**
Min Huang
minhuanghm@163.com

† These authors have contributed equally to this work.

Received: *10 January 2018*
Accepted: *15 May 2018*
Published: *01 June 2018*

Citation:
Huang M, Liang Y, Chen H, Xu B, Chai C and Xing P (2018) The Role of Fluoxetine in Activating Wnt/β-Catenin Signaling and Repressing β-Amyloid Production in an Alzheimer Mouse Model. Front. Aging Neurosci. 10:164. doi: 10.3389/fnagi.2018.00164

INTRODUCTION

Alzheimer's disease (AD) is a chronic neurodegenerative disease characterized by progressive memory decline and cognitive impairment (Scharre and Chang, 2002). AD has various histopathological hallmarks, including neurofibrillary tangles, cerebral amyloid senile plaques, synaptic and neuronal loss in the brain (Suh and Checler, 2002). Senile plaques, one of the important histopathological hallmarks, consist of a dense core of amyloid-β peptide (Aβ) and the

dystrophic neuritis surrounded (Selkoe, 2004). The sequential proteolytic process of β-amyloid precursor protein (APP) through β- and γ-secretases could generate Aβ (Oulès et al., 2012). Previous study shows that Aβ could disrupt synapses and initiate a cascade of toxic events, which might result in neuronal loss (Liu et al., 2014). Another early feature of AD, besides amyloid pathogenesis, is synaptic dysfunction, which might be even prior to Aβ deposition (Miller-Thomas et al., 2016; Zuroff et al., 2017). PP2A plays a core part in dephosphorylation of inactive β-catenin and phosphorylated APP (Seeling et al., 1999; Sontag et al., 2007). Additionally, Aβ generation could also be inhabited simultaneously by drugs that target inactive PP2A (Liu and Wang, 2009; Triaca et al., 2016).

The Wnt/β-catenin signaling pathway has been found to be critical for both neuronal development and maintenance of the nervous system (Patapoutian and Reichardt, 2000). Research shows that Wnt/β-catenin signaling pathway would influence various neuronal processes, such as synaptic differentiation, synaptic function, the function of neuronal circuits, dendrite development, and neuronal plasticity (Rosso and Inestrosa, 2013). Without the activation of the Wnt/β-catenin pathway, β-catenin in the cytoplasm could be phosphorylated by a complex set of proteins, such as glycogen synthase kinase-3β (GSK3β), for ubiquitylation and degradation. However, the GSK3β activity could be inhibited by the activation of the Wnt/β-catenin pathway, which would in term lead to the repression of β-catenin phosphorylation, and, ultimately, result in the degradation of proteasome (Davidson et al., 2005; Zeng et al., 2008). Previous research shows that, in both sporadic and familial AD patients, there could be observed a decreased level of active β-catenin, inactive PP2A, and hyper active GSK3β (Voronkov et al., 2011; Inestrosa and Varela-Nallar, 2014). According to mentioned studies, it could be implied that it would be constructive and therapeutic for AD patients to maintain and rescue Wnt/β-catenin signaling.

Fluoxetine (FLX), as a selective serotonin reuptake inhibitors (SSRIs) antidepressant, could be used to relieve depression and anxiety among AD patients (Modrego, 2010). Moreover, studies suggest another potential application of FLX. For patients with mild cognitive impairment (MCI), which is a prodromal state of AD, Fluoxetine could improve the memory and cognitive function (Mowla et al., 2007). Besides, fluoxetine has been shown to be able to inhibit β-amyloid production, and prevent neuronal degeneration in an APP/PS1 mouse model (Wang et al., 2014; Ma et al., 2017; Sun et al., 2017). Furthermore, Li et al. (2004) have showed that fluoxetine could greatly enhance the phosphorylation of GSK3β. And Pilar-Cuellar et al. (2012) have revealed that fluoxetine could increase the β-catenin level. However, more research would be required to clarify if the neuroprotective effect of fluoxetine is related to the action of Wnt/β-catenin.

The purpose of our research is to explore the role of fluoxetine and its underlying mechanism in alleviating AD symptom. The research would utilize a triple-transgenic mouse model of AD, and measure the AD symptom by PP2A dependent Wnt/β-catenin signaling. Fluoxetine treatment dramatically slowing down the production of Aβ in the hippocampus of AD mouse. Moreover, during the process where fluoxetine positively influences the activation of Wnt/β-catenin signaling, promotion of PP2A activity is found to play a significant role. Ultimately, the mechanisms behind the regulation of fluoxetine in the Wnt/β-catenin signaling pathway were explored.

MATERIALS AND METHODS

Drugs and Reagents

Fluoxetine was manufactured by Sigma-Aldrich (St. Louis, MO, United States). All cell culture reagents were produced from Invitrogen. Penicillin–streptomycin and poly-D-lysine, were manufactured by Sigma-Aldrich (St. Louis, MO, United States). Papain was obtained from Worthington. The Aβ1–42 ELISA kits and Aβ40 ELISA kits were purchased from Nanjing SenBeiJia Biological Technology Co., Ltd. (Nanjing, China). Antibodies information was in the **Table 1**. All other reagents were reagent grade.

Animals and Treatment

This study utilized 3×Tg-AD mice expressing APPswe, PS1M146V, and tauP301L human gene mutants, which were purchased from the Jackson Laboratory (Bar Harbor, ME, United States). In these mice, intracellular Aβ was detected

TABLE 1 | Antibody information.

Antibody	Host	Application	Source	Dilutions
Aβ1–42	Rabbit	WB/IF	Abcam	1:500
APP	Mouse	WB	Abcam	1:3000
CTFβ	Mouse	WB	Santa Cruz	1:500
CTFα	Rabbit	WB	Santa Cruz	1:500
$ADAM_{10}$	Rabbit	WB	Abcam	1:1000
BACE1	Rabbit	WB	Abcam	1:3000
PS1	Mouse	WB	Abcam	1:1000
sAPPα	Mouse	WB	USBiological	1:1000
sAPPβ	Rabbit	WB	Abcam	1:500
C99	Rabbit	WB	Pierce	1:2000
C83	Rabbit	WB	Pierce	1:2000
BDNF	Mouse	WB	Abcam	1:1000
NeuN	Rabbit	IF	Abcam	1:300
Bcl-xL	Rabbit	WB	Abcam	1:1000
Bcl-2	Rabbit	WB	Abcam	1:1000
Cleave-Caspase3	Rabbit	WB	Cell signaling	1:1000
Bax	Rabbit	WB	Abcam	1:1000
PP2Ac	Rabbit	WB	Abcam	1:1000
PP2A pY307	Rabbit	WB	Abcam	1:1000
GSK3β pY216	Rabbit	WB	Abcam	1:1000
GSK3β	Rabbit	WB	Abcam	1:5000
Active β-catenin	Rabbit	WB/IF	Cell signaling	1:2000
Inactive β-catenin	Rabbit	WB	Cell signaling	1:2000
PSD95	Rabbit	WB/IF	Abcam	1:500
Synaptophysin	Rabbit	WB	Abcam	1:1000
GAPDH	Rabbit	WB	Abcam	1:2500

WB, western blot blatting; IF, immunofluorescence.

at ages between 3 and 6 months, and cognitive impairment was detected at the age of 6 months (Oddo et al., 2003a,b; Billings et al., 2005). In the treatment group (Tg + FLX) (n = 12; 6 males and 6 females), fluoxetine was administrated at 10 mg/kg/day, intragastrical injection for 4 months. The fluoxetine administration began at the 4 months of age, just before they developed cognitive impairment and key pathologic features. The dose of fluoxetine was chosen aligning with previous studies (Li et al., 2009), with no gender differences. The rest two groups, the 3×Tg-AD mice group (Tg) (n = 12; 6 males, and 6 females) and male non-transgenic wild-type (WT) mice group (n = 12, 12 males), were treated with drinking water instead. All these three groups were kept under the same standard laboratory conditions with the treatment group, including temperature of 22 ± 2°C, 12-h light/dark cycle, and free access to water and food. Each cage contained 3 or 4 subjects with the same genotype. All experiments were conducted following the *Animal Care and Institutional Ethical Guidelines* in China to minimize animal suffering, for instance, reducing the number of animals used, and utilizing alternatives to *in vivo* techniques, if available. The experiments and procedures utilized in this study were conducted strictly according to the institutional guidelines regarding experimental animal use in Sun Yat-sen University. The protocol was approved by the Animal Ethical and welfare Committee of Sun Yat-sen University (Permit Number: SYXK 2016-0112).

Behavioral Tasks

Morris Water Maze Test

At 8 months of age, all mice were subjected to the Morris water maze task (Mueller et al., 2008) for 5 days (d), as an evaluation of their learning and memory abilities. During the 5-day evaluation, the treatments in both experiment and control groups remained the same. All the apparatus and the test procedure utilized were described before (Vorhees and Williams, 2006). Briefly, the apparatus included a circular white metal pool, whose diameter was 160 cm and height 50 cm, and the pool was filled with 26-cm deep water at constant temperature (22 ± 1°C) throughout the experiment. The water pool was divided into four quadrants by the water maze software, and had a translucent acrylic platform. The translucent acrylic platform was 12 cm in diameter, and 24 cm in height. It was placed in the center of the northwest quadrant, 1∼2.0 cm below the water surface.

Spatial Learning Test

The spatial learning task was conducted for five training days with four consecutive trials per day. The location of platform was remained constant with the starting position chosen among four quadrants in sequence at the pool rim every day. At the beginning of each trial, the mice would be gently released into the water with their noses against the wall at each starting point (north, south, east, and west). Every mouse was given a maximum of 60 s to find the hidden platform. If the mouse failed to find the escape platform within 60 s on the training day, it was then manually guided to the platform for 30 s. A camera was mounted in the ceiling directly above the pool to record the escape trace of each mouse. All trials were recorded using an HVS (human visual system) water maze program for subsequent analyses of escape latency (Water Maze 3, Actimetrics, Evanston, IL, United States). All experimental procedures were performed in a blind method, where investigators were blinded to group assignment of each mouse.

Probe Trial

To evaluate short-term and long-term memory consolidation, probe trials were conducted at 24 and 72h, respectively, after the last trial. To perform the memory consolidation evaluation, the platform was removed at first. Then, the mice were placed into the quadrant of the pool opposite to the one pre-placed with the platform. The mice were given 60 s to swim in each probe trial. Both the time spent in the quadrant preplaced with the platform and the time spent across the platform position were recorded to evaluate short-term and long-term memory.

Primary Culture of Hippocampal Neurons

Primary hippocampal neurons were achieved from postnatal (P0–P1) 3×Tg-AD and WT mice pups born within 24 h. After being dissected from the brain, the hippocampi were then digested with 2 mg/mL papain for 30 min at 37°C. Afterwards, the digested tissue was triturated and suspended in DMEM with 10% FBS. Dissociated cells were cultured in the neurobasal medium with 0.5 mM of L-glutamine, 2% B27 supplement, and 50 U/mL of penicillin–streptomycin. All the cultivation process would be conducted in poly-D-lysine-coated 6-well cell culture plates/culture dishes at a density of 0.5×10^6 cells/per well. The cells were cultured in a 37°C incubator with 95% O_2 and 5% CO_2. The medium was completely replaced after 4 h, and half of the medium was then replaced every 3 days. On day 13, the neurons were treated with 1 μM fluoxetine (diluted from 20 mM fluoxetine stock solution dissolved in culture medium) for 24 h. Neurons from 3×Tg-AD mice treated with the culture medium were set up as the control group.

ELISA for Aβ1–42 and Aβ40 Levels

Aβ1–42 and Aβ40 levels were assessed by ELISA (enzyme-linked immunosorbent assay). Primary cultured hippocampal neurons and medium from WT, 3×Tg-AD and 3×Tg-AD+fluoxetine groups were collected. The levels of extracellular and intracellular Aβ1–42 and Aβ40 were evaluated through a sandwich ELISA kit, following the manufacturer's instruction.

Western Blot Assay

In the brain tissue-based assay, lysis buffer plus 1 mM PMSF and protease inhibitor cocktail were utilized to homogenize brain tissue samples from different group. In the cell-based assay, the utilized cells were harvested after 24 h of 1 μM of fluoxetine treatment. Then, the harvested cells were lysed with lysis buffer. BCA protein assay kit was utilized to measure protein concentration. And SDS-PAGE was used to extract the same amount of total protein (20 μg per well) from each sample. The extracted protein would then be transferred to polyvinylidene fluoride (PVDF) membranes. After blocking with 5% fat-free

milk, corresponding primary antibodies (**Table 1**) were used to probe, which would then be incubated with HRP-conjugated anti-rabbit antibody or HRP-anti-mouse antibody. The blots were developed with ECL detection reagents and visualized with a KODAK Image Station 4000 MM (Carestream Health Inc., New Haven, CT, United States). All band intensities were quantified using Quantity One software.

Immunofluorescence Staining and Histological Analysis

Five-micrometer-thick sagittal paraffin sections of mouse hippocampus were mounted on glass slides. Before incubation, they were pretreated with 0.01 mol/L citrate buffer (pH = 6.0) in hyperthermy for 5 min. 5% goat serum in PBS was used to block the sections for 10 min. After the above pretreatments, there performed two incubations. The first one was performed with primary antibodies at 4°C, overnight. The second incubation was with secondary antibodies (1: 500 in PBS) at 37°C, 1 h. The primary antibodies used were specific to Aβ1–42, NeuN, and β-catenin. The Alexa-Fluor fluorescent dye-conjugated secondary antibodies (anti-mouse and anti-rabbit; Alexa Fluor 488 and 695, Multi Sciences Biotech) were used to detect MAP2 and PSD95. Three equidistant sections including the whole hippocampus were assessed per sample. To analyze and quantify immunoreactive areas, these sections were imaged with fluorescence microscopy (Olympus, Japan) and analyzed with Image-Pro Plus 6.0 software (Media Cybernetics).

TdT-Mediated dUTP Nick-End Labeling

Neurons were washed three times with 0.01 MPBS, 5 min each time. 4% paraformaldehyde was used to fix the neurons for 30 min, and 0.1% Triton X-100 in 0.1% sodium citrate was used to permeate them. The TdT-mediated dUTP nick-end labeling (TUNEL) was conducted via In Situ Cell Death Detection Kit, Fluorescein (Roche), following the manufacturer's protocols. Hoechst 33342 was used to counter stain the neuronal nuclei. Fluorescence images were obtained with an Olympus fluorescent microscope (Olympus), and TUNEL-positive cells were counted under a 20× objective.

Quantitative RT-PCR Analysis (qRT-PCR)

TRIzol reagent (Invitrogen, Carlsbad, CA, United States) was utilized to exact the total RNA from the cells. And a qSYBR-green-containing PCR kit (Qiagen, Germantown, MD, United States) was utilized to conduct reverse transcription and qRT-PCR reactions. The fold change was determined as $2^{-\Delta\Delta C_t}$, where *C*t standard for the number of fractional cycle where the fluorescence of each sample passed the fixed threshold. All of the real-time PCR assays were performed with the Bio-Rad IQTM5 Multicolor Real-Time PCR Detection System (United States).

Statistical Analysis

All data was in the form of mean ± SEM or mean ± SD. All statistical analysis were performed using SPSS 19.0 software (IBM SPSS Inc., Chicago, IL, United States). Two-way repeated ANOVA was used to analyze the latency of MWM test. And two-way ANOVA and Bonferroni's *post hoc* tests were utilized to analyze the rest data. $p < 0.05$ was considered as statistically significant.

RESULTS

Spatial Learning and Memory Test

The general health conditions of the 3×Tg-AD mice during the fluoxetine treatment were carefully monitored during the trial period, and no significant changes were found in the body weight of the mice before and after the trial.

Spatial learning was evaluated by the length of the time to find the hidden platform (i.e., escape latency). The results of all mice during the water maze acquisition training could be found in **Figure 1A** ($p < 0.05$). From the perspective of daily escape latency, the spatial learning ability of the mice was effectively improved in both groups after the 5-day consecutive training period. Compared with the 3×Tg-AD mice group, a significantly shorter escape latency was observed for the fluoxetine-treated 3×Tg-AD mice ($p < 0.05$). However, in *post hoc* multiple comparisons, there was no significant differences across all groups regarding swimming speed (**Figure 1B**, $p > 0.05$). The data suggests that fluoxetine could have a significant influence in attenuating spatial learning deficits in 8-month-old 3×Tg-AD mice.

Following the 5-day training, probe trials were conducted to evaluate short-term (24 h later) and long-term (72 h later) memory on the 6th and 8th day, respectively (**Figures 1C,D**). Compared with the WT mice group, 3×Tg-AD mice group exhibited a longer path distance ($p < 0.01$) across all trial sessions (**Figures 1C,D**). Between the fluoxetine -treated group and the 3×Tg-AD mice group, a statistically significant difference was observed in both short-term and long-term memory test in terms of the length of time searching for target quadrant, and searching for non-target quadrants (**Figure 1C**, $p < 0.05$). When the 3×Tg-AD mice group was compared with WT group, the former spent significantly longer time than the latter group. Based on the assessment of the length of time searching for the pre-placed platform in both short-term and long-term memory test, a statistically significant improvement was observed in the fluoxetine treated group, compared with the 3×Tg-AD mice group (**Figure 1D**, $p < 0.05$). Mice in the treated groups were gender-matched, and no significant gender-specific differences in the results were observed. Compared three groups follow tracks, the fluoxetine treated 3×Tg-AD mice group and WT group were more similar (**Figure 1E**).

Fluoxetine Reduced the Production of Aβ in the Brains of 3×Tg-AD Mice

The effect of fluoxetine on Aβ burden in the brain was also investigated in the 3×Tg-AD mice. **Figures 2A,B** indicated the results of immunofluorescent staining and immunohistochemical staining for β-amyloid in the hippocampus of mice from all three groups. While little aggregation of β-amyloid was found in the WT mice, in the other

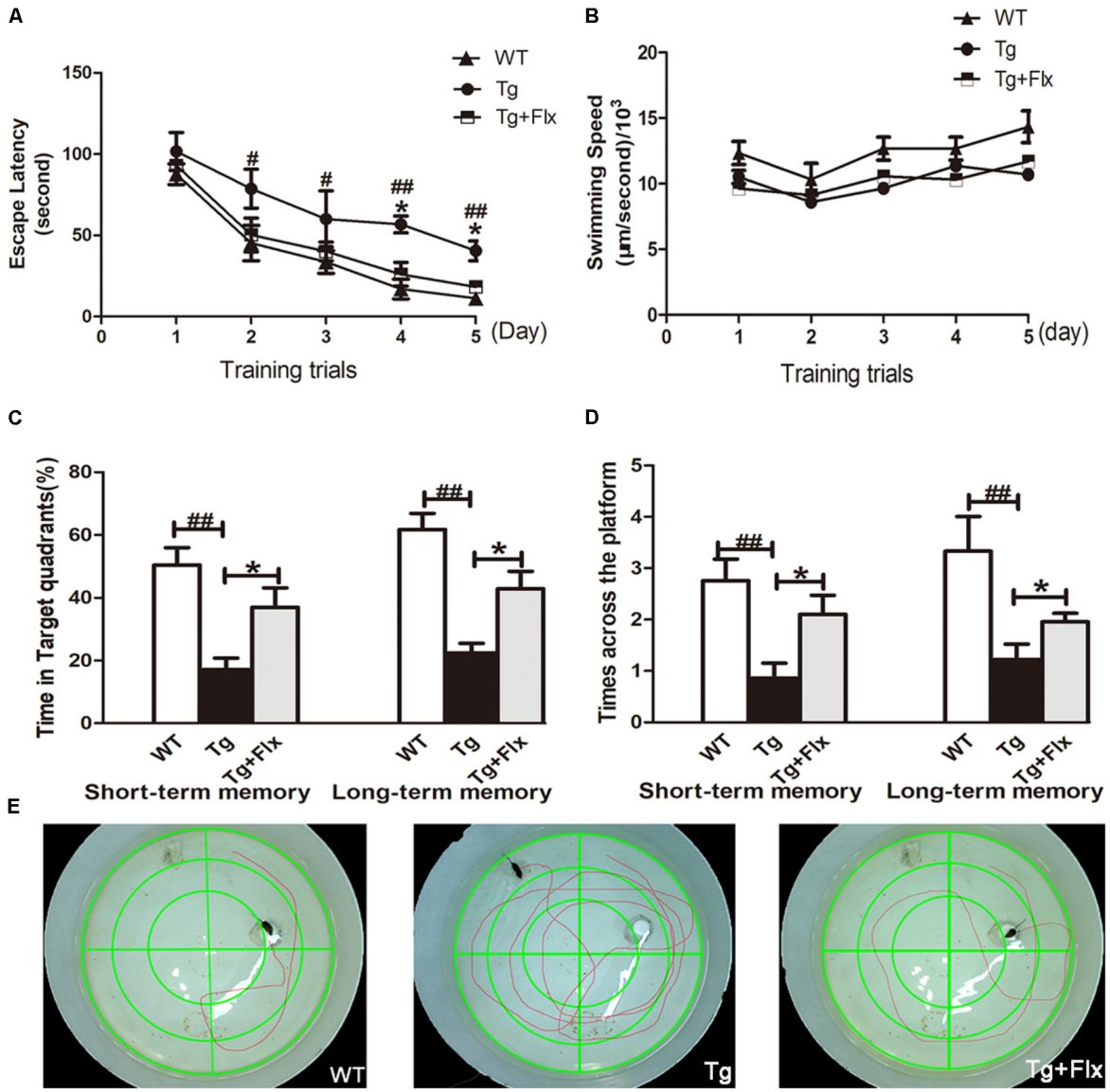


FIGURE 1 | Effects of fluoxetine on spatial learning and memory of 3×Tg-AD mice detected by the Morris water maze task. **(A)** In 5-day training trials, the escaping latencies of mice were measured to evaluate the three groups mouse memory ability. Based on the results, compared with vehicle control 3×Tg-AD mice. **(B)** Regarding the swimming speed, no significant differences were observed in all groups. **(C)** In the probe trail, the frequency that mice crossed the area where the submerged platform was placed in training trials was recorded. **(D)** In terms of the time spent searching for the pre-placed platform in the target quadrant, in both the short-term and long-term memory tests. **(E)** The swimming tracks the mice in the three groups made in the water tank on the last day of the test. WT, wild-type mice; Tg, 3×Tg-AD mice; Tg + FLX, fluoxetine treated 3×Tg-AD mice. Data were shown as mean ± SD, $n = 12$ animals/group. $^{\#}p < 0.05$, 3×Tg-AD group vs. WT group, $^{\#\#}p < 0.01$, 3×Tg-AD group vs. WT group. $^{*}p < 0.05$, fluoxetine treated 3×Tg-AD vs. 3×Tg-AD group.

two groups there could observe β-amyloid aggregation in the hippocampus (**Figures 2A,B**). Moreover, between the 3×Tg AD group and the 3×Tg AD + Flx group, the density of β-amyloid aggregating in the hippocampus was higher in the 3×Tg AD group, and the labeling for β-amyloid was also more intense (**Figure 2B**, $p < 0.05$). These findings were validated by ELISA test. The levels of Aβ42 and Aβ40 increased significantly in the hippocampus of 3×Tg AD mice, when compared with the WT mice. Treatment with fluoxetine could inhibit the level of Aβ42 and Aβ40 in the 3×Tg AD mice (**Figures 2C,D**, $p < 0.01$).

Fluoxetine Enhances Non-amyloidogenic Processing of APP in 3×Tg-AD Mice Brain

To explore the impacts of fluoxetine on APP processing, the study also measured the levels of APP protein in 3×Tg-AD mouse brain with a 4-month fluoxetine treatment. As shown in **Figure 3A**, there was a significant increase in the levels of APP protein in the hippocampus of 3×Tg AD mice, compared with that of the WT mice ($p < 0.01$). Treatment with fluoxetine could

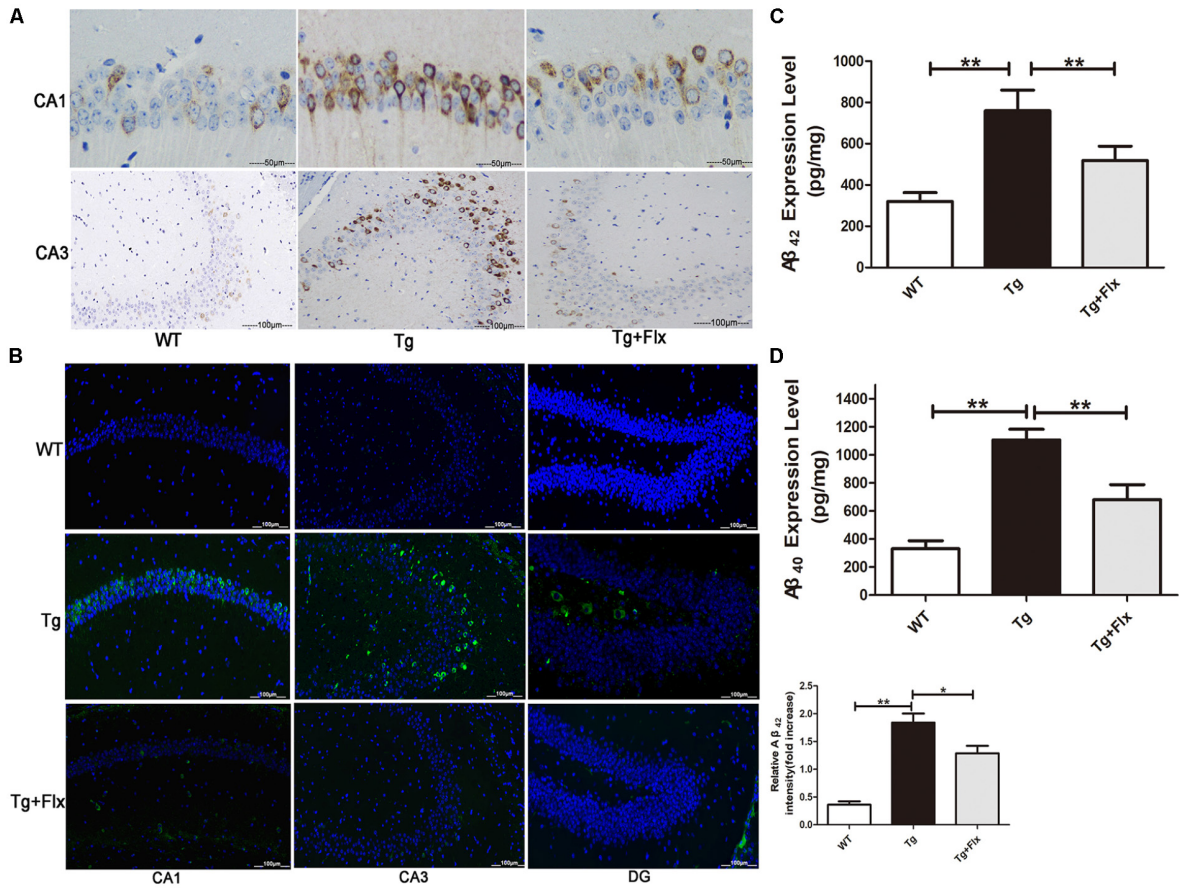


FIGURE 2 | Fluoxetine reduced the production of Aβ in the brains of 3×Tg-AD mice. Four-month old 3×Tg-AD mouse were treated with vehicle or fluoxetine (10 mg/kg/day) every day for 4 months and sacrificed for analysis. **(A)** Immunohistochemical staining for β-amyloid in the hippocampus of mice from the three groups. Scale bars: 100 μm. **(B)** Immunofluorescence of Aβ42 (green) in the hippocampi of mice from the three groups. Scale bars: 100 μm. **(C,D)** The levels Aβ42 and Aβ40 in the brains of three groups were detected by ELISA. WT, wild-type mice; Tg: 3×Tg-AD mice; Tg + FLX: fluoxetine treated 3×Tg-AD mice. Data were shown as mean ± SD, n = 12 animals/group.*$p < 0.05$, **$p < 0.01$.

reduce the level of APP protein in the 3×Tg AD mice (**Figure 3A**, $p < 0.05$). Then, it was investigated if fluoxetine was involved in APP cleavage. Western blot analysis was utilized to detect the APP cleavage enzymes and cleavage fragments in fluoxetine-treated 3×Tg-AD mouse brain (**Figure 3A**). Compared with that of WT mice, the protein levels of CTFs, BACE1, PS1, sAPPβ, and C99 in the hippocampus of 3×Tg AD mice were significantly higher. However, fluoxetine treatment could reduce the levels of protein-CTFs, BACE1, PS1, sAPPβ, and C99 in the hippocampus (**Figures 3A,B**) of the 3×Tg AD mice. We found that, compared with WT mice, 3×Tg AD mice had lower levels of ADAM10, sAPPα, and C83 in the hippocampus of, while fluoxetine treatment markedly enhanced the expression of ADAM10, sAPPα, and C83 in the hippocampus of 3×Tg AD mice.

The Promoting Effect of Fluoxetine on BDNF in the Brain of 3×Tg-AD Mice

The levels of BDNF in brain of three groups mice were measured. As indicated in **Figure 4A**, 3×Tg AD mice had remarkably lower levels of BDNF protein in the hippocampus than that of the WT mice ($p < 0.01$). Treatment with fluoxetine could have a positive impact on increasing the levels of BDNF protein in the 3×Tg AD mice ($p < 0.01$). **Figure 4B** indicated the results of immunofluorescent staining for NeuN in the hippocampus of mice from three groups, there was a decrease the number of cells stained with NeuN antibody in the 3×Tg AD mice compare with WT mice (**Figure 4B**, $p < 0.05$). Treatment with fluoxetine could increase the number of cells stained with NeuN antibody in the 3×Tg AD mice (**Figure 4B**, $p < 0.05$).

Fluoxetine Treatment Inhibited Apoptosis in Hippocampal Primary Neurons

As shown in **Figure 5A**, the 3×Tg AD primary neurons had a larger number of TUNEL-positive cells than the WT primary neurons ($p < 0.01$). Treatment of fluoxetine at 1 μM significantly reduced the number of TUNEL-positive cells ($p < 0.05$) in the 3×Tg AD primary neurons. As proved in previous research, the ratio between Bcl-2/Bcl-xl and Bax is correlated with

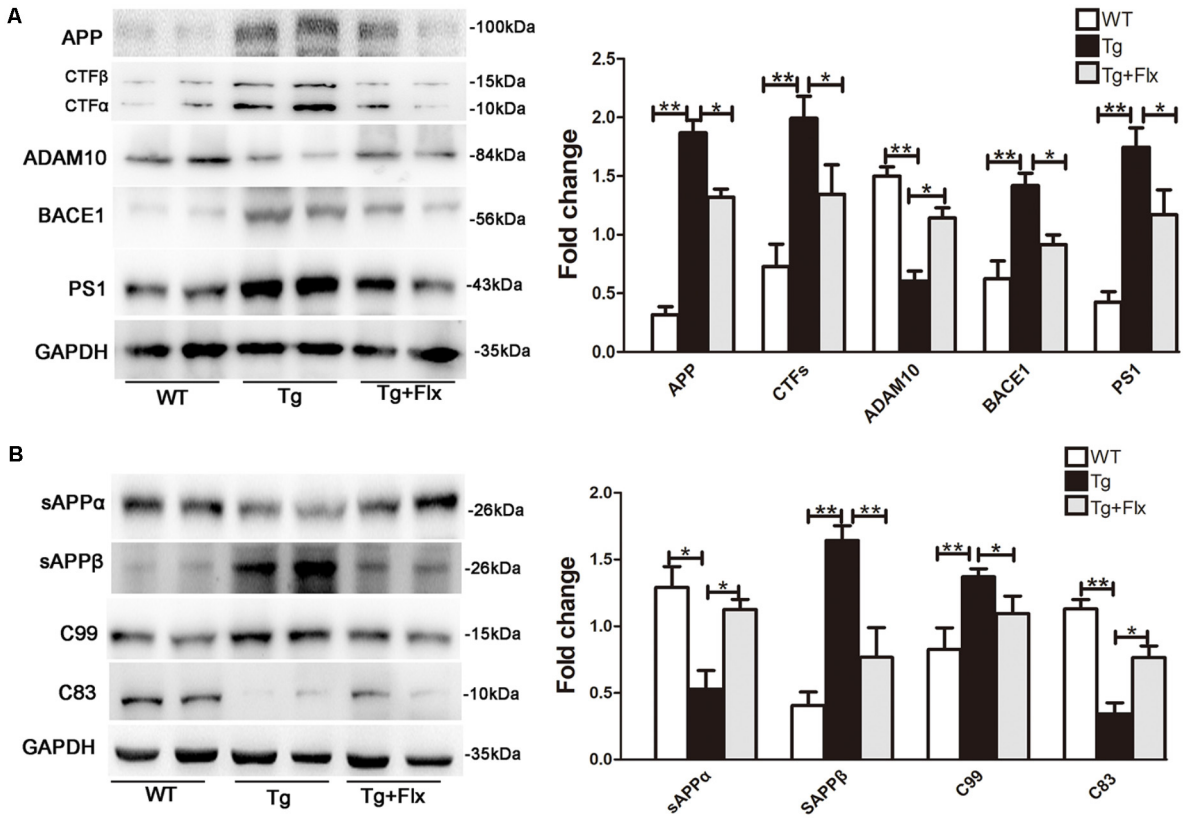


FIGURE 3 | Fluoxetine enhances the non-amyloidogenic pathway in 3×Tg-AD mice brain. **(A)** The western blot analysis was used to examine the expression levels of APP and APP cleavage enzymes, including APP, CTFβ, CTFα, ADAM10, BACE1, and PS1. **(B)** Levels of APP cleavage fragments, including sAPPα, sAPPβ, C83, and C99 generation, in the brain of three groups were assessed and quantified by immunoblotting. WT, wild-type mice; Tg: 3×Tg-AD mice; Tg + FLX: fluoxetine treated 3×Tg-AD mice. All data were shown as mean ± SD, $n = 12$ animals/group. $^{*}p < 0.05$, $^{**}p < 0.01$.

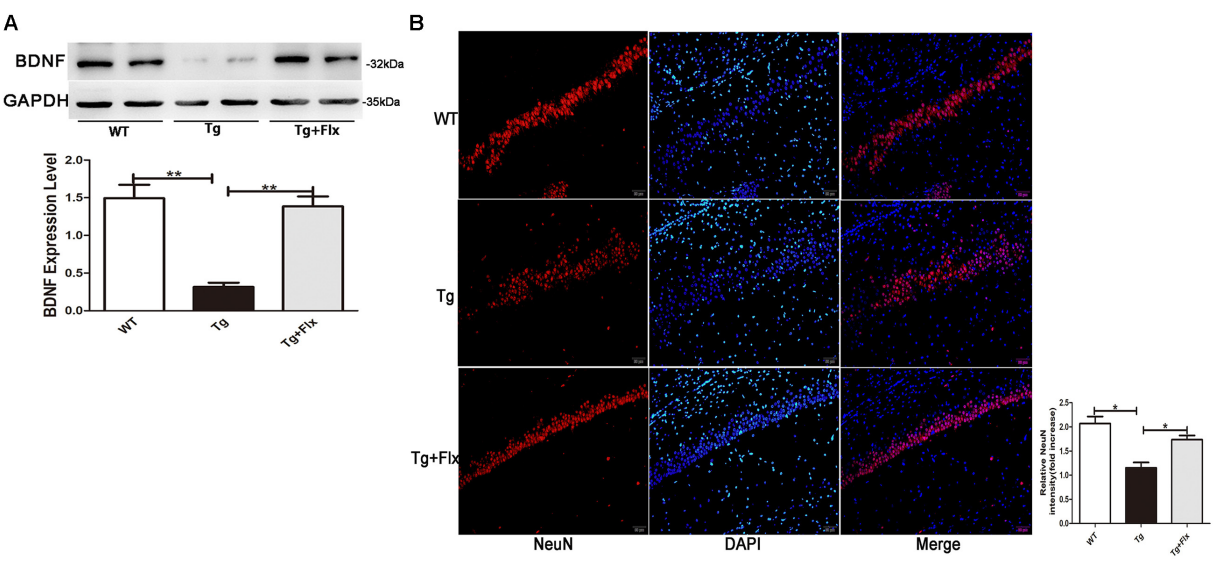


FIGURE 4 | Fluoxetine promotes BDNF in the brain of 3×Tg-AD mice. **(A)** The expression levels of BDNF were examined by western blot analysis. **(B)** Immunofluorescence of NeuN (red) in the hippocampi of mice from the three groups. Scale bars: 100 μm. WT, wild-type mice; Tg, 3×Tg-AD mice; Tg + FLX, fluoxetine treated 3×Tg-AD mice. Data were shown as mean ± SD, $n = 12$ animals/group. $^{*}p < 0.05$, $^{**}p < 0.01$.

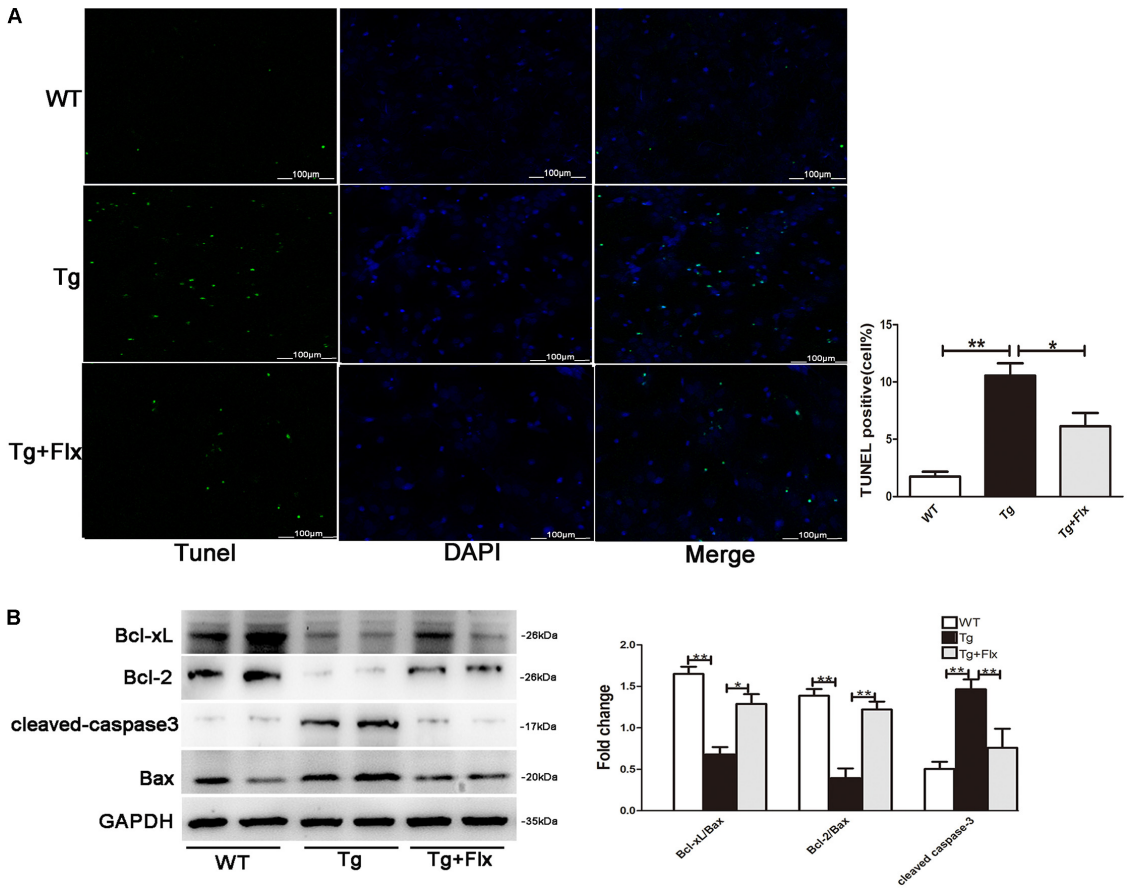


FIGURE 5 | Fluoxetine treatment inhibited apoptosis in hippocampal primary neurons. **(A)** The number of TUNEL-positive neurons (green). The number of TUNEL-positive neurons per 200× field in each group ($n = 6$) was averaged. $^{**}p < 0.001$ vs. control; Scale bar = 100 μm. **(B)** The western blot analysis was adopted to determine the Bcl-2, Bcl-xl cleaved-caspase 3, and Bax protein levels. WT, primarily cultured neurons of wild-type mice; Tg, primarily cultured neurons of 3×Tg-AD mice; Tg + FLX, primarily neurons of 3×Tg-AD mice treated with fluoxetine. Data were expressed as fold of control. $^{*}p < 0.05$ compared with control. $^{**}p < 0.01$ compared with control.

apoptosis (Liu et al., 2005). Thus, to investigate the molecular mechanism of the protective effect of fluoxetine in 3×Tg-AD primary neurons apoptosis, the expression of Bcl-2, Bcl-xl, and Bax was examined. Compared with the WT primary neurons, there could observe significant reduction in both Bcl-xl/Bax and Bcl-2/Bax expression ratio in the 3×Tg AD primary neurons. Treatment with fluoxetine significantly improved the Bcl-xl/Bax and Bcl-2/Bax expression ratio in the 3×Tg AD primary neurons. The levels of cleaved-caspase 3 were up-regulated in the 3×Tg AD primary neurons compared with the WT primary neurons (**Figure 5B**, $p < 0.01$). The results from the 3×Tg AD primary neurons demonstrated that treatment fluoxetine could significantly reverse this change (**Figure 5B**, $p < 0.01$).

Fluoxetine Targeted PP2A to Activate the Wnt/β-Catenin Signaling

The activity of PP2A would be inhibited by its phosphorylation at Tyr307 (Y307) residue of PP2A catalytic subunit (PP2Ac). Inversely, the ratio of PP2A-pY307/PP2Ac could reflect the activity of PP2A *in vivo*. It was observed that this ratio was significantly higher in 3×Tg AD mice than that in the WT mice (**Figure 6A**, $p < 0.05$). This implied that treatment with fluoxetine could reduce the ratio of PP2A pY307/PP2Ac in the 3×Tg AD mice (**Figure 6A**, $p < 0.05$). As the activity of GSK3β would require Y216 phosphorylation, the ratio of GSK3β pY216/GSK3β could then imply the activity of GSK3β *in vivo*. The research provided evidence that fluoxetine could significantly decrease the ratio of GSK3β pY216/GSK3β in the 3×Tg AD mice. A significant reduction in active β-catenin was observed in the hippocampus of 3×Tg AD mice when compared with the WT mice (**Figure 6B**, $p < 0.01$). Treatment with fluoxetine could increase the active β-catenin. The hippocampus of 3×Tg AD mice also demonstrated a significant higher level of active β-catenin, compared with that of WT mice (**Figure 6B**, $p < 0.01$). Thus, treatment with fluoxetine could decrease the inactive β-catenin. It implied that fluoxetine might be sufficient to enhance active β-catenin stabilization. To further confirm the protein expression of active β-catenin in the 3×Tg-AD mice brain,

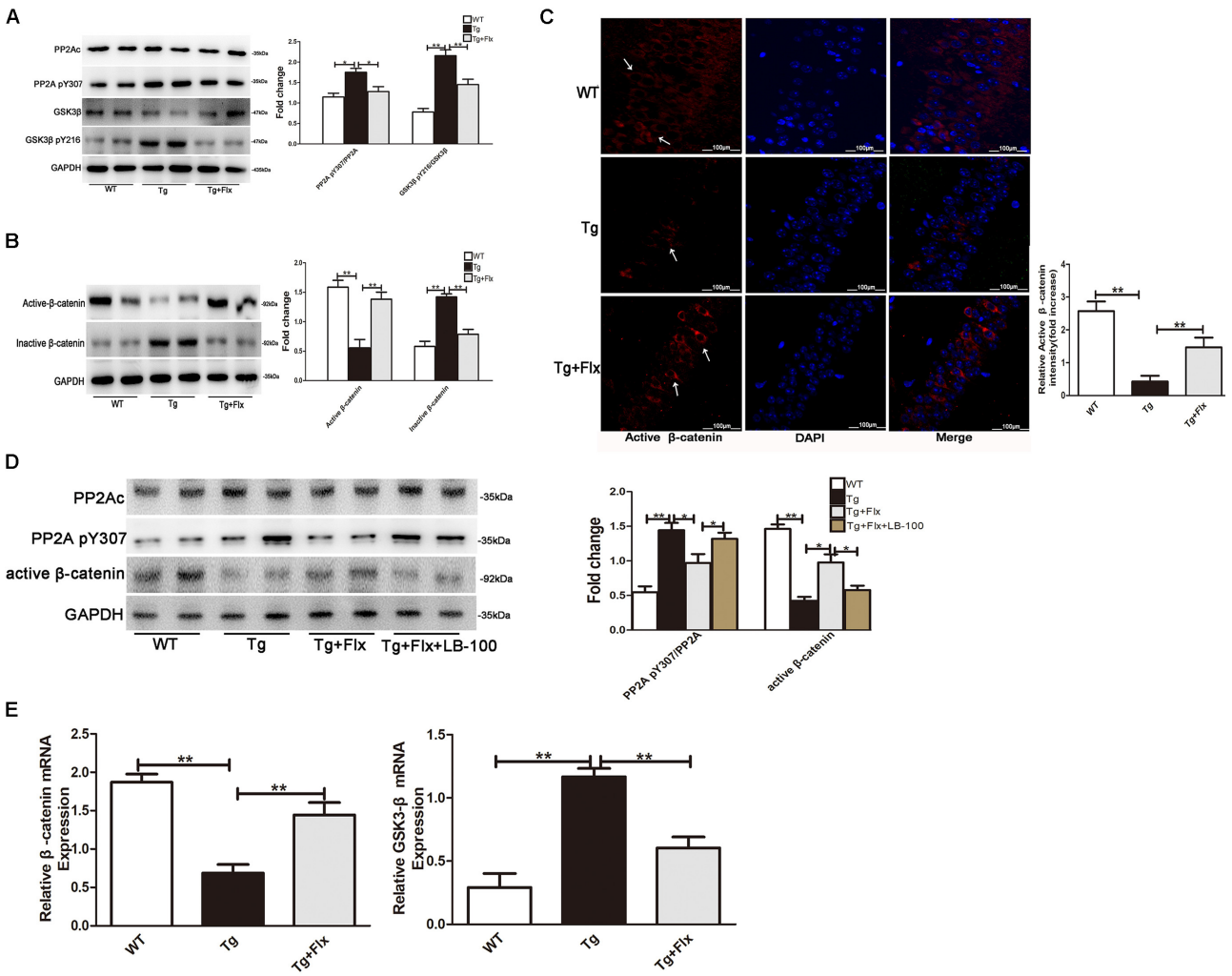


FIGURE 6 | (A) Western blots results that showed the expression levels of GSK3β and PP2A in the brains of mice. **(B)** Active β-catenin, and inactive β-catenin were studied through Western blot. **(C)** Immunofluorescence of β-catenin (red) and DAPI (blue) in the hippocampi of mice. WT, wild-type mice; Tg, 3×Tg-AD mice; Tg + FLX, fluoxetine treated 3×Tg-AD mice. **(D)** Analysis of primarily cultured neurons from mouse hippocampus. WT, primarily cultured neurons of wild-type mice; Tg, primarily cultured neurons of 3×Tg-AD mice; Tg + FLX, primarily neurons of 3×Tg-AD mice treated with fluoxetine. Tg + FLX+LB_100, primarily neurons of 3×Tg-AD mice treated with fluoxetine and LB_100 (an inhibitor of PP2A activity). **(E)** RT-PCR showed active β-catenin and GSK3β expression in the hippocampi of mice. Data are shown as mean ± SD, $n = 12$ animals/group. $^{*}p < 0.05$, $^{**}p < 0.01$.

an immunofluorescence analysis was performed (**Figure 6C**). Based on the immunofluorescence analysis, the level of active β-catenin in 3×Tg-AD mice was markedly increased in the treatment group ($p < 0.01$), compared with the 3×Tg-AD mice group (**Figure 6C**). Quantitative real-time (RT)-PCR analysis also confirmed that β-catenin mRNA expression was increased after fluoxetine treatment (**Figure 6D**, $p < 0.01$), while the mRNA levels of GSK3β were reduced (**Figure 6D**, $p < 0.01$) after fluoxetine treatment. The results suggested that fluoxetine treatment could efficiently activate Wnt/β-catenin signaling through inhibition of GSK3β in the 3×Tg-AD mice brain.

To further investigate if fluoxetine affected the Wnt/β-catenin signaling through PP2A activation, we isolated primarily cultured neurons, respectively, from the hippocampi of WT mouse and 3×Tg AD mouse. The cultured neurons from 3×Tg AD mouse were divided into three groups, which are 3×Tg AD, fluoxetine-treated 3×Tg AD, and fluoxetine-treated 3×Tg AD supplemented with LB-100(Tg+Flx+LB-100). LB-100, a specific inhibitor of PP2A, was used to suppress the activity of PP2A. As shown in **Figure 6E**, the 3×Tg AD primary neurons showed a significantly larger ratio of PP2A pY307/PP2Ac than the WT primary neurons. Treatment fluoxetine significantly decreased the ratio of PP2A pY307/PP2Ac in 3×Tg AD primary neurons, while adding LB-100 extensively eliminated the effect of fluoxetine. The remarkable reduction in active β-catenin between the 3×Tg AD and the WT primary neurons indicated that fluoxetine could raise the active β-catenin. Moreover, the data also demonstrated that adding LB-100 could extensively eliminate this impact from fluoxetine.

Fluoxetine Protection of Synapses

To determine the impact of fluoxetine treatment on synaptic functional protein expression, immunostaining analysis was performed in primary neurons, using synaptic marker PSD95 and MAP2, as shown in **Figure 7A**. A significant reduction in PSD95 was observed in the 3×Tg-AD primary neurons when compared with the WT primary neurons (**Figure 7A**). After fluoxetine treatment, PSD95 expression was partially recovered in the neuritis of 3×Tg-AD primary neurons. In addition, western blot was used to assay the level of synaptophysin and PSD95. Compared with the culture medium 3×Tg-AD primary neurons, the treatment with fluoxetine could increase the level of both synaptophysin (**Figure 7B**, $p < 0.05$) and PSD95 (**Figure 7B**, $p < 0.01$).

DISCUSSION

Although fluoxetine is a well-known neuroprotective agent (Qiao et al., 2016), there exists little information about how fluoxetine influences the Wnt/β-catenin signaling in the hippocampus of AD. Moreover, it remains unconfirmed if the activation of the Wnt/β-catenin signaling pathway has any anti-AD effect.

Utilizing 3×Tg-AD mice with an early-onset AD-like pathology, the study proved that regular administration of fluoxetine could stem the age-related cognitive impairments, as well as Aβ accumulation (Oddo et al., 2003b). Our research provides supports from multiple aspects that fluoxetine could have beneficial impacts on AD. First, utilizing the

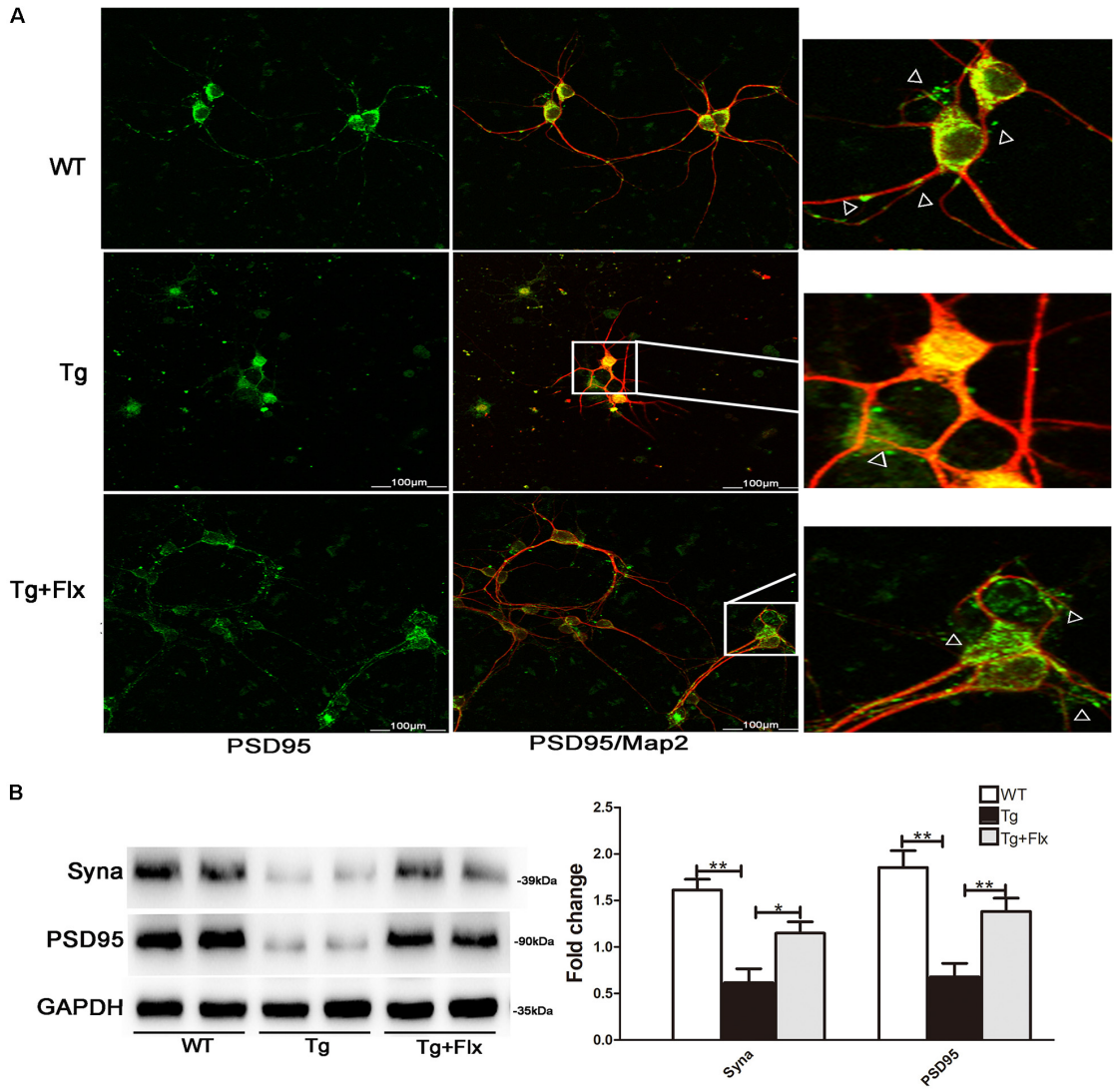


FIGURE 7 | Fluoxetine protection of synapses in 3×Tg-AD neurons. **(A)** Double-labeling analysis results for neurons from WT mice, 3×Tg-AD, and fluoxetine-treated 3×Tg-AD mice. Neuronal marker MAP2 (red) with post synaptic density protein 95 (PSD95) (green). Scale bar = 100 μm. **(B)** The levels of Syna and PSD95 expression were analyzed via Western blot assay. WT, primarily cultured neurons of wild-type mice; Tg, primarily cultured neurons of 3×Tg-AD mice; Tg + FLX, primarily neurons of 3×Tg-AD mice treated with fluoxetine. Data were shown as mean ± SD, $n = 12$ animals/group. $^*p < 0.05$, $^{**}p < 0.01$.

3×Tg-AD mouse model of AD, the study showed that fluoxetine could impact on brain Aβ levels, cognitive deficits, and amyloid neuropathology. Second, fluoxetine could prevent apoptosis in 3×Tg-AD primary neuronal cell. Third, fluoxetine could increase the expression of BDNF. Fourth, the study also demonstrates that fluoxetine could be able to protect neuron synapses. Moreover, our study proves evidence that fluoxetine would upregulates β-catenin expression and inhibits GSK3β expression *in vivo*. It suggests that there might be a correlation between neuroprotective effect of fluoxetine and the regulation of the Wnt signaling pathway in the AD brain.

It is widely accepted that Wnt/β-catenin signaling dysfunction plays a critical role in neurodegeneration process in the AD brain (Inestrosa and Toledo, 2008). GSK3β and β-catenin are two key components of the canonical Wnt/β-catenin signaling pathway. Previous research has demonstrated they could be considerably altered in the AD model mice brains (Zhang et al., 1998; Pei et al., 1999). Also, another study shows that activation of Wnt signaling can play a preventive impact on the neurodegeneration induced by Aβ fibrils (De Ferrari et al., 2003). The dysfunction of Wnt/β-catenin signaling induced by Aβ has been detected in AD and proved to be related to the neuron degeneration and synapse impairment. Researchers have detected the dysfunction of Wnt/β-catenin signaling induced by Aβ among AD. And this dysfunction has been proved to be associated with both neuron degeneration and synapse impairment (Thies and Bleiler, 2011; Inestrosa et al., 2012).

In this study, we showed that, when inactive β-catenin was increased in hippocampus of 3×Tg AD mice, active β-catenin could be reduced significantly. And the 3×Tg AD mouse demonstrated a remarkable reverse of these changes after treatment with fluoxetine. Meanwhile, the treatment of fluoxetine inhibited the cell apoptosis in the hippocampus of 3×Tg ADA primary neurons. These findings suggest that fluoxetine could be capable to activate the Wnt/β-catenin signaling to suppress the pathological hallmarks of AD.

Furthermore, more exploration was conducted regarding the relation across PP2A activity, Wnt/β-catenin signaling, and AD pathology, via utilizing the primarily cultured neurons from the hippocampus of 3×Tg AD mouse. Based on the results, we found that fluoxetine could significantly repair the function of Wnt/β-catenin signaling which had been impaired during the AD progression. LB-100, an inhibitor of PP2A, could extensively eliminated the effect of fluoxetine on β-catenin, which will result in the down-regulation of Wnt/β-catenin signaling and the neuronal apoptosis, Thus, it could be implied that fluoxetine could specifically activate PP2A to dephosphorylate β-catenin on S33/S37/T41 and GSK3β on Y216 for upregulation of Wnt/β-catenin signaling in 3×Tg AD mice.

Deposition of extracellular amyloid plagues in AD would also be subjected to PP2A regulation. PP2A could be capable of regulating the Aβ level through APP phosphorylation and BACE1 activity. Evidence from various aspects shows that APP could be cleaved within the sequence of the Aβ peptide and generate the sAPPα fragment through the α-secretase pathway (Esch et al., 1990). It would be beneficial for neuronal survival (Mattson et al., 1997; Wallace et al., 1997). However, through the β-secretase pathway, APP would be cleaved form neurotoxic Aβ and play a role in the pathogenesis of AD (Haass et al., 1992). This study focused on examining the role of fluoxetine in the APP process, based on the 3×Tg-AD mouse model of AD. The research found that expression level of APP proteins would be dramatically reduced in the fluoxetine-treated 3×Tg-AD mouse brain.

In this study, we examined the effects of fluoxetine on APP processing in the 3×Tg-AD mouse model of AD. Our data showed that the expression level of APP proteins would be dramatically reduced in the fluoxetine-treated 3×Tg-AD mouse brain. In this study, fluoxetine treatment could significantly enhance the expression level of ADAM10, a candidate of α-secretase. This was followed by an increase in the levels of both α-secretase-generated sAPPα and C83 fragments. Activation of the Wnt/β-catenin signaling reduced the transcription of BACE1. In our study, treatment with fluoxetine was shown to activate the Wnt/β-catenin signaling, which in term down regulated the expression of BACE1 in the hippocampus of 3×Tg AD mouse. These processes contributed to the decreased generation of Aβ. The results suggest that the Wnt/β-catenin signaling would play a significant part in regulating BACE1 expression, which then make Wnt/β-catenin signaling a core player in the formation of extracellular amyloid plagues.

Previous study has revealed that mitochondria could play a key role in regulating cell death, especially cell apoptosis (Yu et al., 2015). The dysfunction of mitochondria might become a hallmark of neuronal toxicity in AD (Xi et al., 2012; Zhang et al., 2012, 2016). Several researches also report that Bcl-2 family protein could play a certain role in regulating neuronal apoptotic cell death (Basu et al., 2006; Mancuso et al., 2008; Cartier et al., 2012). One of the key factors for the apoptotic state of cell would be the ratio between pro-apoptotic proteins and anti-apoptotic proteins (Yu et al., 2015). The result of western blot analysis shows that fluoxetine could significantly increase both expression ratios (Bcl-2/Bax and Bcl-xl/Bax) and, at the same time, decrease the number of TUNEL-positive cell compared with the culture treated with culture medium only. Thus, it is suggested that fluoxetine could inhibit the apoptosis, which involves the regulation of Bcl-2 family proteins.

BDNF is a neurotrophic factor, it is well known that BDNF is involved in the growth of neurites and synaptic plasticity (Sandhya et al., 2013). Fluoxetine might preserve synaptic protein expression, thus improve learning and memory abilities. After fluoxetine treatment, PSD95 and synaptic expression were partially recovered in the 3×Tg-AD neurons. The data above and the *in vivo* results together strongly implies that fluoxetine

could be capable to abolish Aβ generation and preserve synaptic functional proteins.

CONCLUSION

Treatment with fluoxetine would significantly enhance the activity of PP2A and repress the pathology of AD significantly. After activated by fluoxetine, the PP2A could increase active β-catenin level and inhibit GSK3β activity in the hippocampus of 3×Tg AD mouse, which then could lead to signal the Wnt/β-catenin signaling. The treatment could relieve the APP cleavage and Aβ generation. Taking all these results into consideration, it could be concluded that fluoxetine could activate Wnt/β-catenin signaling via PP2A to repress the cross-talk among Aβ generation and neuronal apoptosis. These results suggest that fluoxetine could have a potential for the therapy of Alzheimer's disease through the activation of Wnt/β-catenin signaling.

AUTHOR CONTRIBUTIONS

MH, YL, and HC: conceived, designed, and performed the experiments. MH, YL, BX, CC, and PX: analyzed the data. MH: wrote the paper.

FUNDING

This work was supported by the National Natural Science Foundation of China (Grant No. 81503616) and the Project of Administration of Traditional Chinese Medicine of Guangdong Province of China (No.20181064).

REFERENCES

Basu, A., DuBois, G., and Haldar, S. (2006). Posttranslational modifications of Bcl2 family members–a potential therapeutic target for human malignancy. *Front. Biosci.* 11, 1508–1521. doi: 10.2741/1900

Billings, L. M., Oddo, S., Green, K. N., McGaugh, J. L., and LaFerla, F. M. (2005). Intraneuronal Aβ causes the onset of early Alzheimer's disease-related cognitive deficits in transgenic mice. *Neuron* 45, 675–688. doi: 10.1016/j.neuron.2005.01.040

Cartier, J., Marivin, A., Berthelet, J., and Dubrez, L. (2012). IAPs: a central element in the NF-κB activating signaling pathway. *Med. Sci.* 28, 69–75. doi: 10.1051/medsci/2012281019

Davidson, G., Wu, W., Shen, J. L., Bilic, J., Fenger, U., Stannek, P., et al. (2005). Casein kinase 1 gamma couples Wnt receptor activation to cytoplasmic signal transduction. *Nature* 438, 867–872. doi: 10.1038/nature04170

De Ferrari, G. V., Chacon, M. A., Barria, M. I., Garrido, J. L., Godoy, J. A., Olivares, G., et al. (2003). Activation of Wnt signaling rescues neurodegeneration and behavioral impairments induced by beta-amyloid fibrils. *Mol. Psychiatry* 8, 195–208. doi: 10.1038/sj.mp.4001208

Esch, F. S., Keim, P. S., Beattie, E. C., Blacher, R. W., Culwell, A. R., Oltersdorf, T., et al. (1990). Cleavage of amyloid beta peptide during constitutive processing of its precursor. *Science* 248, 1122–1124. doi: 10.1126/science.2111583

Haass, C., Schlossmacher, M. G., Hung, A. Y., Vigo-Pelfrey, C., Mellon, A., Ostaszewski, B. L., et al. (1992). Amyloid beta-peptide is produced by cultured cells during normal metabolism. *Nature* 359, 322–325. doi: 10.1038/359322a0

Inestrosa, N. C., Montecinos-Oliva, C., and Fuenzalida, M. (2012). Wnt signaling: role in Alzheimer disease and schizophrenia. *J. Neuroimmune Pharmacol.* 7, 788–807. doi: 10.1007/s11481-012-9417-5

Inestrosa, N. C., and Toledo, E. M. (2008). The role of *Wnt* signaling in neuronal dysfunction in Alzheimer's disease. *Mol. Neurodegener.* 3:9. doi: 10.1186/1750-1326-3-9

Inestrosa, N. C., and Varela-Nallar, L. (2014). Wnt signaling in the nervous system and in Alzheimer's disease. *J. Mol. Cell Biol.* 6, 64–74. doi: 10.1093/jmcb/mjt051

Li, W. L., Cai, H. H., Wang, B., Chen, L., Zhou, Q. G., Luo, C. X., et al. (2009). Chronic fluoxetine treatment improves ischemia-induced spatial cognitive deficits through increasing hippocampal neurogenesis after stroke. *J. Neurosci. Res.* 87, 112–122. doi: 10.1002/jnr.21829

Li, X., Zhu, W., Roh, M. S., Friedman, A. B., Rosborough, K., and Jope, R. S. (2004). *In vivo* regulation of glycogen synthase kinase-3beta (GSK3beta) by serotonergic activity in mouse brain. *Neuropsychopharmacology* 29, 1426–1431. doi: 10.1038/sj.npp.1300439

Liu, C. C., Tsai, C. W., Deak, F., Rogers, J., Penuliar, M., Sung, Y. M., et al. (2014). Deficiency in LRP6-mediated Wnt signaling contributes to synaptic abnormalities and amyloid pathology in Alzheimer's disease. *Neuron* 84, 63–77. doi: 10.1016/j.neuron.2014.08.048

Liu, R., and Wang, J. Z. (2009). Protein phosphatase 2A in Alzheimer's disease. *Pathophysiology* 16, 273–277. doi: 10.1016/j.pathophys.2009.02.008

Liu, Z., Lu, H., Jiang, Z., Pastuszyn, A., and Hu, C. A. (2005). Apolipoprotein l6, a novel proapoptotic Bcl-2 homology 3-only protein, induces mitochondria-mediated apoptosis in cancer cells. *Mol. Cancer Res.* 3, 21–31.

Ma, J., Gao, Y., Jiang, L., Chao, F. L., Huang, W., and Zhou, C. N. (2017). Fluoxetine attenuates the impairment of spatial learning ability and prevents neuron loss in middle-aged APPswe/PSEN1dE9 double transgenic Alzheimer's disease mice. *Oncotarget* 8, 27676–27692. doi: 10.18632/oncotarget.15398

Mancuso, M., Orsucci, D., Siciliano, G., and Murri, L. (2008). Mitochondria, mitochondrial DNA and Alzheimer's disease. What comes first? *Curr. Alzheimer Res.* 5, 457–468. doi: 10.2174/156720508785908946

Mattson, M. P., Barger, S. W., Furukawa, K., Bruce, A. J., Wyss-Coray, T., Mark, R. J., et al. (1997). Cellular signaling roles of TGF beta, TNF alpha and beta APP in brain injury responses and Alzheimer's disease. *Brain Res. Brain Res. Rev.* 23, 47–61. doi: 10.1016/S0165-0173(96)00014-8

Miller-Thomas, M. M., Sipe, A. L., Benzinger, T. L., McConathy, J., Connolly, S., and Schwetye, K. E. (2016). Multimodality review of amyloid-related diseases of the central nervous system. *Radiographics* 36, 1147–1163. doi: 10.1148/rg.2016150172

Modrego, P. J. (2010). Depression in Alzheimer's disease. Pathophysiology, diagnosis, and treatment. *J. Alzheimers Dis.* 21, 1077–1087. doi: 10.3233/JAD-2010-100153

Mowla, A., Mosavinasab, M., Haghshenas, H., and Borhani Haghighi, A. (2007). Does serotonin augmentation have any effect on cognition and activities of daily living in Alzheimer's dementia? A double-blind, placebo-controlled clinical trial. *J. Clin. Psychopharmacol.* 27, 484–487. doi: 10.1097/jcp.0b013e31814b98c1

Mueller, S. C., Temple, V., Oh, E., VanRyzin, C., Williams, A., Cornwell, B., et al. (2008). Early androgen exposure modulates spatial cognition in congenital adrenal hyperplasia (CAH). *Psychoneuroendocrinology* 33, 973–980. doi: 10.1016/j.psyneuen.2008.04.005

Oddo, S., Caccamo, A., Kitazawa, M., Tseng, B. P., and LaFerla, F. M. (2003a). Amyloid deposition precedes tangle formation in a triple transgenic model of Alzheimer's disease. *Neurobiol. Aging* 24, 1063–1070.

Oddo, S., Caccamo, A., Shepherd, J. D., Murphy, M. P., Golde, T. E., Kayed, R., et al. (2003b). Triple-transgenic model of Alzheimer's disease with plaques and tangles: intracellular Abeta and synaptic dysfunction. *Neuron* 39, 409–421. doi: 10.1016/S0896-6273(03)00434-3

Oulès, B., Del Prete, D., Greco, B., Zhang, X., Lauritzen, I., Sevalle, J., et al. (2012). Ryanodine receptors blockade reduces Amyloid-beta load and memory impairments in Tg2576 mouse model of Alzheimer disease. *J. Neurosci.* 32, 11820–11834. doi: 10.1523/JNEUROSCI.0875-12.2012

Patapoutian, A., and Reichardt, L. F. (2000). Roles of Wnt proteins in neural development and maintenance. *Curr. Opin. Neurobiol* 10, 392–399. doi: 10.1016/S0959-4388(00)00100-8

Pei, J. J., Braak, E., Braak, H., Grundke-Iqbal, I., Iqbal, K., Winblad, B., et al. (1999). Distribution of active glycogen synthase kinase 3beta (GSK-3beta) in brains staged for Alzheimer disease neurofibrillary changes. *J. Neuropathol. Exp. Neurol.* 58, 1010–1019. doi: 10.1097/00005072-199909000-00011

Pilar-Cuellar, F., Vidal, R., and Pazos, A. (2012). Subchronic treatment with fluoxetine and ketanserin increases hippocampal brain-derived neurotrophic factor, beta-catenin and antidepressant-like effects. *Br. J. Pharmacol.* 165, 1046–1057. doi: 10.1111/j.1476-5381.2011.01516.x

Qiao, J., Wang, J., Wang, H., Zhang, Y., Zhu, S., Adilijiang, A., et al. (2016). Regulation of astrocyte pathology by fluoxetine prevents the deterioration of Alzheimer phenotypes in an APP/PS1 mouse model. *GLIA* 64, 240–254. doi: 10.1002/glia.22926

Rosso, S. B., and Inestrosa, N. C. (2013). WNT signaling in neuronal maturation and synaptogenesis. *Front Cell Neurosci.* 7:103. doi: 10.3389/fncel.2013.00103

Sandhya, V. K., Raju, R., Verma, R., Advani, J., Sharma, R., Radhakrishnan, A., et al. (2013). A network map of BDNF/TRKB and BDNF/p75NTR signaling system. *J. Cell Commun. Signal.* 7, 301–307. doi: 10.1007/s12079-013-0200-z

Scharre, D. W., and Chang, S. I. (2002). Cognitive and behavioral effects of quetiapine in Alzheimer disease patients. *Alzheimer Dis. Assoc. Disord.* 16, 128–130. doi: 10.1097/00002093-200204000-00011

Seeling, J. M., Miller, J. R., Gil, R., Moon, R. T., White, R., and Virshup, D. M. (1999). Regulation of beta-catenin signaling by the B56 subunit of protein phosphatase 2A. *Science* 283, 2089–2091. doi: 10.1126/science.283.5410.2089

Selkoe, D. J. (2004). Cell biology of protein misfolding: the examples of Alzheimer's and Parkinson's diseases. *Nat. Cell Biol.* 6, 1054–1061. doi: 10.1038/ncb1104-1054

Sontag, E., Nunbhakdi-Craig, V., Sontag, J. M., Diaz-Arrastia, R., Ogris, E., Dayal, S., et al. (2007). Protein phosphatase 2A methyltransferase links homocysteine metabolism with tau and amyloid precursor protein regulation. *J. Neurosci.* 27, 2751–2759. doi: 10.1523/JNEUROSCI.3316-06.2007

Suh, Y. H., and Checler, F. (2002). Amyloid precursor protein, presenilins, and alphasynuclein: Molecular pathogenesis and pharmacological applications in Alzheimer's disease. *Pharmacol. Rev.* 54, 469–525. doi: 10.1124/pr.54.3.469

Sun, D. S., Gao, L. F., Jin, L., Wu, H., Wang, Q., Zhou, Y., et al. (2017). Fluoxetine administration during adolescence attenuates cognitive and synaptic deficits in adult 3 × TgAD mice. *Neuropharmacology* 126, 200–212. doi: 10.1016/j.neuropharm.2017.08.037

Thies, W., and Bleiler, L. (2011). Alzheimer's association report 2011 Alzheimer's disease facts and figures. *Alzheimers Dement.* 7, 208–244. doi: 10.1016/j.jalz.2011.02.004

Triaca, V., Sposato, V., Bolasco, G., Ciotti, M. T., Pelicci, P., Bruni, A. C., et al. (2016). NGF controls APP cleavage by downregulating APP phosphorylation at Thr668: relevance for Alzheimer's disease. *Aging Cell* 15, 661–672. doi: 10.1111/acel.12473

Vorhees, C. V., and Williams, M. T. (2006). Morris water maze: procedures for assessing spatial and related forms of learning and memory. *Nat. Protoc.* 1, 848–858. doi: 10.1038/nprot.2006.116

Voronkov, M., Braithwaite, S. P., and Stock, J. B. (2011). Phosphoprotein phosphatase 2A: a novel druggable target for Alzheimer's disease. *Future Med. Chem.* 3, 821–833. doi: 10.4155/fmc.11.47

Wallace, W. C., Akar, C. A., and Lyons, W. E. (1997). Amyloid precursor protein potentiates the neurotrophic activity of NGF. *Brain Res. Mol. Brain Res.* 52, 201–212. doi: 10.1016/S0169-328X(97)00258-1

Wang, J., Zhang, Y., Xu, H., Zhu, S., Wang, H., He, J., et al. (2014). Fluoxetine improves behavioral performance by suppressing the production of soluble β-amyloid in APP/PS1 mice. *Curr. Alzheimer Res.* 11, 672–680. doi: 10.2174/1567205011666140812114715

Xi, Y. D., Yu, H. L., Ding, J., Ma, W. W., Yuan, L. H., Feng, J. F., et al. (2012). Flavonoids protect cerebrovascular endothelial cells through Nrf2 and PI3Kfrom â-amyloid peptide-induced oxidative damage. *Curr. Neurovasc. Res.* 9, 32–41. doi: 10.2174/156720212799297092

Yu, T. X., Zhang, P., Guan, Y., Wang, M., and Zhen, M. Q. (2015). Protective effects of luteolin against cognitive impairment induced by infusion of Aβ peptide in rats. *Int. J.Clin. Exp. Pathol.* 8, 6740–6747.

Zeng, X., Huang, H., Tamai, K., Zhang, X. J., Harada, Y., Yokota, C., et al. (2008). Initiation of Wnt signaling: control of Wnt coreceptor Lrp6 phosphorylation/activation via frizzled, dishevelled and axin functions. *Development* 135, 367–375. doi: 10.1242/dev.013540

Zhang, Q., Huang, W. D., Lv, X. Y., and Yang, Y. M. (2012). Puerarin protects differentiated PC12 cells from H2O2-induced apoptosis through the PI3K/Akt signalling pathway. *Cell Biol. Int.* 36, 419–426. doi: 10.1042/CBI20100900

Zhang, X., Liang, D., Lian, X., Jiang, Y., He, H., Liang, W., et al. (2016). Berberine activates Nrf2 nuclear translocation and inhibits apoptosis induced by high glucose in renal tubular epithelial cells through a phosphatidylinositol 3-kinase/Akt-dependent mechanism. *Apoptosis* 21, 721–736. doi: 10.1007/s10495-016-1234-5

Zhang, Z., Hartmann, H., Do, V. M., Abramowski, D., Sturchler-Pierrat, C., Staufenbiel, M., et al. (1998). Destabilization of beta-catenin by mutations in presenilin-1 potentiates neuronal apoptosis. *Nature* 395, 698–702. doi: 10.1038/27208

Zuroff, L., Daley, D., Black, K. L., and Koronyo-Hamaoui, M. (2017). Clearance of cerebral Aβ in Alzheimer's disease: reassessing the role of microglia and monocytes. *Cell Mol. Life. Sci.* 74, 2167–2201. doi: 10.1007/s00018-017-2463-7

Conflict of Interest Statement: The authors declare that the research was conducted in the absence of any commercial or financial relationships that could be construed as a potential conflict of interest.

Copyright © 2018 Huang, Liang, Chen, Xu, Chai and Xing. This is an open-access article distributed under the terms of the Creative Commons Attribution License (CC BY). The use, distribution or reproduction in other forums is permitted, provided the original author(s) and the copyright owner are credited and that the original publication in this journal is cited, in accordance with accepted academic practice. No use, distribution or reproduction is permitted which does not comply with these terms.

frontiers in Aging Neuroscience

ORIGINAL RESEARCH
published: 05 March 2018
doi: 10.3389/fnagi.2018.00050

Royal Jelly Reduces Cholesterol Levels, Ameliorates Aβ Pathology and Enhances Neuronal Metabolic Activities in a Rabbit Model of Alzheimer's Disease

Yongming Pan[1,2], Jianqin Xu[2], Cheng Chen[2], Fangming Chen[2], Ping Jin[3], Keyan Zhu[2], Chenyue W. Hu[4], Mengmeng You[1], Minli Chen[2] and Fuliang Hu[1]**

[1]College of Animal Sciences, Zhejiang University, Hangzhou, China, [2]Comparative Medical Research Center, Experimental Animal Research Center, Zhejiang Chinese Medical University, Hangzhou, China, [3]The First Affiliated Hospital, Zhejiang Chinese Medical University, Hangzhou, China, [4]Department of Bioengineering, Rice University, Houston, TX, United States

Alzheimer's disease (AD) is the most common form of dementia characterized by aggregation of amyloid β (Aβ) and neuronal loss. One of the risk factors for AD is high cholesterol levels, which are known to promote Aβ deposition. Previous studies have shown that royal jelly (RJ), a product of worker bees, has potential neuroprotective effects and can attenuate Aβ toxicity. However, little is known about how RJ regulates Aβ formation and its effects on cholesterol levels and neuronal metabolic activities. Here, we investigated whether RJ can reduce cholesterol levels, regulate Aβ levels and enhance neuronal metabolic activities in an AD rabbit model induced by 2% cholesterol diet plus copper drinking water. Our results suggest that RJ significantly reduced the levels of plasma total cholesterol (TC) and low density lipoprotein-cholesterol (LDL-C), and decreased the level of Aβ in rabbit brains. RJ was also shown to markedly ameliorate amyloid deposition in AD rabbits from Aβ immunohistochemistry and thioflavin-T staining. Furthermore, our study suggests that RJ can reduce the expression levels of β-site APP cleaving enzyme-1 (BACE1) and receptor for advanced glycation end products (RAGE), and increase the expression levels of low density lipoprotein receptor-related protein 1 (LRP-1) and insulin degrading enzyme (IDE). In addition, we found that RJ remarkably increased the number of neurons, enhanced antioxidant capacities, inhibited activated-capase-3 protein expression, and enhanced neuronal metabolic activities by increasing N-acetyl aspartate (NAA) and glutamate and by reducing choline and myo-inositol in AD rabbits. Taken together, our data demonstrated that RJ could reduce cholesterol levels, regulate Aβ levels and enhance neuronal metabolic activities in AD rabbits, providing preclinical evidence that RJ treatment has the potential to protect neurons and prevent AD.

Keywords: royal jelly, Alzheimer's disease, hypercholesterolemia, amyloid plaques, neuronal metabolism activity

OPEN ACCESS

Edited by:
Ghulam Md Ashraf, King Abdulaziz University, Saudi Arabia

Reviewed by:
Homira Behbahani, Karolinska Institute (KI), Sweden
Deep R. Sharma, SUNY Downstate Medical Center, United States

***Correspondence:**
Fuliang Hu
flhu@zju.edu.cn
Minli Chen
cmli991@zcmu.edu.cn

Received: *03 November 2017*
Accepted: *15 February 2018*
Published: *05 March 2018*

Citation:
Pan Y, Xu J, Chen C, Chen F, Jin P, Zhu K, Hu CW, You M, Chen M and Hu F (2018) Royal Jelly Reduces Cholesterol Levels, Ameliorates Aβ Pathology and Enhances Neuronal Metabolic Activities in a Rabbit Model of Alzheimer's Disease. Front. Aging Neurosci. 10:50. doi: 10.3389/fnagi.2018.00050

INTRODUCTION

Alzheimer's disease (AD), the most common type of dementia, is a primary degenerative disease that occurs in the central nervous system (CNS). About 44 million people are currently suffering from AD worldwide, and this population is estimated to exceed 131 million by 2050 (Comas Herrera et al., 2016). Except for 5% of AD cases that are familial, most of the cases are sporadic AD (SAD), the onset of which is largely influenced by both environmental and genetic factors (Selkoe, 2001; Lacher et al., 2018). Though no cure has been found for AD, medications such as cholinesterase inhibitors and N-methyl D-aspartate (NMDA) receptor antagonists are widely used to treat its symptoms. However, the long-term use of these drugs are known to cause serious side-effects (Fereshtehnejad et al., 2014), therefore mandating the development of alternative treatment options.

Since AD is characterized by amyloid β (Aβ) deposition and neuronal loss in the brain (Li et al., 2015), a growing number of studies have been trying to control AD by inhibiting the formation and deposition of Aβ. It was recently found that active ingredients of certain functional foods have anti-aging effects, indicating that dietary intervention may have the potential to prevent or delay the onset of AD (Celik and Sanlier, 2017). One functional food of particular interest is royal jelly (RJ; Ramadan and Al-Ghamdi, 2012), a secretion produced from the hypopharyngeal and mandibular glands of worker bees for feeding to and developing queen bees. Consumed worldwide as a functional food, RJ consists of proteins, carbohydrates, lipids, free amino acids, vitamins (Takenaka, 1982; Nagai and Inoue, 2004; Pourmoradian et al., 2012), as well as a variety of bioactive compounds, including peptides (Fontana et al., 2004), adenosine monophosphate (AMP) N1-oxide (Hattori et al., 2010), acetylcholine (Wei et al., 2010) and fatty acids such as 10-hydroxy-2-decenoic acid (10-HAD; Butenandt and Rembold, 1957; Ramadan and Al-Ghamdi, 2012). RJ has been shown in multiple studies to have anti-aging (Honda et al., 2011), anti-oxidative (Nagai et al., 2006), lipid-lowering (Vittek, 1995) and anti-inflammatory (Kohno et al., 2004) effects. Furthermore, it was recently reported that RJ significantly improves spatial learning and memory in rats with streptozotocin-induced SAD (Zamani et al., 2012), and that RJ attenuates Aβ toxicity in a *C. elegans* model of AD (Wang et al., 2016). Despite these latest research developments in RJ's potential treatment effects related to AD, the mechanism of how RJ regulates Aβ formation and delays the development of AD remains elusive.

One hypothesis is that RJ regulates the formation of Aβ via reducing cholesterol levels. Hypercholesterolemia, a known risk factor for AD, has been shown to promote Aβ neurotoxicity, Aβ accumulation and local neuronal loss across epidemiological (Kivipelto et al., 2001; Gonzalo-Ruiz et al., 2006), animal (Sparks and Schreurs, 2003) and cellular (Galbete et al., 2000) studies. It is thought that hypercholesterolemia can enhance the activities of γ-secretase and β-secretase, facilitate the metabolism of amyloid precursor protein (APP), aggravate Aβ deposition, promote the formation of senile plaques and then lead to AD (Kuo et al., 2015; Loke et al., 2017). The potential mechanism by which hypercholesterolemia causes Aβ formation was revealed by Jaya Prasanthi et al. (2008) in which they found that the hypercholesterolemia-induced production of Aβ was correlated with an increased level of β-site APP cleaving enzyme 1 (BACE1) and receptor for advanced glycation end products (RAGE), as well as a decreased level of insulin degrading enzyme (IDE) and low density lipoprotein receptor-related protein 1 (LRP-1).

In this study, we first investigate whether RJ has an effect on cholesterol and Aβ levels using an AD rabbit model. Though transgenic rodents have been used as the main animal model for AD (e.g., APPswe/PS1dE9 double transgenic mice), this model is unsuitable for SAD due to a lack of correct APP protein sequence and a lack of cleavage enzymes to trigger Aβ peptide formation (Liu et al., 2014). In contrast, rabbits naturally produce cleavage enzymes for Aβ peptides, and their Aβ peptide sequence is identical to that of humans (Johnstone et al., 1991). Notably, the connection between cholesterol levels and Aβ plaques was first reported in rabbits (Sparks et al., 1994), in which rabbits showed a marked response to high cholesterol diets and exhibited Aβ deposition in plaques. Furthermore, Sparks and Schreurs (2003) found that after adding copper to the diet of cholesterol-fed rabbits, the rabbits developed cortical amyloid deposits and exhibited at least 12 other pathological features that are observed in the brain of human AD patients, such as learning deficits. These findings together highlight the usefulness of the rabbit model, and demonstrate the potential of using rabbits for preclinical drug evaluations (Woodruff-Pak et al., 2007).

To provide potential mechanisms of how RJ regulates Aβ deposition and potentially improves AD in rabbit models, we assess the effects of RJ on a variety of biological factors, including the expression of proteins involved in the production, translocation and clearance of Aβ, anti-oxidative capacities, neuronal loss, and neuronal metabolic activities. In particular, the effects of RJ on neuronal metabolic activities are measured using high-field proton magnetic resonance spectroscopy (^{1}H-MRS), which is a non-invasive neuroimaging technique extensively used to quantify metabolic changes in AD pathology (Chen et al., 2012). We use ^{1}H-MRS to evaluate the levels of four main metabolites of AD (i.e., N-acetyl aspartate (NAA), choline (Cho), glutamate (Glu) and myo-inositol (mI)), since numerous studies have shown that NAA and glutamate are decreased in AD, whereas Cho and mI are increased in the early stage of AD (Ackl et al., 2005; Zhang et al., 2014).

MATERIALS AND METHODS

Animals

A total of 24 male White Hair and Black Eyes (WHBE) rabbits (3–4 months old, 1.8–2.0 kg) were purchased from Xin Jian rabbit field (Certificate No. SCXK, Zhejiang, 2015-0004, China), Dashiqu town, Xinchang City (Zhejiang, China). They were housed individually under a 12-h light/dark cycle and were provided with food and water *ad libitum*. All experiments were approved by the Institutional Animal Care and Use Committee

of Zhejiang Chinese Medical University (IACUC Approval No. ZSLL-2016-115), and were performed according to the guidelines from the Laboratory Animal Research Center of Zhejiang Chinese Medical University (Certificate No. SYXK, Zhejiang, 2013-0184, China).

After adaptation to the environment for 14 days, the rabbits were randomly divided into three groups (n = 8 rabbits per group): normal control (NC) group, AD model group and RJ intervention (RJ) group. The NC group rabbits were fed with a regular chow and distilled water (DW), whereas the AD model group was fed with chow plus 2% cholesterol and DW plus cooper (0.12 ppm cooper ion as sulfate) as used by Sparks and Schreurs (2003). The RJ group was fed with chow plus 2% cholesterol and DW plus cooper, and received 200 mg/kg of RJ (Jiangshan, Zhejiang, China) via oral administration twice a day (a total dose of 400 mg/kg RJ daily) in the morning and the afternoon for 12 weeks. This dose was selected based on the previous report that an oral administration of 6 g RJ per day can significantly reduce cholesterol levels in human clinic therapy (Guo et al., 2007). The duration of the experiment procedure was 12 weeks. The experimental designs of biochemical analysis, ^{1}H-MRS assessment and histological examinations are shown in **Figure 1**. After 12 weeks of administration, ^{1}H-MRS assessment, a set of biochemical index in the serum and brain, as well as all AD pathological indices were investigated.

Serum Total Cholesterol (TC), Triglycerides (TG), Low-Density Lipoprotein Cholesterol (LDL-C) and High-Density Lipoprotein Cholesterol (HDL-C) Levels Measurements

After 12-week administration, rabbits (eight per group) would first fast for 12 h, and then blood samples were drawn from their middle auricular artery. Automatic biochemical analyzer (7020, HITACHI, Japan) was used to analyze total cholesterol (TC), triglycerides (TG), low-density lipoprotein cholesterol (LDL-C) and high-density lipoprotein cholesterol (HDL-C) in blood samples by kits corresponding to each component (Shanghai Shenneng-DiaSys Diagnostic Technology Co., Ltd., China).

Quantification of Aβ Levels by ELISA

For ELISA test of Aβ1–40 and Aβ1–42 levels in the rabbit brain (six cortex and hippocampus per group), the wet mass of 100 mg cortex and the hippocampus tissues were sequentially homogenized in a 8× mass of cold 5 M guanidine hydrochloride/50 mM Tris HCl buffer using an IKA ULTRA-TURRAX homogenizer (IKA®-werke Gmbh and Co., KG, German). The homogenates were mixed for 4 h at room temperature. Samples were diluted with Dulbecco phosphate buffered saline with 5% BSA and 0.03% Tween-20 supplemented with 1× protease inhibitor mixture, and were centrifuged at 10,000 rpm for 20 min at 4°C (Jaya Prasanthi et al., 2008). The supernatants were then decanted and stored at −80°C until used. The samples were diluted with at least 1:2 standard dilution buffer, and the ELISA kits (Jiancheng Bioengineering Institute, Nanjing, China) were used to measure Aβ1–40 and Aβ1–42 levels according to the manufacturer's instructions[1]. The protein concentrations of all samples were determined by standard bicinchoninic acid (BCA) assay (Pierce, Rockford, IL, USA; Baptiste et al., 2004). The Aβ levels were normalized to the total protein content in the samples.

Determination of Superoxide Dismutase (SOD) Activities, Malonaldehyde (MDA) Contents and Reactive Oxygen Species (ROS)/Reactive Nitrogen Species (RNS) Levels

The superoxide dismutase (SOD) and malonaldehyde (MDA) contents in the brain (eight per group) were measured using colorimetric commercial kit (Jiancheng Bioengineering Institute,

[1]http://www.njjcbio.com

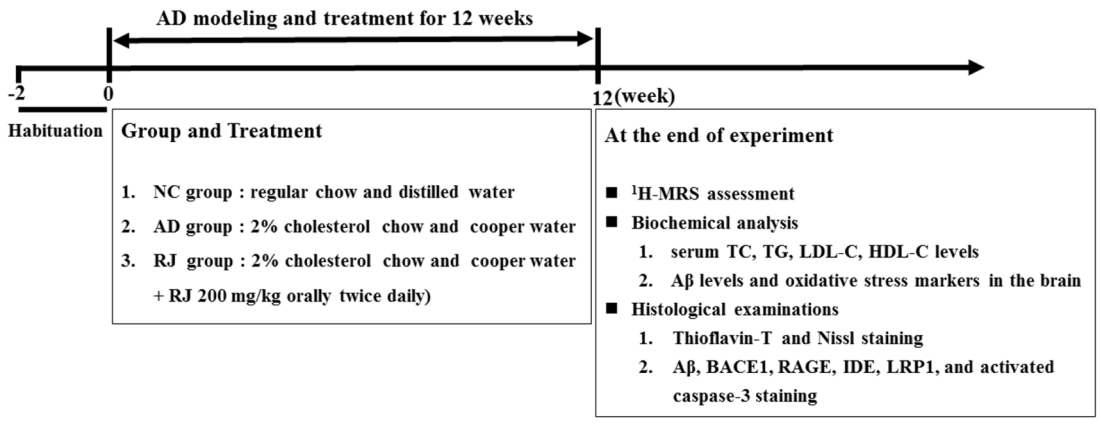


FIGURE 1 | A flowchart of the experimental design in this study.

Nanjing, China). The SOD activity was examined with xanthine oxidase method, and the MDA content was examined with sulfur barbituric acid method (Wang et al., 2005). In addition, reactive oxygen species (ROS)/reactive nitrogen species (RNS) levels in the brain (six per group) were detected with a commercially available ELISA kit (Yuanye Biotech Co., Ltd., Shanghai, China) following the procedure described by the manufacture. Briefly, a 5% w/v cortex and hippocampus homogenates were made in pre-chilled saline using an IKA ULTRA-TURRAX homogenizer (IKA®-werke Gmbh and Co., KG, German). The obtained homogenate was centrifuged at 3000 rpm for 20 min at 4°C. The supernatants were stored at −80°C until used. The protein concentration of all samples was determined by Coomassie brilliant blue method. SOD activities, MDA contents, and ROS/RNS levels were then normalized to the total protein content in the samples.

^{1}H-MRS Assessment

^{1}H-MRS was conducted using a 3.0 T MRI scanner (GE Discovery MR 750, GE, USA) coupled with an 8-channel rabbit dedicated coil (Shanghai Chenguang Medical Technology Co., Ltd., China). All rabbits (six per group) were examined by MRI at 12 weeks. Rabbits were anesthetized by intramuscular injection of 30 mg/kg ketamine and 4 mg/kg xylazine 15 min before imaging. Animals were fixed in prone position in the experiment. During examination, the body temperature was maintained at 36–37°C, and their breathing was kept smooth. T2-weighted fast spin-echo sequence (FSE) was used with the following parameters: TR = 5500 ms, TFE = 100 ms, slice thickness = 3 mm, field of view (FOV) = 100 mm × 100 mm, matrix = 352 × 256, NEX = 2. Images were used to guide MRS subsequent location checks. ^{1}H-MRS scanning used point-resolved water suppression plus sequence (PRESS) with the following parameters: TR = 2000 ms, TE = 35 ms, voxel = 9 mm × 9 mm × 9 mm, total number of scans = 128, NEX = 8. The region of interest (ROI) was positioned in the hippocampus and part of frontal cortex in the brain (**Figure 7A**). Pre-scan, automatic shimming and moisture suppression were performed prior to ^{1}H-MRS. The shimming effect was expressed as full width at half maximum (FWHM). If the FWHM was higher than 20 Hz, a manual shimming was used to obtain good magnetic field uniformity. The spectra of all rabbits were analyzed using an LC Model (version 6.3, Provencher SW; Provencher, 1993). The chemical metabolites, including NAA, glutamate, Cho, mI and creatine (Cr) were identified. Since Cr is consistent in various diseases, it was used as an internal standard to calculate the ratio of NAA/Cr, glutamate/Cr, Cho/Cr and mI/Cr.

Histological Examinations

All rabbits were euthanized with pentobarbital sodium, and were then perfused with 300 ml 4°C PBS solution after cardiac perfusion. The brain was removed, segmented into 5 mm thick parallel coronal slices, and then fixed in formalin solution for at least 24 h. The selected slices were dehydrated with gradient ethanol, embedded in paraffin and cut into 6 μm coronal sections. They were then stained immunohistochemically with Aβ, beta-site APP cleaving enzyme 1 (BACE1), receptor for advanced glycation end products (RAGE), LDL receptor related protein 1(LRP1), insulin-degrading enzyme (IDE), activated caspase-3, thioflavin-T and Nissl.

1. Thioflavin-T staining was used to evaluate the amount of amyloid-β protein (Zhang et al., 2013), with eight samples in each group. Briefly, slides were deparaffinized and rehydrated in descending grades of ethanol, placed in Mayer hematoxylin for 5 min, rinsed twice in double DW, incubated with 1% thioflavin-T (Dalian Meilun Biological Technology Co. Ltd., China) for 10 min and three changes of DW washes, cover-slipped in a neutral glycerol, and examined with the Hg-Lamp for fluorescence excitation by a Zeiss inverted microscope (Axiovert 200, Carl Zeiss, USA).
2. Nissl staining was used to evaluate neuronal loss (Chen et al., 2009), with six samples in each group. Briefly, slides were hydrated and incubated in 1% toluidine blue solution at 56°C for 30 min, washed with PBS, decolorized with 95% ethanol, dehydrated, dried and cover-slipped.
3. Aβ, BACE1, RAGE, IDE, LRP1 and activated caspase-3 staining, with six to eight samples in each group. Briefly, sections were blocked with 3% hydrogen peroxide solution for 10 min, and were then incubated with primary antibodies overnight at 4°C, including BACE1 (1:100, Santa Cruz Biotechnology, USA), RAGE (1:100, Santa Cruz Biotechnology, USA), IDE (1:100, Santa Cruz Biotechnology, USA), LRP1(1:300, Diage Biological Technology co. Ltd., China), activated caspase-3 (1:200, Biosynthesis Biological Technology co. Ltd., China) and β-amyloid (B-4, 1:100, Santa Cruz Biotechnology, USA, which recognizes APP and Aβ). PBS was used as negative control instead of the primary antibody. Subsequently, the sections were washed with PBS three times and were incubated with secondary antibody for 1 h at room temperature. Sections were visualized with DAB (ZSJQ, Beijing, China) and counterstained with hematoxylin.

All sections were scanned using a Hamamatsu Skeleton Scanner (Nanozoomer S210, Hamamatsu, Japan). Since the main pathological feature of early AD is cortical atrophy, especially in the hippocampus and the medial temporal lobe, we examined the pathological changes in the cerebral cortex and hippocampus. The captured images were examined in a blinded manner by an observer who was unware of experimental condition, and were analyzed using the Image pro plus 6.0 software (Media Cybernetics, Rockville, MD, USA). On Nissl-stained sections, five microscopic fields of the hippocampal CA1, CA3 and DG regions, the cortical cone (pyramidal cellular layer, PCL) and the polymorphic cell layer (multiform cellular layers, MCL) were selected. The neuronal counts in each view were calculated at 40× magnification. We counted Aβ and activated caspase-3 immunolabeled positive cells under 40× magnification in three random fields from the cerebral cortex and hippocampal CA1 areas in the three groups and used the averaged value. For quantification, we calculated Aβ, BACE1, RAGE, IDE, LRP1 or activated caspase-3-postive area under 40× magnification in three random fields from the cerebral cortex and hippocampal CA1 areas, and the staining

was quantified as the percent positive staining area as the fraction of immunopositive staining to total area measured. In addition, plaque load was categorized based on the percentage area of tissues positive for deposits labeled by thioflavin-T immunoreactivity.

Statistical Analysis

Data were expressed as means ± SEM. Statistical analyses were performed using GraphPad Prism 6.0 (GraphPad Software, Inc., La Jolla, CA, USA). All quantitative results were analyzed by one-way ANOVA with *post hoc* Tukey's test ($^{*}p < 0.05$, $^{**}p < 0.01$).

RESULTS

RJ Reduced Plasma TC and LDL-C Levels

We first assessed the effects of RJ on blood liquid levels (i.e., TC, HDL-C, LDL-C and TG) in AD rabbits. As shown in **Table 1**, the levels of TC, HDL-C and LDL-C in the AD model group were higher than those in the NC group (ANOVA with *post hoc* Tukey's test, all $p < 0.01$). Compared with the AD model group, plasma TC and LDL-C levels in the RJ group were significantly reduced by 28% and 23% respectively (all $p < 0.05$), while there was no significant difference in plasma HDL-C levels between the RJ group and the AD model group ($p = 0.07$). In addition, there was no significant difference in body weight and TG levels among the three groups (ANOVA, $F = 0.08$, $p = 0.925$; $F = 2.555$, $p = 0.103$, respectively).

RJ Decreased Aβ Levels and Amyloid Burden in the Cortex and the Hippocampus of AD Rabbits

To observe the effects of RJ on Aβ pathology in the brain of AD rabbits, the Aβ level and amyloid burden were assessed in the three groups of rabbits. As shown in **Figure 2A**, the Aβ1–40 and Aβ1–42 levels were significantly increased in the cortex area (ANOVA with *post hoc* Tukey's test, $p < 0.05$ and $p < 0.01$, respectively) and the hippocampus area (ANOVA with *post hoc* Tukey's test, $p < 0.01$ and $p < 0.05$, respectively) in the AD model group compared with the NC group. In contrast, compared with the AD model group, the RJ group showed a 17%–54% reduction in both Aβ1–40 and Aβ1–42 levels in the cortex area ($p < 0.05$ and $p < 0.01$, respectively) and the hippocampus area (all $p < 0.05$).

Next, the Aβ plaque was evaluated using immunohistochemical analysis (**Figure 2B**) and thioflavin-T staining. In the frontal cortex and the hippocampus regions, we found that the expression of Aβ-positive proteins was low in the NC group, upregulated in the AD model group, and suppressed in the RJ group. Quantification analysis showed that the number of Aβ immunolabeled cells were significantly reduced in the cortex and the hippocampus of the RJ group compared to the AD model group (ANOVA with *post hoc* Tukey's test, $p < 0.01$ and $p < 0.05$, respectively). Similarly, the Aβ covered areas were reduced by approximately 45% in the cortex and by 40% in the hippocampus of the RJ group compared to the AD model group (ANOVA with *post hoc* Tukey's test, all $p < 0.01$; **Figure 2C**).

Using thioflavin-T staining, a fluorescein that specifically binds to amyloid deposits and can be excited to produce green fluorescence, we found that the RJ group significantly reduced the amount of thioflavin-T positive plaques in both the cortex and the hippocampus areas compared to the AD model group (**Figure 2D**). Quantitatively, the RJ group reduced the plaques load by 37% in the cortex area (ANOVA with *post hoc* Tukey's test, $p < 0.05$) and by 60% in the hippocampus area relative to the AD model group ($p < 0.01$; **Figure 2E**), demonstrating that RJ could greatly decrease Aβ deposition in AD brains.

RJ Reduced Aβ Accumulation by Decreasing BACE1 and RAGE Expression, and by Increasing IDE and LRP1 Expression

To investigate how RJ reduces Aβ accumulation, the expression of BACE1, RAGE, LRP1 and IDE were measured in the rabbit brains of each group by immunohistochemistry. As shown in **Figure 3**, compared with the NC group, the expression levels of BACE1 and RAGE were significantly increased in the cortex and the hippocampus of the AD model group (ANOVA with *post hoc* Tukey's test, all $p < 0.01$). In specific, the BACE1 covered area in the RJ group was significantly decreased by 65% in the cortex and by 59% in the hippocampus compared with the AD model group (all $p < 0.05$). Similarly, the RAGE covered area in the RJ group was markedly reduced by 68% in the cortex ($p < 0.01$) and by 59% in the hippocampus ($p < 0.05$) relative to the AD model rabbits. In contrast, LRP1 and IDE expression levels were markedly decreased in the AD model group (ANOVA with *post hoc* Tukey's test, all $p < 0.01$). The LRP1 covered area in the RJ group was dramatically increased

TABLE 1 | Effect of royal jelly (RJ) on weight and blood liquid levels in Alzheimer's disease (AD) rabbits at 12 weeks.

Parameters	NC group	AD model group	RJ group
Weight (kg)	2.80 ± 0.07	2.83 ± 0.09	2.85 ± 0.07
TC (mmol/L)	0.62 ± 0.09**	45.79 ± 2.97	33.04 ± 4.07*
HDL-C (mmol/L)	0.28 ± 0.05**	2.91 ± 0.10	2.51 ± 0.17
LDL-C (mmol/L)	0.32 ± 0.04**	32.29 ± 1.97	24.86 ± 2.76*
TG (mmol/L)	0.69 ± 0.04	1.91 ± 0.64	0.95 ± 0.25

*TC, total cholesterol; HDL-C, high-density lipoprotein cholesterol; LDL-C, low-density lipoprotein cholesterol; TG, triglycerides. Data are presented as mean ± SEM from eight rabbits in each group. ANOVA with post hoc Tukey's test was used. *P < 0.05, **P < 0.01 vs. the AD model group.*

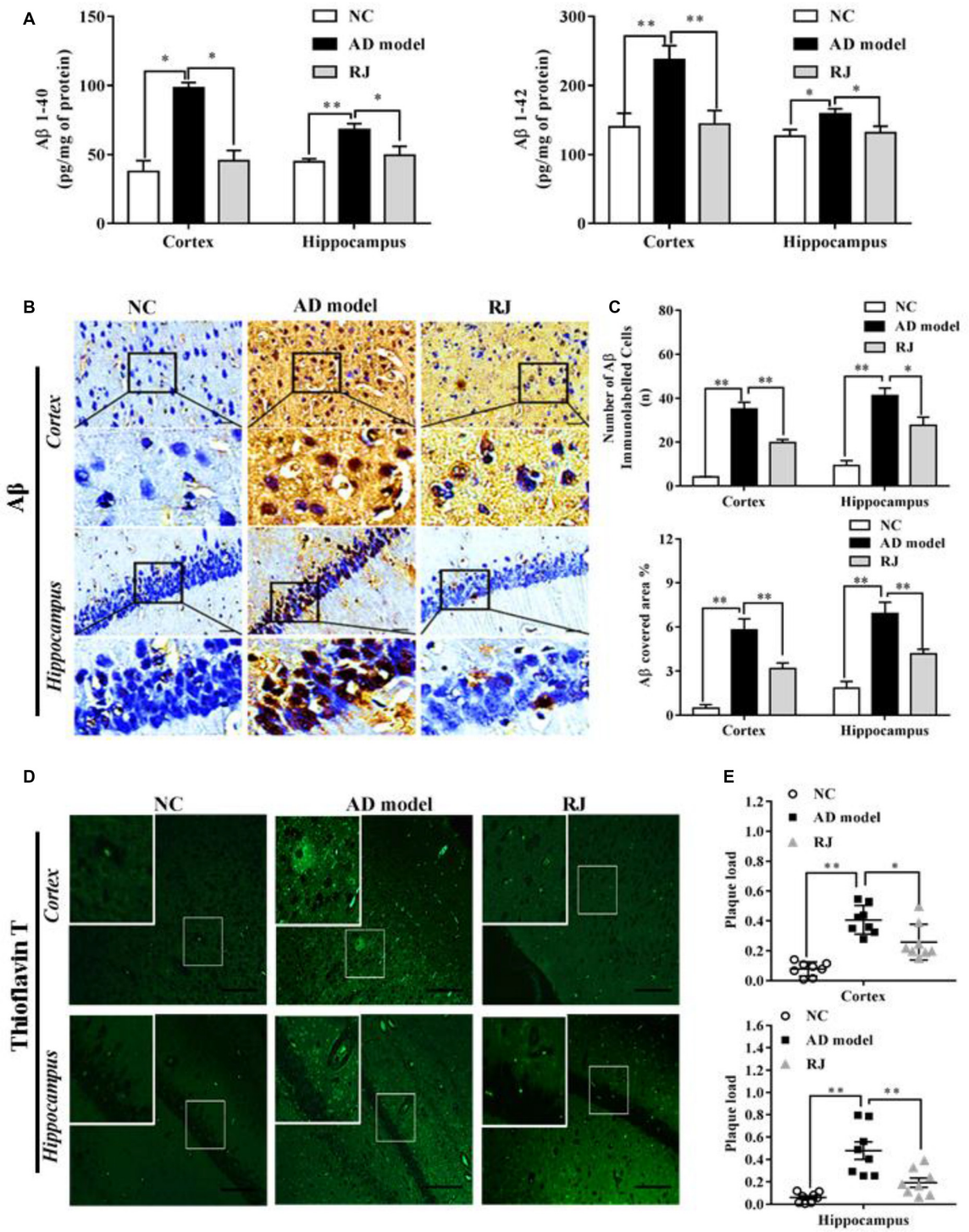


FIGURE 2 | Royal jelly (RJ) decreased brain amyloid β (Aβ) levels and alleviated Aβ pathology in Alzheimer's disease (AD) rabbits. **(A)** The levels of Aβ1–40 and Aβ1–42 in the cortex and the hippocampus of each group measured by ELISA, $n = 6$ rabbits per group. **(B)** Representative Aβ-staining images in the cortex and the hippocampus of each group. Scale bar = 50 μm. Black squares indicate images with higher-magnification. Aβ positive (brown-colored) was detected mainly in the cytoplasm of neuronal cells and the cytoplasm and membranes of endothelia cells. **(C)** The number of Aβ immunolabeled cells per view (40×) and the covered area of Aβ staining in the brain of each group, $n = 6$–8 rabbits per group. **(D)** An example image of Aβ plaque immunoreactivity in the cortex and the hippocampus of each group by thioflavin-T staining. Scale bar = 50 μm. White squares indicate images with higher-magnification. **(E)** Quantification of thioflavin-T positive deposits in the cortex and the hippocampus of the three groups, $n = 8$ rabbits per group. Data are presented as mean ± SEM. ANOVA with *post hoc* Tukey's test was used **(A,C,E)**. $^{*}P < 0.05$, $^{**}P < 0.01$ vs. the AD model group.

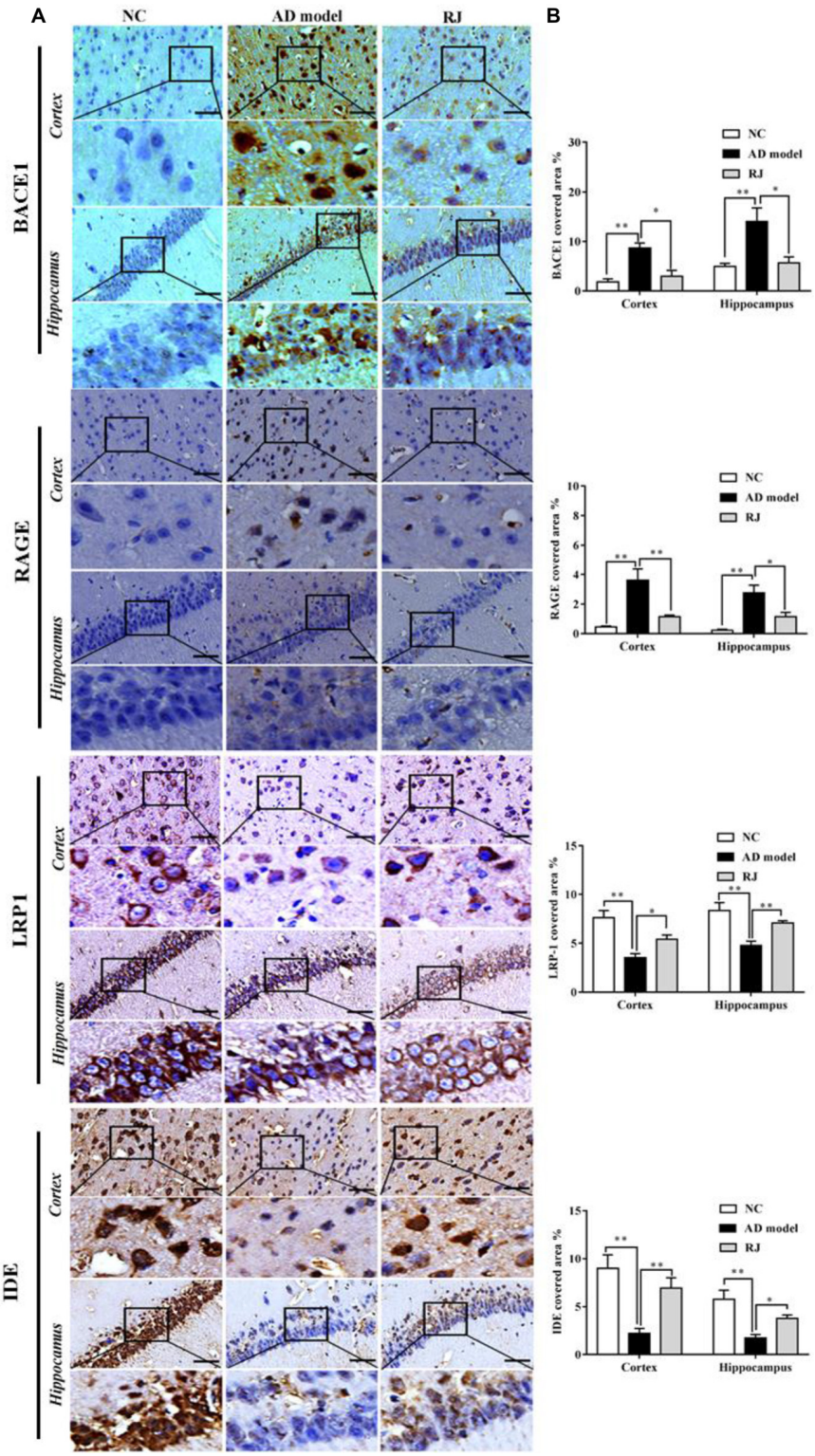


FIGURE 3 | RJ inhibited β-site APP cleaving enzyme-1 (BACE1) and receptor for advanced glycation end products (RAGE) expression levels, and increased lipoprotein receptor-related protein 1 (LRP1) and insulin degrading enzyme (IDE) expression levels, demonstrated by immunohistochemistry. **(A)** Staining for BACE1, RAGE, LRP1 and IDE using specific antibodies in the brain of the AD model, RJ and normal control (NC) group. Scale bar = 50 μm. Black squares indicate images with higher-magnification. **(B)** Quantification of the covered areas of BACE1, RAGE, LRP1 and IDE staining in the frontal cortex and the hippocampus of the three groups, n = 6–8 rabbits per group. Data are presented as mean ± SEM. ANOVA with *post hoc* Tukey's test was used. $^{*}P < 0.05$, $^{**}P < 0.01$ vs. the AD model group.

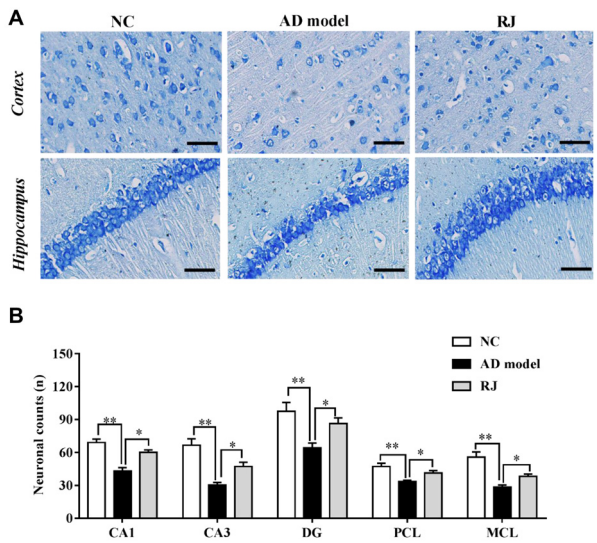


FIGURE 4 | RJ rescued neuronal loss in the brain of AD rabbits. **(A)** Nissl-staining images in the frontal cortex and the hippocampus of the AD model, RJ and NC group. Scale bar = 50 μm. **(B)** Neuronal counts per view (40×) in the hippocampal CA1, CA3, DG regions and cortical pyramidal cellular layer (PCL) and multiform cellular layers (MCL) areas among the three groups, $n = 6$ rabbits per group. Data are presented as mean ± SEM. ANOVA with *post hoc* Tukey's test was used. $^{*}P < 0.05$, $^{**}P < 0.01$ vs. the AD model group.

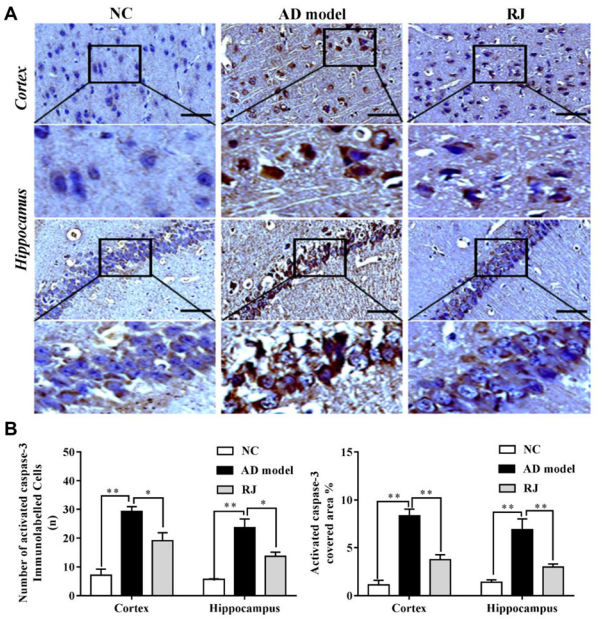


FIGURE 5 | RJ reduced activated caspase-3 expression levels in the brain of AD rabbits. **(A)** Representative activated caspase-3 staining sections in the brain of the AD model, RJ and NC group. Scale bar = 50 μm. Black squares indicate images with higher-magnification. **(B)** The number of activated caspase-3 immunolabeled cells per view (40×) and the covered area of activated caspase-3 staining in the frontal cortex and the hippocampus of the three groups, $n = 6$ rabbits per group. Data are presented as mean ± SEM. ANOVA with *post hoc* Tukey's test was used. $^{*}P < 0.05$, $^{**}P < 0.01$ vs. the AD model group.

by 53% in the cortex and by 67% in the hippocampus relative to the AD model group (all $p < 0.05$). Moreover, the IDE covered area in the RJ group was significantly increased by 2.15 folds in the cortex ($p < 0.01$) and by 1.19 folds in the hippocampus relative to the AD model group ($p < 0.05$). Taken together, these results indicate that RJ may reduce Aβ accumulation in AD brains by inhibiting the expression of BACE1 and RAGE as well as by promoting the expression of LRP1 and IDE.

RJ Reduced Neuronal Loss and Inhibited Apoptosis in AD Rabbit Brains

Nissl staining was performed to evaluate the effects of RJ on neuronal loss in the AD brain. As shown in **Figure 4**, when compared with the NC group, the AD rabbits showed a typical Alzheimer's pathology, including nucleus shrinkage, neuronal loss and disappearance of Nissl bodies in the cortex and the hippocampus (**Figure 4A**). The cell organization was notably improved in the RJ group, in which RJ treatment significantly increased the number of neurons in the hippocampal CA1, CA3, DG regions and cortical PCL and MCL areas by 40%, 56%, 34%, 23% and 34% respectively compared to the AD model group (ANOVA with *post hoc* Tukey's test, all $p < 0.05$; **Figure 4B**). These results suggest that RJ treatment can potentially increase the number of neurons and improve neuronal structures in the AD brain.

To confirm the results above, we assessed the expression level of activated caspase-3 in the brain of each group by immunohistochemistry. As shown in **Figure 5**, the number of activated caspase-3 immunolabeled cells as well as the covered areas of activated caspase-3 were both significantly increased in the cortex and the hippocampus of the AD model group compared to the NC group (ANOVA with *post hoc* Tukey's test, all $p < 0.01$). In contrast, the number of activated caspase-3 immunolabeled cells were notably decreased in the cortex and the hippocampus of the RJ group compared to the AD model group (all $p < 0.05$). Meanwhile, the covered areas of activated caspase-3 were significantly reduced by approximately 55% in the cortex and by 57% in the hippocampus of the RJ group compared to the AD model group (all $p < 0.01$), indicating that RJ can inhibit neuronal apoptosis.

RJ Enhanced Anti-oxidative Capacities in AD Rabbit Brains

The effects of RJ on anti-oxidative capacities of AD rabbit brains were measured. As shown in **Figure 6**, the SOD level was markedly reduced in the cortex and the hippocampus of the AD model group compared to the NC group (ANOVA with *post hoc* Tukey's test, all $p < 0.05$). In contrast, the SOD level in the RJ group was significantly increased by approximately 27% in the cortex and by 13% in the hippocampus relative to the AD model group (all $p < 0.05$). On the other hand, the MDA content was increased in the cortex and the hippocampus of the AD model

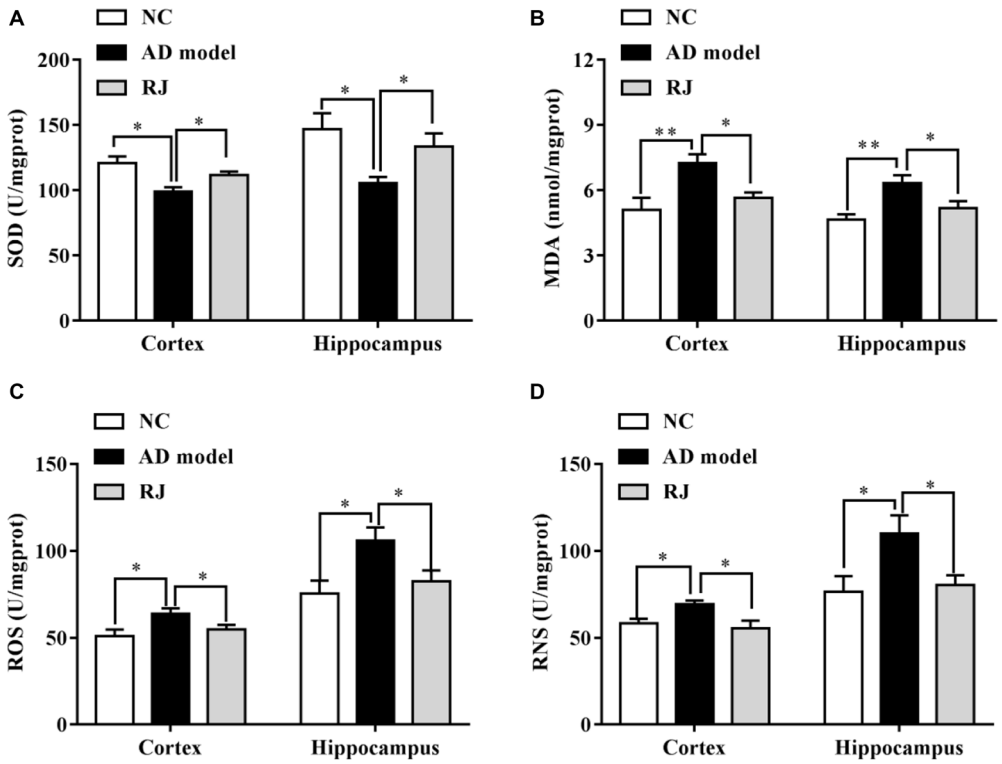


FIGURE 6 | RJ enhanced the anti-oxidative capacities in the brain of AD rabbits. **(A)** Changes of superoxide dismutase (SOD) activities in the cortex and the hippocampus of the three groups, $n = 8$ rabbits per group. **(B)** Changes of malonaldehyde (MDA) contents in the cortex and the hippocampus of the three groups, $n = 8$ rabbits per group. **(C)** Changes of reactive oxygen species (ROS) levels in the cortex and the hippocampus of the three groups, $n = 6$ rabbits per group. **(D)** Changes of reactive nitrogen species (RNS) levels in the cortex and the hippocampus of the three groups, $n = 6$ rabbits per group. Data are presented as mean ± SEM. ANOVA with *post hoc* Tukey's test was used **(A–D)**. $^{*}P < 0.05$, $^{**}P < 0.01$ vs. the AD group.

group compared to that of the NC group (ANOVA with *post hoc* Tukey's test, all $p < 0.01$), and it was significantly reduced by approximately 18% in the cortex and by 22% in the hippocampus of the RJ group relative to the AD model group (all $p < 0.05$). In addition, the ROS/RNS levels were increased in the cortex and the hippocampus of the AD group compared to those of the NC group (ANOVA with *post hoc* Tukey's test, all $p < 0.05$). The ROS level in the RJ group was dramatically decreased by 14.33% in the cortex and by 21.96% in the hippocampus relative to the AD model group (all $p < 0.05$). Moreover, the RNS level in the RJ group was also significantly decreased by 19.79% in the cortex and by 27.17% in the hippocampus relative to the AD group (all $p < 0.05$). These results suggest that RJ treatment can enhance anti-oxidative capacities in the AD rabbit brain.

RJ Improved Neuronal Metabolic Activities in AD Rabbit Brains

We then used ^{1}H-MRS to evaluate the changes of neruonal metabolic activities in rabbit brains, the results from which are presented in **Figure 7**. Compared with the NC group, the AD model group presented with decreased peaks of NAA and glutamate and increased peaks of Cho and mI, while RJ treatment reveresed these changes. Quantification analysis demonstrated that the levels of NAA/Cr and glutamate/Cr were significantly reduced in the brain of the AD model group when compared with the NC group (ANOVA with *post hoc* Tukey's test, $p < 0.05$ and $p < 0.01$, respectively), while the levels of Cho/Cr and mI/Cr were significantly increased (ANOVA with *post hoc* Tukey's test, $p < 0.01$ and $p < 0.05$, respectively). In specific, the levels of NAA/Cr and glutamate/Cr in the RJ group were increased by 18% and 25% respectively, relative to the AD model group (all $p < 0.05$). On the other hand, the levels of Cho/Cr and mI/Cr were markedly decreased by 16% and 26% respectively in the RJ group compared with the AD model group (all $p < 0.05$). These results indicate that RJ can elevate the levels of NAA and glutamate, and can reduce the levels of mI and Cho in the brain of AD rabbits with potential effects of improving neuronal metabolic activities in the AD brain.

DISCUSSION

Our study confirmed in a rabbit AD model that hypercholesterolemia promotes Aβ deposition and leads to neuronal loss, whereas RJ has the effects of reducing plasma TC and LDL-C levels, enhancing anti-oxidative capacities,

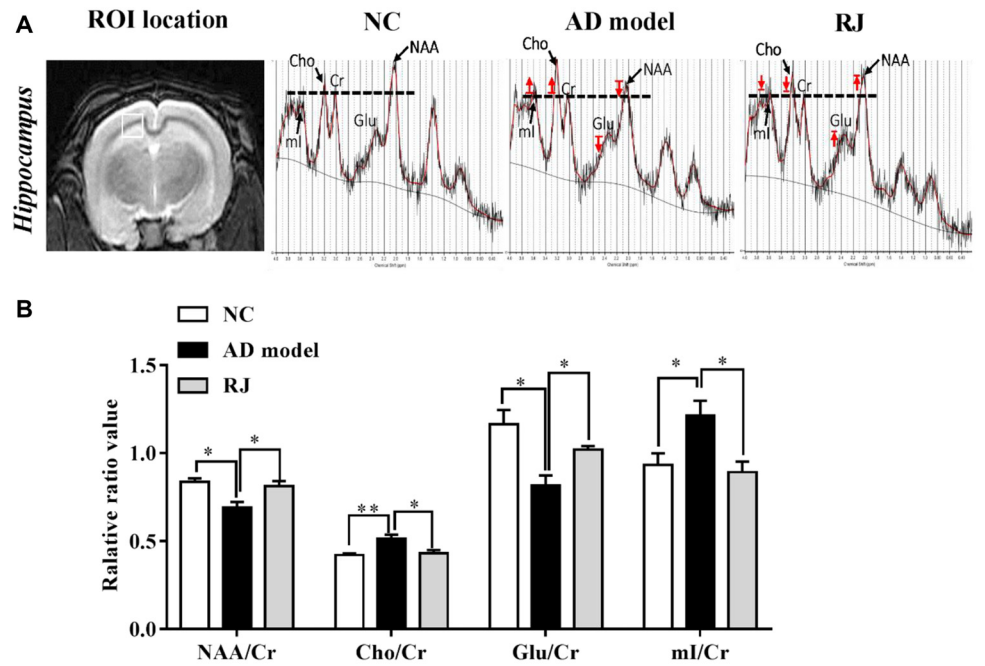


FIGURE 7 | RJ improved brain metabolic activities in AD rabbits. **(A)** Regions of interest (ROI) location in the brain (white box) and representative spectra from the AD model, RJ and NC group rabbits. The red arrow indicates direction of metabolic changes, and the line represents the control level of each metabolite. **(B)** The relative ratios of each metabolite to creatine (Cr) in the brain of the three groups, $n = 6$ rabbits per group. Data are presented as mean ± SEM. ANOVA with *post hoc* Tukey's test was used. $^{*}P < 0.05$, $^{**}P < 0.01$ vs. the AD model group.

ameliorating Aβ pathology and protecting neurons from damage. High cholesterol dietaries are known to promote Aβ generation in human brains, thereby increasing the risk of AD (Panza et al., 2006). Numerous studies have shown that rabbits fed with 1% or 2% cholesterol diet alone or plus trace amounts of copper in drinking water would develop AD pathology, including senile plaques, cognitive impairment and neuronal loss (Larry Sparks, 2004). In this study, we showed that rabbits receiving high cholesterol diets plus copper in drinking water resulted in elevated TC, LDL-C and Aβ (such as Aβ1–40 and Aβ1–42) levels, neuronal loss, and nuclear contraction or disappearance of Nissl bodies, confirming the crucial role of hypercholesterolemia in the development of AD as well as successfully establishing a rabbit AD model. In addition, we observed from an MRI analysis that there was an increase in ventricular volumes in rabbits following 12 weeks on a diet of 2% cholesterol plus copper in drinking water (data not shown), consistent with previous reports (Deci et al., 2012; Schreurs et al., 2013). Furthermore, we showed that RJ significantly reduced the levels of TC and LDL-C in AD rabbits, confirming the previously reported effects of RJ on lowering cholesterol and Aβ levels (Guo et al., 2007).

The effects of RJ on AD rabbits may be explained by its regulatory capabilities of proteins involved in Aβ production, transport, degradation and clearance, such as BACE1, RAGE, LRP1 and IDE. Regarding the regulatory role of RJ in Aβ production, BACE1 is a protease that initiates Aβ production and is mainly located on lipid rafts. Higher BACE1 protein levels were observed in the brain of AD patients (Fukumoto et al., 2002; Holsinger et al., 2002), while *BACE1* gene knocked-out mice were found not to produce Aβ (Vassar et al., 2014; Neumann et al., 2015). The activities of BACE1 are greatly influenced by the metabolism of cholesterol. The increase in Aβ levels caused by high cholesterol diets was found to associate with the up-regulation of BACE1 expression (Jaya Prasanthi et al., 2008). On the other hand, the reduction of cholesterol levels was found to inhibit the BACE1 enzyme activity and reduce Aβ production (Cui et al., 2011). In particular, cholesterol depletion has been shown to reduce the partitioning of APP into lipid rafts, precluding the interaction of BACE1 with lipid rafts and thus lowering Aβ production (Guardia-Laguarta et al., 2009). In this study, we found that BACE1 expression levels as well as cholesterol levels were significantly decreased by RJ, indicating a possible molecular mechanism underlying RJ-mediated decrease of amyloid plaques: RJ inhibits the APP cleavage of amyloid via lowering cholesterol levels and reducing the contact between BACE1 and lipid rafts.

The ability of RJ to reduce the Aβ deposition in the brain may also come from its ability to regulate the transport of Aβ through blood-brain barrier (BBB). Abnormal translocation of Aβ across BBB is considered to be a central link of AD pathogenesis. Recent studies have revealed RAGE and LRP1 as two key Aβ transporters on the BBB: RAGE mediates the transport of Aβ from the peripheral blood to the brain, whereas LRP1 mediates the transport of Aβ from the brain to the blood (Xi et al., 2013;

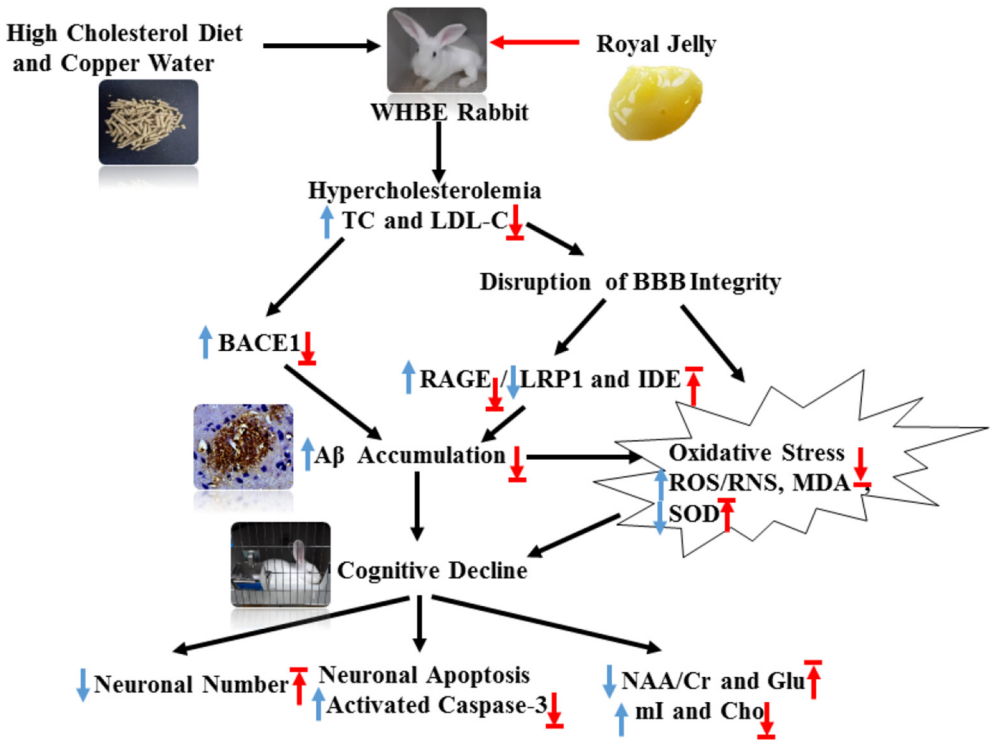


FIGURE 8 | Schematic showing the possible mechanisms by which RJ improves hypercholesterolemia-induced rabbits with AD. AD conditions were induced by feeding rabbits with a high cholesterol diet plus copper in drinking water. RJ can reduce cholesterol levels, down-regulate BACE1 and RAGE expression, increase the expression levels of LRP1 and IDE, promote the degradation and clearance of Aβ, and finally reduce Aβ. Moreover, RJ also has anti-oxidative effects, and it enhances neuronal metabolic activities and prevents neuronal loss. TC, total cholesterol; LDL-C, low-density lipoprotein cholesterol; BACE1, β-site APP cleaving enzyme 1; BBB, Blood-brain barrier; RAGE, receptor for advanced glycation end products; LRP1, LDL receptor related protein 1; IDE, insulin-degrading enzyme; Aβ, amyloid β-protein; ROS, reactive oxygen species; RNS, reactive nitrogen species; MDA, malondialdehyde; SOD, superoxide dismutase; activated caspase-3, activated cysteinyl aspartate specific proteinases 3; NAA, N-acetylaspartata; Glu, glutamate; mI, myo-inositol; Cho, choline. Arrows pointing up or down indicate statistically significant increases or decreases ($p < 0.05$). Blue arrows indicate the changes in AD rabbits, while red arrows indicate the treatment effects of RJ.

Cirillo et al., 2015). In AD patients, the expression of LRP1 was down-regulated, while the expression of RAGE was up-regulated (Shibata et al., 2000; Deane et al., 2004), consistent with what we observed in AD rabbits. Furthermore, we found that RJ could increase the expression levels of LRP1 and inhibit the expression levels of RAGE in the brain of AD rabbits. This effect may be attributed to 10-hydroxy-trans-2-decanoic acid (HDEA), a compound in RJ that can pass through BBB. HDEA has similar effects as brain-derived neurotrophic factor (BDNF), and could potentially promote neurogenesis in mature brains (Hattori et al., 2007). These results suggest that RJ can regulate the translocation of Aβ via RAGE/LRP1 and therefore potentially reduce the Aβ deposition in the brain.

As for the degradation and clearance of Aβ, RJ plays a role in this as well and thereby further reduces the deposition of Aβ. IDE is one of the main enzymes for degrading Aβ in the brain. Increased amyloid plaque and Aβ levels, along with decreased IDE activity, were found in diet-induced insulin resistance APP transgenic mice (Farris et al., 2004). Meanwhile, increased levels of IDE can activate serine/threonine protein kinase B pathway, inhibit the activity of GSK-3β, and decrease abnormal phosphorylation levels of Tau protein (Wang et al., 2006). In addition, the clearance of IDE is related to the BBB transport, and it may contribute to the pathogenesis of AD by influencing insulin signal transduction (Del Campo et al., 2015). We found in this study that the expression levels of IDE were increased by RJ treatment, indicating yet another regulatory path for RJ to reduce Aβ levels.

Apart from Aβ pathology, AD may also benefit from the anti-oxidative effects of RJ. AD is associated with neuronal loss in the brains (Zou et al., 2015), of which apoptosis is a main factor. Oxidative stress was found to promote Aβ aggregation and cause damage to neurons through apoptotic pathways, whereas antioxidant enzymes and vitamin E could antagonize these effects (Mecocci et al., 1994). Known for its anti-oxidative and anti-aging effects, RJ contains rich antioxidant enzymes and vitamins, such as SOD (Min et al., 2004) and vitamin C. In this study, we examined the changes in apoptotic activities and oxidative stress in RJ treated rabbits using five markers: activated caspase-3, a protease involved in apoptosis that has been shown to participate in the pathological process of AD neuronal damage (Zhang et al., 2017); SOD, a free

radical scavenging agent for evaluating free radical production; and MDA, which serves as a sensitive index for evaluating the oxidative stress response (Mancini et al., 2017); ROS/RNS play an important role in the survival and cell death signaling cascades that are essential for neurodegenerative disorders, and an increase in ROS/RNS levels (often associated with AD) will result in lipid and protein oxidation (Limongi and Baldelli, 2016). Studying the neurons in the cortex and the hippocampus of AD rabbits, we found that the number of neurons was significantly increased and that activated caspase-3 expression was markedly inhibited by RJ treatment. Moreover, the SOD level was significantly increased and the MDA content and ROS/RNS were decreased in the brain of AD rabbits after RJ intervention, indicating that RJ has the potential to prevent neuronal loss in AD by enhancing anti-oxidative capacities.

Our assessment of neuronal metabolic activities using ^{1}H-MRS further revealed other potential mechanisms of how RJ may improve AD. First, we found that the levels of NAA and glutamate were notably increased in the brains of RJ-treated rabbits. NAA, a specific marker for neuronal viability and integrity (Chen et al., 2013), was reported to be at markedly reduced levels in AD patients (Moon et al., 2016). Glutamate, a major excitatory neurotransmitter that regulates learning, memory and movement, is a marker for neuronal survival and synaptic plasticity (Alvarez and Ruarte, 2004). The increased levels of NAA and glutamate found in RJ-treated rabbits indicate that RJ treatment can enhance neuronal metabolic activities in the brain of AD rabbits and may ultimately improve the cognitive abilities of AD. Furthermore, we found that RJ also increases the level of Cho and mI in the brain of AD rabbits. Cho, related to phospholipid metabolism of cell membranes, participates in the formation of cell membranes and myelin. Meanwhile, mI is a cell marker of glial since it is associated with the activation or proliferation of astrocytes (Zhang et al., 2014). In AD patients, Cho and mI levels were both reported to have increased due to the damage of brain cell membrane and the reactive proliferation of glial cells (Zhang et al., 2014). Our results confirmed that Cho and mI levels are increased in AD rabbits, and showed that these levels can be decreased by RJ treatment. This suggests that RJ treatment can potentially increase the stability of neural cell membrane and promote the activation of glial cells in the AD brain.

In summary, this study showed that RJ can reduce cholesterol levels, down-regulate BACE1 and RAGE expression, increase the expression levels of LRP1 and IDE, promote the degradation and clearance of Aβ, and finally reduce Aβ (**Figure 8**). Moreover, we found that RJ has anti-oxidative effects and that it enhances neuronal metabolic activities and prevents neuronal loss. These results together suggest possible mechanisms by which RJ reduces Aβ deposition and prevents neuronal loss, providing preclinical evidence of the utility of RJ as a natural product for potentially preventing and treating AD.

AUTHOR CONTRIBUTIONS

FH, MC, YP designed the research project; YP, JX, CC, FC, PJ, MY and KZ performed the experiment; YP and MC analyzed the data; YP, CWH and FH wrote the article.

ACKNOWLEDGMENTS

This work was supported by the earmarked fund for Modern Agro-industry Technology Research System from the Ministry of Agriculture of China (CARS-44), public projects of Zhejiang Province Science and Technology Department (No. 2016C37092) and Zhejiang Chinese Medical University Comparative Medical Innovation Team (No. XTD201301).

REFERENCES

Ackl, N., Ising, M., Schreiber, Y. A., Atiya, M., Sonntag, A., and Auer, D. P. (2005). Hippocampal metabolic abnormalities in mild cognitive impairment and Alzheimer's disease. *Neurosci. Lett.* 384, 23–28. doi: 10.1016/j.neulet.2005.04.035

Alvarez, E. O., and Ruarte, M. B. (2004). Glutamic acid and histamine-sensitive neurons in the ventral hippocampus and the basolateral amygdala of the rat: functional interaction on memory and learning processes. *Behav. Brain Res.* 152, 209–219. doi: 10.1016/j.bbr.2003.10.012

Baptiste, D. C., Hartwick, A. T., Jollimore, C. A., Baldridge, W. H., Seigel, G. M., and Kelly, M. E. (2004). An investigation of the neuroprotective effects of tetracycline derivatives in experimental models of retinal cell death. *Mol. Pharmacol.* 66, 1113–1122. doi: 10.1124/mol.104.001081

Butenandt, A., and Rembold, H. (1957). Royal jelly of the honeybee. I. Isolation, constitution analysis and incidence of 10-hydroxy-Δ^2-decenoi acid. *Hoppe Seylers Z. Physiol. Chem.* 308, 284–289. doi: 10.1515/bchm2.1957.308.1.284

Celik, E., and Sanlier, N. (2017). Effects of nutrient and bioactive food components on Alzheimer's disease and epigenetic. *Crit. Rev. Food Sci. Nutr.* doi: 10.1080/10408398.2017.1359488 [Epub ahead of print].

Chen, S. Q., Cai, Q., Shen, Y. Y., Wang, P. J., Teng, G. J., Li, M. H., et al. (2012). ^{1}H-MRS evaluation of therapeutic effect of neural stem cell transplantation on Alzheimer's disease in AβPP/PS1 double transgenic mice. *J. Alzheimers Dis.* 28, 71–80. doi: 10.3233/JAD-2010-110893

Chen, S. M., Fan, C. C., Chiue, M. S., Chou, C., Chen, J. H., and Hseu, R. S. (2013). Hemodynamic and neuropathological analysis in rats with aluminum trichloride-induced Alzheimer's disease. *PLoS One* 8:e82561. doi: 10.1371/journal.pone.0082561

Chen, S. Q., Wang, P. J., Ten, G. J., Zhan, W., Li, M. H., and Zang, F. C. (2009). Role of myo-inositol by magnetic resonance spectroscopy in early diagnosis of Alzheimer's disease in APP/PS1 transgenic mice. *Dement. Geriatr. Cogn. Disord.* 28, 558–566. doi: 10.1159/000261646

Cirillo, C., Capoccia, E., Iuvone, T., Cuomo, R., Sarnelli, G., Steardo, L., et al. (2015). S100B inhibitor pentamidine attenuates reactive gliosis and reduces neuronal loss in a mouse model of Alzheimer's disease. *Biomed Res. Int.* 2015:508342. doi: 10.1155/2015/508342

Comas Herrera, A., Prince, M., Knapp, M., Karagiannidou, M., and Guerchet, M. (2016). *World Alzheimer Report 2016: Improving Healthcare for People with Dementia. Coverage, Quality and Costs Now and in the Future.* London: Alzheimer's Disease International.

Cui, W., Sun, Y., Wang, Z., Xu, C., Xu, L., Wang, F., et al. (2011). Activation of liver X receptor decreases BACE1 expression and activity by reducing membrane cholesterol levels. *Neurochem. Res.* 36, 1910–1921. doi: 10.1007/s11064-011-0513-3

Deane, R., Wu, Z., and Zlokovic, B. V. (2004). RAGE (yin) versus LRP (yang) balance regulates alzheimer amyloid β-peptide clearance through transport across the blood-brain barrier. *Stroke* 35, 2628–2631. doi: 10.1161/01.str.0000143452.85382.d1

Deci, S., Lemieux, S. K., Smith-Bell, C. A., Sparks, D. L., and Schreurs, B. G. (2012). Cholesterol increases ventricular volume in a rabbit model of Alzheimer's disease. *J. Alzheimers Dis.* 29, 283–292. doi: 10.3233/JAD-2011-111415

Del Campo, M., Stargardt, A., Veerhuis, R., Reits, E., and Teunissen, C. E. (2015). Accumulation of BRI2-BRICHOS ectodomain correlates with a decreased clearance of Aβ by insulin degrading enzyme (IDE) in Alzheimer's disease. *Neurosci. Lett.* 589, 47–51. doi: 10.1016/j.neulet.2015.01.036

Farris, W., Mansourian, S., Leissring, M. A., Eckman, E. A., Bertram, L., Eckman, C. B., et al. (2004). Partial loss-of-function mutations in insulin-degrading enzyme that induce diabetes also impair degradation of amyloid β-protein. *Am. J. Pathol.* 164, 1425–1434. doi: 10.1016/s0002-9440(10)63229-4

Fereshtehnejad, S. M., Johnell, K., and Eriksdotter, M. (2014). Anti-dementia drugs and co-medication among patients with Alzheimer's disease: investigating real-world drug use in clinical practice using the Swedish Dementia Quality Registry (SveDem). *Drugs Aging* 31, 215–224. doi: 10.1007/s40266-014-0154-8

Fontana, R., Mendes, M. A., de Souza, B. M., Konno, K., César, L. L. M. M., Malaspina, O., et al. (2004). Jelleines: a family of antimicrobial peptides from the Royal Jelly of honeybees (*Apis mellifera*). *Peptides* 25, 919–928. doi: 10.1016/j.peptides.2004.03.016

Fukumoto, H., Cheung, B. S., Hyman, B. T., and Irizarry, M. C. (2002). β-secretase protein and activity are increased in the neocortex in Alzheimer disease. *Arch. Neurol.* 59, 1381–1389. doi: 10.1001/archneur.59.9.1381

Galbete, J. L., Martin, T. R., Peressini, E., Modena, P., Bianchi, R., and Forloni, G. (2000). Cholesterol decreases secretion of the secreted form of amyloid precursor protein by interfering with glycosylation in the protein secretory pathway. *Biochem. J.* 348, 307–313. doi: 10.1042/0264-6021:3480307

Gonzalo-Ruiz, A., Pérez, J. L., Sanz, J. M., Geula, C., and Arévalo, J. (2006). Effects of lipids and aging on the neurotoxicity and neuronal loss caused by intracerebral injections of the amyloid-β peptide in the rat. *Exp. Neurol.* 197, 41–55. doi: 10.1016/j.expneurol.2005.06.008

Guardia-Laguarta, C., Coma, M., Pera, M., Clarimãn, J., Sereno, L., Agulló, J. M., et al. (2009). Mild cholesterol depletion reduces amyloid-β production by impairing APP trafficking to the cell surface. *J. Neurochem.* 110, 220–230. doi: 10.1111/j.1471-4159.2009.06126.x

Guo, H., Saiga, A., Sato, M., Miyazawa, I., Shibata, M., Takahata, Y., et al. (2007). Royal jelly supplementation improves lipoprotein metabolism in humans. *J. Nutr. Sci. Vitaminol.* 53, 345–348. doi: 10.3177/jnsv.53.345

Hattori, N., Nomoto, H., Fukumitsu, H., Mishima, S., and Furukawa, S. (2007). Royal jelly and its unique fatty acid, 10-hydroxy-trans-2-decenoic acid, promote neurogenesis by neural stem/progenitor cells *in vitro*. *Biomed. Res.* 28, 261–266. doi: 10.2220/biomedres.28.261

Hattori, N., Nomoto, H., Fukumitsu, H., Mishima, S., and Furukawa, S. (2010). AMP N_1-oxide, a unique compound of royal jelly, induces neurite outgrowth from PC12 cells via signaling by protein kinase A independent of that by mitogen-activated protein kinase. *Evid. Based Complement. Alternat. Med.* 7, 63–68. doi: 10.1093/ecam/nem146

Holsinger, R. M., McLean, C. A., Beyreuther, K., Masters, C. L., and Evin, G. (2002). Increased expression of the amyloid precursor β-secretase in Alzheimer's disease. *Ann. Neurol.* 51, 783–786. doi: 10.1002/ana.10208

Honda, Y., Fujita, Y., Maruyama, H., Araki, Y., Ichihara, K., Sato, A., et al. (2011). Lifespan-extending effects of royal jelly and its related substances on the nematode *Caenorhabditis elegans*. *PLoS One* 6:e23527. doi: 10.1371/journal.pone.0023527

Jaya Prasanthi, R. P., Schommer, E., Thomasson, S., Thompson, A., Feist, G., and Ghribi, O. (2008). Regulation of β-amyloid levels in the brain of cholesterol-fed rabbit, a model system for sporadic Alzheimer's disease. *Mech. Ageing Dev.* 129, 649–655. doi: 10.1016/j.mad.2008.09.002

Johnstone, E. M., Chaney, M. O., Norris, F. H., Pascual, R., and Little, S. P. (1991). Conservation of the sequence of the Alzheimer's disease amyloid peptide in dog, polar bear and five other mammals by cross-species polymerase chain reaction analysis. *Mol. Brain Res.* 10, 299–305. doi: 10.1016/0169-328x(91)90088-f

Kivipelto, M., Helkala, E. L., Laakso, M. P., Hänninen, T., Hallikainen, M., Alhainen, K., et al. (2001). Midlife vascular risk factors and Alzheimer's disease in later life: longitudinal, population based study. *BMJ* 322, 1447–1451. doi: 10.1136/bmj.322.7300.1447

Kohno, K., Okamoto, I., Sano, O., Arai, N., Iwaki, K., Ikeda, M., et al. (2004). Royal jelly inhibits the production of proinflammatory cytokines by activated macrophages. *Biosci. Biotechnol. Biochem.* 68, 138–145. doi: 10.1271/bbb.68.138

Kuo, P. H., Lin, C. I., Chen, Y. H., Chiu, W. C., and Lin, S. H. (2015). A high-cholesterol diet enriched with polyphenols from Oriental plums (*Prunus salicina*) improves cognitive function and lowers brain cholesterol levels and neurodegenerative-related protein expression in mice. *Br. J. Nutr.* 113, 1550–1557. doi: 10.1017/s0007114515000732

Lacher, S. E., Alazizi, A., Wang, X., Bell, D. A., Pique-Regi, R., Luca, F., et al. (2018). A hypermorphic antioxidant response element is associated with increased MS4A6A expression and Alzheimer's disease. *Redox Biol.* 14, 686–693. doi: 10.1016/j.redox.2017.10.018

Larry Sparks, D. (2004). Cholesterol, copper, and accumulation of thioflavine S-reactive Alzheimer's-like amyloid β in rabbit brain. *J. Mol. Neurosci.* 24, 97–104. doi: 10.1385/jmn:24:1:097

Li, X. Y., Bao, X. J., and Wang, R. Z. (2015). Potential of neural stem cell-based therapies for Alzheimer's disease. *J. Neurosci. Res.* 93, 1313–1324. doi: 10.1002/jnr.23555

Limongi, D., and Baldelli, S. (2016). Redox imbalance and viral infections in neurodegenerative diseases. *Oxid. Med. Cell. Longev.* 2016:6547248. doi: 10.1155/2016/6547248

Liu, Q. Y., Chang, M. N., Lei, J. X., Koukiekolo, R., Smith, B., Zhang, D., et al. (2014). Identification of microRNAs involved in Alzheimer's progression using a rabbit model of the disease. *Am. J. Neurodegener. Dis.* 3, 33–44.

Loke, S. Y., Wong, T. H., and Ong, W. Y. (2017). Global gene expression changes in the prefrontal cortex of rabbits with hypercholesterolemia and/or hypertension. *Neurochem. Int.* 102, 33–56. doi: 10.1016/j.neuint.2016.11.010

Mancini, S., Balducci, C., Micotti, E., Tolomeo, D., Forloni, G., Masserini, M., et al. (2017). Multifunctional liposomes delay phenotype progression and prevent memory impairment in a presymptomatic stage mouse model of Alzheimer disease. *J. Control. Release* 258, 121–129. doi: 10.1016/j.jconrel.2017.05.013

Mecocci, P., MacGarvey, U., and Beal, M. F. (1994). Oxidative damage to mitochondrial DNA is increased in Alzheimer's disease. *Ann. Neurol.* 36, 747–751. doi: 10.1002/ana.410360510

Min, L., Li, J., Liu, K., Jiang, Y., Liu, X., and Liu, X. (2004). Isolation, purification and characterization of superoxide dismutase from royal jelly of the Italian worker bee, *Apis mellifera*. *Acta Entomol. Sin.* 47, 171–177.

Moon, C. M., Kim, B. C., and Jeong, G. W. (2016). Effects of donepezil on brain morphometric and metabolic changes in patients with Alzheimer's disease: a DARTEL-based VBM and ^{1}H-MRS. *Magn. Reson. Imaging* 34, 1008–1016. doi: 10.1016/j.mri.2016.04.025

Nagai, T., and Inoue, R. (2004). Preparation and the functional properties of water extract and alkaline extract of royal jelly. *Food Chem.* 84, 181–186. doi: 10.1016/s0308-8146(03)00198-5

Nagai, T., Inoue, R., Suzuki, N., and Nagashima, T. (2006). Antioxidant properties of enzymatic hydrolysates from royal jelly. *J. Med. Food* 9, 363–367. doi: 10.1089/jmf.2006.9.363

Neumann, U., Rueeger, H., Machauer, R., Veenstra, S. J., Lueoend, R. M., Tintelnot-Blomley, M., et al. (2015). A novel BACE inhibitor NB-360 shows a superior pharmacological profile and robust reduction of amyloid-β and neuroinflammation in APP transgenic mice. *Mol. Neurodegener.* 10:44. doi: 10.1186/s13024-015-0033-8

Panza, F., Capurso, C., D'Introno, A., Colacicco, A. M., Vasquez, F., Pistoia, G., et al. (2006). Serum total cholesterol as a biomarker for Alzheimer's disease: mid-life or late-life determinations? *Exp. Gerontol.* 41, 805–806. doi: 10.1016/j.exger.2006.06.005

Pourmoradian, S., Mahdavi, R., Mobasseri, M., Faramarzi, E., and Mobasseri, M. (2012). Effects of royal jelly supplementation on body weight and dietary intake in type 2 diabetic females. *Health Promot. Perspect.* 2, 231–235. doi: 10.5681/hpp.2012.028

Provencher, S. W. (1993). Estimation of metabolite concentrations from localized *in vivo* proton NMR spectra. *Magn. Reson. Med.* 30, 672–679. doi: 10.1002/mrm.1910300604

Ramadan, M. F., and Al-Ghamdi, A. (2012). Bioactive compounds and health-promoting properties of royal jelly: a review. *J. Funct. Foods* 4, 39–52. doi: 10.1016/j.jff.2011.12.007

Schreurs, B. G., Smith-Bell, C. A., and Lemieux, S. K. (2013). Dietary cholesterol increases ventricular volume and narrows cerebrovascular diameter in a rabbit model of Alzheimer's disease. *Neuroscience* 254, 61–69. doi: 10.1016/j.neuroscience.2013.09.015

Selkoe, D. J. (2001). Alzheimer's disease: genes, proteins, and therapy. *Physiol. Rev.* 81, 741–766. doi: 10.1152/physrev.2001.81.2.741

Shibata, M., Yamada, S., Kumar, S. R., Calero, M., Bading, J., Frangione, B., et al. (2000). Clearance of Alzheimer's amyloid-ß$_{(1–40)}$ peptide from brain by LDL receptor-related protein-1 at the blood-brain barrier. *J. Clin. Invest.* 106, 1489–1499. doi: 10.1172/jci10498

Sparks, D. L., and Schreurs, B. G. (2003). Trace amounts of copper in water induce β-amyloid plaques and learning deficits in a rabbit model of Alzheimer's disease. *Proc. Natl. Acad. Sci. U S A* 100, 11065–11069. doi: 10.1073/pnas.1832769100

Sparks, D. L., Scheff, S. W., Hunsaker, J. C. III., Liu, H., Landers, T., and Gross, D. R. (1994). Induction of Alzheimer-like β-amyloid immunoreactivity in the brains of rabbits with dietary cholesterol. *Exp. Neurol.* 126, 88–94. doi: 10.1006/exnr.1994.1044

Takenaka, T. (1982). Chemical compositions of royal jelly. *Honeybee Sci.* 3, 69–74.

Vassar, R., Kuhn, P. H., Haass, C., Kennedy, M. E., Rajendran, L., Wong, P. C., et al. (2014). Function, therapeutic potential and cell biology of BACE proteases: current status and future prospects. *J. Neurochem.* 130, 4–28. doi: 10.1111/jnc.12715

Vittek, J. (1995). Effect of Royal Jelly on serum lipids in experimental animals and humans with atherosclerosis. *Experientia* 51, 927–935. doi: 10.1007/bf01921742

Wang, Z. F., Li, H. L., Li, X. C., Zhang, Q., Tian, Q., Wang, Q., et al. (2006). Effects of endogenous β-amyloid overproduction on tau phosphorylation in cell culture. *J. Neurochem.* 98, 1167–1175. doi: 10.1111/j.1471-4159.2006.03956.x

Wang, X., Min, C., and Dong, Y. (2016). Royal jelly promotes DAF-16-mediated proteostasis to tolerate β-amyloid toxicity in *C. elegans* model of Alzheimer's disease. *Oncotarget* 7, 54183–54193. doi: 10.18632/oncotarget.10857

Wang, S. H., Wang, Y. Z., Zhang, K. Y., Shen, J. H., Zhou, H. Q., and Qiu, X. Y. (2005). Effect of superoxide dismutase and malondialdehyde metabolic changes on carcinogenesis of gastric carcinoma. *World J. Gastroenterol.* 11, 4305–4310. doi: 10.3748/wjg.v11.i28.4305

Wei, W., Wei, M., Kang, X., Deng, H., and Lu, Z. (2010). A novel method developed for acetylcholine detection in royal jelly by using capillary electrophoresis coupled with electrogenerated chemiluminescence based on a simple reaction. *Electrophoresis* 30, 1949–1952. doi: 10.1002/elps.200800721

Woodruff-Pak, D. S., Agelan, A., and Del Valle, L. (2007). A rabbit model of Alzheimer's disease: valid at neuropathological, cognitive, and therapeutic levels. *J. Alzheimers Dis.* 11, 371–383. doi: 10.3233/jad-2007-11313

Xi, Y. D., Li, X. Y., Ding, J., Yu, H. L., Ma, W. W., Yuan, L. H., et al. (2013). Soy isoflavone alleviates Aβ1–42-induced impairment of learning and memory ability through the regulation of RAGE/LRP-1 in neuronal and vascular tissue. *Curr. Neurovasc. Res.* 10, 144–156. doi: 10.2174/1567202611310020007

Zamani, Z., Reisi, P., Alaei, H., and Pilehvarian, A. A. (2012). Effect of Royal Jelly on spatial learning and memory in rat model of streptozotocin-induced sporadic Alzheimer's disease. *Adv. Biomed. Res.* 1:26. doi: 10.4103/2277-9175.98150

Zhang, Y. P., Brown, R. E., Zhang, P. C., Zhao, Y. T., Ju, X. H., and Song, C. (2017). DHA, EPA and their combination at various ratios differently modulated Aβ25–35-induced neurotoxicity in SH-SY5Y cells. *Prostaglandins Leukot. Essent. Fatty Acids* doi: 10.1016/j.plefa.2017.07.003 [Epub ahead of print].

Zhang, Q. Q., Shi, J. Q., Xu, J., Cheng, X. X., Zhu, H. Q., and Chen, J. (2013). Application of thioflavin T staining in detection of β-amyloid. *Zhonghua Bing Li Xue Za Zhi* 42, 764–765. doi: 10.3760/cma.j.issn.0529-5807.2013.11.011

Zhang, N., Song, X., Bartha, R., Beyea, S., D'Arcy, R., Zhang, Y., et al. (2014). Advances in high-field magnetic resonance spectroscopy in Alzheimer's disease. *Curr. Alzheimer Res.* 11, 367–388. doi: 10.2174/1567205011666140302200312

Zou, C., Montagna, E., Shi, Y., Peters, F., Blazquez-Llorca, L., Shi, S., et al. (2015). Intraneuronal APP and extracellular Aβ independently cause dendritic spine pathology in transgenic mouse models of Alzheimer's disease. *Acta Neuropathol.* 129, 909–920. doi: 10.1007/s00401-015-1421-4

Conflict of Interest Statement: The authors declare that the research was conducted in the absence of any commercial or financial relationships that could be construed as a potential conflict of interest.

Copyright © 2018 Pan, Xu, Chen, Chen, Jin, Zhu, Hu, You, Chen and Hu. This is an open-access article distributed under the terms of the Creative Commons Attribution License (CC BY). The use, distribution or reproduction in other forums is permitted, provided the original author(s) and the copyright owner are credited and that the original publication in this journal is cited, in accordance with accepted academic practice. No use, distribution or reproduction is permitted which does not comply with these terms.

frontiers in Neuroscience

ORIGINAL RESEARCH
published: 12 February 2018
doi: 10.3389/fnins.2018.00042

The Histamine H3 Receptor Antagonist DL77 Ameliorates MK801-Induced Memory Deficits in Rats

*Nermin Eissa[1], Nadia Khan[1], Shreesh K. Ojha[1], Dorota Łazewska[2], Katarzyna Kieć-Kononowicz[2] and Bassem Sadek[1]**

[1] Department of Pharmacology & Therapeutics, College of Medicine & Health Sciences, United Arab Emirates University, Al Ain, United Arab Emirates, [2] Department of Technology and Biotechnology of Drugs, Faculty of Pharmacy, Jagiellonian University-Medical College, Kraków, Poland

The role of Histamine H3 receptors (H3Rs) in memory, and the prospective of H3R antagonists in pharmacological control of neurodegenerative disorders, e.g., Alzheimer disease (AD) is well-accepted. For that reason, the procognitive effects of the H3R antagonist DL77 on cognitive impairments induced with MK801 were tested in an inhibitory passive avoidance paradigm (PAP) and novel object recognition (NOR) task in adult male rats, using donepezil (DOZ) as a standard drug. Acute systemic pretreatment with DL77 (2.5, 5, and 10 mg/kg, i.p.) significantly ameliorated memory deficits induced with MK801 in PAP (all $P < 0.05$, $n = 7$). The ameliorative effect of most promising dose of DL77 (5 mg/kg, i.p.) was reversed when rats were co-injected with the H3R agonist *R*-(α)-methylhistamine (RAMH, 10 mg/kg, i.p.) ($p = 0.701$ for MK801-amnesic group vs. MK801+DL77+RAMH group, $n = 6$). In the NOR paradigm, DL77 (5 mg/kg, i.p.) counteracted long-term memory (LTM) deficits induced with MK801 ($P < 0.05$, $n = 6$–8), and the DL77-provided effect was similar to that of DOZ ($p = 0.788$, $n = 6$–8), and was reversed when rats were co-injected with RAMH (10 mg/kg, i.p.) ($p = 0.877$, $n = 6$, as compared to the (MK801)-amnesic group). However, DL77 (5 mg/kg, i.p.) did not alter short-term memory (STM) impairment in NOR test ($p = 0.772$, $n = 6$–8, as compared to (MK801)-amnesic group). Moreover, DL77 (5 mg/kg) failed to modify anxiety and locomotor behaviors of animals innate to elevated-plus maze (EPM) ($p = 0.67$ for percentage of time spent exploring the open arms, $p = 0.52$ for number of entries into the open arms, $p = 0.76$ for percentage of entries into the open arms, and $p = 0.73$ number of closed arm entries as compared to saline-treated groups, all $n = 6$), demonstrating that the procognitive effects observed in PAP or NOR tests were unconnected to alterations in emotions or in natural locomotion of tested animals. These results signify the potential involvement of H3Rs in modulating neurotransmitters related to neurodegenerative disorders, e.g., AD.

Keywords: histamine H3 receptor, antagonist, learning and memory, Alzheimer's disease, neurodegeneration, passive avoidance paradigm, novel object recognition, behavioral research

OPEN ACCESS

Edited by:
Ghulam Md Ashraf, King Abdulaziz University, Saudi Arabia

Reviewed by:
Shahab Uddin, Hamad Medical Corporation, Qatar
Przemysław Rzodkiewicz, National Institute of Geriatrics, Rheumatology and Rehabilitation, Poland

****Correspondence:***
Bassem Sadek
bassem.sadek@uaeu.ac.ae

Specialty section:
This article was submitted to Neurodegeneration, a section of the journal Frontiers in Neuroscience

Received: *17 October 2017*
Accepted: *17 January 2018*
Published: *12 February 2018*

Citation:
Eissa N, Khan N, Ojha SK, Łazewska D, Kieć-Kononowicz K and Sadek B (2018) The Histamine H3 Receptor Antagonist DL77 Ameliorates MK801-Induced Memory Deficits in Rats. Front. Neurosci. 12:42. doi: 10.3389/fnins.2018.00042

INTRODUCTION

Alzheimer's disease (AD) is a life long-lasting brain disorder that is considered by its cognitive deficits, memory impairment, and dementia (Khunnawutmanotham et al., 2016; Shaik et al., 2016). Following a recent report, around 36 million people worldwide were diagnosed with dementia in recent years, and the number is estimated to significantly increase by the double every two decades, ultimately leading to more than 100 million people with AD after four decades (Khunnawutmanotham et al., 2016). The pathogenesis of AD is still complex, though several theories have been established. The multifaceted pathophysiological alterations include deficient cholinergic neurotransmission, malfunctioning metabolic status of β-amyloid protein, irregularities of numerous central neurotransmitters including glutamate, norepinephrine, serotonin and dopamine, and the contribution of neuroinflammation and high oxidative stress to the progression of AD (Doraiswamy, 2002; Khan et al., 2015; Sadek et al., 2016a). Brain histamine is an established neurotransmitter in the central nervous system (CNS) (Arrang et al., 1983, 1985, 1987a,b, 1988, 2007; Schwartz et al., 1986), exerting its biological activities through interaction with four histamine receptor (HR) subtypes (H1-H4R) that belong to the family of G-protein coupled receptors (Schneider and Seifert, 2009; Panula et al., 2015). H1R and H2R are present in the brain and periphery, whereas H4Rs are predominately expressed in mast cells and leukocytes (Schneider and Seifert, 2009; Panula et al., 2015). Contrary, H3Rs are abundant in the CNS (Arrang et al., 1983, 1985, 1987a,b, 1988, 2007; Panula et al., 2015). Moreover, H3Rs acting as auto-receptors in the CNS are coupled to $G\alpha_{i/o}$-proteins and are capable of controlling the synthesis and release of histamine (Arrang et al., 1983, 1985, 1987a,b, 1988, 2007). Furthermore, H3Rs operating as hetero-receptors located on non-histaminergic neurons in different brain regions can also moderate the release of other neurotransmitters including acetylcholine, glutamate, GABA, norepinephrine, serotonin, dopamine (Brown et al., 2001, 2013). Previous preclinical experiments have proposed H3R antagonists to be of characteristic feature by their possible memory-enhancing effects (Panula et al., 1998, 2015; Panula and Nuutinen, 2011; Sadek and Stark, 2015; Sadek et al., 2016b). Accordingly, several H3R antagonists improved cognitive deficits induced with ketamine and MK801 in numerous animal models (Browman et al., 2004), suggesting that these H3R antagonists may also be effective in neurodegenerative disorders, e.g., AD (Witkin and Nelson, 2004; Bardgett et al., 2010; Charlier et al., 2013; Sadek and Stark, 2015; Sadek et al., 2016b). Among a wide range of H3R antagonists investigated so far, H3R antagonists ABT-239 and A-431404 were found to ameliorate cognitive deficits induced by ketamine and MK-801 in rodents, demonstrating enhanced procognitive effects of these compounds compared to standard drugs, e.g., DOZ (Brown et al., 2013). Therefore, the central H3Rs embodies an attractive target for the development of novel H3R antagonists with the prospective therapeutic future in neurodegenerative disorders (Yokoyama et al., 1993; Yokoyama, 2001; Harada et al., 2004; Witkin and Nelson, 2004; Uma Devi et al., 2010; Bhowmik et al., 2012, 2014; Sadek and Stark, 2015; Sadek et al., 2016b). Regardless of the abovementioned experimental observations for the role for H3Rs in the modulation of memory deficits and related behaviors, targeting H3Rs in the CNS is not commonly proposed as a future strategy to treat AD.

In the current study and as a continuation of our research efforts, the procognitive effects of the non-imidazole H3R antagonist, namely DL77 [1-(3-(4-*tert*-pentylphenoxy)propyl)piperidine dihydrogenoxalate], with high *in vitro* selectivity to human H3R, high antagonist affinity in the subnanomolar concentration range and a pK_i-value of 8.03, and high H3R antagonist *in vivo* potency with an ED_{50} value of 2.1 ± 0.2 mg/kg, per oral (p.o.) (Łazewska et al., 2006) has been explored on its procognitive effects on memory deficits induced with MK801 in PAP and NOR paradigms in adult male rats applying DOZ as a reference drug. Moreover, the effects of DL77 on anxiety and locomotor behaviors in EPM was assessed, since anxiety and locomotion could influence the performance of rats in PAP or NOR. Furthermore, the abrogative effects of the histamine H3R agonist RAMH on the memory-enhancing effects provided with DL77 in PAP and NOR paradigms were examined. The non-imidazole H3R antagonist DL77 was selected for testing in the current studies as it in an earlier study proved to exhibit (5–15 mg/kg, i.p.) anticonvulsant properties and procognitive effects on acquisition, consolidation and retrieval in the same animal species (Sadek et al., 2016c). Also, a previous study showed a promising effects of DL77 (3–30 mg/kg, i.p.) on alcohol intake and preference in adult C57BL/6 mice (Bahi et al., 2015).

EXPERIMENTAL PROCEDURES

Animals

Male Wistar rats (inbred of Central Animal Facility of the UAE University, aged 6–8 weeks) of body weight 180–220 g were used for the study. The animals were retained in an air-conditioned animal facility room with controlled temperature (24 ± 2°C) and humidity (55 ± 15%) under a 12 h light/dark cycle, and were provided free access to food and water. Experiments were carried out between 9:00 and 13:00 h, and all procedures were approved by the Institutional Animal Ethics Committee of College of Medicine and Health Sciences/United Arab Emirates University (A30-13). All efforts were made to minimize animal suffering, to reduce the number of animals used. Also, all behavioral studies were conducted in a blinded fashion and by the same experimenter.

Drugs

R-(α)-methylhistamine dihydrochloride (RAMH), donepezil hydrochloride (DOZ), and MK801 hydrogen maleate were purchased from Sigma-Aldrich (St Louis, Missouri, USA). The H3R antagonist 1-(3-(4-*tert*-pentylphenoxy)propyl)piperidine dihydrogenoxalate (DL77, 2.5, 5, 10, mg/kg) was synthesized by

Abbreviations: AD, Alzheimer disease; H3Rs, histamine H3 receptors; RAMH, *R*-(α)-methyl-histamine; DOZ, donepezil; MK801, dizocilpine; PAP, passive avoidance paradigm; STL, step-through latency; NOR, novel object recognition; STM, short-term memory; LTM, long-term memory; EPM, elevated plus maze; p.o., per oral; i.p., intraperitoneal.

us in the Department of Technology and Biotechnology of Drugs (Kraków, Poland) as described previously (Meier et al., 2001; Łazewska et al., 2006). All drugs were dissolved in isotonic saline and injected intraperitoneal (i.p.) at a volume of 1 ml/kg, and all doses were expressed in terms of the free base.

Behavioral Tests

Inhibitory PAP Test

Male adult Wistar rats were tested in a two compartment step-through passive avoidance apparatus (Step-through Cage, 7550, Ugo Basile, Comerio, Italy) as described previously (Izquierdo et al., 1999; Bernaerts et al., 2004; da Silva et al., 2009; Goshadrou et al., 2013; Khan et al., 2015; Sadek et al., 2016a,c; Alachkar et al., 2017; Sultan et al., 2017), with minor modifications. The test was conducted in an automatically operated commercial passive avoidance apparatus as previously described (Khan et al., 2015; Sadek et al., 2016a,c; Alachkar et al., 2017). The experiment consisted of two trials (training and testing) separated by a 24 h interval. Each rat in the first trial was placed in the white compartment (facing the auto guillotine door) and after a 30-s habituation period the door was raised automatically. The rat was given a 60 s cut-off time to step-through to the dark compartment. Rats that failed to move within this time period were excluded from the test session on the following day. Once the rat moved into the dark compartment, the sliding door was lowered and a scrambled foot shock (0.4 mA, 20 Hz, 8.3 ms) was delivered to the grid floor for a duration of 3 s. The power of the delivered foots-hock was designated following confirming the sensitivity threshold that yields the minimal vocalization and jumping responses in tested rats. The rat was removed from the dark chamber directly after receiving the foot-shock, returned to its home cage, and both compartments were cleaned. The animals were trained for 3 consecutive days; in which they were injected with saline i.p. 30–45 min before each training session, with the only modification that the cut-off latency was put at 300 s to move to the dark compartment without delivery of scrambled foot-shock (Khan et al., 2015; Sadek et al., 2016a,c). Rats that did not move into the dark compartment during the training, despite the practices carried out during training sessions, were excluded from the current test. For each separate experiment, 9–11 animals of the same age and weight average were trained on the step-through latency (STL) paradigm. Approximately 2–4 rats failed to demonstrate enhanced performance in a cut-off time of 60 s. In the current series of behavioral experiments, a group of 7 animals was used for each STL task conducted for the PAP. In the test session, animals were turned amnesic with acute systemic injection of MK801 (0.1 mg/kg, i.p.) 30–45 min prior to test session, and the animals were allowed to move to the dark compartment for a maximum period of 300 s. In this test session, the STL time for each rat to enter the dark compartment in 300 s was measured.

Dose regimen

Six groups of seven rats each were used, and were pretreated with Saline+Saline, MK801+Saline, MK801+DL77 (2.5, 5, and 10 mg/kg, i.p.), or MK801+DOZ (1 mg/kg, i.p.) 30–45 min before the test session, and the procognitive effects DL77 (2.5, 5, and 10 mg/kg, i.p.) on amnesia induced with acute systemic injection of MK801 (0.1 mg/kg, i.p.) was investigated by determining the STLs to move into the dark compartment. In an additional experiment, a single group of seven rats received two injections; the first injection contained the most effective dose of DL77 and was administered 30–45 min before the PAP test, and the second injection contained RAMH (10 mg/kg, i.p.) which was administered 15–20 min prior PAP test. The CNS penetrant H3R agonist RAMH was injected 15–20 min before the start of test conduction to ensure its presence in the CNS, as RAMH shows fast metabolism (Krause et al., 2001). Doses of DL77, DOZ, and RAMH were chosen according to previously published results in the same species of rodents (Orsetti et al., 2001, 2002; Khan et al., 2015; Sadek et al., 2016a,c) (**Figures 1**, **2**).

NOR Test

Recognition memory was assessed in a novel object recognition (NOR) test as previously described (Ennaceur and Delacour, 1988; Izquierdo et al., 1999; de Lima et al., 2005; Karasawa et al., 2008; Alachkar et al., 2017). The experiments were conducted in a black open field box (50 × 35 ×50 cm), and the experimental procedure included two sessions of habituation of 1 h interval, whereby the animals were provided 3 min time to explore the apparatus. On the test day and after a 3 min exploration of the apparatus, two novel objects were introduced in two corners (∼30 cm apart from each other). The objects (9 × 5 × 9 cm) used in this study were wood blocks and existed in different shape and color, but were of the same size. They appeared devoid of natural

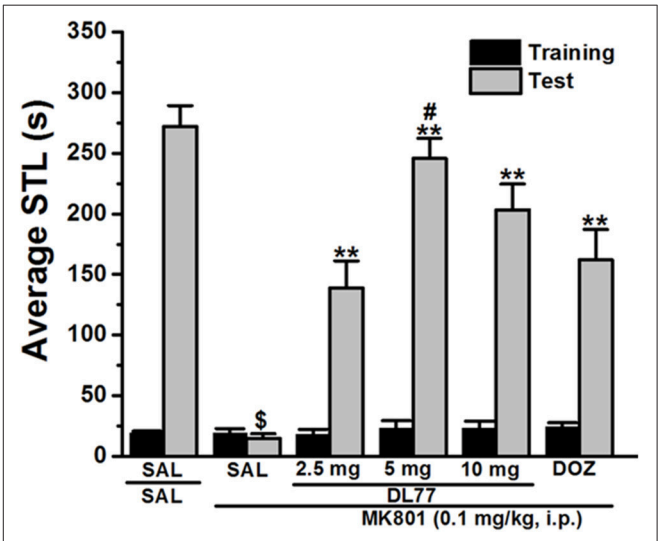


FIGURE 1 | Effects of DL77 on MK801-induced memory deficits in an inhibitory PAP in rats. Gray columns represent the mean STLs measured during the training trial before the delivery of the foot-shock (pre-shock latencies) and black columns the mean STLs measured during the retention test (test latencies). Rats were injected with DL77 (2.5, 5, or 10 mg/kg, i.p.) or donepezil (DOZ, 1 mg/kg, i.p.) 30 min before the test session. $^{\$}P < 0.001$ for mean STLs vs the value of the (saline)-treated group. $^{**}P < 0.001$ for mean STLs vs. the value of the (MK801)-treated group. $^{\#}P < 0.05$ for mean STLs vs. the value of MK801+DOZ-treated group. Data are expressed as mean ± SEM ($n = 7$).

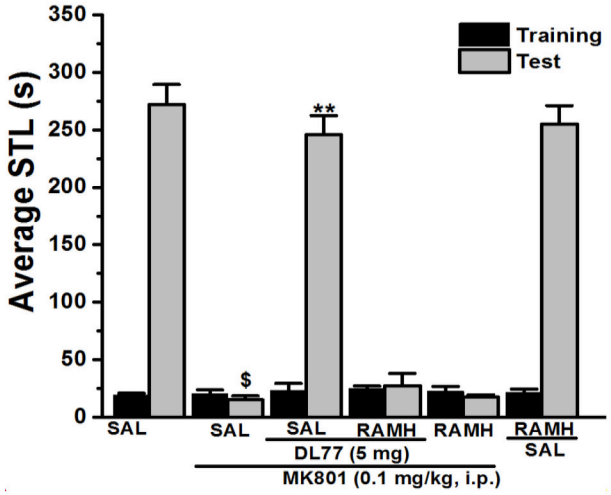


FIGURE 2 | Effect of vehicle, DL77, and RAMH on MK801-induced deficit in an inhibitory PAP in rats. Gray columns represent the mean STLs measured during the training trial before the delivery of the foot-shock (pre-shock latencies) and black columns the mean STLs measured during the retention test (test latencies). Rats were injected with DL77 (5 mg/kg, i.p.), RAMH, or a combination of RAMH (10 mg/kg)+DL77 (5 mg/kg) 15 min (RAMH) or 30 min (DL77) before the test session. $^{\$}P < 0.001$ for mean STLs vs. the value of the (Saline)-treated group. $^{**}P < 0.001$ for mean STLs vs. the value of the (MK801)-treated group. Data are expressed as mean ± SEM ($n = 7$).

significance for the animals and had never been linked with reinforcement. They were adequately heavy to be not displaced by the tested rats. The experimental session consisted of two trials T1 and T2, each lasting for 3 min. In T1, rats were exposed to two identical objects, and those exploring the objects for less than 10 s during T1 were excluded from the tests. In T2, performed 120 min (for STM) or 24 h (for LTM) later, rats were exposed to two objects, one of which was a duplicate of familiar object in order to exclude olfactory traits, and another novel object. The role (familiar or novel object) as well as the relative position of the two objects were counterbalanced and arbitrarily permuted during T2. The principle measure was the time spent by the rat for exploring objects during both trials, namely T1 and T2. The test box as well as all used objects were thoroughly cleaned with 70% (volume/volume; v/v) alcoholic solution. All sessions of NOR test were executed during the light phase (8:00–12:00 a.m.). In order to detect procognitive effects of test compound, MK801 and test compound were dissolved in isotonic saline and injected i.p. at a volume of 1 ml/kg 30–45 min. following T1. The control groups received an equivalent volume of saline injection. The choice of doses and pretreatment times for each compound was decided according to the results of most promising dose in PAP and was derived from previously reported procognitive studies (Bernaerts et al., 2004; da Silva et al., 2009; Goshadrou et al., 2013; Khan et al., 2015; Sadek et al., 2016c; Alachkar et al., 2017; Sultan et al., 2017).

Dose regimen

Six groups of six to eight rats each were used for the detection of a procognitive effect in STM. The groups were injected with Saline, MK801, MK801+DL77 (5 mg/kg, i.p.), MK801+DL77(5 mg/kg)+RAMH (10 mg/kg, i.p.), MK801+DOZ (1 mg/kg, i.p.), or MK801+RAMH (10 mg/kg, i.p.) 30–45 min before T2, respectively, and the counteracting effects of DL77 on cognitive deficits induced with MK801 were assessed by measuring the time spent by the rat in exploring objects in both trials T1 and T2 for STM (**Figure 3**). In an additional experiment, the procognitive effect of DL77 on MK801-induced memory impairments was confirmed by abrogative study in which the respective promising dose (5 mg/kg, i.p.) of DL77 and RAMH (10 mg/kg, i.p.) were co-administered to a separate group of six rats 30–45 min prior to T2 and 24 h after T1. The latter experiment was carried out to confirm the procognitive effect for LTM, whereas control groups received comparable saline injections (**Figure 4**). Doses of MK801, RAMH, and DOZ were chosen according to previous experimental protocols of NOR (Bernaerts et al., 2004; de Lima et al., 2005; da Silva et al., 2009; Goshadrou et al., 2013; Khan et al., 2015; Sadek et al., 2016c; Alachkar et al., 2017; Sultan et al., 2017).

EPM Test

Anxiety-like behaviors were evaluated in an EPM as previously described (Jiang et al., 2016; Alachkar et al., 2017). The EPM apparatus consisted of several parts including one central part (8 × 8 cm), two opposing open and closed arms (30 × 8 cm), and nontransparent walls (30 cm in height). Between every session, both the plat form and the wall were thoroughly cleaned using 10% alcoholic spray. Animals were placed individually in the center arena of the maze (50 cm above the floor) facing an open arm, and test sessions took place in the light phase (9:00–12:00 a.m.). The amount of time spent with head and forepaws on the open arms and closed arms of the maze as well as the number of entries into each arm was manually scored for a session of 5 min. The maze was thoroughly cleaned between sessions using a tissue dampened with 70% (volume/volume; v/v) alcohol to remove the odor after each rat was tested. The total number of entries into the closed arms is usually used as an index of locomotor activity in the test.

Dose regimen

Rats were divided into two groups of six rats each. One group received saline injection i.p. 30–45 min before the test and test group received the H3R antagonist DL77 (5 mg/kg, i.p.) for testing its modulating effects on anxiety and locomotion (**Figure 5**).

Statistical Analysis

IBM® SPSS Statistics® version 24 software (IBM Middle East, Dubai, United Arab Emirates) was used for all statistical comparisons. The results of NOR were expressed as the means and standard errors (SEM) of the exploratory time spent by the rat exploring both objects in T1 and T2. The results of the EPM test were expressed as the means and SEM of the percentage time spent on open arms, number of entries into the open arms, the percentage of entries into the open arms, and number of entries into closed arms. Results of NOR and EPM were analyzed by using a two-way analysis of variance

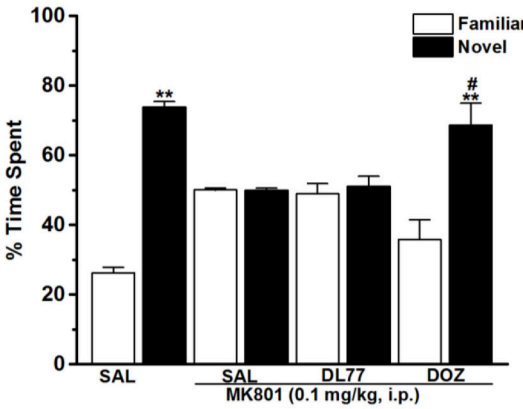


FIGURE 3 | Effects of DL77 on MK801-induced STM cognitive deficits in NOR paradigm in rats. Following training session T1, DL77 (5 mg/kg) or DOZ (1 mg/kg) was administrated i.p., followed 30 min later by i.p. administration of MK801 at a dose of 0.1 mg/kg. The test session T2 was performed 120 min (STM) after the training session T1. Results are calculated as individual percentage of time spent exploring familiar (white columns) and novel (black columns) objects. Data represent mean ± SEM ($n = 6$). $^{**}P < 0.001$ vs. respective familiar object. $^{\#}P < 0.05$ vs. MK801-treated group.

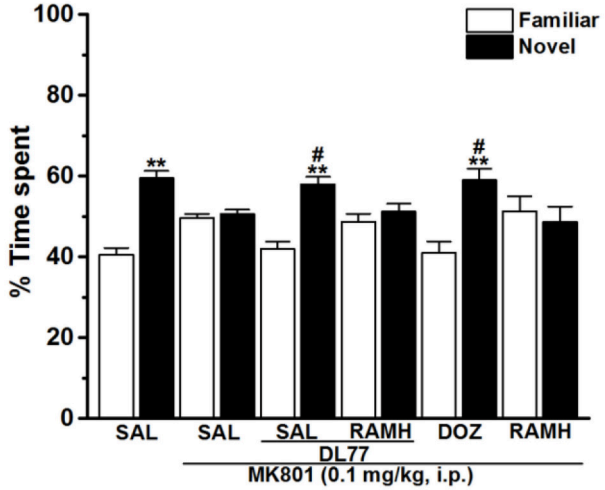


FIGURE 4 | Effects of DL77 on MK801-induced LTM cognitive deficits in NOR paradigm in rats. Following training session T1, DL77 (5 mg/kg) or DOZ (1 mg/kg) was administrated i.p., followed 30 min later by i.p. injection of MK801 at a dose of 0.1 mg/kg. The test session T2 was performed 24 h (LTM) after the training session T1. Results are calculated as individual percentage of time spent exploring familiar (white columns) and novel (black columns) objects. Data represent mean ±SEM ($n = 6$). $^{**}P < 0.001$ vs. respective familiar object. $^{\#}P < 0.05$ vs. MK801-treated group.

(ANOVA). When relevant *post-hoc* comparisons were performed with *Bonferroni's* test in case of a significant main effect. STLs observed in PAP test were expressed as means and SEM. Because of the arbitrary cutoff latency used, the results were evaluated by using nonparametric Kruskal–Wallis ANOVA, and the differences between groups were estimated by individual Mann–Whitney *U*-tests. The criterion for statistical significance was set at *P*-value of <0.05.

RESULTS

Memory-Enhancing Effects of H3R Antagonist DL77 and Standard Drug DOZ on Memory Deficits Induced with MK801 in PAP Task

The effect of acute systemic injection of DL77 at three different doses, namely 2.5, 5, and 10 mg/kg, and DOZ (1 mg/kg) on memory deficits induced with MK801 in an inhibitory PAP test in rats are shown in **Figure 1**. Statistical analysis of observed results indicated that acute systemic pretreatment with the three doses of DL77, and DOZ (1 mg/kg) prior to retention test exhibited a significant memory-enhancing effect on STLs [$H_{(5)} = 28.29$; $P < 0.001$; **Figure 1**]. As shown following pairwise comparisons, MK801 (0.1 mg/kg) decreased STL time when compared to the (saline)-treated control group with ($U = 28.00$, $P < 0.05$). Moreover, DL77 tested in three different doses (2.5, 5, and 10 mg/kg) showed significant improving effect on STLs time when compared to (MK801)-treated group with (all $P < 0.05$). However, pretreatment with DL77 (5 mg/kg, i.p.) was found to be not significantly different from (Saline)-treated control rats ($U = 38.50$, $p = 0.073$) (**Figure 1**). Furthermore, DL77 (5 mg/kg) showed signicantly higher improving effects on STL when compared with the DOZ(1 mg)-provided memory-enhancing efects with ($U = 5.00$, $P < 0.05$) (**Figure 1**).

Abrogative Effects of RAMH on the Memory Improvement Provided with DL77 in MK801-Induced Deficits in PAP Task

For this experiment, a group of seven animals was injected with the most promising dose of DL77 (5 mg/kg, i.p.) 30–45 min prior to test, and also adminstered with the H3R agonist RAMH (10 mg/kg, i.p.) 15 min before the test session (**Figure 2**). As shown in **Figure 2**, statistical analysis revealed that this factor had a significant effect on the STL time [$H_{(5)} = 31.32$; $P < 0.001$]. Moreover, pairwise comparisons indicated that acute systemic pretreatment with DL77 (5 mg/kg, i.p.) enhanced STL time when compared to the (MK801)-amnesic group with ($U = 49.00$; $P < 0.05$). Interestingly, the improvmemnt of observed STL time provided with DL77 was abrogated following acute co-injection of RAMH ($U = 49.00$; $p = 0.701$: MK801-amnesic group vs. MK801+DL77+RAMH group, **Figure 2**). Noteably, acute systemic administration of RAMH (10 mg/kg, i.p.) alone failed to affect the observed STL time in MK801-amnesic group as well as in Saline group with no significant differences ($U = 30.50$; $p = 0.442$) and ($U = 20.50$; $p = 0.620$), respectively (**Figure 2**).

Modulating Effects of H3R Antagonist DL77 and DOZ on the STM Deficits Induced with MK801 in NOR Task

The results observed for the total time exploring both objects during T1 and T2 were not significantly different when

comparing groups pretreated with saline and those injected with MK801 (**Table 1**). The latter experimental observation is substantial to exclude any confounding factors, e.g., that the post-training treatment with the amnesic compound MK801 in the first experiment did not modify sensorimotor considerations such as locomotor activity and motivations of tested animals. Furthermore, statistical results revealed that no significant differences were present in exploratory times between the two identical objects during T1 for each respective experimental group of animals (**Table 1**). The observed results, also, showed that acute systemic pretreatment with DL77 (5 mg/kg, i.p.) and standard drug DOZ (1 mg/kg, i.p.) significantly counteracted time spent exploring objects in T2 with $[F_{(3, 20)} = 13.76; P < 0.001]$ when injected 30–45 min after T1 (**Figure 3**). As revealed by conducted post hoc analyses, MK801 (0.1 mg/kg, i.p.) decreased memory toward the novel object in T2 when compared to the (saline)-treated group with $[F_{(1, 10)} = 140.96; P < 0.001]$, and DOZ (1 mg/kg, i.p.) significantly counteracted this memory deficit in STM in T2 when compared to (MK801)-amnesic group $[F_{(1, 10)} = 7.02; P < 0.05)]$. Contrary, acute systemic administration of DL77 (5 mg/kg, i.p.) did not counteract the decreased STM when compared to (MK801)-amnesic group with $[F_{(1, 10)} = 0.08; p = 0.772]$.

Modulating Effects of H3R Antagonist DL77 and DOZ on the LTM Deficits Induced with MK801 in NOR Task

The results showed that H3R antagonist DL77 (5 mg/kg, i.p.) and standard drug DOZ (1 mg/kg, i.p.) when injected 30–45 min before T2 exhibited a significant counteracting effect on time spent exploring objects in T2 with $[F_{(5, 30)} = 2.67; P < 0.05]$ (**Figure 4**). Moreover, subsequent *post-hoc* analyses revealed that MK801 (0.1 mg/kg, i.p.) decreased memory for the novel object in T2 when compared to the (MK801)-amnesic

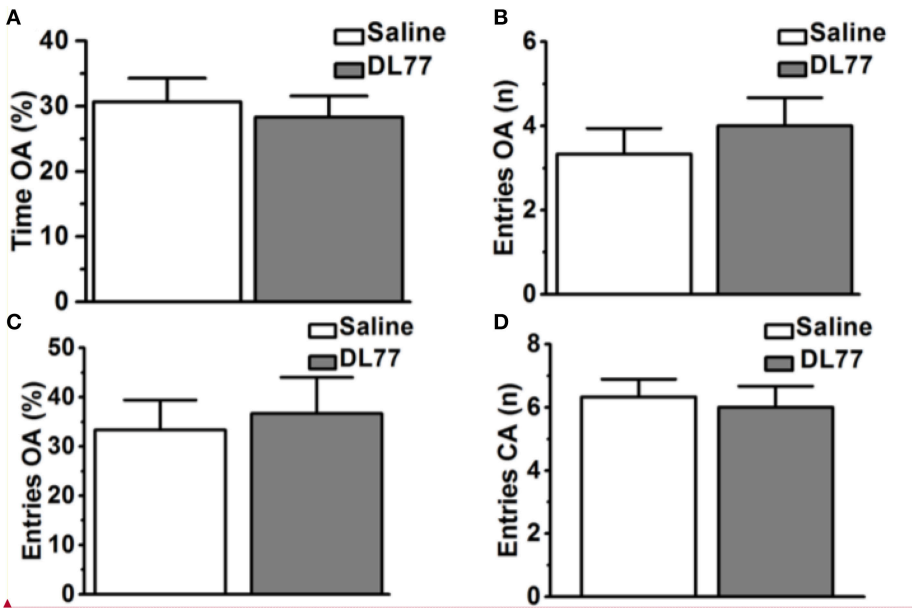


FIGURE 5 | Effects of acute systemic administration of DL77 on exploratory behavior in EPM. DL77 (5 mg/kg) did not alter the percentage of time spent on the open arms of the EPM **(A)**, increase the number of entries into the open arms **(B)** and the percentage of entries into the open arms **(C)**. Acute systemic pretreatment with the H3R antagonist/inverse agonist DL77 (5 mg/kg, i.p.) did not affect the number of closed arm entries **(D)**. Data are expressed as mean ± SEM ($n = 6$).

TABLE 1 | Effects of DL77 on MK801-induced total exploratory time spent with both objects during training and test session in NOR in rats.

Group		Time exploring objects (s)			
	n	Training session STM	Test session STM	Training session LTM	Test session LTM
Saline	6	37.50 ± 3.2	41.83 ± 2.67	36.67 ± 2.93	38.17 ± 3.86
MK801	8	36.00 ± 2.73	42.25 ± 1.57	23.63 ± 2.73	28.88 ± 2.32
MK801 + DL77(5 mg/kg)	8	24.88 ± 2.73	28.17 ± 3.57	23.50 ± 1.71	23.63 ± 2.73
MK801+DL77(5 mg/kg)+RAMH(10 mg/kg)	6	ND	ND	23.63 ± 2.73	23.33 ± 4.87
MK801+DOZ(1 mg/kg)	6	24.83 ± 1.72	25.33 ± 1.88	23.00 ± 3.34	25.33 ± 1.68
MK801+RAMH(10 mg/kg)	6	ND	ND	21.67 ± 1.74	22.67 ± 2.35

Data are expressed as mean ±SEM of 6 or 8 animals per experimental group. There were no significant differences in total exploratory times among treated groups.

group with [$F_{(1, 10)} = 13.92$; $P < 0.05$]. However, acute systemic administration with the H3R antagonist DL77 (5 mg/kg, i.p.) significantly counteracted the induced memory deficits in LTM when compared to (MK801)-amnesic group with [$F_{(1, 10)} = 9.05$; $P < 0.05$] (**Figure 4**). Moreover, the LTM-enhancing procognitive effect provided by DL77 (5 mg/kg, i.p.) was reversed when rats were co-administered with RAMH (10 mg/kg, i.p., i.p.) as compared to the (MK801)-amnesic group with [$F_{(1, 10)} = 0.03$; $p = 0.877$]. Notably, the significant LTM enhancing effect provided with DL77 (5 mg/kg, i.p.) was comparable to the effects observed by the standard drug DOZ (1 mg/kg, i.p.) in T2 with [$F_{(1, 10)} = 0.08$; $p = 0.788$]. Also and similar to the results observed in STM, statistical analyses revealed that RAMH (10 mg/kg, i.p.) alone did not alter LTM in T2 when compared to the MK801-amnesic group with [$F_{(1, 10)} = 0.20$; $p = 0.67$] (**Figure 4**).

Effect of DL77 on Rat Anxiety and Locomotor Activity in EPM Test

Figure 5 shows the observed effects of acute systemic injection of Saline or H3R antagonist DL77 (5 mg/kg, i.p.) on the anxiety parameters of rats exposed to the EPM, namely the percentage of time spent in open arms, the number of entries into open arms, the percentage entries into open arms, and locomotor activity expressed as the number of entries into closed arms. Subsequent *post-hoc* analyses showed that DL77 (5 mg/kg, i.p.) did not alter the percentage of time spent exploring the open arms of the maze during a 5 min session when compared to saline-treated group with [$F_{(1, 10)} = 0.19$, $p = 0.67$] (**Figure 5A**). Moreover, further analyses of data describing the number and percentage of entries into the open arms of the maze [$F_{(1, 10)} = 0.45$, $p = 0.52$; $F_{(1, 10)} = 0.10$, $p = 0.76$, respectively] yielded practically the same results. As depicted in **Figures 5B,C**, no significant differences were obtained between the results in the DL77(5 mg/kg)-treated group and those observed in the saline-treated group (**Figures 5B,C**). Interestingly, the number of closed arm entries following DL77 injection was not significantly changed with [$F_{(1, 10)} = 0.12$, $p = 0.73$], demonstrating that locomotor activity as such was not modulated following acute systemic administration with the H3R antagonist DL77 (5 mg/kg, i.p.) (**Figure 5D**).

DISCUSSION

In the current series of experiments, acute systemic injection of 2.5, 5, and 10 mg/kg of DL77 ameliorated the memory deficits induced by MK801 in an inhibitory PAP in rats. The observed results revealed that DL77 significantly reversed the memory deficits induced by MK801 (**Figure 1**). Since MK801 is a very well-known NMDA receptor antagonist and NMDA receptors were confirmed with their important role in both consolidation and retrieval processes, it is likely that DL77 partially counteracted memory deficits induced with MK801 through direct interaction and activation of NMDA receptors by the increased release of central histamine as a consequence of antagonistic activity of DL77 at histamine H3-auto-receptors. These latter results are in agreement with earlier studies in which histamine enhanced NMDA receptor-mediated neurotransmission in cultured hippocampal cells, indicating that the interaction between histamine and NMDA receptors might facilitate the histamine's capability to counteract MK801-induced amnesic effect (Vorobjev et al., 1993; Xu et al., 2005; Brabant et al., 2013; Sadek et al., 2016a). Notably, the procognitive effect provided by DL77 was dose-dependent, as DL77 at a dose of 5 mg/kg provided significantly higher counteracting effect on decreased STL time when compared to the lower as well as higher dose (2.5 and 10 mg/kg), respectively, indicating that an optimum of DL77-provided memory-enhancing effect might have been reached with a dose of 5 mg/kg, and that off-targets effects could have been present following acute systemic administration of DL77 at a dose of 10 mg/kg (**Figure 1**). Interestingly, the latter observations for the dose dependency are, also, similar to those observed in previous preclinical experiments in rodents (Benetti and Izquierdo, 2013; Benetti et al., 2013; Sadek et al., 2016c). Moreover, the results observed in regard to dose dependency strongly support our previous results detected for the effects of H3R antagonist DL77 (2.5, 5, and 10 mg/kg, i.p.) on different memory stages, namely acquisition, consolidation, and retrieval (Sadek et al., 2016c). Notably, the observed procognitive effects for DL77 (5 mg/kg) were comparable to those obtained for the reference drug DOZ, a procognitive compound available for memory-enhancing effect, since there is up to date no reference drug which is targeting H3Rs (**Figure 1**). Moreover, the procognitive effects found for DL77 (5 mg/kg) were completely reversed when animals were pretreated with the CNS penetrant H3R agonist RAMH, indicating clearly that blockade of H3Rs substantially contributes in the central neurotransmissions associated with retrieval processes of tested animals (**Figure 2**). Unlike the inhibitory PAP, the NOR paradigm in rodents does not involve a reward or a punishment, and it takes advantage of their innate interest for exploring their environment, as it is established on the natural behavior of rodents. Therefore, the behavioral reaction of tested animals is not biased by reinforcement/response interactions of tested rats. Also, the NOR task is a behavioral paradigm used in animal models to evaluate aspects related to cognitive performance, e.g., recognition memory (Jaaro-Peled, 2009; Tseng et al., 2009; Brown et al., 2013; Callahan et al., 2017). Furthermore, previous preclinical studies revealed that NOR paradigm can be utilized in cognitive related experiments due to its sensitivity to both agents capable of impairing (Ennaceur and Delacour, 1988; Ennaceur and Meliani, 1992a,b) as well as enhancing cognition (Lebrun et al., 2000; Barak and Weiner, 2011) following acute systemic pre- and/or post-training administration of the individual agent (King et al., 2004; de Lima et al., 2005; Pichat et al., 2007). In the current study, acute systemic post-training injection of DL77 (5 mg/kg, the most promising dose in PAP test) significantly improved the exploratory time spent with the novel object compared with the familiar objects (**Figure 3**). These observations are in consensus with previous reports revealing that various H3R antagonists belonging to the imidazole-based class, e.g., thioperamide and clobenpropit (Giovannini et al., 1999), and to the non-imidazole-based class, e.g., pitolisant (Ligneau et al., 2007); GSK189254 (Giannoni et al., 2010); SAR110894 (Griebel et al., 2012), and

ABT-239 (Provensi et al., 2016) counteracted the memory-impairing effects of MK801 and scopolamine in NOR tests using different rodents. In our conducted experiments, DL77 potently counteracted the LTM-impairing effects induced with MK801, and these DL77-provided effects were entirely reversed when rats were co-injected with the H3R agonist RAMH (**Figure 3** and **Table 1**). The latter observations are in agreement with an earlier study in which RAMH abolished the memory-enhancing effects provided by H3R antagonist ciproxifan on LTM (Pascoli et al., 2009). Unlike the results observed for DL77 on LTM, acute systemic post-training administration of DL77 did not increase the exploratory time spent with the novel objects in STM when compared with the familiar objects (**Figure 4** and **Table 1**). The latter results are in discrepancy with earlier studies in which H3R antagonist ABT-239 enhanced STM in mice (Provensi et al., 2016). The discrepancy in the results observed in STM might be explained with the different species used or the differences in doses used or in the conduct of experiments. Accordingly, acute systemic post-training administration of MK801 was used in the current study to induce amnesia, whereas natural memory decline as well as presence or absence of histaminergic neurotransmission were examined in the study conducted by Provensi et al. (2016). Moreover, the current experimental findings in NOR obviously point toward profound contribution of histaminergic H3Rs in neuronal circuits associated with the DL77-provided procognitive effects in LTM (**Figure 4** and **Table 1**). The lack of memory-enhancing activity of DL77 in STM is in agreement with previous reports in which no differences were found in time spent exploring novel object in wild type (intact brain histamine) and histidine decarboxylase-knocked out mice (lack of brain histamine) when tested 2 h post-training (STM), but not when testing 24 h post-training (LTM), indicating that histaminergic neurotransmission is more involved the neural circuits which modulate the LTM (Acevedo et al., 2006, 2007; Provensi et al., 2016). Interestingly, several H3R antagonists have in earlier preclinical studies been designated as talented candidates for AD and were suggested to be of possible novel therapeutics due to their capability to interact with H3 auto- and hetero-receptors, modulating the synthesis and release of numerous brain neurotransmitters critical for cognition, including histamine, dopamine, and acetylcholine (Brioni et al., 2011; Sadek and Stark, 2015; Sadek et al., 2016b). The EPM test is considered to be one of the most used animal tests in neuroscience to assess emotionality-related behaviors, e.g., anxiety, based on the innate tendency of animals to avoid open spaces in favor of protected areas, while measuring percent and/or number of closed arms entries reportedly ensures that behavior observed in the maze did not simply reflect drug-induced alterations in locomotor activity (Fernandes and File, 1996; Hogg, 1996; Alachkar et al., 2017). Notably, DL77 at the dose (5 mg/kg) that exhibited the most encouraging procognitive effect in PAP and NOR paradigms did not affect anxiety levels of the adult male Wistar rats (**Figures 5A–D**). Also, DL77 administered at the same dose (5 mg/kg) did not affect the number of closed arm entries, indicating that DL77 failed to modify locomotion of tested rats, demonstrating that enhanced memory performance in PAP as well as NOR is not related to modified emotional responses or altered spontaneous locomotor activity considered as confounding factors when assessing memory-enhancing effects in PAP and NOR (**Figure 5D**) (McGaugh and Roozendaal, 2009; Charlier et al., 2013). The latter results are, also, in line with our earlier results in which acute systemic injection of DL77 (2.5, 5, and 10 mg/kg, i.p.) did not affect spontaneous locomotion of the same animal species when tested in the open field task (Sadek et al., 2016c). Therefore, it is unlikely that acute systemic injection of DL77 (5 mg/kg, i.p.) in the post-training sessions provided memory-enhancing effects in PAP and NOR paradigms due to a nonspecific effect rather than improved learning tasks conducted in the training sessions of both paradigms.

CONCLUSION

The results show that the non-imidazole H3R antagonist DL77 ameliorated cognitive deficits induced by the NMDA receptor antagonist MK801 in an inhibitory PAP and in NOR paradigms in rats (**Figure 6**). Moreover, the results observed in PAP as well as LTM of NOR indicated that DL77 ameliorated cognitive deficits through blockade of H3Rs, demonstrating the therapeutic prospective of H3R antagonists in the future treatment of neurodegenerative diseases, e.g., AD. However, additional preclinical experiments in other behavioral test

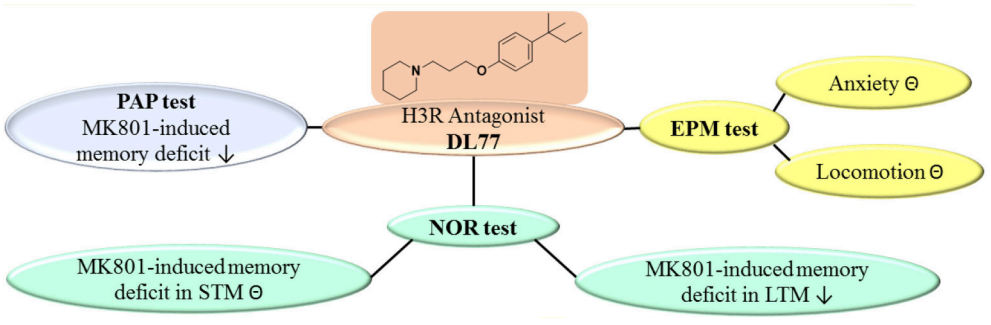


FIGURE 6 | Schematic representation of proposed ameliorative effects for H3R antagonist DL77 in MK801-induced memory deficit in PAP, NOR, and EPM. PAP, passive avoidance paradigm; NOR, novel object recognition; EPM, elevated plus maze; Θ, no effect; ↓, ameliorates.

models and with several rodent species are still warranted to comprehend the translational validity of the prospective use of H3R antagonists in future therapy of neurodegenerative diseases.

AUTHOR CONTRIBUTIONS

BS was responsible for the study concept, design, acquisition, and analysis of animal data; NK provided technical support to the conducted behavioral experiments; NE and NK conducted behavioral experiments; KK-K and DŁ were responsible for the generation, synthesis, and pharmacological *in vitro* characterization the H3R antagonist DL77; BS and NE drafted the manuscript; KK-K, DŁ, and SO provided critical revision for the manuscript; All authors critically reviewed content and approved final version for publication.

ACKNOWLEDGMENTS

The Office of Graduate Studies and Research of UAE University as well as ADEK Award for Research Excellence (AARE) 2017 are highly thanked for the support provided to BS in form of intermural College of Medicine and Health Sciences as well as extramural funds from ADEK. The authors, also, acknowledge the partial support of National Science Center granted on the basis of decision numbers DEC-2011/02/A/NZ4/00031. Support was kindly provided by the EU COST Actions CA151315 (KK-K; DŁ).

REFERENCES

Acevedo, S. F., de Esch, I. J., and Raber, J. (2007). Sex- and histamine-dependent long-term cognitive effects of methamphetamine exposure. *Neuropsychopharmacology* 32, 665–672. doi: 10.1038/sj.npp.1301091

Acevedo, S. F., Pfankuch, T., Ohtsu, H., and Raber, J. (2006). Anxiety and cognition in female histidine decarboxylase knockout (Hdc(-/-)) mice. *Behav. Brain Res.* 168, 92–99. doi: 10.1016/j.bbr.2005.10.016

Alachkar, A., Łazewska, D., Kiec' -Kononowicz, K., and Sadek, B. (2017). The histamine H3 receptor antagonist E159 reverses memory deficits induced by dizocilpine in passive avoidance and novel object recognition paradigm in rats. *Front. Pharmacol.* 8:709. doi: 10.3389/fphar.2017.00709

Arrang, J. M., Devaux, B., Chodkiewicz, J. P., and Schwartz, J. C. (1988). H3-receptors control histamine release in human brain. *J. Neurochem.* 51, 105–108. doi: 10.1111/j.1471-4159.1988.tb04841.x

Arrang, J. M., Garbarg, M., Lancelot, J. C., Lecomte, J. M., Pollard, H., Robba, M., et al. (1987a). Highly potent and selective ligands for histamine H3-receptors. *Nature* 327, 117–123. doi: 10.1038/327117a0

Arrang, J. M., Garbarg, M., and Schwartz, J. C. (1983). Auto-inhibition of brain histamine release mediated by a novel class (H3) of histamine receptor. *Nature* 302, 832–837. doi: 10.1038/302832a0

Arrang, J. M., Garbarg, M., and Schwartz, J. C. (1985). Autoregulation of histamine release in brain by presynaptic H3-receptors. *Neuroscience* 15, 553–562. doi: 10.1016/0306-4522(85)90233-7

Arrang, J. M., Garbarg, M., and Schwartz, J. C. (1987b). Autoinhibition of histamine synthesis mediated by presynaptic H3-receptors. *Neuroscience* 23, 149–157. doi: 10.1016/0306-4522(87)90279-X

Arrang, J. M., Morisset, S., and Gbahou, F. (2007). Constitutive activity of the histamine H3 receptor. *Trends Pharmacol. Sci.* 28, 350–357. doi: 10.1016/j.tips.2007.05.002

Bahi, A., Sadek, B., Nurulain, S. M., Lazewska, D., and Kiec-Kononowicz, K. (2015). The novel non-imidazole histamine H receptor antagonist DL77 reduces voluntary alcohol intake and ethanol-induced conditioned place preference in mice. *Physiol. Behav.* 151, 189–197. doi: 10.1016/j.physbeh.2015.07.012

Barak, S., and Weiner, I. (2011). Putative cognitive enhancers in preclinical models related to schizophrenia: the search for an elusive target. *Pharmacol. Biochem. Behav.* 99, 164–189. doi: 10.1016/j.pbb.2011.03.011

Bardgett, M. E., Davis, N. N., Schultheis, P. J., and Griffith, M. S. (2010). Ciproxifan, an H3 receptor antagonist, alleviates hyperactivity and cognitive deficits in the APP Tg2576 mouse model of Alzheimer's disease. *Neurobiol. Learn. Mem.* 95, 64–72. doi: 10.1016/j.nlm.2010.10.008

Benetti, F., Baldi, E., Bucherelli, C., Blandina, P., and Passani, M. B. (2013). Histaminergic ligands injected into the nucleus basalis magnocellularis differentially affect fear conditioning consolidation. *Int. J. Neuropsychopharmacol.* 16, 575–582. doi: 10.1017/S1461145712000181

Benetti, F., and Izquierdo, I. (2013). Histamine infused into basolateral amygdala enhances memory consolidation of inhibitory avoidance. *Int. J. Neuropsychopharmacol.* 16, 1539–1545. doi: 10.1017/S1461145712001514

Bernaerts, P., Lamberty, Y., and Tirelli, E. (2004). Histamine H3 antagonist thioperamide dose-dependently enhances memory consolidation and reverses amnesia induced by dizocilpine or scopolamine in a one-trial inhibitory avoidance task in mice. *Behav. Brain Res.* 154, 211–219. doi: 10.1016/j.bbr.2004.02.017

Bhowmik, M., Khanam, R., and Vohora, D. (2012). Histamine H3 receptor antagonists in relation to epilepsy and neurodegeneration: a systemic consideration of recent progress and perspectives. *Br. J. Pharmacol.* 167, 1398–1414. doi: 10.1111/j.1476-5381.2012.02093.x

Bhowmik, M., Saini, N., and Vohora, D. (2014). Histamine H3 receptor antagonism by ABT-239 attenuates kainic acid induced excitotoxicity in mice. *Brain Res.* 1581, 129–140. doi: 10.1016/j.brainres.2014.06.012

Brabant, C., Charlier, Y., and Tirelli, E. (2013). The histamine H(3)-receptor inverse agonist pitolisant improves fear memory in mice. *Behav. Brain Res.* 243, 199–204. doi: 10.1016/j.bbr.2012.12.063

Brioni, J. D., Esbenshade, T. A., Garrison, T. R., Bitner, S. R., and Cowart, M. D. (2011). Discovery of histamine H3 antagonists for the treatment of cognitive disorders and Alzheimer's disease. *J. Pharmacol. Exp. Ther.* 336, 38–46. doi: 10.1124/jpet.110.166876

Browman, K. E., Komater, V. A., Curzon, P., Rueter, L. E., Hancock, A. A., Decker, M. W., et al. (2004). Enhancement of prepulse inhibition of startle in mice by the H3 receptor antagonists thioperamide and ciproxifan. *Behav. Brain Res.* 153, 69–76. doi: 10.1016/j.bbr.2003.11.001

Brown, J. W., Whitehead, C. A., Basso, A. M., Rueter, L. E., and Zhang, M. (2013). Preclinical evaluation of non-imidazole histamine H3 receptor antagonists in comparison to atypical antipsychotics for the treatment of cognitive deficits associated with schizophrenia. *Int. J. Neuropsychopharmacol.* 16, 889–904. doi: 10.1017/S1461145712000739

Brown, R. E., Stevens, D. R., and Haas, H. L. (2001). The physiology of brain histamine. *Prog. Neurobiol.* 63, 637–672. doi: 10.1016/S0301-0082(00)00039-3

Callahan, P. M., Bertrand, D., Bertrand, S., Plagenhoef, M. R., and Terry, A. V. Jr. (2017). Tropisetron sensitizes alpha7 containing nicotinic receptors to low levels of acetylcholine *in vitro* and improves memory-related task performance in young and aged animals. *Neuropharmacology* 117, 422–433. doi: 10.1016/j.neuropharm.2017.02.025

Charlier, Y., Brabant, C., Serrano, M. E., Lamberty, Y., and Tirelli, E. (2013). The prototypical histamine H3 receptor inverse agonist thioperamide improves multiple aspects of memory processing in an inhibitory avoidance task. *Behav. Brain Res.* 253, 121–127. doi: 10.1016/j.bbr.2013.07.016

da Silva, A. L., Silva Martins, B., Linck Vde, M., Herrmann, A. P., Mai, N., Nunes, D. S., et al. (2009). MK801- and scopolamine-induced amnesias are reversed by an Amazonian herbal locally used as a "brain tonic". *Psychopharmacology* 202, 165–172. doi: 10.1007/s00213-008-1272-y

de Lima, M. N., Laranja, D. C., Bromberg, E., Roesler, R., and Schroder, N. (2005). Pre- or post-training administration of the NMDA receptor blocker MK-801

impairs object recognition memory in rats. *Behav. Brain Res.* 156, 139–143. doi: 10.1016/j.bbr.2004.05.016

Doraiswamy, P. M. (2002). Non-cholinergic strategies for treating and preventing Alzheimer's disease. *CNS Drugs* 16, 811–824. doi: 10.2165/00023210-200216120-00003

Ennaceur, A., and Delacour, J. (1988). A new one-trial test for neurobiological studies of memory in rats. 1: behavioral data. *Behav. Brain Res.* 31, 47–59. doi: 10.1016/0166-4328(88)90157-X

Ennaceur, A., and Meliani, K. (1992a). Effects of physostigmine and scopolamine on rats' performances in object-recognition and radial-maze tests. *Psychopharmacology* 109, 321–330. doi: 10.1007/BF02245880

Ennaceur, A., and Meliani, K. (1992b). A new one-trial test for neurobiological studies of memory in rats. III. Spatial vs. non-spatial working memory. *Behav. Brain Res.* 51, 83–92. doi: 10.1016/S0166-4328(05)80315-8

Fernandes, C., and File, S. E. (1996). The influence of open arm ledges and maze experience in the elevated plus-maze. *Pharmacol. Biochem. Behav.* 54, 31–40. doi: 10.1016/0091-3057(95)02171-X

Giannoni, P., Medhurst, A. D., Passani, M. B., Giovannini, M. G., Ballini, C., Corte, L. D., et al. (2010). Regional differential effects of the novel histamine H3 receptor antagonist 6-[(3-cyclobutyl-2,3,4,5-tetrahydro-1H-3-benzazepin-7-yl)oxy]-N-methyl-3-pyridine carboxamide hydrochloride (GSK189254) on histamine release in the central nervous system of freely moving rats. *J. Pharmacol. Exp. Ther.* 332, 164–172. doi: 10.1124/jpet.109.158444

Giovannini, M. G., Bartolini, L., Bacciottini, L., Greco, L., and Blandina, P. (1999). Effects of histamine H3 receptor agonists and antagonists on cognitive performance and scopolamine-induced amnesia. *Behav. Brain Res.* 104, 147–155. doi: 10.1016/S0166-4328(99)00063-7

Goshadrou, F., Kermani, M., Ronaghi, A., and Sajjadi, S. (2013). The effect of ghrelin on MK-801 induced memory impairment in rats. *Peptides* 44, 60–65. doi: 10.1016/j.peptides.2013.03.022

Griebel, G., Pichat, P., Pruniaux, M. P., Beeske, S., Lopez-Grancha, M., Genet, E., et al. (2012). SAR110894, a potent histamine H(3)-receptor antagonist, displays procognitive effects in rodents. *Pharmacol. Biochem. Behav.* 102, 203–214. doi: 10.1016/j.pbb.2012.04.004

Harada, C., Hirai, T., Fujii, Y., Harusawa, S., Kurihara, T., and Kamei, C. (2004). Intracerebroventricular administration of histamine H3 receptor antagonists decreases seizures in rat models of epilepsia. *Methods Find. Exp. Clin. Pharmacol.* 26, 263–270.

Hogg, S. (1996). A review of the validity and variability of the elevated plus-maze as an animal model of anxiety. *Pharmacol. Biochem. Behav.* 54, 21–30. doi: 10.1016/0091-3057(95)02126-4

Izquierdo, I., Medina, J. H., Vianna, M. R., Izquierdo, L. A., and Barros, D. M. (1999). Separate mechanisms for short- and long-term memory. *Behav. Brain Res.* 103, 1–11. doi: 10.1016/S0166-4328(99)00036-4

Jaaro-Peled, H. (2009). Gene models of schizophrenia: DISC1 mouse models. *Prog. Brain Res.* 179, 75–86. doi: 10.1016/S0079-6123(09)17909-8

Jiang, Y. M., Li, X. J., Meng, Z. Z., Liu, Y. Y., Zhao, H. B., Li, N., et al. (2016). Effects of xiaoyaosan on stress-induced anxiety-like behavior in rats: involvement of CRF1 receptor. *Evid. Based Complement. Alternat. Med.* 2016:1238426. doi: 10.1155/2016/1238426

Karasawa, J., Hashimoto, K., and Chaki, S. (2008). D-Serine and a glycine transporter inhibitor improve MK-801-induced cognitive deficits in a novel object recognition test in rats. *Behav. Brain Res.* 186, 78–83. doi: 10.1016/j.bbr.2007.07.033

Khan, N., Saad, A., Nurulain, S. M., Darras, F. H., Decker, M., and Sadek, B. (2015). The dual-acting H3 receptor antagonist and AChE inhibitor UW-MD-71 dose-dependently enhances memory retrieval and reverses dizocilpine-induced memory impairment in rats. *Behav. Brain Res.* 297, 155–164. doi: 10.1016/j.bbr.2015.10.022

Khunnawutmanotham, N., Chimnoi, N., Saparpakorn, P., and Techasakul, S. (2016). Synthesis and anti-acetylcholinesterase activity of scopoletin derivatives. *Bioorg. Chem.* 65, 137–145. doi: 10.1016/j.bioorg.2015.12.002

King, M. V., Sleight, A. J., Woolley, M. L., Topham, I. A., Marsden, C. A., and Fone, K. C. (2004). 5-HT6 receptor antagonists reverse delay-dependent deficits in novel object discrimination by enhancing consolidation–an effect sensitive to NMDA receptor antagonism. *Neuropharmacology* 47, 195–204. doi: 10.1016/j.neuropharm.2004.03.012

Krause, M., Stark, H., and Schunack, W. (2001). Azomethine prodrugs of (R)-alpha-methylhistamine, a highly potent and selective histamine H3-receptor agonist. *Curr. Med. Chem.* 8, 1329–1340. doi: 10.2174/0929867013372274

Łazewska, D., Ligneau, X., Schwartz, J. C., Schunack, W., Stark, H., and Kiec-Kononowicz, K. (2006). Ether derivatives of 3-piperidinopropan-1-ol as non-imidazole histamine H3 receptor antagonists. *Bioorg. Med. Chem.* 14, 3522–3529. doi: 10.1016/j.bmc.2006.01.013

Lebrun, C., Pillière, E., and Lestage, P. (2000). Effects of S 18986-1, a novel cognitive enhancer, on memory performances in an object recognition task in rats. *Eur. J. Pharmacol.* 401, 205–212. doi: 10.1016/S0014-2999(00)00429-5

Ligneau, X., Perrin, D., Landais, L., Camelin, J. C., Calmels, T. P., Berrebi-Bertrand, I., et al. (2007). BF2.649 [1-{3-[3-(4-Chlorophenyl)propoxy]propyl}piperidine, hydrochloride], a nonimidazole inverse agonist/antagonist at the human histamine H3 receptor: preclinical pharmacology. *J. Pharmacol. Exp. Ther.* 320, 365–375. doi: 10.1124/jpet.106.111039

McGaugh, J. L., and Roozendaal, B. (2009). Drug enhancement of memory consolidation: historical perspective and neurobiological implications. *Psychopharmacology* 202, 3–14. doi: 10.1007/s00213-008-1285-6

Meier, G., Apelt, J., Reichert, U., Grassmann, S., Ligneau, X., Elz, S., et al. (2001). Influence of imidazole replacement in different structural classes of histamine H_3-receptor antagonists. *Eur. J. Pharm. Sci.* 13, 249–259. doi: 10.1016/S0928-0987(01)00106-3

Orsetti, M., Ferretti, C., Gamalero, R., and Ghi, P. (2002). Histamine H3-receptor blockade in the rat nucleus basalis magnocellularis improves place recognition memory. *Psychopharmacology* 159, 133–137. doi: 10.1007/s002130100892

Orsetti, M., Ghi, P., and Di Carlo, G. (2001). Histamine H(3)-receptor antagonism improves memory retention and reverses the cognitive deficit induced by scopolamine in a two-trial place recognition task. *Behav. Brain Res.* 124, 235–242. doi: 10.1016/S0166-4328(01)00216-9

Panula, P., Chazot, P. L., Cowart, M., Gutzmer, R., Leurs, R., Liu, W. L., et al. (2015). International union of basic and clinical pharmacology. XCVIII. Histamine Receptors. *Pharmacol. Rev.* 67, 601–655. doi: 10.1124/pr.114.010249

Panula, P., and Nuutinen, S. (2011). Histamine and H3 receptor in alcohol-related behaviors. *J. Pharmacol. Exp. Ther.* 336, 9–16. doi: 10.1124/jpet.110.170928

Panula, P., Rinne, J., Kuokkanen, K., Eriksson, K. S., Sallmen, T., Kalimo, H., et al. (1998). Neuronal histamine deficit in Alzheimer's disease. *Neuroscience* 82, 993–997. doi: 10.1016/S0306-4522(97)00353-9

Pascoli, V., Boer-Saccomani, C., and Hermant, J. F. (2009). H3 receptor antagonists reverse delay-dependent deficits in novel object discrimination by enhancing retrieval. *Psychopharmacology* 202, 141–152. doi: 10.1007/s00213-008-1171-2

Pichat, P., Bergis, O. E., Terranova, J. P., Urani, A., Duarte, C., Santucci, V., et al. (2007). SSR180711, a novel selective alpha7 nicotinic receptor partial agonist: (II) efficacy in experimental models predictive of activity against cognitive symptoms of schizophrenia. *Neuropsychopharmacology* 32, 17–34. doi: 10.1038/sj.npp.1301188

Provensi, G., Costa, A., Passani, M. B., and Blandina, P. (2016). Donepezil, an acetylcholine esterase inhibitor, and ABT-239, a histamine H3 receptor antagonist/inverse agonist, require the integrity of brain histamine system to exert biochemical and procognitive effects in the mouse. *Neuropharmacology* 109, 139–147. doi: 10.1016/j.neuropharm.2016.06.010

Sadek, B., Khan, N., Darras, F. H., Pockes, S., and Decker, M. (2016a). The dual-acting AChE inhibitor and H3 receptor antagonist UW-MD-72 reverses amnesia induced by scopolamine or dizocilpine in passive avoidance paradigm in rats. *Physiol. Behav.* 165, 383–391. doi: 10.1016/j.physbeh.2016.08.022

Sadek, B., Saad, A., Sadeq, A., Jalal, F., and Stark, H. (2016b). Histamine H3 receptor as a potential target for cognitive symptoms in neuropsychiatric diseases. *Behav. Brain Res.* 312, 415–430. doi: 10.1016/j.bbr.2016.06.051

Sadek, B., Saad, A., Subramanian, D., Shafiullah, M., Łazewska, D., and Kieć-Kononowiczc, K. (2016c). Anticonvulsant and procognitive properties of the non-imidazole histamine H3 receptor antagonist DL77 in male adult rats. *Neuropharmacology* 106, 46–55. doi: 10.1016/j.neuropharm.2015.10.023

Sadek, B., and Stark, H. (2015). Cherry-picked ligands at histamine receptor subtypes. *Neuropharmacology* 106, 56–73. doi: 10.1016/j.neuropharm.2015.11.005

Schneider, E. H., and Seifert, R. (2009). Histamine H(4) receptor-RGS fusion proteins expressed in Sf9 insect cells: a sensitive and reliable approach for the functional characterization of histamine H(4) receptor ligands. *Biochem. Pharmacol.* 78, 607–616. doi: 10.1016/j.bcp.2009.05.015

Schwartz, J. C., Arrang, J. M., Garbarg, M., and Korner, M. (1986). Properties and roles of the three subclasses of histamine receptors in brain. *J. Exp. Biol.* 124, 203–224.

Shaik, J. B., Palaka, B. K., Penumala, M., Kotapati, K. V., Devineni, S. R., Eadlapalli, S., et al. (2016). Synthesis, pharmacological assessment, molecular modeling and *in silico* studies of fused tricyclic coumarin derivatives as a new family of multifunctional anti-Alzheimer agents. *Eur. J. Med. Chem.* 107, 219–232. doi: 10.1016/j.ejmech.2015.10.046

Sultan, A., Yang, K. S., Isaev, D., Nebrisi, E. E., Syed, N., Khan, N., et al. (2017). Thujone inhibits the function of alpha7-nicotinic acetylcholine receptors and impairs nicotine-induced memory enhancement in one-trial passive avoidance paradigm. *Toxicology* 384, 23–32. doi: 10.1016/j.tox.2017.04.005

Tseng, K. Y., Chambers, R. A., and Lipska, B. K. (2009). The neonatal ventral hippocampal lesion as a heuristic neurodevelopmental model of schizophrenia. *Behav. Brain Res.* 204, 295–305. doi: 10.1016/j.bbr.2008.11.039

Uma Devi, P., Manocha, A., Khanam, R., and Vohora, D. (2010). Beneficial interaction between clobenpropit and pyridoxine in prevention of electroshock-induced seizures in mice: lack of histaminergic mechanisms. *Hum. Exp. Toxicol.* 30, 84–88. doi: 10.1177/0960327110372398

Vorobjev, V. S., Sharonova, I. N., Walsh, I. B., and Haas, H. L. (1993). Histamine potentiates N-methyl-D-aspartate responses in acutely isolated hippocampal neurons. *Neuron* 11, 837–844. doi: 10.1016/0896-6273(93)90113-6

Witkin, J. M., and Nelson, D. L. (2004). Selective histamine H3 receptor antagonists for treatment of cognitive deficiencies and other disorders of the central nervous system. *Pharmacol. Ther.* 103, 1–20. doi: 10.1016/j.pharmthera.2004.05.001

Xu, L. S., Yang, L. X., Hu, W. W., Yu, X., Ma, L., Liu, L. Y., et al. (2005). Histamine ameliorates spatial memory deficits induced by MK-801 infusion into ventral hippocampus as evaluated by radial maze task in rats. *Acta Pharmacol. Sin.* 26, 1448–1453. doi: 10.1111/j.1745-7254.2005.00229.x

Yokoyama, H. (2001). The role of central histaminergic neuron system as an anticonvulsive mechanism in developing brain. *Brain Dev.* 23, 542–547. doi: 10.1016/S0387-7604(01)00261-3

Yokoyama, H., Onodera, K., Iinuma, K., and Watanabe, T. (1993). Effect of thioperamide, a histamine H3 receptor antagonist, on electrically induced convulsions in mice. *Eur. J. Pharmacol.* 234, 129–133. doi: 10.1016/0014-2999(93)90717-V

Conflict of Interest Statement: The authors declare that the research was conducted in the absence of any commercial or financial relationships that could be construed as a potential conflict of interest.

Copyright © 2018 Eissa, Khan, Ojha, Łazewska, Kieć-Kononowicz and Sadek. This is an open-access article distributed under the terms of the Creative Commons Attribution License (CC BY). The use, distribution or reproduction in other forums is permitted, provided the original author(s) and the copyright owner are credited and that the original publication in this journal is cited, in accordance with accepted academic practice. No use, distribution or reproduction is permitted which does not comply with these terms.

frontiers in Aging Neuroscience

ORIGINAL RESEARCH
published: 31 October 2017
doi: 10.3389/fnagi.2017.00347

Sex Differences in the Cognitive and Hippocampal Effects of Streptozotocin in an Animal Model of Sporadic AD

*Jian Bao[1], Yacoubou A. R. Mahaman[1], Rong Liu[1], Jian-Zhi Wang[1,2], Zhiguo Zhang[3], Bin Zhang[4] and Xiaochuan Wang[1,2]**

[1] Key Laboratory of Ministry of Education of China for Neurological Disorders, Department of Pathophysiology, School of Basic Medicine and the Collaborative Innovation Center for Brain Science, Tongji Medical College, Huazhong University of Science and Technology, Wuhan, China, [2] Co-innovation Center of Neuroregeneration, Nantong University, Nantong, China, [3] School of Medicine and Health Management, Tongji Medical College, Huazhong University of Science and Technology, Wuhan, China, [4] Department of Genetics and Genomic Sciences, Icahn School of Medicine at Mount Sinai, New York, NY, United States

More than 95% of Alzheimer's disease (AD) belongs to sporadic AD (sAD), and related animal models are the important research tools for investigating the pathogenesis and developing new drugs for sAD. An intracerebroventricular infusion of streptozotocin (ICV-STZ) is commonly employed to generate sporadic AD animal model. Moreover, the potential impact of sex on brain function is now emphasized in the field of AD. However, whether sex differences exist in AD animal models remains unknown. Here we reported that ICV-STZ remarkably resulted in learning and memory impairment in the Sprague-Dawley male rats, but not in the female rats. We also found tau hyperphosphorylation, an increase of Aβ40/42 as well as increase in both GSK-3β and BACE1 activities, while a loss of dendritic and synaptic plasticity was observed in the male STZ rats. However, STZ did not induce above alterations in the female rats. Furthermore, estradiol levels of serum and hippocampus of female rats were much higher than that of male rats. In conclusion, sex differences exist in this sporadic AD animal model (Sprague-Dawley rats induced by STZ), and this should be considered in future AD research.

Keywords: Alzheimer's disease (AD), animal model, Streptozotocin (STZ), sex differences, learning and memory

OPEN ACCESS

Edited by:
Mohammad Amjad Kamal, King Fahad Medical Research Center, King Abdulaziz University, Saudi Arabia

Reviewed by:
Agnes Lacreuse, University of Massachusetts Amherst, United States
Melita Salkovic-Petrisic, School of Medicine, University of Zagreb, Croatia

****Correspondence:***
Xiaochuan Wang
wxch@mails.tjmu.edu.cn

Received: *18 August 2017*
Accepted: *16 October 2017*
Published: *31 October 2017*

Citation:
Bao J, Mahaman YAR, Liu R, Wang J-Z, Zhang Z, Zhang B and Wang X (2017) Sex Differences in the Cognitive and Hippocampal Effects of Streptozotocin in an Animal Model of Sporadic AD. Front. Aging Neurosci. 9:347. doi: 10.3389/fnagi.2017.00347

INTRODUCTION

Alzheimer's disease (AD) is one of the most common neurodegenerative diseases, affecting about 35 million people all over the world. And its prevalence is expected to reach 115 million by 2050 due to aggravating trend of aging population, unless there are available treatments that can prevent or cure this disease (Mangialasche et al., 2010). Therefore, an appropriate animal model is an important research tool for finding valid AD treatments. Yet, over the last 20 years, many of the potential drugs that target tau and Aβ, the two hallmarks of AD, failed in clinical trials, though some of treatments were effective in AD animal models (Zahs and Ashe, 2010; Shineman et al., 2011; Hall and Roberson, 2012). Thus, it is crucial to re-evaluate the existing animal models of AD.

AD exists mainly in two forms: familial (fAD) and sporadic (sAD). More than 95% of cases belong to sAD, for which aging and metabolic disorders are the main non-genetic risk factors

(Kloppenborg et al., 2008). Intracerebroventricular streptozotocin (ICV-STZ) injection produces cognitive deficits in rats, as well as cholinergic dysfunction, tau hyperphosphorylation, insulin receptor dysfunction, impaired energy metabolism, and oxidative stress (Hong and Lee, 1997; Prickaerts et al., 1999; Salkovic-Petrisic and Hoyer, 2007; Deng et al., 2009). These changes are similar to those observed in the brain of patients with sporadic AD. Therefore, ICV-STZ treated rats have been proposed as a research model of sAD (Lannert and Hoyer, 1998; Mehla et al., 2013). Meanwhile, ICV-STZ animal model has been used to evaluate the therapeutic potential of numerous old and novel drugs and compounds, as well as other non-drug therapies (Jee et al., 2008; Rodrigues et al., 2010; Salkovic-Petrisic et al., 2013). Nevertheless, although effectiveness of the therapeutic strategies has been proved in ICV-STZ model, the therapies failed to achieve similar therapeutic effects on learning and memory deficits in sAD clinical trials, like those with NSAIDs and PPAR agonists or vitamin E and Ginkgo biloba (Woo, 2000; Salkovic-Petrisic et al., 2013; Dysken et al., 2014; Malkki, 2016; Prasad, 2017; Wightman, 2017). Thus, it is necessary to characterize and re-evaluate the ICV-STZ animal model.

Accumulating evidence indicates that there are some differences in structure, development, enzyme activity, and chemistry of the central nervous system (CNS) between female and male mammals (Becker et al., 2005; Cahill, 2006; McCarthy, 2009; Raznahan et al., 2010; Ruigrok et al., 2014; Forger et al., 2016). AD is one of major chronic neurodegenerative disorders that is histopathologically characterized by the intracellular neurofibrillary tangles (NFTs) that are composed of abnormally hyperphosphorylated tau and extracellular senile plaques that are accumulated of insoluble β-amyloid (Aβ), which result in a progressive cognitive impairment (Grundke-Iqbal et al., 1986; Alafuzoff et al., 1987). Although, it has been reported that ICV-STZ induces AD-like pathological changes, however, whether ICV STZ-induced sporadic AD in animal model is stable and universal in different sexes has not been reported. Here, we found that ICV-STZ remarkably induced AD-like pathological changes, including impaired learning and memory capacities; loss of dendritic and synaptic plasticity; tau hyperphosphorylation; increase in Aβ40/42 and increase in both GSK-3β and BACE1 activities in the male but not female STZ treated rats. Our study implies that sex difference should be taken into account during experiments design, results interpretation and drawing conclusions in AD research.

MATERIALS AND METHODS

Chemicals and Antibodies

STZ was from Sigma (Sigma, St. Louis, MO, USA). Antibodies employed in this study are listed in Supplementary Table 1.

Animal Experiments

Two-month-old male ($n = 24$) and female ($n = 24$) Sprague-Dawley (SD) rats were provided by the Experiment Animal Center of Tongji Medical College, Huazhong University of Science and Technology. All animal experiments were performed according to the "Policies on the Use of Animals and Humans in Neuroscience Research" approved by Society for Neuroscience in 1995 and approved by the Experiment Animal Center of Tongji Medical College, Huazhong University of Science and Technology. The animals were individually housed in cages (house temperature 24°C, controlled humidity 40% and 12/12 h inverted light cycle) with free access to water and food.

STZ, soluble in artificial cerebrospinal fluid (aCSF), was injected slowly (1 μl/min) into the ventriculus lateralis cerebri of rats (10 μl, 3 mg/kg). Control animals were identically treated with the same volume of aCSF. After 30 days, morris water maze was employed to train and test spatial learning and memory. After this procedure which lasted for 7 days, mice were sacrificed and other tests were proceeded (**Supplementary Figure 1**).

Morris Water Maze Assay

The water maze used was a circular, steel pool (1.6 m in diameter) that was filled with black water (temperature 25°C) that was non-toxic and contrast to rat. A black-colored, circular platform (12 cm in diameter) was placed below the water surface at a specific location. Distinctive visual cues were stuck to the wall. For spatial training, rats were subjected to 4 trials each day from 2:00 to 5:00 p.m. The training was lasted 6 days and 24 trials were given to every rat. For each trial, the rat was placed at different starting position spaced equally around the perimeter of the pool. Rats were allowed to find the submerged platform within 60 s. If the rat could not find the hidden platform, it was then gently guided to the platform and allowed to stay there for 30 s. The time that each rat took to reach the platform was recorded as the escape latency. For the probe trial test, rats were submitted to the same pool with the platform removed and a probe trial of 60 s was given. The number of crossings and the time in the target quadrant were recorded.

Western Blotting

The protocol was performed as previously described (Xu et al., 2014). Four left hippocampus per group for Western blotting. Hippocampi were rapidly dissected out and homogenized in a buffer containing NaF 50 mM, Tris-Cl (pH 7.6) 10 mM, 1 mM EDTA, 1 mM Na_3VO_4, 1 mM benzamidine, and 1 mM phenylmethylsulfonylfluoride (PMSF), 10 g/ml leupeptin, and 2 g/ml each of pepstatin A and aprotinin. The homogenates were added to one-third of sample buffer containing 200 mM Tris-HCl (pH 7.6), 8% sodium dodecyl sulfate, and 40% glycerol, boiled in a water bath for 10 min, and then centrifuged at 14,510 r for 10 min. Protein concentration of the supernatants were measured by the bicinchoninic acid Protein Assay Kit (Pierce, Rockford, IL, USA). Ten micrograms of protein for DMIA and pS396 antibodies, 20 μg protein for other antibodies, were loaded and separated by SDS-polyacrylamide gel electrophoresis (10% gel), and then transferred to a nitrocellulose membrane. After blocking in 3% non-fat milk for 1 h, the nitrocellulose membranes were incubated with primary antibodies at 4°C overnight. The membranes were then incubated with secondary antibodies conjugated to IRDye (800CW) for 1–2 h and visualized using the Odyssey Infrared Imaging System (LI-Cor Biosciences, Lincoln, NE, USA). Image J software was employed for the quantitative analysis of the western blots.

Golgi Staining

The Golgi staining protocol was performed as previously described (Morest, 1960). Three per group were used for Golgi Staining. The rats were anesthetized with 6% chloral hydrate and perfused with 300 ml of normal saline containing 0.5% sodium nitrite, followed by 400 ml of 4% formaldehyde solution and further by ∼400 ml dying solution (4% formaldehyde, 5% potassium dichromate, and 5% chloral hydrate) for 5 h in the dark. The brains were removed and incubated in the same fixative in the dark. After 3 days, the brains were transferred to a solution containing 1% silver nitrate for 3 days in the dark. The silver solution was changed each day. Thirty-five micrometers of thick coronal brain sections were cut using a vibrating microtome (Leica, VT1000S, Germany).

Immunofluorescence

Three per group were used for Immunofluorescence Staining. The anesthetized rats were immediately perfused through the aorta with 300 ml normal saline, followed by a 300 ml solution containing 4% paraformaldehyde. The brains were dissected and post-fixed in 4% paraformaldehyde for another 48 h. Coronal sections (30 μm thick) were cut using a vibrating microtome. After incubation in 0.3% Triton-X100-PBS for 30 min at room temperature, free floating sections were blocked with 5% goat serum in PBS for 45 min at room temperature. Sections were then incubated overnight at 4°C with primary antibodies: polyclonal anti-MAP2 antibodies obtained from Abcam, (dilution 1:200, Cambridge, MA, USA). This was followed by incubation with secondary antibodies for 2 h at room temperature. The antibody staining was semi-quantitated by mean fluorescence intensities (MFIs) with Image J software.

BACE1 Enzymatic Assay

The protocol was performed as previously described (Qi et al., 2016). Five right hippocampus per group for the assay. Beta-secretase activity was monitored using a commercial kit, from Abnova (Neihu District, Taipei City 114 Taiwan) according to the manufacturer instructions and using a multi-well fluorescence plate reader capable of Ex = 335–355 nm and Em = 495–510 nm. In briefly, 50 μl of 4 μg/μl hippocampus lysate was added to a 96-well plate. Fifty microliters of 2×reaction buffer were added, followed by 2 μl of β-secretase substrate. The reaction mixtures were incubating for 1 h in the dark. Fluorescence was monitored at excitation wave (wavelength = 334–355 nm) and emission wave (emission wavelength = 490–510 nm). β-secretase activity can be expressed as the Relative Fluorescence Units (RFU) per μg of protein sample.

ELISA Quantification of Aβ

The protocol was performed as previously described (Zhang et al., 2015). Five right hippocampus per group for the Elisa assay. To detect the concentration of Aβ in hippocampi lysates, the rat hippocampi were homogenized in buffer (PBS with 5% BSA and 0.03% Tween-20, supplemented with protease inhibitor cocktail), and centrifuged at 16,000 g for 20 min. Aβ1-40 or Aβ1-42 was quantified using the rats Aβ1-40 or Aβ1-42 ELISA Kit (Elabscience, Wuhan, China) in accordance with the manufacturer's instructions. The Aβ concentrations were determined by comparison with the standard curve.

ELISA Quantification of Estradiol

Three right hippocampus per group for the assay. To measure the levels of estradiol in hippocampi lysates and serum, the rat hippocampi were homogenized in 1× PBS and blood is obtained from the orbital vessels, then centrifuged at 1,500 r for 20 min. Estradiol was quantified using the rat estradiol ELISA Kit (CZVV, Nanjing, China). The results were expressed in ng/L.

Statistical Analysis

Data are descriptively presented as means ± *SD* and analyzed by SPSS 17.0. Statistical analysis was performed using either Student's *t*-test (two-group comparison) for behavior test, dendritic plasticity, Western blot, enzymatic activity. For the levels of estradiol in serum and hippocampus, we firstly performed a descriptive analysis in Supplementary Tables 2, 3, and then a Shapiro–wilk test for a normal distribution of the samples from four group, finally a general linear model to be used for two-way ANOVA followed by *post-hoc* comparison, and differences with $P < 0.05$ were considered significant.

RESULTS

Sex Influences Spatial Learning and Memory Deficits in Sporadic AD Animal Model Induced by ICV-STZ

A study showed that a significant cognitive impairment was evoked at the 2nd week onwards, which persisted up to the 14th week with ICV-STZ (3 mg/kg) in rats (Mehla et al., 2013). To investigate whether sex differences exist in cognitive deficits induced by STZ, in the present study, we performed morris water maze to evaluate the memory and learning abilities of rats 30 days after ICV-STZ treatment. For male rats, we found that the escape latency to find a hidden platform dramatically increased while the traversing times and the time in the target quadrant were significantly decreased at the 7th day in ICV-STZ rats when compared to vehicle control (**Figures 1A–C**). This confirmed that ICV-STZ induced learning and memory deficits in male rats. For female rats, to our surprise, we failed to observe any learning and/or memory deficits. The latency to find the hidden platform, the crossing numbers and time spent in the target quadrant also did not change in female rats (**Figures 1E–G**). Both groups in male or female rats exhibited comparable swimming speed (**Figures 1D,H**), indicating that motor function was not affected. Altogether, the findings suggest that ICV-STZ injection induces cognitive impairments in male but not female rats.

Sex Influences Loss of Dendritic and Synaptic Plasticity in the Sporadic AD Animal Model Induced by ICV-STZ

Dendrite complexity (Li et al., 2008) and synaptic plasticity (Kasai et al., 2010) are neurobiological basis for learning and memory. We determined the effect of ICV-STZ on neuronal integrity, by examining levels of the dendritic marker MAP2. For male

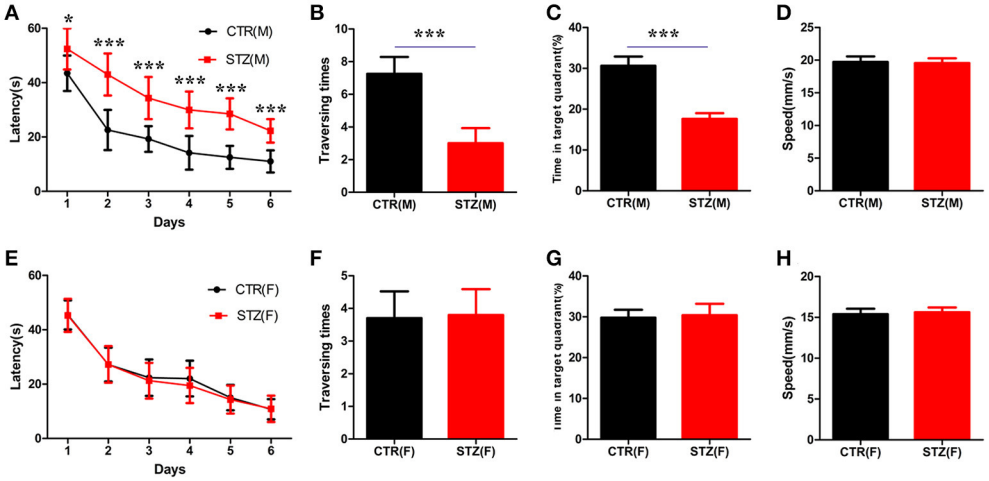


FIGURE 1 | Sex influences spatial learning and memory deficits in sporadic AD animal model induced by ICV-STZ. **(A,E)** Escape latencies to find the hidden platform for male or female rats. **(B,F)** The time spent in the target quadrant and **(C,G)** the crossed times after removing the platform. **(D,H)** The speed of male or female rats. Males are top figures **(A–D),** females bottom figures **(E–H)**. The data were expressed as mean ± *SD* ($n = 12$). ***$P < 0.001$ vs. the vehicle control. Data were analyzed using *t*-test. *$P < 0.05$ vs. the vehicle control.

rats, the semi quantitative results showed a strongly reduced mean fluorescence intensities (MFIs) of MAP2 immunoreactivity in the pyramidal neurons of CA1 region of the hippocampus in ICV-STZ rats compared to vehicle control (**Figures 2A,B**). However, in female rats, MAP2 immunoreactivity showed that ICV-STZ had no effect on dendritic number compared to control (**Figures 2A,C**). We also examined alterations in dendritic spines using Golgi staining. Mushroom-type spines in the CA1 of ICV-STZ treated male rats decreased remarkably compared to control (**Figures 2D,E**), but the number of mushroom-type dendritic spines were not altered in the ICV-STZ treated female rats compared to control (**Figures 2D,F**).

Normal synaptic function is contingent upon the stable expression of synaptic proteins. Therefore, we evaluated several key synapse-associated proteins using Western blotting. ICV-STZ treatment remarkably suppressed the expressions of presynaptic synapsin I, synaptagmin and postsynaptic PSD95, PSD93, NR2A, and NR2B in male rats (**Figures 3A,B**). Nonetheless, there is no any significant difference between vehicle and ICV-STZ treated female rats (**Figures 3C,D**). These data demonstrate that ICV-STZ induces loss of dendritic and synaptic plasticity in male, but not in female rats.

Sex Influences Tau Hyperphosphorylation and GSK-3β Activity in the Sporadic AD Animal Model Induced by ICV-STZ

Abnormal hyperphosphorylation and accumulation of Tau play a key role in AD pathology (Wang and Liu, 2008), and hyperphosphorylated tau causes dendritic loss and neurodegeneration (Wang et al., 2010). In addition, ICV-STZ treatment induces tau hyperphosphorylation in rats (Zhou et al., 2013). In this study, we also explored whether ICV-STZ induces tau hyperphosphorylation in male or female rats, respectively. We detected a significantly increasing tau phosphorylation at the Ser199/202(AT8), Ser262, Ser396, and Ser404 sites in ICV-STZ treated male rats (**Figures 4A,B**). Conversely, in the female rats, ICV-STZ did not induce tau hyperphosphorylation (**Figures 4C,D**).

GSK-3β is the first identified and critical tau kinase (Singh et al., 1995), therefore we evaluated the total level and the activity-dependent phosphorylation of GSK-3β. In male rats, we found that the p-GSK-3β (Ser9) (the inactive form) level was remarkably decreased, while the level of total GSK-3β and p-GSK-3β (Tyr216) (the active form) didn't change (**Figures 5A,B**). In female rats, no significant difference was observed between ICV-STZ treated and vehicle control (**Figures 5C,D**). Taken together, these findings suggest that ICV-STZ activates GSK-3β and consequently leads to hyperphosphorylation of tau protein in male rats, but does not elicit these demonstrable pathological alterations in female rats.

Sex Influences the Activity of BACE1 and Aβ Production in the Sporadic AD Animal Model Induced by ICV-STZ

Another characterized histology of AD is extracellular senile plaques, which are composed of aggregated protein Aβ initiated by β-secretase (BACE1) (Alafuzoff et al., 1987; Vassar et al., 2009). We employed β-secretase Activity Assay Kit and Aβ40/42 Elisa Kit to detect BACE1 activity and Aβ levels of hippocampus. In ICV-STZ treated male rats, both BACE1 activity and Aβ40 level were significantly increased compared to control rats, while Aβ42 showed ascendant trend without significant difference (**Figures 6A,C,D**). However, in female rats, BACE1 activity and Aβ40/42 levels were not altered in both ICV-STZ and vehicle treated rats (**Figures 6B,E,F**). Thus, these data strongly support that ICV-STZ increases BACE1 activity and augments Aβ

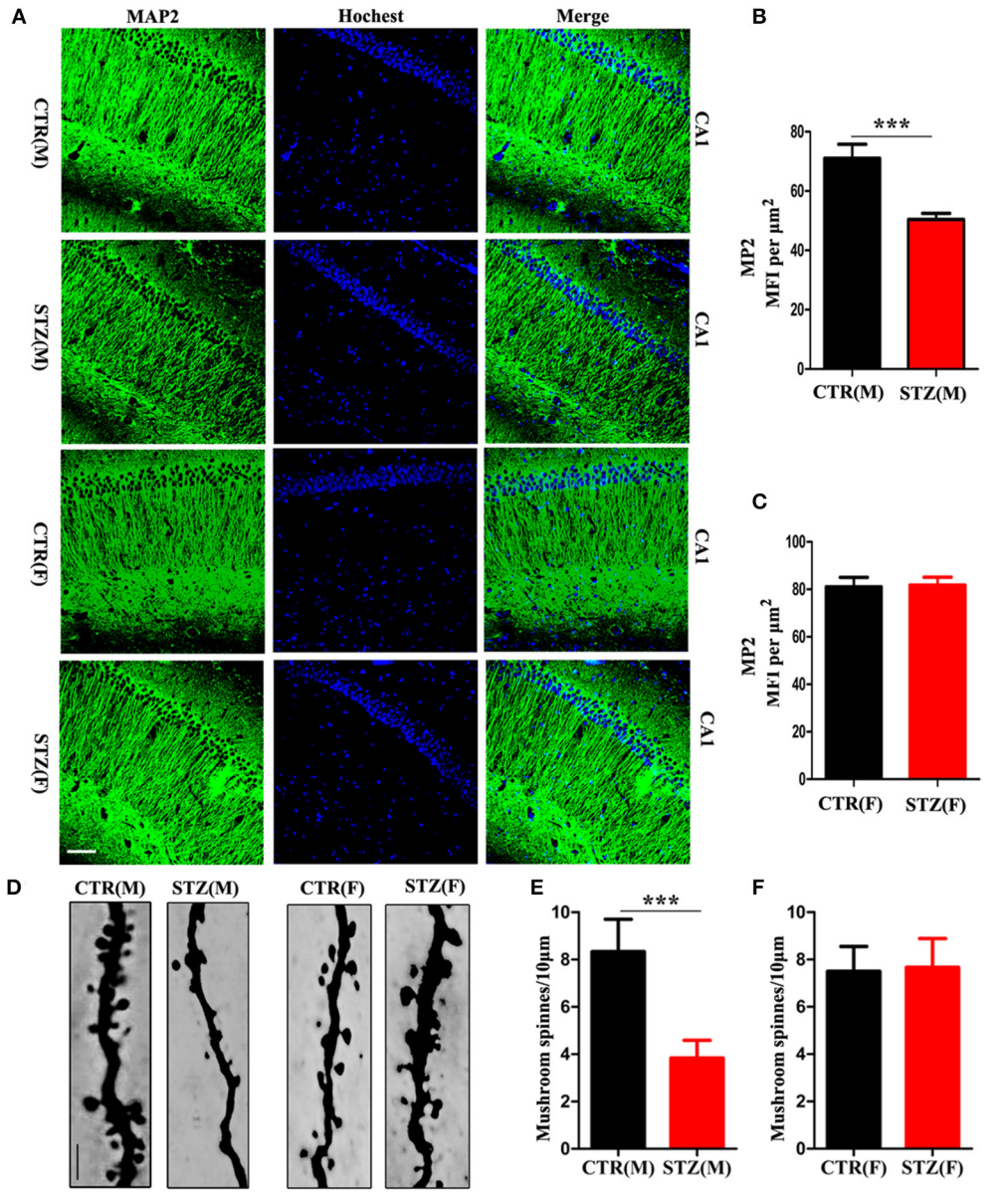


FIGURE 2 | Sex influences loss of dendritic plasticity in sporadic AD animal model. **(A)** MAP2 and DAPI co-staining in the hippocampal CA1 region for male or female rats. Scale bar = 100 μm. **(B,C)** Quantification of MAP2 immunofluorescence. The data were expressed as mean ± *SD* ($n = 3$). **(D)** Representative photomicrographs of dendritic spines in the hippocampal CA1 region. Scale bar = 5 μm. **(E,F)** Quantification of mushroom-type dendritic spines. The data were expressed as mean ± *SD* ($n = 3$). ***$P < 0.001$ vs. the vehicle control. Data were analyzed using *t*-test.

production in male rats, while did not exhibit these toxic effects in female rats.

Estradiol Levels in Serum and Hippocampus of ICV-STZ Treated Male and Female Rats

Previous studies have shown that estradiol reduces Aβ production via reducing total BACE1 activity, and decreases tau hyperphosphorylation by mediated GSK-3β activity (Singh et al., 1999; Zhang et al., 2008). To investigate whether estradiol influences the generation of the sporadic AD animal model induced by ICV-STZ, we measured estradiol levels in serum and hippocampus of ICV-STZ treated male and female rats. Shapiro–wilk test showed that all of the *p*-values were > 0.05, indicating estradiol levels in serum (Supplementary Table 4) and hippocampus (Supplementary Table 5) according with normal distribution from each group. And then, a general linear model was used for two-way ANOVA (Supplementary Tables 6, 7) followed by *post-hoc* comparison. We found that estradiol

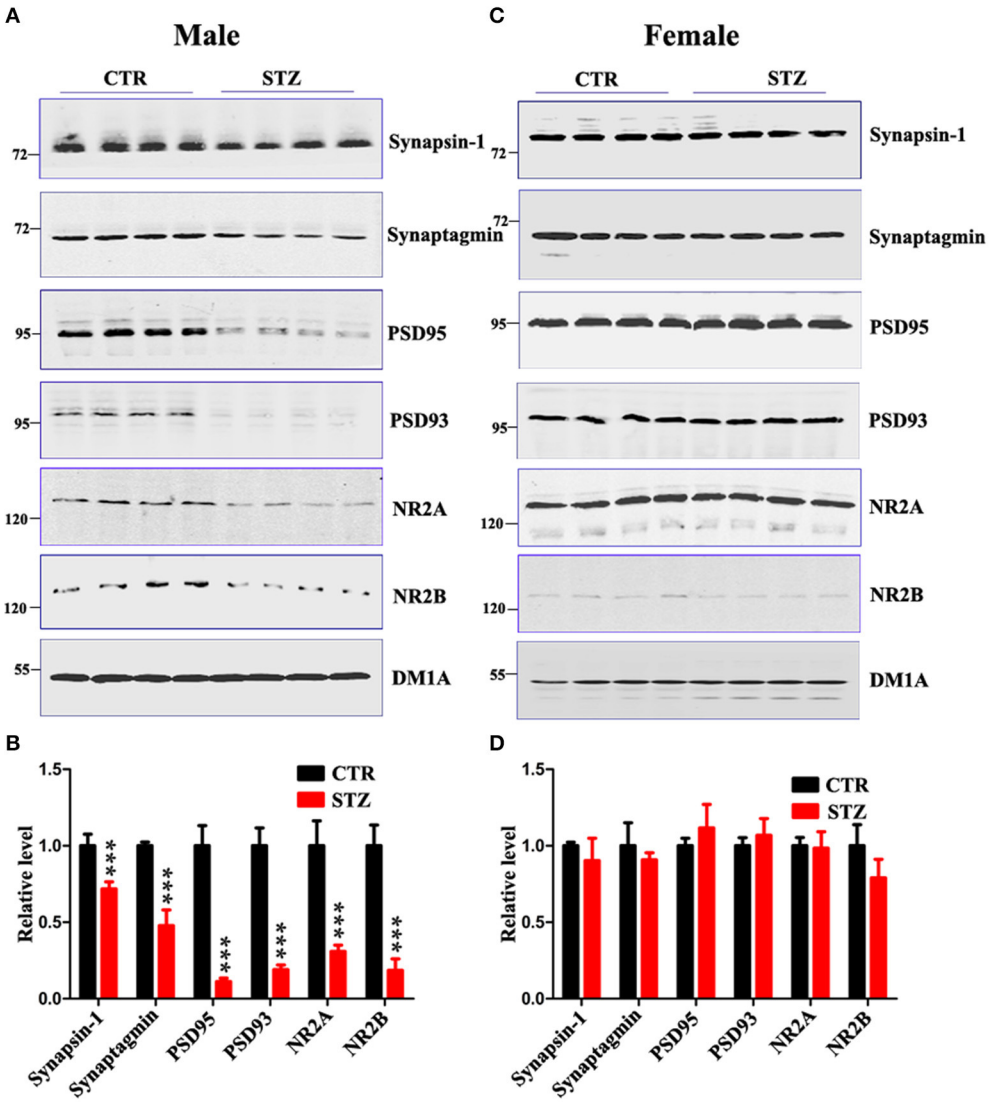


FIGURE 3 | Sex influences synaptic plasticity in the sporadic AD animal model. **(A,C)** Western blot analysis of the protein levels of synapsin-1, synaptagmin, psd95, psd93, NR2A, and NR2B and **(B,D)** their quantitative analysis for male or female rats. DM1A was used as a loading control. The data were expressed as mean ± *SD* ($n = 4$). ***$P < 0.001$ vs. the vehicle control. Data were analyzed using *t*-test.

levels of serum (**Figure 7A**) and hippocampus (**Figure 7B**) of female rats were much higher than that of male rats, while no difference was observed between the groups with same sex. The data suggest that high estradiol might protect from STZ induced neurotoxic effects in female rats.

DISCUSSION

Nowadays, AD is a major public health problem, which has been considered as a multifactorial disease associated with several etiopathogenic mechanisms (Iqbal and Grundke-Iqbal, 2010). The first step for a rational drug design is to study etiopathogenic mechanisms and to develop animal models based on these mechanisms. The late-onset sporadic form of AD, which mechanisms still remain unclear due to its multi-etiopathological factors, accounts for over 95% of all cases. However, few experimental animal model of sporadic AD badly limit the studies on its pathogenesis and drug development (Agrawal et al., 2011; Iqbal et al., 2013).

The majority of current animal models of AD are generated as familial one, which express human genes mutations, such as Aβ and tau related gene manipulation. However, animal model of familial AD cannot sufficiently exhibit all pathological alterations and processes (Chen et al., 2013). Therefore, experimental models that faithfully mimic the pathology of sAD are essential to study its mechanism and assess the effectiveness of the therapeutic strategies. Previous research has showed that sAD

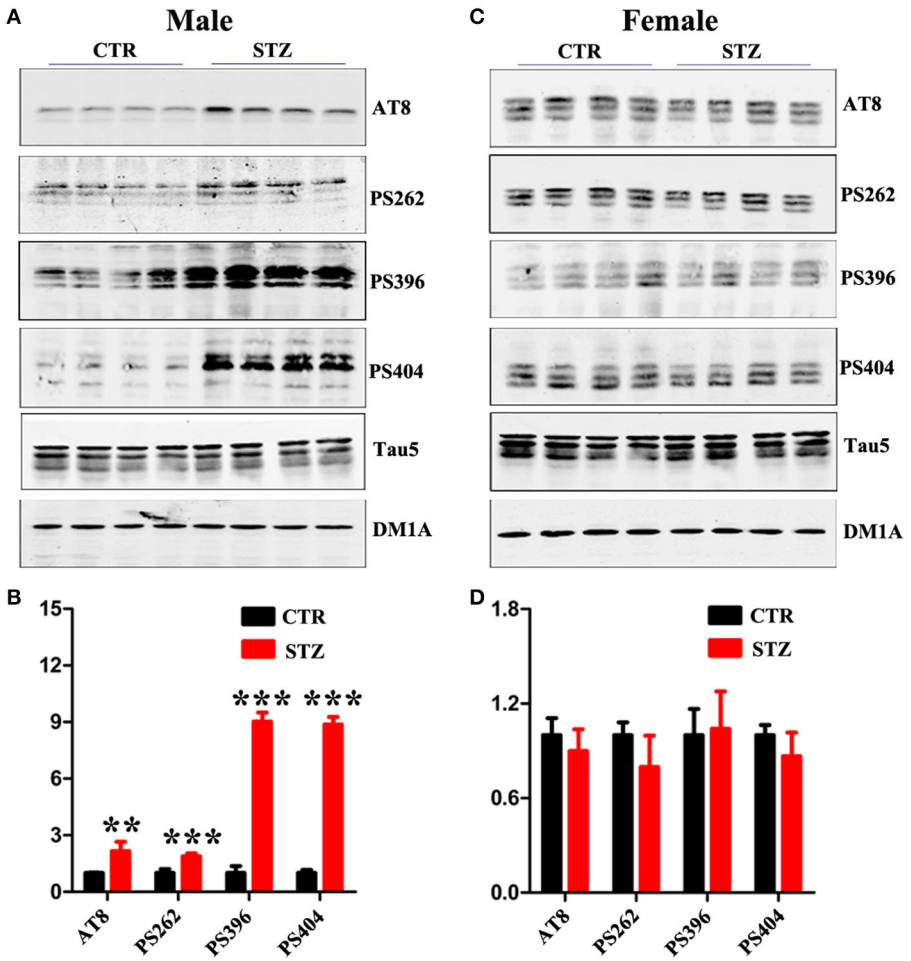


FIGURE 4 | Sex influences tau hyperphosphorylation in the sporadic AD animal model. **(A,C)** Western blot analysis of the protein levels of AT8, PS262, PS396, PS404, and Tau5 and **(B,D)** their quantitative analysis for male or female rats. The data were expressed as mean ± *SD* ($n = 4$). The phosphorylation level of tau was normalized to total tau level probed by tau5. The total level of tau was normalized DM1A. ***$P < 0.001$ vs. the vehicle control. Data were analyzed using *t*-test. **$P < 0.01$ vs. the vehicle control.

is being recognized as an insulin resistant brains state (Valente et al., 2010; Bitel et al., 2012; Kamat et al., 2016). Therefore, a non-transgenic animal model generated by ICV-STZ has been proposed as a representative model of sAD. The ICV-STZ rats develop insulin resistant brains state associated with sAD like neuropathological changes and memory impairment (Carro and Torres-Aleman, 2004; Valente et al., 2010; Agrawal et al., 2011; Bitel et al., 2012; Chen et al., 2013; Iqbal et al., 2013; Kamat et al., 2016). Although, the mechanisms underlying ICV-STZ evoked AD pathology remain unknown, ICV-STZ rats have been used in many labs as an experimental model of sAD. For more than 20 years, although some of therapeutic strategies displayed very good effectiveness for AD in ICV-STZ animal models, the same therapies were hard to be reproduced on memory deficits in clinical trials with sAD patients (Salkovic-Petrisic et al., 2013). Thus, it is necessary to re-evaluate the ICV-STZ animal model once again.

Sex has a regulatory effect on brain functions (Brinton, 2009; Cui et al., 2013). We here investigated sex differences on cognitive deficits in the sporadic AD animal model induced by ICV-STZ. Similar to previous studies, the ICV administration of STZ induced cognitive deficits and loss of synaptic plasticity in male rats, but these neurotoxic effects were not observed in female rats. Thus, the ICV-STZ is only for generating animal model of sAD in male, but not in female rats. Consequently sex differences should be considered in AD researches in the future.

Estrogen reduces Aβ level by down-regulating total β secretase activity through MARK/ERK pathway, and modulates Aβ degradation (Pike, 1999; Singh et al., 1999; Vassar et al., 2009). In the present study, we found that ICV-STZ increased BACE1 activities and Aβ40/42 production in male rats, but these alterations were not observed in female rats. The studies have demonstrated that the number of NFTs consisting of hyperphosphorylated tau is positively correlated with the degree of clinical dementia (Iqbal and Grundke-Iqbal, 1991; Iqbal et al., 2008; Luo et al., 2014). Estrogens attenuate tau hperphosphorylation through kinases and phosphatases, such as the GSK-3β, Wnt, and PKA pathways (Zhang et al., 2008). The

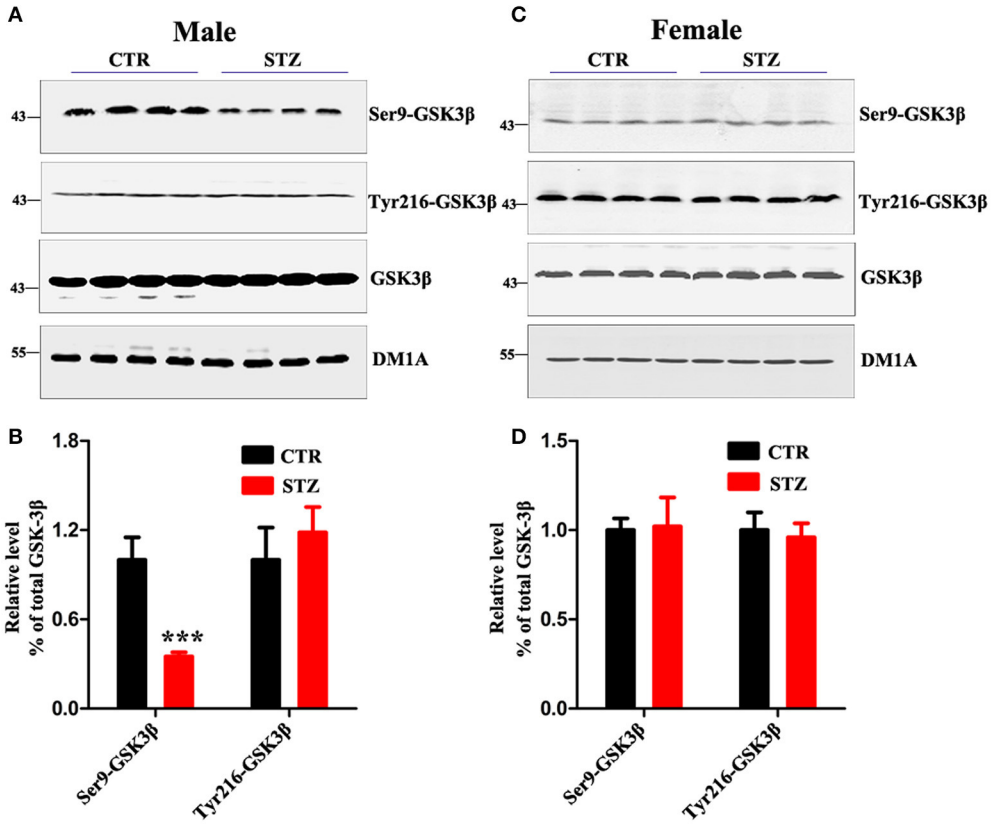


FIGURE 5 | Sex influences activity of GSK-3β in the sporadic AD animal model. **(A,C)** The total GSK-3β, GSK-3β (Ser9), GSK-3β (Tyr216) levels in whole hippocampus extracts were measured using Western blotting and **(B,D)** quantitative analysis. The phosphorylation level of GSK-3β was normalized to total GSK-3β level. The total level of GSK-3β was normalized DM1A. The data were expressed as mean ± *SD* ($n = 4$). ***$P < 0.001$ vs. the vehicle control. Data were analyzed using *t*-test.

ICV-STZ model in male rats shows hyperphosphorylation of tau and an increase of GSK-3β activity, but these tau pathologies are not observed in female rats. Together, sex hormones might account for functional discrepancy of ICV-STZ in the two sexes.

A large body of evidence shows that women have a higher incidence of AD than men happening after menopause, which suggest that estrogen might protect against AD pathology. Hormones have long been known to play key roles in regulating learning and memory and ample evidence has demonstrated that estradiol affects hippocampal morphology, plasticity, and memory (Packard, 1998; Brinton, 2009; Foster, 2012; Cui et al., 2013). Studies in the aromatase knock-out mouse suggest that estradiol induced spine and spine synapse formation in hippocampus, not in the cortex or the cerebellum (Zhou et al., 2014). Previous studies point to a role of hippocampus-derived estradiol in synaptic plasticity in cultured slices and *in vivo*, not just the role of gonads-derived estradiol (Zhou et al., 2010; Vierk et al., 2012). In addition, dendritic spines of CA1 pyramidal neurons vary during estrus cyclicity, which likely results from cycle of estradiol synthesis in the hippocampus, since gonadotropin releasing hormone regulates estradiol synthesis in the hippocampus in a dose-dependent manner (Woolley et al., 1990; Prange-Kiel et al., 2008, 2013). In the present study, 10 rats employed in each group is a small sample size. Therefore, we performed Shapiro–wilk test which showed that samples from each group was in accord with normal distribution. Relatively we found that hippocampal estradiol level of female rats is almost four times higher than that of male rats in both vehicle and ICV-STZ treated groups, which is in accordance with previous studies by using mass spectrometry (Fester et al., 2012). This implies that high estradiol levels in female rats might protect them from the ICV-STZ induced cognitive deficits and neurodegenerative pathologies, including synaptic damage, Aβ deposition, and tau hyperphosphorylation in hippocampus.

In reported literature, optimal female performance occurred during the phase of estrus on the spatial learning and memory, and the least efficient performance occurred during proestrus (Vina and Lloret, 2010). Since we did not determine the estrus stage of the control animals and cognitive ability and synaptic density are optimal during proestrus, the estradiol protective effects on hippocampal plasticity and memory would very likely have been greater if we had had exclusively taken proestrus female rats.

Although, the mouse- and monkey ICV-STZ models have also been developed, ICV-STZ rats are still widely used and employed to evaluate the therapeutic potential of drugs and

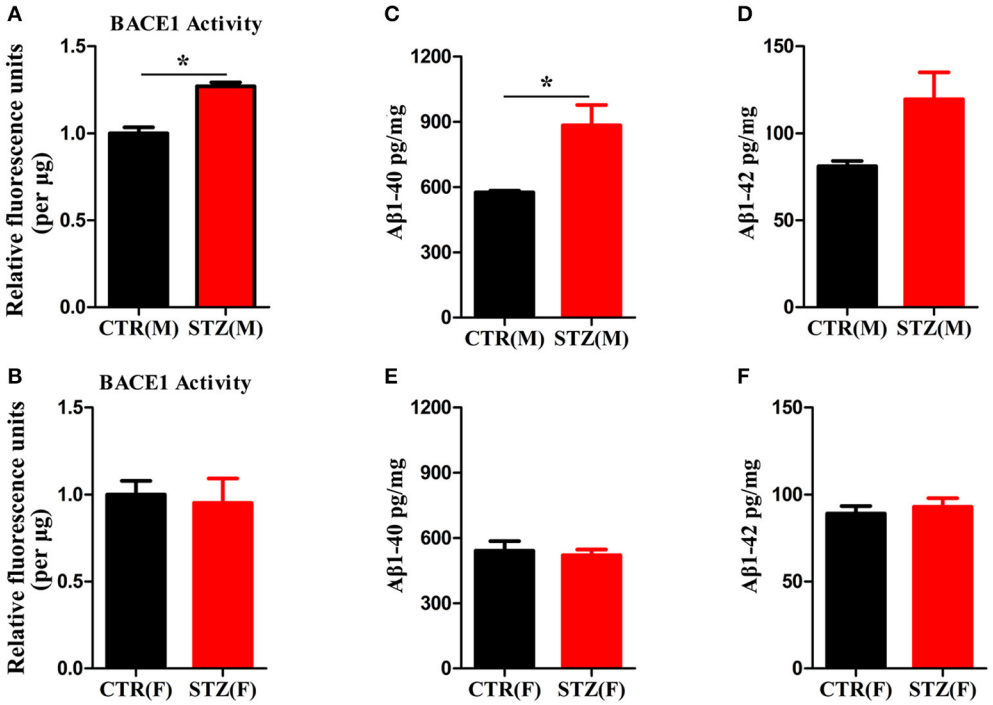


FIGURE 6 | Sex influences activity of BACE1 and Aβ production in the sporadic AD animal model. **(A,B)** BACE1 activity was determined using β-Secretase Activity Assay Kit. **(C–F)** Aβ40/42 levels were quantified through ELISA. The data were expressed as mean ± *SD* ($n = 5$). *$P < 0.05$ vs. the vehicle group. Data were analyzed using *t*-test.

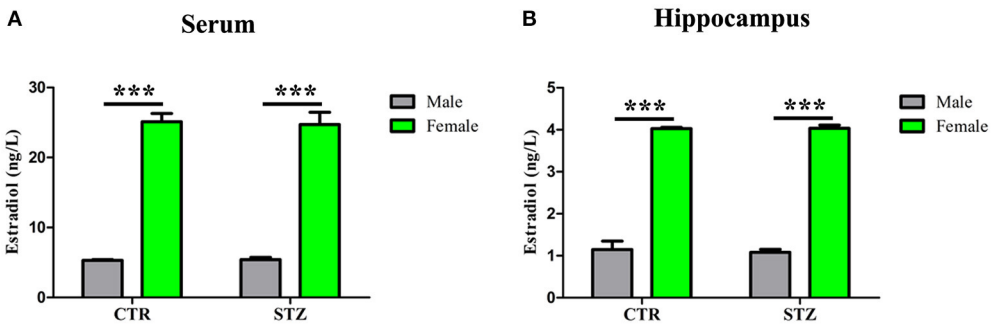


FIGURE 7 | Estradiol levels in serum and hippocampus. The Estradiol levels in the serum **(A)** and hippocampus **(B)** were measured. Estradiol levels of female rats were much higher than that of male rats, while no difference was observed between the groups with same sex. Data were presented as means ± *SD* ($n = 3$). ***$P <$ 0.001 vs. male rats. Data were analyzed using a general linear model was used for two-way ANOVA followed by *post-hoc* comparison.

non-drug therapies in numerous laboratories. Cognitive deficits and AD-like pathology, such as neuroinflammation, brain insulin resistance, tau hyperphosphorylation, Aβ overproduction, have been found both in female mice and monkeys (Chen et al., 2014; Park et al., 2015). Liu et al. have reported that STZ inhibits the Ras/ERK signaling cascade and decreased the phosphorylation of CREB, and induces cognitive impairment in rats (Liu et al., 2013). However, the study from Diao et al. shows the gender- and EC-dependent levels of proteins from the protein synthetic, chaperoning, and degradation machinery (Diao et al., 2007). Accordingly, it is necessary to re-evaluate the STZ-induced cognitive alterations between male and female rats. In the present study, we found that ICV-STZ remarkably results in cognitive impairments and AD like pathological alterations in the Sprague-Dawley male rats, but not in the female rats. It may conceivably be related with the gender- and EC-dependent levels of proteins from the protein synthetic, chaperoning, and degradation machinery, and consequently regulates tau related kinases and APP cleavage. Its molecular mechanism is worth further discussing. Our findings provide novel insights suggesting that sex differences exist in ICV-STZ rats which have been used as sporadic AD animal model for about 20

years. Therefore, our study encourages investigators to comply with National Institutes of Health policies to include females in biomedical research and to be aware that adding females to a study is not as simple as adding just another group.

AUTHOR CONTRIBUTIONS

XW and JW designed the experiments. JB performed the experiments and analyzed data. JB, YM, BZ, RL, ZZ, JW, and XW discussed and interpreted the results. JB, YM, and XW wrote the paper. All authors have approved the final version of the manuscript.

ACKNOWLEDGMENTS

This study was supported in parts by grants from Natural Science Foundation of China (81571255 and 31528010), the Hubei Province Key Technology R&D Program (2015BCE094) and the Academic Frontier Youth Team Project of HUST.

SUPPLEMENTARY MATERIAL

The Supplementary Material for this article can be found online at: https://www.frontiersin.org/articles/10.3389/fnagi.2017.00347/full#supplementary-material

Supplementary Figure1 | The experiments were designed as shown above.

REFERENCES

Agrawal, R., Tyagi, E., Shukla, R., and Nath, C. (2011). Insulin receptor signaling in rat hippocampus: a study in STZ (ICV) induced memory deficit model. *Eur. Neuropsychopharmacol.* 21, 261–273. doi: 10.1016/j.euroneuro.2010.11.009

Alafuzoff, I., Iqbal, K., Friden, H., Adolfsson, R., and Winblad, B. (1987). Histopathological criteria for progressive dementia disorders: clinical-pathological correlation and classification by multivariate data analysis. *Acta Neuropathol.* 74, 209–225. doi: 10.1007/BF00688184

Becker, J. B., Arnold, A. P., Berkley, K. J., Blaustein, J. D., Eckel, L. A., and Hampson, E. (2005). Strategies and methods for research on sex differences in brain and behavior. *Endocrinology* 146, 1650–1673. doi: 10.1210/en.2004-1142

Bitel, C. L., Kasinathan, C., Kaswala, R. H., Klein, W. L., and Frederikse, P. H. (2012). Amyloid-βand tau pathology of Alzheimer's disease induced by diabetes in a rabbit animal model. *J. Alzheimers Dis.* 32, 291–305. doi: 10.3233/JAD-2012-120571

Brinton, R. D. (2009). Estrogen-induced plasticity from cells to circuits: predictions for cognitive function. *Trends Pharmacol. Sci.* 30, 212–222. doi: 10.1016/j.tips.2008.12.006

Cahill, L. (2006). Why sex matters for neuroscience. *Nat. Rev. Neurosci.* 7, 477–484. doi: 10.1038/nrn1909

Carro, E., and Torres-Aleman, I. (2004). The role of insulin and insulin-like growth factor I in the molecular and cellular mechanisms underlying the pathology of Alzheimer's disease. *Eur. J. Pharmacol.* 490, 127–133. doi: 10.1016/j.ejphar.2004.02.050

Chen, Y., Liang, Z., Blanchard, J., Dai, C. L., Sun, S., Lee, M. H., et al. (2013). A non-transgenic mouse model (icv-STZ mouse) of Alzheimer's disease: similarities to and differences from the transgenic model (3xTg-AD mouse). *Mol. Neurobiol.* 47, 711–725. doi: 10.1007/s12035-012-8375-5

Chen, Y., Liang, Z., Tian, Z., Blanchard, J., Dai, C. L., and Chalbot, S. (2014). Intracerebroventricular streptozotocin exacerbates Alzheimer-like changes of 3xTg-AD mice. *Mol. Neurobiol.* 49, 547–562. doi: 10.1007/s12035-013-8539-y

Cui, J., Shen, Y., and Li, R. (2013). Estrogen synthesis and signaling pathways during aging: from periphery to brain. *Trends Mol. Med.* 19, 197–209. doi: 10.1016/j.molmed.2012.12.007

Deng, Y., Li, B., Liu, Y., Iqbal, K., Grundke-Iqbal, I., and Gong, C. X. (2009). Dysregulation of insulin signaling, glucose transporters, O-GlcNAcylation, and phosphorylation of tau and neurofilaments in the brain: implication for Alzheimer's disease. *Am. J. Pathol.* 175, 2089–2098. doi: 10.2353/ajpath.2009.090157

Diao, W. F, Chen, W. Q., Höger, H., Shim, K. S., Pollak, A., and Lubec, G. (2007). The hippocampal protein machinery varies over the estrous cycle. *Proteomics Clin. Appl.* 1, 1462–1475. doi: 10.1002/prca.200700333

Dysken, M. W., Sano, M., Asthana, S., Vertrees, J. E., Pallaki, M., and Llorente, M. (2014). Effect of vitamin E and memantine on functional decline in Alzheimer disease: the TEAM-AD VA cooperative randomized trial. *JAMA* 311, 33–44. doi: 10.1001/jama.2013.282834

Fester, L., Prange-Kiel, J., Zhou, L., Blittersdorf, B.V., Bohm, J., Jarry, H., et al. (2012). Estrogen-regulated synaptogenesis in the hippocampus: sexual dimorphism *in vivo* but not *in vitro*. *J. Steroid Biochem. Mol. Biol.* 131, 24–29. doi: 10.1016/j.jsbmb.2011.11.010

Forger, N. G., Strahan, J. A., and Castillo-Ruiz, A. (2016). Cellular and molecular mechanisms of sexual differentiation in the mammalian nervous system. *Front. Neuroendocrinol.* 40, 67–86. doi: 10.1016/j.yfrne.2016.01.001

Foster, T. C. (2012). Role of estrogen receptor alpha and beta expression and signaling on cognitive function during aging. *Hippocampus* 22, 656–669. doi: 10.1002/hipo.20935

Grundke-Iqbal, I., Iqbal, K., Tung, Y. C., Quinlan, M., Wisniewski, H. M., and Binder, L. I. (1986). Abnormal phosphorylation of the microtubule-associated protein tau (tau) in Alzheimer cytoskeletal pathology. *Proc. Natl. Acad. Sci. U.S.A.* 83, 4913–4917. doi: 10.1073/pnas.83.13.4913

Hall, A. M., and Roberson, E. D. (2012). Mouse models of Alzheimer's disease. *Brain Res. Bull.* 88, 3–12. doi: 10.1016/j.brainresbull.2011.11.017

Hong, M., and Lee, V. M. (1997). Insulin and insulin-like growth factor-1 regulate tau phosphorylation in cultured human neurons. *J. Biol. Chem.* 272, 19547–19553. doi: 10.1074/jbc.272.31.19547

Iqbal, K., Bolognin, S., Wang, X., Basurto-Islas, G., Blanchard, J., Tung, Y. C., et al. (2013). Animal models of the sporadic form of Alzheimer's disease: focus on the disease and not just the lesions. *J. Alzheimers Dis.* 37, p469–p474. doi: 10.3233/JAD-130827

Iqbal, K., Alonso Adel, C, and Grundke-Iqbal, I. (2008). Cytosolic abnormally hyperphosphorylated tau but not paired helical filaments sequester normal MAPs and inhibit microtubule assembly. *J. Alzheimer's Dis.* 14, 365–370. doi: 10.3233/JAD-2008-14402

Iqbal, K., and Grundke-Iqbal, I. (1991). Ubiquitination and abnormal phosphorylation of paired helical filaments in Alzheimer's disease. *Mol. Neurobiol.* 5, 399–410.

Iqbal, K., and Grundke-Iqbal, I. (2010). Alzheimer disease, a multifactorial disorder seeking multi therapies. *Alzheimers Dement.* 6, 420–4. doi: 10.1016/j.jalz.2010.04.006

Jee, Y. S., Ko, I. G., Sung, Y. H., Lee, J. W., Kim, Y. S., and Kim, S. E. (2008). Effects of treadmill exercise on memory and c-Fos expression in the hippocampus of the rats with intracerebroventricular injection of streptozotocin. *Neurosci. Lett.* 443, 188–192. doi: 10.1016/j.neulet.2008.07.078

Kamat, P. K., Kalani, A., Rai, S., Tota, S. K., Kumar, A., and Ahmad, A. S. (2016). Streptozotocin intracerebro ventricular induced neurotoxicity and brain insulin resistance:a therapeutic intervention for treatment of Sporadic Alzheimer's Disease (sAD)-like pathology. *Mol. Neurobiol.* 53, 4548–4562. doi: 10.1007/s12035-015-9384-y

Kasai, H., Fukuda, M., Watanabe, S., Hayashi-Takagi, A., and Noguchi, J. (2010). Structural dynamics of dendritic spines in memory and cognition. *Trends Neurosci.* 33, 121–129. doi: 10.1016/j.tins.2010.01.001

Kloppenborg, R. P., van den Berg, E., Kappelle, L. J., and Biessels, G. J. (2008). Diabetes and other vascular risk factors for dementia: which factor matters most? A systematic review. *Eur. J. Pharmacol.* 585, 97–108. doi: 10.1016/j.ejphar.2008.02.049

Lannert, H., and Hoyer, S. (1998). Intracerebroventricular administration of streptozotocin causes long-term diminutions in learning and memory abilities

and in cerebral energy metabolism in adult rats. *Behav. Neurosci.* 112, 1199–1208. doi: 10.1037/0735-7044.112.5.1199

Li, B., Yamamori, H., Tatebayashi, Y., Shafit-Zagardo, B., Tanimukai, H., and Chen, S. (2008). Failure of neuronal maturation in Alzheimer disease dentate gyrus. *J. Neuropathol. Exp. Neurol.* 67, 78–84. doi: 10.1097/nen.0b013e318160c5db

Liu, P., Zou, L., Jiao, Q., Chi, T., Ji, X., and Qi, Y. (2013). Xanthoceraside attenuates learning and memory deficits via improving insulin signaling in STZ-induced AD rats. *Neurosci. Lett.* 543, 115–120. doi: 10.1016/j.neulet.2013.02.065

Luo, H. B., Xia, Y. Y., Shu, X. J., Liu, Z. C., Feng, Y., and Liu, X. H. (2014). SUMOylation at K340 inhibits tau degradation through deregulating its phosphorylation and ubiquitination. *Proc. Natl. Acad. Sci. U.S.A.* 111, 16586–16591. doi: 10.1073/pnas.1417548111

Malkki, H. (2016). Alzheimer disease: NSAIDs protect neurons and preserve memory in a mouse model of AD. *Nat. Rev. Neurol.* 12, 370–371. doi: 10.1038/nrneurol.2016.79

Mangialasche, F., Solomon, A., Winblad, B., Mecocci, P., and Kivipelto, M. (2010). Alzheimer's disease: clinical trials and drug development. *Lancet Neurol.* 9, 702–716. doi: 10.1016/S1474-4422(10)70119-8

McCarthy, M. M (2009). The two faces of estradiol: effects on the developing brain. *Neuroscientist* 15, 599–610. doi: 10.1177/1073858409340924

Mehla, J., Pahuja, M., and Gupta, Y. K. (2013). Streptozotocin-induced sporadic Alzheimer's disease: selection of appropriate dose. *J. Alzheimers Dis.* 33, 17–21. doi: 10.3233/JAD-2012-120958

Morest, D. K (1960). A study of the structure of the area postrema with Golgi methods. *Am. J. Anat.* 107, 291–303. doi: 10.1002/aja.1001070307

Packard, M. G. (1998). Posttraining estrogen and memory modulation. *Horm. Behav.* 34, 126–139. doi: 10.1006/hbeh.1998.1464

Park, S. J., Kim, Y. H., Nam, G. H., Choe, S. H., Lee, S. R., Kim, S. U., et al. (2015). Quantitative expression analysis of APP pathway and tau phosphorylation-related genes in the ICV STZ-induced non-human primate model of sporadic Alzheimer's disease. *Int. J. Mol. Sci.* 16, 2386–2402. doi: 10.3390/ijms16022386

Pike, C. J. (1999). Estrogen modulates neuronal Bcl-xL expression and beta-amyloid-induced apoptosis: relevance to Alzheimer's disease. *J. Neurochem.* 72, 1552–1563. doi: 10.1046/j.1471-4159.1999.721552.x

Prange-Kiel, J., Jarry, H., Schoen, M., Kohlmann, P., Lohse, C., Zhou, L., et al. (2008). Gonadotropin-releasing hormone regulates spine density via its regulatory role in hippocampal estrogen synthesis. *Cell Biol. J.* 180, 417–426. doi: 10.1083/jcb.200707043

Prange-Kiel, J., Schmutterer, T., Fester, L., Zhou, L., Imholz, P., Brandt, N., et al. (2013). Endocrine regulation of estrogen synthesis in the hippocampus? *Prog. Histochem. Cytochem.* 48, 49–64. doi: 10.1016/j.proghi.2013.07.002

Prasad, K. N (2017). Oxidative stress and pro-inflammatory cytokines may act as one of the signals for regulating microRNAs expression in Alzheimer's disease. *Mech. Ageing Dev.* 162, 63–71. doi: 10.1016/j.mad.2016.12.003

Prickaerts, J., Fahrig, T., and Blokland, A. (1999). Cognitive performance and biochemical markers in septum, hippocampus and striatum of rats after an i.c.v. injection of streptozotocin: a correlation analysis. *Behav. Brain Res.* 102, 73–88. doi: 10.1016/S0166-4328(98)00158-2

Qi, C., Bao, J., Wang, J., Zhu, H., Xue, Y., Wang, X., et al. (2016). Asperterpenes, A., and B, two unprecedented meroterpenoids from *Aspergillus terreus* with BACE1 inhibitory activities. *Chem. Sci.* 7, 6563–6572. doi: 10.1039/C6SC02464E

Raznahan, A., Lee, Y., Stidd, R., Long, R., Greenstein, D., and Clasen, L. (2010). Longitudinally mapping the influence of sex and androgen signaling on the dynamics of human cortical maturation in adolescence. *Proc. Natl. Acad. Sci. U.S.A.* 107, 16988–16993. doi: 10.1073/pnas.1006025107

Rodrigues, L., Dutra, M. F, Ilha, J, Biasibetti, R., Quincozes-Santos, A., and Leite, M. C. (2010). Treadmill training restores spatial cognitive deficits and neurochemical alterations in the hippocampus of rats submitted to an intracerebroventricular administration of streptozotocin. *J. Neural Transm.* 117, 1295–1305. doi: 10.1007/s00702-010-0501-9

Ruigrok, A. N., Salimi-Khorshidi, G., Lai, M. C., Baron-Cohen, S., Lombardo, M. V., and Tait, R. J. (2014). A meta-analysis of sex differences in human brain structure. *Neurosci. Biobehav. Rev.* 39, 34–50. doi: 10.1016/j.neubiorev.2013.12.004

Salkovic-Petrisic, M., and Hoyer, S. (2007). Central insulin resistance as a trigger for sporadic Alzheimer-like pathology: an experimental approach. *J. Neural Transm. Suppl.* 72, 217–233. doi: 10.1007/978-3-211-73574-9_28

Salkovic-Petrisic, M., Knezovic, A., Hoyer, S., and Riederer, P. (2013). What have we learned from the streptozotocin-induced animal model of sporadic Alzheimer's disease, about the therapeutic strategies in Alzheimer's research. *J. Neural Transm.* 120, 233–252. doi: 10.1007/s00702-012-0877-9

Shineman, D. W., Basi, G. S., Bizon, J. L., Colton, C. A., Greenberg, B. D., and Hollister, B. A. (2011). Accelerating drug discovery for Alzheimer's disease: best practices for preclinical animal studies. *Alzheimers Res. Ther.* 3, 28. doi: 10.1186/alzrt90

Singh, M., Sétáló, G., Guan, X., Warren, M., and Toran-Allerand, C. D. (1999). Estrogen-induced activation of mitogen-activated protein kinase in cerebral cortical explants: convergence of estrogen and neurotrophin signaling pathways. *J. Neurosci.* 19, 1179–1188.

Singh, T. J., Zaidi, T., Grundke-Iqbal, I., and Iqbal, K. (1995). Modulation of GSK-3-catalyzed phosphorylation of microtubule-associated protein tau by non-proline-dependent protein kinases. *FEBS Lett.* 358, 4–8. doi: 10.1016/0014-5793(94)01383-C

Valente, T., Gella, A., Fernàndez-Busquets, X., Unzeta, M., and Durany, N. (2010). Immunohistochemical analysis of human brain suggests pathological synergism of Alzheimer's disease and diabetes mellitus. *Neurobiol. Dis.* 37, 67–76. doi: 10.1016/j.nbd.2009.09.008

Vassar, R., Kovacs, D. M., Yan, R., and Wong, P. C (2009). The beta-secretase enzyme BACE in health and Alzheimer's disease: regulation, cell biology, function, and therapeutic potential. *J. Neurosci.* 29, 12787–12794. doi: 10.1523/JNEUROSCI.3657-09.2009

Vierk, R., Glassmeier, G., Zhou, L., Brandt, N., Fester, L., Dudzinski, D., et al. (2012). Aromatase inhibition abolishes LTP generation in female but not in male mice. *Neurosci. J.* 32, 8116–8126. doi: 10.1523/JNEUROSCI.5319-11.2012

Vina, J., and Lloret, A. (2010). Why women have more Alzheimer's disease than men: gender and mitochondrial toxicity of amyloid-beta peptide. *J. Alzheimers Dis.* 20(Suppl. 2), S527–S533. doi: 10.3233/JAD-2010-100501

Wang, J. Z., and Liu, F. (2008). Microtubule-associated protein tau in development, degeneration and protection of neurons. *Prog. Neurobiol.* 85, 148–175. doi: 10.1016/j.pneurobio.2008.03.002

Wang, X., Blanchard, J., Kohlbrenner, E., Clement, N., Linden, R. M., and Radu, A. (2010). The carboxy-terminal fragment of inhibitor-2 of protein phosphatase-2A induces Alzheimer disease pathology and cognitive impairment. *FASEB J.* 24, 4420–4432. doi: 10.1096/fj.10-158477

Wightman, E. L. (2017). Potential benefits of phytochemicals against Alzheimer's disease. *Proc. Nutr. Soc.* 76, 106–112. doi: 10.1017/S0029665116002962

Woo, K. (2000). Is vitamin E the magic bullet for the treatment of Alzheimer's disease (AD)? *Perspectives* 24, 7–10.

Woolley, C. S., Gould, E., Frankfurt, M., and McEwen, B. S. (1990). Naturally-occurring fluctuation in dendritic spine density on adult hippocampal pyramidal neurons. *Neurosci. J.* 10, 4035–4039.

Xu, Z. P., Li, L., Bao, J., Wang, Z. H., Zeng, J., and Liu, E. J. (2014). Magnesium protects cognitive functions and synaptic plasticity in streptozotoc in-induced sporadic Alzheimer's model. *PLoS ONE* 9:e108645. doi: 10.1371/journal.pone.0108645

Zahs, K. R., and Ashe, K. H. (2010). 'Too much good news' - are Alzheimer mouse models trying to tell us how to prevent, not cure, Alzheimer's disease? *Trends Neurosci.* 33, 381–389. doi: 10.1016/j.tins.2010.05.004

Zhang, Q.G., Wang, R., Khan, M., Mahesh, V., and Brann, D. W. (2008). Role of Dickkopf-1, an antagonist of the Wnt/beta-catenin signaling pathway, in estrogen-induced neuroprotection and attenuation of tau phosphorylation. *J. Neurosci.* 28, 8430–8441. doi: 10.1523/JNEUROSCI.2752-08.2008

Zhang, Z., Song, M., Liu, X., Su Kang, S., Duong, D. M., and Seyfried, N. T. (2015). Delta-secretase cleaves amyloid precursor protein and regulates the pathogenesis in Alzheimer's disease. *Nat. Commun.* 9, 8762. doi: 10.1038/ncomms9762

Zhou, L., Fester, L., Haghshenas, S., de Vrese, X., von Hacht, R., Gloger, S., et al. (2014). Oestradiol-induced synapse formation in the female hippocampus:

roles of oestrogen receptor subtypes. *Neuroendocrinol. J.* 26, 439–447. doi: 10.1111/jne.12162

Zhou, L., Fester, L., von Blittersdorff, B., Hassu, B., Nogens, H., Prange-Kiel, J., et al. (2010). Aromatase inhibitors induce spine synapse loss in the hippocampus of ovariectomized mice. *Endocrinology* 151, 1153–1160. doi: 10.1210/en.2009-0254

Zhou, S., Yu, G., Chi, L., Zhu, J., Zhang, W., and Zhang, Y. (2013). Neuroprotective effects of edaravone on cognitive deficit, oxidative stress and tau hyperphosphorylation induced by intracerebroventricular streptozotocin in rats. *Neurotoxicology* 38, 136–145. doi: 10.1016/j.neuro.2013.07.007

Conflict of Interest Statement: The authors declare that the research was conducted in the absence of any commercial or financial relationships that could be construed as a potential conflict of interest.

Copyright © 2017 Bao, Mahaman, Liu, Wang, Zhang, Zhang and Wang. This is an open-access article distributed under the terms of the Creative Commons Attribution License (CC BY). The use, distribution or reproduction in other forums is permitted, provided the original author(s) or licensor are credited and that the original publication in this journal is cited, in accordance with accepted academic practice. No use, distribution or reproduction is permitted which does not comply with these terms.

frontiers in Aging Neuroscience

CORRECTION
published: 15 October 2019
doi: 10.3389/fnagi.2019.00275

Corrigendum: Sex Differences in the Cognitive and Hippocampal Effects of Streptozotocin in an Animal Model of Sporadic AD

Jian Bao[1], *Yacoubou A. R. Mahaman*[1], *Rong Liu*[1], *Jian-Zhi Wang*[1,2], *Zhiguo Zhang*[3], *Bin Zhang*[4] *and Xiaochuan Wang*[1,2]*

[1] Key Laboratory of Ministry of Education of China for Neurological Disorders, Department of Pathophysiology, School of Basic Medicine and the Collaborative Innovation Center for Brain Science, Tongji Medical College, Huazhong University of Science and Technology, Wuhan, China, [2] Co-innovation Center of Neuroregeneration, Nantong University, Nantong, China, [3] School of Medicine and Health Management, Tongji Medical College, Huazhong University of Science and Technology, Wuhan, China, [4] Department of Genetics and Genomic Sciences, Icahn School of Medicine at Mount Sinai, New York, NY, United States

Keywords: Alzheimer's disease (AD), animal model, Streptozotocin (STZ), sex differences, learning and memory

OPEN ACCESS

Edited and reviewed by:
Mohammad Amjad Kamal, King Fahad Medical Research Center, King Abdulaziz University, Saudi Arabia

***Correspondence:**
Xiaochuan Wang
wxch@mails.tjmu.edu.cn

Received: *24 August 2019*
Accepted: *25 September 2019*
Published: *15 October 2019*

Citation:
Bao J, Mahaman YAR, Liu R, Wang J-Z, Zhang Z, Zhang B and Wang X (2019) Corrigendum: Sex Differences in the Cognitive and Hippocampal Effects of Streptozotocin in an Animal Model of Sporadic AD. Front. Aging Neurosci. 11:275. doi: 10.3389/fnagi.2019.00275

A Corrigendum on

Sex Differences in the Cognitive and Hippocampal Effects of Streptozotocin in an Animal Model of Sporadic AD

by Bao, J., Mahaman, Y. A. R., Liu, R., Wang, J.-Z., Zhang, Z., Zhang, B., et al. (2017). Front. Aging Neurosci. 9:347. doi: 10.3389/fnagi.2017.00347

In the original article, due to the authors' oversight, there were several mistakes in **Figure 3C** and **Figure 4C** as published. The image "PSD95 of Female" in **Figure 3C** was inadvertently replaced with the image "GSK3β" in Figure 5C. The images "AT8 of Female" and "PS262 of Female" in **Figure 4C** were inadvertently replaced with image "PS404 of Female" from **Figure 4C**. The image "Tau5 of Female" in **Figure 4C** was inadvertently replaced with image "Tau5 of Male" in **Figure 4A**. The corrected **Figures 3C** and **4C** appear below. The quantification for the above-mentioned blots have been done in the corrected **Figures 3D** and **4D**, which all have no significant difference between control and STZ groups as in the published original version of the article.

The authors apologize for this error and state that this does not change the scientific conclusions of the article in any way. The original article has been updated.

Copyright © 2019 Bao, Mahaman, Liu, Wang, Zhang, Zhang and Wang. This is an open-access article distributed under the terms of the Creative Commons Attribution License (CC BY). The use, distribution or reproduction in other forums is permitted, provided the original author(s) and the copyright owner(s) are credited and that the original publication in this journal is cited, in accordance with accepted academic practice. No use, distribution or reproduction is permitted which does not comply with these terms.

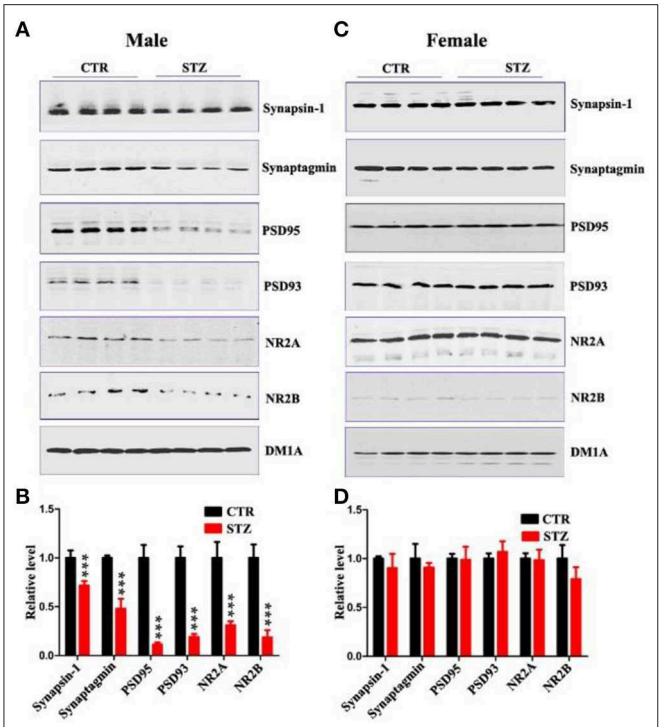


FIGURE 3 | Sex influences synaptic plasticity in the sporadic AD animal model. **(A,C)** Western blot analysis of the protein levels of synapsin-1, synaptagmin, psd95, psd93, NR2A, and NR2B and **(B,D)** their quantitative analysis for male or female rats. DM1A was used as a loading control. The data were expressed as mean ± *SD* ($n = 4$). ***$P < 0.001$ vs. the vehicle control. Data were analyzed using *t*-test.

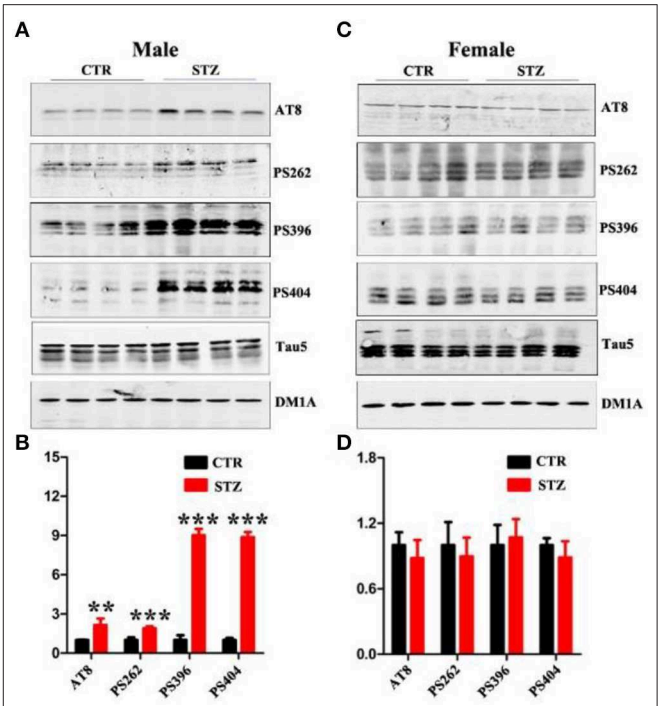


FIGURE 4 | Sex influences tau hyperphosphorylation in the sporadic AD animal model. **(A,C)** Western blot analysis of the protein levels of AT8, PS262, PS396, PS404, and Tau5 and **(B,D)** their quantitative analysis for male or female rats. The data were expressed as mean ± *SD* ($n = 4$). The phosphorylation level of tau was normalized to total tau level probed by tau5. The total level of tau was normalized DM1A. ***$P < 0.001$ vs. the vehicle control. Data were analyzed using *t*-test. **$P < 0.01$ vs. the vehicle control.

frontiers in Aging Neuroscience

ORIGINAL RESEARCH
published: 26 July 2017
doi: 10.3389/fnagi.2017.00245

Differential Roles of Environmental Enrichment in Alzheimer's Type of Neurodegeneration and Physiological Aging

*Vladimir V. Salmin[1], Yulia K. Komleva[2,3], Natalia V. Kuvacheva[2,3], Andrey V. Morgun[4], Elena D. Khilazheva[2,3], Olga L. Lopatina[2,3], Elena A. Pozhilenkova[2,3], Konstantin A. Shapovalov[1], Yulia A. Uspenskaya[3] and Alla B. Salmina[2,3]**

[1] Department of Medical and Biological Physics, Krasnoyarsk State Medical University named after Prof. V.F. Voino-Yasenetsky, Krasnoyarsk, Russia, [2] Department of Biochemistry, Medical, Pharmaceutical and Toxicological Chemistry, Krasnoyarsk State Medical University named after Prof. V.F. Voino-Yasenetsky, Krasnoyarsk, Russia, [3] Research Institute of Molecular Medicine and Pathobiochemistry, Krasnoyarsk State Medical University named after Prof. V.F. Voino-Yasenetsky, Krasnoyarsk, Russia, [4] Department of Pediatrics, Krasnoyarsk State Medical University named after Prof. V.F. Voino-Yasenetsky, Krasnoyarsk, Russia

OPEN ACCESS

Edited by:
Athanasios Alexiou, Novel Global Community Educational Foundation (NGCEF), Hebersham, Australia

Reviewed by:
Daniel Ortuño-Sahagún, Centro Universitario de Ciencias de la Salud, Mexico
Maik Gollasch, Charité Universitätsmedizin Berlin, Germany

***Correspondence:**
Alla B. Salmina
allasalmina@mail.ru

Received: 01 May 2017
Accepted: 14 July 2017
Published: 26 July 2017

Citation:
Salmin VV, Komleva YK, Kuvacheva NV, Morgun AV, Khilazheva ED, Lopatina OL, Pozhilenkova EA, Shapovalov KA, Uspenskaya YA and Salmina AB (2017) Differential Roles of Environmental Enrichment in Alzheimer's Type of Neurodegeneration and Physiological Aging. Front. Aging Neurosci. 9:245. doi: 10.3389/fnagi.2017.00245

Impairment of hippocampal adult neurogenesis in aging or degenerating brain is a well-known phenomenon caused by the shortage of brain stem cell pool, alterations in the local microenvironment within the neurogenic niches, or deregulation of stem cell development. Environmental enrichment (EE) has been proposed as a potent tool to restore brain functions, to prevent aging-associated neurodegeneration, and to cure neuronal deficits seen in neurodevelopmental and neurodegenerative disorders. Here, we report our data on the effects of environmental enrichment on hippocampal neurogenesis *in vivo* and neurosphere-forming capacity of hippocampal stem/progenitor cells *in vitro.* Two models – Alzheimer's type of neurodegeneration and physiological brain aging – were chosen for the comparative analysis of EE effects. We found that environmental enrichment greatly affects the expression of markers specific for stem cells, progenitor cells and differentiated neurons (Pax6, Ngn2, NeuroD1, NeuN) in the hippocampus of young adult rats or rats with Alzheimer's disease (AD) model but less efficiently in aged animals. Application of time-lag mathematical model for the analysis of impedance traces obtained in real-time monitoring of cell proliferation *in vitro* revealed that EE could restore neurosphere-forming capacity of hippocampal stem/progenitor cells more efficiently in young adult animals (fourfold greater in the control group comparing to the AD model group) but not in the aged rats (no positive effect of environmental enrichment at all). In accordance with the results obtained *in vivo*, EE was almost ineffective in the recovery of hippocampal neurogenic reserve *in vitro* in aged, but not in amyloid-treated or young adult, rats. Therefore, EE-based neuroprotective strategies effective in Aβ-affected brain could not be directly extrapolated to aged brain.

Keywords: environmental enrichment, neurogenesis, neurosphere, Alzheimer's disease, aging, time-lag model

INTRODUCTION

Environmental enrichment (EE) is considered as an environment with numerous sensorimotor, cognitive, and social stimulations able to affect brain plasticity, to restore brain functional reserves, and to facilitate establishment of novel connections actual for preventive or rehabilitation strategies. Modeling EE is currently widely used in experiments aimed to study synaptogenesis, neurogenesis, and brain connectivity (Komleva Iu et al., 2013). EE stimulates neurogenesis and synapse turnover, integration of newly-formed cells into neuronal ensembles, modifies epigenetic mechanisms controlling resistance to oxidative stress, modulates production of neurotransmitters and molecules with neurotrophic activity, prevents apoptosis, suppresses neuroinflammation, affects neuron-glia interactions, thereby enhancing cognition, learning, and social communications in animals or humans with or without brain pathology (Herring et al., 2011; Cotel et al., 2012; Komleva Iu et al., 2013; Leger et al., 2015; Grinan-Ferre et al., 2016; Stuart et al., 2017). These effects well-correspond to those observed in people practicing so-called cognitive training because of their professional duties or personal habits and demonstrating good preservation of cognitive functions even at the eldest period of life (Mora, 2013). However, action of EE depends on experimental conditions, duration of exposure, severity of brain injury, age, gender etc., thereby, the observed effects of EE on neuroplasticity might be different and even unexpected (Ming and Song, 2011; Valero-Aracama et al., 2015).

Growing number of experimental and clinical findings suggest that EE might serve as an effective strategy to restore the functional capacity of damaged brain, i.e., in Alzheimer's disease (AD), in neurodevelopmental disorders, after stroke, etc. (Janssen et al., 2014; Polito et al., 2014; Cioni et al., 2016; Rosbergen et al., 2016). Particularly, prevention or treatment of Alzheimer-type neurodegeneration is one of the most challenging questions in the modern neuroscience which is directly linked to the controlled modulation of hippocampal plasticity (Balietti et al., 2012) In such context, EE provides a lot of premises for its effective application: prevention of hippocampal astroglial dysfunction in the AD transgenic mice (Rodriguez et al., 2013), up-regulation of brain-derived growth factor expression in the hippocampus of senescence-accelerated prone mice (Yuan et al., 2012), prevention of amyloid β (Aβ) deposition and memory impairment in AD model mice (Maesako et al., 2012), modulation of hippocampal synaptic proteins expression (Barak et al., 2013).

In contrast, EE action in aging brain is not deciphered in detail, even aging itself is the certain risk for AD development (Avila et al., 2010). Moreover, precise molecular mechanisms of EE effects on neuroplasticity in aged or AD brain remain to be unclear or even contradictory (Herring et al., 2011; Cotel et al., 2012; Bezzina et al., 2015; Huttenrauch et al., 2016). Impairment of hippocampal adult neurogenesis in aging is a well-known phenomenon caused by the shortage of brain stem cell pool, alterations in the local microenvironment within the neurogenic niches, or deregulation of stem cell development (Ali et al., 2015; Moraga et al., 2015). It is well-known that there is an obvious contrast between Alzheimer-type neurodegeneration and physiological aging, however, both of them are associated with progressive cognitive deficits and impairment of brain plasticity. Healthy aging brain is characterized by moderate decline in neurogenesis affecting the structure and function of the entorhinal-hippocampal circuit which is in the focus of neurodegeneration seen in AD due to the toxic action of Aβ, oxidative stress, excitotoxicity, and neuroinflammation (Hollands et al., 2016). In physiologically aging brain, no significant changes in the number of neural stem cells (NSCs) residing within the hippocampal neurogenic niche have been detected (Hattiangady and Shetty, 2008). In contrast, gradual decrease of NSCs and neural progenitor cells (NPCs) number has been reported in the experimental APP/PS1/nestin-GFP triple transgenic mouse model of AD (Zeng et al., 2016). Thus, the earliest stages of adult neurogenesis (stem cell maintenance, self-renewal, and proliferation) are significantly affected in AD neurodegeneration but not in healthy aging. Since enhancing neurogenesis was proposed as a therapeutic approach in neurodegeneration (Hollands et al., 2016), one may assume that EE could produce different effects on aging-associated and AD-compromised hippocampal neurogenesis. Despite several experimental and clinical observations on EE action in elderly subjects with or without AD, little information is available on the comparative efficacy of EE in AD and healthy aging.

So, whether EE-induced changes are equally beneficial in aging brain and in AD? The subject has received increased attention with the deciphering the biological mechanisms of late-life brain alterations: reduced neurogenesis and synapse turnover (Mostany et al., 2013), suppressed release of neuropeptides and neurotrophic factors (Forlenza et al., 2015), appearance of white matter lesions and pathological blood–brain barrier permeability (Marin-Padilla and Knopman, 2011; Firbank et al., 2012). Several studies suggest that EE affects epigenetic mechanisms controlling neuroplasticity, promotes remyelination, or reduces glia-supported neuroinflammation in the neurogenic niches in the aged brain (Williamson et al., 2012; Yang et al., 2012; Neidl et al., 2016). However, alterations in neurogenesis and the capacity of so-called "neurogenic reserve" may have different patterns and degree of progression in normal aging and in AD (Esiri and Chance, 2012).

Assessment of neurogenesis represents an appropriate system to analyze the activity of factors with presumptive neuroprotective properties. *In vivo*, neurogenesis can be studied with the approach based on the detection of markers expression in cells at different stages of development within the neurogenic niches or along their migratory paths in the brain (Roybon et al., 2009). Apart from this, some neurogenesis-associated events are easily reproduced *in vitro* due to ability of neurogenic non-differentiated cells to produce non-adherent spherical clusters of cells known as neurospheres (NS). NS-forming capacity is a parameter which is widely used for the assessment of neurogenic potential of neural stem/progenitor cells as well as the action of regulatory molecules, neurotoxic substances, or drug candidates (Pacey et al., 2006). Positive effects of EE on neurogenesis *in vivo* have been shown (Monteiro et al., 2014; Clemenson et al., 2015),

however, there are very limited data on NS development *in vitro* in AD or aging (Heo et al., 2007; Diaz-Moreno et al., 2013).

Recently, we have demonstrated EE-mediated enhancement of neurosphere-forming capacity of NSCs obtained from the brains of AD rat model (Kuvacheva et al., 2015). It should be mentioned that analysis of data obtained with NS culture systems is hampered by the relative shortage of tools for adequate interpretation within the context of cell cycle- and proliferation-related events. Modeling the cell growth kinetics has been in the focus of researchers for a long time (Baker et al., 1998), but mathematic analysis of kinetic features of stem cells behavior in several subsequent NS generations *in vitro* was undertaken in few studies only (Ma et al., 2007). Development of correct mathematical models of NS establishment in the short-term experimental conditions (when reduction of cell population due to cell death might be contingently neglected) would provide new opportunities for rapid and effective analysis of endogenous and exogenous stimuli targeting neurogenesis. Moreover, current achievements in the application of NS cultures for AD modeling *in vitro* (Choi et al., 2013; Ghate et al., 2014) or novel attempts to restore brain functions with NSCs transplantation therapy (Waldau and Shetty, 2008) determine the needs in the appropriate mathematical modeling of NS-generation *in vitro* to clarify mechanisms underlying neurogenesis modulation in a given microenvironment.

Thus, we may entertain the hypothesis that: (i) effects of EE on neurogenesis are different in healthy brain aging and in brain affected by Alzheimer's type of neurodegeneration; (ii) combination of *in vivo* and *in vitro* approaches to the assessment of neurogenesis with the mathematical modeling of neurogenic reserve could help us to identify the neurogenesis stage which is a main "target" for the action of EE in normal and damaged brain. Therefore, the goal of this study was to compare the effects of *in vivo* EE in the Alzheimer's type of neurodegeneration and physiological brain aging with the special focus on hippocampal neurogenesis *in vivo* and NS-forming capacity of hippocampal stem/progenitor cells *in vitro*.

Experimental Procedures

Modeling Environmental Enrichment *In Vivo*

Wistar male rats ($n = 64$) were maintained in standard cages with water and standard diet with free access to food and water. The following groups of animals were included in the experiment: (i) young adult rats, 7–9 months old ($n = 40$) kept under standard conditions (SC, $n = 20$) or in the environmental enrichment (EE, $n = 20$); (ii) elderly rats, 23–25 months old ($n = 24$) kept under SC or in the EE. In SC, rats were housing in the cages sized 50 cm × 30 cm × 18 cm (five animals in one cage). In EE, rats were housing for 60 days in cages sized 78 cm × 48 cm × 39 cm (10 animals in one cage) equipped with various devices to provide extensive physical and explanatory activity (tunnels, houses, hammocks, stairs, boxes, wheels) (Jankowsky et al., 2003).

Modeling Alzheimer-Type Neurodegeneration

In the group of young adult rats, 10 animals kept under SC and 10 animals kept in EE have been used for modeling AD with intracerebral bilateral stereotaxic-guided (Narishige Scientific Instrument Lab) injections of 5 μl (2 μg/μl) aggregated Aβ1-42 (Sigma-Aldrich) into CA1 zones of hippocampus at the day 60 of SC or EE housing according to the protocol described (Li et al., 2011). For this procedure, anesthesia with chloral hydrate (0.35 g/kg) has been applied, and the following stereotaxic coordinates have been chosen: A/P = 3.0 mm, M/L = ± 2.2 mm, D/V = 2.8 mm. Establishment of AD model (Aβ deposition and cognitive impairment) has been confirmed with Thioflavin S staining of brain tissue and neurobehavioral phenotyping of animals (data not shown).

Assessment of Hippocampal Neurogenesis

Expression of markers in NSCs, progenitor cells and differentiated neurons (Pax6, Neurogenin 2, NeuroD1, NeuN) was assessed in the hippocampus of animals in all experimental groups according to the standard protocol of immunohistochemistry with antigen unmasking (proteinase K) procedure. Briefly, 2 μm hippocampal slices were obtained after transcardial perfusion of anesthesized rats with 0.1 M PBS (pH 7.4) and 4% PFA followed by hippocampus fixation in 10% buffered PFA for 24 h. The following primary antibodies have been used: Pax-6 (Abcam, ab78545, mouse monoclonal), 1:100, Neurogenin2 (Abcam, ab26190, rabbit polyclonal), 1:50, NeuroD1 (Abcam, ab60704, mouse monoclonal), 1:100, NeuN (Millipore, ABN78, rabbit polyclonal), 1:500. Alexa-conjugated secondary antibodies were used in 1:500 dilution: Alexa Fluor 488 chicken anti-mouse (for Pax6 detection), Alexa Fluor 488 donkey anti-rabbit (for Neurogenin2 detection), NeuN (rabbit polyclonal) – Alexa Fluor 488 donkey anti-rabbit (for NeuroD1 detection), and Alexa Fluor 488 chicken anti-rabbit (for NeuN detection) on slices. Images were visualized with Olympus CX41 microscope and analyzed with Image J software. Corrected total cell fluorescence (CTCF) was calculated for all the images.

Isolation of Adult Hippocampal Cells with the NS-Forming Capacity

At the day 70 of housing (10 days after AD modeling in the corresponding group of animals), isolation of hippocampus was performed in anesthesized rats according to the standard protocol described (Kuvacheva et al., 2015). After brain tissue dissociation and isolation of hippocampal cells, counting of the cells for further adjusting the viable cell concentrations was done with the Scepter CellCounter (Millipore). Assessment of proliferation of obtained hippocampal cells *in vitro* has been performed by culturing them in NeuroCult®NS-A Proliferation Medium with bFGF and EGF (Stemcell). On the next day after cell plating, development of neurospheres as transparent free-floating cell aggregates with surface microspikes was assessed with phase-contrast microscopy. At the day 3 of NS culture, cells were carefully harvested from the flasks, centrifuged, and suspended in the fresh NeuroCult®NS-A Proliferation Medium.

Real-Time Analysis of Cell Proliferation *In Vitro*

Further real-time analysis of cell proliferation kinetics was done using xCElligence system (Roche) with the gold microelectrode-covered microtiter plates. This method allows electrical impedance monitoring in the real-time manner. For this,

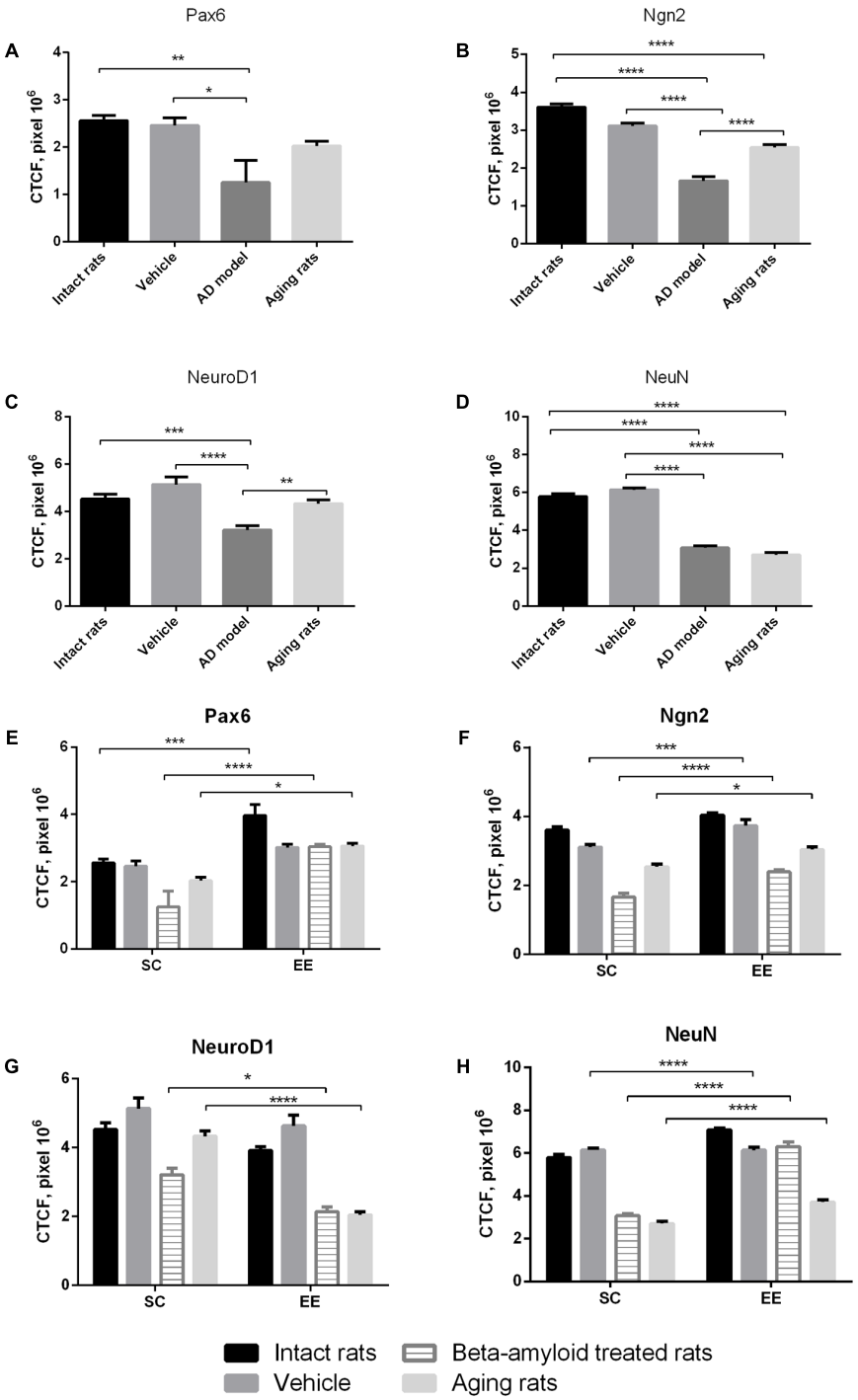


FIGURE 1 | Neurogenesis in the subgranular and granular layers of the dentate gyrus in experimental groups (intact rats, vehicle – sham-operated rats, AD model – Aβ-treated rats, aging rats, SC – standard conditions, EE – environmental enrichment). **(A–D)** Measurement of the CTCF index of different neurogenesis markers between groups under standards conditions (N = 10/per group, one-way ANOVA; Turkey's multiple comparisons test was run between groups). **(A)** Pax6 CTCF index ($p < 0.01$; one-way ANOVA). **(B)** Ngn2 CTCF index ($p < 0.0001$; one-way ANOVA). **(C)** NeuroD1 CTCF index ($p < 0.0001$; one-way ANOVA). **(D)** NeuN CTCF index ($p < 0.0001$; one-way ANOVA). Asterisks indicate statistical differences between groups. *$p < 0.05$; **$p < 0.01$; ***$p < 0.001$; ****$p < 0.0001$. **(E–H)** Measurement of the CTCF index of different neurogenesis markers between groups under standards conditions compared to environmental enrichment (N = 10/per group, statistical significance was determined by two-way ANOVA with a Sidak's test multiple comparisons test). **(E)** Pax6 CTCF index [Interaction $p < 0.05$, $F(3,72) = 2.573$, two-way ANOVA]. **(F)** Ngn2 CTCF index [Interaction ns; environmental factor $p < 0.0001$, $F(1,72) = 68.85$, group factor $p < 0.0001$, $F(3,72) = 130.7$, two-way ANOVA]. **(G)** NeuroD1 CTCF index [Interaction $p = 0.0001$, $F(3,72) = 7.91$, two-way ANOVA]. **(H)** NeuN CTCF index [Interaction $p < 0.0001$, $F(3,72) = 47.92$, two-way ANOVA]. Asterisks indicate statistical differences between groups. *$p < 0.05$; ***$p < 0.001$; ****$p < 0.0001$.

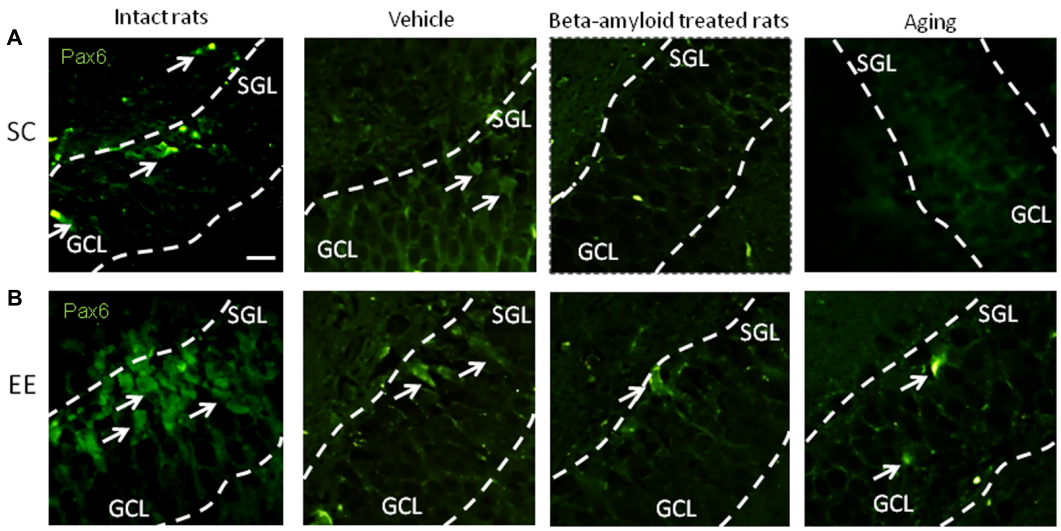


FIGURE 2 | Immunohistochemical (IHC) detection of Pax6 expression in intact, vehicle-, Aβ-treated, and aged rats kept under standard conditions (SC) **(A)** and environmental enrichment (EE) **(B)**. Representative photomicrographs show Pax6 immunostaining in the granular cell layer (GCL) and subgranular layer (SGL) of dentate gyrus. Pax6 was visualized using primary anti-Pax6 monoclonal antibody and secondary chicken anti-mouse IgG conjugated with green fluorescent dye Alexa Fluor 488.

1.2–2.5 × 10^4 cells/ml were cultured in NeuroCult®NS-A Proliferation Medium (100 μl per well, four wells for each series) at +37°C, 5% CO_2 with the measurements intervals of 5 min (from time 0 to 4.5 h) and 15 min (from 4.5 to 24 h).

Statistical Analysis

Non-linear regression analysis was done with the Origin 8.5 software (OriginLab). We applied user-defined function models. All regression models indicate the confidence coefficient χ^2 not worsen than 10^{-4}, and determination coefficient R^2 not less than 0.99. Statistical analysis was performed with the GraphPad Prism 6.0 software. Statistical significance was determined by one-way or two-way ANOVA with a Sidak's test multiple comparisons test. The data are presented as mean and standard deviation.

RESULTS

Immunohistochemical analysis of molecular markers expression in cells at different stages of neurogenesis (Pax6, Neurogenin 2, NeuroD1, NeuN) in the hippocampus revealed that their levels were dramatically affected in Aβ-treated rats and in the group of aging animals (**Figures 1A–D**). Noteworthy, EE did not affect the expression of the markers in the hippocampus of intact or sham-operated rats. EE demonstrated pronounced restorative effect on the impaired neurogenesis in the animals with AD model comparing with the elderly rats (**Figures 1E–H**). Among all the markers, most prominent changes were observed in the expression of NeuroD1 (reduction in all the tested animals subjected to EE).

Expression of Pax6 was efficiently restored by EE in all the groups tested (**Figure 2**). It is well-known that Pax6 is a transcription factor controlling proliferation of multipotent stem/progenitor cells in hippocampus and cortex being predominantly expressed by radial glia. High expression of Pax6 is usually followed by the elevated expression of Neurogenin 2 in amplifying unipotent progenitors, which is later replaced with the expression of NeuroD1 in neuronally committed cells of hippocampus where it is required for their survival (Roybon et al., 2009). At the final stage of neurogenesis, mature neurons in the granule zone of hippocampus are highly enriched in NeuN with the evident elevation in animals kept in EE, particularly in those having AD-type of neurodegeneration (**Figure 3**).

To analyze plausible mechanisms of the observed effect of EE at the initial stage of hippocampal adult neurogenesis, we further used the experimental model suitable for the assessing the kinetic parameters of cell proliferation *in vitro*. Evaluation of NS-forming capacity of hippocampal stem/progenitor cells is rather reliable tool to get the integral pattern of neurogenic cells proliferation and differentiation in the controlled conditions where cell cluster formation and development resemble the events occurring *in vivo* (Malik et al., 2015), particularly at the earliest steps of neurogenesis that were more sensitive to the action of EE *in vivo* (as shown above). We found that being cultured *in vitro,* adult hippocampal stem/progenitor cells produce NS whose appearance could be detected and analyzed with real-time impedance measurements. Recently, we have presented actual impedance traces for NS obtained from the animals with AD model kept under SC or EE (Kuvacheva et al., 2015). For analyzing the kinetic parameters of cell proliferation we applied several assumptions shown below.

Cell index (C) which is the impedance value corresponds to the number of adherent cells, therefore, cell sedimentation leads to the elevation of cell index. If the medium viscosity is not changed, then cell sedimentation to the microplate bottom

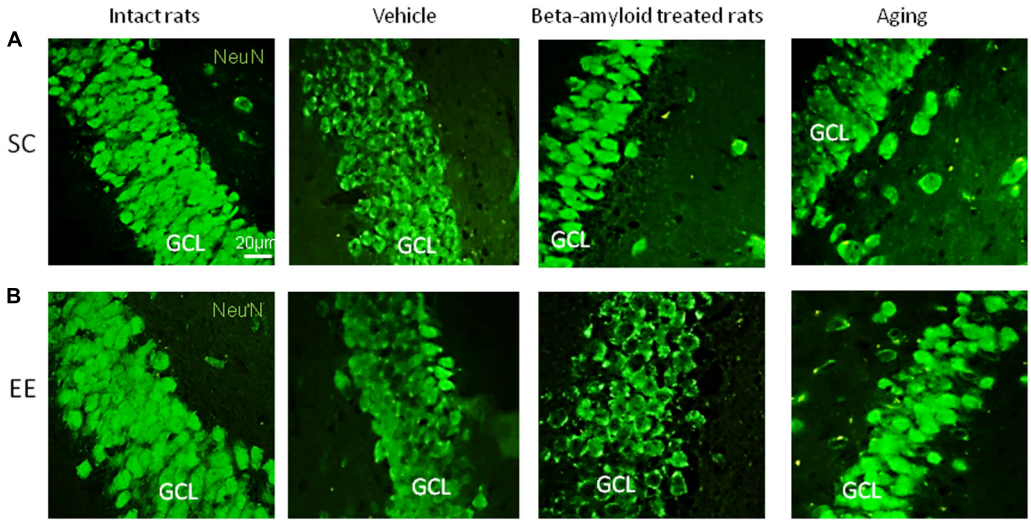


FIGURE 3 | Immunohistochemical (IHC) detection of NeuN expression in intact, vehicle-, Aβ-treated, and aged rats kept under standard conditions (SC) **(A)** and environmental enrichment (EE) **(B)**. Representative photomicrographs show NeuN immunostaining in the granular cell layer (GCL) of dentate gyrus. NeuN was visualized using primary anti-NeuN antibody and secondary donkey anti-rabbit IgG conjugated with green fluorescent dye Alexa Fluor 488.

demonstrates constant velocity, and C is progressively rising at the initial phase of cell culture with the linear dependence on the time:

$$C = \eta t + C_0.$$

Constant parameter η characterizes velocity of cell sedimentation, C_0 is the cell index obtained for the adherent cells at the initial point of measurements. The described process corresponds to the phase A (attachment of cells to the plate). Let assume that cells might be at any phase of cell cycle at this period. Phase I_1 of the impedance trace corresponds to the period after the complete cell adhesion (interphase of the cell cycle) when maximal value of cell index (C_{max}) is not changed. It is well-known that just before mitosis cell adhesion is weakened, and flattened cells acquire round shape (VanHook, 2014), therefore formation of NS leads to decrease of C value. This process corresponds to the mitotic phase M_1. Phase I_2 (interphase) demonstrates stable C value established just before entering mitosis in the 2nd generation of cells. This period is followed by reducing cell adhesion in the 2nd cell generation which corresponds to the mitotic phase M_2 (**Figure 4A**).

Thus, we postulate that in the given experimental conditions: (i) cell proliferation is synchronized; (ii) mitosis-associated loss of cell adhesion leads to C decline; (iii) two generations of cells are present in the system during 24 h of cell culture on microelectrode-covered microplates.

To exclude the impact of cell sedimentation velocity on C kinetics, lets adopt the cell index value as $C=C_{max}$ at the initial phase A. We may use the parameter shown below to take into account all the changes in C caused by the decreasing number of adherent cells:

$$C_N = C_{max} - C$$

Normalization of cell index changes (c_N) allows considering some deviations in cell concentrations in the microplate wells:

$$c_N = \frac{C_N}{C_{N\,max}}$$

Typical curve for c_N kinetics is shown in **Figure 4B**.

In order to analyze the observed changes in c_N, we may apply a lag model developed for explaining the proliferative kinetics of cell population with the synchronized growth (Baker et al., 1998). For this purpose we must use bell-shaped distribution of cells along the different phases of cell cycle. Let's propose that the probability of cell detachment out of microelectrode caused by alterations in adhesion mechanisms would have Boltzmann's distribution of time, whereas normalized changes in c_N value could be covered by the following equation:

$$c_N = c_0 + \frac{A_1}{1 + \exp\left(\frac{t_C - t}{t_M}\right)},$$

where c_0 – value of normalized changes of cell index at the initial point of measurements $t = 0$, A_1 – amplitude of normalized changes of cell index at the point of completing the 1st cycle of proliferation, t_c – duration of cell cycle, t_M – duration of phase M_1 (**Figure 2B**), presumably, corresponding to the duration of mitotic phase in the synchronously proliferating cell population.

The equation given above does not account for any time delay between the cell cycle initiation and beginning of cell index changes. To do this we will introduce another parameter – time-lag t_L, and we will consider a shift from the half-time of mitotic phase duration in the previous cell division (before the

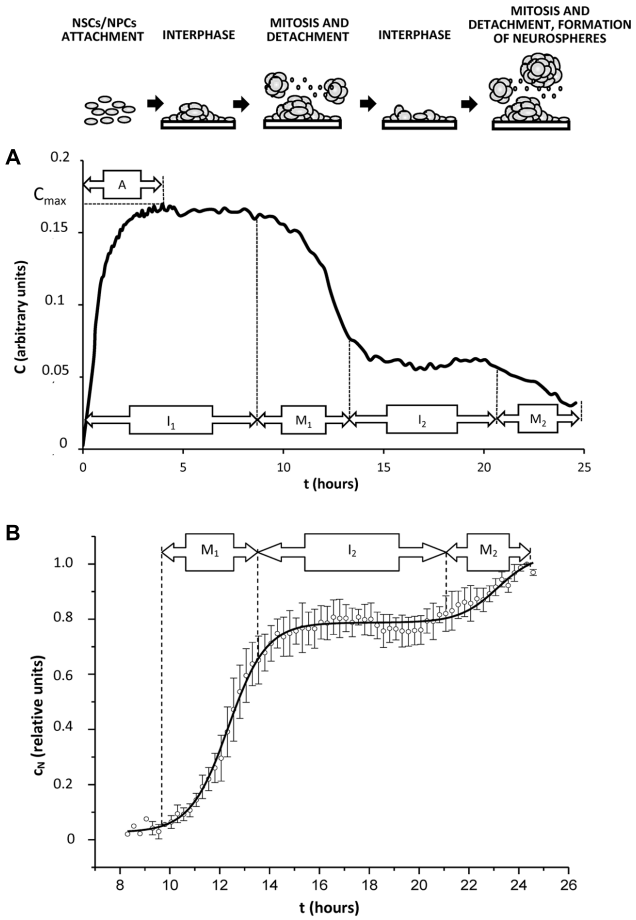


FIGURE 4 | Typical kinetics of cell index in the conditions promoting generation of neurospheres *in vitro*. Cells (NSCs, NPCs) isolated from rat hippocampus were plated in the microelectrode-covered plates of xCELLigence system for impedance measurements as described in Section "Experimental Procedures." Time of incubation is shown as t, hours. **(A)** A representative curve of cell index kinetics (indicated as C, arbitrary units) reflects real impedance trace obtained from the xCELLigence system during 24 h of cell culture. Cell index kinetics corresponds to changes in the number of attached cells during cell cycle progression. A – attachment phase, $I_{1,2}$ – interphase of 1st or 2nd cell cycle (interphasic cells attach to the microelectrode-covered plate), $M_{1,2}$ – mitosis in the 1st or 2nd cell cycle (mitotic cells detach from the microelectrode-covered plate). Corresponding changes in the cell culture are shown schematically at the top of the figure. **(B)** Normalized and approximated cell index (indicated as c_n, relative units) was calculated from the real cell index C as shown in Section "Results," and relates to the number of detached cells. Solid curve corresponds to the best regression model.

measurements). Then, the equation covering cell index changes due to 1st mitosis would be as follows:

$$c_N = c_0 + \frac{A_1}{1 + \exp\left(\frac{t_C - t_L - 0.5t_M - t}{t_M}\right)}$$

Second mitosis will be accounted by introducing the second summand:

$$c_N = c_0 + \frac{A_1}{1 + \exp\left(\frac{t_C - t_L - 0.5t_M - t}{t_M}\right)} + \frac{A_2}{1 + \exp\left(\frac{2*t_C - t_L - 0.5t_M - t}{t_M}\right)}$$

We have used this equation for non-linear regression analysis of experimental data. **Figure 4B** shows regression solid curve corresponding to the applied model for the cells isolated from young adult rats exposed to EE.

At the first round of regression analysis, we determined the mean value of cell cycle duration t_C with kinetic curves for the normalized changes of cell index for the groups of cells with the well-identified phase of 2nd division. This group included data obtained from EE-treated rats as well as from aged rats housed in SC. Then, the obtained value of cell cycle duration for all the cell types was as follows:

$$t_C = 10.8 \pm 2.5 \text{ hr.}$$

At the second round of regression analysis, we fixed the cell cycle duration t_C, and values of t_M have been estimated for all the cell types. The data obtained for the duration of "mitotic phase" t_M are presented in **Table 1**.

Supposing t_M duration as a time of cell cycle "mismatch" in the synchronously proliferating population, we may assume that when the number of cell generations is $N_g = \frac{t_C}{t_M}$ full

TABLE 1 | Parameters of NS-forming capacity of hippocampal progenitors in rats with the Alzheimer-type neurodegeneration (AD) or physiological aging housed in the standard conditions (SC) or in the environmental enrichment (EE).

Experimental group	t_M *(hours)*	*Ng*	*Nc*	*K*
Young adult rats (SC)	1.23 ± 0.07	9	512	
Young adult rats (EE)	0.77 ± 0.03	14	16,384	32
AD model rats (SC)	2.23 ± 0.07	5	32	
AD model rats (EE)	1.42 ± 0.05	8	256	8
Elderly rats (SC)	1.66 ± 0.06	7	128	
Elderly rats (EE)	1.57 ± 0.08	7	128	1

t_M – duration of mitotic phase M.
N_g – number of cell generations produced before full desynchronization of cell growth.
N_c – maximal cluster size obtained before full desynchronization of cell growth.
K – coefficient of cluster size enlargement due to effect of EE.

desynchronization would happen, thereby affecting cells microenvironment and their proliferative capacity. Under the given experimental conditions, desynchronization is most obvious in the cell culture obtained from the group of elderly rats.

Supposing doubling of cell number in every next cell generation, we may adopt that maximal cluster size (number of cells in an aggregate) which might be formed before full desynchronization of cell cycle in the culture is:

$$N_C = 2^{N_g}$$

Therefore, maximal cluster size Nc should be interpreted as neurosphere-forming capacity. It is clearly shown (**Table 1**) that it is dramatically reduced in the elderly rats and – even more visibly – in the rats with AD-type of neurodegeneration. Since NS-forming ability marks the general neurogenic potential (or neurogenic reserve) of cells involved into adult hippocampal neurogenesis, we may conclude that Aβ treatment of young adult rats produces more prominent suppression of neurogenesis than healthy aging. However, the restorative potential of EE might be easily calculated using coefficient K describing changes in Nc:

$$K = \frac{N_C(EE)}{N_C(SC)}$$

As might be expected from our *in vivo* experiments, EE restored Nc more efficiently in young adult animals (fourfold greater in the control group comparing to the AD model group) but not in the elderly rats (no positive effect of EE at all). Thus, 60 days in the conditions of EE produced no any preventive effect on the aging-associated suppression of hippocampal neurogenesis *in vitro*, being, however, relatively effective in the Alzheimer's type of neurodegeneration. This finding well-corresponds to the number of NeuN+ mature neurons in the dentate gyrus in rats kept in SC or EE (**Figure 1H**) where prominent restoration of mature neurons number was evident in the group of amyloid-treated rats but not in the group of aged animals.

DISCUSSION

Our findings clearly indicate that EE restores neurogenesis affected by the toxic action of Aβ or by aging at the earliest stage of niche cell development (before neuronal fate specification) as was evident both *in vivo* and *in vitro*. In contrast to aging brain, amyloid-affected brain was much more susceptible to the action of EE on the neurogenic capacity of cells. These findings confirm our hypothesis that EE may have different efficacy in AD-type of neurodegeneration and healthy aging brain in the context of neurogenesis improvement.

In accordance to previously published data (Hattiangady and Shetty, 2008) we found that expression of Pax6 within the neurogenic niche was not dramatically decreased in aging animals, but demonstrated prominent decline in AD model. However, the number of NeuN-immunopositive mature neurons was reduced both in healthy aging brain and in AD-affected brain in a similar manner. Therefore, it was not surprising that the earliest stages of neurogenesis both *in vivo* and *in vitro* were more sensitive to the action of EE. Particularly, Pax6 expression was greatly improved by EE exposure *in vivo* in Aβ-treated or aging rats, and the expression pattern of the same marker confirmed the highest neurogenic reserve in young adult rats exposed to long-lasting EE.

Unexpectedly, EE promoted obvious reduction in NeuroD1 expression in the hippocampus in AD group or aged group, whereas in the group of young adult animals no significant changes in NeuroD1 expression have been observed upon action of EE. It is known that NeuroD1 controls survival and maturation of neurons born in the adult brain (Gao et al., 2009) being under the control of Wnt-regulated activity of Sox2 and HDAC1 in NSCs (Chen and Do, 2012). This transcription factor may also direct reprogramming of glial cells into functional neurons *in vivo*, particularly, in AD brain (Guo et al., 2014). NeuroD1 overexpression could reduce functional deficits in newly-formed hippocampal neurons in the experimental model of AD (Richetin et al., 2015). In the aging brain, NeuroD expression declines in the hippocampal neurogenic niche (Uittenbogaard and Chiaramello, 2000). Thus, taking into the consideration the role of NeuroD1 in controlling cell fate and differentiation in hippocampal neurogenesis, one may assume that EE-induced reduction of NeuroD1 expression in Aβ-treated or aged rats could relate to some kind of preservation of neurogenic cells in the non-differentiated state, particularly, in the group of aging rats where elevation of NeuN+ neurons number was less evident than in the group with AD model. Since such effect on NeuroD1 expression was not found in young adult animals, changes in NeuroD1-controled cell differentiation might be considered as a "marker" of EE action in Alzheimer-type neurodegeneration or in healthy brain aging.

It should be noted that EE-mediated decline in NeuroD1 expression is in the contrast to the majority of reports on EE-induced expression of main neurogenesis markers, including NeuroD (Terada et al., 2008). However, similar effect was reported in Manuel et al. (2015) where it was attributed to the inhibition of avoidance behavior in fish subjected to EE. Thus, we may conclude that EE-induced reduction in NeuroD1

hippocampal expression in Aβ-treated or aging rats could reflect some adaptive behavioral reactions needed in further investigation.

We also should point out that housing in standard conditions revealed that NeuroD1 expression in healthy aging brain was well-preserved comparing with Aβ-affected brain. In EE-exposed rats, NeuroD1 expression underwent dramatic decline, particularly in the group of aging animals. Different sensitivity of NeuroD1-expressing cells to the action of EE in aging and AD is consistent with the observed effect of EE on the number of NeuN-immunopositive hippocampal mature neurons: stimulatory action of EE was considerably stronger in Aβ-treated rats.

In sum, EE efficiently improves neurogenesis impaired in the Alzheimer-type neurodegeneration (at least in the AD model used in our study) but produces relatively weak effect on neurogenesis in physiologically aging brain. In both cases, earliest stages of neurogenesis (stimuli-induced proliferation of stem cells and progenitors) *in vivo* represent the periods with higher sensitivity to the action of EE.

The essential question now is whether this effect might be reproduced and quantitatively explained *in vitro*? Analysis of neurogenesis *in vivo* is commonly complemented with *in vitro* studies. Along this way, establishment of NS culture *in vitro* is very useful for assessing proliferative and differentiating properties of stem cells and their progeny, however, quantitative insight into the process of NS development and evolution is highly required (Pacey et al., 2006). Characteristic behavior of NSCs/NPCs in NS culture could not be easy interpreted with simple observations and routine statistics. This problem is further complicated when a number of kinetic data appears in the conditions enabling action of various factors *in vivo* (before cell isolation) or *in vitro* (during cell clusters expansion and development). Therefore, we applied original algorithm to produce comparative analysis of EE effects on the neurogenic reserve of NSCs/NPCs obtained from all the tested groups.

We found that mathematical modeling allowed analyzing the kinetics of cell proliferation *in vitro* with high accuracy and in a good correspondence to the data obtained *in vivo*. Moreover, we were able to get the integral parameter (Nc) reflecting neurogenic reserve of stem/progenitor hippocampal cells affected by different factors (aging, amyloid treatment, EE) *in vivo*. We demonstrated that NS-forming capacity of brain stem and progenitor cells was positively affected by EE in young adult animals, aging animals, but not in elderly rats. The observed difference in the effects of EE on aging- or AD-associated impairment of neurospheres generation *in vitro* might be linked to the very recently reported age-related alterations in the duration of cell cycle (particularly, abnormal extension of G1 phase of the cell cycle not associated with a differentiation commitment) in the hippocampal stem cells resulting in neurogenesis decline (Daynac et al., 2016). A rough analogy might be found with G1-lengthening and alterations in G1/S transition in embryonic stem cells leading to imbalance between self-renewal and differentiation (Coronado et al., 2013). Therefore, the observed prevalence of desynchronization-related changes in the neurosphere-forming capacity in the group of elderly rats is very likely caused by the analogous mechanism of cell cycle impairment. Moreover, such alterations in the cell cycle progression that are evident in neurogenic cells derived from the aged brain might contribute to the relative inefficacy of EE in the context of neurogenesis recovery in aging.

In contrast to physiological aging, Aβ is able to increase NSC activity at the earliest steps of AD pathogenesis followed by later decline (Heo et al., 2007; Diaz-Moreno et al., 2013). Furthermore, EE was reported to increase Aβ accumulation in the transgenic AD model mice due to extensive synaptic activity (Jankowsky et al., 2003). Here, we will note that neurospheres-generating capacity of hippocampal stem/progenitor cells might be enhanced by neuronal excitation due to recruitment of latent stem cells into adult neurogenesis (Walker et al., 2008). That is why Aβ-induced alterations in the adult neurogenesis seem to be more profound but at the same time more sensitive to the restorative capacity of EE-provided neuronal excitation than in the healthy aging brain. Thus, it is reasonable to suggest that long-lasting exposure to EE preceding Aβ neurotoxic action results in excitation-mediated mobilization of latent stem cells and partial restoration of neurosphere-forming capacity *in vitro*. However, this effect is less prominent in Aβ-treated rats than in intact young adult animals. In the group of elderly rats, alterations in the duration of cell cycle diminish EE-induced changes in the stem/progenitor cells pool.

Previously, several attempts have been done to get a mathematical model of neurogenesis (Ashbourn et al., 2012; Ziebell et al., 2014). In this study we propose a mathematical model describing early processes in NSCs/NPCs development *in vitro*. Our time-lag model is based on several assumptions and simplifications but proves our data obtained *in vivo* and provides quantitative parameter (Nc) which is suitable for comparative analysis of effects produced by different factors (i.e., age, housing conditions, neurotoxic stimuli). Thus, combination of *in vivo* and *in vitro* approaches with mathematical modeling reveals some important characteristics of EE action on hippocampal neurogenesis in healthy aging brain or in Alzheimer-type neurodegeneration. It is tempting to speculate that the same approach might be further applied for assessing neurogenesis-targeting activity of drug-candidates in preclinical studies.

There is a growing interest to the restoration of impaired neurogenesis and prevention of neurological deficits in physiological aging (Marr et al., 2010; Mattson, 2015), but differential sensitivity of aging brain and Alzheimer's brain to the conditions of EE should be carefully taken into the consideration. Coming back to our initial hypothesis, we may conclude that: (i) early stages of adult hippocampal neurogenesis are more sensitive to the action of EE in the experimental model of Alzheimer-type neurodegeneration or in aging; (ii) EE differently affects neurogenesis in physiological aging and in experimental AD, particularly, Aβ-affected brain is more susceptible to the action of EE comparing with healthy aging brain; (iii) different outcomes of EE action on NSCs/NPCs in AD or in healthy aging brain can be reliably detected with NS-forming assay *in vitro* and time-lag model of synchronized growth.

Thus, it is clear that EE-based neuroprotective strategies effective in the amyloid-affected brain could not be directly

extrapolated to neurodegenerative processes associated with physiological brain aging. Therefore, application of EE strategy aimed to enhance adult neurogenesis should be considered as a personalized and pathogenetically based preventive or therapeutic intervention.

ETHICS STATEMENT

All animal experiments were performed in accordance with the principles of humanity set out in the Directive of the European Community (2010/63/EU). Protocols were reviewed and approved by the Local ethics committee of the Krasnoyarsk State Medical University named after Prof. V.F. Voino-Yasenetsky (35/2011).

AUTHOR CONTRIBUTIONS

VS, YK, and AS conceived and designed the research. All authors performed experiments. VS, YK, NK, AM, EK, and KS analyzed data. VS, YK, OL, and EP prepared figures. VS, YK, YU, EP, and AS prepared the initial draft; VS, YK, OL, and AS revised the manuscript. All authors reviewed the final manuscript and approved its publication.

ACKNOWLEDGMENT

The study is supported by the grant given by the President of Russian Federation for the Leading Scientific Teams (N 10241.2016.7).

REFERENCES

Ali, A. A. H., Schwarz-Herzke, B., Stahr, A., Prozorovski, T., Aktas, O., and von Gall, C. (2015). Premature aging of the hippocampal neurogenic niche in adult Bmal1-deficient mice. *Aging* 7, 435–449. doi: 10.18632/aging.100764

Ashbourn, J. M. A., Miller, J. J., Reumers, V., Baekelandt, V., and Geris, L. (2012). A mathematical model of adult subventricular neurogenesis. *J. R. Soc. Interface* 9, 2414–2423. doi: 10.1098/rsif.2012.0193

Avila, J., Insausti, R., and Del Rio, J. (2010). Memory and neurogenesis in aging and Alzheimer's Disease. *Aging Dis.* 1, 30–36.

Baker, C. T., Bocharov, G. A., Paul, C. A., and Rihan, F. A. (1998). Modelling and analysis of time-lags in some basic patterns of cell proliferation. *J. Math. Biol.* 37, 341–371. doi: 10.1007/s002850050133

Balietti, M., Tamagnini, F., Fattoretti, P., Burattini, C., Casoli, T., Platano, D., et al. (2012). Impairments of synaptic plasticity in aged animals and in animal models of Alzheimer's disease. *Rejuvenation Res.* 15, 235–238. doi: 10.1089/rej.2012.1318

Barak, B., Shvarts-Serebro, I., Modai, S., Gilam, A., Okun, E., Michaelson, D. M., et al. (2013). Opposing actions of environmental enrichment and Alzheimer's disease on the expression of hippocampal microRNAs in mouse models. *Transl. Psychiatry* 3:e304. doi: 10.1038/tp.2013.77

Bezzina, C., Verret, L., Halley, H., Dahan, L., and Rampon, C. (2015). Environmental enrichment does not influence hypersynchronous network activity in the Tg2576 mouse model of Alzheimer's disease. *Front. Aging Neurosci.* 7:178. doi: 10.3389/fnagi.2015.00178

Chen, M., and Do, H. (2012). Wnt Signaling in neurogenesis during aging and physical activity. *Brain Sci.* 2, 745–768. doi: 10.3390/brainsci2040745

Choi, Y. J., Park, J., and Lee, S.-H. (2013). Size-controllable networked neurospheres as a 3D neuronal tissue model for Alzheimer's disease studies. *Biomaterials* 34, 2938–2946. doi: 10.1016/j.biomaterials.2013.01.038

Cioni, G., Inguaggiato, E., and Sgandurra, G. (2016). Early intervention in neurodevelopmental disorders: underlying neural mechanisms. *Dev. Med. Child Neurol.* 58(Suppl. 4), 61–66. doi: 10.1111/dmcn.13050

Clemenson, G. D., Deng, W., and Gage, F. H. (2015). Environmental enrichment and neurogenesis: from mice to humans. *Curr. Opin. Behav. Sci.* 4, 56–62. doi: 10.1016/j.cobeha.2015.02.005

Coronado, D., Godet, M., Bourillot, P.-Y., Tapponnier, Y., Bernat, A., Petit, M., et al. (2013). A short G1 phase is an intrinsic determinant of naïve embryonic stem cell pluripotency. *Stem Cell Res.* 10, 118–131. doi: 10.1016/j.scr.2012.10.004

Cotel, M. C., Jawhar, S., Christensen, D. Z., Bayer, T. A., and Wirths, O. (2012). Environmental enrichment fails to rescue working memory deficits, neuron loss, and neurogenesis in APP/PS1KI mice. *Neurobiol. Aging* 33, 96–107. doi: 10.1016/j.neurobiolaging.2010.02.012

Daynac, M., Morizur, L., Chicheportiche, A., Mouthon, M.-A., and Boussin, F. D. (2016). Age-related neurogenesis decline in the subventricular zone is associated with specific cell cycle regulation changes in activated neural stem cells. *Sci. Rep.* 6:21505. doi: 10.1038/srep21505

Diaz-Moreno, M., Hortiguela, R., Goncalves, A., Garcia-Carpio, I., Manich, G., Garcia-Bermudez, E., et al. (2013). Abeta increases neural stem cell activity in senescence-accelerated SAMP8 mice. *Neurobiol. Aging* 34, 2623–2638. doi: 10.1016/j.neurobiolaging.2013.05.011

Esiri, M. M., and Chance, S. A. (2012). Cognitive reserve, cortical plasticity and resistance to Alzheimer's disease. *Alzheimers Res. Ther.* 4:7. doi: 10.1186/alzrt105

Firbank, M. J., Teodorczuk, A., van der Flier, W. M., Gouw, A. A., Wallin, A., Erkinjuntti, T., et al. (2012). Relationship between progression of brain white matter changes and late-life depression: 3-year results from the LADIS study. *Br. J. Psychiatry* 201, 40–45. doi: 10.1192/bjp.bp.111.098897

Forlenza, O. V., Miranda, A. S., Guimar, I., Talib, L. L., Diniz, B. S., Gattaz, W. F., et al. (2015). Decreased neurotrophic support is associated with cognitive decline in non-demented subjects. *J. Alzheimers. Dis.* 46, 423–429. doi: 10.3233/jad-150172

Gao, Z., Ure, K., Ables, J. L., Lagace, D. C., Nave, K.-A., Goebbels, S., et al. (2009). Neurod1 is essential for the survival and maturation of adult-born neurons. *Nat. Neurosci.* 12, 1090–1092. doi: 10.1038/nn.2385

Ghate, P. S., Sidhar, H., Carlson, G. A., and Giri, R. K. (2014). Development of a novel cellular model of Alzheimer's disease utilizing neurosphere cultures derived from B6C3-Tg(APPswe,PSEN1dE9)85Dbo/J embryonic mouse brain. *Springerplus* 3, 161. doi: 10.1186/2193-1801-3-161

Grinan-Ferre, C., Puigoriol-Illamola, D., Palomera-Avalos, V., Perez-Caceres, D., Companys-Alemany, J., Camins, A., et al. (2016). Environmental enrichment modified epigenetic mechanisms in SAMP8 mouse hippocampus by reducing oxidative stress and inflammaging and achieving neuroprotection. *Front. Aging Neurosci.* 8:241. doi: 10.3389/fnagi.2016.00241

Guo, Z., Zhang, L., Wu, Z., Chen, Y., Wang, F., and Chen, G. (2014). In vivo direct reprogramming of reactive glial cells into functional neurons after brain injury and in an Alzheimer's disease model. *Cell Stem Cell* 14, 188–202. doi: 10.1016/j.stem.2013.12.001

Hattiangady, B., and Shetty, A. K. (2008). Aging does not alter the number or phenotype of putative stem/progenitor cells in the neurogenic region of the hippocampus. *Neurobiol. Aging* 29, 129–147. doi: 10.1016/j.neurobiolaging.2006.09.015

Heo, C., Chang, K. A., Choi, H. S., Kim, H. S., Kim, S., Liew, H., et al. (2007). Effects of the monomeric, oligomeric, and fibrillar Abeta42 peptides on the proliferation and differentiation of adult neural stem cells from subventricular zone. *J. Neurochem.* 102, 493–500. doi: 10.1111/j.1471-4159.2007.04499.x

Herring, A., Lewejohann, L., Panzer, A. L., Donath, A., Kroll, O., Sachser, N., et al. (2011). Preventive and therapeutic types of environmental enrichment counteract beta amyloid pathology by different molecular mechanisms. *Neurobiol. Dis.* 42, 530–538. doi: 10.1016/j.nbd.2011.03.007

Hollands, C., Bartolotti, N., and Lazarov, O. (2016). Alzheimer's Disease and Hippocampal adult neurogenesis; exploring shared mechanisms. *Front. Neurosci.* 10:178. doi: 10.3389/fnins.2016.00178

Huttenrauch, M., Walter, S., Kaufmann, M., Weggen, S., and Wirths, O. (2016). Limited effects of prolonged environmental enrichment on the pathology of

5XFAD Mice. *Mol. Neurobiol.* doi: 10.1007/s12035-016-0167-x [Epub ahead of print].

Jankowsky, J. L., Xu, G., Fromholt, D., Gonzales, V., and Borchelt, D. R. (2003). Environmental enrichment exacerbates amyloid plaque formation in a transgenic mouse model of Alzheimer disease. *J. Neuropathol. Exp. Neurol.* 62, 1220–1227. doi: 10.1093/jnen/62.12.1220

Janssen, H., Ada, L., Bernhardt, J., McElduff, P., Pollack, M., Nilsson, M., et al. (2014). An enriched environment increases activity in stroke patients undergoing rehabilitation in a mixed rehabilitation unit: a pilot non-randomized controlled trial. *Disabil. Rehabil.* 36, 255–262. doi: 10.3109/09638288.2013.788218

Komleva Iu, K., Salmina, A. B., Prokopenko, S. V., Shestakova, L. A., Petrova, M. M., Malinovskaia, N. A., et al. (2013). Changes in structural and functional plasticity of the brain induced by environmental enrichment. *Vestn. Ross. Akad. Med. Nauk.* 39–48.

Kuvacheva, N. V., Morgun, A. V., Komleva, Y. K., Khilazheva, E. D., Gorina, Y. V., Lopatina, O. L., et al. (2015). In Vitro modeling of brain progenitor cell development under the effect of environmental factors. *Bull. Exp. Biol. Med.* 159, 546–549. doi: 10.1007/s10517-015-3012-8

Leger, M., Paizanis, E., Dzahini, K., Quiedeville, A., Bouet, V., Cassel, J. C., et al. (2015). Environmental enrichment duration differentially affects behavior and neuroplasticity in adult mice. *Cereb. Cortex* 25, 4048–4061. doi: 10.1093/cercor/bhu119

Li, X., Yuan, H. F., Quan, Q. K., Wang, J. J., Wang, N. N., and Li, M. (2011). Scavenging effect of Naoerkang on amyloid beta-peptide deposition in the hippocampus in a rat model of Alzheimer's disease. *Chin. J. Integr. Med.* 17, 847–853. doi: 10.1007/s11655-011-0896-7

Ma, B. F., Liu, X. M., Zhang, A. X., Wang, P., Zhang, X. M., Li, S. N., et al. (2007). Mathematical models for the proliferation of neural stem/progenitor cells in clonogenic culture. *Rejuvenation Res.* 10, 205–214. doi: 10.1089/rej.2006.0532

Maesako, M., Uemura, K., Kubota, M., Kuzuya, A., Sasaki, K., Asada, M., et al. (2012). Environmental enrichment ameliorated high-fat diet-induced Abeta deposition and memory deficit in APP transgenic mice. *Neurobiol. Aging* 33, 1011.e11–e23. doi: 10.1016/j.neurobiolaging.2011.10.028

Malik, A., Jamasbi, R. J., Kondratov, R. V., and Geusz, M. E. (2015). Development of circadian oscillators in neurosphere cultures during adult neurogenesis. *PLoS ONE* 10:e0122937. doi: 10.1371/journal.pone.0122937

Manuel, R., Gorissen, M., Stokkermans, M., Zethof, J., Ebbesson, L. O., van de Vis, H., et al. (2015). The effects of environmental enrichment and age-related differences on inhibitory avoidance in zebrafish (Danio rerio Hamilton). *Zebrafish* 12, 152–165. doi: 10.1089/zeb.2014.1045

Marin-Padilla, M., and Knopman, D. S. (2011). Developmental aspects of the intracerebral microvasculature and perivascular spaces: insights into brain response to late-life diseases. *J. Neuropathol. Exp. Neurol.* 70, 1060–1069. doi: 10.1097/NEN.0b013e31823ac627

Marr, R. A., Thomas, R. M., and Peterson, D. A. (2010). Insights into neurogenesis and aging: potential therapy for degenerative disease? *Future Neurol.* 5, 527–541. doi: 10.2217/fnl.10.33

Mattson, M. P. (2015). Lifelong brain health is a lifelong challenge: from evolutionary principles to empirical evidence. *Ageing Res. Rev.* 20, 37–45. doi: 10.1016/j.arr.2014.12.011

Ming, G.-L., and Song, H. (2011). Adult neurogenesis in the mammalian brain: significant answers and significant questions. *Neuron* 70, 687–702. doi: 10.1016/j.neuron.2011.05.001

Monteiro, B. M., Moreira, F. A., Massensini, A. R., Moraes, M. F., and Pereira, G. S. (2014). Enriched environment increases neurogenesis and improves social memory persistence in socially isolated adult mice. *Hippocampus* 24, 239–248. doi: 10.1002/hipo.22218

Mora, F. (2013). Successful brain aging: plasticity, environmental enrichment, and lifestyle. *Dialogues Clin. Neurosci.* 15, 45–52.

Moraga, A., Pradillo, J. M., García-Culebras, A., Palma-Tortosa, S., Ballesteros, I., Hernández-Jiménez, M., et al. (2015). Aging increases microglial proliferation, delays cell migration, and decreases cortical neurogenesis after focal cerebral ischemia. *J. Neuroinflamm.* 12, 87. doi: 10.1186/s12974-015-0314-8

Mostany, R., Anstey, J. E., Crump, K. L., Maco, B., Knott, G., and Portera-Cailliau, C. (2013). Altered synaptic dynamics during normal brain aging. *J. Neurosci.* 33, 4094–4104. doi: 10.1523/jneurosci.4825-12.2013

Neidl, R., Schneider, A., Bousiges, O., Majchrzak, M., Barbelivien, A., de Vasconcelos, A. P., et al. (2016). Late-life environmental enrichment induces acetylation events and nuclear factor kappaB-dependent regulations in the hippocampus of aged rats showing improved plasticity and learning. *J. Neurosci.* 36, 4351–4361. doi: 10.1523/jneurosci.3239-15.2016

Pacey, L., Stead, S., Gleave, J., Tomczyk, K., and Doering, L. (2006). Neural stem cell culture: neurosphere generation, microscopical analysis and cryopreservation. *Protoc. Exch.* doi: 10.1038/nprot.2006.215

Polito, L., Chierchia, A., Tunesi, M., Bouybayoune, I., Kehoe, P. G., Albani, D., et al. (2014). Environmental enrichment lessens cognitive decline in APP23 mice without affecting brain sirtuin expression. *J. Alzheimers. Dis.* 42, 851–864. doi: 10.3233/jad-131430

Richetin, K., Leclerc, C., Toni, N., Gallopin, T., Pech, S., Roybon, L., et al. (2015). Genetic manipulation of adult-born hippocampal neurons rescues memory in a mouse model of Alzheimer's disease. *Brain* 138(Pt 2), 440–455. doi: 10.1093/brain/awu354

Rodriguez, J. J., Terzieva, S., Olabarria, M., Lanza, R. G., and Verkhratsky, A. (2013). Enriched environment and physical activity reverse astrogliodegeneration in the hippocampus of AD transgenic mice. *Cell Death Dis.* 4:e678. doi: 10.1038/cddis.2013.194

Rosbergen, I. C. M., Grimley, R. S., Hayward, K. S., Walker, K. C., Rowley, D., Campbell, A. M., et al. (2016). The effect of an enriched environment on activity levels in people with stroke in an acute stroke unit: protocol for a before-after pilot study. *Pilot Feasibility Stud.* 2:36. doi: 10.1186/s40814-016-0081-z

Roybon, L., Hjalt, T., Stott, S., Guillemot, F., Li, J.-Y., and Brundin, P. (2009). Neurogenin2 directs granule neuroblast production and amplification while NeuroD1 specifies neuronal fate during hippocampal neurogenesis. *PLoS ONE* 4:e4779. doi: 10.1371/journal.pone.0004779

Stuart, K. E., King, A. E., Fernandez-Martos, C. M., Dittmann, J., Summers, M. J., and Vickers, J. C. (2017). Mid-life environmental enrichment increases synaptic density in CA1 in a mouse model of Abeta-associated pathology and positively influences synaptic and cognitive health in healthy ageing. *J. Comp. Neurol.* 525, 1797–1810. doi: 10.1002/cne.24156

Terada, M., Kuzumaki, N., Hareyama, N., Imai, S., Niikura, K., Narita, M., et al. (2008). Suppression of enriched environment-induced neurogenesis in a rodent model of neuropathic pain. *Neurosci. Lett.* 440, 314–318. doi: 10.1016/j.neulet.2008.05.078

Uittenbogaard, M., and Chiaramello, A. (2000). Differential expression patterns of the basic helix-loop-helix transcription factors during aging of the murine brain. *Neurosci. Lett.* 280, 95–98. doi: 10.1016/S0304-3940(00)00761-8

Valero-Aracama, M. J., Sauvage, M. M., and Yoshida, M. (2015). Environmental enrichment modulates intrinsic cellular excitability of hippocampal CA1 pyramidal cells in a housing duration and anatomical location-dependent manner. *Behav. Brain Res.* 292, 209–218. doi: 10.1016/j.bbr.2015.05.032

VanHook, A. M. (2014). De-adhesion for mitotic progression. *Sci. Signal.* 7, ec337. doi: 10.1126/scisignal.aaa3737

Waldau, B., and Shetty, A. K. (2008). Behavior of neural stem cells in the Alzheimer brain. *Cell. Mol. Life Sci.* 65, 2372–2384. doi: 10.1007/s00018-008-8053-y

Walker, T. L., White, A., Black, D. M., Wallace, R. H., Sah, P., and Bartlett, P. F. (2008). Latent stem and progenitor cells in the hippocampus are activated by neural excitation. *J. Neurosci.* 28, 5240–5247. doi: 10.1523/jneurosci.0344-08.2008

Williamson, L. L., Chao, A., and Bilbo, S. D. (2012). Environmental enrichment alters glial antigen expression and neuroimmune function in the adult rat hippocampus. *Brain Behav. Immun.* 26, 500–510. doi: 10.1016/j.bbi.2012.01.003

Yang, S., Lu, W., Zhou, D. S., and Tang, Y. (2012). Enriched environment and white matter in aging brain. *Anat. Rec. (Hoboken)* 295, 1406–1414. doi: 10.1002/ar.22526

Yuan, Z., Wang, M., Yan, B., Gu, P., Jiang, X., Yang, X., et al. (2012). An enriched environment improves cognitive performance in mice from the senescence-accelerated prone mouse 8 strain: role of upregulated neurotrophic factor

expression in the hippocampus. *Neural Regen. Res.* 7, 1797–1804. doi: 10.3969/j.issn.1673-5374.2012.23.006

Zeng, Q., Zheng, M., Zhang, T., and He, G. (2016). Hippocampal neurogenesis in the APP/PS1/nestin-GFP triple transgenic mouse model of Alzheimer's disease. *Neuroscience* 314, 64–74. doi: 10.1016/j.neuroscience.2015.11.054

Ziebell, F., Martin-Villalba, A., and Marciniak-Czochra, A. (2014). Mathematical modelling of adult hippocampal neurogenesis: effects of altered stem cell dynamics on cell counts and bromodeoxyuridine-labelled cells. *J. R. Soc. Interface* 11, 20140144. doi: 10.1098/rsif.2014.0144

Conflict of Interest Statement: The authors declare that the research was conducted in the absence of any commercial or financial relationships that could be construed as a potential conflict of interest.

Copyright © 2017 Salmin, Komleva, Kuvacheva, Morgun, Khilazheva, Lopatina, Pozhilenkova, Shapovalov, Uspenskaya and Salmina. This is an open-access article distributed under the terms of the Creative Commons Attribution License (CC BY). The use, distribution or reproduction in other forums is permitted, provided the original author(s) or licensor are credited and that the original publication in this journal is cited, in accordance with accepted academic practice. No use, distribution or reproduction is permitted which does not comply with these terms.

frontiers in Neuroinformatics

ORIGINAL RESEARCH
published: 23 May 2018
doi: 10.3389/fninf.2018.00026

Analyzing the Behavior of Neuronal Pathways in Alzheimer's Disease Using Petri Net Modeling Approach

Javaria Ashraf[1], *Jamil Ahmad*[1]*, *Amjad Ali*[2] *and Zaheer Ul-Haq*[3]

[1] Research Center for Modeling and Simulation, National University of Sciences and Technology, Islamabad, Pakistan,
[2] Atta-Ur-Rahman School of Applied Biosciences, National University of Sciences and Technology, Islamabad, Pakistan,
[3] Dr. Panjwani Center for Molecular Medicine and Drug Research, International Center for Chemical Sciences, University of Karachi, Karachi, Pakistan

Alzheimer's Disease (AD) is the most common neuro-degenerative disorder in the elderly that leads to dementia. The hallmark of AD is senile lesions made by abnormal aggregation of amyloid beta in extracellular space of brain. One of the challenges in AD treatment is to better understand the mechanism of action of key proteins and their related pathways involved in neuronal cell death in order to identify adequate therapeutic targets. This study focuses on the phenomenon of aggregation of amyloid beta into plaques by considering the signal transduction pathways of Calpain-Calpastatin (CAST) regulation system and Amyloid Precursor Protein (APP) processing pathways along with Ca^{2+} channels. These pathways are modeled and analyzed individually as well as collectively through Stochastic Petri Nets for comprehensive analysis and thorough understating of AD. The model predicts that the deregulation of Calpain activity, disruption of Calcium homeostasis, inhibition of CAST and elevation of abnormal APP processing are key cytotoxic events resulting in an early AD onset and progression. Interestingly, the model also reveals that plaques accumulation start early (at the age of 40) in life but symptoms appear late. These results suggest that the process of neuro-degeneration can be slowed down or paused by slowing down the degradation rate of Calpain-CAST Complex. In the light of this study, the suggestive therapeutic strategy might be the prevention of the degradation of Calpain-CAST complexes and the inhibition of Calpain for the treatment of neurodegenerative diseases such as AD.

Keywords: Calpain, CAST, calcium, PKC, APP, Stochastic petri net, Alzheimer disease, Amyloid beta

OPEN ACCESS

Edited by:
Athanasios Alexiou, Novel Global Community Educational Foundation (NGCEF), Hebersham, Australia

Reviewed by:
Faez Iqbal Khan, Rhodes University, South Africa
Hong Qing, Beijing Institute of Technology, China

***Correspondence:**
Jamil Ahmad
jamil.ahmad@rcms.nust.edu.pk

Received: *11 December 2017*
Accepted: *30 April 2018*
Published: *23 May 2018*

Citation:
Ashraf J, Ahmad J, Ali A and Ul-Haq Z (2018) Analyzing the Behavior of Neuronal Pathways in Alzheimer's Disease Using Petri Net Modeling Approach. Front. Neuroinform. 12:26. doi: 10.3389/fninf.2018.00026

1. INTRODUCTION

Alzheimer's disease (AD) is a neurodegenerative disorder which has impacted nearly 44 million[1] people around the world and this number is still increasing. AD is the leading cause of dementia in the old age (Ashford, 2004). Unfortunately, it is diagnosed only in one out of four people living with the disease[1]. Clinical characterization of AD includes memory loss and cognitive impairment which further lead to damaged behavioral activities and render a person completely dependent

[1]http://www.alzheimers.net/resources/alzheimers-statistics/

on an external aid (Budson and Price, 2005). AD establishes over time with the appearance of pathological emblems which are senile plaques and neurofibrillary tangles. These lesions comprise of extracellular deposits of Amyloid beta ($A\beta$) (Selkoe, 2000; Golde, 2005; Tam and Pasternak, 2012) and intracellular self-gathered clumps of tau proteins (Lee et al., 2001), respectively. $A\beta$ is a 40–42 amino-acids long peptide which is formed after the proteolytic cleavage of Amyloid Precursor Protein (APP) (Selkoe, 2000; Golde, 2005; Tam and Pasternak, 2012). Previous studies have shown that $A\beta$ monomers are initially non-toxic but their conversion to oligomers makes them toxic (Volles and Lansbury, 2002; Walsh and Selkoe, 2004). Eventually, the abnormal accumulation of oligomers form plaques (Walsh et al., 2002) that deposit into neuronal Endoplasmic Reticulum (ER) (Cuello, 2005) and in extracellular space (Trojanowski and Lee, 2000; Walsh et al., 2000). Aggregation of senile plaques and neurofibrillary tangles cause neuronal cell death and synaptic failure (Tiraboschi et al., 2000; Selkoe, 2002). During the last two decades, several lines of studies have pointed toward the imbalance between $A\beta$ production and its clearance plays a central role in pathogenesis of AD. Since 1992, this hypothesis has earned acquiescence (Hardy and Higgins, 1992) and is known as "***Amyloid cascade hypothesis (ACH)***". It suggests that $A\beta$ and processing of APP are crucial in neuro-degeneration. In AD, aggregation of $A\beta$ is the first step leading toward the formation of senile plaques (Hardy and Selkoe, 2002; Vassar, 2005). APP is a type1 trans-membrane protein produced in ER (Greenfield et al., 1999; Roussel et al., 2013). In neurons, production and metabolism of APP occurs rapidly which makes it a crucial element in neuro-pathogenesis (Lee et al., 2008). The main APP proteolytic processing steps occur at the cell surface and Trans-Golgi networks (TGNs). Proteolysis of APP can occur through the so-called *non-amyloidogenic* and *amyloidogenic Pathways* (**Figure 1**). The first step of non-amyloidogenic pathway is carried out by the enzyme alpha (α)-secretase that breaks down APP into soluble Amyloid precursor protein alpha (sAPPα) and alpha C-terminal fragment (αCTF / CTF83). The catalysis by α-secretase is imperative as it cuts APP within $A\beta$ domain which blocks $A\beta$ formation (Lichtenthaler, 2011). This initial step can also be driven by the beta (β)-secretase / β-site APP-cleaving enzyme (BACE), a transmembrane aspartyl protease (Vassar et al., 1999; Haass, 2004) (**Figure 1**), which constitute amyloidogenic pathway. BACE is a crucial enzyme, that acts as a rate limiting protein in $A\beta$ generation. It breaks down the APP into soluble Amyloid precursor protein beta (sAPPβ) and beta C-terminal fragments (βCTF / CTF99) (Cai et al., 2001). The CTFs are intermediate products of the first step in both pathways which remain attached to the membrane and they are further cleaved by

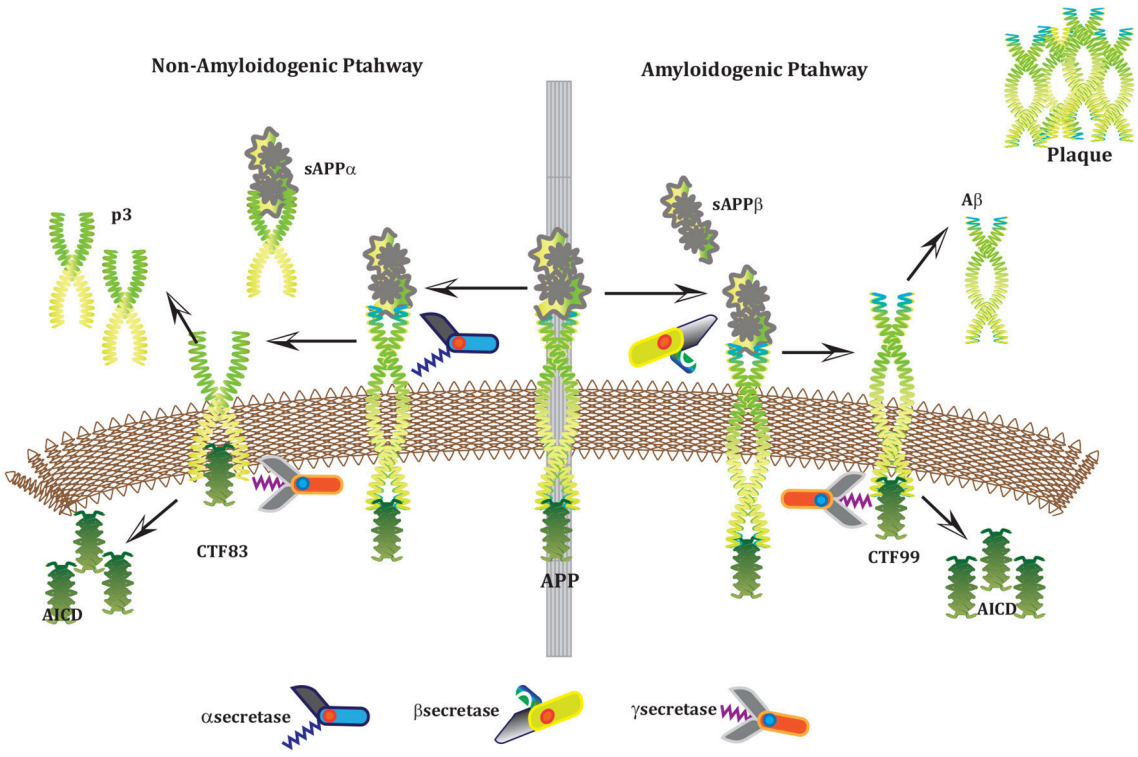


FIGURE 1 | APP and processing products: APP is synthesized in the ER and then transported to the trans-Golgi-network (TGN) where it is cleaved by secretases. In non-amyloidogenic pathway (**left**), cleavage of APP by α-secretase results in the generation of sAPPα and C-terminal fragments CTF83 which is further cleaved by γ-secretase into p3 and AICD. Proteolysis by α-secretase prevents $A\beta$ production as the cleavage site in APP is within the $A\beta$ domain. In amyloidogenic pathway (**right**), APP is cleaved into sAPPβ and CTF99 by $\beta-$secretase / BACE activity. Furthermore, CTF99 breaks down into AICD and $A\beta$ by γ-secretase activity. $A\beta$ fragments oligomerize and fibrillize into plaques.

gamma (γ)-secretase (Zhang et al., 2011). In non-amyliodogenic pathway, the fragment α-CTF is cut down by γ-secretase into p38 and the Amyloid Precursor Protein Intracellular Cytoplasmic / C-terminal Domain (AICD). While in amyloidogenic pathway, γ-secretase degrades the βCTF into $A\beta$ and AICD (O'Brien and Wong, 2011) (**Figure 1**).

The Biological Regulatory Networks (BRN) of APP processing, depicted in **Figure 2**, is also built from **Figure 1**. APP processing depends on sequential cleavage by three secretases (α/β-secretase and γ-secretase). In normal conditions, α-secretase residing at the plasma membrane is constitutively active for APP coming to the cell surface and thus favoring non-amyloidogenic pathway (De Strooper and Annaert, 2000). Though there is an interesting fact about APP proteolysis that none of the secretases show special substrate specificity toward APP. There are several transmembrane proteins such as cell surface receptors and ligand, growth factors and cytokines besides APP which undergo ectodomain shedding by enzymes with α-secretase activity (Annaert and Saftig, 2009). In the same manner, BACE shows low affinity toward APP and it is not its exclusive physiological substrate (DeStrooper et al., 2006; Hu et al., 2006). Many observations highlight that in healthy cells APP is frequently processed through non-amyloidogenic pathway to resist amyloid generation while it is altered in pathological conditions (De Strooper and Annaert, 2000). Abnormal processing of APP is stated to be the first and fundamental step in plaques formation in AD pathogenesis (Jonsson et al., 2012). In neuropathological conditions, BACE affinity toward APP increases two folds which leads to enhanced $A\beta$ production (Yang et al., 2003; Li and Südhof, 2004). Recent studies on transgenic mice model have shown that BACE activity is modulated by Calpain activation in AD pathology (Liang et al., 2010). Calpain-Calpastatin system also plays a key role in neurodegeneration. Transgenic mice models have shown that over expression of APP, increased production of $A\beta$, inhibition of Calpastatin (CAST) and activation of Calpain increase neuronal degeneration in AD (Higuchi et al., 2012).

Calpains are protein clan of cysteine/ thiol proteases and their activity depends on Ca^{2+} concentration (Ferreira, 2012). The most studied Calpains, mu(μ)-Calpain (Calpain1) and m-Calpain (Calpain2) are present abundantly in neurons, central nervous system (CNS) and glial cells. Though their distribution differs, Calpain1 is ubiquitous and expressed more in neurons while Calpain2 is present in glial cells (Ono and Sorimachi, 2012; Santos et al., 2012). Calpain1 requires micro-molar concentration of Ca^{2+} (10–50μM), while Calpain2 is activated by mili-molar concentration of Ca^{2+} (250–350μM) *in vitro* (Goll et al., 2003; Ryu and Nakazawa, 2014). Ca^{2+} plays important role in ensuring the cell's vital functions. In addition to calcium, Calpain is tightly regulated in the cell by CAST which is also ubiquitous and solely

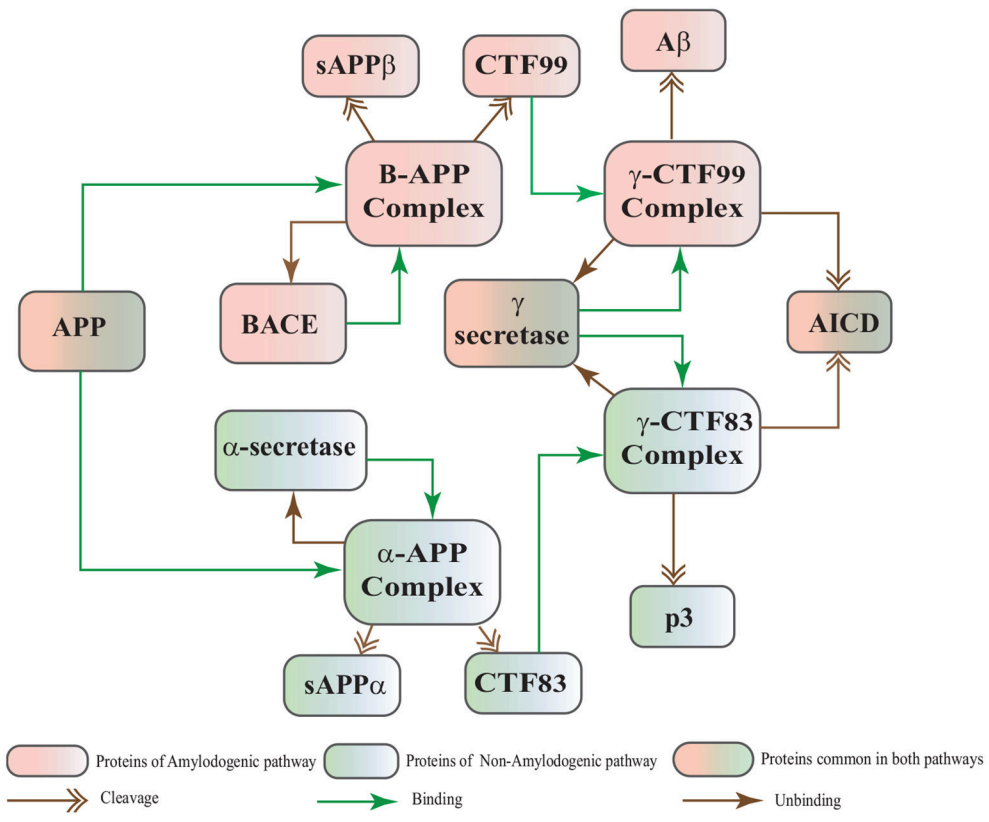


FIGURE 2 | APP processing pathways BRN derived from **Figure 1**.

a specific endogenous inhibitor for both Calpains (Melloni et al., 2006).

CAST is reported as an explicit suicide substrate for Calpain (Yang et al., 2013). The proportion of CAST in a cell is normally larger than Calpain, its ratio with location is crucial in controlling the extent of activation of Calpain within a cell (Todd et al., 2003). CAST interacts with Calpain at different stages i.e., first it constrains Calpain at the membrane where pro-Calpain is attached then it interacts with active Calpain inside cytosol (Hanna et al., 2008). CAST forms a reversible complex with Calpain at both the sites. At membrane, the reversible complex breaks down when Ca^{2+} influx increases to release Calpain. Inside cytosol, Calpain undergoes autolysis to attain active conformation. In response, CAST changes its cellular distribution to make itself widely available in the cytoplasm to counter active Calpain (Todd et al., 2003). Both active Calpain and CAST rejoin in a reversible complex to resist persistent activity of Calpain (De Tullio et al., 1999). Active Calpain modulates CAST by slowly digesting it into small inactive fragments which results in plethora of Calpain in cell leading to pathological condition (Averna et al., 2001b; Tompa et al., 2002) (**Figure 3**). It has been reported that in AD CAST becomes depleted from different regions of the brain as compared to healthy aged brain (Rao et al., 2008). It has also been observed that by controlling Calpain, CAST is indirectly preventing cell membrane damages induced by high Ca^{2+} and $A\beta$ peptide (Vaisid et al., 2008).

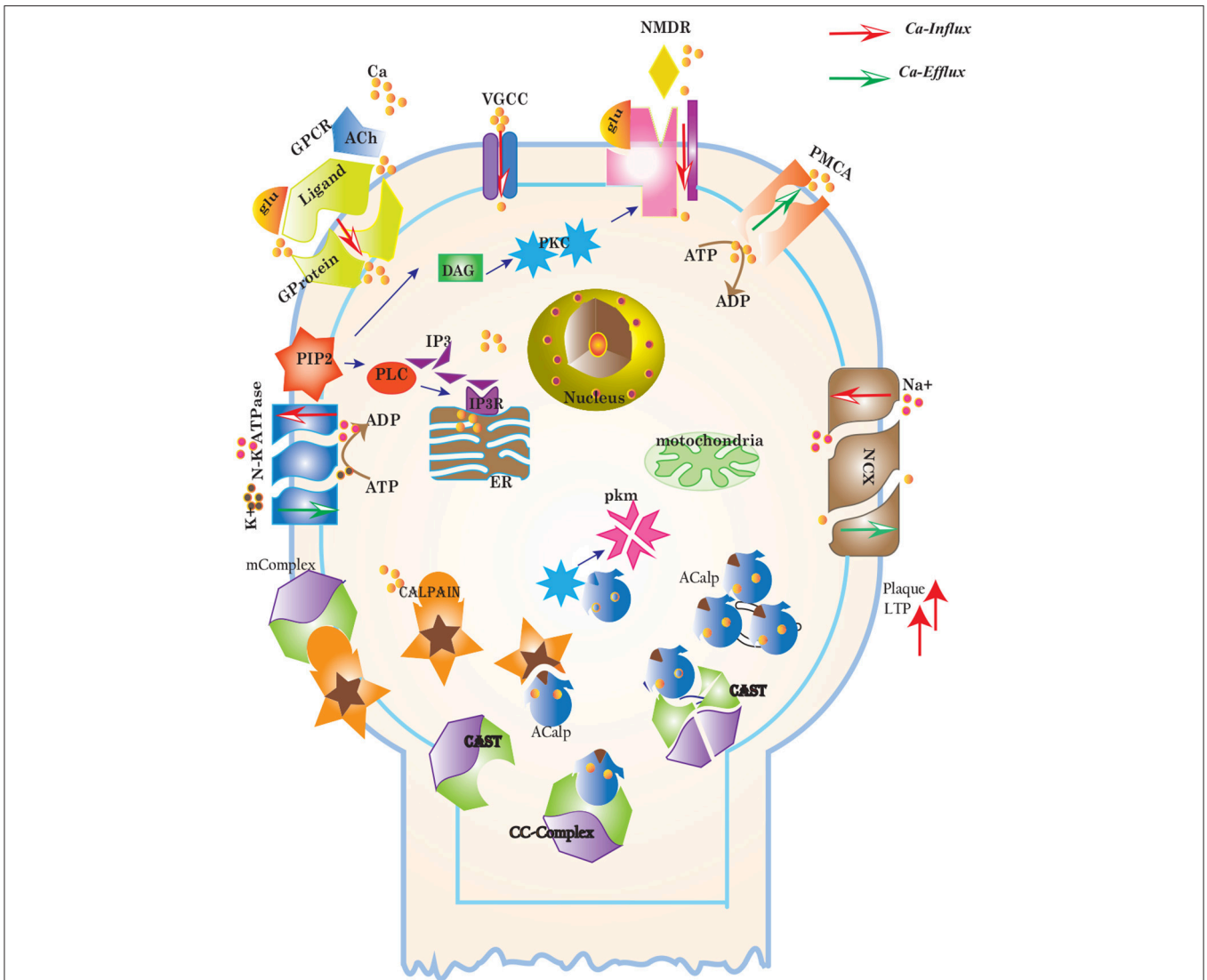


FIGURE 3 | Different calcium channels work in harmony to establish homeostasis in neurons. Calcium influx is controlled by voltage gated (*VGCCs*) or receptor-ligand based (*NMDAR*, *GPCR*) channels. *ER* also release Ca^{2+} into the cytoplasm through inositol-1,4,5-trisphosphate (*IP3R*) and ryanodine receptors. Calcium efflux is carried out by energy (*ATP*) dependent channels such as plasma membrane calcium ATPase (*PMCA*), sodium-potassium ATPase (*NKA*) and sodium-calcium exchanger (*NCX*) channels. Calcium homeostasis influences Calpain-CAST system. At membrane, Calpain is bound to CAST to form *mComplex* at low Ca^{2+} level. At high Ca^{2+} concentration, Calpain is released into cytoplasm and autolysed to active form *ACalp* that again forms complex with CAST (*cComplex*). Gradually the complex breaks down and releases *ACalp* which enhances *Plaque* accumulation and *LTP* events.

CAST pool is regulated by reversible phosphorylation via PKC, which is a Ca^{2+}-activated phospholipid dependent kinase. Moreover, it is de-phosphorylated by protein phosphatases (ppase) (Melloni et al., 2006). Phosphorylation control CAST inhibitory efficiency in brain (Averna et al., 2001a) to regulate its availability for calpain inhibition. Reversible protein phosphorylation regulates many neuronal functions and is important for neuronal signal transduction (Wu and Lynch, 2006). Inactive PKC is converted to Ca^{2+}-bound activated form in the presence of diacylglycerol (DAG) which in turn is activated by receptor based hydrolysis of phosphoinositides 3 (IP3) (Courjaret et al., 2003). The N-terminal region of CAST which is responsible for the function of the protein has a site for phosphorylation by PKC. CAST is phosphorylated by PKC to decrease its inhibitory efficiency toward calpain (Averna et al., 2001a) (**Figure 3**). It has been observed that PKC also regulates APP processing by activating α-secretase (Rossner et al., 2001; Racchi et al., 2003), it promotes non-amylodogenic pathway over β-secretase (Lanni et al., 2004). *In vivo* studies show that in the presence of PKC, secretion of sAPPα increases and $A\beta$ secretion declines (Chen and Fernandez, 2004). Other studies about AD found that PKC has substantial role in AD pathology (Etcheberrigaray et al., 2004; Alkon et al., 2007). Active Calpain also interacts with PKC and converts it into constitutive active enzyme (Yamakawa et al., 2001; Goll et al., 2003). Calpain1 directly starts depletion of PKC from cell by converting it into protein kinase M (PKM) (Yamakawa et al., 2001; Liu et al., 2008). The whole mechanism is also depicted in the form of Calpain-CAST system BRN in **Figure 4**.

The dysregulation of Calcium homeostasis contributes in aging and neurodegeneration (Mattson, 2004; Smith et al., 2005; Stutzmann, 2005). A tremendous deal of work by calcium is tightly regulated in time, space and intensity by intracellular stores, influx and efflux channels (Stutzmann, 2005). At resting stage, extracellular Ca^{2+} concentration ranges from 1.5 to 2.0 mM (Orrenius et al., 2003). While magnitude of Ca^{2+} inside a cell is very low (between 50–100/ 50–300 nM) (LaFerla, 2002; Orrenius et al., 2003) and after activation it can rise to several micromoles. On contrary, inside ER, the level of Ca^{2+} is in the range 100-500μM (LaFerla, 2002) which is approximately 1000 times higher than cytosol concentration at the resting phase. Persistent alteration of Ca^{2+} homeostasis affects production and digestion of pathological proteins such as Calpain, $A\beta$ and tau protein. Dysregulation of cellular Ca^{2+} level is an early and main feature of AD (Mattson et al., 2000; LaFerla, 2002; Small, 2009).

Cytosolic Ca^{2+} is maintained at very low level as compared to extracellular space through several homeostatic mechanisms, working both temporally and spatially (**Figure 3**). These equilibrating apparatuses include voltage-operated channels (VOCs) and receptor operated channels (ROCs) for Ca^{2+} inclusion, Ca^{2+} storage in organelles e.g., ER (Wojda et al., 2008) and Ca^{2+} extrusion to extracellular space. Different ATP-dependent membrane pumps such as plasma membrane calcium ATPase channel (PMCA) and sodium-calcium exchanger (NCX) which are dependent on sodium-potassium ATPase (NKA) (Wojda et al., 2008; Brittain et al., 2012) are used for Ca^{2+} efflux. In different physiological processes, elevation of Ca^{2+} is necessary to switch-on respective proteins. Ca^{2+} inclusion is

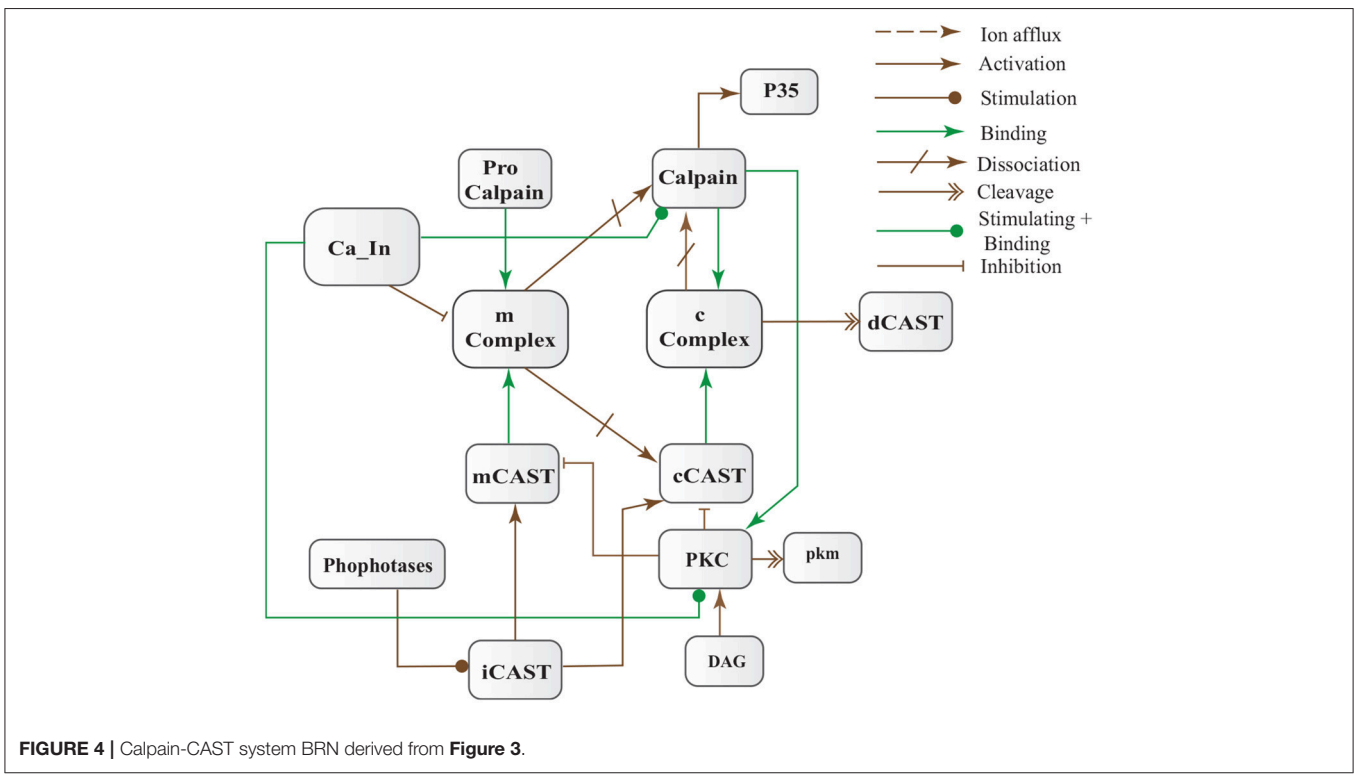


FIGURE 4 | Calpain-CAST system BRN derived from **Figure 3**.

administered by several routes such as N-methyl-D-aspartate receptor (NMDAR), an imperative type of ROCs, which switch into open conformation after binding of endogenous glutamate (glu) as ligand. Another important influx gateway is voltage gated Ca^{2+} channel (VGCC) which is in closed conformation when neuronal membrane is polarized (Schmolesky et al., 2002; Cain and Snutch, 2011). The VGCC adopts open conformation as plasma membrane depolarizes due to Ca^{2+}/ sodium (Na+) influx through ROCs or ion channels (Weber, 2012). Ca^{2+} influx also increases from intracellular stores in ER through store-operated channels. There are two calcium channels in ER which are IP3-sensitive and ryanodine (RyRs)-sensitive Ca^{2+} stores (Berridge, 2009). IP3 driven release of Ca^{2+} starts by binding of G-protein coupled receptor (GPCR) on plasma membrane which induces Phospholipase C (PLC) mediated cleavage of phosphatidylinositol-4,5-bisphosphate (PIP2) on cell membrane into DAG and IP3. IP3 binds to its receptor on ER membrane and stimulate Ca^{2+} release into the cytoplasm (Berridge, 2009; Krebs et al., 2015). Furthermore, depletion of ER stores mediate influx of extracellular Ca^{2+} through store-operated channels (SOCs) (Emptage et al., 2001; Weber, 2012). The mechanism for lowering Ca^{2+} from cell is controlled by PMCA and NCX. Both PMCA and NCX are energy dependent while, NCX is also Na^{+} gradient dependent (Wojda et al., 2008). The BRN of Calcium channels, **Figure 4**, is also helpful in understanding the mechanism underlying the Ca^{2+} homeostasis.

To comprehend the above mentioned neuronal pathways, models are constructed to understand their dynamics. Stochastic

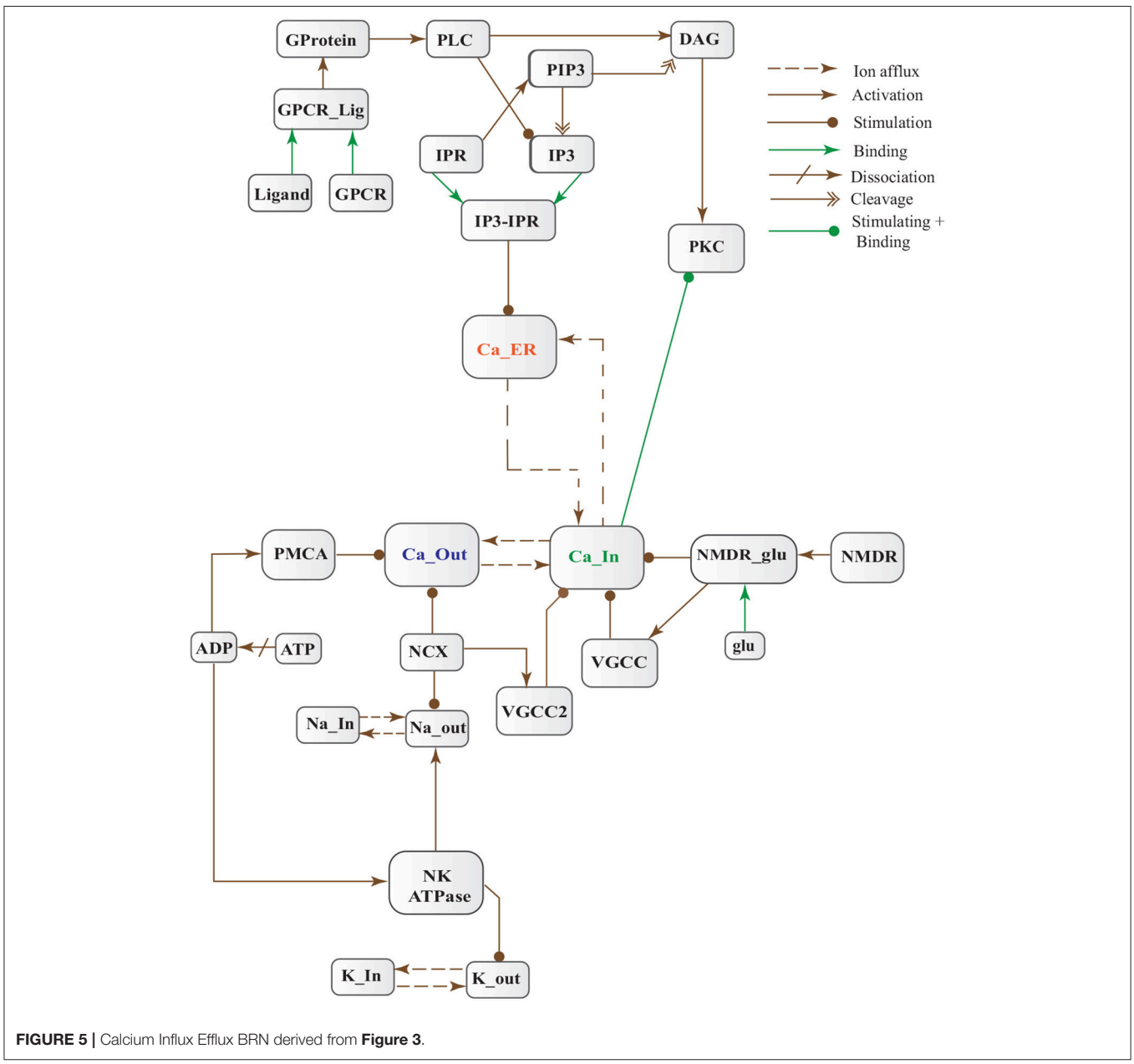


FIGURE 5 | Calcium Influx Efflux BRN derived from **Figure 3**.

approaches describe the randomness of biological system accurately as compared to ordinary differential equations. In BRNs, the activation or inhibition processes take place with random time delays, therefore, stochastic modeling frameworks are more suitable for their modeling. Petri nets provide complementary approach for both qualitative and quantitative modeling and simulation of the dynamical behavior of large systems in an intuitive way (Mounts and Liebman, 1997; Tsavachidou and Liebman, 2002; Tareen and Ahmad, 2015). The study (Tsavachidou and Liebman, 2002) shows that the Petri net models predict the experimental findings which support the soundness of these models. Stochastic petri nets (SPNs) have emerged as a promising tool for modeling and analyzing BRNs in the field of molecular biology (Goss and Peccoud, 1998). The dynamic behaviors of a variety of BRNs have been studied using stochastic simulations (Mura and Csikász-Nagy, 2008; Lamprecht et al., 2011; Castaldi et al., 2012; Marwan et al., 2012).

In this study, we have modeled and analyzed the neuronal physiological system constituting Ca^{2+} channels maintaining homeostasis, CAST regulating Calpain system and APP processing pathways separately and collectively at molecular

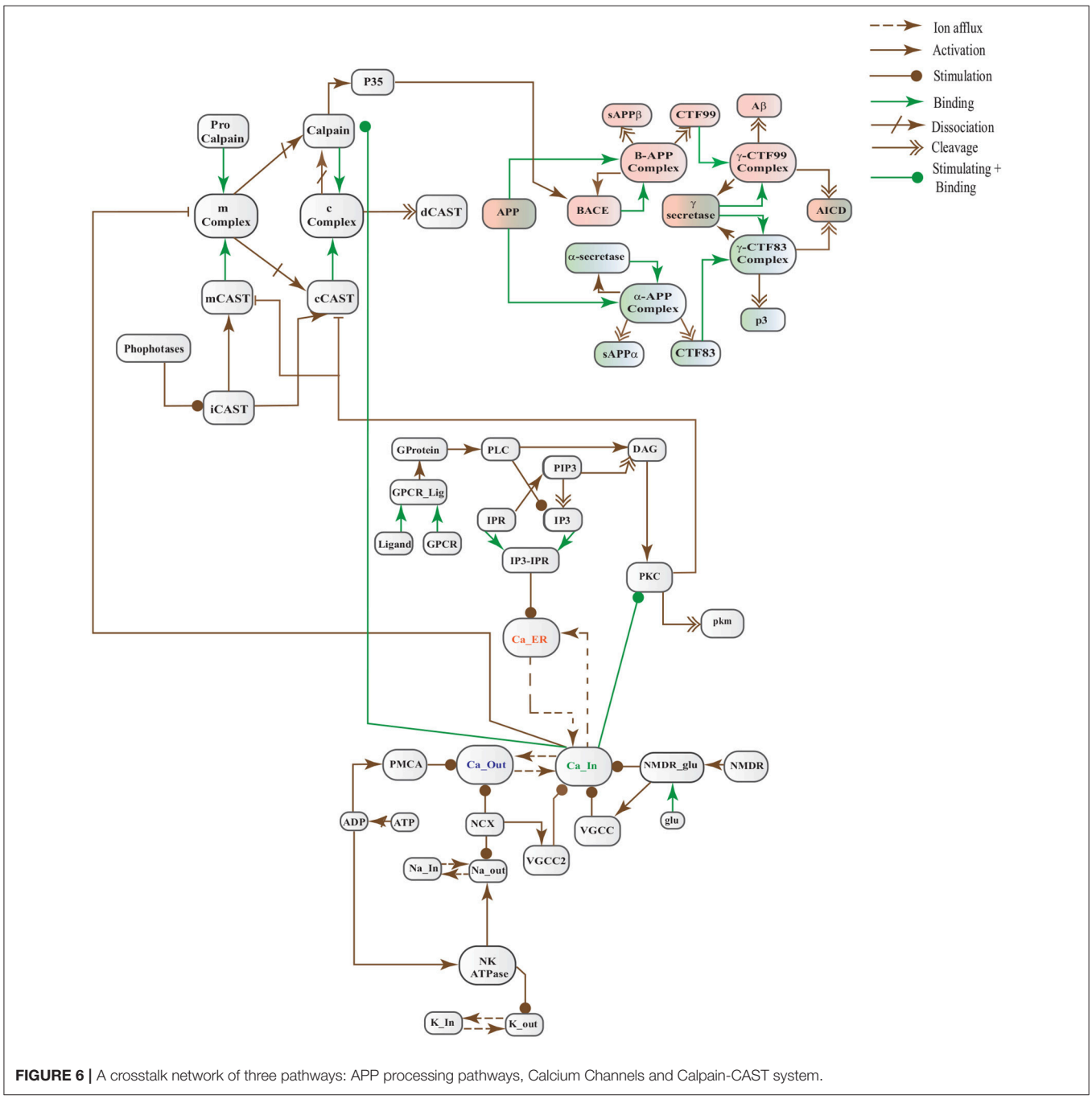


FIGURE 6 | A crosstalk network of three pathways: APP processing pathways, Calcium Channels and Calpain-CAST system.

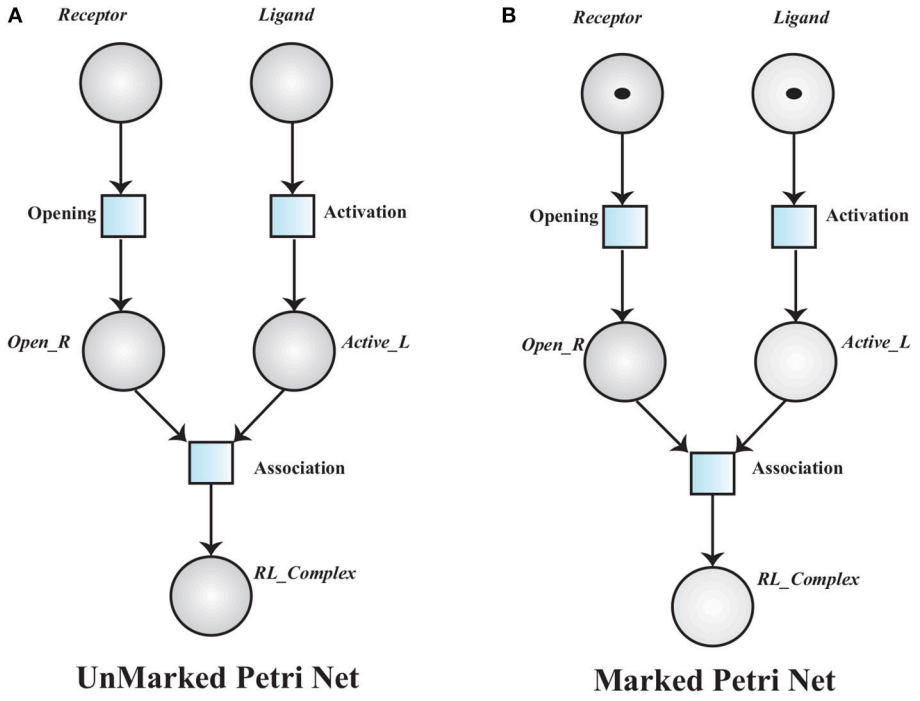


FIGURE 7 | (A) An Unmarked Petri net model of Receptor Ligand binding. *RL_Complex* is formed when *Receptor* is in open conformation (*Open_R*) and *Ligand* is activated into *Active_L*. **(B)**, A marked PN model has tokens which represent initial marking of the Receptor Ligand binding model.

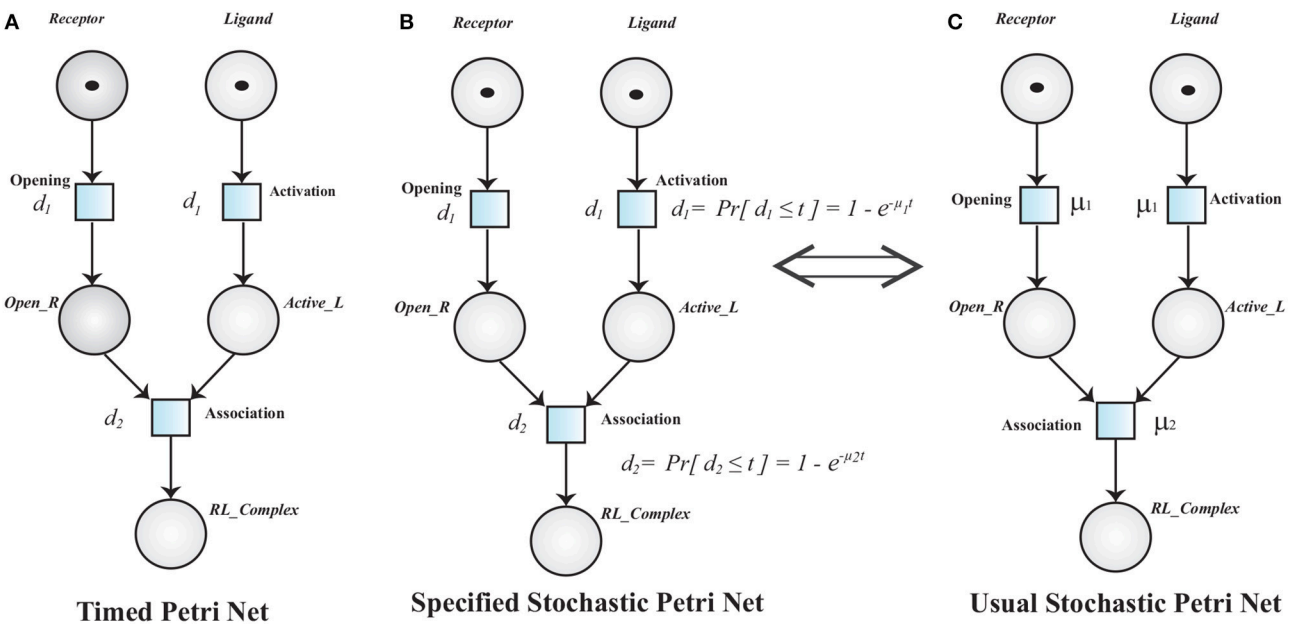


FIGURE 8 | (A) A Timed Petri net model of Receptor Ligand Binding. Initially, the *Receptor* is in close conformation and the *Ligand* is inactive. After enabling of respective transition (*Opening* and *Activation*), *Receptor* adopts open conformation (*Open_R*) and *Ligand* is activated into *Active_L* respectively. The transition *Opening* and *Activation* have an associated time delay d_1. The transitions are fired when the associated time delay is elapsed. *RL_Complex* is formed when *Open_R*, *Active_L* are present and time d_2 is elapsed. **(B,C)** are Specified and Usual Stochastic Petri Nets respectively. The TPN can be converted into SPN when the deterministic firing function *d* changes into a random variable.

level using SPNs to understand the AD progression mechanism. Particularly, we have analyzed neuronal patho-physiological dynamic behaviors causing the development of hallmark lesions in brain to answer many question e.g., how dysregulation of Ca^{2+} triggers AD? When CAST, the sole inhibitor of Calpain, depletes from the brain cells? how $A\beta$ production increases? and when the accumulation of plaques start? The answers to these questions lie in the modeling of the combined BRN **Figure 6**. The model predicts that Calpain is the main cause of dysregulation, which start with the rise in Ca^{2+} levels in the cytosol. Calpain activates different pathways through which $A\beta$ production and accumulation increases. Plaques start building with time at the age of forty and older. Plaques first enter lag phase and then into rapid growth phase. Calpain slowly degrades CAST which depletes from the cell and eventually neuronal degradation progresses. These results suggest that patho-physiological events such as dysregulation of Ca^{2+} homeostasis, Calpain hyper-activation, CAST degradation and abnormal digestion of APP, all are inter-connected and a cumulative study of these processes through SPN was needed.

2. METHODOLOGY

Petri nets (PNs) have three components namely places, transitions and edges. Place and transition are collectively known as nodes/ vertices of a PN. An arc or edge joins nodes such as a place (*pre-place*) to a transition or a transition to a place (*post-place*) to make a bipartite graph (Petri, 1966). Edges are directed and have weights associated with them. In biological systems, such as BRNs, places (○) represent biological

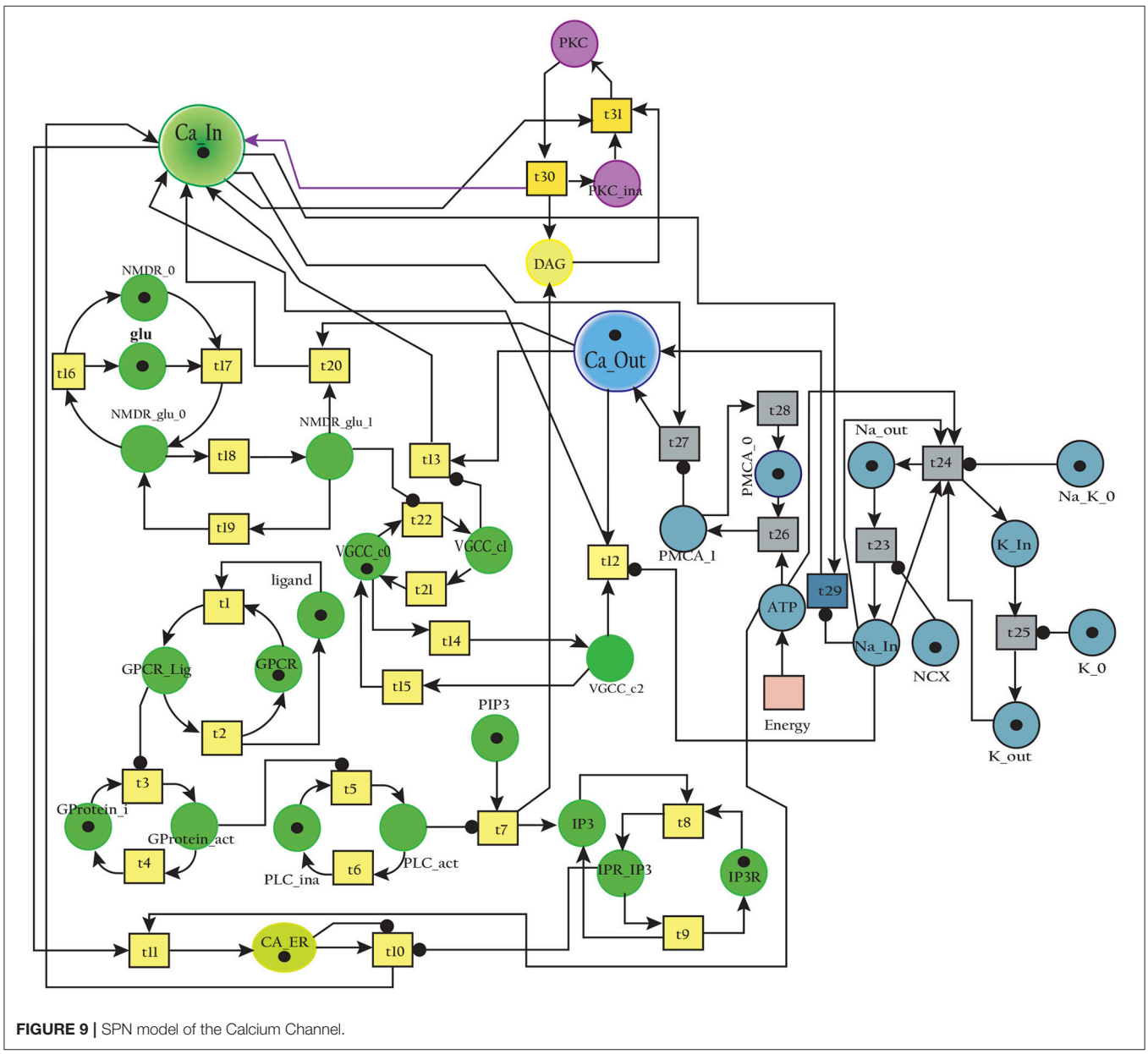


FIGURE 9 | SPN model of the Calcium Channel.

entities e.g., protein or their complexes, gene, mRNA, ions, metabolites and cell or cellular components while transitions (□) represent biochemical reactions e.g., association, activation, decomposition, inhibition, phosphorylation, dephosphorylation and translocation (Tareen and Ahmad, 2015). The weights of edges represent the stoichiometry of reactions. The weight can be one (1) or greater than one (Blätke et al., 2011; Liu et al., 2016). Following are the different types of edges.

- **Standard edge(⟶)** is use to represents a simple biochemical reaction such as synthesis, decomposition, replacement and activation reactions. It is enabled when pre-places have adequate tokens. When the transition is fired, tokens from pre-places are removed and then deposited in post-places according to arc weights.
- **Inhibitor edge**(—○) connects only a pre-place to a transition. If the corresponding pre-place is not adequately marked i.e., it has less tokens than weight of arc, then, the transition is enabled otherwise, it is un-firable. Tokens are not removed from pre-place in the inhibitor edge.
- **Read edge (—●)** connects only a pre-place to a transition. It enables the transition when the corresponding place is adequately marked. The tokens of a place are not altered when the transition is fired.
- **Equal edge (—●—●)** connects pre-place to transition. It may fire a transition when number of tokens in a pre-place is equal to corresponding arc weight. After firing of transition, tokens are not removed from the respective pre-place.

The following definitions are originally given in David and Alla (2010).

Definition 1 (Unmarked Petri Net). *An unmarked Petri Net (PN) is a five-tuple* $\mathbb{P} = \langle \mathcal{P}, \mathcal{T}, \mathcal{E}, \mathfrak{pre}, \mathfrak{post} \rangle$ *where:*

- $\mathcal{P}$ *is a finite set of places i.e.,* $\mathcal{P} = \{\mathcal{P}_1, \mathcal{P}_2, \mathcal{P}_3 \ldots, \mathcal{P}_n\}$,
- $\mathcal{T}$ *is a finite set of transitions i.e.,* $\mathcal{T} = \{\mathcal{T}_1, \mathcal{T}_2, \mathcal{T}_3, \ldots, \mathcal{T}_n\}$,
- $\mathcal{P} \cap \mathcal{T} = \varnothing$, *both* $\mathcal{P}$ *and* $\mathcal{T}$ *are non-empty sets,*
- $\mathcal{E} \subseteq \mathcal{P} \times \mathcal{T} \cup \mathcal{T} \times \mathcal{P}$, *is a set of input and output edges of transitions.*
- $\mathfrak{pre} : \mathcal{P} \times \mathcal{T} \longrightarrow \mathbb{N}$, *is a weight function that assigns non-negative integers to input edges.*
- $\mathfrak{post} : \mathcal{T} \times \mathcal{P} \longrightarrow \mathbb{N}$, *is a weight function that assigns non-negative integers to output edges.*

A simple unmarked PN is given in **Figure 7A**, to model a receptor-ligand association. A receptor is in closed conformation and ligand is in in-active form. The receptor must undergoes open conformation and then the ligand activates to form an association (*RL_Complex*) with receptor. The places in a PN may have tokens (black dots or positive real numbers) which represent marking of the places. In a marked PN, places are initially assigned tokens.

Definition 2 (Marked Petri Net). *A Marked Petri Net (MPN) is a tuple* $\mathbb{MP} = \langle \mathbb{P}, \check{\mathfrak{m}}_0 \rangle$ *where:*

- $\mathbb{P} = \langle \mathcal{P}, \mathcal{T}, \mathcal{E}, \mathfrak{pre}, \mathfrak{post} \rangle$ *is an unmarked PN and*
- $\check{\mathfrak{m}}_0 : \mathcal{P} \longrightarrow \mathbb{Z}_{\geq 0}$, *is an initial marking of the PN.*

The transition associated to a marked place is said to be enabled and it will be fired when the corresponding pre-places have tokens equal or greater than the weight of the associated arc. Receptor opening requires a *Receptor* and ligand activation depends on the presence of an inactive *Ligand*. An active ligand and an opened receptor form a Receptor-Ligand Complex (**Figure 7B**).

TABLE 1 | Transition rates of the SPN model of Calcium Channel.

Tansitions	Rate (μ)	Transitions	Rate (μ)
*t*1	1	*t*17	1
*t*2	1	*t*18	1
*t*3	1	*t*19	1
*t*4	1	*t*20	1
*t*5	1	*t*21	1
*t*6	1	*t*22	1
*t*7	1	*t*23	1
*t*8	1	*t*24	1
*t*9	1	*t*25	1
*t*10	0.65	*t*26	1
*t*11	1	*t*27	1
*t*12	1	*t*28	1
*t*13	1	*t*29	1
*t*14	1	*t*30	1
*t*15	1	*t*31	1
*t*16	1	*Energy*	1

*The transitions (t) from (**Figure 9**) are listed with their rates. The transitions are adjusted to rates which can reproduce the physiological working of calcium channels.*

Definition 3 (Timed Petri Net). *A Timed Petri Net (TPN) is a tuple* $\mathbb{TP} = \langle \mathbb{MP}, \check{\mathfrak{fn}} \rangle$ *where:*

- $\mathbb{MP} = \langle \mathbb{P}, \check{\mathfrak{m}} \rangle$ *is a MPN.*
- $\check{\mathfrak{fn}} : \mathcal{T} \longrightarrow \mathbb{R}^+$ *is a function that associates a positive real value i.e., time delay to each transition.*

A TPN associates a time delay d_i to a transition $\mathcal{T}_i$. The transition $\mathcal{T}_i$ is said to be enabled when it has sufficient tokens in its pre-places and it is fired when its deterministic delay time is elapsed (**Figure 8**). Stochastic Petri Net (SPN) are used when time delays are random variables. SPN (**Figure 8C**) (Marsan et al., 1994; Heiner et al., 2008) are explicitly derived from TPN (**Figure 8A**).

Definition 4 (Stochastic Petri Net). *A marked stochastic petri net is a pair* $\mathbb{SPN} = \langle \mathbb{MP}, \mathfrak{Rate} \rangle$ *where:*

- $\mathbb{MP} = \langle \mathbb{P}, \check{\mathfrak{m}}_0 \rangle$ *is a MPN.*
- $\mathfrak{Rate} : \mathcal{T} \longrightarrow \mathbb{R}^+$, *is a function from the set* $\mathcal{T}$ *of transition to the set of finite positive real numbers.* $\mathfrak{Rate}(\mathcal{T}_i) = \mu_i$, *is the firing rate associated with transition* $\mathcal{T}_i$.
  The random variables d_i *have assigned negative exponential probability distribution function (PDF)* $\check{\mathfrak{fn}}(t)$,

$$\check{\mathfrak{fn}}(t) = Pr[\, d_i \leq t] = 1 - e^{-\mu_i t} \text{ where,}$$

$$Pr[\, d_i \leq t + dt \mid d_i > t] = \mu_i \cdot dt$$

The marking of $\check{\mathfrak{m}}_t$ of SPN is a homogenous Markovanian Chain (HMC) process, which is a class of stochastic processes simply built from the reachability graph of a qualitative PN by

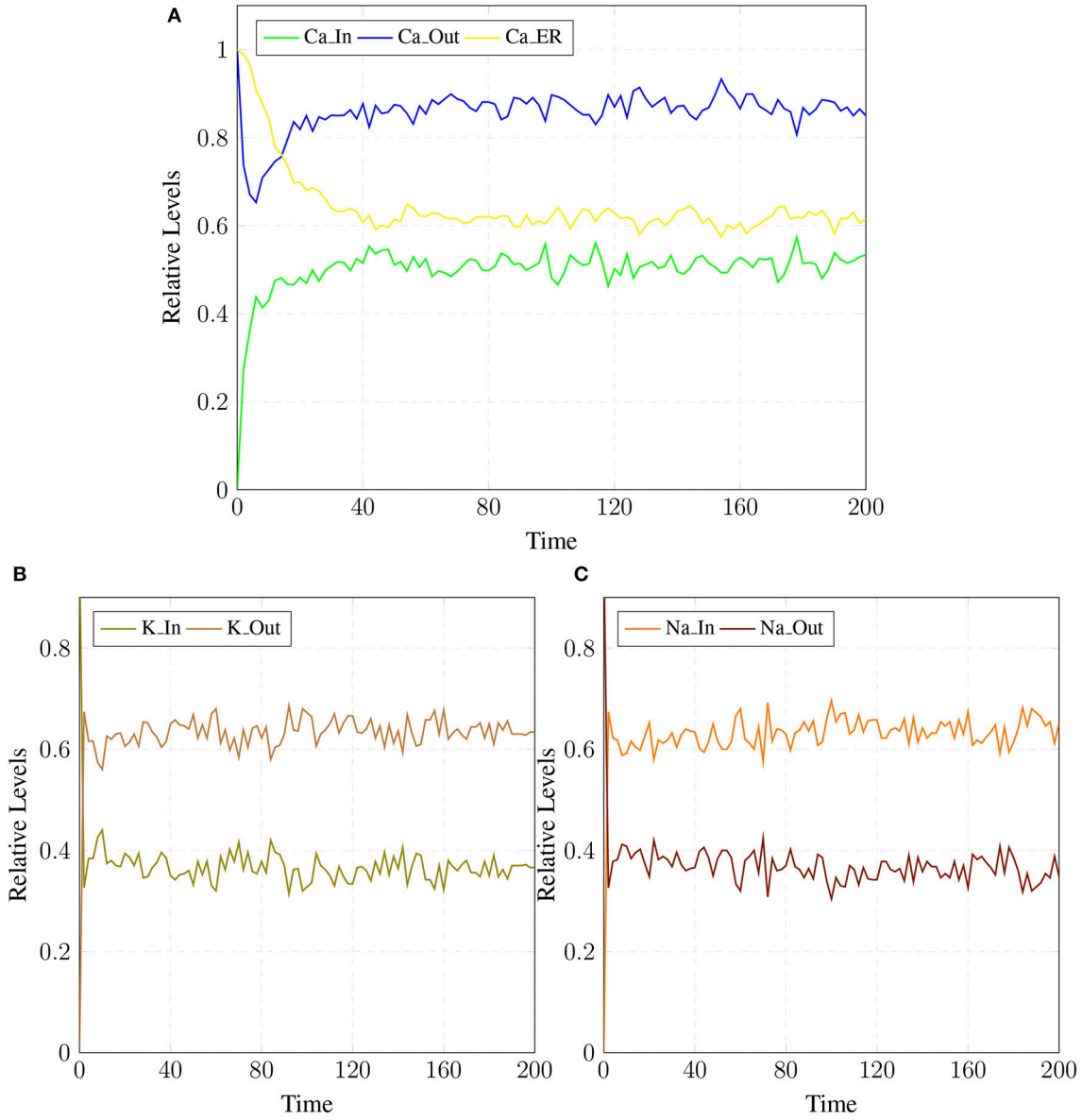


FIGURE 10 | (A) shows Calcium homeostasis which is maintained by influx (***Ca_In***), efflux (***Ca_Out***) and intracellular storage (***Ca_ER***). Calcium efflux is further maintained by coordinated and controlled *in and out* flow of Potassium (***K_In***, ***K_Out***) in **(B)** as well as of the Sodium (***Na_In***, ***Na_out***) ions channels **(C)**.

assigning transition rates to edges between all the states (Heiner et al., 2008). Thus an HMC can be associated with every SPN. Gillespie was the first one who designed special case of Petri nets for reaction networks and called them SPNs (Gillespie, 1976). Snoopy (Marwan et al., 2012) tool is used to design, animate and simulate SPNs of neurodegeneration related BRNs. This tool has been extensively used to model a variety of systems such as software systems, biological systems and production systems. The supplementary file S1 contains a general Enzyme-Substrate BRN that is modeled and simulated through the Petri net modeling tool Snoopy. This file helps to explain the working of the tool (Snoopy).

3. RESULTS

In this study, stochastic modeling and analysis of the neuronal pathways involved in neuro-degradation in AD was carried out. The SPN models of the three main neuronal physiological pathways: Calcium Influx Efflux channels (**Figure 5**), Calpain-CAST regulatory system (**Figure 4**) and APP digesting pathways (**Figure 2**). The SPN model of the crosstalk of these three pathways is also presented.

3.1. SPN of Calcium Influx Efflux Channels

The BRN of Calcium influx efflux channels in **Figure 5** is translated into a SPN model as shown in **Figure 9**. The influx

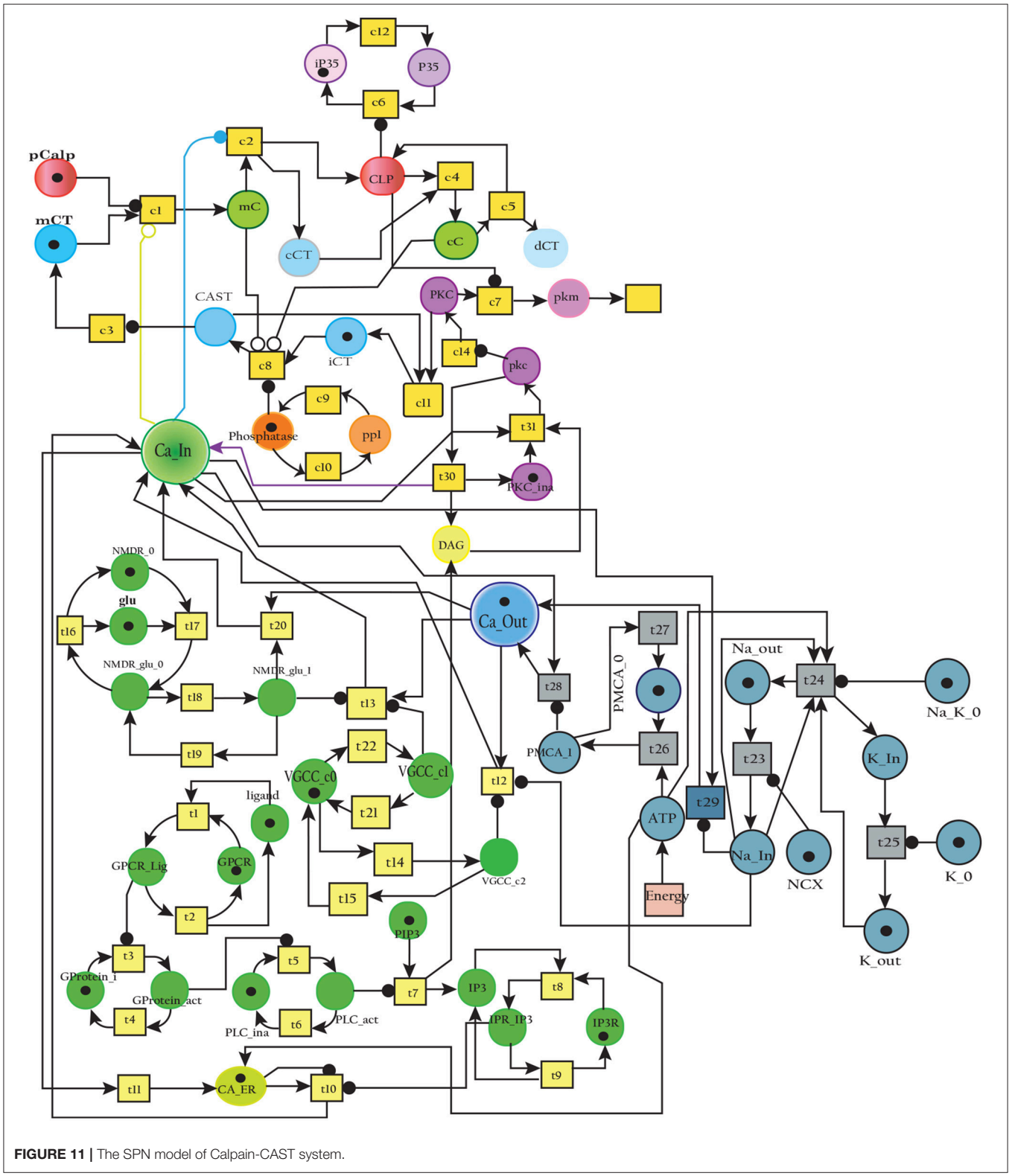


FIGURE 11 | The SPN model of Calpain-CAST system.

channels comprise of receptor based and voltage gated channels (NMDR, VGCC1 / VGCC2). In addition, the GPCR channel regulates intracellular trafficking of Ca^{2+} ions and stimulation of ***PKC*** signaling pathway. The energy dependent efflux channels (e.g., PMCA and Na-K ATPase) work efficiently in a sync with influx channels to maintain equilibrium between in-out flow of

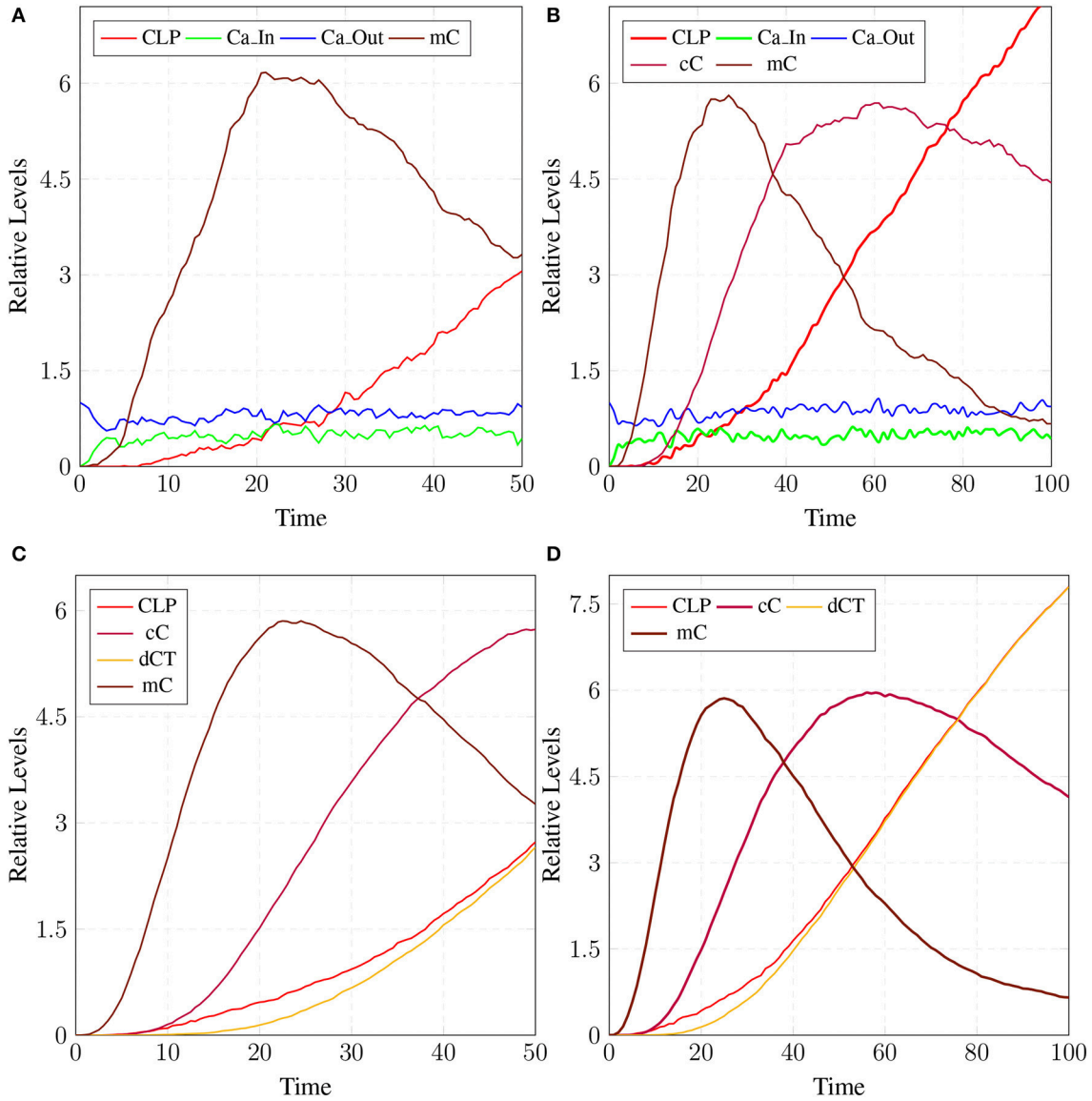


FIGURE 12 | Calpain activation and regulation: In **(A)**, ***CLP*** is bound to CAST in the form of ***mC*** at membrane. As the ***Ca_In*** increases and ***Ca_Out*** decreases the complex ***mC*** breaks down. In an elaborate view **(B)**, ***CLP*** is produced by the break down of the ***mC*** which is again controlled by the formation of ***cC***. In **(C)**, ***mC*** is formed, maintained and eventually degraded into CAST and Calpain. Both Calpain and CAST form complex ***cC*** which decreases the availability of free ***CLP***. *CLP* binding to ***cC*** slowly degrades the CAST which is represented as ***dCT***. **(D)** Both complexes ***mC*** and ***cC*** are formed while ***cC*** is more stable than ***mC***, as rate of degradation of ***mC*** is higher than **(C)**.

Ca^{2+} ions in neurons. Ca^{2+} ions move from ***Ca_In*** place (green) to ***Ca_Out*** place (blue) and vice versa. The places in green colors and transitions (yellow) constitute influx channels. The places in light blue colors and transitions in grey colors make efflux channels. Initially, ***NMDR_0*** place represents that receptor is in close conformation that binds with ***glu*** to form the complex represented by ***NMDR_glu_0*** place. This complex adapts open conformation represented by the place ***NMDR_glu_1*** and then further triggers the opening of VGCC channel represented by the place ***VGCC_c1*** to facilitate Ca^{2+} ions influx. Excess Ca^{2+} ions are deposited into the place ***Ca_ER*** through store-operated channel. The place ***GProtein_i*** represents inactive GPCR, that change into place ***GProtein_act*** by a complex of GPCR and ligand represented by places ***GPCR_Lig*** (complex), ***GPCR*** (receptor) and ***ligand*** respectively. ***GProtein_act*** activates PLC represented by place ***PLC_act***, which mediate cleavage of ***PIP2*** place into ***DAG*** and ***IP3***. The place ***DAG*** activates ***PKC*** by adding Ca^{2+} ion in it. At the surface of ER, IP3 binds with its receptor IP3R, represented by places ***IP3*** and ***IP3R***, which induces Ca^{2+} ions flow into the place ***Ca_ER***. At the same time, Ca outflow is maintained by PMCA, NCX and Na-K ATPase. PMCA channel represented by place ***PMCA_1*** requires ATP (place ***ATP***) to extrude one Ca^{2+} ion into extracellular space. The place ***NCX*** representing NCX pump ensures extrusion of

TABLE 2 | The transition rates of the SPN model of Calpain-CAST regulatory system.

Tansitions	Rate (μ)	Transitions	Rate (μ)	Transitions	Rate (μ)
*t*1	1	*t*17	1	*c*1	0.5
*t*2	1	*t*18	1	*c*2	0.1
*t*3	1	*t*19	1	*c*3	1
*t*4	1	*t*20	1	*c*4	0.02
*t*5	1	*t*21	1	*c*5	0.5
*t*6	1	*t*22	1	*c*6	0.5
*t*7	1	*t*23	1	*c*7	0.3
*t*8	1	*t*24	1	*c*8	0.5
*t*9	1	*t*25	1	*c*9	1
*t*10	0.65	*t*26	1	*c*10	1
*t*11	1	*t*27	1	*c*11	1
*t*12	1	*t*28	1	*c*12	1
*t*13	1	*t*29	1	*c*13	1
*t*14	1	*t*30	1	*c*14	0.5
*t*15	1	*t*31	1		
*t*16	1	*Energy*	1		

*The transitions (t and c) from (**Figure 11**) are listed with their rates. The transitions are adjusted to rates which can reproduce the physiological working of Calpain-CAST regulatory system.*

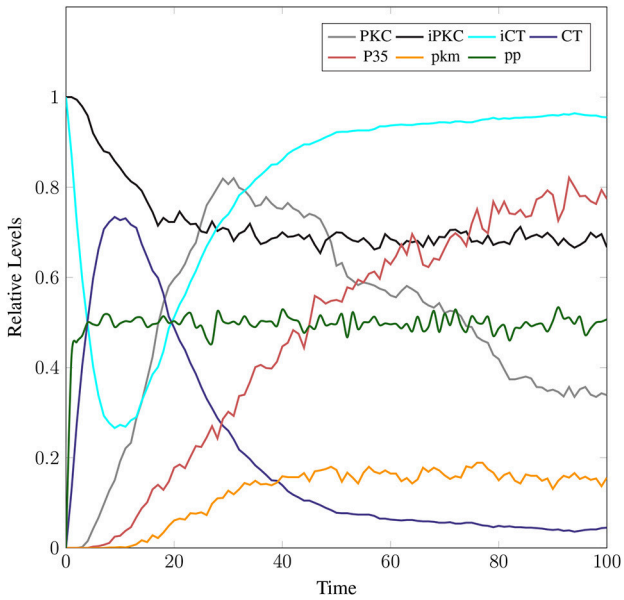


FIGURE 13 | In physiological condition, the helping enzymes (***PKC*** and ***phosphotases***) are periodically activating and deactivating. ***iPKC*** is the dormant form of the cytosol; it activates into ***PKC*** to convert ***mCT*** and ***cCT*** into ***iCT***. Phophotases (***pp***) convert the ***iCT*** into ***CT***. ***PKC*** in the presence of *CLP* is degraded into ***pkm***.

one Ca^{2+} ion by adding three Na ions into the cytoplasm represented by place ***Na_In***. The place ***Na_K_1*** represents active (i.e., depends on ATP) Na-K ATPase pumping that pumps Na out of the neuron (place ***Na_out***) and K into the neuron (place ***K_In***). The place ***VGCC_c2*** representing Ca inflow is also dependent on place ***NCX***, which depolarizes the membrane. The SPN model is simulated after applying and adjusting the rates of transitions in order to reproduce physiological working of the pathway. The transitions are labeled by *t*, transition from ***t1–t22*** are associated with influx channels. ***t1–t10*** are linked to GPCR channel which help in storage of excess Ca^{2+} ions into place ***Ca_ER***. ***t11*** takes Ca^{2+} ions from ***Ca_ER*** into cytoplasm (place ***Ca_In***). Remaining ***t12–t22*** make NMDR and VGCC channels functional. The efflux channels, consisting of NCX, NKA channels and PMCA are connected with transitions ***t23–t29***. The transitions ***t30*** and ***t31*** are involved in activation of PKC which is dependent on calcium. The rates of transitions are shown in parameter in **Table 1**. The simulation results have shown that there is an equilibrium behavior in all channels, which is required to maintain homeostasis in calcium flow. In **Figure 10A**, a stable oscillating behavior can be observed among the places ***Ca_out***, ***Ca_ER*** and ***Ca_In***. Concentration of Ca^{2+} ions in ***Ca_out*** place is higher while it is lower in place ***Ca_In***. Na and K ions, (**Figures 10B,C**) are also oscillating properly, contributing to Ca^{2+} homeostasis and generating nerve impulses through polarization and depolarization. Ca^{2+} homeostasis has pivotal role in cell physiological working. Dysregulation of Ca^{2+} homeostasis will affect the regulation of most of the proteins, enzymes and genes which will have deleterious effects on the physiological processes.

3.2. SPN of Calpain-CAST Regulatory System

The model in **Figure 11** represents Calpain-CAST regulatory system as given in **Figure 4**. In SPN model, due to lower Ca^{2+} level in cytosol, Calpain is in dormant form which is represented by place ***pCalp***. It then attaches to CAST located on membrane (place ***mCT***) to form a reversible complex of CAST and Calpain (place ***mC***). Calpain is activated when cytosolic Ca^{2+} rises to specific concentration (Pal et al., 2001; Ryu and Nakazawa, 2014). Lower level of cytosolic Ca^{2+} represented by place ***Ca_In*** facilitates (place ***mC***), membrane bound inactive reversible Calpain-CAST complex. After the concentration of ***Ca_In*** rises or crosses its threshold, then the short-lived ***mC*** is disintegrated into places ***CLP*** and ***cCT***. The place ***CLP*** shows that Calpain moves to transmembrane and then converts into active form in the presence of Ca^{2+} ions and its autolysis. Now place ***CLP*** shows that Calpain is activated that is free to translocate to cytosol. The place ***cCT*** represents that CAST can again hinder over-activation of ***CLP*** by forming a reversible complex, represented by place ***cC***. The place ***cC***, splits into places ***CLP*** and ***dCT***. In nature, active Calpain breaks down the bounded CAST into small subunits (Rao et al., 2008). The place ***CLP*** shows that it is active and which can be involved in various cellular processes. The place ***CLP*** can cleave place ***P35*** into *p25* which is involved in hyper-activation of cyclin dependent kinase 5 (*cdk5*) (Kusakawa et al., 2000; Lee et al., 2000). The transitions of this system are labeled with *c*. The transition ***c1*** forms complex, place ***mC*** from ***pCalp*** and ***mCT*** at low Ca^{2+} concentration. The ***c2*** breaks complex and activates ***CLP*** when level of Ca^{2+} rises into cytoplasm. The

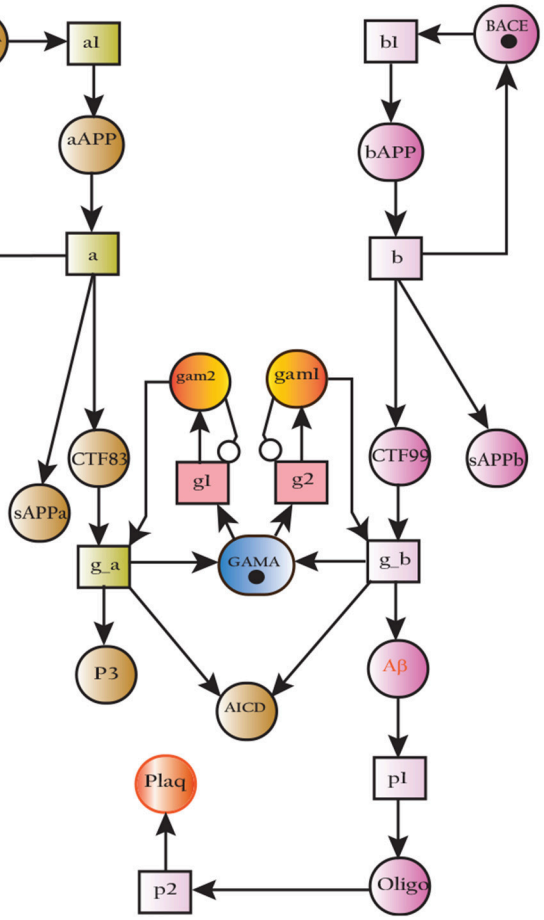


FIGURE 14 | SPN model of non-amyliodogenic (**left**) and amyliodogenic (**right**) of APP processing pathways.

transition ***c4*** forms complex place ***cC*** by binding ***CT*** and ***CLP*** in cytoplasm and ***c5***, at a very low rate (**Table 2**) slowly degrades the CAST into ***dCT*** and makes the ***CLP*** free. Transitions ***c6***, ***c12*** and ***c13*** are linked to ***CLP*** mediated ***P35*** pathway. ***CLP*** also degrades ***PKC*** into ***pkm*** through ***c7***. Remaining transitions ***c3***, ***c8***, ***c9***, ***c10***, ***c11*** and ***c14*** are associated to CAST regulation through ***PKC*** and phosphotases ***pp***. The **Table 2** lists all reaction rates of associated transitions which are obtained after fine tuning. In **Figure 12A**, the simulation shows that when Ca influx, ***Ca_In***, is lower than its threshold then ***pCalp*** is bounded into complex of Calpain-CAST (***mC***) at membrane. When ***Ca_In*** crosses its threshold, the peak of ***mC*** runs down and ***CLP*** rises representing release and activation of Calpain, (**Figure 12B**). These results are according to experimental findings (De Tullio et al., 1999; Todd et al., 2003) (**Figures 12A,B**). To regulate ***CLP*** activation, ***cC*** appears but gradually the complex peak falls down showing that the ***cC*** is broken down into active ***CLP*** and ***dCT***. The results in **Figures 12C,D** show that as ***CLP*** is rising, both the complexes (***mC*** and ***cC***) are gradually degrading causing depletion of CAST from the cytosol (Averna et al., 2001b; Tompa et al., 2002). In **Figure 13**, regulation of ***PKC***, CAST and phophatases (represented as ***pp***) can be observed. ***iPKC*** converted into ***PKC*** in the presence of Ca^{2+}, which further converts into ***pkm*** by the action of ***CLP***. As shown in the graph of **Figure 13**, ***CT*** is regulating through means of reversible phosphorylation and dephosphorylation expedited by ***PKC*** and ***pp***, respectively.

TABLE 3 | The transition rates of the SPN model of APP processing pathways.

Tansitions	Rate (μ)
a	0.5
*a*1	0.5
b	0.3
*b*1	0.3
*g*1	0.5
*g*2	0.5
g_a	0.5
g_b	0.3
*p*1	0.005
*p*2	0.02

*The transitions from **Figure 14** are listed with their rates. The transitions are adjusted to rates which can reproduce the physiological working of amyloidogenic and non-amyloidogenic pathways.*

3.3. APP Processing Pathways

The SPN model of APP processing as shown in **Figure 14** is built by combining both amyliodogenic and non-amyliodogenic pathways (**Figure 2**). APP (place ***aAPP***) is catalyzed by α-secretase (place ***ALPHA***) which produces CTF83 and sAPPα (places ***CTF83*** and ***sAPPa***), whereas digestion of APP (***bAPP***) by β-secretase (place ***BACE***) yields CTF99 and sAPPβ, (represented by places ***CTF99*** and ***sAPPb*** respectively). Further processing is carried out by enzyme γ-secretase (place ***GAMA***) which converts CTF83 into p3 and AICD, while it converts CTF99 into ***Aβ*** and ***AICD***. Aβ accumulate into ***Oligomer*** and finally into ***Plaq***. The transitions ***a***, ***a1*** and ***g_a*** constitute non-amyliodogenic pathway, while transitions ***b***, ***b1*** and ***g_b*** are linked to amyloidogenic pathway. The parameters are set according to **Table 3**, in which the rate of transition of α-secretase (place **ALPHA**) mediated APP processing (***aAPP***) is higher than BACE (***BACE***) driven APP digestion (***bAPP***) ***(μ = 0.5, 0.3 respectively)***. The rates of plaques formation and accumulation (transitions: ***p1*** and ***p2***) are also adjusted according to the observations in literature which predict low $A\beta$ burden in normal healthy brain (Mawuenyega et al., 2010; Rodrigue et al., 2012).

The simulations in **Figure 15A** shows that all the three enzymes (***ALPHA***, ***BACE***, and ***GAMA***) are available for the proteolysis of APP (in the cell to digest the around-the-clock production of) ***APP***. The **Figure 15B** shows that the product ***sAPPa*** of non-amyloidogenic processing pathway is in higher concentration than the product ***sAPPb*** of amyloidogenic pathway. Production rate of ***sAPPa*** is higher than ***sAPPb***. The graph in **Figure 16A** shows that in the healthy brain plaques are produced and accumulated in a linear fashion. $A\beta$ burdens in the form of plaques at elder age i.e., approximately after 60 unit to 100 unit time. In **Figure 16B**, the linear behavior of plaques change to an exponential growth due to the fast accumulation

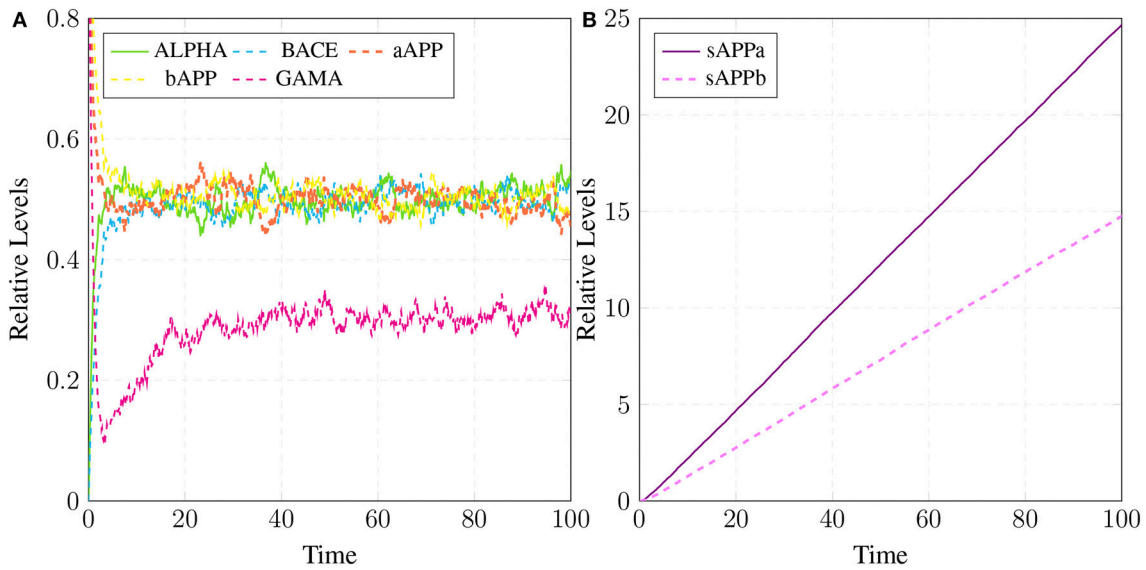


FIGURE 15 | APP processing in physiological conditions: In **(A)**, substrate *aAPP* binds with alpha secretase (***ALPHA***) and ***bAPP*** binds with **BACE**. All the three secretases ***ALPHA*** ,***BACE*** , and ***GAMA*** are oscillating. In **(B)**, concentration of ***sAPPa*** is higher than the concentration of ***sAPPb*** which depicts healthy cell physiology.

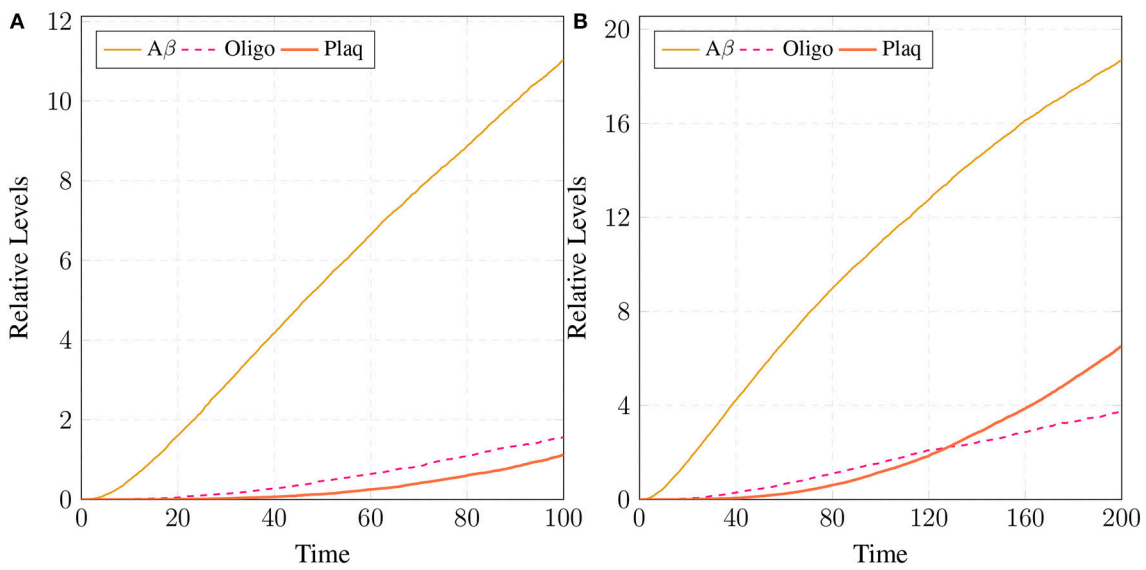


FIGURE 16 | Plaques formation in healthy brain: In **(A,B)** production of plaque is shown over the time period of 100 and 200 unit time, respectively. ***Plaq*** accumulation starts after sixty to eighty unit time. ***Aβ*** and ***Oligo*** show fluctuating behaviors as they start to build-up but degrade with time. First, ***Aβ*** gathers into large quantity to form ***Oligo*** which gradually accumulates into ***Plaq***.

rate with passage of time which depicts the lag phase (no plaques appearance) upto 80 unit time and after it evolves into growth phase (evolution).

3.4. Cross Talk of Calcium Channels, APP and Calpain-CAST Regulatory Pathways

The **Figure 17** represents the SPN model of the crosstalk network in **Figure 6**. The connection that joins the pathways is established through places ***CLP***, ***P35*** and ***BACE***. Active Calpain enhances β-secretase mediated APP cleavage twice than normal (Kusakawa et al., 2000; Liang et al., 2010) which initiates early production and accumulation of plaques (Jack et al., 2010; Braak et al., 2011). As a counter action, PKC ***PKC*** plays its role and enhances the activity of enzyme α-secretase (***ALPHA***) (Skovronsky et al., 2000). In the next connection, Calpain (***CLP***) hinders the functioning of ***PKC*** by degrading it into pkm (place ***pkm***). Aβ

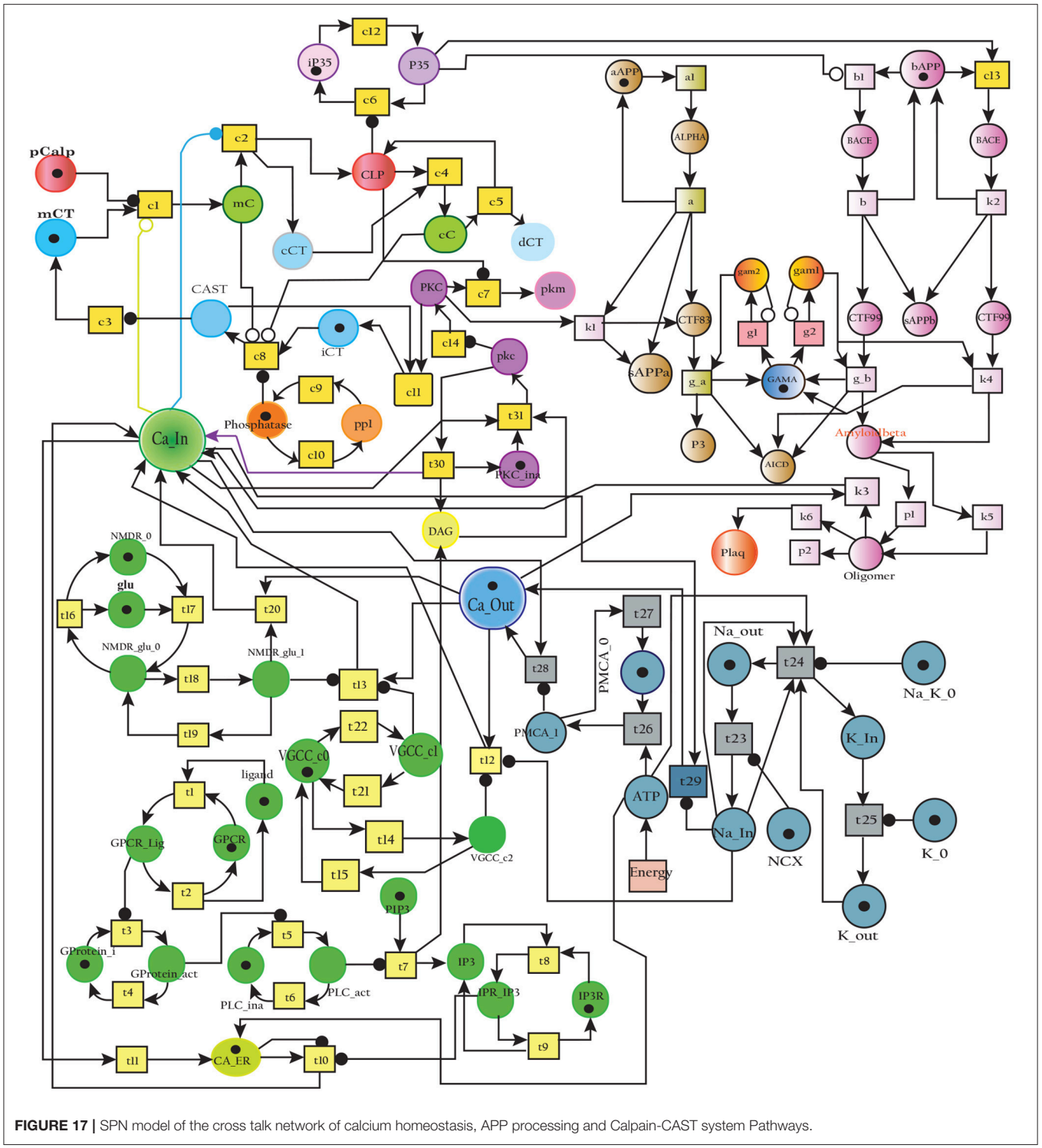


FIGURE 17 | SPN model of the cross talk network of calcium homeostasis, APP processing and Calpain-CAST system Pathways.

oligomers represented by place ***Oligomer*** forms pores into the membrane which instantaneously increases influx of Ca^{2+} ions. The place ***Amyloidbeta*** inhibits the transition **Energy** which indirectly hinders Ca^{2+} extrusion into extracellular space. The new transitions in the crosstalk network are labeled with *k*. The transition ***k1*** connects the place ***PKC*** with ***ALPHA*** while ***P35*** is connected to ***Plaq*** through transitions ***c13***, ***k2***, ***k4***, ***k5***, and ***k6***. The transition ***k3*** joins ***Oligomer*** with ***Ca_In***. The reaction rates of all the transitions are listed in **Table 4**.

The results in **Figure 18** show that ***CLP*** and ***P35*** are accumulating which can directly affect the plaques accumulation process by increase in their deposition rate, as compared to

TABLE 4 | The transitions rates of the SPN model of the crosstalk network.

Tansitions	Rate (μ)	Transitions	Rate (μ)	Transitions	Rate (μ)	Transitions	Rate (μ)
*t*1	1	*t*17	1	*c*1	0.5	*b*	0.3
*t*2	1	*t*18	1	*c*2	0.1	*b*1	0.3
*t*3	1	*t*19	1	*c*3	1	*g*1	0.5
*t*4	1	*t*20	1	*c*4	0.5	*g*2	0.5
*t*5	1	*t*21	1	*c*5	0.02	*g_a*	0.5
*t*6	1	*t*22	1	*c*6	1	*g_b*	0.3
*t*7	1	*t*23	1	*c*7	0.3	*p*1	0.005
*t*8	1	*t*24	1	*c*8	0.5	*p*2	0.02
*t*9	1	*t*25	1	*c*9	1	*k*1	0.5
*t*10	0.65	*t*26	1	*c*10	1	*k*2	0.6
*t*11	1	*t*27	1	*c*11	1	*k*3	1
*t*12	1	*t*28	1	*c*12	0.5	*k*4	0.6
*t*13	1	*t*29	1	*c*13	1	*k*5	0.01
*t*14	1	*t*30	1	*c*14	0.5	*k*6	0.04
*t*15	1	*t*31	1	*a*	0.5		
*t*16	1	*Energy*	1	*a*1	0.5		

*All the transitions from **Figure 17** are listed with their corresponding rate values. As the SPN is a combination of previous three models, it has only three new connections with transition labeled k. All the transitions are adjusted to rates which can reproduce the patho-physiological condition of the brain.*

results in section 3.3 where accumulation of ***Plaq*** is minimal (**Figure 16A**). It can also be observed that ***mC*** and ***cC*** start declining at later stages which indicates depletion of CAST (**Figure 18A**).

In **Figure 18B**, the concentration of ***sAPPb*** is higher than ***sAPPa*** protein, which is contrary to the **Figure 15B**. Hyper activity of ***CLP*** influences more than one processes in the pathological network by enhancing ***BACE*** activity which increases the growth of ***sAPPb***. The decrease in ***PKC*** concentration and calcium dysregulation (***Ca_In*** rises gradually, ***Ca_Out*** and ***Ca_ER*** both lower down) are also due to over-activation of ***CLP*** (**Figure 18C**). Instability in Calcium equilibrium in neurons appear after 60 unit time which also act as a signal indicating the development of AD. Additionally, degradation of ***PKC*** into ***pkm*** by the action of ***CLP*** also have bidirectional effect on the system. First the availability of active ***CT*** in the cell raises and then ***ALPHA*** secretase driven APP processing slows down (**Figure 18B**). **Figure 18D** represents the translocation and regulation of CAST (***cC*** and***cC***) in the brain cell.

3.5. Therapeutic Intervention

The parameter **Table 5** shows that by changing the rate of reaction of two crucial transitions i.e., ***c2*** and ***c5*** (representing degradation rate of Calpain-CAST complex at membrane and cytosol, respectively) would provide effective strategy to control or stop the development of AD and other related neurological disorders. After applying *in silico* intervention, it can be observed that as the rate of transition ***c2*** is decreased the neurological network move toward stability due to basal or low activity of ***CLP*** (**Figure 19A**). Further, the rate of ***c2*** is set to zero which indicates that ***mC*** is made unbreakable or stable which implies that there would be no production of ***CLP*** (**Figure 19B**). In **Figure 19A**, both the complexes (***mC*** and ***cC***) are maintained for longer time duration which result in low production of ***CLP***, ***Aβ*** and ***Plaq***. In **Figure 19B**, there is neither the production of ***CLP*** nor the formation of ***cC*** due to long life of ***mC*** complex occur and there is negligible production of ***Aβ***. The complex (***mC***) also ensures low level of ***sAPPb*** and high concentration of ***sAPPa*** and as a result there is minor accumulation of ***Plaq*** in the neurons.

The stability of ***mC*** have positive effects in maintaining the calcium homeostasis which regains its equilibrium accompanied by substantial concentration of ***PKC*** and no production of ***P35*** **Figure 20A**. The smaller rate of ***c5*** also favors stable condition of system and can delay the production of plaques. **Figures 19C,D** show that as the rate of transition of *c5* decreases the system maintains a stable state due to prolonged life of ***cC*** which causes basal level production of ***CLP*** and eventually guard against rapid ***Plaq*** accumulation in brains. As shown in **Figure 19D**, ***cC*** helps in maintaining a balanced level of **CAST**, ***sAPPa*** and ***sAPPb*** and it lowers down the concentration and accumulation of ***Aβ*** and ***Plaq***. Also it aids in maintaining homeostasis of other proteins and channels into the cell such as ***PKC***, ***pkm***, ***P35*** and calcium homeostasis (**Figure 20B**). Therefore, these complexes are very critical targets since they regulate homeostasis of many crucial proteins.

4. DISCUSSION

This study contributes in achieving long haul goal of AD research i.e., understanding and manipulating pathological conditions which include BACE and Calpain over-activation, Calcium dysregulation, CAST depletion and abnormal production of Aβ. In this study, neuronal pathways comprising Calpain-CAST system, APP processing pathways and Calcium channels were first modeled individually and then their cross-talk was also modeled. The simulation results of these models predicted a more clearer picture of AD pathogenisis also, on the basis of observations interventions were introduced to linger on the AD pathogenesis.

In a healthy physiological model, rate of Ca^{2+} ions inflow should be lower than rate of Ca^{2+} ions outflow with uniform oscillation within the safest level. Moreover, the concentration of Ca^{2+} ions in intracellular store (***Ca_ER***) is greater than (***Ca_In***) (**Figures 10B,C**) (Korol et al., 2008; Gutierrez-Merino et al., 2014). An equilibrated flow is also observed in other important ions channels such as NCX and NKA, which mediate influx and efflux of Na and K ions. Balance in their flow is obligatory for the adequate efflux of Ca^{2+} ions for maintaining homeostasis (Gutierrez-Merino et al., 2014). Another important physiological pathway, Calpain-CAST regulatory system also depends on Ca^{2+}. The calcium influx and efflux channels are required for the activation and regulation of Calpain.

The simulation results in section 3.2, show that when concentartion of Ca^{2+} is lower inside the cytosol then Calpain is bounded in the complex of Calpain-CAST at membrane.

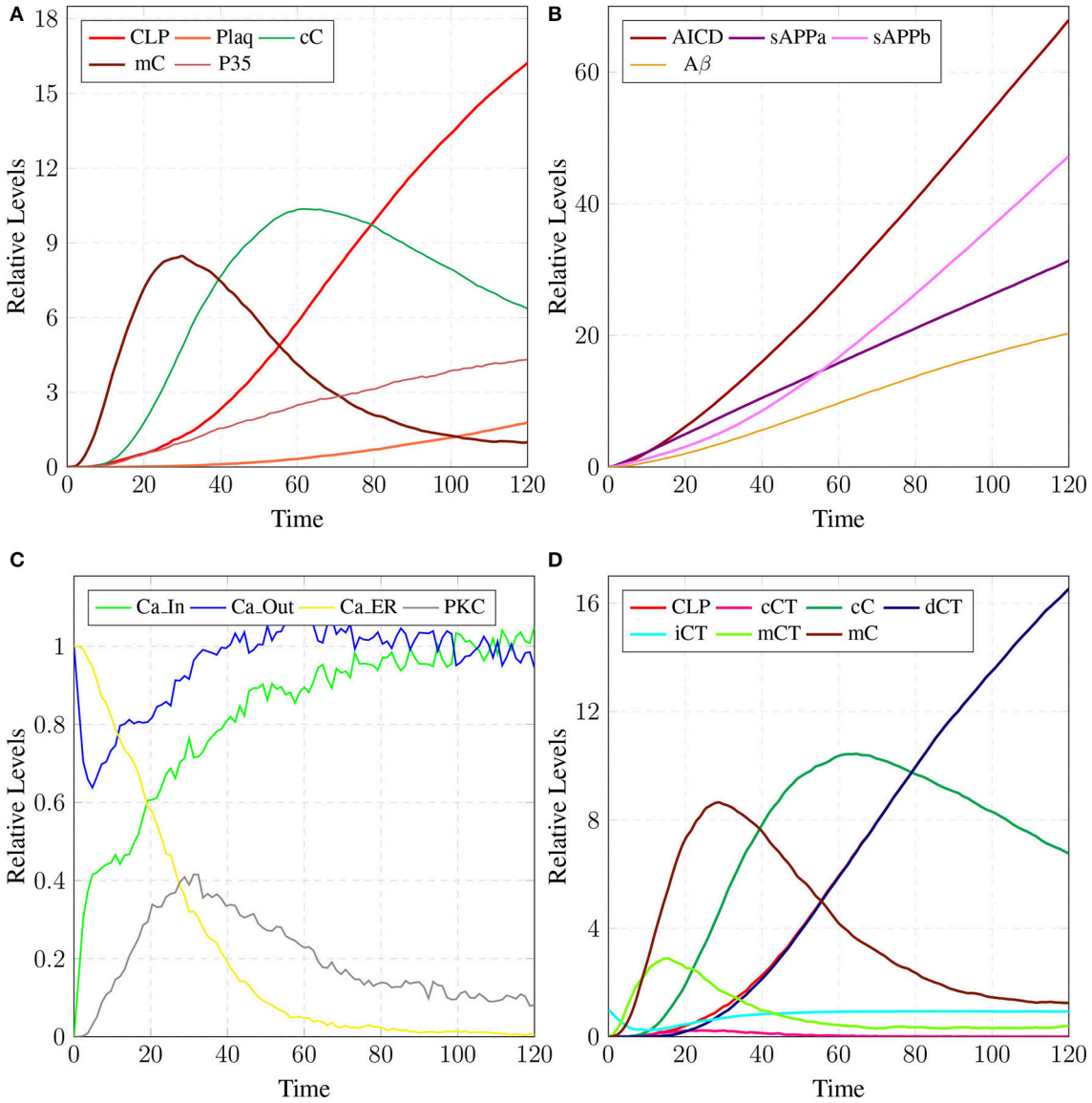


FIGURE 18 | In **(A)**, high concentration of ***CLP*** causes gradual degradation of ***cC*** and further increases the activation of ***P35*** which then activates rapid production of ***Plaq*** leading to the onset of AD. In **(B)**, the production of ***sAPPa*** is lower than the production ***sAPPb*** and ***AICD*** production is higher than both ***sAPPa*** and ***sAPPb***. **(C)** shows slow dysregulation of calcium homeostasis by increase of concentration of ***Ca_In*** from ***Ca_Out*** and ***Ca_ER***. **(D)** shows conversion of ***iCT*** into active form then translocation to membrane ***mCT*** and cytosol ***cCT***. Furthermore, ***cCT*** binds with ***CLP*** to form ***cC***. ***CLP*** gradually degrades CAST into ***dCT***.

TABLE 5 | Transition rate table.

Tansitions	Rate (μ)	Rate (μ)
c2	0.05	0.0
c5	0.005	0.0

*Changing the rate of crucial transitions c2 and c5 to study their effects on crosstalk network model **Figure 17**.*

As concentartion of Ca^{2+} rises, the complex degrades and active Calpain is produced (De Tullio et al., 1999; Todd et al., 2003). To regulate Calpain's activation, CAST appears to form Calpian-CAST complex in cytosol, but gradually its peak falls down which shows release of active Calpain and degradation of CAST. The results in **Figures 12C,D** show that as ***CLP*** rises, both the complexes (***mC*** and ***cC***) gradually degrade which causes depletion of CAST (Averna et al., 2001b; Tompa et al., 2002). PKC also has important role in building a feedback mechanism for Calpain by phosphorylating CAST into inactive form (Averna et al., 2001a). Calpain is also regulating PKC by cleaving it into pkm (Goll et al., 2003) which is persistently active catalytic fragment and quickly disappears (Yamakawa et al., 2001; Liu et al., 2008). PKC also has important roles in the system, it is favoring α-secretase mediated APP cleavage (Rossner et al., 2001; Racchi et al., 2003) and is also involved in inactivation of CAST through phosphorylation

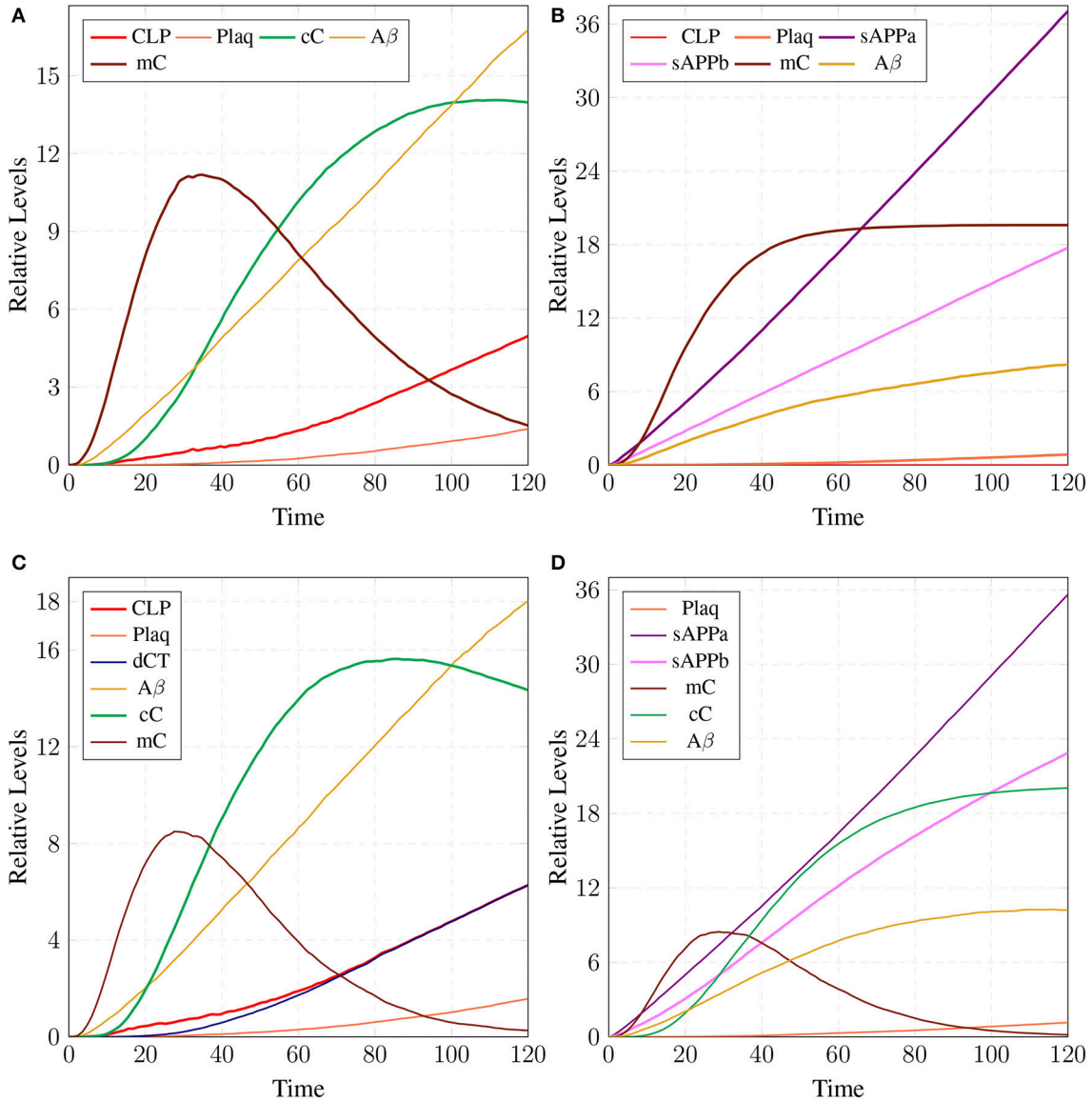


FIGURE 19 | A mild cognitive impairment behavior in **(A,C)**. ***CLP*** is in loosely controlled by ***mC*** and ***cC*** ($c2 = 0.05$ and $c5 = 0.005$). There is low level of ***Plaq*** and significant level of ***Aβ***. By changing the rate of $c2 = 0$ **(B)** there is no conversion of pro-Calpain into ***CLP*** due to long life of ***mC***. Production of ***sAPPb*** and ***Aβ*** are also decreased sufficiently and it lingers on the process of accumulation of ***Plaq***. In **(D)**, $c5$ is set to zero which controls level of ***CLP*** after its activation and saves CAST from depletion into ***dCT***. The production of ***sAPPa*** is higher than production of ***sAPPb*** in **(B,D)**.

(Olariu et al., 2002). The inactive CAST regains its active conformation in the presence of phosphatases (Averna et al., 2001a).

Simulation results of the model APP processing pathways show that in a healthy brain all three enzymes of this pathway are available in the cell to digest the around-the-clock production of APP with α-secretase having high affinity as compared to BACE (De Strooper and Annaert, 2000). Consequently, production rate of sAPPα is higher than sAPPβ (**Figure 15B**) which is a depiction of normal physiological behavior (De Strooper and Annaert, 2000; Lichtenthaler, 2011). Studies showed that in healthy brain, plaques produce and accumulate in a linear fashion which is also observed in our studies. Moreover, $A\beta$ burdens in the form of plaques at elder age. This linear behavior of plaques accumulation can adopt exponential growth due to the high accumulation rate with passage of time. In our results the formation of plaques first enter the lag phase (no plaques appearance) upto 80 unit time and then evolve into growth phase (evolution), which is also experimentally reported (Friedrich et al., 2010; Jack et al., 2010; Sperling et al., 2011).

In neuro-pathological model, simulation revealed that the intermediate product sAPPβ of amyloidogenic pathway rises in the AD brain. Higher concentration of sAPPβ can lead to early occurrence of AD (at age of 40 and onward) due

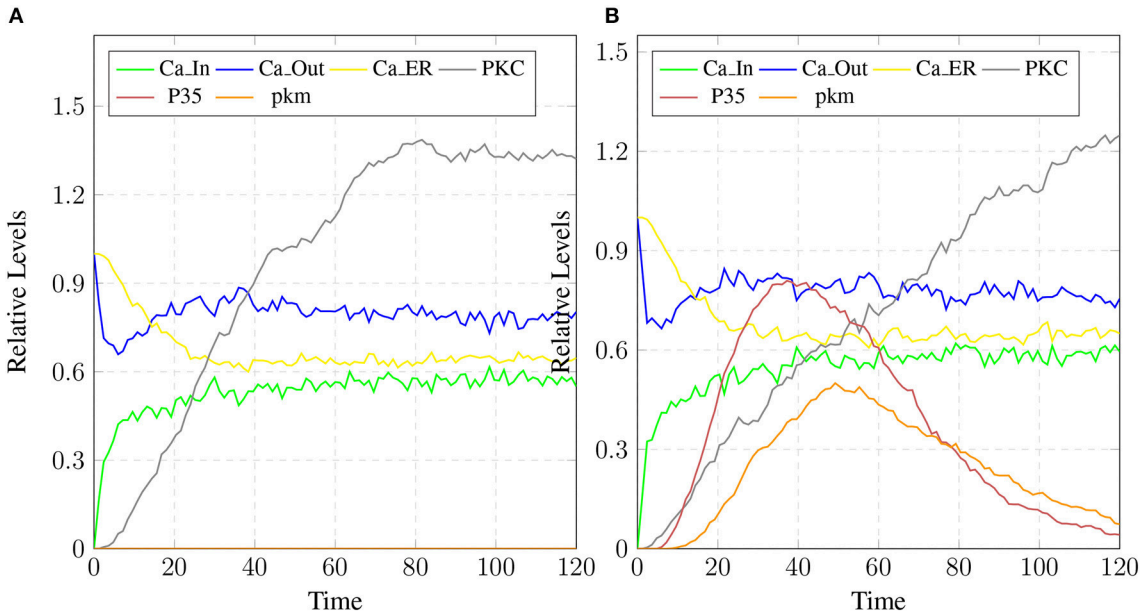


FIGURE 20 | The restoration of Calcium homeostasis. In **(A)**, ***PKC*** is present for longer time and there is no conversion into ***pkm*** also there is no production of ***P35***. In **(B)**, there is less production of ***P35*** and ***pkm***.

to rapid deposition of the plaques in brain of AD patients (Freer et al., 2016). Higher level of sAPPβ also indicate the enhanced activity of BACE which is triggered by over-activation of Calpain. Enhanced activation of Calpain disturbs more than one processes in the pathological network i.e., increased BACE activity, decreased PKC functioning and calcium dysregulation. Initially CAST and its complex with pro-Calpain are in high quantity to control Calpain but with the elevation of calcium influx, the complex starts to degrade. The active Calpain accumulates in cytosol which is then controlled by cytosolic CAST by forming complex with it. After sometime Calpain degrades the CAST in the complex to release itself into the cytosol and eventually CAST and complex deplete from the cell (Higuchi et al., 2012). Depletion of CAST destroys the cell normal functioning and then nervous system deteriorates (Rao et al., 2008, 2014; Kurbatskaya et al., 2016).

After analyzing the neuropathological network, the vague picture of AD development becomes more clear. It provide useful observations such as loss of calcium homeostasis occur after 60 unit time due to intra-neuronal ATP depletion caused by elevation of Calpain (Lipton, 1999; Kurbatskaya et al., 2016) and formation of extracellular ion pores formed by Aβ oligomers (Small et al., 2009). Ca^{2+} disruption increases Calpain concentration in neurons which further elevates the BACE activity toward APP (Liang et al., 2010; Chami and Checler, 2012; Song et al., 2015) via cdk5 dependent pathway as a result of Aβ and sAPPβ levels in neurons built up (Sennvik et al., 2004). In normal healthy brain, the mean burden in the form of plaques are low and it increase in linear fashion from 60 to 90 unit time (Rodrigue et al., 2012; Freer et al., 2016; Kurbatskaya et al., 2016). It is noteworthy that both amyloidogenic and non-amyloidogenic pathways are enabled in an healthy individual but plaques in the brain of AD patient grow rapidly due to increased Calpain mediated cleavage of APP through BACE (Mawuenyega et al., 2010). It can be inferred that all the neuro-pathological events are inter-related where Calpain and its complexes are playing crucial role. Calpain can be called as bone of contention and the complexes are the defenders. This neuropathological network provides valuable knowledge about interventions and offers new therapeutic targets. To stop the Calpain destructive effects, it may be effective strategy to slightly modify the natural process. In the work of Emmaneul and coworkers on cardiovascular remodeling, the Calpain-CAST system has emerged as new effective strategy to prevent angiotension (Letavernier et al., 2008). In our study, Calpain-CAST complexes have also proved to be effective therapeutic targets for delaying the process of neuronal degradation which can save the brains from AD.

5. CONCLUSION

In AD, $A\beta$ has central role as they accumulate into hallmark lesions i.e., plaques. $A\beta$ generates from APP cleavage through amyloidogenic pathway. Progression of the corresponding processing pathway increases due to over-activation of Caplain and depletion of its sole inhibitor CAST. Calpain hyper activation depends on high Calcium concentration in the cytosol. Calpain triggers the production of P35 and the degradation of CAST and PKC. In-Addition, it also triggers the imbalance of calcium homeostasis. All these observations were incorporated into a Stochastic PN models. We gained insight into the mechanism of the AD progression and were able to derive some useful inferences. The first important inference is that under hyper-activation of Calpain, calcium homeostasis dysregulates and CAST starts to degrade gradually. APP processing enzyme

(BACE) increases two folds which starts producing $A\beta$ that slowly accumulates into plaques in AD brains at early age and lesions appear later. The second important inference is about the most crucial protein Calpain that influences many important proteins of neuronal network such as CAST, PKC, P35, and BACE. Furthermore, these proteins together dysregulate calcium homeostasis. Calpain regulation through CAST plays important role in keeping cells safe from neurodegradation. CAST encounters Calpain at two locations in the cell. Initially at membrane, CAST forms complex with inactive Calpain which is short lived and dissociates as the calcium influx increases. In the cytoplasm, active Calpain-CAST complex is long-standing which keeps the Calpain concentration in control but it also degraded slowly by the action of Calpain. From our study, Calpain and Calpain-CAST complexes have emerged as the potential therapeutic targets for the treatment of neurodegenerative pathologies. The pathway modeling of these networks have predicted that we can introduce delays in the production and accumulation of plaques by targeting the Calpain-CAST complexes. The production of Calpain should be kept in safe levels to avoid its hyper activity. It can be achieved implicitly by enhancing activity of Calpain-CAST complexes. The more durable are the complexes, the lesser would be the accumulation of plaques. Another useful strategy can be the designing of inhibitors against the active Calpain using *in silico* methods and *in vitro* experiments. By considering these effective interventions we can increase the chances of healthy life expectancy and can save many lives and families from the adversity of AD.

AUTHOR CONTRIBUTIONS

JAs and JAh conceived research idea, designed and performed the experiments, analyzed the data, wrote the paper, prepared figures and/or tables, reviewed drafts of the paper. AA and ZU-H analyzed the data, prepared tables and/or figures, wrote the paper, reviewed drafts of the paper.

SUPPLEMENTARY MATERIAL

The Supplementary Material for this article can be found online at: https://www.frontiersin.org/articles/10.3389/fninf.2018.00026/full#supplementary-material

REFERENCES

Alkon, D. L., Sun, M.-K., and Nelson, T. J. (2007). Pkc signaling deficits: a mechanistic hypothesis for the origins of alzheimer's disease. *Trends Pharmacol. Sci.* 28, 51–60. doi: 10.1016/j.tips.2006.12.002

Annaert, W. G., and Saftig, P. (2009). Regulated intramembrane proteolysis—a story about sheddases and I-CliPs. *Semin. Cell Dev. Biol.* 20:125. doi: 10.1016/j.semcdb.2009.03.005

Ashford, J. W. (2004). Apoe genotype effects on Alzheimer's disease onset and epidemiology. *J. Mol. Neurosci.* 23, 157–165. doi: 10.1385/JMN:23:3:157

Averna, M., De Tullio, R., Passalacqua, M., Salamino, F., Pontremoli, S., and Melloni, E. (2001a). Changes in intracellular calpastatin localization are mediated by reversible phosphorylation. *Biochem. J.* 354, 25–30. doi: 10.1042/bj3540025

Averna, M., De Tullio, R., Salamino, F., Minafra, R., Pontremoli, S., and Melloni, E. (2001b). Age-dependent degradation of calpastatin in kidney of hypertensive rats. *J. Biol. Chem.* 276, 38426–38432. doi: 10.1074/jbc.M101936200

Berridge, M. J. (2009). Inositol trisphosphate and calcium signalling mechanisms. *Mol. Cell Res.* 1793, 933–940. doi: 10.1016/j.bbamcr.2008.10.005

Blätke, M. A., Heiner, M., and Marwan, W. (2011). *Petri Nets in Systems Biology*. Technical report, Technical Report, Otto-von-Guericke University Magdeburg.

Braak, H., Thal, D. R., Ghebremedhin, E., and Del Tredici, K. (2011). Stages of the pathologic process in alzheimer disease: age categories from 1 to 100 years. *J. Neuropathol. Exp. Neurol.* 70, 960–969. doi: 10.1097/NEN.0b013e318232a379

Brittain, M. K., Brustovetsky, T., Sheets, P. L., Brittain, J. M., Khanna, R., Cummins, T. R., et al. (2012). Delayed calcium dysregulation in neurons requires both the nmda receptor and the reverse Na+/Ca2+ exchanger. *Neurobiol. Dis.* 46, 109–117. doi: 10.1016/j.nbd.2011.12.051

Budson, A. E., and Price, B. H. (2005). Memory dysfunction. *New Engl. J. Med.* 352, 692–699. doi: 10.1056/NEJMra041071

Cai, H., Wang, Y., McCarthy, D., Wen, H., Borchelt, D. R., Price, D. L., et al. (2001). Bace1 is the major β-secretase for generation of aβ peptides by neurons. *Nat. Neurosci.* 4, 233–234. doi: 10.1038/85064

Cain, S. M., and Snutch, T. P. (2011). Voltage-gated calcium channels and disease. *Biofactors* 37, 197–205. doi: 10.1002/biof.158

Castaldi, D., Maccagnola, D., Mari, D., and Archetti, F. (2012). "Stochastic simulation of the coagulation cascade: a petri net based approach," in *European Conference on Parallel Processing* (Rhodos: Springer).

Chami, L., and Checler, F. (2012). Bace1 is at the crossroad of a toxic vicious cycle involving cellular stress and β-amyloid production in Alzheimer's disease. *Mol. Neurodegenerat.* 7:52. doi: 10.1186/1750-1326-7-52

Chen, M., and Fernandez, H. L. (2004). Stimulation of β-amyloid precursor protein α-processing by phorbol ester involves calcium and calpain activation. *Biochem. Biophys. Res. Commun.* 316, 332–340. doi: 10.1016/j.bbrc.2004.02.052

Courjaret, R., Grolleau, F., and Lapied, B. (2003). Two distinct calcium-sensitive and-insensitive pkc up-and down-regulate an α-bungarotoxin-resistant nachr1 in insect neurosecretory cells (dum neurons). *Eur. J. Neurosci.* 17, 2023–2034. doi: 10.1046/j.1460-9568.2003.02644.x

Cuello, A. C. (2005). Intracellular and extracellular aβ, a tale of two neuropathologies. *Brain Pathol.* 15, 66–71. doi: 10.1111/j.1750-3639.2005.tb00101.x

David, R., and Alla, H. (2010). *Discrete, Continuous, and Hybrid Petri Nets*. Grenoble: Springer Science & Business Media.

De Strooper, B., and Annaert, W. (2000). Proteolytic processing and cell biological functions of the amyloid precursor protein. *J. Cell. Sci.* 113, 1857–1870.

De Tullio, R., Passalacqua, M., Averna, M., Salamino, F., Melloni, E., and Pontremoli, S. (1999). Changes in intracellular localization of calpastatin during calpain activation. *Biochem. J.* 343, 467–472. doi: 10.1042/bj3430467

DeStrooper, B., Saftig, P., Birchmeier, C., and Haass, C. (2006). Control of peripheral nerve myelination by the beta-secretase bace1. *Science* 314, 664–666. doi: 10.1126/science.1132341

Emptage, N. J., Reid, C. A., and Fine, A. (2001). Calcium stores in hippocampal synaptic boutons mediate short-term plasticity, store-operated ca 2+ entry, and spontaneous transmitter release. *Neuron* 29, 197–208. doi: 10.1016/S0896-6273(01)00190-8

Etcheberrigaray, R., Tan, M., Dewachter, I., Kuipéri, C., Van der Auwera, I., Wera, S., et al. (2004). Therapeutic effects of pkc activators in alzheimer's disease transgenic mice. *Proc. Natl. Acad. Sci. U.S.A.* 101, 11141–11146. doi: 10.1073/pnas.0403921101

Ferreira, A. (2012). Calpain dysregulation in Alzheimer's disease. *ISRN Biochem.* 2012:728571. doi: 10.5402/2012/728571

Freer, R., Sormanni, P., Vecchi, G., Ciryam, P., Dobson, C. M., and Vendruscolo, M. (2016). A protein homeostasis signature in healthy brains recapitulates tissue vulnerability to Alzheimer's disease. *Sci. Adv.* 2:e1600947. doi: 10.1126/sciadv.1600947

Friedrich, R. P., Tepper, K., Rönicke, R., Soom, M., Westermann, M., Reymann, K., et al. (2010). Mechanism of amyloid plaque formation suggests an intracellular basis of aβ pathogenicity. *Proc. Natl. Acad. Sci. U.S.A.* 107, 1942–1947. doi: 10.1073/pnas.0904532106

Gillespie, D. T. (1976). A general method for numerically simulating the stochastic time evolution of coupled chemical reactions. *J. Comput. Phys.* 22, 403–434. doi: 10.1016/0021-9991(76)90041-3

Golde, T. E. (2005). The aβ hypothesis: Leading us to rationally-designed therapeutic strategies for the treatment or prevention of alzheimer disease. *Brain Pathol.* 15, 84–87. doi: 10.1111/j.1750-3639.2005.tb00104.x

Goll, D. E., Thompson, V. F., Li, H., Wei, W., and Cong, J. (2003). The calpain system. *Physiol. Rev.* 83, 731–801. doi: 10.1152/physrev.00029.2002

Goss, P. J., and Peccoud, J. (1998). Quantitative modeling of stochastic systems in molecular biology by using stochastic petri nets. *Proc. Natl. Acad. Sci. U.S.A.* 95, 6750–6755. doi: 10.1073/pnas.95.12.6750

Greenfield, J. P., Tsai, J., Gouras, G. K., Hai, B., Thinakaran, G., Checler, F., et al. (1999). Endoplasmic reticulum and trans-golgi network generate distinct populations of Alzheimer β-amyloid peptides. *Proc. Natl. Acad. Sci. U.S.A.* 96, 742–747. doi: 10.1073/pnas.96.2.742

Gutierrez-Merino, C., Marques-da Silva, D., Fortalezas, S., and Samhan-Arias, A. K. (2014). "Cytosolic calcium homeostasis in neurons–control systems, modulation by reactive oxygen and nitrogen species, and space and time fluctuations," in *Neurochemistry*, ed T. Heinbockel (Rijeka: InTech), 59–110.

Haass, C. (2004). Take five–bace and the γ-secretase quartet conduct alzheimer's amyloid β-peptide generation. *EMBO J.* 23, 483–488. doi: 10.1038/sj.emboj.7600061

Hanna, R. A., Campbell, R. L., and Davies, P. L. (2008). Calcium-bound structure of calpain and its mechanism of inhibition by calpastatin. *Nature* 456, 409–412. doi: 10.1038/nature07451

Hardy, J., and Selkoe, D. J. (2002). The amyloid hypothesis of Alzheimer's disease: progress and problems on the road to therapeutics. *Science* 297, 353–356. doi: 10.1126/science.1072994

Hardy, J. A., and Higgins, G. A. (1992). Alzheimer's disease: the amyloid cascade hypothesis. *Science* 256, 184. doi: 10.1126/science.1566067

Heiner, M., Gilbert, D., and Donaldson, R. (2008). "Petri nets for systems and synthetic biology," in *International School on Formal Methods for the Design of Computer, Communication and Software Systems*, eds M. Bernardo, P. Degano, and G. Zavattaro (Bertinoro: Springer), 215–264.

Higuchi, M., Iwata, N., Matsuba, Y., Takano, J., Suemoto, T., Maeda, J., et al. (2012). Mechanistic involvement of the calpain-calpastatin system in alzheimer neuropathology. *FASEB J.* 26, 1204–1217. doi: 10.1096/fj.11-187740

Hu, X., Hicks, C. W., He, W., Wong, P., Macklin, W. B., Trapp, B. D., et al. (2006). Bace1 modulates myelination in the central and peripheral nervous system. *Nat. Neurosci.* 9, 1520–1525. doi: 10.1038/nn1797

Jack, C. R., Knopman, D. S., Jagust, W. J., Shaw, L. M., Aisen, P. S., Weiner, M. W., et al. (2010). Hypothetical model of dynamic biomarkers of the Alzheimer's pathological cascade. *Lancet Neurol.* 9, 119–128. doi: 10.1016/S1474-4422(09)70299-6

Jonsson, T., Atwal, J. K., Steinberg, S., Snaedal, J., Jonsson, P. V., Bjornsson, S., et al. (2012). A mutation in app protects against Alzheimer's disease and age-related cognitive decline. *Nature* 488:96. doi: 10.1038/nature11283

Korol, T. Y., Kostyuk, E., and Kostyuk, P., (2008). Disruption of calcium homeostasis in Alzheimer's disease. *Neurophysiology* 40, 385–392. doi: 10.1007/s11062-009-9064-5

Krebs, J., Agellon, L. B., and Michalak, M. (2015). Ca2+ homeostasis and endoplasmic reticulum (er) stress: an integrated view of calcium signaling. *Biochem. Biophys. Res. Commun.* 460, 114–121. doi: 10.1016/j.bbrc.2015.02.004

Kurbatskaya, K., Phillips, E. C., Croft, C. L., Dentoni, G., Hughes, M. M., Wade, M. A., et al. (2016). Upregulation of calpain activity precedes tau phosphorylation and loss of synaptic proteins in Alzheimer's disease brain. *Acta Neuropathol. Commun.* 4:34. doi: 10.1186/s40478-016-0299-2

Kusakawa, G.-i., Saito, T., Onuki, R., Ishiguro, K., Kishimoto, T., and Hisanaga, S.-i. (2000). Calpain-dependent proteolytic cleavage of the p35 cyclin-dependent kinase 5 activator to p25. *J. Biol. Chem.* 275, 17166–17172. doi: 10.1074/jbc.M907757199

LaFerla, F. M. (2002). Calcium dyshomeostasis and intracellular signalling in Alzheimer's disease. *Nat. Rev. Neurosci.* 3, 862–872. doi: 10.1038/nrn960

Lamprecht, R., Smith, G. D., and Kemper, P. (2011). Stochastic petri net models of ca2+ signaling complexes and their analysis. *Nat. Comput.* 10, 1045–1075. doi: 10.1007/s11047-009-9143-y

Lanni, C., Mazzucchelli, M., Porrello, E., Govoni, S., and Racchi, M. (2004). Differential involvement of protein kinase c alpha and epsilon in the regulated secretion of soluble amyloid precursor protein. *Eur. J. Biochem.* 271, 3068–3075. doi: 10.1111/j.1432-1033.2004.04240.x

Lee, J., Retamal, C., Cuitiño, L., Caruano-Yzermans, A., Shin, J.-E., Van Kerkhof, P., et al. (2008). Adaptor protein sorting nexin 17 regulates amyloid precursor protein trafficking and processing in the early endosomes. *J. Biol. Chem.* 283, 11501–11508. doi: 10.1074/jbc.M800642200

Lee, M.-s., Kwon, Y. T., Li, M., Peng, J., Friedlander, R. M., and Tsai, L.-H. (2000). Neurotoxicity induces cleavage of p35 to p25 by calpain. *Nature* 405, 360–364. doi: 10.1038/35012636

Lee, V. M., Goedert, M., and Trojanowski, J. Q. (2001). Neurodegenerative tauopathies. *Annu. Rev. Neurosci.* 24, 1121–1159. doi: 10.1146/annurev.neuro.24.1.1121

Letavernier, E., Perez, J., Bellocq, A., Mesnard, L., de Castro Keller, A., Haymann, J.-P., et al. (2008). Targeting the calpain/calpastatin system as a new strategy to prevent cardiovascular remodeling in angiotensin ii–induced hypertension. *Circul. Res.* 102, 720–728. doi: 10.1161/CIRCRESAHA.107.160077

Li, Q., and Südhof, T. C. (2004). Cleavage of amyloid-β precursor protein and amyloid-β precursor-like protein by bace 1. *J. Biol. Chem.* 279, 10542–10550. doi: 10.1074/jbc.M310001200

Liang, B., Duan, B.-Y., Zhou, X.-P., Gong, J.-X., and Luo, Z.-G. (2010). Calpain activation promotes bace1 expression, amyloid precursor protein processing, and amyloid plaque formation in a transgenic mouse model of alzheimer disease. *J. Biol. Chem.* 285, 27737–27744. doi: 10.1074/jbc.M110.117960

Lichtenthaler, S. F. (2011). Alpha-secretase in Alzheimer's disease: molecular identity, regulation and therapeutic potential. *J. Neurochem.* 116, 10–21. doi: 10.1111/j.1471-4159.2010.07081.x

Lipton, P. (1999). Ischemic cell death in brain neurons. *Physiol. Rev.* 79, 1431–1568. doi: 10.1152/physrev.1999.79.4.1431

Liu, F., Heiner, M., and Yang, M. (2016). Fuzzy stochastic petri nets for modeling biological systems with uncertain kinetic parameters. *PLoS ONE* 11:e0149674. doi: 10.1371/journal.pone.0149674

Liu, J., Liu, M. C., and Wang, K. K. (2008). Calpain in the cns: from synaptic function to neurotoxicity. *Sci. Signal.* 1, re1. doi: 10.1126/stke.114re1

Marsan, M. A., Balbo, G., Conte, G., Donatelli, S., and Franceschinis, G. (1994). *Modelling With Generalized Stochastic Petri Nets*. New York, NY: John Wiley & Sons, Inc.

Marwan, W., Rohr, C., and Heiner, M. (2012). Petri nets in snoopy: a unifying framework for the graphical display, computational modelling, and simulation of bacterial regulatory networks. *Bact. Mol. Netw. Methods Protocols* 804, 409–437. doi: 10.1007/978-1-61779-361-5_21

Mattson, M. P. (2004). Pathways towards and away from alzheimer's disease. *Nature* 430, 631–639. doi: 10.1038/nature02621

Mattson, M. P., LaFerla, F. M., Chan, S. L., Leissring, M. A., Shepel, P. N., and Geiger, J. D. (2000). Calcium signaling in the er: its role in neuronal plasticity and neurodegenerative disorders. *Trends Neurosci.* 23, 222–229. doi: 10.1016/S0166-2236(00)01548-4

Mawuenyega, K. G., Sigurdson, W., Ovod, V., Munsell, L., Kasten, T., Morris, J. C., et al. (2010). Decreased clearance of cns β-amyloid in Alzheimer's disease. *Science* 330, 1774–1774. doi: 10.1126/science.1197623

Melloni, E., Averna, M., Stifanese, R., De Tullio, R., Defranchi, E., Salamino, F., et al. (2006). Association of calpastatin with inactive calpain a novel mechanism to control the activation of the protease? *J. Biol. Chem.* 281, 24945–24954. doi: 10.1074/jbc.M601449200

Mounts, W. M., and Liebman, M. N. (1997). Application of petri nets and stochastic activity nets to modeling biological pathways and processes. *Int. J. Comput. Simul.* 20, 265–281.

Mura, I., and Csikász-Nagy, A. (2008). Stochastic petri net extension of a yeast cell cycle model. *J. Theor. Biol.* 254, 850–860. doi: 10.1016/j.jtbi.2008.07.019

O'Brien, R. J., and Wong, P. C. (2011). Amyloid precursor protein processing and Alzheimer's disease. *Annu. Rev. Neurosci.* 34, 185–204. doi: 10.1146/annurev-neuro-061010-113613

Olariu, A., Yamada, K., Mamiya, T., Hefco, V., and Nabeshima, T. (2002). Memory impairment induced by chronic intracerebroventricular infusion of beta-amyloid (1–40) involves downregulation of protein kinase c. *Brain Res.* 957, 278–286. doi: 10.1016/S0006-8993(02)03608-9

Ono, Y., and Sorimachi, H. (2012). Calpains–an elaborate proteolytic system. *Biochimica et Biophysica Acta* 1824, 224–236. doi: 10.1016/j.bbapap.2011.08.005

Orrenius, S., Zhivotovsky, B., and Nicotera, P. (2003). Calcium: Regulation of cell death: the calcium–apoptosis link. *Nat. Rev. Mol. Cell Biol.* 4, 552. doi: 10.1038/nrm1150

Pal, G. P., Elce, J. S., and Jia, Z. (2001). Dissociation and aggregation of calpain in the presence of calcium. *J. Biol. Chem.* 276, 47233–47238. doi: 10.1074/jbc.M105149200

Petri, C. (1966). *Kommunikation mit Automaten*. Bonn: Institut für Instrumentelle Mathematik, Schriften Des IIM, No. 3 (1962). English Translation: Communication with Automata, Griffiss Air Force Base. Tech. Rep. RADC-TR-65-377, 1.

Racchi, M., Mazzucchelli, M., Pascale, A., Sironi, M., and Govoni, S. (2003). Role of protein kinase $c\alpha$ in the regulated secretion of the amyloid precursor protein. *Mol. Psychiatry* 8, 209–216. doi: 10.1038/sj.mp.4001204

Rao, M. V., McBrayer, M. K., Campbell, J., Kumar, A., Hashim, A., Sershen, H., et al. (2014). Specific calpain inhibition by calpastatin prevents tauopathy and neurodegeneration and restores normal lifespan in tau p301l mice. *J. Neurosci.* 34, 9222–9234. doi: 10.1523/JNEUROSCI.1132-14.2014

Rao, M. V., Mohan, P. S., Peterhoff, C. M., Yang, D.-S., Schmidt, S. D., Stavrides, P. H., et al. (2008). Marked calpastatin (cast) depletion in Alzheimer's disease accelerates cytoskeleton disruption and neurodegeneration: neuroprotection by cast overexpression. *J. Neurosci.* 28, 12241–12254. doi: 10.1523/JNEUROSCI.4119-08.2008

Rodrigue, K., Kennedy, K., Devous, M., Rieck, J., Hebrank, A., Diaz-Arrastia, R., et al. (2012). β-amyloid burden in healthy aging regional distribution and cognitive consequences. *Neurology* 78, 387–395. doi: 10.1212/WNL.0b013e318245d295

Rossner, S., Mendla, K., Schliebs, R., and Bigl, V. (2001). Protein kinase $c\alpha$ and $\beta 1$ isoforms are regulators of α-secretory proteolytic processing of amyloid precursor protein *in vivo*. *Eur. J. Neurosci.* 13, 1644–1648. doi: 10.1046/j.0953-816x.2001.01525.x

Roussel, B. D., Kruppa, A. J., Miranda, E., Crowther, D. C., Lomas, D. A., and Marciniak, S. J. (2013). Endoplasmic reticulum dysfunction in neurological disease. *Lancet Neurol.* 12, 105–118. doi: 10.1016/S1474-4422(12)70238-7

Ryu, M., and Nakazawa, T. (2014). "Calcium and calpain activation," in *Neuroprotection and Neuroregeneration for Retinal Diseases*, eds T. Nakazawa, Y. Kitaoka, and T. Harada (Tokyo: Springer), 13–24.

Santos, D. M., Xavier, J. M., Morgado, A. L., Sola, S., and Rodrigues, C. M. (2012). Distinct regulatory functions of calpain 1 and 2 during neural stem cell self-renewal and differentiation. *PLoS ONE* 7:e33468. doi: 10.1371/journal.pone.0033468

Schmolesky, M. T., Weber, J. T., Zeeuw, C. I., and Hansel, C. (2002). The making of a complex spike: ionic composition and plasticity. *Ann. N.Y. Acad. Sci.* 978, 359–390. doi: 10.1111/j.1749-6632.2002.tb07581.x

Selkoe, D. J. (2000). Toward a comprehensive theory for alzheimer's disease. hypothesis: Alzheimer's disease is caused by the cerebral accumulation and cytotoxicity of amyloid β-protein. *Ann. N.Y. Acad. Sci.* 924, 17–25. doi: 10.1111/j.1749-6632.2000.tb05554.x

Selkoe, D. J. (2002). Alzheimer's disease is a synaptic failure. *Science* 298, 789–791. doi: 10.1126/science.1074069

Sennvik, K., Bogdanovic, N., Volkmann, I., Fastbom, J., and Benedikz, E. (2004). β-secretase-cleaved amyloid precursor protein in Alzheimer brain: a morphologic study. *J. Cell. Mol. Med.* 8, 127–134. doi: 10.1111/j.1582-4934.2004.tb00267.x

Skovronsky, D. M., Moore, D. B., Milla, M. E., Doms, R. W., and Lee, V. M.-Y. (2000). Protein kinase c-dependent α-secretase competes with β-secretase for cleavage of amyloid-β precursor protein in the trans-golgi network. *J. Biol. Chem.* 275, 2568–2575. doi: 10.1074/jbc.275.4.2568

Small, D. H. (2009). Dysregulation of calcium homeostasis in Alzheimer's disease. *Neurochem. Res.* 34, 1824–1829. doi: 10.1007/s11064-009-9960-5

Small, D. H., Gasperini, R., Vincent, A. J., Hung, A. C., and Foa, L. (2009). The role of aβ-induced calcium dysregulation in the pathogenesis of Alzheimer's disease. *J. Alzheimer's Dis.* 16, 225–233. doi: 10.3233/JAD-2009-0951

Smith, I. F., Green, K. N., and LaFerla, F. M. (2005). Calcium dysregulation in alzheimer's disease: recent advances gained from genetically modified animals. *Cell Calc.* 38, 427–437. doi: 10.1016/j.ceca.2005.06.021

Song, W.-J., Son, M.-Y., Lee, H.-W., Seo, H., Kim, J. H., and Chung, S.-H. (2015). Enhancement of bace1 activity by p25/cdk5-mediated phosphorylation in Alzheimer's disease. *PLoS ONE* 10:e0136950. doi: 10.1371/journal.pone.0136950

Sperling, R. A., Aisen, P. S., Beckett, L. A., Bennett, D. A., Craft, S., Fagan, A. M., et al. (2011). Toward defining the preclinical stages of Alzheimer's disease: recommendations from the national institute on aging-alzheimer's association workgroups on diagnostic guidelines for Alzheimer's disease. *Alzheimer's Dement.* 7, 280–292. doi: 10.1016/j.jalz.2011.03.003

Stutzmann, G. E. (2005). Calcium dysregulation, ip3 signaling, and Alzheimer's disease. *Neuroscientist* 11, 110–115. doi: 10.1177/1073858404270899

Tam, J. H., and Pasternak, S. H. (2012). Amyloid and alzheimer's disease: inside and out. *Can. J. Neurol. Sci.* 39, 286–298. doi: 10.1017/S0317167100013408

Tareen, S. H. K., and Ahmad, J. (2015). Modelling and analysis of the feeding regimen induced entrainment of hepatocyte circadian oscillators using petri nets. *PLoS ONE* 10:e0117519. doi: 10.1371/journal.pone.0117519

Tiraboschi, P., Hansen, L., Alford, M., Masliah, E., Thal, L., and Corey-Bloom, J. (2000). The decline in synapses and cholinergic activity is asynchronous in Alzheimer's disease. *Neurology* 55, 1278–1283. doi: 10.1212/WNL.55.9.1278

Todd, B., Moore, D., Deivanayagam, C. C., Chattopadhyay, D., Maki, M., Wang, K. K., et al. (2003). A structural model for the inhibition of calpain by calpastatin: crystal structures of the native domain vi of calpain and its complexes with calpastatin peptide and a small molecule inhibitor. *J. Mol. Biol.* 328, 131–146. doi: 10.1016/S0022-2836(03)00274-2

Tompa, P., Mucsi, Z., Orosz, G., and Friedrich, P. (2002). Calpastatin subdomains a and c are activators of calpain. *J. Biol. Chem.* 277, 9022–9026. doi: 10.1074/jbc.C100700200

Trojanowski, J. Q., and Lee, V. M.-Y. (2000). "fatal attractions" of proteins: a comprehensive hypothetical mechanism underlying Alzheimer's disease and other neurodegenerative disorders. *Ann. N.Y. Acad. Sci.* 924, 62–67. doi: 10.1111/j.1749-6632.2000.tb05561.x

Tsavachidou, D., and Liebman, M. N. (2002). Modeling and simulation of pathways in menopause. *J. Am. Med. Inf. Ass.* 9, 461–471. doi: 10.1197/jamia.M1103

Vaisid, T., Barnoy, S., and Kosower, N. (2008). Calpastatin overexpression attenuates amyloid-β-peptide toxicity in differentiated pc12 cells. *Neuroscience* 156, 921–931. doi: 10.1016/j.neuroscience.2008.07.072

Vassar, R. (2005). beta-secretase, app and abeta in Alzheimer's disease. *Subcell Biochem.* 38, 79–103. doi: 10.1007/0-387-23226-5_4

Vassar, R., Bennett, B. D., Babu-Khan, S., Kahn, S., Mendiaz, E. A., Denis, P., et al. (1999). β-secretase cleavage of alzheimer's amyloid precursor protein by the transmembrane aspartic protease bace. *Science* 286, 735–741. doi: 10.1126/science.286.5440.735

Volles, M. J., and Lansbury, P. T. (2002). Vesicle permeabilization by protofibrillar α-synuclein is sensitive to parkinson's disease-linked mutations and occurs by a pore-like mechanism. *Biochemistry* 41, 4595–4602. doi: 10.1021/bi0121353

Walsh, D. M., Klyubin, I., Fadeeva, J. V., Rowan, M. J., and Selkoe, D. J. (2002). Amyloid-beta oligomers: their production, toxicity and therapeutic inhibition. *Biochem. Soc. Trans.* 30, 552–557. doi: 10.1042/bst0300552

Walsh, D. M., and Selkoe, D. J. (2004). Oligomers on the brain: the emerging role of soluble protein aggregates in neurodegeneration. *Protein Pept. Lett.* 11, 213–228. doi: 10.2174/0929866043407174

Walsh, D. M., Tseng, B. P., Rydel, R. E., Podlisny, M. B., and Selkoe, D. J. (2000). The oligomerization of amyloid β-protein begins intracellularly in cells derived from human brain. *Biochemistry* 39, 10831–10839. doi: 10.1021/bi001048s

Weber, J. T. (2012). Altered calcium signaling following traumatic brain injury. *Front. Pharmacol.* 3:60. doi: 10.3389/fphar.2012.00060

Wojda, U., Salinska, E., and Kuznicki, J. (2008). Calcium ions in neuronal degeneration. *IUBMB Life* 60, 575–590. doi: 10.1002/iub.91

Wu, H.-Y., and Lynch, D. R. (2006). Calpain and synaptic function. *Mol. Neurobiol.* 33, 215–236. doi: 10.1385/MN:33:3:215

Yamakawa, H., Banno, Y., Nakashima, S., Yoshimura, S.-i., Sawada, M., Nishimura, Y., et al. (2001). Crucial role of calpain in hypoxic pc12 cell death: calpain, but not caspases, mediates degradation of cytoskeletal proteins and protein kinase c-α and-δ. *Neurol. Res.* 23, 522–530. doi: 10.1179/016164101101198776

Yang, J., Weimer, R. M., Kallop, D., Olsen, O., Wu, Z., Renier, N., et al. (2013). Regulation of axon degeneration after injury and in development by the endogenous calpain inhibitor calpastatin. *Neuron* 80, 1175–1189. doi: 10.1016/j.neuron.2013.08.034

Yang, L.-B., Lindholm, K., Yan, R., Citron, M., Xia, W., Yang, X.-L., et al. (2003). Elevated β-secretase expression and enzymatic activity detected in sporadic Alzheimer disease. *Nat. Med.* 9, 3–4. doi: 10.1038/nm0103-3

Zhang, Y.-w., Thompson, R., Zhang, H., and Xu, H. (2011). App processing in alzheimer's disease. *Mol. Brain* 4:3. doi: 10.1186/1756-6606-4-3

Conflict of Interest Statement: The authors declare that the research was conducted in the absence of any commercial or financial relationships that could be construed as a potential conflict of interest.

Copyright © 2018 Ashraf, Ahmad, Ali and Ul-Haq. This is an open-access article distributed under the terms of the Creative Commons Attribution License (CC BY). The use, distribution or reproduction in other forums is permitted, provided the original author(s) and the copyright owner are credited and that the original publication in this journal is cited, in accordance with accepted academic practice. No use, distribution or reproduction is permitted which does not comply with these terms.

frontiers in Aging Neuroscience

ORIGINAL RESEARCH
published: 18 May 2018
doi: 10.3389/fnagi.2018.00145

Streptozotocin Impairs Proliferation and Differentiation of Adult Hippocampal Neural Stem Cells *in Vitro*-Correlation With Alterations in the Expression of Proteins Associated With the Insulin System

*Ping Sun[1,2], Gabriela Ortega[2], Yan Tan[3], Qian Hua[3], Peter F. Riederer[2], Jürgen Deckert[2] and Angelika G. Schmitt-Böhrer[2]**

[1]Key Laboratory of Molecular Target & Clinical Pharmacology, School of Pharmaceutical Science & The Fifth Affiliated Hospital, Guangzhou Medical University, Guangzhou, China, [2]Center of Mental Health, Department of Psychiatry, Psychosomatics, and Psychotherapy, University Hospital of Würzburg, Würzburg, Germany, [3]School of Preclinical Medicine, Beijing University of Chinese Medicine, Beijing, China

OPEN ACCESS

Edited by:
Mohammad Amjad Kamal, King Fahad Medical Research Center, King Abdulaziz University, Saudi Arabia

Reviewed by:
Olivier Thibault, University of Kentucky, United States
Muddanna Sakkattu Rao, Department of Anatomy, Faculty of Medicine, Kuwait University, Kuwait

***Correspondence:**
Angelika G. Schmitt-Böhrer
schmitt_a3@ukw.de

Received: 25 February 2018
Accepted: 30 April 2018
Published: 18 May 2018

Citation:
Sun P, Ortega G, Tan Y, Hua Q, Riederer PF, Deckert J and Schmitt-Böhrer AG (2018) Streptozotocin Impairs Proliferation and Differentiation of Adult Hippocampal Neural Stem Cells in Vitro-Correlation With Alterations in the Expression of Proteins Associated With the Insulin System. Front. Aging Neurosci. 10:145. doi: 10.3389/fnagi.2018.00145

Rats intracerebroventricularily (icv) treated with streptozotocin (STZ), shown to generate an insulin resistant brain state, were used as an animal model for the sporadic form of Alzheimer's disease (sAD). Previously, we showed in an *in vivo* study that 3 months after STZ icv treatment hippocampal adult neurogenesis (AN) is impaired. In the present study, we examined the effects of STZ on isolated adult hippocampal neural stem cells (NSCs) using an *in vitro* approach. We revealed that 2.5 mM STZ inhibits the proliferation of NSCs as indicated by reduced number and size of neurospheres as well as by less BrdU-immunoreactive NSCs. Double immunofluorescence stainings of NSCs already being triggered to start with their differentiation showed that STZ primarily impairs the generation of new neurons, but not of astrocytes. For revealing mechanisms possibly involved in mediating STZ effects we analyzed expression levels of insulin/glucose system-related molecules such as the glucose transporter (GLUT) 1 and 3, the insulin receptor (IR) and the insulin-like growth factor (IGF) 1 receptor. Applying quantitative Real time-PCR (qRT-PCR) and immunofluorescence stainings we showed that STZ exerts its strongest effects on GLUT3 expression, as GLUT3 mRNA levels were found to be reduced in NSCs, and less GLUT3-immunoreactive NSCs as well as differentiating cells were detected after STZ treatment. These findings suggest that cultured NSCs are a good model for developing new strategies to treat nerve cell loss in AD and other degenerative disorders.

Keywords: streptozotocin, neural stem cells, proliferation, differentiation, insulin-like growth factor 1 receptor, insulin receptor, glucose transporter, Alzheimer's disease

INTRODUCTION

Streptozotocin (STZ) is a glucosamine derivative of nitrosourea produced by *Streptomyces achromogens* and toxic to the insulin-producing β cells of the pancreas in mammals (Eileen Dolan, 1997). It is used in medicine for treating certain cancers of the Islets of Langerhans (Murray-Lyon et al., 1968; Brentjens and Saltz, 2001) and also used in research to produce animal models for type 1 diabetes mellitus (T1DM) via high dose intraperitoneal (i.p.) injections (Like and Rossini, 1976) and type 2 diabetes mellitus (T2DM) with low doses i.p. injections (Reaven and Ho, 1991; Wang and Gleichmann, 1998; Yuan et al., 2016). STZ treatment causes typical aging-associated changes, such as telomere instability (Paviolo et al., 2015), mitochondrial dysfunction (Raza and John, 2012), genomic instability (Attia et al., 2009), metabolic dysfunction (Rodríguez-Mañas et al., 2009) and cellular senescence (Oubaha et al., 2016). Furthermore, T2DM induced by STZ i.p. injections exhibit increased brain aging and AD-like pathology, such as brain atrophy, Aβ aggregation, and synapse loss (Wang et al., 2014). With moderate to low dosage administration, STZ causes insulin resistance by decreased autophosphorylation of the insulin receptor (IR; Kadowaki et al., 1984; Blondel and Portha, 1989).

IR can be activated by insulin-like growth factor (IGF)-1 and -2 besides insulin (Ward and Lawrence, 2009) and plays a key role in the regulation of glucose homeostasis. Besides the insulin-sensitive glucose transporter (GLUT)4, which is shown to be primarily expressed by cerebellar neurons, the insulin-independent GLUT1 is the main transporter responsible for glucose transport across the blood-brain barrier into the brain and into astrocytes (Leybaert et al., 2007) and GLUT3 is responsible for glucose transport into neurons (for review, see Simpson et al., 2007). Reduced IR signaling may finally results in insulin resistance, accompanied by impaired ability to maintain cell glucose and energy homeostasis (Draznin, 2006; Moloney et al., 2010; Talbot et al., 2012; Talbot, 2014). Insulin resistance in non-neural tissues can be considered as the reason for many peripheral metabolic disorders such as T2DM (Reaven, 1988). Insulin resistance in the brain may trigger pathophysiological key events of neurodegenerative disorders such as Alzheimer's disease (AD) and therefore can be linked to these disorders (Correia et al., 2011; Talbot et al., 2012).

Individuals with diabetes have higher risk for developing dementia syndromes (Ott et al., 1999; Roriz-Filho et al., 2009; Riederer et al., 2017). Epidemiologic studies revealed a significant association between T2DM and AD, and that metabolic dysfunctions like hyperglycemia and hyperinsulinemia and/or hypoinsulinemia are closely correlated with AD pathophysiology (Ryan and Geckle, 2000; Allen et al., 2004; Matsuzaki et al., 2010; Ou et al., 2018). Therefore, disturbances of brain glucose uptake, glucose tolerance and glucose utilization and impairment of the insulin/IR signaling cascade are thought to be key targets for the neuropathology of the sporadic form of AD (sAD) which covers >95% of AD patients (Grünblatt et al., 2007; de la Monte, 2009; Salkovic-Petrisic et al., 2009; Talbot et al., 2012).

STZ intracerebroventricularily (STZ icv) treated rats, which develop an insulin resistant brain state shortly after treatment, have been suggested to act as an animal model for sAD (Grünblatt et al., 2007; de la Monte, 2009; Salkovic-Petrisic et al., 2009). In this animal model, cognitive function was shown to be impaired already a few weeks after STZ icv treatment (Mayer et al., 1990; Blokland and Jolles, 1993) paralleled by cholinergic deficits (Hellweg et al., 1992), oxidative stress (Sharma and Gupta, 2001), neuronal loss (Shoham et al., 2003), amyloid angiopathy (Salkovic-Petrisic et al., 2011), increasing tau protein (Salkovic-Petrisic et al., 2006) as well as insulin signaling pathway damage (Salkovic-Petrisic et al., 2006). Brain glucose metabolism has been found to be dramatically harassed in this animal model including decreased glucose utilization (Duelli et al., 1994) and reduced glycolytic key enzymes activity (Plaschke and Hoyer, 1993), diminished adenosine triphosphate (ATP) and creatine phosphate (Lannert and Hoyer, 1998). The neuron-specific GLUT3 has been found to be significantly reduced in this rat model (Salkovic-Petrisic et al., 2013).

Neural stem cells (NSCs), which were able to give birth to new neurons, astrocytes and oligodendrocytes in the developing as well as in the adult brain, primarily exist in few neurogenic regions in most mammals, including humans (Altman and Das, 1965; Eriksson et al., 1998; Wiskott et al., 2006). Aside from the subventricular zone of the lateral ventricle, the dentate gyrus (DG) of the hippocampus is one of the neurogenic regions in the adult brain (Kempermann and Gage, 2000; Kempermann et al., 2004; Ming and Song, 2005; Von Bohlen Und Halbach, 2011). From a functional point of view, hippocampal adult neurogenesis (AN) plays an important role in structural plasticity and network adaptation and is likely to contribute to learning and memory processes (Aimone et al., 2010). The question of a possible involvement of altered AN in AD etiopathology is not satisfactorily answered, yet. Discrepancies between results of various studies may result from the different AD animal models used in these AN studies. Besides, NSCs can be discussed to have therapeutic potential in the treatment of neurodegenerative disorders such as AD (Abdel-Salam, 2011), Parkinson's disease (Nishimura and Takahashi, 2013), as well as traumatic injuries of the nervous system (Longhi et al., 2005) and aging (Leeman et al., 2018). Hippocampal NSCs transplantation as well as stimulating AN through physical exercise and drugs could rescue cognitive deficits in AD mice (van Praag et al., 1999; Dong S. et al., 2012; Chen et al., 2015) by enhancement of hippocampal synaptic density (Blurton-Jones et al., 2009). Elevating AN may have therapeutic potential for the treatment of AD, e.g., compensation of neuronal as well as synaptic loss observed in the AD brain (Selkoe, 2002). Therefore, it is worth characterizing NSCs and studying their performance and regulation during normal aging as well as in the disease state.

AN is a dynamic process tightly regulated by intrinsic and extrinsic factors, including molecules of the Insulin/IGF-1 signaling pathway (Bateman and McNeill, 2006). IGF-1 is a key factor in the regulation of NSCs, as in the absence of IGF-I neither the epidermal growth factor (EGF) nor the fibroblast growth factor 2 (FGF-2) were able to induce the proliferation of E14 mouse striatal cells (Arsenijevic et al., 2001). Moreover, high

concentrations of insulin promote the differentiation of newborn cells into neurons (Han et al., 2008). However, the impact of the Insulin/IGF-1 signaling pathway on the proliferation of NSCs and the differentiation fate of their progeny has not been uncovered at the cellular level. Our recently published *in vivo* study dealing with the effects of STZ icv injections on AN indicated reduced neuron generation after 3 months predominantly in the septal part of the hippocampus (Sun, 2015; Sun et al., 2015).

Therefore we aimed at uncovering cellular mechanisms underlying the negative effect of STZ on AN. With an *in vitro* approach using hippocampal NSCs we investigated the possible influence of STZ on the proliferation of NSCs, their migration and differentiation, and whether STZ treatment alters the expression levels of genes related to the insulin system such as the IR, IGF-1 receptor (IGF-1R) and GLUT1 and 3.

MATERIALS AND METHODS

Isolation of Neural Stem Cells—Establishment of Primary Adult Neural Stem Cell Cultures of Rat Hippocampi

Adult NSCs were derived from both hippocampi of Wistar rats (in total about 50 rats were used, 2 months ± 1 week old; Charles River, Sulzfeld, Germany). After performing a pilot study using rats of different ages with the result that younger animals generate more neurospheres than older ones we decided to continue working with these young adult rats, even if older animals would have been the better choice to study neurobiological mechanisms of human sAD with an onset around 65 years. In brief, hippocampi were dissected mechanically on ice and enzymatically dissociated in a 0.01% papain–0.1% protease–0.01 DNase I (PPD) solution (each enzyme was obtained from Worthington Biochemicals, USA and dissolved in Hank's Balanced Salt Solution). Cells were collected by centrifugation at 110 *g* for 7 min (RT) and then re-suspended in proliferation cell culture medium composed of NeuroCult^{TM} NS-A Basal medium (containing 0.6% glucose; STEMCELL_Technologies, USA) supplemented with Neurocult^{TM} NS-A proliferation supplement (containing 25 μg/ml insulin; 10%), EGF (20 ng/ml, Peprotech, Germany), basic fibroblast growth factor (bFGF; 10 ng/ml, Peprotech, Germany) and Heparin (2 μg/ml, STEMMCELL, USA). Next, cells were plated onto T25 culture flasks (Corning, USA) and maintained in a humidified incubator with 5% CO_2 at 37°C. In general, proliferation medium was replaced every 7 days. After 2 days of incubation in proliferation medium neurospheres had been formed and were visible.

For the characterization of cells composing such neurospheres immunofluorescence stainings were performed using antibodies detecting nestin, a marker for NSCs. For that, neuroshperes were seeded on poly-L-ornithine/laminin-coated coverslips (Neuvitro, El Monte, CA, USA) in proliferation culture medium. After approximately 2 h of incubation, most neurospheres were attached to the coverslips, a prerequisite for the subsequent immunofluorescence staining. Then, they were fixed with 4% PFA (dissolved in PBS) at RT for 20 min and immunostained for nestin (for details see below).

Treatment With STZ

Stem Cell Proliferation

First, a dilution series of STZ was applied to NSCs to select a suitable STZ concentration. For that, neurospheres (which had been passaged already two times) were enzymatically dissociated using a PPD solution and then obtained single cells were seeded into 96-well plates (Life Technologies, Gaithersburg, MD, USA) with 2000 cells per well in proliferation cell culture medium (see above). A 0.5 M stock solution of STZ diluted in citrate buffer (0.1 M, pH 4.5) was prepared. Cells were incubated in proliferation medium containing five different final STZ concentrations (0, 1.0, 2.5, 5.0 and 10 mM) for 4 days. Then, the number of neurospheres per well (size >5 cells) was estimated under the BX40 microscope (Olympus, Tokyo, Japan) at 10× magnification.

In subsequent experiments (proliferation, migration and differentiation assays) STZ at a concentration of 2.5 mM was used with different incubation times (2–8 days).

Time-Dependency of STZ Influence

For unraveling the time-dependency of STZ effects on the generation of neurospheres, we performed a long-term incubation study with or without 2.5 mM STZ. The same proliferation assay was performed as described above and the number of neurospheres per well was estimated after 2, 4, 6 and 8 days of incubation with 2.5 mM STZ in proliferation cell culture medium under the microscope. Three independent experiments with each experiment stemming from three biological replicates (using the hippocampus of three rats) were performed, but only the results of one experiment were presented.

Effect of STZ on the Size of Newly Generated Neurospheres

For the evaluation of the *percentage of neurospheres of different sizes*, we measured the diameter of each neurosphere (μm). Neurospheres were generated using a single cell suspension (generated via dissecting neurospheres as described above) and then plated in a 96-well plate (2000 cells/well) for 7 days. The number of neurospheres exhibiting certain sizes (<50 μm, 50–99 μm, 100–149 μm, 150–199 μm and ≥200 μm) were estimated with the help of the BX40 microscope and the Image-Pro-Plus 5.0 software (Media Cybernetics, Rockville, MD, USA). We performed these experiments three times, collected all the data and then calculated the mean size ± SD of neurospheres with a certain size.

5-Bromodeoxyuridine (BrdU) Incorporation Assay

For the estimation of the proliferation of NSCs a BrdU incorporation assay was performed. For that, cells of a single cell suspension were generated via dissecting neurospheres (as described above) and were then seeded on pre-coated coverslips in a 24 well plate (10,000 cells per well; Sarstedt, Nümbrecht, Germany). After 2 days of incubation in proliferation medium,

10 μM BrdU (BrdU stock solution contained 10 mM BrdU dissolved in D-PBS) was added to culture medium for 4 h to label proliferating cells. Next, cells were fixed with 4% PFA and a BrdU/DAPI immunofluoresence double staining was performed (for details see below). After picturing of stained cells the percentage of BrdU-positive cells was calculated using 10–15 pictures per group out of three independent experiments.

Migration Assay

Rat hippocampal neurospheres were collected via centrifugation (110 *g*, 7 min) and then re-suspended with differentiation cell culture medium composed of Neurocult™ NS-A basal medium (with 0.6% glucose) and 10% Neurocult™ NS-A differentiation supplement (with 25 μg/ml insulin). Neurospheres were seeded on pre-coated coverslips in a 24-well plate (10–14 neurospheres per well; Sarstedt, Nümbrecht, Germany) and after approximately 2 h (most of the neurospheres should have been attached in the meantime) the differentiation cell culture medium was refreshed with culture medium with or without 2.5 mM STZ. After 2 days of incubation, images were taken using the BX40 microscope and the migration distance was estimated with the help of Image-Pro-Plus 5.0 software. Distance from the cell to the rim of the respective originating neurosphere was defined as the migration distance. Overall, 15–20 images per group out of three independent experiments were analyzed.

Differentiation Assay

For characterization of the cellular phenotype of differentiating newborn cells and the effect of STZ on the differentiation fate, 10–15 neurospheres per well after the second passage were collected and then promoted to differentiate using the same procedure as described in the migration assay above. After 2 days of incubation, we aspired cell culture medium and added 0.5 ml of the fixative (4% PFA dissolved in PBS) for 30 min at RT. Immunofluoresence detection of young neurons and astrocytes with anti-Tuj-1 and GFAP antibodies, respectively, was performed. Finally, a DAPI stain was applied for visualizing of all cultured cells. For quantification of immunoreactive (ir) cells, 15–20 images out of three independent experiments was determined.

Detection of Insulin Receptor and Glucose Transporter 3 Protein in NSCs as Well as in Differentiating Cells

For immunostaining of NSCs, single cells enzymatically dissociated from neurospheres were placed on pre-coated coverslips in a 24-well plate (20,000 cells/well). After exposure to 2.5 mM STZ for 2 days, we fixed obtained cells with 4% PFA and immunostained them with antibodies detecting the IR and the glucose transporter 3 (GLUT3; for details see below).

In order to further characterize differentiating cells, they were generated (as described above in the chapter "differentiation assay"; also with or without 2.5 mM STZ) and processed for immunofluorescence stainings with GLUT3 and IR antibodies (for details see below). A DAPI stain was applied for visualizing all cultured cells. For quantification, we calculated the percentage of IR or GLUT3 positive cells using 15–20 replicate images per group out of three independent experiments.

Single and Double Immunofluorescence Staining

Immunodetection of BrdU

After NSCs had been fixed with 4% PFA (dissolved in PBS), they were washed three times with TBS for 5 min and DNA denaturation was achieved by incubation with 1 N HCl at 37°C for 10 min. Then, we neutralized low pH-values with 0.1 M boric acid (pH 8.5) for 10 min and subsequently rinsed the cells with TBS three times. Non-specific immunoreactions were blocked with 5% normal goat serum for 1.5 h. The mouse anti-BrdU antibody (monoclonal antibody, 1:300; MCA2483; Serotec, Kidlington, UK) was used as the primary antibody, and donkey anti-mouse IgGs conjugated with Alexa 555 (1:600; Life science, Carlsbad, CA, USA) as the secondary antibody. After rinsing remaining cells fixed to coverslips, all nuclei were stained with DAPI (300 nM) for 5 min at RT, and then washed again. Finally, coverslips were mounted to slides with Fluoromount™ Aqueous Mounting Medium (DAKO, Hamburg, Germany).

Single and Double Immunofluorescent Stainings

For immunofluorescent single and double stainings of NSCs as well as differentiating cells with primary antibodies detecting Tuj-1 (monoclonal mouse antibody, 1:250; ab14545, Abcam, Cambridge, MA, USA), GFAP (polyclonal rabbit antibody, 1:500; Z0334, DAKO, Hamburg, Germany), Nestin (polyclonal rabbit antibody, 1:250; ab92391, Abcam, Cambridge, MA, USA), IR (monoclonal mouse antibody, 1:250; ab69508, Abcam, Cambridge, USA) and GLUT3 (polyclonal rabbit, 1:500; ab41525, Abcam, Cambridge, USA) proteins, applied protocols were similar to the BrdU staining described above, but without treatment with 1 N HCl for 10 min and subsequent incubation step with boric acid. For double immunofluorescent stainings we used two primary antibodies produced in different species. Secondary antibodies utilized were the following: donkey anti mouse IgGs conjugated with Alexa 488 and donkey anti-rabbit IgGs conjugated with Alexa 555 (both diluted 1:500, Life science, Carlsbad, CA, USA). DAPI was always used as a nuclear stain.

Quantitative Real Time-PCR

Total RNA was extracted from neurospheres, which had been treated with or without 2.5 mM STZ for 2 days, using RNeasy kit from QIAGEN following manufacturer's instructions. cDNAs were synthesized with the help of the first cDNA synthesis kit (Bio-Rad, Hercules, CA, USA) and 20 ng RNA per sample. QRT-PCR was performed in 384-well plates (life technologies, Gaithersburg, MD, USA) using a CFX384 Real-Time system (Bio-Rad, USA) and SYBR green. The relative amount of the message of interest was normalized to the expression level of the reference gene GAPDH. C_T values of duplicates or triplicates were analyzed with LinRegPCR software.

Statistical Analysis

For the NSCs proliferation assay and the cell migration study with various concentrations of STZ, data analyses were

performed with one-way ANOVA, followed by *post hoc* comparison with Bonferroni *post hoc* test using SPSS software (Version 22.0, IBM Inc., Chicago, IL, USA). For the statistical evaluation of all other experimental data, Student's *t*-test was used. Data were presented as mean ± standard deviation (SD). Significance levels were set at $^{*}p < 0.05$; $^{**}p < 0.01$; $^{***}p$-value < 0.001.

RESULTS

We cultured NSCs using the three-dimensional neurosphere method. NSCs isolated from adult rat hippocampus proliferated quickly forming small free-floating clusters of NSCs first, and then forming larger neurospheres 1 week after seeding (**Figure 1A**). Nestin, a marker protein of neural progenitor cells, was expressed in these neurospheres (**Figure 1B**). After replacing the proliferation cell culture medium by the differentiation cell culture medium [without EGF and bFGF], neurospheres were cultivated for two additional days. Cells originating from such a neurosphere started to migrate and became immunoreactive for Tuj-1 (marker for immature neurons) or GFAP (marker for astrocytes; **Figure 1C**).

STZ Impairs the Proliferation of Neural Stem Cells

To determine the optimal STZ concentration for investigating its effect on the proliferation of NSCs *in vitro*, NSCs (single cells, after the second passage) were seeded in a 96-well plate and treated with increasing concentrations of STZ. Four days of incubation with different STZ concentrations resulted in an overall, but dose-dependent, decrease of the number of neurospheres (ANOVA: $p < 0.001$; *Post hoc* analysis: 1 mM: 29.3%, $p < 0.05$; 2.5 mM: 53.3%, $p < 0.05$; 5 mM: 67.3%, $p < 0.05$ and 10 mM: 79.0%, $p < 0.05$) compared to the control group (0 mM STZ; **Figure 2A**).

As we preferred moderate, but not too strong effects of STZ, we choose 2.5 mM for all subsequent experiments. To determine the time-dependency of the effectiveness of STZ, NSCs were treatment with STZ for different time periods and the number of neurospheres was then counted (**Figure 2B**). STZ significantly decreased the number of neurospheres in a time-dependent manner (ANOVA: $p < 0.05$; *Post hoc* analysis: after 2 days of incubation a reduction of 25.1%, with $p < 0.05$; after 4 days a reduction of 53.85%, $p < 0.05$; after 6 days a reduction of 59.8%, $p < 0.05$; after 8 days a reduction of 62.8%, $p < 0.05$). As it is known that the size of neurospheres is directly related to proliferative capacity, we quantified the diameter of neurospheres after 7 days in the presence or absence of STZ. In cell culture medium with STZ significantly lower numbers of big neurospheres, e.g., with a diameter of ≥200 μm ($p = 0.018$, 4.85 ± 1.43%) and of neurospheres with a diameter between 150 μm and 199 μm ($p = 0.025$, 6.41 ± 1.86%) were detected when comparing to neurospheres in cell culture medium without STZ (≥200 μm: 8.21 ± 2.10%; 150–199 μm: 12.48 ± 4.45%). However, significantly greater number of small neurospheres with a diameters <50 μm were detected in the STZ treatment group ($p = 0.007$, 50.10 ± 5.10%) compared to control group (38.96 ± 4.90%; **Figure 2C**).

The thymidine analog bromodeoxyuridine (BrdU) is widely used to label cell proliferation because it incorporates into replicating DNA of dividing cells and can be immunodetected subsequently (Taupin, 2007). Without STZ treatment about 20% of NSCs had incorporated BrdU after 4 h of incubation (**Figure 2F**). Adding STZ to the cell culture medium resulted in a significant decrease of the percentage of BrdU-positive cells out of the total number of DAPI-positive cells ($p < 0.001$) to 12.9% (**Figures 2D–F**).

STZ Does Not Affect the Migration of Newborn Differentiating Cells

In the subgranular zone of the hippocampal DG, NSCs differentiate into immature neurons which then migrate into the granule cell layer, where they mature into granule cells finally integrating into local neuronal circuitries (Ming and Song, 2005). To study the effect of STZ on this migration process, 10–15 neurospheres after the second passage were directly plated

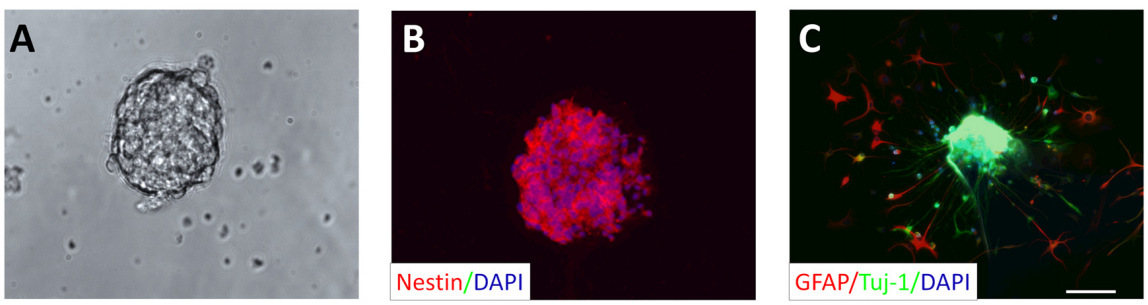


FIGURE 1 | Neural stem cell (NSC) culture: neurosphere generation derived from adult rat hippocampus. **(A)** Culturing of NSCs in proliferation cell culture medium resulted in the formation of neurospheres after 1 week. **(B)** Representative neurosphere after the second passage shows immunoreactivity for nestin, a marker for NSCs (red). All cells composing the neurosphere were counterstained with the cell nucleus stain DAPI (blue). **(C)** Cells originating in a neurosphere, but cultivated in differentiation culture medium for 2 days display positive immunoreactivity for the marker for immature neurons Tuj-1 (green) and the astrocytic marker GFAP (red). DAPI was used to stain all cell nuclei (blue). Scale bar in **(C)** represents 50 μm for **(A–C)**.

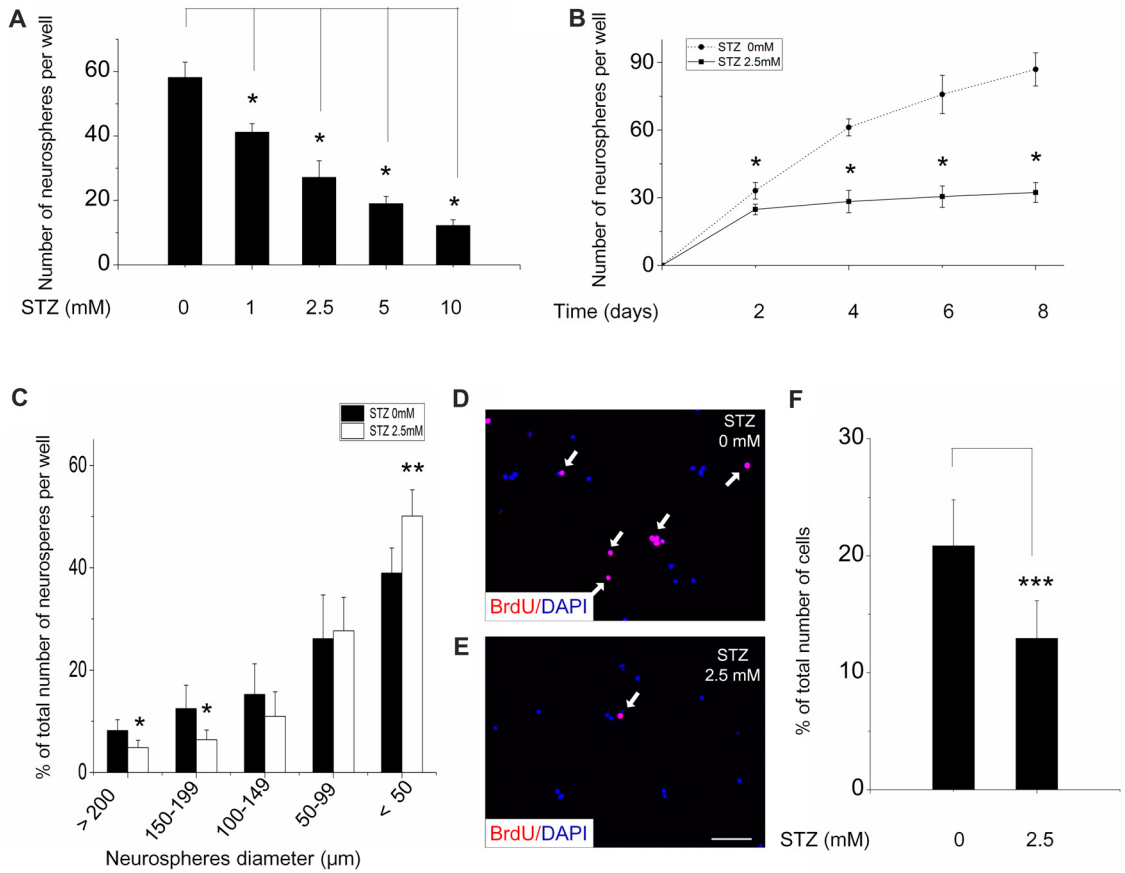


FIGURE 2 | Streptozotocin (STZ) decreases proliferation of neural stem cells and the formation of neurospheres. Cells from neurospheres after the second passage were incubated with various concentrations of STZ for 4 days **(A)** and with 2.5 mM STZ for 8 days **(B)**. **(C)** Size distribution of neurospheres after incubation in culture medium with or without 2.5 mM STZ for 7 days. A significantly lower percentage of large neurospheres was counted in culture media with STZ. **(D–F)** STZ decreases the number and percentage of bromodeoxyuridine (BrdU)-positive NSCs. Data in **(A,B)** are presented as the number of neurospheres per well ± standard deviation (SD). Data in **(C)** are expressed as the percentage of neurospheres of a certain size (% of total number of neurospheres) ± SD. Data in **(F)** are presented as the percentage of BrdU-positive cells (% of total number of DAPI-positive cells) ± SD. **p*-value < 0.05, ***p*-value < 0.01, ****p*-value < 0.001.

on pre-coated coverslips in 24-well plates and incubated in differentiation culture medium with or without STZ (0.1, 0.5, 1, 2.5 mM STZ) for 2 days. The migration distance of newborn cells treatment with STZ were very similar with the control group, which suggested that the STZ-exposure did not affect the ability and speed of newborn cells to migrate (ANOVA; $p = 0.215$; **Figure 3**).

Effect of STZ on the Differentiation Fate of Newborn Cells

The neuronal phenotype of differentiating cells was determined by using Tuj-1 as a marker of immature neurons and GFAP as a marker for astrocytes. After 2 days of incubation in the differentiation medium, Tuj-1- and GFAP-positive cells were found in close vicinity of the neurospheres they originate from (**Figure 1C**). Double immunofluorescence stainings of cells, differentiated for 2 days in cell culture medium with and without STZ, suggested a negative effect of STZ exclusively on the number of Tuj1-positive cells, but not on the number of GFAP-positive cells (**Figures 4A,B**). Quantitative analysis demonstrated that the percentage of cells immunoreactive for Tuj-1 were significantly lower after 2 days of STZ treatment than those incubated in the normal differentiation medium (a decrease of 45.5%; $p = 0.003$; **Figure 4C**). However, the percentages of cells immunopositive for GFAP were not significantly different between the STZ treatment and the control group (**Figure 4D**).

Effect of STZ on Insulin Receptor, Insulin-Like Growth Factor 1 Receptor and Glucose Transporter 1 and 3 mRNA Expression in Neural Stem Cells

In the STZ icv treatment rat model (*in vivo*), brain glucose/energy metabolism abnormalities were found in all hippocampal subfields, such as decreased glucose utilization (Duelli et al., 1994). GLUT3 is most known for its specific expression in neurons and has originally been designated as the neuronal

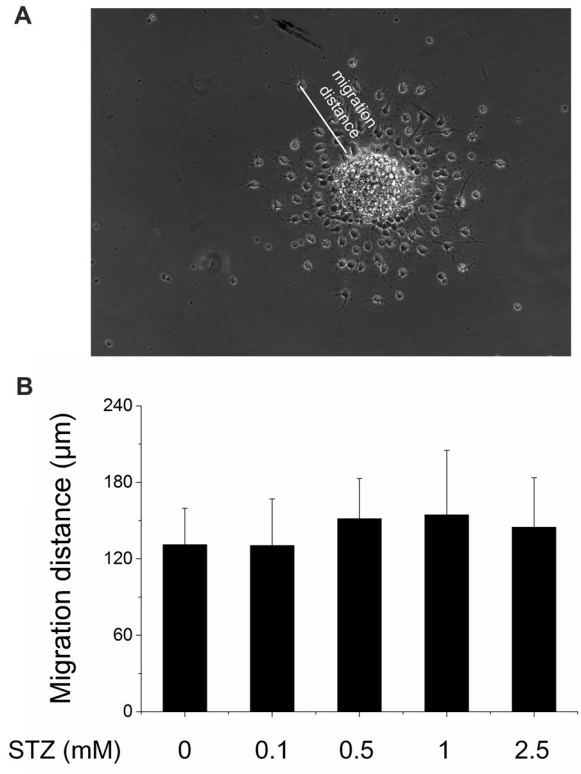


FIGURE 3 | No effect of STZ on the migration capability of newborn differentiating cells. Neurospheres after the second passage were seeded in 24-well plates (10–15 neurospheres) and exposed to different concentrations of STZ in differentiation culture medium. **(A)** Representative image of migrating cells originating from a neurosphere. Scale bar represents 100 μm. **(B)** Migration distances of cells originating from neurospheres exposed to 0.0, 0.1, 0.5, 1.0 and 2.5 mM STZ. Data are expressed as the mean migration distance measured from the differentiating cells to the rim of the neurosphere ± SD.

GLUT (Kayano et al., 1988) and also been found to be expressed in adult NSCs (Maurer et al., 2006). Furthermore, insulin system dysfunction accompanied by diminished IR expression in hippocampus develops in consequence of STZ-icv administration (Grünblatt et al., 2007; Salkovic-Petrisic et al., 2013). In order to study possible STZ effects on the expression of glucose metabolism-related genes such as IR, IGF-1R, GLUT1 and GLUT3, we performed quantitative real time-PCR (qRT-PCR). After 2 days of incubation in cell proliferation medium, STZ remarkably decreased the relative expression levels of GLUT3 mRNA by 46.4% ($p = 0.041$). However, STZ treatment did not affect relative expression levels of IR and GLUT1 in NSCs (**Figure 5**).

Effect of STZ on the Expression of Insulin Receptor and Glucose Transporter 3 Protein Levels in NSCs and Differentiating Cells

We further studied the effects of STZ on IR and GLUT3 protein expression levels in NSCs and differentiating cells via immunostaining with respective antibodies and used DAPI for counterstaining. For immunostaining of NSCs, single cells dissociated from neurospheres were plated on pre-coated coverslips in proliferation medium with and without 2.5 mM STZ for 2 days. For differentiating cells, neurospheres were seeded on pre-coated coverslips in differentiation culture medium with or without 2.5 mM STZ. Nearly all NSCs and differentiating cells express the IR (NSCs: approximately 96%; differentiating cells: approximately 98%; **Figure 6B**) as well as the GLUT3 (NSCs: approximately 91%; differentiating cells: approximately 95%; **Figure 6D**) without STZ treatment. However, STZ treatment reduced the number of NSCs in general as well as the percentage of IR-positive NSCs by 42.2% ($p = 0.003$; **Figures 6A,B**) and GLUT3-positive NSCs by 61.7% ($p = 0.001$; **Figures 6C,D**) compared to the control group. Different from the effect of STZ on NSCs, STZ did not affect the percentage of IR-positive differentiating cells (**Figures 6A,B**). But, treatment of differentiating cells with STZ resulted in a significantly decreased percentage of GLUT3-ir cells by 47.3% compared to controls ($p = 0.015$; **Figures 6C,D**).

DISCUSSION

STZ-treated adult NSCs produce fewer and smaller neurospheres as well as a reduced percentage of BrdU-positive cells. Although we could not exclude the possibility that the decreasing number and size of neurospheres mainly are the result of cell death, the decreased number of BrdU-positive cells indicate that at least the inhibition of cell proliferation is partly participating in the reduction of NSCs numbers. These findings are similar to a study previously reported by Qu et al. (2012), even if they used a much higher concentration of STZ (8 mM) than we did. As shown by Qu et al. (2012) STZ elicits a striking increase of cellular reactive oxygen species (ROS) in NSCs. Although proliferative NSCs maintain high endogenous ROS status and pharmacological or genetic manipulations that diminished cellular ROS levels interfered with normal NSCs function both in *in vitro* and *in vivo* studies (Le Belle et al., 2011), an excess of intracellular ROS induces cell death and inhibits NSCs proliferation (Limoli et al., 2006). Elevated intracellular ROS levels in NSCs caused by the treatment of NSCs with the glutathione synthetase inhibitor buthionine sulfoximine reduces the number of NSCs (Prozorovski et al., 2008).

Different from the results of this *in vitro* study, our previously published *in vivo* study (Sun, 2015; Sun et al., 2015) suggested that STZ significantly affects the survival of newborn cells, but not stem cell proliferation (Sun, 2015; Sun et al., 2015). The micro-environment in an animal's brain is much more complex than in cell culture and this may be the reason for the discrepancy between *in vivo* and *in vitro* study results. *In vivo*, STZ may not only target newborn cells directly (as it certainly happens in cell culture) but also indirectly through acting on other types of cells. *In vivo*, the neurogenic niche, where NSCs give birth to new cells, contains various cell types such as astrocytes, microglial cells, various types of neurons as well as endothelial cells (as NSCs are localized in close proximity of blood vessels) and all these cells form a complex neurogenic micro-environment in

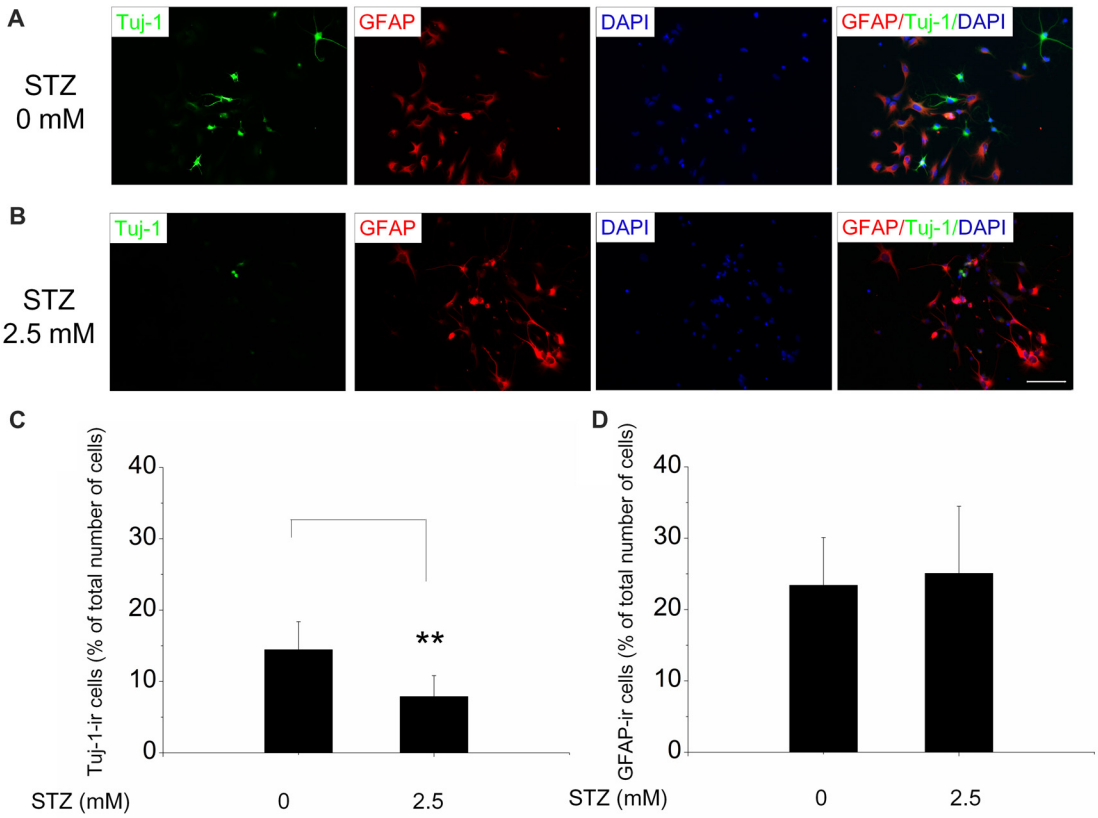


FIGURE 4 | STZ diminishes the generation of new neurons, but has no effect on the number of new astrocytes. Neurospheres after the second passage were exposed to 2.5 mM STZ for 2 days in differentiation medium, and then stained with antibodies. **(A,B)** Representative photomicrographs of early differentiating cells with Tuj-1 (green) and GFAP (red) immunoreactivity exposed to 0 mM **(A)** or 2.5 mM STZ **(B)** for 2 days. All cells were counterstained with DAPI (blue). Scale bar represents 50 μm. **(C,D)** Quantitative analysis of the percentage of Tuj-1- or GFAP-immunoreactive (ir) cells analyzing 10–12 representative images per treatment group. Data are expressed as the percentage of Tuj-1- **(C)** or GFAP- **(D)** -ircells (in relation to the overall number of DAPI-positive cell nuclei) ± SD. $^{**}p$-value < 0.01.

the subgranular zone (Palmer et al., 2000). In consequence, the neurogenic niche plays an important role in the regulation of the survival and self-renewing capacity of stem cells (Kazanis et al., 2008) that depends on the change of vasculature (Palmer et al., 2000), growth and trophic factors (Anderson et al., 2002; Lee et al., 2002) and the support through glial cells (Morrens et al., 2012). A comparable micro-environment for proliferating NSCs is almost missing in a normal cell culture system, as in *in vitro* studies. Besides directly affecting NSCs STZ could also induce neuronal apoptosis (Unsal et al., 2016), astrogliosis and the activation of microglia (Chen et al., 2013). Therefore, NSCs in the brain could be regulated by several factors secreted by apoptotic neurons or activated microglia, such as high mobility group box 1 (HMGB1) and TNF-α, respectively (Kawabata et al., 2010; Shu et al., 2018). Inhibition of cells secreting proinflammatory cytokines (i.e., IL-1β, IL-6, TNF-α and IFN-γ) significantly inhibited neurogenesis in the subventricular zone (Shigemoto-Mogami et al., 2014). Furthermore, AN is shown to be remarkably influenced by several growth and trophic factors such as insulin/IGF (Grünblatt et al., 2007), NGF (Hellweg, 1994) as well as BDNF (Shonesy et al., 2012; Liu et al., 2014) which were suggested to be altered in the STZ icv rat model. We speculate that the discrepancy of results revealed by our recently published *in vivo* study and this cell culture study may be primarily due to the complex micro-environment of an AN niche missing under *in vitro* conditions. Furthermore, although STZ treatment could impair NSCs proliferation directly, the interactions between NSCs, mature neurons and glia cells may compensate this damage in the animal's brain.

Another reason of this discrepancy may derive from different methods for analysis applied in these studies. In our *in vivo* study, we detected stem cell proliferation and the number of newborn cells of the neuronal lineage by immunostaining of the endogenous markers MCM2 and NeuroD, respectively. Newborn cells survived for almost 4 weeks were analyzed with the BrdU integration and detection method. We revealed that 1 month after STZ treatment stem cell proliferation is not affected, but that 3 months after STZ treatment the number of survived BrdU-ir cells was significantly decreased. In the *in vitro* study, however, we counted newly produced neurospheres and BrdU-positive cells after a various number of days of STZ incubation. These different methods applied and different time lines may also induce discrepancies between *in vivo* and *in vitro* studies.

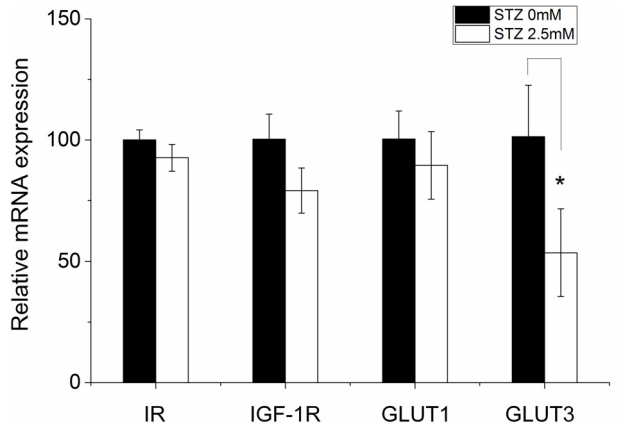


FIGURE 5 | STZ impacts the expression of some metabolism-related genes in neural stem cells. Ten to fifteen neurospheres after the second passage were seeded in a 6-well plate exposed to either 0.0 or 2.5 mM STZ for 2 days. Then, cells were collected and analyzed via quantitative real-time PCR. The relative mRNA expression level of glucose transporter (GLUT) 3 is significantly reduced in neural stem cells (NSCs) by 46.4% ($p = 0.041$) in consequence of 2.5 mM STZ exposure. Expression differences of the insulin receptor (IR), insulin-like growth factor 1 receptor (IGF-1R), and GLUT1 did not reach statistical significance. Data are presented as the mean of relative mRNA expression levels ± SD; *p-value < 0.05.

Migration of NSCs is a prerequisite for the formation of the central nervous system (CNS) and also plays a pivotal role in AN in the CNS of mammals (Hatten, 1999). Molecular mechanisms involved in the migration of NSCs in the adult brain are still poorly understood. Neural progenitors transplanted into mouse brain migrate towards areas of brain damage resulting from stroke (Arvidsson et al., 2002) or glioblastoma (Glass et al., 2005). Such studies support the idea that tumor necrosis factor-α (TNF-α), interferon-γ (IFN-γ) and monocyte chemoattractant protein-1 (MCP-1; Belmadani et al., 2006) secreted by damaged brain areas regulate the migration of these differentiating NSCs towards sites of inflammation. Moreover, it has been shown that STZ icv treatment elevates the level of TNF-α in rat brain (Rai et al., 2014) and IFN-γ in peripheral blood lymphocytes (Pandey and Bani, 2010). Whether these elevated TNF-α and IFN-γ levels then impact the migration of differentiating newborn cells is still an open question. Our *in vitro*-study showed that STZ did not influence the migration distance and migration speed of newborn cells. However, in our study we measured the migration of all kinds of cells (e.g., immature neurons and astrocytes) and cannot provide information about the migration performance of a specific cell type.

Contrary to our *in vivo* results (Sun, 2015; Sun et al., 2015), STZ in cell culture seems to influence the differentiation fate of newborn cells. We used a 2 days differentiation paradigm (cells were kept for 2 days in differentiation medium), which is shown to mimic the initial stage of differentiation with differentiating cells already expressing Tuj1 and GFAP (Aranha et al., 2011). Qu et al. (2012) also found that STZ reduces neuronal differentiation of NSCs using three neuronal markers, Tuj-1, microtubule-associated protein 2 (MAP 2) and neurofilament 150 (NF 150; Qu et al., 2012). Our data show that after 2 days of differentiation 15% of cells were Tuj-1 positive, and this percentage is lower compared to the results of Dong (34%, incubation in differentiation medium for 3 weeks; Dong C. et al., 2012) and of Qu (20%, incubation in differentiation medium for 1 week; Qu et al., 2012). However, besides different incubation times in differentiation medium applied in these studies, they used rats of different ages (postnatal day 0 or embryonic day 17 rats) for the isolation of NSCs. Because we studied AN, we selected young adult rats for this research. Our study showed that the percentage of GFAP-ir cells (20%) did not change in consequence of STZ treatment. Like with the proliferation of NSCs (we already discussed above) ROS may also impact the differentiation of newly produced cells. As high ROS levels seem to reduce new neuron generation, e.g., with differentiation of NSCs for 7 days in the presence of pro-oxidative bothionine sulfoximine or diethyldithiocarbamate, ROS seem to contribute to neural-fate decision (Prozorovski et al., 2008).

Under normal conditions, nearly all NSCs express IR and GLUT3 proteins. Although STZ treatment decreased number of NSCs (**Figure 2F**), remaining cells exhibit even a lower percentage of cells expressing IR and GLUT3 protein. In contrast to the staining results with antibodies detecting IR protein, mRNA expression levels of this receptor were not found to be influenced by STZ. Therefore, STZ may influence the process of IR protein translation, post-translational modification and/or subcellular distribution. As many studies have shown, Insulin/PI3 kinase signaling is necessary to maintain NSCs survival and self-renewal in the adult brain (Groszer et al., 2006; Siegrist et al., 2010).

Glucose transport into adult NSCs mainly relies on GLUT1 and GLUT3 as they do not express GLUT2 and GLUT4 (Maurer et al., 2006). The expression of GLUT1 is relatively stable. However, GLUT3 in NSCs seems to be sensitive to environmental changes. Stress induced by hypoxia and/or hyperglycemia dramatically increases GLUT3 expression at both, protein and mRNA levels, but only slightly up-regulates GLUT1 protein levels in NSCs (Maurer et al., 2006). There exist only few indications in the literature for a relationship between NSCs' proliferation and GLUT3 expression. However, GLUT3 was found to promote tumor cell proliferation in non-small cell lung cancer (Masin et al., 2014). GLUT3 may also increase NSCs' proliferation through the transport of more glucose into NSCs enhancing energy supply.

Differentiation fate of newborn cells may also be affected by the expression of GLUT3. At the stage of NSCs both transporters, GLUT1 and GLUT3, are expressed (Maurer et al., 2006), however, in astrocytes only GLUT1 can be detected, whereas newborn neurons mainly depend on GLUT3 for glucose transport (McCall et al., 1996; Dienel, 2012). The level of GLUT3 and GLUT1 expression may influence the potential of NSCs to differentiate. Decreased GLUT3 expression caused by STZ treatment may thus reduce the potential of NSCs toward neuronal-oriented differentiation without affecting the differentiation to astrocytes.

In summary, our *in vitro* study showed that STZ influences AN at different stages, during NSCs' proliferation as well as

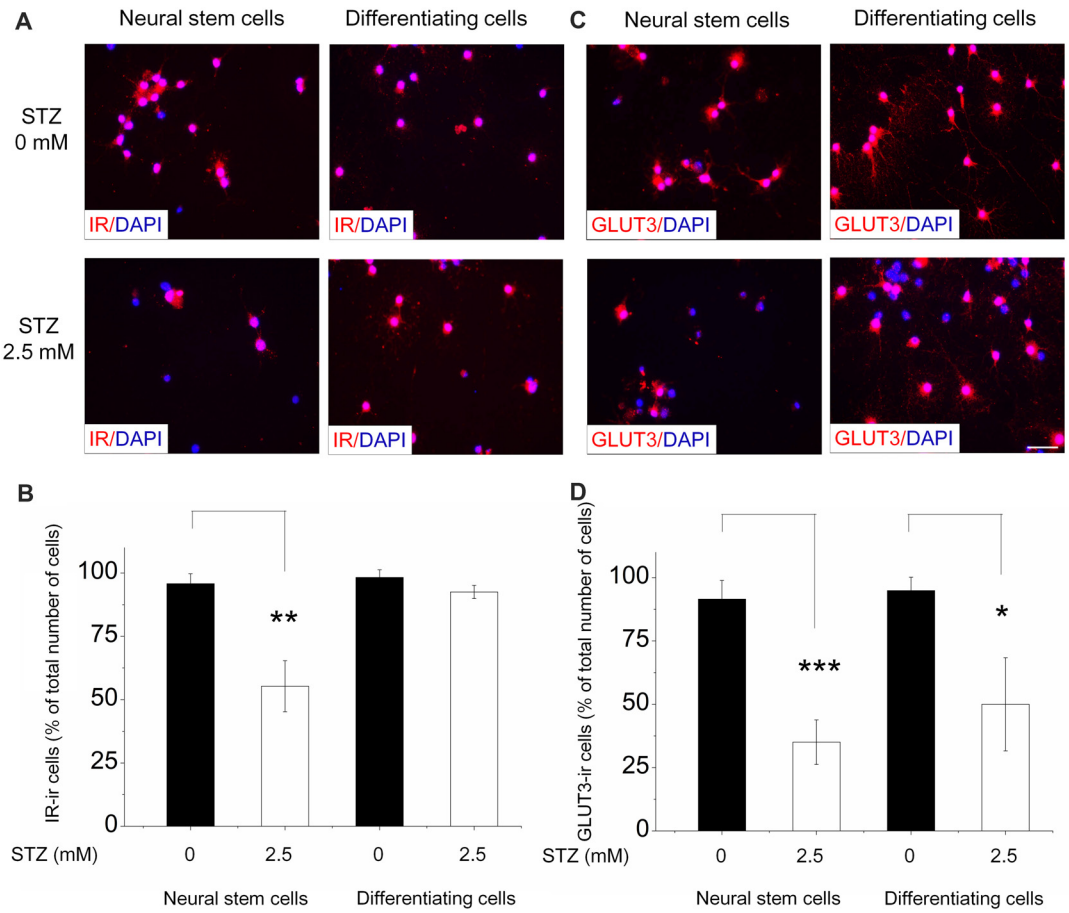


FIGURE 6 | STZ affects IR and GLUT 3 protein levels in neural stem cells and differentiating cells differentially. For the analysis of neural stem cells (NSCs), neurospheres were dissociated and seeded in a 24-well plate (20,000 cells/well). After 2 days of 0.0 or 2.5 mM STZ exposure we immunostained them for the detection of IR and Glucose transporter 3 (GLUT3). For differentiating cells, neurospheres were seeded in a 24-well plate and let them grow in differentiation culture medium with or without 2.5 mM STZ for 2 days. **(A,C)** Immunostaining with IR and GLUT3 antibodies revealed that almost all NSCs and differentiating cells express IR as well as GLUT3. **(B)** STZ treatment resulted in a lower percentage of IR-immunoreactive (ir) NSCs, but not of differentiating cells. **(D)** STZ treatment affects GLUT3 protein expression in NSCs as well as in differentiating cells. Scale bar in **(C)** represents 20 μm for all images. Data in **(B,D)** are expressed as the percentage of IR- or GLUT3-ir cells (in relation to the overall number of DAPI-stained cell nuclei) ± SD. *p-value < 0.05, **p-value < 0.01, ***p-value < 0.001.

during differentiation of their progeny. More detailed, 2.5 mM STZ inhibits the proliferation of NSCs in a dose/time-dependent manner and impairs new neuron generation but not the production of new astrocytes. Furthermore, STZ remarkably affects the expression of metabolism-related genes/proteins such as GLUT3. All these attempts will help to further highlight the role of AN in the etiopathogenesis of dementia and especially of sAD with the overall aim to unravel factors and mechanisms for the treatment of sAD. Beyond that, we hope that cultured NSCs analyzed in this study could be used as a cell model to screen new compounds for the treatment of AD and other aging-related diseases. Establishing a co-culture system would help to improve the study of STZ effects on NSCs as co-culturing of NSCs with multiple other cell types would help to overcome the missing micro-environment influencing STZ treatment. Moreover, rats of 2 months of age used for this *in vitro* study are young adult animals and certainly do not have the best age to study neurobiological mechanisms underlying a neurodegenerative disorder such as sAD. Therefore, using neurospheres derived from 2 months old animals are a limitation of this study and we will use NSCs derived from older animals in the future.

AUTHOR CONTRIBUTIONS

PS and AS-B designed the experiments. PS and GO performed the experiments and analyzed data. PS, YT, QH, PR, JD and AS-B discussed and interpreted the results. PS and AS-B wrote the article. All authors have approved the final version of the manuscript.

FUNDING

This research was supported by the Dr. Edda Neele foundation (to AS-B). This publication was funded by the German Research Foundation (DFG) and the University of Wuerzburg in the funding programme Open Access Publishing.

REFERENCES

Abdel-Salam, O. M. (2011). Stem cell therapy for Alzheimer's disease. *CNS Neurol. Disord. Drug Targets* 10, 459–485. doi: 10.2174/187152711795563976

Aimone, J. B., Deng, W., and Gage, F. H. (2010). Adult neurogenesis: integrating theories and separating functions. *Trends Cogn. Sci.* 14, 325–337. doi: 10.1016/j.tics.2010.04.003

Allen, K. V., Frier, B. M., and Strachan, M. W. (2004). The relationship between type 2 diabetes and cognitive dysfunction: longitudinal studies and their methodological limitations. *Eur. J. Pharmacol.* 490, 169–175. doi: 10.1016/j.ejphar.2004.02.054

Altman, J., and Das, G. D. (1965). Autoradiographic and histological evidence of postnatal hippocampal neurogenesis in rats. *J. Comp. Neurol.* 124, 319–335. doi: 10.1002/cne.901240303

Anderson, M. F., Aberg, M. A., Nilsson, M., and Eriksson, P. S. (2002). Insulin-like growth factor-I and neurogenesis in the adult mammalian brain. *Brain Res. Dev. Brain Res.* 134, 115–122. doi: 10.1016/s0165-3806(02)00277-8

Aranha, M. M., Santos, D. M., Solá, S., Steer, C. J., and Rodrigues, C. M. (2011). miR-34a regulates mouse neural stem cell differentiation. *PLoS One* 6:e21396. doi: 10.1371/journal.pone.0021396

Arsenijevic, Y., Weiss, S., Schneider, B., and Aebischer, P. (2001). Insulin-like growth factor-I is necessary for neural stem cell proliferation and demonstrates distinct actions of epidermal growth factor and fibroblast growth factor-2. *J. Neurosci.* 21, 7194–7202. doi: 10.1523/jneurosci.21-18-07194.2001

Arvidsson, A., Collin, T., Kirik, D., Kokaia, Z., and Lindvall, O. (2002). Neuronal replacement from endogenous precursors in the adult brain after stroke. *Nat. Med.* 8, 963–970. doi: 10.1038/nm747

Attia, S. M., Helal, G. K., and Alhaider, A. A. (2009). Assessment of genomic instability in normal and diabetic rats treated with metformin. *Chem. Biol. Interact.* 180, 296–304. doi: 10.1016/j.cbi.2009.03.001

Bateman, J. M., and McNeill, H. (2006). Insulin/IGF signalling in neurogenesis. *Cell. Mol. Life Sci.* 63, 1701–1705. doi: 10.1007/s00018-006-6036-4

Belmadani, A., Tran, P. B., Ren, D., and Miller, R. J. (2006). Chemokines regulate the migration of neural progenitors to sites of neuroinflammation. *J. Neurosci.* 26, 3182–3191. doi: 10.1523/jneurosci.0156-06.2006

Blokland, A., and Jolles, J. (1993). Spatial learning deficit and reduced hippocampal ChAT activity in rats after an ICV injection of streptozotocin. *Pharmacol. Biochem. Behav.* 44, 491–494. doi: 10.1016/0091-3057(93)90497-H

Blondel, O., and Portha, B. (1989). Early appearance of *in vivo* insulin resistance in adult streptozotocin-injected rats. *Diabete Metab.* 15, 382–387.

Blurton-Jones, M., Kitazawa, M., Martinez-Coria, H., Castello, N. A., Müller, F. J., Loring, J. F., et al. (2009). Neural stem cells improve cognition via BDNF in a transgenic model of Alzheimer disease. *Proc. Natl. Acad. Sci. U S A* 106, 13594–13599. doi: 10.1073/pnas.0901402106

Brentjens, R., and Saltz, L. (2001). Islet cell tumors of the pancreas: the medical oncologist's perspective. *Surg. Clin. North Am.* 81, 527–542. doi: 10.1016/S0039-6109(05)70141-9

Chen, Y., Liang, Z., Blanchard, J., Dai, C. L., Sun, S., Lee, M. H., et al. (2013). A non-transgenic mouse model (icv-STZ mouse) of Alzheimer's disease: similarities to and differences from the transgenic model (3xTg-AD mouse). *Mol. Neurobiol.* 47, 711–725. doi: 10.1007/s12035-012-8375-5

Chen, Y., Pan, C., Xuan, A., Xu, L., Bao, G., Liu, F., et al. (2015). Treatment efficacy of ngf nanoparticles combining neural stem cell transplantation on Alzheimer's disease model rats. *Med. Sci. Monit.* 21, 3608–3615. doi: 10.12659/msm.894567

Correia, S. C., Santos, R. X., Perry, G., Zhu, X., Moreira, P. I., and Smith, M. A. (2011). Insulin-resistant brain state: the culprit in sporadic Alzheimer's disease?. *Ageing Res. Rev.* 10, 264–273. doi: 10.1016/j.arr.2011.01.001

de la Monte, S. M. (2009). Insulin resistance and Alzheimer's disease. *BMB Rep.* 42, 475–481. doi: 10.5483/BMBRep.2009.42.8.475

Dienel, G. A. (2012). Fueling and imaging brain activation. *ASN Neuro* 4:e00093. doi: 10.1042/an20120021

Dong, C., Rovnaghi, C. R., and Anand, K. J. (2012). Ketamine alters the neurogenesis of rat cortical neural stem progenitor cells. *Crit. Care Med.* 40, 2407–2416. doi: 10.1097/ccm.0b013e318253563c

Dong, S., Zeng, Q., Mitchell, E. S., Xiu, J., Duan, Y., Li, C., et al. (2012). Curcumin enhances neurogenesis and cognition in aged rats: implications for transcriptional interactions related to growth and synaptic plasticity. *PLoS One* 7:e31211. doi: 10.1371/journal.pone.0031211

Draznin, B. (2006). Molecular mechanisms of insulin resistance: serine phosphorylation of insulin receptor substrate-1 and increased expression of p85alpha: the two sides of a coin. *Diabetes* 55, 2392–2397. doi: 10.2337/db06-0391

Duelli, R., Schröck, H., Kuschinsky, W., and Hoyer, S. (1994). Intracerebroventricular injection of streptozotocin induces discrete local changes in cerebral glucose utilization in rats. *Int. J. Dev. Neurosci.* 12, 737–743. doi: 10.1016/0736-5748(94)90053-1

Eileen Dolan, M. (1997). Inhibition of DNA repair as a means of increasing the antitumor activity of DNA reactive agents. *Adv. Drug Deliv. Rev.* 26, 105–118. doi: 10.1016/s0169-409x(97)00028-8

Eriksson, P. S., Perfilieva, E., Björk-Eriksson, T., Alborn, A. M., Nordborg, C., Peterson, D. A., et al. (1998). Neurogenesis in the adult human hippocampus. *Nat. Med.* 4, 1313–1317. doi: 10.1038/3305

Glass, R., Synowitz, M., Kronenberg, G., Walzlein, J. H., Markovic, D. S., Wang, L. P., et al. (2005). Glioblastoma-induced attraction of endogenous neural precursor cells is associated with improved survival. *J. Neurosci.* 25, 2637–2646. doi: 10.1523/jneurosci.5118-04.2005

Groszer, M., Erickson, R., Scripture-Adams, D. D., Dougherty, J. D., Le Belle, J., Zack, J. A., et al. (2006). PTEN negatively regulates neural stem cell self-renewal by modulating G0-G1 cell cycle entry. *Proc. Natl. Acad. Sci. U S A* 103, 111–116. doi: 10.1073/pnas.0509939103

Grünblatt, E., Salkovic-Petrisic, M., Osmanovic, J., Riederer, P., and Hoyer, S. (2007). Brain insulin system dysfunction in streptozotocin intracerebroventricularly treated rats generates hyperphosphorylated tau protein. *J. Neurochem.* 101, 757–770. doi: 10.1111/j.1471-4159.2006.04368.x

Han, J., Wang, B., Xiao, Z., Gao, Y., Zhao, Y., Zhang, J., et al. (2008). Mammalian target of rapamycin (mTOR) is involved in the neuronal differentiation of neural progenitors induced by insulin. *Mol. Cell. Neurosci.* 39, 118–124. doi: 10.1016/j.mcn.2008.06.003

Hatten, M. E. (1999). Central nervous system neuronal migration. *Annu. Rev. Neurosci.* 22, 511–539. doi: 10.1146/annurev.neuro.22.1.511

Hellweg, R. (1994). Trophic factors during normal brain aging and after functional damage. *J. Neural Transm.* 44, 209–217. doi: 10.1007/978-3-7091-9350-1_16

Hellweg, R., Nitsch, R., Hock, C., Jaksch, M., and Hoyer, S. (1992). Nerve growth factor and choline acetyltransferase activity levels in the rat brain following experimental impairment of cerebral glucose and energy metabolism. *J. Neurosci. Res.* 31, 479–486. doi: 10.1002/jnr.490310310

Kadowaki, T., Kasuga, M., Akanuma, Y., Ezaki, O., and Takaku, F. (1984). Decreased autophosphorylation of the insulin receptor-kinase in streptozotocin-diabetic rats. *J. Biol. Chem.* 259, 14208–14216.

Kawabata, H., Setoguchi, T., Yone, K., Souda, M., Yoshida, H., Kawahara, K., et al. (2010). High mobility group box 1 is upregulated after spinal cord injury and is associated with neuronal cell apoptosis. *Spine* 35, 1109–1115. doi: 10.1097/brs.0b013e3181bd14b6

Kayano, T., Fukumoto, H., Eddy, R. L., Fan, Y. S., Byers, M. G., Shows, T. B., et al. (1988). Evidence for a family of human glucose transporter-like proteins. Sequence and gene localization of a protein expressed in fetal skeletal muscle and other tissues. *J. Biol. Chem.* 263, 15245–15248.

Kazanis, I., Lathia, J., Moss, L., and Ffrench-Constant, C. (2008). "The neural stem cell microenvironment," in *StemBook*, ed. D. Scadden (Cambridge, MA: Harvard Stem Cell Institute, Massachusetts General Hospital). Available online at: http://www.stembook.org

Kempermann, G., and Gage, F. H. (2000). Neurogenesis in the adult hippocampus. *Novartis Found. Symp.* 231, 220–235; discussion 235–241, 302–306.

Kempermann, G., Wiskott, L., and Gage, F. H. (2004). Functional significance of adult neurogenesis. *Curr. Opin. Neurobiol.* 14, 186–191. doi: 10.1016/j.conb.2004.03.001

Lannert, H., and Hoyer, S. (1998). Intracerebroventricular administration of streptozotocin causes long-term diminutions in learning and memory abilities and in cerebral energy metabolism in adult rats. *Behav. Neurosci.* 112, 1199–1208. doi: 10.1037/0735-7044.112.5.1199

Le Belle, J. E., Orozco, N. M., Paucar, A. A., Saxe, J. P., Mottahedeh, J., Pyle, A. D., et al. (2011). Proliferative neural stem cells have high endogenous ROS levels that regulate self-renewal and neurogenesis in a PI3K/Akt-dependant manner. *Cell Stem Cell* 8, 59–71. doi: 10.1016/j.stem.2010.11.028

Lee, J., Duan, W., and Mattson, M. P. (2002). Evidence that brain-derived neurotrophic factor is required for basal neurogenesis and mediates, in part,

the enhancement of neurogenesis by dietary restriction in the hippocampus of adult mice. *J. Neurochem.* 82, 1367–1375. doi: 10.1046/j.1471-4159.2002.01085.x

Leeman, D. S., Hebestreit, K., Ruetz, T., Webb, A. E., McKay, A., Pollina, E. A., et al. (2018). Lysosome activation clears aggregates and enhances quiescent neural stem cell activation during aging. *Science* 359, 1277–1283. doi: 10.1126/science.aag3048

Leybaert, L., De Bock, M., Van Moorhem, M., Decrock, E., and De Vuyst, E. (2007). Neurobarrier coupling in the brain: adjusting glucose entry with demand. *J. Neurosci. Res.* 85, 3213–3220. doi: 10.1002/jnr.21189

Like, A. A., and Rossini, A. A. (1976). Streptozotocin-induced pancreatic insulitis: new model of diabetes mellitus. *Science* 193, 415–417. doi: 10.1126/science.180605

Limoli, C. L., Giedzinski, E., Baure, J., Doctrow, S. R., Rola, R., and Fike, J. R. (2006). Using superoxide dismutase/catalase mimetics to manipulate the redox environment of neural precursor cells. *Radiat. Prot. Dosimetry* 122, 228–236. doi: 10.1093/rpd/ncl458

Liu, F., Xuan, A., Chen, Y., Zhang, J., Xu, L., Yan, Q., et al. (2014). Combined effect of nerve growth factor and brain-derived neurotrophic factor on neuronal differentiation of neural stem cells and the potential molecular mechanisms. *Mol. Med. Rep.* 10, 1739–1745. doi: 10.3892/mmr.2014.2393

Longhi, L., Zanier, E. R., Royo, N., Stocchetti, N., and McIntosh, T. K. (2005). Stem cell transplantation as a therapeutic strategy for traumatic brain injury. *Transpl. Immunol.* 15, 143–148. doi: 10.1016/j.trim.2005.09.003

Masin, M., Vazquez, J., Rossi, S., Groeneveld, S., Samson, N., Schwalie, P. C., et al. (2014). GLUT3 is induced during epithelial-mesenchymal transition and promotes tumor cell proliferation in non-small cell lung cancer. *Cancer Metab.* 2:11. doi: 10.1186/2049-3002-2-11

Matsuzaki, T., Sasaki, K., Tanizaki, Y., Hata, J., Fujimi, K., Matsui, Y., et al. (2010). Insulin resistance is associated with the pathology of Alzheimer disease: the Hisayama study. *Neurology* 75, 764–770. doi: 10.1212/wnl.0b013e3181eee25f

Maurer, M. H., Geomor, H. K., Burgers, H. F., Schelshorn, D. W., and Kuschinsky, W. (2006). Adult neural stem cells express glucose transporters GLUT1 and GLUT3 and regulate GLUT3 expression. *FEBS Lett.* 580, 4430–4434. doi: 10.1016/j.febslet.2006.07.012

Mayer, G., Nitsch, R., and Hoyer, S. (1990). Effects of changes in peripheral and cerebral glucose metabolism on locomotor activity, learning and memory in adult male rats. *Brain Res.* 532, 95–100. doi: 10.1016/0006-8993(90)91747-5

McCall, A. L., Van Bueren, A. M., Nipper, V., Moholt-Siebert, M., Downes, H., and Lessov, N. (1996). Forebrain ischemia increases GLUT1 protein in brain microvessels and parenchyma. *J. Cereb. Blood Flow Metab.* 16, 69–76. doi: 10.1097/00004647-199601000-00008

Ming, G. L., and Song, H. (2005). Adult neurogenesis in the mammalian central nervous system. *Annu. Rev. Neurosci.* 28, 223–250. doi: 10.1146/annurev.neuro.28.051804.101459

Moloney, A. M., Griffin, R. J., Timmons, S., O'Connor, R., Ravid, R., and O'Neill, C. (2010). Defects in IGF-1 receptor, insulin receptor and IRS-1/2 in Alzheimer's disease indicate possible resistance to IGF-1 and insulin signalling. *Neurobiol. Aging* 31, 224–243. doi: 10.1016/j.neurobiolaging.2008.04.002

Morrens, J., Van Den Broeck, W., and Kempermann, G. (2012). Glial cells in adult neurogenesis. *Glia* 60, 159–174. doi: 10.1002/glia.21247

Murray-Lyon, I. M., Eddleston, A. L., Williams, R., Brown, M., Hogbin, B. M., Bennett, A., et al. (1968). Treatment of multiple-hormone-producing malignant islet-cell tumour with streptozotocin. *Lancet* 2, 895–898. doi: 10.1016/s0140-6736(68)91058-1

Nishimura, K., and Takahashi, J. (2013). Therapeutic application of stem cell technology toward the treatment of Parkinson's disease. *Biol. Pharm. Bull.* 36, 171–175. doi: 10.1248/bpb.b12-00929

Ott, A., Stolk, R. P., van Harskamp, F., Pols, H. A., Hofman, A., and Breteler, M. M. (1999). Diabetes mellitus and the risk of dementia: the rotterdam study. *Neurology* 53, 1937–1942. doi: 10.1212/WNL.53.9.1937

Ou, Z., Kong, X., Sun, X., He, X., Zhang, L., Gong, Z., et al. (2018). Metformin treatment prevents amyloid plaque deposition and memory impairment in APP/PS1 mice. *Brain Behav. Immun.* 69, 351–363. doi: 10.1016/j.bbi.2017.12.009

Oubaha, M., Miloudi, K., Dejda, A., Guber, V., Mawambo, G., Germain, M. A., et al. (2016). Senescence-associated secretory phenotype contributes to pathological angiogenesis in retinopathy. *Sci. Transl. Med.* 8:362ra144. doi: 10.1126/scitranslmed.aaf9440

Palmer, T. D., Willhoite, A. R., and Gage, F. H. (2000). Vascular niche for adult hippocampal neurogenesis. *J. Comp. Neurol.* 425, 479–494. doi: 10.1002/1096-9861(20001002)425:4<479::aid-cne2>3.0.co;2-3

Pandey, A., and Bani, S. (2010). Hydroxychavicol inhibits immune responses to mitigate cognitive dysfunction in rats. *J. Neuroimmunol.* 226, 48–58. doi: 10.1016/j.jneuroim.2010.05.031

Paviolo, N. S., Santiñaque, F. F., Castrogiovanni, D. C., Folle, G. A., and Bolzán, A. D. (2015). The methylating agent streptozotocin induces persistent telomere dysfunction in mammalian cells. *Mutat. Res. Genet. Toxicol. Environ. Mutagen.* 794, 17–24. doi: 10.1016/j.mrgentox.2015.09.007

Plaschke, K., and Hoyer, S. (1993). Action of the diabetogenic drug streptozotocin on glycolytic and glycogenolytic metabolism in adult rat brain cortex and hippocampus. *Int. J. Dev. Neurosci.* 11, 477–483. doi: 10.1016/0736-5748(93)90021-5

Prozorovski, T., Schulze-Topphoff, U., Glumm, R., Baumgart, J., Schroter, F., Ninnemann, O., et al. (2008). Sirt1 contributes critically to the redox-dependent fate of neural progenitors. *Nat. Cell Biol.* 10, 385–394. doi: 10.1038/ncb1700

Qu, Z. Q., Zhou, Y., Zeng, Y. S., Lin, Y. K., Li, Y., Zhong, Z. Q., et al. (2012). Protective effects of a Rhodiola crenulata extract and salidroside on hippocampal neurogenesis against streptozotocin-induced neural injury in the rat. *PLoS One* 7:e29641. doi: 10.1371/journal.pone.0029641

Rai, S., Kamat, P. K., Nath, C., and Shukla, R. (2014). Glial activation and post-synaptic neurotoxicity: the key events in Streptozotocin (ICV) induced memory impairment in rats. *Pharmacol. Biochem. Behav.* 117, 104–117. doi: 10.1016/j.pbb.2013.11.035

Raza, H., and John, A. (2012). Streptozotocin-induced cytotoxicity, oxidative stress and mitochondrial dysfunction in human hepatoma HepG2 cells. *Int. J. Mol. Sci.* 13, 5751–5767. doi: 10.3390/ijms13055751

Reaven, G. M. (1988). Banting lecture 1988. Role of insulin resistance in human disease. *Diabetes* 37, 1595–1607. doi: 10.2337/diabetes.37.12.1595

Reaven, G. M., and Ho, H. (1991). Low-dose streptozotocin-induced diabetes in the spontaneously hypertensive rat. *Metab. Clin. Exp.* 40, 335–337. doi: 10.1016/0026-0495(91)90141-i

Riederer, P., Korczyn, A. D., Ali, S., Bajenaru, O., Choi, M. S., Chopp, M., et al. (2017). The diabetic brain and cognition. *J. Neural Transm.* 124, 1431–1454. doi: 10.1007/s00702-017-1763-2

Rodríguez-Mañas, L., Angulo, J., Peiró, C., Llergo José, L., Sánchez-Ferrer, A., López-Dóriga, P., et al. (2009). Endothelial dysfunction and metabolic control in streptozotocin-induced diabetic rats. *Br. J. Pharmacol.* 123, 1495–1502. doi: 10.1038/sj.bjp.0701749

Roriz-Filho, J. S., Sá-Roriz, T. M., Rosset, I., Camozzato, A. L., Santos, A. C., Chaves, M. L., et al. (2009). (Pre)diabetes, brain aging, and cognition. *Biochim. Biophys. Acta* 1792, 432–443. doi: 10.1016/j.bbadis.2008.12.003

Ryan, C. M., and Geckle, M. (2000). Why is learning and memory dysfunction in Type 2 diabetes limited to older adults?. *Diabetes Metab. Res. Rev.* 16, 308–315. doi: 10.1002/1520-7560(2000)9999:9999<::aid-dmrr141>3.0.co;2-x

Salkovic-Petrisic, M., Osmanovic, J., Grünblatt, E., Riederer, P., and Hoyer, S. (2009). Modeling sporadic Alzheimer's disease: the insulin resistant brain state generates multiple long-term morphobiological abnormalities including hyperphosphorylated tau protein and amyloid-beta. *J. Alzheimers Dis.* 18, 729–750. doi: 10.3233/JAD-2009-1184

Salkovic-Petrisic, M., Osmanovic-Barilar, J., Brückner, M. K., Hoyer, S., Arendt, T., and Riederer, P. (2011). Cerebral amyloid angiopathy in streptozotocin rat model of sporadic Alzheimer's disease: a long-term follow up study. *J. Neural Transm. Vienna* 118, 765–772. doi: 10.1007/s00702-011-0651-4

Salkovic-Petrisic, M., Osmanovic-Barilar, J., Knezovic, A., Hoyer, S., Mosetter, K., and Reutter, W. (2013). Long-term oral galactose treatment prevents cognitive deficits in male Wistar rats treated intracerebroventricularly with streptozotocin. *Neuropharmacology* 77C, 68–80. doi: 10.1016/j.neuropharm.2013.09.002

Salkovic-Petrisic, M., Tribl, F., Schmidt, M., Hoyer, S., and Riederer, P. (2006). Alzheimer-like changes in protein kinase B and glycogen synthase kinase-3 in rat frontal cortex and hippocampus after damage to the insulin signalling pathway. *J. Neurochem.* 96, 1005–1015. doi: 10.1111/j.1471-4159.2005.03637.x

Selkoe, D. J. (2002). Alzheimer's disease is a synaptic failure. *Science* 298, 789–791. doi: 10.1126/science.1074069

Sharma, M., and Gupta, Y. K. (2001). Intracerebroventricular injection of streptozotocin in rats produces both oxidative stress in the brain and cognitive impairment. *Life Sci.* 68, 1021–1029. doi: 10.1016/s0024-3205(00)01005-5

Shigemoto-Mogami, Y., Hoshikawa, K., Goldman, J. E., Sekino, Y., and Sato, K. (2014). Microglia enhance neurogenesis and oligodendrogenesis in the early postnatal subventricular zone. *J. Neurosci.* 34, 2231–2243. doi: 10.1523/JNEUROSCI.1619-13.2014

Shoham, S., Bejar, C., Kovalev, E., and Weinstock, M. (2003). Intracerebroventricular injection of streptozotocin causes neurotoxicity to myelin that contributes to spatial memory deficits in rats. *Exp. Neurol.* 184, 1043–1052. doi: 10.1016/j.expneurol.2003.08.015

Shonesy, B. C., Thiruchelvam, K., Parameshwaran, K., Rahman, E. A., Karuppagounder, S. S., Huggins, K. W., et al. (2012). Central insulin resistance and synaptic dysfunction in intracerebroventricular-streptozotocin injected rodents. *Neurobiol. Aging* 33, 430.e5–430.e18. doi: 10.1016/j.neurobiolaging.2010.12.002

Shu, T., Liu, C., Pang, M., Wang, J., Liu, B., Zhou, W., et al. (2018). Effects and mechanisms of matrix metalloproteinase2 on neural differentiation of induced pluripotent stem cells. *Brain Res.* 1678, 407–418. doi: 10.1016/j.brainres.2017.11.006

Siegrist, S. E., Haque, N. S., Chen, C. H., Hay, B. A., and Hariharan, I. K. (2010). Inactivation of both Foxo and reaper promotes long-term adult neurogenesis in Drosophila. *Curr. Biol.* 20, 643–648. doi: 10.1016/j.cub.2010.01.060

Simpson, I. A., Carruthers, A., and Vannucci, S. J. (2007). Supply and demand in cerebral energy metabolism: the role of nutrient transporters. *J. Cereb. Blood Flow Metab.* 27, 1766–1791. doi: 10.1038/sj.jcbfm.9600521

Sun, P. (2015). *Alzheimer's Disease and Brain Insulin Resistance: The Diabetes Inducing Drug Streptozotocin Diminishes Adult Neurogenesis in the Rat Hippocampus—an in vivo and in vitro Study (Alzheimer-Krankheit und Insulinresistenz im Gehirn: Streptozotocin, das Änderungen im Insulinstoffwechsel Hervorruft, Reduziert die Neubildung von Neuronen im Hippocampus Von Adulten Ratten—in vivo- und in vitro-Untersuchungen).* Würzburg: University of Würzburg.

Sun, P., Knezovic, A., Parlak, M., Cuber, J., Karabeg, M. M., Deckert, J., et al. (2015). Long-term effects of intracerebroventricularstreptozotocin treatment on adult neurogenesis in the rat hippocampus. *Curr. Alzheimer Res.* 12, 772–784. doi: 10.2174/1567205012666150710112147

Talbot, K. (2014). Brain insulin resistance in Alzheimer's disease and its potential treatment with GLP-1 analogs. *Neurodegener. Dis. Manag.* 4, 31–40. doi: 10.2217/nmt.13.73

Talbot, K., Wang, H. Y., Kazi, H., Han, L. Y., Bakshi, K. P., Stucky, A., et al. (2012). Demonstrated brain insulin resistance in Alzheimer's disease patients is associated with IGF-1 resistance, IRS-1 dysregulation, and cognitive decline. *J. Clin. Invest.* 122, 1316–1338. doi: 10.1172/JCI59903

Taupin, P. (2007). BrdU immunohistochemistry for studying adult neurogenesis: paradigms, pitfalls, limitations, and validation. *Brain Res. Rev.* 53, 198–214. doi: 10.1016/j.brainresrev.2006.08.002

Unsal, C., Oran, M., Albayrak, Y., Aktas, C., Erboga, M., Topcu, B., et al. (2016). Neuroprotective effect of ebselen against intracerebroventricular streptozotocin-induced neuronal apoptosis and oxidative stress in rats. *Toxicol. Ind. Health* 32, 730–740. doi: 10.1177/0748233713509429

van Praag, H., Christie, B. R., Sejnowski, T. J., and Gage, F. H. (1999). Running enhances neurogenesis, learning and long-term potentiation in mice. *Proc. Natl. Acad. Sci. U S A* 96, 13427–13431. doi: 10.1073/pnas.96.23.13427

Von Bohlen Und Halbach, O. (2011). Immunohistological markers for proliferative events, gliogenesis and neurogenesis within the adult hippocampus. *Cell Tissue Res.* 345, 1–19. doi: 10.1007/s00441-011-1196-4

Wang, Z., and Gleichmann, H. (1998). GLUT2 in pancreatic islets: crucial target molecule in diabetes induced with multiple low doses of streptozotocin in mice. *Diabetes* 47, 50–56. doi: 10.2337/diabetes.47.1.50

Wang, J. Q., Yin, J., Song, Y. F., Zhang, L., Ren, Y. X., Wang, D. G., et al. (2014). Brain aging and AD-like pathology in streptozotocin-induced diabetic rats. *J. Diabetes Res.* 2014:796840. doi: 10.1155/2014/796840

Ward, C. W., and Lawrence, M. C. (2009). Ligand-induced activation of the insulin receptor: a multi-step process involving structural changes in both the ligand the receptor. *Bioessays* 31, 422–434. doi: 10.1002/bies.200800210

Wiskott, L., Rasch, M. J., and Kempermann, G. (2006). A functional hypothesis for adult hippocampal neurogenesis: avoidance of catastrophic interference in the dentate gyrus. *Hippocampus* 16, 329–343. doi: 10.1002/hipo.20167

Yuan, X., Xiao, Y. C., Zhang, G. P., Hou, N., Wu, X. Q., Chen, W. L., et al. (2016). Chloroquine improves left ventricle diastolic function in streptozotocin-induced diabetic mice. *Drug Des. Devel. Ther.* 10, 2729–2737. doi: 10.2147/DDDT.s111253

Conflict of Interest Statement: The authors declare that the research was conducted in the absence of any commercial or financial relationships that could be construed as a potential conflict of interest.

Copyright © 2018 Sun, Ortega, Tan, Hua, Riederer, Deckert and Schmitt-Böhrer. This is an open-access article distributed under the terms of the Creative Commons Attribution License (CC BY). The use, distribution or reproduction in other forums is permitted, provided the original author(s) and the copyright owner are credited and that the original publication in this journal is cited, in accordance with accepted academic practice. No use, distribution or reproduction is permitted which does not comply with these terms.

frontiers in Neuroscience

REVIEW
published: 30 April 2018
doi: 10.3389/fnins.2018.00275

An Algorithm for Preclinical Diagnosis of Alzheimer's Disease

*Tapan K. Khan**

Center for Neurodegenerative Diseases, Blanchette Rockefeller Neurosciences Institute, West Virginia University, Morgantown, WV, United States

Almost all Alzheimer's disease (AD) therapeutic trials have failed in recent years. One of the main reasons for failure is due to designing the disease-modifying clinical trials at the advanced stage of the disease when irreversible brain damage has already occurred. Diagnosis of the preclinical stage of AD and therapeutic intervention at this phase, with a perfect target, are key points to slowing the progression of the disease. Various AD biomarkers hold enormous promise for identifying individuals with preclinical AD and predicting the development of AD dementia in the future, but no single AD biomarker has the capability to distinguish the AD preclinical stage. A combination of complimentary AD biomarkers in cerebrospinal fluid ($A\beta_{42}$, tau, and phosphor-tau), non-invasive neuroimaging, and genetic evidence of AD can detect preclinical AD in the *in-vivo* ante mortem brain. Neuroimaging studies have examined region-specific cerebral blood flow (CBF) and microstructural changes in the preclinical AD brain. Functional MRI (fMRI), diffusion tensor imaging (DTI) MRI, arterial spin labeling (ASL) MRI, and advanced PET have potential application in preclinical AD diagnosis. A well-validated simple framework for diagnosis of preclinical AD is urgently needed. This article proposes a comprehensive preclinical AD diagnostic algorithm based on neuroimaging, CSF biomarkers, and genetic markers.

Keywords: Alzheimer's disease, neuroimaging (anatomic and functional), CSF, diagnosis, differential, preclinical Alzheimer's disease

OPEN ACCESS

Edited by:
Mohammad Amjad Kamal, King Abdulaziz University, Saudi Arabia

Reviewed by:
Michal Novak, Slovak Academy of Sciences (SAS), Slovakia
Domenico De Berardis, Azienda Usl Teramo, Italy

***Correspondence:**
Tapan K. Khan
tkhan@hsc.wvu.edu

Specialty section:
This article was submitted to Neurodegeneration, a section of the journal Frontiers in Neuroscience

Received: *04 December 2017*
Accepted: *09 April 2018*
Published: *30 April 2018*

Citation:
Khan TK (2018) An Algorithm for Preclinical Diagnosis of Alzheimer's Disease. Front. Neurosci. 12:275. doi: 10.3389/fnins.2018.00275

INTRODUCTION

Therapeutic interventions for Alzheimer's disease (AD) will have a better chance of success if initiated at the earliest stage (preclinical), before the synaptic loss and neuronal death occur. Therefore, an effective disease-modifying clinical trial should target the stage before the manifestation of clinical symptoms of memory loss and cognitive impairment. The term preclinical AD is initially described to classify cognitively normal individuals with evidence of amyloid plaques and hyperphosphorylated tau (p-tau) tangles (hallmarks of AD pathology) at time of brain autopsy (Hubbard et al., 1990). This definition of preclinical AD was built on the existing AD mechanistic hypothesis. Several longitudinal studies predicted the conversion of mild cognitive impairment (MCI) to AD when there is amyloid plaques and p-tau tangles in the brain (Petersen et al., 1999, 2001; Grand et al., 2011). In preclinical familial AD cases, Fox et al. (1999) were the first to use serial structural magnetic resonance imaging (MRI) to detect cerebral atrophy in a longitudinal study of asymptomatic individuals (no cognitive impairment) at high risk of the familial AD (autosomal dominant early-onset before 65 years of age). Since that study, several groups have examined the predictive capacity of various brain biomarkers, such as noninvasive neuroimaging

modalities, and invasive cerebrospinal fluid (CSF) biomarkers ($A\beta_{42}$, tau, and p-tau). These studies concluded that patients who are positive for various AD biomarkers in the preclinical AD stage are at higher risk of progressing to AD dementia (Mintun et al., 2006; Villemagne et al., 2008; Johnson et al., 2012; Dubois et al., 2016). Non-invasive neuroimaging modalities, such as positron emission tomography (PET), functional MRI (fMRI), diffusion tensor imaging (DTI) MRI, and arterial spin labeling (ASL) MRI hold enormous promise for identifying preclinical AD (Mintun et al., 2006; Mosconi et al., 2006; Villemagne et al., 2008; Johnson et al., 2012; Ewers et al., 2013; Dubois et al., 2016) (**Table 2**). CSF biomarkers can predict decreasing cognitive ability in studies of conversion of MCI to AD (Frölich et al., 2017) and predicting memory deficit in longitudinal studies of normal individuals (Fagan et al., 2007; Gustafson et al., 2007; Stomrud et al., 2007; Jansen et al., 2015). AD is a multifactorial disease with several genetic biomarkers are found to be involved (http://www.alzgene.org) in the pathogenesis of AD. Those genes increase the predictability of conversion of preclinical AD to MCI and finally AD. In this perspective review, we describe the utility of combining neuroimaging, CSF, and genetic AD biomarker in the diagnosis of preclinical AD and propose a comprehensive preclinical AD diagnostic algorithm.

Preclinical Stage of Alzheimer's Disease

The National Institute on Aging and Alzheimer's Association (NIA-AA) (2011) introduced the concept of "preclinical AD" that arises before MCI and advanced stages of AD. The most recent definition of preclinical AD, proposed in a joint meeting of NIA-AA and the International Working Group (IWG) in 2015 (Dubois et al., 2016), is the simplest: preclinical AD starts the day that pathological AD lesions appear without any clinical symptoms. The NIA-AA guideline (2011) divides the progression of AD into distinct phases, taking into account both AD pathobiology and clinical symptoms: preclinical, asymptomatic pre-dementia; symptomatic pre-dementia (MCI); and dementia due to AD (McKhann et al., 2011; Sperling et al., 2011). Before that, preclinical stage AD biomarkers were categorized as Stage 1: amyloidosis by PET and CSF $A\beta_{42}$ analysis, and Stage 2: Neurodegeneration by PET and CSF tau (Jack et al., 2010). The preclinical phase can also be separated into "pre-symptomatic" and "asymptomatic at risk" suggested by IGW−2014 (Dubois et al., 2014). The pre-symptomatic preclinical AD refers to individuals with familial AD who will develop AD in the future. Individuals with pre-symptomatic preclinical AD show no clinical symptoms but have at least one mutation in the familial AD genes (APP, PSEN1, PSEN2). Asymptomatic at risk refers to preclinical AD in individuals without clinical symptoms, but positive for AD biomarkers (decreased level of $A\beta_{42}$, increased the level of tau p-tau in CSF) or positive in Aβ-PET (Dubois et al., 2014). According to the NIA-AA (2011) progressive preclinical AD pathological trajectory can be divided into three distinguishable stages: in the first stage, there is evidence of abnormality in Aβ, and individuals in this stage would be positive for Aβ, no dementia or neurodegeneration. The second stage consists of positive for Aβ, plus higher CSF tau (neurodegeneration). In the third stage, individuals begin exhibiting evidence of memory problems along with abnormalities in CSF biomarkers and neuroimaging, but all evidence of memory problems is less than MCI cases (Sperling et al., 2011).

CRITICAL EVALUATION OF IGW AND NIA-AA PRECLINICAL ALZHEIMER'S DISEASE CRITERIA

AD pathology is a continuum process spanning many years of underlying changes in brain morphology due to preclinical AD stage to a clinical AD phase. Hippocampus volume loss, temporoparietal hypometabolism, and neocortical Aβ deposition are the first to be affected in brain areas due to preclinical AD pathology. Metabolic brain networks of these areas are affected by age as well as by preclinical AD. White matter brain network is the primary area that is also affected in preclinical AD. On the cellular level, the synaptic and the axonal degenerations start to occur, but such degenerations would not affect the overall memory at the preclinical AD stage. The critical point is how and when the *in-vivo* AD-related pathology that determines preclinical AD can be measured by AD-biomarkers. The revised IWG definition of a preclinical AD: no clinical sign of AD but has at least one positive pathological AD biomarker (Dubois et al., 2016). In a critical viewpoint, it will be very difficult to distinguish preclinical AD by only one AD-biomarker. On the other hand, the NIA-AA definition of preclinical AD is more generalized (not specific): evidence of amyloidosis and neurodegeneration (Sperling et al., 2011). Here also we need the more specific definition of the role and applicability of AD *in-vivo* pathological biomarkers. The revised IWG definition of preclinical AD is too simplified to find the right condition to diagnose preclinical AD. Therefore, neither of them are perfect for determining *in-vivo* preclinical AD by AD pathological biomarkers. Both IGW and NIA-AA definition of preclinical AD considered amyloidosis ahead of tauopathy. There is evidence that neurodegeneration due to high tau or tauopathy started before amyloidosis (Jack and Holtzman, 2013; Jack et al., 2013). The phenomenon of mixed pathologies (AD with non-AD dementia) underlying the preclinical AD stage of neurodegeneration has been completely ignored by both (IGW and NIA-AA) the definitions of preclinical AD.

HYPOTHETICAL MODEL OF PRECLINICAL ALZHEIMER'S DISEASE AND PROGRESSION OF ALZHEIMER'S DISEASE

A hypothetical model of AD progression in relation to aging and disease severity is shown in **Figure 1**. The disease severity increases as age increases, because age is the most important risk factor for AD dementia. Two trajectories of AD progression are shown, one based on changes in brain morphology (red) and the other is the onset of clinical symptoms of neurodegeneration (blue). Neurodegeneration due to normal aging is shown as a

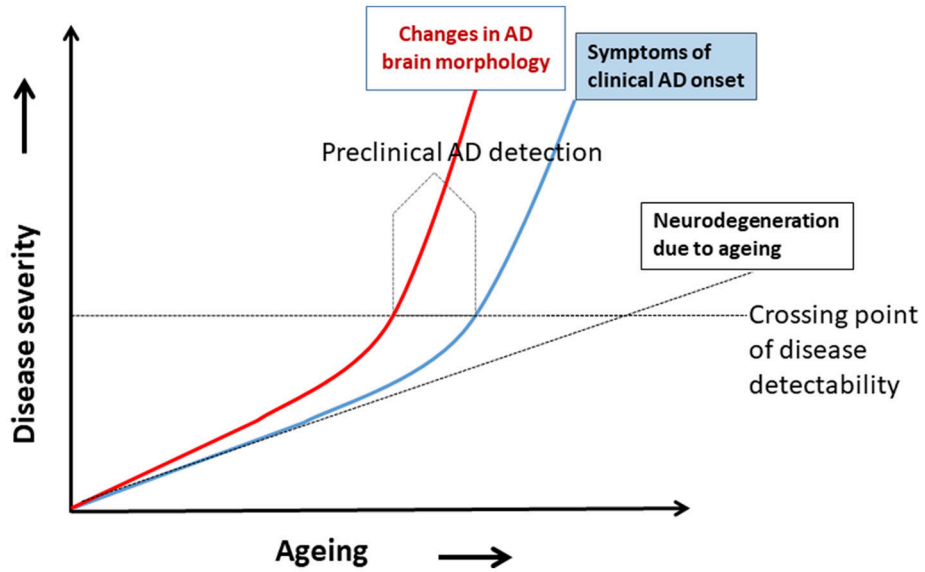


FIGURE 1 | A hypothetical model for detecting preclinical Alzheimer's disease (AD). Disease severity increases with aging, the major risk factor for an AD. Two disease trajectories represent brain morphology changes (red) and clinical AD symptoms (blue). Neurodegeneration due to aging shown by the broken black line. The model shows the hypothetical deviation of the changes in brain morphology trajectory and symptoms trajectory, and where they cross a horizontal line of disease detectability. The preclinical AD can be detected before the onset of AD symptoms (modified from Khan, 2016).

broken black line. The model shows deviations of the brain morphology trajectory and the clinical symptoms trajectory as they cross a hypothetical line of disease detectability. The trajectory of neurodegeneration due to normal aging crosses this line much later in life. Note that the changes in brain morphology increased much earlier than clinical symptoms; this indicates that the pathological changes and abnormalities in brain cell signaling (neuronal network function) occur earlier in disease progression than symptoms, such that CSF biomarkers, for example, would be detectable even in the absence of symptoms. Preclinical AD could thus be detected before the onset of AD symptoms (**Figure 1**). Preclinical diagnosis of AD is possible when brain morphology due to AD pathology started to change (box "Preclinical AD detection" in **Figure 1**), (subtle changes in brain white matters, minute changes in brain metabolites, and abnormalities in the neuronal network by functional MRI) and biomarkers of brain morphology changes can detect such signals. It is at this point in disease progression that advanced non-invasive neuroimaging of morphologic biomarkers with modalities, such as rs-fMRI, DTI MRI, ASL MRI, and PET, have enormous potential for diagnosis of preclinical AD.

The abnormalities in the brain due to the onset of AD pathology start 10–20 years before symptoms of cognitive deficiencies appear in genetically susceptible cases (Morris, 2005; Reiman et al., 2012). In one study, brain MRI was used to image brain atrophy in individuals classified as asymptomatic AD mutation carriers (presymptomatic preclinical). A recent study found that brain atrophy could be detected 1–8 years before the clinical symptoms of familial AD appeared (Kinnunen et al., 2017). A similar approach to detecting preclinical AD based on MRI-measured brain atrophy over time is not as simple for sporadic AD, however. More research is necessary to validate the preclinical AD category of "asymptomatic at risk." Brain amyloidosis (higher Aβ deposition) in a cognitively normal individual has a higher likelihood of progression from preclinical stages to symptomatic stages of AD.

APPLICABILITY OF CEREBROSPINAL FLUID (CSF) BIOMARKERS IN PRECLINICAL ALZHEIMER'S DISEASE DIAGNOSIS

Widely researched CSF AD biomarkers are low $A\beta_{42}$, high tau, and high p-tau (phosphorylated tau) levels compared to age-matched non-demented controls. Three CSF biomarkers represent three different aspects of AD brain pathology, respectively. Low levels of $A\beta_{42}$ reflects higher amyloid plaques (amylolysis), high levels of tau represents neurodegeneration, and high p-tau level correlates with high levels of neurofibrillary tangles (NFTs) in the AD brain. As a single test CSF biomarkers are not accurate to detect conversion of MCI to AD; however, negative CSF results in MCI cases can accurately predict conversion of non-Alzheimer's disease (Ritchie et al., 2017). Moreover, an evaluation of CSF biomarkers found them to have the ability to predict memory decline in individuals with aging (Fagan et al., 2007; Gustafson et al., 2007; Stomrud et al., 2007; Jansen et al., 2015). Therefore, CSF biomarkers can be used as part of a preclinical biomarker panel that can predict developing AD in the future.

CSF biomarker patterns of preclinical AD were found to be different in middle aged asymptomatic cases in a recent

longitudinal study (Sutphen et al., 2015). Besides established AD CSF, ($A\beta_{42}$, tau, and p-tau) there are other CSF biomarkers that are more close to the neurodegeneration in preclinical AD stage. Such recently studied CSF biomarkers are neurofilament light chain, neurogranin, inflammatory markers, and tau fragments. Levels of CSF neurogranin are high in AD and progressive AD cases (Kester et al., 2015). Higher levels of neurogranin represent synaptic dysfunction and neurodegeneration. Neurogranin level was correlated with tau but not Aβ, which indicates it can be a measure of neurodegeneration, not levels of Aβ deposition. The levels of neurofilament light chain concentration were also high in AD progression (Zetterberg et al., 2016). Neurofilament light chain is a measure of axonal degeneration due to underlying preclinical AD. CSF inflammatory markers such as IL-15, MCP-1, VEGFR-1, sICAM1, sVCAM-1, and VEGF-D were found to correlate with the levels of tau and p-tau (Popp et al., 2017). More research and validation is needed for these newly incorporated CSF biomarkers before considering them definitive preclinical AD biomarkers. Longitudinal follow-up of CSF biomarkers in individuals in risk cohort will be more effective than cross-sectional cohort for determining preclinical AD progression.

ADVANCED MRI AND PET-BASED NEUROIMAGING FOR THE DIAGNOSIS OF PRECLINICAL ALZHEIMER'S DISEASE

Non-invasive imaging of the brain is a promising tool for the early detection of AD. The most widely researched neuroimaging biomarkers of AD are summarized in **Table 1**. Advanced neuroimaging techniques are most promising in detecting the disease at its earliest stage for initiating therapeutic intervention and finding individuals at risk of AD. In fact, hippocampus volume is one of the first brain areas affected due to preclinical AD pathology. Advanced MRI-based neuroimaging techniques and protocols have been introduced to detect more subtle changes in brain tissues at the microscopic level (**Table 2**). Tissues and cell damage that precede neurodegeneration include loss of synapses, loss of axonal integrity, demyelination, loss of microtubule assembly, and minute changes in levels of brain metabolites. Resting-state functional MRI (rs-fMRI), DTI, and ASL MRI have been developed to detect these preclinical AD biomarkers and are described here. Longitudinal follow-up of imaging biomarkers in individuals in an at risk cohort will be more effective than a cross-sectional cohort for determining preclinical AD progression.

TABLE 1 | Neuroimaging biomarkers in Alzheimer's disease.

Neuroimaging biomarker	Biomarker readout associated with AD
MRI*	Atrophy
fMRI	Disrupted neural network
^{11}C-PIB PET*	Increased amyloid plaque binding to PIB
^{18}F-Aβ-binding compound-PET**	Higher amount of amyloid in brain
^{18}FDG-PET*	Low brain metabolism measured by decreased glucose uptake

Aβ, amyloid beta; AD, Alzheimer's disease; FDG, fluoro-2-deoxy-D-glucose; fMRI, functional MRI; MRI, magnetic resonance imaging; PET, positron emission tomography; PIB, Pittsburgh compound B.

**Included in the NIA-2011 and IWG−2014 criteria to support diagnosis of AD for research purposes.*

*** Approved by FDA and EMA.*

Resting-State Functional MRI (rs-fMRI)

Resting-state functional MRI was first developed by Biswal et al. (1995) to detect low-frequency fluctuations in the resting brain. In principle, it measures changes in paramagnetic properties of oxyhemoglobin/deoxy-hemoglobin in blood flowing through different brain regions influenced by changes in neuronal network activity. In the resting brain, the neuronal network is linearly dependent on spontaneous low-frequency fluctuations of the blood oxygen-dependent (BOLD) signals detected by fMRI in different brain areas. In a task-free state, functional connectivity analysis can detect subtle changes in brain network differences between individuals with the early-stage disease and healthy controls. The neuronal network and synaptic activities are beginning to change in preclinical AD, before the symptomatic manifestation of AD. Thus, rs-fMRI enables functional connectivity analysis to detect subtle brain network abnormalities in the very beginning of AD pathology in the brain. Recently, lower functional connectivity measured by rs-fMRI has also been demonstrated to be an indicator of pre-MCI and pre-dementia due to AD in longitudinal studies of individuals with preclinical AD (Buckley et al., 2017) (**Table 2**).

Diffusion Tensor Imaging (DTI) With sMRI

DTI, sometimes called diffusion-weighted imaging (DWI), was developed in the last decade of the twentieth century (Moseley et al., 1990; Beaulieu and Allen, 1994; Pierpaoli and Basser, 1996; Pierpaoli et al., 1996). In principle, it measures the probability distribution of diffusion of water molecules in the brain in terms of the diffusion tensor. In the ideal case, if there are no hindrances, the probability distribution of diffusion of water molecules should be isotropic. A brain has nerve fibers and tightly associated axonal bundles; therefore, the distribution of water molecules should be highly anisotropic in non-demented normal brains. The phenomenon of white matter loss starts at the preclinical AD stage. This loss of white matter decreases the anisotropic nature of the diffusion of the water molecules. DTI calculates two measurable quantities from the anisotropic nature of diffusion of water molecules by sMRI in the region of interest in the brain. Those two quantities are fractional anisotropy (FA) and mean diffusion coefficient (MD). Increased MD and decreased FA values indicate loss of white matter in AD and MCI brains indicating that MD and FA may be potential neuroimaging biomarkers of early-stage AD. Several studies have shown that DTI has the ability to distinguish between AD, MCI, and age-matched control case (Chua et al., 2009; a meta-analysis of 41 DTI studies by Sexton et al., 2011) (**Table 2**).

Expanding on this work, DTI technology combined with novel mathematical tools has been used recently to identify preclinical AD cases. New evidence suggests that white matter alterations begin in preclinical AD and can be measured by

TABLE 2 | Preclinical Alzheimer's disease neuroimaging biomarkers.

Modality	Parameter	Values in preclinical AD	Notes	References
rs-fMRI	Paramagnetic property of oxy-hemoglobin/deoxy-hemoglobin in blood flow	Low-frequency spontaneous fluctuation of BOLD signal Reduced functional connectivity	rs-fMRI can detect abnormalities before brain volume loss No regulatory guidelines by FDA or EMA	Machulda et al., 2011; Sheline and Raichle, 2013; Buckley et al., 2017
DTI with sMRI	Diffusion of water molecules in brain	Higher overall mean diffusivity of water molecules Lower fractional anisotropy	Region specificity Detectable abnormality in WM networks in preclinical AD No regulatory guidelines by FDA or EMA	Sexton et al., 2011; Racine et al., 2014; Fischer et al., 2015; Nedelska et al., 2015
ASL/sMRI	CBF traced by magnetically labeled water molecules	Decreased blood flow in brain	Consistent with vascular hypothesis of AD Could be useful biomarker for tracking disease severity and progression No radiotracer or contrast reagents No regulatory guidelines by FDA or EMA	Alsop et al., 2010; Wang et al., 2013; Wierenga et al., 2014; Hays et al., 2016
Aβ-PET	Radiotracer binding to amyloid beta in specific brain regions	Presence of Aβ detected with ^{11}C-PIB or ^{18}F-labeled amyloid-binding agents	Amyloid accumulation occurs before brain atrophy and is hypothesized to be the first pathological event in AD It is not correlated with AD clinical severity and neurodegeneration Can be used for differential diagnosis per FDA or EMA	Jack et al., 2009; Jagust et al., 2009; Scheinin et al., 2009; Okamura et al., 2014
^{18}FDG-PET	Glucose uptake in different brain regions	Glucose uptake using ^{18}FDG	Useful for differential diagnosis of AD and FTD Brain region-specific differentiation capability Can be used for differential diagnosis per FDA or EMA	Mosconi et al., 2006; Ewers et al., 2013, 2014
Tau-^{18}F-T807-PET	Region specific distribution of tau deposition	^{18}F-T807	Progression of AD related to neurodegeneration due to tau deposition	Johnson et al., 2016

Aβ, amyloid beta; AD, Alzheimer's disease; ASL MRI, arterial spin-labeled magnetic resonance imaging; BOLD, blood oxygen level-dependent; CBF, cerebral blood flow; DTI, diffusion tensor imaging; EMA, European Medical Agency; FDA, Food and Drug Administration; FTD, frontotemporal dementia; FDG, fluoro-2-deoxy-D-glucose; fMRI, functional MRI; MRI, magnetic resonance imaging; ^{18}F-T807-PET, Fluorinated tau PET ligand; PET, positron emission tomography; PIB, Pittsburgh Compound B; rs-fMRI, resting state functional MRI; sMRI, structural MRI; WM, white matter.

DTI (Racine et al., 2014; Kantarci et al., 2017). White matter primarily consists of axon and myelin sheets that is altered by AD pathology. Axonal degeneration and deformation of myelin sheets are early events that occur before the wide-spread neuronal loss in the AD brain. Among the neuroimaging techniques, DTI is the best suited to assess degeneration of myelinated nerve fibers in the brain. By applying tractography and graph theory in DTI, a study reported alterations within the entire white matter network in preclinical AD, even before structural markers of significant neurodegeneration, such as atrophy by MRI and reduced cortical glucose utilization by ^{18}FDG-PET, were detected (Fischer et al., 2015). Moreover, the alteration of DTI parameters (FA and MD) were correlated with common risk factors of sporadic AD (Adluru et al., 2014).

Arterial Spin Labeling (ASL) MRI

ASL/MRI imaging of AD is consistent with the hypothesis of vascular abnormality of the AD. ASL was first developed in 1992 for imaging the rat brain using magnetically labeled blood water (arterial spin labeling) followed by MRI (Detre et al., 1992). The principle of ASL is based on imaging magnetically labeled blood water in brain tissues of a region of interest by applying a 180° radio-frequency pulse (Detre et al., 2009, 2012). In the next step, the local changes of magnetization in brain tissue by blood flow with magnetically labeled water are measured by scanning with normal MRI sequence scanning mode. It has the ability to identify vascular factors in neurodegenerative diseases such as AD and vascular dementias (Detre et al., 2012). Cerebral blood flow (CBF) is a possible biomarker of AD that can be measured by ASL MRI. Typical CBF images by ASL MRI measure reduced CBF in AD, and can even differentiate between MCI, and age-matched control groups (Wang et al., 2013). Reduced CBF values measured by ASL MRI were found to be region specific AD patients compared to age-matched control cases. Reduced CBF occurs in the lateral prefrontal cortex, posterior cingulate, precuneus, and inferior parietal areas of AD brains (Alsop et al., 2000, 2010; Johnson et al., 2005; Dai et al., 2009) (**Table 2**). CBF is easy to follow over time and imaging a biomarker can be useful to follow the disease's condition and prognosis. It has been hypothesized that abnormality in CBF occurs much earlier than cognitive deficits appear in AD, possibly earlier than wide-spread brain atrophy or plaque/tangle formation. Recent studies showed that ASL MRI can be extended to detect preclinical AD, at least for research purposes (Wierenga et al., 2014; Hays et al., 2016).

AD BRAIN IMAGING BY POSITRON EMISSION TOMOGRAPHY (PET)

Amyloid Imaging by PET as AD Biomarker

Aβ deposition can be found in the neocortical area of the brain, one of the first areas affected due to preclinical AD pathology. Imaging of amyloid as a biomarker of AD is based on the popular yet controversial "amyloid cascade hypothesis" of AD (Hardy and Allsop, 1991; Hardy and Higgins, 1992). According to this oversimplified hypothesis, toxic deposition of amyloid in the AD brain causes synaptic loss and neuronal apoptosis; thus, measuring Aβ aggregates in antemortem AD brain imaging by PET would give the right AD diagnosis (**Table 2**). This hypothesis also supports the idea that amyloid plaque deposition is the primary pathophysiologic change that occurs in preclinical AD. Since fibrillary tau deposition is common in another neurodegenerative disease (Tauopathy, Frontotemporal dementia, Corticobasal degeneration), amyloid imaging by tau would have higher specificity. Klunk et al. (2004) were first to develop ^{11}C-PIB (2-(4′-[11C] methylaminophenyl)-6-hydroxybenzothiazole or Pittsburgh compound B) as an Aβ PET imaging agents (Klunk et al., 2004). The ^{11}C-PIB-PET imaging biomarker has a limitation in terms of sensitivity specificity. A study found ^{11}C-PIB-PET positive in about 20–30% of cases of cognitively normal individuals (Pike et al., 2007). On the other hand, a report demonstrated that ∼16% of patients with probable AD were PIB PET negative (Shimada et al., 2011). As Aβ plaque is not associated with dementia in AD, the earliest event in preclinical AD, synaptic loss, would not be expected to correlate with ^{11}C-PIB-PET alone. A longitudinal study of PIB-PET found no correlation of PIB uptake depending their dementia status in age-matched control, MCI, and AD individuals (Jack et al., 2009). Therefore, ^{11}C-PIB-PET may provide evidence of amyloid deposit in the brain but may not be useful for diagnosing preclinical AD alone. Another Aβ PET imaging compound, ^{18}F-florbetapir demonstrated greater specificity than CSF $A\beta_{42}$ (Mattsson et al., 2014). The half-life of positron-emitting ^{11}C-PIB (20.33 min) is much lower than that of ^{18}F (109.77 min). While ^{18}F compounds provide a shorter window for conducting an imaging study, this also means that the ^{18}F radiotracer must be made in-house using a cyclotron, or within a range consistent with the 20-min half-life. Other well studied Aβ radiotracers are ^{11}C-BF227 and ^{18}F-NAV4694. A recent study found that Aβ-PET is suitable for defining preclinical AD along with CSF biomarkers (Dubois et al., 2016). Moreover ante mortem ^{11}C-PIB-PET scanning results were correlated with the Thal amyloid deposition stages (Murray et al., 2015). Amyloid plaque score in terms of Thal stage has been incorporated in NIA-AA (2011) AD neuropathological criteria (Hyman et al., 2012).

Biomarker of Glucose Metabolism in AD by PET

Dysfunctional brain glucose metabolism is another hypothesis of AD pathogenesis. Temporoparietal hypometabolism is one of the brain areas first affected due to preclinical AD pathology. [^{18}F]-fluoro-2-deoxy-D-glucose (^{18}FDG) has been extensively used as the PET agent for region-specific brain imaging. ^{18}FDG-PET imaging outcomes from AD patients were appropriately correlated with the mini-mental score examination (MMSE) (Jagust et al., 2009). In fact, among the PET imaging techniques, ^{18}FDG-PET is the most widely researched imaging biomarker for AD. ^{18}FDG-PET showed consistent low signal in the parietal-temporal area and posterior cingulate cortex. In severe AD, the frontal cortex showed lower signal; however, other brain areas unaffected by AD pathologies such as the cerebellum, striatum basal ganglia and the visual and sensory cortex remained unchanged. A differential low glucose metabolism detected at different brain region by ^{18}FDG-PET can be used for differential AD and non-AD dementia diagnosis (Silverman et al., 2001; Mosconi et al., 2008). ^{18}FDG-PET can be used for differential AD diagnosis vs. other non-AD dementia suggested by important regulatory authorities, such as FDA and EMA. In addition to that, International panels for AD diagnostic criteria have included ^{18}FDG-PET as one of the AD biomarkers (Sperling et al., 2011; Dubois et al., 2014). The Centers for Medicare and Medicaid Services (CMS) have allowed the use of ^{18}FDG-PET to establish the diagnosis of dementia due to AD and frontotemporal dementia (FTD). ^{18}FDG-PET also has potential to predict preclinical AD pathology (Ito et al., 2015).

Biomarkers of tau Imaging in AD by PET

The hyperphosphorylated paired helical filament (PHF) that forms NFTs quantified by Braak stages are better correlated with AD severity and neuronal atrophy than amyloid plaques (Bierer et al., 1995; Nelson et al., 2007). Both tau and phosphorylated tau (p-tau) are increased in AD pathology considered to be the measure of neuronal injury. Some studies even showed that neuronal injuries due to tau and p-tau are earlier than abnormalities in amyloidosis (Jack and Holtzman, 2013; Jack et al., 2013). CSF tau is not the same as deposition of NFTs in the AD brain. Moreover, the dynamic ranges of tau and p-tau in CSF AD biomarkers are lower than $A\beta_{42}$. Therefore, tau imaging by PET as AD preclinical should have a higher implication.

Tau-PET imaging for AD was initiated with^{18}FDDNP (a radiofluorinated derivative of the 2-(1-[6-(dimethylamino)-2-naphthyl]ethylidene) malononitrile) showing higher binding in AD and MCI cases (Small et al., 2006). The first human trial of tau radiotracer ^{18}F-T807 by Siemens Molecular Imaging Biomarker Research (Culver City, CA) found higher tau levels in brain areas rich in PHF and very low in white matter (Chien et al., 2013). There are several other new tau-PET tracers that have been developed based on quinolone derivatives (^{18}F-THK-523, ^{18}F-THK-5105, and ^{18}F-THK-5117) (Fodero-Tavoletti et al., 2011; Harada et al., 2013; Okamura et al., 2014). Longitudinal tau-PET cohorts in patients with high-risk preclinical AD provided special distribution of deposition of tau that can allow to staging *in-vivo* neurodegeneration according to tau levels in preclinical AD (Johnson et al., 2016). Special distribution of tau deposition by tau-PET would serve a very important role in determining preclinical AD cases. For example, tau-PET ligand uptake in the neocortex and increase amyloidosis with time in longitudinal studies can find underlining preclinical AD pathology. Tau-PET uptake in the medial temporal lobe can

be due to non-AD pathology preclinical FTD (frontotemporal dementia), CBD (corticobasal degeneration), PSP (progressive supranuclear palsy), or age-related tauopathy (Crary et al., 2014). Tau-PET binding in medial temporal lobe is not useful for preclinical AD diagnosis since it cannot differentiate control from MCI cases. Moreover, Tau-PET binding occurs in media temporal lobe even in asymptomatic elderly cases up to Braak stage 2.

APPLICABILITY OF BRAIN NEUROIMAGING MODALITIES FOR DETECTION OF BIOMARKERS IN PRECLINICAL ALZHEIMER'S DISEASE

A comparison of the different neuroimaging modalities used to detect preclinical AD biomarkers is shown in **Table 3**. ^{18}FDG-PET imaging outcome determines region-specific subtle metabolic changes in the brain. According to metabolic dysfunction hypothesis AD, pathologic changes first occur in the metabolic pathway of a preclinical AD brain. While ^{18}FDG-PET correlates strongly with AD and AD progression, it has the potential to distinguish AD vs. other non-AD dementia, and it strongly correlates with MMSE. Therefore, ^{18}FDG-PET has the capability to distinguish preclinical AD. There will be some disadvantages using ^{18}FDG-PET for the diagnosis of preclinical AD. The ^{18}FDG-PET signal can be affected by inflammation, local ischemia, and the behavior state of the subject (Duara et al., 2010; Shipley et al., 2013). The diagnostic criteria for the preclinical AD by IWG-AA (2015) does not list either MRI or ^{18}FDG-PET as suitable modalities for defining preclinical AD (Dubois et al., 2016). However, IWG-AA recommends^{18}FDG-PET for tracking progress in clinical AD in individuals with asymptomatic preclinical AD (Dubois et al., 2016).

rs-fMRI can detect abnormalities before brain volume loss (atrophy as determined by sMRI). It can be used to detect reduced functional connectivity in the preclinical stage of AD. However, there are no regulatory guidelines by FDA or EMA. DTI/sMRI has the potential to detect abnormalities in white matter networks in preclinical AD. In addition, it has the capability to detect region specificity to detect a specific region affected by preclinical AD. ASL/MRI can detect the abnormality in CBF in the preclinical AD. While Aβ-PET imaging can only be a signature of an amount of Aβ levels in the preclinical AD brain, it may not be used to detect the level of neurodegeneration (**Table 3**).

RISK FACTORS IN PRECLINICAL ALZHEIMER'S DISEASE

Preclinical AD can be classified in terms of degree of the risk factor of developing preclinical AD (except age). Such risk factors are positive amyloidosis, positive neurodegeneration, abnormalities in synaptic function by fMRI, and positive genetic AD risk factors. Individuals with high-risk factors should be included in a longitudinal follow-up in a cohort to find the relationship between risk factor and development of preclinical AD. A longitudinal cohort study showed CSF AD biomarkers ($A\beta_{42}$ and tau) and Aβ-PET can distinguish preclinical AD as high risk and low-risk categories (Vos et al., 2013). In future patients in a high-risk AD category and preclinical categories can be advised to change their lifestyle and food habits to delay the disease. Longitudinal changes with different risk factor in preclinical AD follow-up until cognitively impaired will allow for estimating positive and negative predictive values of the use of AD biomarkers in an at-risk population.

NEED FOR DIAGNOSTIC GUIDELINES FOR PRECLINICAL AD

Ample evidence shows that AD has long prodromal stages (preclinical AD → MCI due to AD pathology → AD-dementia) before the real clinical manifestation of dementia. The earlier treatment of AD begins in the disease course, the more effective it is at slowing the progression of the disease. Therefore, the detection of preclinical AD in asymptomatic individuals has become a major AD research focus. A simple definition of preclinical AD by the International panel (IWG-2014): No clinical symptoms of AD but positive AD biomarker values (in CSF: decreased $A\beta_{42}$, increased tau and/or p-tau in CSF; or in brain imaging: increased fibrillary amyloid on PET; Dubois et al., 2014). This simplistic definition needs more extensive diagnostic guidelines for preclinical AD. Deposition of amyloid plaques in the brain begins decades before clinical manifestation of AD, and the NIA-AA (2011) defines preclinical AD on the basis of pathological changes in the brain that occur before a demonstration of cognitive deficits. Later, IWG and NIA-AA (2015) simplified the definition of preclinical AD as the period of time between the first evidence of neuropathological lesions in the brain to the date of first clinical symptoms of AD. Now the challenge is to find validated biomarkers capable of detecting the first evidence of neuropathological lesions in the brain. Extensive research of AD biomarkers over the last couple decades has shown that preclinical AD is more likely to be diagnosed using multi-modal criteria. There is a need for evidence-based guidance on how to combine validated tests and imaging modalities to diagnose AD before the widespread synaptic loss and irreversible neuronal damage occur.

A combination of early Aβ-PET, ^{18}FDG-PET, and DTI MRI and/or fMRI to detect neurodegeneration, supported by genetic tests of the mutated APP, PSEN1, PSEN2, and APOE4, may be appropriate for preclinical AD diagnosis. Positive Aβ-PET, low ^{18}FDG-PET, and the presence of subtle neurodegeneration on MRI has been detected in familial AD prior to clinical symptoms. In sporadic AD, it would be reasonable to categories individuals with APOE4, positive Aβ-PET, low ^{18}FDG-PET, and subtle neurodegeneration by MRI as having a preclinical AD. Diagnosis of preclinical AD in an individual without genetic markers but with positive Aβ-PET, low ^{18}FDG-PET, and subtle evidence of neurodegeneration on MRI would have to wait until subtle evidence of cognitive decline appears that is not yet equivalent to the level indicative of MCI.

TABLE 3 | Comparison of preclinical Alzheimer's disease neuroimaging modalities.

Neuroimaging modalities	Differences	References
Tau-^{18}F-T807-PET vs. ^{13}C-PIB-PET	Region specific distribution of tau deposition	Johnson et al., 2016
Tau-^{18}F-THK5317-PET vs. ^{18}FDG-PET	Progression of AD is better tracked by ^{18}FDG-PET	Chiotis et al., 2017
^{18}FDG-PET vs. DTI with sMRI	Whole-brain white matter network properties in preclinical AD can be detected by DTI with sMRI before structural markers of significant neurodegeneration such as atrophy (by MRI) or reduced cortical glucose utilization (by ^{18}FDG-PET)	Fischer et al., 2015
^{18}FDG-PET vs. ASL\MRI	ASL MRI is not invasive ^{18}FDG-PET is more expensive than ASL/MRI ASL/MRI operation is simple	Wolk and Detre, 2012

Aβ, amyloid beta; AD, Alzheimer's disease; ASL MRI, arterial spin-labeled magnetic resonance imaging; DTI, diffusion tensor imaging; FDG, fluoro-2-deoxy-D-glucose; fMRI, functional MRI; ^{18}F-T807-PET, Fluorinated tau PET ligand; Tau-^{18}F-THK5317, Fluorinated tau PET ligand; MRI, magnetic resonance imaging; PET, positron emission tomography; PIB, Pittsburgh compound B.

A POSSIBLE ALGORITHM FOR COMPREHENSIVE PRECLINICAL ALZHEIMER'S DISEASE DIAGNOSIS

How and at what point in the lifespan can we begin to detect clear-cut signs of the ongoing neurodegenerative process of AD pathology that is distinct from normal aging? A multidimensional "panel" of preclinical AD biomarkers presents the best chance for a diagnosis and prediction of progression to AD dementia. A combination of three sets of evidence is recommended: (1) neuroimaging to detect early evidence of neurodegeneration in brain areas susceptible to AD pathology; (2) the genetic risk markers that predict AD onset; and (3) evidence of abnormalities in AD biomarkers (e.g., CSF $A\beta_{42}$, tau, and p-tau) (**Figure 2**). Major exclusion criteria would not be useful for preclinical AD diagnosis. Only deposition of tau at the medial temporal lobe by tau-PET can be used as an exclusion of preclinical AD from other tau related preclinical non-AD dementia (preclinical FTD, CBD or age-related tauopathy). Preclinical AD diagnostic algorithm has been proposed based on this combinatorial approach of neuroimaging, genetic testing, and CSF biomarker tests (**Table 4**). Incorporation of biomarkers and genetic information into the preclinical AD diagnostic scheme may also permit prediction of the *in vivo* physiological changes occurring in the brain before a clinical AD diagnosis.

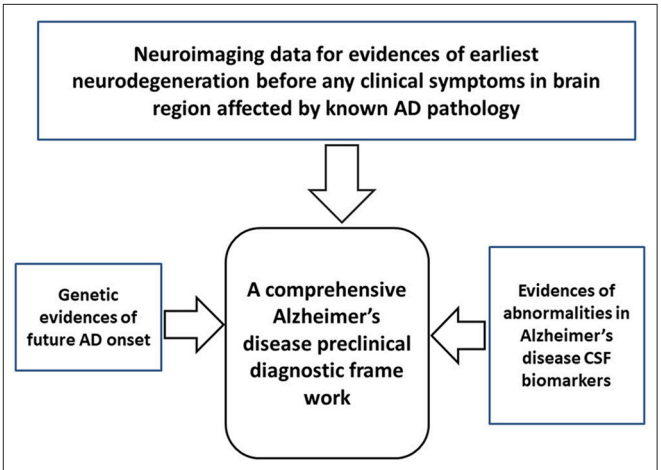


FIGURE 2 | A simple framework for comprehensive diagnosis preclinical Alzheimer's disease (AD). The framework includes three diagnostic modalities: neuroimaging to detect the earliest evidence of neurodegeneration in brain areas susceptible to AD pathology, genetic markers associated with an AD, and biomarker testing to detect abnormalities associated with an AD.

Validation of this framework will require accurate identification of an asymptomatic cohort at risk of AD. Longitudinal follow-up of different risk factors in preclinical AD will allow estimating accuracy, sensitivity, specificity, positive, and negative predictive values of the use of a particular AD biomarker at-risk population. The applicability of this diagnostic algorithm for screening of preclinical case needs extensive validation. Predicting positive and negative predictive values and false positives will depend on how preclinical AD cases will be selected. Standardization of operating procedure, thresholds, and cutoff values of CSF and neuroimaging biomarkers are needed to minimize between-lab and between-batch variability. Despite these challenges, the use of biomarkers holds great promise for the detection of the preclinical AD and the initiation of therapy at earlier stages to slow the progression of the disease. CSF sample collection is highly invasive and neuroimaging biomarkers are expensive; therefore, the ultimate goal for this research area is to find peripheral preclinical biomarkers for AD.

ISSUES CONCERNING PRECLINICAL AD BIOMARKERS

There are several necessary issues of preclinical AD biomarkers to be addressed before application. Most important issues are diagnostic accuracy, patient selection in clinical trial, universal standardization of diagnostic protocols, cost of diagnosis, the complexity of patient selection in clinical trials, and ethical challenges.

TABLE 4 | Algorithm for preclinical Alzheimer's disease diagnosis.

Approach	Preclinical AD biomarkers	Preclinical AD diagnosis
Pre-symptomatic genetic risk factors of familial AD	Familial AD genes: APP, PSEN1, PSEN2	Definite preclinical AD
Combination of sporadic AD risk factor genes (APOE4), CSF biomarkers, and neuroimaging biomarkers	APOE4, TOMM40: Yes CSF: low $A\beta_{42,}$ high tau and p-tau Neuroimaging: high Aβ by PET, neurodegeneration by low ^{18}FDG-PET	Highly probable preclinical AD
Combination of sporadic AD risk factor genes (APOE4), CSF biomarkers, and neuroimaging biomarkers	APOE4: No CSF: low $A\beta_{42}$, high tau and p-tau Neuroimaging: high Aβ by PET, neurodegeneration by low ^{18}FDG-PET	Probable preclinical AD
Combination of sporadic AD risk factor genes from Alzgen data base, CSF biomarkers, and neuroimaging biomarkers	Susceptible gene: Alzgene database CSF: low $A\beta_{42}$, high tau and p-tau Neuroimaging: high Aβ by PET, neurodegeneration by low ^{18}FDG-PET, deposition of tau in cortical region by ^{18}F-T807-PET	Probable preclinical AD
Combination of sporadic AD risk factor genes (APOE4), CSF biomarkers, and neuroimaging biomarkers	APOE4: No CSF: low $A\beta_{42}$, high tau and p-tau Neuroimaging: high Aβ by PET, no neurodegeneration by ^{18}FDG-PET, deposition of tau in cortical region by 18F-T807-PET	Suspected preclinical AD
Combination of sporadic AD risk factor genes (APOE4), CSF biomarkers, and neuroimaging biomarkers	APOE4: No CSF: no $A\beta_{42}$, high tau and p-tau Neuroimaging: low or no Aβ by PET, neurodegeneration by low ^{18}FDG-PET	Suspected preclinical non-AD pathophysiology

Alzgene (http://www.alzgene.org/); Aβ, amyloid beta; APOE, apolipoprotein; CSF, cerebrospinal fluid; FDG, fluoro-2-deoxy-D-glucose; ^{18}F-T807-PET, Fluorinated tau PET ligand; PET, positron emission tomography; TOMM40, translocate of outer mitochondrial membrane 40.

Diagnostic Accuracy and Patient Selection

Improved diagnostic accuracy (sensitivity, specificity, positive predictive value, negative predictive value) and universally accepted unified standard operating procedures (SOP; for sample collection, cut-off values, analysis) are urgently required. The diagnostic sensitivity (SN), specificity (SP), positive likely-hood ratio (LR+), and negative likely-hood ratio (LR–) of all three core CSF biomarkers ($A\beta_{42}$: SN = 79%, SP = 63%, LR+ = 2, and LR– = 0.3; tau: SN = 76%, SP = 58%, LR+ = 2, and LR– = 0.4; p-tau: SN = 78%, SP = 56%, LR+ = 2, and LR– = 0.4; combination of three: $A\beta_{42}$: SN = 84%, SP = 63%, LR+ = 2, and LR– = 0.3) for MCI conversion to AD were found to be moderate by a systemic meta-analysis (Ferreira et al., 2014). The diagnostic sensitivity, specificity, positive likely-hood ratio, and negative likely-hood ratio of ^{18}F-labeled Aβ-PET imaging biomarkers (Florbetapir: SN = 89.6%, SP = 87.2%, LR+ = 7.9 and LR– = 0.108; Florbetaben: SN = 89.3%, SP = 87.6%, LR+ = 6.06 and LR– = 0.141) for distinguishing AD with non-demented control were found to be considerably higher by a systemic meta-analysis (Yeo et al., 2015). The progression of AD in non-demented elderly individuals was predicted with considerable accuracy (SN = 82% and SP = 93%) by studying brain metabolic states by FDG-PET (Ewers et al., 2014). ^{11}C-PIB-PET has higher SN (96%), low SP (58%), moderate LR+ (2.3), and LR– (0.07) for the conversion of MCI-AD (Zhang et al., 2014).

One of the main issues of concern of using this proposed algorithm is how to select potential patients to be screened. The selection of patients should be conducted as described in **Table 4**.

Universal Standardization Diagnostic Protocols

Standard methods of sample collection, reference standards, universal cut-off values for diagnostic tests, and standard operating procedures (SOP) are urgently needed for most advanced AD biomarkers (CSF core biomarkers, Aβ-PET, FDG-PET, and tau-PET). A significant amount of work has been done by an IWG for a universal standardization of AD diagnostic biomarkers (Mattsson and Zetterberg, 2012; Mattsson et al., 2012, 2013; https://aibl.csiro.au/wp-content/uploads/2014/01/sperling.pdf).

Estimated Costs of AD Diagnosis Tests

No doubt, there will be several thousand dollar cost for selecting each patient, and more cost would be during longitudinal follow up. An estimated cost of MRI ($1,694–$3,624) is higher than CSF biomarkers (http://www.comparemricost.com/. Study of 10 cities in the USA show that (Orlando, FL Dallas, TX—MRI Testing Facility A MRI and Dallas, TX—MRI Testing Facility B, San Diego, CA, Salt Lake City, UT, Detroit, MI, New York, NY—MRI Testing Facility A, New York, NY—MRI Testing Facility B, Raleigh, NC, Omaha, NE) fMRI costs are even higher than MRI. Specialized bio-informatics personals with expensive equipment are the main reason for the higher cost of modern neuroimaging AD biomarkers. Moderately invasive PET imaging costs $825–$6,800 (http://www.newchoicehealth.com/procedures/pet-scan-brain: National PET Scan Brain Procedure Pricing Summary). Highly invasive CSF biomarker tests are moderately expensive (∼$450-$1,000 per test) (Fiandaca et al.,

2014; Valcárcel-Nazco et al., 2014), because highly skilled personals are required in specialized medical centers for CSF sample collection (lumbar puncture), three ELISA kits are necessary for ($A\beta_{42}$, tau, and p-tau), and the cost of CSF biomarker tests are much higher than blood-based diagnostic tests. Neuroimaging biomarkers are expensive because modality is a technical sophistication that needs technically trained expert teams of neuroscientists, radiologists, and bioinformatics specialists. A panel of a combination of CSF and neuroimaging biomarkers would increase the predicting power of preclinical AD diagnosis. However, the cost of diagnosis of such AD biomarkers will be much higher. Peripheral AD diagnosis in preclinical AD phase is the best way to decrease this enormous cost.

The Complexity of Patient Selection for Preclinical AD Clinical Trials

A homogeneous set of patients with preclinical AD certainly would not be available by its own characteristic feature of heterogeneity. Therefore, several subgroups of patients with preclinical AD can be separated according to their initial baseline preclinical AD biomarker values and follow longitudinally for a longer time (5–10 years). Such sub-groups are A. genetic sub-group: Asymptomatic high genetic risk with APOE4 and TOMM40 alleles, B. Neurodegeneration subgroup: Asymptomatic neurodegeneration by brain hypometabolism/tau deposition/atrophy, and C. Asymptomatic high-risk Aβ deposition by Aβ-PET and low CSF $A\beta_{42}$ values. Because of longtime follow-up, preclinical AD longitudinal clinical trials should be expensive. Other drawbacks of such clinical trial are patient withdrawal, interference of comorbidity, and lifestyle changes of patients during the longitudinal long follow-up.

Ethical Challenges

Ethical issues to a conclusion and disclosure of a preclinical AD is very complex. The main ethical concerns for an individual are emotional, social, and economical. Emotional issues are feelings, fears, impact on personal motivation, and behavior to family members. A Metlife Foundation survey in 2011 found Americans middle aged and older (≥55 years) are afraid of AD (31%), more than diabetes, heart disease, or stroke and less than cancer (41%) (Metlife Foundation, 2011). Preclinical AD disclosure may induce anxiety and depression. Social issues, such as the social stigma of future development of AD and withdrawal from social events, are an impact on friendship networks. The economic impact will be enormous to an individual with a preclinical AD diagnosis. Health insurance companies may increase the insurance premium. An individual working in higher cognitive performing jobs, such as pilot, clinical practitioners, and nurses need to be reported to a higher authority. Regulatory authorities should develop suitable guidelines for ethical issues for informing individuals about preclinical AD diagnosis.

Keeping all of these issues in mind, one can look at the positive aspect of the disclosure of preclinical AD. More than 90% responded in a survey that they wanted to adopt a healthier lifestyle if they knew they were at risk of AD (Caselli et al., 2014). Individuals who want to take a positive outlook of preclinical AD diagnosis should be influenced to increase social contact, healthy food, and mental exercises such as numerical problem solving, meditation, and yoga.

Feasibility and Utility of the Preclinical AD Diagnostic Algorithm

The main challenge remains how to choose individuals for preclinical AD diagnostic clinical trials. We proposed four different categories of probable preclinical AD cases and definitive preclinical AD category of pre-symptomatic genetic risk factors (**Table 4**) to be longitudinally tested in clinical trials by proposed preclinical AD biomarkers. In longitudinal follow-up trials will produce four different categories of biomarkers results (amyloid+ and neurodegenerative+, amyloid+ and neurodegenerative-, amyloid-and neurodegenerative+, amyloid- and neurodegenerative– (Pereira et al., 2017), and cognitive impairment due to AD. Those results will be complied in a comprehensive AD preclinical diagnostic framework presented in **Figure 2** to generate correlation of AD converters and AD non-converters with preclinical AD biomarkers.

Although challenges of cost, positive predictive values, and ethical issues are substantial this algorithm will provide a frame work of preclinical AD diagnosis, like lipid profiling for an individual in risk of heart disease. In the future individual with a risk of a preclinical AD from this framework should have suggestion from doctors to follow a healthy lifestyle.

AUTHOR CONTRIBUTIONS

The author confirms being the sole contributor of this work and approved it for publication.

ACKNOWLEDGMENTS

Financial assistance from the Intramural Research Program of the Blanchette Rockefeller Neurosciences Institute at West Virginia University, Morgantown, WV (TK), is gratefully acknowledged. The author is indebted to Ms. Cassandra George for assisting in the preparation of this manuscript. The author is grateful to the honorable editor and reviewers for their valuable comments for the improvement of this article.

REFERENCES

Adluru, N., Destiche, D. J., Lu, S. Y., Doran, S. T., Birdsill, A. C., Melah, K. E., et al. (2014). White matter microstructure in late middle-age: effects of apolipoprotein E4 and parental family history of Alzheimer's disease. *Neuroimage Clin.* 4, 730–742. doi: 10.1016/j.nicl.2014.04.008

Alsop, D. C., Dai, W., Grossman, M., and Detre, J. A. (2010). Arterial spin labeling blood flow MRI: its role in the early characterization of Alzheimer's disease. *J. Alzheimers Dis.* 20, 871–880. doi: 10.3233/JAD-2010-091699

Alsop, D. C., Detre, J. A., and Grossman, M. (2000). Assessment of cerebral blood flow in Alzheimer's disease by spin-labeled magnetic resonance imaging. *Ann. Neurol.* 47, 93–100. doi: 10.1002/1531-8249(200001)47:1<93::AID-ANA15>3.0.CO;2-8

Beaulieu, C., and Allen, P. S. (1994). Determinants of anisotropic water diffusion in nerves. *Magn. Reson. Med.* 31, 394–400. doi: 10.1002/mrm.1910310408

Bierer, L. M., Hof, P. R., Purohit, D. P., Carlin, L., Schmeidler, J., Davis, K. L., et al. (1995). Neocortical neurofibrillary tangles correlate with dementia severity in Alzheimer's disease. *Arch. Neurol.* 52, 81–88. doi: 10.1001/archneur.1995.00540250089017

Biswal, B., Yetkin, F. Z., Haughton, V. M., and Hyde, J. S. (1995). Functional connectivity in the motor cortex of resting human brain using echo-planar MRI. *Magn. Reson. Med.* 34, 537–541. doi: 10.1002/mrm.1910340409

Buckley, R. F., Schultz, A. P., Hedden, T., Papp, K. V., Hanseeuw, B. J., Marshall, G., et al. (2017). Functional network integrity presages cognitive decline in preclinical Alzheimer disease. *Neurology* 89, 29–37. doi: 10.1212/WNL.0000000000004059

Caselli, R. J., Langbaum, J., Marchant, G. E., Lindor, R. A., Hunt, K. S., Henslin, B. R., et al. (2014). Public perceptions of presymptomatic testing for Alzheimer disease. *Mayo Clin. Proc.* 89, 1389–1396. doi: 10.1016/j.mayocp.2014.05.016

Chien, D. T., Bahri, S., Szardenings, A. K., Walsh, J. C., Mu, F., Su, M. Y., et al. (2013). Early clinical PET imaging results with the novel PHF-tau radioligand [F-18]-T807. *J. Alzheimers Dis.* 34, 457–468. doi: 10.3233/JAD-122059

Chiotis, K., Saint-Aubert, L., Rodriguez-Vieitez, E., Leuzy, A., Almkvist, O., Savitcheva, I., et al. (2017). Longitudinal changes of tau PET imaging in relation to hypometabolism in prodromal and Alzheimer's disease dementia. *Mol. Psychiatry*. doi: 10.1038/mp.2017.108. [Epub ahead of print].

Chua, T. C., Wen, W., Chen, X., Kochan, N., Slavin, M. J., Trollor, J. N., et al. (2009). Diffusion tensor imaging of the posterior cingulate is a useful biomarker of mild cognitive impairment. *Am. J. Geriatr. Psychiatry* 17, 602–613. doi: 10.1097/JGP.0b013e3181a76e0b

Crary, J. F., Trojanowski, J. Q., Schneider, J. A., Abisambra, J. F., Abner, E. L., Alafuzoff, I., et al. (2014). Primary age-related tauopathy (PART): a common pathology associated with human aging. *Acta Neuropathol.* 128, 755–766. doi: 10.1007/s00401-014-1349-0

Dai, W., Lopez, O. L., Carmichael, O. T., Becker, J. T., Kuller, L. H., and Gach, H. M. (2009). Mild cognitive impairment and Alzheimer disease: patterns of altered cerebral blood flow at MR imaging. *Radiology* 250, 856–866. doi: 10.1148/radiol.2503080751

Detre, J. A., Leigh, J. S., Williams, D. S., and Koretsky, A. P. (1992). Perfusion imaging. *Magn. Reson. Med.* 23, 37–45. doi: 10.1002/mrm.1910230106

Detre, J. A., Rao, H., Wang, D. J., Chen, Y. F., and Wang, Z. (2012). Applications of arterial spin labeled MRI in the brain. *J. Magn. Reson. Imaging* 35, 1026–1037. doi: 10.1002/jmri.23581

Detre, J. A., Wang, J., Wang, Z., and Rao, H. (2009). Arterial spin-labeled perfusion MRI in basic and clinical neuroscience. *Curr. Opin. Neurol.* 22, 348–355. doi: 10.1097/WCO.0b013e32832d9505

Duara, R., Loewenstein, D. A., Greig-Custo, M. T., Raj, A., Barker, W., Potter, E., et al. (2010). Diagnosis and staging of mild cognitive impairment, using a modification of the clinical dementia rating scale: the mCDR. *Int. J. Geriatr. Psychiatry* 25, 282–289. doi: 10.1002/gps.2334

Dubois, B., Feldman, H. H., Jacova, C., Hampel, H., Molinuevo, J. L., Blennow, K., et al. (2014). Advancing research diagnostic criteria for Alzheimer's disease: the IWG-2 criteria. *Lancet Neurol.* 13, 614–629. doi: 10.1016/S1474-4422(14)70090-0

Dubois, B., Hampel, H., Feldman, H. H., Scheltens, P., Aisen, P., Andrieu, S., et al. (2016). Preclinical Alzheimer's disease: definition, natural history, and diagnostic criteria. *Alzheimers Dement.* 12, 292–323. doi: 10.1016/j.jalz.2016.02.002

Ewers, M., Brendel, M., Rizk-Jackson, A., Rominger, A., Bartenstein, P., Schuff, N., et al. (2014). Reduced FDG-PET brain metabolism and executive function predict clinical progression in elderly healthy subjects. *Neuroimage Clin.* 4, 45–52. doi: 10.1016/j.nicl.2013.10.018

Ewers, M., Insel, P. S., Stern, Y., and Weiner, M. W. (2013). Cognitive reserve associated with FDG-PET in preclinical Alzheimer disease. *Neurology* 80, 1194–1201. doi: 10.1212/WNL.0b013e31828970c2

Fagan, A. M., Roe, C. M., Xiong, C., Mintun, M. A., Morris, J. C., and Holtzman, D. M. (2007). Cerebrospinal fluid tau/beta-amyloid (42) ratio as a prediction of cognitive decline in nondemented older adults. *Arch. Neurol.* 64, 343–349. doi: 10.1001/archneur.64.3.noc60123

Ferreira, D., Perestelo-Pérez, L., Westman, E., Wahlund, L. O., Sarría, A., and Serrano-Aguilar, P. (2014). Meta-review of CSF core biomarkers in Alzheimer's disease: the state-of-the-art after the new revised diagnostic criteria. *Front. Aging Neurosci.* 6:47. doi: 10.3389/fnagi.2014.00047

Fiandaca, M. S., Mapstone, M. E., Cheema, A. K., and Federoff, H. J. (2014). The critical need for defining preclinical biomarkers in Alzheimer's disease. *Alzheimers Dement.* 10(Suppl. 3), S196–S212. doi: 10.1016/j.jalz.2014.04.015

Fischer, F. U., Wolf, D., Scheurich, A., and Fellgiebel, A. (2015). Altered whole-brain white matter networks in preclinical Alzheimer's disease. *Neuroimage Clin.* 8, 660–666. doi: 10.1016/j.nicl.2015.06.007

Fodero-Tavoletti, M. T., Okamura, N., Furumoto, S., Mulligan, R. S., Connor, A. R., McLean, C. A., et al. (2011). 18F-THK523: a novel *in vivo* tau imaging ligand for Alzheimer's disease. *Brain* 134, 1089–1100. doi: 10.1093/brain/awr038

Fox, N. C., Warrington, E. K., and Rossor, M. N. (1999). Serial magnetic resonance imaging of cerebral atrophy in preclinical Alzheimer's disease. *Lancet* 353, 2125–2125. doi: 10.1016/S0140-6736(99)00496-1

Frölich, L., Peters, O., Lewczuk, P., Gruber, O., Teipel, S. J., Gertz, H. J., et al. (2017). Incremental value of biomarker combinations to predict progression of mild cognitive impairment to Alzheimer's dementia. *Alzheimers Res. Ther.* 9:84. doi: 10.1186/s13195-017-0301-7

Grand, J. H., Caspar, S., and Macdonald, S. W. (2011). Clinical features and multidisciplinary approaches to dementia care. *J. Multidiscip. Healthc.* 4, 125–147. doi: 10.2147/JMDH.S17773

Gustafson, D. R., Skoog, I., Rosengren, L., Zetterberg, H., and Blennow, K. (2007). Cerebrospinal fluid beta-amyloid 1-42 concentration may predict cognitive decline in older women. *J. Neurol. Neurosurg. Psychiatr.* 78, 461–464. doi: 10.1136/jnnp.2006.100529

Harada, R., Okamura, N., Furumoto, S., Tago, T., Maruyama, M., Higuchi, M., et al. (2013). Comparison of the binding characteristics of [18F]THK-523 and other amyloid imaging tracers to Alzheimer's disease pathology. *Eur. J. Nucl. Med. Mol. Imaging* 40, 125–132. doi: 10.1007/s00259-012-2261-2

Hardy, J. A., and Higgins, G. A. (1992). Alzheimer's disease: the amyloid cascade hypothesis. *Science* 256, 184–185. doi: 10.1126/science.1566067

Hardy, J., and Allsop, D. (1991). Amyloid deposition as the central event in the aetiology of Alzheimer's disease. *Trends Pharmacol. Sci.* 12, 383–388. doi: 10.1016/0165-6147(91)90609-V

Hays, C. C., Zlatar, Z. Z., and Wierenga, C. E. (2016). The utility of cerebral blood flow as a biomarker of preclinical Alzheimer's disease. *Cell. Mol. Neurobiol.* 36, 167–179. doi: 10.1007/s10571-015-0261-z

Hubbard, B. M., Fenton, G. W., and Anderson, J. M. (1990). A quantitative histological study of early clinical and preclinical Alzheimer's disease. *Neuropathol. Appl. Neurobiol.* 16, 111–121.

Hyman, B. T., Phelps, C. H., Beach, T. G., Bigio, E. H., Cairns, N. J., Carrillo, M. C., et al. (2012). National Institute on Aging-Alzheimer's Association guidelines for the neuropathologic assessment of Alzheimer's disease. *Alzheimers Dement.* 8, 1–13. doi: 10.1016/j.jalz.2011.10.007

Ito, K., Fukuyama, H., Senda, M., Ishii, K., Maeda, K., Yamamoto, Y., et al. (2015). Prediction of outcomes in mild cognitive impairment by using 18F-FDG-PET: a multicenter study. *J. Alzheimers Dis.* 45, 543–552. doi: 10.3233/JAD-141338

Jack, C. R. Jr, and Holtzman, D. M. (2013). Biomarker modeling of Alzheimer's disease. *Neuron* 80, 1347–1358. doi: 10.1016/j.neuron.2013.12.003

Jack, C. R. Jr, Knopman, D. S., Jagust, W. J., Shaw, L. M., Aisen, P. S., Weiner, M. W., et al. (2010). Hypothetical model of dynamic biomarkers of the Alzheimer's pathological cascade. *Lancet Neurol.* 9, 119–128. doi: 10.1016/S1474-4422(09)70299-6

Jack, C. R. Jr, Lowe, V. J., Weigand, S. D., Wiste, H. J., Senjem, M. L., Knopman, D. S., et al. (2009). Serial PIB and MRI in normal, mild cognitive impairment and Alzheimer's disease: implications for sequence of pathological events in Alzheimer's disease. *Brain* 132, 1355–1365. doi: 10.1093/brain/awp062

Jack, C. R. Jr., Wiste, H. J., Weigand, S. D., Knopman, D. S., Lowe, V., Vemuri, P., et al. (2013). Amyloid-first and neurodegeneration-first profiles characterize incident amyloid PET positivity. *Neurology* 81, 1732–1740. doi: 10.1212/01.wnl.0000435556.21319.e4

Jagust, W. J., Landau, S. M., Shaw, L. M., Trojanowski, J. Q., Koeppe, R. A., Reiman, E. M., et al. (2009). Relationships between biomarkers in aging and dementia. *Neurology* 73, 1193–1199. doi: 10.1212/WNL.0b013e3181bc010c

Jansen, W. J., Ossenkoppele, R., Knol, D. L., Tijms, B. M., Scheltens, P., Verhey, F. R., et al. (2015). Prevalence of cerebral amyloid pathology in persons without dementia: a meta-analysis. *JAMA* 313, 1924–1938. doi: 10.1001/jama.2015.4668

Johnson, K. A., Fox, N. C., Sperling, R. A., and Klunk, W. E. (2012). Brain imaging in Alzheimer disease. *Cold Spring Harb. Perspect. Med.* 2:a006213. doi: 10.1101/cshperspect.a006213

Johnson, K. A., Schultz, A., Betensky, R. A., Becker, J. A., Sepulcre, J., Rentz, D., et al. (2016). Tau positron emission tomographic imaging in aging and early Alzheimer disease. *Ann. Neurol.* 79, 110–119. doi: 10.1002/ana.24546

Johnson, N. A., Jahng, G. H., Weiner, M. W., Miller, B. L., Chui, H. C., Jagust, W. J., et al. (2005). Pattern of cerebral hypoperfusion in Alzheimer disease and mild cognitive impairment measured with arterial spin-labeling MR imaging: initial experience. *Radiology* 234, 851–859. doi: 10.1148/radiol.23430 40197

Kantarci, K., Murray, M. E., Schwarz, C. G., Reid, R. I., Przybelski, S. A., Lesnick, T., et al. (2017). White-matter integrity on DTI and the pathologic staging of Alzheimer's disease. *Neurobiol. Aging* 56, 172–179. doi: 10.1016/j.neurobiolaging.2017.04.024

Kester, M. I., Teunissen, C. E., Crimmins, D. L., Herries, E. M., Ladenson, J. H., Scheltens, P., et al. (2015). Neurogranin as a cerebrospinal fluid biomarker for synaptic loss in symptomatic Alzheimer disease. *JAMA Neurol.* 72, 1275–1280. doi: 10.1001/jamaneurol.2015.1867

Khan, T. K. (2016). *Biomarkers in Alzheimer's Disease*. London: Academic Press, 37.

Kinnunen, K. M., Cash, D. M., Poole, T., Frost, C., Benzinger, T. L. S., Ahsan, R. L., et al. (2017). Presymptomatic atrophy in autosomal dominant Alzheimer's disease: a serial MRI study. *Alzheimers Dement.* 14, 43–53. doi: 10.1016/j.jalz.2017.06.2268

Klunk, W. E., Engler, H., Nordberg, A., Wang, Y., Blomqvist, G., Holt, D. P., et al. (2004). Imaging brain amyloid in Alzheimer's disease with Pittsburgh Compound-B. *Ann. Neurol.* 55, 306–319. doi: 10.1002/ana.20009

Machulda, M. M., Jones, D. T., Vemuri, P., McDade, E., Avula, R., Przybelski, S., et al. (2011). Effect of APOE epsilon4 status on intrinsic network connectivity in cognitively normal elderly subjects. *Arch. Neurol.* 68, 1131–1136. doi: 10.1001/archneurol.2011.108

Mattsson, N., and Zetterberg, H. (2012). What is a certified reference material. *Biomark. Med.* 6, 369–370. doi: 10.2217/bmm.12.37

Mattsson, N., Andreasson, U., Persson, S., Carrillo, M. C., Collins, S., Chalbot, S., et al. (2013). CSF biomarker variability in the Alzheimer's Association quality control program. *Alzheimers Dement.* 9, 251–261. doi: 10.1016/j.jalz.2013.01.010

Mattsson, N., Insel, P. S., Landau, S., Jagust, W., Donohue, M., Shaw, L. M., et al. (2014). Diagnostic accuracy of CSF Aβ42 and florbetapir PET for Alzheimer's disease. *Ann. Clin. Transl. Neurol.* 1, 534–543. doi: 10.1002/acn3.81

Mattsson, N., Zegers, I., Andreasson, U., Bjerke, M., Blankenstein, M. A., Bowser, R., et al. (2012). Reference measurement procedures for Alzheimer's disease cerebrospinal fluid biomarkers: definitions and approaches with focus on amyloid β42. *Biomark. Med.* 6, 409–417. doi: 10.2217/bmm.12.39

McKhann, G. M., Knopman, D. S., Chertkow, H., Hyman, B. T., Jack, C. R. Jr, Kawas, C. H., et al. (2011). The diagnosis of dementia due to Alzheimer's disease: recommendations from the National Institute on Aging-Alzheimer's Association workgroups on diagnostic guidelines for Alzheimer's disease. *Alzheimers Dement.* 7, 263–269. doi: 10.1016/j.jalz.2011.03.005

Metlife Foundation (2011). *What America Thinks: MetLife Foundation Alzheimer's Survey*. New York, NY: Harris Interactive.

Mintun, M. A., Larossa, G. N., Sheline, Y. I., Dence, C. S., Lee, S. Y., Mach, R. H., et al. (2006). [11C]PIB in a nondemented population: potential antecedent marker of Alzheimer disease. *Neurology* 67, 446–452. doi: 10.1212/01.wnl.0000228230.26044.a4

Morris, J. C. (2005). Early-stage and preclinical Alzheimer's disease. *Alzheimer Dis. Assoc. Disord.* 19, 163–165. doi: 10.1097/01.wad.0000184005.22611.cc

Mosconi, L., Sorbi, S., de Leon, M. J., Li, Y., Nacmias, B., Myoung, P. S., et al. (2006). Hypometabolism exceeds atrophy in presymptomatic early-onset familial Alzheimer's disease. *J. Nucl. Med.* 47, 1778–1786.

Mosconi, L., Tsui, W. H., Herholz, K., Pupi, A., Drzezga, A., Lucignani, G., et al. (2008). Multicenter standardized 18F-FDG PET diagnosis of mild cognitive impairment, Alzheimer's disease, and other dementias. *J. Nucl. Med.* 49, 390–398. doi: 10.2967/jnumed.107.045385

Moseley, M. E., Cohen, Y., Kucharczyk, J., Mintorovitch, J., Asgari, H. S., Wendland, M. F., et al. (1990). Diffusion-weighted MR imaging of anisotropic water diffusion in cat central nervous system. *Radiology* 176, 439–445. doi: 10.1148/radiology.176.2.2367658

Murray, M. E., Lowe, V. J., Graff-Radford, N. R., Liesinger, A. M., Cannon, A., Przybelski, S. A., et al. (2015). Clinicopathologic and 11C-Pittsburgh compound B implications of Thal amyloid phase across the Alzheimer's disease spectrum. *Brain* 138, 1370–1381. doi: 10.1093/brain/awv050

Nedelska, Z., Schwarz, C. G., Boeve, B. F., Lowe, V. J., Reid, R. I., Przybelski, S. A., et al. (2015). White matter integrity in dementia with Lewy bodies: a voxel-based analysis of diffusion tensor imaging. *Neurobiol. Aging* 36, 2010–2017. doi: 10.1016/j.neurobiolaging.2015.03.007

Nelson, P. T., Jicha, G. A., Schmitt, F. A., Liu, H., Davis, D. G., Mendiondo, M. S., et al. (2007). Clinicopathologic correlations in a large Alzheimer disease center autopsy cohort: neuritic plaques and neurofibrillary tangles "do count" when staging disease severity. *J. Neuropathol. Exp. Neurol.* 66, 1136–1146. doi: 10.1097/nen.0b013e31815c5efb

Okamura, N., Furumoto, S., Fodero-Tavoletti, M. T., Mulligan, R. S., Harada, R., Yates, P., et al. (2014). Non-invasive assessment of Alzheimer's disease neurofibrillary pathology using 18F-THK5105 PET. *Brain* 137, 1762–1771. doi: 10.1093/brain/awu064

Pereira, J. B., van Westen, D., Stomrud, E., Strandberg, T. O., Volpe, G., Westman, E., et al. (2017). Abnormal structural brain connectome in individuals with preclinical Alzheimer's disease. *Cereb. Cortex*. doi: 10.1093/cercor/bhx236. [Epub ahead of print].

Petersen, R. C., Doody, R., Kurz, A., Mohs, R. C., Morris, J. C., Rabins, P. V., et al. (2001). Current concepts in mild cognitive impairment. *Arch. Neurol.* 58, 1985–1992. doi: 10.1001/archneur.58.12.1985

Petersen, R. C., Smith, G. E., Waring, S. C., Ivnik, R. J., Tangalos, E. G., and Kokmen, E. (1999). Mild cognitive impairment: clinical characterization and outcome. *Arch. Neurol.* 56, 303–308. doi: 10.1001/archneur.56.3.303

Pierpaoli, C., and Basser, P. J. (1996). Toward a quantitative assessment of diffusion anisotropy. *Magn. Reson. Med.* 36, 893–906. doi: 10.1002/mrm.1910360612

Pierpaoli, C., Jezzard, P., Basser, P. J., Barnett, A., and Di Chiro, G. (1996). Diffusion tensor MR imaging of human brain. *Radiology* 201, 637–648. doi: 10.1148/radiology.201.3.8939209

Pike, K. E., Savage, G., Villemagne, V. L., Ng, S., Moss, S. A., Maruff, P., et al. (2007). β-amyloid imaging and memory in non-demented individuals: evidence for preclinical Alzheimer's disease. *Brain* 130, 2837–2844. doi: 10.1093/brain/awm238

Popp, J., Oikonomidi, A., Tautvydaite, D., Dayon, L., Bacher, M., Migliavacca, E., et al. (2017). Markers of neuroinflammation associated with Alzheimer's disease pathology in older adults. *Brain Behav. Immun.* 62, 203–211. doi: 10.1016/j.bbi.2017.01.020

Racine, A. M., Adluru, N., Alexander, A. L., Christian, B. T., Okonkwo, O. C., Oh, J., et al. (2014). Associations between white matter microstructure and amyloid burden in preclinical Alzheimer's disease: a multimodal imaging investigation. *Neuroimage Clin.* 4, 604–614. doi: 10.1016/j.nicl.2014.02.001

Reiman, E. M., Quiroz, Y. T., Fleisher, A. S., Chen, K., Velez-Pardo, C., Jimenez-Del-Rio, M., et al. (2012). Brain imaging and fluid biomarker analysis in young adults at genetic risk for autosomal dominant Alzheimer's disease in the presenilin 1 E280A kindred: a case-control study. *Lancet Neurol.* 11, 1048–1056. doi: 10.1016/S1474-4422(12)70228-4

Ritchie, C., Smailagic, N., Noel-Storr, A. H., Ukoumunne, O., Ladds, E. C., and Martin, S. (2017). CSF tau and the CSF tau/ABeta ratio for the diagnosis of Alzheimer's disease dementia and other dementias in people with mild cognitive impairment (MCI). *Cochrane Database Syst. Rev.* 3:CD010803. doi: 10.1002/14651858.CD010803.pub2

Scheinin, N. M., Aalto, S., Koikkalainen, J., Lötjönen, J., Karrasch, M., Kemppainen, N., et al. (2009). Follow-up of [11C] PIB uptake and brain volume in patients with Alzheimer disease and controls. *Neurology* 73, 1186–1192. doi: 10.1212/WNL.0b013e3181bacf1b

Sexton, C. E., Kalu, U. G., Filippini, N., Mackay, C. E., and Ebmeier, K. P. (2011). A meta-analysis of diffusion tensor imaging in mild cognitive impairment and Alzheimer's disease. *Neurobiol Aging* 32, 2322.e5–2322.e18. doi: 10.1016/j.neurobiolaging.2010.05.019

Sheline, Y. I., and Raichle, M. E. (2013). Resting state functional connectivity in preclinical Alzheimer's disease. *Biol. Psychiatry* 74, 340–347. doi: 10.1016/j.biopsych.2012.11.028

Shimada, H., Ataka, S., Takeuchi, J., Mori, H., Wada, Y., Watanabe, Y., et al. (2011). Pittsburgh Compound B-negative dementia–a possibility of misdiagnosis of patients with non-Alzheimer disease-type dementia as having AD. *J. Geriatr. Psychiatry Neurol.* 24, 123–126. doi: 10.1177/0891988711409410

Shipley, S. M., Frederick, M. C., Filley, C. M., and Kluger, B. M. (2013). Potential for misdiagnosis in community-acquired PET scans for dementia. *Neurol. Clin. Pract.* 3, 305–312. doi: 10.1212/CPJ.0b013e318296f2df

Silverman, D. H., Small, G. W., Chang, C. Y., Lu, C. S., Kung De Aburto, M. A., Chen, W., et al. (2001). Positron emission tomography in evaluation of dementia: regional brain metabolism and long-term outcome. *JAMA* 286, 2120–2127. doi: 10.1001/jama.286.17.2120

Small, G. W., Kepe, V., Ercoli, L. M., Siddarth, P., Bookheimer, S. Y., Miller, K. J., et al. (2006). PET of brain amyloid and tau in mild cognitive impairment. *N. Engl. J. Med.* 355, 2652–2663. doi: 10.1056/NEJMoa054625

Sperling, R. A., Aisen, P. S., Beckett, L. A., Bennett, D. A., Craft, S., Fagan, A. M., et al. (2011). Toward defining the preclinical stages of Alzheimer's disease: recommendations from the National Institute on Aging-Alzheimer's Association workgroups on diagnostic guidelines for Alzheimer's disease. *Alzheimers Dement.* 7, 280–292. doi: 10.1016/j.jalz.2011.03.003

Stomrud, E., Hansson, O., Blennow, K., Minthon, L., and Londos, E. (2007). Cerebrospinal fluid biomarkers predict decline in subjective cognitive function over 3 years in healthy elderly. *Dement. Geriatr. Cogn. Disord.* 24, 118–124. doi: 10.1159/000105017

Sutphen, C. L., Jasielec, M. S., Shah, A. R., Macy, E. M., Xiong, C., Vlassenko, A. G., et al. (2015). Longitudinal cerebrospinal fluid biomarker changes in preclinical Alzheimer disease during middle age. *JAMA Neurol.* 72, 1029–1042. doi: 10.1001/jamaneurol.2015.1285

Valcárcel-Nazco, C., Perestelo-Pérez, L., Molinuevo, J. L., Mar, J., Castilla, I., and Serrano-Aguilar, P. (2014). Cost-effectiveness of the use of biomarkers in cerebrospinal fluid for Alzheimer's disease. *J. Alzheimers Dis.* 42, 777–788. doi: 10.3233/JAD-132216

Villemagne, V. L., Pike, K. E., Darby, D., Maruff, P., Savage, G., Ng, S., et al. (2008). Abeta deposits in older non-demented individuals with cognitive decline are indicative of preclinical Alzheimer's disease. *Neuropsychologia* 46, 1688–1697. doi: 10.1016/j.neuropsychologia.2008.02.008

Vos, S. J., Xiong, C., Visser, P. J., Jasielec, M. S., Hassenstab, J., Grant, E. A., et al. (2013). Preclinical Alzheimer's disease and its outcome: a longitudinal cohort study. *Lancet. Neurol.* 12, 957–965. doi: 10.1016/S1474-4422(13)70194-7

Wang, Z., Das, S. R., Xie, S. X., Arnold, S. E., Detre, J. A., and Wolk, D. A. (2013). Arterial spin labeled MRI in prodromal Alzheimer's disease: a multi-site study. *Neuroimage Clin.* 2, 630–636. doi: 10.1016/j.nicl.2013.04.014

Wierenga, C. E., Hays, C. C., and Zlatar, Z. Z. (2014). Cerebral blood flow measured by arterial spin labeling MRI as a preclinical marker of Alzheimer's disease. *J. Alzheimers Dis.* 42(Suppl. 4), S411–S419. doi: 10.3233/JAD-141467

Wolk, D. A., and Detre, J. A. (2012). Arterial spin labeling MRI: an emerging biomarker for Alzheimer's disease and other neurodegenerative conditions. *Curr. Opin. Neurol.* 25, 421–428. doi: 10.1097/WCO.0b013e328354ff0a

Yeo, J. M., Waddell, B., Khan, Z., and Pal, S. (2015). A systematic review and meta-analysis of ^{18}F-labeled amyloid imaging in Alzheimer's disease. *Alzheimers Dement.* 1, 5–13. doi: 10.1016/j.dadm.2014.11.004

Zetterberg, H., Skillbäck, T., Mattsson, N., Trojanowski, J. Q., Portelius, E., Shaw, L. M., et al. (2016). Association of cerebrospinal fluid neurofilament light concentration with Alzheimer disease progression. *JAMA Neurol.* 73, 60–67. doi: 10.1001/jamaneurol.2015.3037

Zhang, S., Smailagic, N., Hyde, C., Noel-Storr, A. H., Takwoingi, Y., McShane, R., et al. (2014). (11)C-PIB-PET for the early diagnosis of Alzheimer's disease dementia and other dementias in people with mild cognitive impairment (MCI). *Cochrane Database Syst. Rev.* 7:CD010386. doi: 10.1002/14651858.CD010386.pub2

Conflict of Interest Statement: The author declares that the research was conducted in the absence of any commercial or financial relationships that could be construed as a potential conflict of interest.

Copyright © 2018 Khan. This is an open-access article distributed under the terms of the Creative Commons Attribution License (CC BY). The use, distribution or reproduction in other forums is permitted, provided the original author(s) and the copyright owner are credited and that the original publication in this journal is cited, in accordance with accepted academic practice. No use, distribution or reproduction is permitted which does not comply with these terms.

frontiers in Aging Neuroscience

ORIGINAL RESEARCH
published: 12 April 2018
doi: 10.3389/fnagi.2018.00087

Cognitive Function and Brain Atrophy Predict Non-pharmacological Efficacy in Dementia: The Mihama-Kiho Scan Project2

Ken-ichi Tabei[1,2], Masayuki Satoh[1]*, Jun-ichi Ogawa[3], Tomoko Tokita[4], Noriko Nakaguchi[5], Koji Nakao[6], Hirotaka Kida[1] and Hidekazu Tomimoto[2]*

[1] Department of Dementia Prevention and Therapeutics, Graduate School of Medicine, Mie University, Tsu, Japan, [2] Department of Neurology, Graduate School of Medicine, Mie University, Tsu, Japan, [3] Yamaha Music Foundation, Tokyo, Japan, [4] Department of Health and Welfare, Mihama Town Hall, Mihama, Japan, [5] Department of Health and Welfare, Kiho Town Hall, Kiho, Japan, [6] Department of Neurosurgery, Kinan Hospital, Mihama, Japan

We aimed to determine whether neuropsychological deficits and brain atrophy could predict the efficacy of non-pharmacological interventions. Forty-six participants with mild-to-moderate dementia were monitored for 6 months; 25 underwent an intervention involving physical exercise with music, and 21 performed cognitive stimulation tasks. Participants were categorized into improvement (IMP) and no-IMP subgroups. In the exercise-with-music group, the no-IMP subgroup performed worse than the IMP subgroup on the Rivermead Behavioural Memory Test at baseline. In the cognitive-stimulation group, the no-IMP subgroup performed worse than the IMP subgroup on Raven's Colored Progressive Matrices and the cognitive functional independence measure at baseline. In the no-IMP subgroup, voxel-based morphometric analysis at baseline revealed more extensive gray matter loss in the anterior cingulate gyrus and left middle frontal gyrus in the exercise-with-music and cognitive-stimulation groups, respectively. Participants with mild-to-moderate dementia with cognitive decline and extensive cortical atrophy are less likely to show improved cognitive function after non-pharmaceutical therapy.

Keywords: dementia, exercise with music, cognitive dysfunction, voxel-based morphometry, atrophy, frontal lobe

OPEN ACCESS

Edited by:
Athanasios Alexiou, Novel Global Community Educational Foundation (NGCEF), Australia

Reviewed by:
Sadaf Jahan, Council of Scientific and Industrial Research (CSIR), India
Elizabeta Blagoja Mukaetova-Ladinska, Newcastle University, United Kingdom

****Correspondence:***
Ken-ichi Tabei
tabei@clin.medic.mie-u.ac.jp; kenichi.tabei@gmail.com
Masayuki Satoh
bruckner@clin.medic.mie-u.ac.jp

Received: *26 September 2017*
Accepted: *14 March 2018*
Published: *12 April 2018*

Citation:
Tabei K, Satoh M, Ogawa J, Tokita T, Nakaguchi N, Nakao K, Kida H and Tomimoto H (2018) Cognitive Function and Brain Atrophy Predict Non-pharmacological Efficacy in Dementia: The Mihama-Kiho Scan Project2. Front. Aging Neurosci. 10:87. doi: 10.3389/fnagi.2018.00087

INTRODUCTION

The World Alzheimer Report has estimated that there were 46.8 million people with dementia worldwide in 2015, and that this number will reach 131.5 million by 2050 (Prince et al., 2015). However, pharmacological treatments are relatively ineffective in halting the progression of dementia. The lack of pharmacological options (e.g., vaccines or disease-modifying agents) has shifted the focus of researchers toward non-pharmacological treatments for dementia, such as cognitive training, aerobic physical exercise, and music therapy (Gates and Sachdev, 2014; Groot et al., 2016; Zhang et al., 2017).

Abbreviations: AD, Alzheimer's disease; CS, cognitive stimulation; ExM, exercise with music; GM, gray matter; IMP, improvement; LM, logical memory; MMSE, Mini-Mental State Examination; no-IMP, no-improvement; RBMT, Rivermead Behavioural Memory Test; RCPM, Raven's Colored Progressive Matrices; VaD, vascular dementia; WF, word fluency.

Accumulating evidence suggests that non-pharmacological treatment may maintain or decrease the rate of cognitive decline in adults with mild cognitive impairment and early stage dementia (Rodakowski et al., 2015). Additionally, the protective effects of aerobic physical exercise against the development and/or progression of dementia have been well documented (Laurin et al., 2001; Abbott et al., 2004; Ravaglia et al., 2008; Erickson et al., 2011). Additional studies have suggested that physical exercise combined with cognitive training exerts a greater positive impact on cognitive function than physical exercise alone (Fabre et al., 2002; Oswald et al., 2006; Shatil, 2013; Satoh et al., 2014, 2017; Tabei et al., 2017). In older adults, physical ExM induces greater positive effects on visuospatial function and leads to more extensive neuroanatomical changes (Tabei et al., 2017) than exercise alone. In participants with mild-to-moderate dementia, ExM also exerts greater positive effects on cognitive function and activities of daily living than CS using portable game consoles or drills (e.g., easy calculations, mazes, and mistake-searching in pictures) (Satoh et al., 2017).

Despite recent advancements, few studies have focused on predicting outcomes following non-pharmacological treatment. Knowledge of such predictors may allow clinicians to modify factors that are likely to attenuate the effects of the intervention and to provide more targeted treatment (Hsu et al., 2017). Indeed, previous studies have demonstrated that clinical and demographic factors can influence the effect of non-pharmacological activities on cognition and on the behavioral and psychological symptoms of dementia (Särkämö et al., 2016; Hsu et al., 2017). However, the neuropsychological factors influencing non-pharmacological treatment, as well as the neural basis of its efficacy, remain unknown. Furthermore, no randomized controlled trials have compared such effects among different non-pharmacological treatment options.

Therefore, the purpose of the present study was to determine whether neuropsychological factors and regional brain atrophy [as measured via voxel-based morphometry (VBM)] can predict the rate of improvement following non-pharmacological treatment in participants with mild-to-moderate dementia and to compare the effects of different non-pharmacological interventions.

MATERIALS AND METHODS

Participants

The present study included participants with mild-to-moderate dementia who had utilized nursing services, such as day care or group homes, in the towns of Mihama and Kiho, which are situated at the southern end of the Kii peninsula in Japan. This study received approval from the Kinan Hospital Research Ethics Committee, and conformed to the tenets of the Declaration of Helsinki, and all participants provided written informed consent. This study was registered at UMIN-CTR (UMIN000017066) on April 7, 2015. The present study included the same participants as a previous study, which investigated the effect of non-pharmacological interventions in participants with mild-to-moderate dementia (Satoh et al., 2017). The inclusion criteria were as follows: (a) current diagnosis of intractable dementia by neurological specialists, based on ICD-10 diagnostic criteria (World Health Organization, 1993); (b) score between 16 and 26 on the MMSE; (c) stable physical and psychological condition; and (d) preserved hearing, visual acuity, and physical movement sufficient to enable participation in the intervention. Participants were excluded if they met any of the following criteria: (a) presence of chronic debilitating disease, such as malignancy or infection; (b) presence of severe cardiac, respiratory, and/or orthopedic disabilities that would prevent participation in the intervention; (c) presence of paresis or coordination disturbances that would prevent participation in the intervention; and (d) diagnosis of treatable dementia.

Diagnoses of AD were performed in accordance with criteria established by the National Institute of Neurologic Disorders and Stroke/Alzheimer Disease and Related Disorders Association (McKhann et al., 1984). Diagnoses of VaD were performed in accordance with criteria established by the National Institute of Neurological Disorders and Stroke/Association Internationale pour la Recherche et l'Enseignement en Neurosciences (Román et al., 1993).

All participants received treatment with anti-dementia drugs, the most common of which was donepezil hydrochloride. Pharmacological and non-pharmacological activities performed in the nursing-care facilities remained unchanged during the 6-months intervention period. Neuropsychological assessments and brain MRI were performed at baseline and following the intervention.

Procedures

Detailed descriptions of the procedures for each non-pharmacological intervention and neuropsychological assessment can be found in our previous report (Satoh et al., 2017).

Physical Exercise With Music (ExM)

Participants participated in 40-min physical exercise sessions once per week over the 6-months intervention period (total number of sessions: 24). The exercise program was developed by the Yamaha Music Foundation based on a program used in our previous study, which investigated the efficacy of physical exercise combined with music in older adults with normal cognitive function (Satoh et al., 2014; Tabei et al., 2017). The program consisted of muscle training for the upper and lower extremities, hand clapping to music, breath and voice training, and singing. The exercise trainers were professional musicians who also held private licenses as physical trainers with the Yamaha Music Foundation.

Cognitive Stimulation (CS)

Participants trained using a program called "Yawaraka Atama Juku (flexible thinking club)" developed by Nintendo Co., Ltd., using a portable game console (Nintendo DS LL,

Kyoto, Japan) and performed drills consisting of easy calculations (Kawashima, 2003), mazes, and mistake-searching in pictures. Each session was 40 min long and were conducted once per week over the 6-months intervention period (total sessions: 24). Each session was moderated by nurses, certified care workers, or psychiatric social workers employed at the respective nursing facility.

Neuropsychological Assessment

The MMSE (Folstein et al., 1975) and RCPM (Raven, 1947) were used to quantify cognitive function. In addition to an overall score, the RCPM task measures performance time, which reflects the psychomotor speed of the participants. Memory was evaluated using the LM-I/-II subtests of the RBMT (Wilson et al., 1985), which requires immediate and delayed recall of a short story. The RBMT contains four stories of varying difficulty and different word counts. We used different stories for the pre- and post-test periods to avoid the influence of familiarity with story content.

Visuospatial ability was assessed using methods described by Strub and Black (2001). Participants were shown images of cubes and Necker cubes, and were then asked to draw a picture of each. Each drawing was scored by assigning one of four possible grades (0: poor, 1: fair, 2: good, and 3: excellent).

Frontal lobe function was assessed using two tasks: WF and Trail Making Test -A/-B (Partington and Leiter, 1949). The WF test consists of category and letter domains. In the categorical WF task, participants were asked to name as many animals as possible in 1 min. In the letter WF task, participants were asked to name as many objects as possible in 1 min beginning with each of the following four phonemes: ka, sa, ta, and te (Dohi et al., 1992). The average scores for these four phonemes were used for statistical analyses.

The Functional Independence Measure was used to evaluate functional performance regarding activities of daily living. The Functional Independence Measure consists of both motor and cognitive function domains. Motor function is assessed on thirteen items, including eating, dressing, evacuation, urination, and walking. Cognitive function is assessed on five items associated with understanding, expression, and memory. The maximum motor function, cognitive function, and overall Functional Independence Measure scores are 91, 35, and 126, respectively, with higher scores indicating better function. These neuropsychological assessments were administered to participants in both groups before and after the 6-month intervention period.

Improvement and No-Improvement Groups

Participants were dichotomized into an IMP or no-IMP subgroup based on MMSE scores following the intervention. Participants with an increased MMSE score of 2 points or more were included in the IMP subgroup, while the remaining participants were included in the no-IMP subgroup. The cut-off of 2 points was determined based on the findings of previous studies, which had shown that changes in MMSE scores of 2 points are beyond the threshold of chance (Morris et al., 1993; Bowie et al., 1999; Ballard et al., 2003).

MRI Acquisition

T1-weighted gradient echo MR images were obtained using a 1.5-T MR scanner (Echelon Oval, Hitachi Medical Corporation, Tokyo, Japan). Scan parameters were as follows: repetition time = Shortest (Automatic); echo time = 11 ms; flip angle = 90°; field of view = 230 mm × 230 mm; slice thickness = 4 mm; gapless; in-plane resolution = 0.45 mm × 0.45 mm. Scans were obtained both before and after the 6-month intervention period.

MRI Analysis

MRI data were analyzed using SPM12 (Wellcome Trust Centre for Neuroimaging, University College London, London, United Kingdom) implemented in MATLAB R2012a (MathWorks, Natick, MA, United States). In the pre-processing phase, images were set to match the anterior to posterior commissure line using an automated MATLAB script. The images were then visually inspected to check for possible scan issues such as field distortion and movement artifacts. Reoriented images were corrected for intensity inhomogeneity and segmented into GM, white matter, cerebrospinal fluid, and other tissues outside the brain using SPM12 tissue probability maps. The images were registered to the East Asian Brains International Consortium for Brain Mapping space template via affine regularization. We created a population-specific template

TABLE 1 | Characteristics of study participants.

Characteristics	Total IMP	No-IMP	*p*-value	ExM IMP	No-IMP	*p*-value	CS IMP	No-IMP	*p*-value
No. of participants	18	28	0.183	11	14	0.690	7	14	0.189
Sex (F/M)	17/1	27/1	0.174	11/0	14/0	0.690	6/1	13/1	0.167
Dementia type (AD/VaD)	17/1	22/6	0.522	10/1	11/3	1.000	7/0	11/3	0.481
Age, y, mean (*SD*)	89.4 (4.9)	86.4 (5.1)	0.053	89.1 (5.7)	85.6 (5.8)	0.143	89.9 (3.6)	87.1 (4.4)	0.178
Years of education, mean (*SD*)	7.4 (1.9)	8.0 (2.0)	0.135	7.3 (1.6)	7.1 (2.3)	0.609	7.6 (2.4)	8.9 (1.3)	0.287
MMSE, mean (*SD*)	20.5 (2.9)	20.8 (4.0)	0.726	20.1 (2.5)	20.6 (3.7)	0.716	21.1 (3.6)	21.0 (4.3)	0.913
Change in MMSE score at the 6-month follow up, mean (*SD*)	3.8 (1.6)	−1.5 (2.1)	<0.001	4.4 (1.6)	−1.5 (2.1)	<0.001	3.0 (1.4)	−1.4 (2.1)	<0.001

IMP, improvement; no-IMP, no improvement; ExM, exercise plus music intervention; CS, cognitive stimulation intervention; AD, Alzheimer's disease; VaD, vascular dementia; MMSE, Mini Mental State Examination.

TABLE 2 | Baseline neuropsychological performance in the IMP and no-IMP subgroups.

	Total IMP	No-IMP	*p*-value	ExM IMP	No-IMP	*p*-value	CS IMP	No-IMP	*p*-value
MMSE	20.5 (2.9)	20.8 (4.0)	0.726	20.1 (2.5)	20.6 (3.7)	0.716	21.1 (3.6)	21.0 (4.3)	0.913
RCPM (score)	20.7 (5.3)	16.8 (6.4)	0.040	20.2 (6.0)	17.7 (7.3)	0.373	21.4 (4.3)	15.9 (5.6)	0.034
RCPM (time)	755.3 (497.1)	780.7 (782.0)	0.497	747.6 (471.6)	1054.3 (1041.2)	0.709	766.3 (570.1)	507.1 (157.2)	0.172
LM-I	5.4 (2.6)	3.1 (2.6)	0.004	5.2 (1.7)	3.2 (2.5)	0.025	5.9 (3.7)	3.0 (2.7)	0.059
LM-II	2.8 (3.2)	2.0 (2.8)	0.473	2.1 (2.6)	1.9 (2.9)	0.727	3.9 (4.0)	2.1 (2.8)	0.443
Cube	0.7 (0.5)	0.8 (0.5)	0.620	0.6 (0.5)	0.5 (0.5)	0.572	0.7 (0.5)	1.0 (0.4)	0.360
Necker cube	0.3 (0.5)	0.4 (0.5)	0.686	0.3 (0.5)	0.1 (0.4)	0.609	0.4 (0.5)	0.6 (0.5)	0.443
WF (animal)	9.9 (2.2)	8.6 (2.8)	0.099	9.7 (2.2)	8.4 (2.9)	0.209	10.1 (2.4)	8.8 (2.8)	0.172
WF (letter)	5.3 (2.0)	4.8 (2.1)	0.381	5.4 (1.6)	5.0 (1.9)	0.609	5.3 (2.6)	4.6 (2.3)	0.527
TMT-A	350.9 (184.5)	373.5 (182.9)	0.685	381.0 (211.9)	398.2 (158.3)	0.652	303.7 (131.9)	354.1 (203.8)	0.856
FIM (total)	118.6 (8.5)	112.2 (14.4)	0.038	116.9 (10.2)	114.6 (10.7)	0.373	121.3 (4.2)	109.9 (17.4)	0.034
FIM (motor)	85.9 (7.5)	82.4 (11.9)	0.070	85.0 (9.2)	85.5 (10.0)	0.403	87.4 (3.7)	79.2 (13.2)	0.110
FIM (cognition)	32.7 (3.0)	30.6 (4.5)	0.033	31.9 (3.3)	30.5 (4.7)	0.291	33.9 (1.9)	30.6 (4.5)	0.025

IMP, improvement; no-IMP, no improvement; ExM, exercise plus music intervention; CS, cognitive stimulation intervention; MMSE, Mini Mental State Examination; RCPM, Raven's Colored Progressive Matrices; LM, Logical Memory; WF, word fluency; TMT, Trail-Making Test; FIM, Functional Independence Measure.

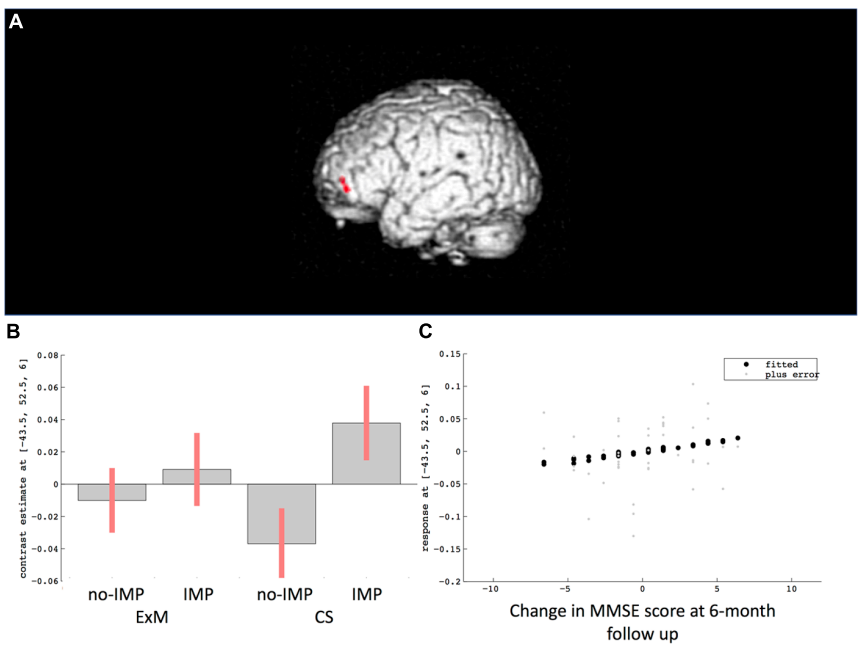


FIGURE 1 | Results of subtraction analysis between the IMP and non-IMP subgroups of the whole cohort **(A,B)**. Correlation between changes in MMSE scores and gray matter (GM) volume **(C)**. IMP, improvement; no-IMP, no-improvement; MMSE, Mini Mental State Examination.

using the SPM12 DARTEL template procedure to directly compare data between the IMP and no-IMP subgroups. We investigated group differences in GM volume, as well as the relationship between neuropsychological assessment results and GM at the whole-brain level. High-dimensional DARTEL was used to create non-linear, modulated-normalized GM and white matter images, which were smoothed using a Gaussian kernel of 8 mm FWHM (full-width at half-maximum). For whole-brain and multiple regression analyses, we assessed the statistical significance at a voxel threshold of $p < 0.005$ (uncorrected), within contiguous clusters of at least 20 voxels. We obtained both MNI and Talairach coordinates to detect the anatomical regions of the clusters. We used a transform from Matthew Brett[1] to convert MNI coordinates to Talairach coordinates, and Talairach Client 2.4.3 (Lancaster et al., 2000) was used to identify the anatomical regions corresponding to Talairach coordinates.

Statistical Analyses

Differences in demographic variables and neuropsychological assessment results between the IMP and no-IMP subgroups were analyzed using independent *t*-tests for continuous data,

[1]http://imaging.mrc-cbu.cam.ac.uk/imaging/MniTalairach

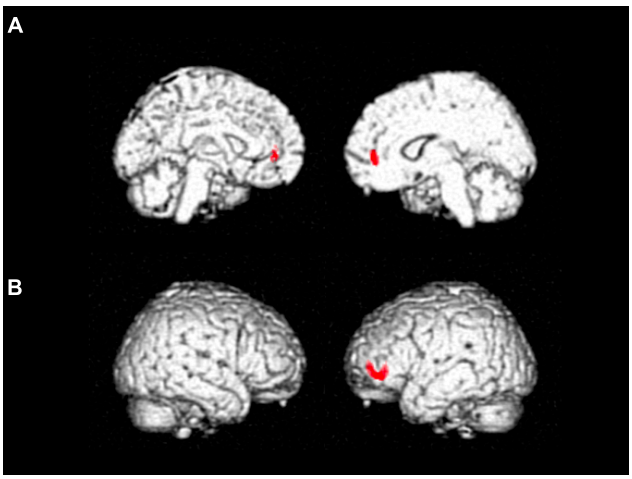


FIGURE 2 | Results of subtraction analysis between the IMP and non-IMP subgroups of the ExM **(A)** and CS groups **(B)**. IMP, improvement; no-IMP, no-improvement; ExM, exercise plus music intervention; CS, cognitive stimulation intervention.

chi-square tests for dichotomous data, and Mann–Whitney *U* tests for non-parametric data. Differences of $p < 0.05$ were considered statistically significant. Statistical analyses were performed using IBM SPSS Statistics software version 20 (IBM Corp., Armonk, NY, United States).

RESULTS

Participant Characteristics

Participants who participated in more than 75% of all sessions (more than 18) and completed the neuropsychological and MRI assessments before and after the intervention were included in the final analysis. Following exclusion of the remaining participants, the ExM and CS groups included 25 and 21 participants, respectively (ExM: AD = 21; VaD = 4; CS: AD = 18, VaD = 3) (**Table 1**). Prior to the intervention, there were no significant differences in sex ratio, dementia type, age, years of education, or MMSE scores between the ExM and CS groups. However, among participants in both ExM and CS groups, MMSE scores were significantly worse in the no-IMP subgroup than in the IMP subgroup at the 6-month follow-up ($p < 0.001$) (**Table 1**).

Neuropsychological Assessments

Baseline cube and Necker cube scores were significantly worse in the ExM group than in the CS group ($p = 0.022$, 0.01), although no significant differences were observed in the other neuropsychological assessments.

Participants in the no-IMP subgroup had significantly poorer baseline scores on the RCPM, LM-I section of the RBMT, and cognitive functional independence than those in the IMP subgroup ($p = 0.04$, 0.004, 0.033) (**Table 2**). Furthermore, baseline scores on the LM-I subtest were significantly worse in the no-IMP subgroup than the IMP subgroup ($p = 0.025$) of the ExM participants. In the CS group, baseline scores on the RCPM test and cognitive functional independence measure were significantly worse in the no-IMP subgroup than in the IMP subgroup ($p = 0.034$, 0.025, respectively) (**Table 2**).

MRI Assessments

Cube and Necker cube scores were used as covariates. Subtraction analysis revealed more extensive loss of GM in the left middle frontal gyrus in the no-IMP subgroup at baseline, relative to the IMP subgroup (**Figures 1A,B** and **Table 3**). Analysis of MMSE scores at the 6-month follow up revealed that changes in MMSE scores were positively correlated with volume in the left middle frontal gyrus (**Figure 1C** and **Table 3**). Subtraction analysis revealed more extensive GM loss in the anterior cingulate gyrus and left middle frontal gyrus in no-IMP participants in both the ExM (**Figure 2A** and **Table 3**) and CS (**Figure 2B** and **Table 3**) groups at baseline, respectively.

DISCUSSION

The present study aimed to determine whether neuropsychological factors and regional brain atrophy can predict the rate of IMP in participants with mild-to-moderate dementia following non-pharmacological intervention. Among ExM participants, the no-IMP subgroup exhibited poorer baseline performance on the LM-I subtest of the RBMT than participants in the IMP subgroup. Among CS participants, the no-IMP subgroup exhibited poorer baseline RCPM and cognitive functional independence measure scores than participants in the IMP subgroup. Such differences may be associated with differences in cognitive resources required to execute each intervention. Proper execution of the ExM protocol requires the participant to remember the exercise patterns from week to week, while proper execution of the CS protocol requires spatial and

TABLE 3 | Cluster sizes, peak locations, and statistical values for regions showing significant pre-intervention differences between the IMP and no-IMP subgroups.

				Talairach coordinates (mm)				
Contrast	**L/R**	**Area**	**BA**	**X**	**Y**	**Z**	***Z*-value**	**Cluster size in voxels**
IMP > no-IMP (Total)	L	Middle Frontal Gyrus	10	−44	46	−4	2.72	49
IMP > no-IMP (ExM)	R	Anterior Cingulate	32	4	44	−2	2.96	209
IMP > no-IMP (CS)	L	Middle Frontal Gyrus	10	−44	50	3	3.20	433

IMP, improvement; no-IMP, no-improvement; ExM, exercise plus music intervention; CS, cognitive stimulation intervention.

mathematical abilities that allow understanding of geometric designs and missing pieces, as well as expressive abilities and memory function to complete calculations, mazes, and search for mistakes in images. Although previous studies have indicated that exercise and ExM tasks enhance memory in participants with dementia (Radak et al., 2010; Intlekofer and Cotman, 2013; Satoh et al., 2017), our results suggest that execution of the intervention requires a certain amount of memory function reserve. These findings highlight the importance of early intervention, when cognitive function may be somewhat preserved (Dubois et al., 2016).

Voxel-based morphometry analysis revealed more extensive loss of GM in the anterior cingulate gyrus in no-IMP participants of the ExM group, and in the left middle frontal gyrus in the CS group at baseline relative to that observed in the IMP subgroup. These findings may also have been associated with the execution of each intervention. Previous studies have demonstrated that the anterior cingulate gyrus plays a key role in music processing in participants with dementia (Omar et al., 2011; Fletcher et al., 2015; Jacobsen et al., 2015), while the left middle frontal gyrus is associated with calculation (Maurer et al., 2016) and visual search (Weidner et al., 2009) in CS tasks. Therefore, our results indicate that the extent and location of brain atrophy at baseline may represent the neural basis of task execution for each intervention. In addition, these parameters may aid in predicting the efficacy of non-pharmacological treatment.

Previous studies have indicated that characteristic impairments across cognitive domains (Mori et al., 2016), Barthel Index (Formiga et al., 2010), and lower pre-treatment regional cerebral blood flow in the right orbitofrontal cortex (Hongo et al., 2008) can be used to predict better responses to cholinesterase inhibitors treatment in older adults with dementia. Our findings suggest that the efficacy of non-pharmacological treatment can also be predicted based on neural characteristics and the extent of cognitive decline.

The present study has some limitations of note. First, as we did not include healthy controls, further studies are required to investigate differences in neuropsychological factors and regional brain atrophy between healthy individuals and participants with mild-to-moderate dementia. Such findings may allow clinicians to predict the most appropriate non-pharmacological treatment for each participant. Second, the intervention period of the present study lasted only 6 months. Explicit differences in neuropsychological factors and regional brain atrophy may be more evident following a longer intervention period. Future studies should also aim to include a larger number of participants to enhance the accuracy of prediction.

CONCLUSION

Our findings suggest that participants with mild-to-moderate dementia who have experienced cognitive decline, reduced ability to perform activities of daily living, and extensive cortical atrophy are less likely to exhibit IMPs in cognitive function following non-pharmacological treatment. Thus, some characteristics of pre-treatment cognitive dysfunction and regional brain atrophy may aid clinicians in determining the most appropriate non-pharmacological intervention for each participant.

AUTHOR CONTRIBUTIONS

MS: conceived and designed the experiments. TT, NN, and KN: conducted the experiments. KT: analyzed the data. KT and MS: wrote the paper. JO: contributed materials. HK: analyzed and interpreted the data. HT: supervised and interpreted the data. All authors read and approved the final version of the paper.

FUNDING

This study was supported by JSPS KAKENHI Grant-in-Aid for Scientific Research (C) (Grant No: 15K08909) and Grant-in-Aid for Young Scientists (B) (Grant Nos: 25870325 and 17K17811).

ACKNOWLEDGMENTS

We would like to thank Keisuke Okamoto who works in the laboratory, Isamu Nonomura in radiology, and Hideshi Kanai in the community cooperation room at Kinan Hospital, and Takayuki Yotsuji at the Yamaha Music Foundation, for their kind contributions to this study.

REFERENCES

Abbott, R. D., White, L. R., Ross, G. W., Masaki, K. H., Curb, J. D., and Petrovitch, H. (2004). Walking and dementia in physically capable elderly men. *J. Am. Med. Assoc.* 292, 1447–1453. doi: 10.1001/jama.292.12.1447

Ballard, C., Rowan, E., Stephens, S., Kalaria, R., and Kenny, R. A. (2003). Prospective follow-up study between 3 and 15 months after stroke: improvements and decline in cognitive function among dementia-free stroke survivors >75 years of age. *Stroke* 34, 2440–2444. doi: 10.1161/01.STR.0000089923.29724.CE

Bowie, P., Branton, T., and Holmes, J. (1999). Should the mini mental state examination be used to monitor dementia treatments? *Lancet* 354, 1527–1528. doi: 10.1016/S0140-6736(99)03486-8

Dohi, N., Iwaya, T., and Kayamori, R. (1992). *Seishin-kinou Hyouka, the Evaluation of Mental Function*. Tokyo: Ishiyaku Publishers, Inc.

Dubois, B., Hampel, H., Feldman, H. H., Scheltens, P., Aisen, P., Andrieu, S., et al. (2016). Preclinical Alzheimer's disease: definition, natural history, and diagnostic criteria. *Alzheimers Dement.* 12, 292–323. doi: 10.1016/j.jalz.2016.02.002

Erickson, K. I., Voss, M. W., Prakash, R. S., Basak, C., Szabo, A., Chaddock, L., et al. (2011). Exercise training increases size of hippocampus and improves memory. *Proc. Natl. Acad. Sci. U.S.A.* 108, 3017–3022. doi: 10.1073/pnas.1015950108

Fabre, C., Chamari, K., Mucci, P., Masse-Biron, J., and Prefaut, C. (2002). Improvement of cognitive function by mental and/or individualized aerobic training in healthy elderly subjects. *Int. J. Sports Med.* 23, 415–421. doi: 10.1055/s-2002-33735

Fletcher, P. D., Downey, L. E., Golden, H. L., Clark, C. N., Slattery, C. F., Paterson, R. W., et al. (2015). Auditory hedonic phenotypes in dementia: a behavioural and neuroanatomical analysis. *Cortex* 67, 95–105. doi: 10.1016/j.cortex.2015.03.021

Folstein, M. F., Folstein, S. E., and McHugh, P. R. (1975). Mini-mental state: a practical method for grading the cognitive state of patients for the clinician. *J. Psychiatr. Res.* 12, 189–198. doi: 10.1016/0022-3956(75)90026-6

Formiga, F., Fort, I., Robles, M. J., Rodriguez, D., and Regalado, P. (2010). Lower Barthel Index scores predict less prescription of pharmacological therapy in elderly patients with Alzheimer disease. *Dement. Geriatr. Cogn.* 29, 198–203. doi: 10.1159/000278348

Gates, N. J., and Sachdev, P. (2014). Is cognitive training an effective treatment for preclinical and early Alzheimer's disease? *J. Alzheimers Dis.* 42(Suppl. 4), S551–S559. doi: 10.3233/JAD-141302

Groot, C., Hooghiemstra, A. M., Raijmakers, P. G. H. M., van Berckel, B. N. M., Scheltens, P., Scherder, E. J. A., et al. (2016). The effect of physical activity on cognitive function in patients with dementia: a meta-analysis of randomized control trials. *Ageing Res. Rev.* 25, 13–23. doi: 10.1016/j.arr.2015.11.005

Hongo, J., Nakaaki, S., Shinagawa, Y., Murata, Y., Sato, J., Tatsumi, H., et al. (2008). SPECT-identified neuroanatomical predictor of the cognitive effects of donepezil treatment in patients with Alzheimer's disease. *Dement. Geriatr. Cogn.* 26, 556–566. doi: 10.1159/000181148

Hsu, T. J., Tsai, H. T., Hwang, A. C., Chen, L. Y., and Chen, L. K. (2017). Predictors of non-pharmacological intervention effect on cognitive function and behavioral and psychological symptoms of older people with dementia. *Geriatr. Gerontol. Int.* 17(Suppl. 1), 28–35. doi: 10.1111/ggi.13037

Intlekofer, K. A., and Cotman, C. W. (2013). Exercise counteracts declining hippocampal function in aging and Alzheimer's disease. *Neurobiol. Dis.* 57, 47–55. doi: 10.1016/j.nbd.2012.06.011

Jacobsen, J. H., Stelzer, J., Fritz, T. H., Chételat, G., La Joie, R., and Turner, R. (2015). Why musical memory can be preserved in advanced Alzheimer's disease. *Brain* 138, 2438–2450. doi: 10.1093/brain/awv135

Kawashima, R. (2003). *Calculation Drill for Adults Which Improves Brain Function*. Tokyo: Kumon Publication.

Lancaster, J. L., Woldorff, M. G., Parsons, L. M., Liotti, M., Freitas, C. S., Rainey, L., et al. (2000). Automated Talairach atlas labels for functional brain mapping. *Hum. Brain Mapp.* 10, 120–131. doi: 10.1002/1097-0193(200007)10:3<120::AID-HBM30>3.0.CO;2-8

Laurin, D., Verreault, R., Lindsay, J., MacPherson, K., and Rockwood, K. (2001). Physical activity and risk of cognitive impairment and dementia in elderly persons. *Arch. Neurol.* 58, 498–504. doi: 10.1001/archneur.58.3.498

Maurer, S., Tanigawa, N., Sollmann, N., Hauck, T., Ille, S., Boeckh-Behrens, T., et al. (2016). Non-invasive mapping of calculation function by repetitive navigated transcranial magnetic stimulation. *Brain Struct. Funct.* 221, 3927–3947. doi: 10.1007/s00429-015-1136-2

McKhann, G., Drachman, D., Folstein, M., Katzman, R., Price, D., and Stadlan, E. M. (1984). Clinical diagnosis of Alzheimer's disease: report of the NINCDS-ADRDA Work Group under the auspices of Department of Health and Human Services Task Force on Alzheimer's disease. *Neurology* 34, 939–944. doi: 10.1212/WNL.34.7.939

Mori, E., Ikeda, M., Nakagawa, M., Miyagishi, H., and Kosaka, K. (2016). Pretreatment cognitive profile likely to benefit from donepezil treatment in dementia with Lewy bodies: pooled analyses of two randomized controlled trials. *Dement. Geriatr. Cogn.* 42, 58–68. doi: 10.1159/000447586

Morris, J. C., Edland, S., Clark, C., Galasko, D., Koss, E., Mohs, R., et al. (1993). The consortium to establish a registry for Alzheimer's disease (CERAD). Part IV. Rates of cognitive change in the longitudinal assessment of probable Alzheimer's disease. *Neurology* 43, 2457–2465. doi: 10.1212/WNL.43.12.2457

Omar, R., Henley, S. M., Bartlett, J. W., Hailstone, J. C., Gordon, E., Sauter, D. A., et al. (2011). The structural neuroanatomy of music emotion recognition: evidence from frontotemporal lobar degeneration. *Neuroimage* 56, 1814–1821. doi: 10.1016/j.neuroimage.2011.03.002

Oswald, W. D., Gunzelmann, T., Rupprecht, R., and Hagen, B. (2006). Differential effects of single versus combined cognitive and physical training with older adults: the SimA study in a 5-year perspective. *Eur. J. Ageing* 3, 179–192. doi: 10.1007/s10433-006-0035-z

Partington, J. E., and Leiter, R. G. (1949). Partington's pathway test. *Psychol. Serv. Center Bull.* 1, 9–20.

Prince, M., Wimo, A., Guerchet, M., Ali, G. C., Wu, Y. T., and Prina, M. (2015). *World Alzheimer Report 2015 - The Global Impact of Dementia: An Analysis of Prevalence, Incidence, Cost and Trends*. London: Alzheimer's Disease International.

Radak, Z., Hart, N., Sarga, L., Koltai, E., Atalay, M., Ohno, H., et al. (2010). Exercise plays a preventive role against Alzheimer's disease. *J. Alzheimers Dis.* 20, 777–783. doi: 10.3233/JAD-2010-091531

Ravaglia, G., Forti, P., Lucicesare, A., Pisacane, N., Rietti, E., Bianchin, M., et al. (2008). Physical activity and dementia risk in the elderly: findings from a prospective Italian study. *Neurology* 70, 1786–1794. doi: 10.1212/01.wnl.0000296276.50595.86

Raven, J. C. (1947). *Coloured Progressive Matrices Sets A, AB, B. Manual Sections A and 2*. Oxford: Oxford Psychologists Press.

Rodakowski, J., Saghafi, E., Butters, M. A., and Skidmore, E. R. (2015). Non-pharmacological interventions for adults with mild cognitive impairment and early stage dementia: an updated scoping review. *Mol. Aspects Med.* 43, 38–53. doi: 10.1016/j.mam.2015.06.003

Román, G. C., Tatemichi, T. K., Erkinjuntti, T., Cummings, J. L., Masdeu, J. C., Garcia, J. A., et al. (1993). Vascular dementia: diagnostic criteria for research studies. Report of the NINDS-AIREN International Workshop. *Neurology* 43, 250–260. doi: 10.1212/WNL.43.2.250

Särkämö, T., Laitinen, S., Numminen, A., Kurki, M., Johnson, J. K., and Rantanen, P. (2016). Clinical and demographic factors associated with the cognitive and emotional efficacy of regular musical activities in dementia. *J. Alzheimers Dis.* 49, 767–781. doi: 10.3233/JAD-150453

Satoh, M., Ogawa, J. I., Tokita, T., Nakaguchi, N., Nakao, K., Kida, H., et al. (2014). The effects of physical exercise with music on cognitive function of elderly people: Mihama-Kiho project. *PLoS One* 9:e95230. doi: 10.1371/journal.pone.0095230

Satoh, M., Ogawa, J. I., Tokita, T., Nakaguchi, N., Nakao, K., Kida, H., et al. (2017). Physical exercise with music maintains activities of daily living in patients with dementia: Mihama-Kiho project part 21. *J. Alzheimers Dis.* 57, 85–96. doi: 10.3233/JAD-161217

Shatil, E. (2013). Does combined cognitive training and physical activity training enhance cognitive abilities more than either alone? A four-condition randomized controlled trial among healthy older adults. *Front. Aging Neurosci.* 5:8. doi: 10.3389/fnagi.2013.00008

Strub, R. L., and Black, F. W. (2001). *The Mental Status Examination in Neurology*, 4th Edn. Philadelphia, PA: F.A. Davis Company.

Tabei, K. I., Satoh, M., Ogawa, J. I., Tokita, T., Nakaguchi, N., Nakao, K., et al. (2017). Physical exercise with music reduces gray and white matter loss in the frontal cortex of elderly people: the Mihama-Kiho scan project. *Front. Aging Neurosci.* 9:174. doi: 10.3389/fnagi.2017.00174

Weidner, R., Krummenacher, J., Reimann, B., Müller, H. J., and Fink, G. R. (2009). Sources of top-down control in visual search. *J. Cogn. Neurosci.* 21, 2100–2113. doi: 10.1162/jocn.2008.21173

Wilson, B., Cockburn, J., and Baddeley, A. (1985). *The Rivermead Behavioural Memory Test*. Bury St Edmunds: Thames Valley Test Company.

World Health Organization (1993). *International Statistical Classification of Diseases and Related Health Problems*, 10th Rev. Geneva: World Health Organization.

Zhang, Y., Cai, J., An, L., Hui, F., Ren, T., Ma, H., et al. (2017). Does music therapy enhance behavioral and cognitive function in elderly dementia patients? A systematic review and meta-analysis. *Ageing Res. Rev.* 35, 1–11. doi: 10.1016/j.arr.2016.12.003

Conflict of Interest Statement: The authors declare that the research was conducted in the absence of any commercial or financial relationships that could be construed as a potential conflict of interest.

Copyright © 2018 Tabei, Satoh, Ogawa, Tokita, Nakaguchi, Nakao, Kida and Tomimoto. This is an open-access article distributed under the terms of the Creative Commons Attribution License (CC BY). The use, distribution or reproduction in other forums is permitted, provided the original author(s) and the copyright owner are credited and that the original publication in this journal is cited, in accordance with accepted academic practice. No use, distribution or reproduction is permitted which does not comply with these terms.

frontiers in Aging Neuroscience

METHODS
published: 10 April 2018
doi: 10.3389/fnagi.2018.00103

A Brainnetome Atlas Based Mild Cognitive Impairment Identification Using Hurst Exponent

Zhuqing Long[1†], Bin Jing[2†], Ru Guo[3†], Bo Li[4], Feiyi Cui[1], Tingting Wang[1] and Hongwen Chen[1]*

[1]*Medical Apparatus and Equipment Deployment, Nanfang Hospital, Southern Medical University, Guangzhou, China,* [2]*School of Biomedical Engineering, Capital Medical University, Beijing, China,* [3]*Department of Tuberculosis, Beijing Chest Hospital Capital Medical University, Beijing, China,* [4]*Department of Traditional Chinese Medicine, Beijing Chest Hospital, Capital Medical University, Beijing Tuberculosis and Thoracic Tumor Research Institute, Beijing, China*

Mild cognitive impairment (MCI), which generally represents the transition state between normal aging and the early changes related to Alzheimer's disease (AD), has drawn increasing attention from neuroscientists due that efficient AD treatments need early initiation ahead of irreversible brain tissue damage. Thus effective MCI identification methods are desperately needed, which may be of great importance for the clinical intervention of AD. In this article, the range scaled analysis, which could effectively detect the temporal complexity of a time series, was utilized to calculate the Hurst exponent (HE) of functional magnetic resonance imaging (fMRI) data at a voxel level from 64 MCI patients and 60 healthy controls (HCs). Then the average HE values of each region of interest (ROI) in brainnetome atlas were extracted and compared between MCI and HC. At last, the abnormal average HE values were adopted as the classification features for a proposed support vector machine (SVM) based identification algorithm, and the classification performance was estimated with leave-one-out cross-validation (LOOCV). Our results indicated 83.1% accuracy, 82.8% sensitivity and 83.3% specificity, and an area under curve of 0.88, suggesting that the HE index could serve as an effective feature for the MCI identification. Furthermore, the abnormal HE brain regions in MCI were predominately involved in left middle frontal gyrus, right hippocampus, bilateral parahippocampal gyrus, bilateral amygdala, left cingulate gyrus, left insular gyrus, left fusiform gyrus, left superior parietal gyrus, left orbital gyrus and left basal ganglia.

Keywords: mild cognitive impairment, range scaled analysis, Hurst exponent, brainnetome atlas, support vector machine

OPEN ACCESS

Edited by:
Mohammad Amjad Kamal, King Fahad Medical Research Center, King Abdulaziz University, Saudi Arabia

Reviewed by:
Zhengyi Yang, The University of Queensland, Australia
Liuqing Yang, Johns Hopkins Medicine, United States

***Correspondence:**
Hongwen Chen
chw47922@126.com

[†]These authors have contributed equally to this work.

Received: *19 December 2017*
Accepted: *27 March 2018*
Published: *10 April 2018*

Citation:
Long Z, Jing B, Guo R, Li B, Cui F, Wang T and Chen H (2018) A Brainnetome Atlas Based Mild Cognitive Impairment Identification Using Hurst Exponent. Front. Aging Neurosci. 10:103. doi: 10.3389/fnagi.2018.00103

INTRODUCTION

Mild cognitive impairment (MCI), which is characterized by memory complaints, attention deficits and other reduced cognitive functions (Petersen, 2007; Han et al., 2011; Zhang et al., 2012), generally represents the transition state between normal aging and the early changes related to Alzheimer's disease (AD; Desikan et al., 2009; Wang et al., 2015).

Abbreviations: AD, Alzheimer's disease; BOLD, blood oxygen level dependent; fMRI, functional magnetic resonance imaging; HCs, healthy controls; HE, Hurst exponent; LOOCV, leave-one-out cross-validation; MCI, mild cognitive impairment; RBF, radial basis function; ROI, region of interest; rs-fMRI, resting-state functional magnetic resonance imaging; SVM, support vector machine.

Overall, MCI patients progress to AD at a rate of 10%–15% per year (Khazaee et al., 2016), and roughly half of them will evolve to AD within 3–5 years (Long et al., 2016). Recently, a great deal of attention from neuroscientists, neurologists and neuroradiologists has been paid to MCI due that efficient AD treatments need early initiation ahead of irreversible brain tissue damages (Davatzikos et al., 2008). Therefore, developing accurate and effective MCI identification methodologies that may be of great importance for clinical interventions of AD are desperately needed.

Functional magnetic resonance imaging (fMRI) has received increasing interests because it could provide a primary method of mechanism detection, diagnostic evaluation or therapeutic monitoring for MCI and AD (Fornito and Bullmore, 2010; Wang et al., 2015). Previous studies demonstrated that the aberrant and spontaneous neuronal activities in MCI or AD could be detected by resting-state fMRI (rs-fMRI; Zhang et al., 2012; Brier et al., 2014), and the abnormal brain regions mainly involved in hippocampus, parahippocampal gyrus, posterior cingulate gyrus and precuneus cortex, etc (Baron et al., 2001; He et al., 2007). In addition, many recent studies employed rs-fMRI data to identify MCI or AD from healthy controls (HCs) by extracting a single type of feature or multi-level characteristics (Chen et al., 2011; Dai et al., 2012; Zhang et al., 2012; Brier et al., 2014; Long et al., 2016), and the recognition accuracies were varied with a wide range, suggesting the MCI or AD discrimination needs to be continued. Generally, an effective rs-fMRI based MCI or AD discrimination method should: (I) exhibit an excellent discrimination accuracy between MCI or AD and HC; (II) specifically quantify fundamental characteristics of Alzheimer's pathology in individuals with MCI or AD.

Prior studies demonstrated that blood oxygen level dependent (BOLD) signals have been shown scale-free dynamics (Ciuciu et al., 2012; Wei et al., 2013), and the power spectrum of fMRI signals can be written as $S(f) \propto 1/|f|^{\beta}$ with $\beta < 1$ (where f represents frequency; Maxim et al., 2005; Gentili et al., 2015), suggesting that the fMRI signals have fractal or fractal-like properties. Hurst Exponent (HE), which has a direct linear relationship with the parameter $\beta = 2HE - 1$, could well display the fractal dynamics of fMRI signals via describing the self-similarity of a time series. In fact, the HE, an index ranging from 0 to 1, could divide the time series into three categories according to its values. A HE bigger than 0.5 indicates a persistent or positively correlated time series, meaning that the time series generally causes changes that fluctuate in the same direction along time. A HE equal to 0.5 stands for a random white noise. A HE smaller than 0.5 implies an anti-correlated or anti-persistent time series. In this case, the dynamics of a time series would keep a reversing pattern in time, and a decrease in the time series generally would be followed an increase and vice versa (Gentili et al., 2015). Recently, HE index has been utilized to measure the changes of BOLD signals related to major depressive disorder, normal and pathological aging, cholinergic modulation, AD, autism disorder and different personality traits (Maxim et al., 2005; Wink et al., 2006; Lai et al., 2010; Lei et al., 2013; Gentili et al., 2015; Jing et al., 2017). However, little information was known about the HE changes in MCI patients, and it still remains unknown whether the HE index could serve as an effective parameter for MCI classification.

In this article, the HE index of fMRI signals were first calculated using range scaled analysis at a voxel level. Then the average HE values of each region of interest (ROI) in brainnetome atlas, a newly structural and functional brain partition scheme, were extracted and compared between MCI and HC groups. At last, the abnormal HE values were adopted as the classification features for a proposed support vector machine (SVM)-based classification method to identify MCI patients from HC.

MATERIALS AND METHODS

Participants

Sixty-nine MCI patients and 63 HC subjects participated in the current study, and none of MCI patients had taken any medications that interfere with cognitive functions. All MCI patients were recruited from the memory outpatient clinic at Nanfang Hospital, and the clinical diagnosis of MCI was made by two experienced neurologists based on the following criteria: (1) memory complaints, confirmed by patient-self or their relatives; (2) normal or near normal performance on cognitive function; (3) normal or near normal activities of daily life; (4) Clinical Dementia Rate equals to 0.5; and (5) absence of dementia according to the DSM-IV (Diagnostic and Statistical Manual of Mental Disorders, 4th edition, revised). The HC participants matched well with MCI patients on gender, age and education level and were collected from local community by print advertisements, and the inclusions for all participants were: (1) no other nervous or psychiatric diseases that can intervene with cognitive functions, such as Parkinson's disease, depressive disorders and encephalitis, etc; (2) no history of stroke or dependence of alcohol; (3) no systemic diseases that cause cognitive impairments; and (4) no medication conditions that can influence cognitive performance. All subjects were undergone several clinical assessments including Clinical Dementia Rate, Mini-Mental State Examination (MMSE) and Auditory Verbal Learning Test (AVLT). This study was approved by the ethics committee of Nanfang Hospital affiliated to Southern Medical University, and the informed written consents from all subjects were obtained in accordance with the Declaration of Helsinki. Five MCI patients and three HC subjects were discarded due to excessive head motion during the scan, and the detailed clinical characteristics of the remaining participants were summarized in **Table 1**.

Data Acquisition

All images were collected on a 3 Tesla Siemens scanner with 8-channel radio frequency coil at Nanfang hospital. Headphones and a foam padding were utilized to reduce the scanner noise and limit the head motion during the scan, and all subjects were instructed to close their eyes, to keep mind relax, to not

TABLE 1 | Participants' demographic and clinical characteristics.

Characteristics	MCI	HC	*P* values
Gender (M/F)	64 (28/36)	60 (26/34)	0.96#
Age (years)	67.14 ± 7.33	65.27 ± 7.30	0.16*
Education (years)	9.73 ± 4.24	10.07 ± 4.27	0.66*
CDR	0.5	0	0*
MMSE	23.16 ± 2.77	27.40 ± 3.15	<0.001*
AVLT-immediate recall	7.99 ± 2.60	12.94 ± 2.94	<0.001*
AVLT-delay recall	3.64 ± 2.89	9.77 ± 2.79	<0.001*
AVLT-recognition	7.11 ± 3.55	11.58 ± 2.23	<0.001*

*Values are mean ± SD unless the SD was not calculated. M, male; F, female. CDR, Clinical Dementia Rating scale; MMSE, Mini-Mental State Examination; AVLT, Auditory Verbal Learning Test. #The P value was obtained by Chi-square test. *The P values were obtained by two-sample two-tailed-t-test.*

fall asleep and to not move their head. Resting-state fMRI were acquired using an echo-planar imaging sequence with the following parameters: repetition time = 2000 ms, echo time = 40 ms, flip angle = 90°, matrix size = 64 × 64, number of slices = 28, field of view = 240 × 240 mm^2, slice thickness = 4 mm, and voxel size = 3.75 × 3.75 × 4 mm^3. Two-hundred and thirty-nine volumes were collected for each subject within 478 s. T1-weighted structural images for all subjects were acquired by using magnetization-prepared rapid gradient echo sequence with the following parameters: repetition time = 1900 ms, echo time = 2.2 ms, inverse time = 900 ms, flip angle = 9°, matrix = 256 × 256, number of slices = 176, slice thickness = 1 mm, and voxel size = 1 × 1 × 1 mm^3.

Data Preprocessing

Data preprocessing for all images were carried out with Statistical Parametric Mapping (SPM8)[1]. The first 10 functional volumes were discarded due to signal equilibrium and participant's adaptation to the scanner environment, and the remaining 229 volumes were corrected for different acquisition time between slices. Then all volumes were realigned to the first volume by using a six-parameters rigid-body spatial transformation to compensate for head movement effects. Eight participants (five MCI patients and three HC subjects) were discarded because of excessive head motion (2 mm and 2°criteria). To improve the spatial normalization accuracy, the realigned images were normalized into the Montreal Neurological Institute space by using the parameters obtained from structural normalization, and all normalized functional images were re-sampled into a voxel size of 3 × 3 × 3 mm^3. Next, all the normalized images were detrended, and the spurious covariates including the six head motion parameters obtained from rigid-body transformation, signals of white matter and ventricular system were regressed. At last, a temporal band-pass filter (0.01–0.10 HZ) was carried out on the time series of each voxel to reduce the effects of low-frequency drifts and high-frequency cardiac and respiratory noise, and the filtered images were smoothed with a 4 mm full width at half maximum Gaussian kernel.

HE Calculation and Feature Selection

The range scaled analysis, which is an effective method to detect the temporal complexity of a time series, was utilized to calculate the HE index of fMRI signals at a voxel level, and the detailed principle of HE calculation was reported in our previous study (Jing et al., 2017). In addition, the brainnetome atlas (**Figure 1**), which partitions the cerebral cortex into 246 ROIs including 210 cortical sub-regions and 36 subcortical sub-regions (Fan et al., 2016), was used to extract the HE index feature for the SVM-based classification algorithm. In this article, the average HE values of each ROI in brainnetome atlas were extracted as the candidate features. Considering that properly and correctly reducing the number of features could not only improve the classification performance but also speed up the computation (De Martino et al., 2008; Pereira et al., 2009). Thus a Fisher score method and two-sample two-tailed-*t*-test ($P < 0.05$, uncorrected) were utilized to select out the discriminative HE features between MCI patients and HC subjects. The detailed Fisher score criterion for each candidate feature is defined as:

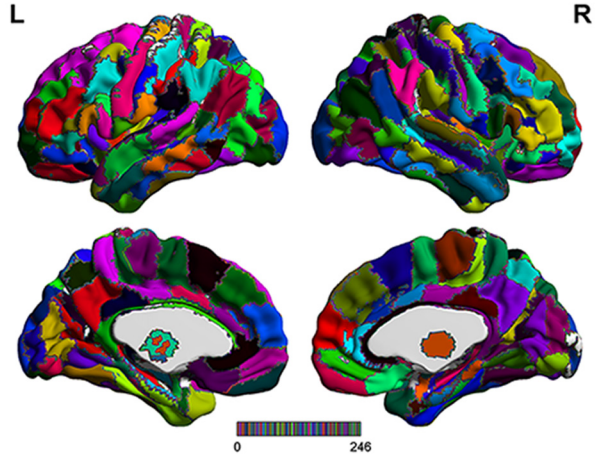


FIGURE 1 | The detailed brainnetome atlas which including 210 cortical sub-regions and 36 subcortical sub-regions.

$$FS = \frac{n_1(m_1 - m)^2 + n_2(m_2 - m)^2}{n_1\sigma_1^2 + n_2\sigma_2^2} \quad (1)$$

Here n_1 and n_2 are the number of the samples on each group, m_1 and m_2 are the respective mean value of the feature, m represents the mean value of the feature, σ_1^2 and σ_2^2 represent the

[1]http://www.fil.ion.ucl.ac.uk/spm

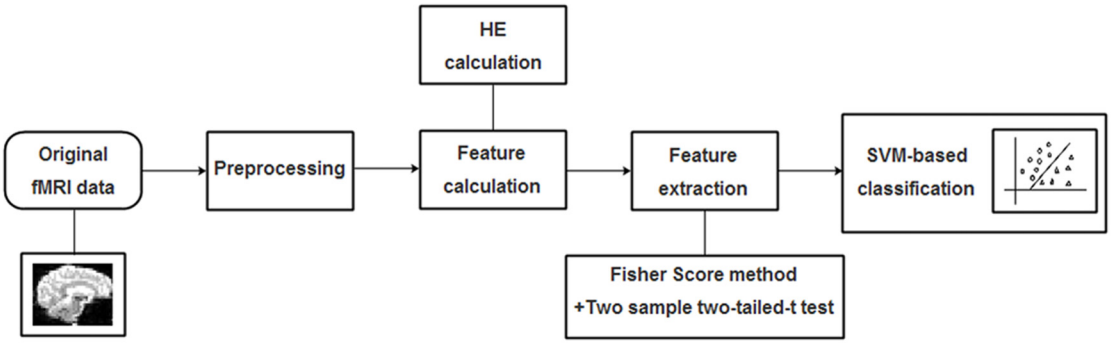


FIGURE 2 | A flowchart of the proposed support vector machine (SVM)-based classification method for mild cognitive impairment (MCI) identification.

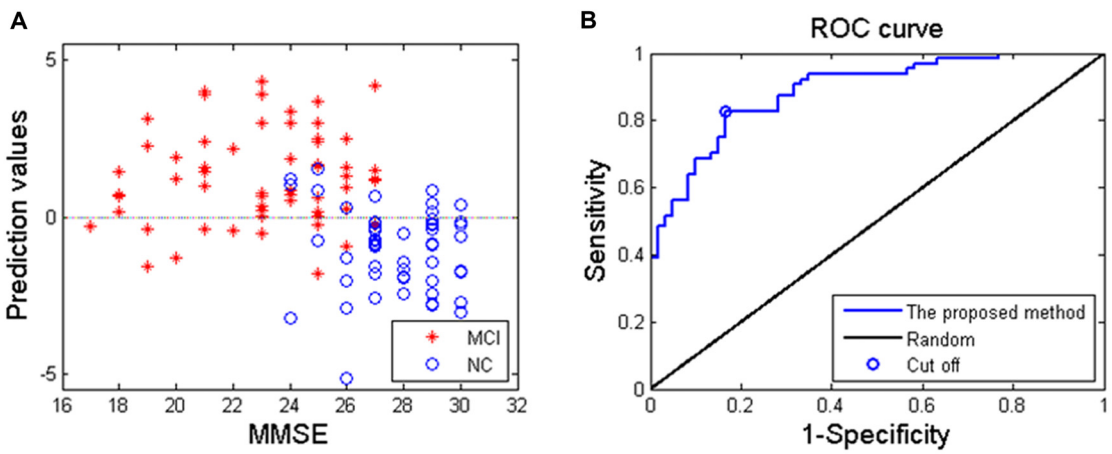


FIGURE 3 | (A) The relationship between the Mini-Mental State Examination (MMSE) score of MCI patients and prediction values; **(B)** receiver operating characteristics curve of the proposed classification method, and the area under curve is 0.88.

variance of the feature on each group. A high Fisher score value indicates a strong discriminative ability of the feature to some degree. At last, it's worth noting that the feature selection was only performed on the training set of per leave-one-out cross-validation (LOOCV) fold, which could reduce the overfitting of the classification algorithm.

SVM-Based Classification Method

The SVM algorithm, which has been widely utilized for its powerful recognition function as well as its simple theory and implementation, was originally proposed for binary classification problems based on statistical learning principles (Beheshti and Demirel, 2016). During the training process, the SVM algorithm seeks the optimal separation hyper-plane in the feature space where the input features were mapped into using a kernel function, and each divided subspace corresponds to one class of training set. In the same way, all the test samples could be labeled depending on which subspace they are mapped into after the training process (Magnin et al., 2009). In this article, the LibSVM toolbox[2] was utilized for SVM implementation.

The radial basis function (RBF) defined as $(X, X_i) \rightarrow K(X, X_i) = e^{\gamma |X - X_i|^2}$ was adopted as the kernel function for the SVM algorithm. To improve classification performance, a grid-search method was utilized to optimize two parameters: the parameter γ representing the width of RBF kernel and the punishment factor C adjusting the importance of error separation. In detail, at each pair of (γ, C), three steps including the above-mentioned feature selection, the training of the SVM-based algorithm and the prediction of the test samples were performed in succession, and the classification performance was estimated with LOOCV. It's worth noting that the feature selection was only carried out on the training set of each LOOCV fold. The whole classification process was repeatedly performed with (γ, C) varying along a grid with $\gamma = 2^{-8}$, $2^{-7.5}$,...,2^{8} and $C = 2^{-8}$, $2^{-7.5}$,...,2^{8}, which is referred as the grid-search method. Considering that each pair of (γ, C)

[2]http://www.csie.ntu.edu.tw/~cjlin/libsvm

TABLE 2 | The number of features retained in per fold of leave-one-out cross-validation (LOOCV) with brainnetome atlas.

Fold	No. of features	Fold	No. of features	Fold	No. of features	Fold	No. of features
1	16	32	17	63	15	94	15
2	15	33	16	64	16	95	15
3	17	34	16	65	15	96	15
4	17	35	14	66	14	97	15
5	16	36	15	67	16	98	15
6	16	37	14	68	16	99	15
7	16	38	15	69	15	100	16
8	15	39	15	70	16	101	14
9	15	40	16	71	15	102	15
10	15	41	16	72	16	103	16
11	15	42	15	73	14	104	14
12	15	43	14	74	15	105	15
13	14	44	14	75	14	106	14
14	16	45	16	76	16	107	15
15	16	46	16	77	16	108	16
16	15	47	16	78	17	109	15
17	14	48	15	79	16	110	16
18	15	49	14	80	16	111	16
19	15	50	17	81	16	112	15
20	15	51	15	82	16	113	15
21	16	52	14	83	15	114	17
22	15	53	14	84	14	115	15
23	16	54	14	85	16	116	16
24	15	55	14	86	16	117	14
25	17	56	15	87	16	118	14
26	15	57	16	88	14	119	15
27	16	58	16	89	16	120	15
28	16	59	15	90	14	121	16
29	16	60	16	91	16	122	15
30	14	61	16	92	16	123	15
31	14	62	14	93	15	124	14

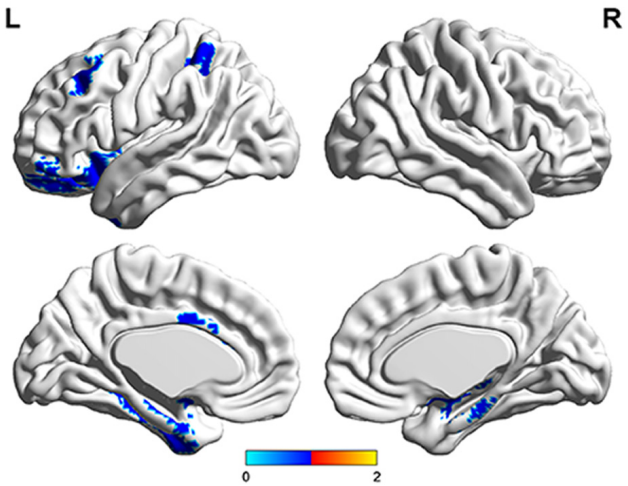


FIGURE 4 | The brain regions with abnormal hurst exponent (HE) values in MCI patients by using brainnetome atlas.

corresponds to an accuracy, the best accuracy rate on the grid of 33 × 33 was acquired as the classification accuracy of the classifier. A flowchart of the detailed classification process was shown in **Figure 2**.

RESULTS

Applying the proposed SVM-based classification method to identify MCI patients from HC subjects, our results indicated 83.1% accuracy, 82.8% sensitivity and 83.3% specificity. Besides, the receiver operating characteristics curve and the relationship between MMSE and prediction values were shown in **Figure 3**, and the area under curve of the classification algorithm is 0.88, indicating a powerful classification performance.

The number of features retained in per fold of LOOCV was shown in **Table 2**. In addition, the abnormal HE brain regions with the retained times of the HE features no less than 118 (124 × 0.95, 124 is the total number of the samples) in the whole LOOCV process were shown in **Figure 4**, and the Fisher score values of these abnormal HE features were displayed in **Figure 5**. Compared to HC subjects, these abnormal HE brain regions in MCI patients were predominately involved in left middle frontal gyrus, right hippocampus, bilateral parahippocampal gyrus, bilateral amygdala, left cingulate gyrus, left insular gyrus, left fusiform gyrus, left superior parietal gyrus, left orbital gyrus and left basal ganglia.

DISCUSSION

This study proposed an effective classification method to identify MCI patients from HC subjects using HE index of rs-fMRI.

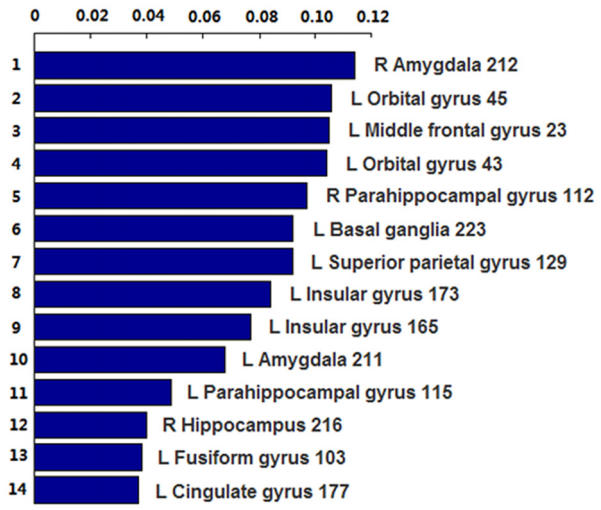


FIGURE 5 | The Fisher score values of these abnormal HE features which were retained no less than 118 times (124 × 0.95, 124 is the total number of the samples) in the whole leave-one-out cross-validation (LOOCV) process.

A promising classification performance was obtained with an accuracy of 83.1% and an area under curve value of 0.88, suggesting that the proposed SVM-based method was effective in identifying MCI from HC subjects, and the calculated HE index could serve as an effective feature for the SVM-based classification algorithm.

To obtain high discrimination accuracy for MCI classification, three steps were taken for the proposed classification method. First, previous studies demonstrated that properly reducing the number of features could not only improve the classification performance but also speed up the computation (Dosenbach et al., 2010; Dai et al., 2012). Thus two-sample two-tailed-*t*-test and Fisher score criteria were both utilized to select out the discriminative HE features in this article, and the classification performance was improved significantly compared to without feature selection. In fact, we firstly tried a total 246 HE features by using the proposed SVM-based algorithm, and the classification accuracy without feature selection was lower than 70%. It needs to note that the feature selection was only performed on the training set, which could reduce the overfitting of the classifier. Second, the RBF kernel function was adopted as the kernel function due that it could deal with the case when the relationship between labels and features is nonlinear (Hsu et al., 2003), which also has an important impact on classification performance. In this article, we also utilized the linear kernel function for MCI classification, and the discrimination rate was 78.2%, which was lower than that with RBF kernel. At last, the grid search method, which has a high learning accuracy and could be implemented with parallel processing (Long et al., 2016), was utilized to optimize the two parameters of SVM, which also improved the classification performance. In addition, to further validate the effectiveness of the proposed MCI classification method, the dataset was randomly split into two subsets including a training subset (42 MCI and 40 HC), a testing subset (22 MCI and 20 HC). The training subset was utilized to train the classification algorithm and optimize the two parameters through an internal cross-validation procedure which averagely divided the training set into two groups to train the algorithm with one group and then predict the other group mutually (Dyrba et al., 2015). Then the final performance of the classification algorithm was estimated with the testing subset. A promising accuracy of 85.71% was obtained, which also indicated that the proposed SVM-based method is effective in identifying MCI patients form HC subjects.

In this article, we found that the abnormal HE brain regions in MCI patients mainly involved in left middle frontal gyrus, right hippocampus, bilateral parahippocampal gyrus, bilateral amygdala, left cingulate gyrus, left insular gyrus, left fusiform gyrus, left superior parietal gyrus, left orbital gyrus and left basal ganglia. Almost all these brain regions were consistent with previous studies that analyzed the structural and functional data of MCI or AD patients with conventional statistical analysis (Hirata et al., 2005; Lerch et al., 2008; Xie et al., 2012). The middle frontal gyrus, hippocampus, parahippocampal gyrus, cingulate gyrus and orbital gyrus belong to the default mode network (Dai et al., 2012; De Vogelaere et al., 2012). Currently, the behavioral correlations of default mode network still remain uncharacterized although some investigators had proposed several potentially inclusive hypotheses that it mediates processes such as reviewing past knowledge and preparing for future actions (Greicius et al., 2004). The abnormal HE values in these brain regions supplementarily supported the abnormalities of default mode network in MCI patients. In addition, the amygdala and insular gyrus were labeled with significant atrophy in MCI patients in previous voxel-based morphometry studies (Hämäläinen et al., 2007), and the fusiform gyrus showed significantly aberrant amplitude of low-frequency fluctuations of BOLD signals in MCI (Wang et al., 2015). Furthermore, the basal ganglia was associated with cognitive functions such as mood swings or disorders (de Oliveira and de Oliveira, 2013). All the above-mentioned evidences suggested that these abnormal brain regions were related to the mechanisms underlying MCI patients.

The HE analysis has already been utilized to describe complex properties of biological signals including electroencephalogram and electrocardiogram (Costa and McCrae, 1992; Ignaccolo et al., 2010). By applying the HE analysis method to BOLD signals, some investigators found that the HE value of fMRI signals in gray matter was higher than in white gray (Maxim et al., 2005), and decreased with cholinergic transmission enhancement and augmented in hippocampus with aging (Wink et al., 2006). Nevertheless, these findings could not conclude that a higher HE value is associated with worse brain functioning. It seems to reflect some inherent patterns of spontaneous discharge and the HE could be modulated by different psychotic or psychological variables (Gentili et al., 2015). In this article, the HE analysis was applied in MCI patients, and some core brain regions were detected with HE abnormalities. It demonstrated that the

persistent behavior of brain activities in these abnormal regions were changed, which may provide some information for the mechanisms underlying MCI patients. However, the physiological significance of HE index still remains unknown currently, and future studies should pay more attention to confirm it through the multi-modal imaging validation in animal models.

Several issues need to be addressed in this article. First, some other structural or functional brain partition atlases exist and these brain parcellation atlases could also be used for identifying different psychiatric disorders. Different parcellation schemes may lead to different classification results. Compared to the widely used automated anatomical labeling atlas, the brainnetome atlas that simultaneously combines information from structural and functional connections obtained better classification performance in differentiating major depressive disorder from HC in our previous study (Jing et al., 2017). Thus the brainnetome atlas was adopted to discriminate MCI from HC subjects in this work. Second, deep learning plays an increasing important role in identifying different psychiatric disorders as it could acquire powerful identification performance from high dimension feature data. Future studies could extract the HE features or other multi-level characteristics at a voxel level for deep learning algorithm to obtain better classification accuracy and more comprehensive explanations for abnormalities in psychiatric disorders.

AUTHOR CONTRIBUTIONS

ZL, BJ and RG made substantial contributions to the conception, design, analysis and interpretation of data and drafted the manuscript. ZL, BJ, BL and HC made contributions to the revision of the manuscript. ZL, FC and TW made contributions to the data acquisition. HC, the corresponding author, made contributions to conception and interpretation of data, and determined the final version to be submitted for publishing. All authors read and approved the final manuscript.

ACKNOWLEDGMENTS

There is no any competing interest among all authors, and thanks very much for all editors and reviewers of our manuscript. BJ was supported by the Beijing Natural Science Foundation (No.7174282).

REFERENCES

Baron, J. C., Chételat, G., Desgranges, B., Perchey, G., Landeau, B., Sayette, V., et al. (2001). *In vivo* mapping of gray matter loss with voxel-based morphometry in mild Alzheimer's disease. *Neuroimage* 14, 298–309. doi: 10.1006/nimg.2001.0848

Beheshti, I., and Demirel, H. (2016). Feature-ranking-based Alzheimer's disease classification from structural MRI. *Magn. Reson. Imaging* 34, 252–263. doi: 10.1016/j.mri.2015.11.009

Brier, M. R., Thomas, J. B., Fagan, A. M., Hassenstab, J., Holtzman, D. M., Benzinger, T. L., et al. (2014). Functional connectivity and graph theory in preclinical Alzheimer's disease. *Neurobiol. Aging* 35, 757–768. doi: 10.1016/j.neurobiolaging.2013.10.081

Chen, G., Ward, B. D., Xie, C., Li, W., Wu, Z., Jones, J. L., et al. (2011). Classification of Alzheimer disease, mild cognitive impairment, and normal cognitive status with large-scale network analysis based on resting-state functional MR imaging. *Radiology* 259, 213–221. doi: 10.1148/radiol.10100734

Ciuciu, P., Varoquaux, G., Abry, P., Sadaghiani, S., and Kleinschmidt, A. (2012). Scale-free and multifractal time dynamics of fMRI signals during rest and task. *Front. Physiol.* 3:186. doi: 10.3389/fphys.2012.00186

Costa, P. T., and McCrae, R. R. (1992). Normal personality assessment in clinical practice: the NEO personality inventory. *Psychol. Assess.* 4, 5–13. doi: 10.1037/1040-3590.4.1.5

Dai, Z., Yan, C., Wang, Z., Wang, J., Xia, M., Li, K., et al. (2012). Discriminative analysis of early Alzheimer's disease using multi-modal imaging and multi-level characterization with multi-classifier (M3). *Neuroimage* 59, 2187–2195. doi: 10.1016/j.neuroimage.2011.10.003

Davatzikos, C., Fan, Y., Wu, X., Shen, D., and Resnick, S. M. (2008). Detection of prodromal Alzheimer's disease via pattern classification of MRI. *Neurobiol. Aging* 29, 514–523. doi: 10.1016/j.neurobiolaging.2006.11.010

De Martino, F. D., Valente, G., Staeren, N., Ashburner, J., Goebel, R., and Formisano, E. (2008). Combining multivariate voxel selection and support vector machines for mapping and classification of fMRI spatial patterns. *Neuroimage* 43, 44–58. doi: 10.1016/j.neuroimage.2008.06.037

de Oliveira, J. R. M., and de Oliveira, M. F. (2013). Basal ganglia calcification as a putative cause for cognitive decline. *Dement. Neuropsychol.* 7, 151–154. doi: 10.1590/s1980-57642013dn70200003

Desikan, R. S., Cabral, H. J., Hess, C. P., Dillon, W. P., Glastonbury, C. M., Weiner, M. W., et al. (2009). Automated MRI measures identify individuals with mild cognitive impairment and Alzheimer's disease. *Brain* 132, 2048–2057. doi: 10.1093/brain/awp123

De Vogelaere, F., Santens, P., Achten, E., Boon, P., and Vingerhoets, G. (2012). Altered default-mode network activation in mild cognitive impairment compared with healthy aging. *Neuroradiology* 54, 1195–1206. doi: 10.1007/s00234-012-1036-6

Dosenbach, N. U., Nardos, B., Cohen, A. L., Fair, D. A., Power, J. D., Church, J. A., et al. (2010). Prediction of individual brain maturity using fMRI. *Science* 329, 1358–1361. doi: 10.1126/science.1194144

Dyrba, M., Grothe, M., Kirste, T., and Teipel, S. J. (2015). Multimodal analysis of functional and structural disconnection in Alzheimer's disease using multiple kernel SVM. *Hum. Brain Mapp.* 36, 2118–2131. doi: 10.1002/hbm.22759

Fan, L., Li, H., Zhuo, J., Zhang, Y., Wang, J., Chen, L., et al. (2016). The human brainnetome atlas: a new brain atlas based on connectional architecture. *Cereb. Cortex* 26, 3508–3526. doi: 10.1093/cercor/bhw157

Fornito, A., and Bullmore, E. T. (2010). What can spontaneous fluctuations of the blood oxygenation-level-dependent signal tell us about psychiatric disorders? *Curr. Opin. Psychiatry* 23, 239–249. doi: 10.1097/yco.0b013e328337d78d

Gentili, C., Vanello, N., Cristea, I., David, D., Ricciardi, E., and Pietrini, P. (2015). Proneness to social anxiety modulates neural complexity in the absence of exposure: a resting state fMRI study using hurst exponent. *Psychiatry Res.* 232, 135–144. doi: 10.1016/j.pscychresns.2015.03.005

Greicius, M. D., Srivastava, G., Reiss, A. L., and Menon, V. (2004). Default-mode network activity distinguishes Alzheimer's disease from healthy aging: evidence from functional MRI. *Proc. Natl. Acad. Sci. U S A* 101, 4637–4642. doi: 10.1073/pnas.0308627101

Hämäläinen, A., Tervo, S., Grau-Olivares, M., Niskanen, E., Pennanen, C., Huuskonen, J., et al. (2007). Voxel-based morphometry to detect brain atrophy in progressive mild cognitive impairment. *Neuroimage* 37, 1122–1131. doi: 10.1016/j.neuroimage.2007.06.016

Han, Y., Wang, J., Zhao, Z., Min, B., Lu, J., Li, K., et al. (2011). Frequency-dependent changes in the amplitude of low-frequency fluctuations in amnestic mild cognitive impairment: a resting-state fMRI study. *Neuroimage* 55, 287–295. doi: 10.1016/j.neuroimage.2010.11.059

He, Y., Wang, L., Zang, Y., Tian, L., Zhang, X., Li, K., et al. (2007). Regional coherence changes in the early stages of Alzheimer's disease: a combined

structural and resting-state functional MRI study. *Neuroimage* 35, 488–500. doi: 10.1016/j.neuroimage.2006.11.042

Hirata, Y., Matsuda, H., Nemoto, K., Ohnishi, T., Hirao, K., Yamashita, F., et al. (2005). Voxel-based morphometry to discriminate early Alzheimer's disease from controls. *Neurosci. Lett.* 382, 269–274. doi: 10.1016/j.neulet.2005.03.038

Hsu, C. W., Chang, C. C., and Lin, C. J. (2003). A practical guide to support vector classification. Available online at: https://www.csie.ntu.edu.tw/∼cjlin/papers/guide/guide.pdf

Ignaccolo, M., Latka, M., Jernajczyk, W., Grigolini, P., and West, B. J. (2010). The dynamics of EEG entropy. *J. Biol. Phys.* 36, 185–196. doi: 10.1007/s10867-009-9171-y

Jing, B., Long, Z., Liu, H., Yan, H., Dong, J., Mo, X., et al. (2017). Identifying current and remitted major depressive disorder with the hurst exponent: a comparative study on two automated anatomical labeling atlases. *Oncotarget* 8, 90452–90464. doi: 10.18632/oncotarget.19860

Khazaee, A., Ebrahimzadeh, A., and Babajani-Feremi, A. (2016). Application of advanced machine learning methods on resting-state fMRI network for identification of mild cognitive impairment and Alzheimer's disease. *Brain Imaging Behav.* 10, 799–817. doi: 10.1007/s11682-015-9448-7

Lai, M. C., Lombardo, M. V., Chakrabarti, B., Sadek, S. A., Pasco, G., Wheelwright, S. J., et al. (2010). A shift to randomness of brain oscillations in people with autism. *Biol. Psychiatry* 68, 1092–1099. doi: 10.1016/j.biopsych.2010.06.027

Lei, X., Zhao, Z., and Chen, H. (2013). Extraversion is encoded by scale-free dynamics of default mode network. *Neuroimage* 74, 52–57. doi: 10.1016/j.neuroimage.2013.02.020

Lerch, J. P., Pruessner, J., Zijdenbos, A. P., Collins, D. L., Teipel, S. J., Hampel, H., et al. (2008). Automated cortical thickness measurements from MRI can accurately separate Alzheimer's patients from normal elderly controls. *Neurobiol. Aging* 29, 23–30. doi: 10.1016/j.neurobiolaging.2006.09.013

Long, Z., Jing, B., Yan, H., Dong, J., Liu, H., Mo, X., et al. (2016). A support vector machine-based method to identify mild cognitive impairment with multi-level characteristics of magnetic resonance imaging. *Neuroscience* 331, 169–176. doi: 10.1016/j.neuroscience.2016.06.025

Magnin, B., Mesrob, L., Kinkingnéhun, S., Pélégrini-Issac, M., Colliot, O., Sarazin, M., et al. (2009). Support vector machine-based classification of Alzheimer's disease from whole-brain anatomical MRI. *Neuroradiology* 51, 73–83. doi: 10.1007/s00234-008-0463-x

Maxim, V., Sendur, L., Fadili, J., Suckling, J., Gould, R., Howard, R., et al. (2005). Fractional gaussian noise, functional MRI and Alzheimer's disease. *Neuroimage* 25, 141–158. doi: 10.1016/j.neuroimage.2004.10.044

Pereira, F., Mitchell, T., and Botvinick, M. (2009). Machine learning classifiers and fMRI: a tutorial overview. *Neuroimage* 45, S199–S209. doi: 10.1016/j.neuroimage.2008.11.007

Petersen, R. C. (2007). Mild cognitive impairment: current research and clinical implications. *Semin. Neurol.* 27, 022–031. doi: 10.1055/s-2006-956752

Wang, Y., Zhao, X., Xu, S., Yu, L., Wang, L., Song, M., et al. (2015). Using regional homogeneity to reveal altered spontaneous activity in patients with mild cognitive impairment. *Biomed Res. Int.* 2015:807093. doi: 10.1155/2015/807093

Wei, M., Qin, J., Yan, R., Li, H., Yao, Z., and Lu, Q. (2013). Identifying major depressive disorder using hurst exponent of resting-state brain networks. *Psychiatry Res.* 214, 306–312. doi: 10.1016/j.pscychresns.2013.09.008

Wink, A. M., Bernard, F., Salvador, R., Bullmore, E., and Suckling, J. (2006). Age and cholinergic effects on hemodynamics and functional coherence of human hippocampus. *Neurobiol. Aging* 27, 1395–1404. doi: 10.1016/j.neurobiolaging.2005.08.011

Xie, C., Bai, F., Yu, H., Shi, Y., Yuan, Y., Chen, G., et al. (2012). Abnormal insula functional network is associated with episodic memory decline in amnestic mild cognitive impairment. *Neuroimage* 63, 320–327. doi: 10.1016/j.neuroimage.2012.06.062

Zhang, Z., Liu, Y., Jiang, T., Zhou, B., An, N., Dai, H., et al. (2012). Altered spontaneous activity in Alzheimer's disease and mild cognitive impairment revealed by regional homogeneity. *Neuroimage* 59, 1429–1440. doi: 10.1016/j.neuroimage.2011.08.049

Conflict of Interest Statement: The authors declare that the research was conducted in the absence of any commercial or financial relationships that could be construed as a potential conflict of interest.

Copyright © 2018 Long, Jing, Guo, Li, Cui, Wang and Chen. This is an open-access article distributed under the terms of the Creative Commons Attribution License (CC BY). The use, distribution or reproduction in other forums is permitted, provided the original author(s) and the copyright owner are credited and that the original publication in this journal is cited, in accordance with accepted academic practice. No use, distribution or reproduction is permitted which does not comply with these terms.

frontiers in Aging Neuroscience

MINI REVIEW
published: 07 February 2018
doi: 10.3389/fnagi.2018.00021

Use of Peptides for the Management of Alzheimer's Disease: Diagnosis and Inhibition

*Mohammad H. Baig, Khurshid Ahmad, Gulam Rabbani and Inho Choi**

Department of Medical Biotechnology, Yeungnam University, Gyeongsan, South Korea

Alzheimer's disease (AD) is a form of dementia and the most common progressive neurodegenerative disease (ND). The targeting of amyloid-beta (Aβ) aggregation is one of the most widely used strategies to manage AD, and efforts are being made globally to develop peptide-based compounds for the early diagnosis and treatment of AD. Here, we briefly discuss the use of peptide-based compounds for the early diagnosis and treatment of AD and the use of peptide-based inhibitors targeting various Aβ aggregation checkpoints. In addition, we briefly discuss recent applications of peptide-based inhibitors against various AD targets including amyloid beta, β-site amyloid precursor protein cleaving enzyme 1 (BACE1), Glyceraldehyde-3-phosphate dehydrogenase (GAPDH), tyrosine phosphatase (TP) and potassium channel KV1.3.

Keywords: Alzheimer's disease, peptides, amyloid beta, BACE-1, GAPDH, inhibitors, diagnosis

INTRODUCTION

Alzheimer's disease (AD) is the most common fatal neurodegenerative disease (ND), and is characterized by the structural and functional loss of neurons. During the last few decades, AD and its associated risk factors have become major healthcare concerns in most developed countries. Furthermore, it has been reported AD is the fifth-leading cause of death among those aged more than 65 years, and that its incidence exceeds five million cases per year in the United States (Alzheimer's Association, 2017). The World Health Organization (WHO) estimated that the prevalence of AD worldwide will quadruple to reach approximately 114 million by 2050 (Alzheimer's Association, 2017).

Pathological hallmarks of AD include the progressive accretion of plaque outside neurons (extracellular amyloid plaque) and of neurofibrillary tangles inside neurons (hyperphosphorylated tau protein accumulations; VanItallie, 2015). These pathological changes gradually result in neuronal loss and eventual neuron death. Although the etiology and pathogenesis of AD remain imprecise, the amyloid cascade theory is widely accepted and supported by several studies (Drachman, 2014; Herrup, 2015). This hypothesis was further reinforced by the identification of a protective amyloid precursor protein (APP) mutation near the protein's beta-cleavage site, which protects against the development of late onset dementia (Jonsson et al., 2012).

Amyloid-beta (Aβ) is a 39–43 amino acid residue peptide and a key component of extracellular amyloid plaque, and its expression is considered a key event in AD progression (Li et al., 2017). Aβ is the peptide product of the sequential proteolytic cleavages (by β- and γ-secretases) of APP (a type-I transmembrane protein). These proteolytic cleavages result in the generations of two types of Aβ isoforms (Aβ40 and Aβ42), and though Aβ40 is more abundant than Aβ42 in human fluids, Aβ42 aggregates faster and is considered to be the more lethal in terms of neuron survival.

Abbreviations: Aβ, Amyloid-beta; AD, Alzheimer's disease; BACE1, β-site APP cleaving enzyme 1; GAPDH, Glyceraldehyde-3-phosphate dehydrogenase; ND, Neurodegenerative disease; TP, Tyrosine phosphatase.

OPEN ACCESS

Edited by:
Ghulam Md Ashraf, King Abdulaziz University, Saudi Arabia

Reviewed by:
Mohd Shahnawaz Khan, King Saud University, Saudi Arabia
Preeti Vishwakarma, King George's Medical University, India

***Correspondence:**
Inho Choi
inhochoi@ynu.ac.kr

Received: *31 October 2017*
Accepted: *18 January 2018*
Published: *07 February 2018*

Citation:
Baig MH, Ahmad K, Rabbani G and Choi I (2018) Use of Peptides for the Management of Alzheimer's Disease: Diagnosis and Inhibition. Front. Aging Neurosci. 10:21. doi: 10.3389/fnagi.2018.00021

It has been reported oligomers of diffusible Aβ, such as, protofibrils, prefibrillar aggregates and Aβ-derived diffusible ligands (ADDLs), are the main toxic players during the development and progression of AD (Haass and Selkoe, 2007; Shankar et al., 2008; Funke and Willbold, 2012). Numerous amyloid reduction therapy (ART) clinical trials have failed to provide expected clinical improvements in AD patients, and these failures raise genuine concerns regarding the validity of the amyloid cascade hypothesis and the merits of further research on ART (Extance, 2010; Grundman et al., 2013; Cheng et al., 2017).

Today, due to the extensive efforts of researchers and pharmaceutical companies, peptide-based drugs have emerged as a major class of therapeutics, and as a result, the last decade has witnessed extraordinary scientific and industrial interest in their therapeutic uses (Vlieghe et al., 2010). Such studies are very much on-going and currently, a number of natural and synthetic therapeutic peptides are undergoing clinical trials (Mandal et al., 2014). Generally, these drugs have several advantages over small molecule therapeutics, particularly in terms of their efficacies and fewer side effects (Craik et al., 2013).

Many other fatal NDs, such as, Parkinson's disease (PD), amyotrophic lateral sclerosis (ALS), prion diseases and Huntington's diseases (HD) share the AD characteristic of misfolded protein aggregation. Peptides have proven to be vital tools for ND research, and can be used to study the properties of misfolded proteins and/or peptides. In this review article, we discuss some of the available peptide-based therapeutics used to treat AD, the use of peptide inhibitors to target different aspects of AD, and the use of peptides for the diagnosis and early detection of AD.

THE USE OF PEPTIDES AS DIAGNOSTIC PROBES

Currently, the number of *in vivo* diagnostic techniques available for detection of AD is limited, but early detection of the disease is crucial for effective treatment, because preemptive treatment might control or eliminate early stage disease. Investigations on AD patients have shown amyloid plaque appears several years before cognitive symptoms (Silverman et al., 1997; Thal et al., 2002; Funke and Willbold, 2012). Accordingly, early stage detection and the quantification of amyloid in brain are viewed as important from the prognostic point of view and for evaluating the effects of therapies, and several molecular imaging techniques, including, magnetic resonance imaging (MRI), positron emission tomography (PET) and single-photon emission computed tomography (SPECT) provide means of doing so. These molecular imaging techniques have been reported to be useful for detecting biomarkers of AD (mainly Aβ) and for monitoring the expression of Aβ (Frisoni et al., 2017), and thus, have attracted considerable attention in the AD research field. Furthermore, amyloid ligands have been used as contrast agents to estimate amyloid plaque load, and been shown to stain amyloid plaque specifically in the brain tissues of AD patients, which make these peptides suitable probes for *in vivo* imaging (Kang et al., 2003).

D-enantiomeric peptides (also known as derivatives of ACI-80) are another set of peptides that have been reported to bind Aβ1–42. In one study, ACI-80 also was found to bind Aβ1–42 with high affinity (in the submicromolar range; Funke et al., 2012; Gulyás et al., 2012), and is currently being used as a molecular probe to monitor Aβ1–42 plaque load in the living brain. Findings show when ACI-80 is injected into the brain, it specifically binds to Aβ1–42 and stains dense amyloid deposits in brain but not diffuse plaque (van Groen et al., 2009), which makes it a suitable molecular probe for *in vivo* imaging in AD. In addition, recent studies have described a series of D-enantiomeric peptides that also specifically bind to aggregated Aβ1–42 (Funke et al., 2012), but have greater stabilities and Aβ binding properties than ACI-80. To confirm binding by these peptide derivatives, *ex vivo* immunochemistry was performed using transgenic mouse models of AD, and the ACI-80 derivatives ACI-87-Kφ, ACI-88-Kφ and ACI-89-Kφ were found to bind to aggregated Aβ1–42 with greater affinity than parent ACI-80. These findings suggest these compounds might be useful probes for specific types of Aβ aggregation and plaque *in vivo*.

Larbanoix et al. (2010) used a phage display technique to search for peptide ligands with carrying ability to vectorize an AP-targeting contrast agent, and identified 12 peptide ligands from among 22 sequenced phage clones with high affinity against Aβ42. Two peptides were selected (C-FRHMTEQ-C and C-IPLPFYN-C) as both were found to be present in several copies and to have K_d-values in the picomolar range. For example, C-IPLPFYN-C was found to have a K_d value of 2.2×10^{-10} M, and C-FRHMTEQ-C a K_d value 5.45×10^{-10} M against mouse Aβ42. Both peptides were also tested on human Aβ42, and C-FRHMTEQ-C demonstrated similar affinity against human Aβ42, whereas C-IPLPFYN-C demonstrated greater affinity against human than mouse Aβ42. In addition, a preliminary *in vivo* MRI study on a transgenic mouse model of AD, showed both C-FRHMTEQ-C and C-IPLPFYN-C acted as excellent contrast agents (Larbanoix et al., 2010).

USE OF PEPTIDES AS INHIBITORS AGAINST ALZHEIMER'S DISEASE

Peptide Inhibitors of Amyloid β

Amyloid plaque accumulation and Aβ fibrillation are clinical hallmarks of AD (Hajipour et al., 2017), and thus, the inhibition of amyloid aggregation has been the subject of much research over the last two decades, and the use of peptide-based inhibitors represents a major part of these efforts (Goyal et al., 2017; Folch et al., 2018; **Figure 1**). A large number of these studies have focused on the design of peptide fragments capable of binding to Aβ regions critical for aggregation (Ladner et al., 2004). The peptides designed function by binding to Aβ to either prevent fibril formation or Aβ elongation to

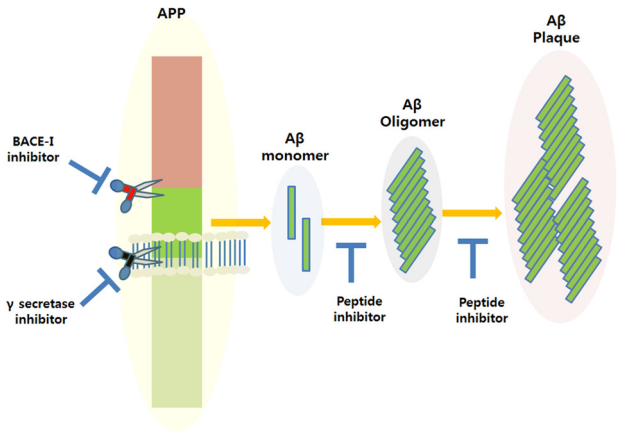


FIGURE 1 | Amyloidogenic amyloid precursor protein (APP) processing and the possible applications of peptide inhibitors to prevent amyloid-beta (Aβ) plaque formation at different disease stages.

prevent the formation of monomers/oligomers. A long list of peptides that specifically target Aβ have been designed (Doig, 2007; Eskici and Gur, 2013), but here, we discuss some of the more recently reported peptides inhibitors of Aβ. **Table 1** shows some of the important peptides described in the literature as inhibitors of AD. Peptide inhibitors that share sequence similar with hydrophobic segments of Aβ are capable of altering Aβ aggregation and reducing the cytotoxicity of Aβ (Wasmer et al., 2008). Austen et al. (2008) described two peptide inhibitors of Aβ, that is, RGKLVFFGR (OR1) and RGKLVFFGR-NH2 (OR2), which were produced by modifying the KLVFF amino acid sequence of Aβ by incorporating RG–/–GR residues at its N- and C-terminals. These inhibitors were both reported to effectively inhibit Aβ fibril formation.

In another study, Wei et al. (2011), reported some new peptide inhibitors based on modifications of the hydrophobic KLVFF amino acid sequence of Aβ, and synthesized a conjugate of the pentapeptide KLVFF and ferrocenoyl (Fc) to improve the lipophilicity and proteolytic stability of peptide inhibitors. In another study, Rangachari et al. (2009) designed two α, β-dehydroalanine (ΔAla) containing peptides based on KLVFF, and found two novel ΔAla-containing peptides (KLVF-ΔA-I-ΔA and KF-ΔA-ΔA-ΔA-F) disrupted Aβ aggregation, though by quite different mechanisms.

Another group of researchers designed and synthesized a decapeptide inhibitor of Aβ1–40 aggregation. This inhibitor (RYYAAFFARR) was designated RR, and unlike other inhibitors was designed to target the extended region of Aβ (Aβ11–23), which consists of a GAG-binding site, a hydrophobic core, and a salt bridge region. RR was found to have high binding affinity for Aβ1–40 (K_d = 1.10 μM), and its binding affinity was markedly greater than that of the known β-sheet breaker peptide iAβ5 (K_d = 156 μM; Liu et al., 2014).

Chalifour et al. (2003) reported results obtained by replacing L-amino acids with D-amino acids with the aims of increase peptide stability and therapeutic potential. The effect of chiral reversal (D-enantiomers) was assessed for five peptides (KKLVFFA, KLVFFA, KIVFFA, KFVFFA and KVVFFA), and it was found they inhibited Aβ aggregation better than L-peptides. In particular, the D-enantiomer of KKLVFFA was found to inhibit the neurotoxic effect of Aβ significantly more than its L counterpart.

Jagota and Rajadas (2013) synthesized three short D-peptides, that is, KKLVFFARRRRA, PGKLVYA and KKLVFFA, based on residues of the central hydrophobic core of Aβ (residues 16–20), and examined their effects on Aβ aggregation. Observations suggested these D-peptides effectively inhibited Aβ fibrillogenesis, and two of the three (KKLVFFA and PGKLVYA) were found to improve survival in transgenic *C. elegans*.

β-Site APP Cleaving Enzyme 1 (BACE1)

Beta-site APP cleaving enzyme 1 (BACE1) is a human aspartyl protease, which is believed to play a prime role in the generation of beta amyloid peptides (Aβ) in AD. BACE1 has characteristic bilobal structure and is a membrane-bound aspartyl protease with an open active site, which is less hydrophobic than those of other aspartic proteases and allows up to 11 substrate residues to be accommodated (Hong et al., 2000; Turner et al., 2005). BACE1 levels are elevated in the brain tissues of AD patients and its overexpression in cerebrospinal fluid offers a possible biomarker of early stage disease. When BACE1 is overexpressed it competes with γ-secretase to initiate the cleavage of APP at its β-position. Furthermore, BACE1 inhibition halts Aβ formation at the first step of APP amyloidogenic processing. BACE1 is composed of two signature peptides, that is, DTGS at position 93–96 and DSGT at position 289–292, which come together to form an active site and have the ability to inhibit APP (Yan et al., 2016). Peptides derived from the sequence of BACE1 have also been reported to inhibit APP processing. BACE1 possess a catalytic domain containing a pair of aspartic acid residues at its active site, and Aβ production is blocked by BACE1 inhibition, which reduces Aβ production by depleting C99, acting as a substrate of γ-secretase. The observation that Aβ production was diminished in BACE1 deficient mice supports the view that BACE1 inhibitors reduce Aβ levels (Vassar, 2002).

Glyceraldehyde-3-Phosphate Dehydrogenase (GAPDH)

Glyceraldehyde-3-phosphate dehydrogenase (GAPDH) is a glycolytic enzyme of considerable interest in ND research, especially in AD. Recently, it was revealed that GAPDH interacts with APP, which is known to be involved in AD (Sunaga et al., 1995; Bertram et al., 2007; Butterfield et al., 2010). GAPDH can undergo diverse oxidative modifications that control its structure, function, and activity, and in AD, when exposed to oxidative stress Aβ forms amyloid-like aggregates, which reduce neuron and synapse numbers. Furthermore, insoluble aggregates of GAPDH accelerate Aβ amyloidogenesis and neuronal cell death *in vitro* and *in vivo* (Itakura et al., 2015), and GAPDH aggregation caused by cysteine oxidation and intermolecular disulfide bonding reduces its catalytic

TABLE 1 | List of peptide-based inhibitors reported to be effective against Alzheimer's disease (AD).

Peptides	Description	Reference
RGKLVFFGR (OR1) RGKLVFFGR-NH2 (OR2)	Based on the Aβ (16–20) sequence	Austen et al. (2008)
Fc-KLVFF	Based on the Aβ (16–20) sequence and conjugated with ferrocenoyl (Fc)	Wei et al. (2011)
KLVF-ΔA-I-ΔAKF-ΔA-ΔA-ΔA-F	Based on the Aβ (16–20) sequence and ΔAla	Wei et al. (2011)
RYYAAFFARR	Based on Aβ (11–23)	Liu et al. (2014)
KLVFFA, KKLVFFA, KFVFFA, KIVFFA and KVVFFA	Based on the Aβ (16–20) sequence and replacement of L- with D-amino acids	Chalifour et al. (2003)
PGKLVYA, KKLVFFARRRRA and KKLVFFA	d-peptides of Aβ (16–20)	Jagota and Rajadas (2013)
AuNPs@POMD-pep	Aβ peptide conjugates with gold nanoparticles (AuNPs)	Gao et al. (2015)
IGLMVG-NH2	Based on Aβ (32–37)	Bansal et al. (2016)
HKQLPFFEED	A β-sheet blocker peptide based on the stereochemical structure and characteristic of aggregation of Aβ (1–42)	Lin et al. (2014)
Nonhemolytic 11-residue peptide (NAVRWSLMRPF)	Modified analog of NIVNVSLVK from the E-protein sequence of SARS coronavirus	Ghosh et al. (2017)
AP90	A 23 residue long hairpin peptide (with alternating D- and L-amino acids) reported to inhibit Aβ aggregation.	Kellock et al. (2016)

activity (Nakajima et al., 2007, 2009). Glycyl-L-histidyl-L-lysine-Copper (GHK-Cu) is naturally occurring peptide in human plasma with a stunning array of actions that appear to counter aging-associated diseases and conditions. In plasma the concentration of GHK-Cu is about 200 ng/ml (10^{-7} M^{-1}) at age 20, but decreases to 80 ng/ml at age 60 (Pickart et al., 2015), and interestingly, the enzyme primarily involved in GAPDH gene silencing also belongs to the histone deacetylase (HDACs) protein family. Selective HDAC inhibitors have been shown to possess neuroprotective properties in animal models of brain disease, and have been suggested as potential therapeutics for AD (Fischer et al., 2010). Gly-Pro-Glu (GPE) is present in plasma and brain tissues, and it has been shown to have neuroprotective effects in animal models of NDs, such as, HD, PD and AD (Alexi et al., 1999). Basic structural studies suggest that GPE can interact with single or several Glu receptor types and bind to N-methyl-D-aspartate (NMDA) receptor (Sara et al., 1989). Furthermore, the C-terminal (Glu) GPE is required for NMDA receptor binding and this binding induces the potassium-evoked release of dopamine from nigrostriatal dopaminergic terminals and acetylcholine through an unknown mechanism via NMDA receptor (Sara et al., 1989; Alonso De Diego et al., 2005).

Tyrosine Phosphatase (TP)

STriatal-Enriched tyrosine phosphatase (STEP) is expressed in neurons of the striatum, neocortex, hippocampus and related structures (Pelkey et al., 2002), and targets signaling pathways in the postsynaptic terminals of excitatory glutamatergic synapses (Lombroso et al., 1991; Boulanger et al., 1995). STEP regulates various synaptic actions including glutamate receptor trafficking, which plays critical functions in learning and memory (Karasawa and Lombroso, 2014). Interestingly, it was recently suggested STEP is overactive in AD and schizophrenia (Carty et al., 2012). Endogenous STEP levels also influence the susceptibility of neurons to excitotoxicity and affect the regulation of synaptic proteins by changing synaptic conductivities via the synchronized dephosphorylations of multiple substrates that regulate synaptic plasticity. STEP is an intracellular tyrosine phosphatase (TP) encoded by the *ptpn5* gene, and contains a signature consensus sequence [I/V]HCxAGXXR[S/T]G at its C-terminus that is required for its catalytic activity (Bult et al., 1996), and the active motif (I/V)HCXAGXGR(S/T), also called the P-loop, which houses catalytic Cys for nucleophilic attack is a hallmark of the PTP super-family. Furthermore, a neuroprotective, endogenous tripeptide GPE was reported to protect and rescue cells from Aβ-induced death, and modified analogs of GPE, including modifications at Pro and/or Glu residues, have been synthesized and evaluated (Guan and Gluckman, 2009). Binding of NNZ-2566 (glycyl-L-2-methylprolyl-L-glutamic acid) analogs with Aβ was found to have better neuroprotective effects in infant rats, as compared with GPE (Cacciatore et al., 2012).

Peptide Based Inhibitors Against Potassium Channel KV1.3

Potassium channel KV1.3 was recently identified as a potential target in AD (Rangaraju et al., 2015; Lowinus et al., 2016). Rangaraju et al. (2015) conducted a study on AD and non-AD patients and found Kv1.3 overexpression in the frontal cortices of AD patients, thus suggesting potassium channel KV1.3 to considered a therapeutic target in AD. BmKTX-R11-T28-H33 (ADWX-1), OsK1-K16-D20 and HsTx1 [R14A] are examples of peptides subsequently designed to target Kv1.3 (Norton and Chandy, 2017).

CONCLUSION AND FUTURE PERSPECTIVES

A large amount of research effort has resulted in advancements in the diagnosis and treatment of AD, the etiology of which is considered by most to be explained by the amyloid cascade hypothesis. Furthermore, it is generally considered the early detection of AD is likely to facilitate

its treatment using advanced therapeutic approaches, and that the use of peptides for the diagnosis of AD offers an effective means of doing so. Nevertheless, these peptide-based approaches require further development to enable early AD to be efficiently diagnosed and properly treated.

AUTHOR CONTRIBUTIONS

IC and MHB conceived the idea. MHB, KA and GR drafted the review manuscript. IC, MHB, KA and GR critically reviewed the article. IC edited the language and corrected the errors within the manuscript.

REFERENCES

Alexi, T., Hughes, P. E., van Roon-Mom, W. M., Faull, R. L., Williams, C. E., Clark, R. G., et al. (1999). The IGF-I amino-terminal tripeptide glycine-proline-glutamate (GPE) is neuroprotective to striatum in the quinolinic acid lesion animal model of Huntington's disease. *Exp. Neurol.* 159, 84–97. doi: 10.1006/exnr.1999.7168

Alonso De Diego, S. A., Muñoz, P., González-Muñiz, R., Herranz, R., Martín-Martínez, M., Cenarruzabeitia, E., et al. (2005). Analogues of the neuroprotective tripeptide Gly-Pro-Glu (GPE): synthesis and structure-activity relationships. *Bioorg. Med. Chem. Lett.* 15, 2279–2283. doi: 10.1016/j.bmcl.2005.03.015

Alzheimer's Association. (2017). Alzheimer's disease facts and figures. *Alzheimers Dement.* 13, 325–373. doi: 10.1016/j.jalz.2017.02.001

Austen, B. M., Paleologou, K. E., Ali, S. A., Qureshi, M. M., Allsop, D., and El-Agnaf, O. M. (2008). Designing peptide inhibitors for oligomerization and toxicity of Alzheimer's β-amyloid peptide. *Biochemistry* 47, 1984–1992. doi: 10.1021/bi701415b

Bansal, S., Maurya, I. K., Yadav, N., Thota, C. K., Kumar, V., Tikoo, K., et al. (2016). C-terminal fragment, Aβ32–37, analogues protect against aβ aggregation-induced toxicity. *ACS Chem. Neurosci.* 7, 615–623. doi: 10.1021/acschemneuro.6b00006

Bertram, L., McQueen, M. B., Mullin, K., Blacker, D., and Tanzi, R. E. (2007). Systematic meta-analyses of Alzheimer disease genetic association studies: the AlzGene database. *Nat. Genet.* 39, 17–23. doi: 10.1038/ng1934

Boulanger, L. M., Lombroso, P. J., Raghunathan, A., During, M. J., Wahle, P., and Naegele, J. R. (1995). Cellular and molecular characterization of a brain-enriched protein tyrosine phosphatase. *J. Neurosci.* 15, 1532–1544.

Bult, A., Zhao, F., Dirkx, R. Jr., Sharma, E., Lukacsi, E., Solimena, M., et al. (1996). STEP61: a member of a family of brain-enriched PTPs is localized to the endoplasmic reticulum. *J. Neurosci.* 16, 7821–7831.

Butterfield, D. A., Hardas, S. S., and Lange, M. L. (2010). Oxidatively modified glyceraldehyde-3-phosphate dehydrogenase (GAPDH) and Alzheimer's disease: many pathways to neurodegeneration. *J. Alzheimers Dis.* 20, 369–393. doi: 10.3233/JAD-2010-1375

Cacciatore, I., Cornacchia, C., Baldassarre, L., Fornasari, E., Mollica, A., Stefanucci, A., et al. (2012). GPE and GPE analogues as promising neuroprotective agents. *Mini Rev. Med. Chem.* 12, 13–23. doi: 10.2174/138955712798868995

Carty, N. C., Xu, J., Kurup, P., Brouillette, J., Goebel-Goody, S. M., Austin, D. R., et al. (2012). The tyrosine phosphatase STEP: implications in schizophrenia and the molecular mechanism underlying antipsychotic medications. *Transl. Psychiatry* 2:e137. doi: 10.1038/tp.2012.63

Chalifour, R. J., McLaughlin, R. W., Lavoie, L., Morissette, C., Tremblay, N., Boule, M., et al. (2003). Stereoselective interactions of peptide inhibitors with the β-amyloid peptide. *J. Biol. Chem.* 278, 34874–34881. doi: 10.1074/jbc.M212694200

Cheng, Y. S., Chen, Z. T., Liao, T. Y., Lin, C., Shen, H. C., Wang, Y. H., et al. (2017). An intranasally delivered peptide drug ameliorates cognitive decline in Alzheimer transgenic mice. *EMBO Mol. Med.* 9, 703–715. doi: 10.15252/emmm.201606666

Craik, D. J., Fairlie, D. P., Liras, S., and Price, D. (2013). The future of peptide-based drugs. *Chem. Biol. Drug Des.* 81, 136–147. doi: 10.1111/cbdd.12055

Doig, A. J. (2007). Peptide inhibitors of β-amyloid aggregation. *Curr. Opin. Drug Discov. Devel.* 10, 533–539.

Drachman, D. A. (2014). The amyloid hypothesis, time to move on: amyloid is the downstream result, not cause, of Alzheimer's disease. *Alzheimers Dement.* 10, 372–380. doi: 10.1016/j.jalz.2013.11.003

Eskici, G., and Gur, M. (2013). Computational design of new Peptide inhibitors for amyloid β (Aβ) aggregation in Alzheimer's disease: application of a novel methodology. *PLoS One* 8:e66178. doi: 10.1371/journal.pone.0066178

Extance, A. (2010). Alzheimer's failure raises questions about disease-modifying strategies. *Nat. Rev. Drug Discov.* 9, 749–751. doi: 10.1038/nrd3288

Fischer, A., Sananbenesi, F., Mungenast, A., and Tsai, L. H. (2010). Targeting the correct HDAC(s) to treat cognitive disorders. *Trends Pharmacol. Sci.* 31, 605–617. doi: 10.1016/j.tips.2010.09.003

Folch, J., Ettcheto, M., Petrov, D., Abad, S., Pedrós, I., Marin, M., et al. (2018). Review of the advances in treatment for Alzheimer disease: strategies for combating β-amyloid protein. *Neurologia* 33, 47–58. doi: 10.1016/j.nrl.2015.03.012

Frisoni, G. B., Boccardi, M., Barkhof, F., Blennow, K., Cappa, S., Chiotis, K., et al. (2017). Strategic roadmap for an early diagnosis of Alzheimer's disease based on biomarkers. *Lancet Neurol.* 16, 661–676. doi: 10.1016/S1474-4422(17)30159-X

Funke, S. A., Bartnik, D., Glück, J. M., Piorkowska, K., Wiesehan, K., Weber, U., et al. (2012). Development of a small D-enantiomeric Alzheimer's amyloid-β binding peptide ligand for future *in vivo* imaging applications. *PLoS One* 7:e41457. doi: 10.1371/journal.pone.0041457

Funke, S. A., and Willbold, D. (2012). Peptides for therapy and diagnosis of Alzheimer's disease. *Curr. Pharm. Des.* 18, 755–767. doi: 10.2174/138161212799277752

Gao, N., Sun, H., Dong, K., Ren, J., and Qu, X. (2015). Gold-nanoparticle-based multifunctional amyloid-β inhibitor against Alzheimer's disease. *Chemistry* 21, 829–835. doi: 10.1002/chem.201404562

Ghosh, A., Pradhan, N., Bera, S., Datta, A., Krishnamoorthy, J., Jana, N. R., et al. (2017). Inhibition and degradation of amyloid β (Aβ40) fibrillation by designed small peptide: a combined spectroscopy, microscopy, and cell toxicity study. *ACS Chem. Neurosci.* 8, 718–722. doi: 10.1021/acschemneuro.6b00349

Goyal, D., Shuaib, S., Mann, S., and Goyal, B. (2017). Rationally designed peptides and peptidomimetics as inhibitors of amyloid-β (Aβ) aggregation: potential therapeutics of Alzheimer's disease. *ACS Comb. Sci.* 19, 55–80. doi: 10.1021/acscombsci.6b00116

Grundman, M., Dibernardo, A., Raghavan, N., Krams, M., and Yuen, E. (2013). 2012: a watershed year for Alzheimer's disease research. *J. Nutr. Health Aging* 17, 51–53. doi: 10.1007/s12603-013-0002-2

Guan, J., and Gluckman, P. D. (2009). IGF-1 derived small neuropeptides and analogues: a novel strategy for the development of pharmaceuticals for neurological conditions. *Br. J. Pharmacol.* 157, 881–891. doi: 10.1111/j.1476-5381.2009.00256.x

Gulyás, B., Spenger, C., Beliczai, Z., Gulya, K., Kása, P., Jahan, M., et al. (2012). Distribution and binding of ^{18}F-labeled and ^{125}I-labeled analogues of ACI-80, a prospective molecular imaging biomarker of disease: a whole hemisphere post mortem autoradiography study in human brains obtained from Alzheimer's disease patients. *Neurochem. Int.* 60, 153–162. doi: 10.1016/j.neuint.2011.10.010

Haass, C., and Selkoe, D. J. (2007). Soluble protein oligomers in neurodegeneration: lessons from the Alzheimer's amyloid β-peptide. *Nat. Rev. Mol. Cell Biol.* 8, 101–112. doi: 10.1038/nrm2101

Hajipour, M. J., Santoso, M. R., Rezaee, F., Aghaverdi, H., Mahmoudi, M., and Perry, G. (2017). Advances in Alzheimer's diagnosis and therapy: the implications of nanotechnology. *Trends Biotechnol.* 35, 937–953. doi: 10.1016/j.tibtech.2017.06.002

Herrup, K. (2015). The case for rejecting the amyloid cascade hypothesis. *Nat. Neurosci.* 18, 794–799. doi: 10.1038/nn.4017

Hong, L., Koelsch, G., Lin, X., Wu, S., Terzyan, S., Ghosh, A. K., et al. (2000). Structure of the protease domain of memapsin 2 (β-secretase) complexed with inhibitor. *Science* 290, 150–153. doi: 10.1126/science.290.5489.150

Itakura, M., Nakajima, H., Kubo, T., Semi, Y., Kume, S., Higashida, S., et al. (2015). Glyceraldehyde-3-phosphate dehydrogenase aggregates accelerate amyloid-β amyloidogenesis in Alzheimer disease. *J. Biol. Chem.* 290, 26072–26087. doi: 10.1074/jbc.M115.669291

Jagota, S., and Rajadas, J. (2013). Synthesis of D-amino acid peptides and their effect on β-amyloid aggregation and toxicity in transgenic *Caenorhabditis elegans*. *Med. Chem. Res.* 22, 3991–4000. doi: 10.1007/s00044-012-0386-2

Jonsson, T., Atwal, J. K., Steinberg, S., Snaedal, J., Jonsson, P. V., Bjornsson, S., et al. (2012). A mutation in APP protects against Alzheimer's disease and age-related cognitive decline. *Nature* 488, 96–99. doi: 10.1038/nature11283

Kang, C. K., Jayasinha, V., and Martin, P. T. (2003). Identification of peptides that specifically bind $A\beta_{1-40}$ amyloid *in vitro* and amyloid plaques in Alzheimer's disease brain using phage display. *Neurobiol. Dis.* 14, 146–156. doi: 10.1016/s0969-9961(03)00105-0

Karasawa, T., and Lombroso, P. J. (2014). Disruption of striatal-enriched protein tyrosine phosphatase (STEP) function in neuropsychiatric disorders. *Neurosci. Res.* 89, 1–9. doi: 10.1016/j.neures.2014.08.018

Kellock, J., Hopping, G., Caughey, B., and Daggett, V. (2016). Peptides composed of alternating L- and D-amino acids inhibit amyloidogenesis in three distinct amyloid systems independent of sequence. *J. Mol. Biol.* 428, 2317–2328. doi: 10.1016/j.jmb.2016.03.013

Ladner, R. C., Sato, A. K., Gorzelany, J., and de Souza, M. (2004). Phage display-derived peptides as therapeutic alternatives to antibodies. *Drug Discov. Today* 9, 525–529. doi: 10.1016/s1359-6446(04)03104-6

Larbanoix, L., Burtea, C., Laurent, S., Van Leuven, F., Toubeau, G., Vander Elst, L., et al. (2010). Potential amyloid plaque-specific peptides for the diagnosis of Alzheimer's disease. *Neurobiol. Aging* 31, 1679–1689. doi: 10.1016/j.neurobiolaging.2008.09.021

Li, C.-z., Grajales, S., Shuang, S., Dong, C., and Nair, M. (2017). β-amyloid biomarker detection for Alzheimer's disease. *Zhonghua Yi Xue Za Zhi* 1:15. doi: 10.1007/s41664-017-0014-8

Lin, L. X., Bo, X. Y., Tan, Y. Z., Sun, F. X., Song, M., Zhao, J., et al. (2014). Feasibility of β-sheet breaker peptide-H102 treatment for Alzheimer's disease based on β-amyloid hypothesis. *PLoS One* 9:e112052. doi: 10.1371/journal.pone.0112052

Liu, J., Wang, W., Zhang, Q., Zhang, S., and Yuan, Z. (2014). Study on the efficiency and interaction mechanism of a decapeptide inhibitor of β-amyloid aggregation. *Biomacromolecules* 15, 931–939. doi: 10.1021/bm401795e

Lombroso, P. J., Murdoch, G., and Lerner, M. (1991). Molecular characterization of a protein-tyrosine-phosphatase enriched in striatum. *Proc. Natl. Acad. Sci. U S A* 88, 7242–7246. doi: 10.1073/pnas.88.16.7242

Lowinus, T., Bose, T., Busse, S., Busse, M., Reinhold, D., Schraven, B., et al. (2016). Immunomodulation by memantine in therapy of Alzheimer's disease is mediated through inhibition of Kv1.3 channels and T cell responsiveness. *Oncotarget* 7, 53797–53807. doi: 10.18632/oncotarget.10777

Mandal, S. M., Roy, A., Ghosh, A. K., Hazra, T. K., Basak, A., and Franco, O. L. (2014). Challenges and future prospects of antibiotic therapy: from peptides to phages utilization. *Front. Pharmacol.* 5:105. doi: 10.3389/fphar.2014.00105

Nakajima, H., Amano, W., Fujita, A., Fukuhara, A., Azuma, Y. T., Hata, F., et al. (2007). The active site cysteine of the proapoptotic protein glyceraldehyde-3-phosphate dehydrogenase is essential in oxidative stress-induced aggregation and cell death. *J. Biol. Chem.* 282, 26562–26574. doi: 10.1074/jbc.M704199200

Nakajima, H., Amano, W., Kubo, T., Fukuhara, A., Ihara, H., Azuma, Y. T., et al. (2009). Glyceraldehyde-3-phosphate dehydrogenase aggregate formation participates in oxidative stress-induced cell death. *J. Biol. Chem.* 284, 34331–34341. doi: 10.1074/jbc.M109.027698

Norton, R. S., and Chandy, K. G. (2017). Venom-derived peptide inhibitors of voltage-gated potassium channels. *Neuropharmacology* 127, 124–138. doi: 10.1016/j.neuropharm.2017.07.002

Pelkey, K. A., Askalan, R., Paul, S., Kalia, L. V., Nguyen, T. H., Pitcher, G. M., et al. (2002). Tyrosine phosphatase STEP is a tonic brake on induction of long-term potentiation. *Neuron* 34, 127–138. doi: 10.1016/s0896-6273(02)00633-5

Pickart, L., Vasquez-Soltero, J. M., and Margolina, A. (2015). GHK peptide as a natural modulator of multiple cellular pathways in skin regeneration. *Biomed. Res. Int.* 2015:648108. doi: 10.1155/2015/648108

Rangachari, V., Davey, Z. S., Healy, B., Moore, B. D., Sonoda, L. K., Cusack, B., et al. (2009). Rationally designed dehydroalanine ($^{\Delta}$Ala)-containing peptides inhibit amyloid-β (Aβ) peptide aggregation. *Biopolymers* 91, 456–465. doi: 10.1002/bip.21151

Rangaraju, S., Gearing, M., Jin, L. W., and Levey, A. (2015). Potassium channel Kv1.3 is highly expressed by microglia in human Alzheimer's disease. *J. Alzheimers Dis.* 44, 797–808. doi: 10.3233/JAD-141704

Sara, V. R., Carlsson-Skwirut, C., Bergman, T., Jornvall, H., Roberts, P. J., Crawford, M., et al. (1989). Identification of Gly-Pro-Glu (GPE), the aminoterminal tripeptide of insulin-like growth factor 1 which is truncated in brain, as a novel neuroactive peptide. *Biochem. Biophys. Res. Commun.* 165, 766–771. doi: 10.1016/s0006-291x(89)80032-4

Shankar, G. M., Li, S., Mehta, T. H., Garcia-Munoz, A., Shepardson, N. E., Smith, I., et al. (2008). Amyloid-β protein dimers isolated directly from Alzheimer's brains impair synaptic plasticity and memory. *Nat. Med.* 14, 837–842. doi: 10.1038/nm1782

Silverman, W., Wisniewski, H. M., Bobinski, M., and Wegiel, J. (1997). Frequency of stages of Alzheimer-related lesions in different age categories. *Neurobiol. Aging* 18, 377–379; discussion 389–392. doi: 10.1016/s0197-4580(97)00051-1

Sunaga, K., Takahashi, H., Chuang, D. M., and Ishitani, R. (1995). Glyceraldehyde-3-phosphate dehydrogenase is over-expressed during apoptotic death of neuronal cultures and is recognized by a monoclonal antibody against amyloid plaques from Alzheimer's brain. *Neurosci. Lett.* 200, 133–136. doi: 10.1016/0304-3940(95)12098-o

Thal, D. R., Rub, U., Orantes, M., and Braak, H. (2002). Phases of A β-deposition in the human brain and its relevance for the development of AD. *Neurology* 58, 1791–1800. doi: 10.1212/WNL.58.12.1791

Turner, R. T. III., Hong, L., Koelsch, G., Ghosh, A. K., and Tang, J. (2005). Structural locations and functional roles of new subsites S5, S6, and S7 in memapsin 2 (β-secretase). *Biochemistry* 44, 105–112. doi: 10.1021/bi048106k

van Groen, T., Kadish, I., Wiesehan, K., Funke, S. A., and Willbold, D. (2009). *In vitro* and *in vivo* staining characteristics of small, fluorescent, Aβ42-binding D-enantiomeric peptides in transgenic AD mouse models. *ChemMedChem* 4, 276–282. doi: 10.1002/cmdc.200800289

VanItallie, T. B. (2015). Biomarkers, ketone bodies and the prevention of Alzheimer's disease. *Metabolism* 64, S51–S57. doi: 10.1016/j.metabol.2014.10.033

Vassar, R. (2002). β-secretase (BACE) as a drug target for Alzheimer's disease. *Adv. Drug Deliv. Rev.* 54, 1589–1602. doi: 10.1016/S0169-409X(02)00157-6

Vlieghe, P., Lisowski, V., Martinez, J., and Khrestchatisky, M. (2010). Synthetic therapeutic peptides: science and market. *Drug Discov. Today* 15, 40–56. doi: 10.1016/j.drudis.2009.10.009

Wasmer, C., Lange, A., Van Melckebeke, H., Siemer, A. B., Riek, R., and Meier, B. H. (2008). Amyloid fibrils of the HET-s(218–289) prion form a β solenoid with a triangular hydrophobic core. *Science* 319, 1523–1526. doi: 10.1126/science.1151839

Wei, C. W., Peng, Y., Zhang, L., Huang, Q., Cheng, M., Liu, Y. N., et al. (2011). Synthesis and evaluation of ferrocenoyl pentapeptide (Fc-KLVFF) as an inhibitor of Alzheimer's $A\beta_{1-42}$ fibril formation *in vitro*. *Bioorg. Med. Chem. Lett.* 21, 5818–5821. doi: 10.1016/j.bmcl.2011.07.111

Yan, R., Fan, Q., Zhou, J., and Vassar, R. (2016). Inhibiting BACE1 to reverse synaptic dysfunctions in Alzheimer's disease. *Neurosci. Biobehav. Rev.* 65, 326–340. doi: 10.1016/j.neubiorev.2016.03.025

Conflict of Interest Statement: The authors declare that the research was conducted in the absence of any commercial or financial relationships that could be construed as a potential conflict of interest.

Copyright © 2018 Baig, Ahmad, Rabbani and Choi. This is an open-access article distributed under the terms of the Creative Commons Attribution License (CC BY). The use, distribution or reproduction in other forums is permitted, provided the original author(s) and the copyright owner are credited and that the original publication in this journal is cited, in accordance with accepted academic practice. No use, distribution or reproduction is permitted which does not comply with these terms.

frontiers in Human Neuroscience

METHODS
published: 09 January 2018
doi: 10.3389/fnhum.2017.00643

A Novel Early Diagnosis System for Mild Cognitive Impairment Based on Local Region Analysis: A Pilot Study

Fatma E. A. El-Gamal[1,2], Mohammed M. Elmogy[1,2], Mohammed Ghazal[2,3], Ahmed Atwan[1], Manuel F. Casanova[4], Gregory N. Barnes[5], Robert Keynton[6], Ayman S. El-Baz[2†] and Ashraf Khalil[7†] for the Alzheimer's Disease Neuroimaging Initiative [‡]*

[1] Faculty of Computers and Information, Information Technology Department, Mansoura University, Mansoura, Egypt, [2] BioImaging Laboratory, Department of Bioengineering, University of Louisville, Louisville, KY, United States, [3] Department of Electrical and Computer Engineering, College of Engineering, Abu Dhabi University, Abu Dhabi, United Arab Emirates, [4] School of Medicine, University of South Carolina, Greenville, SC, United States, [5] University of Louisville Autism Center, Department of Neurology, University of Louisville, Louisville, KY, United States, [6] Department of Bioengineering, University of Louisville, Louisville, KY, United States, [7] Department of Computer Science and Information Technology, College of Engineering, Abu Dhabi University, Abu Dhabi, United Arab Emirates

OPEN ACCESS

Edited by:
Mohammad Amjad Kamal, King Abdulaziz University, Saudi Arabia

Reviewed by:
Chun-Hsien Hsu, Institute of Linguistics, Academia Sinica, Taiwan
Zhen Yuan, University of Macau, China

***Correspondence:**
Ayman S. El-Baz
aselba01@louisville.edu

[†] These authors have contributed equally to this work as senior authors.

[‡] Data used in preparation of this article were obtained from the Alzheimer's Disease Neuroimaging Initiative (ADNI) database (adni.loni.usc.edu). As such, the investigators within the ADNI contributed to the design and implementation of ADNI and/or provided data but did not participate in analysis or writing of this report. A complete listing of ADNI investigators can be found at: http://adni.loni.usc.edu/wp-content/uploads/how_to_apply/ADNI_Acknowledgement_List.pdf

Received: *12 July 2017*
Accepted: *18 December 2017*
Published: *09 January 2018*

Citation:
El-Gamal FEA, Elmogy MM, Ghazal M, Atwan A, Casanova MF, Barnes GN, Keynton R, El-Baz AS and Khalil A for the Alzheimer's Disease Neuroimaging Initiative (2018) A Novel Early Diagnosis System for Mild Cognitive Impairment Based on Local Region Analysis: A Pilot Study. Front. Hum. Neurosci. 11:643. doi: 10.3389/fnhum.2017.00643

Alzheimer's disease (AD) is an irreversible neurodegenerative disorder that accounts for 60–70% of cases of dementia in the elderly. An early diagnosis of AD is usually hampered for many reasons including the variable clinical and pathological features exhibited among affected individuals. This paper presents a computer-aided diagnosis (CAD) system with the primary goal of improving the accuracy, specificity, and sensitivity of diagnosis. In this system, PiB-PET scans, which were obtained from the ADNI database, underwent five essential stages. First, the scans were standardized and de-noised. Second, an Automated Anatomical Labeling (AAL) atlas was utilized to partition the brain into 116 regions or labels that served for local (region-based) diagnosis. Third, scale-invariant Laplacian of Gaussian (LoG) was used, per brain label, to detect the discriminant features. Fourth, the regions' features were analyzed using a general linear model in the form of a two-sample *t*-test. Fifth, the support vector machines (SVM) and their probabilistic variant (pSVM) were constructed to provide local, followed by global diagnosis. The system was evaluated on scans of normal control (NC) vs. mild cognitive impairment (MCI) (19 NC and 65 MCI scans). The proposed system showed superior accuracy, specificity, and sensitivity as compared to other related work.

Keywords: AD, CAD, PiB-PET, statistical analysis, personalized diagnosis

1. INTRODUCTION

Alzheimer's disease (AD) is a chronic neurodegenerative disorder marked by cognitive and behavioral impairments (Hodler et al., 2012; WHO, 2017). Statistically, 42% of AD sufferers are people over 85 years of age with the percentage decreasing to only 6% for people of 70–74 years old. Although the probability is small, younger individuals may also be affected (Brown, 2013).

AD is characterized by clinical symptoms and pathological features, both of which vary among patients (Lu and Bludau, 2011). In the clinical presentation, the patient faces progressive deficits in cognition as well as disturbances in thought, perception, and behavior. Neuropathological abnormalities include the formation of neurofibrillary tangles and neuritic plaques as well

as neuronal loss and granulovacuolar degeneration. Indeed, the quantity and location of neurofibrillary tangles and neuritic plaques represent neurodegenerative features that distinguish AD from other types of dementia. Efforts to establish an early diagnosis of AD have been thwarted by the fact that pathological features of the disease occur 10–15 years before the emergence of clinical symptoms.

Mild cognitive impairment (MCI) can lead to AD. MCI can be defined as an impairment of cognition that is more severe than expected from normal aging and a persons education with objective evidence of impairment in one or more cognitive domains including memory, executive function, attention, language, or visuospatial skills. MCI does not interfere with his/her independence and daily activities including social or occupational functioning (Yaffe, 2013). In this regard, MCI represents an intermediate stage between the cognitive decline observed with normal aging and the severe impairment observed in dementia (Anderson et al., 2012; Yaffe, 2013). It is important to note that not all MCI cases proceed to AD, although studies have found that it increases the risk of later developing AD (Anderson et al., 2012; NIH, 2017). MCI due to AD is a progressive decline in cognition over months to years. MCI due to AD has a lack of significant vascular factors, vascular imaging findings, parkinsonism, visual hallucinations, prominent behavioral, or language disorders (Langa and Levine, 2014).

There are a number of tests that have to be considered when trying to establish a diagnosis of AD. These tests include: neuropsychological screening (to measure related cognitive impairments), patients medical history, and mental/physical examination. In addition, blood tests as well as brain imaging are usually evaluated to rule out other neurological or physiological disorders (Turkington and Harris, 2001; Wegrzyn and Rudolph, 2012). In general, these tests help to classify the subjects along the disease cascade into MCI, when the appearance of some cognitive decline does not fulfill dementia criteria, and other stages of AD (Wegrzyn and Rudolph, 2012). A recent meta-analysis of neuropsychological measures suggested that verbal memory measures and other language tests yield high predictive accuracy for those MCI subjects who will progress to AD. Other domains including executive function and visual memory showed better specificity than sensitivity (Belleville et al., 2017). These data show that there is a clinical need to identify biomarkers of neural circuits involved in MCI, which ultimately lead to the development of AD.

Brain biomarkers have been postulated to help in the diagnosis of AD throughout the diseases natural history. For example, Jack et al. (2010) presented a study in which positron emission tomography (PET) amyloid imaging and cerebrospinal fluid (CSF) amyloid beta 42 (Aβ42) revealed Aβ abnormalities in the brain. These abnormalities are the earliest pathological features observed in the AD-related disease cascade. Additionally, the study reported that both the increase in CSF tau and cerebral atrophy serve as biomarkers of neuronal injury and neurodegeneration. Finally, the decrease in 2-[^{18}F]fluoro-2-deoxy-D-glucose PET (FDG-PET), as demonstrated by the study, helps in revealing the synaptic dysfunction that accompanies the neurodegeneration. Therefore, according to this study, sMRI measures abnormalities of the brain's structure, and FDG-PET/CSF-tau identifies tau-mediated neuronal injury and dysfunction. The authors concluded that PET amyloid imaging could be considered an early identifier of AD-related abnormalities.

PET is a main scanning application of the emission computed tomography (ECT) methodology. Despite the role of the PET amyloid imaging in the early diagnosis of AD, arguments for and against the implementation of this scan modality in clinics should be carefully considered. False positive diagnoses of AD may occur since normal elderly subjects can have elevated Aβ levels. Fortunately, the introduction of carbon-11 labeled Pittsburgh compound B (^{11}C PiB), a neutral analog of the thioflavin T, caused a noteworthy conversion in studies related to AD (Johnson et al., 2013). The compound assists in visualizing the pathological hallmarks related to AD and consequently helps in quantitating the neuropathological burden during subsequent AD stages (Varghese et al., 2013).

Numerous research efforts have been proposed to help in the differentiation between normal control (NC), MCI, and AD utilizing PET scans. These efforts include studies focused on testing computer-aided diagnosis (CAD) systems, such as the automatic classification system proposed by Illán et al. (2010). For this purpose, principal component analysis (PCA) and support vector machines (SVM) were utilized. To evaluate the system, the PiB and FDG related scans were used to compare their results regarding early diagnosis. Although PiB and FDG showed similar accuracies, the PiB had a higher power of discrimination in the very early cases. Again, Illán et al. (2011) utilized PET scans to construct a CAD system that relied on eigenimage framework and composed of feature extraction, dimensionality reduction, and classification stages. In this system, PCA and independent component analysis (ICA) were utilized for image projection (feature reduction), eigenimage based decomposition for feature reduction, and SVM for classification. Through these stages, the system achieved an accuracy of 88.24%. Another study by Jiang et al. (2015) demonstrated a CAD system that improved the classification accuracy of AD using the PCA, ICA, and SVM. The PCA was used for dimension reduction, ICA for feature extraction, and SVM using linear and radial basis function (RBF) kernels for classification. The results of their study showed either better or equivalent performance as compared to the competitive CAD methods with higher accuracy than the traditional visual assessment methods.

In the same context, López et al. (2011) proposed a CAD system aimed at improving the accuracy of three-way classification between NC, MCI, and AD. The study used PCA and linear discriminant analysis/Fisher discriminant ratio for the feature selection process followed by artificial neural network/SVM for the classification purpose. Testing this methodology with FDG PET scans led to a classification accuracy of 89.52%. Martínez-Murcia et al. (2012) presented a CAD system composed of three stages: Mann-Whitney-Wilcoxon *U*-Test for voxel selection in order to exclude outliers, factor analysis for feature extraction, and linear SVM for classification. Testing this system on PET scans achieved an accuracy of 92.9%. Also,

Chaves et al. (2012) exploited association rule mining in a CAD system used in the early diagnosis of AD. Testing the system using two datasets, including PET scans, showed better results as compared to other related work. Padilla et al. (2012) introduced a CAD system to serve the early diagnosis of AD by combining nonnegative matrix factorization (NMF) for feature selection and reduction, and SVM with confidence bounds for classification. Application of the system led to an accuracy of 86%.

In addition to the aforementioned studies, various researchers have used voxel analysis for the early diagnosis of AD. For example, Morbelli et al. (2012) performed voxel-wise interregional correlations through statistical parametric mapping to extract relevant information. The study's results illustrated the association between the pathophysiological process of AD and alterations of the functional brain networks. According to the study, the default mode network (DMN) and memory function-related networks are the main causes of such alterations. Kemppainen et al. (2006) compared AD vs. NC subjects to find the brain regions that showed significant increases in the uptake of ^{11}C PiB by applying voxel-based analysis. A Statistical Parametric Mapping (SPM) analysis was performed using automated region of interest (ROI). The study found that the voxel-based analysis showed widespread distribution regarding the increased ^{11}C PiB uptake. Ziolko et al. (2006) statistically evaluated the amyloid imaging agents' (i.e., PiB) retention differences throughout the brain. In addition, they compared the PiB results with the FDG-based scans of glucose metabolism. The results revealed that the statistical significance of the PiB analysis was both greater than others and had a larger spatial extent. The results also showed that the PiB significance was retained after corrections of family-wise error and false discovery rate.

Forsberg et al. (2008) studied the amyloid deposition in patients with MCI. They used ^{11}C PiB and FDG based PET scans with AD, which were compared with NC scans. The analysis showed an intermediate retention of the mean cortical PiB in the MCI as compared to NC and AD. Also, the study found significantly higher PiB retention in the MCI conversion to AD group, comparable to that of AD patients ($p > 0.01$) and much less in MCI subjects who did not convert to AD. Shin et al. (2010) presented a voxel-based analysis relying on the FDG, PiB along with another tracer known as 2-(1-6-[(2-(^{18}F)fluoroethyl) (methyl) amino]-2-naphthylethylidene) malononitrile (FDDNP). These tracers were utilized to address the pathological hallmarks of AD, beta amyloid plaques, potential neurofibrillary tangles, and glucose metabolism related impairments. The experimental results demonstrated the available capacity to develop and test disease-modifying drugs targeting both tau and amyloid pathology, and/or energy metabolism when using the same subject based PET imaging with these three tracers.

Despite the achievements of the aforementioned investigations, the studies only supported a global diagnosis that indicate whether or not the subject belongs to a certain studied group. The main objectives of this paper are summarized in the following points. First, it provides a personalized diagnosis to help individualize diagnostic options as well as monitoring the disease progression. Second, it improves the final global diagnosis results as compared with previously published studies. To achieve these goals, our system utilized PiB PET scans due to the superior role of this brain imaging modality, as compared to other scanning modalities, when applied to the early diagnosis of the disease. Therefore, the paper is organized as follows. Section 2 (vide infra) starts by describing the materials used for the preparation of the paper and defines the methods used in the proposed CAD system. In section 3, different experimental results are presented to evaluate the performance as well as the efficiency of our system. Finally, the discussion of the applied tests and the future work are highlighted in section 4.

2. MATERIALS AND METHODS

2.1. Materials

A set of ^{11}C PiB-PET scans were used to validate the proposed framework. These scans were collected from the Alzheimer's Disease Neuroimaging Initiative (ADNI) database (adni.loni.usc.edu). The database of ADNI was initially launched in 2003 as a public-private partnership, led by principal investigator Michael Weiner, MD. The goal of demonstrating ADNI was to test whether serial MRI, PET, or other markers, in addition to clinical and neuropsychological assessment, can measure the progression of MCI and AD by combining them. For further advance information, please see www.adni-info.org. The used dataset was obtained from ADNI 1 where it contains a total number of 84 scans obtained from 19 NC and 65 MCI subjects. NC comprises those subjects who do not show any signs of depression, cognitive impairment, or dementia. The MCI group, in general, comprises those subjects with subjective memory concerns, whether self-reported or through an informant or a clinician. Those subjects display neither significant impairment levels in other cognitive domains nor signs of dementia. The Logical Memory II subtest of the Wechsler Memory Scale (WMS) was performed on the participants to document the normality/abnormality of their memory function with respect to their level of education. The demography of the used dataset is presented in **Table 1**.

2.2. Methods

The main aim of this article is to present local (i.e., region) based diagnosis of the MCI regarding AD, to assist clinicians in the personalized treatment of the disease. To achieve this goal, five main steps were performed, as illustrated in **Figure 1**. First, the scans were preprocessed through data standardization and de-noising. Data standardization aimed to prepare the scans for the labeling step, while the de-noising process aimed to improve the scan's quality and consequently the systems accuracy. Second, the atlas of Automated Anatomical Labeling (AAL) was used for brain parcellation to serve the local diagnosis goal. After labeling the brain, we used a Laplacian of Gaussian (LoG) with the automatic scale to extract the discriminant features from the scans. Then, a statistical analysis was performed to determine the significant brain regions to analyze rather than using all the labeled regions in the decision-making process. Finally, these regions were used to construct two decision-making levels using a probabilistic version of SVM (pSVM) and standard SVM to

TABLE 1 | The demographic data of the NC and MCI groups of the ^{11}C PiB-PET scans.

(*N* = 84)	Average Age ± SD	Gender N (%)		WMS logical memory II results (based on years of education)		
		Male	Female	≥16 years	8–15 years	0–7 years
NC (19)	78.3 ± 5.01	11 (57.89)	8 (42.1)	≥ 9	≥ 5	≥ 3
MCI (65)	75.78 ± 7.67	44 (67.69)	21 (32.30)	≥ 8	≥ 4	≥ 2

provide local followed by global diagnosis. The details of the proposed system are presented in the following subsections.

2.2.1. Preprocessing

Scans underwent some preprocessing to orient the data and reduce noise. For orienting the data in a standard coordinate system, the SPM MATLAB toolbox (NeuroImaging, 2017) was used to perform re-orientation, co-registration, spatial normalization, and re-slicing. Noise reduction was accomplished through wavelet shrinkage. Details are as follows: PET scans' associated sMRI data were re-oriented so that the anterior-posterior axis coincides with the AC-PC line. This differs from the ADNI pipeline, which only ensures the axis is parallel to the AC-PC line. The associated PiB-PET scan was re-oriented to the resulting sMRI scan to produce a re-orientation matrix that was then used to re-orient the remaining PiB-PET scans. Precise co-registration between the PET scans and the previously used sMRI scan was performed using rigid body transformations (translations and rotations) to maximize the mutual information. Then, the spatial normalization and re-slicing were applied to the sMRI and PET scans to align the scans to the MNI-152 standard space. In this step, general affine transformation (translations, rotations, non-uniform scaling, and shears) was used, followed by nonlinear deformations. After data standardization, wavelet based de-noising was applied using the symlet8 mother wavelet with Steins unbiased risk estimate as a threshold selection rule and soft thresholding (Bagci and Mollura, 2013). The aim was to retain image detail while removing artifacts of image acquisition and/or transmission (Agrawal and Bahendwar, 2011). At this point, the scans were ready for voxel-wise comparison and labeling steps.

2.2.2. Brain Labeling

Due to the local diagnosis based goal of the proposed system, the brain labeling/partitioning needs to be performed. Through this aim, a detailed diagnosis of the subjects could be achieved. For this purpose, any of the detailed based brain atlases can be used, such as AAL, Talairach Daemon, and Brodmann areas atlases (Su et al., 2014; Zhang et al., 2015; Salas-Gonzalez et al., 2016). In this paper, the AAL atlas was used to label each of the preprocessed scans voxel's positions to the matched anatomical regions. The AAL atlas provides a total of 116 brain regions: 45 per cerebral hemisphere, 9 per cerebellar hemisphere, and 8 in the vermis of the cerebellum. AAL provides a detailed parcellation of the brain and is recommended for use with PET scans. To accomplish the labeling procedure, the xjView MATLAB toolbox (Alivelearn.net, 2017) was utilized.

2.2.3. Blob Detection Based Feature Extraction

Each of the labeled regions is individually fed to the scale-invariant blob detector, which employs LoG with automatic scale selection, for the purpose of feature extraction. Blob detection aims to separate structures (i.e., blobs) from the image background. Each blob is itself a radially symmetric distribution of image intensity about a local minimum or maximum (Toennies, 2012). Blobs corresponding to local maxima could reveal the targeted abnormalities, given that significantly greater retention of PiB in a brain region is linked with greater incidence of Aβ plaques within that region (Shin et al., 2010). **Figure 2** shows a sample of the extracted features with a 3 Dimensional (3D) smoothed histogram showing the local maxima locations that are targeted through the detector.

2.2.4. Statistical Analysis

AAL regions where mean PiB uptake differs significantly in MCI with respect to NC was determined using two-sample *t*-tests. Each atlas region was tested independently. The Bonferroni method was applied to identify a region as "significant" when the *p*-value was less than 0.00043 (i.e., 0.05/116). Significant regions were subsequently used in building a classifier.

2.2.5. Diagnosis

A two-level diagnosis was performed to make local (region-specific abnormalities) and global (level of cognitive impairment) diagnoses. For this purpose, SVM and one of its variant (pSVM) were utilized. Standard SVM is an abstract machine learning technique where the training data are used for the learning followed by a generalization attempt for correct prediction on other novel data (Campbell and Ying, 2011). In SVM, a hyperplane (known as maximal margin hyperplane) is used for the binary separation of the labeled training data. The goal is to build a decision function $f : R^S \rightarrow \pm 1$, according to S-dimensional training patterns p_i and t_i, capable to perform classification for new example (p, t): $(p_1, t_1), (p_2, t_2), ..., (p_s, t_s) \in R^S \pm 1$. The decision hyperplanes in multidimensional feature space can be defined through either using a linear separation of the training data, using linear discriminant functions, or combining SVM with kernel techniques that produce a non-linear decision boundary (hyperplane) in the input space (Illán et al., 2011). Beside its classification power, a variation of SVM, which produces a posterior probability output of the classifier (pSVM), is useful to allow further post processes.

In the proposed system, a separate pSVM model was constructed, in the first diagnosis level, for each significant region. Each pSVM produces a probabilistic result for the

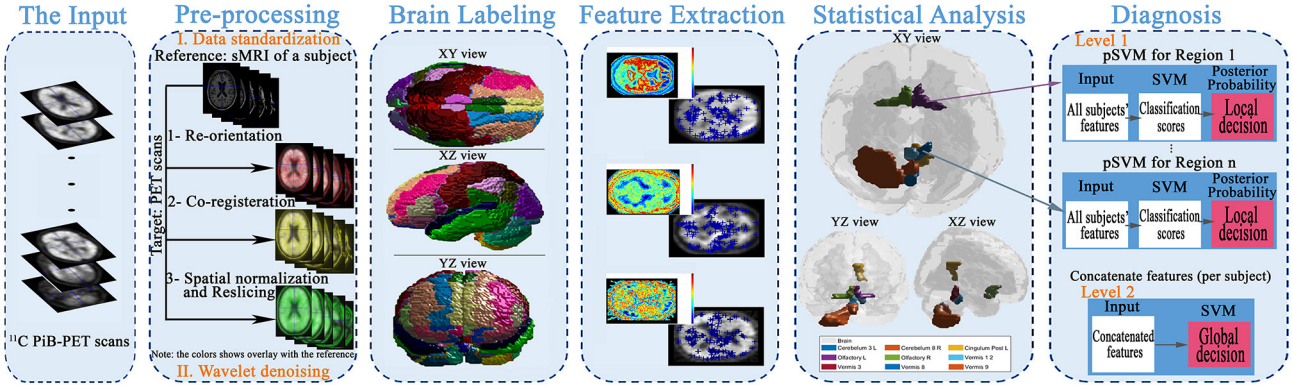


FIGURE 1 | The framework of the proposed early diagnosis system for AD based on local and global region analysis using ^{11}C PiB PET scans.

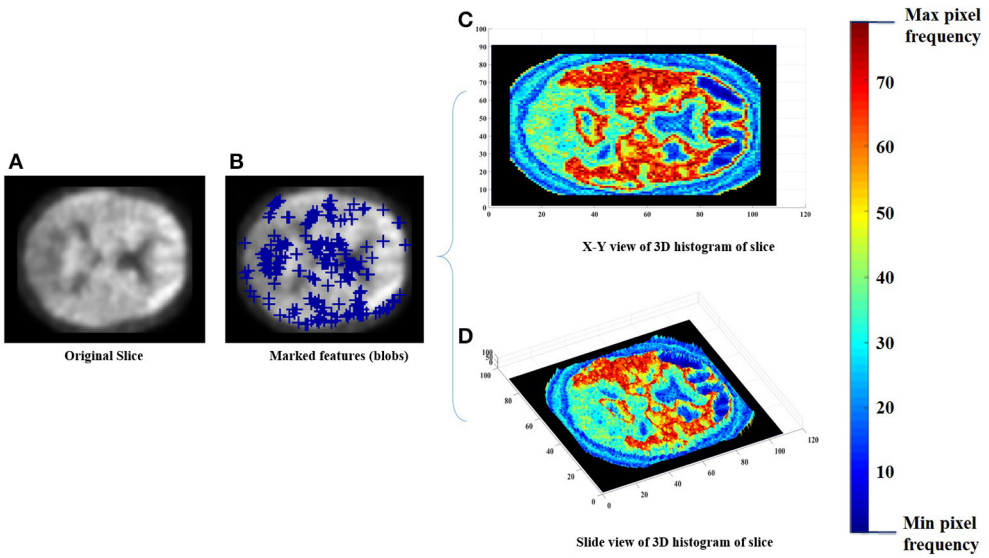


FIGURE 2 | An example of the feature extraction step, **(A)** the original slice, **(B)** the obtained features (blue pluses), **(C,D)** a 3D histogram representation of the slice to indicate the targeted local maxima/minima locations.

incidence of MCI given the features from its brain region independently of all others. In the second level, the scores obtained from the first level were fused with respect to each subject and used to train and test a single SVM model to produce the global diagnosis. Classifier performance, i.e., accuracy, sensitivity, and specificity, were estimated using both leave-one-subject-out (LOSO) and K-fold cross-validation, with two- and four-fold.

3. RESULTS

According to the Bonferroni corrected two-sample *t*-tests, the AAL brain regions of significance, nine regions, were Cerebelum_3_L (left alar central lobule), Cerebelum_8_R (right biventer lobule), Cingulum_Post_L (left posterior cingulate gyrus), Olfactory_L and Olfactory_R (bilateral olfactory cortex), plus Vermis_1_2, Vermis_3, Vermis_8, and Vermis_9 (lobules I, II, III, VIII, and IX of the vermis) as visualized in **Figure 3**. The performance of the resulting classifier was evaluated under a number of different kernels selected for the SVM, with best results being obtained when the linear kernel was used at both level 1 and level 2 (**Table 2**). This classifier was used to compare three cases, using data from all brain regions, using all regions except the significant ones, and using pre-selected, specific regions. The third case found to outperform the other two cases (**Table 3**).

The efficiency of the proposed system was compared to two other published methods (Chaves et al., 2012; Jiang et al., 2015). Our methodology was found to distinguish MCI from NC as well or better than either previous techniques (**Table 4**). Note that performance of the compared classifiers is taken directly from the respective publications since each of them used the same database (i.e., ^{11}PiB PET scans from ADNI), and LOSO cross-validation. Finally, **Figures 4**, **5** provide examples of the



FIGURE 3 | The significant regions as obtained through the two sample *t*-test.

TABLE 2 | Evaluation of SVM classifier performance when different kernels are used.

			Level 2								
			LOSO			K-fold					
						$K = 2$			$K = 4$		
			RBF	Linear	Polynomial	RBF	Linear	Polynomial	RBF	Linear	Polynomial
Level 1	RBF	ACC	72.61	50	22.61	59.52	22.61	77.38	77.38	22.61	77.38
		Spec.	26.31	57.89	100	57.89	100	0	0	100	0
		Sens.	86.15	47.69	0	60	0	100	100	0	100
	Linear	ACC	77.38	**88.09**	95.23	77.38	**79.76**	77.38	77.38	**89.28**	77.38
		Spec.	0	**47.36**	78.94	0	**10.52**	0	0	**52.63**	0
		Sens.	100	**100**	100	100	**100**	100	100	**100**	100
	Polynomial	ACC	77.38	88.09	77.38	77.38	80.95	76.19	77.38	88.09	77.38
		Spec.	0	47.36	0	0	26.31	0	0	47.36	0
		Sens.	100	100	100	100	96.92	98.46	100	100	100

Classifier accuracy (ACC), sensitivity (Sens.) and specificity (Spec.), respectively in %, were estimated over all the labeled regions using LOSO and K-fold cross-validation. The bolded results (linear-pSVM linear-SVM) indicates the best combination of kernels used in the two levels.

local diagnostic results (i.e., the results of the first diagnosis level). **Figure 4** illustrates the local diagnosis of two NC and two MCI cases. While **Figure 5** shows examples of five different MCI subjects. The color bar in both figures represent the degree of abnormality starting from 0 (unaffected) to 1 (indicative of MCI). These examples indicate the varying abnormality effects in each significant region for each case independently. The implementation of the proposed CAD system can be found in the Supplementary Material.

4. DISCUSSION

This paper discusses a personalized MCI diagnosis system while improving the diagnostic performance as compared to other available methods. The personalized diagnosis is achieved through regional/local measurements, using the AAL atlas, which reflects how the disease affects different brain regions. To enhance this procedure, a statistical analysis was initially performed to determine the salient brain regions and consequently analyze the influence of the disease on them through the first diagnosis level, as shown in **Figures 4**, **5**. Apart from being the first stage of the MCI diagnosis procedure, the reported local diagnoses are helpful assistance in the personalized management of the disease. This has been represented through the color bar that shows the degree of abnormality from 0 (unaffected) to 1 (indicative of MCI) in each one of the nine significant regions separately. Finally, the system fuses the regional based probabilistic results obtained from the first diagnosis level to produce the final global diagnosis of each subject.

Regarding the cerebellar regions identified as significant, there have been several studies that focused on cerebellar abnormalities in dementia. Some of these studies were neuropathological-based studies that found that the neuronal shrinkage and loss represent well-known changes that accompany AD (Baldaçara et al., 2011). Morphological studies have targeted the prominent neuropathological AD-related hallmarks, like amyloid plaques (Cole et al., 1993; Wang et al., 2002). According to Wang et al. (2002), most AD-based pathological features that are found in the cerebellum include diffuse Aβ deposits. Considering the later finding and since the regions with increased Aβ plaques are represented as the high retention in the PiB, we could justify this finding in the early stage of AD. In addition to these findings

TABLE 3 | Using LOSO and K-fold cross-validation methods to evaluate the classification results, in %, (using linear-pSVM linear-SVMs) using the features of different cases of input regions: all the labeled regions, all the regions except the significant ones, and the significant regions only.

		LOSO	K-fold	
			$K = 2$	$K = 4$
All labeled regions	ACC	88.09	79.76	89.28
	Spec.	47.36	10.52	52.63
	Sens.	100	100	100
The resulting significant regions	ACC	100	97.61	98.80
	Spec.	100	94.73	94.73
	Sens.	100	98.46	100
Excluding the significant regions	ACC	82.14	77.38	83.33
	Spec.	21.05	0	26.31
	Sens.	100	100	100

TABLE 4 | The comparison of the proposed system's performance results, in %, against other related studies using LOSO cross-validation method.

	ACC	Spec.	Sens.
Chaves et al., 2012	90.48	100	87.69
Jiang et al., 2015	89.17	–	–
The proposed system	100	100	100

and according to Sjöbeck and Englund (2001), structural based changes, mainly involved in the vermis, were judged to represent the progression of the disease.

Dysfunction in the olfactory cortex was found, through some studies, to probably be one of the earliest symptoms that are clinically obtained regarding AD (Serby et al., 1991; Devanand et al., 2000). According to Velayudhan (2015), the combination of the olfactory function tests along with the conventional diagnostic methods provides the ability to improve the sensitivity as well as the specificity of diagnosing AD. This consequently facilitates both the early recognition and diagnosis of AD. More details about the research progress and the future directions of the olfactory dysfunction in AD could be found in Zou et al. (2016).

Finally, as regards the posterior cingulate gyrus, some neuroimaging studies, which targeted several cortical regions, have identified that the posterior cingulate regions of the medial parietal cortex are among the earliest regions affected in AD (Scheff et al., 2015). These studies include one that supports the involvement of the posterior cingulate in the very early progression of AD (Rami et al., 2012).

In general, as shown in **Table 2**, the linear kernel shows best results either using it on both levels of the classifier or along with the polynomial kernel, while the RBF kernel performed poorly even when used conjointly with another kernel. The ability of the extracted features to differentiate the two groups (NC and MCI) and consequently make them linearly separate could justify the highest results of the linear kernel. For the polynomial as well as the RBF kernels, nonlinear kernels, the obtained separable features in addition to the small size of the dataset caused the outperformance of the polynomial kernel as compared to the RBF kernel that can show better results with large size of the dataset. According to these results and since linear-linear SVM-based classifiers show in general the best results, they were used to build the CAD system.

As expected, the significant region-based diagnostic performance outperforms that of the other two trial classifiers (**Table 3**) with a maximum performance of 100% of accuracy, specificity, and sensitivity. This finding could be due to the discrimination power of the features extractor in addition to the demonstration of alpha that helped in obtaining these salient regions. Regarding the two other tests, using all the labels shows better results than excluding the significant regions but worse than using the significant regions. This finding could be due to the presence of the labeled regions that are not significant enough to differentiate between the groups and consequently led to misclassification results that could finally affect the overall performance of the system. In addition, this is the same case when excluding the significant regions, but in addition to the presence of these not well significant regions, the significant regions are excluded causing this drop of performance results as compared with the other two tested cases.

The fact that our system improved performance with respect to other techniques while using the same dataset is of crucial consideration. The superior results of the proposed system over prior work (**Table 4**) could be justified through the capabilities of the combined components of the system that could extract the most discriminant features, identify the significant brains regions and then perform the classification using the SVM along with the linear kernel.

Since the primary goal of the paper was to provide local diagnosis, **Figures 4**, **5** illustrated various examples that demonstrate the variability of the abnormality in each of the salient regions among the subjects. **Figure 4** showed sample cases of NC and MCI groups proving this point where the color bar indicates the degree of the diseases effect starting with the dark blue, no effect, to the dark red, total effect. **Figure 5** shows additional illustration source of the local diagnosis. The figure includes five different MCI subjects where the abnormalities' degree differ from one subject to another. Both figures demonstrate the power of the proposed system to reveal the local diagnosis of the disease on the significant brain regions. The analysis results that could be derived from the figures show the ability of the proposed analysis to reflect the current degree of the dysfunctionality that each region achieved through the disease. This visualization consequently can be considered an effective assistant for the individualized/personalized diagnosis process.

According to the above results, the proposed system may be of assistance in the diagnosis of MCI. In other words, the system offers a personalized diagnosis of the subjects in a short computation time using a subset of the brain's regions rather than using all regions. Additionally, the system provides high global diagnosis results compared to other related studies. Due

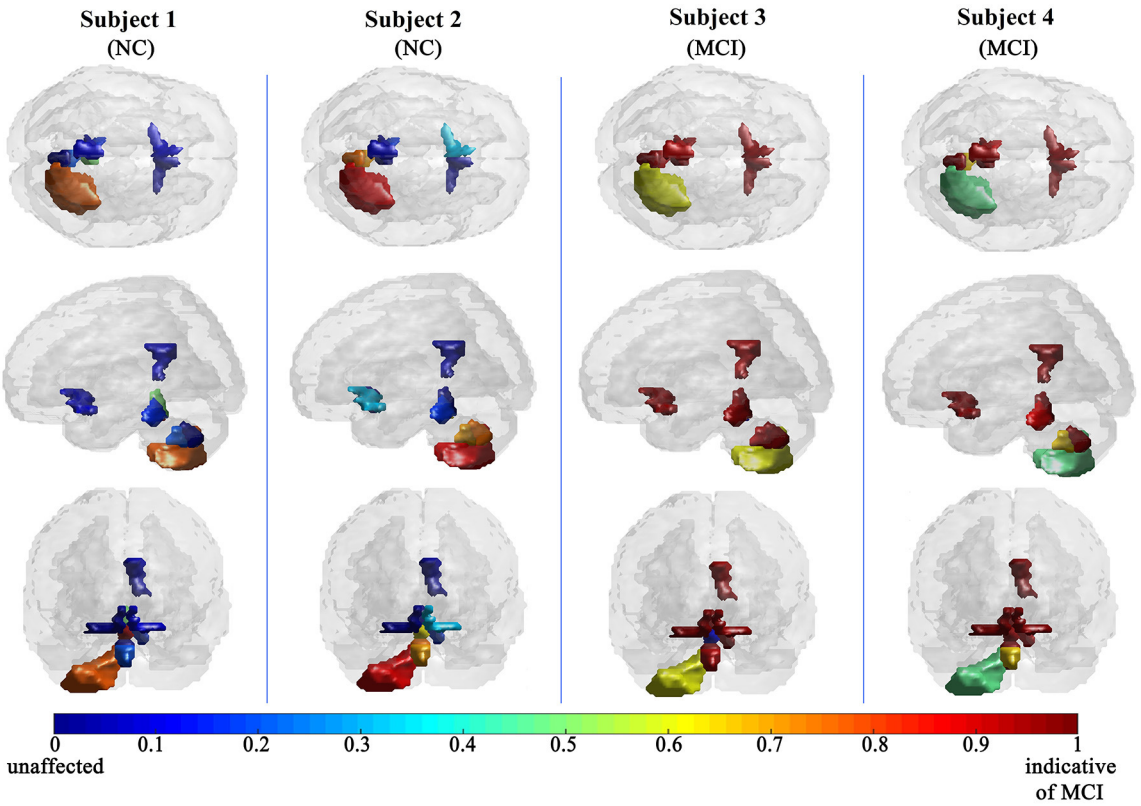


FIGURE 4 | Examples of local diagnosis results for NC vs. MCI classification problem.

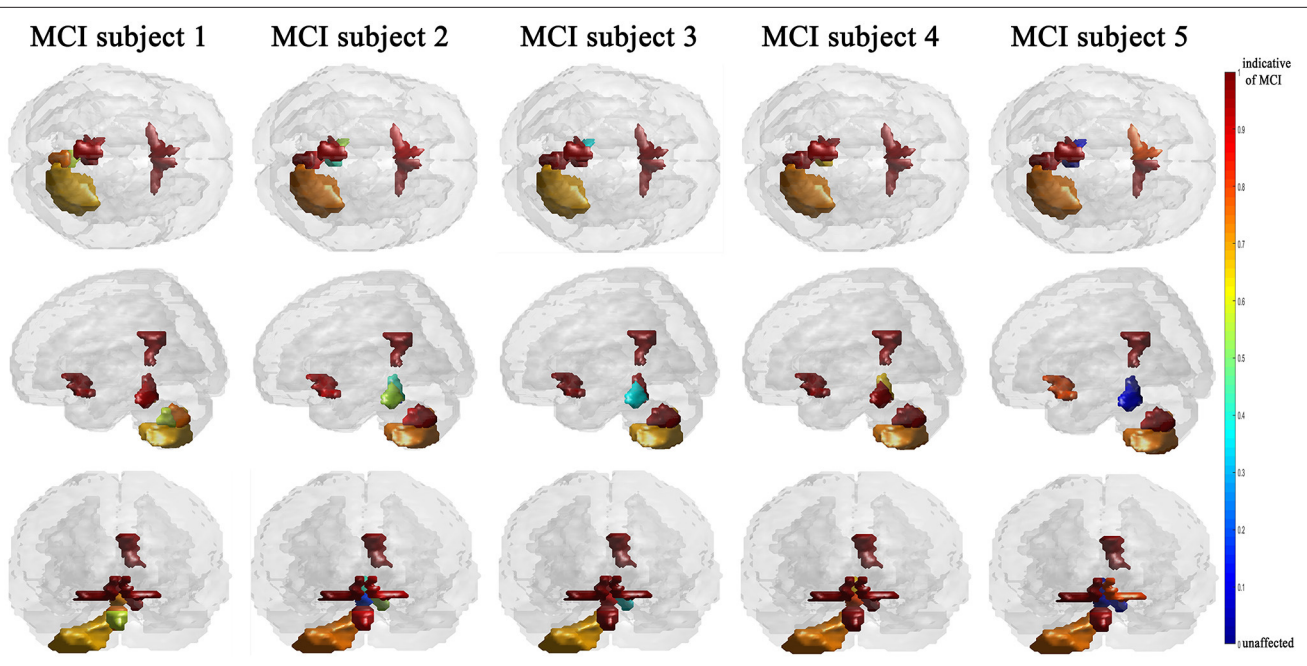


FIGURE 5 | Examples of local diagnosis results of different MCI subjects.

to the promising results of the proposed system and pilot nature of our data, we plan to examine two goals in the future work. First, the system's performance will be evaluated on larger PET scan datasets. Second, the results will be incorporated with other AD-related scanning modalities, to provide more analysis based assistance for the early diagnosis of AD.

AUTHOR CONTRIBUTIONS

FE-G: writing the manuscript and conducting the experiments. ME: advising, designing the experiments, developing the algorithm, and reviewing the entire paper. MG, RK, and AK: advising and financial support. AA: advising and reviewing the entire paper. MC: emphasizing the clinical aspect of the paper and reviewing the entire paper. GB: advising, reviewing the clinical aspect of the paper, reshaping the paper, and extensively editing it. AE-B: advising, designed the experiments, developing the algorithm, and reviewing the entire paper.

ACKNOWLEDGMENTS

The fund of the collected and shared data of this article was done by Alzheimer's Disease Neuroimaging Initiative (ADNI) (National Institutes of Health Grant U01 AG024904) and DOD ADNI (Department of Defense award number W81XWH-12-2-0012). ADNI is funded by the National Institute on Aging, the National Institute of Biomedical Imaging and Bioengineering, and through generous contributions from the following: AbbVie, Alzheimer's Association; Alzheimer's Drug Discovery Foundation; Araclon Biotech; BioClinica, Inc.; Biogen; Bristol-Myers Squibb Company; CereSpir, Inc.; Cogstate; Eisai Inc.; Elan Pharmaceuticals, Inc.; Eli Lilly and Company; EuroImmun; F. Hoffmann-La Roche Ltd and its affiliated company Genentech, Inc.; Fujirebio; GE Healthcare; IXICO Ltd.; Janssen Alzheimer Immunotherapy Research & Development, LLC.; Johnson & Johnson Pharmaceutical Research & Development LLC.; Lumosity; Lundbeck; Merck & Co., Inc.; Meso Scale Diagnostics, LLC.; NeuroRx Research; Neurotrack Technologies; Novartis Pharmaceuticals Corporation; Pfizer Inc.; Piramal Imaging; Servier; Takeda Pharmaceutical Company; and Transition Therapeutics. The Canadian Institutes of Health Research is providing funds to support ADNI clinical sites in Canada. Private sector contributions are facilitated by the Foundation for the National Institutes of Health (www.fnih.org). The grantee organization is the Northern California Institute for Research and Education, and the study is coordinated by the Alzheimer's Therapeutic Research Institute at the University of Southern California. ADNI data are disseminated by the Laboratory for Neuro Imaging at the University of Southern California.

The first author FE-G appreciates the financial support from the Cultural Affairs & Mission Sector, Ministry of Higher Education (MOHE), Egypt.

SUPPLEMENTARY MATERIAL

The Supplementary Material for this article can be found online at: https://www.frontiersin.org/articles/10.3389/fnhum.2017.00643/full#supplementary-material

REFERENCES

Agrawal, S., and Bahendwar, Y. (2011). Denoising of MRI images using thresholding techniques through wavelet transform. *Int. J. Comput. Appl. Eng. Sci.* 1, 361–364.

Alivelearn.net (2017). *xjview | A Viewing Program for SPM*. Available online at: http://www.alivelearn.net/xjview/

Anderson, N., Murphy, K., and Troyer, A. (2012). *Living with Mild Cognitive Impairment: A Guide to Maximizing Brain Health and Reducing Risk of Dementia*. New York, NY: Oxford University Press.

Bagci, U., and Mollura, D. J. (2013). Denoising PET images using singular value thresholding and stein's unbiased risk estimate. *Int. Conf. Med. Image Comput. Comput. Assist. Interv.* 6(Pt 3), 115–122. doi: 10.1007/978-3-642-40760-4_15

Baldaçara, L., Borgio, J. G., Moraes, W. A., Lacerda, A. L., Montano, M. B., Tufik, S., et al. (2011). Cerebellar volume in patients with dementia. *Rev. Bras. Psiquiatr.* 33, 122–129. doi: 10.1590/S1516-44462011000200006

Belleville, S., Fouquet, C., Hudon, C., Zomahoun, H. T. V., Croteau, J., and Consortium for the Early Identification of Alzheimer's disease-Quebec. (2017). Neuropsychological measures that predict progression from mild cognitive impairment to Alzheimer's type dementia in older adults: a systematic review and meta-analysis. *Neuropsychol. Rev.* 27, 328–353. doi: 10.1007/s11065-017-9361-5

Brown, D. (2013). *Brain Diseases and Metalloproteins*. Singapore: Pan Stanford.

Campbell, C., and Ying, Y. (2011). *Learning with Support Vector Machines. Synthesis Lectures on Artificial Intelligence and Machine Learning.* Corvallis, OR: Morgan & Claypool.

Chaves, R., Ramirez, J., Górriz, J., Illán, I., and Salas-Gonzalez, D. (2012). "FDG and PIB biomarker PET analysis for the Alzheimer's disease detection using association rules," in *Nuclear Science Symposium and Medical Imaging Conference (NSS/MIC), 2012 IEEE* (Anaheim, CA), 2576–2579.

Cole, G., Neal, J. W., Singhrao, S. K., Jasani, B., and Newman, G. R. (1993). The distribution of amyloid plaques in the cerebellum and brain stem in down's syndrome and Alzheimer's disease: a light microscopical analysis. *Acta Neuropathol.* 85, 542–552.

Devanand, D., Michaels-Marston, K. S., Liu, X., Pelton, G. H., Padilla, M., Marder, K., et al. (2000). Olfactory deficits in patients with mild cognitive impairment predict Alzheimer's disease at follow-up. *Am. J. Psychiatry* 157, 1399–1405. doi: 10.1176/appi.ajp.157.9.1399

Forsberg, A., Engler, H., Almkvist, O., Blomquist, G., Hagman, G., Wall, A., et al. (2008). PET imaging of amyloid deposition in patients with mild cognitive impairment. *Neurobiol. Aging* 29, 1456–1465. doi: 10.1016/j.neurobiolaging.2007.03.029

Hodler, J., Schulthess, G., and Zollikofer, C. (2012). *Diseases of the Brain, Head & Neck, Spine 2012-2015: Diagnostic Imaging and Interventional Techniques*. Milan: Springer Science & Business Media.

Illán, I. A., Górriz, J. M., López, M. M., Ramírez, J., Salas-Gonzalez, D., Segovia, F., et al. (2011). Computer aided diagnosis of Alzheimer's disease using component based SVM. *Appl. Soft Comput.* 11, 2376–2382. doi: 10.1016/j.asoc.2010.08.019

Illán, I., Gorriz, J., Ramirez, J., Chaves, R., Segovia, F., López, M., et al. (2010). "Machine learning for very early Alzheimer's disease diagnosis; a 18 F-FDG and pib PET comparison," in *Nuclear Science Symposium Conference Record (NSS/MIC), 2010 IEEE* (Knoxville, TN), 2334–2337.

Illán, I., Górriz, J., Ramírez, J., Salas-Gonzalez, D., López, M., Segovia, F., et al. (2011). 18F-FDG PET imaging analysis for computer aided Alzheimer's diagnosis⋆. *Inform. Sci.* 181, 903–916.

Jack, C., Knopman, D., Jagust, W., Shaw, L., Aisen, P., Weiner, M., et al. (2010). Hypothetical model of dynamic biomarkers of the Alzheimer's

pathological cascade. *Lancet Neurol.* 9, 119–128. doi: 10.1016/S1474-4422(09)70299-6

Jiang, J., Shu, X., Liu, X., and Huang, Z. (2015). "A computed aided diagnosis tool for Alzheimer's disease based on 11C-PIB PET imaging technique," in *IEEE International Conference on Information and Automation*.

Johnson, K., Minoshima, S., Bohnen, N., Donohoe, K., Foster, N., Herscovitch, P., et al. (2013). Appropriate use criteria for amyloid PET: a report of the amyloid imaging task force, the society of nuclear medicine and molecular imaging, and the alzheimer's association. *Alzheimer's Dement.* 9, E1–E16. doi: 10.1016/j.jalz.2013.01.002

Kemppainen, N., Aalto, S., Wilson, I., Någren, K., Helin, S., Brück, A., et al. (2006). Voxel-based analysis of PET amyloid ligand [11c] PIB uptake in Alzheimer disease. *Neurology* 67, 1575–1580. doi: 10.1212/01.wnl.0000240117.55680.0a

Langa, K. M., and Levine, D. A. (2014). The diagnosis and management of mild cognitive impairment: a clinical review. *JAMA* 312, 2551–2561. doi: 10.1001/jama.2014.13806

López, M., Ramírez, J., Górriz, J. M., Álvarez, I., Salas-Gonzalez, D., Segovia, F., et al. (2011). Principal component analysis-based techniques and supervised classification schemes for the early detection of Alzheimer's disease. *Neurocomputing* 74, 1260–1271. doi: 10.1016/j.neucom.2010.06.025

Lu, L., and Bludau, J. (2011). *Alzheimer's Disease, 1st Edn.* Westport, CT: ABC-CLIO.

Martínez-Murcia, F., Górriz, J., Ramírez, J., Puntonet, C., and Salas-González, D. (2012). Computer aided diagnosis tool for Alzheimer's disease based on Mann-Whitney-Wilcoxon U-test. *Expert Syst. Appl.* 39, 9676–9685. doi: 10.1016/j.eswa.2012.02.153

Morbelli, S., Drzezga, A., Perneczky, R., Frisoni, G. B., Caroli, A., van Berckel, B. N., et al. (2012). Resting metabolic connectivity in prodromal Alzheimer's disease. a european Alzheimer disease consortium (EADC) project. *Neurobiol. Aging* 33, 2533–2550. doi: 10.1016/j.neurobiolaging.2012.01.005

NeuroImaging, W. (2017). *Spm12 - Statistical Parametric Mapping. fil.ion.ucl.ac.uk.* Available online at: http://www.fil.ion.ucl.ac.uk/spm/software/spm12//

NIH (2017). *National Institute on Aging.* Available online at: http://www.nia.nih.gov/

Padilla, P., Lopez, M., Gorriz, J., Ramirez, J., Salas-Gonzalez, D., and Alvarez, I. (2012). NMF-SVM based CAD tool applied to functional brain images for the diagnosis of Alzheimer's disease. *IEEE Trans. Med. Imaging* 31, 207–216. doi: 10.1109/TMI.2011.2167628

Rami, L., Sala-Llonch, R., Solé-Padullés, C., Fortea, J., Olives, J., Lladó, A., et al. (2012). Distinct functional activity of the precuneus and posterior cingulate cortex during encoding in the preclinical stage of Alzheimer's disease. *J. Alzheimer's Dis.* 31, 517–526. doi: 10.3233/JAD-2012-120223

Salas-Gonzalez, D., Segovia, F., Martínez-Murcia, F. J., Lang, E. W., Gorriz, J. M., and Ramırez, J. (2016). An optimal approach for selecting discriminant regions for the diagnosis of Alzheimer's disease. *Curr. Alzheimer Res.* 13, 838–844. doi: 10.2174/1567205013666160415154852

Scheff, S. W., Price, D. A., Ansari, M. A., Roberts, K. N., Schmitt, F. A., Ikonomovic, M. D., et al. (2015). Synaptic change in the posterior cingulate gyrus in the progression of Alzheimer's disease. *J. Alzheimer's Dis.* 43, 1073–1090. doi: 10.3233/JAD-141518

Serby, M., Larson, P., and Kalkstein, D. (1991). The nature and course of olfactory deficits in Alzheimer's disease. *Am. J. Psychiatry* 148:357.

Shin, J., Lee, S.-Y., Kim, S. J., Kim, S.-H., Cho, S.-J., and Kim, Y.-B. (2010). Voxel-based analysis of Alzheimer's disease PET imaging using a triplet of radiotracers: PIB, FDDNP, and FDG. *Neuroimage* 52, 488–496. doi: 10.1016/j.neuroimage.2010.04.013

Sjöbeck, M., and Englund, E. (2001). Alzheimer's disease and the cerebellum: a morphologic study on neuronal and glial changes. *Dement. Geriatr. Cogn. Disord.* 12, 211–218. doi: 10.1159/000051260

Su, S.-S., Chen, K.-W., and Huang, Q. (2014). Discriminant analysis in the study of Alzheimer's disease using feature extractions and support vector machines in positron emission tomography with 18F-FDG. *J. Shanghai Jiaotong Univ.* 19, 555–560. doi: 10.1007/s12204-014-1540-4

Toennies, K. D. (2012). *Guide to Medical Image Analysis: Methods and Algorithms*. London: Springer Science & Business Media.

Turkington, C., and Harris, J. (2001). *The Encyclopedia of the Brain and Brain Disorders*. New York, NY: Infobase Pub.

Varghese, T., Sheelakumari, R., James, S. J., and Mathuranath, P. (2013). A review of neuroimaging biomarkers of Alzheimer's disease. *Neurol. Asia* 18, 239–248.

Velayudhan, L. (2015). Smell identification function and Alzheimer's disease: a selective review. *Curr. Opin. Psychiatry* 28, 173–179. doi: 10.1097/YCO.0000000000000146

Wang, H.-Y., D'Andrea, M. R., and Nagele, R. G. (2002). Cerebellar diffuse amyloid plaques are derived from dendritic aβ42 accumulations in purkinje cells. *Neurobiol. Aging* 23, 213–223. doi: 10.1016/s0197-4580(01)00279-2

Wegrzyn, R., and Rudolph, A. (2012). *Alzheimer's Disease: Targets for New Clinical Diagnostic and Therapeutic Strategies*. Boca Raton, FL: CRC Press.

WHO (2017). *World Health Organization.* Available online at: http://www.who.int/

Yaffe, K. (2013). *Chronic Medical Disease and Cognitive Aging: Toward a Healthy Body and Brain*. New York, NY: Oxford University Press.

Zhang, Y., Dong, Z., Phillips, P., Wang, S., Ji, G., Yang, J., et al. (2015). Detection of subjects and brain regions related to Alzheimer's disease using 3D MRI scans based on eigenbrain and machine learning. *Front. Comput. Neurosci.* 9:66. doi: 10.3389/fncom.2015.00066

Ziolko, S. K., Weissfeld, L. A., Klunk, W. E., Mathis, C. A., Hoge, J. A., Lopresti, B. J., et al. (2006). Evaluation of voxel-based methods for the statistical analysis of PIB PET amyloid imaging studies in Alzheimer's disease. *Neuroimage* 33, 94–102. doi: 10.1016/j.neuroimage.2006.05.063

Zou, Y.-M., Lu, D., Liu, L.-P., Zhang, H.-H., and Zhou, Y.-Y. (2016). Olfactory dysfunction in Alzheimer's disease. *Neuropsychiatr. Dis. Treat.* 12, 869–875. doi: 10.2147/NDT.S104886

Conflict of Interest Statement: The authors declare that the research was conducted in the absence of any commercial or financial relationships that could be construed as a potential conflict of interest.

Copyright © 2018 El-Gamal, Elmogy, Ghazal, Atwan, Casanova, Barnes, Keynton, El-Baz and Khalil for the Alzheimer's Disease Neuroimaging Initiative. This is an open-access article distributed under the terms of the Creative Commons Attribution License (CC BY). The use, distribution or reproduction in other forums is permitted, provided the original author(s) or licensor are credited and that the original publication in this journal is cited, in accordance with accepted academic practice. No use, distribution or reproduction is permitted which does not comply with these terms.

Advantages of publishing in Frontiers

OPEN ACCESS
Articles are free to read for greatest visibility and readership

FAST PUBLICATION
Around 90 days from submission to decision

HIGH QUALITY PEER-REVIEW
Rigorous, collaborative, and constructive peer-review

TRANSPARENT PEER-REVIEW
Editors and reviewers acknowledged by name on published articles

Frontiers
Avenue du Tribunal-Fédéral 34
1005 Lausanne | Switzerland

Visit us: www.frontiersin.org
Contact us: info@frontiersin.org | +41 21 510 17 00

REPRODUCIBILITY OF RESEARCH
Support open data and methods to enhance research reproducibility

DIGITAL PUBLISHING
Articles designed for optimal readership across devices

FOLLOW US
@frontiersin

IMPACT METRICS
Advanced article metrics track visibility across digital media

EXTENSIVE PROMOTION
Marketing and promotion of impactful research

LOOP RESEARCH NETWORK
Our network increases your article's readership